

MOLECULAR PHYSICS

VOLUME 3

1960

Printed and Published by

TAYLOR & FRANCIS LTD

RED LION COURT, FLEET STREET, LONDON, E.C.4

CONTENTS OF VOLUME 3

NUMBER 1—JANUARY 1960	Page
An electron spin resonance study of a γ -irradiated single crystal of glycollic acid. N. M. ATHERTON and D. H. WHIFFEN	1
The Renner effect and spin-orbit coupling. J. A. POPLE	16
Some temperature-dependent effects on the optical absorption line shape of paramagnetic ions. R. ENGLMAN	23
A thermodynamic discriminant for the Lennard-Jones potential. W. B. BROWN and J. S. ROWLINSON	35
Charge transfer states and optical absorption in octahedrally hydrated paramagnetic salts. ROBERT ENGLMAN	48
Thermodynamic properties of clathrates: II. The heat capacity and entropy of methane in the methane quinol clathrates. N. G. PARSONAGE and L. A. K. STAVELEY	59
The influence of paramagnetic molecules on singlet-triplet transitions. G. J. HOIJINK	67
The fluorescence and excitation spectra of anthracene vapour at low pressures. B. STEVENS and E. HUTTON	71
Some investigations in the theory of open-shell ions. Part I. The spin-Hamiltonian. J. S. GRIFFITH	79
Ionic interactions in solutions of electrolytes as studied by ultra-violet spectroscopy. T. R. GRIFFITHS and M. C. R. SYMONS	90
RESEARCH NOTE	
Electron resonance study of the carboxylate hydroxy methyl radical ion. N. M. ATHERTON and D. H. WHIFFEN	103
 NUMBER 2—MARCH 1960 	
Intramolecular charge-transfer absorption spectra of formamide and acrolein. S. NAGAKURA	105
High resolution hydrogen resonance spectra of some substituted ethylenes. E. O. BISHOP and R. E. RICHARDS	114
Magnetic properties of Co^{2+} ions in octahedral interstices of an oxide lattice. P. COSSEE	125
The redistribution of charge in naphthalene caused by methyl substitution. I. Partial rate factors for hydrogen-deuterium exchange in α , α and β , β -dimethylnaphthalenes. G. DALLINGA, P. J. SMIT and E. L. MACKOR	130
An interpretation of potential interaction constants in terms of low-lying excited states. R. F. W. BADER	137

CONTENTS OF VOLUME 3

	Page
Ultra-violet absorption spectra and π -electron structures of nitromethane and the nitromethyl anion. SABURO NAGAKURA	152
Cobalt nuclear resonance measurements of rate processes and a system in equilibrium. R. P. H. GASSER and R. E. RICHARDS	163
High-resolution nuclear-magnetic-resonance spectra of hydrocarbon groupings. III. An analysis of the spectrum of liquid propane using ^{13}CH satellites. N. SHEPPARD and J. J. TURNER	168
Studies of ion-solvent and ion-ion interactions using nuclear magnetic resonance spectroscopy. A. CARRINGTON, F. DRAVNICKS and M. C. R. SYMONS	174
The effect of strong electric and magnetic fields on the depolarization ratios of gases. A. L. ANDREWS and A. D. BUCKINGHAM	183
Paramagnetic resonance in phosphorescent aromatic hydrocarbons. II. Determination of zero-field splitting from solution spectra. M. S. DE GROOT and J. H. VAN DER WAALS	190

RESEARCH NOTES

New interpretations of the orbital energy differences in hexafluorides. C. K. JØRGENSEN	201
On the surface tension of regular mixtures. A. BELLEMANS and J. STECKI	203

NUMBER 3—MAY 1960

Unstable intermediates. Part X. Aliphatic carbonium ions. J. ROSENBAUM and M. C. R. SYMONS	205
Nuclear magnetic shielding of a hydrogen atom in (1) an electric field-gradient and (2) a cage. A. D. BUCKINGHAM and K. P. LAWLEY ..	219
The redistribution of charge in naphthalene caused by methyl substitution. II. The magnetic shielding of protons in α , α - and β , β -dimethyl-naphthalenes. C. MACLEAN and E. L. MACKOR	223
Self-consistent field theory of the electron spin distribution in π -electron radicals. A. D. McLACHLAN	233
Solvent effects in the proton resonance spectra of dimethyl-formamide and dimethyl-acetamide. J. V. HATTON and R. E. RICHARDS ..	253
A test of the Lennard-Jones potential for nitrogen and methane. J. S. ROWLINSON	265
The temperature-independent paramagnetism of permanganate and related complexes. A. CARRINGTON	271
On a non-linear law of the irreversible phenomena with stationary constraints. P. GLANDSORFF	277
Some investigations in the theory of open-shell ions. Part II. V , W and X coefficients. J. S. GRIFFITH	285

RESEARCH NOTES

Semiconductivity in organic molecular complexes. Miss J. A. VAN DER HOEK, J. H. LUPINSKI and L. J. OOSTERHOFF	299
Discrete sites in liquids. G. WILSE ROBINSON	301

NUMBER 4—JULY 1960

Intermolecular forces from optical spectra of impurities in molecular crystals. R. W. ZWANZIG	305
Statistical mechanics of solid and liquid mixtures of ortho- and para-hydrogen: II. AGNESSA BABLOYANTZ and A. BELLEMANS .. .	313
The effect of paramagnetic molecules on the intensity of spin-forbidden absorption bands of aromatic molecules. J. N. MURRELL .. .	319
The absorption spectra of permanganate, manganate and related oxyions. A. CARRINGTON and D. S. SCHONLAND	331
Nuclear magnetic shielding and diamagnetic susceptibility of interacting hydrogen atoms. T. W. MARSHALL and J. A. POPE	339
High resolution nuclear-magnetic-resonance spectra of hydrocarbon groupings. IV. ABC spectra of vinyl compounds. C. N. BANWELL and N. SHEPPARD	351
Polarizations of electronic transitions in aromatic hydrocarbon molecules and their mono- and di-valent ions. G. J. HOIJTINK and P. J. ZANDSTRA	371
The helix-coil transition in charged macromolecules. BRUNO H. ZIMM and STUART A. RICE	391

NUMBER—5 SEPTEMBER 1960

Helix-coil transformation and titration curve of poly-L-glutamic acid. AKIYOSHI WADA	409
The use of complex wiggle-beat patterns for the estimation of small splittings in NMR spectra. J. J. TURNER	417
Fluorescence self-quenching in aromatic vapours; the role of excited dimers. B. STEVENS and P. J. McCARTIN	425
Spin decoupling in high resolution proton magnetic resonance. R. FREEMAN	435
The calculation of dispersion forces. L. SALEM	441
The effect of bond length variations in molecular orbital calculations of π -electron spectra – aniline. T. E. PEACOCK	453
Some investigations in the theory of open-shell ions. Part III. The calculation of matrix elements. J. S. GRIFFITH	457
Some investigations in the theory of open-shell ions. Part IV. The basis of intensity theory. J. S. GRIFFITH	477

CONTENTS OF VOLUME 3

	Page
The proton resonance spectrum of <i>m</i> -dinitrobenzene, an AB ₂ X system. R. J. ABRAHAM, E. O. BISHOP and R. E. RICHARDS	485
Properties of the self-consistent field treatment of conjugated molecules. H. H. GREENWOOD and T. H. J. HAYWARD	495
RESEARCH NOTE	
The nuclear magnetic resonance spectrum of N-vinyl pyrrolidone. C. N. BANWELL	511
NUMBER 6—NOVEMBER 1960	
A semi-empirical theory of the electronic structure of ethylene with particular reference to the ionization potential. Y. I'HAYA ..	513
A further study on the electronic structure and spectrum of ethylene. Y. I'HAYA	521
Correlations between the electronic spectra of alternant hydrocarbon molecules and their mono- and di-valent ions. II. Hydrocarbons with symmetry D _{2h} . G. J. HOJTINK, N. H. VELTHORST and P. J. ZANDSTRA	533
The analysis of complex nuclear magnetic resonance spectra. I. Systems with one pair of strongly coupled nuclei. J. A. POPLE and T. SCHAEFER	547
The analysis of complex nuclear magnetic resonance spectra. II. Some further systems with one strong coupling constant. P. DIEHL and J. A. POPLE	557
Equilibrium properties of crystalline argon, krypton and xenon. E. A. GUGGENHEIM and M. L. McGLASHAN	563
The properties of argon at its triple point. E. A. GUGGENHEIM and M. L. McGLASHAN	571
Electron spin correlation and the ethane barrier. HARRY G. HECHT, DAVID M. GRANT and HENRY EYRING	577
The proton resonance spectra of metal bis-cyclopentadienyls. D. A. LEVY and L. E. ORGEL	583
The collisional stabilization of excited β-naphthylamine molecules by the paraffin hydrocarbons in the gas phase. B. STEVENS	589
RESEARCH NOTES	
The anomalous temperature dependence of the sound velocity in water. J. SCHUYER	597
Dynamical Jahn-Teller effect in molecules possessing one four-fold symmetry axis. M. S. CHILD	601
Vibrational-electronic coupling in IrF ₆ , OsCl ₆ ²⁻ and IrCl ₆ ²⁻ . M. S. CHILD	605
Rotational isomerism in aldehydes. R. J. ABRAHAM and J. A. POPLE ..	609
Index of Authors (with the Titles of Papers)	613

An electron spin resonance study of a γ -irradiated single crystal of glycollic acid

by N. M. ATHERTON and D. H. WHIFFEN
Chemistry Department, University of Birmingham

(Received 13 July 1959)

Measurements have been made of the electron spin resonance spectrum of a γ -irradiated single crystal of glycollic acid as a function of crystal orientation. These confirm that the trapped radicals are carboxy hydroxy methyl radicals, HOCHCOOH. The results are expressed in the form of a spin Hamiltonian which includes a coupling tensor for the hydrogen attached to the central carbon atom and a tensor for the hydroxyl hydrogen. A special feature of the spectra is that the relative intensities of the hyperfine lines are non-integral, and this is explained by a derivation of the transition moments which shows that the usual selection rule $\Delta M_I = 0$ is inapplicable to the solid state. The anisotropic g tensor is also evaluated. The tensors are briefly discussed in relation to the orientation of the radicals in the crystal and their electronic structure.

1. INTRODUCTION

The interest in the electron resonance spectra of organic free radicals lies principally in their hyperfine structure, which arises through the coupling between the odd electron and neighbouring nuclei. The interpretation of such spectra can yield precise information as to the structure of the radicals and the distribution of the odd electron. Because of the dipole-dipole interaction the coupling is anisotropic, and is most conveniently expressed as a tensor. However, many of the measurements on free radicals have been made on systems in solution, for which state it has been shown that the anisotropic part of the coupling is averaged to zero by the comparatively fast tumbling of the radicals [1], and such spectra have been interpreted solely in terms of the 'contact' interactions, which are isotropic [2]. The hyperfine interactions have then been described by scalar coupling constants. In the case of radicals trapped in amorphous and polycrystalline solids the summation, over all orientations, of the anisotropic term results in broadening of the individual lines so that hyperfine structure may be blurred out and the spectra may have a false simplicity. It has become apparent that the interpretation of such spectra must be approached with reserve.

In order to obtain the couplings in a radical as a tensor, and thus derive the maximum amount of information, it is necessary that the radicals be trapped in specific orientations. This condition may be fulfilled for the radicals produced on γ -irradiation of single crystals, and Ghosh and Whiffen [3] have recently made a detailed study of the oriented radicals trapped in irradiated single crystals of glycine. The radical orientations were found to be quite precise and the couplings were evaluated as tensors and the structure of the radical discussed.

The present contribution is a similar study of the radicals trapped on the γ -irradiation of single crystals of glycollic acid, HOCH₂COOH. A previous

investigation by Grant, Ward and Whiffen [4], who examined the polycrystalline acid and its deuterated derivatives, showed that the radicals remaining trapped were carboxy-hydroxy-methyl, HOCHCOOH, and the present results confirm that conclusion. The couplings to two protons have been analysed, and the *g*-factor, which is also anisotropic, has been evaluated as a tensor.

2. EXPERIMENTAL

2.1. Crystal symmetry and choice of axes

Grown from acetone solution, either by slow cooling or slow evaporation, the glycollic acid crystal is a somewhat elongated hexagonal plate (M.Pt. 75–78°C). Right-handed Cartesian reference axes were chosen against the faces of individual crystals such that *x* and *y* were parallel and perpendicular respectively to the longest edge, and *z* perpendicular to the plate. These axes and the form of the crystals are illustrated in figure 1.

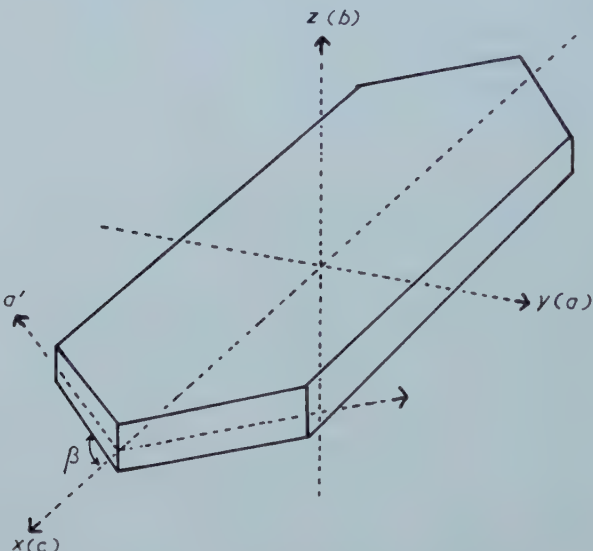


Figure 1. Appearance of crystal showing choice of reference axes.

The elements of symmetry have been described by Groth [5], who gives monoclinic symmetry with $\beta=115^\circ$. This was confirmed by x-ray measurements made by Hughes and Small [6], who found that the space-group is $P2_1/c$ and that the unit cell dimensions are $a'=8.95\text{ \AA}$, $b=10.50\text{ \AA}$ and $c=7.76\text{ \AA}$, with $\beta=115^\circ 44'$. The relation of these axes to the arbitrarily assigned *xyz* system is also shown in figure 1. The asymmetric units of the structure are pairs of molecules, and there are four pairs in the unit cell, but the x-ray measurements [6] were not sufficiently comprehensive to indicate the orientations of individual molecules either to the axes or to each other.

The x-ray measurements [6] indicate that the *c*-axis is almost an axis of symmetry so that the crystal almost has orthorhombic symmetry. The *a*, *b* and *c* axes then correspond to the *y*, *z* and *x* axes, respectively. In this pseudo-orthorhombic representation there are eight pairs of molecules in the unit cell,

with $a = 16.13 \text{ \AA}$ and the other two dimensions identical with those of the monoclinic unit cell. Unfortunately it was not possible to determine whether the a' axes had direction cosines $(\cos \beta, \sin \beta, 0)$ or $(\cos \beta, -\sin \beta, 0)$ since the crystals used for the resonance spectra were too large for x-ray studies.

Throughout the investigation all measurements were referred to the xyz axes and unless it is specifically stated otherwise this will be the case in the present discussion. The magnetic field is conveniently taken to define a direction **Z**, with associated **X** and **Y**, and this will be used to specify the field orientation in terms of the direction cosines (l, m, n) of **Z** with respect to the crystal axes.

2.2. Materials and measurements

Commercial glycollic acid was used to grow large (*c.* 200 mg) crystals from acetone solution. These were dried by pumping under high vacuum at room temperature for at least 24 hours, sealed off in glass phials, and irradiated *in vacuo* at room temperature in a 200 Curie ^{60}Co γ -ray source. The dose varied between 2×10^{20} and 4×10^{20} ev cm^3 . Glycollic acid is very hygroscopic and after irradiation the crystals were painted with shellac as a protection against atmospheric moisture while measurements were being made. The irradiated crystals were stored in a desiccator at room temperature.

The spectra were taken on a 9200 Mc/sec reflection spectrometer [7]. This instrument uses magnetic field modulation at 490 c/s and phase sensitive detection to present the first derivative of the absorption on a pen-recorder. The crystals were mounted on a Perspex rod at the centre of a rectangular H_{012} tuneable cavity, using lanolin as adhesive. The rod extended through the narrow side of the cavity and thus the crystal could be rotated about an axis perpendicular to the applied magnetic field, and the angle of rotation was measured by a small brass scale. This angle could be measured to 2° and the crystals could be mounted reproducibly to $\pm 3^\circ$.

Spectra were taken at room temperature at 10° intervals during rotation about each of the axes x, y, z , and measurements of the hyperfine splittings were made directly from the derivative spectra and are estimated to be accurate to ± 3 per cent. Numerical integration was used to recover the actual absorption line shapes from the recorder traces.

The g -values were measured by comparing the position of the centre of the radical spectrum with that of the α, α -diphenyl β -picryl hydrazyl (DPPH) line. The DPPH was very finely ground, so as to avoid asymmetry of the line in respect of its own anisotropic g -value [8], and a smear put on the crystal so that the superimposed spectra were recorded. The difference between the centres of the pattern was measured in frequency units and the g -values calculated from

$$g = \left(1 + \frac{\Delta\nu}{\nu}\right) g_D$$

where $g = g$ -value of radicals, $g_D = g$ -value of DPPH, $\Delta\nu =$ frequency difference, between centres and $\nu =$ frequency of measurement. The sign convention for this equation is that shifts to higher fields than DPPH are negative.

The DPPH used had been recrystallized from carbon disulphide and its g -value was taken as -2.0036 ± 0.0002 , after Holden, Kittel, Merrit and Yager [9]. DPPH is known to form complexes with some other organic solvents [10] and this may affect the apparent g -value [11].

3. THE SPIN HAMILTONIAN

The spin Hamiltonian may be written

$$\mathcal{H} = -\beta \mathbf{S} \cdot \mathbf{g} \cdot \mathbf{H}_0 + \sum_j \mathbf{S} \cdot \mathbf{T}^j \cdot \mathbf{I}^j - \sum_j (\mu^j / I^j) \mathbf{I}^j \cdot \mathbf{H}_0.$$

In this, the first term is the coupling of the odd electron to the magnetic field and when expressed in frequency units, is about 9200 Mc/s. The second term contains the electron-nuclei couplings of up to 100 Mc/s and the third term expresses the coupling of the nuclei to the magnetic field, of 14.0 Mc/s per proton in 3300 Gauss.

The transition frequencies and intensities derived from this Hamiltonian may be quite complicated and it is not feasible to derive the coupling coefficients directly from the spectra. However, a process of trial and error leads to coupling coefficients which give theoretical spectra agreeing with the experimental.

In computing the hyperfine structure g may be taken as isotropic to a good approximation and off-diagonal elements connecting the $M_S = +\frac{1}{2}$ and $-\frac{1}{2}$ states may be neglected in comparison with the transition frequency, 9200 Mc/s. With this approximation $\mathbf{S} = M_S \mathbf{Z}$ and the nuclear spin section of the Hamiltonian is given by

$$\sum_j M_S \mathbf{Z} \cdot \mathbf{T}^j \cdot \mathbf{I}^j - \nu^j \mathbf{I}^j \cdot \mathbf{Z}$$

where ν^j is the normal nuclear resonance frequency in the magnetic field, i.e.

$$\nu^j \mathbf{Z} = (\mu^j / I^j) \mathbf{H}_0.$$

The Hamiltonian is now separable in the nuclei, j , and the eigenstates can be expressed as products of states of each nucleus. For each nucleus the Hamiltonian may be expressed in terms of the resolved spin operators I_X , I_Y and I_Z where \mathbf{X} and \mathbf{Y} are arbitrary directions perpendicular to each other and \mathbf{Z} . The resultant Hamiltonian for each nucleus is

$$(M_S \mathbf{Z} \cdot \mathbf{T} \cdot \mathbf{Z} - \nu) I_Z + M_S \mathbf{Z} \cdot \mathbf{T} \cdot \mathbf{X} I_X + M_S \mathbf{Z} \cdot \mathbf{T} \cdot \mathbf{Y} I_Y.$$

If

$$\mathbf{Z} \cdot \mathbf{T} \cdot \mathbf{Z} = T_{||} \quad \text{and} \quad (\mathbf{Z} \cdot \mathbf{T} \cdot \mathbf{X})^2 + (\mathbf{Z} \cdot \mathbf{T} \cdot \mathbf{Y})^2 = T_{\perp}^2$$

the energy levels, for nuclei of spin $\frac{1}{2}$, are given by

$$E = \pm \frac{1}{2} [(M_S T_{||} - \nu)^2 + (M_S T_{\perp})^2]^{1/2}.$$

In a representation in which I_Z is diagonal the unnormalized eigenvectors are given by

$$(2E + M_S T_{||} - \nu) |+\rangle + M_S T_{\perp} |-\rangle.$$

It can be seen that both the eigenvalues and eigenvectors depend on M_S . For a transition $M_S = \frac{1}{2} \leftrightarrow -\frac{1}{2}$ there will in general be four hyperfine lines which occur in pairs of equal and opposite frequency with respect to the centre of the pattern, and of equal intensity. The relative intensities are proportional to the square of the overlap of the nuclear eigenvectors.

One pair of transitions have zero intensity: (i) If $T_{\perp} = 0$, that is \mathbf{Z} lies along a principal direction of \mathbf{T} . This case covers all directions for an isotropic coupling tensor, as in solution work. (ii) If the magnetic field tends to zero so that ν can be neglected. (iii) If the magnetic field is very large so that the electron-nuclei couplings can be neglected. Case (iii) corresponds to a Paschen-Back effect in atomic spectroscopy and the general case to a partial effect. In the general case

the two pairs of lines may be of comparable intensity. The hyperfine pattern is also field dependent through its variation with ν .

For coupling to more than one nucleus the transition frequencies are additive and the intensities multiplicative by virtue of the separability of the nuclear coordinates. This separability ensures that the spectra are independent of the relative signs of the two tensors. The calculation is equivalent to that of Trammell, Zeldes and Livingston [12, 13] who discuss case (iii) particularly in terms of the magnetic field of the electron at the position of the nucleus. The present discussion in terms of a spin Hamiltonian appears simpler and more suited to numerical calculation.

4. RESULTS

4.1. Preliminary results and interpretation

The radical stability seemed to vary slightly between different crystals, but was good for at least two months, at room temperature. The decay can be greatly reduced by storing the crystals at liquid air temperature when not in use.

For $\mathbf{Z} = (1, 0, 0)$ the observed spectrum was a doublet, separation 55 ± 2 Mc/s (figure 2 *a*) and for rotation about $(0, 0, 1)$ the lines broadened and eventually split, giving a well resolved quartet at $\mathbf{Z} = (0, 1, 0)$ (figure 2 *d*). Spectra for two of the intermediate orientations are shown in figures 2 *b* and *c*. The changes in the spectrum were symmetrical with respect to $(1, 0, 0)$ and $(0, 1, 0)$ so that the pattern at $\mathbf{Z} = (l, m, 0)$ was identical with that at $(-l, m, 0)$. Similar symmetry was retained during rotation about $(0, 1, 0)$, for which the spectrum remained principally a doublet, the separation increasing to 75 ± 2.5 Mc/s at $\mathbf{Z} = (0, 0, 1)$ (figure 2 *g*). Figures 2 *e* and *f* show spectra at two intermediate orientations and illustrate the appearance of weak satellite lines on either side of each of the main lines. The minimum line width $\Delta H_{\text{m.s.}}$ was 12 Mc/s at $\mathbf{Z} = (2^{-1/2}, 0, 2^{-1/2})$. The analysis in § 4.2 suggests these lines to be an unresolved doublet of 2 Mc/s so that the inherent single line would have $\Delta H_{\text{m.s.}} \sim 10$ Mc/s.

Rotation about $(1, 0, 0)$ produced a much more complicated series of spectra, which are illustrated in figure 3 *a* to *h*. These spectra comprise up to eight resolved lines in some cases, and there is considerable asymmetry, while the changes produced by rotations of 10° are of greater magnitude than for similar intervals during rotation about $(0, 0, 1)$ and $(0, 1, 0)$. However the symmetry of the patterns between $(0, m, n)$ and $(0, -m, n)$ was retained. The hyperfine couplings are therefore consistent with orthorhombic symmetry.

These observations are in accordance with the assignment of the spectrum of the γ -irradiated polycrystalline glycollic acid to the carboxy-hydroxy-methyl radical, HOCHCOOH [4]. The presence of a strong doublet at many orientations is attributed to strong coupling to the remaining proton of the original methylene group, which will be designated H(C). The further splitting of the doublet into four lines near $\mathbf{Z} = (0, 1, 0)$ suggests that there is weaker coupling to a second proton, which will be designated H(O). The obvious choice for this proton is that of the hydroxyl group, and it will be shown that the experimental observations support this choice, in preference to a proton in a neighbour molecule, or the one associated with the carboxyl group.

The complex asymmetric spectra obtained on rotation about $(1, 0, 0)$ suggest that there are two types of radical present. However, the symmetry and

simplicity of the patterns for rotation about the other two reference axes suggest that in fact these are not chemically different species, but merely similar radicals having different orientations, when asymmetry of the *g*-values produces an asymmetric pattern. The two radicals are related by the twofold screw axis, *b*, and therefore their tensors differ only in the sign of their *zx* and *yz* elements.

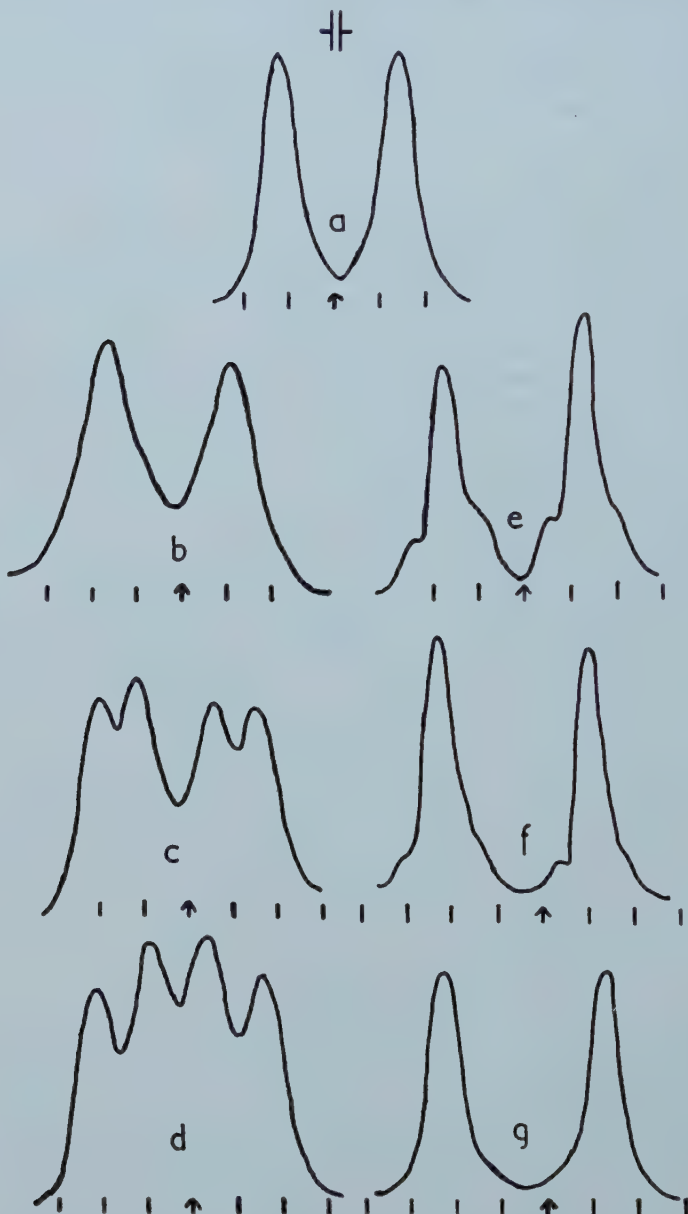


Figure 2. Integrated spectra for rotation about $(0, 0, 1)$ and $(0, 1, 0)$. Magnetic field increasing to the right. Arrow at $g = -2.0023$, marks at 20 Mc/s intervals therefrom. **Z** directions:

- (a) $(1, 0, 0)$; (b) $(3^{1/2}, 2^{-1}, 2^{-1}, 0)$; (c) $(2^{-1}, 3^{1/2}, 2^{-1}, 0)$; (d) $(0, 1, 0)$; (e) $(3^{1/2}, 2^{-1}, 0, 2^{-1})$; (f) $(2^{-1}, 0, 3^{1/2}, 2^{-1})$; (g) $(0, 0, 1)$.

		Tensor in relation to <i>xyz</i> axes		Isotropic component		Anisotropic components	
		Principal values		Principal values		Direction cosines	
H(C)	(-)	+55 0 0	0 +47 ±26	0 ±26 +69	(-)86 (-)55 (-)30	(-)57	(-)29 (+)2 (+)27
H(O)	(+)	+4 0 0	0 +25 ±9	0 ±9 -4	(+)28 (+)4 (-)7	(+)8	(+)20 (-)4 (-)15
<i>g</i>	(-)	+2.0020 +0.0007 0	+0.0007 +2.0038 ±0.0006	0 ±0.0006 +2.0050	-2.0053 -2.0038 -2.0017		(-0.08, -0.41, ±0.91) (+0.33, +0.85, ±0.42) (+0.94, -0.34, ±0.06)

Table 1. Coupling tensors (Mc/s) and *g*-tensors.

4.2. The nuclear coupling tensors

The nuclear tensors finally adopted are shown in table 1. The H(C) couplings for the $\mathbf{Z} = (1, 0, 0), (0, 1, 0)$ and $(0, 0, 1)$ positions give approximate values for the xx , yy and zz components of the H(C) tensor, as for this nucleus the coupling is approximately $\mathbf{Z} \cdot T \cdot \mathbf{Z}$. For rotations about $(0, 1, 0)$ the differently oriented radicals have the same spectra showing both the zx elements to be zero. Non-zero values would need to be of opposite sign for the different radicals. The fact that for rotations about $(0, 0, 1)$ the spectra are symmetrical to the x , y axes

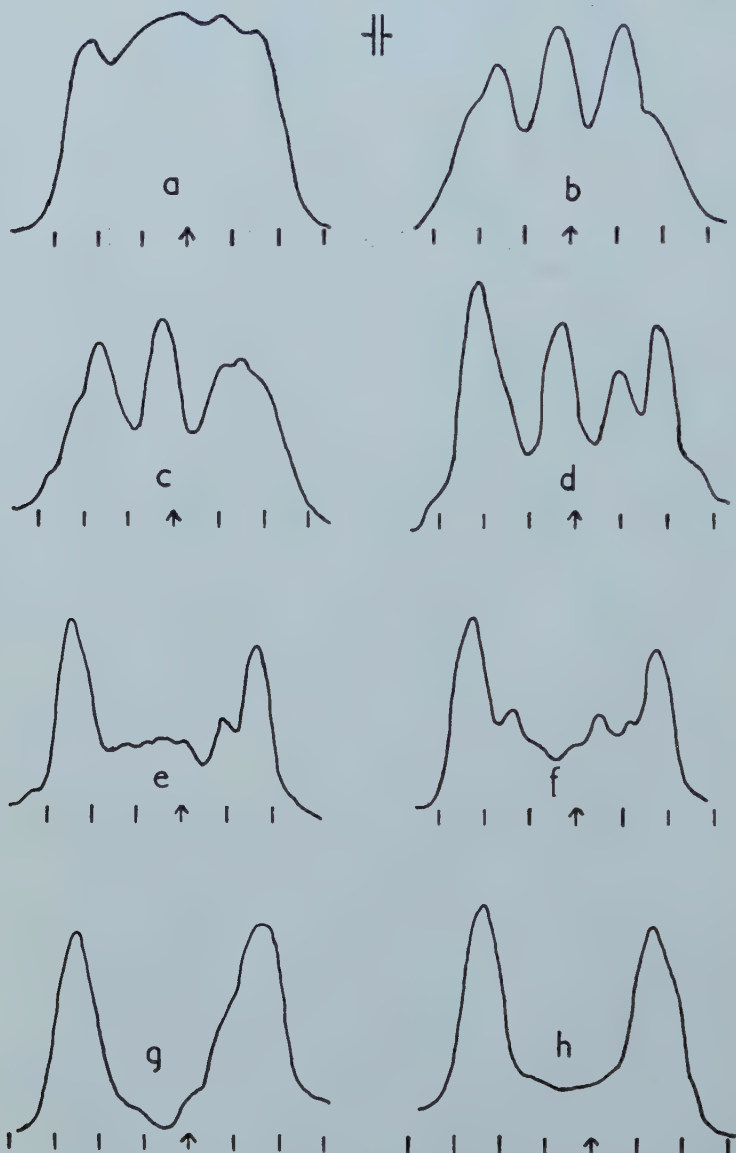


Figure 3. Integrated spectra for rotation about $(1, 0, 0)$. Magnetic field increasing to the right. Arrow $g = -2.0023$, marks at 20 Mc/s intervals therefrom. \mathbf{Z} given by $(0, \cos \theta, \sin \theta)$ with θ having the values (a) 10° ; (b) 20° ; (c) 30° ; (d) 40° ; (e) 50° ; (f) 60° ; (g) 70° ; (h) 80° .

Z	Figure	Hyperfine pattern (upper signs)		Centre
$(\pm 2^{-1}, 3^{1/2}, 2^{-1}, 0)$	2_c	$\pm 44, \pm 12, 27,$	$\pm 36, \pm 21, 66,$	$\pm 19, \pm 4, 5,$
$(3^{1/2}, 2^{-1}, \pm 2^{-1}, 0)$	2_b	$\pm 43, \pm 13, 13,$	$\pm 32, \pm 23, 84,$	$\pm 18, \pm 9, 3,$
$(1, 0, 0)$	2_a	$\pm 42, \pm 14, 9,$	$\pm 30, \pm 26, 100,$	$\pm 16, \pm 12, 0,$
$(3^{1/2}, 2^{-1}, 0, \pm 2^{-1})$	2_e	$\pm 45, \pm 16, 5,$	$\pm 31, \pm 29, 93,$	$\pm 14, \pm 13, 2,$
$(\pm 2^{-1}, 0, 3^{1/2}, 2^{-1})$	2_f	$\pm 50, \pm 20, 19,$	$\pm 36, \pm 34, 86,$	$\pm 14, \pm 12, 4,$
$(0, 0, 1)$	2_g	$\pm 52, \pm 22, 11,$	$\pm 39, \pm 35, 87,$	$\pm 15, \pm 11, 2,$
$\theta = -80$	3_h	$\pm 49, \pm 18, 18,$	$\pm 34, \pm 33, 77,$	$\pm 13, \pm 12, 4,$
-70	3_g	$\pm 45, \pm 14, 23,$	$\pm 31, \pm 28, 69,$	$\pm 13, \pm 11, 6,$
-60	3_f	$\pm 41, \pm 8, 25,$	$\pm 29, \pm 20, 59,$	$\pm 16, \pm 7, 9,$
-50	$3_e, 4$	$\pm 37, \pm 3, 30,$	$\pm 27, \pm 13, 51,$	$\pm 19, \pm 5, 12,$
-40	3_d	$\pm 33, \pm 0, 29,$	$\pm 26, \pm 7, 44,$	$\pm 22, \pm 4, 16,$
-30	3_c	$\pm 31, \pm 0, 32,$	$\pm 27, \pm 4, 43,$	$\pm 25, \pm 2, 14,$
-20	3_b	$\pm 34, \pm 5, 32,$	$\pm 32, \pm 6, 45,$	$\pm 26, \pm 1, 13,$
-10	3_a	$\pm 38, \pm 9, 36,$	$\pm 36, \pm 10, 50,$	$\pm 25, \pm 1, 9,$
0	2_d	$\pm 44, \pm 12, 38,$	$\pm 39, \pm 17, 51,$	$\pm 23, \pm 1, 5,$
10	3_a	$\pm 49, \pm 16, 38,$	$\pm 41, \pm 23, 57,$	$\pm 21, \pm 3, 2,$
20	3_b	$\pm 53, \pm 20, 35,$	$\pm 43, \pm 30, 62,$	$\pm 19, \pm 6, 1,$
30	3_c	$\pm 56, \pm 23, 31,$	$\pm 44, \pm 35, 68,$	$\pm 17, \pm 8, 1,$
40	3_d	$\pm 58, \pm 26, 25,$	$\pm 44, \pm 40, 75,$	$\pm 16, \pm 12, 0,$
50	$3_e, 4$	$\pm 58, \pm 28, 14,$	$\pm 44, \pm 42, 86,$	$\pm 15, \pm 14, 0,$
60	3_f	$\pm 58, \pm 28, 8,$	$\pm 45, \pm 41, 92,$	$\pm 16, \pm 12, 0,$
70	3_g	$\pm 56, \pm 28, 1,$	$\pm 45, \pm 39, 99,$	$\pm 17, \pm 11, 0,$
80	3_h	$\pm 54, \pm 26, 8,$	$\pm 43, \pm 37, 90,$	$\pm 17, \pm 10, 2,$

Table 2.

$\theta = 70$ etc., correspond to $\mathbf{Z} = (0, \cos \theta, \sin \theta)$. All frequencies in Mc/s. Relative intensities in italics. Where two centres are given they correspond to \pm signs in \mathbf{Z} . The alternative radical with tensors of lower sign of table 1 has the transitions quoted here for $-\theta$. The actual pattern is the superposition of the two. Centres quoted are in Mc/s relative to the free spin frequency, for which $g = -2.0023$.

shows that both xy elements are zero. The lack of splitting due to $H(O)$ for rotation about $(0, 1, 0)$ shows that the xx and zz elements of its tensor must be nearly zero, while the splitting at $\mathbf{Z}=(0, 1, 0)$ must be somewhat greater than the yy element. The yz elements are less easily found. A complete set of spectra was calculated for approximate tensors and compared with the observations. In the light of this comparison small changes were made and the spectra recalculated using the tensors of table 1. The results, for the orientations whose spectra are shown in figures 2 and 3, are given in table 2. Figure 4 shows the fit of calculated and observed spectra for $\mathbf{Z}=(0, \cos 50, \sin 50)$, and exemplifies the agreement found throughout. This cannot be readily indicated in the smaller figures.

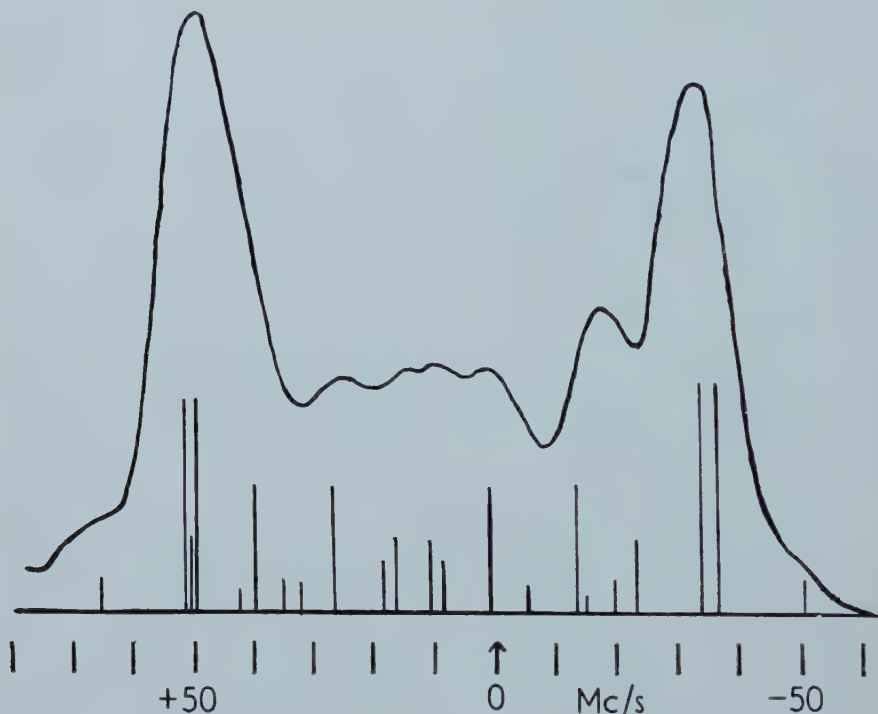


Figure 4. Enlargement of figure 3e showing calculated spectrum. Arrow $g = -2.0023$ and marks 10 Mc/s therefrom.

4.3. The g -tensor

Since $(\Delta g)^2/g^2 \ll 1$ the position of the centre of the hyperfine pattern is given by $\mathbf{Z}.g.\mathbf{Z}$, to a good approximation. The elements on the diagonal of the g -tensor were measured directly from the comparison with DPPH at orientations $\mathbf{Z}=(1, 0, 0)$, $(0, 1, 0)$ and $(0, 0, 1)$ for g_{xx} , g_{yy} and g_{zz} respectively. The variation of the g -value for rotation about $(0, 0, 1)$ and $(0, 1, 0)$ is shown in figure 5, whence the g_{xy} and g_{zx} elements were determined. Since the centres of the overlapping spectra obtained during rotation about $(1, 0, 0)$ were so difficult to pick out, the variation during rotation about that axis was not measured directly. The fit of the calculated to the observed spectra gave the difference in g -value between the two radicals and hence the g_{yz} element of the tensor. The values

are given in table 1, together with the principal values and their directions. In assessing the probable errors account was taken of the uncertainty of ± 0.0002 in the g -value of DPPH, and the overall errors of ± 0.0005 are thereby partially linked. In contrast to the hyperfine couplings, the g -value tensor is not consistent with orthorhombic symmetry, though it is consistent with the true monoclinic symmetry of the crystal.

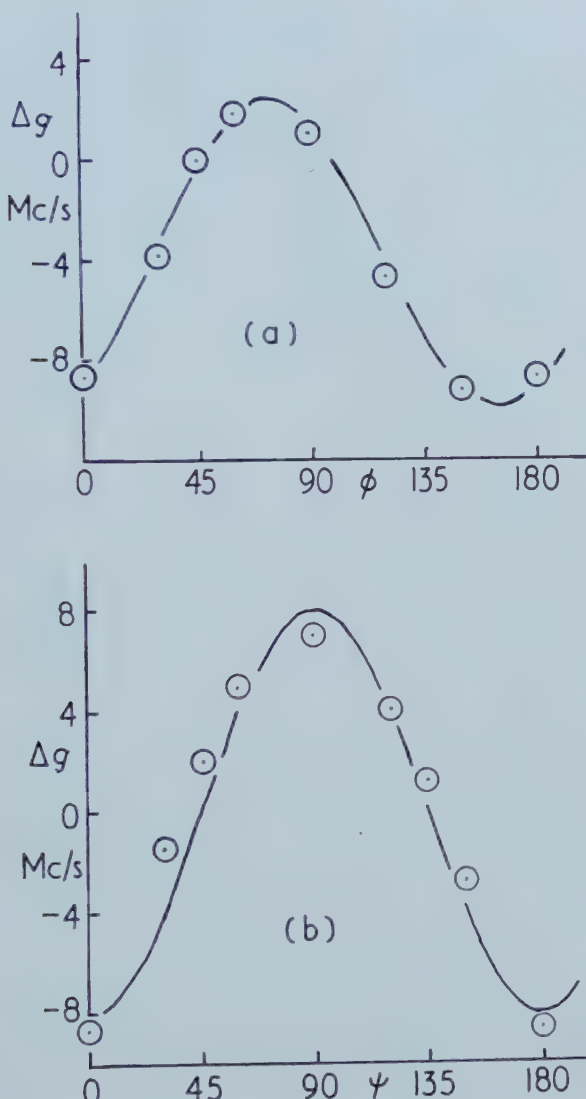


Figure 5. Shift of g (in Mc/s) from that of DPPH. (a) Rotation about $(0, 0, 1)$, i.e. $\mathbf{z} = (\cos \phi, \sin \phi, 0)$; (b) Rotation about $(0, 1, 0)$, i.e. $\mathbf{z} = (\cos \psi, 0, \sin \psi)$.

5. DISCUSSION

The isotropic and principal anisotropic couplings are shown separately in table 1, where the directions of the principal axes are also given.

Figure 4 provides a typical example of the agreement between the observed and calculated spectra, and the approximation discussed in §3 is quite satisfactory in the present case. The omission of the term $\nu \mathbf{I} \cdot \mathbf{Z}$ in §3 would have led to the often quoted selection rule $\Delta M_I = 0$. Such a simplified theory does not even predict the number of hyperfine components correctly and would therefore be useless as regards matching their positions and intensities.

5.1. The $H(C)$ coupling

The contribution of the contact term to the hyperfine interaction in π -electron radicals has been considered by McConnell and Chesnut [19] and by Jarrett [20], who have shown that the coupling in a C–H aromatic fragment is proportional to the probability of the odd electron being located in a p -orbital on the carbon atom. The constant of proportionality is observed and calculated to be -65 ± 10 Mc/s, the negative sign being assigned on both theoretical and experimental [3, 21] grounds. In the present case the average value of the trace of the $H(C)$ coupling tensor, which represents the isotropic part of the interaction, is 57 Mc/s. This suggests that the C–H part of the radical can be considered in the same way as an aromatic fragment, with the odd electron located in a p -orbital perpendicular to the C–H bond. The fact that the observed coupling agrees closely with the accepted constant of proportionality also suggests that the electron is strongly localized in such a p -orbital.

A qualitative discussion of the nature of the dipole–dipole part of the interaction of such a radical fragment has been given by Ghosh and Whiffen [3], whence it is expected that the most positive contribution will arise with \mathbf{Z} along the C–H direction, the most negative with \mathbf{Z} along the axis perpendicular to both the C–H direction and the p -orbital, and that with \mathbf{Z} along the direction of the p -orbital the contribution will be small. On these grounds, remembering that the total coupling is negative, the C–H bond is along $(0, 0.83 \mp 0.56)$, where the anisotropic contribution is +27 Mc/s and the $(1, 0, 0)$ direction is parallel to the axis of the p -orbital.

For the odd electron to reside in a p -orbital on the methylene carbon suggests that the O–C(H)–C part of the radical is roughly planar, the central carbon being trigonally hybridized. The C–COO group must itself also be planar, and by analogy with the glycine case the whole O–C(H)–COO system is probably planar. The $(1, 0, 0)$ direction is then perpendicular to this plane, which will be called the plane of the radical.

5.2. The $H(O)$ coupling

The theoretical work of Chesnut [22] and McLachlan[23] suggests that the isotropic coupling to methyl protons in substituted aromatic radicals is positive, and that it is related to the spin density in a p -orbital on the ring carbon by about the same proportionality constant as for ring protons, except for a change of sign. Ghosh and Whiffen [3] have taken the positive sign in discussing the couplings to the N-protons in the $-\text{OOCCHNH}_3^+$ radicals produced on the γ -irradiation of glycine crystals, and by analogy with these cases it appears that the $H(O)$ couplings should be positive. The value of the isotropic part of the coupling, 8 Mc/s, is very small compared to the 65 Mc/s for methyl substituted aromatic radicals and the 53 Mc/s for the N-protons in glycine [3]. This would be expected if the $H(O)$ proton were in the nodal plane of the p -orbital, i.e. in the

plane of the radical, since it would not then be favourably placed for hyperconjugative overlap.

The qualitative analysis of the signs and magnitudes of the anisotropic couplings can again be applied to this part of the radical. It is to be expected that as the proton is removed to greater distances from the carbon atom then the couplings in the two directions perpendicular to the C . . . H direction will tend to become equal and negative, while that along the C . . . H direction will be positive, tending to twice the numerical value of either of the others. The values for the H(O) couplings, shown in table 1, exhibit this tendency when compared against the H(C) coupling, whence it would appear that the C . . . H(O) direction is along (0, 0.95, ∓ 0.32). As (1, 0, 0) is perpendicular to the plane of the radical, the most negative coupling is now in the (0, 0.32, ± 0.95) direction, which is mutually perpendicular to the *p*-orbital and the C . . . H(O) direction. It is true that the two most negative values are by no means equal, and this may be the result of some unpaired electron character on the oxygen atom. Nevertheless it would be more difficult to justify a reversed sign to the anisotropies, since there would be one large negative and two positive couplings. This argument therefore supports the positive sign taken for the isotropic term.

As discussed for the radical in glycine [3] the most negative coupling provides a rough measure of $[\langle r^3 \rangle_{av}]^{1/3}$ where r is the electron-hydrogen atom distance. For H(O) this is 1.7 Å which is shorter than the expected H(O) . . . C distance but is acceptable if there is delocalization of the unpaired electron to the oxygen atom. It seems far too short for the carboxyl proton and the assignment of the second tensor to the hydroxyl proton rests principally on its large anisotropy.

Splittings attributable to a hydroxyl proton, when this group is attached to a free radical carbon, have not been previously observed. Radicals containing this >COH grouping are probably formed by the attack of OH radicals on alcohol glasses [14, 15] and by irradiation of such glasses with γ -rays [16], x-rays or electrons [17]. The lack of splitting has been discussed [18] in terms of a proton in the plane of the carbon radicals, which would be unfavourable for couplings. The present results confirm this view as the isotropic splitting, 8 Mc/s, is so small. The anisotropy is large and the consequent broadening in amorphous materials would prohibit the resolution of such coupling.

5.3. Spin densities

Integrated spin densities can readily be derived from the isotropic couplings since the spin density is defined as unity at a hydrogen nucleus, for which the coupling is 1420 Mc/s. The calculated values are -0.040 at H(C) and +0.006 at H(O), the signs indicating the relation of the unpaired electron character at the nuclei to that of the whole radical, for which the integrated spin density is +1. These are to be compared with the values -0.053 and +0.037 for the CH and NH protons in the +NH₂CHCOO⁺ radicals in glycine [3]. The values for the H(C) protons are in approximate agreement, which is to be expected for strong localization of the electron in a *p*-orbital on the carbon.

5.4. Orientation of the radicals

The establishment of the C H direction enables the radicals to be laid in the crystallographic axes with an uncertainty of 180° in rotation about C-H. If the C . . . H(O) direction is also required to be as near as possible to the principal

axis of anisotropic coupling of +20 Mc/s the most satisfactory arrangement is that shown in figure 6, which relates to the upper signs of table 1. Two principal axes of the *g*-tensor lie nearly in the plane and their projections are also indicated.

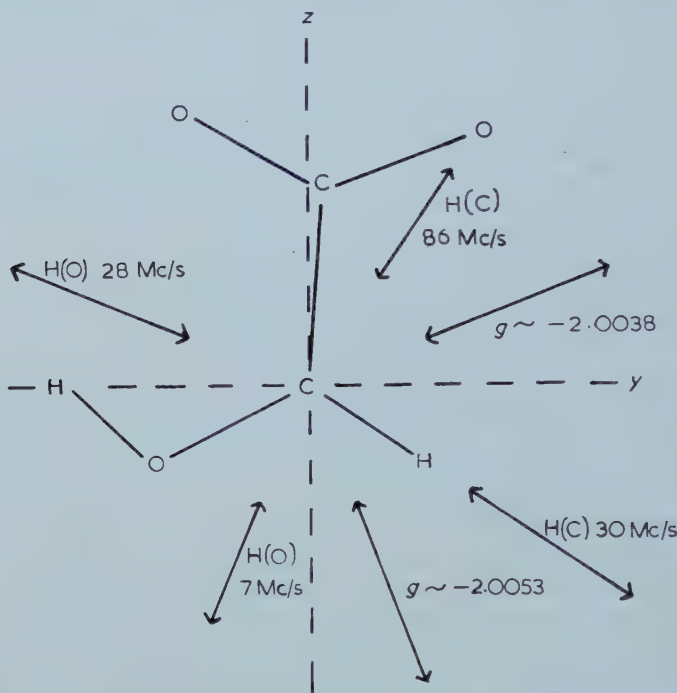


Figure 6. Suggested radical orientation (upper signs). Double arrows indicate the directions of the principal axes of the tensors. For *g* the directions shown are the projections onto the *yz* plane.

By analogy with the glycine case [3] it is to be expected that the C-C-O plane in the radicals will be the same as that in the parent molecules, since the heavy atom skeleton should not be significantly changed by the γ -irradiation. This plane is then the *ab* plane of the pseudo-orthorhombic crystal (figure 1), being perpendicular to *c*. The C-H bond in the radical then makes an angle of 56° with *b*, 90° with *c*. The two radicals having different orientations are related by rotation through 180° about an axis parallel to *b*, plus translation, which is not detectable magnetically. It further appears that all eight molecules in the unit cell are parallel to each other. Apart from this there remains a simplicity of orientation not dictated by the crystal symmetry and it is possible that the asymmetric unit of two molecules is a head to head carboxylic acid dimer and that this unit has a centre of symmetry so that the two halves were indistinguishable in the resonance experiments.

5.5. The *g*-tensor

The axis of the *g*-tensor with the smallest numerical value lies 20° from the perpendicular to the radical plane. Its value -2.0017 is numerically less than that of a free electron, -2.0023, by an amount which only slightly exceeds the limits of error. The other principal directions lie approximately in the plane

and the values are numerically greater than the free spin value, and their projections are indicated in figure 6. It is believed that this is the first determination of the anisotropy in *g*-factor for magnetically dilute organic free radicals.

6. CONCLUSIONS

The present work supports that on the related radical in glycine [3] especially as regards the H(C) coupling tensor which was less accurately measured in the earlier case. The negative spin density on this hydrogen again seems reasonable although x-ray evidence on the molecular structure of the crystal which would confirm this feature is lacking. The positive density on H(O) is less firmly established. It can be seen that quite complicated, field dependent, spectra can arise from coupling to only two hydrogen nuclei and that the usual assumption for interpreting electron resonance spectra, namely $\Delta M_I = 0$, does not hold in the solid. This seems discouraging for the interpretation of spectra in polycrystalline or amorphous materials, but it must be admitted that the spectrum of a polycrystalline sample of this material [4] was correctly interpreted. The peak separation on a polycrystalline sample is† ~ 61 Mc/s which is nearly the isotropic coupling of 57 Mc/s.

We wish to thank the Royal Society for the grant for the purchase of the magnet and N. M. A. wishes to acknowledge the support given by D.S.I.R. We are extremely grateful to Mr. D. Hughes and Dr. R. W. H. Small for their investigation of the crystal symmetry, and for useful discussions. Mr. B. P. Goddard has rendered valuable technical assistance with the maintenance of the spectrometer and the preparation of a sample of DPPH.

REFERENCES

- [1] WEISSMAN, S. I., 1954, *J. chem. Phys.*, **22**, 1378.
- [2] FERMI, E., 1930, *Z. Physik.*, **60**, 320.
- [3] GHOSH, D. K., and WHIFFEN, D. H., 1959, *Mol. Phys.*, **2**, 285.
- [4] GRANT, P. M., WARD, R. B., and WHIFFEN, D. H., 1958, *J. chem. Soc.*, 4635.
- [5] GROTH, P., 1910, *Chem. Kryst.*, **3** (Leipzig : Engelmann).
- [6] HUGHES, D., and SMALL, R. W. H. (private communication).
- [7] ABRAHAM, R. J., OVENALL, D. W., and WHIFFEN, D. H., 1958, *Trans. Faraday Soc.*, **54**, 1128.
- [8] WEIDNER, R. T., and WHITMER, C. A., 1953, *Phys. Rev.*, **91**, 1279.
- [9] HOLDEN, A. N., KITTEL, C., MERRITT, F. R., and YAGER, W. A., 1950, *Phys. Rev.*, **77**, 147.
- [10] LOTHE, J. J., and EIA, G., 1958, *Acta. chem. scand.*, **12**, 1535.
- [11] WAHLER, B. E. (private communication).
- [12] TRAMMELL, G. T., ZELDES, H., and LIVINGSTON, R., 1958, *Phys. Rev.*, **110**, 630.
- [13] LIVINGSTON, R., ZELDES, H., and TAYLOR, E. H., 1955, *Disc. Faraday Soc.*, **19**, 116.
- [14] FUJIMOTO, M., and INGRAM, D. J. E., 1958, *Trans. Faraday Soc.*, **54**, 1304.
- [15] GIBSON, J. F., SYMONS, M. C. R., and TOWNSEND, M. G., 1959, *J. chem. Soc.*, 269.
- [16] ZELDES, H., and LIVINGSTON, R., 1959, *J. chem. Phys.*, **30**, 40.
- [17] ALGER, R. S., ANDERSON, T. H., and WEBB, L. A., 1959, *J. chem. Phys.*, **30**, 695.
- [18] SYMONS, M. C. R., 1959, *J. chem. Soc.*, 277.
- [19] McCONNELL, H. M., and CHESNUT, D. B., 1959, *J. chem. Phys.*, **28**, 107.
- [20] JARRETT, H. S., 1956, *J. chem. Phys.*, **25**, 1289.
- [21] GUTOWSKY, H. S., KUSUMOTO, H., BROWN, T. H., and ANDERSON, D. H., 1959, *J. chem. Phys.*, **30**, 860.
- [22] CHESNUT, D. B., 1958, *J. chem. Phys.*, **29**, 43.
- [23] McLACHLAN, A. D., 1958, *Mol. Phys.*, **1**, 233.

† In reference [4] a value of 25 gauss = 70 Mc/s was quoted, but improved calibration of the field sweep has shown the earlier figure to be rather high as are all values in [3].

The Renner effect and spin-orbit coupling

by J. A. POPLE

Communication from the National Physical Laboratory

(Received 13 July 1959)

The Renner theory of vibrational-electronic interaction in linear triatomic molecules in Π electronic states is extended to take account of coupling between an odd electron spin and the electron orbital angular momentum. Perturbation expressions for the splittings and shifts of energy levels are obtained on the assumption that the Renner splittings and the spin-orbit coupling energy are of the same order of magnitude, but less than the energy quantum of the bending vibrations.

1. INTRODUCTION

Linear triatomic molecules in orbitally degenerate electronic states ($\Pi, \Delta, \Phi \dots$) have a rather complex vibrational-electronic interaction due to the separation of the two components of the electronic state by the bending vibration. The theory of this effect was first developed by Renner [1] who gave an expansion for the splitting of the vibronic levels if this interaction was small. Recently a detailed study of the electronic spectrum of the NH_2 radical by Dressler and Ramsay [2] has suggested that this is an example of the Renner effect with large coupling and some calculations of Pople and Longuet-Higgins [3] based on a modified version of the Renner theory have given satisfactory quantitative agreement with the experimental term values.

For systems with a free electron spin as well as an electronic orbital moment, the effect of spin-orbit coupling should also be taken into account. This is small in NH_2 but it will have to be considered if it is comparable with the splittings caused by the Renner effect. In this paper an extended theory is developed to allow for a moderate coupling between the electron spin and the component of orbital electronic angular momentum along the axis of the molecule.

2. CLASSIFICATION OF LEVELS FOR A SIMPLIFIED MODEL

Suppose we consider a triatomic linear molecule with an odd electron in an orbital of π symmetry. In the absence of any coupling between the angular motion of this electron, the bending vibration and the electron spin, the states of the system can be classified by quantum numbers Λ' ($= \pm 1$) for the electronic orbital angular momentum along the axis, S_z' ($= \pm \frac{1}{2}$) for the corresponding component of spin angular momentum, l ($= 0, 1, 2 \dots$) for the angular momentum of the bending vibration and n ($= |l| + 1, |l| + 3, |l| + 5, \dots$) for the total number of vibrational quanta (including zero-point motion). The energy of the state $|\Lambda', n, l, S_z'\rangle$ is then n in units of the vibrational quantum. Further quantum numbers will be associated with other degrees of freedom such as end-over-end rotation, but we shall not consider any coupling with these in the present paper.

The Renner effect follows if we introduce a coupling between the electronic orbital motion and the plane of the bent molecule. Under these circumstances,

Λ' and l are no longer quantum numbers, but the total *orbital* angular momentum component represented by

$$K = \Lambda' + l \quad (2.1)$$

is still conserved, so that vibronic states may be labelled Σ , Π , Δ , ... according as $K = 0, 1, 2, \dots$. This coupling leads to a splitting of the states $|1, n, K-1, S_z'\rangle$ and $| -1, n, K+1, S_z'\rangle$ which are degenerate in the unperturbed system. For Σ states ($K=0$) the appropriate wave functions are

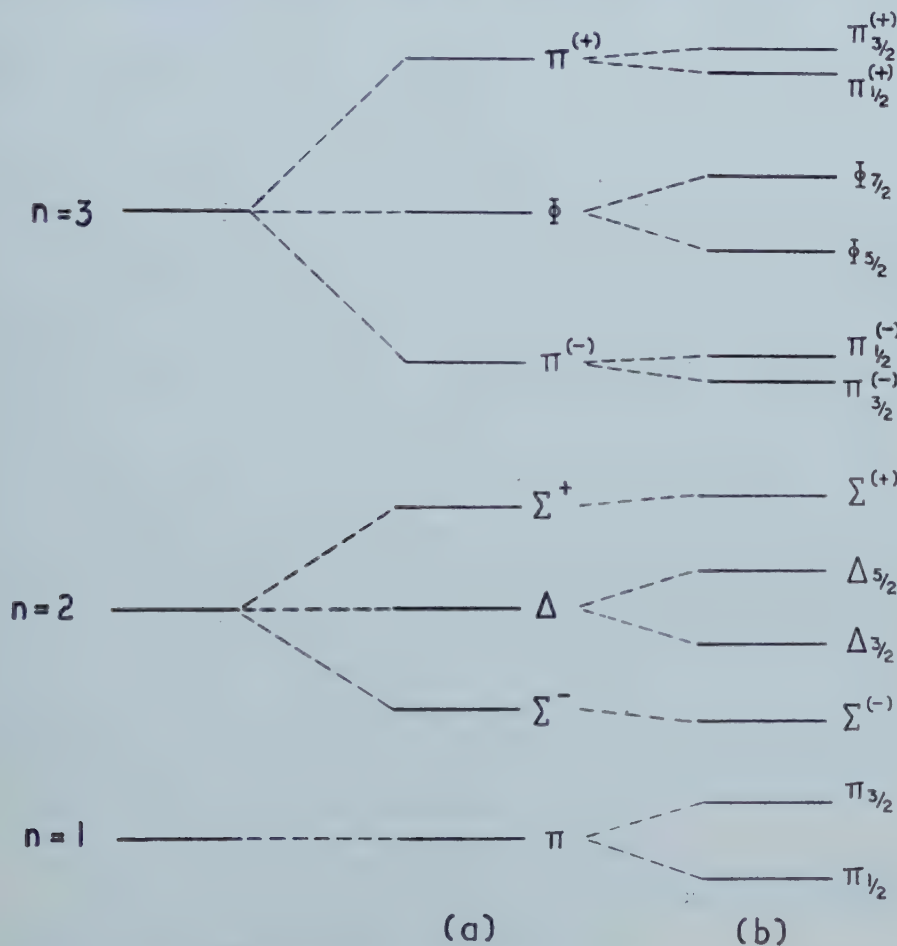
$$\{|1, n, -1, S_z'\rangle + | -1, n, 1, S_z'\rangle\}/\sqrt{2}$$

and

$$\{|1, n, -1, S_z'\rangle - | -1, n, 1, S_z'\rangle\}/\sqrt{2}$$

which have symmetries Σ^+ and Σ^- respectively. For $K \neq 0$, the correct combinations are also approximately sums and differences in this way. The splittings due to this effect, which are dealt with in detail by Renner, are shown in the first part of the figure.

Even after the Renner splitting, each vibronic state with $|K| > 0$ remains four-fold degenerate because of the two possible values of the spin quantum



Level splittings caused by (a) Renner effect alone, (b) Renner effect and spin-orbit coupling.

number $S_z' = \pm \frac{1}{2}$ and the two possible signs of K . We now wish to investigate how these splittings are modified and extended if there is also a coupling between the electron orbital angular momentum and the electron spin. The coupling between the vibrational angular momentum and the electron spin will be much smaller and will be ignored. The simplest approximate representation of this coupling is by a Hamiltonian proportional to ΛS_z where Λ and S_z are now appropriate operators. This represents a positive energy if the two components of angular momentum along the molecular axis are in the same direction. Since components of orbital angular momentum perpendicular to the molecular axis are largely quenched, a Hamiltonian of this sort takes account of the most important part of the spin-orbit coupling.

To the approximation of this simple Hamiltonian, the quantum number S_z' is conserved, since the operator S_z cannot mix α and β electron spin functions. We may therefore continue to classify states by the symbols Σ , Π , Δ ... and in addition by the total angular momentum $K + S_z'$ as a subscript. Thus $\Pi_{3/2}$ and $\Pi_{1/2}$ represent states in which an orbital and spin angular momenta are parallel and antiparallel respectively. All states with $|K| > 0$ get split in this manner as illustrated in the figure (b). It should be noted that the Σ levels can no longer be classified as Σ^+ or Σ^- since, for a particular value of S_z' , the two directions of rotation are no longer equivalent. In the next section we shall derive quantitative expressions for these splittings and shifts, assuming them to be small compared with the vibrational interval.

3. QUANTITATIVE THEORY

We shall only deal with the one-electron model, following the notation of Pople and Longuet-Higgins [3]. r will denote the amplitude of the bending vibration, ϕ the angle of the plane of bending with a fixed plane through the axis of the unbent molecule and θ the angular distance of the electron from the same plane. If the bending potential is harmonic and if there is no coupling between the angles θ and ϕ and the electron spin, the various degrees of freedom can be separated and the wave functions written in the form

$$|\Lambda', n, l, S_z' \rangle = \exp(i\Lambda'\theta)\rho_{nl}(r) \exp(il\phi)^{\{\alpha}_{\beta}} \quad (3.1)$$

where $\Lambda' = \pm 1$, $\rho_{nl}(r) \exp(il\theta)$ is the wave function for the two-dimensional harmonic oscillator and α and β are the usual spin functions for $S_z' = \pm \frac{1}{2}$. It is convenient to choose the unit of energy equal to the vibrational quantum and the unit of distance such that the unperturbed vibrational potential energy is $\frac{1}{2}r^2$.

Following Renner, we now introduce the Hamiltonian

$$H' = \epsilon r^2 \cos 2(\theta - \phi) \quad (3.2)$$

to couple the electronic and vibrational angular momenta. This splits the potential function into upper and lower branches

$$\left. \begin{aligned} U^+ &= \frac{1}{2}(1 + \epsilon)r^2, \\ U^- &= \frac{1}{2}(1 - \epsilon)r^2. \end{aligned} \right\} \quad (3.3)$$

We also introduce a second perturbing Hamiltonian

$$H'' = \xi \Lambda S_z \quad (3.4)$$

to allow for spin-orbit coupling.

Since the quantum number K is conserved, we need to diagonalize the total energy matrix for the complete set of functions (3.1) with $\Lambda' + l = K$. For convenience we shall suppose $K \geq 0$. These functions are conveniently collected in pairs $|1, n, K-1, S_z'\rangle$ and $| -1, n, K+1, S_z'\rangle$ which are degenerate in the absence of the perturbation. For $|K| > 0$, however, the state corresponding to lowest unperturbed energy $|1, K, K-1, S_z'\rangle$ will be non-degenerate. The matrices of $\epsilon^{-1}H'$ will be the same for both values of S_z' and have been evaluated by Renner using a rather different notation. A typical block of this matrix is shown on p. 20. All elements in blocks further removed from the diagonal are zero. If $K > 0$, the first row and column corresponding to $|1, K, K-1\rangle$ are not paired and the top left-hand corner of the matrix has the form

	$ 1, K, K-1\rangle$	$ 1, K+2, K-1\rangle$	$ -1, K+2, K+1\rangle$
$\langle 1, K, K-1 $	0	0	$\frac{1}{2}\sqrt{[K(K+1)]}$
$\langle 1, K+2, K-1 $	0		
$\langle -1, K+2, K+1 $	$\frac{1}{2}\sqrt{[K(K+1)]}$		

If $K=0$, however, this row and column do not occur.

The next step is to add the matrices of H' and H'' and then treat them as a perturbation on the unperturbed energy matrix (which has diagonal elements equal to n). The matrix of H'' is diagonal and has the form

$\xi S_z'$	0	0		
0	$\xi S_z'$	0	0	0
0	0	$-\xi S_z'$	0	0
	0	0	$\xi S_z'$	0
	0	0	0	$-\xi S_z'$

(the first row and column again being absent if $K=0$).

To apply perturbation theory, we first have to apply an orthogonal transformation to the total energy matrix which will remove off-diagonal elements between states which are degenerate in the unperturbed situation. In the absence of spin-orbit coupling, this is accomplished by replacing the pair of functions $|1, n, K-1\rangle$ and $| -1, n, K+1\rangle$ by their sum and difference (normalized) if $n > K$ and leaving $|1, K, K-1\rangle$ unaltered ($K \neq 0$). Our problem is slightly more complicated for the corresponding 2×2 block of the perturbation matrix is now

$$\begin{bmatrix} \xi S_z' & \frac{1}{2}\epsilon\sqrt{[n^2 - K^2]} \\ \frac{1}{2}\epsilon\sqrt{[n^2 - K^2]} & -\xi S_z' \end{bmatrix}$$

$ 1, n-2, K-1\rangle$	$ -1, n-2, K+1\rangle$	$ 1, n, K-1\rangle$	$ -1, n, K+1\rangle$	$ 1, n+2, K-1\rangle$	$ -1, n+2, K+1\rangle$
$\begin{Bmatrix} 1, n-2, K-1 \\ -1, n-2, K+1 \end{Bmatrix}$		$\begin{Bmatrix} 0 & \frac{1}{4}\sqrt{[(n+K-2)(n+K)]} \\ \frac{1}{4}\sqrt{[(n-K)(n-K-2)]} & 0 \end{Bmatrix}$		$\begin{Bmatrix} 0 & 0 \\ 0 & 0 \end{Bmatrix}$	
		$\begin{Bmatrix} 0 & \frac{1}{2}\sqrt{[n^2-K^2]} \\ \frac{1}{2}\sqrt{[n^2-K^2]} & 0 \end{Bmatrix}$		$\begin{Bmatrix} \frac{1}{4}\sqrt{[(n+K)(n+K+2)]} & 0 \\ \frac{1}{4}\sqrt{[(n-K)(n-K)]} & 0 \end{Bmatrix}$	
		$\begin{Bmatrix} 0 & \frac{1}{4}\sqrt{[(n+K+2)(n+K)]} \\ \frac{1}{4}\sqrt{[(n+K)(n+K+2)]} & 0 \end{Bmatrix}$		$\begin{Bmatrix} 0 & \frac{1}{4}\sqrt{[(n-K+2)(n-K)]} \\ \frac{1}{4}\sqrt{[(n+K)(n+K+2)]} & 0 \end{Bmatrix}$	

If we define an angle $\gamma(n, K, S_z')$ between 0 and π by

$$\cos 2\gamma(n, K, S_z') : \sin 2\gamma(n, K, S_z') : 1 = \xi S_z' : \frac{1}{2}\epsilon\sqrt{[n^2 - K^2]} : \frac{1}{2}\sqrt{[\xi^2 + \epsilon^2(n^2 - K^2)]} \quad (3.5)$$

then the appropriate transformation matrix is

$$S = \begin{vmatrix} 1 & 0 & 0 \\ 0 & \cos\gamma(n, K, S_z') & -\sin\gamma(n, K, S_z') \\ 0 & \sin\gamma(n, K, S_z') & \cos\gamma(n, K, S_z') \end{vmatrix} \quad (3.6)$$

where elements outside each 2×2 diagonal block are zero. If $K=0$, the first row and column are omitted. If H is the energy matrix for the original functions, $S^{-1}HS$ now has the required property and the perturbation can be carried out to second order.

If $K>0$ ($\Pi, \Lambda, \Phi \dots$ states) and $n>K$, the four states corresponding to a given value of n are separated, the energies to second order being

$$\left. \begin{aligned} E_{n, K, \pm 1/2}^{(+)} &= n + \frac{1}{2}\sqrt{[\xi^2 + \epsilon^2(n^2 - K^2)]} - \frac{1}{8}\epsilon^2 \left\{ n \mp \frac{K\xi}{\sqrt{[\xi^2 + \epsilon^2(n^2 - K^2)]}} \right\}, \\ E_{n, K, \pm 1/2}^{(-)} &= n - \frac{1}{2}\sqrt{[\xi^2 + \epsilon^2(n^2 - K^2)]} - \frac{1}{8}\epsilon^2 \left\{ n \pm \frac{K\xi}{\sqrt{[\xi^2 + \epsilon^2(n^2 - K^2)]}} \right\}. \end{aligned} \right\} \quad (3.7)$$

The notation is that the indicial (+) or (-) indicates the upper or lower state for the Renner splitting, and the third suffix gives the value of the spin angular momentum S_z' . For example $E_{3, 1, \pm 1/2}^{(+)}$ is the upper $\Pi_{3/2}$ state originating in the unperturbed level $n=3$. This is the highest level shown in the figure (b) and is designated $\Pi_{3/2}^{(+)}$.

If the spin-orbit coupling parameter ξ is small compared with ϵ , these formulae simplify to

$$\left. \begin{aligned} E_{n, K, \pm 1/2}^{(+)} &= n + \frac{1}{2}\epsilon\sqrt{[(n^2 - K^2)]} - \frac{1}{8}\epsilon^2 n \pm \frac{1}{8}\epsilon\xi K/\sqrt{[(n^2 - K^2)]}, \\ E_{n, K, \pm 1/2}^{(-)} &= n - \frac{1}{2}\epsilon\sqrt{[(n^2 - K^2)]} - \frac{1}{8}\epsilon^2 n \mp \frac{1}{8}\epsilon\xi K/\sqrt{[(n^2 - K^2)]}. \end{aligned} \right\} \quad (3.8)$$

If $n=K>0$, the two states are split, the corresponding energies being

$$E_{K, K, \pm 1/2} = K \pm \frac{1}{2}\xi - \frac{1}{8}\epsilon^2 K(K+1). \quad (3.9)$$

For $K=1$, the two levels are $\Pi_{3/2}$ and $\Pi_{1/2}$ as shown at the bottom of the figure (b). The splitting of these levels to the order of this calculation is ξ as it would be if there were no Renner effect.

For $K=0$ (Σ states), the two directions of the spin give the same energy and the four states split into two pairs

$$\left. \begin{aligned} E_{n, 0, \pm 1/2}^{(+)} &= n + \frac{1}{2}\sqrt{[\xi^2 + \epsilon^2 n^2]} - \frac{1}{8}\epsilon^2 n, \\ E_{n, 0, \pm 1/2}^{(-)} &= n - \frac{1}{2}\sqrt{[\xi^2 + \epsilon^2 n^2]} - \frac{1}{8}\epsilon^2 n. \end{aligned} \right\} \quad (3.10)$$

The separation of the two Σ levels is $\sqrt{[\xi^2 + \epsilon^2 n^2]}$. For $n=2$, these are the two lowest Σ levels shown in the figure (b) (designated $\Sigma^{(+)}$ and $\Sigma^{(-)}$ rather than Σ^+ and Σ^- since the appropriate symmetry is reduced).

4. DISCUSSION

The principal modifications of the Renner theory caused by spin-orbit coupling may be summarized as follows.

(1) The Renner effect causes pairs of Σ levels to split into levels of symmetries Σ^+ and Σ^- . Spin-orbit coupling increases the separation of these pairs (equation (3.10)) and the classification as Σ^+ and Σ^- ceases to be precise.

(2) The lowest vibronic levels of $\Pi, \Delta, \Phi \dots$ symmetries are little changed by the Renner effect, but they are split into pairs (e.g. $\Pi_{3/2}$ and $\Pi_{1/2}$) by the spin-orbit coupling. These splittings are all equal to the spin-orbit coupling energy ξ (equation (3.9)).

(3) All other $\Pi, \Delta, \Phi \dots$ vibronic states are split into pairs (designated $\Pi^{(+)}, \Pi^{(-)}$, etc.) by the Renner effect. Spin-orbit coupling causes further splitting to groups of four ($\Pi_{3/2}^{(+)}, \Pi_{1/2}^{(+)}, \Pi_{1/2}^{(-)}, \Pi_{3/2}^{(-)}$, etc.). However, the second splittings are small (being of order $\epsilon\xi$).

REFERENCES

- [1] RENNER, E., 1934, *Z. Phys.*, **92**, 172.
- [2] DRESSLER, K., and RAMSAY, D. A., 1959, *Phil. Trans. roy. Soc. A.*, **251**, 553.
- [3] POPLE, J. A., and LONGUET-HIGGINS, H. C., 1958, *Mol. Phys.*, **1**, 372.

Some temperature dependent effects on the optical absorption line shape of paramagnetic ions

by R. ENGLMAN

Department of Physics, Technion-Israel Institute of Technology,
Haifa, Israel

(Received 26 February 1959)

The temperature variations of the total intensity and of the mean energy of optical absorption in hydrated paramagnetic salts are calculated on the assumption that the absorbing ion and its coordinated ligands form an isolated complex. These calculations take into account the anharmonicities in the vibrational motion of the ligands. Comparison with experimental data indicates a rather large amount of anharmonicity.

1. INTRODUCTION

The absorption of light by hydrated paramagnetic salts is now known to be mainly due to electric dipole transitions taking place in the ion together with a vibrational motion, of odd type, of the water molecules surrounding the ion. This has been confirmed by calculations of the absorption intensities for Cu^+ and Ti^{2+} [1] and in greater detail for Mn^{2+} [2] and for Ni^{2+} (Englman and Pryce, unpublished).

On the other hand, the data in existence [3] showing the temperature variation of the absorption intensity have not so far been exploited (in a rigorous way, at any rate) to yield information about the mechanism of absorption or even adequately explained in terms of the model proposed. This variation is connected with the nuclear motions accompanying the absorption of light. It will be shown that a number of important facts may be accounted for by regarding each ion and its surrounding six ligands as an isolated complex, in weak thermal interaction with the rest of the crystal. This is unlikely to be the whole truth and a complete treatment of the absorption shape would have to include the coupling of the complex with the crystal. But if the limitations of the model have to be recognized, its potentialities must also be exhausted.

Regarding the complex as interacting weakly with its surroundings, the motion of the nuclei can in the first approximation, the only one we are concerned with, be analysed into independent normal modes. In the next section we discuss the effect of the electronic transition on the normal modes. This is of course nothing but the application of the Franck-Condon principle to the problem in hand. We shall see that this treatment, when developed so as to take into account the anharmonicity of the vibrational motion of the nuclei, satisfactorily explains the temperature variation of the peak of absorption (§ 3). To explain the variation of the total intensity we again invoke the anharmonicity, this time of the odd vibrational modes (§ 4).

For quantitative deductions and comparison with experiment we shall repeatedly refer to salts in which the cation is nickel. Whereas this is a convenient situation to take as an example for various reasons, the general conclusions are applicable to other situations as well.

2. THE CHANGE IN THE CONFIGURATIONAL PARAMETERS

Since the configuration† of the nuclei in a molecule or a complex ion depends on the state of the electrons, a change occurring in the latter due to absorption or emission will in general affect the former. Also, since the electronic velocities are much greater than those of the nuclei, the change in the electronic configuration takes place practically instantaneously; later the nuclei will relax from excited states into energetically lower states with the emission of energy.



Figure 1

We now draw the potential curves corresponding to such a situation (figure 1). The absorption is the optical absorption from the ground state ${}^3A_2[F]$ to the excited ${}^3T_1[P]$ state in Ni^{2+} . The resulting change in the nuclear configuration can be described fairly fully by the change in the equilibrium positions of the normal modes A_{1g} and E_g (figure 2). The Jahn-Teller effect for the excited states [4] introduces also the possibility of a trigonal distortion of the octahedron. We ignore this, because in our case this effect is undoubtedly smaller than that leading to tetragonal distortion.

Figure 1 refers to the 'breathing' mode A_1 and the abscissa is the mean nickel-water distance. It is seen that the two potential curves corresponding to two electronic eigenstates differ by a displacement of their minima and also in

† This word will be used in its literal sense, 'arrangement', and not in its technical meaning.

their curvatures. For many purposes, however, and in the neighbourhood of the minima, it is reasonable to regard both potentials as approximately the same.

Now we show how this diagram came to be constructed.

In the ground electronic state the equilibrium ion-ligand distance is estimated at

$$R_0 = 2.2 \text{ \AA},$$

and the frequency of the symmetrical mode as

$$\omega/2\pi \approx 300 \text{ cm}^{-1}.$$

In the following section we deduce an estimate for the anharmonic term. With $V_0(R)$ the ground state potential of the complex in its symmetrical configuration,

$$\left[\frac{\partial^3 V_0}{\partial R^3} \right]_{R=R_0} \simeq -4.5 \times 10^{14} \text{ erg cm}^{-3}.$$

Corresponding to a changed configuration potential

$$V = V_0 + \delta V$$

of the excited state, the equilibrium distance becomes $R_1 = R_0 + \delta R$. We want to find this and the change in frequency $\delta\omega$. We note that

$$\left[\frac{\partial V_0}{\partial R} \right]_{R_0} = 0, \quad \left[\frac{\partial^2 V_0}{\partial R^2} \right]_{R_0} = 6M\omega^2$$

(M = mass of a water molecule). Also

$$\begin{aligned} \left[\frac{\partial V}{\partial R} \right]_{R_1} &= 0 \\ &\simeq \left[\frac{\partial^2 V_0}{\partial R^2} \right]_{R_0} \delta R + \left[\frac{\partial \delta V}{\partial R} \right]_{R_0}. \\ 12M\omega\delta\omega &\simeq \left[\frac{\partial^2 V}{\partial R^2} \right]_{R_1} - \left[\frac{\partial^2 V_0}{\partial R^2} \right]_{R_0}, \\ &\simeq \left[\frac{\partial^3 V}{\partial R^3} \right]_{R_0} \delta R + \left[\frac{\partial^2 \delta V}{\partial R^2} \right]_{R_0}. \end{aligned}$$

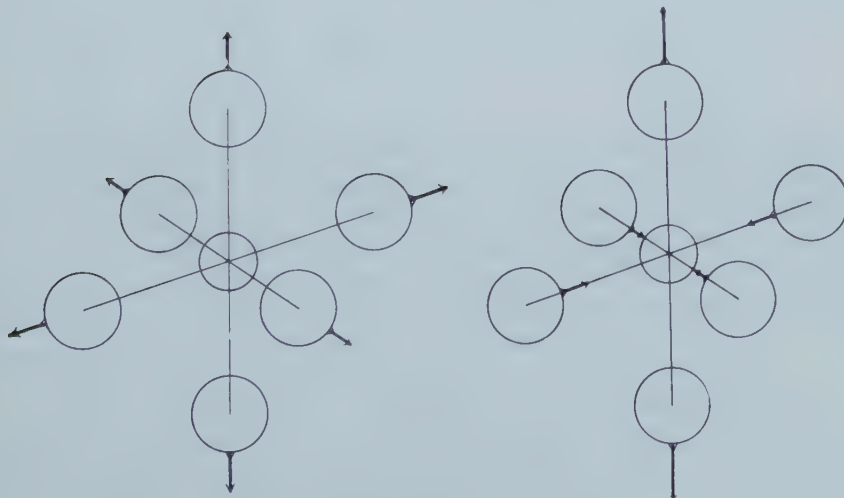


Figure 2. The two even vibrational modes whose equilibrium position is most affected by electronic absorption.

δV as a function of R depends on the crystal field parameter

$$\Delta = \frac{25}{3} \frac{e\mu}{R^2} \frac{\langle r^4 \rangle}{R^4}.$$

This quantity is derivable from experiments. The slope and curvature of the energy lines in the Orgel diagram [5] will then supply all that is necessary to calculate δR and $\delta\omega$.

We list estimates of these for the three nearest excited states (of the same spin multiplicity as the ground state)

	${}^3T_2[F]$	${}^3T_1[F]$	${}^3T_1[P]$
$\delta\omega/\omega$	-0.27	-0.44	-0.37
δR in Å	0.12	0.2	0.16
$2a$	4	6.6	5.4
δZ in Å	0	0.24	0.37
$\delta X, \delta Y$ in Å	0.18	0.17	0.06
$2a'$	3	0.5	4.6

$2a$ gives δR in units of the amplitude of zero point motion ($\hbar/6M\omega$)^{1/2}. The fourth and fifth rows represent the distortion of the equilibrium position of the system from an octahedron due to the excited electronic configuration. These calculations are essentially similar to those for δR , except that now the quantity $\langle r^2 \rangle/R^2$ also enters the expression for the potential energy between ion and ligand. Past experience and various related data have led us to take

$$\frac{\langle r^2 \rangle}{R_0^2} / \frac{\langle r^4 \rangle}{R_0^4} = 4.$$

Note that $\frac{1}{4}(2\delta Z - \delta X - \delta Y)$ is the equilibrium value of the E_g vibrational coordinate. $2a'$ refers to the absolute value of this quantity in units of the amplitude of the zero point motion. This latter is $(3\hbar/16M\omega)^{1/2}$ for the E_g coordinate as defined. Its value is approximately equal to that for the symmetric mode, ≈ 0.03 Å.

3. THE TEMPERATURE VARIATION OF THE ABSORPTION PEAKS

3.1

The data of Holmes and McClure for the peaks of various absorption curves in a number of salts show consistently a downward shift in the position of the peak with increasing temperature. In the region 200–300°K this shift is of the order of 100 cm⁻¹. We now explain this phenomenon by the anharmonicity of the potential. To be quite precise we should add that what we really calculate is the position of the mean energy of absorption \bar{E} , rather than the peak (i.e. the mode). As regards the *shifts* in these quantities due to temperature changes, the difference between mean and mode is unlikely to be significant.

It will be shown that the anharmonicity enters the expression \bar{E} in two ways. First through the difference of the anharmonicities in the initial and final potentials, and secondly through the difference in vibrational frequencies, which itself arises *mainly* (see § 2) from the anharmonic term (Professor Pryce pointed this out to me). At the same time it can be proved (and was first suggested by Huang and Phys [6]) that neither the peak nor the mean position is subject to temperature change for transitions between displaced but otherwise identical parabolae.

We consider first the case when the vibrational Hamiltonians H and H_1 of the ground and excited states differ only by having different vibrational frequencies. Then the mean energy of transition in excess of E_{pr} the energy of the precursor (this terminology is due to Professor Pryce; it denotes the energy separating the minima of the potentials) is given by

$$\begin{aligned}\bar{E} - E_{pr} &= \text{Tr}(H_1 - H) \exp(-H/kT) / \text{Tr} \exp(-H/kT) \\ &= -\frac{\hbar(\omega^2 - \omega_1^2)}{2\omega} [\exp(\hbar\omega/kT) - 1]^{-1}.\end{aligned}$$

We next turn to a potential whose anharmonic term introduces a perturbation in the wave functions of the even vibrations. The energy of the zero point motion is $\frac{1}{2}\hbar\omega$; its amplitude (as defined above, namely, $\sqrt{2} \times$ the root mean square displacement of the zero point motion) is Q_0 , and the minima of the potentials in the ground and excited states are displaced by a distance $2aQ_0$. The anharmonic terms in these potentials have the coefficients λ and λ_1 respectively. We shall obtain for \bar{E} an expression correct to the first order in the anharmonicities; to a good approximation we can now treat the frequencies as identical in the ground and excited states. An indication will be found in the Appendix, how this expression is derived.

In the formula which follows both the anharmonic term and the changes in frequency have been taken into account to the first order:

$$\begin{aligned}\bar{E} - E_{pr} &= 2a^2\hbar\omega + \frac{a}{2\sqrt{2}} Q_0^3 [8a^2\lambda_1 - 3\lambda] \\ &\quad - \left[\frac{3a}{\sqrt{2}} Q_0^3 (\lambda - \lambda_1) - \frac{\delta\omega}{\omega} \right] (\exp(\hbar\omega/kT) - 1)^{-1}.\end{aligned}$$

The last term gives the entire temperature dependence. Taking for the frequency the value 290 cm^{-1} , which is appropriate for the even vibration in question (either the A_{1g} or E_g mode), and adjusting the coefficient of this term we can fit the experimental points as in figure 3.

3.2

In order to give a quantitative measure of the anharmonicity we have chosen the data for the blue band of nickel; the shift in the peak over the range 200° – 300°K has been assessed as 75 cm^{-1} . (The other bands are insufficiently distinct for a quantitative estimate.) Rather arbitrarily we have assumed that the shift is due to the A_{1g} and E_g modes in equal proportions. We then find for either of these the number $2\lambda(\hbar\omega)^{-1}Q_0^3$, which is a good measure of the anharmonicity,

$$\frac{\lambda Q_0^3}{2\hbar\omega} \simeq \frac{1}{15}, \quad \lambda \simeq 0.75 \times 10^{14} \text{ erg cm}^{-3}.$$

In the calculations we have assumed, for simplicity, that $\lambda - \lambda_1 \sim \lambda$. The justification for this procedure is that the distance of the ligands from the hard core of the ion is greater in the excited than in the ground state, so that the anharmonicities are expected to be (numerically) less. The contribution to the temperature dependence due to this term is about half that due to change in frequencies.

3.3

We pass over to consideration of the other terms in $\bar{E} - E_{pr}$. The term $2a^2\hbar\omega$ corresponds in an obvious manner to a mean transition to the energy level vertically above the minimum of the lower potential. On the other hand the second term, which represents a further shift in the mean observed energy, has not been hitherto considered. Supposing that λ_1 , though smaller than, is not much different from λ we find that this term is positive. With the relatively high anharmonicity just found, and using the estimated values of a , this additional energy may well amount to 1200 cm^{-1} .

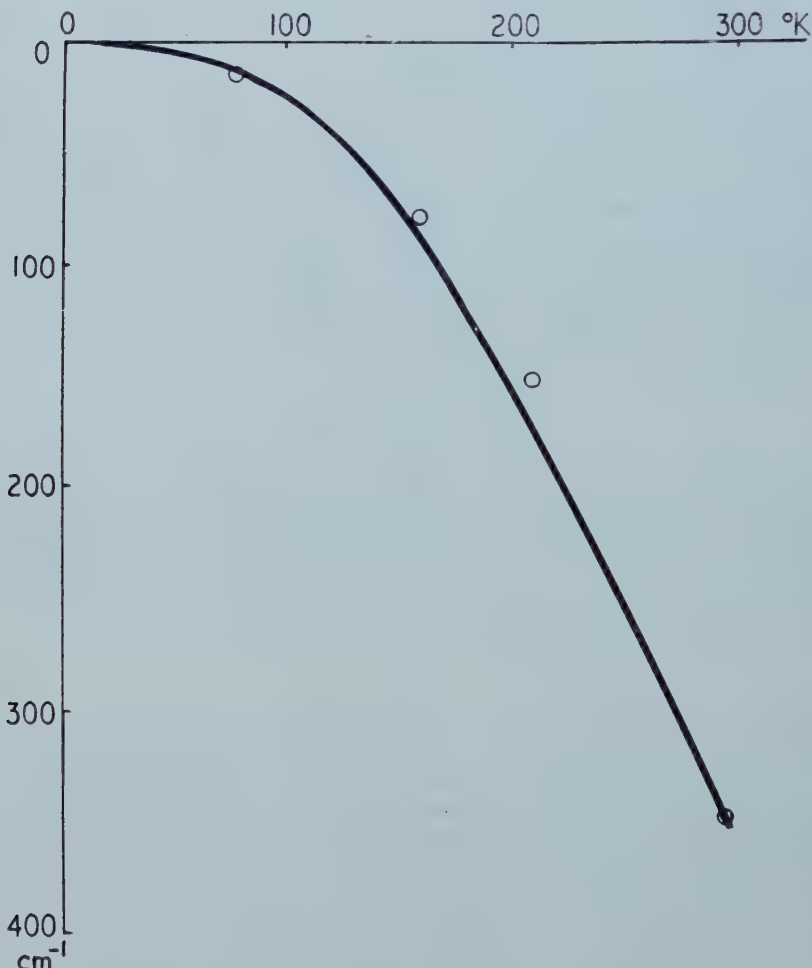


Figure 3. The peak of the absorption line shape as a function of temperature. Circles are experimental results for $\text{KCr}(\text{SO}_4)_2 \cdot 12\text{H}_2\text{O}$.

The consequences of this extra term for the crystal-field theory are two-fold. First, the effective value of the crystal-field parameter Δ for the ground state has to be readjusted. This (or Dq) is usually identified with that abscissa

of the Orgel diagram where the energy-difference of the two lowest levels of the same multiplicity equals the (mean) observed energy of absorption. This identification is valid if, and only if, the two potentials are parabolic. Otherwise, the energy due to anharmonicity must be subtracted before measuring the observed energy on the ordinates of the Orgel diagram. Secondly, the values of Δ for different excited states may be different, decreasing presumably with increasing ligand-ion equilibrium distance.

The simple crystal-field theory, that is without covalency effects, predicts transition energies which for some excited states are in excess of empirical results by about 1500 cm^{-1} . Now, in nickel at any rate, both of these effects would tend to a relative reduction in the observed energies of the higher (as compared to the lowest) excited states. It is now tentatively suggested that part of the observed discrepancy is caused by the anharmonic forces in the ground state. Further experiments aimed at varying the anharmonicities, by the application of pressure or by other means, should prove very useful.

4. THE TEMPERATURE VARIATION OF THE TOTAL INTENSITY OF ABSORPTION

4.1

In common with the peak versus temperature measurements the observed total intensities also follow a pattern which seems independent of the particular band or substance. There is this important difference, however, that the temperature variation of the intensity is now due to that *odd* vibration which is responsible for the transition. In fact, for a purely harmonic vibration a factor $\coth h\nu/2kT$ enters the oscillator strength, ν being the frequency of the odd vibration in question. The approximate values of these frequencies are as noted (figure 4).

The experimental points are in fact quite well covered by the curve $\coth h\nu/2kT$, using $\nu = 350 \text{ cm}^{-1}$. Unfortunately, the detailed theory of these transitions (as given in the works that are listed at the beginning of this paper), assures us that it is the modes with the unmistakably lower frequencies (the 'pumping' modes) which are effective, and it is hard to see how some sort of coupling between odd and even (or odd-odd) vibrations could account for such a substantial discrepancy. It seems that a re-examination of the theory may be desirable on various theoretical grounds. Nevertheless, in the present position (i.e. with the successes of the existing interpretation and the absence of any alternatives) it appears worth while to consider a model which fits into the current theory.

4.2

The solution we offer now is based once again on the existence of strong anharmonicities in the vibrations. In the pumping modes with which we are here concerned, the motion of ligands is perpendicular to the line joining them to the ion. The lowest order anharmonicities are quartic in the displacement; we assume them to be of such sign as to strengthen the restoring force.

Immediately two questions arise. One concerns the origin, the other the treatment of these anharmonicities.

The same problem of pumping modes was considered in a descriptive way by Eley and Evans [7]. They suggested that the water molecules surrounding a positive ion might be moving in a parabolic potential well terminating in a hard

core potential at the molecular radius of the neighbouring water molecule. A suitable description of this situation is provided by the Pöschl-Teller [8] potential

$$V_{PT}(r) = \frac{\hbar^2 \alpha(\alpha - 1)}{2M\rho^2} \operatorname{cosec}^2 2r/\rho$$

which is symmetric about $r = \frac{1}{4}\pi\rho$.

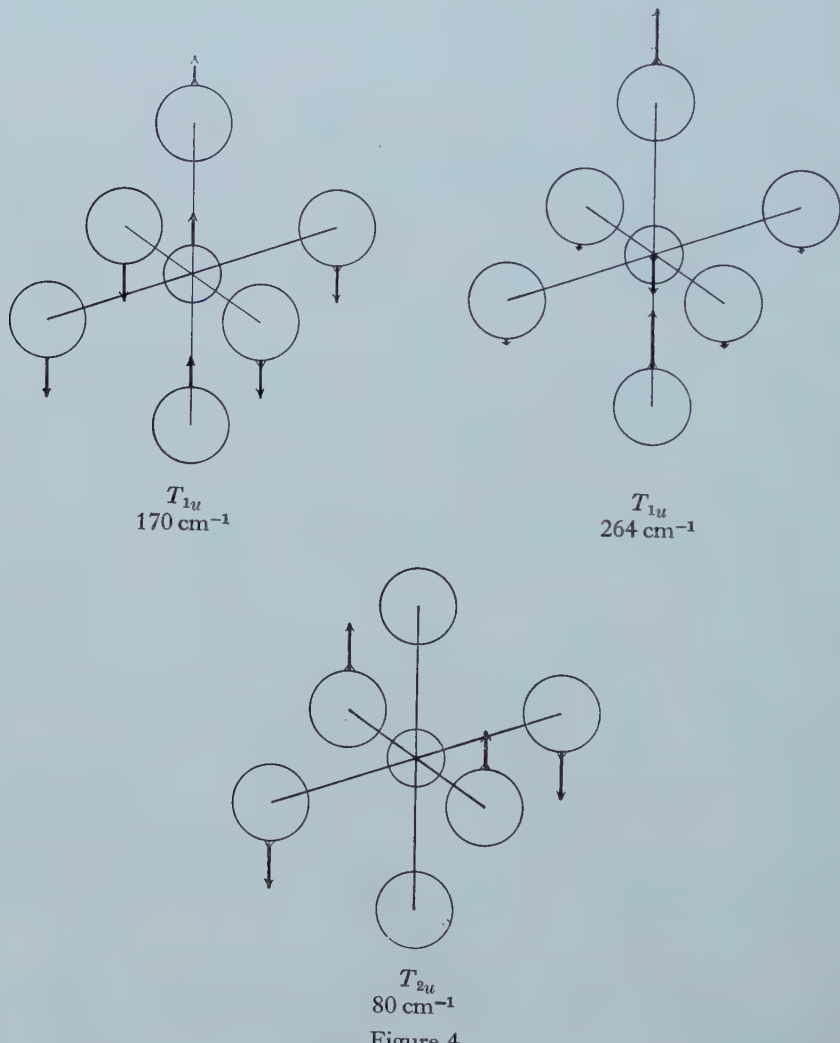


Figure 4

The point that is worth making here is that it would be rather useless to treat the anharmonicities by perturbation theory, since these now enter the energy in the *first* order (in contrast with the case of § 3) and rapidly begin to dominate it for higher energies. In opposition, the Schrödinger equation with the Pöschl-Teller potential can be solved exactly. The form of the *n*th solution is

$$\sin^\alpha(r/\rho) \times \cos^\alpha(r/\rho) \sum_{k=0}^n a_k \sin^k(r/\rho)$$

and the corresponding energy

$$E_n = \frac{\hbar^2}{2M\rho^2} (\alpha + n)^2.$$

The total transition intensity has then the temperature dependent factor

$$\tilde{r}(T) = \frac{\sum_{mn} |\langle m|r|n \rangle|^2 \exp(-E_n/kT)}{\sum_n \exp(-E_n/kT)}.$$

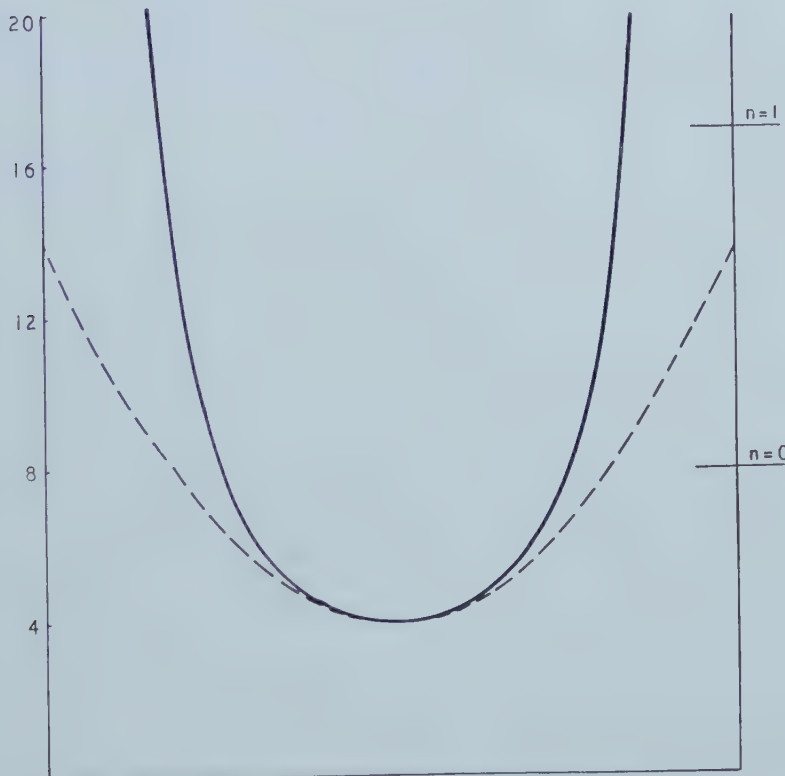


Figure 5. The Pöschl-Teller potential (full line). The broken curve represents the corresponding parabolic potential.

4.3

Plotting this against temperature and adjusting the constant electron dipole factor at 150°K, we secure fairly satisfactory agreement with experimental data (which themselves are not altogether unambiguous). Having chosen $\alpha = 2$, we put

$$\frac{1}{4}\pi\rho = 0.11 \times 10^{-8} \text{ cm},$$

since this value leads in the harmonic approximation to a frequency of 150 cm^{-1} . Also, this is the distance of the wall from the 'edge' of the moving water molecule. In terms of the Eley and Evans conception of hard cores at molecular radii, this corresponds to a molecular radius for water of 1.5×10^{-8} . This compares with the quoted value of 1.4×10^{-8} cm.

We shall not elaborate on the details of the numerical work that arise from this particular choice of the parameters (and which could be improved upon) except to say that only the matrix elements $\langle n|r|n\pm 1\rangle$ are important on the whole and that their increase with n was slower than for harmonic motion.

The ratio of quartic and quadratic terms at the root mean square distance of zero point motion was in the given case $\frac{1}{4}$.

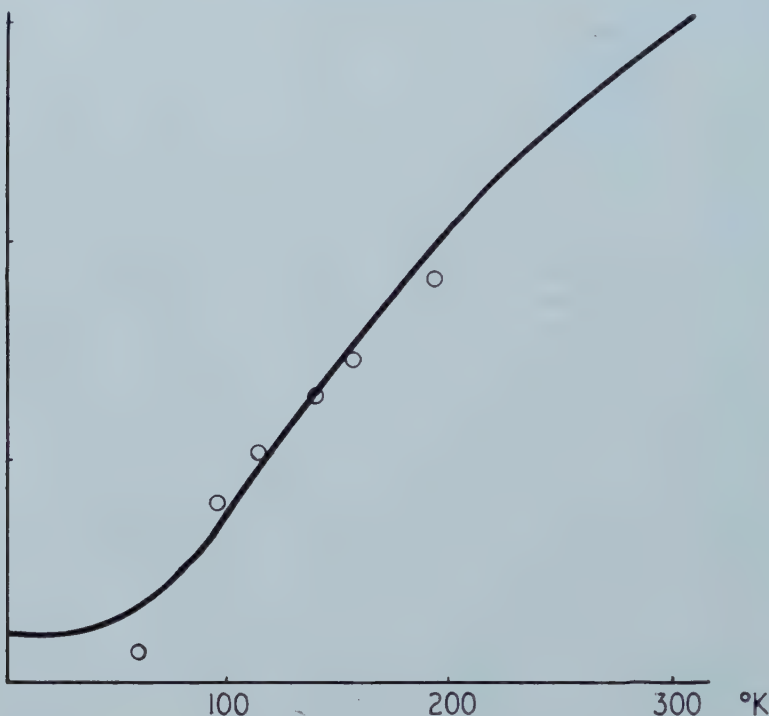


Figure 6. The total intensity of absorption as function of temperature. Arbitrarily vertical scale. Theoretical curve based on Teller-Pöschl potential. Circles are experimental values for red band of nickel.

Most of this work was done while I was in the H. H. Wills Physical Laboratory, Bristol. I am indebted to Professor M. H. L. Pryce, F.R.S., to Dr. N. S. Hush and to Dr. S. Koide for advice and exchange of ideas.

APPENDIX

We indicate now how the mean energy of absorption can be derived for transitions between eigenstates of two potentials which have, in addition to the common quadratic term, small cubic terms in the displacement from the equilibrium positions; namely

$$-\lambda Q^3 \quad \text{and} \quad -\lambda' Q'^3$$

respectively for the ground and excited states. As before the oscillation frequency is written as $\omega/2\pi$, the zero point motion amplitude as Q_0 and the distance between the equilibrium positions as $2aQ_0$.

The energy of the oscillators is not changed in the first order of λ or λ' . The perturbed kets written as superpositions of harmonic oscillator kets become

$$|\hat{n}\rangle = |n\rangle - \frac{\lambda}{\hbar\omega} \sum_m |m\rangle \frac{\langle m|Q^3|n\rangle}{n-m}.$$

A similar equation holds for bras of the displaced potential, distinguished by primed symbols. Then we evaluate

$$\frac{E - E_{pr}}{\hbar\omega} = \frac{\sum_{r,n} |\langle \hat{r}'|\hat{n}\rangle|^2 (r-n) \exp(-xn)}{\sum_{r,n} |\langle \hat{r}'|\hat{n}\rangle|^2 \exp(-xn)} \quad \left(x = \frac{\hbar\omega}{kT} \right).$$

More than one bird may be killed with the same stone, by considering the function

$$G(x, y) = \sum_{r,n} |\langle \hat{r}'|\hat{n}\rangle|^2 \exp(-xn - yr)$$

which equals

$$\begin{aligned} \sum_{r,n} |\langle r'|n\rangle|^2 \exp(-xn - yr) &= \frac{2\lambda}{\hbar\omega} \sum_{r,n,m} \frac{\langle r'|n\rangle \langle n|Q^3|m\rangle \langle m|r'\rangle}{n-m} \exp(-xn - yr) \\ &\quad - \frac{2\lambda'}{\hbar\omega} \sum_{r,n,m} \frac{\langle n|r'\rangle \langle r'|Q'^3|m'\rangle \langle m'|n\rangle}{r-m} \exp(-xn - yr) \end{aligned}$$

to the first order in the perturbation, if a real representation is used for which $\langle r'|n\rangle = \langle n|r'\rangle$.

It is the last term, that involving λ' , which is essential for our purposes. Since the evaluation of this is a rather lengthy business we confine ourselves to an outline of the procedure. The quantities $\langle r'|Q'^3|m'\rangle$ should be evaluated first; the resulting expressions can then be summed with the aid of formal methods. We obtain the sum as a closed analytical expression, in which we put $y=0$ after the appropriate differentiations.

The first two terms may be tackled by the method of diagonal sums. Thus, for example, the sum contained in the second term can be re-written as

$$\sum_{r,n,m} \frac{\langle r'|n\rangle \langle n|Q^3|m\rangle \langle m|r'\rangle \exp(-yH'/\hbar\omega)|r'y\rangle}{n-m}.$$

where H' is the Hamiltonian operator for the excited configuration.

Using the invariance property of the trace, we can carry out the summation over r by summing the diagonal elements in the unprimed representation. This sum is

$$\sum_{n,m} \frac{\langle n|Q^3|m\rangle \langle m|\exp(-yH'/\hbar\omega)|n\rangle}{n-m} \exp(-xn + \frac{1}{2}y).$$

This is clearly zero for $y=0$.

Differentiating with respect to y , putting $y=0$, and noting that

$$H' = H - 2\hbar\omega/Q_0 \cdot aQ + 2\hbar\omega a^2$$

we find

$$\begin{aligned} \frac{2a}{Q_0} \sum_{n,m} \frac{\langle n|Q^3|m\rangle \langle m|Q|n\rangle}{n-m} \exp(-xn) &= -\frac{3a}{4\sqrt{2}} Q_0^3 \sum_n (1+2n) \exp(-xn) \\ &= \frac{3a}{4\sqrt{2}} Q_0^3 \{[1-\exp(-x)]^{-1} - 2[1-\exp(-x)]^{-2}\}. \end{aligned}$$

REFERENCES

- [1] LIEHR, A. D., and BALLHAUSEN, C. J., 1957, *Phys. Rev.*, **106**, 1161.
- [2] KOIDE, S., and PRYCE, M. H. L., 1958, *Phil. Mag.*, **3**, 607.
- [3] HOLMES, O. G., and McCLURE, D. S., 1957, *J. chem. Phys.*, **26**, 1686.
- [4] ÖPIK, U., and PRYCE, M. H. L., 1957, *Proc. roy. Soc. A*, **238**, 425.
- [5] ORGEL, L. E., 1955, *J. chem. Phys.*, **23**, 1004.
- [6] HUANG, KUN, and RHYS, AVRIL, 1950, *Proc. roy. Soc. A*, **204**, 406.
- [7] ELEY, D. D., and EVANS, M. G., 1938, *Trans. Faraday Soc.*, **34**, 1093.
- [8] PÖSCHL, G., and TELLER, E., 1933, *Z. Phys.*, **83**, 143.

A thermodynamic discriminant for the Lennard-Jones potential

by W. B. BROWN and J. S. ROWLINSON

Department of Chemistry, University of Manchester

(Received 16 June 1959)

It is shown that for an assembly of molecules interacting with the Lennard-Jones $n : 6$ pair potential the classical fluctuation discriminant Δ of the configurational energy \mathcal{U} and the virial \mathcal{V} , defined by

$$\Delta = [\overline{\delta \mathcal{U}^2} \overline{\delta \mathcal{V}^{-2}} - (\overline{\delta \mathcal{U} \delta \mathcal{V}^{-1}})^2]/(kT)^2,$$

can be related exactly to configurational thermodynamic properties and the repulsion exponent n . The condition that the discriminant is essentially positive (Schwarz's inequality) provides an experimental lower bound for n .

The experimental behaviour of the discriminant for argon is examined for solid, liquid and gas states. It is found that the assumption of a 12:6 potential leads to negative values of Δ over certain temperature and pressure ranges of the fluid. It appears that a value of n between 13 and 14 would be sufficient to satisfy the inequality for the liquid, but that a much higher value is indicated by the less reliable results for the gas at high temperatures.

The theoretical behaviour of the discriminant is discussed, and it is shown that Δ should tend to zero rapidly at high temperatures and at high densities.

A brief account is given of the appropriate quantal analogue of Δ which unfortunately appears to be experimentally inaccessible.

1. INTRODUCTION

Since accurate potential energy functions for the interaction of molecules are too difficult to calculate by quantum mechanics, much effort has been devoted to obtaining information about intermolecular forces from the bulk properties of matter. Unfortunately it is impossible to invert even the simplest statistical integrals for the thermodynamic and transport properties of a substance to obtain the intermolecular potential. The usual procedure is therefore to choose, on the basis of theory and convenience, a simple functional form for the potential involving various parameters. The values of these parameters are then determined by comparing the experimental results for a simple bulk property with those calculated statistically, and the adequacy of the chosen functional form is assessed by comparing the parameters obtained from different properties.

The function most frequently used to represent central and additive interactions is that of Lennard-Jones,

$$u(r) = \lambda r^{-n} - \nu r^{-m} \quad (\lambda, \nu > 0; \quad n > m). \quad (1.1)$$

The leading characteristics of $u(r)$, namely the minimum interaction energy and the corresponding intermolecular separation, are fixed by the constants λ and ν once the form is determined by n and m . The attraction exponent m is almost invariably set equal to 6, in accordance with the asymptotic form of the London dispersion forces. There is no corresponding theoretical basis for the repulsion term λr^{-n} , but it is found that almost any value of n between 10 and 14 leads to

adequate agreement between the calculated and experimental results for low-energy properties (e.g. second virial coefficient, but not molecular beam scattering). The value $n = 12$ has been widely used [1], partly because it sometimes appears to fit the experimental results best, and partly for mathematical convenience.

The object of this paper is to describe a method of obtaining more precise information about the repulsion exponent n directly from the experimental results and without the need for statistical calculations. The method is based on an inequality for a statistical fluctuation discriminant, which can be expressed in terms of thermodynamic properties for the Lennard-Jones potential, and which leads to a lower bound for n . The reasonableness of this lower bound then checks the adequacy of the Lennard-Jones form itself.

The paper falls naturally into two parts: a theoretical part in which the inequality involving the repulsion exponent n is derived, and a part in which the theory is applied to the experimental results for argon.

2. CLASSICAL CONFIGURATIONAL FLUCTUATION DISCRIMINANT

In this section we consider the statistical fluctuations of configurational quantities in a canonical ensemble of assemblies each containing N identical monatomic molecules confined to a volume V . If the assembly can be treated by classical statistical mechanics, configurational thermodynamic properties can be defined and obtained from the configurational partition function

$$\exp(-F^*/kT) = \frac{1}{N!} \int_V \dots \int_V \exp(-\mathcal{U}/kT) d^3\mathbf{r}_1 \dots d^3\mathbf{r}_N, \quad (2.1)$$

where $F^*(T, V, N)$ is the configurational Helmholtz free-energy, and $\mathcal{U}(\mathbf{r}_1, \dots, \mathbf{r}_N)$ is the potential energy. The two most important configurational functions of an assembly are the potential energy \mathcal{U} and the virial \mathcal{V} , which we shall define by

$$\mathcal{V} = -\frac{1}{3} \sum_{i=1}^N \mathbf{r}_i \cdot \text{grad}_i \mathcal{U}. \quad (2.2)$$

The average values of these functions in the ensemble are most easily obtained by differentiating (2.1) with respect to T and V , and are given by

$$\left. \begin{aligned} \bar{\mathcal{U}} &= F^* - T(\partial F^*/\partial T)_V = U^*, \\ \bar{\mathcal{V}} &= -V(\partial F^*/\partial V)_T - NkT = PV - NkT. \end{aligned} \right\} \quad (2.3)$$

Both functions, and therefore their averages, vanish for a perfect gas.

The fluctuations of \mathcal{U} and \mathcal{V} about their average values can be found by differentiating equations (2.3) with respect to T and V , and are [2],

$$\left. \begin{aligned} \overline{\delta \mathcal{U}^2}/kT &= TC_v^*, \\ \overline{\delta \mathcal{U} \delta \mathcal{V}}/kT &= TV\gamma_v - NkT, \\ \overline{\delta \mathcal{V}^2}/kT &= \bar{\mathcal{W}} + PV - V/\beta_T, \end{aligned} \right\} \quad (2.4)$$

where $\delta \mathcal{U} = \mathcal{U} - \bar{\mathcal{U}}$, etc., C_v^* is the configurational heat capacity at constant volume, γ_v is the thermal pressure coefficient $(\partial p/\partial T)_v$, and β_T is the isothermal compressibility. The configurational function \mathcal{W} appearing in the virial fluctuation is defined by

$$\mathcal{W} = -\frac{1}{3} \sum_{i=1}^N \mathbf{r}_i \cdot \text{grad}_i \mathcal{V}, \quad (2.5)$$

and therefore bears the same relations to \mathcal{V} that \mathcal{W} bears to \mathcal{U} . However, unlike \mathcal{U} and \mathcal{V} , its average value $\overline{\mathcal{W}}$ cannot in general be related to configurational thermodynamic properties of the assembly, which means that the virial fluctuation $\overline{\delta\mathcal{W}^2}$ is generally an experimentally inaccessible quantity.

The fluctuations $\overline{\delta\mathcal{W}^2}$ and $\overline{\delta\mathcal{V}^2}$ must, of course, be positive or zero (all three fluctuations in (2.4) vanish for a perfect gas), so that

$$C_V^* \geq 0, \quad \overline{\mathcal{W}} \geq V/\beta_T - PV. \quad (2.6)$$

The first of the inequalities is related to the thermal stability condition $C_V \geq 0$, but the second is solely a statistical condition, and is not directly related to the requirement of thermodynamic stability, namely $\beta_T \geq 0$. However, it can be shown by using equation (3.1) that this condition on $\overline{\mathcal{W}}$ is not very strong in actual systems.

A stronger inequality is that the fluctuation discriminant for \mathcal{W} and \mathcal{V} is essentially positive. This discriminant may be defined as

$$\Delta = [\overline{\delta\mathcal{W}^2 \delta\mathcal{V}^2} - (\overline{\delta\mathcal{W}\delta\mathcal{V}})^2]/(kT)^2 \geq 0, \quad (2.7)$$

and the inequality is that of Schwarz [3]. When equations (2.4) for the fluctuations are substituted into Δ it becomes

$$\Delta = TC_V^*(\overline{\mathcal{W}} + PV - V/\beta_T) - (TV\gamma_V - NkT)^2; \quad (2.8)$$

it is not in general experimentally accessible since it involves $\overline{\mathcal{W}}$.

3. LENNARD-JONES POTENTIAL

For an assembly of molecules which interact additively with the Lennard-Jones pair potential (1.1) the function \mathcal{W} is linearly related to \mathcal{U} and \mathcal{V} by [2]

$$\mathcal{W} - \frac{1}{3}(n+m)\mathcal{V} + \frac{1}{9}nm\mathcal{U} = 0. \quad (3.1)$$

Therefore $\overline{\mathcal{W}}$ is related to the accessible quantities $\overline{\mathcal{U}}$ and $\overline{\mathcal{V}}$ given by equation (2.3), and hence by substitution equation (2.8) for Δ becomes

$$\Delta = TC_V^*[-\frac{1}{9}nmU^* + PV + \frac{1}{3}(n+m)(PV - NkT) - V/\beta_T] - (TV\gamma_V - NkT)^2. \quad (3.2)$$

If the attraction exponent m is put equal to 6, as usual, then since the configurational energy U^* is usually large and negative, the Schwarz inequality $\Delta \geq 0$ provides an experimental lower bound for the repulsion exponent n . For a satisfactory value of n the discriminant Δ must be positive (or zero) under all conditions of temperature and pressure.

It is interesting to note that (3.1) still holds if the attraction and repulsion coefficients λ and ν in the potential (1.1) depend on the orientations of the molecules. This suggests that the application of the discriminant might usefully be extended to non-polar substances with slightly non-central forces.

Another complicating feature of actual intermolecular forces is their non-additivity [1]; that is, the total potential energy is not exactly equal to the sum of pair potentials, as we have assumed, but contains terms peculiar to the interaction of three and more molecules. However, it is shown in an appendix that the true value of $\overline{\mathcal{W}}$ will probably be less than that given by (3.1), so that (3.2) will still give a lower bound for n . If non-additivity is important, an acceptable value of the repulsion exponent n will thus be even greater than that required by (3.2).

It is worth pointing out that (3.1) is true also for a mixture of Lennard-Jones molecules which have the same exponent n , so that the discriminant given by (3.2) still provides a check on this exponent.

4. VIRIAL EXPANSION AT HIGH TEMPERATURES

The behaviour of the fluctuation discriminant Δ can be analysed theoretically at low densities and high temperatures, and is of particular interest in view of the results found for argon in § 8.

The fluctuations given by (2.4) can all be expanded as power series in the density $\rho = N/V$ the leading terms being

$$\left. \begin{aligned} \overline{\delta U^2}/kT &= -\rho N k \cdot T^2 b'', \\ \overline{\delta U \delta V}/kT &= \rho N k \cdot T b', \\ \overline{\delta V^2}/kT &= \rho N k \cdot \left(\frac{nm}{9} \right) \left[T b' - \left(1 - \frac{3}{n} \right) \left(1 - \frac{3}{m} \right) b \right], \end{aligned} \right\} \quad (4.1)$$

where $N_0 b(T)/T$ is the second virial coefficient $B(T)$ and the primes denote differentiation with respect to T . The discriminant Δ can therefore be expanded as a power series in the density beginning with ρ^2 :

$$\Delta(\rho, T) = \sum_{l=2} \rho^l \Delta_l(T); \quad (4.2)$$

It follows from (4.1) that the leading coefficient is given by

$$\Delta_2 = (NkT)^2 \left\{ -\left(\frac{nm}{9} \right) b'' \left[T b' - \left(1 - \frac{3}{n} \right) \left(1 - \frac{3}{m} \right) b \right] - (b')^2 \right\}. \quad (4.3)$$

The exact form of $b(T)$ is of course known as an infinite series appropriate to high temperatures [1]. On substituting this series into (4.3) it is found that the first two terms of the corresponding high temperature series for Δ_2 vanish identically. This feature is also found in the higher coefficients, and means that at all densities for which (4.2) converges the discriminant Δ (or more exactly, its square root) should vanish more rapidly than the individual fluctuations as the temperature is increased. This suggests that the inequality for the experimental discriminant defined by (3.2) should provide a sensitive criterion for n at high temperatures.

The explanation of this feature is straightforward, and shows it to be peculiar to the Lennard-Jones potential. Let us put

$$U = -A + B \quad (4.4)$$

where $-A$ is the total intermolecular attraction energy and B is the total repulsion energy, and similarly put

$$V = -A_1 + B_1. \quad (4.5)$$

Then the discriminant defined by (2.7) becomes

$$\begin{aligned} \Delta(kT)^2 &= [\overline{\delta B^2} \overline{\delta B_1^2} - (\overline{\delta B \delta B_1})^2] \\ &+ 2[\overline{\delta B \delta B_1} (\overline{\delta B \delta A_1} + \overline{\delta B_1 \delta A}) - \overline{\delta B^2} \overline{\delta B_1 \delta A_1} - \overline{\delta B_1^2} \overline{\delta B \delta A}] \\ &+ [\overline{\delta B^2} \overline{\delta A_1^2} - 2\overline{\delta B \delta B_1} \overline{\delta A \delta A_1} + \overline{\delta B_1^2} \overline{\delta A^2} - (\overline{\delta B \delta A_1})^2 \\ &\quad - 2\overline{\delta B \delta A_1} \overline{\delta B_1 \delta A} + 4\overline{\delta B \delta A} \overline{\delta B_1 \delta A_1} - (\overline{\delta B_1 \delta A})^2] \\ &+ 2[(\overline{\delta B \delta A_1} + \overline{\delta B_1 \delta A}) \overline{\delta A \delta A_1} - \overline{\delta B \delta A} \overline{\delta A_1^2} - \overline{\delta B_1 \delta A} \overline{\delta A^2}] \\ &+ [\overline{\delta A^2} \overline{\delta A_1^2} - (\overline{\delta A \delta A_1})^2]. \end{aligned} \quad (4.6)$$

In this formidable expression the terms in square brackets are in the order of the number of repulsion factors $\delta\mathcal{B}$ they contain. Therefore, since intermolecular repulsions dominate configuration properties at high temperatures, they are also in the order of importance at high temperatures. Only the first square bracket, involving $\delta\mathcal{B}^2\delta\mathcal{B}_1^2$, will contribute to the leading term in the high temperature series for Δ , and so on with successive brackets. In general none of these brackets will vanish; for example, all differ from zero for the Buckingham exp: six potential. However, in the case of the Lennard-Jones form, (1.1), it is easily seen that

$$\mathcal{A}_1 = \frac{1}{3}m\mathcal{A}, \quad \mathcal{R}_1 = \frac{1}{3}n\mathcal{B}, \quad (4.7)$$

so that (4.6) reduces to

$$\Delta = [(n-m)/3kT]^2 [\overline{\delta\mathcal{A}^2} \overline{\delta\mathcal{B}^2} - (\overline{\delta\mathcal{A}\delta\mathcal{B}})^2]. \quad (4.8)$$

The two leading high-temperature terms thus vanish identically, and Δ becomes essentially the fluctuation discriminant of the attraction energy \mathcal{A} and the repulsion energy \mathcal{B} .

It is a corollary that the discriminant is identically zero under all conditions if intermolecular attraction is absent and repulsion has the inverse-power form. Now an assembly of Lennard-Jones molecules will effectively approach this condition at high densities, whatever the temperature. This means that the sign of Δ defined by (3.2) will be sensitive to the value of n , not only at high temperatures, but also at high densities.

5. SIMPLE CELL THEORY

In the simplest version of the cell theory of liquids the molecules move independently in their cells, so that the potential energy is approximated by

$$\mathcal{U} = \mathcal{U}^0(R) + \sum_{i=1}^N \xi(s_i; R), \quad (5.1)$$

where $\xi(s; R)$ is the energy of a molecule distant s from the centre of its cell, and R is the distance between nearest cell centres. The corresponding virial function is

$$\mathcal{V} = \mathcal{V}^0(R) - \frac{1}{3} \sum_{i=1}^N \eta(s_i; R), \quad (5.2)$$

where the cell virial η is given by [2]

$$\eta = s(\partial\xi/\partial s) + R(\partial\xi/\partial R). \quad (5.3)$$

when (5.1) and (5.2) are substituted into (2.7), the fluctuation discriminant becomes

$$\Delta = N[\overline{\delta\xi^2} \overline{\delta\eta^2} - (\overline{\delta\xi\delta\eta})^2]/(3kT)^2, \quad (5.4)$$

where the average need only be over the configurational distribution of a single molecule.

At comparatively high densities the cell energy ξ and virial η will become proportional to s^2 , and therefore to each other. Under these conditions the discriminant Δ will vanish. The simple cell model is, of course, a gross approximation, but it does suggest that Δ may become small for liquids at low temperatures, especially under pressure. This agreement cannot in general be extended to solids, since quantum effects will usually be important.

6. QUANTAL FLUCTUATION DISCRIMINANT

In this section we consider the more fundamental fluctuations and discriminants of quantal statistical mechanics. In this respect the chief difference between the classical and quantal formulae for canonical ensembles is that only in the former is it possible to separate thermodynamic quantities into kinetic and configurational parts, corresponding to the parts of the Hamiltonian

$$\mathcal{H} = \mathcal{K} + \mathcal{U}. \quad (6.1)$$

The Helmholtz free energy F is given by the total partition function

$$\exp(-F/kT) = \sum_{\lambda} \exp(-E_{\lambda}/kT), \quad (6.2)$$

where E_{λ} is the energy of eigenstate λ of the assembly. The total energy E and pressure P can be obtained from (6.1) by differentiation and are merely the canonical averages of E_{λ} and $P_{\lambda} = -dE_{\lambda}/dV$; according to the virial theorem P_{λ} is equal to the expectation value $(\mathcal{P})_{\lambda}$ of the operator \mathcal{P} defined by

$$\mathcal{P}V = \frac{2}{3}\mathcal{K} + \mathcal{V}. \quad (6.3)$$

The fluctuations of E_{λ} and P_{λ} about their average values can be found by differentiating the latter with respect to T and V , which gives [4]

$$\left. \begin{aligned} \overline{\delta E_{\lambda}^2}/kT &= TC_V, \\ \overline{\delta E_{\lambda} \delta P_{\lambda}}/kT &= T\gamma_V, \\ \overline{\delta P_{\lambda}^2}/kT &= (\partial P/\partial V)_T - (\overline{dP_{\lambda}/dV}), \end{aligned} \right\} \quad (6.4)$$

where C_V is the total heat capacity at constant volume. The term (dP_{λ}/dV) is given by [5]

$$-V^2(dP_{\lambda}/dV) = (\mathcal{W})_{\lambda} + P_{\lambda}V + \frac{4}{9}(\mathcal{K})_{\lambda} - J_{\lambda}, \quad (6.5)$$

where \mathcal{W} is defined as before by (2.5), and

$$J_{\lambda} = 2 \sum_{\kappa \neq \lambda} |(\mathcal{P}V)_{\kappa\lambda}|^2 / (E_{\kappa} - E_{\lambda}). \quad (6.6)$$

If the Lennard-Jones potential is obeyed, so that \mathcal{W} is given by (3.1), then the pressure fluctuation may be written in the form

$$\overline{(\delta P_{\lambda}V)^2}/kT = -\frac{1}{9}nmE + \left(1 + \frac{n+m}{3}\right)PV - V/\beta_T + \frac{1}{9}(n-2)(m-2)K - \overline{J}_{\lambda}. \quad (6.7)$$

As this expression involves the average kinetic energy K and the positive quantity \overline{J}_{λ} , both of which are experimentally inaccessible in general, this fluctuation cannot be obtained from experimental quantities, and therefore neither can the fluctuation discriminant

$$\Delta_{\text{qu}} = [\overline{\delta E_{\lambda}^2} \overline{\delta P_{\lambda}^2} - (\overline{\delta E_{\lambda} \delta P_{\lambda}})^2](V/kT)^2. \quad (6.8)$$

It should be pointed out that (6.8) is not the closest analogue of the classical discriminant (2.7). This would be

$$\Delta_{\text{qu}'} = \{[\overline{(\delta \mathcal{H})_{\lambda}^2}] [\overline{(\delta \mathcal{P})_{\lambda}^2}] - [(\overline{\delta \mathcal{H} \delta \mathcal{P}})_{\lambda}]^2\} (V/kT)^2. \quad (6.9)$$

where $\delta \mathcal{P} = \mathcal{P} - P$, whereas Δ_{qu} corresponds classically to first taking micro-canonical averages of \mathcal{H} and \mathcal{P} , and then considering the fluctuations of these. However, $\Delta_{\text{qu}'}$ is also inaccessible to experiment, and it can easily be shown that $\Delta_{\text{qu}'} \geq \Delta_{\text{qu}}$, so that Schwarz's inequality for Δ_{qu} is stronger than that for $\Delta_{\text{qu}'}$. Both discriminants vanish for a monatomic perfect gas.

7. PERFECT CRYSTAL

It is interesting to consider the form of the quantal fluctuation discriminant (6.8) for a perfect crystal, since this case can be analysed theoretically. The free energy can be obtained from (6.2) and is

$$F(T, V) = \mathcal{U}^0(V) + \sum_{\alpha=1}^{3N} [\frac{1}{2}\hbar\omega_{\alpha} + kT \ln[1 - \exp(-x_{\alpha})]] \quad (7.1)$$

where $\mathcal{U}^0(V)$ is the classical potential energy of the crystal when the molecules are at rest, $\omega_{\alpha}(V)$ is the angular frequency of the α th normal vibrational mode, and $x_{\alpha} = \hbar\omega_{\alpha}/kT$. After some straightforward mathematics Δ_{qu} reduces to the essentially positive form

$$\Delta_{\text{qu}} = \left[\sum_{\alpha} (g_{\alpha} X_{\alpha})^2 \sum_{\alpha} X_{\alpha}^{-2} - \left(\sum_{\alpha} g_{\alpha} X_{\alpha}^{-2} \right)^2 \right] (kT)^2, \quad (7.2)$$

where $X_{\alpha} = (x_{\alpha}/2) \operatorname{cosech}(x_{\alpha}/2)$ and $g_{\alpha}(V)$ is the dimensionless Grüneisen parameter

$$g_{\alpha}(V) = -d \ln \omega_{\alpha} / d \ln V. \quad (7.3)$$

Now Grüneisen's hypothesis is that all normal frequencies vary with volume in the same way [7], so that†

$$g_{\alpha}(V) = g(V) \quad (\alpha = 1, 2, \dots, 3N). \quad (7.4)$$

This is precisely the condition that the discriminant (7.2) vanishes for all T, V . The Debye approximation for the distribution of the normal modes implies (7.4), and therefore also leads to $\Delta_{\text{qu}} = 0$. Unfortunately this result does not provide a means of testing Grüneisen's hypothesis directly, since it is only on this condition that Δ_{qu} can be expressed in terms of experimental quantities. Nor does it provide a means of testing the Lennard-Jones repulsion exponent n even if this hypothesis is assumed, as Δ_{qu} only involves the intermolecular forces through the dependence of the normal frequencies on the volume.

The usual way of testing the adequacy of the Lennard-Jones potential is through the direct calculation of $\mathcal{U}^0(V)$ and g , [7]. Another method is suggested by the relation (3.1), which leads to the following equation for the dependence of the normal frequencies on the volume:

$$\omega_{\alpha}^{-2}(V) = -A_{\alpha}V^{-(m+2)/3} + B_{\alpha}V^{-(n+2)/3}, \quad (\alpha = 1, 2, \dots, 3N) \quad (7.5)$$

where A_{α} and B_{α} are constants depending on the particular mode α . This relation implies that the Grüneisen parameters satisfy the equation

$$\left(g_{\alpha} - \frac{n+2}{3} \right) \left(g_{\alpha} - \frac{m+2}{3} \right) = \frac{1}{18} (dg_{\alpha}/d \ln V). \quad (7.6)$$

Unfortunately this relation is not easy to test experimentally even if Grüneisen's hypothesis is assumed, since g only varies slowly with volume [7].

8. APPLICATION TO ARGON

The properties of solid, liquid and gaseous argon are better known than those of any other simple substance. Many comparisons of theory and experiment [1, 7-13] have shown that the Lennard-Jones 12:6 pair potential provides an acceptable representation of the energy of interaction of argon atoms. It follows from §3 that the $n:m$ potential, (1.1) may be tested by calculating the discriminant Δ , or the modified discriminant D , defined by

$$D = [(\overline{\delta \mathcal{U}^2 \delta V^2})^{1/2} - |\overline{\delta \mathcal{U} \delta V}|]/kT \geq 0. \quad (8.1)$$

† This is Grüneisen's constant and is usually denoted by γ .

D has necessarily the same sign as the discriminant Δ , (2.7), and is calculated here in kilojoules mole⁻¹. For an $n:6$ potential

$$D(n) = (TC_V^*)^{1/2} \left[-\frac{2n}{3} U^* + PV + \left(2 + \frac{n}{3}\right)(PV - RT) - V/\beta_T \right]^{1/2} - |TV\gamma_V - RT|. \quad (8.2)$$

8.1. Solid argon

Dobbs and Jones [7] have recently compiled critical tables of the thermodynamic properties of solid argon in equilibrium with its vapour, from which $D(n)$ has been calculated from 40°K to the triple-point at 83.8°K. The results are shown in figure 1 for $n=12$, 13 and 14. It is seen that $D(n)$ is always positive

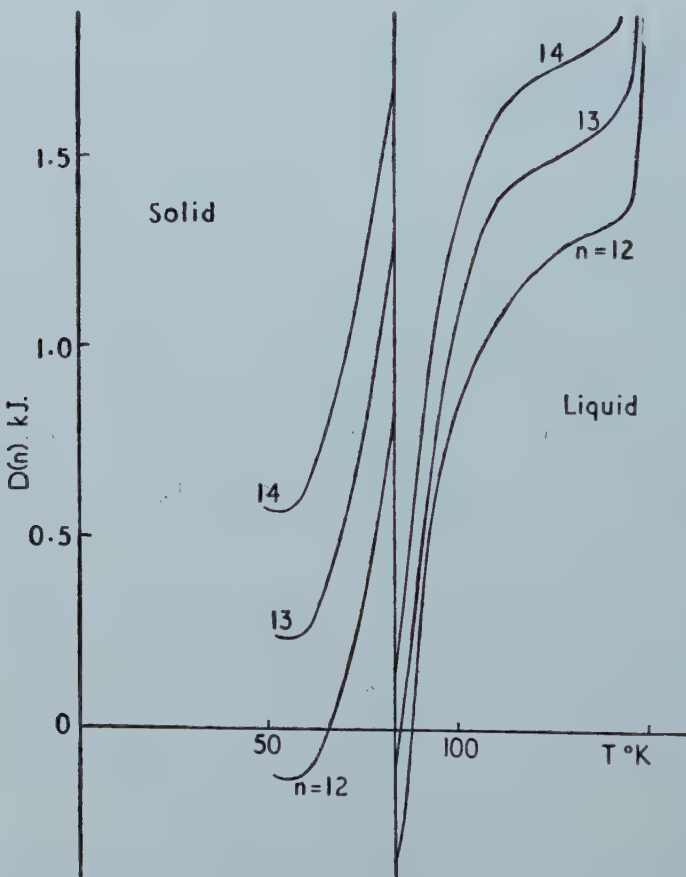


Figure 1. The function $D(n)$, (8.2), for orthobaric solid and liquid argon.

for $n=13$ or 14, but that the curve for $n=12$ cuts the axis at about 65°K. Unfortunately it is clear from an inspection of a graph of C_V against T that the quantal corrections cannot be neglected in the solid state even at a temperature as high as 65°K, and so no test of the $n:6$ potential can be made by using this classical discriminant.

8.2. Orthobaric liquid argon

One of us has recently compiled smoothed tables of the thermodynamic and configurational properties of orthobaric liquid argon from the triple-point to the critical point [14]. These tables are based on the following principal sources,

P, V, U	Din [15].
C_P, C_V, C_σ	Clusius [16], Jones and Walker [17].
γ_V, β_S	Jones and Walker [17], van Itterbeek and Verhaegen [18], Liepmann [19], Galt [20].

where C_σ is the heat capacity at saturation, and β_S is the adiabatic compressibility derived from the velocity of sound. These tables are consistent [14] with the recent results of Michels and his colleagues [21], although they are not based upon them.

The calculated values of the discriminant are shown in figure 1, where it is seen that $D(n)$ becomes negative for the liquid near the triple point if n is less than 13.3. The failure of the potential with $n=12$ to satisfy Schwarz's inequality, $D \geq 0$, appears to be outside the probable experimental error of the thermodynamic properties. The least certain of the properties of the liquids is β_T , the isothermal compressibility. This is used for the calculation of γ_V , the thermal pressure coefficient, and for the calculation of C_V from C_σ . The experimental values of β_T near the triple-point are based upon three consistent measurements of the velocity of sound (that is, β_S).

$D(12)$ is about +5 kJ at the gas-liquid critical point.

8.3. Fluid argon

The thermodynamic properties of the homogeneous fluid have been derived over wide ranges of temperature and pressure by Michels and his colleagues [21, 22], and by Din [15]. Michels' primary measurements are of the pressure as a function of the temperature along isochores. His maximum density is 640 Amagat ($35.0 \text{ cm}^3 \text{ mole}^{-1}$). He and his colleagues have computed extensive tables of all the required thermodynamic properties as functions both of temperature and density and of temperature and pressure. Din's tables are based partly on Michels' results from 0–150 °C and partly on other measurements of the compressibility and on direct measurements of the Joule-Thomson coefficient.

Figure 2 shows the calculated values of $D(12)$ along a typical isobar at a pressure above that of the critical point. Values calculated from Michels' tables have a discontinuity at 0 °C which is due to a discontinuity in his derived values of C_V^* . The poor agreement between the values based on Michels' results and those based on the tables of Din is due to the sensitivity of the discriminant to small errors in the thermodynamic properties. The disagreement is most marked at high temperatures when it is due, almost entirely, to their very different estimates of C_V^* . The disagreement is less marked at low temperatures, where the tables are entirely independent. Here the results of Michels' agree better with those for the orthobaric liquid. All the results make it clear, however, that $D(12)$ becomes negative near the melting point and at high temperatures. Figure 3 shows the boundaries of the regions for which $D(12) \geq 0$, on a P, T plane.

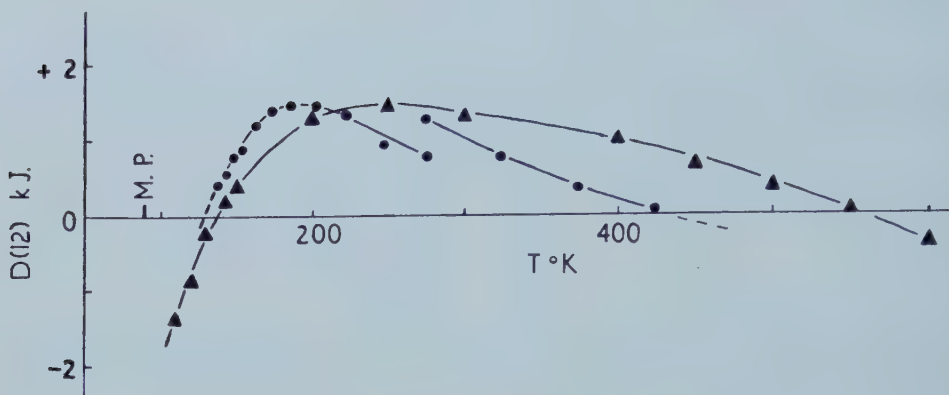


Figure 2. The function $D(12)$ along the 200 atm isobar for argon. Circles, calculated from the results of Michels and his colleagues; triangles, calculated from the tables of Din.

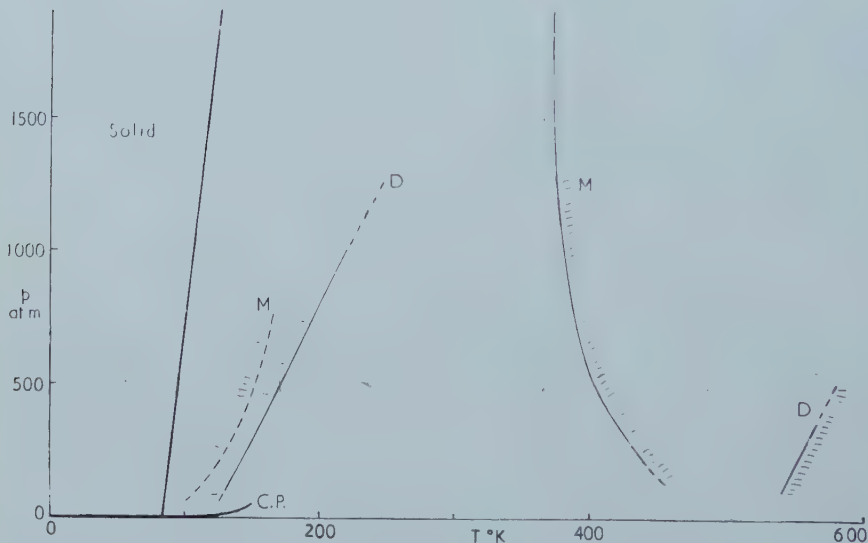


Figure 3. The boundaries of the regions where $D(12) \geq 0$. Lines marked M and D are based, respectively, on the tables of Michels and Din. The lines are dashed where small extrapolations have been made beyond the range of the tables. The lines are shaded on the side on which $D(12)$ is negative.

8.4. The second virial coefficient

It was shown in §4 that the second virial coefficient provides a sensitive test for n at very high temperatures. Let $[VD]_0$ be the limiting value of $[VD]$ at zero density, then it follows from (4.3) that

$$[VD(12)]_0/RT = (-2TB' - T^2B'')^{1/2}(5B + 8TB')^{1/2} - |B + TB'|. \quad (8.3)$$

Whalley, Lupien and Schneider [23] have fitted an empirical equation to their own and other measurements of B as a function of temperature. Figure 4 shows that $[VD(12)]_0$ is satisfactorily positive at all temperatures covered by experiment.

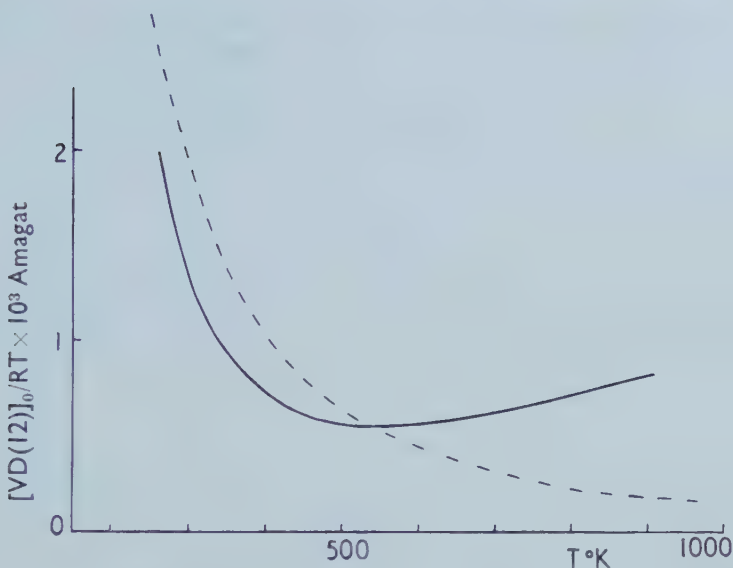


Figure 4. The function $[VD(12)]_0/RT$, (8.3). The full curve is calculated from the experimental results and the dashed curve for a 12:6 potential.

However, the experimental curve for $[VD(12)]_0/RT$ does not show the monotonic decrease with temperature required by a 12:6 potential. The dashed curve in figure 4 is calculated for a 12:6 potential with parameters related to the critical constants of argon by [1]

$$kT^c = 1.25\epsilon, \quad V^c = 3.14N\sigma^3$$

where ϵ and σ are the greatest depth and the collision diameter for this potential.

9. CONCLUSIONS

The best values of the thermodynamic functions that can be derived from the existing measurements on fluid argon produce a negative discriminant $D(12)$ at high densities and at high temperatures. It is shown in §§ 4 and 5 that these are the regions where the discriminant is most useful for testing the Lennard-Jones potential, as it is in these regions that the repulsive forces are most important. The potential would be satisfactory at low temperatures if n were greater than 13, but no reasonable value of n will produce a positive discriminant at high temperatures. For example, at 600°c and 200 atm (Din's tables) the minimum value of n is 21. Such a high value would be incompatible with the properties of the crystal and with the transport properties of the gas at high temperatures [7, 10]. Michels' results require even higher values of n at high temperatures. It must be concluded that the best measurements of the thermodynamic properties of argon cannot be reconciled with a Lennard-Jones potential.

APPENDIX ON NON-ADDITIONITY

If molecular interactions are additive, then by definition the potential energy is given by

$$\mathcal{U}_0 = \sum_{i>j} \sum u(ij) \quad (A 1)$$

where $u(ij) = u(r_{ij})$ is the pair potential. The leading correction to (A 1) is for the potential energy $u(ijk)$ of groups of three molecules, and is

$$\begin{aligned} u'(ijk) &= u(ijk) - u(ij) - u(ik) - u(jk) \\ &= a(3 \cos \theta_i \cos \theta_j \cos \theta_k + 1)/(r_{ij} r_{ik} r_{jk})^3, \end{aligned} \quad (\text{A } 2)$$

where $\theta_i = \widehat{kij}$, etc., and a is a positive constant. The potential energy now has an extra term

$$\mathcal{U}' = \sum_{i>j>k} \sum u'(ijk) \quad (\text{A } 3)$$

which is homogeneous of degree -9 in the position coordinates $\mathbf{r}_1, \dots, \mathbf{r}_N$. If the pair potentials have the Lennard-Jones $n:6$ form and $\mathcal{U} = \mathcal{U}_0 + \mathcal{U}'$, then in place of (3.1) one finds that

$$\mathcal{U} - \frac{1}{3}(n+6)\mathcal{V} + \frac{2n}{3}\mathcal{U}' = -\frac{1}{3}(n-9)\mathcal{U}'. \quad (\text{A } 4)$$

This means that equation (3.2) for Δ should have an extra term $-\frac{1}{3}(n-9)TC_V^* \overline{\mathcal{U}'}$.

It is probably difficult to prove whether or not $\overline{\mathcal{U}'}$ is always positive, but it is fairly easy to show that it is positive in two special cases. The first is that of a gas at low densities and high temperatures. Under these conditions the general expression

$$\overline{\mathcal{U}'} = \frac{1}{6}N^2V^2 \int \int u'(123)g^{(3)}(123)d(1)d(2)d(3) \quad (\text{A } 5)$$

can be approximated by replacing the correct correlation function $g^{(3)}$ with that for hard spheres with collision diameter σ . This leads to the simple result

$$\overline{\mathcal{U}'} = N\sigma^{-9}CV^{-2}, \quad (\text{A } 6)$$

where $C = 5\pi^2 N^2 \sigma^6 / 18$ is the third virial coefficient for hard spheres, so that $\overline{\mathcal{U}'}$ is clearly positive. The second case is the simple cell-lattice model of § 5. Non-additivity enters here chiefly through the configurational lattice energy \mathcal{U}^0 , and it follows from Axilrod's calculations [24] that the contribution of non-additivity is positive for all the basic lattices. Thus $\overline{\mathcal{U}'}$ is positive in the two density and temperature regions of greatest practical interest.

REFERENCES

- [1] HIRSCHFEDLER, J. O., CURTISS, C. F., and BIRD, R. B., 1954, *Molecular Theory of Gases and Liquids* (New York : Wiley).
- [2] BROWN, W. B., 1957, *Phil. Trans. roy. Soc.*, **250**, 221.
- [3] JEFFREYS, H., and JEFFREYS, B. S., 1950, *Methods of Mathematical Physics* (Cambridge : University Press) 2nd Ed., p. 54.
- [4] HILL, T. L., 1956, *Statistical Mechanics* (New York : McGraw-Hill), Chap. 4.
- [5] BROWN, W. B., 1958, *Proc. Camb. phil. Soc.*, **54**, 251.
- [6] BORN, M., and HUANG, K., 1954, *Dynamical Theory of Crystal Lattices* (Cambridge : University Press).
- [7] DOBBS, E. R., and JONES, G. O., 1957, *Rep. Progr. Phys.*, **20**, 216.
- [8] GUGGENHEIM, E. A., 1953, *Rev. Pure appl. Chem.*, **3**, 1.
- [9] KIHARA, T., 1953, *Rev. mod. Phys.*, **25**, 831; 1955, *Ibid.*, **28**, 412.
- [10] WHALLEY, E., and SCHNEIDER, W. G., 1955, *J. chem. Phys.*, **23**, 1644.
- [11] CORNER, J., 1948, *Trans. Faraday Soc.*, **44**, 914.
- [12] DOMB, C., and ZUCKER, I. J., 1956, *Nature, Lond.*, **187**, 484.
- [13] ZUCKER, I. J., 1956, *J. chem. Phys.*, **25**, 915.
- [14] ROWLINSON, J. S., 1959, *Liquids and Liquid Mixtures* (London : Butterworths), pp. 50, 64, 78.
- [15] DIN, F., 1956, *Thermodynamic Functions of Gases* (London : Butterworths), Vol. 2, p. 146.

- [16] CLUSIUS, K., 1936, *Z. phys. Chem.*, B, **31**, 459.
- [17] JONES, G. O., and WALKER, P. A., 1956, *Proc. phys. Soc. Lond.*, B, **69**, 1348; WALKER, P. A., 1956, *Thesis*, London.
- [18] VAN ITTERBEEK, A., and VERHAEGEN, L., 1949, *Proc. phys. Soc. Lond.*, B, **62**, 800.
- [19] LIEPMANN, H. W., 1939, *Helv. phys. acta*, **12**, 421.
- [20] GALT, J. K., 1948, *J. chem. Phys.*, **16**, 505.
- [21] MICHELS, A., LEVFLT, J. M., and DE GRAAFF, W., 1958, *Physica*, **24**, 659; MICHELS, A., LEVLET, J. M., and WOLKERS, G. J., 1958, *Physica*, **24**, 769.
- [22] MICHELS, A., WIJKER, HUB., and WIJKER, HK., 1949, *Physica*, **15**, 627; MICHELS, A., LUNBECK, R. J., and WOLKERS, G. J., 1949, *Physica*, **15**, 689; MICHELS, A., LUNBECK, R. J., and WOLKERS, G. J., 1951, *Appl. sci. Res.*, Hague, A, **2**, 345.
- [23] WHALLEY, E., LUPIEN, Y., and SCHNEIDER, W. G., 1953, *Canad. J. Chem.*, **31**, 722.
- [24] AXILROD, B. M., and TELLER, E., 1943, *J. chem. Phys.*, **11**, 299; AXILROD, B. M., 1951, *J. chem. Phys.*, **19**, 724.

Charge transfer states and optical absorption in octahedrally hydrated paramagnetic salts

by ROBERT ENGLMAN

Department of Physics, Technion-Israel Institute of Technology,
Haifa, Israel

(Received 6 June 1959)

A comprehensive theory is given for all observed optical absorptions which do not involve a spin-change in the paramagnetic ion. Except for the anomalous behaviour of the vanadous ion, good agreement is found between the calculated and the observed oscillator strengths. The operative mechanism in the absorption is the vibrational motion of the ligands, enabling virtual transitions to odd-parity charge transfer states to take place. In these states the central ion loses an electron to the ligands; this situation is also analysed in the paper.

1. INTRODUCTION

Our understanding of the medium intensity optical absorptions in hydrated paramagnetic salts is at present roughly as follows. The transitions involved in the absorption are mainly electric dipole transitions. The energy gain in the absorption is expended by the crystal by a change within the same configuration of the electronic state of the paramagnetic ions. Calculation of the absorption energies on the basis of the ligand field theory were made by Orgel [1] and Tanabe and Sugano [2]. In octahedral ionic complexes with a centre of inversion, the vibrational motion of the ligands adds small odd-parity components to the even $3d$ wave-functions: it is these components which participate in the transition. The most direct evidence for the rôle of the vibrational motion are the intensity measurements, whose temperature variation reflects the statistical population of the vibrational states [3].

The nature of the odd-parity electronic components is not so well established. Since they represent a small fraction in the electronic wave functions (of the order of the fourth root of the ratio of the electronic and ionic masses), they do not significantly enter the energy level calculations. In contrast, for the mechanism of absorption the odd-parity components are vital and would be expected to feature in the expression for the absorption intensities. Actually, in the calculations of absolute intensities of some octahedral complexes [4, 5, 6] the closure property of the electronic wave functions spares one the worry, what exactly the odd-components are made up of; in these investigations it was considered sufficient to regard them as arising from the odd excited electronic states of the central (gaseous) ion.

In this paper we radically depart from this assumption and associate the odd-parity components with the state of charge transfer between the ion and the ligand. The absorption bands corresponding to these states are of very high intensity (their oscillator strengths may be up to order unity). The position of the peak of these bands is in the ultra-violet; their edge for some of the ions appears in the intensity graphs of Holmes and McClure [7] at about $38\ 000\ \text{cm}^{-1}$ (see figure 1);

for other ions the edge is outside the figure but appears in the absorption curves of Dainton [8] at about $50\,000\text{ cm}^{-1}$. The first thing that strikes the eye in figure 1 is the definite correlation between the position of the charge transfer band and the strength of the optical band, in the sense that, the nearer the two bands the higher, as a rule, the intensity of the latter. It will be seen that, while other factors have to be taken into account as well, this correlation follows from our interpretation. Another consequence of the theory is that it fixes the direction of the electron transfer as from the central ion into the ligand.

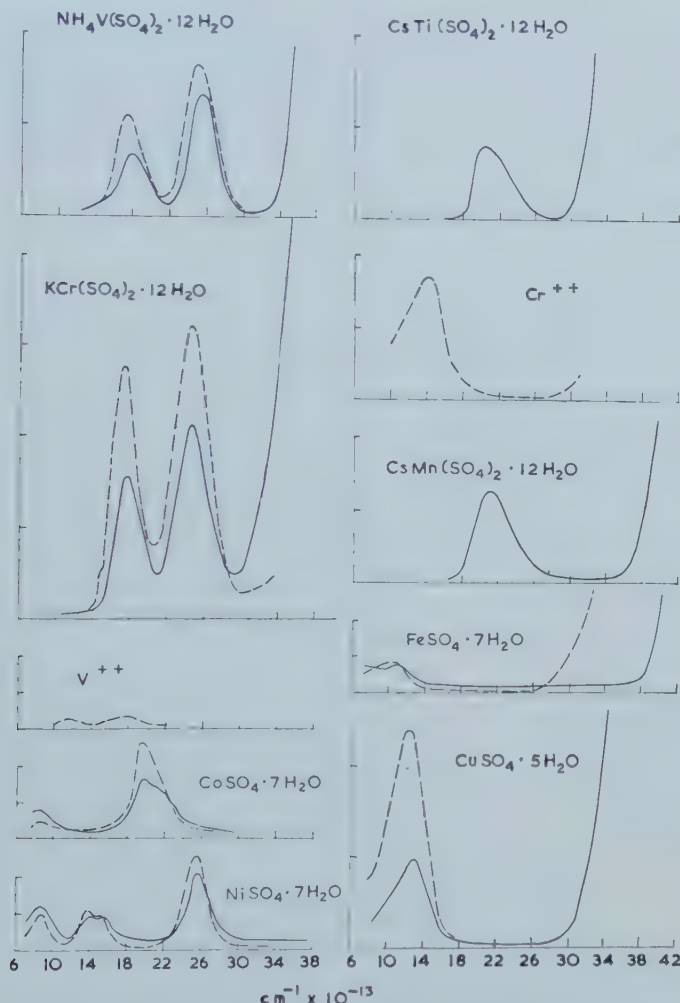


Figure 1. Absorption coefficient. Full lines: Crystal spectra, broken lines: Solution spectra. (From Holmes and McClure.)

Another feature to the credit of the theory is that the theoretical oscillator strengths of *all* the paramagnetic ions (except Fe^{3+} and Mn^{2+}) in octahedral hydrous surroundings are given with the minimum of assumptions, and the relative intensities in different ions are also accounted for. Also, the temperature variation of the total intensity is now in accord with whatever experimental data there are. This is very gratifying, since hitherto experiments showed a much too

slow variation as compared to theory. Now, while it has been shown [3] that this may be the consequence of the strongly anharmonic motion of the ligands, the situation was none too satisfactory. Anticipating what follows, we find now that it is the high-frequency vibrational modes of the ligands which are most effective for the absorption. This is in fair agreement with the temperature dependence of the absorption intensity [7].

2. THE VIBRATIONAL HAMILTONIAN

The first stage in the determination of the transition probabilities is the calculation of the wave functions of the ground and of the relevant excited states of the complex, including the components which are of odd parity in the electronic coordinates. The motion of the ionic masses which gives rise to such components is represented in Cartesian coordinates by the vibrational Hamiltonian

$$\begin{aligned}
 H_v = & \frac{1}{2}(X_1 + X_4 - 2X_0) \frac{\partial}{\partial x} (V_1 + V_4) \\
 & + \frac{1}{4}(X_2 + X_3 + X_5 + X_6 - 4X_0) \frac{\partial}{\partial x} (V_2 + V_3 + V_5 + V_6) \\
 & + \frac{1}{4}(X_2 - X_3 + X_5 - X_6) \frac{\partial}{\partial x} (V_2 - V_3 + V_5 - V_6) + \dots
 \end{aligned}$$

The explanation of the symbols is facilitated by reference to figure 2, which is partly taken from Koide and Pryce. Their notation is also adhered to, as far as possible.

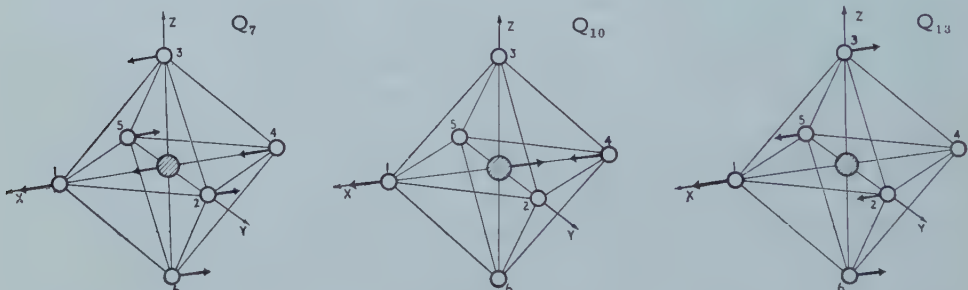


Figure 2.

X_0 denotes the x -coordinate of the central ion, X_i ($i = 1 \dots 6$) the displacements from equilibrium position of the i th ligand. Thus, each ligand, consisting of ions and electrons, is supposed to move as a whole, the internal motion of the ligand being neglected. V_i is the potential due to the i th ligand in its equilibrium position acting on an electron. H_v is that part of the perturbation Hamiltonian on the Born-Oppenheimer approximation which is odd in the electronic coordinates (x, y, z). Later we shall have occasion to consider another Hamiltonian which is of the same order, but even in (x, y, z). The first term in H_v represents to a very good approximation the vibrational mode Q_{10} (T_{1u} -type), the second a mixture of Q_{10} and $Q_7(T_{1u})$, the third $Q_{13}(T_{2u})$, ([4], equation 4.15).

We settle now the nomenclature of the wavefunctions as well. For the $3d$ electrons on the central ions we use the cubic wavefunctions of Tanabe and Sugano. The three $d\epsilon$ and two dy functions are denoted by ξ, η, ζ and u, v . These transform as yz, zx, xy and $1/\sqrt{3}(3z^2 - r^2), x^2 - y^2$. For most hydrated paramagnetic ions the cubic field is sufficiently strong that, barring covalency effects which are not essential for the calculation of transition probabilities, each of the $3d$ electrons will be almost entirely in one of these states. The exceptions are the nickel ion and possibly the vanadous ion.

An excited state of the complex may be formed by the transfer of a $3d$ electron to the ligand (or in principle by the reverse process). This state is at least six-fold degenerate. The degeneracy will be removed by the interaction between the transferred electron and the ions, accompanied by the tendency of the complex to distort itself. The situation, which is quite complicated, will be treated later by the application of the methods of Öpik and Pryce [9].

For the time being we wish to stay within the Born-Oppenheimer approximation. We consider the two charge-transfer states in which an extra electron is at ligands 1 and 4 respectively, and analyse them into an odd electronic state α and an orthogonal even state. As regards the optical transition probabilities, this simplification is justified. We shall prove this statement in § 6.

The calculated oscillator strengths for ten ions are given in table 1. The ion chosen to demonstrate the method is the chromic ion, Cr^{3+} ; for the rest we shall only quote the results and the energy values used in the working.

A further word concerns the high-energy odd states of the (gaseous) paramagnetic ion, which have no place in the theory. Is the neglect of these not inconsistent with the description of the even states in terms of the states of the gaseous ion? Probably not, because in the complex the greater spatial extension of these odd states will either make them merge with the charge transfer states or cause them to shrink considerably, with a consequent increase in energy.

3. THE MATRIX ELEMENT OF THE ELECTRIC DIPOLE MOMENT

Cr^{3+}

The basic electronic states of the chromic ion are

$(d\epsilon)^3$	$\{\xi \eta \zeta\}$	A_2	
$(d\epsilon)^2 dy$	$\{\xi \eta v\}$	T_2	$17\ 600\ \text{cm}^{-1}$
$(d\epsilon)^2 d\gamma$	$\{\xi \eta u\}$	T_1	$24\ 700\ \text{cm}^{-1}$
C	$\{\xi \eta \alpha\}$		$\sim 36\ 000\ \text{cm}^{-1}$

Curly brackets denote Slater determinants. The symmetry type of the state is given, together with its energy. C denotes any one of the charge transfer states; its energy value is taken from Holmes and McClure's curve (figure 1).

Perturbation theory now gives as a correction to these states

$$\begin{aligned}|A_2\rangle' &= |A_2\rangle + \sum_C |C\rangle \frac{\langle C|H_v|A_2\rangle}{E_{A_2} - E_C}, \\ |T_2\rangle' &= |T_2\rangle + \sum_C |C\rangle \frac{\langle C|H_v|T_2\rangle}{E_{T_2} - E_C} \quad \text{etc.}\end{aligned}$$

The matrix element of $P = e \sum \mathbf{r}$, the electric dipole moment is found as

$$\begin{aligned} \langle A_2; n' | P | T_2; n \rangle' &= \sum_C \frac{\langle A_2; n' | H_v | C; n \rangle \langle C; n | P | T_2; n \rangle}{E_{A_2} - E_C} \\ &\quad + \sum_C \frac{\langle A_2; n' | P | C; n' \rangle \langle C; n' | H_v | T_2; n \rangle}{E_{T_2} - E_C}, \end{aligned}$$

where n, n' stands for a set of vibrational quantum numbers. Similarly, of course, for T_1 .

We want to show now that one term dominates the matrix element and that all others can be neglected. It is sufficient to consider the transition to the z -component of T_2 or T_1 (that one written down); the transition probability to any other component will necessarily be the same. For the matrix element of the y -component of the dipole moment we now assert that, disregarding for the moment vibrational matrix elements, the dominant term is

$$\frac{1}{E_{T_2} - E_C} \langle \zeta | ey | \alpha_x \rangle \langle \alpha_x | (\partial/\partial x) (V_1 + V_4) | v \rangle.$$

The contributions due to the second and third terms of H_v are neglected, since these give rise to integrals in which the integrand contains three factors: each large in a different region. (v 'sits' on the central ion, α_x on the axial ligands and the potential on four transverse ligands.) The overlap of the factors is thus necessarily less than that in the retained term.

It remains to consider the following term,

$$\begin{aligned} (E_{A_2} - E_C)^{-1} \langle \zeta | (\partial/\partial x) (V_1 + V_4) | \alpha_y \rangle \langle \alpha_y | ey | v \rangle \\ = -(E_{A_2} - E_C)^{-1} \langle \zeta | (\partial/\partial y) (V_2 + V_5) | \alpha_x \rangle \langle \alpha_x | ex | v \rangle. \end{aligned}$$

Note on the one hand that the derivative increases much more steeply than linearly on moving away from the centre. On the other hand v has a lobe along the x -axis, whereas ζ has a node. It follows therefore that in the latter term we have in terms of overlap of factors a very 'wasteful' disposition of the integrands, as compared to the earlier term.

An analogous term, obtained by interchanging x and y , gives the matrix element of x -component of P . The z -component of P has no non-zero matrix element for the z -component of T_2 .

The square of the P matrix between A_2 and one component of T_2 is

$$\frac{1}{4} |\langle n | X_1 + X_4 - 2X_0 | n \pm 1 \rangle|^2 \cdot 2e^2 (E_{T_2} - E_C)^{-2} \cdot 3I^2 Q^2.$$

Here

$$\begin{aligned} Q &= |\langle \zeta | y | \alpha_x \rangle|, \\ \sqrt{3}I &= |\langle v | (\partial/\partial x) (V_1 + V_4) | \alpha_x \rangle|. \end{aligned}$$

Three important results are added,

$$\begin{aligned} |\langle u | (\partial/\partial x) (V_1 + V_4) | \alpha_x \rangle| &= I, \\ |\langle u | (\partial/\partial z) (V_3 + V_6) | \alpha_z \rangle| &= 2I, \\ |\langle v | (\partial/\partial z) (V_3 + V_6) | \alpha_z \rangle| &= 0. \end{aligned}$$

The first is used to calculate the square of the P matrix between A_2 and one component of T_1 . This is

$$\frac{1}{4} |\langle n | X_1 + X_4 - 2X_0 | n \pm 1 \rangle|^2 \cdot 2e^2 (E_{T_1} - E_C)^{-2} \cdot I^2 Q^2.$$

The relation (Koide and Pryce)

$$X_1 + X_4 - 2X_0 \approx \sqrt{(10/3)Q_{10}}$$

gives

$$|\langle n | X_1 + X_4 - 2X_0 | n+1 \rangle|^2 = \frac{10}{3} \frac{n+1 \cdot h}{4\pi M \nu}$$

M is the ligand mass and ν the frequency of the Q_{10} mode, about 300 cm^{-1} .

The oscillator strength is defined as

$$\text{o.s.} = \frac{2m}{3\hbar^2 e^2} \sum \frac{E_f - E_i}{2j+1} |\langle f | P | i \rangle|^2$$

for transitions between the initial states i of degeneracy $2j+1$ and final states f . The summation is over all initial and final states. For Cr^{3+} the ground state is non-degenerate (apart from spin).

For the optical transitions under consideration

$$\text{o.s.} = \left\{ \frac{2m}{3\hbar^2} \cdot \frac{10}{12} \cdot \frac{n+1 \cdot h}{4\pi M \nu} Q^2 I^2 \right\} \frac{E_f - E_i}{(E_f - E_C)^2} N.$$

At the absolute zero of temperature no vibrational quanta are initially present, so that $n=0$. For non-zero temperatures the statistical averaging over initial states introduces a factor $\coth(\hbar\nu/2kT)$ or 1.6 at room temperature. This factor gives theoretically the main temperature dependence of the absorption intensity. When compared with the results of Holmes and McClure the agreement is reasonable, provided the high frequency value corresponding to Q_{10} is used for ν . The temperature variation due to mechanisms Q_7 and Q_{13} are, on the other hand, too fast by at least a factor two at room temperatures.

N is an integer given by the theory

$$\begin{aligned} N &= 18 \text{ for } A_2 \rightarrow T_2 \\ &= 6 \quad \rightarrow T_1. \end{aligned}$$

Similarly for other transitions

$$N = \begin{array}{cccccc} A_2 \rightarrow T_2, & A_2 \rightarrow T_1; & T_1 \rightarrow T_2, & T_1 \rightarrow T_1; & T_2 \rightarrow E; & E \rightarrow T_2. \\ 18, & 6; & 10, & 6; & 8; & 12. \end{array}$$

4. OSCILLATOR STRENGTHS

Without making further assumptions about $Q^2 I^2$ we can compare intensities of different transitions in the same ion. Thus for Cr^{3+} the ratio of intensities is 1.2. Compare this with the measured ratio of 1.37.

If we assume that $Q^2 I^2$ has one value in all divalent ions and another value for all trivalent ions we can make further comparisons (table 2). The calculations of the next paragraph show that the curly bracket in the oscillator strength has the value (at room temperatures) of 0.9 cm^{-1} for divalent ions and 0.14 cm^{-1} for trivalent ions. The reason for the considerable difference is that, whereas the ligand-ion distances are roughly the same ($2-2.2 \text{ \AA}$) in either kind, the more compact trivalent ions overlap the charge-transfer states to a markedly lesser extent.

In table 1 we give details of the calculations for ten ionic complexes. These include the peaks of the optical absorption bands and the edge of the charge transfer spectra. Both may be read off from figure 1. Using the energies of the absorption edge may at first glance seem arbitrary and likely to introduce error.

Ion	State	Type	Energy in cm^{-1}	Oscillator strength $\times 10^4$	
				Calculated	Observed
Ti^{3+}	$\{\zeta\}$	T_2	20,300 38,000	0.72	0.8
	$\{u\}$	E			
	$\{\alpha\}$	C			
V^{3+}	$\{\xi\eta\}$	T_1	17,800 25,700 40,000	0.49 1.06	0.6 1.1
	$\{\xi u\}$	T_2			
	$\{\xi v\}$	T_1			
	$\{\xi \alpha\}$	C			
V^{2+}	$\{\xi\eta\zeta\}$	A_2	11,800 12,500 40,000(?)	2.4 1.9	0.1 0.2
	$\{\xi\eta\sigma\}$	T_2			
	$\{\xi\eta u\}$	T_1			
	$\{\xi\eta\alpha\}$	C			
Cr^{3+}	$\{\xi\eta\zeta\}$	A_2	17,600 24,700 36,500	1.2 1.5	1.6 2.2
	$\{\xi\eta v\}$	T_2			
	$\{\xi\eta u\}$	T_1			
	$\{\xi\eta\alpha\}$	C			
Cr^{2+}	$\{\xi\eta\zeta u\}$	E	14,000 40,000	2.2	1.8
	$\{\xi\eta\sigma u\}$	T_2			
	$\{\xi\eta\alpha u\}$	C			
Mn^{3+}	$\{\xi\eta\zeta u\}$	E	21,000 43,000	0.73	1.1
	$\{\xi\eta\sigma u\}$	T_2			
	$\{\xi\eta\alpha u\}$	C			
Fe^{2+}	$\{\xi\eta\zeta\xi uv\}$	T_2	10,000 45,000	0.58	0.4
	$\{\xi\eta\zeta\bar{u}uv\}$	E			
	$\{\xi\eta\zeta\bar{\alpha}uv\}$	C			
Co^{2+}	$\{\xi\eta\zeta\bar{\xi}\bar{\eta}uv\}$	T_1	8,350 19,800 60,000	0.28 0.68	0.3 0.9
	$\{\xi\eta\zeta\bar{\xi}\bar{u}uv\}$	T_2			
	$\{\xi\eta\zeta\bar{\xi}\bar{v}uv\}$	T_1			
	$\{\xi\eta\zeta\bar{\xi}\bar{\alpha}uv\}$	C			
Ni^{2+}	$\{\xi\eta\zeta\bar{\xi}\bar{\eta}\bar{\xi}uv\}$	A_2	8,600 14,700 25,500 60,000	0.49 0.20 0.6	0.45 0.35 0.6
	$\{\xi\eta\zeta\bar{\xi}\bar{\eta}\bar{v}uv\}$	T_2			
	$\{\xi\eta\zeta\bar{\xi}\bar{\eta}\bar{u}uv\}$	T_1			
	$\{\xi\eta\zeta\bar{\xi}\bar{\eta}\bar{\alpha}uv\}$	T_1			
Cu^{2+}	$\{\xi\eta\zeta\bar{\xi}\bar{\eta}\bar{\xi}uvu\}$	E	13,000 38,000	2.2	1.4
	$\{\xi\eta\zeta\bar{\xi}\bar{\eta}\bar{v}uvu\}$	T_2			
	$\{\xi\eta\zeta\bar{\xi}\bar{\eta}\bar{\alpha}uvu\}$	C			

Table 1. Oscillator strengths in optical transitions. (Observed values from Holmes and McClure.)

(a) The assumed values of the integrals I, Q are as estimated in § 5.

(b) For the nickel ion it follows from the energy matrix, that the given $(d\epsilon)^5(d\gamma)^3$ cubic state is shared very nearly equally between the two T_1 states.

We shall presently estimate this error. Now we suggest two arguments of entirely different kinds to justify the choice of the absorption edge.

The first is that, by our choice, this part of the theory uses parameters which are empirically given. Choosing the parameters consistently makes it very likely that the errors, albeit of varying proportions, would all lie in the same direction and would not change the results qualitatively.

Ion	Ti ³⁺	V ³⁺		Cr ³⁺		Mn ³⁺	
	Observed	Calculated	0·8 0·72	0·6 0·5	1·1 1·1	1·6 1·2	2·2 1·5

Ion	V ²⁺		Cr ²⁺	Fe ²⁺	Co ²⁺		Ni ²⁺		Cu ²⁺		
	Observed	Calculated	0·1 2·4	0·2 1·9	1·8 2·2	0·4 0·6	0·3 0·3	0·9 0·7	0·45 0·5	0·35 0·2	0·6 0·6

Table 2. Comparison of experimental and calculated values of the oscillator strength ($\times 10^4$) for ions of the same valency.

Secondly, the energy value of the edge may well be more representative than that of the peak. This seems likely, since for the optical absorption we really seek first the weighted average of $(E_f - E_c)^{-1}$ over all C and then of $(E_f - E_c)^{-2}$ over all f . Both these averaging processes result in the reduction of the effective E_c relative to the peak of the absorption line.

We regard the maximum possible error in E_c as the difference between the peak and edge of the charge transfer band. To calculate this error, the assumption is made that the main cause for the broadening of both the optical and the charge transfer absorptions is the distortion in the equilibrium configuration of the complex in the excited states (the Frank-Condon principle). The relation between the extent of the distortion and the change in the configuration potential due to the excited electronic state is discussed elsewhere [3]; in a rough way one may now plausibly reason that the ratio of the distortions in the charge-transfer and the optical transition $d\epsilon \rightarrow d\gamma(u)$ is of the order of the ratio of the corresponding energies. The ratio of the peak-edge distances is the square of the former ratio, on the basis of a model involving parabolic potentials. This allows us to estimate the error (taking the force constants of potentials as equal, one introduces a generous maximum in the estimated error).

The numbers for two extreme examples are as follows: for the highest optical absorption bands of Cr³⁺ and Ni²⁺ the maximum errors in E_c are 6000 and 11 000 cm⁻¹ respectively, the percentage errors in the oscillator strengths 50 and 40 per cent respectively.

The vanadous ion is a striking exception to the good agreement with observation, both as regards the relative strength of the bands and as regards the absolute value. The reason for this is not known. Concerning the other ions one might add that the oscillator strengths depend on a very high power (the fourteenth) of the ratio, ionic radius/ligand-ion distance, so that the exact calculated values should be accepted with some caution.

The following point should be noted, too. We have assumed that in the charge transfer the central ion loses an electron. If the transfer process were to take place in the opposite direction, the analysis of the oscillator strength would be changed as follows. Taking the chromic ion of § 3 as example, the basic electronic states would for the transition $A_2 \rightarrow T_2$ be

$$\begin{array}{ll} \{\xi\eta\zeta\alpha\} & A_2 \\ \{\xi\eta\nu\alpha\} & T_2 \\ \{\xi\eta\zeta\nu\} & C, \end{array}$$

where α represents now an electronic state located in the ground state on the ligand. The procedure of § 3 can be adapted quite easily to show that, to the approximation used there, the only difference in the oscillator strength would arise from there being a factor $(E_i - E_c)^{-2}$ instead of $(E_f - E_c)^{-2}$ as before. There would be no possibility of agreeing that formula with the experimental data. We are thus given strong reasons for assuming that for these ions in a characteristic charge transfer process the electron moves *from* the ion *to* the ligands.

5. THE CHARGE TRANSFER WAVE-FUNCTIONS

The knowledge of these is required by the presence of the integrals I, Q in the oscillator strength. This poses a difficult problem, since the charge transfer states cannot even approximately be considered orbitals of isolated ligands, as most likely no such *bound* orbitals exist at all. The problem thus becomes the finding of an excited state in a complicated molecular system. Consequently, we have been forced to make a number of simplifications.

The potential field of the O^{2-} immediately next to the paramagnetic ion is taken as that due to an effective charge $-0.88e$ placed at the centre of the oxygen ion. This is the total screened charge (according to Slater) at a distance 1.47 \AA from the centre. There will also be other attractive potentials from the ions surrounding the O^{2-} . The question is now: how can we make an electron stay near a repulsive field, when it can slide down to the neighbouring attractive centres? The artifice which provides the answer is shown in Figure 3. The rigid wall potentials at a distance of 2.1 \AA 'ensure' that the electron has a bound state centring on O^{2-} . At the same time the resulting wave-functions vanish at the wall, so that the excited states are at least nearly orthogonal to the more stable states. For simplicity the potential round O^{2-} has been taken as spherically symmetric. This is far from being true for hydrous complexes. On the other hand, this is a reasonable starting point for some oxides where O^{2-} is octahedrally surrounded (e.g. NiO). The optical absorption of many of these oxides are very similar to those of the corresponding hydrated salts.

The p -like wave function on the oxygen ion, pointing towards the paramagnetic ion, was deemed most effectual in promoting optical transitions. A variational calculation gave the form of this as

$$\frac{x}{r} \sin \pi \frac{x}{R_0} \exp \frac{3r}{8R_0},$$

with a radial density maximum at $r = 1.47\text{ \AA}$ from the centre of O^{2-} ($R_0 = 2.1\text{ \AA}$).

The form of the $3d$ wave-functions was fixed by assuming that all divalent ions have ionic radii 0.80 \AA and trivalent ions 0.66 \AA . There is actually some spread about these values [10]. The ligand potentials V_i were supposed to be

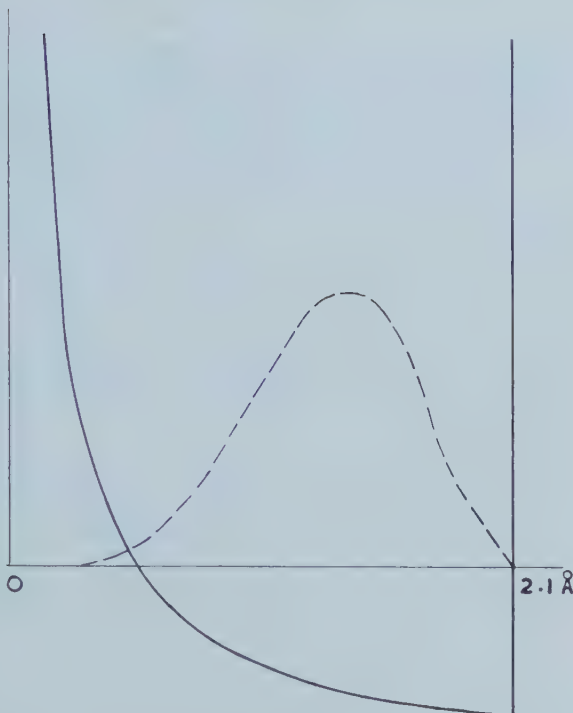


Figure 3. Potential *versus* radial distance from oxygen ion. Broken curve : Charge transfer radial density function.

those due to dipoles. The dipole moment (containing on top of the intrinsic dipole moment of water a considerable induced component) was taken as 4×10^{-18} e.s.u. in complexes of divalent ions [4] and 5.5×10^{-18} in trivalent ion complexes.

We have thus obtained :

$$\begin{aligned} Q^2 &= |\langle \alpha_x | y | \zeta \rangle|^2 \\ &= 0.02 R_0^2 \text{ for divalent ions} \\ &= 0.008 R_0^2 \text{ for trivalent ions;} \\ I^2 &= |\langle \alpha_x | (\partial/\partial x)(V_1 + V_4) | u \rangle|^2 \\ &= 1.66 \times 10^{-22} R_0^{-2} \text{ for divalent ions} \\ &= 0.5 \times 10^{-22} R_0^{-2} \text{ for trivalent ions.} \end{aligned}$$

It may be noted that the oscillator strength of a charge transfer transition ($u \rightarrow \infty$) is with these parameters found to be

$$\begin{aligned} &\sim 0.3 \text{ for divalent ions;} \\ &\sim 0.08 \text{ for trivalent ions.} \end{aligned}$$

There exists no experimental datum for comparison.

6. THE JAHN-TELLER EFFECT

We briefly indicate now, along the lines of Öpik and Pryce [9], Longuet-Higgins *et al.* [11], Moffitt and Liehr [12], how the electron configuration interaction affects the charge transfer wave functions. A familiarity with the first of these papers is desirable for this section.

The charge-transfer electronic wave functions have the representation in the cubic group: A_{1g} , E_g , T_{1u} . The wave functions with the with the totally symmetric (A_{1g}) and the two-fold (E_g) representations are even and do not concern us. Suffice it to say about them, that their degeneracy is lifted by the configuration-interaction of the even vibrational modes A_{1g} , E_g of the complex, accompanied by the distortion of the octahedron in these modes (see § 8 of Öpik and Pryce).

The three odd states (α_x , α_y , α_z) are affected by both the even and the odd type interaction Hamiltonian (§ 4 of Öpik and Pryce). The first will bring about a tetragonal distortion of the complex, the trigonal distortion being negligible since the different T_{1u} states hardly overlap. Finally, H_v the odd interaction Hamiltonian considered earlier will remove any remaining degeneracy. Once again we expect, by consideration of the overlap integrals, that the Q_{10} -type interaction will be most effective.

The summary of this discussion is that for an electronic α_z state the three ionic masses on the z -axis will be displaced in some way from their regular position. It need hardly be said, that in an electronic transition there is not enough time for this reorientation to take place; instead the Franck-Condon principle will be operative. It is however, necessary for us to take the displacement into account in the sum

$$\sum_{C\bar{n}} \frac{\langle A_2; n' | P | C; \bar{n} \rangle \langle C; \bar{n} | H_v | T_2; n \rangle}{E_{T_2} - E_{C; \bar{n}}}$$

since the configuration eigenfunctions, denoted by \bar{n} , of the charge-transfer states C will not be orthogonal to the eigenfunctions n or n' . However, the vibrational energies will be very small compared to $E_{Cn} - E_{T_2}$ so that to a good approximation we can sum over \bar{n} in the numerator. Because of the invariance of the trace, we are left with

$$\sum_C \frac{\langle A_2; n' | P | C; n' \rangle \langle C; n' | H_v | T_2; n \rangle}{E_{T_2} - E_C}$$

This is the expression which has been used earlier, in § 3, for the matrix element of the dipole moment. We have here justified its use, even when the Jahn-Teller effect of the charge transfer states is taken into account.

REFERENCES

- [1] ORGEL, L. E., 1955, *J. chem. Phys.*, **23**, 1004.
- [2] TANABE, T., and SUGANO, S., 1954, *J. phys. Soc., Japan*, **9**, 766; **11**, 864.
- [3] ENGLMAN, R., 1960, *Mol. Phys.*, **3**, 23.
- [4] KOIDE, S., and PRYCE, M. H. L., 1958, *Phil. Mag.*, **3**, 607.
- [5] KOIDE, S., 1959, *Phil. Mag.*, **4**, 243.
- [6] ENGLMAN, R., and PRYCE, M. H. L., 1958 (unpublished calculations).
- [7] HOLMES, O. Y., and MCCLURE, D. S., 1957, *J. chem. Phys.*, **26**, 1686.
- [8] ORGEL, L. E., 1954, *Quart. Rev.*, **8**, 423.
- [9] ÖPIK, U., and PRYCE, M. H. L., 1957, *Proc. roy. Soc. A*, **238**, 425.
- [10] HUSH, N. S., and PRYCE, M. H. L., 1957, *J. chem. Phys.*, **26**, 143.
- [11] LONGUET-HIGGINS, H. C., ÖPIK, U., PRYCE, M. H. L., and SACK, R. A., 1958, *Proc. roy. Soc. A*, **244**, 1.
- [12] MOFFITT, W., and LIEHR, A. D., 1957, *Phys. Rev.*, **106**, 1195.

Thermodynamic properties of clathrates:

II. The heat capacity and entropy of methane in the methane quinol clathrates

by N. G. PARSONAGE and L. A. K. STAVELEY
Inorganic Chemistry Laboratory, Oxford

(Received 13 May 1959)

Measurements have been made of the heat capacity C_p from ~ 13 to $\sim 298^\circ\text{K}$ of three clathrates of methane and β -quinol, in which 75.5, 45.7 and 16.5 per cent of the cavities were occupied by methane. Over the entire temperature range C_p is found to be a linear function of composition. The contribution made to the heat capacity by a mole of methane has been analysed with the aid of the theory of J. H. van der Waals, and the rotational contribution found to be $\frac{3}{2}R$, within experimental error, from about 150°K upwards, showing that rotation of the methane molecules is almost unrestricted.

The heats of formation of several methane clathrates have also been measured calorimetrically.

1. INTRODUCTION

The object of this work was to investigate the motion of methane molecules trapped in the cavities of the β -quinol clathrate. Since the methane molecule is small and highly symmetrical it might be expected that at higher temperatures, at least, it would undergo something approaching free three-dimensional rotation in the cavities. Whether this is so can in principle be found by an analysis of the contribution, C_{CH_4} , made by the methane to the total heat capacity of the clathrate. In the first paper of this series [1] we considered experimental heat capacity results for argon clathrates in the light of the theory of van der Waals [2]. On the basis of this work it is possible to make an estimate of the contribution to the molar heat capacity of methane in the clathrate from the translational degrees of freedom, and hence, by subtraction from C_{CH_4} , of the amount contributed by the rotational degrees of freedom. (At higher temperatures a small correction has to be made for the heat capacity contributed from the internal vibrations of the methane molecules.)

2. EXPERIMENTAL

In the experiments on the argon clathrates five samples were studied in all, since it was found that the total heat capacity C_p did not appear to be a linear function of x at all temperatures, where x is the number of moles of gas trapped in three moles of quinol and C_p refers to the quantity $3\text{C}_6\text{H}_4(\text{OH})_2 \cdot xA$. The position with regard to the methane clathrates is altogether simpler. Three samples were studied with $x = 0.755$, 0.457 and 0.165, and at all temperatures C_p was a linear function of x within experimental error.

The methane clathrates were prepared in the same way as the argon clathrates using cylinder methane of the highest available purity, and the same low-temperature calorimeter was used as before.

To estimate the contribution to C_p from the translational degrees of freedom of the methane molecules it is necessary to give values to two parameters associated with the interaction between the gas molecules and the quinol lattice. These values can be estimated using well-known approximate combination rules together with information about the intermolecular energies of pairs of gas molecules. A knowledge of the two parameters needed for the C_p analysis also makes it possible to calculate the heat of formation of the clathrate. Since this quantity for the methane system has not yet been determined, we have thought it worth while to measure it. This has been done using a differential calorimeter similar to that described by Evans and Richards [3], constructed by Mr. G. Saville.

M1. $3\text{C}_6\text{H}_4(\text{OH})_2 \cdot 0.755\text{CH}_4$ (0.05195 moles in the calorimeter)					
T ($^{\circ}\text{K}$)	C_p	T ($^{\circ}\text{K}$)	C_p	T ($^{\circ}\text{K}$)	C_p
14.24	3.00	90.74	39.53	176.42	64.72
16.81	4.82	95.94	41.07	182.82	66.76
19.92	7.18	101.11	42.40	189.25	68.72
23.36	9.73	106.10	43.82	196.43	70.99
27.52	12.79	111.22	45.36	204.33	73.48
32.01	15.86	116.20	46.74	212.02	75.94
36.96	18.88	121.31	48.23	219.72	78.37
42.57	22.16	126.54	49.75	227.95	81.07
48.53	25.02	131.63	51.19	235.96	83.78
54.56	28.04	136.61	52.67	245.43	86.90
60.93	30.52	142.79	54.52	254.11	89.80
66.60	32.25	148.25	56.14	262.57	92.61
71.44	33.66	153.81	57.84	270.82	95.36
76.02	35.34	159.26	59.55	279.23	98.20
81.39	36.79	164.81	61.13	287.79	101.27
86.16	38.34	170.46	62.95		
M2. $3\text{C}_6\text{H}_4(\text{OH})_2 \cdot 0.165\text{CH}_4$ (0.04539 moles in the calorimeter)					
T ($^{\circ}\text{K}$)	C_p	T ($^{\circ}\text{K}$)	C_p	T ($^{\circ}\text{K}$)	C_p
13.94	2.46	80.74	32.39	170.60	58.21
16.82	4.24	85.37	33.89	176.66	60.16
17.04	4.43	89.79	35.03	183.45	62.20
19.89	6.17	93.98	36.01	190.51	64.35
20.11	6.33	99.13	37.39	197.38	66.48
23.69	8.51	104.43	38.84	204.57	68.80
24.11	8.70	109.85	40.44	212.04	71.16
28.09	11.32	115.41	42.03	220.04	73.66
32.45	13.77	121.08	43.60	228.39	76.38
37.26	16.31	126.87	45.24	236.53	79.10
42.71	19.19	132.49	46.81	244.89	81.80
48.55	21.60	137.84	48.34	253.69	84.81
54.47	24.08	143.19	49.87	262.67	87.78
60.59	26.57	148.42	51.51	271.62	90.81
65.60	28.08	153.78	53.14	280.26	93.76
70.68	29.49	159.28	54.77	288.75	96.78
75.86	30.93	164.77	56.74	296.62	99.66

Table 1. Experimental values of the heat capacities of the samples of methane clathrate in cal deg^{-1} mole $^{-1}$.

M3. $3\text{C}_6\text{H}_4(\text{OH})_2 \cdot 0.457\text{CH}_4$ (0.04368 moles in the calorimeter)					
T ($^{\circ}\text{K}$)	C_p	T ($^{\circ}\text{K}$)	C_p	T ($^{\circ}\text{K}$)	C_p
15.08	3.11	91.43	37.53	177.75	62.53
17.39	4.82	96.25	38.83	183.96	64.50
20.01	6.58	101.29	40.20	191.36	66.83
23.47	9.02	106.46	41.56	198.61	68.89
27.64	11.95	111.78	43.08	205.73	71.49
32.07	14.74	117.22	44.63	214.15	74.23
36.89	17.66	122.50	46.15	221.47	76.49
42.31	20.49	127.92	47.65	229.08	79.05
48.10	22.98	133.46	49.26	236.98	82.02
54.11	25.69	139.18	50.84	245.25	84.54
61.20	28.73	144.45	52.42	253.85	87.67
66.11	30.13	149.85	54.19	262.34	90.45
71.11	31.58	155.38	55.98	271.05	93.23
76.22	33.02	160.80	57.48	280.47	96.45
81.42	34.47	166.34	59.04	289.27	99.40
86.73	36.26	171.99	61.00	297.83	102.39

Table 1. Experimental values of the heat capacities of the samples of methane clathrate in $\text{cal deg}^{-1} \text{mole}^{-1}$.

It is worth noting that in none of the low-temperature calorimetric experiments with the methane clathrates was there any indication of the decomposition to which the argon clathrates were susceptible. The considerable stability of the methane clathrates has been noted by Peyronel and Barbieri [4].

3. DISCUSSION

The precision of the C_p values, expressed as the root mean square percentage deviation from the smooth curve, is 0.17 per cent from 60 to 300°K and 0.32 per cent below 60°K . Within these limits C_p proved to be a linear function of x . From such plots made at regular temperature intervals using C_p values read from the smoothed C_p vs. T curves, the value of C_{CH_4}' , the molar heat capacity of methane in the clathrate, and C_p^Q , the heat capacity of three moles of pure β -quinol, were obtained. These are recorded in table 2.

C_{CH_4}' is plotted against temperature in figure 1. It is first necessary to estimate the contribution, C_{vib} , made to C_{CH_4}' by the vibrational motion of the molecule in the cell. To do this we have used the heat capacity expression given in our first paper on the argon clathrate and derived from the treatment of van der Waals. We have taken for the energy and distance parameters for methane the values of $\epsilon/k = 148.2^{\circ}$ and $\sigma = 3.817 \text{ \AA}$, respectively, quoted by Hirschfelder *et al.* [5]. The values for the corresponding parameters for the quinol lattice were those chosen by van der Waals [2]. The calculated values for C_{vib} are plotted in figure 1 (open circles). With the argon clathrates it was found that when the temperature was high enough for classical statistics to be applicable the experimental values of C_{vib} (called C_A in the previous paper) were less than the calculated values by about 8.6 per cent of the latter. We have therefore also plotted at higher temperatures values of C_{vib}' equal to the theoretical values of C_{vib} reduced by 8.6 per cent, which may perhaps give a more realistic estimate of the

T ($^{\circ}$ K)	C_{vib}	C_{CH_4}	$(C_p)_Q_{\text{CH}_4}$	$(C_p)_Q_A$
15		0.68	2.97	
20		1.72	5.88	5.85
25	5.8658	2.71	8.88	
30		3.51	11.87	11.22
35		4.12	14.59	
40		4.98	16.93	16.15
45	5.8008	5.49	19.19	
50		5.96	21.33	
55		6.28	23.34	
60		6.51	25.15	
65		6.55	26.84	
70	5.7285	6.62	28.31	
75		6.94	29.61	
80		7.06	31.02	
90		7.26	33.79	
100		7.41	36.55	
110		7.51	39.18	38.89
120	5.6079	7.57	42.02	41.75
130		7.75	44.79	44.61
140		7.89	47.64	47.49
150		7.99	50.59	50.39
160		7.88	53.68	53.55
170		7.80	56.78	56.55
180		7.84	59.80	59.45
190		7.97	62.85	62.60
200	5.4565	8.04	65.99	66.06
210		7.99	69.18	69.14
220		8.11	72.33	72.35
230		8.15	75.65	75.60
240		8.05	78.99	78.90
250		8.12	82.30	82.20
260		8.05	85.64	85.49
270		8.06	89.00	88.81
280		8.00	92.46	
290		7.99	95.97	
298.16	5.3206	7.85	98.90	
300		7.84	99.55	

Table 2. Analysis of the heat capacity results.

C_{vib} =the calculated contribution of the vibrational motion of the methane molecules in the holes (in cal deg^{-1} mole $^{-1}$)

C_{CH_4} =the experimental value of the contribution of the methane molecules to the total heat capacity (in cal deg^{-1} mole $^{-1}$)

$(C_p)_Q_{\text{CH}_4}$ =the heat capacity of three moles of β -quinol calculated from the methane experiments (in cal deg^{-1} per three moles quinol)

$(C_p)_Q_A$ =the heat capacity of three moles of β -quinol calculated from the argon experiments (in cal deg^{-1} per three moles quinol)

contribution to C_{CH_4} from the vibrational motion†. Clearly, in this respect, it is desirable to have more information about the rare gases and measurements on the krypton clathrate are at present in progress. Also plotted in figure 1 is the contribution C_{int} from the internal degrees of freedom of the methane molecule (full circles). The values of the quantity $C_{\text{rot}} (= C_{\text{CH}_4} - C_{\text{vib}'} - C_{\text{int}})$ are plotted as crosses and it will be seen that these are grouped closely around the dotted line representing a constant contribution of $\frac{3}{2}R$. There therefore seems no doubt that at least above 150°K the methane molecules virtually rotate freely in their cells.

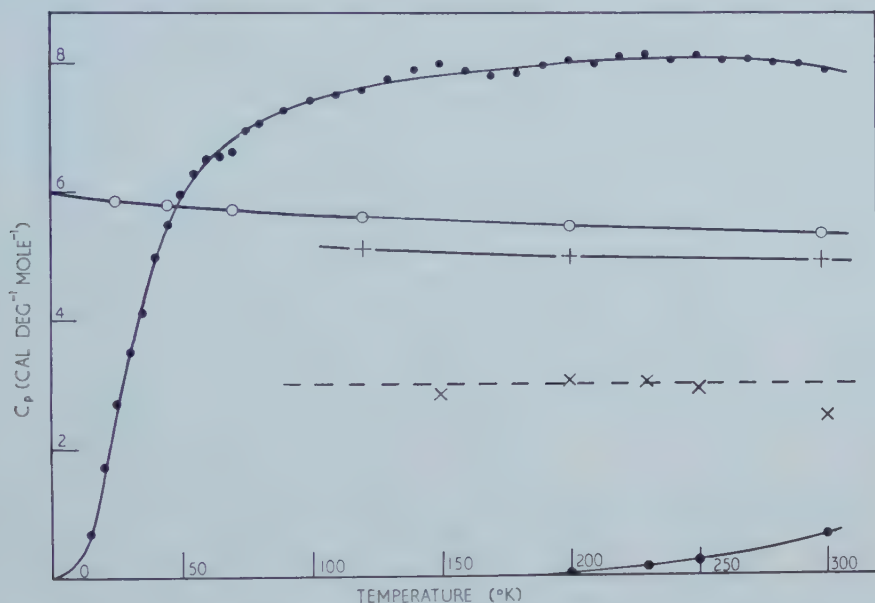


Figure 1. Graphical analysis of the heat capacity of methane in the quinol clathrate as a function of temperature. Full circles upper curve, C_{CH_4} , the total heat capacity per mole of methane. Open circles, values of C_{vib} calculated from van der Waals' theory. +, values of $C_{\text{vib}'}$, i.e. C_{vib} reduced by 8.6 per cent (see text). Full circles, bottom curve, C_{int} (the contribution from the intramolecular vibrations). \times , values of $C_{\text{rot}} (= C_{\text{CH}_4} - C_{\text{vib}'} - C_{\text{int}})$. The dotted line corresponds to $3/2R$.

C_{rot} cannot be accurately evaluated at lower temperatures because the complicated nature of the force field makes it impossible to calculate C_{vib} where the system departs from classical behaviour. Some indication of the course taken by C_{rot} at lower temperatures may be obtained as follows. The Lennard-Jones

† This reduction of C_{vib} by 8.6 per cent may seem rather arbitrary. However, Dr. J. H. van der Waals has kindly indicated to us an alternative and more satisfactory approach. The calculated values of C_{vib} depend upon the values chosen for $\bar{\epsilon}$ and $\bar{\sigma}$, and are very much more sensitive to the value of $\bar{\sigma}$ than to that of $\bar{\epsilon}$. C_{vib} for argon and methane was calculated using $\bar{\sigma}/2 = 1.65 \text{ \AA}$, the value originally adopted by van der Waals, but a re-examination of available data makes it seem likely that this value is too high (Platteeuw and van der Waals, *Advances in Chemical Physics*, 1959, 2). Dr. van der Waals has pointed out that a value of $\bar{\sigma}/2 = 1.50 \text{ \AA}$ gives better agreement between theory and experiment for C_{vib} for argon, and that if the same value of $\bar{\sigma}$ is then used for methane the calculated values of C_{vib} are then about 6.3 per cent less than those estimated using $\bar{\sigma}/2 = 1.65 \text{ \AA}$.

and Devonshire potential which governs the movement of the particle in the cell can be expanded in terms of even powers of the distance x of the particle from the centre of the cell. The dominant term at low temperatures is that in x^2 which corresponds to simple harmonic oscillation. The coefficient of x^2 is given by the expression

$$\frac{\Lambda^*}{a^2} \left\{ 22 \left(\frac{V^*}{V_0} \right)^4 - 10 \left(\frac{V^*}{V_0} \right)^2 \right\},$$

where the symbols are those used by van der Waals and in our previous paper (I). This coefficient can be evaluated using the same values of the energy and distance parameters needed to work out C_{vib} . Regarding the motion at low temperatures as three-dimensional simple harmonic motion, the vibration frequency can be evaluated and C_{vib} calculated. We have done this for argon, for which $\nu = 33.1 \text{ cm}^{-1}$, and the calculated and experimental values for $C_{vib} (= C_A)$ are compared from 0 to 60°K in figure 2. Naturally above this temperature the calculated values asymptotically approach $3R$, while the experimental values

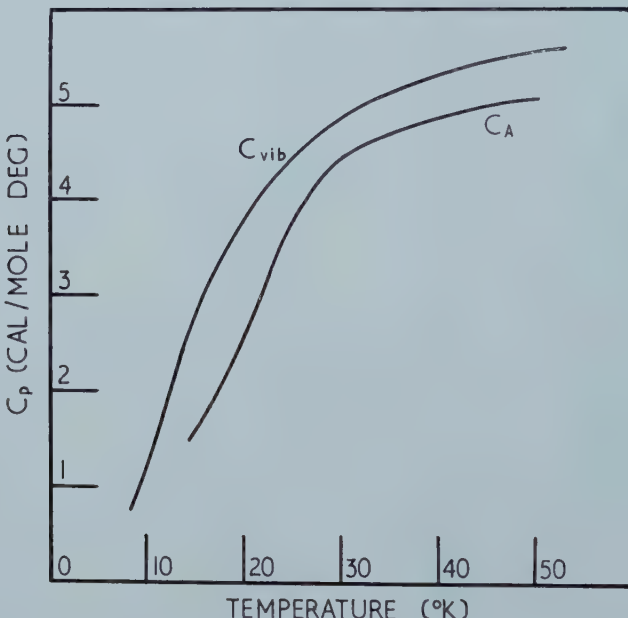


Figure 2. Comparison of the experimental values of C_A (the heat capacity of a mole of argon in the argon clathrate) with C_{vib} , the values of this quantity calculated for the simple harmonic oscillation approximation.

decrease at about the rate predicted by van der Waals. (For reasons given in our previous paper the experimental values for argon cannot be reliably assessed below 20°K.) The corresponding calculation for methane leads to the expected higher value of ν (96.2 cm^{-1}) and to values of C_{vib} which are plotted against temperature from 0 to 80°K in figure 3. The derived values of C_{rot} , i.e. the experimental values of C_{CH_4} less the calculated values of C_{vib} , are also shown in figure 3, together with the calculated curve for the rotational heat capacity of gaseous methane assuming equilibrium between the ortho, meta, and para forms [6].

It is interesting to note that below 20°K the observed contribution made by the methane molecules to the total heat capacity is due almost entirely to their rotational movement, showing again that the restriction on the freedom of rotation of the molecules must be relatively small.

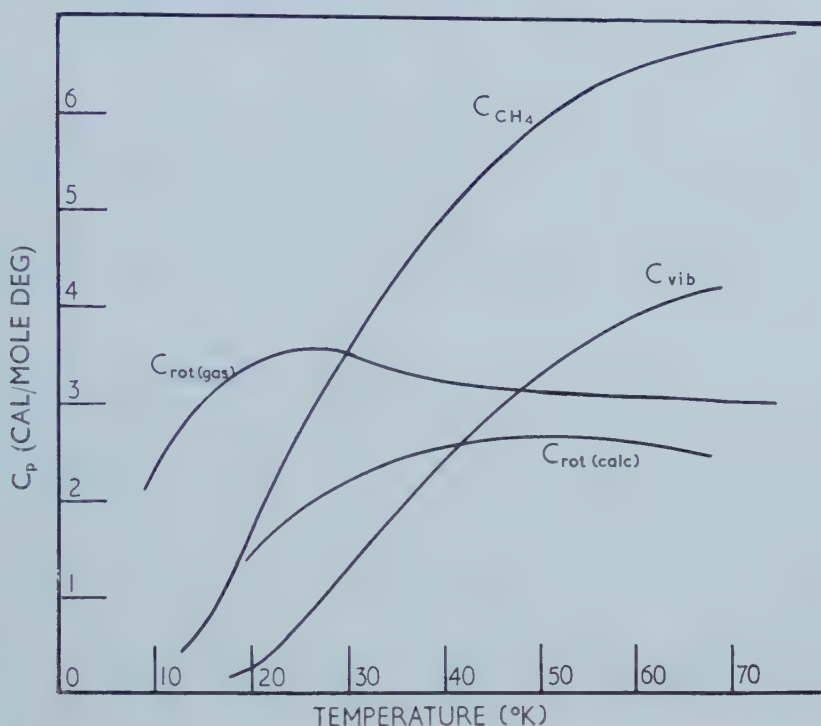


Figure 3. Graphical analysis of the heat capacity of methane at low temperatures.
 C_{CH_4} =measured heat capacity per mole of methane in the quinol clathrate.
 C_{vib} =the contribution from the vibrational movement of the molecules calculated from the simple harmonic oscillator approximation. $C_{rot(cal)}=C_{CH_4}-C_{vib}$.
 $C_{rot(gas)}$ =the calculated rotational contribution to the molar heat capacity of gaseous methane for an equilibrium mixture of the ortho, meta and para forms.

Since C_p was always a linear function of x , the fraction of holes filled, values of C_p^Q , the heat capacity of three moles of pure β -quinol, can be obtained by extrapolation to zero methane content. These values are given in table 2, where they are compared with those values of C_p^Q which could be similarly obtained from the work on the argon clathrates. Over most of the temperature range where comparison is possible agreement is satisfactory, but the differences of ~ 5 per cent at 30° and 40°K are well outside the limits of experimental error, and can only mean that the molecules in the cavities do to some extent interfere with the dynamics of the quinol lattice, presumably with the low-frequency deformation vibrations, which make a relatively large contribution to C_p^Q at low temperatures. The new values of C_p^Q lead to a value of $100.40\text{ cal deg}^{-1}$ for the entropy of 3 moles of pure β -quinol at 298.16°K, in fair agreement with the figure of 99.8 cal deg^{-1} from the argon measurements

When the heats of solution given in table 3 are plotted against x a straight line is obtained which on extrapolation to $x=0$ gives 0.36 kcals. as the heat content difference between three moles of α - and β -quinol, in good agreement with the

x	ΔH (kcal)	Mean ΔH (kcal)
0.165	-0.91	-0.86
	-0.92	
	-0.75	
0.527	-3.44	-3.38
	-3.29	
	-3.40	
0.907	-6.32	-6.23
	-6.13	
	-6.23	

Table 3. The heat content change in the formation of one mole of methane clathrate from α -quinol and gaseous methane at constant pressure.

mean value of 0.48 kcals found by Evans and Richards. From the slope of the line a value of 6.63 kcals is obtained for ΔU_m , the heat of formation of the clathrate per mole of methane at constant volume. This quantity can be calculated from the equations given by van der Waals. Using the parameters in the heat capacity calculations, the estimated value of ΔU_m is 6.04 kcals, in only moderate agreement with the experimental figure.

Finally, we will compare the experimental and theoretical values of the contribution made to the entropy of the clathrate by the non-configurational entropy of a mole of methane, S_{CH_4} . The contribution to S_{CH_4} from the quasi-translational motion of the molecules is estimated from van der Waals' equations to be 9.66 cal deg⁻¹ mole⁻¹, while the contributions from the internal vibrations and completely free rotation are 0.11 and 10.14, respectively. (In estimating the rotational entropy the moment of inertia was taken as 5.330×10^{-40} c.g.s. units.) The calculated value of S_{CH_4} is thus 19.91 cal deg⁻¹ mole⁻¹ as compared with the experimental figure of 17.42, derived from the C_{CH_4} figures of table 2. In the argon clathrates the calculated and experimental values were 14.61 and 12.80, respectively. Thus for both systems the calculated entropy is somewhat greater than the experimental value.

One of us (N. G. P.) thanks the British Oxygen Company for a Fellowship, and we are also indebted to this Company for constructing the high-pressure crystallization apparatus for us and for defraying the cost of the evaluation of the integrals. We are also grateful to Imperial Chemical Industries Ltd. for financial assistance.

REFERENCES

- [1] PARSONAGE, N. G., and STAVELEY, L. A. K., 1959, *Mol. Phys.*, **2**, 212.
- [2] VAN DER WAALS, J. H., 1956, *Trans. Faraday Soc.*, **52**, 184.
- [3] EVANS, D. F., and RICHARDS, R. E., 1954, *Proc. roy. Soc. A*, **223**, 238.
- [4] PEYRONEL, G., and BARBIERI, G., 1958, *Chemistry of the Coordinate Compounds* (a symposium) (London: Pergamon Press), p. 582.
- [5] HIRSCHFELDER, J. O., CURTISS, C. F., and BIRD, R. B., 1954, *Molecular Theory of Gases and Liquids* (New York: Wiley)
- [6] MACDOUGALL, D. P., 1931, *Phys. Rev.*, **38**, 2296.

The influence of paramagnetic molecules on singlet-triplet transitions

by G. J. HOIJTINK

Chemical Laboratory of the Free University, Amsterdam

(Received 5 June 1959)

It is shown that singlet-triplet transitions may obtain a finite probability when exchange interaction occurs between the absorbing molecule and a paramagnetic molecule.

According to this mechanism no quantitative relation exists between the transition dipole strength and the paramagnetic susceptibility of the perturbing molecule.

1. INTRODUCTION

Evans [1] has found that singlet-triplet absorptions of aromatic molecules are strongly induced by paramagnetic substances. According to this author the observed singlet-triplet transitions are very likely due to a spin-orbit perturbation in the aromatic molecule under the influence of the magnetic field of the paramagnetic molecule.

The present study gives an alternative explanation of this phenomenon based on exchange interaction between the singlet and paramagnetic molecules.

2. THEORETICAL

Let us consider a singlet molecule M , the ground and excited state configurations of which are described by anti-symmetrized products of one-electron functions (m.o.'s), say

$$\phi_l, l=a, b, c, \dots \quad (1)$$

In addition we consider a paramagnetic molecule P with the m.o.'s:

$$\phi_\lambda, \lambda=\alpha, \beta, \gamma, \dots \quad (2)$$

For a good understanding of the influence of paramagnetic molecules on singlet-triplet transitions the electronic states of the collision complex between the molecules M and P must be considered. In accordance with Evans' work the following restrictions can be made:

(a) The bonding between M and P is very weak. Investigations by Ketelaar and Dijkgraaf [2] on the benzene oxygen complex have shown the bonding energy to be slightly lower than kT at room temperature.

(b) Electronic transitions in the paramagnetic molecule P as well as charge transfer transitions in the complex MP give rise to absorption of light at shorter wavelengths than the singlet-triplet transitions in the molecule M .

2.1. Perturbation of singlet-triplet transitions by doublet molecules

Owing to the restriction (a) the doublet ground state of the complex MP can be satisfactorily described by an anti-symmetrized product of the m.o.'s (1) and (2) of the unperturbed systems†:

$$^2\Psi_N = |\phi_k \bar{\phi}_k \phi_\mu| \quad (3)$$

† Throughout this paper all m.o.'s which remain doubly occupied are omitted.

in which μ denotes the m.o. of the doublet molecule in which the odd electron is moving.

The lower excited states in the complex MP are due to the electron excitation, $k \rightarrow m$ say, which in the unperturbed molecule M gives rise to transitions from the ground state to the lowest singlet and triplet excited states. One finds two doublet excited states described by ($S_z = \frac{1}{2}$) [3]:

$$^2\Psi_1 = \frac{1}{\sqrt{6}} \{2|\phi_k \phi_m \bar{\phi}_\mu| - |\bar{\phi}_k \phi_m \phi_\mu| - |\phi_k \bar{\phi}_m \phi_\mu|\}, \quad (4)$$

$$^2\Psi_2 = \frac{1}{\sqrt{2}} \{|\bar{\phi}_k \phi_m \phi_\mu| - |\phi_k \bar{\phi}_m \phi_\mu|\}. \quad (5)$$

If one neglects the small energy terms due to the interaction between M and P the energies of the excited states with respect to the ground state and the corresponding dipole moments become:

$$E_1 \approx E_T; \quad M_{N,1} = 0; \quad (6)$$

$$E_2 \approx E_S; \quad M_{N,2} = M_{S \rightarrow S} \quad (7)$$

where E_S and E_T stand for the singlet-singlet and singlet-triplet transition energies of the unperturbed molecule M and $M_{S \rightarrow S}$ denotes the singlet-singlet transition dipole moment.

So far the spectral behaviour of the complex MP does not differ from that of the molecule M . However, when electron exchange between M and P takes place, the matrix element for the interaction between the two doublet excited states (4) and (5):

$$H_{1,2} = \frac{1}{2} \sqrt{3} \{K_{m\mu} - K_{k\mu}\} \quad (8)$$

where

$$K_{k\mu} = \int \int \phi_k(1) \phi_\mu(1) \frac{e^2}{r_{12}} \phi_k(2) \phi_\mu(2) d\tau_1 d\tau_2 \quad (9)$$

does not vanish, unless accidentally the two exchange integrals are equal.

According to the Franck-Condon principle the nuclear framework of the molecule M in the excited states will be practically the same as in the ground state (vertical excited states). We assume that restriction (a) also holds good for the excited states (4) and (5), so that the matrix element (8) will be small in comparison with the singlet-triplet separation of M . Under this condition first-order perturbation theory leads to a finite dipole moment for the transition from the ground state to the lower doublet excited state:

$$M_{N,1}' = \frac{H_{1,2}}{E_S - E_T} M_{S \rightarrow S}. \quad (10)$$

The energy and dipole strength for the lowest singlet-triplet transition in the molecule M under the influence of a doublet molecule P thus become:

$$E_1' \approx E_T, \\ D_{N,1}' = \frac{M_{N,1}'}{e^2} = D_{S \rightarrow T} = \frac{3}{4} \left[\frac{K_{m\mu} - K_{k\mu}}{E_S - E_T} \right]^2 D_{S \rightarrow S}. \quad (11)$$

2.2. Perturbation by a triplet molecule

For triplet molecules the treatment is closely similar to the foregoing one. When the m.o.'s of the triplet molecule P are again denoted by Greek indices

the triplet ground and lower excited states of the collision complex may approximately be described by ($S_z=1$):

$${}^3\Psi_N = |\phi_k \bar{\phi}_k \phi_\mu \phi_\nu|, \quad (12)$$

$${}^3\Psi_1 = \frac{1}{2} \{ |\bar{\phi}_k \phi_m \phi_\mu \phi_\nu| + |\phi_k \bar{\phi}_m \phi_\mu \phi_\nu| - |\phi_k \phi_m \bar{\phi}_\mu \phi_\nu| - |\phi_k \phi_m \phi_\mu \bar{\phi}_\nu| \}, \quad (13)$$

$${}^3\Psi_2 = \frac{1}{\sqrt{2}} \{ |\bar{\phi}_k \phi_m \phi_\mu \phi_\nu| - |\phi_k \bar{\phi}_m \phi_\mu \phi_\nu| \}, \quad (14)$$

$${}^3\Psi_3 = \frac{1}{\sqrt{2}} \{ |\phi_k \phi_m \bar{\phi}_\mu \phi_\nu| - |\phi_k \phi_m \phi_\mu \bar{\phi}_\nu| \}. \quad (15)$$

The transition energies and dipole moments become:

$$E_1 \approx E_T; \quad M_{N,1} = 0; \quad (16)$$

$$E_2 \approx E_S; \quad M_{N,2} = M_{S \rightarrow S}; \quad (17)$$

$$E_3 \approx E_T + 2K_{\mu\nu}; \quad M_{N,3} = 0. \quad (18)$$

Exchange interaction between the molecules M and P gives rise to a non-vanishing matrix element for the interaction between the excited states (13) and (14):

$$H_{1,2} = \frac{1}{\sqrt{2}} \{ K_{m\mu} + K_{m\nu} - K_{k\mu} - K_{k\nu} \}. \quad (19)$$

As a consequence the transition from the ground state to the lowest excited state becomes allowed.

Since the energy of this transition is practically equal to the singlet-triplet transition energy of the molecule M one may say that singlet-triplet transitions obtain a finite probability when the molecule undergoes a weak interaction with the paramagnetic molecule. The dipole-strength following from first-order perturbation theory is given by:

$$D_{N,1}' = D_{S \rightarrow T} = \frac{1}{2} \left[\frac{K_{m\mu} + K_{m\nu} - K_{k\mu} - K_{k\nu}}{E_S - E_T} \right]^2 D_{S \rightarrow S}. \quad (20)$$

Though the foregoing treatment has been restricted to doublet and triplet molecules similar results are found for paramagnetic molecules of higher multiplicity.

3. DISCUSSION

The results of the present considerations as summarized in the formulae (11) and (20) make it clear that singlet-triplet transitions become allowed when the absorbing molecule undergoes a weak exchange interaction with a paramagnetic molecule.

By analogy with Mulliken's discussion of charge transfer complexes [4] one may expect that electron exchange will be stronger between the m.o.'s m and μ than between k and μ , since 'higher' m.o.'s possess more anti-bonding character than 'lower' ones and therefore will give more overlap with orbitals of the complex partner. In view of this it seems reasonable to suppose that the difference $K_{m\mu} - K_{k\mu}$ is of the order of magnitude of $K_{m\mu}$ and the same will hold true, *mutatis mutandis*, for the difference $K_{m\nu} - K_{k\nu}$.

For weak complexes, such as the benzene-oxygen complexes, the equilibrium distance between the two partners will be determined by their van der Waals radii. At such a distance a value of 0.01 ev for the exchange integrals $K_{m\mu}$ and

$K_{m\mu}$ seems not unreasonable, so that the dipole strength for the singlet-triplet transition, for a singlet-triplet separation of about 1 ev, would become:

$$D_{S \rightarrow T}/D_{S \rightarrow S} \approx 10^{-4} \text{ to } 10^{-5}.$$

In comparison with this exchange perturbation the direct influence of the magnetic moment of the paramagnetic molecule on the dipole strength of singlet-triplet transitions will be of minor significance. One can hardly believe that the magnetic moment induced in the molecule M by a neighbouring paramagnetic molecule would be strong enough to cause a sufficient breakdown of the spin selection rule. In this connection Evans' remark that "the perturbing effect of oxygen seems to be greater than one would expect from its magnetic moment" provides an argument in favour of the exchange mechanism, since according to the present considerations no quantitative relation exists between the magnetic moment of the paramagnetic molecule and the dipole strength of singlet-triplet transitions.

Indirectly the present view is supported by recent work of Porter and Wright [5] on the deactivation of triplet states by paramagnetic molecules. This subject will be discussed more in detail in a separate paper.

Note added in proof†.—It is very likely that the experiments by Kasha [6] on the singlet-triplet transitions of α -chloro-naphthalene in ethyl iodide can also be explained by the present mechanism, since one may expect the heavy iodine atom in methyl iodide to cause a strong spin-orbit coupling.

In that case the ground state of the perturbing molecule may formally be described as a superposition of the lowest singlet configuration and excited triplet configurations. The dipole strength (20) for the singlet-triplet transition in the perturbed molecule should then be multiplied by a factor accounting for the triplet fraction of the ground state of the perturbing molecule.

REFERENCES

- [1] EVANS, D. F., 1956, *Nature, Lond.*, **178**, 534; 1957, *J. chem. Soc.*, 1351, 3885.
- [2] KETELAAR, J. A. A., and DIJKGRAAF, C., work in progress.
- [3] SCHIFF, L. I., 1955, *Quantum Mechanics* (New York: McGraw-Hill), p. 235.
- [4] MULLIKEN, R. S., 1956, *Rec. Trav. chim. Pays-Bas*, **75**, 845.
- [5] PORTER, G., and WRIGHT, M. R., 1959, *Disc. Faraday Soc.*, **27**.
- [6] KASHA, M., 1952, *J. chem. Phys.*, **20**, 71; see also McGLYNN, S. P., 1958, *Chem. Revs.*, **58**, 1113.

† The author thanks Mr. Dieleman, who kindly drew his attention to this phenomenon.

The fluorescence and excitation spectra of anthracene vapour at low pressures

by B. STEVENS and E. HUTTON

Department of Chemistry, The University, Sheffield, 10

(Received 14 August 1959)

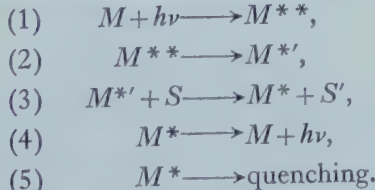
The dependence of fluorescence intensity on the wavelength of exciting radiation has been recorded for anthracene vapour at 0.09 mm and 170°C over the range 230–366 m μ . It is shown that whereas the photon cascade theory cannot account for the much higher intensity excited in the 250 m μ band than excited in the band at 363 m μ , this behaviour is precisely that expected if the fluorescent state is populated by internal conversion following excitation in the short-wave band.

Since the excited molecules are collisionally unperturbed under these conditions, the fluorescence spectrum exhibits a marked dependence on the wavelength of exciting radiation; an increase in the energy of the absorbed quantum produces an appreciable red-shift and loss of vibrational structure.

1. INTRODUCTION

Weber and Teale [1] have recently shown how a comparison of absorption and fluorescence excitation spectra may be used to detect small variations in the quantum yield q of fluorescent solutions with exciting wavelength λ . If however the excitation spectrum involves a transition to a higher electronic state than that responsible for the observed emission, the validity of such a comparison will depend on the mechanism of the ‘cascade’ process whereby the electronic state M^{**} initially excited is transferred to the lowest excited singlet state M^* .

It is generally accepted that the cascade mechanism involves an extremely efficient internal conversion represented by process (2) of the following scheme:



The product M^* of internal conversion is a vibrationally excited molecule in the fluorescent state which loses its excess vibrational energy on collision with a solvent molecule S . If $I(\lambda)$ is the intensity of the incident beam of wavelength $\lambda = c/\nu$ and $A(\lambda)$ is the fraction of incident radiation absorbed by the fluorescent solute, this simple scheme leads to the expression for the measured intensity of fluorescence $F(\lambda)$ used by Weber and Teale, i.e.

$$F(\lambda) = \mathbf{k} q(\lambda) I(\lambda) A(\lambda)$$

where \mathbf{k} is an instrumental constant independent of λ in so far as the fluorescence spectrum is independent of λ , and the quantum yield of fluorescence

$$q(\lambda) = k_4 / (k_4 + k_5).$$

If the maximum of the long-wave absorption band lies at $\bar{\lambda}$ then

$$F(\bar{\lambda}) = \mathbf{k}q(\bar{\lambda})I(\bar{\lambda})A(\bar{\lambda})$$

whence if q is independent of λ

$$\frac{F(\lambda)/I(\lambda)}{F(\bar{\lambda})/I(\bar{\lambda})} = \frac{A(\lambda)}{A(\bar{\lambda})},$$

i.e. after correction for the variation of incident intensity with wavelength, the measured fluorescence intensity is proportional only to the fraction of light absorbed, and absorption and excitation spectra coincide regardless of the electronic state initially excited.

In 1954 however, Birks [2] proposed the 'photon cascade' theory as an alternative in which a very fast primary emission from the initially excited higher electronic state M^{**} undergoes successive reabsorption and re-emission to populate a series of lower energy levels culminating in the fluorescent state M^* from which emission of frequency ν_0 is observed. This theory requires that the molecular fluorescence spectrum extends down to the ionization limit but is completely reabsorbed in the region of the absorption spectrum; some support for this model was adduced from the increased intensity of the short-wave fluorescence band as the optical density of the medium in this region is decreased [3, 4, 5] and the objection that the escape of the primary emission has not yet been observed is not serious provided its reabsorption cross section is high. However, according to this mechanism the rate at which the fluorescent state is populated is controlled by the fractional absorption coefficient $A(\bar{\lambda})$ in the long-wave absorption band at $\bar{\lambda}$, thus excitation in the short-wave band at λ cannot produce a more intense fluorescence than that following direct excitation in the long-wave band even though $A(\lambda)$ may be an order of magnitude greater than $A(\bar{\lambda})$.

Although several successive emissions and re absorptions are postulated [2], the photon cascade mechanism may be schematically written

- (1) $M + h\nu \longrightarrow M^{**},$
- (6) $M^{**} \longrightarrow M + h\bar{\nu},$
- (7) $M + h\bar{\nu} \longrightarrow M^*,$
- (4) $M^* \longrightarrow M + h\nu_0,$
- (5) $M^* \longrightarrow \text{quenching},$

where for the sake of simplicity, processes (6) and (7) illustrate the emission and reabsorption of a quantum of wavelength $\bar{\lambda} = c/\bar{\nu}$ coincident with the absorption maximum of the long-wave band. Under photo-stationary conditions the intensity of fluorescence $F(\lambda)$ intercepted by the detector is given by

$$F(\lambda) = \mathbf{k}k_4[M^*]$$

where

$$[M^*] \leq I(\bar{\lambda})A(\bar{\lambda})/(k_4 + k_5)$$

and

$$I(\bar{\lambda}) = k_6[M^{**}] = I(\lambda)A(\lambda).$$

Thus

$$F(\lambda) \leq k q(\lambda) I(\lambda) A(\lambda) A(\bar{\lambda})$$

and

$$\frac{F(\lambda)/I(\lambda)}{F(\bar{\lambda})/I(\bar{\lambda})} \leq A(\lambda) \leq 1$$

if q is again independent of λ ; i.e.

$$F(\lambda)/I(\lambda) \leq F(\bar{\lambda})/I(\bar{\lambda})$$

despite the fact that $A(\lambda)$ may be very much greater than $A(\bar{\lambda})$.

It should therefore be possible to discriminate between these two mechanisms of the cascade process from an examination of the excitation spectrum of a fluorescent molecule which has

- (i) a short-wave absorption band of greater intensity than the long-wave band, i.e. $A(\lambda) > A(\bar{\lambda})$;
- (ii) a constant quantum yield of fluorescence over both bands.

The coincidence of excitation and absorption spectra of 1-dimethylamino-naphthalene 5-(N-benzyl) sulphonamide, of chlorophylls **a** and **b**, and of pheophytin **a** in solution over the more intense short-wave absorption bands [1] provides strong support for the internal conversion mechanism since it is unlikely that q increases in the short-wave band. However since the variation of q with λ was not determined directly it was decided to investigate the excitation spectrum of anthracene vapour at very low pressures since this molecule satisfies conditions (i) and (ii) above and in addition;

- (iii) the quantum yield of fluorescence excited by absorption in the long-wave band is close to unity [6] and therefore cannot be exceeded at shorter wavelengths;
- (iv) the excited molecule is not collisionally perturbed and second-order processes involving it may be neglected.

Since however it is precisely under these conditions that a dependence of the emission spectrum on exciting wavelength may be expected, it is necessary to investigate this dependence in order to estimate the change in instrumental constant k with λ .

2. EXPERIMENTAL

The apparatus used to record the variation of fluorescence intensity with wavelength has been described by Weber and Teale [1]. The box containing the cuvette was replaced by an evacuated electrically-heated cylindrical quartz cell containing anthracene vapour at a pressure controlled as previously described [6]. To obtain a measurable fluorescence intensity at the low anthracene pressures used it was necessary to use a xenon arc source (Neron spectralamp) and a monochromator slit width of 0.6 mm which provided an effective band-width of 20 Å. A sodium nitrite filter was placed between the cell and the EMI 6255 photomultiplier to remove scattered exciting radiation.

Fluorescence spectra were photographed on a small Hilger quartz spectrograph using the same quartz cell and furnace; the wavelengths of exciting radiation used were

254 m μ isolated from a low pressure Hg vapour lamp by 2 cm of Bowen's filter solution *L* [7];

$313\text{ m}\mu$ isolated from a 125 w high pressure Hg vapour lamp by a Barr and Stroud interference filter together with 2 cm of solution L ;

$366\text{ m}\mu$ isolated from the high-pressure Hg vapour lamp by a Chance OX1 filter.

The fluorescence spectra and intensity measurements were recorded along a direction at right angles to the exciting beam.

3. RESULTS

Figure 1 shows the recorded intensity $F(\lambda)$ of anthracene vapour fluorescence as a function of λ at various temperatures and pressures; the traces are not corrected for the variation in source intensity $I(\lambda)$ with λ . At the highest pressure (0.29 mm) the $250\text{ m}\mu$ excitation band is weak (figure 1a) due to the almost complete absorption at the front surface of the cell which is shielded from the detector by the furnace. However at 0.09 mm (figure 1b) the $250\text{ m}\mu$ band is enhanced relative to the $366\text{ m}\mu$ band and the relative intensities are not changed further when the pressure is reduced to 0.05 mm (figure 1c). Unfortunately at these low pressures the amount of scattered light transmitted by the sodium nitrite filter is considerable, especially in the long-wave region where the incident radiation is most intense.

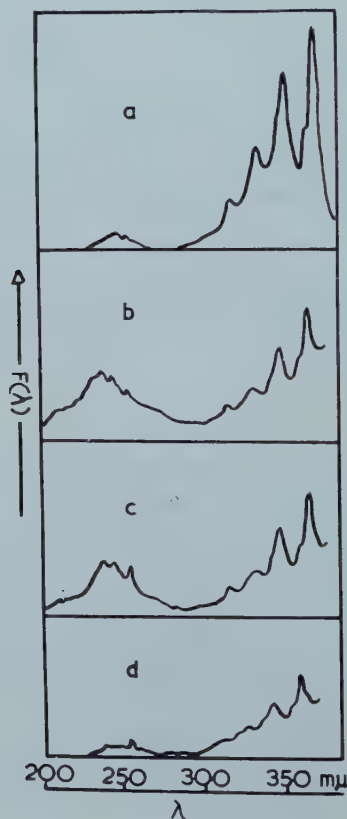


Figure 1. Recorded variation of fluorescence intensity $F(\lambda)$ with incident wavelength λ , (a) at 0.29 mm and 170°C ; (b) at 0.09 mm and 170°C ; (c) at 0.05 mm and 170°C ; (d) at 0.10 mm and 300°C .

At 300°C (figure 1*d*) the short-wave excitation band is greatly reduced in intensity; this is almost certainly due to the predominance of an energy-dependent process which competes with fluorescence emission at this temperature and wavelength, and provides a strong indication that the detected emission excited in this region is not due to the quartz cell.

Micro-densitometer tracings of anthracene vapour fluorescence spectra excited by the Hg lines at 254, 313 and 366 m μ at 0.29 mm and 170°C are shown in figure 2. No emission was observed from the quartz cell alone when excited by the 254 m μ line under the same conditions. At this pressure the excited

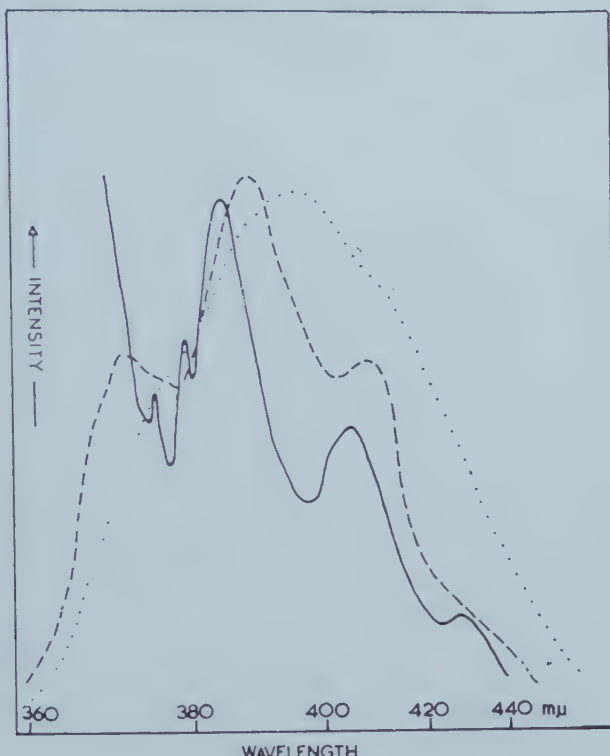


Figure 2. Fluorescence spectra of anthracene vapour at 0.29 mm and 170°C excited by 366 m μ (—), 313 m μ (---) and 254 m μ (.....).

molecules do not collide and a slight red-shift and loss of vibrational structure accompany an increase in the energy of the absorbed quantum. It is estimated that the nitrite filter transmits 49 per cent of the fluorescence spectrum excited by the 254 m μ line and 29 per cent of that excited by the 366 m μ line, thus

$$\mathbf{k(254\text{ m}\mu)/k(366\text{ m}\mu) \sim 1.7.}$$

4. DISCUSSION

An inspection of figure 1*b* and 1*c* shows that at 0.09 mm and 170°C the wavelength dependence of $F(\lambda)$ is independent of pressure, hence the distribution of fluorescence intensity along the exciting beam may be assumed to be independent of λ . The experimental curve shown in figure 1*b* is corrected for

the intensity $I(\lambda)$ of incident radiation in figure 3 in which the quotient $F(\lambda)/I(\lambda)$ as a function of λ drawn as a dotted curve would represent the true excitation spectrum if \mathbf{k} were independent of λ . Since however \mathbf{k} varies considerably with λ a correction for this variation should be made to obtain the true excitation spectrum; this would require a detailed investigation of the wavelength dependence of the emission spectrum since there is no reason to believe that

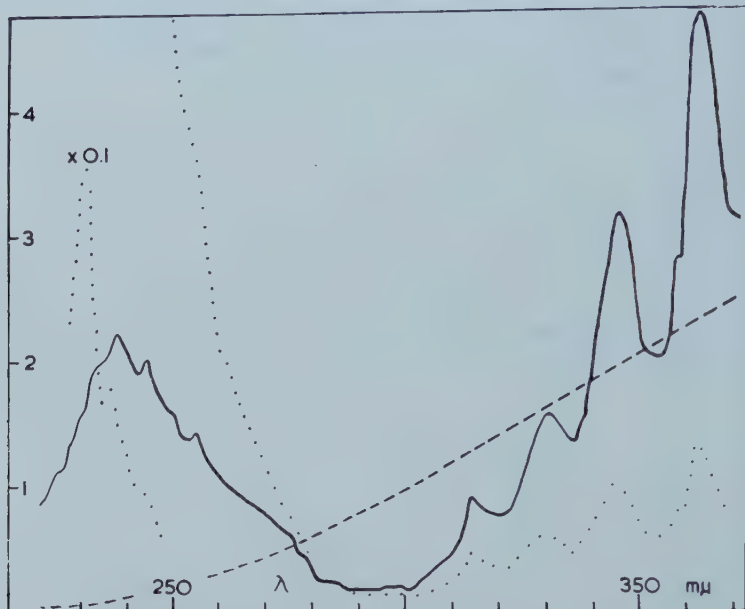


Figure 3. Variation of $F(\lambda)$ (—), $I(\lambda)$ (---) and $F(\lambda)/I(\lambda)$ (.....) with incident wavelength λ . $F(\lambda)$ is that of figure 1 b.

this is a linear function of λ . It would be experimentally more expedient to record the variation in $F(\lambda)$ with λ in the presence of an inert gas which would be expected to remove the excess vibrational energy of the excited molecules and produce a constant emission spectrum.

From figure 3 it is seen that for

$$\lambda = 250 \text{ m}\mu \text{ band maximum,}$$

$$\bar{\lambda} = 363 \text{ m}\mu \text{ band maximum,}$$

$$\frac{F(\lambda)/I(\lambda)}{F(\bar{\lambda})/I(\bar{\lambda})} \sim 28 = \frac{\mathbf{k}(\lambda)q(\lambda)}{\mathbf{k}(\bar{\lambda})q(\bar{\lambda})} \phi A(\lambda)$$

where

$$\phi A(\lambda) = A(\lambda)/A(\bar{\lambda}) \text{ for internal conversion,}$$

$$\leq A(\lambda) \leq 1 \text{ for photon cascade.}$$

$$\text{Since [6]} q(\bar{\lambda}) = 1.0 \pm 0.2,$$

$$q(\lambda)/q(\bar{\lambda}) \leq 1.25;$$

$$\text{whence with } \mathbf{k}(\lambda)/\mathbf{k}(\bar{\lambda}) \sim 1.7,$$

$$\phi A(\lambda) \geq 28/(1.7 \times 1.25) = 13;$$

i.e. the photon cascade mechanism is clearly not operative in this case since it cannot accommodate a value of $\phi A(\lambda)$ greater than unity. Moreover, even at the very low anthracene concentrations used (*c.* 10^{-6} M) the escape of primary emission excited by the $254\text{ m}\mu$ line was not observed.

Since scattered light contributes some 50 per cent of the total signal recorded at $363\text{ m}\mu$ (figure 1*b*), use of a corrected value of $F(\bar{\lambda})$ would approximately double the experimental value of $\phi A(\lambda)$. This would then be in good agreement with the value expected for internal conversion since under the prevailing conditions

$$A(\lambda)/A(\bar{\lambda}) \sim \epsilon(\lambda)/\epsilon(\bar{\lambda}) \sim 25$$

taking values of ϵ from solution data [8].

At a pressure of 0.09 mm the average time between collisions of anthracene molecules with a diameter of 8.0 \AA in the ground state is *c.* 10^{-7} sec . whereas the mean lifetime of the excited molecules is $c. 3.0 \times 10^{-9}\text{ sec}$ [6, 9]. Thus unless the collision diameter for the process



is of the order of 40 \AA , the collision-induced internal conversion process (8) may be considered as extremely unlikely. The dependence of the fluorescence spectrum on exciting wavelength at even higher pressures (0.29 mm) indicates the absence of collisional perturbation of the excited molecules under these conditions.

No infra-red emission in the region of $8\text{--}900\text{ m}\mu$ was observed from anthracene vapour or crystal [10] excited by the Hg $254\text{ m}\mu$ line. It is therefore unlikely that the radiative internal conversion process (9)



takes place since the emitted quantum would be expected to lie in this region.

It is concluded that in anthracene vapour at low pressures, the second excited singlet state is transferred to the first excited singlet (fluorescent) state by the first-order radiationless process (2), referred to as internal conversion [11]. That this process is extremely fast and efficient is apparent from the identity of O_2 quenching constants measured at $265\text{ m}\mu$ and $366\text{ m}\mu$ within an experimental error of 5 per cent [9] which places an upper limit of $1.2 \times 10^{-10}\text{ sec}$ on the lifetime of the second excited singlet state. The actual lifetime is probably shorter than this by a factor of 10^2 since internal conversion competes effectively with re-emission of the absorbed quantum which would be expected to take place in approximately 10^{-11} sec [2].

In so far as any cascade mechanism must be valid for vapours at low pressures where the photophysical properties are virtually those of isolated molecules, the introduction of environmental processes to account for this phenomenon in condensed phases is unwarranted and, in view of the high efficiency of internal conversion, unnecessary.

The authors are deeply indebted to Dr. Gregorio Weber for placing his apparatus at their disposal and for his assistance in making the intensity recordings; they also express their thanks to The Royal Society for a research grant, to the Department of Safety in Mines for the loan of the spectrograph, and to the Department of Scientific and Industrial Research for a maintenance grant to E. H. Department of Scientific and Industrial Research for a maintenance grant to E. H.

REFERENCES

- [1] WEBER, G., and TEALE, F. W. J., 1958, *Trans. Faraday Soc.*, **54**, 640.
- [2] BIRKS, J. B., 1954, *Phys. Rev.*, **94**, 1567.
- [3] BIRKS, J. B., 1953, *Scintillation Counters* (London: Pergamon Press Ltd.).
- [4] BIRKS, J. B., and WRIGHT, G. T., 1954, *Proc. phys. Soc. Lond. B*, **67**, 657.
- [5] BIRKS, J. B., and CAMERON, A. J. W., 1959, *Proc. roy. Soc. A*, **249**, 297.
- [6] STEVENS, B., 1955, *Trans. Faraday Soc.*, **51**, 610.
- [7] BOWEN, E. J., 1946, *The Chemical Aspects of Light* (Oxford: University Press), Appendix II.
- [8] FRIEDEL, R. A., and ORCHIN, M., 1951, *Ultra-violet Spectra of Aromatic Compounds* (New York: John Wiley and Sons).
- [9] STEVENS, B., 1959, *Disc. Faraday Soc.* (in the press).
- [10] STEVENS, B., and HARDWICK, E. R. (unpublished investigation).
- [11] KASHA, M., 1950, *Disc. Faraday Soc.*, **9**, 14.

Some investigations in the theory of open-shell ions

Part I. The spin-Hamiltonian

by J. S. GRIFFITH

Department of Theoretical Chemistry, University Chemical Laboratory,
Lensfield Road, Cambridge

(Received 11 September 1959)

It is shown that second-order perturbation theory leads to the usual quadratic and bilinear terms in the spin-Hamiltonian for a spatially non-degenerate state even when excited states differing in multiplicity from the ground states are included. The form of the spin-Hamiltonian adequate to represent arbitrary splittings of the ground manifold is considered and explicit results given for the fine structure and for those interactions with nucleus and external magnetic field which are linear in \mathbf{I} and \mathbf{H} respectively.

I. INTRODUCTION

The spin-Hamiltonian is by now a very well-known device, introduced originally in a particular form by Pryce [1]. The idea is to take an n -dimensional manifold of states, usually eigenstates of an approximate Hamiltonian, and regard it as the eigenmanifold for \mathbf{S}^2 with $S = \frac{1}{2}(n-1)$ of a spin vector \mathbf{S} . The states are usually classified by writing a basis of the manifold as $|M\rangle$, where M is the S_z value of \mathbf{S} and the $|M\rangle$ are correctly connected in phase [2]. Then the matrix elements of parts \mathcal{H}_j of the true Hamiltonian are represented by operator equivalents, polynomial in the components of \mathbf{S} , which have the same matrix elements as the \mathcal{H}_j within the manifold. The coefficients in the polynomials involve quantities like the components of the external magnetic field \mathbf{H} or even of the nuclear spin \mathbf{I} . In the latter case we consider the direct product of the n -dimensional manifold for the electronic functions with a $(2I+1)$ -dimensional manifold for the ground level of the nucleus and then \mathbf{I} may be regarded as just a number within the electronic manifold.

We should be clear at once that in the general formulation of the concept there is no implication about the behaviour of \mathbf{S} or the $|M\rangle$ under rotations. \mathbf{S} should be regarded as something like the isotopic spin τ which does not operate in ordinary space. For this reason it is often called a fictitious spin vector. However, there is a real danger of confusion here because \mathbf{S} is often very closely related to the real spin vector. Unlike isotopic spin space, in practice fictitious spin space is usually chosen to approximate as closely as possible to real spin space.

There are two main approaches to the theoretical determination of a spin-Hamiltonian. The first uses an 'unperturbed' Hamiltonian which is diagonal within the ground manifold, calculates the actual splittings to a certain order in perturbation theory and finally represents these calculated splittings

by means of operator equivalents [1, 3]. The second is to express a general splitting of the ground manifold as a power series in external quantities such as the components of \mathbf{H} and \mathbf{I} and to determine operator equivalents for the coefficients in the power series which are adequate to represent any splitting [3-6]. Naturally the two approaches are complementary and an investigation of any particular problem usually uses both kinds of approach.

Pryce [1] took a spin-independent unperturbed Hamiltonian and calculated the form of spin-Hamiltonian with fictitious spin S for a spatially non-degenerate state with actual spin S by second-order perturbation theory. However, he assumed that the ground and excited manifolds in his calculation were each contained in the ground term of the free ion. Especially he neglected matrix elements to excited states differing in multiplicity from the ground states. It is the main purpose of this paper to rectify that neglect and to show that the general form

$$\mathcal{H}(S) = \sum (\beta g_{ij} H_i S_j + D_{ij} S_i S_j + A_{ij} S_i I_j) \quad (1)$$

that he obtained for the spin-Hamiltonian remains unchanged. The modification of his proof for the first-order terms is, of course, quite trivial. Therefore I merely consider that part of the calculation which is second-order in the spin-orbit coupling \mathcal{H}_1 or first-order in both \mathcal{H}_1 and either a nuclear moment or the external magnetic field. I use the methods introduced by Racah [7] into the theory of angular momenta because I think they give the required new results in the simplest and most straightforward way. I then show that my results are equivalent to Pryce's when we add his restrictive assumptions, although of course the method of this paper is rather a roundabout one in that particular case.

Finally I discuss the determination of a least general spin-Hamiltonian necessary to represent any splitting independent of \mathbf{H} or \mathbf{I} or linear in one of them. The treatment is general and simple and easily extensible to other terms in the power series. For convenience I break up the true Hamiltonian into three parts. \mathcal{H}_1 is the spin-orbit coupling energy. \mathcal{H}_2 is that part of the nuclear hyperfine interaction which is linear in both \mathbf{I} and one of the spin vectors for the electrons. \mathcal{H}_3 is the sum of the remainder of the hyperfine interaction and the part $\beta \mathbf{H} \cdot \mathbf{L}$ of the interaction with the external magnetic field. The other part $2\beta \mathbf{H} \cdot \mathbf{S}$ causes no difficulty and we do not mention it again. \mathcal{H}_3 does not include any spin vector. Other small terms in the Hamiltonian are not discussed. The perturbation procedure adopted means we consider that part of the matrix.

$$-\sum_{j, M''} E_j^{-1} \langle MO | \sum \mathcal{H}_i | M'' j \rangle \langle M'' j | \sum \mathcal{H}_i | M' O \rangle \quad (2)$$

which is quadratic or linear in \mathcal{H}_1 (see Pryce [1]). The unperturbed energy E_0 is taken zero, M , M'' , M' classify S_z values, O is the ground manifold and j numbers the $(2S'+1$ dimensional) excited manifolds.

2. PROPERTIES OF THE MATRIX ELEMENTS

We have to show that our spin-Hamiltonian is real. For this and other reasons it is desirable to specify the corresponding properties for the kets occurring in the calculations. We use the operator introduced by Kramers [8] into the theory of magnetic properties (which is related also to time-reversal [9])

and denote its effect by an asterisk. It applies to kets and linear operators. I use a bar to denote the other type of conjugate. Thus $\bar{\mathbf{l}} = -\mathbf{l}^* = \mathbf{l}$, $\mathbf{s} = -\mathbf{s}^* = \mathbf{s}$ for orbital and spin angular momentum vectors, while for any number c we always have $\bar{c} = c^*$. Our unperturbed kets are written $|Mj\rangle$ where $j=0$ gives the ground states and otherwise Mj give the quantum numbers of excited states. M refers always to S_z and $|Mj\rangle$ for fixed j are correctly connected in phase. Finally, as is always possible, we define

$$|Mj\rangle^* = (-1)^M | -Mj \rangle \quad (3)$$

for all j . This implies also

$$\langle Mj|^* = (-1)^{-M} \langle -Mj |. \quad (4)$$

Clearly $\overline{\mathcal{H}}_1 = \mathcal{H}_1^* = \mathcal{H}_1$. However, we choose to suppose that neither spatial rotations nor the Kramers operator affect the kets referring to nuclear properties. So the nuclear moment \mathbf{l} and the kets $|M_l\rangle$ are left unaltered. With this definition we have

$$\overline{\mathcal{H}}_2 = -\mathcal{H}_2^* = \mathcal{H}_2.$$

We now determine the dependence of the matrix elements of \mathcal{H}_1 and \mathcal{H}_2 on the spin quantum numbers. I depend heavily here on results in the general theory of angular momenta and use the notation of the book by Fano and Racah [7] (henceforth referred to as FR). However, I differ slightly in that I adopt Racah's earlier definition [10] of the phases of the components of a vector \mathbf{a} when expressed as a tensor operator, writing

$$\mathbf{a}_0 = \mathbf{a}_z, \quad \mathbf{a}_{\pm 1} = \frac{1}{\sqrt{2}} (\mp \mathbf{a}_x - i\mathbf{a}_y). \quad (5)$$

This means that the reduced matrix element for the spin vector \mathbf{s} is

$$\langle \alpha S || S^{(1)} || \alpha' S' \rangle = \delta_{\alpha\alpha'} \delta_{SS'} \{S(S+1)(2S+1)\}^{1/2} \quad (6)$$

in place of FR, equation (14.9).

The spin-orbit coupling is

$$\mathcal{H}_1 = \sum_{\kappa\nu} (-1)^\nu u_{\kappa\nu} s_{\kappa-\nu} \quad (7)$$

where κ numbers the electrons and ν the components†. Therefore

$$\begin{aligned} \langle MO | \mathcal{H}_1 | M''j \rangle &= \sum_{\kappa\nu n} (-1)^\nu \langle MO | u_{\kappa\nu} | Mn \rangle \langle Mn | s_{\kappa-\nu} | M''j \rangle \\ &= \sum_\nu (-1)^{\nu+S-M} Y_\nu \bar{V} \left(\begin{array}{ccc} 1 & S' & S \\ -\nu & M'' & -M \end{array} \right), \end{aligned} \quad (5)$$

where the Y_ν are numbers independent of M and M'' (use FR, equation (14.4)). Therefore

$$\overline{\langle MO | \mathcal{H}_1 | M''j \rangle} = \sum_\nu (-1)^{\nu+S-M} \bar{Y}_\nu \bar{V} \left(\begin{array}{ccc} 1 & S' & S \\ -\nu & M'' & -M \end{array} \right)$$

but this is just a number and so also equal to

$$\begin{aligned} \langle MO | \mathcal{H}_1 | M''j \rangle^* &= (-1)^{M''-M} \langle -MO | \mathcal{H}_1 | -M''j \rangle \\ &= \sum_\mu (-1)^{\mu+M''+S} Y_\mu \bar{V} \left(\begin{array}{ccc} 1 & S' & S \\ -\mu & M'' & M \end{array} \right) \\ &= \sum_\nu (-1)^{\nu+M''+1-S'} Y_{-\nu} \bar{V} \left(\begin{array}{ccc} 1 & S' & S \\ -\nu & M'' & -M \end{array} \right) \end{aligned} \quad (9)$$

† We are not assuming that \mathbf{u} is necessarily $\xi(r)\mathbf{l}$, see Stevens [11].

where we have used (8) and the symmetry properties of \tilde{V} . It then follows from the orthonormality relations (FR equation (10.17)) for the \tilde{V} that

$$\bar{Y}_\nu = (-1)^{1+S'-S+\nu} Y_{-\nu}. \quad (10)$$

In just the same way we write

$$\langle MO|\mathcal{H}_2|M''j\rangle = \sum_\nu (-1)^{\nu+S-M} Y_\nu' \tilde{V} \begin{pmatrix} 1 & S' & S \\ -\nu & M'' & -M \end{pmatrix} \quad (11)$$

and find

$$\bar{Y}'_\nu = (-1)^{S'-S+\nu} Y_{-\nu}'. \quad (12)$$

As in FR, equation (7.10), we now define the elements of irreducible product sets by writing

$$(S \times S)_\gamma^{(c)} = \sum_{\mu\nu} \langle 11\mu\nu | 11c\gamma \rangle S_\mu S_\nu \quad (13)$$

and from (6) and FR, equation (15.15), have

$$\langle \alpha S | (S \times S)^{(c)} | \alpha S \rangle = (-1)^{c+2S} S(S+1)(2S+1)(2c+1)^{1/2} \bar{W} \begin{pmatrix} S & S & c \\ 1 & 1 & S \end{pmatrix}. \quad (14)$$

In a strictly analogous manner we define $(Y \times Y)_\gamma^{(c)}$, $(Y \times Y')_\gamma^{(c)}$ and $(Y' \times Y)_\gamma^{(c)}$. It then follows from the properties of the Wigner coefficients that $(Y \times Y)_\gamma^{(1)}$ is identically zero, while $(Y \times Y')_\gamma^{(c)} - (Y' \times Y)_\gamma^{(c)}$ is identically zero for $c=0$ or 2. Finally $(Y' \times Y)_\gamma^{(1)} = -(Y \times Y')_\gamma^{(1)}$.

3. DERIVATION OF THE SPIN-HAMILTONIAN BY PERTURBATION THEORY

Considering \mathcal{H}_1 and \mathcal{H}_2 , the matrix (2) has the two kinds of second-order parts

$$- \sum_{jM'} E_j^{-1} \langle MO|\mathcal{H}_1|M''j\rangle \langle M''j|\mathcal{H}_1|M'O\rangle \quad (15)$$

which gives the fine structure and

$$- \sum_{jM''} E_j^{-1} \{ \langle MO|\mathcal{H}_1|M''j\rangle \langle M''j|\mathcal{H}_2|M'O\rangle + \langle MO|\mathcal{H}_2|M''j\rangle \langle M''j|\mathcal{H}_1|M'O\rangle \} \quad (16)$$

which gives the hyperfine structure. We abbreviate these to $- \sum_j E_j^{-1} X_{MM'}^j$ and $- \sum_j E_j^{-1} Z_{MM'}^j$ respectively.

Then using (8) and (10) and the symmetry properties of the \tilde{V} we find

$$\begin{aligned} X_{MM'}^j &= \sum_{M''} \langle MO|\mathcal{H}_1|M''j\rangle \langle M''j|\mathcal{H}_1|M'O\rangle \\ &= \sum_{M'\mu\nu} (-1)^{\nu+S-S'+1} Y_\mu Y_\nu \tilde{V} \begin{pmatrix} 1 & S & S' \\ -\mu & -M & M' \end{pmatrix} \tilde{V} \begin{pmatrix} S & 1 & S' \\ M' & -\nu & -M'' \end{pmatrix}, \end{aligned}$$

and then with the help of FR, equation (11.18):

$$\begin{aligned} X_{MM'}^j &= \sum_{\mu\nu\gamma} (-1)^{\nu+S+1-M'} (2c+1) \bar{W} \begin{pmatrix} S & S & c \\ 1 & 1 & S' \end{pmatrix} \tilde{V} \begin{pmatrix} S & S & c \\ M' & -M & -\gamma \end{pmatrix} \tilde{V} \begin{pmatrix} 1 & 1 & c \\ \mu & \nu & -\gamma \end{pmatrix} Y_\mu Y_\nu \\ &= \sum_{c\gamma} (-1)^{c+1+S-M'} (2c+1)^{1/2} \bar{W} \begin{pmatrix} S & S & c \\ 1 & 1 & S' \end{pmatrix} \tilde{V} \begin{pmatrix} S & S & c \\ M' & -M & -\gamma \end{pmatrix} (Y \times Y)_\gamma^{(c)}. \end{aligned} \quad (17)$$

We now show that the $X_{MM'}^j$ are the matrix elements in a spin-Hamiltonian of the quantity

$$R = \sum_{c\gamma} (-1)^\gamma T_\gamma^{(c)} (S \times S)_{-\gamma}^{(c)} \quad (18)$$

for suitable $T_{\gamma}^{(c)}$. Clearly, using (14):

$$\langle MO|R|M'O\rangle = \sum_{c\gamma} (-1)^{\gamma+s-M} T_{\gamma}^{(c)} S(S+1)(2S+1)(2c+1)^{1/2} \\ W\left(\begin{matrix} S & S & c \\ 1 & 1 & S \end{matrix}\right) V\left(\begin{matrix} S & S & c \\ M' & -M & -\gamma \end{matrix}\right), \quad (19)$$

which is identical with (17) providing we put

$$T_{\gamma}^{(c)} = (-1)^{c+1} \alpha \{S(S+1)(2S+1)\}^{-1} (Y \times Y)_{\gamma}^{(c)}$$

where

$$\alpha = \bar{W}\left(\begin{matrix} S & S & c \\ 1 & 1 & S' \end{matrix}\right) / \bar{W}\left(\begin{matrix} S & S & c \\ 1 & 1 & S \end{matrix}\right)$$

is easily deduced from the known expressions for \bar{W} for the relevant values of S' and c [12]. It is given in the table. $T_{\gamma}^{(c)}=0$ for $c=1$ so R gives the usual symmetrical quadratic expression in the spin-Hamiltonian when we multiply by $-E_j^{-1}$ and sum over j . Further, using (10) and $\bar{S}_i = (-1)^i S_{-i}$, we easily deduce that R is real. This concludes the derivation for the fine structure. I mention here the obvious fact that the term with $c=0$ only shifts the centre of gravity (downward, use (10)); that with $c=2$ does not affect it.

		S'	
		$S-1$	S
α		-1	1
c	0	-1	1
	1	$-(S+1)$	1
	2	$(S+1)/(2S-1)$	1
			$S/(2S+3)$

The quantity $\alpha = \bar{W}\left(\begin{matrix} S & S & c \\ 1 & 1 & S' \end{matrix}\right) / \bar{W}\left(\begin{matrix} S & S & c \\ 1 & 1 & S \end{matrix}\right)$ as a function of S for the relevant values of S' , c .

For the case $S'=S$ we use the identity

$$\sum_{c\gamma} (-1)^{\gamma} (Y \times Y)_{\gamma}^{(c)} (S \times S)_{-\gamma}^{(c)} = (\mathbf{Y} \cdot \mathbf{S})^2$$

to deduce

$$R = -\{S(S+1)(2S+1)\}^{-1} (\mathbf{Y} \cdot \mathbf{S})^2.$$

If the spin-orbit coupling can be correctly represented as $\lambda \mathbf{L} \cdot \mathbf{S}$ then (8) gives

$$\mathbf{Y} = (-1)^{2S+1} \lambda \{S(S+1)(2S+1)\}^{1/2} \langle 0 | \mathbf{L} | n \rangle \quad (20)$$

so, remembering that for $S'=S$ we have $\bar{\mathbf{Y}} = -\mathbf{Y}$, the fine structure Hamiltonian becomes $-\lambda^2 \sum_{ij} \Lambda_{ij} S_i S_j$ where i and j now refer to the x , y and z components and

$$\Lambda_{ij} = \sum_n E_n^{-1} \langle 0 | L_i | n \rangle \langle n | L_j | 0 \rangle$$

is real and symmetric. Thus we have recovered the expression derived by Pryce [1] under these particular restrictions.

The expression for R in terms of \mathbf{Y} and \mathbf{S} simplifies also for $S'=S \pm 1$. We have

$$S'=S+1: \quad R = \{S(S+1)(2S+1)(2S+3)\}^{-1} [(S+1)\mathbf{Y}^2 \mathbf{S}^2 - S(\mathbf{Y} \cdot \mathbf{S})^2]$$

$$S'=S-1: \quad R = \{S(S+1)(4S^2-1)\}^{-1} [S\mathbf{Y}^2 \mathbf{S}^2 - (S+1)(\mathbf{Y} \cdot \mathbf{S})^2]$$

with the vector \mathbf{Y} now real. The reader who is familiar with the theory of invariants of the orthogonal group will recognize that the fact that R is in each case linearly dependent on the products $(\mathbf{Y} \cdot \mathbf{S})^2$ and $\mathbf{Y}^2 \mathbf{S}^2$ of scalar products is not accidental but is a necessary consequence of one of the central theorems of that subject (see Weyl [13], Theorem T_m^n , page 53). The expression (21) including the ϵ_{jlm} for the hyperfine energy is to be related also to that theorem, the quantity $\sum_{jkl} S_j I_k$ corresponding to an odd orthogonal invariant because the five constituent vectors are actually all pseudo-vectors.

The calculation for the nuclear magnetic hyperfine interaction is a trivial modification of the preceding one. Remembering the difference of sign between (10) and (12), we have merely to replace $Y_\mu Y_\nu$ in the first line of (17) by $Y_\mu' Y_\nu - Y_\mu Y_\nu'$. We remarked earlier that $(Y' \times Y)_\gamma^{(c)} - (Y \times Y')_\gamma^{(c)}$ is zero unless $c=1$ when it is equal to $2(Y' \times Y)_\gamma^{(c)}$. Hence we now have

$$T_\gamma^{(1)} = 2\alpha \{S(S+1)(2S+1)\}^{-1} (Y' \times Y)_\gamma^{(1)}$$

with α in the table as before. One soon verifies, using (10), (12) and the definition of $(Y' \times Y)^{(1)}$ that R satisfies $R = \bar{R} = -\bar{R}^*$ as it should. Also

$$(S \times S)_\gamma^{(1)} = -\frac{1}{\sqrt{2}} S_\gamma$$

and so R is homogeneous and linear in each of \mathbf{S} and \mathbf{I} which completes the derivation. The part of the nuclear hyperfine interaction which commutes with \mathbf{S} was incorporated in \mathcal{H}_3 and will be discussed shortly.

If we calculate only within states arising from a ground 1^n term of the ion and write

$$\mathcal{L}_\gamma^{(2)} = (\mathbf{L} \times \mathbf{L})_\gamma^{(2)}$$

where \mathbf{L} is the total orbital angular momentum vector, we have

$$\mathcal{H}_2 = -P\kappa \mathbf{S} \cdot \mathbf{I} - 3\sqrt{5}\xi P(I \times \mathcal{L}^{(2)} \times S)^{(0)}$$

according to FR, formula (10.5), and Abragam and Pryce [1]. The latter authors showed the second-order effects of the last term in \mathcal{H}_2 to give $3P\lambda\xi \sum_{jk} u_{jk} S_j I_k$ in the spin-Hamiltonian (there is a misprint in their equation (3.4) but not (3.7)) where

$$u_{jk} = -\frac{1}{2}i \sum_{lmn} \epsilon_{jlm} E_n^{-1} \langle 0 | L_m | n \rangle \langle n | (L_k L_l + L_l L_k) | 0 \rangle, \quad (21)$$

with the j, k, l, m referring to Cartesian coordinates and $n \neq 0$. ϵ_{jlm} is the usual alternating tensor. We have

$$Y_\nu' = \sqrt{(15)P\xi} \{S(S+1)(2S+1)\}^{1/2} (-1)^{2S+1} (I \times \langle 0 | \mathcal{L}^{(2)} | n \rangle)_\nu^{(1)}$$

and a corresponding spin-Hamiltonian

$$\mathcal{H}(S) = \sqrt{(30)P\xi} \sum_{ny} E_n^{-1} (-1)^y ((I \times \langle 0 | \mathcal{L}^{(2)} | n \rangle)^{(1)} \times \langle 0 | L | n \rangle)_\gamma^{(1)} S_{-\gamma}.$$

This is easily shown to be the same as Abragam and Pryce's expression by using the identity

$$\sum_\gamma (-1)^y (a \times b)_\gamma^{(1)} c_{-\gamma} = \frac{1}{2}i\sqrt{2} \sum_{lmj} \epsilon_{jlm} a_l b_m c_j$$

for the three vectors $a^{(1)} = (I \times \langle 0 | \mathcal{L}^{(2)} | n \rangle)^{(1)}$, $b = \langle 0 | \mathbf{L} | n \rangle$ and $c = \mathbf{S}$. In making this comparison, note that their $L_k L_l + L_l L_k$ is not a multiple of the irreducible tensorial quantity $\mathcal{L}^{(2)}$ but has a non-zero trace whose matrix elements between $|0\rangle$ and $|n\rangle$ are always zero with their assumptions.

The part \mathcal{H}_3 of the Hamiltonian is easier to deal with because it commutes with \mathbf{S} . Therefore the only excited states which contribute have the same multiplicity as the ground manifold and hence the matrix elements of \mathcal{H}_1 are proportional to those of \mathbf{S} . Symbolically

$$\langle MO|\mathcal{H}_1|M''j\rangle = \langle MO|\mathbf{Z} \cdot \mathbf{S}|M''j\rangle$$

for some \mathbf{Z} depending on j but independent of M, M'' . The matrix elements of \mathcal{H}_3 are diagonal in M and independent of it. Hence we arrive immediately at the appropriate terms in equation (1), the only difference from Pryce's derivation lying in the details of the formulae for the g_{ij} and this contribution to the A_{ij} .

4. THE GENERAL SPIN-HAMILTONIAN

We now consider the following problem. Given a set of $2S+1$ states ψ_i for an n -electron system with $n+2S$ even, such that

$$\psi_i^* = \sum_{j=1}^{2S+1} a_{ij} \psi_j$$

for some matrix A , to construct a spin-Hamiltonian adequate to express completely arbitrary matrices of zero-field splitting, magnetic field energy and hyperfine energy within the set ψ_i . This has been discussed in particular cases by several authors [3-5] and with some generality by Koster and Statz [6]. However, the extreme simplicity of the general problem does not seem to have been fully appreciated. This has been obscured somewhat by the tendency to introduce group-theoretic considerations too early in the discussion. We suppose at first no restrictions of this kind on the real Hamiltonian and therefore the only conditions upon the matrix elements are those implied by the use of the Kramers operator.

It follows from the usual properties of the Kramers operator that we can find linear combinations of the ψ_i , which we write in ket notation, satisfying

$$|M\rangle^* = (-1)^M | -M \rangle,$$

where M runs from $-S$ to S . Our spin-Hamiltonian will have fictitious spin S and these basic states as eigenstates of the fictitious spin vector, which we write \mathbf{S} because there is no danger of confusion with the real \mathbf{S} .

Suppose now that we have an operator ρ whose matrix elements within the $|M\rangle$ are given. It follows from the usual decomposition of tensors of rank two under the orthogonal group that the quantity

$$X = \sum_{\epsilon\gamma} (-1)^\gamma Q_\gamma^{(c)} S_{-\gamma}^{(c)} \quad (22)$$

is adequate to represent the $(2S+1)^2$ matrix elements of ρ for suitable choices of the numbers $Q_\gamma^{(c)}$ providing the reduced matrix elements of the $S_{-\gamma}^{(c)}$ are all non-zero (generalizing the method of reference [4]). Here c runs through the integers from 0 to $2S$ and the $Q_\gamma^{(c)}$ are uniquely determined by ρ for a given choice of the $S_{-\gamma}^{(c)}$. The $S_{-\gamma}^{(c)}$ are irreducible tensor operators of degree c and the simplest choice for each is to take the irreducible product of degree c of c spin vectors S_γ . Then $\overline{S_\gamma^{(c)}} = (-1)^c S_\gamma^{(c)*} = (-1)^\gamma S_{-\gamma}^{(c)}$ and we assume this. It is usual to take \mathbf{S}^2 rather than 1 for $S_0^{(0)}$ and then to combine it with the term of degree 2 to give a homogeneous quadratic expression.

Because of the crucial importance of the expansion (22) for our argument it is perhaps desirable to give a straightforward proof of its validity. We do this by observing that (FR, equation (14.4)):

$$\langle M|S_{-\gamma}^{(c)}|M'\rangle = \alpha(c)(-1)^{S-M}\bar{V}\begin{pmatrix} S & S & c \\ -M & M' & -\gamma \end{pmatrix}.$$

Therefore a typical matrix element of X is

$$\langle M|X|M'\rangle = \sum_{c\gamma} \alpha(c)(-1)^{S-M'}Q_{\gamma}^{(c)}\bar{V}\begin{pmatrix} S & S & c \\ -M & M' & -\gamma \end{pmatrix}$$

and therefore the matrix elements of X considered as a set of $(2S+1)^2$ quantities are a non-singular transform of the set of $(2S+1)^2$ quantities $\alpha(c)Q_{\gamma}^{(c)}$. (The minus signs do not affect this.) Provided, therefore, that $\alpha(c)$ is non-zero for each c , either set determines the other uniquely. This establishes (22).

We only need the case in which $\rho = \bar{\rho} = \epsilon\rho^*$ for $\epsilon = \pm 1$. This introduces the restrictions $\bar{Q}_{\gamma}^{(c)} = (-1)^c Q_{-\gamma}^{(c)}$ always, and also $Q_{\gamma}^{(c)} = 0$ for $\epsilon = +1$ and c odd or $\epsilon = -1$ and c even as one readily sees. Expressed in a different notation these properties are well known.

Let us consider what this means, first for the fine structure Hamiltonian. The sum (22) now extends over even c from 0 to $2S$. Therefore for $S \leq 1\frac{1}{2}$ a symmetrical quadratic form in S_x , S_y and S_z with real coefficients is always adequate. For $S=2$ or $2\frac{1}{2}$ the addition of a quartic term is sufficient, while for $S=3$ or $3\frac{1}{2}$ we may need a sextic term. In these particular cases at least these results are known [3, 4, 14].

The interaction with the magnetic field requires the specification of three matrices, one for each component of \mathbf{H} , and with $\epsilon = -1$. Therefore we must put

$$V_1 = \sum_{c\gamma\delta} (-1)^c Q_{\gamma}^{(c)}(\delta) S_{-\gamma}^{(c)} H_{\delta} \quad (23)$$

into the spin-Hamiltonian with $c \leq 2S$ and odd. Therefore the usual term $g_{ij}H_iS_j$ is always adequate for $S \leq 1$ but not, in general, for higher S . Similar remarks apply to the nuclear hyperfine interaction (there we have one matrix for each component of \mathbf{I}).

Having dealt with the general problem, the restrictions imposed by a site symmetry group G are easily derived. First we remark that the classification symbols in the kets $|M\rangle$ do not necessarily give any indication of the behaviour of those kets under the operations of G . If a set of states with true spin S breaks up into the irreducible representations $\sum \Gamma_i$ under G there is no need for our set of $(2S+1)$ states to span the same set of Γ_i . They often do however, or at least the sets of matrix elements of any operator ρ have the same transformation properties as if they did†, so we consider that case now. We also suppose the elements of G operate also on the nuclear moment vector \mathbf{I} and the external magnetic field \mathbf{H} . Then the terms \mathcal{H}_j in the Hamiltonian may be regarded as belonging to the unit representation of G .

Let the transformation matrix between an SM and an $S\Gamma_1M_1$ scheme for eigenkets of the true spin vector be $\langle SM|S\beta\Gamma_iM_1\rangle$, where β is inserted if Γ_i is

† i.e. like $2S+1\Gamma$ with Γ a representation of degree one. When Γ is not the unit representation the argument given in the text is only trivially modified. Another kind of set of states is one related to a level of the free ion, e.g. in the rare earth series.

repeated. Then, by hypothesis, there exist linear combinations of our $(2S+1)$ states which may be written $|a\beta\Gamma_i M_i\rangle$, one for each choice of $\beta\Gamma_i M_i$, and having the indicated behaviour under G . Then write

$$|M\rangle = \sum_{\beta\Gamma_i M_i} \langle S\beta\Gamma_i M_i | SM \rangle |a\beta\Gamma_i M_i\rangle \quad (24)$$

for the states of the spin-Hamiltonian with M classifying the eigenstates of the fictitious spin. The \mathcal{H}_j now satisfy

$$\langle a\beta\Gamma_i M_i | \mathcal{H}_j | a\beta'\Gamma'_i M'_i \rangle = f(\beta\beta')\delta(\Gamma_i\Gamma'_i)\delta(M_i M'_i). \quad (25)$$

Let g belong to G . Then because g effects an orthonormal transformation on $|a\beta\Gamma_i M_i\rangle$ but does not alter β or Γ_i , and the spin-Hamiltonian $\mathcal{H}(S)$ must satisfy (25) in place of \mathcal{H}_j , we find

$$\langle a\beta\Gamma_i M_i | g\mathcal{H}(S) | a\beta'\Gamma'_i M'_i \rangle = f(\beta\beta')\delta(\Gamma_i\Gamma'_i)\delta(M_i M'_i),$$

where g now operates only on $\mathcal{H}(S)$. From the orthogonality properties for group representations (see Weyl [13], especially section IV.1.2) it follows that if ϵ is an irreducible idempotent referring to any component other than that of the unit representation then $\epsilon\mathcal{H}(S)$ has all its matrix elements zero. Therefore the only non-zero matrix elements of $\mathcal{H}(S)$ arise from that part which is invariant under G and therefore the most general spin-Hamiltonian that we need take is that part of our previous spin-Hamiltonian which belongs to the unit representation of G .

We have established our result without using the relation (24). However, we need (24) to be true if we go on to determine the precise form of $\mathcal{H}(S)$ as a function of the fictitious spin \mathbf{S} , because then we must know how \mathbf{S} behaves under the elements of G and (24) assures us that we may without inconsistency define it to behave in the same way as a real vector would. This can be proved in the following way.

If the $|M\rangle$ and the $|a\beta\Gamma_i M_i\rangle$ are connected according to (24) then the matrix of any element of G within the $|M\rangle$ uniquely defines its matrix within the $|a\beta\Gamma_i M_i\rangle$ and conversely. The same is true for the matrix of the Kramers operator. Therefore providing we can choose the $|a\beta\Gamma_i M_i\rangle$ so that they give the right matrices for all these operators simultaneously, the same will be true for the $|M\rangle$ and we may define $\mathbf{S}^* = -\mathbf{S}$ and \mathbf{S} to transform under G (but not necessarily under any larger group) in the same way as the true spin vector.

We choose our $|a\beta\Gamma_i M_i\rangle$ to transform correctly under G , as of course we may because of the definition of irreducible representation. Write $|a\beta\Gamma_i M_i\rangle$ as a row vector Ψ . Then if ΨT also transforms correctly under G we have

$$\Psi T R = \Psi R T$$

for all matrices of the representation. Therefore by Schur's lemma T is a multiple ϵ of the unit matrix. $|\epsilon|=1$ because Ψ and ΨT are normalized. We now consider the effect of the Kramers operator on Ψ . The transformed vector Ψ^* forms a basis for the irreducible representation $\bar{\Gamma}$, having matrices \bar{R} which are the complex conjugates of the R . It is well known that there are three possible types of relationship of $\bar{\Gamma}$ to Γ , and the representations Γ_i can be divided accordingly into three categories [16]. In the first category R can be taken always real and by choosing ϵ appropriately we can always take the row vector ΨT

to be real. This shows that the functions of any representation Γ_i of this category can be chosen to conform simultaneously to a standard behaviour under G and the Kramers operator.

In the second category $\bar{\Gamma}_i$ is equivalent to Γ_i but the matrices R cannot be chosen wholly real. Here we insist that $\psi^* = \psi S$ for some S . It can be shown that this is always possible if one accepts the corresponding assumption at the beginning of the section [17]. Suppose now φ with $\varphi^* = \varphi U$ defines the standard behaviour of Γ_i under the various operators. We assume ψ behaves under G in the same way as φ and prove that there is a number $\epsilon = \exp(i\alpha)$ such that $(\epsilon\psi)^* = (\epsilon\psi)U$. First we note that $\varphi^* \bar{R} = \varphi RU = \varphi U \bar{R}$ and so we have both

$$RU = U\bar{R} \quad \text{and} \quad RS = S\bar{R}.$$

Hence

$$RSU^{-1} = S\bar{R}U^{-1} = SU^{-1}R$$

for all R and so $S = \lambda U$ for some number λ . Because φ and ψ are normalized we have $|\lambda| = 1$, so $\lambda = \exp(i\beta)$. Therefore

$$(\epsilon\psi)^* = \exp(-i\alpha)\psi \exp(i\beta)U = \exp[i(\beta - 2\alpha)](\epsilon\psi)U$$

and we put $\beta = 2\alpha$ to give our result.

Finally in the third category Γ_i and $\bar{\Gamma}_i$ are inequivalent so there is no difficulty. Again we require that ψ^* is among our set of kets when ψ is.

For G the octahedral group we now deduce that as the total magnetic field operator and the total nuclear hyperfine operator transform as A_1 , the electronic parts must transform as T_1 . It then follows from the known breakdown of irreducible representations of the three dimensional rotation group under G [15] that, in the most general case, we need $(\lambda+1)^2$ parameters for each of these operators when $S = 2\lambda + \frac{1}{2}$ or $2\lambda + 1$ and $\lambda(\lambda+1)$ when $S = 2\lambda$ or $2\lambda - \frac{1}{2}$. In particular we need two for $S = 1\frac{1}{2}$, four for $S = 2\frac{1}{2}$ and six for $S = 3\frac{1}{2}$ as has been remarked, in part, elsewhere [5, 6]. The general solution for the fine structure is equally easy to obtain but does not give quite such a succinct formula. For $S \leq 1\frac{1}{2}$ we need one parameter, i.e. merely a choice of energy zero which would usually be taken to be zero. For $S = \lambda$ or $\lambda + \frac{1}{2}$, greater than $\frac{1}{2}$ and less than six, we need λ parameters. Thus we need two for $S = 2\frac{1}{2}$ and three for $S = 3\frac{1}{2}$ as is well known [3].

I conclude by remarking that in calculating the spin-Hamiltonian $\mathcal{H}(S)$ by the second-order perturbation treatment of §3 we can again assume that $\mathcal{H}(S)$ belongs to the unit representation of the site spinor symmetry group G . This is because we can take our states as $|a\Gamma_i M_i\rangle$ where Γ_i is an irreducible representation of G and M_i a component. Then allowing G to operate also on \mathbf{H} and \mathbf{I} we have equation (25) for a part \mathcal{H}_j of \mathcal{H} , i.e. the perturbation matrix is diagonal in Γ_i, M_i and independent of M_i . It follows immediately that among our ground set of states $\mathcal{H}(S)$ is diagonal in Γ_i and M_i and, for fixed a, Γ_i , independent of M_i . Therefore we may assume $\mathcal{H}(S)$ belongs to the unit representation of G .

REFERENCES

- [1] PRYCE, M. H. L., 1950, *Proc. phys. Soc., Lond. A*, **63**, 25; ABRAGAM, A., and PRYCE, M. H. L., 1951, *Proc. roy. Soc. A*, **205**, 135.
- [2] CONDON, E. U., and SHORTLEY, G. H., 1953, *Theory of Atomic Spectra* (Cambridge: University Press), p. 48.
- [3] BLEANEY, B., and STEVENS, K. W. H., 1953, *Rep. Prog. Phys.*, **16**, 108.
- [4] STEVENS, K. W. H., 1952, *Proc. roy. Soc. A*, **214**, 237.

- [5] GRIFFITH, J. S., 1958, *Disc. Faraday Soc.*, **26**, 178. (Note misprint, line 4 should read d^3 not d^1); BLEANEY, B., 1959, *Proc. phys. Soc., Lond.*, **73**, 939.
- [6] KOSTER, G. F., and STATZ, H., 1959, *Phys. Rev.*, **113**, 445.
- [7] FANO, U., and RACAH, G., 1959, *Irreducible Tensorial Sets* (New York: Academic Press).
- [8] KRAMERS, H. A., 1930, *Proc. K. Akad. Wetensch.*, **33**, 959.
- [9] WIGNER, E. P., 1932, *Nachr. Ges. Wiss. Göttingen*, 546.
- [10] RACAH, G., 1942, *Phys. Rev.*, **62**, 442.
- [11] STEVENS, K. W. H., 1953, *Proc. roy. Soc. A*, **219**, 546.
- [12] EDMONDS, A. R., 1957, *Angular Momentum in Quantum Mechanics*, Table 5 (Princeton: University Press), p. 130.
- [13] WEYL, H., 1946, *Classical Groups* (Princeton: University Press).
- [14] HUTCHISON, C. A., JUDD, B. R., and POPE, D. F. D., 1957, *Proc. phys. Soc., Lond. B*, **70**, 514.
- [15] BETHE, H., 1929, *Ann. Phys.*, **3**, 133.
- [16] FROBENIUS, G., and SCHUR, I., 1906, *Sitzungsberichte Akad. Berlin*, **1**, 186.
- [17] GRIFFITH, J. S., 1960, *The theory of transition-metal ions*, Section 8.6 (Cambridge: University Press) (in the press).

Ionic interactions in solutions of electrolytes as studied by ultra-violet spectroscopy

by T. R. GRIFFITHS and M. C. R. SYMONS

Department of Chemistry, The University, Southampton

(Received 24 August 1959)

Spectrophotometric evidence for the formation of contact ion-pairs in solutions of tetra-alkylammonium iodides in certain solvents of poor ion-solvating power, such as carbon tetrachloride, is presented.

Since the band ascribed to contact ion-pairs is not detected for solutions in other solvents, such as chloroform, it is concluded that the ion-pairs detectable by other techniques in such solvents are separated by solvent molecules.

1. INTRODUCTION

Ionic interactions in solutions of electrolytes have been studied recently by spectrophotometry in the visible and ultra-violet region [1-5], and the results have been interpreted in a variety of ways. Ambiguity arises partly because the concept of ion-pair formation is ill-defined and partly because different types of electronic transitions can be affected in different ways by changes in environment [4, 6].

1.1. *Ion-pair formation*

For example, Fuoss defines an ion-pair as a pair of ions in physical contact, and all ions not in immediate contact are described as free ions [7]. This simple picture, based on thermodynamic calculations of Denison and Ramsey [8], has been criticized by Prue and Otter [9] who favour the original theory of Bjerrum as extended by Guggenheim [10], in which a distance of closest approach of free ions (d) is introduced, in addition to the contact distance (a). When ions are closer than d they are described as ion-pairs and treated as neutral molecules: for separations greater than d they are deemed free and treated by Debye-Hückel theory. These authors appear to ignore the results of relaxation spectrometry where well-defined effects have been interpreted in terms of a series of specific interactions at close distances in which one or more solvent molecules separate the ions, and a general interaction at larger distances [11].

1.2. *Definitions*

For clarity, we define the following terms relating to interactions between cations and anions:

- (1) *Complexes.* Two or more ions, in contact, held together by covalent bonds.
- (2) *Contact ion-pairs.* Ions, in contact, but with no covalent bonding between them.
- (3) *Solvent shared ion-pairs.* Pairs of ions, linked electrostatically by a single (oriented) solvent molecule.
- (4) *Solvent separated ion-pairs.* Pairs of ions, linked electrostatically but separated by more than one solvent molecule.

(5) *Ion-pairs.* This term includes classes (2), (3) and (4) and will be used when distinction between them cannot be made.

Classes (1) and (2) are extremes, and in certain cases classification may be arbitrary. We have endeavoured to eliminate the chance of complex formation by studying tetra-alkylammonium iodides. A less well-defined example is that of substituted pyridinium iodides: characteristic bands are found when these ions are in contact [12], but, since a variety of partially covalent structures can then be written one cannot be certain that the absorbing unit is a contact ion-pair and not a complex. Weak 'covalent' forces must also play some part whenever charge-transfer between the ions in contact can occur: this must be true for alkali halide contact ion-pairs in the gas phase and probably even of the tetra-alkylammonium iodide contact ion-pairs discussed in § 4.1. In the ground state, however, this contribution to bonding must be small, and is ignored in the following discussion.

Classes (3) and (4) must be distinguished from the symmetrical interactions which occur in any solution. Solvent separated or solvent shared ion-pairs have axial symmetry and should be well separated from like units in dilute solutions.

1.3. Ultra-violet spectrophotometry

The differences of opinion relating to the worth of spectrophotometric methods in the study of ion-pair formation arises because, at times, insufficient attention is given to the nature of the electronic transitions involved. It has often been concluded that the spectra of ion-pairs are identical with those of the free ions [5, 13]. This may well be true for certain intramolecular transitions of either cations or anions [4], but as a generalization it is quite false. On the other extreme, a change in optical density at an arbitrary wavelength with change in the ionic strength of a solution is sometimes attributed to ion-pair formation, even though no attempt has been made to decide whether this change is caused by the growth and decay of bands, or simply the shift or broadening of a band [2, 3]. Since the location of absorption bands may be very sensitive to environmental changes [6, 12] there can be little justification in such an arbitrary assignment. A further objection to this approach is that the electrolytes used are often known to form covalent complexes quite readily, and therefore the changes studied could equally well be due to complex formation.

In this study we have extended some work reported earlier relating to the effect of high concentrations of electrolytes on the spectrum of aqueous iodide and, in particular, we have measured the spectra of solutions of tetra-alkyl-ammonium iodides in solvents of very low ionic solvating power. An attempt has been made to detect contact ion-pairs by seeking for a new absorption band not attributable to solvated iodide [14], and the effect of excess tetra-alkyl-ammonium perchlorate on the iodide band in such solvents has been examined.

2. EXPERIMENTAL

2.1. Materials

When possible all materials were AnalaR or Spectrograde. Where necessary salts were dried and stored under vacuum. Tetra-*n*-butylammonium iodide was

purified by recrystallizing several times from acetone and drying under vacuum. Found m.p. 146·5° (lit. 145°). Tetra-*n*-butylammonium perchlorate was prepared by mixing solutions in acetone of a slight excess of an equivalent of tetra-*n*-butylammonium iodide with an equivalent of silver perchlorate. The mixture was refluxed, filtered hot three times and the acetone removed under vacuum. The resulting salt was recrystallized four times from pure *n*-butanol and dried under high vacuum. Found m.p. 207–8° (lit. 203–4°).

Solvents were dried with calcium sulphate or sodium wire and fractionated, when necessary, up a 50 cm Vigreux column. Benzene (B.D.H. 'M.A.R.' quality) was distilled from phosphorus pentoxide after standing for several weeks. Dioxan was refluxed with fused stannous chloride, fractionated, and then refluxed over sodium prior to final fractionation. Anhydrous 1:3-dioxolane (kindly donated by Brotherton Ltd.) was freed from peroxides by fractionation alone.

The solvents used, and wavelength limits to which these solvents can be used in the ultra-violet region are given in table 1.

Solvent	Cell length when optical density against air is 1·0		
	1 cm	0·1 cm	0·01 cm
CCl ₄	265	248	245
C ₆ H ₆	282	280	278
Et ₂ O		200	
Tetra-hydrofuran		208	
Dioxan	240	215	210
1:2-dimethoxyethane	215	205	
CHCl ₃	245	235	223
1:3-dioxolane		200	

Table 1. Limits of transparency of solvents in $\text{m}\mu$.

2.2. Preparation of solutions

Tetra-*n*-butylammonium iodide was readily soluble in 1:3-dioxolane, chloroform and 1:2-dimethoxyethane. Solutions in dioxan, carbon tetrachloride, diethyl ether and tetrahydrofuran were prepared by standing with occasional shaking in the dark for about one week. Solutions in benzene were prepared by refluxing in the dark for 24 hr and pipetting hot into 1 cm cells already heated to 40° in the cell housing in order to prevent loss of solute by recrystallization. I₃[–] was formed in some solvents (detectable by its characteristic absorption spectrum) and this was removed by adding small amounts of anhydrous ammonium thiosulphate and leaving for times varying from a few hours to a week until the spectrum of I₃[–] was completely lost. Ammonium thiosulphate was insoluble in these solvents and had no effect on the iodide spectra.

Prolonged refluxing of tetra-*n*-butylammonium iodide in hexane, cyclohexane and iso-octane showed that the solubility in these solvents was vanishingly small. The spectra of the hot solvents, after refluxing, all showed a very weak band in the 290 $\text{m}\mu$ region together with a rising absorption at lower wavelengths comparable with that found for monoethers. However, optical densities were less than 0·1 in 1 cm cells and no definite conclusions are drawn.

2.3. Spectrophotometric measurements

The procedures were as described earlier [14] except that the Unicam SP.500 spectrophotometer was used in conjunction with an S.Z.G. 500 photomultiplier attachment of Präzisions-messgeräte R.S.V., Icking, Germany, incorporating a 1P28 multiplier tube, which enabled us to use relatively small slit-widths thus decreasing errors due to stray light.

Optical densities at peak maxima were obtained in the 0.2 to 0.8 region by a suitable choice of cells and concentrations. In the particular case of benzene the onset of absorption by solvent was very much steeper than for any other solvent and readings below $284\text{ m}\mu$ were unreliable. In the 225 to $235\text{ m}\mu$ region, despite the high optical density of the solvent in 0.01 cm cells (1.3–2.0), it was possible to obtain readings that appeared to be genuine. However, the range was too small to establish the position of any band maxima and we conclude only that iodide absorbs relatively strongly in this region.

In order to obtain the spectrum of saturated aqueous tetra-*n*-butylammonium iodide (7.33×10^{-2} moles l.⁻¹) a drop of the solution was placed between two quartz plates held together by a spring retaining clip in the cell carriage, the effective cell length being about 10^{-3} cm.

Extinction coefficients (ϵ_{\max}) for tetra-*n*-butylammonium iodide in carbon tetrachloride, benzene and dioxan were obtained as follows. Solutions in dioxan were diluted with a large excess of water and the optical density at the peak was compared with the known value for aqueous iodide, since small concentrations of dioxan have a negligible effect. Iodide was extracted from carbon tetrachloride

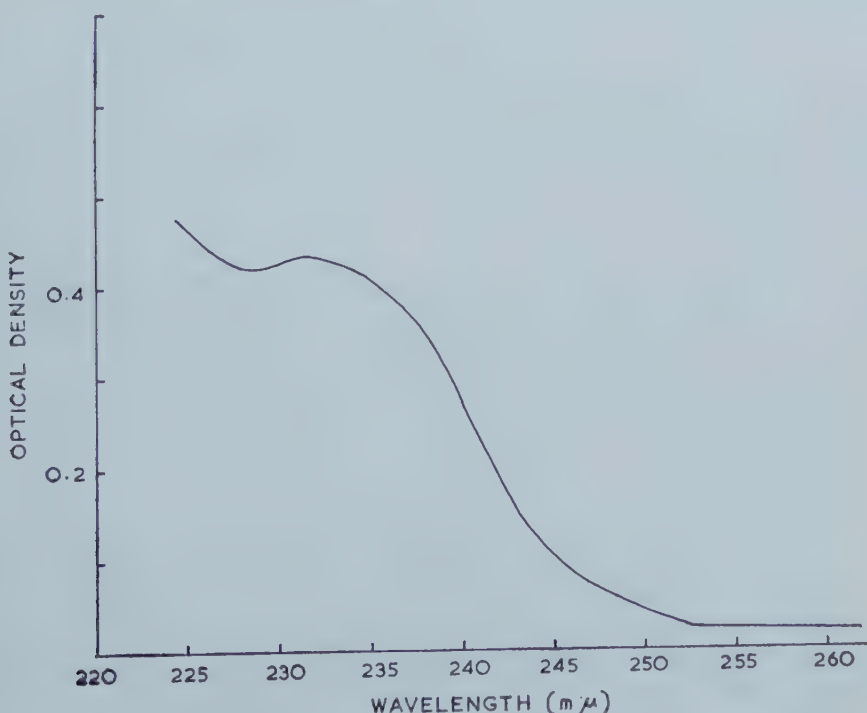


Figure 1. Diffuse reflectance spectrum of $(n\text{-Bu})_4\text{NI}$ diluted with LiF against LiF.

and benzene with four successive aliquots of water. In all cases extinction coefficients were close to that for iodide in water.

2.4. Diffuse reflectance spectra

The Unicam SP.570 attachment for the SP.500 spectrophotometer was used, taking the precautions described elsewhere [15]. The spectra of tetra-*n*-butylammonium and tetra-ethylammonium iodides were measured after suitable dilution with lithium fluoride and using a lithium fluoride reference surface (figure 1).

An attempt was also made to measure the transmission spectrum of a thin film of molten tetra-*n*-butylammonium iodide held between two silica plates and supercooled to room temperature. The result was quite comparable with the diffuse reflectance spectrum.

3. RESULTS

The results are summarized in tables 1-3 and figures 1-6.

3.1. Concentrated aqueous electrolytes

The experimental limits of λ_{\max} recorded in table 3 are $\pm 0.05 \text{ m}\mu$ and were obtained by the method of mid-points. All spectra were recorded in 0.1 cm cells to reduce the optical density due to chloride ion to less than 0.2 in the peak region. The result obtained for tetra-ethylammonium chloride is subject to slightly greater limits of error because its optical density was greater, presumably due to trace impurities. The result was confirmed using 0.01 cm cells.

3.2. Pure solvents

Values for $\lambda_{\max}^{20^\circ}$ which were identical with those given in table 2 were obtained using tetra-*n*-propylammonium iodide in chloroform and tetra-ethylammonium iodide in chloroform and 1:3-dioxolane. However, in carbon tetrachloride,

Solvent	$\lambda_{\max}^{20^\circ}$ ($\text{m}\mu$)	dE_{\max}/dT ($\text{cal}/^\circ$)	'Theoretical' dE_{\max}/dT ($\text{cal}/^\circ$)
CCl_4	293	0	124
C_6H_6	290†	—	124
Et_2O	290	—	124
Tetra-hydrofuran	290†	—	124
Dioxan	237	14 ± 3	45
1:2-dimethoxyethane	245	62 ± 5	59
CHCl_3	240-245‡	—	50-60
1:3-dioxolane	236	45 ± 5	43

† Shoulder; hence dE_{\max}/dT unobtainable but probably zero.

‡ A positive shift occurs, but owing to the breadth of this band dE_{\max}/dT was not accurately obtainable.

Table 2. Band maxima of, and effect of temperature on, the spectrum of tetra-*n*-butylammonium iodide in various solvents.

tetra-*n*-propylammonium iodide gave a band at 268 m μ and tetra-ethylammonium iodide, after refluxing in the dark for a week, gave evidence of a band below 267 m μ (compare table 1). In general alkali metal iodides were insoluble in these solvents; however, after prolonged shaking in the dark with dioxan, caesium iodide gave a band at 235 m μ , identical with that from the tetra-alkylammonium iodides.

3.3. Mixed solvents

Detailed spectroscopic studies have been made on tetra-*n*-butylammonium iodide in the following mixed solvents: carbon tetrachloride/chloroform; *cyclo*-hexane/*iso*-propanol; dioxan *iso*-propanol; dioxan/methyl cyanide, and dioxan acetone. Of these mixtures only carbon tetrachloride/chloroform gave any evidence for the rise of one band and the diminution of another with change in solvent composition (figure 3). For the other mixed solvents, a progressive

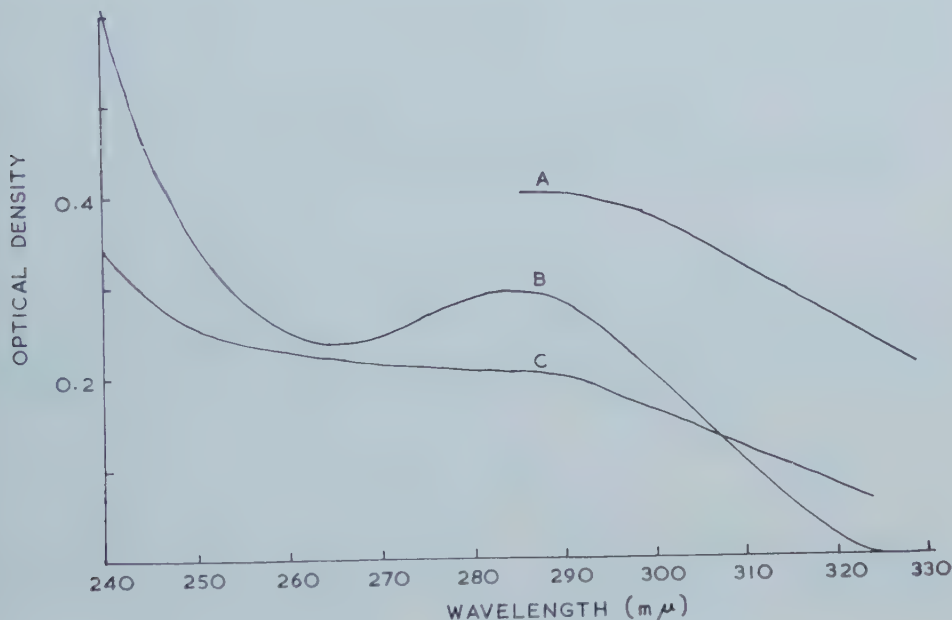


Figure 2. A, (*n*-Bu)₄NI in benzene; B, (*n*-Bu)₄NI in diethyl ether;
C, (*n*-Bu)₄NI in tetrahydrafuran.

Identical spectra obtained in the presence of excess (*n*-Bu)₄NClO₄.

shift of the iodide band was observed (figure 6) quite comparable with the shifts for water-solvent mixtures [14]. Constructed curves have been drawn for mixtures containing dioxan, e.g. the spectrum resulting from the addition of the iodide bands in pure dioxan and pure methyl cyanide in no way resembles any of the spectra obtained from any of the dioxan/methyl cyanide mixtures. It was established that the bands from all mixtures except those containing carbon tetrachloride and cyclohexane could not be reproduced by the addition, in various proportions, of the bands obtained from iodide in the two components.

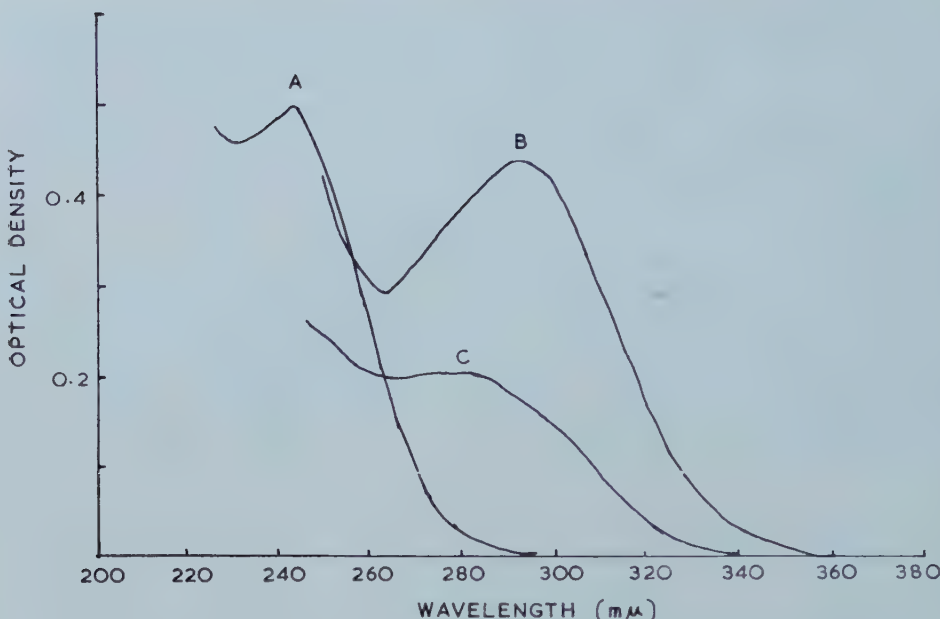


Figure 3. A, $(n\text{-Bu})_4\text{NI}$ in chloroform; B, $(n\text{-Bu})_4\text{NI}$ in carbon tetrachloride; C, $(n\text{-Bu})_4\text{NI}$ in chloroform/carbon tetrachloride mixture (90 per cent by vol. CCl_4).

3.4. Addition of tetra-*n*-butylammonium perchlorate

When tetra-*n*-butylammonium perchlorate was added to dioxan the $237\text{ m}\mu$ band was shifted to the ultra-violet in the normal way (compare table 3), and a shoulder appeared in the $280\text{ m}\mu$ region. However, when added to 1:3-dioxolane the $236\text{ m}\mu$ band was again shifted in the expected way but no shoulder appeared.

Salt	Concentration in moles l. ⁻¹		$r^+ (\text{\AA})$
	1 M	2 M	
NH_4Cl	225.5	225.2	1.03
NaCl	225.4	224.7	0.98
KCl	225.2	224.5	1.33
CsCl	224.9	223.9†	1.65
Et_4NCl	223.8		2.28‡
$(n\text{-Bu})_4\text{NI}$	225.6§		4.4‡

† 1.8 M. ‡ Estimated from a model. § 7.33×10^{-2} M.

Table 3. Comparison of λ_{max} ($\text{m}\mu$) for iodide in aqueous salt solutions of electrolytes with crystallographic cation radius (r^+).

With 1:2-dimethoxyethane the $245\text{ m}\mu$ band broadens and then sharpens to a band at $235\text{ m}\mu$ as progressive amounts of the perchlorate are added. An examination of the band-width at half-height, the shape and relative heights of the bands at comparable concentrations suggests very strongly that the $245\text{ m}\mu$

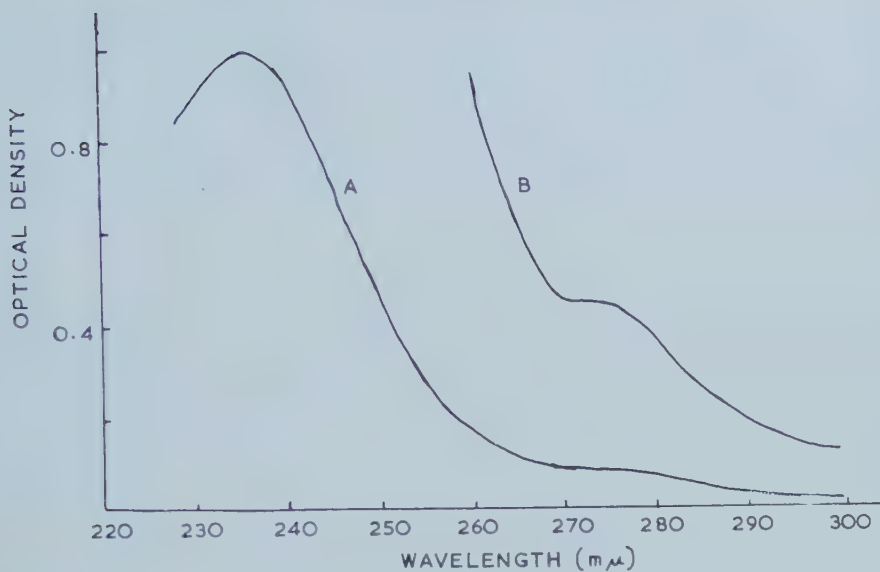


Figure 4. $(n\text{-Bu})_4\text{NI} + \text{excess } (n\text{-Bu})_4\text{NClO}_4$ in dioxan.
A, 0.1 cm cells; B, 1.0 cm cells.

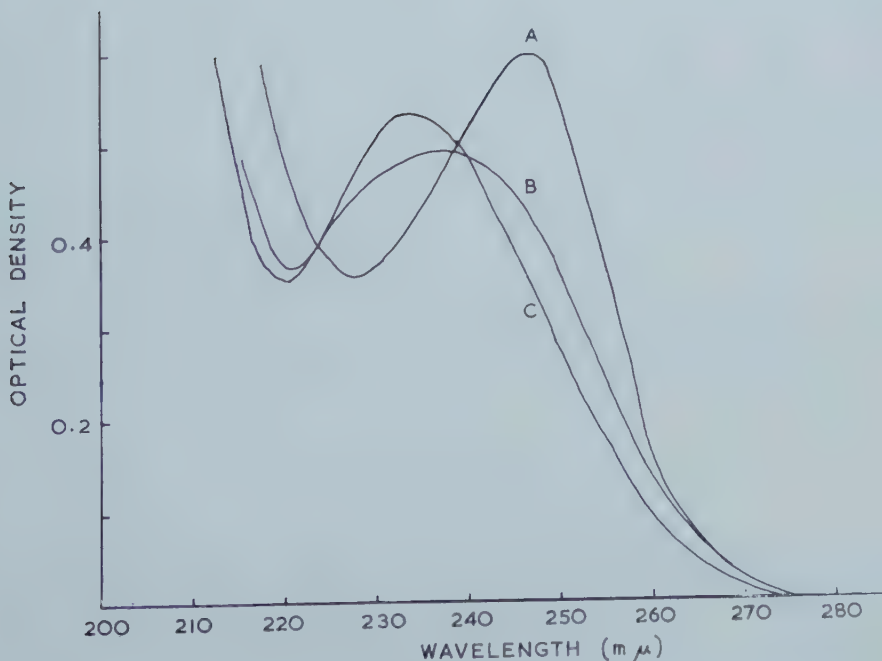


Figure 5. A, $(n\text{-Bu})_4\text{NI}$ in 1:2-dimethoxyethane; B, $(n\text{-Bu})_4\text{NI} + \text{some } (n\text{-Bu})_4\text{NI}$ in 1:2-dimethoxyethane; C, $(n\text{-Bu})_4\text{NI} + \text{excess } (n\text{-Bu})_4\text{NI}$ in 1:2-dimethoxyethane.

band falls as the $235 \text{ m}\mu$ band rises (figure 5). A large shift to high energy together with a marked broadening was also found when the perchlorate was added to a solution of iodide in chloroform. However the resolution of the bands was poor and precise measurements impossible.

Addition of the perchlorate to benzene or diethyl ether produced no effect on the shoulder at $290 \text{ m}\mu$ (figure 2).

4. DISCUSSION

4.1. Contact ion-pairs

The main feature of these results is that, in solvents of very low ion-solvating power such as carbon tetrachloride, a band in the $290 \text{ m}\mu$ region is found which has the following characteristics. (a) The band is not strongly solvent-dependent, in contrast with that due to solvated iodide ions [14]. In fact, the spectrum in certain mixed solvents (figure 3) is composed of two superimposed bands suggesting that two distinct species are present. This behaviour is quite different from that found with solvent mixtures containing only solvated iodide ions (figure 6). (b) Again in contrast with the band due to iodide ions in more polar solvents, the peak position is practically independent of temperature. If the semi-empirical correlation depicted in figure 1 of reference [14] (Part 2)

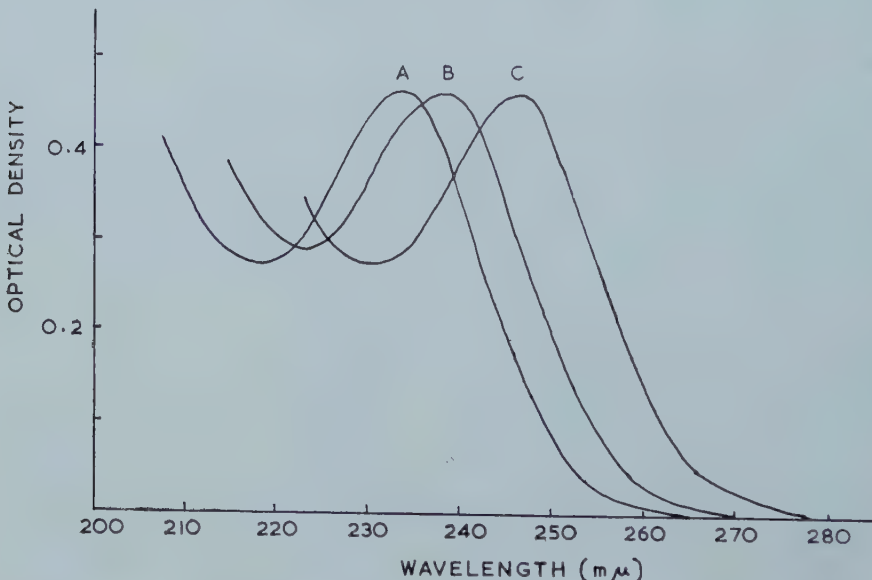


Figure 6. A, $(n\text{-Bu})_4\text{NI}$ in dioxan; B, $(n\text{-Bu})_4\text{NI}$ in dioxan/methyl cyanide mixture; C, $(n\text{-Bu})_4\text{NI}$ in methyl cyanide.

were obeyed, then a shift of $20 \text{ m}\mu$ would be predicted for a 50° change in temperature. (c) The band can be developed by addition of an excess of tetra-*n*-butylammonium perchlorate to a solution of tetra-*n*-butylammonium iodide in dioxan (figure 4). (d) The band maximum is found at progressively shorter wavelengths as the alkyl group (*R*) in R_4N^+ is reduced in size. Such dependence upon the nature of the cation is not detected in dilute solvents of iodides in more polar solvents [14] (compare § 3.1 and table 3).

Accordingly, we conclude that the new band in the $290\text{ m}\mu$ region is characteristic of the contact ion-pair $(n\text{-Bu})_4\text{N}^+\text{I}^-$ (and the $268\text{ m}\mu$ band of the contact ion-pair $(n\text{-Pr})_4\text{N}^+\text{I}^-$). If this conclusion is correct, then the prevalence of contact ion-pairs in solutions of electrolytes in solvents of low dielectric constant is far smaller than is commonly supposed. Since it is generally agreed that there is extensive ionic association in many of the solvents in which contact ion-pairs were not detected by our method it would seem that, contrary to recent conclusions [7, 8], solvent shared and solvent separated ion-pairs are distinct entities in these solutions.

This is our main conclusion; however, other aspects of the results require consideration. The solvents in which small concentrations of tetra-alkyl-ammonium iodide exist mainly as contact ion-pairs (CCl_4 and C_6H_6) have small or zero permanent dipole-moments and are therefore expected to be very poor ionic solvators. They are fairly polarizable, however, and it is probably this property which enables these solvents to retain contact ion-pairs in solution.

4.2. Solvent shared ion-pairs

Two features of the results with diethers are noteworthy. Addition of excess tetra-*n*-butylammonium perchlorate to iodide in 1:2-dimethoxyethane results, not in the usual salt shift, but in the formation of a new band at $235\text{ m}\mu$ (figure 5). Also, when excess perchlorate is added to iodide in dioxan, there is a *small* shift of the main band to higher energies, together with the development of a new band in the $280\text{ m}\mu$ region, characteristic of contact ion-pairs.

We tentatively conclude that the new band in 1:2-dimethoxyethane is due to solvent shared ion-pairs, since our previous discussion rules out contact ion-pairs and since by far the most probable alternative unit with sufficient specificity to give rise to a distinct band is the solvent-shared ion-pair.

There is further evidence that ion-pairs, other than contact ion-pairs, can give rise to unique absorption spectra. Since dioxan solutions give contact ion-pairs when excess tetra-*n*-butylammonium ions are added, it may be supposed that the iodide band at $235\text{ m}\mu$ is, at least in part, due to solvent shared ion-pairs. This band is far less sensitive to changes in temperature than would be expected for freely solvated iodide [14], in contrast with the bands for iodide in 1:3-dioxolane and 1:2-dimethoxyethane (see table 2).

We thus distinguish four classes of solvent: (i) in which contact ion-pairs predominate, (ii) in which solvent shared ion-pairs predominate but in which contact ion-pairs can form, (iii) in which solvent separated ion-pairs can form, and (iv) in which neither contact nor solvent shared ion-pairs can be detected under our conditions.

4.3. Solvent separated ion-pairs

Since conductivity studies suggest that some unspecified form of ion-pairing occurs in some solvents of class (iv) our results show that these ion-pairs are solvent separated and, indeed, that this form of loose association is probably more common than any other. It is noteworthy that solvents of class (iv), in which ionic association is thought to be important have low bulk dielectric constants but relatively large dipole moments.

4.4. *Nature of the electronic transition in contact ion-pairs*

The ultra-violet spectrum of solvated iodide has been discussed, and an approximate theory presented, which seems to explain qualitatively the large shifts which occur on changing environment [14]. This theory is probably also satisfactory for crystalline alkali iodides [16] and the transition has been described as charge-transfer to solvent (C.T.T.S.) [14]. In a crystal, the orbital containing the excited electron probably resembles the ground state orbital of an F-centre [17], the important feature being that it is symmetrical. For alkali halide contact ion-pairs in the gas phase, the transition, which almost certainly involves electron-transfer from the halide to the alkali metal ion, is found to be quite a different region of the spectrum [18]. If such an ion-pair existed in solution we would predict a shift of this band to higher energies, since solvation should stabilize the ground state more than the excited state. It is most unlikely that this effect would be large enough to shift the band into the 215–245 m μ region where most bands attributable to solvated iodide ions occur.

In the case of tetra-alkylammonium iodide contact ion-pairs it is postulated that the excitation is not C.T.T.S. but electron-transfer from iodide to the cation, the electron being held in an expanded orbital possibly similar to that described by Becker *et al.* [19] for the electron in metal-ammonia solutions. Since the intensity of these transitions is large, ϵ_{max} being greater than 10^4 , there must be considerable overlap between the postulated orbital of the cation and the iodide ion. Hence the cation-orbital must be very diffuse.

In this way the dependence upon the nature of the cation can be qualitatively understood although we can offer no quantitative explanation.

The appearance of a new band for solvent shared ion-pairs is less readily understood. We consider that the transition is C.T.T.S. since if it involved electron-transfer to the cation the intensity would surely be small in this case. The close proximity of the cation will distort the solvent shell surrounding iodide from spherical to axial symmetry: such distortions are known to shift the first excitation band for crystalline alkali iodides [20].

Since the iodide bands in solvents of classes (iii) and (iv) have properties similar to those of freely solvated iodide ions, it seems probable that in these cases the transition is C.T.T.S., and the cations are sufficiently far removed to have negligible influence.

4.5. *Concentrated aqueous electrolytes*

The results now described (table 3) confirm the view [6] that shifts to high energy found when iodide spectra are measured in aqueous solutions containing simple electrolytes in high concentration are not caused by specific ion-pairing. Thus, there is no evidence for the presence of any new band, which would be expected on the low-energy side of the main band for contact ion-pairs. Also, the bands are still sensitive to temperature, in contrast with the band ascribed to contact ion-pairs, and this temperature sensitivity fits the general correlation given earlier [14].

The earlier work, in which sodium and potassium salts were used, did not reveal the very slight differences now recorded for different positive ions. These differences were first observed by Stein and Treinin [21]. Any attempt to explain these specific effects is hindered by the fact that differences are very small compared with the overall shift for a given concentration of salt relative to aqueous iodide.

Taking dilute aqueous iodide as a reference, one could argue that the effect of positive ions increases with ionic radius. However, if one took a hypothetical 'ideal' solution containing electrolyte which did not interact with iodide in any specific manner, then one could suppose that this reference band would lie on the high energy side of all bands obtained from real solutions. In that case the deviation from ideality would increase with decreasing size of the cation. In view of these considerations no definite conclusions can be reached (however, see §4.6).

4.6. Relation to other work

The behaviour of the iodide band in concentrated aqueous electrolytes is thought to be due to a combination of effects including dehydration, fortuitous contacts and general polarization. Far more pronounced shifts have been found for the ^{133}Cs nuclear resonance line of aqueous caesium ions and the ^{19}F line of aqueous fluoride ions on the addition of other electrolytes. These shifts will be discussed in detail in a future paper [22].

What appears to be a similar effect to that reported here is found for hexamine cobaltic iodide and related compounds [23, 24]. Since the metal ions are already octahedrally bonded and exchange ligands slowly, the interaction, detected spectrophotometrically in the form of a new band in the $270\text{ m}\mu$ region, is thought to be due to charge-transfer between $\text{Co}(\text{NH}_3)_6^{3+}$ and I^- , when in contact. The small values estimated for the extinction coefficients of these bands suggests that the excited state does not resemble that postulated for tetra-alkylammonium iodide contact ion-pairs. Probably the electron is transferred to an orbital somewhat localized on the central metal atom and hence the transition probability reduced: however, it is also possible that the extinction coefficients reported [23, 24] are too small [25].

Finally, some reference should be made to a considerable body of work relating to ion-pair formation derived from studies of organic reaction mechanisms. Ingold and co-workers have made extensive kinetic studies of the reactions of triarylmethyl compounds in benzene [26]. An essential aspect of this work is that electrolytes are present as contact ion-pairs. Our work confirms this postulate, in the particular case of tetra-alkylammonium halides. Contact ion-pairs are likely to be still more favoured when triarylmethyl carbonium ions are one component, since the high acceptor power of these cations should make charge-transfer forces of considerable importance. These forces probably contribute to the stability of the carbonium ion ion-pairs shown to occur in solvents of low dielectric constant by Evans and co-workers [27].

In these studies [26, 27] only contact ion-pairs are considered as specific entities. By studying salt effects on the rates of solvolysis and racemization of various organic compounds, Winstein and co-workers have found evidence both for contact and solvent separated ion-pairs [28]. It is remarkable that these results yield values for the solvating power of the solvents used which closely parallel those given by Kosower derived from the effects of solvent upon the spectra of substituted pyridinium iodide charge-transfer complexes [12].

We are grateful to the University of Southampton for a maintenance grant to
T. R. G.

REFERENCES

- [1] AMES, D. P., and WILLARD, J. E., 1953, *J. Amer. chem. Soc.*, **75**, 3267.
- [2] GIMBLETT, F. G. R., and MONK, C. B., 1955, *Trans. Faraday Soc.*, **51**, 793.
- [3] DAVIES, W. G., OTTER, R. J., and PRUE, J. E., 1957, *Disc. Faraday Soc.*, **24**, 103.
- [4] SMITHSON, J. M., and WILLIAMS, R. J. P., 1958, *J. chem. Soc.*, p. 457.
- [5] POPOV, H. I., and HUMPHREY, R. E., 1959, *J. Amer. chem. Soc.*, **81**, 2043.
- [6] SMITH, M., and SYMONS, M. C. R., 1957, *Disc. Faraday Soc.*, **24**, 206.
- [7] FUOSS, R. M., 1958, *J. Amer. chem. Soc.*, **80**, 5059.
- [8] DENISON, J. T., and RAMSEY, J. B., 1955, *J. Amer. chem. Soc.*, **77**, 2615.
- [9] PRUE, J. E., and OTTER, R. J., 1957, *Disc. Faraday Soc.*, **24**, 123.
- [10] GUGGENHEIM, E. A., 1957, *Disc. Faraday Soc.*, **24**, 53.
- [11] EIGEN, M., 1957, *Disc. Faraday Soc.*, **24**, 25, 119.
- [12] KOSOWER, E. M., 1956, *J. Amer. chem. Soc.*, **78**, 5700.
- [13] KOLTHOFF, I. M., STOCESOCA, D., and LEE, T. S., 1953, *J. Amer. chem. Soc.*, **75**, 1834.
- [14] SMITH, M., and SYMONS, M. C. R., 1958, *Trans. Faraday Soc.*, **54**, 338, 346.
- [15] GRIFFITHS, T. R., LOTT, K. A. K., and SYMONS, M. C. R., 1959, *Analyt. Chem.*, **31**, 1338.
- [16] RHODES, E., and UBBELOHDE, A. R., 1959, *Proc. roy. Soc. A*, **251**, 156.
- [17] DOYLE, W. T., and SYMONS, M. C. R., 1960, *Quart. Rev.* (in the press).
- [18] ORGEL, L. E., 1954, *Quart. Rev.*, **8**, 422.
- [19] BECKER, E., LINDQUIST, R. H., and ALDER, B. J., 1956, *J. chem. Phys.*, **25**, 971.
- [20] MARTIENSSSEN, W., 1957, *J. Phys. Chem. Solids*, **2**, 257.
- [21] STEIN, G., and TREININ, A. (private communication).
- [22] CARRINGTON, A., and SYMONS, M. C. R., 1960, *Mol. Phys.* (in press).
- [23] LINHARD, M., and WEIGEL, M., 1951, *Z. anorg. Chem.*, **266**, 49.
- [24] EVANS, M. G., and NANCILLAS, G. H., 1953, *Trans. Faraday Soc.*, **49**, 363.
- [25] KING, E. L., ESPENSON, J. H., and VISCO, R. E., 1959, *J. phys. Chem.*, **63**, 755.
- [26] HUGHES, E. D., INGOLD, C. K., PATAI, S., and POCKER, Y., 1957, *J. chem. Soc.*, p. 1206.
- [27] BAYLES, J. W., EVANS, A. G., and JONES, J. R., 1955, *J. chem. Soc.*, p. 206
- [28] WINSTEIN, S., 1955, *Experientia Supplementum*, II, 152.

RESEARCH NOTE

Electron resonance study of the carboxylate hydroxy methyl radical ion

by N. M. ATHERTON and D. H. WHIFFEN

Chemistry Department, The University, Birmingham, 15

(Received 27 August 1959)

In a recent paper [1] results were given for an electron resonance study of the carboxy hydroxy methyl radical HOCHCOOH . Earlier work [2] suggested that gamma-rays decomposed glycollic acid and its calcium salt in a similar manner and it is of interest to compare the coupling parameters of the carboxylate hydroxy methyl radical ion, HOCHCO_2^- with those of the acid.

A single crystal of potassium glycollate was grown from water and irradiated with $^{60}\text{Co} \gamma$ -rays. This was examined and the spectra interpreted in a manner entirely analogous to that used for the acid [1]. The spectra show many resemblances and the coupling tensors of the salt shown in the table are similar to those for the acid. The crystal was elongated along the x direction but as the faces were not well developed and the crystal structure is unknown, the y and z directions were chosen in a manner which led to simplicity in expression of the results and analogy with the acid. The tensors are consistent with orthorhombic symmetry.

Tensor in Cartesian axes			Principal values	Isotropic component	Anisotropic components		
					Value	Direction cosines	
H(C)	+50	0	0	(-) 80	(-) 51	(-) 29	(0, 0.71, ± 0.70)
	(-)	0	+52 ± 29	(-) 50		(+) 1	(1, 0, 0)
	0	± 29	+51	(-) 23		(+) 28	(0, 0.70, ∓ 0.71)
H(O)	+12	0	0	(+?) 18	(+?) 7	(+?) 11	(0, 0.97, ∓ 0.23)
	(+?)	0	+17 ∓ 6	(+?) 12		(+?) 5	(1, 0, 0)
	0	∓ 6	-7	(-?) 8		(-?) 15	(0, 0.23, ± 0.97)
g	2.0021	0	0	2.0054	2.0038	(0, 0.13, ± 0.99)	
	(-)	0	2.0039 ± 0.0002	2.0039		(0, 0.99, ∓ 0.13)	
	0	± 0.0002	2.0054	2.0021		(1, 0, 0)	

Coupling tensors (Mc/s) and g -tensor.

Upper and lower signs refer consistently to the magnetically distinguishable sites in the unit cell.

A comparison between the acid and the salt shows the anisotropic H(C) couplings to be the same within experimental error and consistent with the theory [3]. The isotropic coupling for H(C) appears to be slightly smaller

for the salt (-51 Mc/s) than for the acid (-57 Mc/s). The H(O) isotropic couplings agree in magnitude (7 Mc/s for the salt, 8 Mc/s for the acid) and this confirms the earlier attribution of the coupling to the hydroxyl hydrogen, as opposed to that of the carboxylic acid group. The anisotropic H(O) components differ appreciably. This may be a consequence of a different position for the hydrogen; such a change might arise because of the requirement of intermolecular hydrogen bonding. It can be seen that in the salt the largest anisotropic component is of the opposite sign to the isotropic component whereas in the acid they were of the same sign. This curious reversal makes it difficult to be confident of the absolute sign of the H(O) couplings in either radical. Either the isotropic components are of the same sign and the anisotropic components differ markedly or the anisotropies are similar in magnitude and the isotropic components are reversed in sign. The second alternative is less likely as it would remove the approximate agreement (to 15°) which exists in the relative directions of corresponding principal axes in the two radicals. The ion resembles the radical in having a smaller g value for magnetic fields perpendicular to its plane than for fields lying in the plane.

All the radicals appear to lie parallel to each other and perpendicular to the direction of elongation of the crystal. It is to be expected that the undamaged glycolate host ions are similarly arranged.

N. M. A. wishes to acknowledge support from the D.S.I.R.

REFERENCES

- [1] ATHERTON, N. M., and WHIFFEN, D. H., 1960, *Mol. Phys.*, **3**, 1.
- [2] GRANT, P. M., WARD, R. B., and WHIFFEN, D. H., 1958, *J. chem. Soc.*, 4635.
- [3] McCONNELL, H. M., and STRATHDEE, J., 1959, *Mol. Phys.*, **2**, 129.

Intramolecular charge-transfer absorption spectra of formamide and acrolein†

by S. NAGAKURA‡

Laboratory of Molecular Structure and Spectra, Department of Physics,
University of Chicago

(Received 30 September 1959)

To test further Nagakura and Tanaka's conception of intramolecular charge-transfer absorption, an improved calculation based on Longuet-Higgins and Murrell's method was carried out for the π -electron structures of formamide and acrolein. This shows that the 1717 Å band of formamide and 1935 Å band of acrolein can be regarded as intramolecular charge-transfer absorption bands in the sense that the excited state wave functions for these two bands are mainly constructed of the charge-transfer configuration, and that the transitions corresponding to these bands are accompanied by a large amount of electron transfer from electron donor towards acceptor. The 1717 Å band of formamide can *not* be interpreted as a shifted 1560 Å formaldehyde band. The latter band must shift to *shorter* wavelengths as the result of interaction with non-bonding electrons of the nitrogen atom. Similar blue shifts occur in acrolein for the C=C and C=O $\pi \rightarrow \pi^*$ bands relative to the corresponding bands of ethylene and formaldehyde. Similar causes operate in the blue shifts of the non-charge-transfer bands of donor-acceptor molecular complexes.

1. INTRODUCTION

Appearance of an absorption band characteristic of a molecular compound between an electron donor and acceptor has been well known since in 1949 Benesi and Hildebrand found it for the iodine complex with benzene [1]. This kind of band has been observed with various molecular compounds, such as iodine complexes with mesitylene [2], pyridine [3], ethyl ether [4], and triethylamine [5]. Mulliken interpreted it as a transition between two levels caused by resonance of no-bond and dative structures, with an electron transferred from donor to acceptor and a covalent bond formed between them in the dative structure, and called the band an (intermolecular) charge-transfer absorption band [6].

It seems reasonable to expect that a similar phenomenon occurs within a molecule which is composed of electron donating and accepting groups. More precisely, when an electron donating group, say an amino group, and an electron accepting group, say a carbonyl or nitro group, combine with each other directly or through a bridge of conjugated double bonds, so that π electrons are able to migrate from the former to the latter, it may be expected that the system gives rise to a special absorption band inherent to neither of the components. By analogy with the case of molecular compounds, it may be called an intra-molecular charge-transfer absorption. In fact, Nagakura showed in previous papers that strong

† This work was assisted by the Office of Ordnance Research Under Project TB2-0001 (505) of Contract DA-11-022-ORD-1002 with the University of Chicago.

‡ Permanent address: The Institute for Solid State Physics, The University of Tokyo, Merguro-ku, Tokyo.

absorption bands observed with a number of molecules containing the nitro or carbonyl group can be interpreted as intramolecular charge-transfer absorption bands [7]. Further, Murrell and Longuet-Higgins showed that the $253 \text{ m}\mu$ band of aniline may be regarded as due to charge-transfer absorption [8]†.

In Nagakura's previous calculation, some rough approximations were used to simplify the computation and to make it possible to apply it to complex molecules like nitrostyrene and nitroaniline. The purpose of the present paper is to re-enforce the previous calculations and interpretation by applying an improved method to rather simple molecules like formamide ($\text{H}_2\text{N}-\text{HC}=\text{O}$) and acrolein ($\text{H}_2\text{C}=\text{CH}-\text{HC}=\text{O}$). In addition, some discussion will be given of the blue shift shown by bands characteristic of the electron accepting molecule or group when the latter becomes a part of either an inter- or an intramolecular charge-transfer system.

2. METHOD OF CALCULATION

Let us consider a molecule composed of two groups, D and A, joined by a single bond. Here D and A designate an electron donor and an electron acceptor radical. In the present treatment, only π electrons are taken into account, and the wave function for the molecule as a whole is constructed from π MO (molecular orbital) wave functions of D and A, and for this purpose it is assumed that π -electron functions of DH and AH molecules can be used. Here AH is formaldehyde ($\text{H}_2\text{C}=\text{O}$), and we employ the LCAO MO wave functions evaluated by Kon [9] by combining Pariser and Parr's method [10] with Roothaan's SCF procedure [11]. These are as follows:

$$\left. \begin{aligned} \phi_{\text{C}=\text{O}}^f &= 0.5472 \chi_{\text{C}} + 0.8370 \chi_{\text{O}} \\ \phi_{\text{C}=\text{O}}^v &= 0.8370 \chi_{\text{C}} - 0.5472 \chi_{\text{O}} \end{aligned} \right\} \quad (1)$$

where $\phi_{\text{C}=\text{O}}^f$ and $\phi_{\text{C}=\text{O}}^v$ are the highest occupied and the lowest vacant π MO, respectively, and χ_{C} and χ_{O} are $2p\pi$ AO's (atomic orbitals) on carbon and oxygen, respectively. The DH molecules are NH_3 and $\text{CH}_2=\text{CH}_2$ for formamide and acrolein respectively. For NH_3 , the required donor MO is the $2p\pi$ non-bonding AO (χ_{N}) of nitrogen itself [12]‡, and for $\text{CH}_2=\text{CH}_2$ the highest occupied ($\phi_{\text{C}=\text{C}}^f$) and the lowest vacant ($\phi_{\text{C}=\text{C}}^v$) MO's in LCAO approximation are:

$$\phi_{\text{C}=\text{C}}^f = \frac{1}{\sqrt{2}} (\chi_{\text{C}1} + \chi_{\text{C}2}); \quad \phi_{\text{C}=\text{C}}^v = \frac{1}{\sqrt{2}} (\chi_{\text{C}1} - \chi_{\text{C}2}). \quad (2)$$

From the above-mentioned MO's, a number of electron configurations can be constructed for each molecule. Let us take three and four of these configurations for formamide and acrolein, respectively, as shown in figure 1 §.

† In these papers, the authors adopted the term electron-transfer instead of charge-transfer.

‡ In order that the non-bonding orbital of nitrogen may be a pure $2p\pi$ orbital, the formamide molecule must be planar. From microwave work, it is evident that this condition is completely satisfied.

§ Besides these, several others could be considered in a more exact treatment. For example, for acrolein, the charge-transfer configuration in which an electron is transferred from the $\text{C}=\text{O}$ towards $\text{C}=\text{C}$ should be taken into account. However, since this configuration is thought to have appreciably higher energy than the others, it may reasonably be neglected. This neglect corresponds to the view that acrolein can be fairly well described in terms of resonance between two structures, $\text{H}_2\text{C}=\text{CH}-\text{HC}=\text{O}$, $\text{H}_2\text{C}^+-\text{CH}=\text{HC}-\text{O}^-$, omitting the structure $\text{H}_2\text{C}^--\text{CH}=\text{HC}-\text{O}^+$.

In this figure, the term 'locally excited configuration' is due to Longuet-Higgins and Murrell [8].

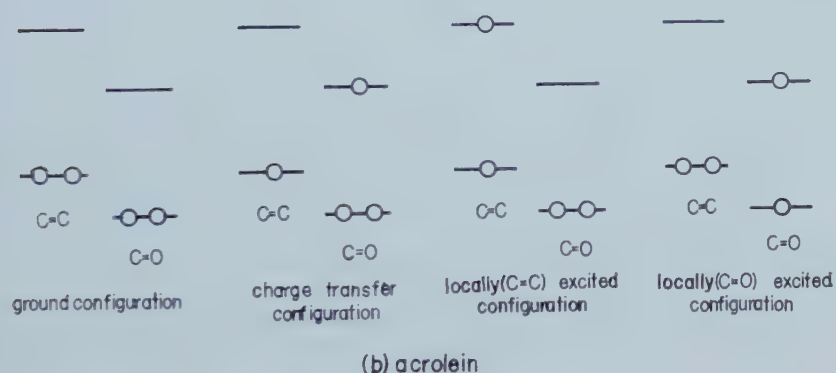
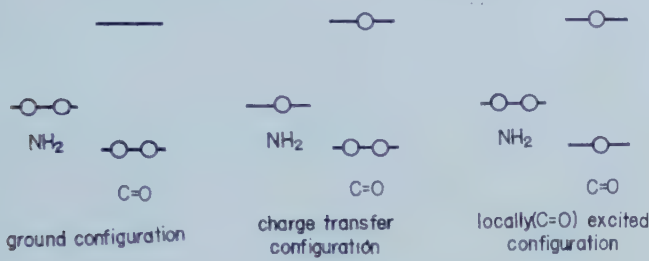


Figure 1. Electron configurations for formamide and acrolein.

The wave function for each configuration can be written as an antisymmetrized product of occupied MO's†. For example, the wave function (ψ)^F_{CT} for the charge-transfer configuration of formamide can be represented as follows:

$$\psi^F_{CT} = \frac{1}{\sqrt{(4!)}} \sum (-1)^n P \{ \phi^f_{C=O}(1)\alpha(1) \phi^f_{C=O}(2)\beta(2) \phi^v_{C=O}(3)\alpha(3) \chi_N(4)\beta(4) \}. \quad (3)$$

Here $\sum (-1)^n P$ is the usual antisymmetrizing summation over all permutations of the electrons. Taking the energy of the ground configuration as the standard, the energy values of the locally excited configurations can be determined by using experimental results on ultra-violet absorption spectra of DH and AH. From the position of the absorption band corresponding to the $\pi - \pi^*$ transition in formaldehyde [13], the energy of the locally (C=O) excited configuration ($E_{C=O}$) is assigned at 7.918 ev. This value is here used for both formamide and acrolein. In a similar way, the locally (C=C) excitation energy ($E_{C=C}^A$) is determined as 7.60 ev [14]‡. The energy for the charge-transfer configuration can be evaluated using wave functions like equation (3), assuming zero differential

† In the present treatment the triplet state is not taken into account.

‡ The peak of the $\pi - \pi^*$ absorption band of ethylene appears at 1625 Å.

overlap [10] and neglecting the penetration integrals [9]. The actual form in the case of formamide is as follows:

$$E_{CT}^F = I_D - A_{C=O} - (0.5472)^2[CC|NN] - (0.8370)^2[OO|NN]. \quad (4)$$

Here I_D and $A_{C=O}$ are the ionization potential of DH and the electron affinity of AH, respectively. The former is taken from data published by Watanabe [15]. The latter is regarded as an experimental parameter and assumed as -1.20 eV for both formamide and acrolein†. Two-centre repulsion integrals of the type ($[CC|NN] = \int \chi_C(\mu)\chi_N(\nu)(e^2/r_{\mu\nu})\chi_C(\mu)\chi_N(\nu)d\tau$) in equation (4), are calculated by combining Pariser and Parr's [10] and Pariser's [16] approximation for the one-centre repulsion integral with the uniformly charged sphere approximation [17]. Valence-state ionization potentials and electron affinities for carbon, oxygen, and nitrogen necessary for evaluating one-centre repulsion integrals are taken from Pritchard and Skinner's table [18]. The values of two-centre repulsion integrals for the appropriate bond distances of the molecules under consideration are given in table 1, together with energy values for charge-transfer configurations (E_{CT}).

Formamide‡	Acrolein‡
$[CC NN]_{1.38} = 7.842$	$[CC C_1C_1]_{1.46} = 7.245$
$[OO NN]_{2.28} = 6.429$	$[CC C_2C_2]_{2.44} = 5.423$
$I_O = 10.25$	$[OO C_1C_1]_{2.32} = 5.800$
$A_{C=O} = -1.20$	$[OO C_2C_2]_{3.53} = 3.964$
$E_{CT}^F = 10.25 + 1.20 - 6.85 = 4.60$	$E_{CT}^A = 10.52 + 1.20 - 5.32 = 6.40$

† Distances between atoms are taken from the data by Kimura and Aoki (Kimura, M., and Aoki, M., 1953, *Bull. chem. Soc. Japan*, 36, 429).

‡ Distances between atoms are taken from the data by Mackle and Sutton (Mackle, H., and Sutton, L. E., 1951, *Trans. Faraday Soc.*, 47, 691).

Table 1. Two-centre repulsion integrals, ionization potentials of electron donors, and energies of charge-transfer configurations (in eV).

$$\begin{array}{ll} H_{G, CT}^F = 1.184\beta_{CN} & H_{CT, C=C}^A = 0.8370\beta_{CC}/\sqrt{2} \\ H_{CT, C=O}^F = -0.5472\beta_{CN} & H_{CT, C=O}^A = -0.5472\beta_{CC}/\sqrt{2} \\ H_{G, C=O}^F = H_{G, C=O}^A = H_{G, C=C}^A = 0 & H_{C=O, C=C}^A = -0.0064 \text{ eV} \\ H_{G, CT}^A = 1.184\beta_{CC}/\sqrt{2} & \end{array}$$

Superscripts F and A refer to formamide and acrolein, respectively

Table 2. Values of off-diagonal matrix elements.

When two groups D and A approach each other to form DA, the π -electron structure of each group is thought to change appreciably. To understand the ground and excited states of DA, it is necessary to consider interaction among the several configurations shown in figure 1. For this purpose, the off-diagonal matrix elements of the total electronic Hamiltonian, each of which represents the magnitude of the interaction between two different configurations, are needed in addition to the diagonal matrix elements whose evaluation has already been described. The evaluation of the off-diagonal element ($H_{A, B}$) is carried out by the aid of the formulation by Pople [19] and by Longuet-Higgins and Murrell [8]. The results are shown in table 2.

† This value is also applicable to explaining the charge-transfer absorption of benzaldehyde.

Here β_{CN} and β_{CC} are the core exchange integral for the C—N bond of formamide and for the C—C bond of acrolein, respectively. The latter is assigned as -1.70 ev. This value seems to be reasonable in comparison with that for butadiene (-1.68 ev)†. Concerning the value of β_{CN} , a value of 2.60 ev is employed†.

Solving the secular equation constructed for each molecule by the use of the matrix elements evaluated above, energy levels and wave functions of formamide and acrolein are obtained as shown in table 3. The relation of the energy levels of each molecule as finally evaluated to those of the original configurations is depicted in figure 2.

Formamide

$$\begin{aligned} W^F_0 &= -1.5866, \quad \Psi^F_0 = 0.8868\psi_G^F + 0.4571\psi_{CT}^F - 0.0685\psi_{C=O}^F \\ W^F_1 &= 5.4907, \quad \Psi^F_1 = 0.4352\psi_G^F - 0.7762\psi_{CT}^F + 0.4563\psi_{C=O}^F \\ W^F_2 &= 8.6059, \quad \Psi^F_2 = 0.1553\psi_G^F + 0.4342\psi_{CT}^F + 0.8874\psi_{C=O}^F \end{aligned}$$

Acrolein

$$\begin{aligned} W^A_0 &= -0.3101, \quad \Psi^A_0 = 0.9766\psi_G^A + 0.2128\psi_{CT}^A + 0.0271\psi_{C=C}^A - 0.0170\psi_{C=O}^A \\ W^A_1 &= 5.9231, \quad \Psi^A_1 = -0.1945\psi_G^A + 0.8098\psi_{CT}^A + 0.4851\psi_{C=C}^A - 0.2665\psi_{C=O}^A \\ W^A_2 &= 7.7934, \quad \Psi^A_2 = 0.0234\psi_G^A - 0.1279\psi_{CT}^A + 0.6405\psi_{C=C}^A + 0.7569\psi_{C=O}^A \\ W^A_3 &= 8.5036, \quad \Psi^A_3 = 0.0886\psi_G^A + 0.5293\psi_{CT}^A - 0.6002\psi_{C=C}^A + 0.5930\psi_{C=O}^A \end{aligned}$$

ψ_G , ψ_{CT} , $\psi_{C=C}$ and $\psi_{C=O}$ designate the wave functions for the ground, charge-transfer, locally (C=C) excited, and locally (C=O) excited configurations, respectively. Supercripts F and A refer to formamide and acrolein respectively.

Table 3. Energy levels (W in ev) and wave functions (Ψ) obtained for formamide and acrolein.

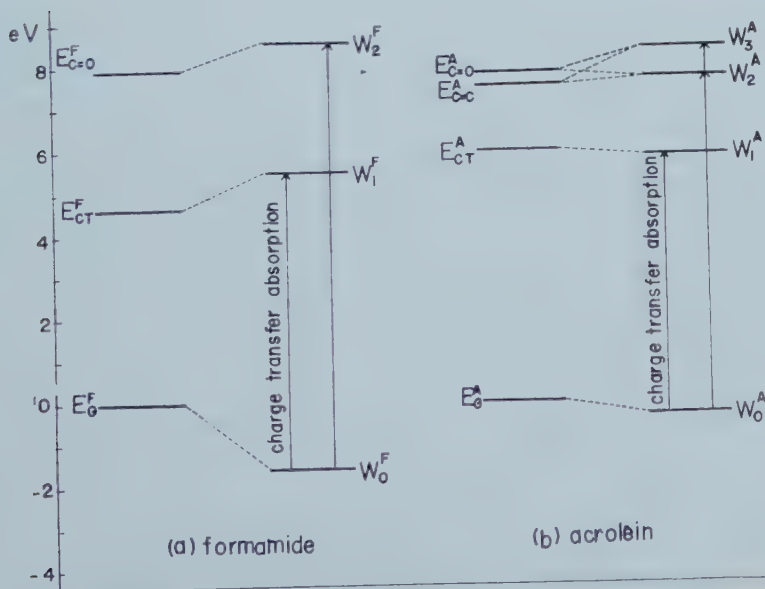


Figure 2. Energy level diagrams for formamide and acrolein.

† Pariser and Parr [10] estimated the core exchange integral value for the C—N bond of s-triazine as -2.576 ev. This value is very close to the β_{CN} value used in the present paper.

3. RESULTS AND DISCUSSION

3.1. Formamide

Looking at the results on formamide given in table 3 and figure 2 (*a*) it is seen that the ground state is lower by 1.587 ev (36.6 kcal/mol) than the unperturbed ground configuration. This stabilization energy, which clearly is mainly brought about by the interaction between the ground and charge-transfer configurations, may be regarded as corresponding to the vertical resonance energy due to the resonance hybrid between following two structures:—



Before the theoretical value is compared with the observed, the compression energy contribution must be considered. This was estimated by Tanaka as 13 kcal/mol [20]. Making allowance for it, the net calculated resonance energy is 23.6 kcal/mol. This agrees well with the value of 21~22 kcal/mol estimated from the heat of combustion [21].

Let us now turn to the excitation energy. According to table 3, the excitation energy corresponding to the $W^F_0 \rightarrow W^F_1$ transition is 7.08 ev. The ultra-violet absorption spectrum of formamide was measured in the gaseous state by Hunt and Simpson [22]. Their results show strong $\pi \rightarrow \pi^*$ bands at 1717 Å (7.19 ev) and 1345 Å (9.19 ev). The former band evidently corresponds to the $W^F_0 \rightarrow W^F_1$ transition of the present calculation. On the basis of the wave functions in table 3, the contributions of the charge-transfer configuration to the ground and excited states Ψ^F_0 and Ψ^F_1 amount to 20 per cent and 60 per cent respectively. This means that the $W^F_0 \rightarrow W^F_1$ transition involves a large amount of electron transfer from the electron-donating group toward the electron-accepting group, so that the absorption due to this transition may properly be called an intramolecular charge-transfer absorption by analogy with Mulliken's nomenclature in the case of a molecular complex between an electron donor and acceptor [6].

A polarized ultraviolet absorption study of the myristamide crystal carried out by Peterson and Simpson [23] gives additional support to the above interpretation. They find the direction of the transition moment of the 1860 Å band,

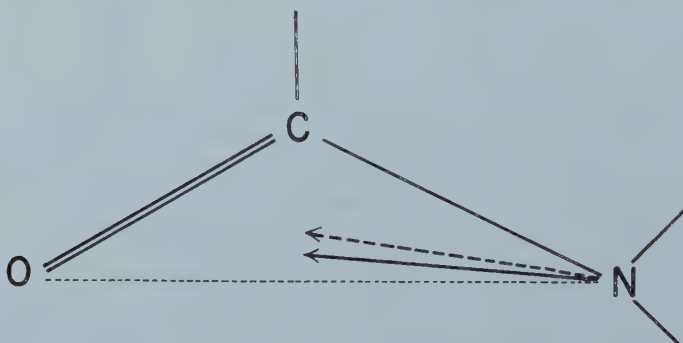


Figure 3. Direction of the transition moment for the intramolecular charge transfer band of amide.

→ theoretical

→ observed (by Peterson and Simpson [23]).

which undoubtedly corresponds to the 1717 Å band of formamide, to be inclined away from the nitrogen-oxygen axis by 9·1° toward the carbon-nitrogen axis. The present theoretical calculation leads to the conclusion that this angle should be 5°. The fact that the experimental and theoretical directions of the transition moment are fairly well coincident, as is seen from figure 3, and lie between the C—N and O—N axes, shows that our interpretation of the 1717 Å band of formamide as intramolecular charge-transfer absorption is more reasonable than that of regarding it as analogous to the 1560 Å band of formaldehyde. In our opinion, the latter band shifts to shorter wavelengths in formamide as the result of interaction with the non-bonding orbital of nitrogen. In fact, the 1345 Å formamide band can be interpreted as a shifted 1560 Å band of formaldehyde.

3.2. Acrolein

The calculations on acrolein summarized in table 3 indicate that the magnitude of the contribution of the charge-transfer configuration to the ground state is about 5 per cent and that the stabilization energy due to this contribution amounts to 7·2 kcal mol†. This energy may approximately be regarded as the vertical resonance energy of acrolein, namely, the energy stabilization caused by resonance between the following two structures:



In this connection, it is a matter of interest to refer to the Stark effect microwave-spectroscopic work carried out by Wagner *et al.* [24]. According to their measurements, acrolein has respective dipole moment components of 3·06D and of 0·54D in directions parallel and perpendicular to the $\text{C}=\text{O}$ bond. From this experimental result, assuming that the total dipole moment of acrolein is composed of (a) the moment inherent to the $\text{C}=\text{O}$ bond [25]‡, and (b) the resonance moment caused by the contribution of the polar structure, it is derived that the amount of polar structure in the resonance hybrid is 7~9 per cent [25]‡, somewhat larger than the above theoretical value of 5 per cent. However, too much importance should not be attached to this discrepancy, because of several approximations both in the theoretical calculation and in the estimation from the experimental dipole moment.

Turning attention to excited states of acrolein, one finds from the results given in table 3 that the contribution of the charge-transfer configurations to the lowest excited state (W_{11}^A) amounts to 65 per cent, as compared with 5 per cent in the ground state. Thus, the absorption due to the transition between these two

† In order to compare this value with the experimental resonance energy it is necessary to consider the compression energy, which may amount to 2~3 kcal/mol. Although the resonance energy of crotonaldehyde ($\text{H}_2\text{CCH}=\text{CH}-\text{HC}=\text{O}$) is estimated at 2·4 kcal/mol from the heat of hydrogenation (ref. 21, p. 85) unfortunately an estimated value has not been found for acrolein.

‡ In this estimation the reasonable value of 2·3D was taken as the dipole moment of the $\text{C}=\text{O}$ bond.

states may be called an intramolecular charge transfer absorption in the same sense as for the 1717 Å band to formamide.

The ultra-violet absorption spectrum of acrolein shows several bands in the near and far ultra-violet [26]. The longest wavelength band, which appears at 3300 Å, is undoubtedly due to an $n \rightarrow \pi^*$ transition. The strong band, which was assigned as an NV ($\pi \rightarrow \pi^*$) transition band by Walsh, appears at 1935 Å. Since the corresponding excitation energy (6.32 ev) is very close to the presently calculated energy difference (6.23 ev) between the ground and the lowest excited state, it seems sure that the strong band under consideration corresponds to the $W^A_0 \rightarrow W^A_1$ transition and therefore can be interpreted as the intramolecular charge-transfer absorption. Other shorter wavelength bands of acrolein will be discussed in the following section.

3.3. Blue shift of the absorption band of the C=O bond

In this section, consideration will be given to absorption bands other than those described in §§ 3.1 and 3.2. Let us first consider the $W^F_0 \rightarrow W^F_2$ transition (cf. figure 2 and table 3) of formamide. Since in the excited state of this transition, according to table 3, the contribution of the locally (C=O) excited configuration is overwhelmingly large, the corresponding band may be obviously regarded as a shifted 1560 Å band of formaldehyde. The calculated excitation energy (10.19 ev) for this transition is certainly larger than that (7.918 ev) for the $\pi \rightarrow \pi^*$ transition of formaldehyde itself. It is expected from this that, as the result of the interaction between π electrons of the C=O bond and non-bonding electrons of nitrogen, the band due to the former shifts toward shorter wavelengths. In fact, it seems sure that the 1345 Å band of formamide observed by Hunt and Simpson [22] corresponds to the $W^F_0 \rightarrow W^F_2$ transition and may be regarded as a shifted 1560 Å band of formaldehyde.

For acrolein, two absorption bands corresponding to $\pi \rightarrow \pi^*$ transitions were found at 1480 Å (8.35 ev) and 1460 Å (8.46 ev) by Walsh [26]. Although assignments of these two bands are not conclusive, the present result seems to support the interpretation that the longer and shorter wavelength bands correspond to the $W^A_0 \rightarrow W^A_2$ and $W^A_0 \rightarrow W^A_3$ transitions, respectively†. It is difficult to determine which of these two bands is the characteristic one of the C=O bond, because the locally excited configurations $E^A_{C=C}$ and $E^A_{C=O}$ in figure 2 (b) mix with each other to almost equal extents in both excited states W^A_2 and W^A_3 according to table 3. At any rate, it is clear that both of the above-mentioned absorption band of acrolein appear at shorter wavelengths than the 1560 Å band of formaldehyde.

It is worthy of remark that similar phenomena have been observed in the case of molecular complex formation between electron donors and acceptors. For example, the visible band of iodine shifts to shorter wavelengths when it enters into molecular complex formation with various electron donors, [27] for example benzene [1], pyridine [3], triethylamine [5] and pyridine N-oxide [28]. Thus, in addition to the appearance of charge-transfer absorption, another parallelism between intra- and inter-molecular interactions is found with respect to the shift

† For acrolein, Walsh [26] observed six absorption bands at 3300 Å, 1935 Å, 1750 Å, 1640 Å, 1480 Å and 1460 Å. According to the assignment by him, the third and fourth bands correspond to the $n-\sigma$ and Rydberg transitions, respectively. Therefore, these two bands are not of concern in the present paper.

of the absorption band of the electron acceptor. Looking at figure 2, it is seen that the energy stabilization of the ground configuration E_u caused by interaction with the charge-transfer configuration plays an important rôle in the blue shift phenomenon observed in the intramolecular cases. It should play a similar rôle in the intermolecular case, although other factors may also be important, especially in the iodine complexes [27].

ACKNOWLEDGMENTS

The author wishes to express his sincere thanks to Professor R. S. Mulliken for his kindness in reading and suggesting changes in the manuscript and in other helpful suggestions. His thanks are also due to Professor J. R. Platt and other members of the Laboratory for the hospitality shown during his stay at Chicago.

REFERENCES

- [1] BENESI, H. A., and HILDEBRAND, J. H., 1949, *J. Amer. chem. Soc.*, **71**, 2703.
- [2] ANDREWS, L. J., and KEEFER, R. M., 1952, *J. Amer. chem. Soc.*, **74**, 4500.
- [3] REID, C., and MULLIKEN, R. S., 1954, *J. Amer. chem. Soc.*, **76**, 3869.
- [4] deMAINE, P. A. D., 1957, *J. chem. Phys.*, **26**, 1192.
- [5] NAGAKURA, S., 1958, *J. Amer. chem. Soc.*, **80**, 520.
- [6] MULLIKEN, R. S., 1950, *J. Amer. chem. Soc.*, **72**, 600; 1952, *Ibid.*, **74**, 811; 1952, *J. phys. Chem.*, **56**, 801.
- [7] NAGAKURA, S., and TANAKA, J., 1953, *J. chem. Phys.*, **22**, 236; NAGAKURA, S., 1955, *J. chem. Phys.*, **23**, 1441; TANAKA, J., and NAGAKURA, S., 1956, *Ibid.*, **24**, 1274.
- [8] MURRELL, J. N., 1955, *Proc. phys. Soc., Lond. A*, **68**, 969; 1955, LONGUET-HIGGINS, H. C., and MURRELL, J. N., 1955, *Proc. phys. Soc., Lond. A*, **68**, 601.
- [9] KON, H., 1955, *Bull. chem. Soc. Japan*, **28**, 275.
- [10] PARISER, R., and PARR, R. G., 1953, *J. chem. Phys.*, **21**, 466, 767.
- [11] ROOTHAAN, C. C. J., 1951, *Rev. mod. Phys.*, **23**, 69.
- [12] KURLAND, R. J., 1957, *J. chem. Phys.*, **27**, 585.
- [13] WALSH, A. D., 1946, *Trans. Faraday Soc.*, **42**, 66.
- [14] PLATT, J. R., KLEVENS, H. B., and PRICE, W. C., 1949, *J. chem. Phys.*, **17**, 466.
- [15] WATANABE, K., 1954, *J. chem. Phys.*, **22**, 1564; 1957, *Ibid.*, **26**, 542.
- [16] PARISER, R., 1953, *J. chem. Phys.*, **21**, 568.
- [17] PARR, R. G., 1952, *J. chem. Phys.*, **20**, 1499.
- [18] PRITCHARD, H. O., and SKINNER, H. A., 1955, *Chem. Rev.*, **55**, 745.
- [19] POPLE, J. A., 1953, *Trans. Faraday Soc.*, **49**, 1375; 1955, *Proc. phys. Soc., Lond. A*, **68**, 81.
- [20] TANAKA, J., 1958, *J. chem. Soc. Japan*, **78**, 1636.
- [21] WHELAND, G. W., 1955, *Resonance in Organic Chemistry* (New York: John Wiley & Sons), p. 99.
- [22] HUNT, H. D., and SIMPSON, W. T., 1953, *J. Amer. chem. Soc.*, **75**, 4540.
- [23] PETERSON, D. L., and SIMPSON, W. T., 1957, *J. Amer. chem. Soc.*, **79**, 2375.
- [24] WAGNER, R., FINE, J., SIMMONS, J. W., and GOLDSTEIN, J. H., 1957, *J. chem. Phys.*, **26**, 634.
- [25] SMYTH, C. P., 1955, *Dielectric Behavior and Structure* (New York: McGraw-Hill), p. 245.
- [26] WALSH, A. D., 1945, *Trans. Faraday Soc.*, **41**, 498.
- [27] MULLIKEN, R. S., 1956, *Rec. Trav. chim. Pays-Bas.*, **75**, 845.
- [28] KUBOTA, T., 1957, *J. Chem. Soc.*, **78**, 196.

High resolution hydrogen resonance spectra of some substituted ethylenes

by E. O. BISHOP and R. E. RICHARDS

Physical Chemistry Laboratory, South Parks Road, Oxford

(Received 2 October 1959)

The olefinic proton resonance spectra of a number of mono- and 1, 2 di-substituted ethylenes have been analysed as AB, ABC or ABX systems to obtain the coupling constants and chemical shifts. The values of J_{trans} (range observed 13.7 to 18.0 c/s in 14 compounds) were significantly larger than J_{cis} in similar molecules. The values of J_{cis} (range observed 6.5 to 12.3 c/s in 8 compounds) are abnormally large when the olefinic bond is conjugated to an aromatic ring. Coupling between adjacent protons in an olefinic methylene group (J_{gem}) is much smaller, and sometimes negative. The shielding of the lone vinyl proton in mono-substituted ethylenes is smaller than that of the methylene group and in two cases (the vinyl group directly bonded to an oxygen atom) the difference is so great as to give an approximation to the ABX condition, so that the methylene protons appear to be shielded to an unusually large extent.

1. INTRODUCTION

Previous reports on the hydrogen resonance spectra of olefines have indicated that the coupling constants across the C=C bond between nuclei mutually trans is appreciably greater than that between nuclei mutually cis [1-4]; this effect has been predicted also from theoretical considerations [5]. The same trend has been observed for F-F and H-F coupling constants where the values of J are generally much larger [6].

In the present investigation, a number of substituted olefines has been examined to obtain coupling constants and chemical shifts. The individual cis trans isomers of type CHX=CHY constitute an AB system for which the spin interaction Hamiltonian is represented as a 2×2 matrix, which is capable of solution in closed algebraic form [7]. The spectrum consists of four lines, symmetrical in spacing and intensity. The vinyl compounds constitute either the ABC or ABX case [7]. In the ABC case the matrix representation of the spin coupling Hamiltonian contains two 3×3 sub-matrices so that the roots and vectors cannot be expressed in simple algebraic form. The twelve principal lines of the spectrum are however assignable as three quartets symmetrical in spacing but not in intensity, each due predominantly to spin change of one nucleus. The mid-point of each quartet may then be considered as a first approximation to the chemical shift of the corresponding nucleus, the true value being somewhat nearer to the weighted centre of the complete spectrum. Each pair of quartets contains a common line spacing repeated four times in all, which provides an approximation to the coupling constant between

the appropriate nuclei. An approximate matrix may thus be set up, and the roots compared with the true eigenvalues (relative to an arbitrary zero) determined from the spectrum. The input parameters are then repeatedly modified, using a computer, until convergence to the experimental eigenvalues is attained. The transition probabilities are then derived from the corresponding vectors [8]. The absolute signs of the coupling constants cannot be determined but their relative values can be differentiated. Thus there are four solutions to the eigenvalue problem, viz. that for which all three coupling constants have the same sign, and those in which each in turn has opposite sign from the others. Convergence to each solution in turn is usually attained by appropriately modifying the line assignment and the sign of the approximate parameters mentioned above.

When the chemical shift of one nucleus (X) is widely different from that of the other two (the ABX case), then mixing between states differing in spin of that nucleus may be neglected, and the problem reduces to diagonalization of 2×2 sub-matrices [7]. The case of two coincident shifts has also been analysed (ABB') [9].

2. EXPERIMENTAL

The high resolution spectra were obtained with the instrument constructed in this laboratory, which has been described previously [10]. The resonance frequency for protons is 29.92000 Mc/s.

Most of the compounds were obtained commercially. Cis and trans-o-cyano-cinnamic acid and N-vinyl phthalimide were kindly given to us by the Dyestuffs Division of I.C.I. Limited. Cis-cinnamic acid was prepared by ultra-violet irradiation of the trans isomer in methanol solution as described by Vaidya [11]. The product was unfortunately not well characterized, probably due to contamination with traces of the trans isomer, but there is little doubt from the spectrum and comparison with the above cis and trans compounds that the results quoted are correct.

ABC analyses were carried out on the University Mercury Ferranti computer. One of the analyses was also performed by hand calculating machine and a different iterative procedure. The results agreed satisfactorily after three stages of iteration in each case. Nomenclature for line assignment follows that of reference [7], and in each case the shielding of the nuclei is considered to increase in the order A, B, C. Line separations and derived parameters are quoted in c/s (100 c/s = 3.342 p.p.m.) with an estimated accuracy of ± 0.2 c/s.

Absolute chemical shifts are rather difficult to measure [12, 13] and so an external standard was used. The chemical shifts were measured in dilute solution (5 per cent) in carbon tetrachloride relative to a benzene external standard in a sealed capillary. A correction of -3.5 c/s was applied to the benzene resonance to allow for the difference in diamagnetic susceptibility of the medium (assumed to be that of carbon tetrachloride) and the standard. The corrected benzene resonance position, to an estimated accuracy of ± 1 c/s is indicated on the diagrams. It should be noted that the conditions of measurement are not intended to give a comparison between the aromatic resonance in the compound studied and the benzene standard.

3. RESULTS AND DISCUSSION

3.1. 1, 2 disubstituted olefines

All the compounds were derivatives of cinnamic acid. These fulfil the necessary conditions, since coupling from side chain to nucleus was undetectable. Specimen traces are given in figure 1 and the data obtained by AB analysis are listed in table 1. Where unspecified, the data refer to the stable trans isomer. A check on the interpretation is given by comparison of the theoretical relative intensities of the outer to inner line pairs with the experimental values measured approximately from peak heights.

In the case of trans-o-cyano cinnamic acid, dimethyl sulphoxide was found to be the only suitable solvent. The resonance lines are abnormally broadened, and the derived data are of lower accuracy than in the remaining cases (± 0.3 c/s).



Figure 1. H resonance spectra of 1, 2-di-substituted olefines. Trans-isomers: (a) Cinnamic acid; (b) Methyl cinnamate; (c) Cinnamoyl chloride; (d) Benzylidene acetone; (e) ω -bromo styrene; (f) ω -nitro styrene; (g) ortho-cyano cinnamic acid. Cis-isomers: (h) ortho-cyano cinnamic acid; (i) Cinnamic acid. Full line indicates corrected position of external benzene standard.

The spectrum of trans-cinnamaldehyde is readily interpreted as an ABX spectrum in terms of coupling between the protons AB of the olefinic group and X of the aldehyde group. The mean of the four line pairs -62.4 ± 0.3 ; -55.7 ± 0.3 ; $+0.3 \pm 0.3$; $+16.2 \pm 0.3$ c/s may be regarded as the basic AB spectrum unperturbed by interaction with X, of repeated spacing 15.9 c/s which is equal to J_{trans} . Coupling of X to B then causes splitting of each of the B lines by 6.7 c/s and of the X resonance by the same amount. Very weak coupling to A then causes hyperfine splitting of the A and X peaks by 0.6 c/s. Since spin-spin interaction usually attenuates rapidly with increasing number of bonds between

Compound	J_{trans}	J_{cis}	$\eta H_0 (\sigma_B - \sigma_A)$	Inner and outer line intensities	
				Theor. ratio	Exptl. ratio
Trans-cinnamic acid (in acetone)	15.8		34.8	0.42	0.45
Cis-cinnamic acid (in acetone)		12.3	27.7	0.42	0.43
ω -cyano cinnamic acid					
Trans (in Me_2SO)	15.8 ± 0.3		30.2 ± 0.3	0.37	0.44 ± 0.05
Cis (in dioxane)		12.3	28.7	0.43	0.50
Methyl cinnamate (in CCl_4)	15.9		36.6	0.38	0.41
Cinnamoyl chloride (in CCl_4)	15.9		35.6	0.37	0.47
Benzylidene acetone (in CCl_4)	16.3		23.4	0.27	0.28
ω -bromo styrene	14.5		12.8	0.20	0.19
ω -nitro styrene	14.0		10.8	0.17	0.16

Table 1. AB spectra.

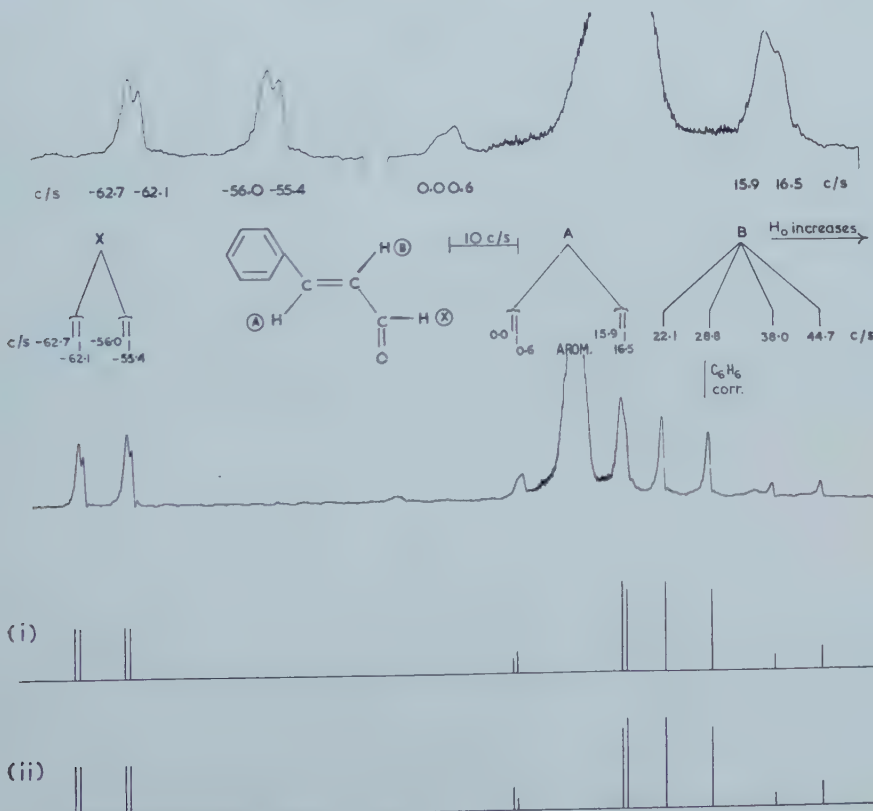


Figure 2. Trans-cinnamaldehyde: H resonance spectrum. Top and inset: experimental traces. (i) and (ii): theoretical spectra (see text).

the nuclei [14], nuclei A and B can be identified with protons H_A , H_B , in figure 2, with the most shielded proton, B, remote from the aromatic ring. It is probable that the assignment of the protons to A and B found for cinnamaldehyde is also true for the derivatives of cinnamic acid discussed above. The spectrum has been analysed for all four sign assignments (*v. infra*) by both ABC and ABX methods; the coupling constants agreeing to within 0.1 c/s throughout. They lead consistently to the values: J_{trans} 15.9; J_{BX} 7.7 ± 0.1 ; $\eta H_0(\sigma_B - \sigma_A)$ 19.1; $\eta H_0(\sigma_A - \sigma_X)$ 70.1 c/s; corrected benzene resonance = +28 c/s. The much lower shielding of X and very weak coupling between A and X renders the calculated value of J_{AX} very sensitive to the input parameters, and makes determination of the relative signs of the coupling constants difficult. 'ABX' intensity pattern (i) (figure 2) for $J_{\text{AB}}: J_{\text{BX}}: J_{\text{AX}} = \pm 15.9: 7.6: -0.3$ c/s respectively shows slightly better agreement with experiment than does (2) for $15.9: \pm 7.7: \pm 1.7$. Experimental peak heights in the close line pairs are increased somewhat by partial overlap. These values accord reasonably with those of a recent account [15], in which splitting of A to X coupling was not recorded.

3.2. Vinyl derivatives

The spectra of six compounds of this type have been evaluated as outlined above. In all of the compounds the lone vinyl proton (A) was less shielded than the methylene group. A specimen trace is shown for each compound for comparison with the theoretical results for all possible signs of the coupling constants. The numbering of the peaks follows the nomenclature used by Bernstein *et al.* [7]. The line positions (denoted by ν) are given in cycles per second relative to the lowest field olefine line of each spectrum as an arbitrary zero. The general ABC spectrum has three combination lines arising from simultaneous spin change of all three nuclei. These will be of low intensity for the present spectra and were observed only in one case. Further compounds investigated (acrylic acid, methyl acrylate, methyl vinyl ketone, divinyl sulphone) yielded strongly coupled ABC spectra rising steeply to three high intensity lines at the centre. Under these conditions interpretation depends on very low intensity lines far removed from the centre, and furthermore the combination lines are relatively strong and cause difficulty in assignment. It was found impracticable to give an unambiguous analysis for these compounds and it is hoped to reinvestigate the spectra at 60 Mc/s.

3.3. *N*-vinyl phthalimide

This compound was studied in solution in nitromethane. Although only moderate signal-to-noise ratio was obtainable, all 12 principal lines of the ABC spectrum were distinct. (Figure 3.) The repeated line spacings (16.3, 0.9, 9.1 c/s) were taken as first approximations for J_{AB} , J_{BC} , J_{CA} respectively, and the results for all four line assignments are given in table 2.

The relatively large separation of the chemical shifts means that the variation between line intensities for the various assignments is rather small. Assignments (2) and (3) can be rejected, but final decision between (1) and (4) requires examination at a lower applied field. Assignment (1) with all J values positive seems the most probable one at the moment. The low intensity line within the A quartet does not match up with a theoretical combination line (6→3 transition) which is predicted at 38.8 c/s but not observed.

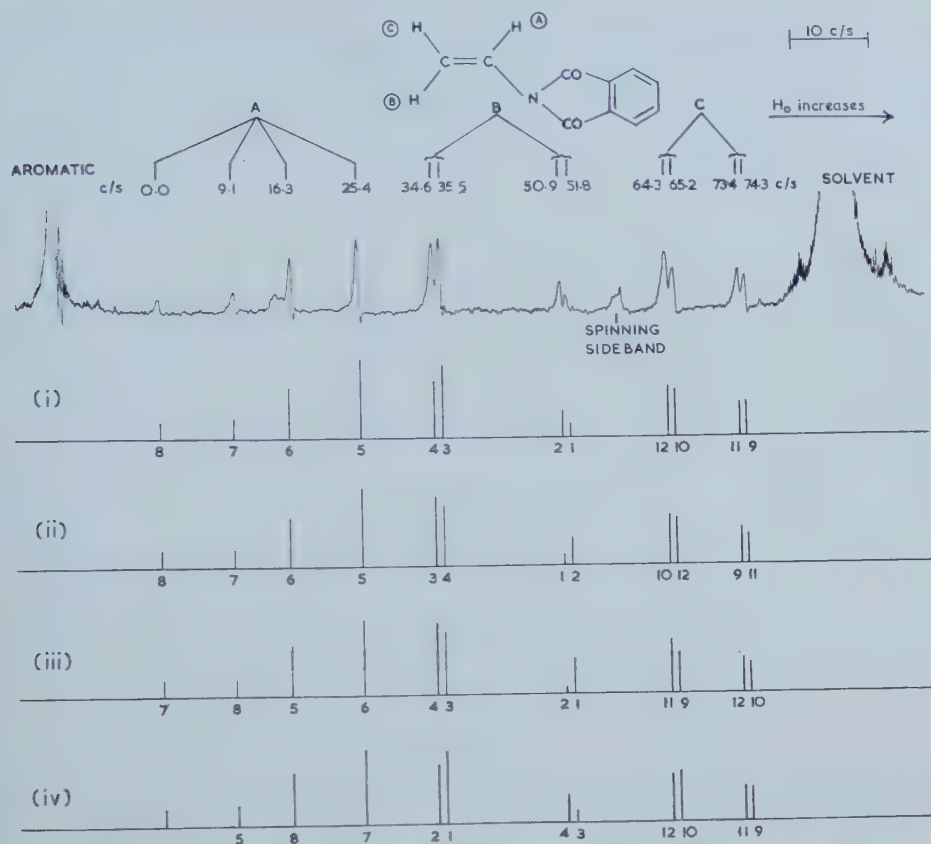


Figure 3. N-vinyl phthalimide: H resonance spectrum. Top : experimental trace. (i) All J values positive. (ii) J_{gem} negative. (iii) J_{cis} negative. (iv) J_{trans} negative.

	J_{AB}	J_{BC}	J_{CA}	ν_A	ν_B	ν_C
(1) All J values positive	16.4	0.0	9.9	15.6	40.8	68.8
(2) J_{gem} negative	16.7	-2.0	9.8	15.7	40.7	68.8
(3) J_{cis} negative	16.7	1.9	-10.5	15.8	40.7	68.6
(4) J_{trans} negative	-16.5	0.3	9.9	15.6	40.8	68.8

Table 2.

3.4. Vinyl mesitylene

The compound gave an ABC spectrum (figure 4) of repeated line separations 11.9, 3.1, 16.8 c/s as approximations to J_{AB} , J_{BC} , J_{CA} respectively. The A line quartet was partially obscured by the aromatic proton resonance, and each component abnormally broadened. This effect persisted even when the sample was diluted with carbon tetrachloride to lower its viscosity. The accurate line positions for analysis were therefore completed by interpolation and comparison with the remainder of the spectrum. The results for three line assignments are given in table 3.

There appears to be no reasonable solution for J_{CA} negative. The chemical shifts of the methylene protons are unusually close, hence the variation in line intensities between the assignments is considerable (see figure 4). Comparison with the experimental values shows clearly that assignment (1), with all the J values positive, is correct.

	J_{AB}	J_{BC}	J_{CA}	ν_A	ν_B	ν_C
(1) All J values positive	11.6	2.3	18.0	17.1	52.2	60.1
(2) J_{gem} negative	13.4	-4.0	16.2	17.1	52.1	60.1
(3) J_{cis} negative	-12.1	3.5	16.7	16.9	51.9	60.5

Table 3. Corrected benzene shift = +15 c/s.

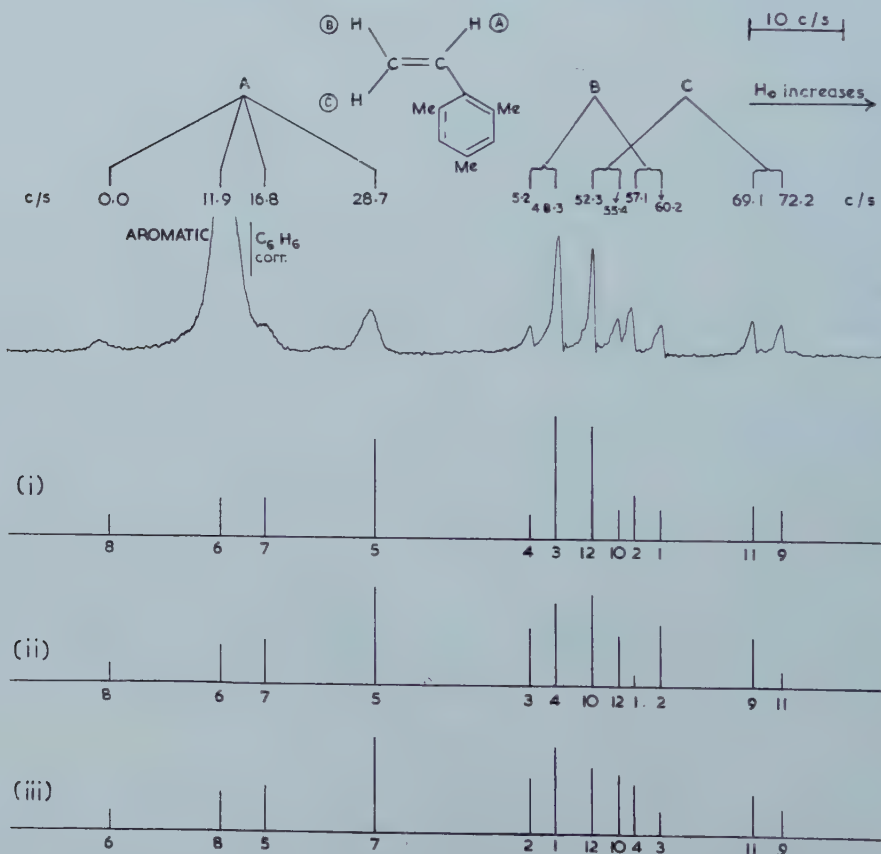


Figure 4. Vinyl Mesitylene: H resonance spectrum. Top: experimental trace. (i) All J values positive. (ii) J_{gem} negative. (iii) J_{cis} negative.

3.5. Styrene

During the present work, Professor Waugh very kindly sent us a copy of a complete analysis of the styrene spectrum at various applied fields [16]. Our results are entirely in agreement with his work, the values obtained by us for the

coupling constants being J_{AB} 17.8, J_{BC} 1.1, J_{CA} 11.0 c/s. There are two cases of line coincidence at 29.92 Mc/s and the line at lowest field underlies the aromatic proton resonance. The chemical shifts relative to the lowest field olefine peak are $\nu_A = 17.1$ c/s, $\nu_B = 46.2$ c/s, $\nu_C = 61.8$ c/s, that of the corrected benzene external standard lying at +16 c/s. It should be noted that the inferred dispositions of nuclei B and C relative to the lone vinyl proton (A) are opposite from those in vinyl mesitylene.

3.6. Vinyl bromide

This compound gave a compact ABC spectrum (figure 5), with iterated spacings 5.8, 0.5 and 15.2 c/s. These are the approximate values of J_{AB} , J_{BC} , J_{CA} respectively. The A quartet ascends much more rapidly towards the centre of the spectrum than in previous cases, corresponding to a more strongly coupled spectrum. The combination line due to the 6 > 3 transition is clearly visible within this quartet. The system has a long relaxation time and accurate measurements of intensities in the close line pairs require lower H_1 fields and slower sweep rates than were used for the whole trace shown in figure 5. Portions of the spectrum run under the necessary conditions are shown in the upper part of figure 5.

The theoretical intensities for all four possible assignments are shown in figure 5 and the calculated parameters are given in table 4.

	J_{AB}	J_{BC}	J_{CA}	ν_A	ν_B	ν_C
(1) All input J values positive	6.8	-0.8	15.5	14.0	28.8	32.8
(2) J_{gem} negative	7.3	-1.9	15.1	13.9	28.8	32.9
(3) J_{cis} negative	-6.3	0.9	15.4	13.8	28.6	33.1
(4) J_{trans} negative	5.9	0.5	-15.3	13.7	28.5	33.4

Table 4. Corrected benzene shift = +9 c/s.

In case (1) in which all input J values were taken as positive, the sign of J_{BC} was reversed on iteration (+0.5 to -0.8 c/s). This has not been observed with any other vinyl spectrum and it is not clear whether the effect is real or due to rounding errors. Comparison with the experimental spectrum however clearly shows that assignment (2) is correct.

3.7. Vinyl acetate

The spectrum consists of eleven lines, assigned as an ABC spectrum with two of the lines overlapping (figure 6). The repeated line separations of 13.9, 1.4 and 6.6 c/s are taken as approximate values of J_{AB} , J_{BC} and J_{CA} respectively. The lone vinyl proton resonance is widely separated to low field from the BC region so that the spectrum approximates to the ABX condition. The differences for the various line assignments are slight under these conditions however and so the spectrum has been analysed rigorously as ABC to obtain accurate intensity values. The results are shown in table 5.

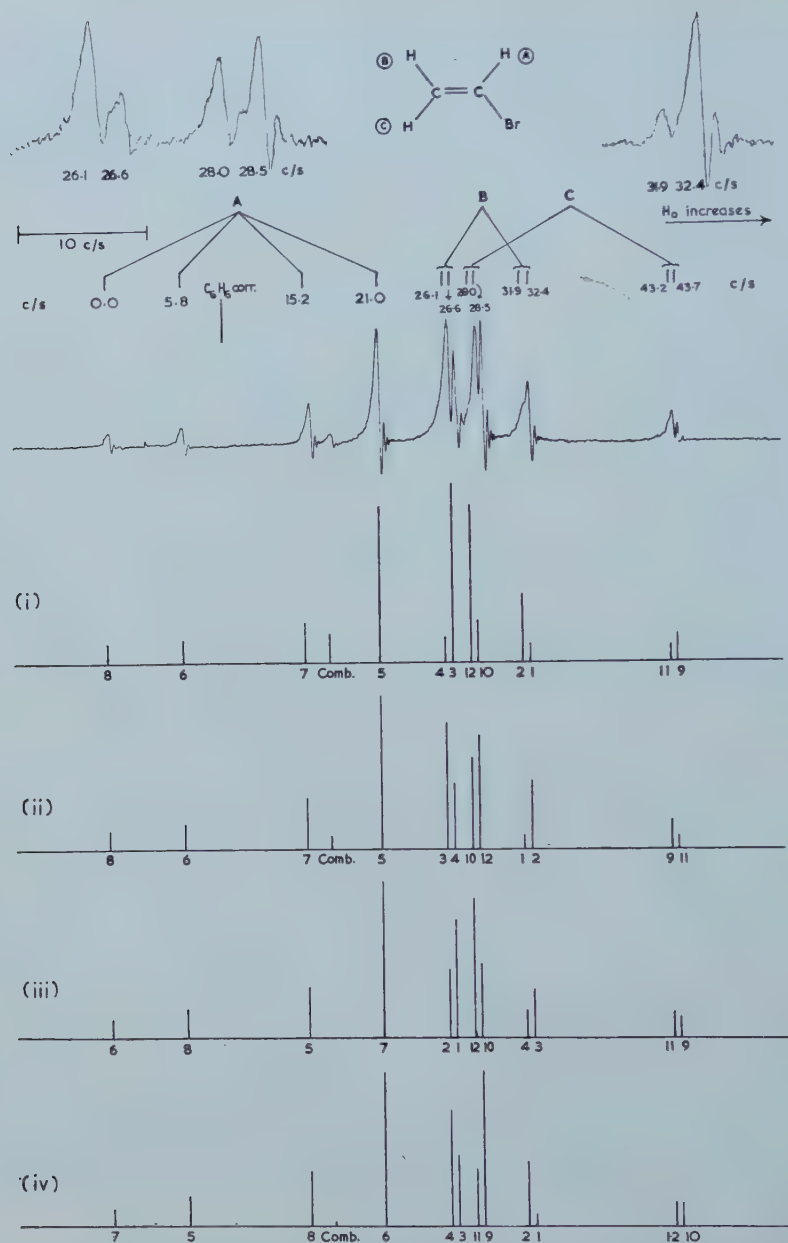


Figure 5. Vinyl bromide: H resonance spectrum. Top and inset: experimental traces. (i) All input J values positive. (ii) J_{gem} negative. (iii) J_{cis} negative. (iv) J_{trans} negative.

No reasonable solution was obtained for negative values of J_{CA} . Comparison with the experimental results shows that assignment (2) with J_{gen} negative is almost certainly correct.

The corrected benzene external reference falls at +28 c/s from the low field end of the spectrum, and so the large separation between A and BC regions

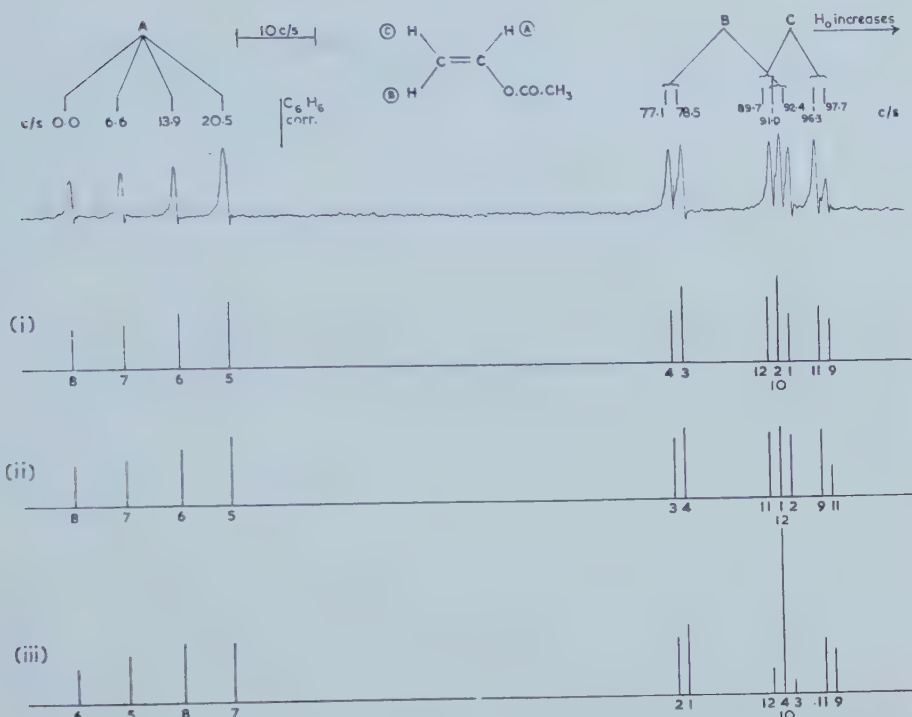


Figure 6. Vinyl acetate: H resonance spectrum. Top: experimental trace. (i) All J values positive. (ii) J_{gem} negative. (iii) J_{trans} negative.

arises from an abnormally large displacement of the methylene resonance to high field; the lone vinyl proton appearing not far below its usual position (compare ethyl vinyl ether).

	J_{AB}	J_{BC}	J_{CA}	ν_A	ν_B	ν_C
(1) All J values positive	13.9	1.3	6.7	11.0	84.1	93.5
(2) J_{gem} negative	14.1	-1.5	6.5	11.1	84.2	93.5
(3) J_{trans} negative	-13.7	1.4	6.4	11.0	84.1	93.6

Table 5. Corrected benzene shift = +28 c/s.

3.8. Ethyl vinyl ether

The olefine resonance is very similar to that of vinyl acetate, with the lone vinyl proton quartet widely separated to low field from the methylene region. The olefine resonance does however overlap the methylene resonance of the ethyl group at the magnetic field used, and so a detailed analysis of the spectrum was not possible. Approximate values of the coupling constants can however be obtained and are found to be $J_{AB} = 13.7$ (trans), $J_{BC} = \pm 1.8$, $J_{CA} = 7.5$ (cis) c/s. The chemical shifts are 9.6, 80, and 88 c/s for the A, B, and C nuclei respectively. The corrected benzene resonance lies at +1 c/s.

4. GENERAL DISCUSSION

The cis coupling constants of 12.3 c/s found for cinnamic and o-cyano cinnamic acids are apparently the highest which have been recorded for cis proton coupling constants in olefines. As abnormally high values were found also for styrene and vinyl mesitylene (11.0 and 11.6 c/s), it appears that this feature may be due to conjugation of the olefinic double bond to an aromatic nucleus. However, there is no overlap between the ranges of the coupling constants found for cis (6.5–12.3 c/s) and trans (13.7–18.0 c/s) coupling and so these values are of considerable value in structural investigations. The very much smaller values of J_{gem} may be of positive or negative sign.

The wide separation between the lone vinyl and methylene protons in vinyl acetate and ethyl vinyl ether is associated with direct linkage of an oxygen atom to a carbon atom in the double bond. Thus the spectrum of vinyl acetate is completely different from that of methyl acrylate, although the pair are structurally isomeric. It is not clear why the abnormal separation appears to be due to movement of the methylene group resonance to high field rather than of the lone vinyl proton in the opposite direction.

We are particularly grateful to Dr. J. S. Rollett of the Oxford University Computing Laboratory for his help and guidance in preparing the computer programme for ABC spectra. We also thank Dr. L. Pratt for examining the spectrum of ethyl vinyl ether at 40 Mc/s, and I.C.I. Limited Dyestuffs Division for generous gifts of chemicals. We thank the Department of Scientific and Industrial Research for a maintenance grant to one of us (E. O. B.) and the Hydrocarbon Research Group of the Institute of Petroleum and the National Coal Board for grants in aid of apparatus. We thank Professor J. Waugh, Dr. N. Sheppard and Professor Gutowsky for allowing us to see certain of their results in advance of publication.

REFERENCES

- [1] ALEXANDRA, S., 1958, *J. chem. Phys.*, **28**, 358.
- [2] VARIAN ASSOCIATES, CALIFORNIA, 1958, *Tech. Infv. Bull.*, **2**, 9.
- [3] COHEN, SHEPPARD, and TURNER, 1958, *Proc. Chem. Soc.*, April.
- [4] FESSENDEN, and WAUGH, 1959, *J. chem. Phys.*, **30**, 944.
- [5] KARPLUS, M., 1959, *J. chem. Phys.*, **30**, 11.
- [6] McCONNELL, REILLY, and MCLEAN, 1956, *J. chem. Phys.*, **24**, 479.
- [7] BERNSTEIN, POPPLE, and SCHNEIDER, 1957, *Canad. J. Chem.*, **35**, 65.
- [8] McCONNELL, MCLEAN and REILLY, 1955, *J. chem. Phys.*, **23**, 1152.
- [9] RICHARDS, and SCHAEFER, 1958, *Mol. Phys.*, **1**, 331.
- [10] LEANE, RICHARDS, and SCHAEFER, 1959, *J. sci. Instrum.*, **36**, 230.
- [11] VAIDYA, 1930, *Proc. roy. Soc. A*, **129**, 299.
- [12] BATH, D. (unpublished work).
- [13] BOTHNER-BY, and GLICK, 1957, *J. chem. Phys.*, **26**, 1647, 1651.
- [14] GUTOWSKY, MEYER, and McCALL, 1955, *J. chem. Phys.*, **23**, 982.
- [15] SHIMIZU, MATSUOKA, HATTORI, and SENDA, 1959, *J. Phys. Soc. Japan*, **14**, 683.
- [16] FESSENDEN, and WAUGH (private communication).

Magnetic properties of Co^{2+} ions in octahedral interstices of an oxide lattice

by P. COSSEE†

(Laboratorium voor Anorganische en Physische Chemie,
Rijks-Universiteit Leiden)

(Received 17 September 1959)

The magnetic properties of Co^{2+} ions in octahedral environment are discussed in relation to the energy-level scheme. It appears that the three low-lying levels arising from the ${}^4\text{F}(\Gamma_4)$ triplet as a consequence of spin-orbit coupling are responsible for a temperature-dependent magnetic moment.

The expected departure from the Curie-Weiss law is demonstrated by susceptibility measurements on mixed-crystals of CoO and MgO between 300° and 1200°K . From the experimental data the spin-orbit coupling constant for Co^{2+} in these compounds is estimated to be -136 cm^{-1} .

1. INTRODUCTION

It is to be expected that Co^{2+} ions in the octahedral interstices of a close-packed oxygen lattice will exhibit interesting magnetic properties in particular at elevated temperatures.

The ${}^4\text{F}$ ground state of Co^{2+} , which is seven-fold orbitally degenerate, is split by the action of a cubic electric field of octahedral symmetry into two triplets and a singlet [1, 2]. The distances between these levels are of the order of $10\,000 \text{ cm}^{-1}$; consequently only the lowest triplet (Γ_4) will be of immediate importance for the magnetic properties. In the Co^{2+} ion with three unpaired electrons this orbital triplet is twelve-fold degenerate. Under the influence of spin-orbit coupling it is further split into a doublet, a quartet and a sextet. The distances of the quartet and sextet to the lower doublet are $9\lambda'/4$ and $6\lambda'$ respectively, where λ' is the spin-orbit coupling constant in the crystal. Its value for the free-ion Co^{2+} is -180 cm^{-1} . (A detailed discussion of the energy levels may be found in ref. [3, 4].)

These levels contribute to the actual state of the ion according to Boltzmann's distribution law. Since the orbital contribution to the magnetic moment belonging to each level will be different, the mean magnetic moment which is found by χ -measurements will be temperature-dependent.

The theoretical predictions may be checked by making χ -measurements on mixed-crystals of CoO and MgO between 300 and 1200°K ‡. These substances crystallize in a rock-salt structure in which the Co^{2+} ions occupy octahedral interstices. In the following, our measurements will be described, and it will be shown how they enabled us to confirm the predicted deviations from the Curie-Weiss law.

† Present address: Koninklijke/Shell-Laboratorium, Amsterdam.

‡ For a study of Co^{2+} ions in tetrahedral interstices, see ref. [5]; for Co^{3+} ions in octahedral interstices, see ref. [6].

2. EXPERIMENTAL

The mixed crystals of (Co, Mg)O were prepared according to the method described in ref. [5] with the following slight modification of the procedure: The solution of nitrates was not directly evaporated to dryness, but the metals were first simultaneously precipitated as carbonates with $(\text{NH}_4)_2\text{CO}_3$ and the precipitate together with the supernatant solution were evaporated to dryness. This modification was necessary for obtaining homogeneous products. The firing of the samples at 950–1200 °C was repeated several times until the room-temperature susceptibility remained constant on further firing.

Samples of the following compositions were subjected to magnetic measurements: $\text{Co}_{0.049}\text{Mg}_{0.951}\text{O}$, $\text{Co}_{0.119}\text{Mg}_{0.881}\text{O}$, $\text{Co}_{0.196}\text{Mg}_{0.804}\text{O}$ and $\text{Co}_{0.493}\text{Mg}_{0.507}\text{O}$.

Susceptibility measurements were carried out with a Faraday torsion balance (see ref. [5]). Diamagnetic corrections were calculated by using a value of $\chi = -0.020 \times 10^{-3} \text{ erg gauss}^{-2} \text{ mole}^{-1}$ for MgO, determined by direct measurements on this substance between 300 and 1200 °K†.

Co _{0.493} Mg _{0.507} O			Co _{0.196} Mg _{0.804} O			Co _{0.049} Mg _{0.951} O		
T °K	$\chi_M \times 10^3$	C_0	T °K	$\chi_M \times 10^3$	C_0	T °K	$\chi_M \times 10^3$	C_0
294	7.36	3.19	291	9.22	3.17	292	10.22	3.07
388	5.89	3.12	528	5.27	2.99	415	7.24	3.03
489	4.92	3.02	691	3.99	2.87	489	6.13	3.00
607	4.03	2.90	803	3.41	2.79	540	5.40	2.90
836	3.00	2.78	888	3.07	2.75	582	5.04	2.90
893	2.83	2.76	1066	2.55	2.69	600	4.88	2.90
956	2.65	2.73	1190	2.29	2.67	639	4.52	2.84
1014	2.51	2.72				677	4.26	2.83
1087	2.34	2.68				741	3.96	2.87
1193	2.15	2.66				804	3.59	2.81
						863	3.36	2.81
						914	3.14	2.77
						990	2.88	2.73

Susceptibility of (Co, Mg)O mixed crystals in erg/gauss² per gram atom of Co, corrected for diamagnetic contribution, as a function of absolute temperature. C_0 is the extrapolated Curie constant at infinite dilution.

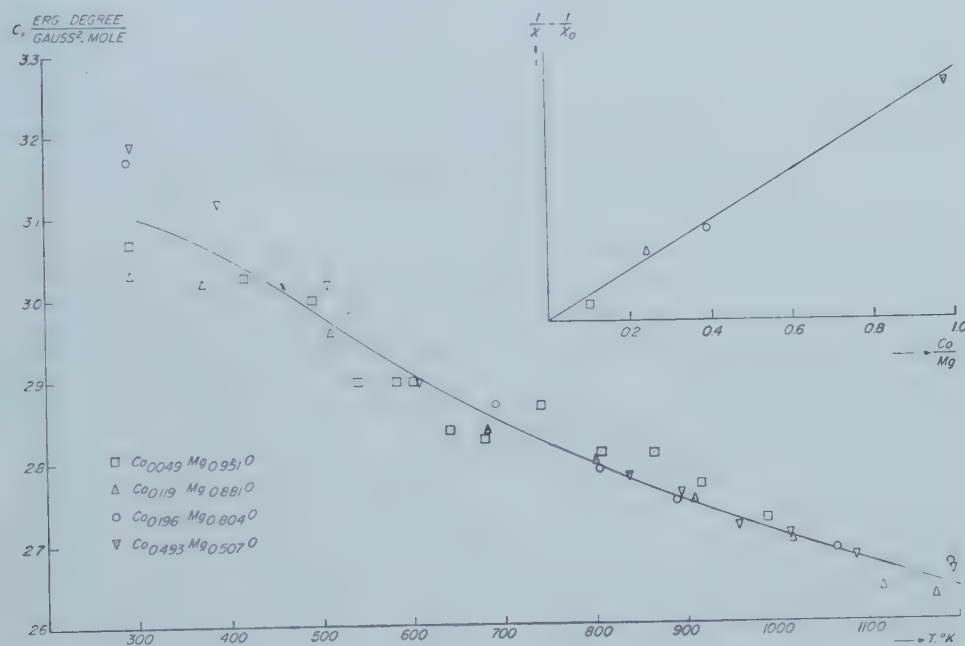
† In the author's thesis (Leiden, 1956) a wrong diamagnetic correction for MgO was used.

The experimental results are summarized in the table, where for each substance the susceptibility per gram atom of Co, corrected for the diamagnetic contribution is given as a function of absolute temperature.

In the third column the extrapolated Curie constant at infinite dilution is given.

3. DISCUSSION

Several investigations into the magnetic properties of Co^{2+} ions have been made on either CoO [7] or mixed crystals of CoO and MgO [8, 9]. The agreement between individual χ -values obtained in this investigation and those measured by Elliott [9] is very good. The present investigation, however, owing to the much larger temperature range covered, revealed a deviation from the Curie-Weiss law, which is thought to be due to the presence of the three low energy levels in the Co^{2+} ion.



Plot of the extrapolated Curie constant $(\chi_0 - a)T$ per gram atom of Co^{2+} against absolute temperature for four different $(\text{Co}, \text{Mg})\text{O}$ mixed crystals. In the inset: The linear relationship of the differences in $1/\chi$ with concentration.

The plots of $1/\chi$ against T appeared to be slightly S-shaped. For the four samples with different Co-concentrations they were perfectly parallel and their mutual distances were proportional to the differences in the Co-concentrations.

In the inset of the figure the linear relationship between the differences in $1/\chi$ and concentration is shown. Apparently the general characteristics of the three low-lying energy levels are not influenced by super-exchange. We therefore extrapolated the $1/\chi$ values to infinite dilution in order to obtain not only the right shape of the curves but also the right absolute value of χ , free from anti-ferromagnetic effects. It may be pointed out that this extrapolation is a purely empirical procedure.

From the χ values at infinite dilution, χ_0 , the Curie constant $C_0 = (\chi_0 - a)T$ could be obtained as a function of absolute temperature. The constant a is a temperature-independent paramagnetic term for which the value 0.15×10^{-3} erg gauss $^{-2}$ mole $^{-1}$ was introduced. This value of the constant term was proposed by Pryce [10] who has also given the following formula for the Curie constant C_0 :

$$C_0 = 0.375 \left[\left\{ \frac{(5+\alpha)^2}{9} + \frac{10(2+\alpha)^2}{27} \frac{T}{T_1} \right\} + \left\{ \frac{2(11-2\alpha)^2}{45} - \frac{88(2+\alpha)^2}{675} \frac{T}{T_1} \right\} \exp\left(-\frac{3T_1}{T}\right) \right. \\ \left. + \left\{ \frac{7(3-\alpha)^2}{5} - \frac{6(2+\alpha)^2}{25} \frac{T}{T_1} \right\} \exp\left(-\frac{8T_1}{T}\right) \right] \\ \times \left\{ 1 + 2 \exp\left(-\frac{3T_1}{T}\right) + 3 \exp\left(-\frac{8T_1}{T}\right) \right\}^{-1}.$$

In this formula, which was derived for non-interacting Co^{2+} ions in a cubic electric field of octahedral symmetry, the Boltzmann distribution over three energy levels is reflected in the three terms of the numerator. Each term consists of a temperature-independent and a temperature-dependent part, of which the former corresponds to the magnetic moment and the latter to the Van Vleck paramagnetic term of that particular level. The denominator is a normalization factor which reflects the fact that the levels are a doublet, a quartet and a sextet respectively.

The parameter T_1 equals $3\lambda'/4k$ (λ' is the spin-orbit coupling constant in the crystal).

The parameter α is a measure of the contamination of the ground state ${}^4\text{F}(\Gamma_4)$ by the higher ${}^4\text{P}$ -level. This parameter is defined as follows $\alpha = \frac{3}{2}\epsilon^2 - \tau^2$, where ϵ and τ are the coefficients of the ${}^4\text{F}(\Gamma_4)$ and ${}^4\text{P}$ wave functions in the total wave function $\psi = \epsilon\psi_{\text{F}} + \tau\psi_{\text{P}}$. When α has its maximum value 1.5 the ground state is the pure ${}^4\text{F}(\Gamma_4)$ triplet.

The agreement between the experimental results and the theory is very satisfactory. This is demonstrated by the figure where the experimental values for the extrapolated Curie constants of four different mixed crystals are plotted against the absolute temperature. The drawn curve is the theoretical one for $\alpha = 1.28$ and $T_1 = 146^\circ\text{K}$.

These values for the parameters correspond to a 9 per cent admixture of the ${}^4\text{P}$ -level and a spin-orbit coupling constant $\lambda' = -136 \text{ cm}^{-1}$ respectively (free-ion value for Co^{2+} is -180 cm^{-1}).

Recently Griffith published a formula for the susceptibility of Co^{2+} ions in octahedra [11], which turns out to be a simplified version of the formula proposed by Pryce. For $\alpha = 1$ the latter becomes identical with that of Griffith. Thus one needs an admixture of 20 per cent ${}^4\text{P}$ (corresponding to $\alpha = 1$) to the ${}^4\text{F}(\Gamma_4)$ ground state in the weak-field approximation of Pryce to obtain the result of the strong-field approximation of Griffith. It may easily be shown that a linear combination of one particular wave function of the ${}^4\text{F}(\Gamma_4)$ triplet with the corresponding wave function of the ${}^4\text{P}$ triplet in the appropriate ratio $\sqrt{\frac{4}{5}} : \sqrt{\frac{1}{5}}$ is equivalent to one of the three strong-field wave functions.

4. CONCLUSION

The deviation at elevated temperatures of the magnetic properties of the $(\text{Co}, \text{Mg})\text{O}$ mixed crystals from an ideal Curie-Weiss behaviour can be satisfactorily explained by the occurrence of three low-lying levels in a Co^{2+} ion

when this ion is surrounded by six negative ions. This is shown by the very good agreement between the experimental data and Pryce's theory.

The value of the parameter λ' which must be introduced to give this agreement is of the right order of magnitude. A reduction of the spin-orbit coupling constant to about 75 per cent of the free-ion value seems quite reasonable [12].

The parameter α may also be estimated from optical data. A value of 1.40 corresponding to an admixture of 4 per cent ^4P is found [4]. This is appreciably smaller than the 9 per cent ^4P admixture derived from our susceptibility measurements. In relation to this one has to realize that the admixture of the ^4P level results in a reduction of the orbital contribution. However, a reduction of orbital magnetic moment can also be caused by partial covalent bonding, which is not taken into account in the approximation given here. It may thus be that an effect which is now explained by assuming 9 per cent admixture of ^4P , is due to a much smaller contribution of this level, together with a contribution of the ligand wave functions. It is not possible to distinguish between these two types of admixture by χ measurements only.

The author wishes to thank Professor M. H. L. Pryce for his interest and for communicating the susceptibility formula, and Professor Dr. A. E. van Arkel and Ir. L. L. van Reyen for valuable discussions.

REFERENCES

- [1] BETHE, H., 1929, *Ann. Phys.*, **3**, 133.
- [2] SCHLAPP, R., and PENNEY, W. G., 1932, *Phys. Rev.*, **42**, 666.
- [3] ABRAGAM, A., and PRYCE, M. H. L., 1951, *Proc. roy. Soc. A*, **206**, 173.
- [4] LOW, W., 1958, *Phys. Rev.*, **109**, 256.
- [5] COSSEE, P., and VAN ARKEL, A. E., *J. Phys. Chem. Solids* (to be published).
- [6] COSSEE, P., 1958, *J. Inorg. Nucl. Chem.*, **8**, 483.
- [7] HENRY LA BLANCHETAIS, C., 1951, *J. Phys. Radium*, **12**, 765.
- [8] PERAKIS, N., and SERRES, A., 1957, *J. Phys. Radium*, **18**, 47.
- [9] ELLIOTT, N., 1954, *J. chem. Phys.*, **22**, 1924.
- [10] PRYCE, M. H. L., private communication.
- [11] GRIFFITH, J. S., 1958, *Trans. Faraday Soc.*, **54**, 1109.
- [12] OWEN, J., 1955, *Proc. roy. Soc. A*, **227**, 183.
- [13] VAN SANTEN, J. H., and VAN WIERINGEN, J. S., 1952, *Rec. Trav. chim.*, **71**, 420.

The redistribution of charge in naphthalene caused by methyl substitution

I. Partial rate factors for hydrogen-deuterium exchange in α , α - and β , β -dimethylnaphthalenes

by G. DALLINGA, P. J. SMIT and E. L. MACKOR

Koninklijke/Shell-Laboratorium, Amsterdam
(Shell Internationale Research Maatschappij N.V.)

(Received 5 October 1959)

The partial rate factors k^i for H-D exchange in α , α - and β , β -dimethylnaphthalenes were measured in $\text{CF}_3\text{COOD}-\text{HPO}_2\text{F}_2-\text{CCl}_4$ mixtures. The values of $\log k^i$ correlate well with the excess of electron charge on the carbon atoms calculated on the basis of the inductive effect of the methyl group.

1. INTRODUCTION

As was reported in previous publications, methyl substituents produce an increase of the rate constants of hydrogen deuterium exchange [1, 2] and of the basicity constants [3] of aromatic hydrocarbons. It was concluded that the inductive effect of the methyl group provides a satisfactory basis for a semi-quantitative discussion of reactivity. This discussion was complicated, however, by the fact that compounds of widely different structures and reactivities were used—necessitating measurements under different conditions—and by the possibility that steric interactions in the molecules would affect reactivity.

For this reason we have measured the hydrogen-deuterium exchange of the α , α - and β , β -dimethylnaphthalenes. These form a group of closely related compounds which can be studied under identical conditions. They also yield a large number of data, since each of the six isomers contains three different groups of two hydrogen atoms.

2. EXPERIMENTAL

2.1. Materials

The 1, 8- and 1, 5-dimethylnaphthalenes were prepared by J. Boekholtz in this laboratory according to the methods of Bailey [4] and Beyler and Sarett [5]. The other isomers were available in the laboratory. Melting or boiling points and ultra-violet spectra of all hydrocarbons were determined. The purity proved to be 99 per cent or better, except for 2, 3-dimethylnaphthalene which contained a few per cent of an impurity, but as this was not an isomer, it did not affect the results of the mass spectrometric analysis.

Deutero-trifluoroacetic acid was prepared from the anhydride by adding the calculated amount of D_2O , refluxing for 30 min and distilling.

Bisfluoro phosphinic acid anhydrous (Ozark-Mahoning Co.) was redistilled once.

2.2. Measurements and analysis

312 mg (2 mmole) of hydrocarbon was dissolved in 5 g of carbon tetrachloride. The solution was added to *ca.* 15 g of a solution of 1·08 per cent by weight of $\text{F}_2\text{PO}_2\text{H}$ in CF_3COOD (0·1 mole $\text{F}_2\text{PO}_2\text{H}$, 1000 g CF_3COOD ; acid strength of the solution before addition of hydrocarbon solution: $H_0 = -3\cdot85$ using 2, 4-dinitroaniline as the indicator). The temperature was kept constant at 20·0 °C (for 2, 3-dimethylnaphthalene; 26·0 °C). At suitable time intervals samples were taken. The hydrocarbon was recovered by pouring the sample into a dilute sodium hydroxide solution, separating the organic layer, drying the carbon tetrachloride solution on anhydrous sodium sulphate, and evaporating the solvent.

The deuterium content was determined by mass spectrometry. A low electron-accelerating voltage was used (~6v) to avoid fragmentation of the molecules and the mass peaks were corrected for ^{13}C contributions. The result of the analysis is a series of numbers

$$d_0, d_1, \dots d_6 \quad \left(\sum_{j=0}^6 d_j = 1 \right),$$

which represents the mole fractions of hydrocarbon containing 0, 1, ... 6 deuterium atoms per molecule.

No exchange takes place in the methyl groups.

3. ANALYSIS OF EXPERIMENTAL DATA

3.1. Calculation of rate constants

The procedure for calculating rate constants from the time-dependence of the mole fractions d_j ($j = 0, 1, \dots 6$) has been given elsewhere [6] and will only be summarized in a form adapted to the present problem. All molecules considered here contain three groups which we shall call u , v and w of two hydrogen atoms each. In each group the distribution of deuterium during the reaction is given by an equation of the form (e.g. for group u):

$$D_0^u = (1 - D^u)^2, \quad D_1^u = 2D^u(1 - D^u), \quad D_2^u = (D^u)^2, \quad (1)$$

where $D^u = \frac{1}{2}D_1^u + D_2^u$ is the mean deuterium content of the group.

For the whole molecule, the deuterium distribution is given by

$$d_j = \sum_{i+k+l=j} D_i^u D_k^v D_l^w, \quad j = 0, 1, \dots 6; \quad 0 \leq i, k, l \leq 2, \quad (2)$$

u , v and w denoting the three groups in order of decreasing reactivity. By means of an iterative process using equations (1) and (2) values of D^u , D^v and D^w are obtained that give the best fit to the experimental values of the d_j .

D^u , D^v and D^w are related in good approximation to the rate constants k^i by the equations†

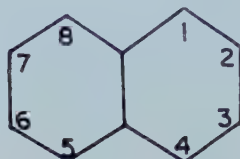
$$\begin{aligned} 2\cdot303 \frac{1+A}{1+2A} \log \frac{D_{\text{eq}}^u}{D_{\text{eq}}^u - D^u} &= k^u t, & 2\cdot303 \frac{1+2A}{1+4A} \log \frac{D_{\text{eq}}^v}{D_{\text{eq}}^v - D^v} &= k^v t, \\ 2\cdot303 \frac{1+4A}{1+6A} \log \frac{D_{\text{eq}}^w}{D_{\text{eq}}^w - D^w} &= k^w t, \end{aligned} \quad (3)$$

where A = moles of hydrocarbon/g equivalent of acid, D_{eq} = 'equilibrium' value of D , equal to $s_0/(1+2A)$, $s_0/(1+4A)$ and $s_0/(1+6A)$ for the groups u , v and w , respectively, s_0 = isotopic purity of the acid mixture before reaction.

† The exact, and very complicated expressions for the k^i are given in ref. [6] where it is also shown that application of the approximate equations (3), obtained by assuming that $k^u \gg k^v \gg k^w$ causes an error in k^i of 2 per cent or less.

3.2. Assignment of rate constants to positions in the molecule

A reliable assignment can be made on the basis of the difference in reactivity between α - and β -positions and an estimate of the inductive effect. In 2, 3-dimethylnaphthalene, for instance, the α -atoms 1 and 4 are by far the most reactive as a strong inductive effect of the neighbouring methyl groups is present. The inductive effect is small and about equal for the atoms in the unsubstituted ring; consequently, 5 and 8, being α -atoms, will be more reactive than the β -atoms 6 and 7.



I	II	III	IV	V		VI	VII	VIII
No.	Positions of methyl-substitution	k in (hours) $^{-1}$	$3 + \log k$	Assignment of carbon atoms		$\log(k/k_0)$	$\sum_r Q_r$	δq_s
				α -atoms	β -atoms			
1	2, 3	5.50†	3.74	1, 4		3.23	0.364	0.059
2		0.174†	2.24	5, 8		1.73	0.091	0.010
3		0.030†	1.48		6, 7	1.85	0.125	0.010
4	2, 6	4.76	3.68	1, 5		3.17	0.364	0.062
5		0.10	2.00	4, 8		1.49	0.091	0.005
6		0.031	1.49		3, 7	1.86	0.125	0.033
7	2, 7	12.9	4.11	1, 8		3.60	0.455	0.074
8		0.148	2.17		3, 6	2.54	0.250	0.043
9		0.037	1.57	4, 5		1.06	0	-0.008
10	1, 4	0.32	2.51		2, 3	2.88	0.500	0.059
11		0.030	1.48	5, 8		0.97	0.091	-0.001
12		0.0054	0.73		6, 7	1.10	0.125	0.008
13	1, 5	1.24	3.09	4, 8		2.58	0.364	0.034
14		0.166	2.22		2, 6	2.59	0.500	0.061
15		0.0067	0.83		3, 7	1.20	0.125	0.005
16	1, 8	0.77	2.89	4, 5		2.38	0.455	0.049
17		0.77	2.89		2, 7	3.26	0.625	0.074
18		0.0027	0.43		3, 6	0.80	0	-0.008
19	—	0.00324	0.51	1, 4, 5, 8		0	—	—
20	—	0.00043	-0.37		2, 3, 6, 7	0	—	—

Rate constants of H-D exchange, for the carbon atoms in naphthalene and symmetrical dimethylnaphthalenes.

† For 2, 3-dimethylnaphthalene k was measured at 26.0°C; k_{H-D} at 20.0°C was calculated using the value of the enthalpy of activation of naphthalene (16 kcal/mole). The measurements for this compound were made by Mr. W. IJ. Aalbersberg.

In a few cases where the argument is less straightforward the tentative assignment was confirmed by measurements of the proton resonance spectra of the partially deuterated compounds as discussed in Part II [7]. Our results are given in the table.

The two monomethylnaphthalenes and the α , β -dimethylnaphthalenes, although a potential source of information, have not been investigated. Owing to their lack of symmetry, these molecules contain 7 or 6 hydrogen atoms of different reactivity. For such a complicated system both the kinetic analysis and the assignment of rate constants are practically impossible.

4. DISCUSSION

In earlier work [6] we assumed that the transition state for H-D exchange of aromatic hydrocarbons resembles the corresponding conjugate acid formed by addition of a proton to a carbon atom of the molecule. In both cases the configuration at the reacting carbon atom is approximately tetrahedral and in consequence the π -electronic structures of transition state and conjugate acid will be similar. This picture is consistent with the fact that the logarithms of both the rate constant of H-D exchange and the basicity constant are linear functions of the energy ΔE_{π} necessary for localizing an electron pair at the reacting carbon atom.

From such a model one would expect that it should be possible to express the rate constant of H-D exchange, k^i , for carbon atom i in a dimethylnaphthalene as:

$$\log(k^i/k_0^i) = \rho \delta E_{\pi}^i / \beta, \quad (4)$$

in which k_0^i is the rate constant for the same position i ($=\alpha$ or β) in unsubstituted naphthalene; ρ is a constant, β is the resonance integral and δE_{π}^i is the difference in localization energy, for position i , between the substituted and the unsubstituted molecule. In the following the superscript i will be omitted; it should be borne in mind that k_0 is different for α - and β -positions.

According to Longuet-Higgins [8]

$$\delta E_{\pi} = -\delta\alpha \sum_r Q_r, \quad (5)$$

where $\delta\alpha$ is the change in Coulomb energy of a carbon atom caused by methyl substitution and Q_r is the net positive charge on carbon atom r in the transition state of the unsubstituted molecule; the summation extends over the methyl-substituted carbon atoms.

By combining equations (4) and (5) one obtains

$$\log(k/k_0) = -\rho(\delta\alpha/\beta) \sum_r Q_r. \quad (6)$$

On plotting the experimental values of $\log(k/k_0)$ against $\sum_r Q_r$ for the three different positions in all dimethylnaphthalenes one would expect the points to fall on a straight line with slope $\rho\delta\alpha/\beta$. Figure 1 shows that this is not true: two approximately parallel straight lines are obtained, the upper one passing through the points of the β , β -dimethylnaphthalenes. Neither of the lines passes through the origin, which probably means that the reactivity of carbon atoms in 'meta' positions with respect to the methyl groups is increased by a factor of about 5-10, an effect which was not predicted. That methyl groups in β -position

enhance reactivity more than those in α -position is in agreement with the fact that β -methylnaphthalene is more basic than the α -isomer [3]: the latter isomerizes to yield the former in acid solution.

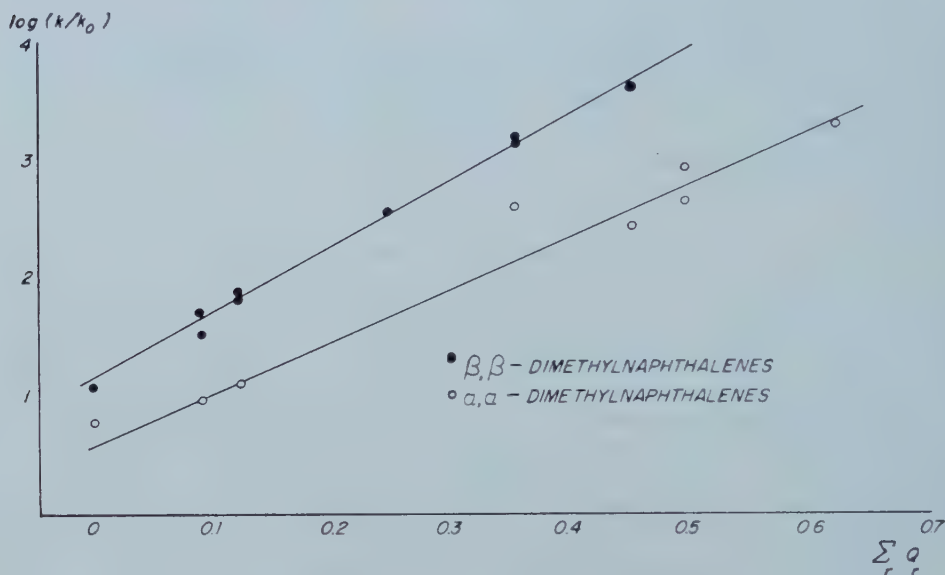


Figure 1. Rate of H-D exchange against $\sum_r Q_{r,r}$.

As there seems to be no systematic way in which one may account for the observed phenomena on the basis of steric factors, the possibility that the first-order perturbation technique might be inadequate was investigated. If one includes second-order terms in equation (6) one arrives at

$$\log(k/k_0) = -\rho(\delta\alpha/\beta) \left\{ \sum_r Q_{r,r} - \frac{1}{2}\delta\alpha\delta\pi_{rr} \right\} \quad (7)$$

where $\delta\pi_{rr} = \pi_{rr}(\text{ion}) - \pi_{rr}(\text{molecule})$, is the difference in self-polarizability of atom r in the transition state and in the molecule [9]. The values of $\pi_{rr}(\text{ion})$ were calculated for all atoms in the two possible naphthalenium ions†.

The calculations showed that for carbon atoms for which first-order perturbation theory predicts equal enhancement of the reactivity, the second-order term predicts the higher reactivity in the β,β -substituted molecules. To a certain extent this explains the anomalies of figure 1, but a quantitative agreement could not be obtained.

A striking correlation was noted between the observed partial rate factors and the magnetic shielding constants of the corresponding hydrogen atoms obtained from nuclear magnetic resonance spectra (cf. Part II [7]). Both effects are connected with the redistribution of π -electronic charge in the molecule, caused by the methyl group. This suggested that the present experimental results might well be interpreted on the basis of the Coulson and Longuet-Higgins model, in which differences in chemical reactivity are related to differences in local electronic charge. Their theory predicts the presence of an excess negative charge on the carbon atoms ortho or para with respect to the methyl group.

† The calculations were made by Dr. J. P. Colpa and Mr. G. ter Maten, to whom we extend our cordial thanks.

The net negative charge, δq_s , on carbon atom s , calculated from

$$\delta q_s = \sum_r \pi_{rs} \cdot \delta \alpha_r, \quad (8)$$

is given in the table, last column. The summation of the mutual atom-atom polarizabilities π_{rs} [9] extends over the methyl substituted atoms r ; $\delta \alpha_r$ was taken equal to -0.3β [3].

Figure 2 demonstrates that there is indeed a satisfactory correlation between $\log(k/k_0)$ and δq_s . The slope of the line indicates that a charge one-twentieth of an electron causes the free energy of activation to be lowered by about 4 kcal/mole.

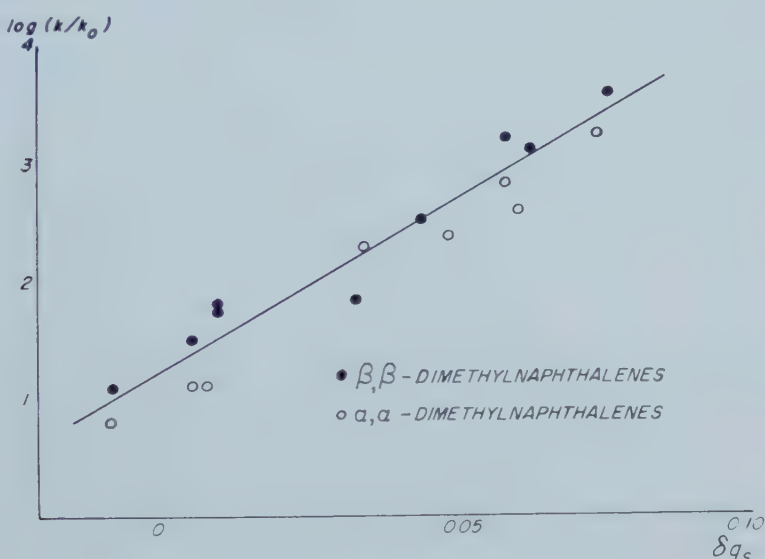


Figure 2. Rate of H-D exchange against δq_s

One may ask whether the order of magnitude of this result is compatible with the Coulomb energy between a proton and a carbon atom carrying a charge of 0.05 electron. Let us suppose by way of a very rough approximation that in the transition state of the exchange reaction the C-H distance in the bond being formed is of the order of 1.5 Å. Depending on the choice of the dielectric constant—which is between 1 and 7—one calculates for the Coulomb interaction between a proton and a charge of 0.05 electron, localized at the centre of the carbon atom, a value between 11 and 1.5 kcal/mole. This qualitative argument indicates that our estimate of the excess electronic charge is physically reasonable.

The line in figure 2 does not pass through the origin which means that the reactivity of carbon atoms in 'meta' positions is increased by a factor of about 10. Similar effects have been found for the meta positions in alkyl-substituted benzenes [1, 10]. In the present argument it must mean that carbon atoms in meta position with respect to the substituent have acquired a small excess of negative charge, a phenomenon which is not predicted by the LCAO MO—

or by the SCF, treatments according to Pariser and Parr or Pople, but which can be understood from the model proposed by Wheland and Mann [11].

REFERENCES

- [1] MACKOR, E. L., SMIT, P. J., and VAN DER WAALS, J. H., 1957, *Trans. Faraday Soc.*, **53**, 1309.
- [2] DALLINGA, G., SMIT, P. J., and MACKOR, E. L., 1958, Proceedings of a Symposium on " Steric effects in conjugated systems ", Hull 15-17 July, p. 150.
- [3] MACKOR, E. L., HOFSTRA, A., and VAN DER WAALS, J. H., 1958, *Trans. Faraday Soc.*, **54**, 186.
- [4] BAILEY, A. S., *et al.*, 1947, *J. Inst. Petr.*, **33**, 503.
- [5] BEYLER, R. E., and SARETT, L. H., 1952, *J. Amer. chem. Soc.*, **74**, 1406.
- [6] DALLINGA, G., VERRIJN STUART, A. A., SMIT, P. J., and MACKOR, E. L., 1957, *Z. Elektrochem.*, **61**, 1019.
- [7] MACLEAN, C., and MACKOR, E. L., *Mol. Phys.* (to be published).
- [8] LONGUET-HIGGINS, H. C., 1951, *Proc. roy. Soc. A*, **207**, 121.
- [9] COULSON, C. A., and LONGUET-HIGGINS, H. C., 1947, *Proc. roy. Soc. A*, **192**, 16.
- [10] LAUER, W. M., MATSON, G. W., and STEDMAN, G., 1958, *J. Amer. chem. Soc.*, **80**, 6437.
- [11] WHELAND and MANN, 1949, *J. chem. Phys.*, **17**, 264.

An interpretation of potential interaction constants in terms of low-lying excited states

by R. F. W. BADER

Department of Chemistry, University of Ottawa

(Received 22 October 1959)

This paper examines the use of second-order perturbation theory in the interpretation and prediction of the signs of the interaction constants which are appended to the simple valence force potential functions. It is shown, for the large number of molecules considered here, that complete agreement with the observed signs can be obtained by expanding the electronic Hamiltonian in terms of the normal coordinates of motion and by then assuming that the lowest of the excited electronic states makes the most important contribution to the second-order sum in the expression for the energy. A knowledge of the symmetry of the transition density between the ground and the first excited electronic states is thus sufficient to determine which of the vibrations in a molecule is energetically favoured and thus to determine the sign of the interaction constant.

1. INTRODUCTION

The simple valence force potential function used for the description of the vibrational frequencies of a molecule may be greatly improved if a number of appropriately chosen interaction constants are included in the expression. Such interaction constants then take into account the fact that the *restoring force* acting on one atom may depend upon the relative simultaneous displacements of other atoms in the molecule. Thus the stretching of one bond may increase or decrease the equilibrium lengths of other bonds present in the molecule. A large number of interaction constants have been determined and it is of interest to see whether one can interpret their direction and magnitude.

Coulson *et al.* [1] have stated that the sign and magnitude of the interaction constant will be dependent upon three effects: resonance, interactions between non-bonded atoms and changes in hybridization. Duchesne [2] has used a Lennard-Jones potential to interpret a number of results in terms of non-bonded effects. Linnett and Hoare [3] have related the sign of the interaction constant in triatomic molecules ABC to the change in the bond AB when the bond BC is broken; if k_{12} is positive, AB becomes shorter and stronger when BC is broken and if k_{12} is negative AB becomes longer and weaker when BC is broken. In all cases they found a positive k_{12} to be associated with the presence of electrons unlocalized over the region of the two bonds and a negative k_{12} when only localized electrons were involved.

Coulson and Longuet-Higgins [4] have found that the interaction constants in unsaturated hydrocarbons are proportional to the mutual polarizability of two unsaturated bonds and at the same time are dependent upon their mobile orders. No account was taken of sigma bond interactions. Their results suggest that the interactions between unsaturated bonds arise primarily from the mobile electrons.

K

2. THE INTERACTION WITH LOW-LYING EXCITED STATES

We are concerned with how the relative potential energies of the nuclei change when they are displaced from their equilibrium positions and this suggests that we should treat the nuclear displacements as perturbations and determine what effect these perturbations have on the electronic energy and wave function as determined by the Born-Oppenheimer procedure for the equilibrium configuration. Therefore, we expand the Hamiltonian about the equilibrium configuration in terms of the normal coordinates of motion of the nuclei (which have the same symmetry properties as do the electronic wave functions). For the extension of the system in the i th normal coordinate q_i the electronic Hamiltonian is

$$H = H_0 + H_i q_i + \frac{1}{2} H_{ii} q_i^2 \quad (1)$$

where

$$\left. \begin{aligned} H_i q_i &= (\partial H / \partial q_i)_0 q_i = \sum_{\nu} (\partial H / \partial r_{\nu})_0 \frac{\partial r_{\nu}}{\partial q_i} q_i \\ H_{ii} q_i^2 &= (\partial^2 H / \partial q_i^2)_0 q_i^2 = \sum_{\mu} \sum_{\nu} (\partial^2 H / \partial r_{\mu} \partial r_{\nu})_0 \frac{\partial r_{\mu}}{\partial q_i} \frac{\partial r_{\nu}}{\partial q_i} q_i^2 \end{aligned} \right\} \quad (2)$$

where r_{ν} is the displacement of the ν th nucleus in the i th normal coordinate. The unperturbed electronic wave functions are those obtained by solving the wave equation for a fixed nuclear configuration corresponding to that found in the *equilibrium* position of the ground state,

$$\langle 0 |, \langle 1 |, \dots, \langle k |, \dots$$

and the corresponding eigenvalues of H_0 are:

$$\epsilon_0, \epsilon_1, \dots, \epsilon_k, \dots$$

The remaining terms in H are potential energy changes arising from nuclear displacements, and so

$$\partial H / \partial r_{\nu} = \partial V / \partial r_{\nu}$$

and equation (1) may be written as

$$H = H_0 + V_i q_i + \frac{1}{2} V_{ii} q_i^2.$$

The energy of the distorted configuration for extension in the i th normal coordinate, correct to the second order is

$$E(q_i) = \epsilon_0 + \frac{1}{2} V_{00}^{ii} q_i^2 + \sum_k' \frac{V_{0k}^i V_{k0}^i}{\epsilon_0 - \epsilon_k} q_i^2 \quad (3)$$

The perturbation terms may be expressed in terms of the static densities and transition densities, ρ_{00} and ρ_{0k} respectively (Longuet-Higgins [5]), as

$$V_{00}^{ii} = \int \rho_{00}(r) \frac{\partial^2 \phi(r)}{\partial q_i^2} dr = \sum_{\mu} \sum_{\nu} \frac{\partial r_{\mu}}{\partial q_i} \frac{\partial r_{\nu}}{\partial q_i} \int \rho_{00}(r) \frac{\partial^2 \phi(r)}{\partial r_{\mu} \partial r_{\nu}} dr, \quad (4)$$

$$V_{0k}^i = \int \rho_{0k}(r) \frac{\partial \phi(r)}{\partial q_i} dr = \sum_{\nu} \frac{\partial r_{\nu}}{\partial q_i} \int \rho_{0k}(r) \frac{\partial \phi(r)}{\partial r_{\nu}} dr \quad (5)$$

in which $\phi(r)$ is the potential due to the nuclei and

$$\rho_{0k}(r) = \langle 0 | \rho(r) | k \rangle$$

where

$$\rho(r) = -e \{ \sum_j \delta(r - r_j) \}.$$

The operator $\rho(r)$ is a function only of the electronic coordinates r_j .

The term $\frac{1}{2}V_{00}q_i^2$ corresponds to moving the nuclei and holding the electrons fixed. The terms $V'_{0k}q_i$ allow for a relaxation of the electron distribution (permitting them to follow the nuclei) and thus significantly reduce the increase in the potential energy accompanying the nuclear displacements. It is evident from the denominator in equation (3) that the lowering in energy will be greatest for that normal mode of vibration which allows for an interaction with the lowest of the excited states if the corresponding numerators are of comparable or equal magnitude. When the ground state electronic wave function $\langle 0 |$ is totally symmetric the transition density $\rho_{0k}(r)$ will possess the symmetry of the excited state $\langle k |$. In order that the second order terms $V'_{0k}q_i$ be different from zero, the symmetries of $\langle k |$ and q_i must be identical. (The multiplicities of $\langle 0 |$ and $\langle k |$ must also be identical if the transition density is to be non-vanishing.) If we assume that only the lowest lying excited state contributes significantly to the summation in equation (3) then we are immediately in a position to predict the sign of the interaction constant which appears in the modified valence potential functions. To do this we simply determine which of the normal coordinates possesses a symmetry identical with that of the transition density for a transition to the lowest of the excited electronic states. When the nuclei are displaced in this mode which allows for an interaction with the lowest lying of these excited states, then the increase in potential energy is not as great as it otherwise would have been if this mixing had not occurred. If this particular normal mode is one in which all relative internuclear distances are increased, then the interaction constant will be negative, while if some bonds are increased in length and others decreased during the execution of this vibration, the interaction constant will be positive. We shall apply this method to a large number of molecules representing a variety of electronic structures.

3. TRIATOMIC MOLECULES CONTAINING 16 VALENCE ELECTRONS

All of the known triatomic molecules with 16 valence electrons are linear. The most general potential function for a linear symmetrical triatomic molecule A_2B is

$$2V = k(\Delta r_1^2 + \Delta r_2^2) + 2k_{12}(\Delta r_1\Delta r_2) + k_\delta\delta^2$$

where Δr_1 , Δr_2 and δ are internal displacement coordinates, the latter for the bending of the molecule and k_{12} is an interaction constant. If there are no bond-bond interactions ($k_{12}=0$), then the ratio of the two stretching frequencies is given simply as a ratio of the masses as the force constants are then identical for each motion, i.e.

$$\nu_1^2/\nu_3^2 = m_B/(m_B + 2m_A).$$

It is found, however, in almost all cases that this relationship does not hold true and that the force constants governing the two linear motions are, therefore, not identical. When the interaction constants are taken into account the ratio of the frequencies is given by

$$\nu_1^2/\nu_3^2 = \frac{m_B}{2m_A + m_B} (k + k_{12})/(k - k_{12}).$$

The increase in energy for both the symmetric normal mode, equal to $(1/2m_A)(k + k_{12})q_1^2$, and for the antisymmetric normal mode, equal to

$$\frac{1}{2m_B} \left(1 + \frac{2m_A}{m_B}\right) (k - k_{12})q_3^2,$$

may be equated to the right-hand side of equation (3). The symmetric stretching mode has the symmetry \sum_g^+ and if the lowest lying excited electronic state possesses the same symmetry, we should expect the force constant for this motion to be lowered over that for the antisymmetric mode of symmetry \sum_u^- . Thus $(k - k_{12}) > (k + k_{12})$ and this is true only if k_{12} is negative. The same result is obtained if one simply considers the potential expression given above. For the symmetric mode both Δr_1 and Δr_2 are positive and the increase in potential energy for any symmetrical extension of the bonds may be lessened only if k_{12} is negative. Similarly, it is easily seen that if the lowest lying excited state is of symmetry \sum_u^+ , then the interaction constant should be positive.

The electronic structure of the sixteen-electron triatomic molecules may be expressed in terms of molecular symmetry orbitals which are given below in the order of decreasing term value:

$$(1\sigma_g)^2(1\sigma_u)^2(2\sigma_g)^2(2\sigma_u)^2(\pi_u)^4(\pi_g)^4; \quad ^1\sum_g^+.$$

According to Walsh the observed electronic spectra of these molecules are best interpreted [6] by supposing that the lowest lying of the excited orbitals is $\bar{\pi}_u\dagger$. Mulliken in an earlier paper [7] assumed the excited $\bar{\sigma}_g$ orbital to be lower than the $\bar{\pi}_u$. The two authors, therefore, differ in their interpretations of some of the observed bands. The excitation of an electron from the π_g to an upper orbital almost invariably results in a bent upper state of C_{2v} symmetry [6]. However, the wavelength of maximum absorption should, according to the Frank Condon principle, correspond to the energy necessary for a vertical transition, i.e. one in which the nuclei retain the linear configuration of the ground electronic state. These are the energies of interest here, and they are the $\epsilon_0 - \epsilon_k$ as obtained by the fixed nucleus approximation for the ground state equilibrium configuration.

A transition of an electron from the π_g orbital to the $\bar{\pi}_u$ antibonding orbital will, in the vertical transition, give rise to three possible transitions,

$$\begin{aligned} & ^1\Delta_u \leftarrow ^1\sum_g^+ \quad (\text{I}), \\ & ^1\sum_u^- \leftarrow ^1\sum_g^+ \quad (\text{II}), \\ & ^1\sum_u^+ \leftarrow ^1\sum_g^+ \quad (\text{III}). \end{aligned}$$

(For the bent upper state, $^1\Delta_u$ correlates with $^1A_2 + ^1B_1$, $^1\sum_u^+$ with 1B_1 and $^1\sum_u^-$ with 1A_2 of C_{2v} symmetry)‡. Of these three transitions only (III) is allowed electronically. Carbon dioxide has a weak band at $\lambda_{\max} = 1490 \text{ \AA}$ and this is identified by Walsh [6] as a transition to a 1B_1 correlating with (I). The second band, $\lambda_{\max} = 1335 \text{ \AA}$ is much more intense and is identified with (III). A third much weaker band with λ_{\max} at approximately 1700 \AA is to be identified with the remaining part of (I), to the 1A_2 state. In this case Mulliken [7] feels that the band at 1335 \AA is to the $\bar{\sigma}_g$ orbital and thus the transition is a $^1\pi_g \leftarrow ^1\sum_g^+$. This is, however, not an allowed transition and does not agree with the observed intensity. Carbon disulphide follows the same pattern of bands. The weak absorption at 3200 \AA is to a 1B_1 state correlating with (I). Both Walsh and Mulliken agree that the band at 1970 \AA is transition (III).

In both these cases the interaction constant should be positive as the lowest lying state of proper symmetry, as determined by the symmetries of the two vibrations, is the $^1\sum_u^+$ state. As noted in the table this is the observed result.

† A bar over the symbol for a molecular orbital denotes antibonding character.

‡ Our species notation for the C_{2v} group is that given in reference [19].

The azide ion possesses a similar electronic structure as it is another 16-electron molecule. It is to be expected that the lowest lying state of proper symmetry in this molecule will also be ${}^1\Sigma_u^+$ and that its interaction constant should be positive as is observed.

Molecule	Symmetry of ρ_{0k}	Predicted sign of k_{12}	Observed k_{12} md/Å	Reference
CO ₂	Σ_u^+	+	+1.3	[19]
CS ₂	Σ_u^+	+	+0.6	[19]
N ₃ ⁻	Σ_u^+	+	+1.6	[20] (*)
N ₂ O	Σ^+	+	+1.36	[19]
COS	Σ^+	+	+2.0	[21]
ClCN	Σ^+	+	+1.0	[2] (*)
UO ₂ ²⁻	Σ_g^+	-	-0.30	[8] (*)
NpO ₂ ⁻²	Σ_g^+	-	-0.54	[8] (*)
PuO ₂ ⁻²	Σ_g^+	-	-0.89	[8] (*)
AmO ₂ ⁻²	Σ_g^+	-	-1.66	[8] (*)
NO ₂	B_1	+	+1.45	[25]
SO ₂	B_1	+	+0.024	[23]
O ₃	B_1	+	+1.52	[24]
ClO ₂	B_1	+	(±)	[11]
OCl ₂	B_1	+	(+)	[11] (*)
OF ₂	B_1	+	+1.1	[2] (*)
H ₂ O	A_1	-	-0.10	[19] (*)
H ₂ S	A_1	-	-0.22	[3] (*)
H ₂ Se	A_1	-	-0.25	[3] (*)
BF ₃	E'	+	+0.78	[19]
BCl ₃	E'	+	+0.31	[19]
BBr ₃	E'	+	+0.61	[17]
PF ₃	E	+	+0.39	[22] (*)
PCl ₃	E	+	+0.27	[22] (*)
PBr ₃	E	+	+0.03	[22] (*)
AsF ₃	E	+	+0.34	[22] (*)
SbCl ₃	E	+	+0.16	[22] (*)
BiCl ₃	E	+	+0.15	[22] (*)
AsCl ₃	E	+	+0.19	[22] (*)

(*) An asterisk implies that the excited state appearing in ρ_{0k} either cannot be, or has not been, observed experimentally.

Comparison of predicted and observed signs of potential interaction constants

3.1. The transition density ρ_{gu}

The transition density required for the evaluation of the V_{0k}^i term (as given by equation (5)) in the case of the $D_{\infty h}$ molecules is

$$\rho_{gu} = \langle {}^1\Sigma_g^+ | \rho(r) | {}^1\Sigma_u^+ \rangle. \quad (6)$$

We need consider only the four electrons directly involved in the transition as the remaining ones stay paired,

$$\dots (\pi_g)^3(\bar{\pi}_u); {}^1\Sigma_u^+ \leftarrow \dots (\pi_g)^4; {}^1\Sigma_g^+.$$

The molecule possesses cylindrical symmetry in both the ground and excited states and thus the π_g and $\bar{\pi}_u$ orbitals may be written as functions of the cylindrical coordinates r, z and ϕ as

$$\pi_g = g(r, z) \exp(i\phi); \bar{\pi}_u = u(r, z) \exp(i\phi).$$

The determinantal wave function for the ${}^1\Sigma_g^+$ state is

$$\langle {}^1\Sigma_g^+ \rangle = |g \exp(i\phi)\alpha \cdot g \exp(i\phi)\beta \cdot g \exp(-i\phi)\alpha \cdot g \exp(-i\phi)\beta|$$

and for the ${}^1\Sigma_u^+$ state

$$\begin{aligned} \langle {}^1\Sigma_u^+ \rangle &= \frac{1}{2} \times [u \exp(i\phi)\alpha \cdot g \exp(i\phi)\beta \cdot g \exp(-i\phi)\alpha \cdot g \exp(-i\phi)\beta] \\ &\quad + [g \exp(i\phi)\alpha \cdot u \exp(i\phi)\beta \cdot g \exp(-i\phi)\alpha \cdot g \exp(-i\phi)\beta] \\ &\quad + [g \exp(i\phi)\alpha \cdot g \exp(i\phi)\beta \cdot u \exp(-i\phi)\alpha \cdot g \exp(-i\phi)\beta] \\ &\quad + [g \exp(i\phi)\alpha \cdot g \exp(i\phi)\beta \cdot g \exp(-i\phi)\alpha \cdot u \exp(-i\phi)\beta] \end{aligned}$$

When these wave functions are substituted into equation (6) the result is

$$\rho_{gu}(r, z) = 4 \times \frac{1}{2} g(r, z) \exp(-i\phi) \cdot u(r, z) \exp(i\phi) = 2g(r, z)u(r, z).$$

The radial functions $g(r, z)$ and $u(r, z)$ are of the forms



and their product ρ_{gu} may be pictured as



The perturbation term $V_{gu}^{(3)}q_3$ may be pictured as the interaction



The dipole created by the displacement of the carbon atom in the vibration v_3 will thus interact strongly with the electronic charge distribution ρ_{gu} and the energy will be lowered. The superposition of the symmetric mode v_1 on the same asymmetric charge distribution



results in the two nuclear motions nullifying one another and the overall result is zero. This is an illustration of the fact that ρ_{0k} and q_i must be of identical symmetries if the perturbation $V_{0k}q_i$ is to possess a non-zero value.

It is to be expected that the electronic structure and behaviour of the unsymmetrical sixteen electron triatomic molecules such as COS and NNO will not differ markedly from that observed for the symmetrical cases. The uppermost filled π orbital in the unsymmetrical case (corresponding to the π_g orbital of the $D_{\infty h}$ group) is now best described as $(a\pi + b\pi - c\pi)$ where the antibonding is between the central atom and the most electronegative of the end atoms, oxygen in OCS and NNO and Cl in ClCN. The greatest concentration of charge is also centred on this most electronegative atom. The orbital corresponding to the antibonding orbital $\bar{\pi}_u$ is now represented as $(-a'\pi + b'\pi + c'\pi)$ and the charge is now centred on the remaining end atom. The transition density resulting from $a(\bar{\pi})(\pi)^3$; ${}^1\Sigma^+ \leftarrow (\pi)^4$; ${}^1\Sigma^+$ transition will, aside from a finite amount of charge now residing on the central atom, resemble very strongly that found in the linear symmetric triatomic molecules. The overall result is still a

parallel transition moment with the charge concentrated mainly on the two end atoms.

Since both of the linear vibrations of the $C_{\infty v}$ point group molecules belong to the same irreducible representation, symmetry arguments alone cannot be employed to predict the sign of the interaction constant as was done previously. However, the two stretching modes of the $C_{\infty v}$ molecules still bear an important resemblance to those of the $D_{\infty h}$ molecules in that in ν_1 , both Δr_1 and Δr_2 are still of the same sign while in ν_3 they differ in sign. Thus we still have a situation in which one mode results in the stretching of both bonds, and the other mode in the lengthening of one and the contracting of the other. The relative amplitudes of the three atoms in the modes ν_1 and ν_3 are shown in figure 1 for ClCN [22] and NNO [27]. The motions in COS will be very similar. It is evident that in ν_3 the relative amplitude of motion of the central atom is greater than that of either of the two end atoms, while in ν_1 the motions of the two end atoms are either comparable to or greater than that of the central atom. Furthermore, in ν_1 the motions of the two end atoms are opposed as in the symmetric stretch of the $D_{\infty h}$ molecules, while in ν_3 they move in phase. Thus, as in the case of the linear symmetric molecules, the charge density will overlap most effectively with the dipole of the central atom and this will be most effective in the 'antisymmetric' mode ν_3 where one bond is lengthened and the other is shortened. The interaction constant should, therefore, be positive. As noted in the table this is the observed result for COS, NNO and ClCN. The $^1B_1 \leftarrow ^1\Sigma^-$ transition (correlating with $^1\Sigma^-$) has a λ_{max} of 1510 Å for COS and one of the bands in the absorption region extending from 3000 to 1760 Å of NNO is also to the bent upper state correlating with $^1\Sigma^+$ [6]. The same should be true for ClCN. (It is important to note that in all of the 16 electron molecules so far considered, even if $\bar{\sigma}_g$ did lie lower than $\bar{\pi}_u$, in some cases this would not invalidate any of the above arguments. Transitions to $\bar{\sigma}_g$ do not give a state of proper symmetry for mixing with either of the stretching vibrations and the $^1\Sigma_u^+$ or $^1\Sigma^+$ states would certainly be the next lowest in energy.)

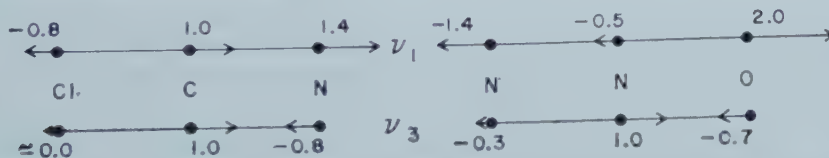


Figure 1. The relative atomic displacements in the linear vibrations ν_1 and ν_3 of ClCN and NNO.

Uncertainty exists as to the sign of the interaction constants in the mercuric dihalides. However, their electronic spectra have been interpreted with some certainty [26], and it is thus of interest to apply the present theory to these molecules. Duchesne and Burnelle [2] have found positive values for k_{12} in the molecules ClHgBr and BrHgI . These authors state, with good reason, that the negative values of k_{12} calculated by Linnett and Hoare for the symmetric halides HgI_2 , HgBr_2 and HgCl_2 are probably in error. Linnett and Hoare were forced, because of a lack of experimental data, to employ in their calculation values of the bending mode frequency obtained from the excited states of the molecules. The present theory also predicts positive values of k_{12} for the HgX_2 molecules. They possess an electronic structure similar to that of the other linear triatomic molecules

with 16 valence electrons, except that the π_u and π_g orbitals are now best described as weakly interacting atomic orbitals on the two end halogen atoms with no contribution from the central mercury atom. The three symmetric halides (chloride, bromide and iodide) all possess a long wavelength absorption continuum which Walsh [6] ascribes to the transition ${}^1B_1 \leftarrow {}^1\Sigma_g^+$ (the 1B_1 state correlating with ${}^1\Delta_u$) and another absorption at shorter wavelengths which Sponer and Teller [26] have definitely identified as the ${}^1\Sigma_u^- \leftarrow {}^1\Sigma_g^+$ transition. The stretching frequencies are decreased in the ${}^1\Sigma_u^-$ state, but there is only slight departure from linearity. The transition density is thus of Σ_u^+ symmetry and we thus predict the interaction constants to be positive. The mixed halides of $C_{\infty v}$ symmetry should also possess positive interaction constants for the same reasons as given previously for the other 16 valence electron molecules of $C_{\infty v}$ symmetry.

4. LINEAR TRIATOMIC IONS OF THE ACTINIDE ELEMENTS

Jones [8] has determined the interaction constants for the linear triatomic ions UO_2^{+2} , NpO_2^{+2} , PuO_2^{+2} and AmO_2^{+2} and found them to be negative. Thus unlike the triatomic molecules considered previously, the ions must possess a low lying excited state of symmetry Σ_g^+ . The presence of such a state may be accounted for if one invokes 'df' hybridization for the actinide elements. There are numerous references in the literature to the presence of df hybridization in uranyl and uranyl-like ions and also to the fact that in such compounds the f orbitals of the metal participate in covalent bonding.

Eisenstein and Price [9, 10] have considered in detail the electronic structure of UO_2^{+2} , NpO_2^{+2} and PuO_2^{+2} . We may consider these compounds as composed of a metal ion M(VI) of electronic configuration $(Th^{+4}) (5f)^n$ (where $n=0, 1, 2, 3$ respectively for U, Np, Pu and Am) with two O^{-2} ions arranged, one either side of the metal ions in a linear fashion. The axially symmetric field of the two O^{-2} ions will partially remove the degeneracy of the d and the f orbitals of the metal ion, the d orbitals splitting into levels of symmetries σ_g , π_g and δ_g , and the f orbitals into levels of σ_u , π_u , δ_u and ϕ_u symmetries. The symmetric and antisymmetric combinations of the oxygen p_z orbitals (the z axis being the molecular symmetry axis) may overlap with the d_σ and f_σ orbitals of the metal ion respectively and thus account for the covalent sigma bond formation in these complexes. There is also a possibility of π bond formation, between the p_x and p_y orbitals of the oxygens and the d_π and f_π orbitals of the metal ion. Pryce and Eisenstein [9] ignore this possibility but quote evidence that the metal-oxygen bond in these molecules is approximately double, which would correspond to an intermediate state between full π bond formation and its complete absence. We shall construct our molecular symmetry orbitals assuming at least weak π bonding between the metal ion and the oxygens. Its omission does not affect the argument. The resulting molecular orbitals and energy levels are illustrated in figure 2. The ϕ_u and δ_u orbitals of the metal ion do not participate in the bonding, but their term values are still shifted by the crystal field.

In the case of UO_2^{+2} the twelve electrons, all paired, are accommodated in the six lowest molecular orbitals giving the observed diamagnetism of this compound. (We have assumed for simplicity that the four electrons in the oxygen 2s orbitals are tightly held and contribute little to the sigma bonding.) The NpO_2^{+2} ion will possess one unpaired 5f electron. Eisenstein and Pryce [9] have shown that the spin-orbit coupling is sufficiently weak in these compounds

(the coupling constant $\zeta_f \approx 1300 \text{ cm}^{-1}$) that a molecular type of Russell-Saunders coupling may be employed in the description of their electronic behaviour. We thus have J_z , L_z and S_z , the axial components of the total, orbital and spin angular momentum all as good quantum numbers. The ground state of UO_2^{+2} is thus a $^1\Sigma_g^+$ state. In NpO_2^{+2} the single unpaired electron will be found in a ϕ orbital as this will allow it to be furthest away from the central core of electrons. The resulting four-fold degenerate $^2\Phi$ level ($L_z = \pm 3, S_z = \pm \frac{1}{2}$) is further split by the spin-orbit interaction into two Kramers spin doublets, a lower level $^2\Phi \pm \frac{5}{2}$ and a level $^2\Phi \pm \frac{7}{2}$, some $3\zeta_f$ above it. The Δ_u levels and the antibonding combinations of the π and σ levels are also split by the spin-orbit coupling but this need not concern us here.

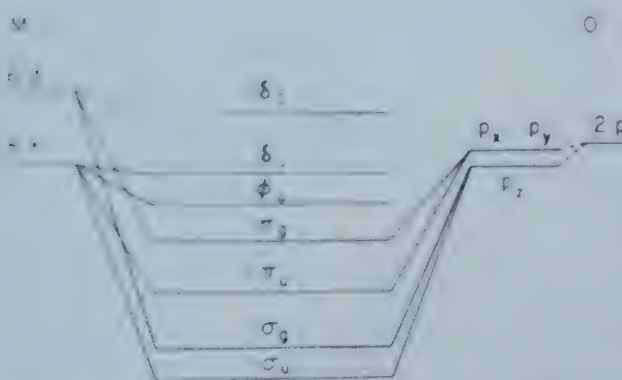


Figure 2. The molecular symmetry orbitals for the uranyl-like ions, $\text{MO}_{\frac{1}{2}}^{+2}$. The antibonding orbitals are not included in the figure.

The PuO_2^{+2} ion has two unpaired $5f$ electrons and due to the electronic repulsion between them they are forced to occupy orbitals of different L_z values, the electronic configuration being $(\phi)^1(\Delta)^1$. The resulting level is one with $L_z = 5$, or a 3H level. The spin-orbit coupling will again split the possible combinations of L_z and S_z and leave a doublet with a total axial component of angular momentum of ± 4 . The ground state is thus 3H_4 with the levels 3H_4 and 3H_6 lying approximately 3000 and 6000 cm^{-1} above it [10].

The lowest transition of the UO_2^{+2} ion which possesses a symmetry identical to that of one of the linear vibrations is

$$(\pi_g)^3(\bar{\pi}_g)^1; ^1\Sigma_g^+ \leftarrow \dots (\pi_g)^4; ^1\Sigma_g^+$$

which gives a transition density of symmetry Σ_g^+ . Transitions to the intervening ϕ and δ levels will be irrelevant as they will not possess transition densities of the proper symmetries. In the NpO_2^{+2} , PuO_2^{+2} and AmO_2^{+2} ions the only relevant transitions are again those involving an excitation of a π_g electron to the antibonding $\bar{\pi}$ orbital, which gives a transition density of symmetry Σ_g^+ . All of these ions should possess negative interaction constants as is observed.

5. BENT TRIATOMIC MOLECULES WITH 17, 18, 19 AND 20 VALENCE ELECTRONS

Nitrogen dioxide (NO_2) is a 17 electron molecule. Its molecular symmetry orbitals may be written as



according to Mulliken [7]. The transition of longest wavelength with a λ_{\max} of 3900 Å is



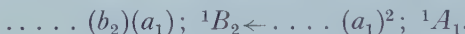
The transition of next lowest energy is



with a λ_{\max} of 4400 Å.

Since the symmetry of the transition density for the first transition is B_1 , the interaction constant should be positive. This is the observed result as listed in the table.

Sulphur dioxide and ozone are 18 electron molecules and their electronic configurations aside from the upwards displacement of the $2b_1$ orbital to above the $3a_1$ orbital are the same as that given above for NO_2 but with one more electron in the $4a_1$ orbital [6, 7]. The lowest transition for SO_2 is

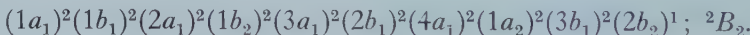


This has a λ_{\max} of 3740 Å. The next lowest transition is



with a λ_{\max} of 2940 Å. Only the second of these two electronic excitations gives a transition density of proper symmetry for mixing with one of the vibrational modes. Since it is a B_1 state the interaction constant should be positive. The observed ones for SO_2 and O_3 as recorded in the table are positive.

Chlorine dioxide is a 19 electron molecule and due to the significant change in its bond–bond angle, some of the low-lying symmetry orbitals have interchanged from what they were in NO_2 . Mulliken [7] gives the electronic configuration of ClO_2 as



The first three predicted transitions for ClO_2 give transition densities of either A_2 or B_2 symmetry. These, of course, cannot mix with either of the vibrational symmetries. The next transition (and it is observed) occurs at λ_{\max} of 3400 Å and is



This gives a transition density of symmetry B_1 and thus the interaction constant k_{12} should be positive. Due to the uncertainty in the value of the frequency for ν_2 the sign of the interaction constant is not known. Both positive and negative values give real values for the other frequencies [11].

The electronic structure of the 20 electron molecules, e.g. Cl_2O and F_2O correspond to the addition of one electron to the $2b_2$ orbital. The next lowest lying molecular orbital is the $5a_1$. The first excited state will be of symmetry B_2 which will not mix with any of the vibrational modes. The second is



of symmetry B_1 and thus the B_1 vibration should mix and k_{12} be positive. This is observed for F_2O [2]. Again due to the uncertainty in ν_2 the sign of k_{12} is uncertain as in the case of Cl_2O [11] but it seems safe to assume, in analogy with F_2O , that it is positive.

6. THE HYDRIDES AH_2 OF SYMMETRY C_{2v}

The most general potential function for C_{2v} triatomic molecules is

$$2V = k(\Delta r_1^2 + \Delta r_2^2) + k_{12}\Delta r_1\Delta r_2 + k_\delta\delta^2 + k_{\delta r}\delta(\Delta r_1 + \Delta r_2).$$

The stretching mode ν_1 and the bending mode ν_2 belong to symmetry A_1 and the antisymmetric stretch ν_3 to B_1 . In these cases the bending and stretching motions may interact since they possess the same symmetry in A_1 . The interaction constant k_{12} is expected to be negative if the lowest lying state is of symmetry 1A_1 and positive if it is of symmetry 1B_1 .

The molecular symmetry orbitals for $C_{2v} AH_2$ molecules may be written as

$$(1a_1)^2(2a_1)^2(1b_1)^2(3a_1)^2(1b_2)^2; {}^1A_1.$$

In the case of water, for example, the a_1 orbitals involve the H(1s), the O(1s), O(2s) and O($2p_z$), $1b_1$ involves the antisymmetric combinations of the H(1s) with the O($2p_x$) and $1b_2$ is simply the O(p_y) orbital. The above order of the orbitals, in the order of decreasing term values, is given by Mulliken [12], Price and Sudgen [13] and by Ellison and Shull [14]. The latter authors have calculated the ionization potentials using LCAO SCF MO's and for the three highest energy orbitals these values are in the order of their appearance above, -16.2 , -14.5 , -12.6 e.v. Walsh [15] has reversed the order of $3a_1$ and $1b_1$ but he admits that it might well fall in the order we have given. He was not concerned with this point as it did not alter any of his interpretations of the electronic spectra.

Everyone agrees that the first transition is from the $1b_2$ orbital to either the $3s$ (symmetry a_1) orbital on oxygen or to the antibonding intra-valency shell orbital made up of the out-of-phase overlap of oxygen with the hydrogen 1s orbitals. This is also of symmetry a_1 . The absorption from 1830 to 1500 Å probably involves both transitions

$$\dots (1b_2)(1\bar{a}_1); {}^1B_2 \leftarrow \text{or} \dots (1b_2)(3s); {}^1B_2 \leftarrow \dots (3a_1)^2(1b_2)^2; {}^1A_1$$

which are not of the correct symmetry to mix with either of the vibrational modes†. There are no more observed transitions but the next one of lowest energy should be that of an electronic transition from $3a_1$ to either of the two excited a_1 orbitals described above. Both of these will give rise to an upper state of proper symmetry,

$${}^1A_1 \leftarrow {}^1A_1.$$

The important point is that the $3a_1$ orbital lies above the $1b_1$ orbital for otherwise the upper state would be of symmetry B_1 .

The symmetry of the first excited state of proper symmetry is, therefore, most likely A_1 and the interaction constant k_{12} should be negative. This is the observed result. The molecules H_2S and H_2Se may be expected to have the same electronic structure and behaviour and they too possess interaction constants k_{12} of negative sign.

Linnett and Heath [16] have given a different interpretation of the signs of the interaction constants in the water molecule. They have shown that the negative value for the k_{12} interaction constant and the positive value for $k_{\delta r}$ cannot

† Mulliken agrees with all of the above, but when he writes the electronic structure for the excited state he changes the nomenclature of the remaining p_y electron from b_2 to a_1 which must be an error. Thus the symmetry of the upper state becomes A_1 and he terms the transition as ${}^1A_1 \leftarrow {}^1A_1$.

be accounted for in terms of interactions between non-bonded atoms. They feel that the observed signs of the interaction constants can be interpreted in terms of the changes in the *sp* hybridization when the molecule undergoes a vibration. The greater the amount of *s* character in the bonds, the stronger and shorter will the OH bonds be. Thus an increase in the HOH angle should, since it implies an increase in the amount of *s* character, lead to a shortening of the OH bonds and thus to a positive value for $k_{\delta r}$. Furthermore, the stretching of either OH bond will lead to an increase in the amount of *p* character and thus a lengthening of each, or a negative interaction constant.

7. PLANAR AB_3 MOLECULES, SYMMETRY D_{3h}

This group includes the following 24 electron molecules; BF_3 , BCl_3 , BBr_3 . The structure of the representation of the internal coordinates is

$$\Gamma = A_1' + A_2'' + 2E'.$$

The vibration of species A_1' is a totally symmetric stretch, of species A_2'' an out-of-plane bend, and those of species E' are compounded of antisymmetric stretches and in-plane bending motions. Anderson, Larsettre and Yost [17] have determined the constants in the following potential expression for the above three boron trihalides;

$$2V = k \sum \Delta r_i^2 + k_\alpha r_0^2 \sum \Delta \alpha_{ij}^2 + k_\beta r_0^2 \sum \Delta \beta_i^2 + 2k_{12} \sum \Delta r_i \Delta r_j$$

where r_0 is the equilibrium bond length, β_i is the angle between AB_i and the B_3 plane and α_{ij} is the angle B_iAB_j . The bond-bond interaction constant was found to be positive for all three of these molecules as shown recorded in the table.

According to Walsh [18], the ground state electronic structure may be written in terms of molecular symmetry orbitals

$$(a_1')^2(1e')^4(a_2'')^2(2e')^4(2e'')^4(a_2')^2; {}^1A_1'.$$

The two lowest excited molecular orbitals are of symmetries \bar{a}_1' and \bar{a}_2'' where the bar denotes their antibonding character. The lowest excited state of proper symmetry is obtained by the following transition

$$\dots (2e'')(a_2')^2(\bar{a}_2''); {}^1E' \leftarrow \dots (2e'')^4(a_2')^2; {}^1A_1'.$$

The symmetry of the transition density is thus E' (this would be an allowed transition). The data on the observed transitions of these molecules are meagre, and since both of the excited orbitals are strongly antibonding, the spectra are continuous in nature. There is little doubt, however, that the first excited state of proper symmetry will be the ${}^1E'$ one. Thus k_{12} should be positive, as is observed.

8. PYRAMIDAL AB_3 MOLECULES

The 26 electron molecules PF_3 , PCl_3 , PBr_3 , AsF_3 , $AsCl_3$, $SbCl_3$ and $BiCl_3$ all belong to the point group C_{3v} . They possess one stretching mode ν_1 and one bending mode ν_2 of symmetry A_1 , and one doubly degenerate stretching mode ν_3 and a doubly degenerate bending mode ν_4 of symmetry E .

While we agree with the description of the electronic structure of the planar AB_3 molecules as given by Walsh [18] his description of the pyramidal AB_3 molecules is not acceptable as he does not allow for any mixing of the *s* and *p* orbitals on the *A* atom. Walsh treats the pyramidal AB_3 molecules as having

pure p bonds between the A and B atoms with no s character. Thus when the planar AB_3 is bent to give the corresponding orbitals of the pyramidal form, a p_z orbital in the planar form (\tilde{a}_2'') becomes an s orbital on the A atom in the pyramidal form and the s orbital in the planar form becomes the p_z orbital in the pyramidal form. Furthermore, Walsh does not give the relative order of the orbitals in the pyramidal form and does not discuss the spectra for such molecules.

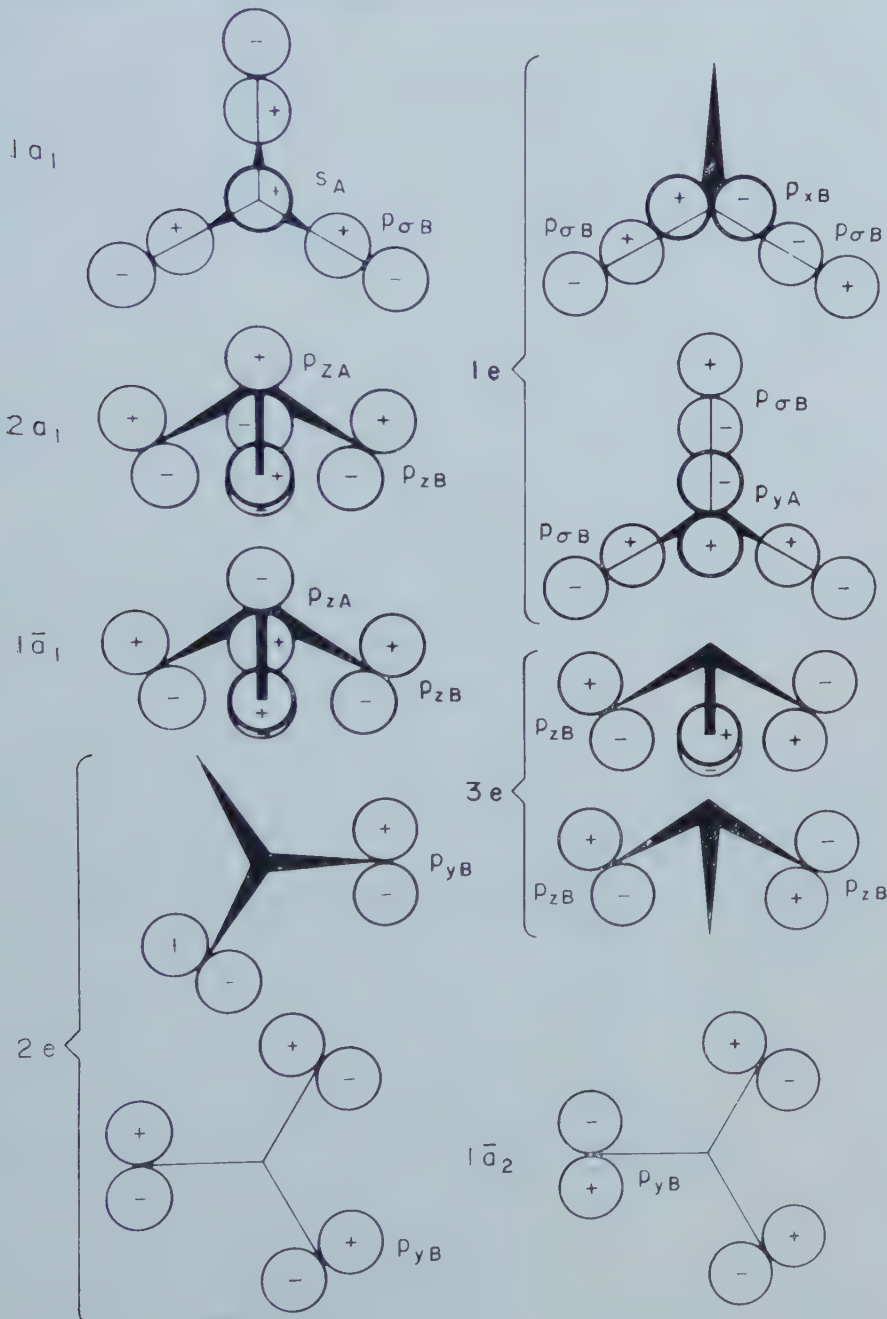


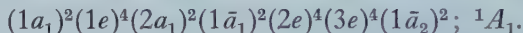
Figure 3. The molecular symmetry orbitals for pyramidal AB_3 molecules.

By constructing molecular symmetry orbitals with allowances for *s-p* mixing on atom *A*, we can assign the order of the molecular orbitals with some certainty and arrive at conclusions regarding the symmetries of the excited states.

The orbitals may be considered as built up in the manner illustrated in figure 3.

The $1a_1$ orbital is best considered as also possessing some contribution from the p_z orbital of atom *A*. The $2a_1$ orbital will consist of the orbital, labelled as such in figure 3, with some admixture of the $1a_1$ orbital. The $1\bar{a}_1$ orbital is the same as the $2a_1$ orbital but the p orbitals on the *B* atoms are now out of phase with the p_z on *A*. Thus, the $1\bar{a}_1$ orbital is weakly *A-B* antibonding in this sense, but still *A-B* bonding with the p_{zA} and the $p_{\sigma B}$'s. It is also *B-B* bonding. The $2e$ orbitals are composed of the p orbitals of the *B* atoms which lie in the B_3 plane. The $3e$ orbitals are composed of the out of phase overlapping of the *B* atom p orbitals which are perpendicular to the *A-B* bonds. The $1\bar{a}_2$ orbital is the third member of the set made up from the *B* atom p orbitals which lie in the B_3 plane. Since all of the *B* atoms are now out of phase it will lie higher in energy than the other two from this set, the $2e$ orbitals. The first vacant orbital, $3a_1$ will be the next highest *s* orbital on the *A* atom.

We may write the electronic configuration of the pyramidal AB_3 molecules as



The first excited state would be of symmetry 1A_2 arising from the excitation of a $1\bar{a}_2$ electron to the $3a_1$ orbital. This is not of the proper symmetry to mix with a vibration. The next lowest excited state should arise from the transition



The transition density will belong to the symmetry species *E*, and thus k_{12} and $k_{\delta\delta}$ (the bending mode interaction constant) should be positive, as is observed for all of the molecules of this type so far reported.

9. CONCLUSIONS

The complete agreement between the predicted and observed signs of the potential interaction constants would seem to justify their interpretation in terms of the modified second-order perturbation theory which has been employed. The assumption that the lowest of the excited electronic states (of the proper symmetry) makes the most important contribution to the second-order sum in the expression for the energy is a sound one. The decrease in energy due to the second-order term may be visualized as arising from the interaction of a charge density which corresponds to a state of transition between the ground and excited states with the nuclear dipoles which arise from the vibrational motion.

Our results show, as noted by other authors, that molecules of similar electronic structure possess interaction constants of like sign. However, the sign of k_{12} depends not only upon the configuration of the ground state, but on that of the excited states as well and it is only due to the fact that the similarity of electronic states between isoelectronic molecules applies generally to the excited as well as to the ground states that the observation noted above holds true. Thus, all of the molecules with 16 valence electrons (aside from UO_2^{++}) have positive interaction constants since the first excited state of proper symmetry is in each case one which gives rise to an asymmetric charge distribution in the distorted molecule and thereby to a lessening of the potential energy increase for motion in the asymmetrical vibrational mode.

The observation of Linnett and Hoare [3] that a positive k_{12} is associated with unlocalized electrons and a negative k_{12} with localized ones is not a general one, the UO_2^{+2} ion being an example of an exception. The valence electrons of the uranyl ion are certainly unlocalized and yet it possesses a negative k_{12} , since the relevant transition density possesses full symmetry in this case.

Another apparent failure of the rule of Linnett and Hoare is provided by the mercuric dihalides. In these molecules the electrons are best considered as localized and according to their rule these molecules should possess negative interaction constants. In point of fact, as noted in § 3 of this paper, the interaction constants are most probably positive.

I wish to thank Professor H. C. Longuet-Higgins and Dr. L. E. Orgel for kindly suggesting this problem and for their help and discussions. I also gratefully acknowledge an award from the National Research Council of Canada.

REFERENCES

- [1] COULSON, C. A., DUCHESNE, J., and MANNEBACK, C., 1947, *Nature, Lond.*, **160**, 793.
- [2] DUCHESNE, J., and MONFILS, A., 1949, *J. chem. Phys.*, **17**, 586; DUCHESNE, J., and BURNELLE, L., 1951, *J. chem. Phys.*, **19**, 1191.
- [3] LINNETT, J. W., and HOARE, M. F., 1949, *Trans. Faraday Soc.*, **45**, 844.
- [4] COULSON, C. A., and LONGUET-HIGGINS, H. C., 1948, *Proc. roy. Soc. A*, **193**, 456.
- [5] LONGUET-HIGGINS, H. C., 1956, *Proc. roy. Soc. A*, **235**, 537.
- [6] WALSH, A. D., 1953, *J. chem. Soc.*, 2266.
- [7] MULLIKEN, R. S., 1942, *Rev. mod. Phys.*, **14**, 204.
- [8] JONES, L. H., 1955, *J. chem. Phys.*, **23**, 2105.
- [9] EISENSTEIN, J. C., and PRYCE, M. H. L., 1955, *Proc. roy. Soc. A*, **229**, 20.
- [10] EISENSTEIN, J. C., and PRYCE, M. H. L., 1956, *Proc. roy. Soc. A*, **238**, 31.
- [11] HEDBERG, K., 1951, *J. chem. Phys.*, **19**, 509.
- [12] MULLIKEN, R. S., 1935, *J. chem. Phys.*, **3**, 506.
- [13] PRICE, W. C., and SUDGEN, T. M., 1948, *Trans. Faraday Soc.*, **44**, 108, 116.
- [14] ELLISON, F. O., and SHULL, H., 1953, *J. chem. Phys.*, **21**, 1420.
- [15] WALSH, A. D., 1953, *J. chem. Soc.*, 2260.
- [16] LINNETT, J. W., and HEATH, D. F., 1948, *Trans. Faraday Soc.*, **44**, 556.
- [17] ANDERSON, T. F., LARSETTRE, E. N., and YOST, D. M., 1936, *J. chem. Phys.*, **4**, 703.
- [18] WALSH, A. D., 1953, *J. chem. Soc.*, 2301.
- [19] WILSON, E. B., DECUS, J. C., and CROSS, P. C., 1955, *Molecular Vibrations* (New York: McGraw-Hill Book Co. Inc.), p. 178.
- [20] SUTHERLAND, G. B. B. M., and PENNEY, W. G., 1936, *Proc. roy. Soc. A*, **156**, 678.
- [21] CALLOMAN, H. J., McKEAN, D. C., and THOMPSON, H. W., 1951, *Proc. roy. Soc. A*, **208**, 541.
- [22] HERZBERG, G., 1954, *Molecular Spectra and Molecular Structure*, Vol. II (New York: D. Van Nostrand Co., Inc.), pp. 187, 177.
- [23] POLO, S. R., and WILSON, M. K., 1954, *J. chem. Phys.*, **22**, 900, 904.
- [24] PIERCE, L., 1956, *J. chem. Phys.*, **24**, 139.
- [25] WESTON, R. E., 1957, *J. chem. Phys.*, **26**, 1248.
- [26] SPONER, H., and TELLER, E., 1941, *Rev. mod. Phys.*, **13**, 106.
- [27] GILL, K. E., and LAIDLER, K. J., 1958, *Canad. J. Chem.*, **36**, 1570.

Ultra-violet absorption spectra and π -electron structures of nitromethane and the nitromethyl anion†

by SABURO NAGAKURA‡

Laboratory of Molecular Structure and Spectra, Department of Physics,
the University of Chicago and the Institute for Solid State Physics,
the University of Tokyo

(Received 30 September 1959)

The ultra-violet absorption spectrum of nitromethane was measured under various conditions. Besides the weak band at $270 \text{ m}\mu$, a strong band, which may be regarded as due to the longest wavelength $\pi \rightarrow \pi^*$ transition band, was observed at $198 \text{ m}\mu$ in the gaseous state. Further, the absorption spectrum of nitromethane was measured in aqueous solutions with several different pH values, and a strong band was observed at $233 \text{ m}\mu$. From the fact that the pK_a value evaluated on the basis of the pH dependence of the absorption intensity is equal to that obtained electrometrically, it was concluded that the $233 \text{ m}\mu$ band is to be ascribed to the nitromethyl anion ($\text{H}_2\text{C}^-\text{NO}_2$). This band was found to shift to $238 \text{ m}\mu$ in alcoholic KOH solution.

The π -electron structure of the anion was studied theoretically by taking into account configuration interaction in terms of the ground, charge transfer, and locally excited configurations. It is shown that the $233 \text{ m}\mu$ band of the anion may be interpreted as an intramolecular charge-transfer absorption involving a large electron transfer from CH_2^- toward NO_2^- . It is suggested that electron donating substituent groups like NH_2 , OH , and CH_2^- should cause the $198 \text{ m}\mu$ band of the nitro group to shift toward shorter wavelengths, in marked contrast to the case of substituted benzene molecules like aniline and phenol.

1. INTRODUCTION

It has been well recognized that aliphatic nitro compounds like nitromethane exhibit some interesting properties from both physical and chemical points of view. These molecules are generally represented by a resonance hybrid between the two following structures, and they have an unusually large dipole moment ($3.5 \sim 3.8 \text{ D}$) [1]:



Further, concerning the ultra-violet absorption spectra of these nitro compounds, a weak band at $270 \text{ m}\mu$ has been extensively studied by several authors [2, 3, 4, 5, 6] and reasonably assigned to an $n \rightarrow \pi^*$ transition. However, no strong band which

† This work was assisted by the Office of Ordnance Research Under Project TB2-0001 (505) of Contract DA-11-022-ORD-1002 with the University of Chicago.

‡ Permanent address: The Institute for Solid State Physics, The University of Tokyo, Meguro-ku, Tokyo.

can be associated with the allowed $\pi \rightarrow \pi^*$ transition has ever been observed with simple nitroalkanes[†]. In the present study of the ultra-violet absorption spectrum of nitromethane, the author found a new band whose molar extinction coefficient is about 5000 and which may safely be assigned to the allowed $\pi \rightarrow \pi^*$ transition.

From the chemical point of view, aliphatic nitro compounds are well known to be typical carbon acids (pseudo-acids). That is to say, they show acid dissociation represented by the following equation[‡] [8]:



The acid dissociation constant (pK_a) of nitromethane has been determined as 10.2 at 25 °C by the aid of electrometric measurement [8]. Since the nitromethyl anion, the ionization product, is isoelectronic with nitramide ($\text{H}_2\text{N}-\text{NO}_2$) whose strong band at 243 m μ has been shown to be satisfactorily explained as an intramolecular charge transfer absorption [9], it seems interesting to compare the absorption spectra of these two entities. Furthermore, as was pointed out by Leffler [10], electronic structures of anions of this kind are important in discussing the relationship between the equilibrium constant and the rate constant for the acid dissociation reactions of several nitroalkane molecules. Under these circumstances, it was undertaken to measure the ultra-violet absorption spectrum of the nitromethyl anion and to make some theoretical study of its electronic structure.

2. EXPERIMENTAL

2.1. Materials

Commercial nitromethane was dried with calcium chloride. Before use it was fractionally distilled (b.p. 101~102 °C). Methanol used as a solvent was dried by the use of magnesium foil activated by iodine, and then fractionally distilled. The buffer solutions were Fisher Certified Reagent, Standard Buffer Solution.

2.2. Measurement

Most of the near ultra-violet absorption spectra were measured with a Beckman spectrophotometer model DU. The measurements of the absorption spectra in the wavelength region 2300 Å to 1900 Å were made with a Cary self-recording spectrophotometer model 14, using a set of special fused silica cells especially transparent to ultra-violet light below 2000 Å. In both instruments the temperature of the cell compartment was kept constant during the measurement by circulating water at a constant temperature.

3. EXPERIMENTAL RESULTS

3.1. Ultra-violet absorption spectrum of nitromethane

The ultra-violet absorption spectrum of nitromethane was measured in the gaseous state and in aqueous and alcoholic solutions. The results are shown in

[†] Matsen stated that nitromethane exhibits a strong band at 210 m μ . However, the data to which he referred show no definite absorption maximum (see reference [5]).

[‡] Hantzsch believed that the ionization of nitromethane could not take place directly, but only by the intermediate formation of the aci-form $\left(\text{H}_2\text{C}=\text{N}^+ \begin{array}{c} \text{OH} \\ \backslash \\ \text{O} \end{array} \text{O}_- \right)$. However, it is now believed that the ionization occurs by a single step, as above. Concerning this problem, see reference [7].

figure 1. In addition to the well-known weak band at $270\text{ m}\mu$, a new band was observed at $198\text{ m}\mu$ in the gaseous state^{†‡}. This band shifts to $201\text{ m}\mu$ in the aqueous and alcoholic solutions, only a small red shift. Its peak molar extinction coefficient amounts to 5007 in the aqueous solution. In view of this large molar extinction coefficient, the band may reasonably be assigned to an allowed $\pi \rightarrow \pi^*$ transition. More detailed discussion on this point will be given in § 4.

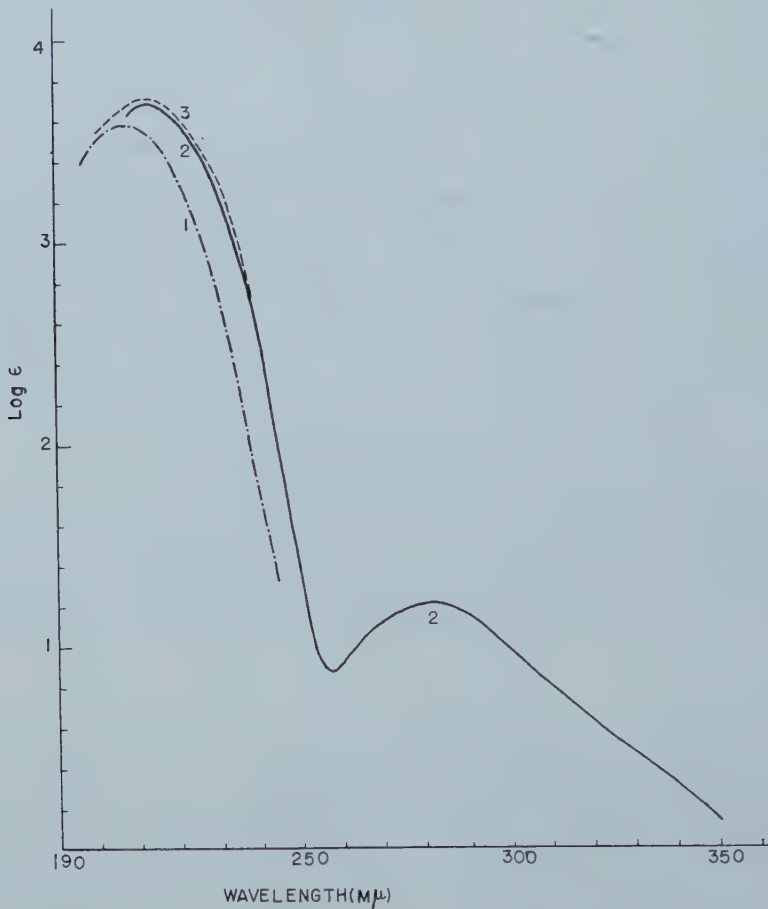


Figure 1. The ultra-violet absorption spectrum of nitromethane.
Curve 1: in the gaseous state; curve 2: in methanol; curve 3: in water.

† It is known that there exists a tautomeric equilibrium between the usual and aci-forms of nitromethane. However, the possibility that this new band may be due to the aci-form can be almost completely neglected, because the concentration ratio of this form to the usual form is known to be negligibly small ($K_r = [\text{aci-form}] / [\text{usual-form}] = 1.1 \times 10^{-7}$ at 25°C (reference [8])).

‡ The vapour pressure of nitromethane necessary for evaluating the molar extinction coefficients in the gaseous state was obtained by the aid of the following equation (see reference [11]):

$$\log_{10} p = 7.274 - 1441.6/(t + 226.9),$$

where p is the vapour pressure (mm Hg) and t is the temperature ($^\circ\text{C}$).

3.2. The ultra-violet absorption spectrum of the nitromethyl anion

The above-mentioned ultra-violet absorption spectrum of nitromethane changes to a great extent in aqueous alkaline solution. As is seen from curve 5 in figure 2, which is the absorption spectrum of nitromethane in 0.01 N aqueous sodium hydroxide solution, the 270 m μ band becomes blurred and a strong band appears at 233 m μ . This result is very similar to that obtained by Kortüm under almost the same experimental conditions [2]. Since it may be expected that nitromethane acts as acid and exists in the form of the anion of this acid, it is reasonable to consider that the 233 m μ band should be ascribed to the anion. In order to make sure of this point, it was undertaken to measure the absorption

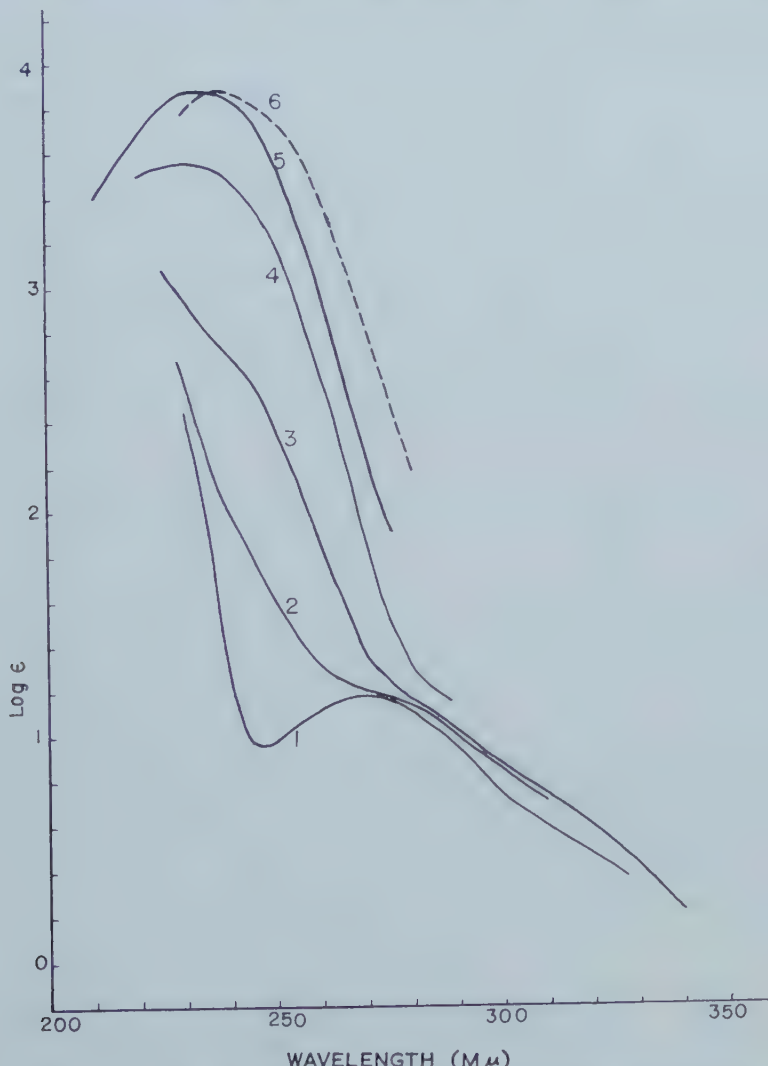


Figure 2. The ultra-violet absorption spectrum of nitromethane in aqueous solutions with different pH values and in alcoholic KOH solution.

Curve 1: in water; curve 2: in pH 8 buffer solution; curve 3: in pH 9 buffer solution; curve 4: in pH 10 buffer solution; curve 5: in 0.01 N NaOH aqueous solution; curve 6: in 0.01 N KOH alcoholic solution.

spectrum of nitromethane in buffer solutions with different pH values ranging from 6 to 10 and to obtain quantitative information on the dependence of 233 m μ band intensity on the pH value of the solution†. The results are shown in figure 2. From the absorption curves given in this figure, the acid dissociation constant (pK_a) of nitromethane was determined as 10·1 at 25°C‡. This value is in fairly good agreement with that determined by the electrometric measurement (10·21 at 25°C). This fact furnishes substantial evidence that the 233 m μ band observed in the present investigation is due to the nitromethyl anion.

A similar experiment was carried out with an alcoholic potassium hydroxide solution of nitromethane, for the purpose of obtaining some information about the solvent effect upon the absorption spectrum of the anion. As is seen from curve 6 in figure 2, the strong band of the anion appears at 238 m μ in the alcoholic solution.

4. THEORETICAL CONSIDERATIONS ON THE ELECTRONIC STRUCTURE OF THE NITROMETHYL ANION

In the previous papers [9, 13], it was shown that a number of strong absorption bands observed with a series of compounds containing the nitro or the carbonyl group as electron acceptor can be regarded as due to intramolecular charge transfer absorptions§ [14]: namely, as due to a transition involving a large electron transfer from an electron donor toward an electron acceptor. From this point of view, peak absorption wavelengths and intensities of a series of strong bands observed with nitramide, nitrobenzene, nitroethylene, *p*-nitrophenol, etc. could be interpreted at least semiquantitatively with the aid of the simple LCMO method.

Moreover, from the experimental point of view, some interesting results have been obtained on this problem. For example, Tanaka has measured the polarized ultra-violet absorption spectrum of a single crystal of *p*-nitroaniline [15]. Combining his result with x-ray crystal analysis data, it was concluded that the transition moment corresponding to the 370 m μ band of *p*-nitroaniline is directed parallel to the molecular axis joining the two nitrogen atoms. This is what may be expected if the band is an intramolecular charge transfer absorption including a large electron transfer from the amino group to the nitro group. On the other

† The ion is not stable and the absorption spectrum changes with time. This change is conspicuous in solutions of high concentration in the nitromethane anion. This is because the anions react with each other to form methayonate ions, O₂NCH₂CHNO⁻ (see reference [12]). However, in such dilute solutions as are used in the present measurements, it is fairly stable, at least enough so to give reproducible results. Further, the above-mentioned change in the absorption spectrum caused by adding alkali is completely reversible. When the solution was neutralized with hydrochloric acid within 30 min after preparation, the absorption spectrum of the solution completely returned to that of the nitromethane molecule.

‡ The pK_a value can be represented by the following equation:

$$pK_a = \text{pH} - \log [\text{H}_2\text{C}-\text{NO}_2]/[\text{H}_3\text{CNO}_2]$$

where [CH₃NO₂] and [CH₂⁻NO₂] are the concentrations of nitromethane and of its anion respectively in the solution of a fixed pH value. With the aid of absorption curves 1 and 5 and an absorption curve for a solution of fixed pH, [CH₃NO₂]/[CH₂⁻NO₂] in the above equation can be determined. The above pK_a value is the average obtained on the basis of the absorption curves for the solutions of pH values 8, 9 and 10.

§ This terminology was given in analogy with Mulliken's for the case of molecular complex formation between electron donor and acceptor.

hand, if the band were a shifted 260 m μ band of benzene, the direction of the transition moment should be perpendicular to the molecular axis in the ring plane.

Since the nitromethane anion is undoubtedly isoelectronic with nitramide, it may reasonably be supposed that the 233 m μ band of the former corresponds to the 225 m μ band [16] of the latter, and that both of them can be interpreted as due to intramolecular charge transfer absorption. However, there is a possibility of an alternative interpretation, namely that the band under consideration is a shifted 198 m μ band of the nitro group. Such a red shift caused by an electron-donating substituent group (in this case CH₂⁻) has been observed with various aromatic compounds like aniline and phenol [17]. However, theoretical considerations described below indicate that the 198 m μ band of the nitro group should shift toward *shorter* wavelengths as the result of interaction with a substituent group such as the amino or CH₂⁻ group.

First let us consider the π -electron structure of the nitro group. According to calculations made by Tanaka using Roothaan's LCAO SCF method [18] combined with Pariser and Parr's method [19], the π -electron molecular orbitals of this group are as shown in table 1.

Symmetry†	Energy (ev)	Wave function‡
b_1	$E_0 = -18.86$	$\phi_0 = 0.7133\chi_N + 0.7009(\chi_{O_1} + \chi_{O_2})/\sqrt{2}$
a_2	$E_1 = -15.63$	$\phi_1 = (\chi_{O_1} - \chi_{O_2})/\sqrt{2}$
b_1	$E_2 = 0.40$	$\phi_2 = 0.7009\chi_N - 0.7133(\chi_{O_1} + \chi_{O_2})/\sqrt{2}$

Wave functions and energy values of nitro group π -electron orbitals calculated for nitromethane [20].

† The symmetry of the nitro group is C_{2v} .

‡ χ_N , χ_{O_1} and χ_{O_2} are $2p\pi$ atomic orbitals of the nitrogen atom and the oxygen atoms 1 and 2, respectively.

Since, in the ground state, the two orbitals E_0 and E_1 are filled, the transition between E_1 and E_2 orbitals may be expected to be associated with the longest wavelength $\pi-\pi^*$ transition band, which was found at 198 m μ . Consideration of the absorption intensity of this band from both experimental and theoretical points of view supports this assignment. The oscillator strength is calculated as 0.38 and 0.06 for the $E_1 \rightarrow E_2$ and $E_0 \rightarrow E_2$ transitions, respectively [20]. On the other hand, from the absorption curve of nitromethane in aqueous solution (curve 3 in figure 1), the measured oscillator strength is 0.18. Taking into account that the calculated value of this quantity is usually larger than the observed, it seems reasonable to assign the 198 m μ band to the $E_1 \rightarrow E_2$ transition.

Now let us turn to the electronic structure of the nitromethyl anion. If one regards this ion as constructed from the electron donor CN₃₋ and the electron acceptor NO₂, and if the atoms are all coplanar, with overall symmetry C_{2v} , as seems very probable, the π -electron structure of the system as a whole can be described on the basis of the orbitals of the component groups by considering the resonance, inductive, and electron interaction effects. As pointed out by Murrell and Longuet-Higgins [21], these effects can be evaluated in terms of configuration interaction among the electron configurations which are schematically shown

in figure 3†. The configurations (A) and (B) in this figure represent the ground and charge-transfer configurations, and the configurations (C) and (D) the locally excited ones.

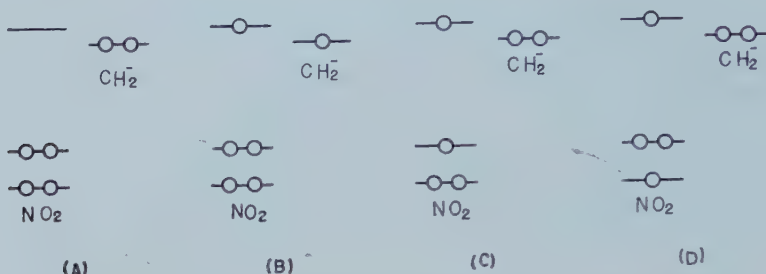


Figure 3. Electron configurations for the nitromethane anion.

(A) the ground configuration; (B) the charge transfer configuration; (C) the locally excited ($E_1 \rightarrow E_2$) configuration; (D) the locally excited ($E_0 \rightarrow E_2$) configuration.

Configuration (A) has a closed-shell (1A_1) wave function. Configurations (B) and (D) each give a 1A_1 and a 3A_1 state, of which the 1A_1 can interact with (A). Configuration (C) gives 1B_2 and 3B_2 states, which cannot interact with the others. However, we shall include configuration (C) in the following calculations, since it is important for a consideration of the position of the analogue of the $198\text{ m}\mu$ band of nitromethane. On the other hand, the interaction of configuration (D), whose energy was evaluated [20] to be higher by 2 or 3 ev than that of (C), with (A) and (B) will be considered only qualitatively.

Now one must determine the energy values of configurations (A), (B), and (C). It is useful to explain this procedure in two steps. The first step is to determine the energy values of configurations (B) and (C) relative to that of (A), neglecting the electrostatic interaction between the CH_2^- and NO_2 groups. This procedure can easily be accomplished using the electron affinity of the nitro group†, the ionization potential of the $2p$ orbital of the carbon anion§ [22], and the observed excitation energy of nitromethane $E_1 \rightarrow E_2$ transition ($198\text{ m}\mu = 6.235\text{ ev}$). The result is shown in figure 4 (a). Looking at this figure, it is seen that the energy values of the ground and charge-transfer configurations are very close to each other in this stage of the evaluation.

In the second step, electrostatic interaction between the CH_2^- and NO_2 groups must be considered for the ground and locally excited configurations. It may be expected that this interaction brings about energy stabilization in these two configurations, because the nitro group in its ground state has a large heterogeneity in the π -electron distribution and the nitrogen atom is positively charged to a great extent||. In fact, using the wave functions given in table 1, the π -electron distributions in configurations (A) and (C) can be evaluated with results as shown in figure 5 (a) and (b), respectively. In configuration (D), on

† In the present treatment only the single excited configurations are taken into account. The doubly excited ones are neglected.

‡ Tanaka determined theoretically the electron affinity of the nitro group as 0.4 ev.

§ 0.58 ev. This was taken from Pritchard and Skinner's table.

|| On the basis of this π -electron distribution, the contribution of the π -electrons to the dipole moment of the nitromethane molecule is evaluated as $2.8D$. This value amounts to 80 per cent of the observed dipole moment of this molecule ($3.5D$).

the other hand, the distribution is nearly the same as in (A). From the π -electron distributions of configurations (A) and (C), corresponding electrostatic interaction energies can be calculated by assuming a suitable geometry for the nitromethane anion† [23]. The stabilization energy caused by this interaction amounts to 2.883 ev and 1.441 ev in configurations (A) and (C), respectively. The energy values thus obtained for the ground (E_G'), charge transfer (E_{CT}'), and first locally excited (E_E') configurations are given in table 2 and figure 4 (b).

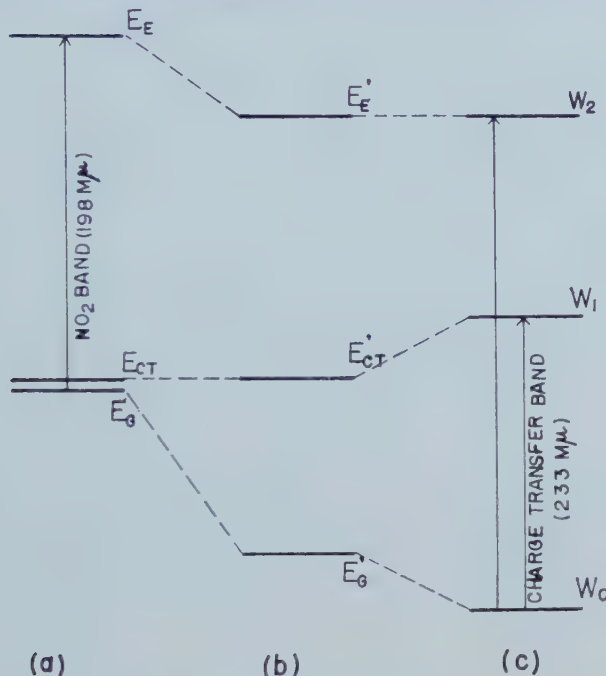


Figure 4. Energy level diagram.

- (a) energy levels of the ground (E_G), charge transfer (E_{CT}), and locally excited (E_E) configurations, without considering the electrostatic interaction; (b) energy levels of the three electron configurations with considering the electrostatic interaction; (c) energy levels of the nitromethane anion.

Next one must take into account the resonance interaction between configurations (A) and (B); as already noted, (C) being of different symmetry, does not interact further. The calculation of the resonance interaction can easily be done by the aid of the method presented by Pople [24] and by Murrell and Longuet-Higgins [21]. Three energy levels (W_0 , W_1 and W_2) and corresponding wave functions (Ψ_0 , Ψ_1 and Ψ_2) thus evaluated are given in table 2 and figure 4. The value of the resonance integral between the $2p\pi$ orbitals belonging to the carbon and nitrogen atoms was assumed as 2.576 ev, which is equal to that in the case of triazine [19]. From the coefficients of the component wave functions

† The following values were assumed: $d_{CN} = 1.35 \text{ \AA}$, $d_{NO} = 1.21 \text{ \AA}$, $\angle ONO = 120^\circ$. The two-centre coulomb integrals necessary for the evaluation of the electrostatic interaction energy were determined as 9.401 and 6.466 ev for $[C^- C^- | NN]$ and $[C^- C^- | OO]$, respectively, by the aid of Roothaan's table. The effective nuclear charge was taken as 1.45, 2.125, and 2.187 for the carbon, nitrogen, and oxygen atoms, respectively.

in Ψ_0 and Ψ_1 , it is concluded that the wave functions of the W_0 and W_1 levels are principally constructed from the ground and the charge-transfer configuration, respectively, with 25 per cent of the charge-transfer configuration in the W_0 level and 75 per cent in W_1 level. More accurately, configuration (D) of figure 3 should be somewhat mixed with the wave functions of W_0 and W_1 , but this effect is probably much less important than the mixing of (A) and (B), since (D) should be rather high in energy (above E_E of figure 4(a)). At any rate mixing with (D) cannot change the qualitative conclusions described below.

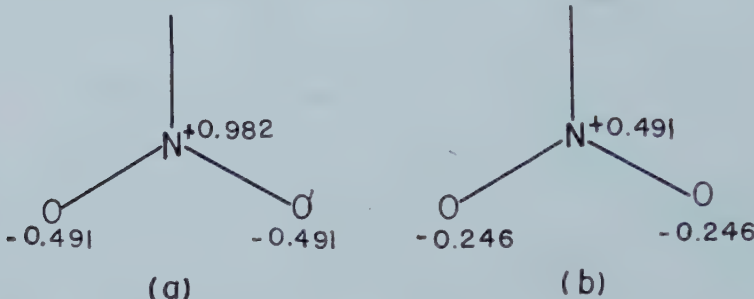


Figure 5. π -electron distribution of the nitro group.

(a) in the ground configuration, (A) of figure 3; (b) in the locally excited configuration, (C) of figure 3.

$E_G = 0$	$E_G' = -2.883 \text{ ev}$
$E_{CT} = 0.18 \text{ ev}$	$E_{CT}' = 0.18 \text{ ev}$
$E_E = 6.235 \text{ ev}$	$E_E' = 4.794 \text{ ev}$
$W_0 = -4.3290 \text{ ev}$	$\Psi_0 = 0.8701\psi_G + 0.4928\psi_{CT}$
$W_1 = 1.6260 \text{ ev}$	$\Psi_1 = 0.4928\psi_G - 0.8701\psi_{CT}$
$W_2 = 4.7940 \text{ ev}$	$\Psi_2 = \psi_E$

Table 2†. The energy levels and the wave functions calculated with the nitromethyl anion.

† In this table, ψ_G , ψ_{CT} and ψ_E designate the antisymmetrized wave functions for the ground, charge-transfer, and first locally excited configurations, respectively.

From the preceding discussion, it is seen that transition from level W_0 to level W_1 is undoubtedly accompanied by a large electron transfer from the electron donor (CH_2^-) toward the electron acceptor (NO_2). In this sense, the longest wavelength $\pi \rightarrow \pi^*$ transition band corresponding to this transition may be regarded as an intramolecular charge-transfer absorption. The theoretically calculated excitation energy for this transition, 5.955 ev, is a little larger than for the strong band observed with the nitromethyl anion ($233 \text{ m}\mu = 5.30 \text{ ev}$). This result supports the identification of the latter as an intramolecular charge-transfer band. Too much importance should not be attached to the rather small discrepancy between the calculated and observed positions of the band in view of several rough approximations made in the calculation.

Since the wave function of the W_2 level coincides in the present approximate calculation with that of the locally excited configuration, the $W_0 \rightarrow W_2$ transition band of the anion should be of the same nature as the $198 \text{ m}\mu$ band of nitromethane. As is seen from figure 4, however, the excitation energy for the $W_0 \rightarrow W_2$

transition must be larger than that for the corresponding transition in nitromethane itself. That is to say, the $198\text{ m}\mu$ band of nitromethane is expected to show a large blue shift in the nitromethyl anion. Since the absorption spectrum of the anion in the wavelength region below $190\text{ m}\mu$ is difficult to measure, the predicted rather large blue shift cannot be verified by comparison with experiment. However, since the theoretical argument is qualitatively conclusive, it strongly supports the interpretation that the $233\text{ m}\mu$ band observed with the nitromethane anion cannot be regarded as shifted $198\text{ m}\mu$ band of nitromethane but is the intramolecular charge transfer absorption band.

One of the reasons for the occurrence of the above-mentioned blue shift phenomenon is that the contribution of the electrostatic interaction between the CH_2 and NO_2 groups is larger in the ground configuration than in the locally excited configurations. Another reason is that the ground configuration is considerably further stabilized by the interaction with the charge-transfer configuration (see figure 4). For the above-mentioned second reason, it may be expected that nitro compounds like nitramide and nitric acid (HONO_2), where the nitro group is capable of interacting with the electron donating groups, should show a blue shift, like the nitromethyl anion. Thus it would seem to be interesting to investigate the vacuum ultra-violet absorption spectra of these compounds.

The author wishes to express his sincere thanks to Professor R. S. Mulliken for his kindness in reading and suggesting changes in the manuscript and in other helpful suggestions. His thanks are also due to Professor J. R. Platt and other members of the Laboratory for the hospitality shown during his stay at Chicago.

REFERENCES

- [1] WHELAND, G. W., 1955, *Resonance in Organic Chemistry* (New York: John Wiley & Sons), pp. 205 and 213.
- [2] KORTÜM, G., 1939, *Z. phys. Chem. B*, **43**, 271.
- [3] BAYLISS, N. S., and MCRAE, E. G., 1954, *J. phys. Chem.*, **58**, 1006.
- [4] HASZELDINE, R. N., 1953, *J. chem. Soc.*, p. 2525.
- [5] WEST, W., 1956, *Chemical Applications of Spectroscopy* (New York: Interscience Publishers), p. 664.
- [6] DEMAINE, P. A. D., DEMAINE, M. M., and GOBLE, A. G., 1957, *Trans. Faraday Soc.*, **53**, 427.
- [7] BELL, R. P., 1953, *Acids and Bases* (London: Methuen & Co.), p. 72.
- [8] PEARSON, R. G., and DILLON, R. L., 1953, *J. Amer. chem. Soc.*, **75**, 2439; TURNBULL, D., and MARSON, S. H., 1943, *J. Amer. chem. Soc.*, **65**, 212.
- [9] NAGAKURA, S., 1955, *J. chem. Phys.*, **23**, 1441.
- [10] LEFFLER, J. E., 1956, *The Reactive Intermediates of Organic Chemistry* (New York: Interscience Publishers), p. 188.
- [11] MAKOVKY, A., and LENJI, L., 1958, *Chem. Rev.*, **58**, 627.
- [12] DREW, C. M., McNESBY, J. R., and GORDON, A. S., 1955, *J. Amer. chem. Soc.*, **77**, 2622.
- [13] NAGAKURA, S., and TANAKA, J., 1954, *J. chem. Phys.*, **22**, 236; TANAKA, J., NAGAKURA, S., and KOBAYASHI, M., 1956, *J. chem. Phys.*, **24**, 311.
- [14] MULLIKEN, R. S., 1952, *J. phys. Chem.*, **56**, 801; 1956, *Rec. Trav. chim. Pays-Bas*, **75**, 845.
- [15] TANAKA, J., 1958, *J. chem. Soc. Japan (Nippon Kagaku Zasshi)*, **79**, 1373.
- [16] JONES, R. N., and THÖRN, G. D., 1949, *Canad. J. Res. B*, **27**, 828.

- [17] MATSEN, F. A., 1950, *J. Amer. chem. Soc.*, **72**, 5243; HERZFELD, K. F., 1947, *Chem. Rev.*, **41**, 233; NAGAKURA, S., and BABA, H., 1952, *J. Amer. chem. Soc.*, **74**, 5693.
- [18] ROOTHAAN, C. C. J., 1951, *Rev. mod. Phys.*, **23**, 69.
- [19] PARISER, R., and PARR, R. G., 1953, *J. chem. Phys.*, **21**, 466, 767.
- [20] TANAKA, J., 1957, *J. chem. Soc. Japan (Nippon Kagaku Zasshi)*, **78**, 1643.
- [21] MURRELL, J. N., and LONGUET-HIGGINS, H. C., 1955, *Proc. phys. Soc. Lond. A*, **68**, 329; MURRELL, J. N., 1955, *Proc. phys. Soc. Lond. A*, **68**, 969.
- [22] PRITCHARD, H. O., and SKINNER, H. A., 1955, *Chem. Rev.*, **55**, 745.
- [23] ROOTHAAN, C. C. J., 1955, Special Technical Report, Laboratory of Molecular Structure and Spectra, The University of Chicago.
- [24] POPE, J. A., 1955, *Proc. phys. Soc. Lond. A*, **68**, 81.

Cobalt nuclear resonance measurements of rate processes and a system in equilibrium

by R. P. H. GASSER and R. E. RICHARDS

Physical Chemistry Laboratory, South Parks Road, Oxford

(Received 24 October 1959)

The intensities of cobalt nuclear resonance spectra have been used to study the rate of exchange at various temperatures between ethylenediamine and the cobalt hexammine (III) ion. The variation of the relative intensities of the two lines from sodium cobaltinitrite solutions with temperature has been studied and interpreted in terms of an isomerization equilibrium. The rates of both electron and ligand exchange in solutions of cobalt complexes have been found to be slow.

1. INTRODUCTION

The intensity of a nuclear resonance absorption curve, recorded under the correct conditions, is proportional to the number of the particular nuclei present, and therefore to their concentration. Unlike most other branches of spectroscopy the proportionality constant is the same for a given nucleus under fixed experimental conditions in all its compounds. A reaction can thus be followed, in principle, by measuring the rate of diminution of a peak due to the reacting species and/or the rate of growth of a peak due to the product. Two difficulties in applying such a procedure, are the significant time required to make a nuclear resonance measurement and the lack of accuracy of intensity measurements with present instruments.

Some aspects of the nuclear resonance spectra of cobalt complexes have previously been studied by Freeman *et al.* [1], who interpreted the shifts between different complexes in terms of the Crystal Field theory. An unexplained phenomenon was the presence of two lines from a solution of very pure sodium cobaltinitrite [2].

The experiments to be described extend previous measurements on cobalt compounds to the study of an equilibrium and of a rate process.

2. EXPERIMENTAL

2.1. Nuclear resonance spectrometer

The measurements were performed on the nuclear resonance apparatus which has been described previously [1].

Measurements at elevated temperatures were made using a vacuum jacketed air flow cryostat. The temperature was measured with a copper-constantan thermocouple in a glass sheath dipping into the solution. It was found to be constant to about $\pm 1^\circ\text{C}$ during the period of an experiment.

2.2. Compounds

The sodium cobaltinitrite, nitrite and bromide used were 'Analar' grade.

Aqueous solutions of potassium hexacyanocobaltate (III), carbonato-tetramminecobalt (III) nitrate, tris-ethylenediaminecobalt (III) chloride, sodium hexanitrocobaltate (III), carbonato-bis-ethylenediaminecobalt (III) bromide,

trans-di-chloro-bis-ethylenediaminecobalt (III) chloride and hexamminocobalt (III) chloride were made up from commercial salts. To these a solution of the paramagnetic cobalt (II) chloride was added. A solution of pentammine-aquocobalt (III) chloride was prepared by the method of Biltz [4], by dissolving purpureo-cobalt chloride, $[Co(NH_3)_5Cl]Cl_2$, in dilute ammonia.

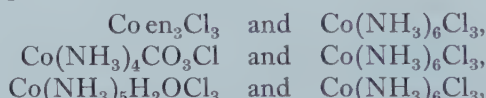
3. RESULTS

3.1. Rate processes

The nuclear quadrupole moment of ^{59}Co provides an efficient relaxation mechanism, though it is not so large as to make the lines from most of the complexes wider than the field inhomogeneity of the magnet on which the measurements were made.

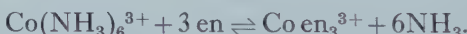
The addition of cobaltous salts to the complexes up to an equimolar ratio caused no increase in the line widths of the resonances from any of the cobalt (III) complexes.

Mixtures of the pairs of complexes



showed a separate resonance from each of the complexes. These two resonances were observed to be unchanged even on boiling the mixtures and cooling to room temperature. There was no sign of any ligand exchange in a solution of potassium hexacyanocobaltate (III) in strong ethylenediamine, even after maintaining the solution near the boiling point for two hours.

On the other hand exchange of the ligands was observed in the replacement of ammonia in the hexammine-cobalt (III) ion by ethylenediamine, according to the overall equation



The reaction was carried out in a large excess of ethylenediamine, and throughout it only two lines were obtained, each of width equal to the field inhomogeneity, one corresponding to $Co(NH_3)_6^{++\tau}$ and the other to $Co\ en_3^{++\tau}$. The reaction was followed by plotting the heights of the derivative curves against time, when two typical exponential curves were obtained for the diminution of the cobalt hexammine line and the growth of the cobalt ethylenediamine line. The point at which the curves cross corresponds to the halfway stage of the reaction, and the log of the time for this to be reached, $\log t_{1/2}$, is plotted as a function of temperature in figure 1.

The graph gives a value for the activation energy of the reaction of 22 kcal/mole.

3.2. Equilibrium measurement

It was found on warming a solution of sodium cobaltinitrite that the relative intensities of the two lines altered, the higher frequency peak, which is the smaller at room temperature, increasing as the temperature was raised. The widths of the two lines were different, that of the lower frequency peak being equal to the field inhomogeneity, while the higher frequency peak had a width greater than this. The heights of the derivative curves are therefore no longer a measure of the concentration, so that this must be obtained by numerical integration. The temperature dependence of the ratio of the intensity of the low frequency to the

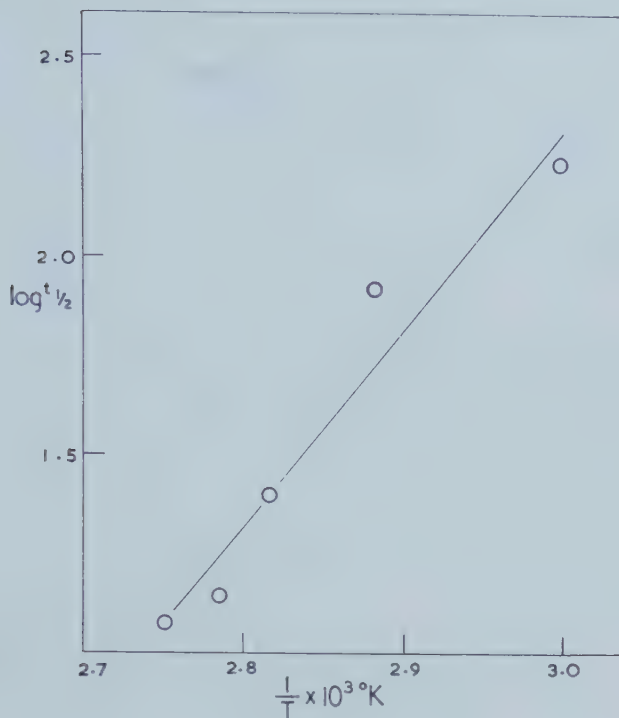


Figure 1.

high frequency peak is plotted in figure 2. Solutions of sodium cobaltinitrite decompose in water, and at high temperatures the solutions effervesced briskly. On cooling, the original relative intensities were regained, though with a diminished absolute intensity. The effects on the equilibrium of adding sodium nitrite to a concentration of 2.60 M to a 0.70 M solution of cobaltinitrite, or of adding sodium bromide to a concentration of 3.69 M to a 0.65 M solution of cobaltinitrite, are also shown in figure 2.

4. DISCUSSION.

4.1. Rate processes

The rate of electron exchange between cobalt (II) and cobalt (III) in these solutions is such that there is no increase in the line width. Moreover the ligands appear to be so securely attached to each individual cobalt atom that complexes in mixtures retain their identity even after prolonged heating.

The reaction between the cobalt hexammine ion and ethylenediamine must proceed by a stepwise substitution, although the intermediate complexes do not appear to be present in any appreciable concentration. This implies that the mixed complexes are more reactive than the hexammine and therefore in the presence of a large excess of ethylenediamine react quickly to give the fully substituted complex. If this is the case, the rate determining step will be the first substitution and the reaction will be expected to show first-order kinetics. The exponential rate curves show that this is indeed the case.

The principal sources of error in these measurements are probably the appreciable time taken to make a measurement and the difficulty of extrapolating the rate curve to zero time. These both become more acute as the temperature

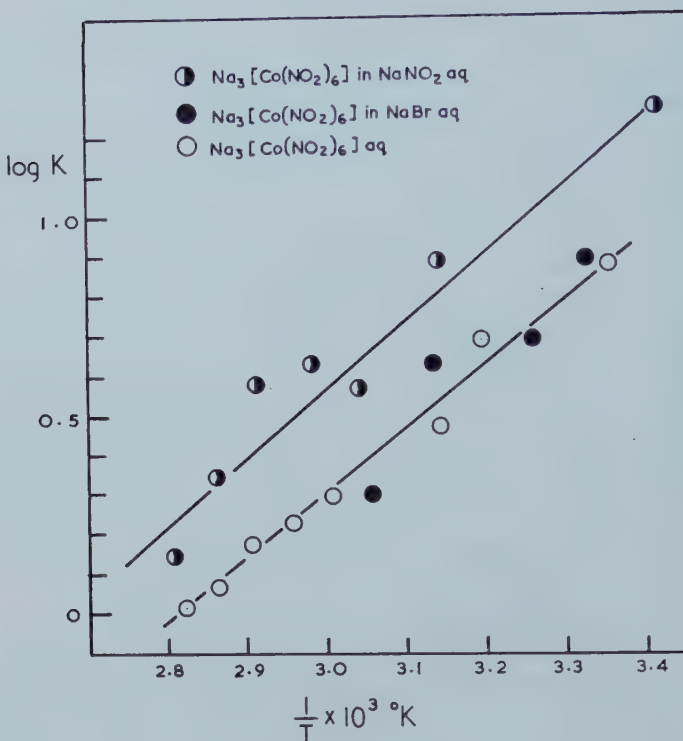


Figure 2.

is raised. The rate of exchange at room temperature is very slow and it does not become measurable in a reasonable time until about 60°C , when $t_{1/2}$ is nearly three hours. At this temperature the time taken to go over a peak (about 1 min) is very small compared with $t_{1/2}$. However, at 90°C , $t_{1/2}$ is reduced to about 12 min, and this is no longer the case.

The solutions were prepared at room temperature by mixing the ethylenediamine with hexammine cobaltic chloride solution and then warmed to the required temperature. During the warming and equilibration, the reaction is proceeding at an untypical rate so that measurements cannot be made. The longer this time is compared with $t_{1/2}$, the greater becomes the error in the extrapolation to zero time. The considerable heat of mixing of ethylenediamine and water prohibits the breaking of a bulb of one solution into the other at the desired temperature.

The combination of these errors is estimated to lead to a total error of about 10 per cent, so that the activation energy is $22 \pm 2 \text{ kcal/mole}$.

4.2. Sodium cobaltinitrite solution

On warming a solution of sodium cobaltinitrite, the relative intensities of the two lines change. The equilibrium constant for the interconversion of the two forms is expressed as the ratio of the areas under the low and high frequency peaks. When the solution contains sodium nitrite the higher frequency line is reduced, an effect which must be attributed to the presence of the nitrite ions because sodium bromide has no effect.

The possibility of chemical impurity having been eliminated, three explanations for the presence of two lines suggest themselves.

(i) That there are two closely spaced electronic energy levels in the cobaltinitrite complex between which the molecules are distributed according to a Boltzmann distribution. The work of Freeman *et al.* [1] shows that there would probably be a chemical shift between these species, while the intensity of the line corresponding to the upper level would be expected to become more intense on heating.

(ii) That there is a chemical equilibrium between the hexanitrocobaltate ion and a hydrolysis product derived from it. The position of such an equilibrium would alter in accordance with the van't Hoff relation.

(iii) That there is an isomerism equilibrium between the 'nitro' form characteristic of the hexanitrocobaltate and a 'nitrito' form.

Of these explanations, the first can be ruled out immediately, because at high temperature the equilibrium constant is less than one, which implies that the upper level becomes more populated than the lower. This would mean that the statistical weight of the upper level would have to have an improbably large value. Neither of the other two possibilities seems to be satisfactory on its own, though a combination of them provides a plausible explanation. A reversible chemical hydrolysis cannot be the complete explanation, because it would produce nitrite ions and therefore be virtually completely repressed by the addition of sodium nitrate. Moreover it seems unlikely [3] that such a process would be completely reversible. On the other hand a nitro-nitrito equilibrium would be expected to be reversible [4], but would not be altered by the addition of nitrite ions.

The following combination is therefore proposed. At any temperature the high frequency line is attributed to a mixture of the nitrito form of the complex ion and a hydrolysis product. The addition of sodium nitrite represses the hydrolysis but does not affect the isomerization. After heating and cooling the original relative intensities are obtained by the reversion of the nitrito to the nitro form, the hydrolysis products having decomposed into species making no contribution to the resonance.

The slopes of the graphs with and without the addition of sodium nitrite are equal, and lead to a value of the heat of reaction of 8.4 kcal. The scatter of the points is considerable and the estimated error is about 10 per cent, so that this should be written as 8.4 ± 1 kcal/mole.

It is proposed to study the nitrogen resonances in these solutions to provide more evidence for the mechanisms proposed.

We wish to thank the Hydrocarbon Research Group of the Institute of Petroleum, the National Coal Board, and the Department of Scientific and Industrial Research for grants in aid of apparatus. We are also grateful to the Department of Scientific and Industrial Research for a maintenance grant for one of us (R. P. H. G.).

REFERENCES

- [1] FREEMAN, R., MURRAY, G., and RICHARDS, R. E., 1957, *Proc. roy. Soc. A*, **242**, 455.
- [2] PROCTOR, W. G., and YU, F. C., 1951, *Phys. Rev.*, **81**, 20.
- [3] VENANZI, L., private communication.
- [4] BASOLO, F., and PEARSON, R. G., 1958, *Mechanisms of Inorganic Reactions* (New York: Wiley).

High-resolution nuclear-magnetic-resonance spectra of hydrocarbon groupings

III. An analysis of the spectrum of liquid propane using ^{13}CH satellites

by N. SHEPPARD and J. J. TURNER

University Chemical Laboratory, Lensfield Road, Cambridge

(Received 26 November 1959)

Previous studies on ^{13}CH satellite features in the hydrogen nuclear-magnetic-resonance spectra of symmetrical molecules are extended to include the complex spectrum of liquid propane ($\text{CH}_3\text{CH}_2\text{CH}_3$). The exact Hamiltonian for the nuclear system $A_3B_2A_3'$ and its simplification using group theoretical methods are described. A precise solution of the spectrum at 40 Mc/s, aided by the satellite features, is presented; the values of the AB chemical shift and AB coupling constant which produce the best agreement between experimental and theoretical spectra at 40 Mc/s are 17.50 ± 0.05 c/s and 7.4 ± 0.1 c/s respectively.

1. INTRODUCTION

The hydrogen nuclear-magnetic-resonance (N.M.R.) spectrum of liquid propane ($\text{CH}_3\text{CH}_2\text{CH}_3$) at 40 Mc/s is very complex due both to the small internal chemical shift (δ) between CH_3 and CH_2 groups relative to the coupling constant (J) between these groups, and to the large number of magnetic nuclei. Narasimhan *et al.* [1] have attempted an analysis of the spectra obtained at 40 and 60 Mc/s using the multiplet moment method and second order perturbation theory. We wish to illustrate the application of ^{13}CH satellite [2, 3] analysis to aid a precise solution of the spectrum at 40 Mc/s.

2. SYMMETRY PROPERTIES AND THE EXACT HAMILTONIAN

The application of the group theoretical methods described by McConnell *et al.* [4] and by E. Bright Wilson, Jr. [5] allows a considerable simplification of the equations for the propane eight-spin system. Using the notation of Pople *et al.* [6] we can represent the propane nuclear spin system as $A_3B_2A_3'$. Because of averaging due to internal rotation about the C—C bonds and the symmetry of the molecule, $J_{AB}(=J_{A'B})$ is the same between all A's (and A' s) and B's; also $J_{AA'}$, which will be small, is the same for all pairs of A and A' nuclei. Thus those operators which commute with the Hamiltonian include the covering operations for the whole molecule, for the groups A_3 and A_3' and for group B_2 . The zero order eigenfunctions which are simultaneous eigenfunctions for all these operators are obtained by standard group theoretical methods. The nuclear groups A_3 , A_3' and B_2 belong effectively to the point groups C_{3v} , C_{3v} and C_{2v} respectively, and in addition the eigenfunctions can be classified as symmetrical or anti-symmetrical with respect to interchange of A_3 and A_3' . In this way the largest of the submatrices in the exact Hamiltonian is of order 6×6 , whereas without application of the symmetry properties the largest submatrix is of order 70×70 .

There are certain important consequences of the nuclear symmetry. The *intra*-group coupling constants for the nuclear groups A_3 , A_3' and B_2 and the coupling constant $J_{AA'}$ have no effect on the spectrum. There is thus only one parameter which determines the shape of the spectrum, i.e. the ratio J_{AB}/δ .

Since mixing can only occur between states of the same symmetry, there are many eigenfunctions in the complete set which are unperturbed. Two such functions, with total spin 2 and 1 respectively, are:

$$\frac{1}{2\sqrt{3}} [\alpha\alpha\alpha(\alpha\beta - \beta\alpha)(\alpha\alpha\beta + \alpha\beta\alpha + \beta\alpha\alpha) - (\alpha\alpha\beta + \alpha\beta\alpha + \beta\alpha\alpha)(\alpha\beta - \beta\alpha)\alpha\alpha\alpha] (F_z = 2),$$

$$\frac{1}{2\sqrt{3}} [\alpha\alpha\alpha(\alpha\beta - \beta\alpha)(\beta\beta\alpha + \beta\alpha\beta + \alpha\beta\beta) - (\beta\beta\alpha + \beta\alpha\beta + \alpha\beta\beta)(\alpha\beta - \beta\alpha)\alpha\alpha\alpha] (F_z = 1).$$

These two eigenfunctions have the same symmetry in every respect so that the transition between the two eigenstates is allowed and gives rise to a line at the chemical shift value of a CH_3 group. In a similar way certain transitions result in lines at the centre of the CH_2 resonance so that, provided these lines are correctly assigned, the value of δ can be determined directly from the experimental spectrum.

3. ^{13}CH SATELLITE-BANDS

It has been demonstrated previously [2, 3] that the features in the hydrogen resonance spectra of hydrocarbon groupings caused by the 1 per cent natural abundance of ^{13}C nuclei, can be most useful for the determination of nuclear spin-spin coupling constants. The technique has been applied to molecules such as dioxan, $\text{O}(\text{CH}_2\text{CH}_2)_2\text{O}$, where molecular symmetry otherwise gives rise to a single-line spectrum. The coupling constants between the adjacent CH_2 groups have been determined by analysing the ^{13}CH satellite features in the main spectrum due to groups such as $-\text{CH}_2-\text{CH}_2-$. A_2B_2 theory [6] was used and the effective chemical shift in c/s between the two CH_2 groups is identical to one half of the coupling constant between a ^{13}C nucleus and its bonded protons.

In order to verify that this method will give reliable results for more complex spectra, the values of the CH_3-CH_2 and CH_3-CH coupling constants in ethyl chloride and ethylidene dichloride respectively have been determined in two ways. The presence of the halogen atoms produces a large chemical shift between the hydrocarbon groups and hence the spectra of the two compounds are analysable using A_3X_2 and A_3X theory respectively. Satellite features occur in the spectra due to molecules such as $^{13}\text{CH}_3^{12}\text{CH}_2\text{Cl}$ and $^{13}\text{CH}_3^{12}\text{CHCl}_2$ and analysis of these also provides values of the two coupling constants. The two methods furnish identical values of the coupling constants $-\text{CH}_3\text{CH}_2\text{Cl}(J = 7.3 \pm 0.2 \text{ c/s})$; $\text{CH}_3\text{CHCl}_2(J = 6.0 \pm 0.2 \text{ c/s})$.

There are, in propane, a small percentage of molecules of formula



the $^{13}\text{CH}_3$ group gives rise to a spectrum consisting essentially of a widely spaced doublet of separation approximately 124 c/s, i.e. the value of $J_{^{13}\text{CH}}$. Each component of this doublet consists of a triplet caused by coupling between CH_3 and CH_2 groups and the separation between the lines in the triplets gives the value of this coupling constant to a first approximation. The two triplets will not be quite identical however because the small internal chemical shift (δ) between

CH_3 and CH_2 groups makes the 'effective' chemical shift between $^{13}\text{CH}_3$ and $^{12}\text{CH}_2$ groups either $\frac{1}{2}J_{13\text{CH}} + \delta$ for one triplet or $\frac{1}{2}J_{13\text{CH}} - \delta$ for the other. In the previous studies δ was always zero, so that the two satellites were identical and also easily observable since the main spectrum was a single line.

In addition there is a perturbation due to the second CH_3 group which gives rise to second order effects in the $^{13}\text{CH}_3$ spectrum. An estimate of this perturbing effect has been evaluated by calculating exact theoretical spectra for the nuclear systems ABCX , ABC_2X , ABC_3X , and $\text{AB}_2\text{C}_3\text{X}$; here X corresponds to a ^{13}C nucleus. A typical calculation involved computing the theoretical spectrum of



with $J_{\text{AX}} = 124 \text{ c/s}$, $J_{\text{AB}} = 7.4 \text{ c/s}$, $J_{\text{BC}} = 7.4 \text{ c/s}$, $J_{\text{AC}} = J_{\text{BX}} = J_{\text{CX}} = 0 \text{ c/s}$ and $\delta_{\text{AB}} = \delta_{\text{CB}} = 17.5 \text{ c/s}$. The spectrum of A, which corresponds to the $^{13}\text{CH}_3$ spectrum of propane, is shown in figure 1. The separation (i.e. XY or X'Y') is 7.1 c/s ; thus the perturbation due to the C nucleus is 0.3 c/s . It was found that the greater the number of nuclei at site C, the greater was the perturbing effect on the measured approximate value of the AB coupling constant.

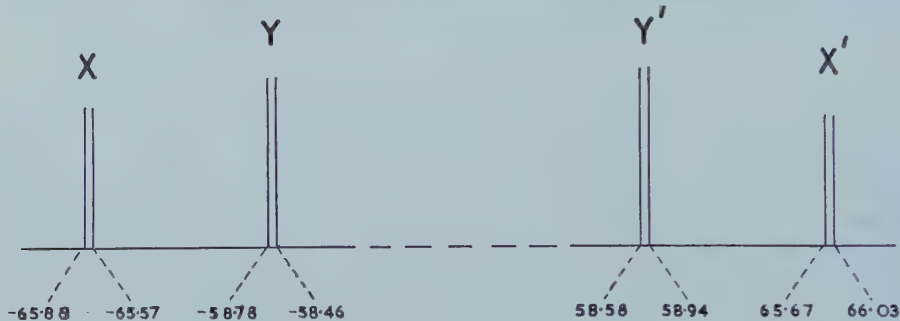


Figure 1. Theoretical A spectrum of ABCX group with $J_{\text{AX}} = 124 \text{ c/s}$, $J_{\text{AB}} = J_{\text{BC}} = 7.4 \text{ c/s}$, $J_{\text{AC}} = J_{\text{BX}} = J_{\text{CX}} = 0 \text{ c/s}$ and $\delta_{\text{AB}} = \delta_{\text{CB}} = 17.5 \text{ c/s}$.

4. EXPERIMENTAL

The liquid propane was carefully distilled under vacuum, degassed to remove dissolved oxygen and sealed in a 5 mm o.d. tube. The spectra were obtained using a Varian Associates V4300B high resolution NMR spectrometer operating at 40 Mc/s and equipped with flux stabilizer. Line positions were measured relative to the large central peak as zero, using sidebands generated by a Muirhead Decade oscillator. It was possible to measure accurately the ^{13}CH satellite triplet on the high field side of the main resonance to give an approximate value of the coupling constant. The internal chemical shift was measured directly from the spectrum after the correct assignment of lines had been found.

5. RESULTS

The overall separation between the outside pair of lines in the satellite triplet to the high-field side of the main resonance is $13.56 \pm 0.20 \text{ c/s}$ giving $J \approx 6.8 \text{ c/s}$. The perturbation calculations mentioned above suggest that with $J_{13\text{CH}} = 124 \text{ c/s}$ and $\delta \approx 15.5 \text{ c/s}$ [1] the actual coupling constant is approximately 0.7 c/s greater, i.e. 7.5 c/s . The exact theoretical spectrum for propane was then calculated on the electronic Digital Computer EDSAC 2 using $J = 7.5 \text{ c/s}$ and $\delta = 15.5 \text{ c/s}$.

Although the detailed agreement between the observed and calculated spectra for these values was not very good, the correct assignment of lines in the observed spectrum could then be made easily and the internal chemical shift measured precisely ($\delta = 17.50 \pm 0.05$ c/s). Further computed spectra for $\delta = 17.50$ c/s and $J = 6.8$, 7.4 and 8.5 c/s are shown together with the experimental spectrum in figure 2.

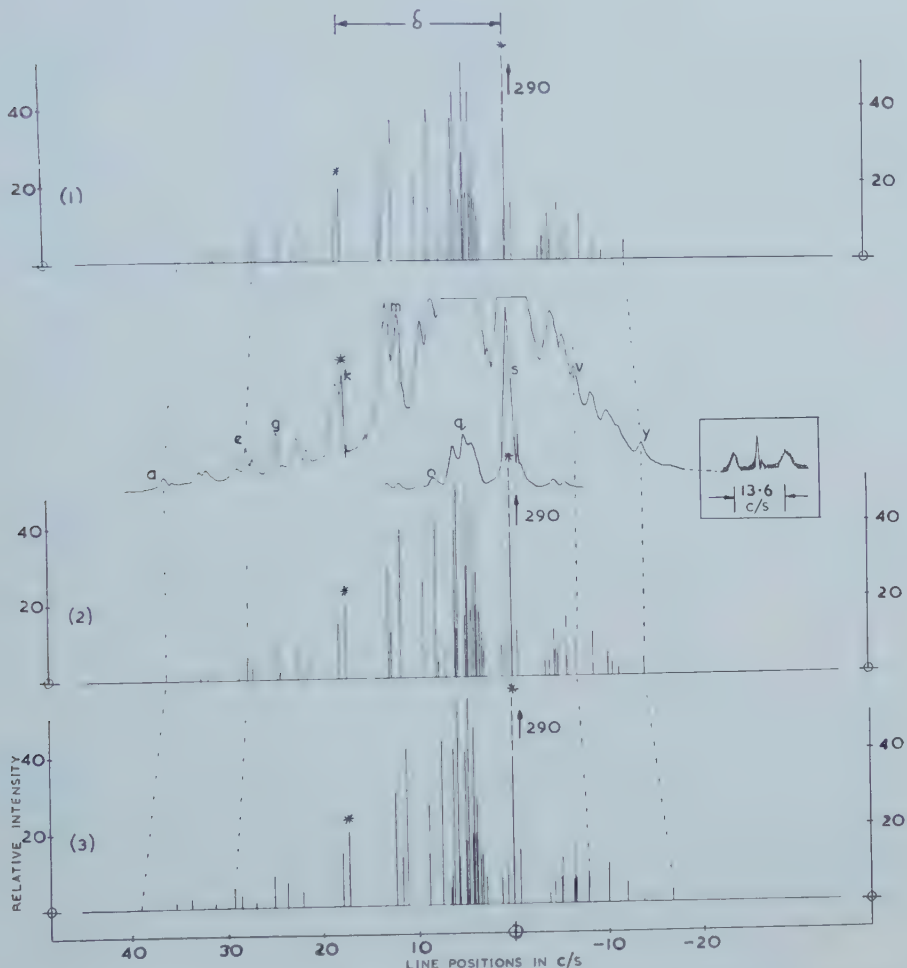


Figure 2. Theoretical $A_3B_2A'_3$ ' spectra with $\delta_{AB} = 17.50$ c/s and (1) $J_{AB} = 6.8$ c/s; (2) $J_{AB} = 7.4$ c/s; (3) $J_{AB} = 8.5$ c/s. Also shown are the experimental propane spectrum, and one ^{13}CH satellite band.

The ^{13}CH satellite triplet on the high field side of the main resonance is also shown greatly magnified. The value of 7.4 c/s for J is obtained by comparing experimental and theoretical spectra for $J = 6.8$ c/s and 8.5 c/s, and interpolating between them. The dotted lines connect lines of analogous assignment and it is clear that the theoretical spectrum with $J = 7.4$ c/s and $\delta = 17.5$ c/s provides a very close fit to the experimental spectrum. The fit is good, not only for overall spacings, but also for certain lines whose positions are very sensitive to small

changes in J . The peaks in the spectrum whose separation provides the value of δ are also indicated. One of these is exceedingly strong, the other is of moderate intensity but is particularly sharp.

Line number	Experimental† position	Theoretical positions $\delta = 17.50$ c/s		
		$J = 6.8$ c/s	$J = 7.4$ c/s	$J = 8.5$ c/s
a	36.1 ± 0.1	34.40	36.13	39.16
b	32.50 ± 0.15	30.93	32.59	35.45
c	31.8 ± 0.2	30.69	31.88	33.90
d	28.5 ± 0.1	27.03	28.65	31.47
e	27.5 ± 0.1	26.61	27.63	29.40
f	27.1 ± 0.1	26.26	27.13	28.73
g	24.4 ± 0.1	23.83	24.34	25.21
h	22.3 ± 0.1	21.51	22.30	23.85
i	21.3 ± 0.1	20.85	21.30	22.22
j	18.15 ± 0.05	18.16	18.11	18.02
k	17.50 ± 0.05	17.50	17.50	17.50
l	12.6 ± 0.1	13.10	12.75	12.45
m	11.6 ± 0.1	11.94	11.61	11.19
n	9.35 ± 0.10	9.57	9.25	8.84
o	7.95 ± 0.20	8.15	7.87	7.55
p	5.85 ± 0.20	5.5	5.8	6.0
q	4.8 ± 0.1	4.5	4.7	4.8
r	3.9 ± 0.3	3.9	4.0	4.2
s	0	0	0	0
t	-4.8 ± 0.1	-4.47	-4.70	-5.00
u	-5.9 ± 0.1	-5.44	-5.80	-6.29
v	-6.9 ± 0.1	-6.31	-6.84	-7.73
w	-8.7 ± 0.1	-7.77	-8.57	-9.93
x	-10.2 ± 0.1	-9.10	-10.14	-11.90
y	-14.0 ± 0.1	-12.40	-14.00	-16.76

†Measured relative to large central peak in c/s. Positive sign indicates low field side of centre.

Table 1. Experimental and theoretical spectra for liquid propane at 40 Mc/s.

	Internal chemical shift (δ) in c/s	Coupling constant J in c/s	Chemical shifts	$J_{^{13}\text{CH}}$ ¶ in c/s
60 Mc/s†	16.5§	7.25		
40 Mc/s†	14.5	5.6		
40 Mc/s‡	17.50 ± 0.05	7.4 ± 0.1	$(\text{CH}_3) + 0.530 \pm 0.005$ $(\text{CH}_2) + 0.093 \pm 0.005$	124 ± 1

† See reference [1].

‡ This work.

§ Corrected to 40 Mc/s.

|| In p.p.m. for a 10 per cent solution in CCl_4 with internal cyclohexane as reference. Positive sign indicates high field side of standard.

¶ CH_3 group.

Table 2. N.M.R. parameters for liquid propane.

Table 1 shows the experimental and theoretical line positions relative to the CH_3 resonance; the intensities are more easily compared in figure 2 due to the considerable overlap in the experimental spectrum.

Table 2 compares the results obtained by Narasimhan *et al.* with those from these studies.

6. CONCLUSION

These results show that analysis of ^{13}CH satellites in a complex spectrum of a hydrocarbon grouping can furnish by direct experimental measurement reasonably accurate values of coupling constant parameters.

One of us (J. J.T.) is indebted to the Department of Scientific and Industrial Research for a Research Studentship, and to King's College, Cambridge for a Harold Fry Studentship. This research has been carried out on a nuclear-magnetic-resonance spectrometer bought with a generous grant to this Laboratory from the Wellcome Foundation and has been aided by a grant from the Hydrocarbon Research Group of the Institute of Petroleum.

We are particularly grateful to Dr. M. V. Wilkes, F.R.S., of the University Mathematical Laboratory for enabling us to carry out a series of calculations on the EDSAC 2 digital computer, and to Mr. H. P. F. Swinnerton-Dyer for assistance with programming.

Note added in proof.—Since this paper was submitted, Whitman *et al.* [7] have also published a detailed solution of the spectrum of liquid propane. They find, at 40 Mc/s, the values $J = 7\cdot26$ c/s and $\delta = 17\cdot5$ c/s which agree closely with the values obtained in this work.

REFERENCES

- [1] NARASIMHAN, P. T., LAINE, N., and ROGERS, M. T., 1958, *J. chem. Phys.*, **28**, 1257; **29**, 1184.
- [2] COHEN, A. D., SHEPPARD, N., and TURNER, J. J., 1958, *Proc. chem. Soc.*, p. 118.
- [3] SHEPPARD, N., and TURNER, J. J., 1959, *Proc. roy. Soc. A*, **252**, 506.
- [4] MCCONNELL, H. M., MCLEAN, A. D., and REILLY, C. A., 1955, *J. chem. Phys.*, **23**, 1152.
- [5] WILSON, E. B., Jr., 1957, *J. chem. Phys.*, **27**, 60.
- [6] POPPLE, J. A., SCHNEIDER, W. G., and BERNSTEIN, H. J., 1959, *High Resolution Nuclear Magnetic Resonance* (New York: McGraw-Hill Book Company, Inc.).
- [7] WHITMAN, D. R., ONSAGER, L., SAUNDERS, M., and DUBB, H. E., 1960, *J. chem. Phys.*, **32**, 67.

Studies of ion-solvent and ion-ion interactions using nuclear magnetic resonance spectroscopy

by A. CARRINGTON†, F. DRAVNICKS‡ and M. C. R. SYMONS

Department of Chemistry, The University, Southampton

(Received 29 October 1959)

Chemical shifts of the fluorine nuclear resonance have been measured for fluoride ion in a variety of environments. The shift varies linearly with the mole-fraction of organic solvent and is dependent upon the nature and concentration of added cations and anions. In contrast, the value for the caesium resonance from solutions of caesium salts is independent of the choice of solvent. Large, linear, chemical shifts are observed when other electrolytes are added, the effect being almost entirely due to the anions.

1. INTRODUCTION

When studying ion-solvent and ion-ion interactions in solutions of electrolytes two alternative procedures are commonly used. In one, changes in some property relating to the whole solution are considered and in the other specific changes in a property of the particular ion under consideration are measured, the latter approach being, in principle, more direct.

Two techniques of potential use in the latter category both suffer from severe limitations. Changes in the ultra-violet spectra of certain simple anions are sometimes very large when the environment is varied, but, since both the ground and electronically excited states are affected, interpretation of these changes is dependent upon the choice of a model for the excited state [1, 2].

Variations in the nuclear resonance of a given ion is a more delicate probe, in that only the ground state is directly involved, but unfortunately relatively high ionic concentrations have to be used (usually ≥ 0.1 M) and interpretation of the shifts is limited by the complexity of the general theory of chemical shifts as developed by Ramsey [3].

We report a study of relative shifts in the nuclear resonance bands of fluoride and caesium ions when temperature, ionic strength and solvent are varied systematically. The fluoride results have already been reported in summary [4]. Singly charged rare-gas ions were selected in order to reduce specific ionic association to a minimum: caesium and fluoride were then chosen after a preliminary survey had revealed that the nuclear resonance bands from these ions were relatively narrow and did, in fact, shift when the environment was changed.

The resonance band for caesium ions was studied by Gutowsky and McGarvey [5] who observed a shift when the concentration of aqueous caesium chloride was

† Present address : Department of Theoretical Chemistry, University Chemical Laboratory, University of Cambridge.

‡ Department of Physical Chemistry, University of Minnesota, Minneapolis.

changed. Similarly, Shoolery and Alder commented briefly on the concentration dependence of the fluoride resonance band from aqueous potassium fluoride [6]. Wertz and co-workers have discussed the shifts and broadening which are found for ^{23}Na and ^{35}Cl resonance bands for sodium and chloride ions when the counter ion is changed [7, 8].

Complex fluorides have been studied by Connick and Poulsen [9] and the Tl resonance from thallous ion complexes has been studied by Richards and co-workers [10]. Also relevant is the work of Gutowsky and McGarvey on the relative shifts of the caesium resonance bands in crystalline caesium halides [11], which has recently been extended and interpreted by Bloembergen and Sorokin [12].

2. EXPERIMENTAL

2.1. Apparatus

The spectrometer of Professor John E. Wertz at the Department of Chemistry, the University of Minnesota, was used throughout this work.

2.2. Fluoride resonance

Measurements were made at a resonance frequency of 30 Mc/s. The test solutions were contained in glass tubes of 6 mm diameter and the shifts were measured relative to $\text{C}_6\text{H}_5\text{CF}_3$ contained in a sealed capillary immersed in the test solutions. The side-band method was employed to measure the shifts.

Most measurements were made at 30° and the shifts, σ_F , are reported relative to 0.4 M aqueous potassium fluoride, a positive value of σ indicating a shift to higher field. The shift is expressed as

$$\sigma_F = \frac{H_s - H_r}{H_r} \times 10^6 \quad (1)$$

where H_s and H_r are the resonance fields in gauss of the sample and reference solutions respectively. The minor corrections for changes in bulk diamagnetism have been made to the results reported. Some of the measurements were repeated at 40 Mc/s, the results being identical within experimental error.

2.3. Caesium resonance

A resonance frequency of 3 Mc/s was used. The sample was contained in the central compartment of a thin double-walled tube, the reference solution being permanently enclosed in the outer compartment. This reference was a saturated aqueous solution of caesium chloride containing a trace of ferric chloride to reduce the relaxation time. The shifts σ_{Cs} are reported relative to 1.8 M aqueous caesium chloride as reference zero, and σ_{Cs} is defined as in equation (1).

3. RESULTS

3.1. Fluoride ion

The results are summarized in figures 1 to 4. Figure 1 shows the effect of adding various organic solvents to aqueous potassium fluoride, the concentration of the fluoride being constant at 0.4 M. (The change in mole-fraction of

potassium fluoride as the mole-fraction of the organic component changes is negligible.) For each organic solvent, measurements were made to the limit of miscibility. Unfortunately for most of the solvents of relatively low dielectric constant such as acetone, methyl cyanide and dioxane, the solute began to separate in the 0.2 mole-fraction region and, for these solvents, little or no shift in the resonance frequency was detected.

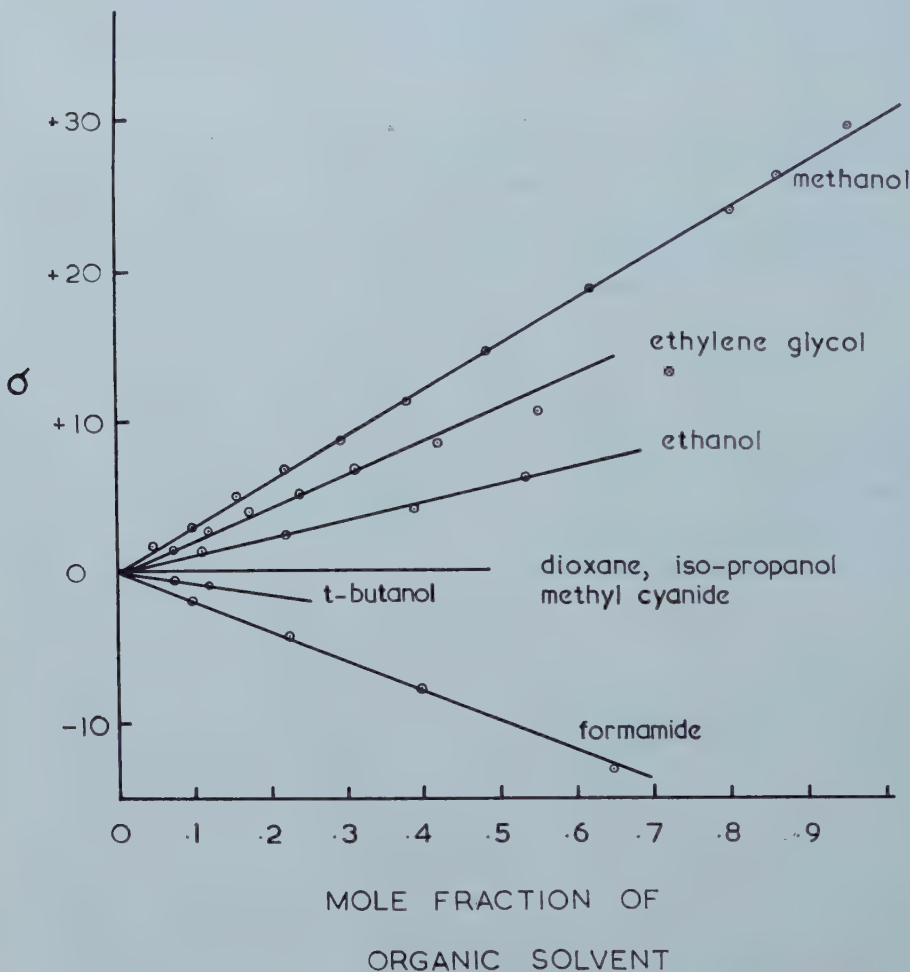


Figure 1. Variation of chemical shift with mole-fraction of solvent for fluoride ion in solvents composed of water and the solvents named in the figure.

Figure 2 shows the effect of changing the concentration of potassium fluoride in various mixtures of water and methanol. In all cases there was an initial linear shift to low field, but at very high concentrations there is a minimum followed by a trend back towards high fields. The overall shifts increase as the methanol content increases, but the minimum is unaltered. In aqueous formamide the effect is very small indeed, and no defined minimum was detected.

In figure 3 the effect of adding various electrolytes other than fluorides is depicted. In all cases for which high concentrations could be reached, there was a departure from linearity on the high field side in very concentrated solutions.

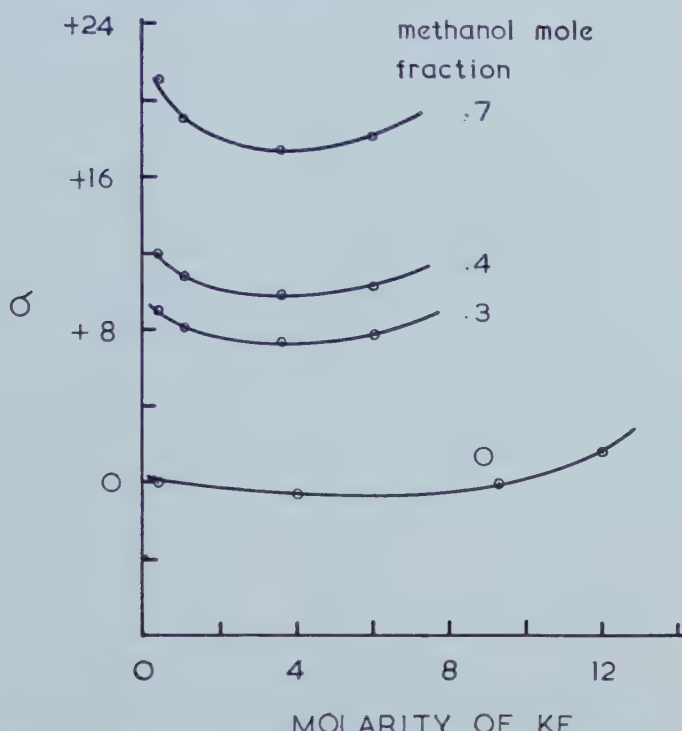


Figure 2. The effect of varying the concentration of potassium fluoride in various water-methanol mixtures.

From the results shown in figure 3 shift parameters σ^+ and σ^- can be derived for cations and anions relative to some fixed value for any one ion. Such values, derived from the equation

$$\sigma_F = m(n^+ \sigma^+ + n^- \sigma^-) \quad (2)$$

where σ_F is the net shift, m the molarity and n^+ the charge on the ions, are given in the table, the value for sodium ion having been arbitrarily set equal to zero.

Ion	σ^-	Ion	σ^+
F^-	+0.75	Na^+	0
Cl^-	+0.62	K^+	-0.90
Br^-	+0.58	Rb^+	-1.12
I^-	+0.30	Cs^+	-2.13

Relative molar shifts of the fluorine resonance for anions and cations. (The value of zero for sodium ion is arbitrarily chosen.)

Figure 4 shows the observed shifts on addition of a weak acid (acetic acid) and a strong acid (trifluoroacetic acid).

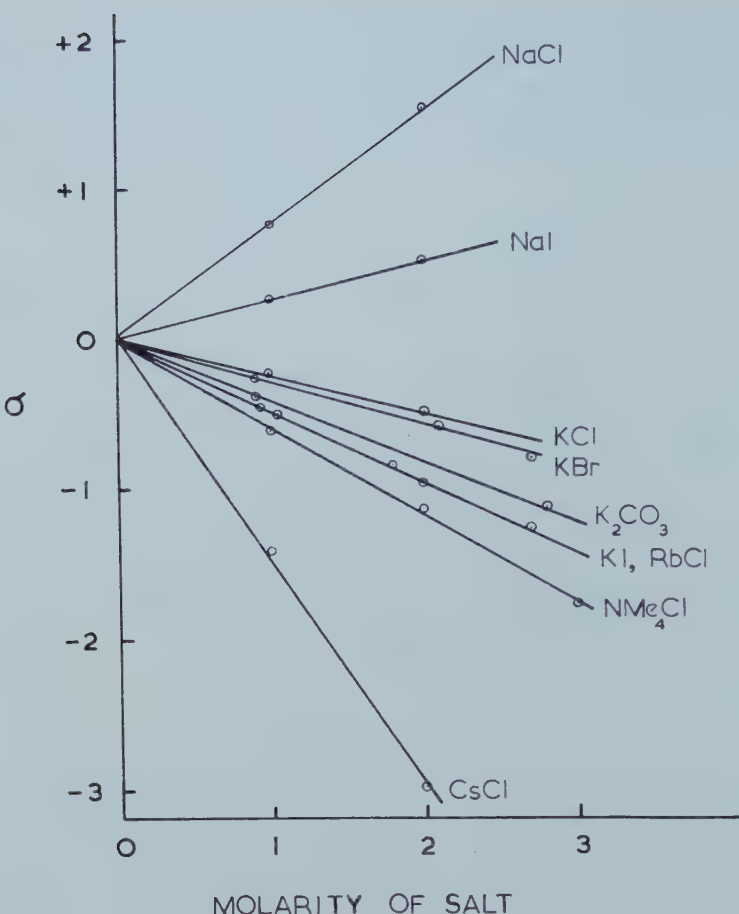


Figure 3. The effect of added salts on the fluoride ion resonance in aqueous potassium fluoride.

A qualitative study of the effect of temperature changes on the fluoride resonance has been made. In every case, an increase in temperature gave a shift to higher field but the effect was relatively small.

A brief survey has also been made of certain polyatomic ions containing fluorine, namely $CF_3CO_2^-$, $CF_3SO_3^-$, PF_6^- and AlF_2^+ . In each case addition of methanol to aqueous solutions resulted in a shift to high field and addition of formamide in a shift to low field, but these shifts were very much smaller than for the fluoride ion and in some cases were close to experimental error.

However, these results are thought to be of some importance since they show that the solvent shifts for fluoride ion are not a unique property of the closed shell ion. However, they also give some idea about the size of shifts to be expected if fluoride were specifically bonded to one cation or one solvent molecule, rather than solvated in the usual sense.

3.2. Caesium ion resonance

Figure 5 shows how the caesium resonance shifts upon addition of electrolytes. In all solutions the mole-fraction of caesium chloride was constant at 0.035. In contrast with the results obtained with fluoride, there is relatively little dependence

upon the nature of the positive ion and hence one can approximate by setting σ^+ equal to zero, the difficulty of differentiating between positive and negative ions then being avoided.

Also, in marked contrast with fluoride, there is no detectable effect on the resonance when the solvent is changed.

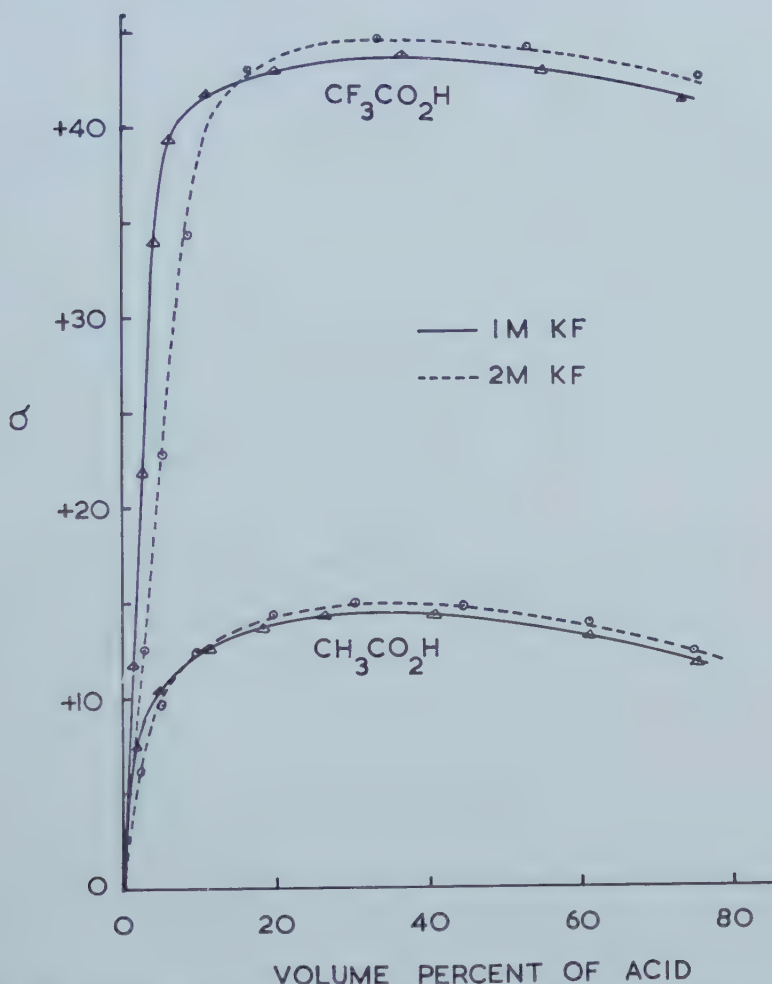


Figure 4. The effect of acids on the fluoride ion resonance in aqueous potassium fluoride.

4. DISCUSSION

4.1. Caesium ion shifts

The most important features are the marked dependence upon the nature of the negative ion and the linearity of the mole-fraction plots. The sequence amongst the halide ions is the same as that for crystalline caesium halides, but if the linear plots of shift against mole-fraction of added salt are extrapolated to a mole-fraction of one, the shifts predicted for the solids are far greater than observed.

Since a change in solvent has no effect on the resonance, we conclude that the anion shift is not simply an ionic atmosphere effect, giving rise to an increased polarization of solvent molecules. We therefore suggest that it is fortuitously

formed contact ion-pairs (cf. [13]) that are responsible for the large shifts. If this is correct, then the shift is primarily due to an increase in the paramagnetic circulation which can occur *via* excited states of the contact ion-pairs. If a specific reaction rather than chance collisions were important, one would not expect the closely linear plots recorded. Deviations from linearity have been observed for thallous salts [10] for which complexing is expected to be far more important.

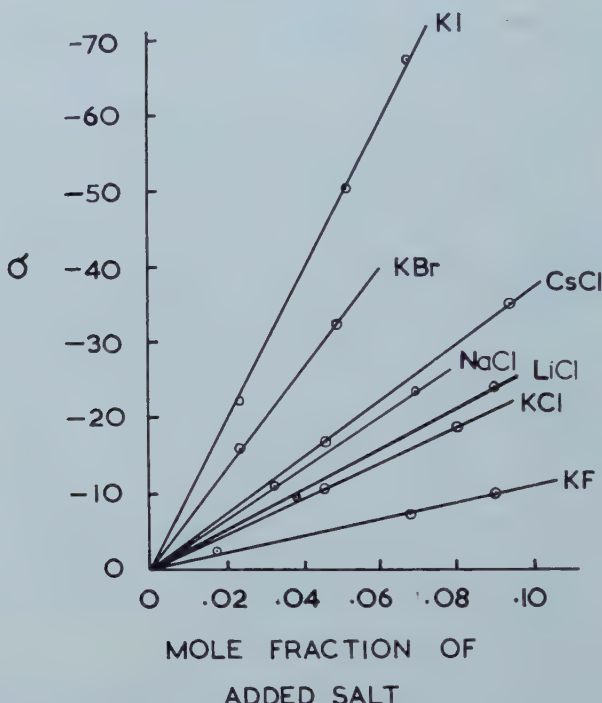


Figure 5. Variation of chemical shift with concentration of added salt for aqueous caesium ion.

4.2. Fluoride resonance shifts

Since the fluoride resonance is a function of the nature and concentration of added cations and anions and one cannot add one without the other, it is only possible to assign specific values for the effect of individual ions if a value for one is assumed. The shifts caused by potassium, rubidium and caesium are increasingly paramagnetic relative to sodium ion, which is the same order of cations found for the iodide resonance in alkali iodide crystals [12].

Since the fluoride resonance is strongly solvent dependent, there will be at least two superimposed effects from added electrolytes, namely the contact ion-pair effect considered for caesium from cations, and a general solvent effect from both cations and anions. If in the low mole-fraction region, anions affect the fluoride ion indirectly by polarising the solvent molecules, we would expect this effect to increase from iodide to fluoride. There is a diamagnetic trend in the resonance line on going from iodide to fluoride, so we conclude that an increase in the polarization of solvent molecules results in a shift to high field, that is, towards the value for aqueous hydrogen fluoride.

A similar trend is found within the series of alcohols studied. As the acid-strength of the alcohol increases, so a strong shift to high field is found, while with acetic and trifluoroacetic acids, when actual formation of hydrogen fluoride is expected, the trend to high fields is very strong indeed. Since hydrogen fluoride has its resonance on the high field side of solvated fluoride, it is unlikely that the solvent effects arise from a specific hydrogen bonding effect involving only one solvent molecule: more likely it is a relatively minor interaction with many protons which is responsible for the chemical shifts.

Some other aspects of the shifts will now be touched on. The upward trend for concentrated electrolytes is probably connected with the fact that the trend must, ultimately, be to the value for the solid. These are not known with sufficient accuracy to warrant comparison.

The strong acid, trifluoroacetic acid, evidently converts fluoride into hydrogen fluoride, the subsequent shift being a solvent shift on this molecule. Since ammonium fluoride shifts in the opposite sense with increasing concentration it would seem that the ion HF_2^- has a resonance to low field of aqueous fluoride. The intermediate position for fluoride in acetic acid may reflect the presence of both hydrogen fluoride and HF_2^- in these solutions.

The definite shift to high field with increase in temperature is further evidence for strong interactions with the solvent, which are presumably decreased as the temperature increases.

4.4. Linearity of shifts

In many ways the most remarkable feature of the present results is the good linearity of the plots of shift against mole-fraction. This linearity implies a surprising simplicity in the underlying physical laws. For mixed solvents the implication is that the immediate environment of each fluoride ion has a solvent composition which, on average, is exactly that of the bulk medium. In other words, there is no preferential solvation by one component. This seems to be true of the fluoride-water-alcohol systems and of the fluoride-water-formamide system. When no shift is detected, for example when dioxane is added to aqueous fluoride, it is very probable that water remains specifically in contact with fluoride. Other solvents for which this happens are indicated in figure 1. Unfortunately the sparing solubility of fluorides in these relatively poorly solvating media has prevented measurements over much of the mole-fraction range.

In contrast, the shift for ethylene glycol indicates preferential solvation by the glycol (figure 1). This is understandable if the glycol solvates the fluoride ion with both hydroxyl protons, thus being effectively chelated.

From a study of the ultra-violet spectrum of solvated iodide ion in similar mixtures of solvents, it was concluded that some preferential solvation by water generally occurred [1]. This was very much less marked for the alcohols than for methyl cyanide and especially dioxane, but nevertheless the plots of shift against mole-fraction for the alcohols were curved. However, as the temperature was raised, so the curvature decreased and at about 70° the plots were linear. It has now been found that addition of a large excess of potassium fluoride, to simulate conditions used in the present experiments, also tends to straighten the plots [14]. This is understandable since the added electrolyte will compete for solvent molecules so that a far greater proportion of the total must be engaged in solvating the ions, and hence individual ions will be less selective.

4.5. Comparison of fluoride with caesium ions

To the extent that fortuitous contact ion-pairs are important, these ions behave similarly. However, the electron donating power of fluoride ion can manifest itself in its interaction with solvent as well as with cations, whereas the electron accepting power of caesium is apparently only important in the contact ion-pair. That is to say, charge-transfer from solvent to the cation does not seem to be important, nor does it seem likely that covalent bonding between caesium ion and solvent is significant.

The experimental work described was carried out in the University of Minnesota and was supported in part by the United States Air Force Office of Scientific Research under contract AF 18-(600)-479. One of us (A.C.) is indebted to Professor J. E. Wertz for the award of a Research Fellowship at the University of Minnesota. Thanks are due to Dr. J. A. Pople for helpful discussions.

REFERENCES

- [1] SMITH, M., and SYMONS, M. C. R., 1958, *Trans. Faraday Soc.*, **54**, 339, 346.
- [2] STEIN, G., and TREININ, A., 1959, *Trans. Faraday Soc.*, **55**, 1086, 1091.
- [3] RAMSEY, N. F., 1952, *Phys. Rev.*, **86**, 243.
- [4] CARRINGTON, A., and HINES, T., 1958, *J. chem. Phys.*, **28**, 727.
- [5] GUTOWSKY, H. S., and McGARVEY, B., 1953, *Phys. Rev.*, **91**, 81.
- [6] SHOOLERY, J. N., and ALDER, B. J., 1955, *J. chem. Phys.*, **23**, 805.
- [7] WERTZ, J. E., 1957, *J. phys. Chem.*, **61**, 51.
- [8] WERTZ, J. E., and JARDETZKY, O., 1956, *J. chem. Phys.*, **25**, 357.
- [9] CONNICK, R. E., and POULSON, R. E., 1957, *J. Amer. chem. Soc.*, **79**, 5153.
- [10] FREEMAN, R., GASSER, R., RICHARDS, R. E., and WHEELER, D. H., 1959, *Mol. Phys.*, **2**, 75.
- [11] GUTOWSKY, H. S., and McGARVEY, B., 1953, *J. chem. Phys.*, **21**, 1423.
- [12] BLOEMBERGEN, N., and SOROKIN, R., 1958, *Phys. Rev.*, **110**, 865.
- [13] GRIFFITHS, T. R., and SYMONS, M. C. R., 1960, *Mol. Phys.*, **3**, 90.
- [14] GRIFFITHS, T. R., unpublished results.

The effect of strong electric and magnetic fields on the depolarization ratios of gases

by A. L. ANDREWS and A. D. BUCKINGHAM

The Inorganic Chemistry Laboratory, The University of Oxford

(Received 26 October 1959)

The influence of a strong electric field F on the polarization of light scattered elastically by small gaseous molecules is investigated. Two effects are found:

(i) The field distorts the molecules, thereby changing their polarizabilities. If they are isotropically polarizable when $F=0$, and hence capable of scattering only polarized light from a parallel beam, this distortion may lead to depolarization. For inert gas atoms, this depolarization is proportional to F^4 , and hence normally very small, but for tetrahedral molecules it is proportional to $\beta^2 F^2$, where β is the first hyperpolarizability of the molecule.

(ii) F tends to orientate anisotropic molecules, thereby affecting the polarization of the scattered light; this effect is related to the anisotropy in the molecular polarizability, and to the dipole moment, but is not likely to lead to information that is not obtainable by simpler means.

The effect of a strong magnetic field, in place of F , is also discussed.

1. INTRODUCTION

The light scattered elastically by small molecules is partly polarized. Thus if a parallel beam is travelling in the x -direction and the light scattered along the y -axis is observed, its partial intensity I_x (with electric vector parallel to the x -axis) is zero if the scattering molecules are isotropic. This is because the induced oscillating dipole is in the yz plane. However, if the molecule has different polarizabilities in different directions, the oscillating dipole is not in general parallel to the instantaneous electric field acting on it, and hence there may be an oscillating dipole in the x -direction, and a non-zero I_x . The ratio $I_x/I_z = \rho_0$ is called the depolarization ratio. For incident light which is plane polarized with its electric vector parallel to the z -direction [1]

$$\rho_0 = \frac{3\kappa^2}{5 + 4\kappa^2} \quad (1)$$

and for ordinary light

$$\rho_0' = I_x'/I_z' = \frac{2I_x}{I_z + I_x} = \frac{6\kappa^2}{5 + 7\kappa^2} \quad (2)$$

where

$$\kappa^2 = \frac{3\alpha_{\alpha\beta}\alpha_{\alpha\beta} - \alpha_{\alpha\alpha}\alpha_{\beta\beta}}{2\alpha_{\alpha\alpha}\alpha_{\beta\beta}} \quad (3)$$

$\alpha_{\alpha\beta}$ being the polarizability tensor. For axially symmetric molecules

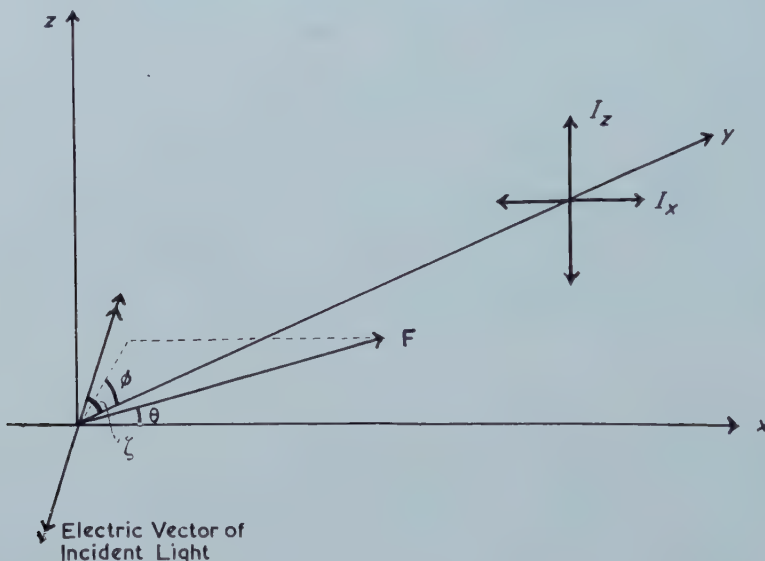
$$\kappa^2 = \frac{(\alpha_{||} - \alpha_{\perp})^2}{(\alpha_{||} + 2\alpha_{\perp})^2}$$

so that κ is the anisotropy. Thus depolarization measurements, particularly if made on gases, lead to valuable information about the anisotropy of molecules.

If a strong static electric or magnetic field is applied to a molecule, there will be two main effects influencing the depolarization ratio ρ :

(i) The molecules will be distorted by the field, and if they are isotropically polarizable in the absence of F (e.g. argon, methane) they will depolarize the light only when the field is present. Thus the higher order polarizabilities ('hyperpolarizabilities') might be measured by observing this induced depolarization.

(ii) The field will orientate the molecules if they are dipolar or anisotropically polarizable, and this will clearly influence ρ . This effect, which is temperature dependent, could lead to information about the polarizability tensor.



The effect is in some respects similar to that produced by molecular interactions on the depolarization ratios of compressed gases, and may be of value in interpreting measurements made on dense media. The two effects may easily be separated by application of an alternating field, leading to a component of the depolarization ratio with twice the applied frequency. The effect due to molecular interactions is frequency independent.

Heller [5] has considered the effects of fields on the scattering from large molecules.

2. THEORY

Consider polarized light travelling in the \mathbf{i} direction ($\mathbf{i}, \mathbf{j}, \mathbf{k}$ are unit vectors in the x, y, z directions) with electric vector at an angle ζ to \mathbf{j} . Suppose the molecule is in a strong electric field $\mathbf{F} = F\mathbf{f}$ where

$$f_\alpha = \cos \theta i_\alpha + \sin \theta \cos \phi j_\alpha + \sin \theta \sin \phi k_\alpha. \quad (4)$$

Then, since ρ must be an even function of F

$$\rho = \rho_0 + \rho_2 F^2 + \rho_4 F^4 + \dots = I_x / I_z \quad (5)$$

where [2]

$$I_x = \pi_{\alpha\gamma} \pi_{\beta\delta} i_\alpha i_\beta (\sin \zeta k_\gamma + \cos \zeta j_\gamma) (\sin \zeta k_\delta + \cos \zeta j_\delta) \quad (6)$$

and

$$I_z = \pi_{\alpha\gamma} \pi_{\beta\delta} k_\alpha k_\beta (\sin \zeta k_\gamma + \cos \zeta j_\gamma) (\sin \zeta k_\delta + \cos \zeta j_\delta) \quad (7)$$

the bar denoting a statistical average over all molecular orientations τ :

$$\bar{X} = \int X \exp(-u/kT) d\tau / \int \exp(-u/kT) d\tau.$$

The potential energy, dipole moment and polarizability of a molecule in a field F are [4]

$$\left. \begin{aligned} u &= u^{(0)} - \mu_\alpha F_\alpha - \frac{1}{2} \alpha_{\alpha\beta} F_\alpha F_\beta - \frac{1}{6} \beta_{\alpha\beta\gamma} F_\alpha F_\beta F_\gamma - \frac{1}{24} \gamma_{\alpha\beta\gamma\delta} F_\alpha F_\beta F_\gamma F_\delta - \dots \\ m_\alpha &= -\partial u / \partial F_\alpha = \mu_\alpha + \alpha_{\alpha\beta} F_\beta + \frac{1}{2} \beta_{\alpha\beta\gamma} F_\beta F_\gamma + \frac{1}{6} \gamma_{\alpha\beta\gamma\delta} F_\beta F_\gamma F_\delta + \dots \\ \pi_{\alpha\beta} &= \partial m_\alpha / \partial F_\beta = \alpha_{\alpha\beta} + \beta_{\alpha\beta\gamma} F_\gamma + \frac{1}{2} \gamma_{\alpha\beta\gamma\delta} F_\gamma F_\delta + \dots \end{aligned} \right\} \quad (8)$$

μ_α is the permanent dipole moment, $\alpha_{\alpha\beta}$ the polarizability tensor, and β, γ are 'hyperpolarizabilities' describing departure from a linear relation between the induced dipole moment and F .

Hence

$$\begin{aligned} (I_x)_{F=0} &= \langle \alpha_{\alpha\gamma} \alpha_{\beta\delta} i_\alpha i_\beta (\cos^2 \zeta j_\gamma j_\delta + \sin^2 \zeta k_\gamma k_\delta) \rangle \\ &= \frac{\alpha_{\alpha\gamma} \alpha_{\beta\delta}}{30} \{ 4\delta_{\alpha\beta} \delta_{\gamma\delta} - \delta_{\alpha\gamma} \delta_{\beta\delta} - \delta_{\alpha\delta} \delta_{\beta\gamma} \} \\ &= \frac{1}{30} \{ 3\alpha_{\alpha\beta} \alpha_{\alpha\beta} - \alpha_{\alpha\alpha} \alpha_{\beta\beta} \} \end{aligned} \quad (9)$$

where the angular brackets denote an unweighted average over all orientations. (For the required values of the unweighted averages of the various products of $i_\alpha, j_\beta, k_\gamma$ see the Appendix.)

$$\begin{aligned} (I_z)_{F=0} &= \langle \alpha_{\alpha\gamma} \alpha_{\beta\delta} k_\alpha k_\beta (\cos^2 \zeta j_\gamma j_\delta + \sin^2 \zeta k_\gamma k_\delta) \rangle \\ &= \frac{\alpha_{\alpha\gamma} \alpha_{\beta\delta}}{30} \{ (4 \cos^2 \zeta + 2 \sin^2 \zeta) \delta_{\alpha\beta} \delta_{\gamma\delta} - (\cos^2 \zeta - 2 \sin^2 \zeta) (\delta_{\alpha\gamma} \delta_{\beta\delta} + \delta_{\alpha\delta} \delta_{\beta\gamma}) \} \\ &= \frac{1}{30} \{ \alpha_{\alpha\beta} \alpha_{\alpha\beta} (4 - \cos^2 \zeta) + \alpha_{\alpha\alpha} \alpha_{\beta\beta} (2 - 3 \cos^2 \zeta) \}. \end{aligned} \quad (10)$$

Hence

$$\rho_0 = \frac{3\alpha_{\alpha\beta} \alpha_{\alpha\beta} - \alpha_{\alpha\alpha} \alpha_{\beta\beta}}{(4 - \cos^2 \zeta) \alpha_{\alpha\beta} \alpha_{\alpha\beta} + (2 - 3 \cos^2 \zeta) \alpha_{\alpha\alpha} \alpha_{\beta\beta}}. \quad (11)$$

If $\zeta = \pi/2$ this reduces to (1), and if the incident light is unpolarized, $\sin^2 \zeta$ and $\cos^2 \zeta$ can be replaced by $\frac{1}{2}$ so that

$$\begin{aligned} \rho_0' &= \frac{6\alpha_{\alpha\beta} \alpha_{\alpha\beta} - 2\alpha_{\alpha\alpha} \alpha_{\beta\beta}}{7\alpha_{\alpha\beta} \alpha_{\alpha\beta} + \alpha_{\alpha\alpha} \alpha_{\beta\beta}} \\ &= \frac{6\kappa^2}{5 + 7\kappa^2}. \end{aligned} \quad (12)$$

Also

$$\rho_2 = \frac{1}{2} \left(\frac{d^2 \rho}{dF^2} \right)_{F=0} = \frac{1}{2(I_z)_{F=0}} \left\{ \frac{d^2 I_x}{dF^2} - \rho_0 \frac{d^2 I_z}{dF^2} \right\} \quad (13)$$

$$\begin{aligned} &= \frac{1}{2(I_z)_{F=0}} \left\{ \left[2\alpha_{\alpha\gamma} \gamma_{\beta\delta\epsilon\phi} + 2\beta_{\alpha\gamma\epsilon} \beta_{\beta\delta\phi} + \frac{\alpha_{\alpha\gamma}}{kT} \left\{ 4\beta_{\beta\delta\epsilon} \mu_\phi + \alpha_{\beta\delta} \left(\alpha'_{\epsilon\phi} + \frac{\mu_\epsilon \mu_\phi}{kT} \right) \right\} \right] \right. \\ &\quad \times \left. (i_\alpha i_\beta - \rho_0 k_\alpha k_\beta) \{ \cos^2 \zeta j_\gamma j_\delta + \sin \zeta \cos \zeta (j_\gamma k_\delta + j_\delta k_\gamma) + \sin^2 \zeta k_\gamma k_\delta \} f_\epsilon f_\phi \right\} \end{aligned} \quad (14)$$

where $f_\epsilon f_\phi$ is obtainable from (4), and $\alpha'_{\epsilon\phi}$ is the polarizability tensor for the frequency of the applied field F ; $\alpha_{\epsilon\phi}$ is the polarizability for the optical frequency of the light.

2.1. Case (i): spherical molecules

For spherical molecules (e.g. argon and the other inert gases)

$$\mu_\alpha = \beta_{\alpha\beta\gamma} = 0; \quad \alpha_{\alpha\beta} = \alpha\delta_{\alpha\beta}, \quad \gamma_{\alpha\beta\gamma\delta} = \frac{1}{3}\gamma\{\delta_{\alpha\beta}\delta_{\gamma\delta} + \delta_{\alpha\gamma}\delta_{\beta\delta} + \delta_{\alpha\delta}\delta_{\beta\gamma}\}$$

whence

$$(I_z)_{F=0} = \alpha^2 \sin^2 \zeta$$

and

$$\rho_0 = \rho_2 = 0. \quad (15)$$

Thus the depolarization produced by spherical molecules is proportional to $\gamma^2 F^4$ and is therefore likely to be small under normal conditions.

2.2. Case (ii): tetrahedral molecules

For molecules with tetrahedral symmetry (e.g. CH₄, Ni(CO)₄) $\mu_\alpha = 0$; $\alpha_{\alpha\beta} = \alpha\delta_{\alpha\beta}$ and there is one non-zero β -tensor, namely $\beta_{123} = \beta$, where the 1, 2, 3 directions are the three axes of a cube whose three diagonals from a corner form the sides of the tetrahedron. In this case, (14) reduces to

$$\rho = \rho_2 F^2 = \frac{\beta^2 F^2}{35 \alpha^2 \sin^2 \zeta} [8 - 3 \sin^2 \theta (\cos^2 \zeta \sin^2 \phi + \sin^2 \zeta \cos^2 \phi)] \quad (16)$$

which for unpolarized light becomes

$$\rho' = \frac{2\beta^2 F^2}{35 \alpha^2} (8 - \frac{3}{2} \sin^2 \theta). \quad (17)$$

2.3. Case (iii): zero hyperpolarizability

For highly anisotropic molecules (e.g. CO₂, C₆H₅NO₂) the effects of hyperpolarizability are probably negligible (except at high temperatures) and (14) leads to

$$\begin{aligned} \rho_2 = & \frac{1}{420 k T (I_z)_{F=0}} \left[\left(\alpha'_{\alpha\alpha} + \frac{\mu_\alpha \mu_\alpha}{kT} \right) (\alpha_{\beta\gamma} \alpha_{\beta\gamma} [5 + 6 \sin^2 \theta (\cos \zeta \sin \phi - \sin \zeta \cos \phi)^2 \right. \right. \\ & - \rho_0 \{ \cos^2 \zeta (5 + 6 \cos^2 \theta) + (12 - 8 \sin^2 \theta \sin^2 \phi) \sin^2 \zeta - 8 \sin \zeta \cos \zeta \sin^2 \theta \sin \phi \right. \\ & \times \cos \phi \}] \\ & - \alpha_{\beta\beta} \alpha_{\gamma\gamma} [1 + 4 \sin^2 \theta (\cos \zeta \sin \phi - \sin \zeta \cos \phi)^2 - \rho_0 \{ \cos^2 \zeta (1 + 4 \cos^2 \theta) \\ & - \sin^2 \zeta (6 - 4 \sin^2 \theta \sin^2 \phi) + 4 \sin \zeta \cos \zeta \sin^2 \theta \sin \phi \cos \phi \}] \\ & + \left(\alpha'_{\alpha\beta} + \frac{\mu_\alpha \mu_\beta}{kT} \right) (\alpha_{\alpha\gamma} \alpha_{\beta\gamma} [6 - 18 \sin^2 \theta (\cos \zeta \sin \phi - \sin \zeta \cos \phi)^2 - \rho_0 \{ \cos^2 \zeta \right. \\ & \times (6 - 18 \cos^2 \theta) - \sin^2 \zeta (8 - 24 \sin^2 \theta \sin^2 \phi) + 24 \sin \zeta \cos \zeta \sin^2 \theta \sin \phi \cos \phi \}] \\ & - \alpha_{\alpha\beta} \alpha_{\gamma\gamma} [4 - 12 \sin^2 \theta (\cos \zeta \sin \phi - \sin \zeta \cos \phi)^2 \\ & - \rho_0 \{ \cos^2 \zeta (4 - 12 \cos^2 \theta) + \sin^2 \zeta (4 - 12 \sin^2 \theta \sin^2 \phi) \\ & \left. \left. - 12 \sin \zeta \cos \zeta \sin^2 \theta \sin \phi \cos \phi \} \right] \right]. \end{aligned} \quad (18)$$

For polarized light with $\zeta = \pi/2$, (18) becomes

$$\begin{aligned} \rho_2 = & \frac{1}{14kT(2x_{\xi\eta}x_{\xi\eta} + x_{\xi\xi}x_{\eta\eta})} \left[(x'_{\alpha\alpha} + \mu^2/kT)\{(3\sin^2\theta - 2)x_{\beta\gamma}x_{\beta\gamma} \right. \\ & + (\cos^2\theta - \sin^2\theta\cos^2\phi)x_{\beta\beta}x_{\gamma\gamma}\} + \left(x'_{\alpha\beta} + \frac{\mu_\alpha\mu_\beta}{kT} \right) \right. \\ & \times \{(1 - 3\sin^2\theta\cos^2\phi)(3x_{\alpha\gamma}x_{\beta\gamma} - 2x_{\alpha\beta}x_{\gamma\gamma}) + \\ & \left. \left. + 2\rho_0(1 - 3\sin^2\theta\sin^2\phi)(2x_{\alpha\gamma}x_{\beta\gamma} + x_{\alpha\beta}x_{\gamma\gamma})\right\} \right]. \end{aligned} \quad (19)$$

For axially symmetric molecules, (19) leads to the result

$$\begin{aligned} \rho = \rho_0 \left[1 + \left(\frac{x'_{\parallel\parallel} - x'_{\perp\perp} + \mu^2/kT}{7kT} \right) F^2 \left\{ \sin^2\theta(1 - 2\cos^2\phi) + \right. \right. \\ \left. \left. + \frac{(1 - 3\sin^2\theta\sin^2\phi)(3x_{\parallel\parallel}^2 + 2x_{\parallel\parallel}x_{\perp\perp})}{3x_{\parallel\parallel}^2 + 4x_{\parallel\parallel}x_{\perp\perp} + 8x_{\perp\perp}^2} \right\} + O(F^4) \right]. \end{aligned} \quad (20)$$

For ordinary light $\cos^2\zeta = \sin^2\zeta = \frac{1}{2}$; $\sin\zeta\cos\zeta = 0$, and (18) yields

$$\begin{aligned} \rho'_2 = & \frac{1}{7kT(7x_{\xi\eta}x_{\xi\eta} + x_{\xi\xi}x_{\eta\eta})} \left[(x'_{\alpha\alpha} + \mu^2/kT)\{x_{\beta\gamma}x_{\beta\gamma}[5 + 3\sin^2\theta \right. \\ & - \rho'_0(17/2 + 3\cos^2\theta - 4\sin^2\theta\sin^2\phi)] - x_{\beta\beta}x_{\gamma\gamma}[1 + 2\sin^2\theta \right. \\ & + \rho'_0(5/2 - 2\cos^2\theta - 2\sin^2\theta\sin^2\phi)]\} + \left(x'_{\alpha\beta} + \frac{\mu_\alpha\mu_\beta}{kT} \right) \{x_{\alpha\gamma}x_{\beta\gamma} \right. \\ & \times [3(2 - 3\sin^2\theta) + \rho'_0(1 + 9\cos^2\theta - 12\sin^2\theta\sin^2\phi)] - x_{\alpha\beta}x_{\gamma\gamma} \right. \\ & \times [2(2 - 3\sin^2\theta) - \rho'_0(4 - 6\cos^2\theta - 6\sin^2\theta\sin^2\phi)]\} \end{aligned} \quad (21)$$

which for axial symmetry leads to the result

$$\begin{aligned} \rho' = \rho'_0 \left[1 + \frac{3(x'_{\parallel\parallel} - x'_{\perp\perp} + \mu^2/kT)F^2}{14kT(7(x_{\parallel\parallel} - x_{\perp\perp})^2 + 5(x_{\parallel\parallel} + 2x_{\perp\perp})^2)} \{8x_{\parallel\parallel}^2 + 2x_{\perp\perp}^2 \right. \\ \left. - (6x_{\parallel\parallel}^2 - 2x_{\parallel\parallel}x_{\perp\perp} + 11x_{\perp\perp}^2)\sin^2\theta - 4(3x_{\parallel\parallel}^2 + x_{\parallel\parallel}x_{\perp\perp} - 4x_{\perp\perp}^2)\sin^2\theta\sin^2\phi\} \right. \\ \left. + O(F^4) \right]. \end{aligned} \quad (22)$$

If \mathbf{F} is perpendicular to \mathbf{i} and \mathbf{j} , $\sin\theta = \sin\phi = 1$ and

$$\rho' = \rho'_0 \left[1 - \frac{(x'_{\parallel\parallel} - x'_{\perp\perp} + \mu^2/kT)F^2}{14kT(4x_{\parallel\parallel}^2 + 2x_{\parallel\parallel}x_{\perp\perp} + 9x_{\perp\perp}^2)} (10x_{\parallel\parallel}^2 + 2x_{\parallel\parallel}x_{\perp\perp} - 7x_{\perp\perp}^2) + O(F^4) \right]. \quad (23)$$

3. MAGNETIC FIELDS

If the strong uniform electric field \mathbf{F} is replaced by a strong magnetic field \mathbf{H} , then the analogue of (5) is

$$\rho_H = \rho_0 + \rho_{H_s} H^2 + \rho_{H_4} H^4 + \dots \quad (24)$$

Also, instead of (8), we have, for diamagnetic materials

$$\begin{aligned} u = u^{(0)} - \frac{1}{2}\chi_{\alpha\beta}H_\alpha H_\beta, \\ \pi_{\alpha\beta} = \alpha_{\alpha\beta} + \frac{1}{2}\eta_{\alpha\beta;\gamma\delta}H_\gamma H_\delta, \end{aligned} \quad (25)$$

where $\chi_{\alpha\beta}$ is the diamagnetic susceptibility tensor of the molecule, and the η tensor plays the role of γ in the electric field case [3].

The analogous equation to (22) is obtained by replacing

$$\{\alpha_{\parallel}' - \alpha_{\perp}' + \mu^2/kT\}F^2 \text{ by } \{\chi_{\parallel} - \chi_{\perp}\}H^2.$$

However, since an electric field alone cannot induce a magnetic moment (for it cannot give rise to a circulation of charge), there is no term in ρ_H , corresponding to the terms in β in ρ_2 .

4. DISCUSSION

The intensity I_x of the 'depolarized' component of the scattered light is approximately related to that of the incident light I_0 by [1]

$$I_x = \left(\frac{2\pi}{\lambda}\right)^4 \frac{N\alpha^2\rho}{R^2} I_0$$

where λ is the wavelength of the light, N the number of scattering molecules, and R is the distance of the detector from the scatterer.

Typical parameters would be $\lambda = 5 \times 10^{-5}$ cm, $\alpha = 3 \times 10^{-24}$ cm³, $R = 10$ cm, $N = 10^{19}$ and $I_0 = 10^6$ ergs cm⁻² sec⁻¹, whence $I_x \sim 5 \times 10^7 \rho$ photons cm⁻² sec⁻¹.

A photomultiplier tube can detect and measure a minimum of about 50 photons cm⁻² sec⁻¹, so that changes in depolarization ratios of the order of 10^{-6} should be detectable.

To pick out $\rho_2 F^2$ from ρ , it would presumably be most convenient to apply an alternating field $F = F_0 \exp(2\pi i v t)$ to the gas, and to amplify the photocurrent from the photomultiplier tube receiving the scattered light by means of a narrow band amplifier tuned to frequency $2v$. With this device, $\rho_2 F^2$ could be singled out from a possibly much larger ρ_0 . Thus in the case of CH₃F, $\kappa = 0.11$, and hence $\rho_0' = 0.014$, while (23) indicates that for fields of the order of 10³ e.s.u. (300 000 volts/cm) attainable in methyl fluoride if it is compressed to a few atmospheres, $\rho' = \rho_0' [1 - 10^{-4}]$.

Thus it is probable that ρ_2 could be measured for gaseous polar molecules using present-day equipment. However, such measurements would be of little value, as they would merely lead to information about the anisotropy in $\alpha_{\alpha\beta}$, and this could be obtained more readily from observations of ρ_0 or of the Kerr constant.

It is of interest to note that (22) can lead either to a positive or negative ρ_2' , the sign depending on the direction of \mathbf{F} . Thus if the molecule is polarizable only along its axis (i.e. $\kappa = 1$, $\rho_0' = \frac{1}{2}$), $\theta = \phi = \pi/2$ leads to an orientation of the molecules parallel to the z -axis, thereby reducing the polarizability—and hence I_x —in the x -direction. Also, if $\theta = 0$, I_x will be increased by the tendency for the polarizability in the x -direction to be raised.

In the case of tetrahedral molecules, $\rho_0 = \rho_0' = 0$ and all of I_x arises from the field.

If $\beta^2/\alpha^2 \sim 10^{-12}$, then for ρ' to be of the order of 10^{-6} , \mathbf{F} must be $\sim 5 \times 10^5$ volts cm⁻¹. This is by no means an impossibly-large field, so measurements of the first hyperpolarizability β of the molecule would seem to be feasible for tetrahedra. The second hyperpolarizability of the molecule γ can easily be obtained from Kerr effect measurements [4]; for CH₄

$$\gamma = 2.6 \times 10^{-36} \text{ e.s.u.}$$

APPENDIX

Averaging over all orientations of a molecule in the absence of any external constraints (the averages signified by the angular brackets $\langle \dots \rangle$ in the above are

of this kind) is equivalent to fixing the molecule and averaging over all possible directions of the co-ordinate axes. Such averaging leads, after straightforward trigonometrical analysis, to the following results, which were used to obtain the above formulae :

$$\begin{aligned}\langle i_\alpha i_\beta \rangle &= \langle j_\alpha j_\beta \rangle = \langle k_\alpha k_\beta \rangle = \langle f_\alpha f_\beta \rangle = \frac{1}{3} \delta_{\alpha\beta}, \\ \langle i_\alpha i_\beta i_\gamma i_\delta \rangle &= \frac{1}{15} \{ \delta_{\alpha\beta} \delta_{\gamma\delta} + \delta_{\alpha\gamma} \delta_{\beta\delta} + \delta_{\alpha\delta} \delta_{\beta\gamma} \}, \\ \langle i_\alpha i_\beta j_\gamma j_\delta \rangle &= \frac{1}{30} \{ 4 \delta_{\alpha\beta} \delta_{\gamma\delta} - \delta_{\alpha\gamma} \delta_{\beta\delta} - \delta_{\alpha\delta} \delta_{\beta\gamma} \}, \\ \langle i_\alpha i_\beta i_\gamma i_\delta i_\epsilon i_\phi \rangle &= \frac{1}{105} [\delta_{\alpha\beta} \delta_{\gamma\delta} \delta_{\epsilon\phi} + \delta_{\alpha\beta} \delta_{\gamma\epsilon} \delta_{\delta\phi} + \delta_{\alpha\beta} \delta_{\gamma\phi} \delta_{\delta\epsilon} + \delta_{\alpha\gamma} \delta_{\beta\delta} \delta_{\epsilon\phi} + \delta_{\alpha\gamma} \delta_{\beta\epsilon} \delta_{\delta\phi} \\ &\quad + \delta_{\alpha\gamma} \delta_{\beta\phi} \delta_{\delta\epsilon} + \delta_{\alpha\delta} \delta_{\beta\gamma} \delta_{\epsilon\phi} + \delta_{\alpha\delta} \delta_{\beta\epsilon} \delta_{\gamma\phi} + \delta_{\alpha\delta} \delta_{\beta\phi} \delta_{\gamma\epsilon} + \delta_{\alpha\epsilon} \delta_{\beta\gamma} \delta_{\delta\phi} \\ &\quad + \delta_{\alpha\epsilon} \delta_{\beta\delta} \delta_{\gamma\phi} + \delta_{\alpha\epsilon} \delta_{\beta\phi} \delta_{\gamma\delta} + \delta_{\alpha\phi} \delta_{\beta\gamma} \delta_{\delta\epsilon} + \delta_{\alpha\phi} \delta_{\beta\delta} \delta_{\gamma\epsilon} + \delta_{\alpha\phi} \delta_{\beta\epsilon} \delta_{\gamma\delta}], \\ \langle j_\alpha j_\beta i_\gamma i_\delta i_\epsilon i_\phi \rangle &= \frac{1}{35} \delta_{\alpha\beta} (\delta_{\gamma\delta} \delta_{\epsilon\phi} + \delta_{\gamma\epsilon} \delta_{\delta\phi} + \delta_{\gamma\phi} \delta_{\delta\epsilon}) \\ &\quad - \frac{1}{210} \{ \delta_{\alpha\gamma} \delta_{\beta\delta} \delta_{\epsilon\phi} + \delta_{\alpha\gamma} \delta_{\beta\epsilon} \delta_{\delta\phi} + \delta_{\alpha\gamma} \delta_{\beta\phi} \delta_{\delta\epsilon} + \delta_{\alpha\delta} \delta_{\beta\gamma} \delta_{\epsilon\phi} + \delta_{\alpha\delta} \delta_{\beta\epsilon} \delta_{\gamma\phi} \\ &\quad + \delta_{\alpha\delta} \delta_{\beta\phi} \delta_{\gamma\epsilon} + \delta_{\alpha\epsilon} \delta_{\beta\gamma} \delta_{\delta\phi} + \delta_{\alpha\epsilon} \delta_{\beta\delta} \delta_{\gamma\phi} + \delta_{\alpha\epsilon} \delta_{\beta\phi} \delta_{\gamma\delta} + \delta_{\alpha\phi} \delta_{\beta\gamma} \delta_{\delta\epsilon} \\ &\quad + \delta_{\alpha\phi} \delta_{\beta\delta} \delta_{\gamma\epsilon} + \delta_{\alpha\phi} \delta_{\beta\epsilon} \delta_{\gamma\delta} \}, \\ \langle i_\alpha i_\beta j_\gamma j_\delta k_\epsilon k_\phi \rangle &= \frac{8}{105} \delta_{\alpha\beta} \delta_{\gamma\delta} \delta_{\epsilon\phi} - \frac{1}{42} \{ \delta_{\alpha\beta} (\delta_{\gamma\epsilon} \delta_{\delta\phi} + \delta_{\gamma\phi} \delta_{\delta\epsilon}) \\ &\quad + \delta_{\gamma\delta} (\delta_{\alpha\epsilon} \delta_{\beta\phi} + \delta_{\alpha\phi} \delta_{\beta\epsilon}) + \delta_{\epsilon\phi} (\delta_{\alpha\gamma} \delta_{\beta\delta} + \delta_{\alpha\delta} \delta_{\beta\gamma}) \} \\ &\quad + \frac{1}{105} \{ \delta_{\alpha\gamma} \delta_{\beta\epsilon} \delta_{\delta\phi} + \delta_{\alpha\gamma} \delta_{\beta\phi} \delta_{\delta\epsilon} + \delta_{\alpha\delta} \delta_{\beta\epsilon} \delta_{\gamma\phi} + \delta_{\alpha\delta} \delta_{\beta\phi} \delta_{\gamma\epsilon} \\ &\quad + \delta_{\alpha\epsilon} \delta_{\beta\gamma} \delta_{\delta\phi} + \delta_{\alpha\epsilon} \delta_{\beta\delta} \delta_{\gamma\phi} + \delta_{\alpha\phi} \delta_{\beta\gamma} \delta_{\delta\epsilon} + \delta_{\alpha\phi} \delta_{\beta\delta} \delta_{\gamma\epsilon} \}.\end{aligned}$$

REFERENCES

- [1] BHAGAVANTAM, S., 1942, *Scattering of Light and the Raman Effect* (Brooklyn).
- [2] BUCKINGHAM, A. D., and STEPHEN, M. J., 1957, *Trans. Faraday Soc.*, **53**, 884.
- [3] BUCKINGHAM, A. D., 1957, *Proc. phys. Soc. Lond. B*, **70**, 753.
- [4] BUCKINGHAM, A. D., and POPPLE, J. A., 1955, *Proc. phys. Soc. Lond. A*, **68**, 905.
- [5] HELLER, W., 1942, *Rev. mod. Phys.*, **14**, 390.

Paramagnetic resonance in phosphorescent aromatic hydrocarbons. II: Determination of zero-field splitting from solution spectra

by M. S. DE GROOT and J. H. VAN DER WAALS
Koninklijke/Shell-Laboratorium, Amsterdam

(Received 16 November 1959)

Electron paramagnetic resonance spectra are given of glassy solutions of triphenylene, 1, 3, 5-triphenylbenzene, coronene and naphthalene excited into their lowest triplet state by ultra-violet irradiation at liquid-nitrogen temperature. For each substance two spectra were measured: one with the r.f. magnetic field parallel to the constant field, the other with the fields at right angles.

A method is suggested for analysing the spectra of those molecules having a trigonal symmetry axis and values of the zero-field splitting parameter are derived. A complete treatment for molecules of lower symmetry has not been given, but it is shown that our results on a glassy solution of naphthalene are in agreement with those obtained by Hutchison and Mangum with single crystals.

1. INTRODUCTION

In 1958 Hutchison and Mangum [1] succeeded to show e.p.r. absorption of the lowest triplet (phosphorescent) state of naphthalene in single crystals of a solid solution of naphthalene in durene. The spectra obtained by these authors are due to transitions between neighbouring sub-levels of the triplet and from their results it is apparent that the anisotropy of these transitions is so great that no measurable e.p.r. signal can be expected from a sample of randomly oriented naphthalene molecules as occur in the glassy solutions normally used in phosphorescence studies.

Further work on naphthalene [2] has led to the conclusion that the transition between the highest and the lowest sub-levels of the triplet—corresponding to $\Delta m = \pm 2$ in the atomic case—also has a considerable intensity and that its anisotropy is small. It could therefore be observed in a solution of naphthalene in glycerol when this was irradiated with ultra-violet light at liquid nitrogen temperature. This result should not be specific for naphthalene but hold more generally for triplet state molecules with a zero-field splitting of the order of a few tenths of the quantum of r.f. energy used.

In the present paper experiments are reported on rigid glass solutions of phosphorescent aromatic molecules having a three- or six-fold symmetry axis. If one chooses a coordinate system with its z axis perpendicular to the plane of such a molecule, the x and y axes then belong to a degenerate representation of the point group D_3 . This implies [2] that in the absence of an external magnetic field spin-spin (or spin-orbit) interaction can only split the triplet into two components, one of which remains degenerate. For molecules with a trigonal axis the zero-field splitting is thus defined by a single energy difference, the value of which can be easily derived from a solution spectrum.

The general case of molecules of lower symmetry, where the zero-field splitting is defined by two parameters, will not be considered in detail. In principle, values of both these parameters can still be derived from suitable solution spectra, but this would involve a laborious numerical analysis. An approximate value of one of the parameters, however, can again be obtained in a simple manner.

2. EXPERIMENTAL

A Varian V-4500 e.p.r. spectrometer was used. Two spectra were recorded of each sample: the first with the r.f. magnetic field parallel to the constant field and the second with both fields perpendicular to each other. The 'parallel' spectra were obtained with the arrangement described earlier and at a frequency of 9422 Mc s. The 'perpendicular' spectra were obtained in the same way except that the reflection cavity was replaced by a similar one having a different (i.e. normal) orientation relative to the constant field and operating at 9387 Mc/s.

Alphanol 79, a commercially available mixture of primary alkanols containing seven to nine carbon atoms was used as a solvent. At room temperature this is a rather viscous liquid in which many organic compounds are reasonably soluble; on cooling it readily forms a glass. The ultra-violet light absorption of this solvent, though being small down to 2500 Å, could be reduced somewhat by hydrogenation at 100°C with Raney nickel as a catalyst.

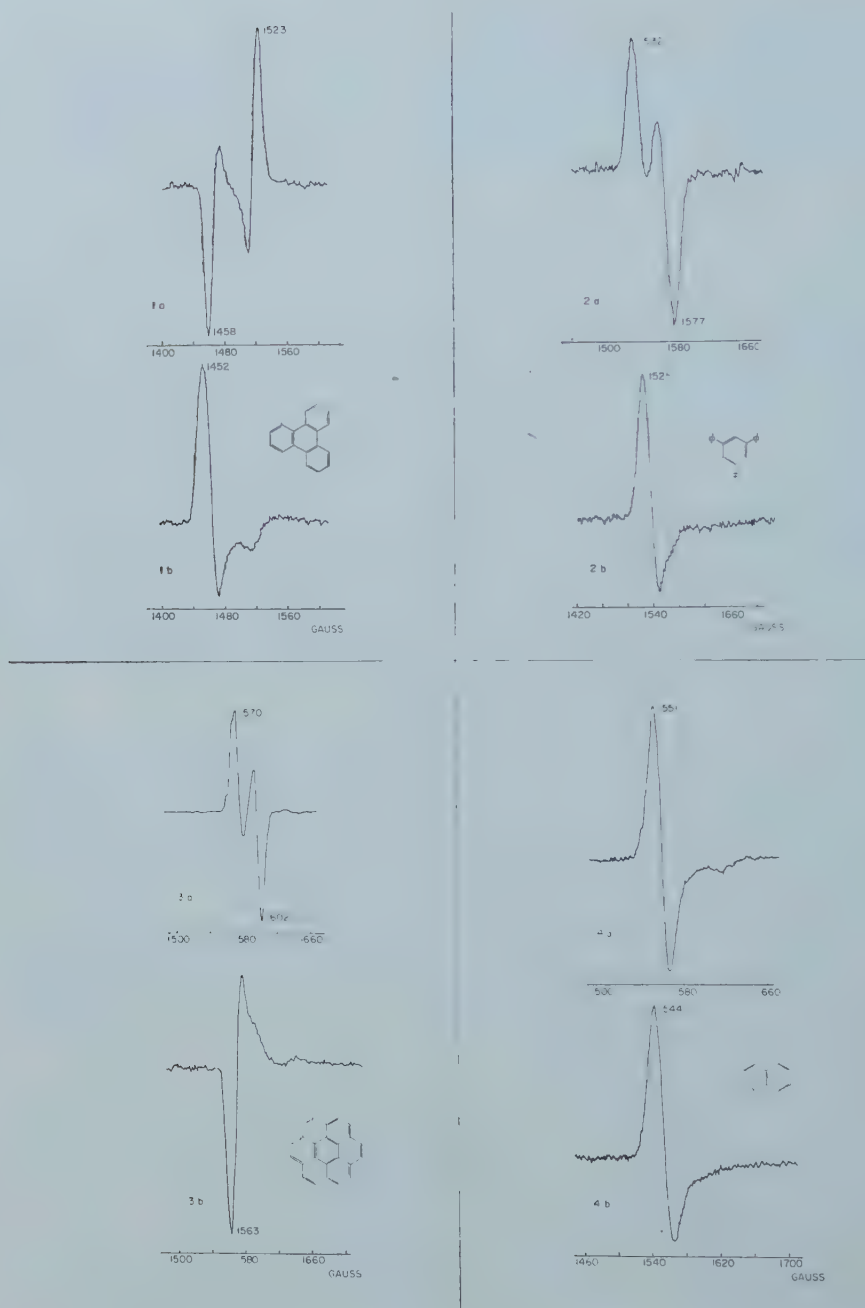
Dilute solutions of polynuclear aromatic hydrocarbons in Alphanol 79 were contained in thin-walled quartz tubes of 3.0–3.5 mm diameter. These sample tubes were placed in a slightly wider vacuum-jacketed quartz tube which passed through the cavity. As before, nitrogen gas, at liquid nitrogen temperature, was introduced as a cooling agent. No optical filter was employed after preliminary experiments had shown this to be unnecessary.

Figures 1–4 show the electron spin resonance spectra in derivative form recorded for glassy solutions of triphenylene, 1, 3, 5-triphenylbenzene, coronene and naphthalene when irradiated with ultra-violet light at liquid-nitrogen temperature. Decay times for the disappearance of the signals when the light was switched off are given in table 1.

Solute	Concentration, mole/1000 g solution	Decay time, seconds
Triphenylene	0.0043	13.3
1, 3, 5-Triphenylbenzene	0.0018	5.1
Coronene	0.0008	7.9
Naphthalene	0.0159	3.0

Table 1. Decay time of electron paramagnetic resonance signal for solutions in Alphanol 79 at liquid-nitrogen temperature.

It may be mentioned at this point that boric acid glass is not suitable for this type of experiment. Aromatic hydrocarbons dissolved in it rapidly produce coloured products when irradiated with ultra-violet light.



Figures 1-4. Spectra of rigid glass solutions of phosphorescent polyaromatic hydrocarbons (derivative of absorption line; modulation 400 c/s, 7-12 gauss).

Upper curves (a): $H_1 \parallel H$, frequency 9422 Mc/s.

Lower curves (b): $H_1 \perp H$, frequency 9387 Mc/s.

- | | |
|----------------------------|---------------------|
| 1. Triphenylene, | 0·0043 mole/1000 g. |
| 2. 1,3,5-Triphenylbenzene, | 0·0018 mole/1000 g. |
| 3. Coronene, | 0·0008 mole/1000 g. |
| 4. Naphthalene, | 0·0159 mole/1000 g. |

3. DISCUSSION

3.1. Molecules with a threefold (or higher) symmetry axis

The parallel spectra of figures 1–3 are mutually very similar, and so are the perpendicular spectra. But, whereas the former on integration render a roughly symmetrical resonance doublet, the latter correspond to a single asymmetrical line. This is illustrated by figure 5 in which the full curves are the absorption lines for triphenylene, as derived from figure 1 by graphical integration.

For a given molecule the value of the magnetic field at which resonance occurs depends on its orientation relative to the field. In order to explain a solution spectrum as shown in figure 5 one has to perform an integration over all possible orientations of the phosphorescent molecules. When one restricts oneself to the case of molecules with a three-fold (or higher) axis this can be done in the following manner.

For phosphorescent naphthalene Hutchison and Mangum could interpret their results with the spin Hamiltonian

$$\mathcal{H} = g\beta \mathbf{H} \cdot \mathbf{S} + DS_z^2 + E(S_x^2 - S_y^2). \quad (1)$$

The constants D and E determine the zero-field splitting and g was reported to be equal to 2.0140.

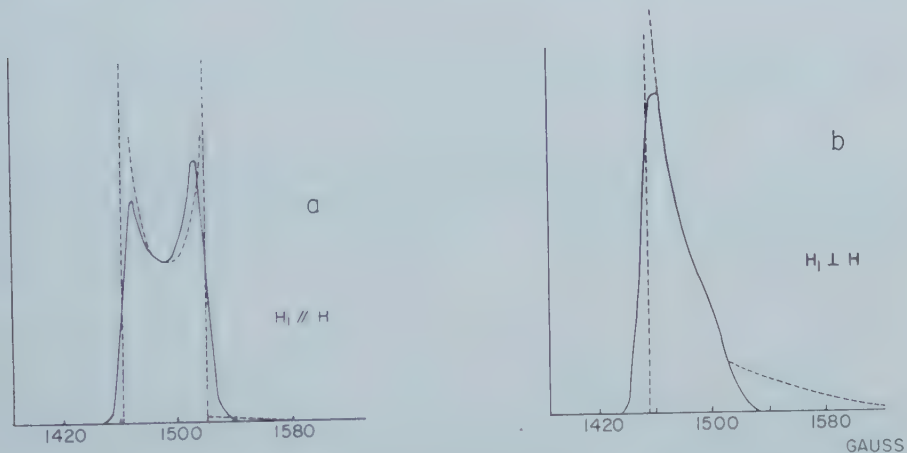


Figure 5. E.P.R. absorption curves of a glassy solution of triphenylene.
— experimental results obtained by integration of the spectra of figure 1.
- - - theoretical results following from equation (15).

In molecules with a trigonal axis, however, the x and y directions are physically equivalent. Hence $E=0$, and without loss of generality one may further assume that the coordinate system is chosen such that the magnetic field lies in the plane $y=0$. By substituting

$$H_x = H \sin \theta, \quad H_y = 0, \quad H_z = H \cos \theta \quad (2)$$

the spin Hamiltonian is thus reduced to

$$\mathcal{H} = g\beta H (\sin \theta S_x + \cos \theta S_z) + DS_z^2. \quad (3)$$

Although it is not necessary to choose a specific representation for the spin operators and zero-order wave functions to find the eigenvalues of \mathcal{H} , it is convenient to think in the same physical scheme as used in Part I [2]. We therefore

take again as basis a set of orthonormal triplet spin functions [3] T_x , T_y , T_z , which transform like x , y , z under the operations of the group D_3 and which obey the following relations

$$\mathbf{S}_x T_x = 0, \quad S_y T_x = -iT_z, \quad S_z T_x = iT_y, \quad (4)$$

etc. by cyclic permutation. From the definitions (4), it follows in particular that

$$\mathbf{S}^2 T_\nu = 2T_\nu \quad (\nu = x, y, z),$$

i.e. the T_ν are indeed eigenfunctions of \mathbf{S}^2 with eigenvalue $S(S+1)=2$. Substituting (4) into (3), we obtain the matrix

$$\mathcal{H} = \begin{bmatrix} D & -ig\beta H \cos \theta & 0 \\ ig\beta H \cos \theta & D & -ig\beta H \sin \theta \\ 0 & ig\beta H \sin \theta & 0 \end{bmatrix}, \quad (5)$$

with as corresponding secular equation

$$\epsilon^3 - 2D\epsilon^2 + \{D^2 - (g\beta H)^2\}\epsilon + (g\beta H)^2 D \sin^2 \theta = 0. \quad (6)$$

In the present experiments one has to deal with transitions between the highest and lowest levels of the triplet, involving a fixed quantum of r.f. energy δ . Hence, in order to explain the absorption curves of figure 5 the eigenvalues ϵ_j and eigenfunctions

$$\phi_j = \sum_\nu c_{j\nu} T_\nu \quad (\nu = x, y, z) \quad (7)$$

of (5) have to be found subject to the condition that the difference between the largest and smallest root of (6) is equal to δ ,

$$\epsilon_1 - \epsilon_3 = \delta. \quad (8)$$

When, for the moment, all line-broadening due to interaction of the electrons with nuclear moments or relaxation effects is neglected, the mathematical consequences of condition (8) are

- (a) it restricts the values of H for which resonance can occur to within a narrow range;
- (b) for a given value of H within this range it limits θ to one or two specific values.

By a combination of equations (6) and (8) and some algebra† it is found that the possible values of $\cos \theta$, i.e. orientations of the molecule for which resonance occurs at the given field H , follow from

$$\left. \begin{aligned} \cos^2 \theta(H) = & \frac{2D^3 + 9D(g\beta H)^2 \pm \{3\delta^2 - D^2 - 3(g\beta H)^2\} \sqrt{[-3\delta^2 + 4D^2 + 12(g\beta H)^2]}}{27D(g\beta H)^2} \\ & 0 \leq \cos \theta \leq 1. \end{aligned} \right\} (9)$$

† Equation (9) is obtained in the following manner. By first substituting $\epsilon = \epsilon_1$ into (6) and subsequently $\epsilon = \epsilon_1 - \delta$ one gets a pair of equations, which on subtraction from one another yield:

$$3\delta\epsilon_1^2 - (3\delta^2 + 4D\delta)\epsilon_1 + \delta^3 + 2D\delta^2 + \{D^2 - (g\beta H)^2\}\delta = 0.$$

The roots of this equation are given by

$$\epsilon_1 = \frac{1}{6} \{3\delta + 4D \pm \sqrt{(-3\delta^2 + 4D^2 + 12(g\beta H)^2)}\}. \quad (10)$$

For resonance ϵ_1 must be a root of the secular equation (6) as well as obey (10), which followed from the condition (8). By eliminating $\epsilon = \epsilon_1$ from (6) and (10) one thus obtains (9).

In figure 6 the values of $\cos \theta$ following from (9) have been plotted as a function of $g\beta H/\delta$ and for different values of the ratio D/δ . It is seen that for zero-field splittings $D < \frac{3}{4}\delta$ the function $\cos \theta(H)$ is not uniquely defined in a certain region of field strengths, but possesses two distinct values. The constant D is assumed to be positive; its sign cannot be determined in the present type of experiment.

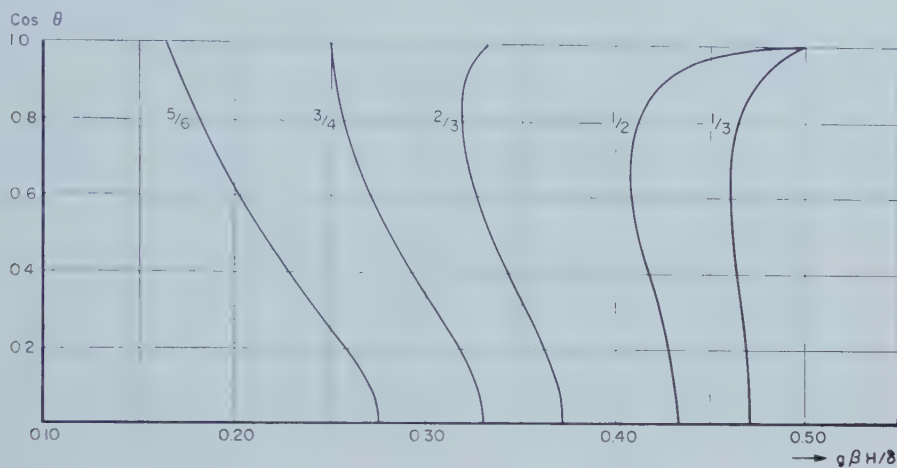


Figure 6. Graphical representation of $\cos \theta(H)$ according to equation (9) as a function of $g\beta H/\delta$. The curves have been labelled with the values of the ratio D/δ .

Suppose we now consider a triplet molecule in a suitable field H , so oriented that the angle $\theta(H)$ between the field and the molecular z axis obeys equation (9). In this situation the molecule has three stable eigenstates characterized by the eigenenergies $\epsilon_1 \geq \epsilon_2 \geq \epsilon_3$ and eigenvectors

$$\mathbf{C}_j = \begin{bmatrix} c_{jx} \\ c_{jy} \\ c_{jz} \end{bmatrix}, \quad j = 1, 2, 3.$$

These energies and vectors—all of which are functions of H and $\theta(H)$ —can be numerically calculated in the usual way from (5)–(7).

Under the influence of an r.f. field with energy quanta δ , transitions between the states $1 \leftrightarrow 3$ can be induced in the molecule. The relative transition probability for these magnetic dipole transitions is given by

$$B_R = \sum_{v=x, y, z} \gamma_v^2 |\langle \phi_1 | S_v | \phi_3 \rangle|^2, \quad (11)$$

in which $\gamma_x, \gamma_y, \gamma_z$ are the direction cosines of the r.f. magnetic field relative to the molecular axes. For an r.f. magnetic field parallel to the constant field (2) one has in particular

$$B_{||} = \sin^2 \theta |\langle \phi_1 | S_x | \phi_3 \rangle|^2 + \cos^2 \theta |\langle \phi_1 | S_z | \phi_3 \rangle|^2; \quad (12)$$

whilst for the average transition probability in r.f. magnetic fields perpendicular to (2) one obtains

$$B_{\perp} = \frac{1}{2} \{ \cos^2 \theta |\langle \phi_1 | S_x | \phi_3 \rangle|^2 + |\langle \phi_1 | S_y | \phi_3 \rangle|^2 + \sin^2 \theta |\langle \phi_1 | S_z | \phi_3 \rangle|^2 \}. \quad (13)$$

It may be noted, that once the eigenvectors \mathbf{C}_1 and \mathbf{C}_3 are known for the given values of H and $\theta(H)$, the calculation of the matrix elements occurring in (12) and (13) is an easy matter. By virtue of (4) and (7) one simply has

$$\langle \phi_1 | \mathbf{S} | \phi_3 \rangle = -i(\mathbf{C}_1 \times \mathbf{C}_3). \quad (14)$$

By way of illustration figure 7 gives a graphical representation of the results of some numerical calculations which are thought to be representative for our experiments on triphenylene. In this figure the function $\cos \theta(H)$ following from (9) and the two transition probabilities $B_{\parallel}(H)$ and $B_{\perp}(H)$ have been plotted as a function of H and for the parameter values (energies are expressed in cm^{-1} by leaving out a factor hc):

$$g = 2.0023 \text{ (spin-only value, i.e. } g\beta = 0.9351 \times 10^{-4} \text{ cm}^{-1} \text{ gauss}^{-1}),$$

$$D = 0.134 \text{ cm}^{-1},$$

$$\delta = 0.3143 \text{ cm}^{-1} \quad (\nu = 9422 \text{ Mc/s}).$$

In those regions of the variable H where the function $\cos \theta(H)$ is two-valued, the functions $B_{\parallel}(H)$ and $B_{\perp}(H)$ also are two-valued.

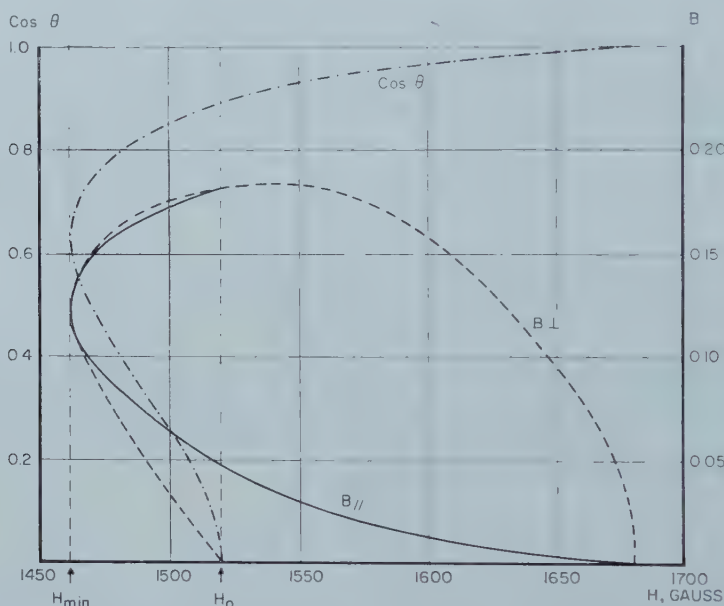


Figure 7. Graphical representation of the expressions for $\cos \theta$ (9), and for the transition probabilities B_{\parallel} (12) and B_{\perp} (13) as a function of magnetic field strength.

$$g = 2.0023, D = 0.134 \text{ cm}^{-1} \text{ and } \delta = 0.3143 \text{ cm}^{-1}.$$

The results obtained thus far hold for a single molecule of known orientation; we now have to average over all possible orientations. In a random solution the number of molecules having azimuthal angles between θ and $\theta + d\theta$, is proportional to $\sin \theta d\theta$. Hence, the relative intensity of the e.p.r. absorption between the fields H and $H + dH$ must be equal to

$$dI = \sum_{\theta} B(H, \theta(H)) \sin \theta(H) \left| \frac{d\theta(H)}{dH} \right| dH,$$

where the summation is over one or two possible values of $\theta(H)$. Expressing this result as intensity absorbed per unit of magnetic field strength one obtains:

$$\frac{dI}{dH} = \sum_{\theta} B(H, \theta(H)) \left| \frac{d\cos \theta(H)}{dH} \right|. \quad (15)$$

For the present type of molecules (D/δ well below $\frac{3}{4}$) the derivative $d \cos \theta/dH$ according to figures 6 and 7 becomes infinite for two values of H . Firstly, for the lower limiting value of H at which resonance can occur (H_{\min}) and, secondly, for the field H_0 at which $\cos \theta(H_0) = 0$. In the former singularity both dI_{\parallel}/dH and dI_{\perp}/dH tend to infinity, whereas in the latter singularity dI_{\parallel}/dH becomes infinite but the contribution to dI_{\perp}/dH can be shown to go to zero. These infinities, of course, arise owing to the fact that all sources of line-broadening have been neglected, but the maxima they represent are thought to give rise to the two peaks of figure 5 (a) and the single peak of figure 5 (b).

For triphenylene we calculated the e.p.r. absorption curves that must be expected according to (15); the results have been indicated by the dotted lines in figure 5. The value $D = 0.134 \text{ cm}^{-1}$ used in our numerical calculations was chosen so as to obtain a good fit for this molecule. The characteristic features of the two experimental curves are all displayed by the theoretical model; the tails of low intensity predicted at the high field side are thought to be submerged in 'noise'.

On the basis of this agreement it is suggested that, for the molecules under consideration, values of the zero-field splitting parameter D can simply be determined by assigning the peaks in their derivative spectra which are labelled in figures 1-3 to the infinities H_{\min} and H_0 of the model. From (9) it follows that this equation has two coinciding roots (i.e. vertical tangent in figure 6) if

$$-3\delta^2 + 4D^2 + 12(g\beta H_{\min})^2 = 0$$

or

$$g\beta H_{\min}/\delta = \sqrt{\left[\frac{1}{4} - \frac{1}{3}(D/\delta)^2\right]} \quad (16)$$

provided $D/\delta < \frac{3}{4}$.

It can further be verified that

$$g\beta H_0/\delta = \frac{1}{2}\sqrt{[1 - (D/\delta)^2]} \quad (17)$$

on substitution into (9) gives a solution $\cos \theta(H_0) = 0$. The expressions (16) and (17) have been drawn as functions of D/δ in figure 8; the extra set of scales (in cm^{-1} and gauss) to the right and at the top holds for the special case that $g = 2.0023$, and $\delta = 0.3143 \text{ cm}^{-1}$ which corresponds to the frequency of the parallel spectra. By substituting the magnetic field values of the pairs of peaks of figures 1 (a) 3(a) in equations (16) and (17) one obtains the zero-field splittings recorded in table 2†. The location of the single peaks of the perpendicular spectra leads to the same results; because of the somewhat lower value of δ (0.3131 cm^{-1}) these peaks occur at slightly lower fields. It is seen that the result for triphenylene is essentially the same as that following from the much more laborious procedure required for the construction of the integrated spectra given in figure 5.

Notwithstanding numerous attempts to observe e.p.r. absorption in phosphorescent benzene, xylene or mesitylene, we have, so far, been unsuccessful. It is believed that this is due to a zero-field splitting close to, or even exceeding, the quantum of r.f. energy used in our experiments (0.3143 cm^{-1}). Even if the splitting were somewhat smaller than the experimental quantum of r.f. energy the present technique would probably fail, because of the broadness of the solution spectra predicted by figure 8 for values of D/δ exceeding about 0.6.

† Theoretical calculations of the zero-field splitting due to spin-spin interaction are in progress for the molecules listed in table 2. The calculations are similar to those reported for some related substances by Gouterman and Moffitt [4] and Hameka [5].

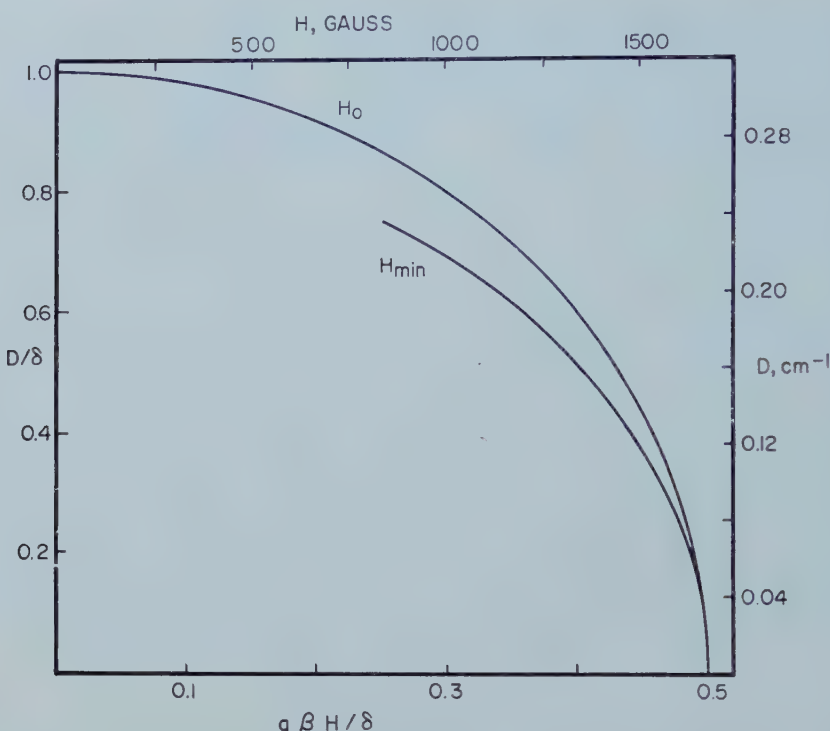


Figure 8. Graphical representation of equations (16) and (17). The extra set of scales gives the values of H_{\min} and H_0 in gauss, corresponding to the maxima in the e.p.r. absorption curves, as a function of the zero-field splitting D in cm^{-1} for $g = 2.0023$ and a radio-frequency of 9422 Mc/s.

	Orientation of $H_{\text{r.f.}}$	Peak position, gauss	Zero-field splitting D , cm^{-1}
Triphenylene		$\left\{ \begin{array}{l} H_{\min} = 1458 \\ H_0 = 1523 \end{array} \right.$	0.135
	\perp	$H_{\min} = 1452$	0.133
1, 3, 5-triphenylbenzene		$\left\{ \begin{array}{l} H_{\min} = 1532 \\ H_0 = 1577 \end{array} \right.$	0.112
	\perp	$H_{\min} = 1525$	0.109
Coronene		$\left\{ \begin{array}{l} H_{\min} = 1570 \\ H_0 = 1602 \end{array} \right.$	0.097
	\perp	$H_{\min} = 1563$	0.095
			0.097

Table 2. Values of zero-field splitting parameter D as derived from peak positions in figures 1-3 by means of equations (16) and (17); $\delta_{||} = 0.3143 \text{ cm}^{-1}$ and $\delta_{\perp} = 0.3131 \text{ cm}^{-1}$.

3.2. Molecules of lower symmetry

For molecules of lower than threefold symmetry the parameter E is no longer identically zero and the x and y axes are fixed relative to the molecular frame by the requirement that in the absence of an external field the spin Hamiltonian

has the diagonal form (1). Hence, the magnetic field \mathbf{H} can, in general, not be assumed to lie in the xz plane but must be represented by

$$H_x = H \sin \theta \cos \phi; \quad H_y = H \sin \theta \sin \phi; \quad H_z = H \cos \theta. \quad (18)$$

The mathematical consequences of these complications will not be discussed in detail, but for molecules for which both parameters D and E are appreciably smaller than δ —that is for naphthalene and probably for all other polyaromatic molecules—the picture briefly is as follows. Resonance will again be limited to a certain range of H values. For each value of H within this range ϕ can have any value, but θ is restricted by a condition similar to (9)†. That is to say that the single curve $\cos \theta(H)$ of figure 7 is now replaced by a family of curves $\cos \theta(H, \phi)$. This family has the important property that all curves have a common vertical tangent (envelope) at

$$\frac{g\beta H_{\min}}{\delta} = \sqrt{\left(\frac{1}{4} - \frac{1}{3} \frac{D^2 + 3E^2}{\delta^2}\right)}, \quad (19)$$

as well as a common end point at which $\cos \theta = 1$. The position H_0 of the other end point at which $\cos \theta = 0$ and $|d \cos \theta / dH| \rightarrow \infty$, on the contrary, depends strongly on the quantity $E \cos 2\phi$.

When we consider an integrated absorption curve the effect of this situation must be the following. The energy absorbed per unit of field strength is now proportional to

$$\frac{dI}{dH} = \int_{\phi} \sum_{\theta} B(H, \theta(H, \phi)) \left| \frac{d \cos \theta(H, \phi)}{dH} \right| d\phi. \quad (20)$$

The derivative $d \cos \theta(H, \phi) / dH$ will become infinite for $H = H_{\min}$, independent of the value of ϕ , and consequently dI/dH will tend to infinity at this point. Hence, the sharp rise at low field strength found for the solution spectra of molecules possessing a trigonal axis may be expected to occur also for molecules of lower symmetry. Again attributing the first peak in the recorded derivative spectra to this infinity, one can derive a value of

$$\sqrt{D^2 + 3E^2} = D\sqrt{1 + 3E^2/D^2} \quad (21)$$

from such a spectrum by means of (19). The respective values $H_{\min} = 1551$ and $H_{\min} = 1544$ gauss for the parallel and perpendicular spectra of naphthalene (cf. figure 4) both lead to $\sqrt{D^2 + 3E^2} = 0.1048 \text{ cm}^{-1}$. This result is in nice agreement with the value of 0.1034 cm^{-1} following from Hutchison and Mangum's experiments on oriented single crystals ($|D| = 0.1006 \text{ cm}^{-1}$, $|E| = 0.0137 \text{ cm}^{-1}$). The correction factor $\sqrt{1 + 3E^2/D^2}$ in (21), which equals 1.028 for naphthalene, may be expected to be close to unity for aromatic molecules in general.

Electron paramagnetic resonance was also found in rigid solutions of some other phosphorescent polyaromatic hydrocarbons of low symmetry. In the case of chrysene the spectra closely resemble those of figure 4 for naphthalene, but for biphenyl and fluorene the value of E/D seems to be so small that the very distinctive shape of figures 1–3 is again obtained.

† Explicitly the condition is

$27(g\beta H)^2(D - E \cos 2\phi)(\cos^2 \theta - 1) = 2D(4D^2 - 3k^2) \pm (3\delta^2 - k^2)(-3\delta^2 + 4k^2)^{1/2}$
where $k^2 = D^2 + 3E^2 + 3(g\beta H)^2$.

We are greatly indebted to Miss M. J. Wiggers de Vries and Mr. J. F. Benders for their assistance with the mathematical analysis and numerical calculations, and to Professor D. Polder for a stimulating discussion.

REFERENCES

- [1] HUTCHISON, C. A., and MANGUM, B. W., 1958, *J. chem. Phys.*, **29**, 952. (Some numerical values have been altered slightly according to a private communication from Dr. Hutchison.)
- [2] VAN DER WAALS, J. H., and DE GROOT, M. S., 1959, *Mol. Phys.*, **2**, 333. (Part 1.)
- [3] HAMEKA, H. F., and OOSTERHOFF, L. J., 1958, *Mol. Phys.*, **1**, 358.
- [4] GOUTERMAN, M., and MOFFITT, W., 1959, *J. chem. Phys.*, **30**, 1107; GOUTERMAN, M., 1959, *J. chem. Phys.*, **30**, 1369.
- [5] HAMEKA, H. F., 1959, *J. chem. Phys.*, **31**, 315.

RESEARCH NOTES

New interpretations of the orbital energy differences in hexafluorides

by CHR. KLIXBÜLL JØRGENSEN

Chemistry Department A, Technical University of Denmark, Copenhagen†

(Received 17 October 1959)

The absorption spectra of ReF_6 , OsF_6 , IrF_6 and PtF_6 were recently reported by Moffitt *et al.* [1]. The narrow bands of these gaseous compounds in the infra-red and the red were successfully interpreted by ligand field theory as due to transitions from the lowest level to the other levels of the M.O. configuration γ_5'' , assuming intermediate coupling. The table includes the values of $(3B+C)$, derived from these spin-forbidden transitions (or more exactly, the integral $K(4,5)$) if hydrogenic angular dependence [2], i.e. $l=2$ is not assumed), for a series of complexes of the 4d and 5d groups. The values of B , derived from the spin-allowed bands, and of the Landé parameter ζ_{nd} and the orbital energy difference Δ between the three equivalent γ_5 and two equivalent γ_3 orbitals, are also given.

The nephelauxetic effect [3–5] of decreased parameters of interelectronic repulsion (compared to the gaseous ion) is clearly seen to become more important with increasing oxidation number and, for a given central ion, with the ligands fluoride, chloride, and bromide. As also emphasized by Dunn [6], the inter-electronic repulsion parameters and the ζ_{nd} assume in complexes values which are close to those known from the neutral atoms. Unfortunately, the atomic spectroscopy data are very meagre for ions of the 5d group. Hence the data in the table are extrapolated from the corresponding 3d ions, assuming 0·60 times larger values of B and (somewhat less certain) 7·5 times larger values of ζ_{nd} . Only for neutral gaseous Re Trees [7] has estimated direct values. However, no doubt can be raised against a considerable decrease of $(3B+C)$ and ζ_{nd} in the gaseous hexafluorides to about half the values for the gaseous ions with the charge +6.

The present author [8] has previously predicted the band positions of several hexafluorides. Thus, IrF_6 has its narrow bands [1] at wavenumbers some 3–10 per cent higher than predicted. The broad bands in the ultra-violet occur nearly at the positions predicted for the spin-allowed ligand field transitions, having wavenumbers close to Δ . However, the present author does not agree with the latter identification except for ReF_6 , where the band groups near $32\ 500\ \text{cm}^{-1}$ presumably represent a ligand field transition (perhaps broadened by the inherent Jahn–Teller instability of the molecule).

The electron transfer bands, caused by transitions of π electrons (mainly delocalized in the ligands) to the partly filled γ_5 shell, are expected to occur at nearly the same wavenumbers as the ‘ligand field’ $\gamma_5 \rightarrow \gamma_3$ transitions in OsF_6 , IrF_6 , and at lower wavenumber in PtF_6 . When the treatment of hexahalides [9] is followed, the band positions of all the hexafluorides can be extrapolated from the band at $57\ 000\ \text{cm}^{-1}$ of WF_6 [10], assuming the parameters $D=3000$ and $E-A=9000\ \text{cm}^{-1}$. D is related to the spin-pairing energy in the central ion

† On leave as Head of the Section for Pure and Applied Science, the Office of the Science Adviser, N.A.T.O., Paris.

and $E - A$ to the decreasing energy difference between γ_5 and π orbitals for an increasing number of electrons in the partly filled shell. The values [9] for the series ReCl_6^{--} , OsCl_6^{--} , IrCl_6^{--} , is $D = 3000$ and $E - A = 6000 \text{ cm}^{-1}$. If only terms with maximum value of the seniority number are considered in the case of a d shell, D equals $\frac{5}{2}B + C$.

		$3B + C$	B	ζ_{nd}	Δ	Ref.
3d ³	Mn^{+4}	7500	1064†	400	—	[8]
	MnF_6^{---}	5400	600	—	21 800	[8]
4d ³	MoCl_6^{---}	3100	440	700	19 200	[5]
	TcCl_6^{---}	3000	—	—	—	[13]
5d	ReF_6^{--}	—	—	3400	31 000	[1]
5d ²	Os^{+6} , ext.	5500	780	(4800)	—	—
	OsF_6^{--}	2600	—	3400	—	[1]
5d ³	Re^{+4} , ext.	4500	640	(3000)	—	—
	ReF_6^{--}	3400	—	2600	31 000	[13]
	ReCl_6^{--}	2800	—	2300	27 500	[4]
	ReBr_6^{--}	2600	—	2400	—	[4]
	Ir^{+6} , ext.	5700	810	(6000)	—	—
5d ⁴	IrF_6^{--}	2200	—	3400	—	[1]
	OsCl_6^{---}	2500	—	2800	—	[4]
	OsBr_6^{--}	2300	—	2800	—	[4]
	PtF_6^{--}	1800	—	3400	—	[1]
5d ⁶	IrCl_6^{---}	—	280	(2000)	25 000	[3]
	PtF_6^{--}	—	350	—	33 000	[8]
—	Re^0	3300	480	2400	—	[7]

Parameters in cm^{-1} for the energy levels of hexahalide complexes and the gaseous ions.

ext. = extrapolated values for the gaseous ions.

† This value was erroneously given in ref. [8].

Goodman and Fred [11] assume that the orbital energy difference between γ_2 and γ_4 of 5f in NpF_6 is $21\ 350 \text{ cm}^{-1}$, explaining some bands at $23\ 000$ and $28\ 000 \text{ cm}^{-1}$. However, since UF_6 exhibits similar bands at $27\ 000 \text{ cm}^{-1}$, they must probably be described as electron transfer transitions to the 5f shell. It is interesting to see how much lower the energy is of the empty 5f shell of UF_6 than of the empty 5d shell of WF_6 . Arguments have previously been advanced [12] for the orbital energy differences being some 10–20 times smaller within the 5f shell, than in the 5d complexes.

REFERENCES

- [1] MOFFITT, W., GOODMAN, G. L., FRED, M., and WEINSTOCK, B., 1959, *Mol. Phys.*, **2**, 109.
- [2] JØRGENSEN, C. K., 1958, *Acta Chem. Scand.*, **12**, 903.
- [3] SCHÄFFER, C. E., and JØRGENSEN, C. K., 1958, *J. inorg. nucl. Chem.*, **8**, 143.
- [4] JØRGENSEN, C. K., 1958, *Disc. Faraday Soc.*, **26**, 110 and 175.
- [5] JØRGENSEN, C. K., 1960, *Absorption Spectra and the Chemical Bonding in Complexes* (London: Pergamon Press).
- [6] DUNN, T. M., 1959, *J. chem. Soc.*, p. 623.
- [7] TREES, R. E., 1958, *Phys. Rev.*, **112**, 165.
- [8] JØRGENSEN, C. K., 1958, *Acta Chem. Scand.*, **12**, 1539.
- [9] JØRGENSEN, C. K., 1959, *Mol. Phys.*, **2**, 309.
- [10] TANNER, K. N., and DUNCAN, A. B. F., 1951, *J. Amer. chem. Soc.*, **73**, 1164.
- [11] GOODMAN, G. L., and FRED, M., 1959, *J. chem. Phys.*, **30**, 849.
- [12] JØRGENSEN, C. K., 1959, *Mol. Phys.*, **2**, 96.
- [13] DUNN, T. M., and PEACOCK, R. D., private communication.

On the surface tension of regular mixtures

by A. BELLEMANS and J. STECKI†

Université Libre de Bruxelles, Belgique

(Revised MS. received 29 August 1959)

The surface tension of regular solutions was calculated by Guggenheim [1] using a monomolecular layer model. Prigogine and Defay [2] extended this treatment by considering two layers of compositions different from that of the bulk liquid. Recently one of us [3] pointed out that, in principle at least, it is not necessary to specify any layers in which the composition differs from that of the bulk phase and that the surface tension γ can directly be calculated from the free energy F (including boundary conditions) by means of the formula:

$$\gamma = \left(\frac{\partial F}{\partial A} \right)_{T, V, N_A, N_B} \quad (1)$$

(T : temperature, V : volume, A : area; N_A, N_B : numbers of molecules of species A and B). For the quasicrystalline model (regular solutions) without holes this reduces to

$$\gamma a = \left(\frac{\partial F}{\partial N_c} \right)_{T, N_A, N_B}, \quad (2)$$

where N_c is the total number of molecules in contact with the vapour phase (which we shall treat as a vacuum) and a is the area occupied by one molecule on the surface ($A = N_c a$).

The configurational partition function of a regular solution including surface effects, has been calculated by applying the expansion method of Kirkwood [4] up to second-order terms. Let z and $z(1-m)$ be respectively the number of first neighbours of a molecule in the bulk phase and on the surface; further let ϵ_{AA} , ϵ_{AB} and ϵ_{BB} be the interaction energies of neighbouring pairs AA, AB, and BB, and define:

$$w = \epsilon_{AB} - \frac{1}{2}\epsilon_{AA} - \frac{1}{2}\epsilon_{BB}. \quad (3)$$

The configurational free energy is given by

$$\begin{aligned} \frac{F}{kT} &= -\ln \sum \exp(-E/kT) \\ &= -\ln g + \frac{\langle E \rangle}{kT} - \frac{1}{2} \frac{\langle E^2 \rangle - \langle E \rangle^2}{(kT)^2} + \dots; \end{aligned} \quad (4)$$

E is the energy of a given configuration; g is equal to $N!/(N_A! N_B!)$ (N being the total number of molecules) and the brackets denote averages over all configurations. By direct counting we found

$$\langle E \rangle = \frac{1}{2}z(N - N_c m)(\epsilon_{AA}x_A^2 + 2\epsilon_{AB}x_Ax_B + \epsilon_{BB}x_B^2) + O(1/N), \quad (5)$$

† On leave of absence from the Laboratory of Physical Chemistry, University of Warsaw, Poland.

$$\langle E^2 \rangle - \langle E \rangle^2 = 2z(N - N_c m)w^2 x_A^2 x_B^2 + N_c(zm)^2 [w(x_A - x_B) + \frac{1}{2}(\epsilon_{BB} - \epsilon_{AA})]^2 x_A x_B + O(1/N), \quad (6)$$

(x_A , x_B : mole fractions of A and B).

Now γ is easily obtained from the above formulae by applying relation (2); noting that the surface tensions of pure A and B are respectively

$$\gamma_A a = -\frac{1}{2} z m \epsilon_{AA}, \quad \gamma_B a = -\frac{1}{2} z m \epsilon_{BB} \quad (7)$$

we get

$$\begin{aligned} \gamma a &= (\gamma_A x_A + \gamma_B x_B) a - zmw x_A x_B + \frac{zmw^2}{kT} x_A^2 x_B^2 \\ &\quad - \frac{1}{2kT} [(\gamma_B - \gamma_A)a + zmw(x_B - x_A)]^2 x_A x_B + \dots \end{aligned} \quad (8)$$

Incidentally the two first terms correspond to the 'dynamic' surface tension [5]. The quantity

$$\gamma^E = \gamma - x_A \gamma_A - x_B \gamma_B \quad (9)$$

which, to a certain extent, plays the rôle of an 'excess surface tension', is given by

$$\frac{\gamma^E a}{x_A x_B} = -z mw - \frac{1}{2kT} [(\gamma_B - \gamma_A)a + zmw(x_B - x_A)]^2 + \frac{zmw^2}{kT} x_A x_B + \dots \quad (10)$$

This is a particular case of a more general expression given by one of us [3] for conformal solutions. It is an exact result as far as terms of third and higher order in w and $(\gamma_B - \gamma_A)$ may be neglected.

It is interesting to compare (10) with Guggenheim's calculations [1]; by expanding his expressions up to the second order one finds

$$\frac{\gamma^E a}{x_A x_B} = -z mw - \frac{1}{2kT} [(\gamma_B - \gamma_A)a + zmw(x_B - x_A)]^2 + \dots \quad (11)$$

Comparing with (10) one sees that the monolayer model leads to a substantially correct value of γ^E up to the second order, apart from a small term

$$\frac{zmw^2}{kT} x_A^2 x_B^2$$

which is of the same magnitude as the order-disorder terms for the bulk solution.

However, this excellent agreement between (10) and (11) is not maintained for higher order terms. Preliminary calculations have shown that quite large differences already appear in third-order terms. Also the detailed structure of the lattice needs to be specified by some new parameters besides z and m .

The authors are indebted to Professor I. Prigogine for his constant interest and advice.

One of us (J. S.) is indebted to the Polish Academy of Sciences for a grant.

REFERENCES

- [1] GUGGENHEIM, E. A., 1945, *Trans. Faraday Soc.*, **41**, 150; 1952, *Mixtures* (Oxford: University Press).
- [2] PRIGOGINE, I., and DEFAY, R., 1950, *Trans. Faraday Soc.*, **46**, 199.
- [3] BELLEMANS, A., 1957, *Bull. Acad. Belg. Cl. Sci.*, **43**, 663.
- [4] KIRKWOOD, J. G., 1938, *J. chem. Phys.*, **6**, 70.
- [5] PRIGOGINE, I., and DEFAY, R., 1951, *Tension Superficielle et Adsorption* (Liège: Desoer).

Unstable intermediates

Part X. Aliphatic carbonium ions

by J. ROSENBAUM and M. C. R. SYMONS
Chemistry Department, University, Southampton

(Received 30 December 1959)

The preparation of solutions thought to contain simple aliphatic carbonium ions is described and their spectra recorded. Alternative explanations are considered, and the nature of the electronic transition is discussed.

1. INTRODUCTION

Reactions which occur between strong acids and simple aliphatic olefins, alcohols and related compounds have been reviewed recently [1, 2, 3]. Extensive study has centred on solutions in dilute aqueous acids and hardly at all on solutions in concentrated acids, probably because oxidation and polymerization may occur in the latter media.

It has been concluded that in concentrated sulphuric acid alkyl hydrogen sulphates are first formed and that the equilibrium



is the main cause of subsequent dis-proportionation, polymerization, etc. However, it has been stated that "there is no evidence which would lead us to suppose that the degree of ionization is large and it seems reasonable to presume that in every case the equilibrium lies well on the side of the un-ionized hydrogen sulphate" [2].

It has long been known that solutions of many alcohols and olefins in sulphuric acid become yellow on standing. Visible and ultra-violet spectra of concentrated solutions of certain tertiary alcohols were reported by Lavrushin [4], who found a shoulder in the $450 \text{ m}\mu$ region and a broad band at about $300 \text{ m}\mu$. A similar band at $300 \text{ m}\mu$ was reported by Gonzalez-Vidal *et al.* [5], for solutions of octene-1 in sulphuric acid. They established that sulphur dioxide and certain saturated hydrocarbons were formed under these conditions and ascribed the band at $300 \text{ m}\mu$ to unspecified oxidation products.

It has been inferred from a study of monoaryl carbonium ions [6] that, provided very dilute solutions are used and care is taken to prevent interaction between carbonium ions and uncharged solute during the process of dissolution, relatively stable solutions of these ions can be obtained. Our main aim has been to discover if aliphatic carbonium ions could be formed in detectable quantities under similar conditions.

2. EXPERIMENTAL AND RESULTS

2.1. Materials

Solvents and solutes were highest grade commercial products, further purified when necessary by standard methods and characterized by boiling or melting points and refractive indices. Sulphuric acid (98 per cent) was either 'AnalalR'

grade or further purified by distillation. Oleums were prepared as described previously [7]. 'AnalaR' grade *n*-hexane was shaken repeatedly with sulphuric acid, washed with distilled water, dried over sodium and distilled, b.p. 80–81°. *Tert.* butanol, twice distilled from anhydrous calcium sulphate, had b.p. 82° and m.p. 25·3°.

Trimethylborine was prepared by the action of methyl magnesium iodide on boron trifluoride, in a nitrogen atmosphere, according to the method of Brown [8]. The gaseous product was passed into degassed *n*-hexane, samples of which were run off periodically and their ultra-violet spectra recorded. The concentration of trimethylborine in these solutions was estimated using 1:2:5:8-tetrahydroxy-anthraquinone [9].

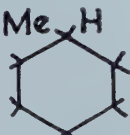
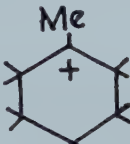
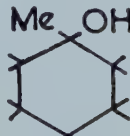
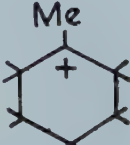
Compound	Probable ion	λ_{\max} (m μ)	$\epsilon_{\max} \times 10^3$	$\Delta H \text{ cm}^{-1}\dagger$
<i>n</i> PrOH	Me ₂ CH ⁺	296	‡	5300
<i>iso</i> -PrOH	"	291	"	"
Me ₂ C: CH ₂	Me ₃ C ⁺	291	6·0	5000
<i>n</i> -BuOH	"	290	6·4	4500
<i>iso</i> -BuOH	"	290	6·3	4800
<i>sec</i> .BuOH	"	292	6·1	4900
<i>tert.BuOH</i>	"	293	6·4	4800
Me ₃ CCl	"	292	6·3	4600
Me ₃ CBr	"	292	6·3	4400
Me ₃ COAc	"	293	6·4	4700
Me ₂ C: CHMe	Me ₂ C ⁺ Et	295	2·4	5100
Me ₂ C(OH)Et	"	296	2·8	5200
CH ₂ =C·Et ₂	MeC ⁺ Et ₂	297	2·1	5000
		293	5·1	5100
		293	4·9	6000
Et ₃ COH	Et ₃ C ⁺	298	4·4	5200
		300	4·9	4400
Me ₃ C: CH: CMe ₂	Me ₃ C ⁺	292	10·4	5500

Table 1. Details of the ultra-violet absorption spectra of carbonium ions in sulphuric acid.

† Total band width at half height.

‡ About 500 in 100 per cent sulphuric acid, and strongly dependent on acidity.

2.2. Preparation of solutions

The reactants used were olefins and their corresponding alcohols and halides (see table 1). The procedure for preparing stable solutions in sulphuric acid was as described earlier [6], that involving preliminary solution in acetic acid being the most satisfactory. Concentrations were generally less than 10^{-3} M, and were estimated by direct weighing for alcohols and halides. Stock solutions of olefins in acetic acid were treated with an excess of a standardized solution of bromine in acetic acid and the decrease in optical density at $407\text{ m}\mu$ was used to estimate the olefin concentration.

2.3. Spectrophotometric measurements

These were made using a Unicam S.P. 500 quartz spectrophotometer and S.P. 700 recording spectrophotometer, pure solvents being used for reference. When possible stoppered cells were used.

For most olefins, spectra were recorded with freshly prepared solutions, and showed no change over a period of days. In contrast, the $293\text{ m}\mu$ band rapidly increased in intensity for alcohols and alkyl halides but remained constant after about three days. The results recorded in table 1 relate to solutions for which spectra were invariant.

Within experimental error, the spectra from $\text{Me}_2\text{C}:\text{CH}_2$, the four butanols, Me_3CCl , Me_3CBr and Me_3COAc were identical: in other cases the olefins and their corresponding alcohols gave the same spectra. The bands from the butanols were fully developed after a few hours. In contrast, several weeks were required before the band was developed from *sec.* butyl chloride.

Propyl compounds behaved erratically. A band at about $296\text{ m}\mu$ developed from solutions of the alcohols at rates comparable with the butanols. The apparent extinction coefficient was strongly dependent upon acidity and was not very reproducible. Extinction coefficients as high as 2.2×10^3 were obtained using dilute oleums. *Iso*-propyl chloride gave no band in the $296\text{ m}\mu$ region after several weeks in sulphuric acid.

Di-iso-butylene was the only olefin studied whose spectrum changed with time. Initially an extinction coefficient of 5.0×10^3 was calculated, which increased quite rapidly to 10.4×10^3 .

2.4. Spectrum of trimethylborine

In early work, solutions in hexane, prepared as described above, had an intense band with a maximum at $260\text{ m}\mu$ [10]. However, it was found that in the presence of oxygen this band increased in intensity, and further study showed that, despite care taken to exclude air during preparation, this band was due to some oxidation product. Very scrupulous removal of oxygen from the solvent and exclusion of air during the preparation and spectral measurements gave solutions whose spectra showed that trimethylborine itself has no peak at $260\text{ m}\mu$. These spectra are characterized by intense absorption in the 200 – $220\text{ m}\mu$ region and the shape of the curve suggests that there is a maximum at wavelengths just below $200\text{ m}\mu$. This result is in accord with unpublished results of Dr. John Murrell, who measured the spectrum of trimethylborine in the gas phase. It is also in agreement with the results of Davies *et al.* on more complex trialkylborines [11].

2.5. Spectra of concentrated solutions

Spectra of solutions more concentrated than about 10^{-3} M changed markedly with time, and in general, a new band in the $350\text{ m}\mu$ region appeared. Sometimes a hydrocarbon layer separated on standing. A typical spectrum is shown in figure 3. Matsen *et al.* have shown that under these conditions sulphur dioxide is formed [5].

2.6. Dependence on acidity

Solutions of *tert.* butanol in sulphuric acid were stored until their ultra-violet spectra were invariant. Aliquots were diluted with aqueous sulphuric acids and the composition of the resulting solutions determined by measuring their densities and comparing with standard tables. The spectra of these solutions were measured, and the results are recorded in figure 4, as a plot of the acidity function H_0 against $\log Q$, where Q is defined by equation 2 [12]:

$$Q = \frac{[\text{carbonium ion}]}{[\text{olefin}]} = \frac{\epsilon_{\text{exp}}}{\epsilon_{\text{max}} - \epsilon_{\text{exp}}} \quad (2)$$

(ϵ_{exp} is the apparent extinction coefficient at $293\text{ m}\mu$ at a given value of H_0 , and ϵ_{max} is the extinction coefficient in 98% sulphuric acid).

Although there is considerable experimental error, the results follow a line having unit slope fairly closely. This is a necessary property of an equilibrium involving proton transfer but not of one involving hydration. The spectra of solutions in dilute aqueous sulphuric acid were transparent above $210\text{ m}\mu$, but reacidification with concentrated sulphuric acid resulted in an immediate and quantitative reappearance of a band at $293\text{ m}\mu$.

2.7. Other solvents

Addition of dilute oleum to solutions of *tert.* butanol in sulphuric acid did not alter their spectra. Solutions in perchloric acid (72 per cent w.w.), methanesulphonic, and trifluoroacetic acids also gave bands at $293\text{ m}\mu$ but in the last two

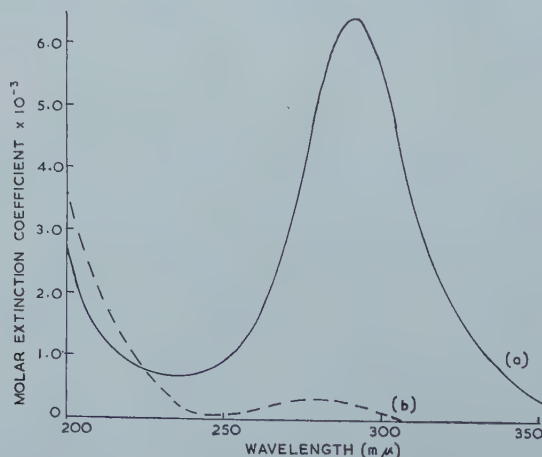


Figure 1. Absorption spectrum of (a) *tert.* butanol, and (b) sulphur dioxide in 98 per cent sulphuric acid.

solvents the rate of growth was slow and the apparent extinction coefficients were smaller than usual.

2.8. Possibility of oxidation

If the postulate that this band is a property of carbonium ions is wrong, then the most probable alternative is that it is due to an oxidation product. This could have been formed by direct oxidation by solvent to give sulphur dioxide, by reaction with dissolved oxygen, or by disproportionation, such as that shown in equation (3):



Accordingly, we have endeavoured to develop sensitive methods for the detection of sulphur dioxide in sulphuric acid. The reaction rate for *tert.* butanol has been measured in the absence of oxygen, and the behaviour of saturated hydrocarbons in sulphuric acid has been studied. In addition, a wide range of the more simple possible oxidation products in sulphuric acid have been studied by spectrophotometry.

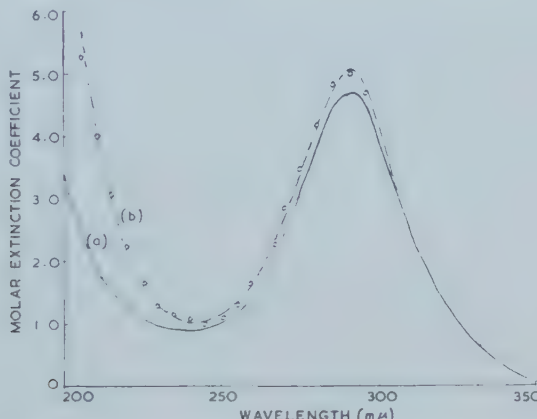


Figure 2. Absorption spectrum of (a) 1-methyl-cyclo-hexane-1-ol and (b) methyl-cyclohexane in 98 per cent sulphuric acid. The circles represent points calculated by the addition of curve (b) figure 1 to curve (a) figure 2.

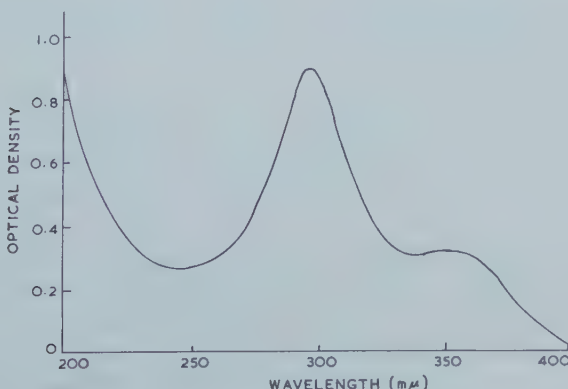


Figure 3. Absorption spectrum of *tert.* butanol (10^{-2} M) in 98 per cent sulphuric acid.

Methyl-*cyclo*-hexane (spectrograde), dissolved in sulphuric acid by the procedures developed earlier [6], reacted slowly to give a product whose spectrum was identical with that for 1-methyl-*cyclo*-hexane-1-ol except that in the 220 m μ region, the long wavelength edge of an intense band was detected (figure 2). A reconstruction of this spectrum by addition of the spectra of sulphur dioxide and 1-methyl-*cyclo*-hexane-1-ol in sulphuric acid is also shown in figure 2, from which it may be seen that about one equivalent of sulphur dioxide was formed during the reaction. If the reaction is written as



then there should be a one to one equivalence between the number of moles of carbonium ion and sulphur dioxide formed.

As a further check on the possibility that sulphur dioxide is formed, solutions obtained from methyl-*cyclo*-hexane and *tert.* butanol were treated with an excess of a solution formed by reaction between iodine and iodic acid in sulphuric acid. These brown solutions, thought to contain the tri-iodide positive ion [13, 14] react slowly with sulphur dioxide in sulphuric acid, with liberation of iodine. Iodine was only precipitated from solutions derived from methyl-*cyclo*-hexane, thus further establishing that sulphur dioxide is not a product of the reaction between sulphuric acid and tertiary alcohols.

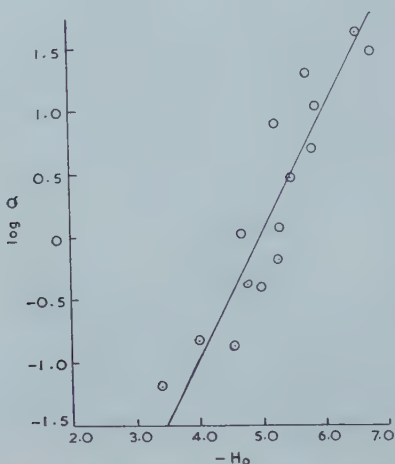


Figure 4. The concentration of trimethylcarbonium ions as a function of acidity. Q is defined in the experimental section: H_0 is the Hammett acidity function. The straight line is drawn with unit slope.

To check the possibility that oxygen was involved, solutions of *tert.* butanol were de-gassed by repeated partial freezing and warming under high vacuum. The rate of build up of the 293 m μ band was identical with that found under ordinary conditions.

Had a disproportionation occurred, such as that shown in equation (3), our results with methyl-*cyclo*-hexane establish that the *iso*-butane formed would be reoxidized by the solvent. Since sulphur dioxide would then be a product, this reaction can also be eliminated.

Solutions of a wide range of possible oxidation products in sulphuric acid have been studied spectrophotometrically in an endeavour to discover what product

might have a band at $293 \text{ m}\mu$. These included 2-methyl propane, -1, 2-diol, 2-methyl allyl alcohol; *iso*-butyric acid, 2-hydroxy-*iso*-butyric acid, acetone and acetic acid. Solutions of these compounds in sulphuric acid prepared by our procedure had spectra from which the $293 \text{ m}\mu$ band was completely absent. Some of these spectra were of considerable interest and will be the subject of a subsequent paper. The spectrum of acetone in aqueous acids is discussed by Nagakura, Minegishi and Stanfield [15], who found that in concentrated sulphuric acid condensation occurred. Dilute solutions prepared as above showed no evidence of condensation, the salient feature being a rising absorption below $230 \text{ m}\mu$. Dilute solutions of the carboxylic acids listed above were transparent above $210 \text{ m}\mu$, as also was acetic anhydride. (Since the latter is thought to be converted into the ion MeCO^+ under these conditions this result suggests that MeCO^+ has no absorption band in the near ultra-violet region.)

Since side reactions occur in solutions more concentrated than 10^{-3} M , it was considered impracticable to isolate reaction products after dilution with water.

2.9. Reaction rates

The band at $293 \text{ m}\mu$ developed at a measurable rate with alcohols and certain alkyl halides. An approximate measure of the rate of formation of the compound responsible for this band was obtained in the following way. Solutions in sulphuric acid preheated to 25° were prepared by procedures 1 (*a*) or 1 (*b*) of [6] as rapidly as possible, and transferred to a stoppered 1 cm cell contained in a cell housing thermostated at 25° . Optical densities at the peak position were measured periodically and the final, constant value ($O.D._\infty$) was used to obtain the first-order rate constant from a plot of $\log(O.D._\infty - O.D._t)$ against time t . It was established that solvent cyclohexane gave no band in the 200 – $300 \text{ m}\mu$ region under these conditions. However, when procedure 1 (*a*) was used the solutions were cloudy and it was necessary to de-gas the solutions by partial freezing under high vacuum to remove the solvent. A typical plot is shown in figure 5, and the results summarized in table 2.

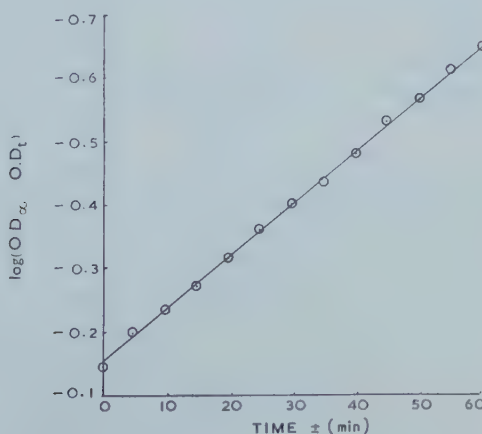


Figure 5. The rate of growth of the absorption band at $293 \text{ m}\mu$ at 25° .

3. DISCUSSION

3.1. Nature of the species having an absorption band at 293 m μ

Since solutions of both methanol and ethanol in 98 per cent sulphuric acid are transparent above about 200 m μ , the 293 m μ band cannot be ascribed to alkyl hydrogen sulphates, which are formed under these conditions. Also, since methyl sulphonic acid has no absorption in this region, it is unlikely that alkyl sulphonate acids are responsible. There is no apparent reason why alkyl oxonium ions, such as Me₃COH₂⁺ should absorb in the near ultraviolet region, and since solutions of *tert.* butanol have no absorption in this region at zero time but have an extrapolated *i* factor of two at zero time [16], it is probable that Me₃COH₂⁺ is formed very rapidly, and is, indeed, transparent in this region.

Other than carbonium ions, it is difficult to understand what compound could be formed in sulphuric acid which has an absorption band at 293 m μ , unless it is an oxidation product, as postulated by Matsen *et al.* [5]. This has been considered in detail (§ 2.7) and we conclude that both oxidation and disproportionation are insignificant under our conditions.

The relative rates of formation from corresponding olefins, alcohols and alkyl halides are in accord with the carbonium ion postulate and detailed comparison of the rates for butyl halides with rates for S_N1 reactions of these compounds in water seem also to support the postulate (§ 3.4). The dependence upon the H₀ acidity function rather than on the J₀ function [17] suggests that the equilibrium being followed is loss of a proton to give isobutene, rather than addition of water to give the alcohol. This observation is strongly supported by the rapid reformation of the 293 m μ band on re-acidification: had alcohol or polymer been formed this should have been a slow process.

In order to utilize the results for trimethylborine, a search has been made for other compounds of similar structure, differing only in the atomic number of the central atom. A suitable series is borate, carbonate and nitrate. The first electronic absorption band for borate is well below 200 m μ , that for carbonate is at about 220 m μ and that for nitrate is in the 310 m μ region. The energy difference between the carbonate and nitrate bands is 14 000 cm⁻¹ which is close to that now postulated for trimethylborine and trimethyl carbonium ions (15 800 cm⁻¹). This comparison is only valid if the transitions involved are comparable: this is discussed in § 3.3.

Since we can discover no other explanation for the spectra reported we will assume, in the following, that our postulate is correct.

3.2. Structure and solvation of carbonium ions

Before considering the nature of the electronic transition, it seems desirable to discuss the structure of alkyl carbonium ions, and the influence of solvent on their structure.

Bethell and Gold [3] have discussed carbonium ions in terms of 'classical' and 'non-classical' bridged structures such as (1), and (2) or (3)



By analogy with trimethylborine, it seems most likely that (1) is the best representation [18], and that (2) or (3) are better described as transition states for the

rearrangement of the ion $\text{Me}_2\text{CHCH}_2^+$ to Me_3C^+ . From another viewpoint one can say that, in so far as structures such as (4) make an important contribution to the ground state of (1), the structures (2) or (3) are less probable because one only of the nine β -hydrogen atoms has been selected.

Comparison of the spectra of Me_3C^+ and Et_3C^+ shows that there is a very small shift to lower energy when methyl is replaced by ethyl. This could involve changes in either ground or excited states or both, and is too small to warrant discussion. The marked decrease in intensity when methyl is replaced by ethyl is discussed in § 3.3.

Recently, the spectrum of an ion thought to have the structure (V, R = Me) has been reported [19]:



The ultra-violet spectrum was characterized by an intense band at $295 \text{ m}\mu$ having an extinction coefficient of 7.5×10^3 , in 60 per cent sulphuric acid. The authors infer that this is the spectrum of a bridged carbonium ion (VI, R = Me). Their spectrum, however, is closely similar to that assigned to the tri-methyl carbonium ions, which suggests that, if the double bond does interact with the positive carbon, ground and excited states are equally stabilized. In view of the conclusion drawn in the next section, that the transition involves movement of electrons from methyl towards the central carbon, this coincidence would appear to be unlikely. Leal and Pettit's conclusion regarding the bridged structure is based largely on an analogy with the corresponding ion in which methyl is replaced by phenyl (V, R = Ph). The *cis*-isomer gave, in 60 per cent sulphuric acid, a spectrum closely similar to that for phenyl dimethyl carbonium ions [6], the intense band at $390 \text{ m}\mu$ assigned to the latter ions being split into a doublet at 390 and $405 \text{ m}\mu$. In this instance, the *trans* isomer was also studied, but in 60 per cent sulphuric acid, no band could be detected in the $400 \text{ m}\mu$ region. In view of the results for simple monoaryl carbonium ions [6], we conclude that the difference in behaviour of the *cis*- and *trans*-compounds is to be understood not so much in terms of delocalization of electrons and consequent spectral modification implied in the 'non-classical' structure (VI, R = Ph), but in the different reactivities expected for the two compounds. Thus, the *cis*-ion, for steric and electrostatic reasons, will not be readily protonated on the double bond, and hence dimerization or other reactions which may occur when the *trans*-compound is dissolved in 60 per cent sulphuric acid are avoided. Indeed, it is conceivable that carbonium ion formation from the *cis*-alcohol proceeds via initial protonation of the double bond followed by the formation of an internal ether.

Our results with secondary alcohols are not clear cut. Secondary butanol almost certainly rearranges to give trimethyl carbonium ions but the band at

297 m μ obtained from *isopropanol* (and from *n*-propanol after an induction period), is either due to a tertiary carbonium ion derived from a rearranged dimer or polymer, or to dimethyl carbonium ions. The marked sensitivity of the apparent extinction coefficient to change in acidity in 90–100 per cent sulphuric acid in contrast with the behaviour of trimethyl carbonium ions, is in accord with the expected increase in reactivity for secondary carbonium ions. However the proximity of the band to that found for tertiary carbonium ions is unexpected.

3.3. Nature of the electronic transition

Since neither methyl nor ethyl carbonium ions could be detected, even in 65 per cent oleum, electron release from alkyl groups must play an important role in stabilizing these ions. The conclusive proof that, in similar free-radicals, hyperconjugation is of considerable importance [20, 21] strongly suggests that it is also the main source of stability in these ions [22]. We have postulated that the electronic transition involves β -C–H bonding electrons, already delocalized by hyperconjugation, and that the transition consists of charge transfer from methyl towards the central carbon atom [10].

The shift of 15 800 cm $^{-1}$ to higher energies when carbon is replaced by boron is in accord with this description of the transition. Indeed, the energy gap is close to that between the first bands for nitrate and carbonate (see above). The transition for these ions is thought to involve transfer of electrons in non-bonding orbitals on oxygen to a π -type level largely on the central atom [23], and is thus very similar to that proposed for the carbonium ions.

A further check on the reasonableness of the assignment may be obtained by computing the energy of a cycle in which an electron is withdrawn from methyl and placed on the central carbon. This can be effected, albeit crudely, by subtracting the ionization potential for *tert.* butyl or *isopropyl* radicals from that for methane. This gives 5.57 and 5.1 ev respectively for the transition, which may be compared with the experimental value of 4.23 ev.

Muller and Mulliken have used a procedure based on the LCAO MO approximation to calculate hyperconjugation energies in alkyl radicals and carbonium ions, the very large stabilization energies found for carbonium ions being attributed to the combined effects of hyperconjugation and charge redistribution [22]. Using their model, it would seem that we are concerned with transitions involving electrons in quasi- π group orbitals having nodes in the plane of the carbon atoms. For the trimethyl carbonium ion, six π -electrons are assigned to three such orbitals, and will be largely localized on the three methyl groups, whilst the excited level will be largely localized on the central carbon, being similar to the half-filled orbital in the corresponding radical. Of the three occupied levels, one is symmetrical, and the transition would be forbidden: the other two form a degenerate pair, and it is this level that is thought to be involved in the observed transition.

Using the results of Muller and Mulliken for trimethyl carbonium ions and the corresponding radicals, we estimate a transition energy of about 3.87 ev. Again, our approach is very approximate, but the result does suggest that our assignment is reasonable.

The extinction coefficient for triethyl carbonium ions is about two-thirds that of trimethyl carbonium ions. This may be linked to the conformational requirements for suitable overlap between orbitals involved in the transition.

The small value for dimethyl ethyl carbonium ions, which has been confirmed in numerous experiments, is then anomalous, but may possibly be linked to the suggestion that the orbital involved for trimethyl carbonium ions is doubly degenerate. A change in symmetry might lift this degeneracy, but the decrease, also observed for diethylmethyl carbonium ions (table 1), is not found for methylcyclohexyl carbonium ions.

3.4. Reaction rates

Our original aim in measuring the rates of growth of the band at 293 m μ was to shed further light on the postulate that this band is due to carbonium ions, rather than to compare rates within the context of this postulate. For this reason a detailed presentation and discussion of reaction rates is deferred to a future report.

The observations that, from isobutene the band is developed within less than a minute of the time of mixing, grows according to a first-order rate law over a period of several hours from *tert.* butyl chloride and only appears at all after 24 hours for solutions of *sec.* butyl chloride, are all in qualitative accord with the carbonium ion postulate. Detailed comparison with rates reported for reactions thought to proceed by rate determining ionization of alkyl halides (S_N1 mechanism) is not possible since S_N1 reaction rates are markedly dependent upon the solvent polarity. However, some relevant data are listed in table 2, and it may be noted that the rate of hydrolysis of *tert.* butyl chloride in water is very close to the rate of growth of the band at 293 m μ in sulphuric acid. Since both water and sulphuric

Compound	Medium	Rate $\times 10^4$ sec $^{-1}$	Induction period	S_N1 rate $\times 10^4$ sec $^{-1}$
<i>n</i> -BuOH	98 per cent H ₂ SO ₄	3.1	5–10 min	
<i>iso</i> -BuOH	"	7.0	"	
<i>sec</i> .BuOH	"	3.8	Very small	
<i>tert.BuOH</i>	80 per cent H ₂ SO ₄	3.5	"	
	98 per cent H ₂ SO ₄	3.5	Nil	
	80 per cent H ₂ SO ₄	3.3	"	
<i>tert.BuCl</i>	98 per cent H ₂ SO ₄	8.0	"	13†
<i>sec</i> .BuCl	"	ca. 10 ⁻³ –10 ⁻⁴ ‡		ca. 10 ⁻⁴ ‡

Table 2. Rate constants for the formation of carbonium ions in sulphuric acid and relevant data for solvolyses.

† An approximate value based on readings taken over a period of days.

‡ The rate for *tert.* butyl chloride refers to 60 per cent aqueous ethanol (Ingold, *Structure and Mechanism in Organic Chemistry*, Bell and Sons Ltd., London, 1953, p. 349), and the rate for *sec.* butyl chloride has been estimated approximately from the rate data for the corresponding bromides in formic acid (*ibid.*, p. 321).

acid have very high dielectric constants and since the rate of growth of the band is insensitive to addition of water within the region 80–100 per cent sulphuric acid, we conclude that this close agreement is further evidence for the validity of our postulate.

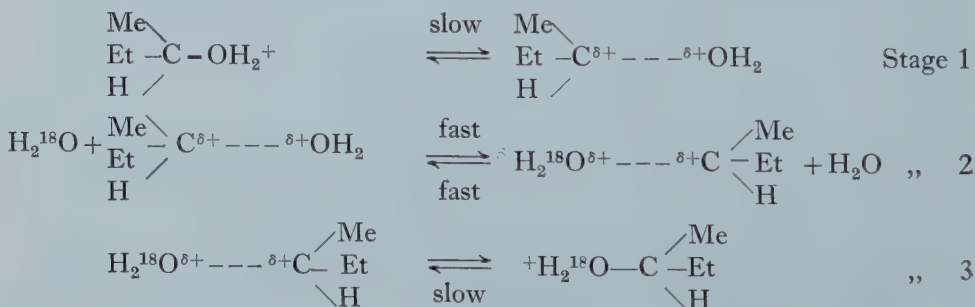
The rates of growth of the $293 \text{ m}\mu$ band from solutions of the butanols are less readily interpreted. Dostrovsky and Klein measured the rate of oxygen exchange for *tert.* butanol in dilute aqueous sulphuric acid [24], and from their data one can obtain an approximate value for the first-order rate constant assigned to reaction (5):



The value obtained is at least one-hundred fold greater than the rate constant derived from our data. To obtain this result we have used a value of -3.0 for the pK of *tert.* butanol [25]: this value is extrapolated from data for primary and secondary alcohols but it is very unlikely to be in error by as much as two pK units. The rate of growth of the band at $293\text{ m}\mu$ is almost independent of the concentration of sulphuric acid in the 80–100 per cent region but falls off rapidly at lower acidities. This result is in accord with a pK of about -3.0 for *tert.* butanol since protonation would then be effectively complete in 80 per cent sulphuric acid. If these assignments are correct it would seem that the pK value for *tert.* butanol and *isobutene* are quite similar.

The first order rate constant for *sec.* butanol is remarkably close to that for *tert.* butanol (table 2). In contrast, the rate of oxygen exchange and racemization in aqueous perchloric acid reported by Bunton *et al.* [26] is very slow compared with that of oxygen exchange for *tert.* butanol [24], though the rate still appears to be somewhat faster than we would predict from our results. It is conceivable that *sec.* butanol is converted into *sec.* butyl hydrogen sulphate by a direct displacement process prior to carbonium ion formation: this is, however, rather improbable because formation of alkyl hydrogen sulphates involves attack by the free alcohol on sulphuric acid. Under our conditions the alcohol is largely converted into its conjugate acid, ROH_2^+ , which would probably not react.

It is noteworthy that Bunton *et al.* found that each step involving oxygen exchange was accompanied by an inversion of configuration. Nevertheless, they describe the reaction as of the S_N1 type: their formulation, modified in order to comply with symmetry requirements, being



The S_N1 assignment is based largely on the observation that the rate follows Hammett's acidity function, H_0 , rather than the acid concentration. This is commonly thought to establish that a molecule of water does not enter into the kinetic expression for the rate-determining step [17], and hence they rejected the alternative that stage 2 of their mechanism was rate-determining. There are so many exceptions to this generalization that, taken alone, such evidence is not compelling [27]. If our results are correct, then it seems probable that, for

protonated alcohols, but not halides, these displacements are not S_N1 in type, and that stage 2 of the above mechanism is rate-determining. However, results over a far wider range of conditions are required before this can be verified.

3.5. Polymerization and rearrangements

The results with *di-iso* butylene give good evidence that polymerization is not an important reaction under our conditions. The 'instantaneous' build up of a band in the $293\text{ m}\mu$ region, followed by a further relatively slow growth until the apparent extinction coefficient had grown from about 5×10^{-3} to 10.4×10^3 is most readily explained by the postulate that depolymerization occurred to give, finally, two moles of *tert.* butyl carbonium ions per mole of *di-iso* butylene :



Finally, the results with *normal*, *iso*, and *sec.* butanols are best understood in terms of the postulate that, in each case, rearrangement to trimethyl carbonium ions occurs. For the two primary alcohols there is an induction period during which no absorption in the near ultra-violet can be detected: it is hoped that detailed kinetic studies will shed some light on these rearrangements.

Thanks are offered to Drs. J. Murrell and A. G. Davies for drawing our attention to their results related to trialkylborines, to Professors H. C. Longuet-Higgins, F.R.S., and R. C. Cookson for helpful discussions, and to D.S.I.R. for a maintenance grant to J. R.

REFERENCES

- [1] BURTON, H., and PRAILL, P. F. G., 1952, *Quart. Rev.*, **6**, 302.
- [2] GILLESPIE, R. J., and LEISTEN, J. A., 1954, *Quart. Rev.*, **8**, 44.
- [3] BETHELL, D., and GOLD, V., 1958, *Quart. Rev.*, **9**, 173.
- [4] LAVRUSHIN, V. F., VERKHOUD, N. N., and MOVEHAN, P. K., 1956, *J. gen. Chem., Moscow*, **26**, 3005.
- [5] GONZALEZ-VIDAL, J., KOHN, E., and MATSEN, F. A., 1956, *J. chem. Phys.*, **25**, 181.
- [6] GRACE, J. A., and SYMONS, M. C. R., 1959, *J. chem. Soc.*, 958.
- [7] SYMONS, M. C. R., 1957, *J. chem. Soc.*, 387.
- [8] BROWN, H. C., 1945, *J. Amer. chem. Soc.*, **67**, 375.
- [9] HOPKIN-WILLIAMS MONOGRAPHS: *Organic Reagents for Metals*, Vol. **1**, 139.
- [10] ROSENBAUM, J., and SYMONS, M. C. R., 1959, *Proc. chem. Soc.*, 92.
- [11] DAVIES, A. G., HARE, D. G., and LARKWORTHY, L. F., 1959, *Chem. Ind.* **48**, 1519.
- [12] DENO, N. C., JARUZELSKI, J. J., and SCHREISHEIM, A., 1955, *J. Amer. chem. Soc.*, **77**, 3044.
- [13] MASSON, I., and ARGUMENT, C., 1938, *J. chem. Soc.*, 1702.
- [14] SYMONS, M. C. R., 1957, *J. chem. Soc.*, 2186.
- [15] NAGAKURA, S., MINEGISHI, A., and STANFIELD, K., 1957, *J. Amer. chem. Soc.*, **79**, 1033.
- [16] DENO, N. C., and NEWMAN, M. S., 1949, *J. Amer. chem. Soc.*, **71**, 869.
- [17] PAUL, M. A., and LONG, F. A., 1957, *Chem. Rev.*, **57**, 935.
- [18] LEVY, H. A., and BROOKWAY, L. O., 1937, *J. Amer. chem. Soc.*, **59**, 2085.
- [19] LEAL, G., and PETTIT, R., 1959, *J. Amer. chem. Soc.*, **81**, 3160.
- [20] GIBSON, J. F., INGRAM, D. J. E., SYMONS, M. C. R., and TOWNSEND, M. G., 1957, *Trans. Faraday Soc.*, **53**, 914.
- [21] MATHESON, M. S., and SMALLER, B., 1958, *J. chem. Phys.*, **28**, 1169.
- [22] MULLER, N., and MULLIKEN, R. S., 1958, *J. Amer. chem. Soc.*, **80**, 3489.
- [23] WALSH, J. R., 1953, *J. chem. Soc.*, 2301; McCONNELL, H. 1952, *J. chem. Phys.*, **20**, 700.
- [24] DOSTROVSKY, I., and KLEIN, T. S., 1955, *J. chem. Soc.*, **791**.
- [25] BARTLETT, P. D., and MCCOLLUM, S. D., 1956, *J. Amer. chem. Soc.*, **78**, 1441.
- [26] BUNTON, C. A., KONASIEWICZ, A., and LLEWELLYN, D. R., 1955, *J. chem. Soc.*, 604.
- [27] TAFT, R. W., Jr., DENO, N. C., and SKELL, P. S., 1958, *Ann. Rev. phys. Chem.*, **9**, 287.

Nuclear magnetic shielding of a hydrogen atom in (1) an electric field-gradient and (2) a cage

by A. D. BUCKINGHAM and K. P. LAWLEY

The Inorganic Chemistry Laboratory, The University of Oxford

(Received 19 December 1959)

The ground state wave function of a hydrogen atom in an electric field-gradient \mathbf{F}' is obtained, correct to the first power in \mathbf{F}' , and the nuclear magnetic screening constant σ evaluated. The \mathbf{F}' contribution to σ vanishes if all directions of \mathbf{F}' relative to the applied magnetic field are equally probable. In part (2), the influence of a uniform compression of the H-atom on σ is examined. This effect, which will predominate at sufficiently high pressures, causes a decrease in the electronic polarizability but an increase in σ .

1. A HYDROGEN ATOM IN AN ELECTRIC FIELD-GRADIENT

The effect of a uniform electric field \mathbf{F} on the nuclear magnetic screening constant σ of an atom must, by symmetry, be proportional to \mathbf{F}^2 [1], but the contribution arising from a field-gradient \mathbf{F}' is a first order one. It is worthwhile to compare the orders of magnitude of these two effects in a well-defined case with values of \mathbf{F} and \mathbf{F}' that an atom or ion might experience in a condensed phase or in a molecule because of the presence of nearby polar groups. The problem is exactly soluble for the ground state of the H-atom (neglecting electron spin).

Let the perturbed wave function ψ be expanded as a power series in the field gradient (first subscript) and the magnetic field (second subscript)

$$\psi = \psi_{00} + \psi_{10} + \psi_{01} + \psi_{11} + \dots \quad (1)$$

where

$$(a) \quad F'_{\parallel} = F'_{zz} = -2F'_{xx} = -2F'_{yy},$$

$$(b) \quad F'_{\perp} = F'_{xx} = -2F'_{yy} = -2F'_{zz},$$

and

$$H = H_z.$$

Since we are considering an effect proportional to F' and H , only ψ_{01} , ψ_{10} and ψ_{11} will be required. It is well known that ψ_{01} is zero and since we are concerned with the ground state, $E_{10}=0$, so that ψ_{10} and ψ_{11} must satisfy the following differential equations [2]

$$(H_{00} - E_{00})\psi_{10} + H_{10}\psi_{00} = 0, \quad (2)$$

$$(H_{00} - E_{00})\psi_{11} + H_{01}\psi_{10} = E_{11}\psi_{00}, \quad (3)$$

where

$$H_{00} = -\left(\frac{\hbar^2}{2m}\right)\nabla^2 - e^2/r,$$

$$E_{00} = -e^2/2a, \quad E_{11} = 0,$$

$$(a) \quad \psi_{00} = \exp(-r')$$

$$H_{10} = \frac{er'^2}{4} (3 \cos^2 \theta - 1) F_{\parallel}'$$

$$(b) \quad H_{10} = \frac{er'^2}{4} (3 \sin^2 \theta \sin^2 \phi - 1) F_{\perp}'$$

$$H_{01} = -i(\hbar e/2mc) \mathbf{H} \frac{\partial}{\partial \phi}$$

and $r' = r/a$ (a is the Bohr radius $= h^2/e^2m$) and θ is the angle between the radius vector of the electron and the direction of the magnetic field. In (a) the axis of symmetry of the field gradient is parallel, and in (b) perpendicular, to \mathbf{H} .

The solutions of equation (2) are

$$\psi_{10}^{(a)} = -\frac{1}{8}(a^3/e)r'^2(1 + \frac{2}{3}r')(3 \cos^2 \theta - 1)F_{\parallel}' \exp(-r'), \quad (4a)$$

$$\psi_{10}^{(b)} = -\frac{1}{8}(a^3/e)r'^2(1 + \frac{2}{3}r')(3 \sin^2 \theta \sin^2 \phi - 1)F_{\perp}' \exp(-r'). \quad (4b)$$

The diamagnetic screening constant σ^d is given by [3, 1]

$$\sigma^d = \frac{e^2}{2mc^2 a} \int \sin^2 \theta r'^{-1} \psi^* \psi d\tau / \int \psi^* \psi d\tau. \quad (5)$$

Thus (4a) and (4b) lead to

$$\sigma_{\parallel}^d = \frac{e^2}{3mc^2 a} \left[1 + \frac{7}{20} \frac{a^3}{e} F_{\parallel}' \right], \quad (6a)$$

$$\sigma_{\perp}^d = \frac{e^2}{3mc^2 a} \left[1 - \frac{7}{40} \frac{a^3}{e} F_{\perp}' \right]. \quad (6b)$$

The paramagnetic screening constant σ^p is given by (see, for example, [1])

$$\sigma^p = \frac{e\hbar}{2mc i H} \int \left(\psi^* \frac{\partial \psi}{\partial \phi} - \psi \frac{\partial \psi^*}{\partial \phi} \right) r^{-3} d\tau / \int \psi^* \psi d\tau \quad (7)$$

and is related to the hindering of the free precession of the electrons about \mathbf{H} . Thus $\sigma_{\parallel}^p = 0$, and to the first order in F' ,

$$\sigma_{\perp}^p = \frac{e\hbar}{mc i H} \int \psi_{00} \frac{\partial \psi_{11}}{\partial \phi} r^{-3} d\tau / \int \psi_{00}^2 d\tau. \quad (8)$$

From (3) and (4b)

$$\psi_{11} = -\frac{i}{16} \left(\frac{a^5}{hc} \right) r'^2 \left(\frac{13}{2} + \frac{13}{3}r' + r'^2 \right) \exp(-r') \sin^2 \theta \sin \phi \cos \phi H F_{\perp}'. \quad (9b)$$

On substituting (9b) into (8), it is found that σ_{\perp}^p is zero to the first order in \mathbf{F}' .

Thus, from (6a, b), the \mathbf{F}' contribution to the magnetic shielding of an atom in an environment where the axis of the field gradient is randomly orientated with respect to the fixed magnetic field (as for the intramolecular field-gradient in a freely rotating molecule or ion pair) is

$$\sigma_{F'} = \frac{1}{3}(\sigma_{\parallel}^d + 2\sigma_{\perp}^d) = 0. \quad (10)$$

For an H-atom distant r' atomic units from a singly charged positive ion, the ratio of the \mathbf{F}' contribution to σ_{\parallel} to that proportional to \mathbf{F}^2 (see [1]) is

$$\frac{\sigma_{F'}}{\sigma_{F^2}} = \frac{\frac{7}{10} r'^{-3}}{\frac{439}{40} r'^{-4}} = \frac{28}{439} r'.$$

Thus, the field-gradient effect, although of the first order, will normally be negligible compared to the second order \mathbf{F}^2 effect whenever \mathbf{r}' is small enough to make σ_{F^2} significant. Cancellation of the σ_{\parallel} and σ_{\perp} components causes the mean $\sigma_{F'}$ effect to be even smaller, and it will only be non-zero for asymmetric atoms (as found in chemical bonds involving H-atoms). However, in certain ionic crystals a field-gradient exists at lattice points where $F=0$, and by orientating the crystal in the magnetic field the $\sigma_{F'}$ constants could possibly be determined, although the broad lines normally associated with solids would presumably render the chemical shifts difficult to measure.

2. A HYDROGEN ATOM IN A 'CAGE'

It is possible that an intermolecular effect known as the 'cage effect' might influence the magnetic shielding of a nucleus. The model assumes that the presence of a shell of neighbouring molecules in a condensed medium provides a barrier which is impenetrable to the electrons of the enclosed molecule. It has been used by Michels *et al.* [4] to describe the effects of high pressures on the electronic polarizabilities of atoms. These authors took a hydrogen atom in its ground state at the centre of an impenetrable spherical shell of radius r_0' and obtained the following wave function (to the first order in β)

$$\psi = \exp\{-r'/(1+\beta)\} \left[1 - \beta \sum_{s=1}^{\infty} b_s r'^{(s-1)} \right]; \quad (0 \leq r' \leq r_0') \quad (11)$$

where

$$\beta = \left[\sum_{s=1}^{\infty} b_s r_0'^{(s-1)} \right]^{-1} \quad \text{and} \quad b_1 = 1, \quad b_s = 2^{s-1}/(s-1)! \ s!, \quad \text{and} \quad r_0' = r_0/a.$$

On substituting (11) into Ramsey's equation (5) for the diamagnetic screening constant (there is obviously no paramagnetic contribution to σ) one obtains

$$\sigma^d = \frac{e^2}{3mc^2a} \frac{\int_0^{r_0'} \exp\{-2r'/(1+\beta)\} \left[1 - 2\beta \sum_{s=1}^{\infty} b_s r'^{(s-1)} \right] r' dr'}{\int_0^{r_0'} \exp\{-2r'/(1+\beta)\} \left[1 - 2\beta \sum_{s=1}^{\infty} b_s r'^{(s-1)} \right] r'^2 dr'}. \quad (12)$$

For $r_0' = 5$, the magnitudes of the effects are:

$p_{\text{atms.}}$	β	$\Delta\alpha/\alpha$	$\Delta\sigma/\sigma$
4860	3.45×10^{-3}	-22.7 per cent	+1.42 per cent

(using the simplest cage model of a liquid, internal pressures of the order of 1000 atms are predicted).

It is seen that the change in σ is of the opposite sign to the change in α . However, although it is fairly general to observe a decrease in the polarizability on liquefaction of a gas, σ also usually decreases. It is suggested by the above figures that the cage effect will have a larger influence on the polarizability than on σ ; the dispersion forces in the liquid may tend to decrease σ below the gas value.

But at sufficiently high pressures the cage effect, or the more general effect of non-bonded electron-electron repulsions which it represents, presumably predominates and a positive value for $\partial\sigma/\partial p$ should be observed.

REFERENCES

- [1] MARSHALL, T. W., and POPLE, J. A., 1958, *Mol. Phys.*, **1**, 199.
- [2] BUCKINGHAM, A. D., and POPLE, J. A., 1957, *Proc. Camb. phil. Soc.*, **53**, 262.
- [3] RAMSEY, N. F., 1950, *Phys. Rev.*, **77**, 567; **78**, 699.
- [4] MICHELS, A., DE BOER, J., and BIJL, A., 1937, *Physica*, **4**, 981.

The redistribution of charge in naphthalene caused by methyl substitution

II. The magnetic shielding of protons in α , α - and β , β -dimethylnaphthalenes

by C. MACLEAN and E. L. MACKOR

Koninklijke/Shell-Laboratorium, Amsterdam
(Shell Internationale Research Maatschappij N.V.)

(Received 5 October 1959)

The proton resonance spectra at 40 Mc/s of solutions of symmetrically substituted dimethylnaphthalenes in carbon disulphide have been measured and interpreted. Methyl substitution causes changes of the chemical shifts of the various ring protons, which are discussed in terms of the inductive effect of the methyl group. It is shown that a correlation exists between the variations of these chemical shifts and the partial rate factors for H-D exchange.

1. INTRODUCTION

In Part I [1] the rates of H-D exchange in acid solution of symmetrically substituted dimethylnaphthalenes were discussed. It was shown that the considerable enhancement of the rates by methyl substitution can be interpreted in terms of displacements of electronic charge in the aromatic rings by the methyl groups.

The present study was undertaken to investigate how far the nuclear magnetic resonance spectra of these compounds bear out such charge displacements. As a systematic study of the influence of the induction effect on the magnetic shielding has been made to a limited extent only, it seemed desirable to carry out such an investigation. The spectra form interesting examples of the application of recently published theories, because the coupling constants and the chemical shifts are comparable. Some of them require an analysis on the basis of the ABC case.

2. EXPERIMENTAL

The spectra of 1,4-, 2,3-, 2,6-, 2,7-, 1,5- 1,8-dimethylnaphthalene and acenaphthene were recorded at room temperature with a Varian V4300 high resolution spectrometer operating at 40 Mc/sec. Peak separations were measured with the aid of side bands. The external reference was a mixture of 92 per cent of D₂O and 8 per cent of H₂O, which was contained in the annulus between two concentric tubes, the inner one of which (diameter = 3 mm) contained the hydrocarbon solution under investigation. The concentration of the hydrocarbon solutions was invariably 8.1 ± 0.1 mole per cent in carbon disulphide. Since the diamagnetic susceptibilities of these isomers are nearly equal, the shifts were not corrected for bulk susceptibility. The internal reference was benzene dissolved

in small amounts in the solutions. Apart from a constant the chemical shifts were identical for both references. The benzene resonance is located at -97.2 c/s from the water reference.

The origin of the hydrocarbons used is described in Part I.

3. RESULTS

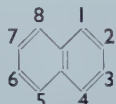
Tables 1 and 3 contain the values of the coupling constants and the chemical shifts as derived from the spectra. Apparently the coupling constants are, within the experimental error, not influenced by methyl substitution as they are identical with those in naphthalene [2]. In those cases for which the coupling could not be determined from the spectrum (1, 5- and 1, 8-dimethylnaphthalene) they have been taken to be identical with those of naphthalene.

The influence of methyl substitution on the chemical shifts has been found to be considerable, as can be seen from table 3.

4. INTERPRETATION OF THE SPECTRA

1, 4- and 2, 3-dimethylnaphthalene (figure 1(f) and (b))

The unsubstituted compound, naphthalene,



has a complicated NMR spectrum (figure 1(a)), which has been discussed by Pople *et al.* [2]. The spectrum is symmetrically arranged about a centre and consists, under the available resolution, of 12 lines. Explicit formulae to derive three coupling constants and the two chemical shifts from the spectrum are given in [2].

The coupling between protons of different rings can be neglected. Consequently, the spectra of 1, 4- and 2, 3-dimethylnaphthalene are expected to consist of a superposition of a 'naphthalene' spectrum of the unsubstituted ring and a single sharp peak of the aromatic protons in the substituted ring.

Figure 1(f) shows the aromatic part of the spectrum of 1, 4-dimethylnaphthalene. It consists on the low field side of a 'naphthalene' spectrum and on the high field side of a single peak due to the protons in the 2- and 3-positions. The shielding of the ring protons in the β -positions of the substituted ring is increased by 13 c/s, whereas the relative shift of the α - and β -protons in the unsubstituted ring has increased from 13.1 to 17.7 c/s. This difference in chemical shift has been found to be somewhat dependent on concentration—14.5 c/s in the pure compound—probably due to association effects [3].

The spectrum of 2, 3-dimethylnaphthalene (figure 1(b)) can be interpreted in the same way; for this compound, however, the peak due to the ring protons in α -positions in the substituted ring falls nearly in the centre of the 'naphthalene' spectrum, which gives rise to a less well-resolved spectrum.

2, 6- and 2, 7-dimethylnaphthalene (figure 1(c) and (d))

The spectra of these compounds are very similar. Let us discuss that of 2, 7-dimethylnaphthalene, which, to a good approximation, can be treated as a superposition of a single peak due to the α protons in the 1- and 8-positions and

a quadruplet due to the two adjacent protons in each of the two rings. The absolute value (8.5 c/s) of the coupling constant between the ortho protons ($J_{34}=J_{56}$) was derived from the separation of either the right-hand pair or the left-hand pair of lines in the quadruplet and is equal to that of naphthalene. The relative shift of the same protons could then be obtained from the overall separation of the quadruplet lines.

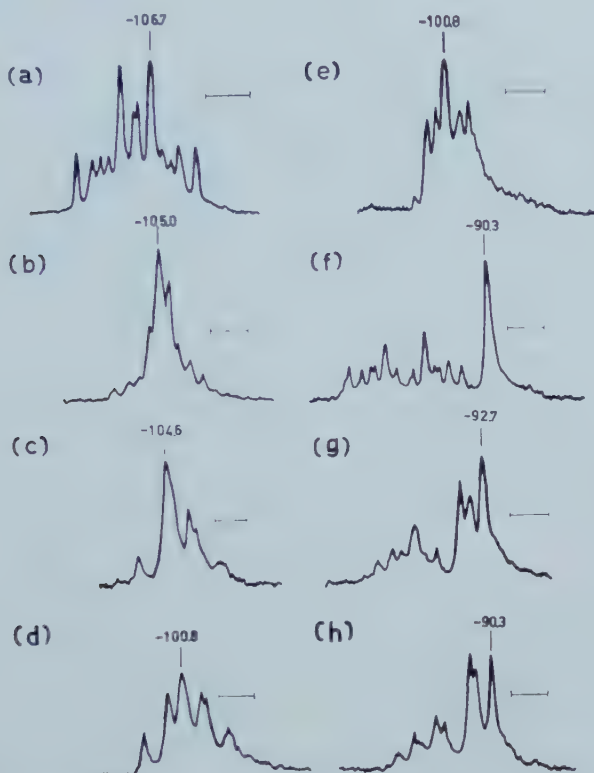


Figure 1. NMR spectra of the ring protons of 8.1 per cent solutions in carbon disulphide of (a) naphthalene; (b) 2,3-dimethylnaphthalene; (c) 2,6-dimethylnaphthalene; (d) 2,7-dimethylnaphthalene; (e) acenaphthene; (f) 1,4-dimethylnaphthalene; (g) 1,5-dimethylnaphthalene, and (h) 1,8-dimethylnaphthalene. Magnetic field increases from left to right. The spectra are approximately on the same absolute scale which is indicated by a horizontal bar (10 c/s). Vertical bars and numbers indicate the separation from the water reference.

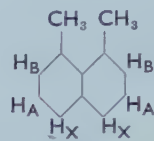
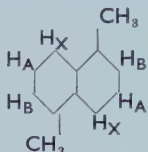
The small coupling between the two protons in the 1- and 3-positions causes a small splitting of about 1.7 c/s in each of the two lines at the high field side of the quadruplet. This indicates that the β -protons in the 3- and 6-positions are more shielded than the α -protons in the 4- and 5-positions.

The analysis of the spectrum of 2,6-dimethylnaphthalene proceeds in the same way.

1,5- and 1,8-dimethylnaphthalene (figure 1(g) and (h))

The spectra of these compounds consist of two fairly well separated parts with intensity ratio of approximately 2:1, the former falling on the high field side. Consequently an ABX analysis seems feasible [4].

Since the X-proton gives rise to the transitions on the low field side one would expect it to be the α -proton. Furthermore, of the β -protons the one in ortho position to the methyl group is expected to have the greatest shielding and thus the assignment would be as follows:



The AB part of the spectrum is very simple; it consists of an intense triplet with a weak shoulder on the high field side wing. The AB part of the spectrum is predicted by the ABX approximation, when the relative chemical shift of the AB protons is equal to half the difference between the coupling constants J_{AX} and J_{BX} ($D_- = \frac{1}{2}J_{AB}$ in Pople's notation) [4].

However, the intensities cannot be interpreted satisfactorily in the ABX approximation. A complete ABC analysis is required since the mixing of all three wave functions of the spin states $+\frac{1}{2}$ or $-\frac{1}{2}$, respectively, was found to be considerable.

A number of calculations using an electronic digital computer (Ferranti mark 1*) were made, taking different combinations of chemical shifts. The coupling constants were taken to be $J_{2,3} = 6.0$ c/s, $J_{2,4} = 1.4$ c/s and $J_{3,4} = 8.6$ c/s, approximately equal to the values in table 1.

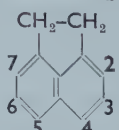
	$J_{\alpha\beta}$ (ortho)	$J_{\alpha\beta}$ (meta)	$J_{\beta\beta}$
Naphthalene	8.3	1.6	6.1
1, 4-dimethylnaphthalene	8.5	1.3	6.2
2, 6-dimethylnaphthalene	8.5	~ 1.7	—
2, 7-dimethylnaphthalene	8.5	~ 1.7	—
2, 3-dimethylnaphthalene	sum = 9.85		—

Table 1. Coupling constants between α - and β -ring protons in ortho- and meta-positions in c/s.

Table 2 demonstrates that an excellent fit is obtained with the ABC analysis whereas the ABX analysis is particularly inadequate for the interpretation of the relative intensities for the X-part.

The recent measurements of Leane and Richards [5] on substituted furanes and thiophenes also demonstrate that an ABX analysis is not sufficient when the relative shifts between X and AB protons is smaller than about 25 c/s.

Acenaphthene (figure 1(e))



The spectrum of acenaphthene is concentrated in a narrow range of about 12 c/s. The fact that it contains only six peaks, one of which is very small, suggests that the three chemical shifts are nearly equal. The lack of detail in the spectrum renders the analysis and the assignments difficult. An attempt was

Energy (c/s)			Relative intensity		
Calculated ABX	Calculated ABC	Observed	Calculated ABX	Calculated ABC	Observed
1, 5-dimethylnaphthalene ($\sigma_B - \sigma_A = 4.0$ c/s; $\sigma_B - \sigma_C = 21.4$ c/s)					
+6.03	—	—	0.01	<0.01	—
+2.85	+2.30	+2.8	0.38	0.31	Weak
+0.03	+0.12	0.0	1.95	1.43	Very strong
-0.03	-0.12	0.0	1.95	1.45	
-3.15	-3.54	-3.7	1.60	1.91	Very strong
-6.03	-5.72	—	0.01	0.06	—
-6.85	-6.62	-6.3	1.60	2.25	Very strong
-12.85	-12.46	-12.9	0.38	0.59	Medium
-14.02	-16.27	-15.8	0.14	0.42	Weak
-16.90	-18.45	-18.7	1.00	1.56	Strong
-20.08	-21.86	-22.2	0.86	0.86	Medium
-23.72	-25.20	-24.9	0.86	0.57	Medium
-26.90	-28.61	-28.7	1.00	0.51	Medium
-29.78	-30.79	—	0.14	0.08	—

The chemical shifts of the B, A and C protons, relative to the zero of this spectrum are -1.0, -5.0 and -22.4 c/s respectively. With respect to the water reference these values are -93.8, -97.8 and -115.2 c/s.

Calculated ABX	Calculated ABC	Observed	Calculated ABX	Calculated ABC	Observed
1, 8-dimethylnaphthalene ($\sigma_B - \sigma_A = 1.8$ c/s; $\sigma_B - \sigma_C = 16.4$ c/s)					
+6.13	+5.97	—	0.04	0.02	—
+2.04	+1.48	—	0.26	0.16	—
+0.13	+0.17	0.0	1.96	1.18	Very strong
-0.13	-0.16	0.0	1.96	1.30	
-3.96	-4.31	-4.5	1.74	2.16	Very strong
-6.04	-5.88	-5.7	1.74	2.52	Very strong
-6.13	-5.95	—	0.04	0.26	—
-10.83	-11.67	—	0.05	0.40	—
-12.04	-13.18	-12.4	0.26	0.59	Medium
-13.00	-14.82	-14.8	1.00	1.68	Strong
-17.09	-19.31	-19.2	0.95	0.66	Medium
-18.91	-20.54	-20.9	0.95	0.53	Medium
-23.00	-25.03	-25.0	1.00	0.44	Medium
-25.17	-26.66	—	0.05	0.10	—

The chemical shifts of the B, A and C protons relative to the zero of this spectrum are -2.3, -4.1 and -18.7 c/s respectively. With respect to the water reference these values are -92.5, -94.3 and -108.9 c/s.

Table 2. Observed and calculated spectra of 1,5- and 1,8-dimethylnaphthalene.

Compound	Aromatic protons					δq_s	Methyl protons
	Shift H ₂ O	Assignment	No.	Log k _{H-D}	$\delta \sigma_s$		
Naphthalene	-117.0	α		0.51	0	0	—
Figure 1 (a)	-103.9	β		-0.37	0	0	—
2, 3-dimethylnaphthalene	-105.0	α (1.4)	1	3.74	+12.0	0.059	
Figure 1 (b)	-110.4	α (5.8)	2	2.24	+ 6.6	0.010	+ 99.3
	- 99.3	β (6.7)	3	1.48	+ 4.6	0.010	
2, 6-dimethylnaphthalene	-104.6	α (1.5)	4	3.68	+12.4	0.062	
Figure 1 (c)	-107.0	α (4.8)	5	2.00	+10.0	0.005	+ 94.1
	- 91.8	β (3.7)	6	1.49	+12.1	0.033	
2, 7-dimethylnaphthalene	-100.8	α (1.8)	7	4.11	+16.2	0.074	
Figure 1 (d)	- 93.0	β (3.6)	8	2.17	+10.9	0.043	
	-110.5	α (4.5)	9	1.57	+ 6.5	-0.008	+ 94.8
1, 4-dimethylnaphthalene	- 90.3	β (2.3)	10	2.51	+13.6	0.059	
Figure 1 (f)	-121.0	α (5.8)	11	1.48	- 4.0	-0.001	
	-103.3	β (6.7)	12	0.73	+ 0.6	0.008	+ 88.7
1, 5-dimethylnaphthalene	-115.2	α (4.8)	13	3.09	+ 1.8	0.034	
Figure 1 (g)	- 93.8	β (2.6)	14	2.22	+10.1	0.061	
	- 97.8	β (3.7)	15	0.83	+ 6.1	0.005	
1, 8-dimethylnaphthalene	-108.9	α (4.5)	16	2.89	+ 8.1	0.049	
Figure 1 (h)	- 92.5	β (2.7)	17	2.89	+11.4	0.074	+ 78.7
	- 94.3	β (3.6)	18	0.43	+ 9.6	-0.008	
Acenaphthene	-105	α (4.5)	19	4.19	+12	—	+ 59.9
Figure 1 (e)	- 99	β (2.7)	20	3.83	+ 5	—	
	-101.8	β (3.6)	21	0.76	+2.1	—	

Table 3. Chemical shifts in c/s of aromatic and aliphatic proton resonance lines relative to external water reference (uncorrected for bulk-susceptibility). Negative values correspond to resonances at a lower field value. $\delta \sigma_s$: Relative chemical shift in c/s as compared with unsubstituted compound. δq_s : Calculated excess electronic charge on adjacent carbon atom.

made to interpret this spectrum as an ABB' case [6]. This treatment proved to be unsatisfactory because ambiguities in the intensities arise.

From the NMR spectrum of the partly deuterated compound (next paragraph) one can conclude that the chemical shift of the protons in the 3- and 6-positions lies at 1·0 c/s to the low field side from the intense central peak in the acenaphthene spectrum.

Tentative values of the chemical shifts of the protons in acenaphthene are given in table 3.

5. CHECKS OF THE ASSIGNMENTS BY H-D SUBSTITUTION

As can be seen in the fifth column of table 3 the rates of H-D exchange vary considerably for different positions in each isomer. For instance, if 1, 4-dimethylnaphthalene is partly deuterated in acid solution—as described in Part I—the β -carbon atoms in the substituted ring will exchange rapidly, whereas the β -carbon atoms in the other ring will hardly exchange at all. The spectrum of this isomer containing about 70, 25 and 3 mole per cent of deuterium in the three sub-groups displayed a spectrum in which the single peak due to the β -protons in the substituted ring is practically absent. This spectrum had the appearance of a broadened doublet in which the peak due to the β -protons in the unsubstituted ring is the more intense. In this manner one may see whether the assignment of the order of reactivities, as made in Part I, is correct.

The influence of deuteration on the spectra of 1,5- and 1,8-dimethylnaphthalene and acenaphthene was similarly studied. The positions of the peaks of deuterated samples of 1,5- and 1,8-dimethylnaphthalene were within 1·5 c/s in agreement with the calculated chemical shifts of the A-protons given in table 3. For acenaphthene this enabled us to find the chemical shift of the least reactive proton which is given by the position of the peak of the deuterated sample at 102·9 c/s with respect to the water reference, again within 1·5 c/s from the value calculated from the spectrum.

6. DISCUSSION

The inductive effect of a methyl group causes a redistribution of electronic charge over the carbon atoms in the aromatic nuclei. These charge densities can be calculated in first approximation by the theory—based on the LCAO MO approximation—of Coulson and Longuet-Higgins [9] (see Part I). It is commonly argued that an increase in the charge density on a carbon atom will cause an increase in reactivity in electrophilic reactions as well as an increase in the magnetic shielding of the nearby proton. In Part I it was shown that the partial rate factors for H-D exchange, $\log k$ (table 3, column 5) change proportionally with the calculated net negative charges δq_s (table 3, column 7).

The magnetic shielding of the aromatic protons varies over a range of about 20 c/s. Apart from one exception, the magnetic shielding of both α - and β -protons is always increased as compared with the protons in the parent compound (table 3, column 6). Figure 2 shows that there is a rough linear correlation between the chemical shifts and the partial rate factors. The points in the figure fall along two parallel lines: one for the α -protons (open circles) and another one for the β -protons (dots). The points at the extreme left of both lines represent the values for the unsubstituted molecule. The magnetic shielding increases with increasing

reactivity as expected. It may be stressed that the behaviour of the $\alpha\alpha$ - and the $\beta\beta$ -dimethylnaphthalenes is equivalent.

Both 1,4- and 1,5-dimethylnaphthalene possess two α -protons which are hindered sterically by the methyl groups. It has been observed [7] that this effect displaces the resonance of the relevant protons to a lower field, which is in accordance with the relatively low value of the chemical shifts for these protons (points 1, 4 and 1, 5 in figure 2).

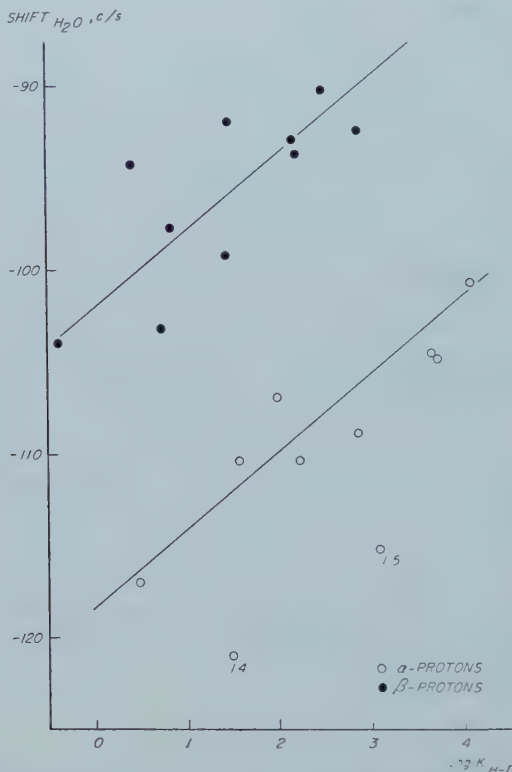


Figure 2. Chemical shifts of α - and β -protons plotted against the rate of H-D exchange.

The question arises whether there is also a direct proportionality between the charge densities (δq_s) and the chemical shifts ($\delta \sigma_s$). Figure 3 shows that the points scatter considerably along a straight line. For instance, the shifts of the protons in 2,7-dimethylnaphthalene show the expected pattern. An increase of δq_s by 0.04 electron causes an increment in $\delta \sigma_s$ of about 5 c/s. In the closely related molecule 2,6-dimethylnaphthalene, on the other hand, the values of $\delta \sigma_s$, of all three protons are nearly equal (11.7 ± 1.0 c/s). Both the partial rate factors and the calculated δq_s of the three unsubstituted carbon atoms on the other hand have a variation only slightly smaller than those in 2,7-dimethylnaphthalene.

Our measurements seem to indicate, therefore, that the redistribution of charge, caused by the substitution of methyl groups, can only be one aspect in a discussion of the variations in magnetic shielding thereby produced. Other factors, such as changes in induced second-order paramagnetism, in bond hybridization, etc. may contribute considerably.

In the light of this conclusion we can discuss the observations on mono-substituted benzenes made by Corio and Dailey [8]. They found that the aromatic part of the spectrum of toluene consists of one single line. This phenomenon, which is similar to the nearly constant value of $\delta\sigma_s$ in 2, 6-dimethylnaphthalene, was interpreted as indicating that the charge densities on meta-carbon atoms in toluene are equal to those on the para- and ortho-carbon atoms. A preliminary study of the NMR spectrum of para-deuterotoluene revealed that the aromatic peak is considerably broadened, although, under the available resolution, the line

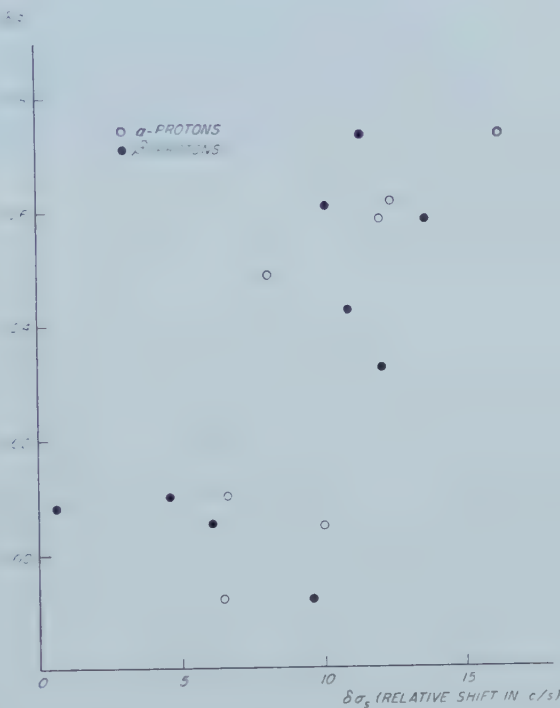


Figure 3. Net negative charges plotted against relative chemical shifts.

remains single. The line width of 3.4 c/s indicates that there is a difference in chemical shifts between the meta- and ortho-protons of the order of 3 c/s. The spectrum of the ring protons of metaxylene has been found to consist of at least 16 lines spread out over a frequency interval of approximately 13 c/s. These observations are illustrative of the non-equivalence of the various species of ring protons in methylsubstituted benzenes.

Furthermore, Chamberlain [10] has shown that in the series benzene, toluene, metaxylene, mesitylene the magnetic shielding of the aromatic protons increases by about 6 c/s for each methyl group introduced into the ring. This points to an increase of electronic charge on the carbon atoms in the substituted ring caused by the methyl groups.

The calculated charge densities, as used in the discussion of our own experiments, have been obtained by choosing the induction parameter of the methyl group in accordance with information obtained from other phenomena such as the enhancement of basicity and reactivity by methyl substitution (see Part I).

If one accepts this value one would infer an increase in chemical shielding of about 20 c/s (at 40 Mc/sec) per 0·1 of an electron charge on the adjacent carbon atom. We have investigated the NMR spectra of a number of aromatic molecules and carbonium ions which are known to possess an unequal distribution of charge over the carbon atoms in the conjugated system. Examples are azulene [3], pyridine [11], acridine and the proton complexes of pentamethylbenzene and anthrone [12]. Our tentative conclusion is that the magnetic shielding of the protons in these molecules changes by about 20–40 c/s per 0·1 of an electron charge. A detailed account will be given in a subsequent publication.

The differences in the magnetic shielding of the methyl protons given in table 3 can be understood on the basis of a ring current model of aromatic molecules [13]. One will notice, however, that the considerable steric strain in 1, 8-dimethylnaphthalene and acenaphthene makes itself felt in the shift to lower fields of the aliphatic protons in comparison with those in 1, 4- and 1, 5-dimethylnaphthalene.

The experimental assistance of Mr. J. Gaaf is gratefully acknowledged. We also wish to thank Dr. J. P. Colpa and Mr. G. ter Maten for their help in the computer calculations.

REFERENCES

- [1] DALLINGA, G., SMIT, P. J., and MACKOR, E. L., 1960, *Mol. Phys.*, **3**, 130.
- [2] POPLE, J. A., SCHNEIDER, W. G., and BERNSTEIN, H. J., 1957, *Canad. J. Chem.*, **35**, 1060.
- [3] SCHNEIDER, W. G., BERNSTEIN, H. J., and POPLE, J. A., 1958, *J. Amer. chem. Soc.*, **80**, 3497.
- [4] BERNSTEIN, H. J., POPLE, J. A., and SCHNEIDER, W. G., 1957, *Canad. J. Chem.*, **35**, 65.
- [5] LEANE, J. B., and RICHARDS, R. E., 1958, *Trans. Faraday Soc.*, **55**, 518.
- [6] RICHARDS, R. E., and SCHAEFFER, T., 1958, *Mol. Phys.*, **1**, 332.
- [7] REID, C., 1957, *J. mol. Spectroscopy*, **1**, 18.
- [8] CORIO, P. L., and DAILEY, B. P., 1956, *J. Amer. chem. Soc.*, **78**, 3043.
- [9] COULSON, C. A., and LONGUET-HIGGINS, H. C., 1947, *Proc. roy. Soc.*, **192**, 16.
- [10] CHAMBERLAIN, N. F., 1959, *Analyt. Chem.*, **31**, 56.
- [11] SCHNEIDER, W. G., BERNSTEIN, H. J., and POPLE, J. A., 1957, *Canad. J. Chem.*, **35**, 1487.
- [12] MACLEAN, C., VAN DER WAALS, J. H., and MACKOR, E. L., 1958, *Mol. Phys.*, **1**, 247.
- [13] BERNSTEIN, H. J., SCHNEIDER, W. G., and POPLE, J. A., 1956, *Proc. roy. Soc. A*, **236**, 515.

Self-consistent field theory of the electron spin distribution in π -electron radicals

by A. D. McLACHLAN†

Department of Theoretical Chemistry, University Chemical Laboratory,
Lensfield Road, Cambridge

(Received 17 November 1959)

In a radical the single determinant wave function which gives the lowest electronic energy is one where electrons of opposite spins occupy different sets of molecular orbitals and thereby lower the 'exchange' part of the energy. The unpaired spin density may be negative in a wave function of this type and is easily found by perturbation theory if certain exchange integrals are small. We show that the spin density is then almost the same as one finds by combining the usual single determinant function (with one unpaired electron, and $2n$ paired ones in n orbitals) with its singly excited doublet configurations. In alternant hydrocarbons the Pariser and Parr theory leads to a simple formula for the spin density: $\rho_r = c_{ro}^2 - \lambda \sum_s \pi_{rs} c_{so}^2$, where c_{ro} is the Hückel coefficient of the odd orbital on atom r , π_{rs} is the mutual polarizability of atoms r and s , and λ is a constant derived from the theory. The observed hyperfine structure in the electron resonance spectra of naphthalene, anthracene, perylene, diphenyl, phenanthrene, and pyrene negative ions agrees well with this formula, provided the constant Q defined by McConnell is about -24.2 gauss. The non-alternant negative ions of acenaphthylene and fluoranthene also agree, but not acepleiadylene. The theory predicts identical spin densities in corresponding positive and negative ions. In neutral alternant radicals we find negative spin densities on all the unstarred atoms of triphenylmethyl, perinaphthyl, allyl, and benzyl. The calculated negative densities are a little too small to fit the spectra of the first two radicals, but fit just as well as valence bond ones.

1. INTRODUCTION

It is now well established that the hyperfine splittings from ring protons in the electron resonance spectrum of an aromatic free radical in solution are closely proportional to the unpaired spin densities on the ring carbon atoms [1, 2]. The main point of interest in understanding these spectra is how to account for the unpaired spin distribution over the carbon atoms in each radical. This distribution has been treated in two ways. A simple molecular orbital treatment gives a highly successful account of the spectra of many alternant hydrocarbon ions [3], but is unable to explain the negative spin densities which occur in some of them, notably the pyrene negative ion. This is because the molecular orbital wave function makes no allowance for the correlation of electrons with opposite spins. On the other hand the valence bond method, which does allow for this effect, is only practicable for neutral radicals, where polar structures are not necessary, and is even then a laborious and inflexible theory. In the first part of this paper we show how the self-consistent field theory can combine the best

† Now at Gates and Crellin Laboratories of Chemistry, California Institute of Technology, Pasadena, U.S.A. (Contribution No. 2526). Harkness Fellow of the Commonwealth Fund, 1959-61.

features of both the first methods, and lead to a simple perturbation treatment of alternant radicals. In the second, we give some examples of its application in neutral radicals and some of the negative hydrocarbon ions studied by de Boer and Weissman [3].

In a radical the conventional single determinant wave function with one unpaired electron and $2n$ other electrons paired in n molecular orbitals is less useful than in a closed shell molecule. This is because the motions of electrons of α and β spins are affected in different ways by the odd electron. To allow for this difference one must use a modified type of wave function which automatically brings in negative spin densities. One type uses the conventional determinant with a small admixture of excited configurations, while the other uses a single determinant with different orbitals for electrons of α and β spins. There is a good theoretical reason why both these methods will lead to nearly the same π electron spin distribution, and the second has a simple physical interpretation which makes it very suitable.

PART A. THEORY

2. SELF-CONSISTENT WAVE FUNCTIONS

Our starting point will be a single determinant wave function

$$\chi_0 = \|\psi_1^2 \psi_2^2 \dots \psi_n^2 \psi_0^\alpha\| \quad (2.1)$$

in which $2n$ electrons occupy the orbitals $\psi_1 \dots \psi_n$ in pairs and the odd electron of spin α occupies ψ_0 . These molecular orbitals are found by a variational method and we express them in L.C.A.O. form with atomic orbitals $\phi_1 \dots \phi_m$. In a molecule with all its electrons paired $\psi_0 \dots \psi_n$ would be self-consistent orbitals and satisfy the Hartree-Fock equations. For such molecules Roothaan [4] has derived L.C.A.O. equations which are equivalent to the Hartree-Fock theory, and in alternant hydrocarbons Pople [5] has made assumptions which take Roothaan's equations into a form very similar to the Hückel equations

$$\left. \begin{aligned} \psi_i &= \sum_r C_{ri} \phi_r \\ \sum_s \beta_{rs} C_{si} &= (E_i - \alpha_r) C_{ri} \end{aligned} \right\} \quad (2.2)$$

The chief difference is that the effective values of the Coulomb integrals α_r and resonance integrals β_{rs} depend on the electron distribution in the molecule. In a molecule with unpaired electrons none of these equations hold strictly, but Longuet-Higgins and Pople [6] obtained exact variational equations on the assumption that the wave function is of the form (2.1) and the orbitals are chosen to give the lowest energy. Theirs is thus the 'best' function of simple form and the natural starting point for a perturbation calculation.

An important characteristic of the self-consistent wave function of a closed shell molecule is that it has no energy matrix elements with any of its singly excited configurations. This property does not hold in radicals, and even when the orbitals are chosen to give it the lowest energy χ_0 of (2.1) can always mix with singly excited doublet configurations

$$\chi_i^r = \|\psi_1^2 \dots \psi_i \psi_r \dots \psi_n^2 \psi_0\| \frac{1}{\sqrt{6}} (2\alpha\alpha\beta - \alpha\beta\alpha - \beta\alpha\alpha), \quad (2.3)$$

in which one electron from orbital i is placed in the empty orbital r . The matrix element between these states is an exchange integral

$$\langle \chi_0 | \mathcal{H} | \chi_i^r \rangle = \frac{-3}{\sqrt{6}} \int \int \psi_0^* \psi_r(1) \frac{e^2}{r_{12}} \psi_i^* \psi_0(2) d\tau_1 d\tau_2. \quad (2.4)$$

Thus in a radical the simple wave function (2.1) is not self-consistent in the full sense, and we are forced to use a more elaborate form.

Hoijtink [7] met this difficulty by taking Ψ to be

$$\Psi = \chi_0 + \sum_{i,r} \lambda_{ir} \chi_i^r, \quad (2.5)$$

and treated the exchange energy of (2.4) as a small perturbation. He used his method to calculate the spin densities in hydrocarbon ions, taking ψ_i to be the Hückel orbitals. Hoijtink's function is better than χ_0 but it is no longer easy to calculate the best form of this wave function by successive approximations. This is a serious drawback if the method is to be used instead of the Hartree-Fock one for exact numerical calculations on radicals. Another point is the great number of excited configurations in a large molecule.

Pople and Nesbet [8] tried to avoid these difficulties and proposed a self-consistent wave function

$$\Phi = ||\psi_1^\alpha \psi_1'^\beta \dots \psi_n^\alpha \psi_n'^\beta \psi_0^\alpha|| \quad (2.6)$$

in which electrons of α and β spin occupy independent sets of orbitals $\psi_0, \psi_1 \dots \psi_n$ and $\psi_1' \dots \psi_n'$. The orbitals are those which minimize the energy. In a wave function like Φ the effective field produced by the other electrons is different for electrons of different spin owing to the exchange term in the energy. Electrons of the same spin attract one another through the exchange force, as Hund's rule for multiplets shows in atoms. This 'exchange polarisation' effect is evident in a wave function like (2.6), but appears in (2.5) also through the excited doublet configurations introduced by the exchange integral (2.4).

Unfortunately (2.6) is not an eigenfunction of S^2 , and so is unsuitable for treating the electronic spectra of radicals [6]. However, Löwdin [9] has developed a projection method by which the part of any wave function which represents states belonging to a particular value of S^2 can be picked out. He dealt with the case of $2n$ electrons in $2n$ orthonormal orbitals having $S=0$. We have extended his treatment to deal with Pople and Nesbet's wave function for a radical, but the formulae are so complicated when nonorthogonal orbitals are involved that one cannot apply them to actual molecules. We have also derived formulae for finding the best possible set of orbitals $\psi_0 \dots \psi_n$ with which one can construct a wave function of the form proposed by Hoijtink. Here again the theory could only be used with elaborate computations, so we now limit ourselves to seeing what the two simpler methods can tell us about the spin densities in a radical.

3. THE SPIN DENSITIES

In a simple wave function like (2.1) the spin density ρ is just equal to $|\psi_0|^2$ and is everywhere positive. However, in Pople and Nesbet's function it is

$$\rho = |\psi_0|^2 + \sum_1^n \{ |\psi_i|^2 - |\psi_i'|^2 \}, \quad (3.1)$$

so that if $|\psi_i'|^2$ exceeds $|\psi_i|^2$ at a node of ψ_0 ρ becomes negative. McConnell [2] has used this type of wave function to derive the relation

$$a_H = Q\rho \quad (3.2)$$

between proton splitting constants and π electron densities. Wood [10] too has used it to calculate the s -electron hyperfine splitting in iron group metals. In (2.5) the spin density is

$$\rho = \rho_0 + 2 \sum_{i,r} \langle \chi_0 | \rho | \chi_i^r \rangle \quad (3.3)$$

and can again be negative. In fact, as we mentioned before, its value is practically the same whether one uses (3.1) or (3.3). To see this we examine the form of the two wave functions in a simple system, treating the exchange energy as a small perturbation.

Consider a radical in which three electrons can move among three atomic orbitals and are in a state with $S_z = \frac{1}{2}$. We first form three new orthogonal orbitals, a , b , c , from them such that the best wave function of the type (2.1) for the ground state is

$$D_0 = \|aab\|(\alpha\beta\alpha) \quad (3.4)$$

and the orbital c is empty. The other two types of wave function differ from D_0 by including components from two singly excited doublet configurations and one quartet:

$$\left. \begin{aligned} D_1 &= \|abc\| \frac{1}{\sqrt{6}} (\beta\alpha\alpha + \alpha\alpha\beta - 2\alpha\beta\alpha), \\ D_2 &= \|ccb\|(\alpha\beta\alpha), \\ Q &= \|abc\| \frac{1}{\sqrt{3}} (\alpha\beta\alpha + \beta\alpha\alpha + \alpha\alpha\beta). \end{aligned} \right\} \quad (3.5)$$

The extended Hartree-Fock wave function (2.6) with

$$\psi_0 = b, \quad \psi_1 = a + \lambda c, \quad \psi_1' = a - \lambda c, \quad (3.6)$$

is equivalent in form to

$$\Phi = D_0 + \frac{1}{3}\lambda(2Q\sqrt{3} + D_1\sqrt{6}) - \lambda^2 D_2. \quad (3.7)$$

Varying λ to obtain the least possible energy one obtains

$$\lambda = \frac{-\sqrt{(2/3)H_{01}}}{(2/3)(E_1 - E_0) + (4/3)(E_Q - E_0) - 2H_{02}}, \quad (3.8)$$

and the spin density is

$$\rho = \rho_0 + 4\lambda \langle a | \rho | c \rangle. \quad (3.9)$$

The corresponding wave function like (2.5) is

$$\Psi = D_0 + 2\sqrt{(3/2)\lambda'} D_1, \quad (3.10)$$

where first order perturbation theory gives

$$\lambda' = \frac{-\sqrt{(2/3)H_{01}}}{2(E_1 - E_0)}, \quad (3.11)$$

and the spin density is again given by (3.9). The two methods differ only in the effective excitation energy of the doublet state. H_{02} is always positive, and generally the quartet has lower energy than the doublet, so that spin densities calculated by the extended Hartree-Fock method tend to be too large. In the allyl radical, for example, the excitation energies of the first doublet and quartet

states have been estimated theoretically [6] to be 7.74 and 4.51 ev. The method also seriously underestimates the effect of these excited doublet configurations on the total energy of the radical. In the first theory the difference in energy between Φ and D_0 when λ takes its best value (3.8) is

$$\frac{-(H_{01})^2}{(E_1 - E_0) + 2(E_Q - E_0) - 3H_{02}} + \text{terms in } (H_{01})^4, \quad (3.12)$$

while the second order perturbation energy correction in (3.9) is

$$\frac{-(H_{01})^2}{(E_1 - E_0)}, \quad (3.13)$$

about three times as large.

In the Hückel approximation the energies of doublet and quartet configurations are the same, so that the methods of configuration interaction or of different orbitals for different spins will give identical spin densities.

4. THE EXTENDED HARTREE-FOCK METHOD

In section 3 we showed that the extended Hartree-Fock wave function (2.6) is for many purposes as good as the complicated form (2.5). Also it embodies the essential physical difference between radicals and closed shells in a simple way. We shall now apply it to calculate the spin distribution of the π electrons in even alternant hydrocarbon ions and neutral odd radicals.

We shall use the L.C.A.O. semiempirical method of Pariser and Parr [12] with the notation and approximations of Pople and Brickstock [11]. The only change is that we call their ψ_i^α and ψ_i^β ψ_i and ψ'_i , and write β_{rr} instead of $U_{\mu\mu}$. Usually the orbitals ψ_0 , ψ_i , and ψ'_i are very similar to the corresponding orbitals of χ_0 , so that we can still speak of the 'odd' orbital and the 'odd' electron, and group the other orbitals into pairs ψ_i , ψ'_i . The L.C.A.O. coefficients of the two sets of orbitals

$$\psi_0 = c_{or}\phi_r, \quad \psi_i = c_{ir}\phi_r, \quad \psi'_i = c_{ir'}\phi_r \quad (4.1)$$

are determined by the equations

$$\left. \begin{aligned} \sum_s F_{rs} c_{is} &= E_i c_{ir}, \\ \sum_s F'_{rs} c'_{is} &= E'_i c_{ir}, \end{aligned} \right\} (s = 1 \dots 2n+1) \quad (4.2)$$

$$\sum_s F_{rs}^0 c_{os} = E_o c_{or} \quad \text{or} \quad \sum_s F_{rs}^0 c'_{os} = E'_o c_{or}. \quad (4.3)$$

The quantities F , F' and F^0 describe the self-consistent field for the α , β and odd electrons in the atoms and bonds of the molecule, and depend on the bond orders and electron densities for electrons of α and β spin, defined to be:

$$P_{rs} = \sum_{i=1}^n c_{ir} c_{is}, \quad P_{rs}' = \sum_{i=1}^n c_{ir'} c'_{is}, \quad P_{rs}^0 = c_{or} c_{os}. \quad (4.4)$$

We may then write the operators F and F' as the sum of three terms

$$\left. \begin{aligned} F &= V + K - J, \\ F' &= V + K - J', \end{aligned} \right\} \quad (4.5)$$

where V represents the field of the core of nuclei and σ electrons, K the Coulomb field of all the π electrons, and J, J' the exchange field for π electrons of α and β

spins. F^0 is the field of all the π electrons except the odd one, and is obtained by omitting from F all the terms proportional to P^0 .

$$\left. \begin{aligned} V_{rs} &= \beta_{rs} - \delta_{rs} \sum_{t \neq r} \gamma_{rt}, \\ K_{rs} &= \delta_{rs} \sum_t (P_{tt} + P_{tt}' + P_{tt}^0) \gamma_{rt}, \end{aligned} \right\} \quad (4.6)$$

and

$$J_{rs} = (P_{rs} + P_{rs}^0) \gamma_{rs}, \quad J_{rs}' = P_{rs}' \gamma_{rs}. \quad (4.7)$$

We notice that the difference between F and F' arises from the exchange field ($J' - J$) of the odd electron. The wave function of any molecule would be found by a series of successive approximations, starting with values of F based on Hückel orbitals. This has been done for the allyl radical [13] and the orbital coefficients are given below:

Self-consistent orbitals of allyl		
ψ_0	(0.7071, 0.0000, -0.7071)	
ψ_1	(0.5595, 0.6115, 0.5595)	
ψ_1'	(0.4324, 0.7912, 0.4324)	
Spin density	0.6260, -0.2521, 0.6260.	

In this small molecule the orbitals for α and β spins are quite close to the ordinary S.C.F. ones, so that the exchange term ($J' - J$) can be treated as a small perturbation. The spin density on the central atom is negative, as predicted by the valence bond theory.

The well-known pairing property [14] of Hückel orbitals in an alternant hydrocarbon follows also in a modified form from Pople and Brickstock's equations (4.2). The two sets of orbitals, ψ_i^+ , $\psi_i'^+$ and ψ_i^- , $\psi_i'^-$ in the corresponding positive and negative ions of an alternant hydrocarbon M with n atoms are closely related. If ψ_i^+ is the i th bonding orbital of α spin in M^+ its pair is ψ_{n-i}^- , the i th antibonding one of β spin in M^- . It immediately follows that the spin densities in the two ions are identical, as is well known from the experiments of Weissman and de Boer (see also [15]).

5. THE PERTURBATION METHOD

An iterative solution of equations (4.2) is possible for a negative ion if we know the self-consistent orbitals of the neutral molecule. We calculate P , P' , and P^0 from these orbitals, and use them to make a first approximation to F , F' and F^0 . In a neutral radical the proper starting point for the process is the wave function of Longuet-Higgins and Pople [6]. As the exchange integrals have fairly small effects a single iteration is often sufficient, and we can then use perturbation theory.

If the 'unperturbed' molecule is alternant $P_{rr} = P_{rr}' = \frac{1}{2}$. Also $P_{rs} = P_{rs}'$ and vanishes when atoms r, s belong to the same set. The operator F therefore starts with the values

$$\left. \begin{aligned} F(0)_{rr} &= \beta_{rr} + \frac{1}{2} \gamma_{rr}, \\ F(0)_{rs} &= \beta_{rs} - P(0)_{rs} \gamma_{rs}, \end{aligned} \right\} \quad (5.1)$$

Renaming the odd orbital ψ_0 , we now find that the first corrections to $F(0)$ are given by

$$K(1)_{rs} - K(0)_{rs} = \sum_t P^0(0)_{rt} \gamma_{rt} \delta_{rs}, \quad (5.2)$$

$$\left. \begin{aligned} J(1)_{rs} - J(0)_{rs} &= P^0(0)_{rs} \gamma_{rs} = G_{rs} \\ J'(1)_{rs} - J'(0)_{rs} &= \end{aligned} \right\} \quad (5.3)$$

and

$$F^0(1)_{rs} = F^0(0)_{rs}. \quad (5.4)$$

G_{rs} is the exchange potential of the odd electron, which causes electrons of α and β spin to move in different orbitals. Both sets of orbitals alter equally under the influence of the Coulomb field of the odd electron. In this first iteration the orbital of the odd electron is completely unchanged, but it will usually undergo a small change in a second iteration. To calculate the spin density we can treat the effect of Coulomb and exchange terms as independent small perturbations.

If the radical is neutral the starting values of F are

$$\left. \begin{aligned} F(0)_{rr} &= \beta_{rr} + \frac{1}{2} \gamma_{rr} \\ F(0)_{rs} &= \beta_{rs} - (P + \frac{1}{2} P^0)_{rs} \gamma_{rs} \end{aligned} \right\} \quad (5.5)$$

instead of (5.1), but equations (5.3) hold with the same quantities G_{rs} as before. One can show easily that in the first iteration :

- (i) The odd orbital does not change.
- (ii) The total electron density at each atom does not alter either.
- (iii) The change of spin density is caused entirely by the exchange term G_{rs} of (5.3), just as it is in an even alternant ion.

Hoijtink [7] obtained slightly different results for radicals and ions because he started from a wave function like (2.6) in ions, whereas the self-consistent wave function of the neutral molecule is the natural choice.

The exchange potential G of the odd electron alters the spin density by changing the effective values of Coulomb integrals α_r and resonance integrals β_{rs} for electrons of α spin. The correction to the spin density can therefore be found by the method one uses to find the changes of π electron density caused by substituents in the molecule [14]. These depend on the mutual polarizability coefficients $\pi_{rs, tu}$, and the perturbed spin density is

$$\rho_{rs} = \rho(0)_{rs} - \frac{1}{2} \sum_{tu} \pi_{rs, tu} G_{tu}. \quad (5.6)$$

We usually only need the spin densities on the atoms. Since the atom-bond polarizabilities in an alternant hydrocarbon vanish when atoms t, u are in different sets we can neglect most of the terms where $t \neq u$. We shall in fact neglect them all and assume that the γ_{rr} are all equal, obtaining the simple equation

$$\rho_r = c_{or}^2 - \frac{1}{2} \gamma \sum_s \pi_{rs} c_{os}^2, \quad (5.7)$$

where π_{rs} is the mutual polarizability of the two atoms.

From equations (4.2) it follows that π_{rs} should be calculated from the expression

$$\pi_{rs} = -4 \sum_i \sum_j \frac{c_{ri} c_{sj} c_{si} c_{rj}}{E_j - E_i} \quad (5.8)$$

where i, j are occupied and vacant orbitals, and E_i are the Hartree-Fock energy

parameters of (4.2). The origin of negative spin densities is closely linked with the law of alternating polarity in alternant molecules. A high spin density on atom r tends to induce a yet higher value on that atom, and negative values on the next neighbours. In neutral radicals this tendency is most evident, because the odd orbital is confined to the starred atoms only, and induces large negative spins on all the unstarred atoms.

6. NUMERICAL CALCULATIONS

In the two previous sections we have described two approximate ways of estimating spin densities by the molecular orbital method. The first is an iterative method which starts from known self-consistent orbitals. The second is a perturbation method based on these orbitals and neglecting the exchange integrals of the bonds. It is useful to compare them by sample calculations to see not only whether perturbation theory is adequate but also whether the orbitals and energies one uses in (5.8) make much difference to the final result.

Brickstock [13] has calculated the self-consistent orbitals and energy parameters E of naphthalene, using values of the β and γ integrals obtained by Pariser and Parr [12]. Lefèvre [16] also has calculated the orbitals of the benzyl radical. In both cases the coefficients of the orbitals, especially the odd one, are almost identical with Hückel's, although their relative energies are very different. In naphthalene negative ion for example, the odd electron densities at the α and β positions are

	S.C.F.	Hückel
α	0.18055	0.18088
β	0.06954	0.06910

Next we carried out the first two stages of the iterative method for the naphthalene negative ion. After the first stage the spin densities had changed to $\rho_\alpha = 0.2257$, $\rho_\beta = 0.0471$ and $\rho_\gamma = -0.0453$ on each of the other two carbon atoms. The total electron density changed by less than $0.02e$ on each atom. In the second iteration the changes of the odd electron density caused by these charge shifts were less than $0.01e$. We therefore conclude that perturbation theory is quite adequate in this case, though the same need not be true in neutral radicals with large negative spin densities. It also turned out that the bond terms in G_{rs} had a negligible effect on the final spin densities.

The use of Hückel orbitals in (5.8) instead of self-consistent ones will not make much difference, since they are so alike, but it also seems that Hückel energies can be used safely, provided that we choose a proper value of the resonance integral β . According to the self-consistent theory the resonance integral is

$$\beta_{rs}(\text{eff.}) = \beta_{rs} - \frac{1}{2} P_{rs} \gamma_{rs}, \quad (6.1)$$

where P_{rs} is the *total* bond order. We therefore take β to be the average of this quantity for all the bonds in the molecule. Using Pariser and Parr's parameters $\gamma = 10.53 \text{ ev}$, $\beta_{12} = -2.39 \text{ ev}$, $\gamma_{12} = 7.30 \text{ ev}$, β is about -4.5 ev in most cases, and

$$\frac{1}{2}\gamma/\beta \approx -1.2 = -\lambda. \quad (6.2)$$

The spin densities deduced in this way by the perturbation method with S.C.F.

and Hückel energies are almost identical with one another and with the iterative method:

S.C.F. energies	Hückel energies
$\rho_\alpha = 0.2231$	$\rho_\alpha = 0.222$
$\rho_\beta = 0.0462$	$\rho_\beta = 0.047$
$\rho_\gamma = 0.0386$	$\rho_\gamma = 0.037$

We finally conclude that the Hückel approximation gives just as reliable results as the more elaborate methods, and adopt instead of (5.7) the expression

$$\rho_r = c_{or}^2 - \lambda \sum_s \pi_{rs} c_{os}^2, \quad (6.3)$$

where π_{rs} is the numerical value (without β), and the only adjustable parameter is λ . Finally we note that if an automatic computer is available to solve the secular equations one need not calculate the π_{rs} directly, but find ρ from (3.1), where $\psi_0, \psi_1 \dots \psi_n'$ are the ordinary Hückel orbitals, and $\psi_1 \dots \psi_n$ are calculated with β_{rs} unchanged but $\alpha_r = +2\lambda c_{or}^2 \beta$.

PART B. COMPARISON WITH EXPERIMENT

7. THE VALUES OF Q AND λ

To predict the hydrogen hyperfine splittings a_H for the different ring positions we shall assume that they are proportional to the unpaired spin density ρ on the nearest carbon atom, so that

$$a_H = Q\rho. \quad (7.1)$$

McConnell [17] showed theoretically that the sign of Q should be negative, and this has been confirmed by recent experiments on irradiated single crystals of malonic acid [18]. The numerical value must be found empirically. If Q were a constant for all C–H bonds the best estimate would be McConnell's value of 22.5 gauss from the spectrum of the benzene negative ion [20], since here the spin density is certainly one sixth at each carbon atom. A similar estimate is obtained from the methyl and malonic radicals [18, 19]. The validity of equation (7.1), which was first suggested by McConnell, was first tested experimentally on the semiquinone radicals [21]. Since then it has been further examined theoretically by McConnell and Chesnut [2]†, who conclude that Q should be a good constant, and tested many times experimentally in radicals whose spin distributions have been calculated by the molecular orbital or valence bond methods. It fits the observed electron resonance spectra very well, provided that Q is given a suitable value which varies between –20 and –30 gauss for different radicals. Recent experiments by Carrington [22] on the positive and negative ions of anthracene, naphthacene, and perylene, led him to conclude that Q is accurately constant except for a small variation with the electric charge on the carbon atom. In these compounds the pairing of the electronic states in alternant hydrocarbons [14, 15] makes it likely that the spin densities are almost identical in the corresponding pairs of positive and negative ions, so that any differences in their spectra are caused by variations of Q . The spectra are indeed almost identical, except that the splitting constants on the positive ions tend to be larger, and the difference between positive and negative ions is greatest at the positions with high positive (or negative) charges. A rough estimate is that $Q = -23\text{--}24$ gauss for a neutral carbon atom, and varies in a range of ± 10 per cent between the different positions.

† Further work by the author greatly strengthens their theory.

A possible explanation is that a negative charge makes the electron cloud of the C-H bond expand and decreases the hyperfine interaction, while a positive one has the opposite effect.

De Boer and Weissman were able to understand most of their negative ion spectra [3] with a simple Hückel treatment of the π electron spin distribution, except that each radical needed a different value of Q .

According to the arguments above the actual variations of Q are too small to agree with their results, and we shall now try to reinterpret their spectra with a single value of Q and improved calculations of the spin densities, ignoring the small changes which may arise from the uneven charge distribution of these ions. In the present calculations each splitting constant depends on the parameter λ as well as Q , and both quantities are found empirically. If our theory is correct λ should be close to the value in (6.2), while if Hückel theory alone were adequate it will be very small. We used the total widths of the spectra to find Q and λ , since this quantity will not be much affected by variations of Q from one position to another or by disagreement between the calculated and experimental spin densities. The first stage was to calculate widths with $Q = -22.5$ gauss and the λ 's given by the procedure of (6.1). Then we multiplied each λ by a constant x , and each Q by another, y , and calculated new widths, choosing x and y by the method of least squares to fit the observed widths of nine negative ion spectra. The result was that $x = 1.00$ and $Q = -24.2$ gauss, showing that the corrections given by the extended Hartree-Fock wave function are indeed important, and the Pariser-Parr theory estimates their magnitude rather well. In the table below we compare the observed widths with our best theoretical estimate.

Ion	Obs. width (gauss)	Calc. width (gauss)
Benzene	22.5	24.2
Naphthalene	26.9	26.0
Diphenyl	23.8	22.4
Anthracene	28.4	26.9
Phenanthrene	24.5†	27.1
Perylene	28.3	28.1
Pyrene	31.2†	29.5
Acenaphthylene	29.2†	28.1
Fluoranthene	21.9†	21.5

Table 1. Widths of negative ion spectra.

† Spectra incompletely resolved. Width is average of that between the ends of the derivative curve and that between the extreme peaks.

8. ALTERNANT HYDROCARBON NEGATIVE IONS

In this section we compare the spectrum of each of the ions in table 1 with our calculations and discuss the results. To compare spin densities and splitting constants Q was taken equal to -24.2 gauss, and λ was given the value derived from (6.1). Figure 1 shows our labelling of the different ring positions, and in the table below each row lists the splitting constant at each position (in gauss) as the upper entry, and the spin density as the lower one. Since Q has a negative sign splitting constants are negative too, unless the spin density itself is negative. To avoid confusion we give only the magnitudes of the splitting constants.

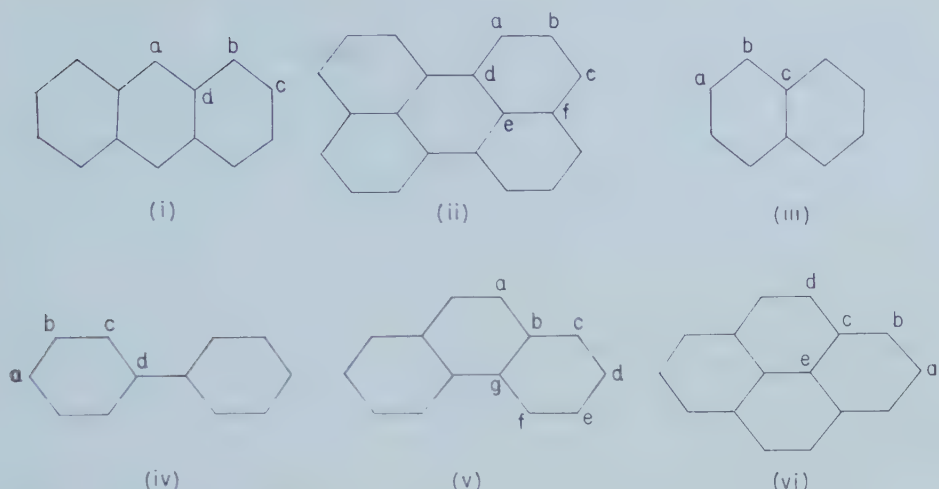


Figure 1. Alternant hydrocarbon negative ions. (i) Anthracene, (ii) perylene, (iii) naphthalene, (iv) diphenyl, (v) phenanthrene, (vi) pyrene.

In these ions the extended Hartree-Fock method gives a π electron spin distribution in which the largest part is due to the electron in the lowest anti-bonding orbital, while the unpaired spins of the underlying half-filled electron shell give a small correction which can sometimes lead to negative spin densities. Negative spin densities play an important part in the pyrene negative ion, as De Boer and Weissman suspected from its inexplicable spectrum, but they are also predicted in the spectra of diphenyl, phenanthrene, and perylene. In these ions one would have to measure the signs of the splitting constants, as simple molecular orbital theory gives almost the same numerical values.

Anthracene

Method	Width (gauss)	H.F.S. and spin densities			
		<i>a</i>	<i>b</i>	<i>c</i>	<i>d</i>
Experiment [22]	28.4	5.56 0.230	2.74 0.113	1.57 0.064	— (-0.042)
Theory $(\lambda = 1.14)$	26.9	6.18 0.256	2.85 0.118	0.77 0.032	— -0.028

Perylene

Method	Width (gauss)	H.F.S. and spin densities					
		<i>a</i>	<i>b</i>	<i>c</i>	<i>d</i>	<i>e</i>	<i>f</i>
Experiment [22]	28.3	3.09 0.128	0.46 0.019	3.53 0.146	—	—	—
Theory $(\lambda = 1.00)$	28.1	2.78 0.115	0.75 -0.031	3.49 0.145	— 0.034	— -0.028	0.003

In anthracene and perylene the observed and calculated spectra clearly agree quite well, but the other ones need more detailed discussion.

Naphthalene

Method	Width (gauss)	H.F.S. and spin densities			Ratio $b:a$
		a	b	c	
Experiment [22]	26.9	1.83 0.076	4.90 0.203	— (-0.058)	2.7
Theory ($\lambda=1.00$) β 's equal	26.0	1.14 0.047	5.37 0.222	— -0.037	4.7
Theory ($\lambda=1.00$) β 's variable	25.7	1.33 0.055	5.10 0.211	— -0.032	3.8

Our first calculation, for a molecule with all resonance integrals equal, gives spin densities similar to those found by Hoijink [7]. In contrast to the simple Hückel treatment, which correctly predicts the ratio $\rho_b:\rho_a=2.61$, ours gives a much higher value. The induced part of the spin density increases ρ_b and lowers ρ_a so that $b:a$ becomes too large. This is due to the law of alternating polarity, and seems to be an essential feature of our theory. One possible reason for the poor agreement with experiment may be that the short and long bonds have different resonance integrals, β_{rs} . We therefore repeated the calculation, allowing for the variation of β with bond length according to an empirical formula suggested by Longuet-Higgins and Salem [23]:

$$\beta(r) = \beta_0 \exp [-(r - 1.40 \text{ \AA})/a]$$

with $a=0.311 \text{ \AA}$ and the bond lengths found from x-ray data [24]. The new results do fit better, but are still not satisfactory.

Both calculations predict a negative spin density of about -0.035 at position c , which might show itself if ^{13}C were substituted there.

Diphenyl

Method	Width (gauss)	H.F.S. and spin densities			
		a	b	c	d
Experiment [22]	23.8	5.50 0.227	0.45 0.019	2.75 0.113	— (0.085)
Theory ($\lambda=1.09$), planar	22.3	5.04 0.208	0.55 -0.023	2.52 0.105	— 0.128
Theory ($\lambda=1.09$), twisted	16.6	4.95 0.205	0.10 -0.004	1.58 0.065	— 0.172

The two rings of diphenyl do not lie in one plane, but are twisted relative to one another both in the vapour and in solutions [25]. This should affect the resonance integral β' of the central bond, and it is interesting to see whether the

electron resonance spectrum of the negative ion differs from what we expect in a planar molecule. Our first calculation, for a planar molecule with all resonance integrals equal, fits Carrington's spectrum almost perfectly; the second, for a twisted one with $\beta' = \frac{1}{2}\beta$, fails completely. Admittedly these are crude calculations, but we conclude that the conjugation across the rings of diphenyl is not seriously affected by its twisted shape, or else that the ion is planar. This configuration might allow more of the excess charge to migrate to opposite ends of the molecule and lower its energy. (Hoijtink's spin densities [7] require correction because they do not add up to one.)

Phenanthrene

Method	Width (gauss)	H.F.S. and spin densities						
		a	b	c	d	e	f	g
Theory ($\lambda=1.16$)	27.1	4.75 0.196	— 0.003	3.84 0.159	1.02 -0.042	3.02 0.125	0.91 0.038	— 0.021

De Boer's spectrum [3, 26] is not completely resolved, so that its analysis is uncertain. The 29 lines fall into seven main groups with a total width of 24.5 gauss. Our calculation overestimates this width, but the theoretical ratios $a:c:d:e:f=5:4:1:3:1$ lead to a reconstruction of the spectrum which fits De Boer's in every detail (see figure 2).

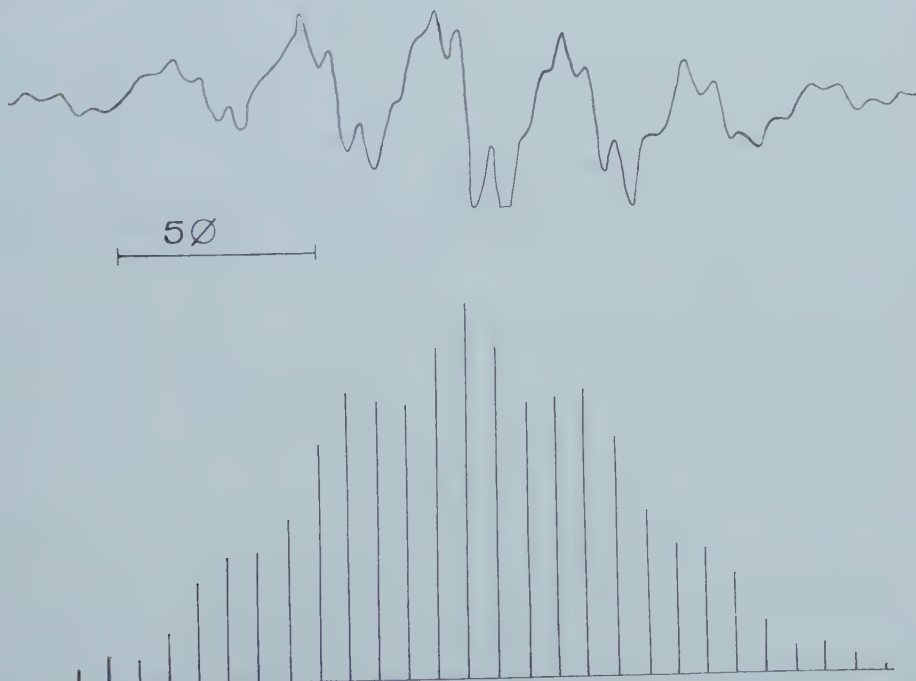


Figure 2. Electron resonance spectrum of phenanthrene⁻ and its theoretical reconstruction.

Pyrene

Method	Width (gauss)	H.F.S. and spin densities				
		a	b	c	d	e
Experiment [3]	31·2	1·3 -0·054	5·8 0·240	— —	1·3 0·054	— —
Theory ($\lambda = 1\cdot16$)	29·5	1·25 -0·052	4·52 0·187	— 0·002	2·23 0·092	— -0·012

The spectra we have met so far can all be interpreted reasonably well by simple Hückel theory, but pyrene is an important exception. Here the odd orbital has a node through (a) and (e), and the hyperfine splitting should all be from the hydrogens at (b) and (d), giving a spectrum of at most 25 lines [3]. In fact there are 35, forming five equidistant septets, so that the Hückel theory is wrong, and there is an appreciable unpaired spin density at (a). De Boer showed by comparison with deuterated compounds that the splitting at (b) is 5·8 gauss. In view of this the simplest explanation of the spectrum is that (a) and (d) are equivalent with splittings of $\pm 1\cdot3$ gauss.

Our extended Hartree-Fock wave function immediately explains the spin density at (a), which is negative, and gives a good estimate of its value.

9. NON-ALTERNANT IONS

In these compounds with odd-numbered rings of carbon atoms the electronic states cannot be paired as they are in alternant hydrocarbons. This has two effects. First there is no longer any reason why the spectra from the positive and negative ions of a non-alternant molecule should be alike. Secondly many of the features which make the theoretical treatment of alternant radicals specially simple disappear. The electron density is not uniform in the neutral molecule, and there are bond orders between atoms which are second neighbours. Although much of the theory in the first part of this paper is perfectly general, these differences affect some of the details. Equations (5.1) and (5.5) no longer hold, and we are no longer justified in neglecting atom-bond polarizabilities in the derivation of (5.7) from (5.6).

In spite of this objection we did in fact use (5.7) for simplicity, and believe that the bond terms will not affect the spin densities very much. The 12×12 or 16×16 secular equations for the molecular orbitals of different spins were solved quickly and easily on the Ferranti Pegasus electronic computer at Southampton University, with the kind cooperation of Mr. Ray Hardiman and Dr. Alan Carrington.

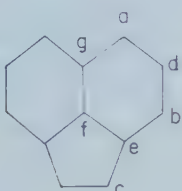
The ring positions are labelled in figure 3.

Acenaphthylene-

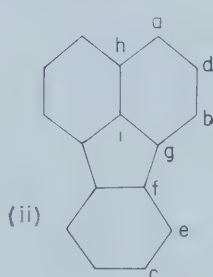
The spectrum is not fully resolved, but the observed pattern of 11 lines is consistent with splitting constants in the ratio $a:b:c:d=2:2:1:0$ given by the Hückel theory. The numerical values in the table then agree with the total width. Our calculated splitting constants fit fairly well, although their ratios are closer to $a:b:c:d=5:4:2:$

Acenaphthylene⁻

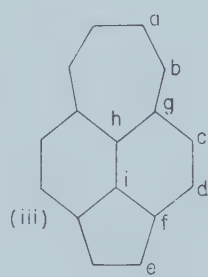
Method	Width (gauss)	H.F.S. and spin density						
		a	b	c	d	e	f	g
Experiment [3]	29·2	5·4 0·223	5·4 0·223	2·7 0·112	0·0 0·000	—	—	—
Theory ($\lambda = 1\cdot00$)	28·1	5·92 0·245	4·74 0·196	2·90 0·101	0·99 -0·041	— 0·027	— -0·012	— -0·045



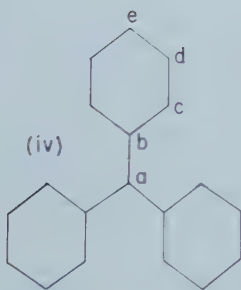
(i)



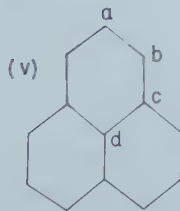
(ii)



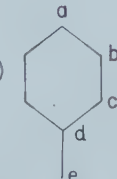
(iii)



(iv)



(v)



(vi)

Figure 3. Non-alternant negative ions and odd alternant radicals. (i) Acenaphthylene, (ii) fluoranthene, (iii) acepleiadylene, (iv) triphenylmethyl, (v) perinaphthetyl, (vi) benzyl.

Fluoranthene⁻

Method	Width (gauss)	H.F.S. and spin density				
		a	b	c	d	e
Experiment [3]	21·9	5·2 0·215	3·9 0·161	1·3 0·054	0·0 0·000	0·0 0·000
Theory ($\lambda = 1\cdot00$)	21·5	5·49 0·227	3·79 0·157	0·90 0·037	0·54 -0·023	0·00 0·000
		f	g	h	i	
		0·064	0·063	-0·039	-0·013	

Theory and experiment agree quite well if we accept this interpretation of the 17 line spectrum, which gives $a:b:c:d:e$ the ratio 4:3:1:0:0 predicted by Hückel theory.

Acepleiadylene \pm

The spectra of these two ions are quite different, as is expected for non-alternant radicals. However, they do not agree at all with either Hückel or extended Hartree-Fock calculations, which is more surprising. While the negative ion has about the expected width, and its spectrum may arise from a spin distribution bearing some resemblance to the calculated ones, the enormous width of the positive one suggests a far more serious divergence. The Hückel orbitals occupied by the odd electrons in both ions are almost degenerate, so that a distortion of the carbon skeleton may be possible. We assumed that the odd orbital was always the antisymmetrical member of the almost degenerate pair, and then calculated the following results.

Ion	Width (gauss)	H.F.S. and spin density								
		<i>a</i>	<i>b</i>	<i>c</i>	<i>d</i>	<i>e</i>	<i>f</i>	<i>g</i>	<i>h</i>	<i>i</i>
Negative ion ($\lambda=1.00$)	21.8 (obs. 25.0)	2.51 0.104	0.05 0.002	1.14 -0.047	4.45 0.184	2.30 0.095	- 0.007	- 0.175	- -0.033	- 0.006
Positive ion ($\lambda=1.00$)	21.8 (obs. 45.9)	1.18 0.049	3.38 0.140	4.41 0.183	0.83 -0.034	1.41 0.058	- 0.143	- -0.021	- -0.004	- -0.029

10. NEUTRAL ALTERNANT RADICALS

The electron resonance spectra of odd alternant radicals like triphenylmethyl or perinaphthetyl are explained very nicely by the valence bond theory [27, 28, 29]. The absence of odd-membered rings allows the formation of a ground state in which every canonical structure has the same sign [30] and as a result the spin density alternates in sign across each bond, being positive on all the starred atoms and negative on the others. The calculated spin distributions agree well with the spectra, although they slightly exaggerate the alternations of sign.

The extended Hartree-Fock treatment leads to similar conclusions. The odd electron in these radicals occupies a non-bonding orbital with nodes on every unstarred atom, so that Hückel theory gives a positive spin density on each starred atom and zero on the others. If, however, electrons of different spins are allowed to move in different sets of orbitals, the energy is lowest when there is an excess of α spin on the starred atoms and of β spin on the others. According to (6.3) the spin densities would alternate in sign on every odd alternant radical if the mutual polarizabilities π_{rs} obeyed the law of alternating polarity. Unfortunately this law does not hold generally in radicals, but we expect that the spin distribution will often alternate in spite of this.

We now compare the calculated and observed splitting constants in detail. (The ring positions are shown in figure 3.)

Perinaphthyl

Method	Width (gauss)	H.F.S. and spin density			
		a	b	c	d
Experiment [31]	50.4	2.2 -0.091	7.3 0.302	—	—
Hartree-Fock ($\lambda = 1.15$)	37.9	1.68 -0.070	5.48 0.226	-0.052	0.006
Valence bond [29]	59.9	4.25 -0.176	7.86 0.325	—	—

Both calculations account for the main features of the spectrum. The first underestimates the width, but gives the correct ratio of $\rho_a : \rho_b$; the second overestimates the width but predicts ρ_b correctly.

Triphenylmethyl

Method	Width (gauss)	Ratio $c:d:e$	H.F.S. and spin density				
			a	b	c	d	e
Experiment [32]	36	2:1:2	— 0.68	— —	3.0 0.124	1.5 -0.062	3.0 0.124
Hartree-Fock (planar, $\lambda = 1.14$)	30.3	2.6:1:2.3	— 0.413	— -0.045	2.76 0.114	1.06 -0.044	2.44 0.101
Valence bond (planar)	57.2	1.9:1:1.8	— 0.564	— -0.230	4.83 0.200	2.51 -0.104	4.40 0.182
Hartree-Fock (twisted, $\lambda = 1.14$)	26.9	2.5:1:2.2	— 0.516	— -0.047	2.44 0.101	0.99 -0.041	2.10 0.087
Valence bond (twisted)	54.3	1.9:1:1.8	— 0.616	— -0.226	4.54 0.188	2.39 -0.099	4.23 0.175

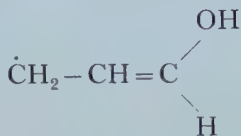
Jarrett's complicated spectrum [32] still defies complete analysis, but the 21 main lines can be accounted for on the assumption that the ratio $c:d:e$ is approximately 2:1:2. This interpretation agrees with Brovetto and Ferroni's valence bond calculations and is also supported by recent experiments on deuterated compounds [33]. One then obtains the 'experimental' splitting constants given above. The spin density at the centre was deduced by Adam and Weissman from ^{13}C hyperfine structure in solution and dipolar broadening in crystals. It is harder to judge the accuracy of this value.

Brovetto and Ferroni assumed a planar molecule with all exchange integrals equal for their calculation, which overestimates the spin densities on the rings, while Adam and Weissman obtained better results by allowing for twisted central bonds with $J' = 0.85J$. Our Hartree-Fock calculation for a planar molecule

succeeds fairly well, although the spin densities on the rings are a little too small, but the calculation for twisted central bonds with $\beta' = 0.8660\beta$ (angle of twist 30°) gives far too narrow a spectrum. Both calculations account for the essential features of the spin distribution, but the results are too inaccurate to support any reliable conclusion about the shape of this radical.

Allyl

Our contribution to the ever-increasing number of computations on this radical [34, 35] gives spin densities of 0.594, -0.187 and 0.594 on the three carbon atoms ($\lambda = 1.06$). The radical



which is similar to allyl is believed to be formed by the ultra-violet irradiation of allyl alcohol in a glass containing hydrogen peroxide frozen at 70°K [36]. The spectrum is a 1-3-3-1 quartet with a width of 30 gauss, and suggests splittings of 10 gauss from each of the end hydrogens. The lines are too broad to reveal any splitting from the central position.

Benzyl

No spectra have yet been reported for this radical, but a radical with similar electronic structure is the nitrobenzene negative ion [37], in which the odd orbital is probably a linear combination of the symmetric antibonding π orbital of the nitro group with the $2p_z$ orbitals of the benzene ring. The hyperfine splittings at (a), (b) and (c) are found to be 3.7, < 0.65, and 3.7 gauss, in agreement with simple Hückel theory. This is surprising, since for benzyl itself we calculate the following values with a negative spin density at b.

Position	a	b	c	d	e
Splitting constant (gauss)	3.30	1.51	3.88	—	18.60
Spin density ($\lambda = 1.00$)	0.137	-0.063	0.161	-0.102	0.770

11. CONCLUSIONS

While it would be rash to claim that the electronic structure of these hydrocarbon radicals is completely understood, the extended Hartree-Fock method accounts for the essential features of all the spectra for which calculations have been made, with the exception of the acepleiadylene ions. It shows that the occurrence of negative spin densities is perfectly normal in ions as well as neutral radicals, although the special form of the non-bonding orbital in a neutral radical favours a spin distribution which alternates in sign from starred to unstarred atoms, and often leads to large negative values. Alternant hydrocarbons are a class of compounds whose peculiar 'paired' electronic structure can be treated successfully by simple theories, so that we cannot hope to obtain such good

results with other types of free radical. Some of the discrepancies in the spectra of the negative ions might be removed by allowing for the variable strength of different bonds, but one cannot expect a crude theory to give exact numerical results. In neutral radicals our assumption that the negative spin densities arise from a small perturbation effect is questionable, and a new theory midway between the molecular orbital and valence bond ones would be useful. Lowdin's projection operator formalism might be suitable if the difficulties with nonorthogonal orbitals were overcome.

The extended Hartree-Fock method has the advantages of flexibility and physical simplicity, and could be applied to substituted hydrocarbon radicals like the methylnaphthalene ions, and heterocyclic ones like the phenazine negative ion.

I would like to thank Dr. Alan Carrington and Mr. Ray Hardiman of Southampton University for computing many of the molecular orbitals required, especially those in the non-alternant ions; Professor C. A. Coulson, F.R.S. for the use of his tables of molecular orbital coefficients and mutual polarizabilities; Professor H. C. Longuet-Higgins, F.R.S. for many ideas and suggestions at all stages of this work, and the Department of Scientific and Industrial Research for a maintenance grant in 1957-58.

REFERENCES

- [1] McCONNELL, H. M., 1956, *J. chem. Phys.*, **24**, 362; DE BOER, E., 1956, *J. chem. Phys.*, **25**, 190; TUTTLE, T. R., WARD, R. L., and WEISSMAN, S. I., 1956, *J. chem. Phys.*, **25**, 189.
- [2] McCONNELL, H. M., and CHESNUT, D. B., 1958, *J. chem. Phys.*, **28**, 107.
- [3] DE BOER, E., and WEISSMAN, S. I., 1958, *J. Amer. chem. Soc.*, **80**, 4549.
- [4] ROOTHAN, C. C. J., 1951, *Rev. mod. Phys.*, **23**, 69.
- [5] POPLE, J. A., 1953, *Trans. Faraday Soc.*, **49**, 1375.
- [6] LONGUET-HIGGINS, H. C., and POPLE, J. A., 1955, *Proc. phys. Soc. Lond.*, A, **68**, 591.
- [7] HOIJTINK, G. J., 1958, *Mol. Phys.*, **1**, 157.
- [8] POPLE, J. A., and NESBET, R. K., 1954, *J. chem. Phys.*, **22**, 571.
- [9] LÖWDIN, P. O., 1955, *Phys. Rev.*, **97**, 1509.
- [10] WOOD, J. H., and PRATT, G. W., 1957, *Phys. Rev.*, **107**, 995.
- [11] BRICKSTOCK, A., and POPLE, J. A., 1954, *Trans. Faraday Soc.*, **50**, 901.
- [12] PARISER, R., and PARR, R. G., 1953, *J. chem. Phys.*, **21**, 466, 767.
- [13] BRICKSTOCK, A., 1954, Ph.D. Thesis, Cambridge.
- [14] COULSON, C. A., and LONGUET-HIGGINS, H. C., 1947, *Proc. roy. Soc. A*, **191**, 39; **192**, 16.
- [15] McLACHLAN, A. D., 1959, *Mol. Phys.*, **2**, 271.
- [16] BRION, H., LEFÈVRE, R., and MOSER, C., 1958, *J. Chim. phys.*, **54**, 363.
- [17] McCONNELL, H. M., 1956, *J. chem. Phys.*, **24**, 764.
- [18] COLE, T., HELLER, C., and McCONNELL, H. M., 1959, *Proc. nat. Acad. Sci., Wash.*, **45**, 525.
- [19] COLE, T., PRITCHARD, H. O., DAVIDSON, N. R., and McCONNELL, H. M., 1958, *Mol. Phys.*, **1**, 406.
- [20] WEISSMAN, S. I., TUTTLE, T. R., and DE BOER, E., 1957, *J. phys. Chem.*, **61**, 28.
- [21] McCONNELL, H. M., 1956, *J. chem. Phys.*, **24**, 632.
- [22] CARRINGTON, A., DRAVNIEKS, F., and SYMONS, M. C. R., 1959, *J. chem. Soc.*, 947.
- [23] LONGUET-HIGGINS, H. C., and SALEM, L., 1959, *Proc. roy. Soc. A*, **251**, 172.
- [24] AHMED, F. R., and CRICKSHANK, D. W. J., 1952, *Acta cryst.*, **5**, 852.
- [25] BASTIANSEN, O., 1949, *Acta chem. scand.*, **3**, 408.
- [26] DE BOER, E., 1957, Ph.D. Thesis, Amsterdam.
- [27] BROVETTO, P., and FERRONI, S., 1957, *Nuovo cim.*, **5**, 142.

- [28] ADAM, F., and WEISSMAN, S. I., 1958, *J. Amer. chem. Soc.*, **80**, 2057.
- [29] McCONNELL, H. M., and DEARMAN, H. H., 1958, *J. chem. Phys.*, **28**, 51.
- [30] McLACHLAN, A. D., 1959, *Mol. Phys.*, **2**, 223.
- [31] SOGO, P. B., NAKAZAKI, M., and CALVIN, M., 1957, *J. chem. Phys.*, **26**, 1343.
- [32] JARRETT, H. S., and SLOAN, G. J., 1954, *J. chem. Phys.*, **22**, 1783.
- [33] REITZ, D. C., 1959, *J. chem. Phys.*, **30**, 1364.
- [34] CHALVET, O., and DAUDEL, R., 1952, *J. Chim. phys.*, **49**, 629.
- [35] McCONNELL, H. M., 1958, *J. chem. Phys.*, **28**, 1188; 1959, **30**, 328; 1958, **29**, 244.
- [36] SYMONS, M. C. R., *et al.*, 1957, *Trans. Faraday Soc.*, **53**, 914.
- [37] WEISSMAN, S. I., 1955, *Disc. Faraday Soc.*, **19**, 147; WARD, R. L., and KLEIN, M. P., 1958, *J. chem. Phys.*, **28**, 518; WARD, R. L., 1959, *J. chem. Phys.*, **30**, 852.

Solvent effects in the proton resonance spectra of dimethyl-formamide and dimethyl-acetamide

by J. V. HATTON and R. E. RICHARDS

Physical Chemistry Laboratory, South Parks Road, Oxford

(Received 4 February 1960)

Changes in the nuclear magnetic resonance spectra of dimethyl-formamide and dimethyl-acetamide have been studied in various solvents over a range of concentrations. It is shown that addition of aromatic solvents causes the relative chemical shifts of the two methyl resonances to change sign. This shows that no rapid reorientation of the dimethyl amino group occurs in these solutions at room temperature, and the shifts observed are interpreted in terms of the formation of loose complexes between the amide and the aromatic molecule.

1. INTRODUCTION

In liquid dimethyl-formamide, and dimethyl-acetamide, the resonance of the hydrogen atoms of the methyl groups attached to the nitrogen atom is a doublet, the two lines being separated by 5.2 c/s at 29.92 Mc/s. These doublets have been attributed [1] to the planar structure of the molecules, resulting in a difference between the methyl groups, one being closer to the carbonyl oxygen atom than the other.

Certain interesting changes in the spectra of these N-dimethyl groups have been observed in these compounds by varying the temperature [2] or by the addition of solvents [3]. As the temperature is raised, the doublet resonance gradually coalesces, and this has been interpreted [2] in terms of interchange of the methyl groups by rotation about the C-N bond. From this work Gutowsky and Holm [2] deduce potential barriers to rotation about the C-N bond of 22 and 19 k cal/mole for dimethyl-formamide and dimethyl-acetamide respectively.

Interaction with a solvent can also produce changes in the spectra even at room temperature [3]. Fraenkel and Niemann [4] have measured shifts of dimethyl-formamide and dimethyl-acetamide in solutions in water, heavy water, pure sulphuric acid and heavy sulphuric acid, and conclude that protonation at the oxygen atom is favoured in some circumstances. Berger, *et al.* [5] interpret changes in the nuclear magnetic resonance spectra of dimethyl-acetamide in solutions of different pH as due to protonation at the nitrogen or oxygen atom, depending on the nature of the solution. In very acid conditions, they believe that protonation occurs predominantly at the oxygen atom, but that both species are in equilibrium. Kumler [6], however, has obtained strong evidence from infra-red spectroscopic data of the hydro and deutero chlorides of many amides that protonation or deuteration occurs only at the nitrogen atom. Effects of environment on the nuclear resonance spectra of dimethyl-formamide and of dimethyl-acetamide have therefore been studied in greater detail in order to resolve these difficulties.

2. EXPERIMENTAL

The nuclear resonance spectra were recorded at 29.9200 Mc/s on the high resolution spectrometer described previously [7]. Chemical shifts were measured with respect to cyclohexane as an internal standard and are quoted in c/s. The instrument was adjusted to repeat the recording of the doublet resonance about 25 times and the mean value of the spacings was taken. The base line was calibrated using the conventional side band technique.

The dimethyl-formamide, dimethyl-acetamide and liquid solvents were all purified before use. Solutions were prepared to include mole fractions of amide in the range 0.05–0.90, but in some cases the range was limited by the solubilities.

3. RESULTS

The resonances of the methyl groups of dimethyl-formamide can be distinguished because each component of the doublet is itself split into a closely spaced doublet by spin–spin coupling with the hydrogen atom of the formyl group. The coupling constants to the methyl groups are not equal and are found to be 0.65 ± 0.05 c/s and ≈ 0.3 c/s as shown in figure 1. The high field resonance in a pure liquid is most strongly coupled to the formyl hydrogen and this resonance line will be referred to as the β line; the resonance lying at lower fields in the pure material will be referred to as the α line.

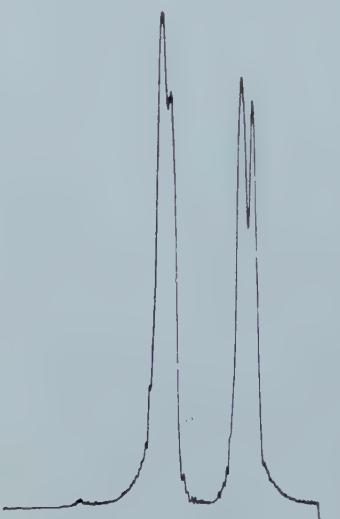


Figure 1. The methyl resonances of liquid dimethyl formamide.

In dimethyl-acetamide, the two methyl resonances are also distinguishable, because the β line is broader than the α line; they are presumably unresolved quartets in which the coupling constants are different.

The behaviour of these resonances in solutions can be classified according to the type of solvent. Aliphatic solvents and water produce only small effects, whereas aromatic substances cause marked changes in the spectrum.

3.1. Aliphatic solvents

The chemical shifts of the N-dimethyl groups of dimethyl-formamide and dimethyl-acetamide were measured at various concentrations in chloroform, cyclohexane, propargyl chloride and water. In each case the mean shift of the doublet resonance with respect to cyclohexane internally, remained constant. The doublet separation became smaller as the mole fraction of amide was reduced. The results are shown in the table. Addition of water produces very little change in the spectra, but for the solvents of relatively low dielectric constant, the doublet closes from a separation of 5.2 c/s in the pure liquid to about 2.5 c/s at 0.1 mole fraction of amide.

Dimethyl-formamide			Dimethyl-acetamide		
Solvent	Mole fraction Dimethyl-formamide	Doublet separation (c/s)	Solvent	Mole fraction Dimethyl-acetamide	Doublet separation (c/s)
Cyclohexane	0.81	5.16	Water	0.43	5.05
	0.55	2.69		0.20	4.70
	0.19	2.75		0.13	4.95
Water	0.58	5.00	Chloroform	0.65	4.70
	0.47	5.10		0.39	4.00
	0.15	4.70		0.18	2.80
Propargyl chloride	0.94	5.10	Cyclohexane	0.75	5.10
	0.76	4.70		0.61	5.00
	0.43	4.50		0.24	4.20
	0.14	3.50			
Chloroform	0.68	4.50			
	0.46	4.00			
	0.23	3.40			
	0.06	2.50			

3.2. Aromatic solvents

The behaviour of the methyl resonances in aromatic solvents is more complicated. As the proportion of aromatic solvent is increased the resonances of both methyl groups shift to higher fields, but the α resonance shifts by a greater amount than the β , so that the two lines appear to coalesce at a certain concentration and then to cross over as the amide concentration is reduced still further. The results are presented in figures 2-10, in which the magnetic field increases from left to right. Figure 11 shows the changes in the methyl resonances in two typical cases, in concentration ranges over which the two lines coalesce.

4. DISCUSSION

4.1. The pure liquids

The two chemically shifted methyl resonances with a field dependent separation, arise from the planar character of the molecules. One methyl group is closer to the carbonyl group than the other and has a different chemical shift.

Figure 2.

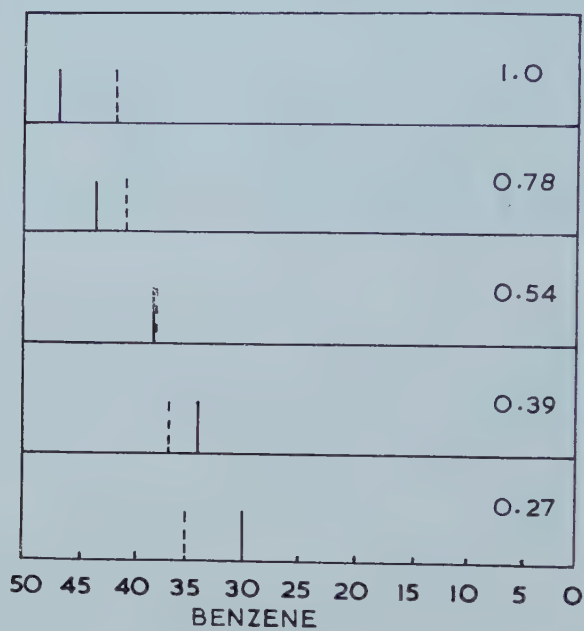
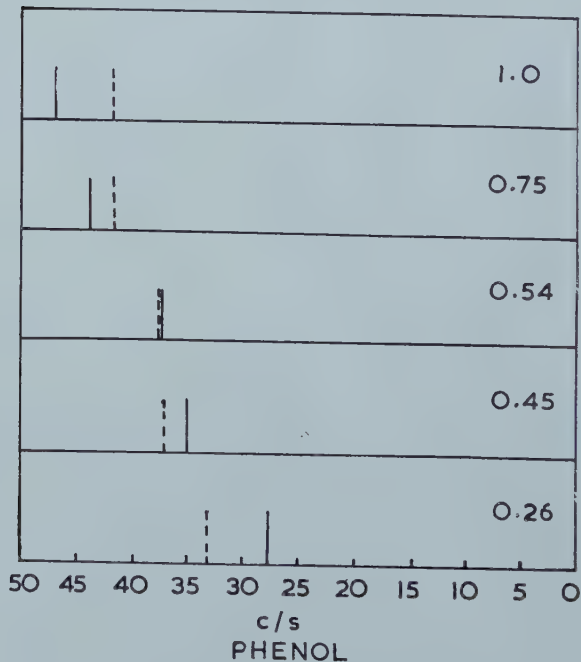


Figure 3.



Figures 2 and 3. Effects of concentration on the shifts of N-methyl resonances of N,N-dimethyl formamide. Shifts are in c/s from cyclohexane used as an internal standard. Mole fractions of amide are given with each spectrum.

Figure 4.

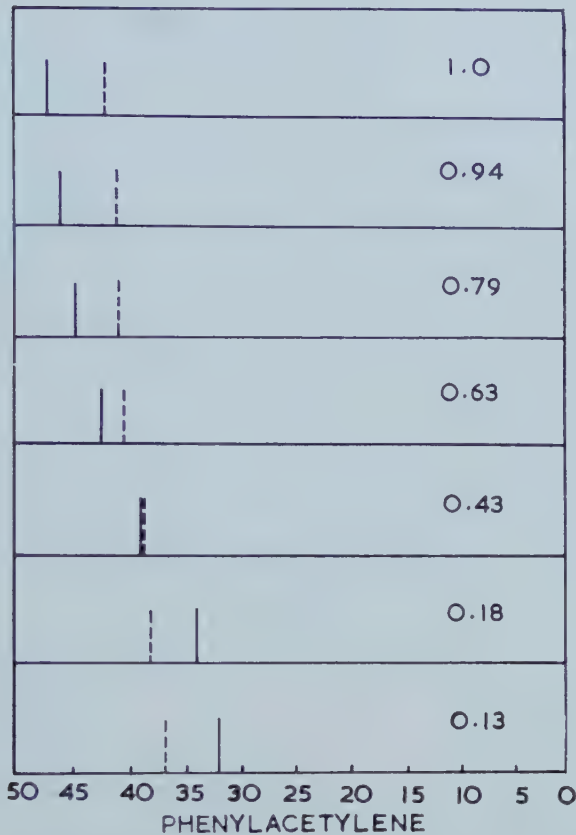
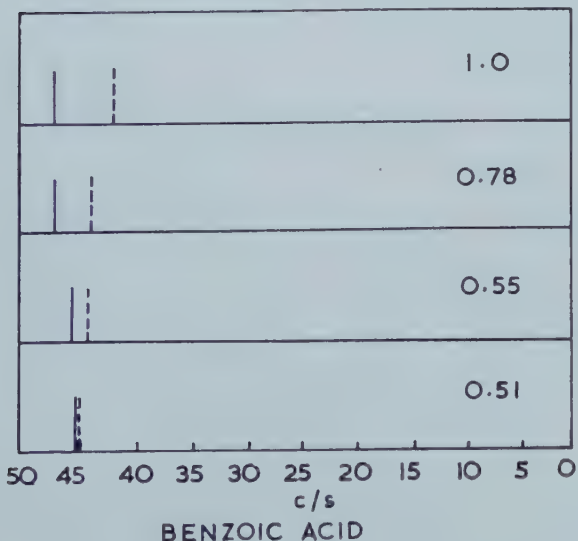


Figure 5.



Figures 4 and 5. Effects of concentration on the shifts of N-methyl resonances of N, N-dimethyl formamide. Shifts are in c/s from cyclohexane used as an internal standard. Mole fractions of amide are given with each spectrum.

Figure 6.

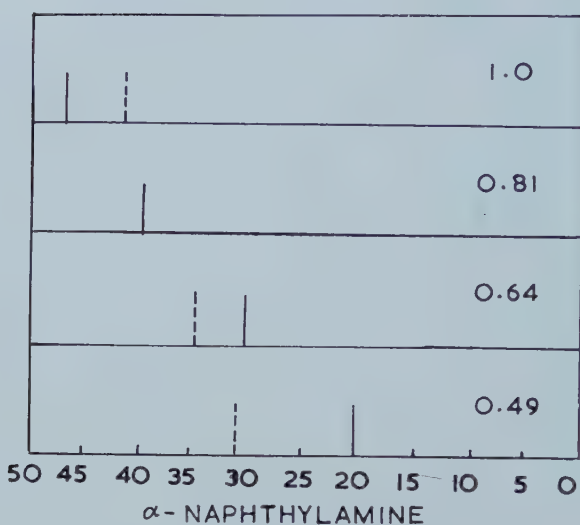
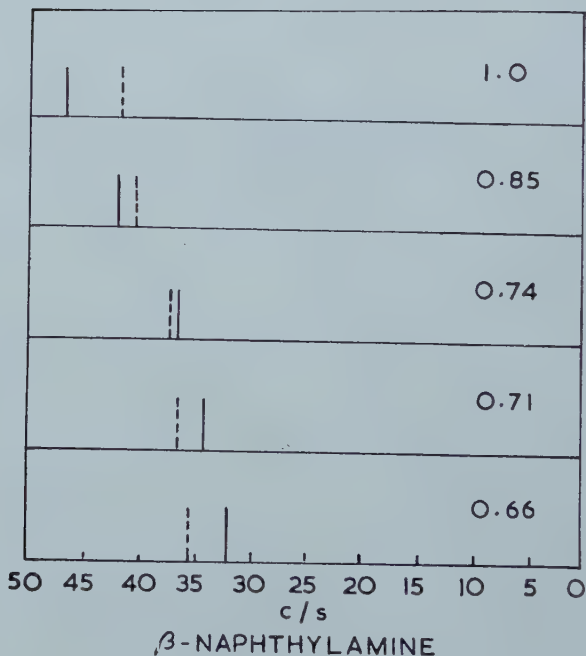


Figure 7.



Figures 6 and 7. Effects of concentration on the shifts of N-methyl resonances of N, N-dimethyl formamide. Shifts are in c/s from cyclohexane used as an internal standard. Mole fractions of amide are given with each spectrum.

Figure 8.

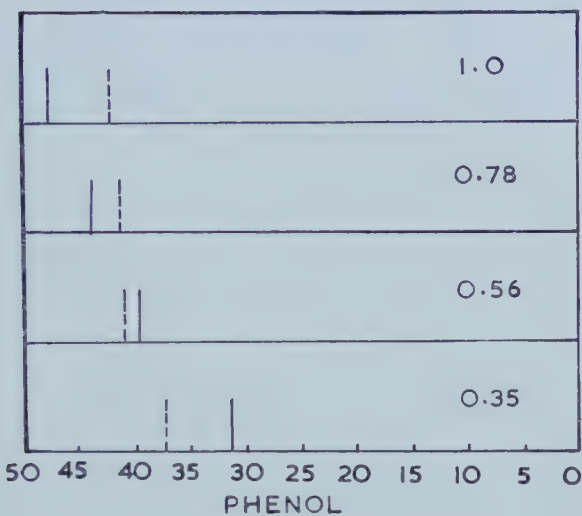
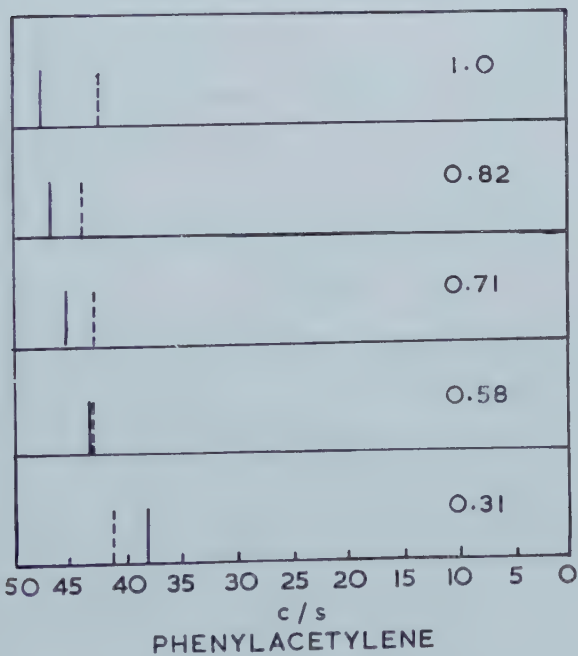


Figure 9.



Figures 8 and 9. Effects of concentration on the shifts of the N-methyl resonances of N,N-dimethyl acetamide. Shifts are in c/s from cyclohexane used as an internal standard. Mole fractions of amide are given with each spectrum.

The spin-spin coupling constant between the hydrogen of the HCO group in dimethyl-formamide and the two methyl groups are different and it is probable [8] that the largest coupling constant is associated with the methyl group *trans* to the hydrogen of the CHO group. We can therefore assign the α and the β methyl resonances as follows:

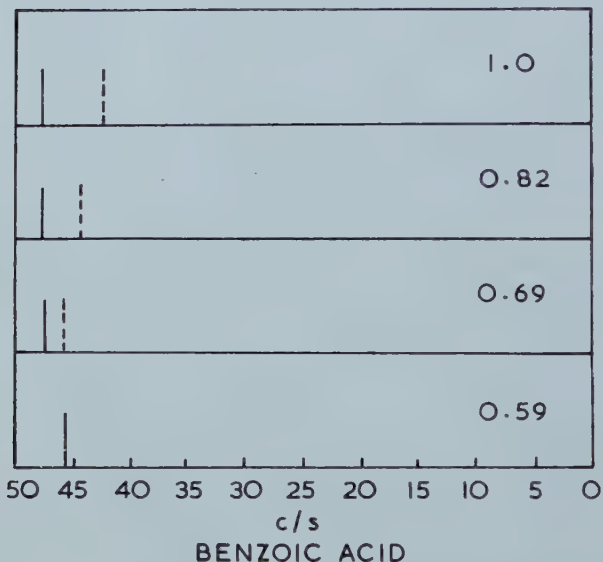
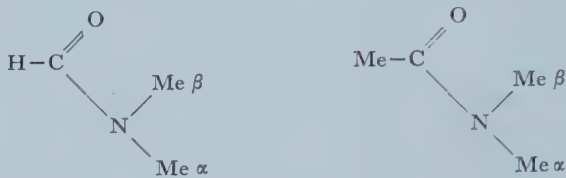


Figure 10. Effects of concentration on the shifts of the N-methyl resonances of N,N-dimethyl acetamide. Shifts are in c/s from cyclohexane used as an internal standard. Mole fractions of amide are given with each spectrum.

4.2. Non-aromatic solvents

Dilution of the amides with non-aromatic solvents causes a small reduction in the separation of the two methyl resonances. It is therefore likely that some contribution to their relative chemical shifts comes from the mutual interaction of the dimethyl-formamide molecules by dipolar association. It is not immediately obvious that the methyl group nearest to the carbonyl group should give the high field resonance, because there are so many factors affecting the chemical shifts of these hydrogens. The paramagnetic moment induced in the molecular plane is clearly smaller than in aldehydes, because the CH resonance lies at higher fields in the amides. The chemical shift of the methyl groups will be affected by this as well as by the moments induced on the nitrogen atom and the effect of the electric field from the oxygen atom. A theoretical study of chemical shifts in these amides [9] did not permit an assignment of the methyl resonances to particular methyl groups.

4.3. Aromatic solvents

The shifts of the methyl resonances have been measured with respect to the internal standard, cyclohexane. Any changes which are observed as the fraction of aromatic solvent changes therefore reflect interactions which are in addition to the normal bulk shift produced by aromatic molecules.

Both methyl resonances shift to higher fields as the fraction of aromatic component increases, and this indicates some association between the amide and

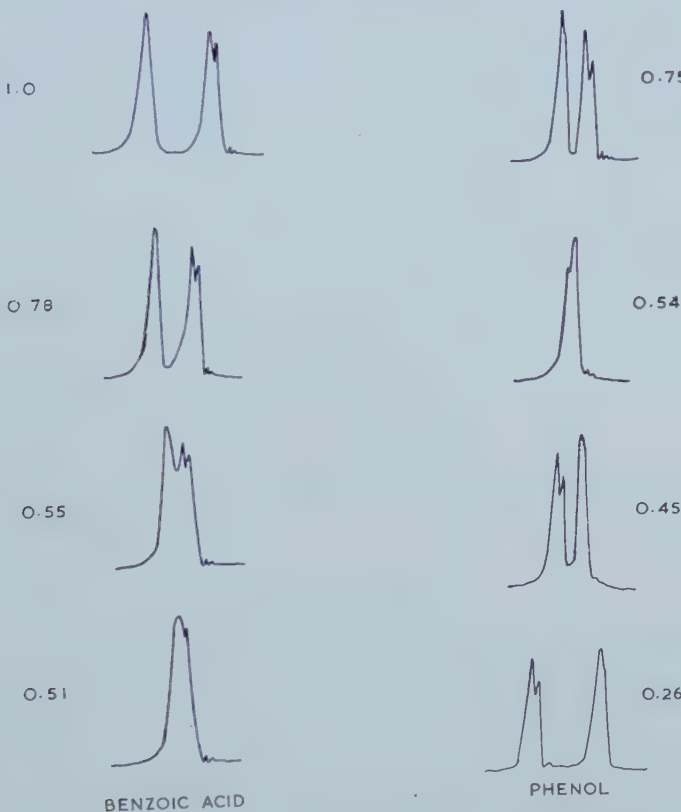
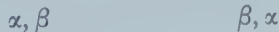


Figure 11. Methyl resonances in mixtures of phenol and of benzoic acid with N, N-dimethyl formamide.

aromatic molecules in which an orientation is preferred with the planes of the two molecules parallel. The progressive change (figure 11) in the spectrum can be interpreted in terms of an equilibrium



In the amide molecule the line due to the α methyl group lies at lower fields and in the weak associative complex between the amide and aromatic molecule the α methyl group resonance is shifted more to higher fields than that of the β methyl resonance. Their order is therefore changed. Owing to rapid exchange between the two sides of this equilibrium, the observed spectrum is a weighted intermediate between the two extremes.

The question remains as to why the relative chemical shifts of the two methyl groups change when the amide becomes associated with the aromatic molecule. It is well known [10] that some molecules such as hydrogen chloride, chloroform, and substituted acetylenes associate with aromatic substances in such a way that the positive end of the molecular dipole is situated above or below the plane of the aromatic ring. It may be that amides also associate in this way, so that the preferred arrangement is with the nitrogen, with its fractional positive charge, over the benzene ring, and with the negatively charged carbonyl oxygen as far away from the centre of the ring as possible, whilst retaining the planar association, figure 12. All arrangements of this kind leave the α methyl group near the centre of the aromatic ring and the β methyl group near the edge. The strong induced diamagnetic moment at the centre of the ring would then produce a very much bigger high field shift on the α methyl group than on the β methyl group as observed.

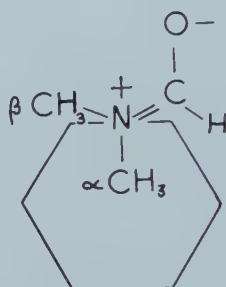
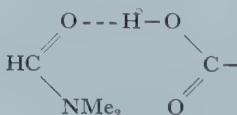


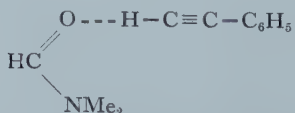
Figure 12. Possible association of amide with aromatic substance.

In accordance with this explanation, the shifts produced by naphthalene derivatives are much greater than by benzene derivatives. In naphthalene, the induced currents in the two rings reinforce one another causing a correspondingly greater diamagnetic moment at right angles to the molecular plane.

On the other hand, the effect of adding benzoic acid and phenyl acetylene is much smaller. These two molecules are expected to associate with amides by a different mechanism involving the substituent rather than the ring. Benzoic acid probably associates by hydrogen bonds, for example,



and phenyl acetylene in a similar manner



This type of association is much less likely to lead to close proximity of the aromatic ring and dimethyl amino group and so the effects on the chemical shifts of the hydrogen resonances of the methyl groups are correspondingly smaller.

The shift of the aldehyde hydrogen in dimethyl-formamide provides further information regarding the association. In the aromatic mixtures the hydrogen atom of the aldehyde group shifts to higher fields but by a smaller amount than either of the methyl resonances. For example, in a mixture of 0·61 mole fraction benzene, it shifts by 2·5 c/s to high fields. This must mean that in the associated complexes the aldehyde hydrogen is nearer the edge of the aromatic ring as it would have to be if the oxygen atom of the carbonyl group tends to lie as far away from the centre of the ring as possible. Addition of phenyl acetylene causes no shift of the hydrogen of the aldehyde group, because of the different type of association. Addition of benzoic acid causes the hydrogen resonance of the aldehyde group to shift to *lower* fields by 4 c/s at a mole fraction of benzoic acid of 0·45. This clearly implies that in this mixture the amide molecule is associated in such a way as to lie roughly in the plane of the aromatic molecule as indicated above.

Addition of benzoic acid caused no shift in the mean position of the two methyl resonances and no mixture studied showed an actual crossing over of the lines. This may be accounted for by the limited solubility of benzoic acid in dimethyl-formamide, or it is possible that in this case the change in the appearance of the methyl resonances may be due to more rapid reorientation of the dimethyl amino group permitted by the association. This question can be resolved by extending the measurements to lower and to higher temperatures, and it is hoped to do this in the near future.

In the examples where crossing over of the lines is observed, however, it is clear that rapid reorientation of the dimethyl amino group does not occur at room temperature.

ACKNOWLEDGMENTS

We are grateful to the Hydrocarbon Research Group of the Institute of Petroleum and to the Coal Board for grants in aid of apparatus. We also thank the Department of Scientific and Industrial Research for a Maintenance Grant to one of us (J.V.H.).

REFERENCES

- [1] PHILLIPS, W. D., 1955, *J. chem. Phys.*, **23**, 1363.
- [2] GUTOWSKY, H. S., and HOLM, C. H., 1956, *J. chem. Phys.*, **25**, 1228.
- [3] HUMBLE OIL N. M. R. CATALOGUE, 1958.
- [4] FRAENKEL, G., and NIEMANN, C., 1958, *Proc. nat. Acad. Sci., Wash.*, **44**, 688.
- [5] BERGER, A., LOEWENSTEIN, A., and MEIBOOM, S., 1959, *J. Amer. chem. Soc.*, **81**, 62.
- [6] KUMLER, W. D. (private communication).
- [7] LEANE, J. B., RICHARDS, R. E., and SCHAEFER, T. P., 1959, *J. sci. Instrum.*, **36**, 230.
- [8] BISHOP, E. O., and RICHARDS, R. E. (to be published).
- COHEN, A. D., SHEPPARD, N., and TURNER, J. J., 1958, *Proc. chem. Soc.*, p. 118.
- [9] NARASIMHAN, P. T., and ROGERS, M. T., 1959, *J. phys. chem.*, **63**, 1388.
- [10] REEVES, L. P. T., and SCHNEIDER, M. T. G., 1957, *Canad. J. chem.*, **35**, 251.

A test of the Lennard-Jones potential for nitrogen and methane

by J. S. ROWLINSON

Department of Chemistry, University of Manchester

(Received 7 January 1960)

The experimental behaviour of the classical fluctuation discriminant of the configurational energy and the virial is examined for the fluid states of nitrogen and methane. This discriminant must be essentially positive. It is found that the assumption of a Lennard-Jones 12 : 6 potential leads to negative values of the discriminant for the orthobaric liquids at low temperatures, for the liquids at high pressures, and, probably, for the gases at high temperatures. These results confirm those found previously for argon, and demonstrate the inadequacy of the 12 : 6 potential at high densities and temperatures.

1. INTRODUCTION

It was shown recently that the classical fluctuation discriminant of the configurational energy \mathcal{U} and virial \mathcal{V} provides a sensitive test of the Lennard-Jones 12:6 potential. A discriminant D can be defined by

$$D = [(\delta\mathcal{U}^2\delta\mathcal{V}^2)^{1/2} - |\delta\mathcal{U}\delta\mathcal{V}|]/kT. \quad (1)$$

This may be expressed in terms of the thermodynamic properties of the fluid and the repulsive index, n , of the potential [1],

$$D(n) = [TC_V^*]^{1/2} \left[-\frac{2n}{3} U^* + (PV - V/\beta_T) + \left(2 + \frac{n}{3}\right)(PV - RT) \right]^{1/2} - |TV\gamma_V - RT| \quad (2)$$

where C_V^* and U^* are the configurational heat capacity and energy, where β_T is the coefficient of isothermal compressibility, and where γ_V is $(\partial P/\partial T)_V$.

The condition that $D(n)$ is positive or zero (Schwarz's inequality) provides an experimental lower bound for n , since U^* is negative.

The best experimental results for argon suggested that $D(12)$ is negative for the orthobaric liquid near the triple point, for the fluid at high pressures and low temperatures, and for the gas at high temperatures. There is no other inert gas for which there are sufficiently good measurements for the calculation of D over wide ranges of pressure and temperature. However, nitrogen and methane are substances which, according to the criterion provided by the principle of corresponding states, have intermolecular potentials that resemble closely that of argon. Their small departures from spherical symmetry should not invalidate this method of testing the Lennard-Jones potential [1]. The discriminant $D(12)$ has therefore been calculated for the fluid states of these substances to see how closely they resemble argon.

1.1. Nitrogen

The discriminant has been calculated for the following states:

- (1) The orthobaric liquid from the triple point at 63.18°K to 80°K [2].

(2) The fluid from -125°C to $+150^{\circ}\text{C}$ and at pressures up to 3000–6000 atm, depending on the temperature. The tables of Lunbeck, Michels and Wolkers [3] are calculations of the thermodynamic properties over this range from their own experimental results and from those of Benedict [4].

(3) The gas from 200 to 800°C and at densities up to 180–240 Amagat, depending on the temperature. The tables of Saurel and Lecocq [5, 6] give the pressure as a function of temperature along the isochores. The derivatives $(\partial P/\partial T)_V$ and $(\partial^2 P/\partial T^2)_V$ were obtained by numerical differentiation, and integrated to give U^* and C_V^* . The values of C_V^* agreed well with those derived by the authors within the accuracy with which their graph could be read.

The discriminant $D(12)$ was found to be negative for the orthobaric liquid near the triple point (table 1). A repulsive index of 13·2 or more is required for D to be positive at the triple point. The regions in which $D(12)$ was found to be negative from the tables of Lunbeck, Michels and Wolkers are shown in figure 1. The sign of the discriminant is hard to determine at very high pressures where the experimental errors are the greatest, but it appears that $D(12)$ is negative above about 5500 atm at all temperatures covered by these tables. The low-temperature branch of the curve $D(12)=0$ may be extrapolated smoothly to meet the orthobaric curve between 70 and 80°K , in agreement with the results in table 1. The upper branch of the curve $D(12)=0$ is not changed significantly by increasing n to 13 or 14, since U^* is here only a small part of the term for the fluctuation of \mathcal{V} .

Temperature ($^{\circ}\text{K}$)	63·18	70	80
Pressure (atm)	0·124	0·382	1·346
$D(12)$ (J mole^{-1})	-340	-90	+120
$D(13)$ (J mole^{-1})	-50	+190	+370

Table 1. The discriminants $D(12)$ and $D(13)$ for liquid nitrogen.

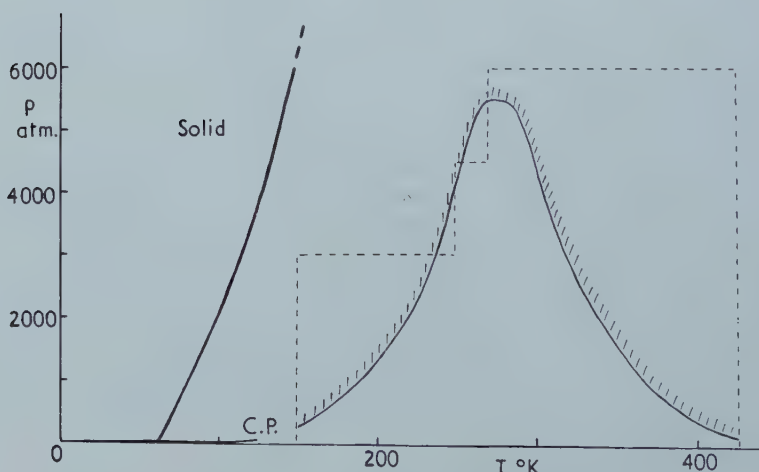


Figure 1. The curve $D(12)=0$ for nitrogen, calculated from the tables of Lunbeck, Michels and Wolkers. The line is shaded on the side on which D is negative. The dashed line is the boundary of the region of pressure and temperature covered by these tables.

The results of Saurel and Lecocq give positive values of $D(12)$ at all temperatures and pressures. This disagreement with the results of Michels is shown for two isobars in figure 2. This discrepancy is similar to, but more pronounced than, that found in the calculations for argon between the values of $D(12)$ based upon Michels' results and those based upon the tables of Din [7]. The differences are accounted for almost entirely by differences in the values of C_V^* . It is most probable that Michels' values of C_V^* are too low at high temperatures.

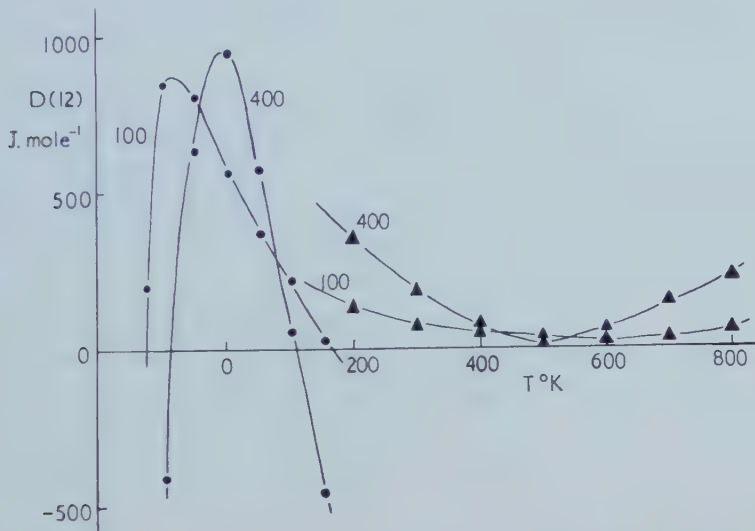


Figure 2. The discriminant $D(12)$ for nitrogen along the 100 and 400 atm isobars. Circles: from tables of Lunbeck, Michels and Wolkers; triangles: from tables of Saurel and Lecocq.

1.2. Methane

The discriminant has been calculated for two regions:

- (1) The orthobaric liquid from the triple point $90\cdot66^\circ\text{K}$ to the normal boiling point $111\cdot67^\circ\text{K}$ [2].
- (2) The fluid from 240°K to 470°K and at pressures up to 1000 atm, from the tables of Tester [8]. These are based on all experimental results published up to 1958.

The tables of the American Petroleum Institute, Project 44, cover $110\text{--}1500^\circ\text{K}$ and pressures up to 1000 atm. However, they could not be used for these calculations for two reasons. First, the properties at high temperatures are values calculated from virial equation of state in which the coefficients are themselves calculated from the 12:6 potential. Secondly, the entries in the tables at lower temperatures (below 500°K) were not smooth enough to give reliable values of C_V^* by numerical differentiation. However the values of C_V^* obtained from these tables were never larger than those of Tester and so could not have led to larger values of $D(12)$.

The values found for the discriminants $D(12)$ and $D(14)$ are shown in table 2. The maximum in D was unexpected and may be a reflection of errors in the experimental results, since D must ultimately rise along the orthobaric curve to

a large positive value at the critical point. The calculations for argon showed a point of inflection above the boiling point, but no maximum. It is possible that the heat capacity of liquid methane is a little lower than that of the classical fluid, since methane has a light mass and a very small moment of inertia. A low heat capacity would explain the low values of D .

Temperature ($^{\circ}\text{K}$)	90.66	100	111.67
Pressure (atm)	0.115	0.340	1.000
$D(12)$ (J mole^{-1})	-780	-690	-760
$D(14)$ (J mole^{-1})	-50	+10	-150

Table 2. The discriminants $D(12)$ and $D(14)$ for liquid methane.

The curve $D(12)=0$ at higher temperatures is shown in figure 3, which resembles closely the curve for argon derived from the tables of Din. Too little of the upper branch of this curve falls within the range of present experimental results for its course to be properly determined.

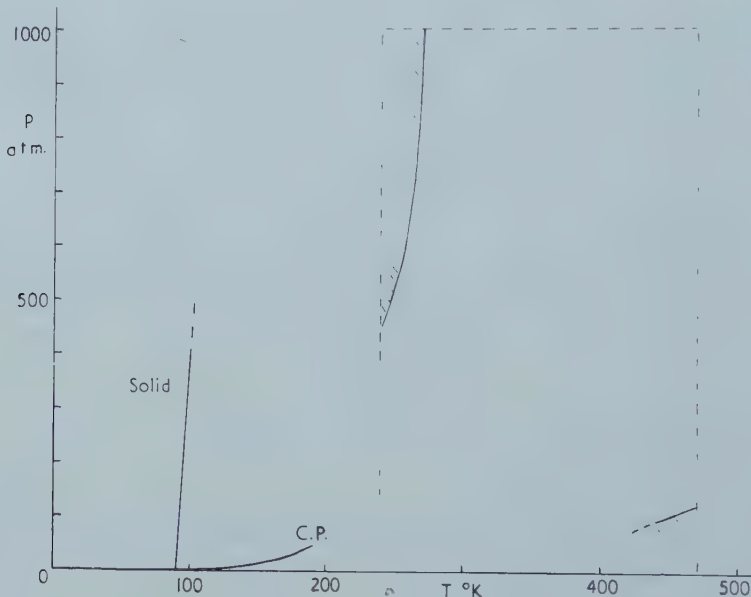


Figure 3. The curves $D(12)=0$ for methane, calculated from the tables of Tester. The lines are shaded on the side on which D is negative. The dashed line is the boundary of the region of pressure and temperature covered by these tables.

2. CONCLUSIONS

There are uncertainties in the experimental results for both gases which make it impossible to determine accurately the regions of pressure and temperature for which $D(12)$ is negative. However, the results confirm generally the conclusions drawn from the single case of argon, namely that the discriminant tends to be negative under those conditions where the form of the repulsive forces is most important. These are the liquid at low temperature and high pressures and the gas at high temperature. The discriminant can be made positive in the

low temperature region by choosing a value of n of 13–14, but at high temperatures the value would have to be 20–30. It appears, therefore, that the best experimental results for gases at high temperatures are not compatible with a Lennard-Jones potential with a reasonable repulsive index. A more satisfactory test of the potential cannot be made by this method until there are more reliable values of the configurational heat capacity at constant volume.

I wish to thank Dr. H. E. Tester of the British Petroleum Company for permission to use his tables of the properties of methane before their publication.

REFERENCES

- [1] BROWN, W. B., and ROWLINSON, J. S., 1960, *Mol. Phys.*, **3**, 35.
- [2] ROWLINSON, J. S., 1959, *Liquids and Liquid Mixtures*, tables 2.7, 2.9, 2.13 and 2.15 (London: Butterworths).
- [3] LUNBECK, R. J., MICHELS, A., and WOLKERS, G. J., 1953, *Appl. sci. Res.*, Hague, A, **3**, 197.
- [4] BENEDICT, M., 1937, *J. Amer. chem. Soc.*, **59**, 2224, 2233.
- [5] SAUREL, J., and LECOCQ, A., 1958, *Compt. Rend.*, **246**, 2586, 3025; 1959, *Ibid.*, **248**, 653; *J. Phys. Radium*, **20**, 443.
- [6] SAUREL, J., 1958, *J. Rech. C.N.R.S.*, No. 42, p. 21 (tables 4–6).
- [7] DIN, F., 1956, *Thermodynamic Functions of Gases* (London: Butterworths), Vol. 2, p. 146.
- [8] TESTER, H. E., 1959, *Thermodynamic Properties of Methane* (London: British Petroleum Co.).

The temperature-independent paramagnetism of permanganate and related complexes

by A. CARRINGTON

Department of Theoretical Chemistry,
University Chemical Laboratory, Lensfield Road, Cambridge

(Received 12 February 1960)

The temperature-independent paramagnetism of permanganate is discussed in terms of molecular orbital theory. It is shown that the major contribution to the paramagnetism arises from electrons in metal d orbitals, and that the amount of charge-transfer from the ligands to the metal ion can be estimated. The theory is applicable to any complex in which the metal ion possesses vacant low-lying d orbitals.

1. INTRODUCTION

The magnetic susceptibility of a molecule in which all the electrons are paired depends on the relative magnitude of a diamagnetic contribution χ_D and a paramagnetic contribution χ_T , which arises from high-frequency matrix elements of the angular momentum. In contrast to the paramagnetism due to unpaired electron spins, χ_T does not depend on the temperature and if it is bigger than χ_D the molecule is said to show 'temperature-independent', 'residual' or 'feeble' paramagnetism. Many molecules fall into this category, particularly transition-metal complexes possessing paired d electrons.

The contribution of the temperature-independent paramagnetism to the magnetic susceptibility may be written [1]

$$\chi_T = \frac{2}{3}N \sum_{n \neq 0} \frac{|\mathbf{m}^0(0; n)|^2}{E(0; n)} \quad (1)$$

where N is Avogadro's number, $E(0; n)$ is the energy difference between the ground and n th excited state and $\mathbf{m}^0(0; n)$ is the matrix element of $\sum_i (e/2mc)l_i$ between the ground and n th excited state. l_i is the angular momentum operator for electron i , the summation extending over all the electrons.

The calculation of χ_T thus involves the determination of these matrix elements. Almost the only quantitative treatment is that of Griffith and Orgel [2] who dealt with octahedral cobaltic complexes. The cobalt ion has the d electron configuration $(t_{2g})^6 : ^1A_{1g}$ and the angular momentum operator has matrix elements between the $^1A_{1g}$ ground state and the excited $^1T_{1g}$ state, formed by promoting a t_{2g} electron into an e_g orbital. Equation (1) shows that the magnitude of the paramagnetic contribution is inversely proportional to the energy separation between the $^1A_{1g}$ and $^1T_{1g}$ states.

In this paper we are concerned primarily with the permanganate ion, although the treatment is appropriate for any tetrahedral complex in which the metal ion does not possess d electrons, but does have relatively low-lying d orbitals available for bonding.

2. MOLECULAR-ORBITAL THEORY

We begin by constructing molecular orbitals for MnO_4^- , making use of manganese $3d$ and $4s$ orbitals and oxygen $2p$ orbitals. The precise form of the molecular orbitals depends upon the choice of axes and relative orientations of the oxygen orbitals. We make use of the set derived by Wolfsberg and Helmholz [3] in which πx_1 , πy_1 , etc., are oxygen $2p\pi$ orbitals and σ_1 , σ_2 , etc., are oxygen $2p\sigma$ orbitals. The axes x , y and z have their origin at the manganese atom and pass through the mid-points of the tetrahedron edges.

The molecular orbitals for a tetrahedral molecule are classified according to the irreducible representation of T_d to which they belong and the low-lying ones are of four different types. The t_1 orbitals are fully determined by symmetry and are non-bonding combinations of oxygen $2p_\pi$ orbitals. Under the operations of T_d , the three degenerate members of the t_1 set, t_x , t_y and t_z , transform like the components l_x , l_y and l_z of the angular momentum \mathbf{l} . The t_2 orbitals transform like xy , xz and yz respectively and are combinations of the metal d_{xy} , d_{xz} and d_{yz} orbitals with oxygen $2p_\sigma$ and $2p_\pi$ orbitals. The e orbitals e_a and e_b transform like $x^2 - y^2$ and $3z^2 - r^2$ respectively and are π combinations of the $d_{x^2-y^2}$ and d_{z^2} orbitals with oxygen $2p_\pi$ orbitals. Finally the a_1 orbital is a σ combination of the metal $4s$ and oxygen $2p\sigma$ orbitals.

The four O^{2-} ions provide 24 electrons which are fed into the molecular orbitals to give the ground state electron configuration

$$(1a_1)^2(1t_2)^6(1e)^4(2t_2)^6(t_1)^6: ^1A_1.$$

The order of the t_2 and e orbitals is not established but fortunately it is not too important for our present purposes.

In order to account for the temperature-independent paramagnetism of permanganate we seek non-vanishing matrix elements of \mathbf{l} between the ground state and excited states, and since \mathbf{l} transforms under the T_1 representation of T_d , we need only to consider T_1 states. It has been established that the first two vacant orbitals are of types e and t_2 respectively [4-7] and we will demonstrate the method of calculation by considering the contribution to χ_T from the $(t_1)^5(2e)^1: ^1T_1$ state, formed by promoting a t_1 electron to the vacant e orbital.

The first stage is to derive wave functions for the three components of the 1T_1 state and by use of standard group theoretical methods these are found to be

$$\Phi_1 = t_0^z e_b,$$

$$\Phi_2 = \frac{1}{2}(t_0^y e_b + \sqrt{3}t_0^y e_a),$$

$$\Phi_3 = \frac{1}{2}(t_0^x e_b - \sqrt{3}t_0^x e_a).$$

Here we are using an abbreviated notation in which $t_0^z e_b$, for example, represents the wave function formed by removing an electron from t_z and putting it in e_b . The complete singlet wave function Φ_1 is written in determinantal form

$$\Phi_1 = \frac{1}{\sqrt{6!}} \frac{1}{\sqrt{2}} \left\{ |t_x(\alpha) t_x(\beta) t_y(\alpha) t_y(\beta) t_z(\alpha) e_b(\beta)| - |t_x(\alpha) t_x(\beta) t_y(\alpha) t_y(\beta) t_z(\beta) e_b(\alpha)| \right\}.$$

The wave functions Φ_2 and Φ_3 are treated in the same manner.

We now seek matrix elements of the components of \mathbf{l} between these wave functions and the ground state wave function

$$\frac{1}{\sqrt{6!}} |t_x(\alpha)t_x(\beta)t_y(\alpha)t_y(\beta)t_z(\alpha)t_z(\beta)|.$$

In fact, l_z , l_y and l_x connect Φ_1 , Φ_2 and Φ_3 respectively with the ground state. Each matrix element has the value $\sqrt{2}\mathbf{a}$ where \mathbf{a} is the integral $\langle t_z|l_z|e_b\rangle$. (Matrix elements of l_x and l_y can be converted into matrix elements of l_z by using appropriate symmetry operations of T_d .) Hence the sum of squares of the matrix elements of l between the 1A_1 ground state and the 1T_1 excited states is $6\mathbf{a}^2$.

In order to evaluate \mathbf{a} we must decide on the explicit forms of the molecular orbitals t_z and e_b . With our choice of axes the expressions for these orbitals are

$$t_z = \frac{1}{4}\{\pi y_2 + \pi y_3 - \pi y_1 - \pi y_4 + \sqrt{3}(\pi x_2 + \pi x_3 - \pi x_1 - \pi x_4)\},$$

$$e_b = \lambda d_{z^2} - \mu \frac{1}{4}\{\pi x_1 + \pi x_2 + \pi x_3 + \pi x_4 + \sqrt{3}(\pi y_1 + \pi y_2 + \pi y_3 + \pi y_4)\}.$$

If we neglect terms involving two different atoms (which depend on overlap), \mathbf{a} can be reduced to the expression

$$\mathbf{a} = -\frac{1}{4}\mu\{\langle\pi y_2|l_z|\pi x_2\rangle + \sqrt{3}\langle\pi y_2|l_z|\pi y_2\rangle + \sqrt{3}\langle\pi x_2|l_z|\pi x_2\rangle + 3\langle\pi x_2|l_z|\pi y_2\rangle\}.$$

The integrals occurring in this expression are readily evaluated and \mathbf{a} is found to have the value $-[(\sqrt{3}/2)\mu\hbar]$. Hence the contribution to χ_T is

$$\frac{2}{3}N\left(\frac{e\hbar}{2mc}\right)^2 \frac{9}{2}\mu^2/\Delta E = 0.1738 \times \frac{9}{2}\mu^2/\Delta E.$$

Electric dipole transitions to T_1 states are forbidden but the spectrum of permanganate in sites of lower symmetry [8] suggests that $\Delta E = 15\,000\text{ cm}^{-1}$. Electron resonance studies on manganate [5, 6], and the intensity of the $(t_1)^6 \rightarrow (t_1)^5 2e : ^1T_2$ absorption band in permanganate [4], both suggest that μ is small (~ 0.18). Hence the contribution to χ_T is 1.7×10^{-6} c.g.s. electromagnetic units, whereas the experimental value [9] is 58.5×10^{-6} . Even if the e orbitals were spread evenly over the whole molecule the contribution to χ_T would be less than 10×10^{-6} .

The contribution from the excited state $(t_1)^5 3t_2 : ^1T_1$ can be calculated in a similar manner. Writing one of the $3t_2$ orbitals in the form

$$t_{yz} = \alpha d_{yz} - \beta \frac{1}{2}(\sigma_1 + \sigma_3 - \sigma_2 - \sigma_4) - \gamma \frac{1}{4}(\pi x_4 + \pi x_2 - \pi x_1 - \pi x_3 + \sqrt{3}(\pi y_4 + \pi y_2 - \pi y_1 - \pi y_3))$$

we find that the contribution to χ_T is $0.1738(2\beta^2 + \gamma^2)/\Delta E$. Spectroscopic studies [4] suggest that ΔE is approximately $25\,000\text{ cm}^{-1}$ and that γ is very small, while electron resonance studies of manganate indicate that the $3t_2$ orbitals are spread over the whole molecule. If we regard the $3t_2$ orbitals as being full σ -type orbitals (putting $\alpha = \beta$, $\gamma = 0$ and choosing a reasonable value for the overlap integral) we find that the contribution to χ_T is 8.7×10^{-6} .

Hence we see that the lowest-lying excited 1T_1 states of permanganate cannot be responsible for the temperature-independent paramagnetism. Consideration of the cobaltic complexes mentioned earlier provides a clue however. If electrons can get into metal t_2 -type d orbitals, the excited 1T_1 state formed by promoting an electron from the t_2 orbital to the vacant $2e$ orbital will give a substantial contribution to χ_T . Calculation shows that the contribution from the excited state

$(1t_2)^5(2e)^1: ^1T_1$ is $0.1738 \times 24\alpha^2\lambda^2/\Delta E$ if we take the $1t_2$ and $3t_2$ orbitals to be the members of a fully σ -bonding and antibonding pair [4, 7]. We can only guess at the value of ΔE but $60\,000\text{ cm}^{-1}$ is probably not far out. Using the values of α and λ introduced earlier (see also table), the contribution to χ_T is 42×10^{-6} .

3. DISCUSSION

In the table we give expressions for the main contributions to χ_T and approximate estimates of their values. The significant point is that the major contribution to χ_T arises as a result of covalent bonding. Thus the presence of temperature-independent paramagnetism in this type of complex is very direct evidence for charge transfer from the ligands (O^{2-}) to the metal ion (Mn^{7+}).

Excited T_1 state	Contribution to χ_T	Numerical estimate
$(t_1)^52e$	$0.1738 \times \frac{9}{2}\mu^2/15\,000$	1.7×10^{-6}
$(t_1)^53t_2$	$0.1738 \times (2\beta^2 + \gamma^2)/25\,000$	8.7×10^{-6}
$(t_1)^52a_1$	0	0.0
$(1t_2)^52e$	$0.1738 \times 24\alpha^2\lambda^2/60\,000$	42.0×10^{-6}
$(2t_2)^52e$	0	0.0
$(1t_2)^53t_2$	$0.1738 \times 12 \left(\alpha^4 + \frac{4}{9}\beta^4 - \frac{4}{3}\alpha^2\beta^2 \right) / 70\,000$	1.4×10^{-6}
$(2t_2)^53t_3$	$0.1738 \times 12 \times \frac{2}{9}\gamma^2 / 50\,000$	9.3×10^{-6}
	Total	63.1×10^{-6}

Contributions to the temperature-independent paramagnetism of MnO_4^- .

Ground state electron configuration
 $(1a_1)^2(1t_2)^6(1e)^4(2t_2)^6(1t_1)^6(2e)^0(3t_3)^0(2a_1)^0$.

We have chosen the $1t_2$ and $3t_2$ orbitals to be a full σ -bonding and antibonding pair with $\alpha = \beta = 0.79$. These values of α and β are derived using a value for the group overlap integral (3) of 0.2. t_2 is essentially non-bonding with $\alpha = \beta = 0$, $\gamma = 1$. Terms involving two different atoms are neglected throughout.

It does not, however, distinguish between σ and π transfer and it can only be used to give a quantitative estimate of the charge transfer if there is some way of measuring or calculating the ${}^1A_1-{}^1T_1$ energy separation†.

We would expect these effects to be important in other complexes which possess low-lying vacant d orbitals and the series of ions Mn^{VII} , Cr^{VI} , V^V and Ti^{IV} illustrate this conclusion. Chromium trioxide [10] vanadium pentoxide [9] and titanium dioxide [9] are all feebly paramagnetic.

Octahedral complexes can be treated in much the same manner. The e_g -type orbitals are capable of forming σ bonds with ligand p_g orbitals, and the excited ${}^1T_{1g}$ state, formed by promoting an electron from the e_g bonding orbital into the antibonding t_{2g} orbital, will give the major contribution to χ_T . Examples are WF_6 [11] and WCl_6 [12] in which the values of χ_T are 2×10^{-6} and 64×10^{-6} respectively.

† It should also be emphasized that χ_T cannot be measured directly, but only calculated after the diamagnetic contribution to the measured susceptibility has been allowed for.

Finally it is of interest to note that KMnO_4 , TiCl_4 and TiBr_4 all show an anomalous magnetic rotation [13], the Verdet constants being negative, and it seems probable that this effect is also due to charge transfer.

I should like to thank Professor H. C. Longuet-Higgins, F.R.S. and Dr. L. E. Orgel for valuable discussions.

REFERENCES

- [1] VAN VLECK, 1931, *Electric and Magnetic Susceptibilities* (Oxford: University Press).
- [2] GRIFFITH, and ORGEL, 1957, *Trans. Faraday Soc.*, **53**, 601.
- [3] WOLFSBERG, and HELMHOLZ, 1952, *J. chem. Phys.*, **20**, 837.
- [4] CARRINGTON, and SCHONLAND, 1960, *Mol. Phys.* (to be published).
- [5] CARRINGTON, INGRAM, LOTT, SCHONLAND, and SYMONS, 1960, *Proc. roy. Soc. A*, **254**, 101.
- [6] SCHONLAND, 1960, *Proc. roy. Soc. A*, **254**, 111.
- [7] BALLHAUSEN, and LIEHR, 1958, *J. Mol. Spectroscopy*, **2**, 342.
- [8] TELTOW, 1938, *Z. phys. Chem. B*, **40**, 397.
- [9] RAYCHAUDHURI, and SENGUPTA, 1936, *Indian J. Phys.*, **10**, 245.
- [10] GREY, and DAKERS, 1931, *Phil. Mag.*, **11**, 237.
- [11] HENKEL, and KLEMM, 1935, *Z. anorg. Chem.*, **222**, 71.
- [12] BERKMAN, and ZOCHER, 1926, *Z. phys. Chem. A*, **124**, 321.
- [13] FRITSCH, 1943, *Compt. Rend.*, **217**, 447.

On a non-linear law of the irreversible phenomena with stationary constraints

by P. GLANSDORFF

Polytechnic Faculty of Mons and Brussels University, Belgium

(Received 10 December 1959)

In 1954, I. Prigogine and the present author established that the time derivative of the entropy production, for constant values of the fluxes, is always negative or zero when the boundary conditions of the system are stationary. However, mechanical equilibrium was postulated and it follows that the dissipative forces were not taken into consideration but only the other cases of irreversibility (chemical reactions, heat and diffusion). In this work the above limitation is eliminated. The system, however, is assumed to be in mechanical steady flow during the whole process.

List of symbols

- e Internal energy per unit mass.
- \mathbf{F}_γ External force (per unit mass) acting on the γ th component.
- h Enthalpy per unit mass.
- M_γ Molecular mass of component γ .
- N_γ Mass fraction of γ .
- \mathbf{p} Pressure tensor.
- p Pressure.
- s Entropy per unit mass.
- T Thermodynamic temperature.
- $\mathbf{v}, \mathbf{v}_\gamma$ Barycentric velocity and peculiar velocity of component γ .
- v Specific volume (ρ^{-1}).
- \mathbf{W} Heat flow.
- Δ_γ Diffusion velocity of γ : $\mathbf{v}_\gamma - \mathbf{v}$.
- δ Variation.
- ρ Density; also index of chemical reaction.
- ρ_γ Density of γ ; (ρN_γ) .
- μ_γ Chemical potential per unit mass.
- χ Isothermal compressibility coefficient: $-v^{-1}(\partial v / \partial p)_T$.
- $\nu_{\gamma\rho}$ Stoichiometric coefficient of γ in reaction ρ .
- $\mathbf{:}$ Double product of two tensors: $\mathbf{p}:\nabla\mathbf{v} = \sum \sum p_{ij} (\partial v_i / \partial x_j)$.
- \mathbf{U} Unit tensor:
$$\begin{bmatrix} 1 & 0 & 0 \\ 0 & 1 & 0 \\ 0 & 0 & 1 \end{bmatrix}.$$

The other symbols are defined in the text.

1. INTRODUCTION

In the present discussion of irreversible phenomena, the applicability of Gibbs's law is assumed, and hence processes which are too far removed from equilibrium are excluded [1]. Under these conditions, the rate of entropy production σ per unit volume can be expressed as a bilinear form in the generalized forces X_i and the conjugate rates J_i of the irreversible phenomena [2, 3]. The second principle of thermodynamics introduces the local condition:

$$\sigma = \sum_i X_i J_i \geq 0 \quad (1.1)$$

and hence the rate of entropy production P in the entire volume V is

$$P = \int_V \sigma dV = \int_V \sum_i X_i J_i dV \geq 0. \quad (1.2)$$

In (1) and (2), the equality sign corresponds to the equilibrium state. If the differential $d\sigma$ is split into two parts:

$$d_X \sigma = \sum_i J_i dX_i \quad \text{and} \quad d_J \sigma = \sum_i X_i dJ_i \quad (1.3)$$

we obtain:

$$d\sigma = d_X \sigma + d_J \sigma \quad \text{and} \quad dP = d_X P + d_J P. \quad (1.4)$$

I. Prigogine and the present author [4] showed that *under stationary boundary conditions*, the irreversible evolution of the system obeys the relation:

$$d_X P \leq 0 \quad (1.5)$$

regardless of the kinetic behaviour of the system. Here the equality sign corresponds to equilibrium or non-equilibrium *stationary states*.

Two interesting special cases may be pointed out. The first is the case where linear relations between the forces and fluxes prevail, i.e. $J_i = \sum_j L_{ij} X_j$, where, because of the nearness to equilibrium conditions, the phenomenological coefficients L_{ij} are constant ($L_{ij} = L_{ij}^{eq}$). From the Onsager reciprocal relations: $L_{ij}^{eq} = L_{ji}^{eq}$, the elements $d_X \sigma$ and $d_J \sigma$ become exact differentials, and we obtain $d\sigma = 2d_X \sigma = 2d_J \sigma$. In the same manner, the relation (5) reduces to

$$dP \leq 0. \quad (1.6)$$

This condition expresses the well-known theorem of *minimum entropy production in the stationary state*; it is clear from its derivation that the validity of the theorem is limited to stationary states which are sufficiently close to equilibrium for the foregoing assumption of linearity to hold.

The second special case occurs when the sole irreversible flux is the chemical reaction. The inequality (5) then reduces to the scalar form in the configuration space of the system:

$$d_X \sigma = \sum_\rho u_\rho dA_\rho \leq 0 \quad (\rho = 1, \dots, r). \quad (1.7)$$

Here the generalized forces X_i become the affinities A_ρ of the r chemical reactions, and the conjugate rates J_i become the rates of reaction u_ρ . It is clear that condition (7) is of interest principally in open systems, since the only stationary state possible in a closed system without transport phenomena is the trivial state of equilibrium.

Because of its extreme simplicity, the inequality (7) was also derived directly in a separate publication [5] using an adaptation to open systems of the line of reasoning applied to closed systems by Prigogine [6]. In contrast with the first

case, the linear differential form (7) is not in general an exact differential, and hence the matrix of the coefficients $l_{\rho\rho'} = \partial u_\rho / \partial A_{\rho'}$, contains an antisymmetric component. Prigogine and Balescu [7, 8], showed that this antisymmetric component implies that the representative point in the space of the affinities can rotate about a non-equilibrium steady state, in a direction determined by the inequality (7).

The moderation of the entropy production expressed by the *differential law* (5) contains as a particular case the theorem of minimum entropy production expressed by the *variational law* (6). This moderation law (5) is, according to its previous derivation [4], applicable to the irreversible phenomena of chemical reaction (including phase changes), heat flow and diffusion. However, only systems in mechanical equilibrium (zero barycentric velocity at all points), were taken into consideration in this derivation and hence irreversibility arising from dissipative mechanical forces was excluded. The purpose of the present work is to derive this law free from the restriction of mechanical equilibrium.

We consider now a system having stationary boundary conditions which prevent its attaining equilibrium in any sense—mechanical, chemical, thermal or diffusion—although non-equilibrium steady states are permitted. The only remaining limitation will be the assumption that the mechanical stationary state is already established. Indeed, the first stationary state to be attained is mostly the mechanical stationary state; otherwise the principle (5) would be invalidated, since it would be necessary to add to $d_X\sigma$, terms of the type $J_i'dX_i'$ which have no counterpart in the entropy production equation (1).

However, the basic method remains the same since it is based on the sign properties of the quadratic forms introduced in the study of the stability of the equilibrium state. Because of continuity properties, these forms retain their sign outside the immediate neighbourhood of equilibrium, throughout the entire range of validity of the Gibbs relations.

2. FUNDAMENTAL RELATIONS

The derivations which follow are based on the following fundamental equations [2, 3]:

Mass balance for each of the c components

$$\frac{\partial \rho_\gamma}{\partial t} = -\nabla \cdot \rho_\gamma \mathbf{v}_\gamma + \sum_\rho \nu_{\gamma\rho} M_\rho u_\rho \quad (\gamma=1, \dots, c; \rho=1, \dots, r). \quad (2.1)$$

Energy balance

$$\frac{\partial pe}{\partial t} = -\nabla \cdot (\mathbf{W} + \rho e \mathbf{v}) - \mathbf{p} : \nabla \mathbf{v} + \sum_\gamma \rho_\gamma \Delta_\gamma \cdot \mathbf{F}_\gamma. \quad (2.2)$$

Relations deduced from Euler's theorem on homogeneous functions:

The enthalpy (homogeneous of degree one):

$$pe + p = \rho h = \sum_\gamma \rho_\gamma (\partial h / \partial N_\gamma)_{T, p, (n)} = \sum_\gamma \rho_\gamma h_\gamma. \quad (2.3)$$

The chemical potential (homogeneous of degree zero):

$$\sum_{\gamma'} N_{\gamma'} (\partial \mu_\gamma / \partial N_{\gamma'})_{T, p, (n)} = 0 \quad (2.4)$$

known as the Gibbs–Duhem formula; the subscript (n) indicates differentiation with constant masses of all components other than the one being varied.

Derivatives of the chemical potential:

$$(\partial\mu_\gamma/\partial T)_{p,n} = -s_\gamma \quad \text{and} \quad (\partial\mu_\gamma/\partial p)_{T,n} = v_\gamma \quad (2.5)$$

the first, may also be written:

$$(\partial\mu_\gamma T^{-1}/\partial T)_{p,n} = -h_\gamma T^{-2} \quad (2.6)$$

directly deducible in this form, from the Gibbs–Helmholtz formula. Here the subscript n denotes differentiation with the masses of all components held constant.

The Kelvin formula:

$$(\partial h/\partial p)_{T,n} = v - T(\partial v/\partial T)_{p,n}. \quad (2.7)$$

The heat capacity relation connecting the specific heat at constant volume c with that at constant pressure c_p :

$$c_v - c_p = T(\partial v/\partial T)_{p,n}^2 (\partial v/\partial p)_{T,n}^{-1}. \quad (2.8)$$

3. THE QUADRATIC FORM

If the two members of (2.1) are multiplied by $-(\partial\mu_\gamma T^{-1}/\partial t)_{p,n}$ and those of (2.2) by $\partial T^{-1}/\partial t$, and then the relations thus obtained added member by member, the left member of the sum will be expressed as:

$$\phi \equiv \frac{\partial \rho e}{\partial t} \frac{\partial T^{-1}}{\partial t} - \sum_\gamma \frac{\partial \mu_\gamma T^{-1}}{\partial t} \frac{\partial \rho_\gamma}{\partial t}. \quad (3.1)$$

Let us show that ϕ can be put into a negative definite quadratic form†. We obtain first (variables T, p, N_γ):

$$\frac{\partial h}{\partial t} = c_p \frac{\partial T}{\partial t} + \left(\frac{\partial h}{\partial p} \right)_{T,n} \frac{\partial p}{\partial t} + \sum_\gamma h_\gamma \frac{\partial N_\gamma}{\partial t}$$

and hence, using also (2.3) and (2.7), (variables T, p, ρ_γ):

$$\frac{\partial \rho e}{\partial t} = \rho c_p \frac{\partial T}{\partial t} - \rho T \left(\frac{\partial v}{\partial T} \right)_{p,n} \frac{\partial p}{\partial t} + \sum_\gamma h_\gamma \frac{\partial \rho_\gamma}{\partial t}. \quad (3.2)$$

One likewise obtains, due to (2.4), (2.5) and (2.6):

$$\frac{\partial \mu_\gamma T^{-1}}{\partial t} = -\frac{h_\gamma}{T^2} \frac{\partial T}{\partial t} + \frac{v_\gamma}{T} \frac{\partial p}{\partial t} + \frac{1}{T} \sum_\gamma \frac{\partial \mu_\gamma}{\partial \rho_\gamma} \frac{\partial \rho_\gamma}{\partial t}. \quad (3.3)$$

If we introduce (2) and (3) into (1) we obtain, after reduction of similar terms:

$$\phi = -\frac{\rho c_p}{T^2} \left(\frac{\partial T}{\partial t} \right)^2 + \frac{\rho}{T} \left(\frac{\partial v}{\partial T} \right)_{p,n} \frac{\partial p}{\partial t} \frac{\partial T}{\partial t} - \frac{1}{T} \frac{\partial p}{\partial t} \sum_\gamma v_\gamma \frac{\partial \rho_\gamma}{\partial t} - \frac{1}{T} \sum_\gamma \sum_{\gamma'} \frac{\partial \mu_\gamma}{\partial \rho_{\gamma'}} \frac{\partial \rho_{\gamma'}}{\partial t} \frac{\partial \rho_\gamma}{\partial t}.$$

Now we have:

$$\begin{aligned} \sum_\gamma v_\gamma \frac{\partial \rho_\gamma}{\partial t} &= \frac{\partial \rho}{\partial t} \sum_\gamma N_\gamma v_\gamma + \rho \sum_\gamma v_\gamma \frac{\partial N_\gamma}{\partial t} = -\rho \left(\frac{\partial v}{\partial t} - \sum_\gamma v_\gamma \frac{\partial N_\gamma}{\partial t} \right) \\ &= -\rho \left[\left(\frac{\partial v}{\partial T} \right)_{p,n} \frac{\partial T}{\partial t} + \left(\frac{\partial v}{\partial p} \right)_{T,n} \frac{\partial p}{\partial t} \right] = -\rho \left(\frac{\partial v}{\partial t} \right)_n; \end{aligned}$$

whence:

$$\phi = -\frac{\rho c_p}{T^2} \left(\frac{\partial T}{\partial t} \right)^2 + \frac{2\rho}{T} \left(\frac{\partial v}{\partial T} \right)_{p,n} \frac{\partial p}{\partial t} \frac{\partial T}{\partial t} + \frac{\rho}{T} \left(\frac{\partial v}{\partial p} \right)_{T,n} \left(\frac{\partial p}{\partial t} \right)^2 - \frac{1}{T} \sum_\gamma \sum_{\gamma'} \frac{\partial \mu_\gamma}{\partial \rho_{\gamma'}} \frac{\partial \rho_{\gamma'}}{\partial t} \frac{\partial \rho_\gamma}{\partial t}.$$

Finally, by introducing (2.8) and regrouping, we find:

$$\phi = - \left[\frac{\rho c_p}{T^2} \left(\frac{\partial T}{\partial t} \right)^2 + \frac{\rho^2}{T} \left(\frac{\partial v}{\partial t} \right)_n^2 + \frac{1}{T} \sum_\gamma \sum_{\gamma'} \frac{\partial \mu_\gamma}{\partial \rho_{\gamma'}} \frac{\partial \rho_{\gamma'}}{\partial t} \frac{\partial \rho_\gamma}{\partial t} \right] \quad (3.4)$$

† It will be seen that ϕ represents the quadratic part in the development of $\partial^2 s/\partial t^2$ in variables ρe , $\rho N_\gamma = \rho$ and $\rho v = 1$.

which is the negative definite quadratic form sought, by virtue of the well known conditions on the stability of equilibrium:

$$c_v > 0 \quad (\text{thermal stability}),$$

$$\chi > 0 \quad (\text{mechanical stability}),$$

$$\sum_{\gamma} \sum_{\gamma'} \frac{\partial \mu_{\gamma}}{\partial \rho_{\gamma'}} \frac{\partial \rho_{\gamma'}}{\partial t} \frac{\partial \rho_{\gamma}}{\partial t} > 0 \quad (\text{diffusion stability, including chemical stability}).$$

Because of continuity, the negative sign of ϕ will necessarily extend to a finite region in the field of the irreversible phenomena surrounding a state of equilibrium. We shall therefore have in this field the local condition:

$$\phi \leq 0 \quad (3.5)$$

and for the whole system:

$$\Phi \equiv \int_V \phi dV \leq 0. \quad (3.6)$$

The sign of equality refers to the stationary states of equilibrium or of non-equilibrium within the region, since the local derivatives are all equal to zero for such states. It is noteworthy that when ϕ is expressed in the form (4), the terms which correspond to the physical variables T and v , and the terms which correspond to the mass changes appear separately, without mixed terms. The latter, in fact, would have introduced supplementary conditions restricting the generality of (5) and of (6).

4. THE MODERATION OF IRREVERSIBLE PROCESSES

Let us now examine the right member of the sum which produced (3.1). By taking into account the first equality (2.3) we obtain:

$$\begin{aligned} \phi = & - \frac{\partial T^{-1}}{\partial t} \nabla \cdot (\mathbf{W} + \rho h \mathbf{v}) + \frac{\partial T^{-1}}{\partial t} [(\rho \mathbf{U} - \mathbf{p}) : \nabla \mathbf{v}] + \frac{\partial T^{-1}}{\partial t} \mathbf{v} \cdot \nabla p \\ & + \frac{\partial T^{-1}}{\partial t} \sum_{\gamma} \rho_{\gamma} \Delta_{\gamma} \cdot \mathbf{F}_{\gamma} + \sum_{\gamma} \frac{\partial \mu_{\gamma} T^{-1}}{\partial t} \nabla \cdot \rho_{\gamma} \mathbf{v}_{\gamma} + \sum_{\rho} u_{\rho} \frac{\partial (T^{-1} A_{\rho})}{\partial t} \leq 0. \end{aligned} \quad (4.1)$$

Now let us integrate over the volume V of the whole system and introduce the following stationary boundary conditions on the surface Ω of V :

$$(\partial T^{-1} / \partial t)_{\Omega} = 0; \quad (\partial \mu_{\gamma} T^{-1} / \partial t)_{\Omega} = 0. \quad (4.2)$$

If we assume moreover that the system has already reached its stationary mechanical state, we have:

$$\partial \mathbf{v} / \partial t = 0; \quad \partial p / \partial t = 0. \quad (4.3)$$

which necessarily implies:

$$\partial \mathbf{F}_{\gamma} / \partial t = 0 \quad (4.4)$$

for the field of long-range forces. Let us introduce these conditions into (1). We have, after partial integration of the first and penultimate terms, and after cancellation of the terms at the limits in accordance with (2):

$$\begin{aligned} \Phi = & \int_V [(\mathbf{W} + \rho h \mathbf{v}) \frac{\partial}{\partial t} (\nabla T^{-1}) + (\rho \mathbf{U} - \mathbf{p}) : \frac{\partial}{\partial t} (T^{-1} \nabla \mathbf{v}) + \mathbf{v} \frac{\partial}{\partial t} (T^{-1} \nabla p) \\ & + \sum_{\gamma} \rho_{\gamma} \Delta_{\gamma} \cdot \frac{\partial}{\partial t} (T^{-1} \mathbf{F}_{\gamma}) - \sum_{\gamma} \rho_{\gamma} \mathbf{v}_{\gamma} \cdot \frac{\partial}{\partial t} (\nabla \mu_{\gamma} T^{-1}) + \sum_{\rho} u_{\rho} \frac{\partial}{\partial t} (T^{-1} A_{\rho})] dV \leq 0 \end{aligned} \quad (4.5)$$

the operations ∇ and $\partial / \partial t$ being commutative.

We shall write (5) in the abbreviated form:

$$\Phi = \int_V \sum_i J_i X'_i dV \leq 0 \quad (4.6)$$

with the table of the rates J_i and of the generalized forces X_i :

Rates J_i	Generalized forces X_i
$\mathbf{W} + \rho h \mathbf{v}$	∇T^{-1}
$p\mathbf{U} - \mathbf{p}$	$T^{-1}\nabla \mathbf{v}$
\mathbf{v}	$T^{-1}\nabla p$
$\rho_\gamma \Delta_\gamma$	$T^{-1}\mathbf{F}_\gamma$
$\rho_\gamma \mathbf{v}_\gamma$	$-\nabla \mu_\gamma T^{-1}$
u_ρ	$T^{-1}A_\rho$

It must be remembered that the equality sign in (6) relates to the stationary states of equilibrium or non-equilibrium.

Let us now compare these values with the contributions to the local entropy production σ . A well known bilinear expression for this production is [3]:

$$\begin{aligned} \sigma = & \mathbf{W} \cdot \nabla T^{-1} + (p\mathbf{U} - \mathbf{p}) : (T^{-1}\nabla \mathbf{v}) + \sum_\gamma \rho_\gamma \Delta_\gamma \cdot [T^{-1}\mathbf{F}_\gamma - \nabla(\mu_\gamma T^{-1})] \\ & + \sum_\rho u_\rho (T^{-1}A_\rho) \geq 0 \end{aligned} \quad (4.7)$$

the sign of equality relating here only to equilibrium states. However, the choice of the conjugate forces and rates is not unique; we shall transform this expression so as to include the forces and rates given in the above table. For this purpose, we shall use the Gibbs-Duhem linear differential form:

$$s\delta T - v\delta p + \sum_\gamma N_\gamma \delta \mu_\gamma = 0 \quad (4.8)$$

applicable over the entire region under consideration, since we have limited ourselves to irreversible phenomena in which the entropy remains a function of the independent macroscopic variables T, p, N_γ , and where its differential coefficients are given by Gibbs's law. We shall employ the gradients as variational elements, and thus deduce immediately from (8) the equality:

$$\rho h \nabla T^{-1} + T^{-1} \nabla p - \sum_\gamma \rho_\gamma \nabla(\mu_\gamma T^{-1}) = 0. \quad (4.9)$$

Let us multiply by the barycentric velocity \mathbf{v} and introduce into (7). We have, after regrouping the terms:

$$\begin{aligned} \sigma = & (\mathbf{W} + \rho h \mathbf{v}) \nabla T^{-1} + (p\mathbf{U} - \mathbf{p}) : (T^{-1}\nabla \mathbf{v}) + \mathbf{v} (T^{-1}\nabla p) \\ & + \sum_\gamma \rho_\gamma \Delta_\gamma (T^{-1}\mathbf{F}_\gamma) - \sum_\gamma \rho_\gamma \mathbf{v}_\gamma (\nabla \mu_\gamma T^{-1}) + \sum_\rho u_\rho (T^{-1}A_\rho) \geq 0 \end{aligned} \quad (4.10)$$

which is the bilinear form sought. Consequently, comparing (5) with (10) our moderation theorem of entropy production is established in the form:

$$\Phi = \partial_X P / \partial t \leq 0 \quad (4.11)$$

for stationary boundary conditions. In particular, at mechanical equilibrium the barycentric velocity \mathbf{v} is nil ($\mathbf{v}_\gamma = \Delta_\gamma$), the two forms (7) and (10) become the same and the inequality (5) then leads to the result reported in our previous work [4]. The present generalization stresses the role of the barycentric velocity which is shown in (10) as a rate coupled to the gradient of the pressure, while the irreversible terms of the pressure tensor appear as rates coupled to the speeds of deformation.

REFERENCES

- [1] PRIGOGINE, I., 1949, *Physica*, **15**, 272.
- [2] PRIGOGINE, I., 1947, *Etude thermodynamique des phénomènes irréversibles* (Liège : Desoer) ch. IX.
- [3] HIRSCHFELDER, J. O., CURTISS, CH., F., and BYRON BIRD, R., 1954, *Molecular Theory of Gases and Liquids* (New York : John Wiley & Sons), § 11.
- [4] GLANSDORFF, P., and PRIGOGINE, I., 1954, *Physica*, **20**, 773.
- [5] GLANSDORFF, P., 1956, *Bull. Acad. Belg. Cl. Sci.*, **42**, 628.
- [6] PRIGOGINE, I., 1955, *Introduction to Thermodynamics of Irreversible Processes* (Springfield, Illinois: C. C. Thomas), Appendix.
- [7] PRIGOGINE, I., and BALESCU, R., 1955, *Bull. Acad. Belg. Cl. Sci.*, **41**, 917.
- [8] PRIGOGINE, I., and BALESCU, R., 1956, *Bull. Acad. Belg. Cl. Sci.*, **42**, 257.

Some investigations in the theory of open-shell ions

Part II. V , W and X coefficients

by J. S. GRIFFITH

Department of Theoretical Chemistry, University Chemical
Laboratory, Lensfield Road, Cambridge

(Received 13 January 1960)

V , W , and X coefficients analogous to Racah's \bar{V} , \bar{W} and \bar{X} coefficients and Wigner's $3j$, $6j$ and $9j$ symbols are defined for certain finite groups and their properties examined. Tables of values of these coefficients are given for the one-valued representations of the octahedral group.

1. INTRODUCTION

In the theory of angular momenta the Wigner coefficients $\langle j_1 j_2 j_3 m_3 | j_1 j_2 m_1 m_2 \rangle$ are known to possess symmetry with respect to the interchange of any pair of the three momenta j_1 , j_2 and j_3 . This symmetry is made particularly obvious by the expression of the Wigner coefficients in terms of certain 'reduced' quantities, the Wigner $3j$ symbols or Racah \bar{V} coefficients. Like the $\langle j_1 j_2 j_3 m_3 | j_1 j_2 m_1 m_2 \rangle$, these give the numerical details of the reduction to irreducible components of the direct product of two irreducible representations of the unitary unimodular group U_2 . Alternatively, and more significantly, they show the way in which the unit representation occurs in the decomposition of the direct product of three irreducible representations.

Because of their relationship to the unit representation, the \bar{V} coefficients may be regarded as three-suffix tensors. We can think of such a unit representation as an invariant which is the inner product of a \bar{V} tensor with three 'vectors' $|j_1 m_1\rangle$, $|j_2 m_2\rangle$ and $|j_3 m_3\rangle$. From this point of view it is natural to consider invariants constructed solely from the \bar{V} . The two simplest non-trivial invariants of this kind are the \bar{W} and \bar{X} coefficients ($6j$ and $9j$ symbols respectively). They prove to be extremely useful for two main reasons. First, most matrix elements of interest in systems containing coupled angular momenta can be expressed very simply in terms of them and the \bar{V} . Secondly, although they are related to recoupling matrix elements and satisfy similar equations they have the great advantage of being highly symmetrical with respect to permutation of their constituent j symbols.

The preceding description is phrased so as to suggest that analogous quantities might be defined for finite groups and their properties usefully investigated. This is done in the present paper, chiefly for the octahedral group, although the V coefficients in § 2 are defined with somewhat greater generality. Before doing this I will expose the two essential facts upon which our analysis is founded. First, for the (one-valued) representations of the octahedral group as for those of U_2 , the direct product of any three irreducible representations contains the unit representation at most once. Secondly it is possible to choose the phases of

the coupling coefficients in such a way that the V coefficients have a highly symmetric and simple behaviour under permutation of their constituent representation symbols.

The theoretical scheme I develop in this paper is, then, largely a straightforward adaptation to the theory of ions with finite symmetry groups of a theory which has already proved itself for systems with spherical symmetry. The general equations satisfied by the V , W and X are consequently similar in form to those satisfied by Racah's coefficients and their proofs are similar. Consequently I do not give most of the proofs in detail here but merely sketch their methods. I recommend the reader who has any difficulty to read the first half of *Irreducible Tensorial Sets* by Fano and Racah ([1], henceforward referred to as FR), although in my proofs I depend much less heavily on the properties of recoupling transformations.

2. DEFINITION OF V COEFFICIENTS

With application to the one-valued representations of the octahedral group O , of D_4 and of D_3 especially in mind we assume that we have three irreducible representations a , b and c such that each is equivalent to a real representation and ab contains c just once. Then we choose bases $|a\alpha\rangle$, $|b\beta\rangle$ and $|c\gamma\rangle$ which are real, write the product $|a\alpha\rangle|b\beta\rangle|c\gamma\rangle=|a\alpha, b\beta, c\gamma\rangle$ and suppose a , b , c to refer respectively to independent parts (or particles) of the system. We also make a definite choice for the matrices of each irreducible representation a and require that any set of kets, $|a\alpha\rangle$ say, spanning a shall span it according to our choice rather than to an equivalent one. We can then define coupling coefficients and take them all to be real. Finally if i is the unit representation we define always

$$\begin{aligned}\langle aai|aa\alpha\alpha'\rangle &= \delta_{\alpha\alpha'}\lambda(a)^{-1/2}, \\ \langle iaax|ia\alpha\alpha'\rangle &= \langle aiax|aix'i\rangle = \delta_{\alpha\alpha'},\end{aligned}\quad (1)$$

where $\lambda(a)$ is the degree of the representation a . The symmetric expression for $\langle aai|aa\alpha\alpha'\rangle$ is a consequence of our assumption that a is equivalent to a real representation (see Frobenius and Schur [2]).

By hypothesis ab contains c once and therefore, apart from a numerical factor, there is just one linear combination of the products $|a\alpha, b\beta, c\gamma\rangle$ which is an invariant for the group, i.e. which forms a basis for the unit representation. In no matter what order we couple the kets $|a\alpha\rangle$, $|b\beta\rangle$ and $|c\gamma\rangle$ to form an invariant, that invariant is always the same apart perhaps from a numerical factor. Let us couple a to b first and then to c to give

$$|ab, c\rangle = \sum_{\alpha\beta\gamma} \lambda(c)^{-1/2} \langle ab\alpha\beta|abc\gamma\rangle |a\alpha, b\beta, c\gamma\rangle, \quad (2)$$

where we have used (1). It follows immediately that $|ab, c\rangle$ satisfies $\langle ab, c|ab, c\rangle = 1$. As the coupling coefficients are real we must therefore have, for a' , b' , c' any permutation of a , b , c , $|a'b', c'\rangle = \pm |ab, c\rangle$. Hence if we define

$$V \begin{pmatrix} a & b & c \\ \alpha & \beta & \gamma \end{pmatrix} = \lambda(c)^{-1/2} \langle ab\alpha\beta|abc\gamma\rangle, \quad (3)$$

then V is real and can at most have its sign changed by any permutation of its columns. For fixed a , b , c the sign change is independent of α , β and γ . The coupling coefficients $\langle ab\alpha\beta|abc\gamma\rangle$ are only partly determined by the constituent representations. For each distinct ordered trio abc there is an arbitrary phase

factor common to all the coefficients and the factors for different ordered trios can be chosen entirely independently of one another. Similar remarks therefore apply to the V symbols.

We now define the phases of the coupling coefficients so as to exhibit the natural symmetry of V as clearly as possible. Three cases arise according to the extent to which the representations in V are the same. First if a, b and c are all different then each V is a multiple of a different coupling coefficient so we can choose the phases so that V is invariant to all permutations of its columns. However, we can also choose the phases so that V is multiplied by the parity of a permutation and it is sometimes advantageous to adopt this apparently perverse choice.

Next let $a=b \neq c$. Then c must belong either to the symmetrized square $[a^2]$ or the antisymmetrized square (a^2) of a . So

$$V \begin{pmatrix} a & a & c \\ \beta & \alpha & \gamma \end{pmatrix} = \epsilon V \begin{pmatrix} a & a & c \\ \alpha & \beta & \gamma \end{pmatrix}$$

where $\epsilon = +1$ if c belongs to $[a^2]$ and -1 otherwise. We now define the phases of the coupling of ac to a and ca to a so that

$$V \begin{pmatrix} c & a & a \\ \gamma & \beta & \alpha \end{pmatrix} = \epsilon V \begin{pmatrix} a & a & c \\ \alpha & \beta & \gamma \end{pmatrix} = \epsilon V \begin{pmatrix} a & c & a \\ \beta & \gamma & \alpha \end{pmatrix}.$$

It then easily follows that V is invariant to all permutations P of its columns when $\epsilon = +1$ and is multiplied by the parity of P when $\epsilon = -1$.

Lastly suppose $a=b=c$ and that the sets of kets $|ax\rangle, |a\beta\rangle, |a\gamma\rangle$ are identical. Then a permutation P of α, β and γ must multiply $|aa, a\rangle$ by ± 1 . Hence $|aa, a\rangle$ is a basis for a representation of degree one of the symmetric group S_3 . So it is either the unit or the alternating representation. Therefore V is either invariant to permutations P of its columns or multiplied by the parity of P , this behaviour depending on a but being independent of α, β and γ .

We have given V the required high degree of symmetry. The associative property of Racah's \bar{V} (FR, equation (10.4)) reads $|ab, c\rangle = |bc, a\rangle$ in our notation and is true because V is always invariant to even permutation of its columns. The fact that the definition (3) of V does not contain any minus signs while the definition of \bar{V} does so even for j integral is simply a consequence of our assumption that our representations are actually real and not merely equivalent to real ones.

For the groups D_3 , D_4 and O the change of sign of V under odd permutations necessarily occurs for each group for A_2E^2 and for O also for T_1^3 and $T_1T_2^2$. For O we also define it to happen for ET_1T_2 . This enables us to give a simple explicit formula for the effect of an odd permutation on V for each of these groups.

$$V \begin{pmatrix} a & b & c \\ \alpha & \beta & \gamma \end{pmatrix}$$

is multiplied by $(-1)^{a+b+c}$, where we interpret a representation symbol, a say, as 0 in this context unless $a=A_2$ or T_1 when we interpret it as 1. For example $(-1)A_2 = -1$, but $(-1)T_2 = +1$. Clearly $(-1)^{2a} = 1$ always. One should note that the high symmetry we have assumed for V is inconsistent with the universal rule

$$\langle abc\gamma | ab\alpha\beta \rangle = \langle bac\gamma | ba\beta\alpha \rangle$$

for $a \neq b$, just as for Wigner coefficients in U_g .

For example we must have

$$\langle A_2 E E \theta | A_2 E a \epsilon \rangle = -\langle E A_2 E \theta | E A_2 \epsilon a \rangle$$

for O (see table 1).

The V satisfy the relations

$$\left. \begin{aligned} \sum_{\alpha\beta\gamma} V \begin{pmatrix} a & b & c \\ \alpha & \beta & \gamma \end{pmatrix} V \begin{pmatrix} a & b & c' \\ \alpha & \beta & \gamma' \end{pmatrix} &= \lambda(c)^{-1} \delta_{cc'} \delta_{\gamma\gamma'} \delta(a, b, c), \\ \sum_{c\gamma} \lambda(c) V \begin{pmatrix} a & b & c \\ \alpha & \beta & \gamma \end{pmatrix} V \begin{pmatrix} a & b & c \\ \alpha' & \beta' & \gamma \end{pmatrix} &= \delta_{\alpha\alpha'} \delta_{\beta\beta'}, \end{aligned} \right\} \quad (4)$$

where $\delta(a, b, c) = 1$ when abc contains the unit representation and $\delta(a, b, c) = 0$ otherwise. $\lambda(c)$ is the degree of the representation c and corresponds to the quantity $2j+1$ in the theory of angular momenta. Equations (4) follow immediately from the orthonormality properties of the coupling coefficients (compare FR, equations (10.17) and (10.18)). $V = 0$ when c is not contained in ab . Summation of the first equation of (4) over γ yields the equation

$$\sum_{\alpha\beta\gamma} V \begin{pmatrix} a & b & c \\ \alpha & \beta & \gamma \end{pmatrix}^2 = \delta(a, b, c). \quad (5)$$

When c is the unit representation i we deduce from (1) that

$$V \begin{pmatrix} a & b & i \\ \alpha & \beta & i \end{pmatrix} = \delta_{ab} \delta_{\alpha\beta} \lambda(a)^{-1/2}. \quad (6)$$

Another equation which is sometimes useful is obtained by putting $c' = i$ in the first of equations (4) and is

$$\sum_{\alpha} V \begin{pmatrix} a & a & c \\ \alpha & \alpha & \gamma \end{pmatrix} = \lambda(a)^{1/2} \delta_{ci}. \quad (7)$$

Thus far we have described properties of the V which exactly parallel those of Racah's \bar{V} . As well as these the V possess further symmetry and of a kind quite different from that discussed earlier. Suppose a group possesses a representation of degree one (assumed real) distinct from the unit representation and let a function η be a basis for it. For example A_2 is such a representation for the octahedral group. Then η^2 is a basis for the unit representation and

$$|a'\alpha'\rangle = \eta|a\alpha\rangle = |\eta a\alpha\rangle,$$

say, is a basis for an irreducible representation a' which may or may not be the same as a . The components, classified by α' , are not necessarily in accord with the standard choice for components of a' . If $a = a'$ it may not be possible to choose them so. We now show that V symbols for abc are simply related to those for $a'b'c$, $ab'c'$ and $a'bc'$.

Multiply the invariant $|ab, c\rangle$ of equation (2) through by η^2 to give

$$\begin{aligned} |ab, c\rangle' &= \sum_{\alpha\beta\gamma} V \begin{pmatrix} a & b & c \\ \alpha & \beta & \gamma \end{pmatrix} |\eta a\alpha, \eta b\beta, c\gamma\rangle \\ &= \sum_{\alpha'\beta'\gamma} V \begin{pmatrix} a & b & c \\ \alpha' & \beta' & \gamma \end{pmatrix} |a'\alpha', b'\beta', c\gamma\rangle. \end{aligned}$$

So $|ab, c\rangle'$ is, apart perhaps from sign, the invariant corresponding to $a'b'$ coupled with c . Therefore

$$V \begin{pmatrix} a' & b' & c \\ \alpha' & \beta' & \gamma \end{pmatrix} = \omega V \begin{pmatrix} a & b & c \\ \alpha & \beta & \gamma \end{pmatrix},$$

where $\omega = \pm 1$ is independent of α, β and γ but may depend on the ordered set (a, b, c) . An equation of analogous form holds if we incorporate η not with ab but with either ac or bc . It is convenient to write

$$V \begin{pmatrix} a & b & c \\ \alpha & \beta & \gamma \end{pmatrix}'_{\mu\nu}$$

to indicate that the μ th and ν th columns have been ‘dashed’. Generalizing the last equation we have

$$V \begin{pmatrix} a & b & c \\ \alpha & \beta & \gamma \end{pmatrix}'_{\mu\nu} = \omega(abc)_{\mu\nu} V \begin{pmatrix} a & b & c \\ \alpha & \beta & \gamma \end{pmatrix}. \quad (8)$$

Because the V coefficients are invariant to even permutations of their columns it follows that $\omega(abc)_{\mu\nu}$ is invariant to even permutations applied simultaneously to a, b, c and to $\mu\nu$, i.e. for example

$$\omega(abc)_{12} = \omega(bca)_{13}.$$

The order of μ and ν is irrelevant.

We now pass from this somewhat formal and abstract discussion to consider the octahedral group O. Here A_2 is the unique non-trivial representation of degree one and $A_1' = A_2$, $E' = E$, $T_1' = T_2$. Of course $a'' = a$ always. For the group O the relation $a \rightarrow a'$ is the same, via the isomorphism with the permutation group S_4 , as the well-known passage between associated representations obtained by reflecting the Young tableau corresponding to the representation in its main diagonal.

We can define our components so that $|T_1'M'\rangle = |T_2M\rangle$, $|T_2'M'\rangle = |T_1M\rangle$ and of course $|A_1'a'\rangle = |A_2a\rangle$ and $|A_2'a'\rangle = |A_1a\rangle$. However, for the self-associated representation E we must make a choice such as $\theta' = \epsilon$, $\epsilon' = -\theta$ (θ, ϵ transform as $d_{z^2}, d_{x^2-y^2}$ respectively.) We make the obvious definition here that

$$V \begin{pmatrix} E & b & c \\ -\theta & \beta & \gamma \end{pmatrix} = -V \begin{pmatrix} E & b & c \\ \theta & \beta & \gamma \end{pmatrix}; \text{ etc.}$$

Consider for example $a = b = c = E$. There are four non-zero V which we take as

$$V \begin{pmatrix} E & E & E \\ \theta & \epsilon & \epsilon \end{pmatrix} = V \begin{pmatrix} E & E & E \\ \epsilon & \theta & \epsilon \end{pmatrix} = V \begin{pmatrix} E & E & E \\ \epsilon & \epsilon & \theta \end{pmatrix} = -V \begin{pmatrix} E & E & E \\ \theta & \theta & \theta \end{pmatrix} = \frac{1}{2}. \quad (9)$$

Then replacing the first two columns of V we find

$$\frac{1}{2} = V \begin{pmatrix} E & E & E \\ \theta & \epsilon & \epsilon \end{pmatrix} = \omega V \begin{pmatrix} E & E & E \\ \theta' & \epsilon' & \epsilon \end{pmatrix} = -\omega V \begin{pmatrix} E & E & E \\ \epsilon & \theta & \epsilon \end{pmatrix} = -\frac{1}{2}\omega$$

and so $\omega = -1$. Therefore we have also

$$V \begin{pmatrix} E & E & E \\ \theta & \theta & \theta \end{pmatrix} = -V \begin{pmatrix} E & E & E \\ \theta' & \theta' & \theta \end{pmatrix} = -V \begin{pmatrix} E & E & E \\ \epsilon & \epsilon & \theta \end{pmatrix}$$

agreeing with equation (9). In this case $\omega = -1$ for replacement of either of the other pairs of columns also. On the other hand for V symbols involving only the representations A_1 , A_2 , T_1 and T_2 we can insist that $|ab, c\rangle'$ is identical in form with $|ab, c\rangle$ and then have the simpler relations

$$V \begin{pmatrix} a & b & c \\ \alpha & \beta & \gamma \end{pmatrix}'_{\mu\nu} = V \begin{pmatrix} a & b & c \\ \alpha & \beta & \gamma \end{pmatrix}. \quad (10)$$

We conclude this section by tabulating a set of values of V and ω . For the rest of the paper only the octahedral group O without inversion is explicitly treated. The inclusion of inversion is, of course, trivial. First, then, the V .

Taking the components of T_1 to transform as x, y and z we obtain the useful formulae

$$\left. \begin{aligned} V\begin{pmatrix} T_1 & T_1 & T_1 \\ \alpha & \beta & \gamma \end{pmatrix} &= V\begin{pmatrix} T_2 & T_2 & T_1 \\ \alpha & \beta & \gamma \end{pmatrix} = -\frac{1}{\sqrt{6}} \epsilon_{\alpha\beta\gamma}, \\ V\begin{pmatrix} T_1 & T_1 & T_2 \\ \alpha & \beta & \gamma \end{pmatrix} &= V\begin{pmatrix} T_2 & T_2 & T_2 \\ \alpha & \beta & \gamma \end{pmatrix} = -\frac{1}{\sqrt{6}} |\epsilon_{\alpha\beta\gamma}|, \end{aligned} \right\} \quad (11)$$

where $\epsilon_{\alpha\beta\gamma} = \pm 1$ or 0 is the usual alternating tensor in three variables. Note that the components of T_2 are also labelled x, y and z not, as previously, ξ, η and ζ . The V which are not included in equations (6) and (11) are given in table 1. $\omega(abc)_{\mu\nu} = 1$ unless at least one of a, b, c is E . Remembering the invariance to even permutations, table 2 gives a sufficient collection of values of ω .

A_2EE			EEE			$A_2T_1T_2$					
$\alpha\beta$	γ		θ	ϵ		$\alpha\beta$	γ		x	y	z
$a\theta$			0	$1/\sqrt{2}$		$\theta\theta$			ax	$1/\sqrt{3}$.
$a\epsilon$			$-1/\sqrt{2}$	0		$\theta\epsilon$			ay	.	$1/\sqrt{3}$
						$\epsilon\theta$			az	.	$1/\sqrt{3}$
						$\epsilon\epsilon$					

T_2ET_1				T_1ET_1			
	x	y	z		x	y	z
$x\theta$	$-\frac{1}{2}$.	.	$x\theta$	$1/2\sqrt{3}$.	.
$y\theta$.	$\frac{1}{2}$.	$y\theta$.	$1/2\sqrt{3}$.
$z\theta$.	.	.	$z\theta$.	.	$-1/\sqrt{3}$
$x\epsilon$	$-1/2\sqrt{3}$.	.	$x\epsilon$	$-\frac{1}{2}$.	.
$y\epsilon$.	$-1/2\sqrt{3}$.	$y\epsilon$.	$\frac{1}{2}$.
$z\epsilon$.	.	$1/\sqrt{3}$	$z\epsilon$.	.	.

Table 1. Values of $V\begin{pmatrix} abc \\ \alpha\beta\gamma \end{pmatrix}$. For those containing three T representations see equation (11).

a	b	c	12	ij	23
E	E	A_2	1	1	-1
E	A_2	E	-1	1	1
A_2	E	E	1	-1	1
E	E	E	-1	-1	-1
E	T_1	T_1	1	-1	1
E	T_1	T_2	1	1	-1
E	T_2	T_1	-1	-1	-1
E	T_2	T_2	-1	1	1

Table 2. Values of $\omega(abc)_{ij}$.

3. W COEFFICIENTS

The W coefficients are defined by the formula

$$W\begin{pmatrix} a & b & c \\ d & e & f \end{pmatrix} = \sum_{\alpha\beta\gamma\delta\epsilon\phi} V\begin{pmatrix} a & b & c \\ \alpha & \beta & \gamma \end{pmatrix} V\begin{pmatrix} a & e & f \\ \alpha & \epsilon & \phi \end{pmatrix} V\begin{pmatrix} b & f & d \\ \beta & \phi & \delta \end{pmatrix} V\begin{pmatrix} c & d & e \\ \gamma & \delta & \epsilon \end{pmatrix}. \quad (12)$$

Strictly W should be defined so as to be invariant in form with respect to orthonormal transformations of the basic kets $|a\alpha\rangle$, etc., in analogy with equation (11.6) of FR for \bar{W} . This can easily be done but W is then a more complicated expression and, as we shall not consider such orthonormal transformations, we use the simpler formula (12).

It follows immediately from (12) that W is invariant both to even permutations of its columns and to turning any pair of columns upside down. For example

$$W\begin{pmatrix} a & b & c \\ d & e & f \end{pmatrix} = W\begin{pmatrix} b & c & a \\ e & f & d \end{pmatrix} = W\begin{pmatrix} d & b & f \\ a & e & c \end{pmatrix},$$

etc. Next, W is multiplied by $(-1)^{2(a+b+c+d+e+f)} = 1$, i.e. is also invariant, on odd permutation of its columns. These symmetry operations are all well-known for \bar{W} .

The other symmetry operations for W are the ‘dashing’ of any of the four trios (def) , (dbc) , (eca) , (fab) or the three quartets $(abde)$, $(bcdf)$, $(acdf)$. Each such operation multiplies W by ± 1 and those W which do not involve an E representation are left invariant. Thus

$$W\begin{pmatrix} T_1 & T_1 & T_1 \\ T_1 & T_1 & T_1 \end{pmatrix} = W\begin{pmatrix} T_1 & T_2 & T_2 \\ T_1 & T_2 & T_2 \end{pmatrix} = W\begin{pmatrix} T_1 & T_1 & T_1 \\ T_2 & T_2 & T_2 \end{pmatrix}.$$

When an E is present we use the values of ω in table 2 to deduce the relation between W and W' . For example

$$\begin{aligned} W\begin{pmatrix} E & T_2 & T_1 \\ T_2 & T_1 & T_1 \end{pmatrix} &= \omega(ET_2T_1)_{12}\omega(ET_1T_1)_{12}W\begin{pmatrix} E & T_1 & T_1 \\ T_1 & T_2 & T_1 \end{pmatrix} \\ &= -W\begin{pmatrix} E & T_1 & T_1 \\ T_1 & T_2 & T_1 \end{pmatrix}, \end{aligned}$$

where we simply multiply together those ω which involve an E . The minus sign in the relation $\epsilon' = -\theta$ causes no difficulty because when it occurs in (12) it always appears twice and hence cancels out.

When one of the symbols in W is the unit representation it is easy to show that

$$W\begin{pmatrix} a & b & A_1 \\ d & e & f \end{pmatrix} = (-1)^{a+d+f}\lambda(a)^{-1/2}\lambda(d)^{-1/2}\delta_{ab}\delta_{de}\delta(a,d,f). \quad (13)$$

Next, using the relation

$$\sum_{\alpha} \epsilon_{\alpha\beta\gamma} \epsilon_{\alpha\epsilon\phi} = \delta_{\beta\epsilon} \delta_{\gamma\phi} - \delta_{\beta\phi} \delta_{\gamma\epsilon}, \quad (14)$$

for the alternating tensor (do not confuse the two kinds of ϵ), we deduce from (11) that

$$\begin{aligned} W\begin{pmatrix} T_1 & T_1 & T_1 \\ h & T_1 & T_1 \end{pmatrix} &= \frac{1}{6} \sum_{\beta\gamma\epsilon\phi\theta} (\delta_{\beta\epsilon}\delta_{\gamma\phi} - \delta_{\beta\phi}\delta_{\gamma\epsilon}) V\begin{pmatrix} T_1 & T_1 & h \\ \beta & \phi & \theta \end{pmatrix} V\begin{pmatrix} T_1 & h & T_1 \\ \gamma & \theta & \epsilon \end{pmatrix} \\ &= \frac{1}{6} \sum_{\beta\gamma\theta} V\begin{pmatrix} T_1 & T_1 & h \\ \beta & \gamma & \theta \end{pmatrix}^2 - \frac{1}{6} \sum_{\beta\gamma\theta} V\begin{pmatrix} T_1 & T_1 & h \\ \beta & \beta & \theta \end{pmatrix} V\begin{pmatrix} T_1 & T_1 & h \\ \gamma & \gamma & \theta \end{pmatrix} \\ &= \frac{1}{6} - \frac{1}{2}\delta_{hA_1}, \end{aligned} \quad (15)$$

where we used (5) and (7), except for $h=A_2$ when $W=0$. Apart from the W given by formulae (13) and (15) there are only eight other genuinely distinct ones except those which are zero because of $\delta(a, b, c)\delta(a, e, f)d(b, f, d)\delta(c, d, e)=0$. All others can be turned into one of these by the symmetry operations described earlier for the W . These eight and a few other useful values are given in table 3.

$$\begin{aligned} W\left(\begin{matrix} E & E & E \\ E & E & A_2 \\ E & E & A_2 \end{matrix}\right) &= W\left(\begin{matrix} E & E & A_2 \\ E & E & A_2 \\ E & E & E \end{matrix}\right) = \frac{1}{2}, \quad W\left(\begin{matrix} E & E & E \\ E & E & E \\ T_1 & T_2 & T_1 \end{matrix}\right) = 0, \quad W\left(\begin{matrix} E & E & A_2 \\ T_1 & T_2 & T_1 \\ T_1 & T_2 & T_1 \end{matrix}\right) = -\frac{1}{\sqrt{6}}, \\ W\left(\begin{matrix} E & E & E \\ T_1 & T_1 & T_1 \\ T_1 & T_1 & T_2 \end{matrix}\right) &= W\left(\begin{matrix} E & E & E \\ T_1 & T_1 & T_2 \\ T_1 & T_1 & T_1 \end{matrix}\right) = -W\left(\begin{matrix} E & T_2 & T_1 \\ T_1 & T_1 & T_1 \end{matrix}\right) = \frac{1}{2\sqrt{3}}, \quad W\left(\begin{matrix} E & T_2 & T_1 \\ E & T_1 & T_1 \end{matrix}\right) = 0, \\ W\left(\begin{matrix} E & T_1 & T_1 \\ E & T_1 & T_1 \end{matrix}\right) &= \frac{1}{3}, \quad W\left(\begin{matrix} E & T_1 & T_1 \\ T_1 & T_1 & T_1 \end{matrix}\right) = W\left(\begin{matrix} E & T_2 & T_1 \\ T_2 & T_2 & T_1 \end{matrix}\right) = -W\left(\begin{matrix} E & T_1 & T_1 \\ T_2 & T_1 & T_1 \end{matrix}\right) \\ &= -W\left(\begin{matrix} E & T_2 & T_1 \\ T_1 & T_2 & T_1 \end{matrix}\right) = \frac{1}{6}. \end{aligned}$$

Table 3. Values of $W\left(\begin{matrix} a & b & c \\ d & e & f \end{matrix}\right)$. All W with six T representations equal $\frac{1}{6}$.

There are a number of important equations satisfied by V and W . We lead into these by considering the relationship between the matrix element

$$\langle e, fb(d)c\gamma | ef(a), bc'\gamma' \rangle$$

representing the recoupling of the three representations e, f and b . For group-theoretic reasons it has a factor $\delta_{ee'}\delta_{\gamma\gamma'}$ and is independent of γ . Expansion in terms of the V coefficients then gives the two relations

$$\langle e, fb(d)c\gamma | ef(a), bc\gamma' \rangle = \lambda(a)^{1/2}\lambda(d)^{1/2}(-1)^{b+c+e+f}W\left(\begin{matrix} a & b & c \\ d & e & f \end{matrix}\right), \quad (16)$$

$$\sum_{\alpha\beta\delta\epsilon\phi} V\left(\begin{matrix} a & b & c' \\ \alpha & \beta & \gamma' \end{matrix}\right) V\left(\begin{matrix} a & e & f \\ \alpha & \epsilon & \phi \end{matrix}\right) V\left(\begin{matrix} b & f & d \\ \beta & \phi & \delta \end{matrix}\right) V\left(\begin{matrix} c & d & e \\ \gamma & \delta & \epsilon \end{matrix}\right) = \lambda(c)^{-1}\delta_{ee'}\delta_{\gamma\gamma'}W\left(\begin{matrix} a & b & c \\ d & e & f \end{matrix}\right). \quad (17)$$

From (17), using equations (4), we can deduce a series of other equations. Multiply through by

$$\lambda(c')V\left(\begin{matrix} a & b & c' \\ \alpha' & \beta' & \gamma' \end{matrix}\right)$$

and sum over c' and γ' . Dropping the dashes on α and β this yields

$$\sum_{\delta\epsilon\phi} V\left(\begin{matrix} a & e & f \\ \alpha & \epsilon & \phi \end{matrix}\right) V\left(\begin{matrix} b & f & d \\ \beta & \phi & \delta \end{matrix}\right) V\left(\begin{matrix} c & d & e \\ \gamma & \delta & \epsilon \end{matrix}\right) = W\left(\begin{matrix} a & b & c \\ d & e & f \end{matrix}\right) V\left(\begin{matrix} a & b & c \\ \alpha & \beta & \gamma \end{matrix}\right).$$

Using equations (4) we then obtain successively

$$\sum_{\phi} V\left(\begin{matrix} a & e & f \\ \alpha & \epsilon & \phi \end{matrix}\right) V\left(\begin{matrix} b & f & d \\ \beta & \phi & \delta \end{matrix}\right) = \sum_{c\gamma} \lambda(c)W\left(\begin{matrix} a & b & c \\ d & e & f \end{matrix}\right) V\left(\begin{matrix} a & b & c \\ \alpha & \beta & \gamma \end{matrix}\right) V\left(\begin{matrix} c & d & e \\ \gamma & \delta & \epsilon \end{matrix}\right), \quad (19)$$

$$\begin{aligned} \delta_{fg}\lambda(f)^{-1}\delta(a, e, f)V\left(\begin{matrix} b & g & d \\ \beta & \eta & \delta \end{matrix}\right) &= \sum_{c\gamma\alpha\epsilon} \lambda(c)W\left(\begin{matrix} a & b & c \\ d & e & f \end{matrix}\right) V\left(\begin{matrix} a & b & c \\ \alpha & \beta & \gamma \end{matrix}\right) \\ &\quad V\left(\begin{matrix} c & d & e \\ \gamma & \delta & \epsilon \end{matrix}\right) V\left(\begin{matrix} a & e & g \\ \alpha & \epsilon & \eta \end{matrix}\right), \end{aligned} \quad (20)$$

$$\sum_c \lambda(c)W\left(\begin{matrix} a & b & c \\ d & e & f \end{matrix}\right) W\left(\begin{matrix} a & b & c \\ d & e & g \end{matrix}\right) = \lambda(f)^{-1}\delta_{fg}\delta(a, e, f)\delta(b, d, f). \quad (21)$$

As well as (21) there are other equations satisfied by the W alone which may sometimes be useful. From its connection with recoupling transformations

(FR, p. 57) the first may be called the associative law. We prove it as follows:

$$\begin{aligned} \sum_c (-1)^c \lambda(c) W \begin{pmatrix} a & b & c \\ d & e & f \end{pmatrix} W \begin{pmatrix} a & b & c \\ e & d & g \end{pmatrix} \\ = \sum_{\alpha\beta\gamma} (-1)^{\gamma} \lambda(\gamma) W \begin{pmatrix} a & b & c \\ d & e & f \end{pmatrix} V \begin{pmatrix} a & b & c \\ \alpha & \beta & \gamma \end{pmatrix} W \begin{pmatrix} a & b & c \\ e & d & g \end{pmatrix} V \begin{pmatrix} a & b & c \\ \alpha & \beta & \gamma \end{pmatrix} \\ = (-1)^{f+g} W \begin{pmatrix} a & d & g \\ b & e & f \end{pmatrix}, \end{aligned} \quad (22)$$

using equation (18). On putting $g = A_1$ we obtain the useful result

$$\sum_c \lambda(c) W \begin{pmatrix} a & b & c \\ a & b & f \end{pmatrix} = \delta(a, b, f). \quad (23)$$

Our final equation is the analogy in our theory of an equation for the \bar{W} obtained by Biedenharn and Elliott (FR, p. 159). It can be proved in very similar way to the associative law, using first (+) then successively (18) twice, (19) once, (18) twice and finally (4) again giving

$$\begin{aligned} & (-1)^{a+b+c+d+e+f+\tilde{d}+\tilde{e}+\tilde{f}} W \begin{pmatrix} a & b & c \\ d & e & f \end{pmatrix} W \begin{pmatrix} a & b & c \\ d & \tilde{e} & \tilde{f} \end{pmatrix} \\ & = \sum_g (-1)^g \lambda(g) W \begin{pmatrix} g & \tilde{e} & e \\ a & f & \tilde{f} \end{pmatrix} W \begin{pmatrix} g & \tilde{f} & f \\ b & d & \tilde{d} \end{pmatrix} W \begin{pmatrix} g & \tilde{d} & d \\ c & e & \tilde{e} \end{pmatrix}. \end{aligned} \quad (24)$$

4. X COEFFICIENTS

The X coefficients are defined by the formula

$$X \begin{bmatrix} a & b & c \\ d & e & f \\ g & h & k \end{bmatrix} = \sum_{\alpha\beta\gamma\delta\epsilon\phi\eta\theta\kappa} V \begin{pmatrix} a & b & c \\ \alpha & \beta & \gamma \end{pmatrix} V \begin{pmatrix} d & e & f \\ \delta & \epsilon & \phi \end{pmatrix} V \begin{pmatrix} g & h & k \\ \eta & \theta & \kappa \end{pmatrix} \\ V \begin{pmatrix} a & d & g \\ \alpha & \delta & \eta \end{pmatrix} V \begin{pmatrix} b & e & h \\ \beta & \epsilon & \theta \end{pmatrix} V \begin{pmatrix} c & f & k \\ \gamma & \phi & \kappa \end{pmatrix}. \quad (25)$$

It follows from (25) that X is invariant to transposition, i.e. reflection in its main diagonal, and to even permutation of rows or columns. Odd permutations of the rows or columns multiply it by $(-1)^{a+b+c+d+e+f+g+h+k}$. Evidently X has some similarity with a 3×3 determinant and we see, for example, that

$$X \begin{bmatrix} T_1 T_1 T_1 \\ T_1 T_1 T_1 \\ T_1 T_1 T_1 \end{bmatrix} = 0$$

because of this. Quite a number of X can be shown to be zero by the same sort of elementary argument which shows certain determinants to be zero. All the X in table 4(a) may be evaluated by such procedures supplemented, on occasion, by the dashing operation. This latter symmetry operation on X involves dashing the four symbols which represent the intersections of any pair of rows with any pair of columns or any six symbols which are such that the remaining three lie one in each row and one in each column. As with W , we have $X' = X$ when X contains no E and $X' = \pm X$ otherwise with \pm the product of the relevant ω values. For example

$$X \begin{bmatrix} A_2 E & E \\ E & A_2 E \\ E & E & A_2 \end{bmatrix} = X \begin{bmatrix} A_2 E & E \\ E & A_1 E \\ E & E & A_1 \end{bmatrix}$$

because

$$\{\omega(EA_2E)_{23}\omega(EEA_2)_{23}\}^2 = 1.$$

When one of the symbols in X , say k , is A_1 , equation (25) simplifies to give

$$X \begin{bmatrix} a & b & c \\ d & e & f \\ g & h & A_1 \end{bmatrix} = \lambda(c)^{-1/2} \lambda(g)^{-1/2} \delta_{cf} \delta_{gh} (-1)^{b+d+f+h} W \begin{pmatrix} a & b & c \\ e & d & g \end{pmatrix}. \quad (26)$$

Equation (26) together with the dashing operation means that we can easily obtain the value of any X which contains at least one A_1 or A_2 representation. Another special case, analogous to equation (15), is

$$X \begin{bmatrix} a & b & T_1 \\ d & e & T_1 \\ T_1 & T_1 & T_1 \end{bmatrix} = \frac{1}{6} \lambda(b)^{-1} \delta_{bd} - \frac{1}{6} \lambda(a)^{-1} \delta_{ae} (-1)^{b+d}, \quad (27)$$

providing that $\delta(a, b, T_1) \delta(d, e, T_1) \delta(a, d, T_1) \delta(b, e, T_1) = 1$. A general X can be evaluated in terms of the W using the relation

$$X \begin{bmatrix} a & b & c \\ d & e & f \\ g & h & k \end{bmatrix} = \sum_p \lambda(p) W \begin{pmatrix} a & b & c \\ h & p & e \end{pmatrix} W \begin{pmatrix} d & e & f \\ p & g & a \end{pmatrix} W \begin{pmatrix} g & h & k \\ c & f & p \end{pmatrix}, \quad (28)$$

which follows from (25) together with (19), (18) and (4). The sum in (28) is over at most four values of p and hence any X is calculated without difficulty. Another useful formula for calculating X is given by putting $a=f$ and $b=k$ in (25), multiplying by $\lambda(c)$ and summing over c , whence

$$\sum_c \lambda(c) X \begin{bmatrix} a & b & c \\ d & e & a \\ g & h & b \end{bmatrix} = \lambda(e)^{-1} \delta_{eg} \delta(b, e, h). \quad (29)$$

I have tabulated a sufficient collection of X in table 4 so that any X which does not contain A_1 can be turned into one of this collection, or into one containing A_1 , by permutation of rows and columns, transposition and dashing. Those containing A_1 are readily calculated using equation (26).

There is a series of equations involving V and X paralleling (17)–(20). A typical one is

$$\begin{aligned} & \sum_{\alpha\beta\delta\epsilon} V \begin{pmatrix} a & b & c \\ \alpha & \beta & \gamma \end{pmatrix} V \begin{pmatrix} d & e & f \\ \delta & \epsilon & \phi \end{pmatrix} V \begin{pmatrix} a & d & g \\ \alpha & \delta & \eta \end{pmatrix} V \begin{pmatrix} b & e & h \\ \beta & \epsilon & \theta \end{pmatrix} \\ &= \sum_{k\kappa} \lambda(k) X \begin{bmatrix} a & b & c \\ d & e & f \\ g & h & k \end{bmatrix} V \begin{pmatrix} c & f & k \\ \gamma & \phi & \kappa \end{pmatrix} V \begin{pmatrix} g & h & k \\ \eta & \theta & \kappa \end{pmatrix}. \end{aligned} \quad (30)$$

It can be proved by a straightforward but lengthy series of operations. First express the right-hand side in terms of W by (28) and then eliminate the W using equations (18) and (19). Having obtained (30) we can deduce the rest of the series from it using (4). The most useful ones are

$$\begin{aligned} & \sum_{\alpha\beta\delta\epsilon\eta\theta} V \begin{pmatrix} a & b & c \\ \alpha & \beta & \gamma \end{pmatrix} V \begin{pmatrix} d & e & f \\ \delta & \epsilon & \phi \end{pmatrix} V \begin{pmatrix} g & h & k \\ \eta & \theta & \kappa \end{pmatrix} V \begin{pmatrix} a & d & g \\ \alpha & \delta & \eta \end{pmatrix} V \begin{pmatrix} b & e & h \\ \beta & \epsilon & \theta \end{pmatrix} \\ &= X \begin{bmatrix} a & b & c \\ d & e & f \\ g & h & k \end{bmatrix} V \begin{pmatrix} c & f & k \\ \gamma & \phi & \kappa \end{pmatrix}, \end{aligned} \quad (31)$$

(a) X which are zero for symmetry reasons

$$\begin{bmatrix} \cdot & \cdot & \cdot \\ E & E & E \\ T_2 & \cdot & \cdot \\ \cdot & \cdot & \cdot \end{bmatrix} \begin{bmatrix} T_2 & \cdot & \cdot \\ \cdot & T_2 & \cdot \\ \cdot & \cdot & T_2 \\ \cdot & \cdot & \cdot \\ A_2 & E & E \\ E & E & E \\ E & E & E \end{bmatrix} \begin{bmatrix} E & T_2 & \cdot \\ \cdot & \cdot & \cdot \\ \cdot & \cdot & \cdot \\ \cdot & \cdot & \cdot \\ A_2 & E & E \\ E & T_2 & \cdot \\ E & T_2 & \cdot \end{bmatrix} \begin{bmatrix} E & T_2 & \cdot \\ \cdot & \cdot & \cdot \\ \cdot & \cdot & \cdot \\ \cdot & \cdot & \cdot \\ A_2 & E & E \\ E & T_2 & \cdot \\ E & T_2 & \cdot \end{bmatrix}$$

(b) X with an A_2 .

$$\begin{bmatrix} A_2 & E & E \\ E & A_2 & E \\ E & E & E \end{bmatrix} = \frac{1}{4}, \quad \begin{bmatrix} A_2 & E & E \\ E & A_2 & E \\ E & E & A_2 \end{bmatrix} = -\frac{1}{4}, \quad \begin{bmatrix} A_2 & E & E \\ \cdot & A_2 & E \\ T_2 & E & \cdot \end{bmatrix} = \frac{1}{6}, \quad \begin{bmatrix} A_2 & E & E \\ T_2 & E & \cdot \\ \cdot & E & T_2 \end{bmatrix} = -\frac{1}{6\sqrt{2}}, \quad \begin{bmatrix} A_2 & E & E \\ T_2 & E & T_2 \\ \cdot & E & T_2 \end{bmatrix} = -\frac{1}{6\sqrt{2}}, \quad \begin{bmatrix} A_2 & E & E \\ T_2 & E & T_2 \\ T_2 & E & \cdot \end{bmatrix} = \frac{1}{6\sqrt{2}},$$

$$\begin{bmatrix} A_2 & E & E \\ T_2 & T_2 & \cdot \\ \cdot & T_2 & \cdot \end{bmatrix} = \frac{1}{6\sqrt{6}}, \quad \begin{bmatrix} A_2 & E & E \\ E & T_2 & \cdot \\ E & T_2 & \cdot \end{bmatrix} = \frac{1}{6},$$

(c) X without A_1 or A_2 .

$$\begin{bmatrix} T_2 & \cdot & \cdot \\ \cdot & T_2 & \cdot \\ \cdot & \cdot & T_2 \\ \cdot & \cdot & \cdot \\ E & T_2 & \cdot \\ \cdot & E & T_2 \\ E & \cdot & E \end{bmatrix} = \begin{bmatrix} T_2 & T_2 & T_2 \\ \cdot & T_2 & \cdot \\ \cdot & \cdot & T_2 \\ \cdot & \cdot & \cdot \\ E & T_2 & \cdot \\ \cdot & E & T_2 \\ E & \cdot & E \end{bmatrix} = \begin{bmatrix} E & \cdot & \cdot \\ \cdot & T_2 & \cdot \\ \cdot & \cdot & T_2 \\ \cdot & \cdot & \cdot \\ E & E & E \\ E & E & E \\ E & E & E \end{bmatrix} = -\frac{1}{18},$$

$$\begin{bmatrix} E & T_2 & \cdot \\ \cdot & T_2 & \cdot \\ \cdot & \cdot & E \\ \cdot & \cdot & \cdot \\ E & T_2 & \cdot \\ \cdot & E & T_2 \\ E & \cdot & E \end{bmatrix} = \begin{bmatrix} E & T_2 & \cdot \\ \cdot & T_2 & \cdot \\ \cdot & \cdot & E \\ \cdot & \cdot & \cdot \\ E & E & E \\ E & E & E \\ E & E & E \end{bmatrix} = \frac{1}{12}, \quad \begin{bmatrix} E & T_2 & \cdot \\ \cdot & T_2 & \cdot \\ \cdot & \cdot & E \\ \cdot & \cdot & \cdot \\ E & E & E \\ E & E & E \\ E & E & E \end{bmatrix} = -\frac{1}{12\sqrt{3}},$$

$$\begin{bmatrix} E & T_2 & \cdot \\ \cdot & E & T_2 \\ \cdot & \cdot & E \\ \cdot & \cdot & \cdot \\ E & T_2 & \cdot \\ \cdot & E & T_2 \\ E & \cdot & E \end{bmatrix} = 0, \quad \begin{bmatrix} E & T_2 & \cdot \\ \cdot & E & T_2 \\ \cdot & \cdot & E \\ \cdot & \cdot & \cdot \\ E & E & E \\ E & E & E \\ E & E & E \end{bmatrix} = \frac{1}{6\sqrt{3}}, \quad \begin{bmatrix} E & E & E \\ E & E & E \\ E & E & E \end{bmatrix} = \frac{1}{4}.$$

Table 4. Values of X . A dot always signifies T_1 and the symbol X is omitted.

$$\begin{aligned} & \sum_{\alpha\delta} V \begin{pmatrix} a & b & c \\ \alpha & \beta & \gamma \end{pmatrix} V \begin{pmatrix} d & e & f \\ \delta & \epsilon & \phi \end{pmatrix} V \begin{pmatrix} a & d & g \\ \alpha & \delta & \eta \end{pmatrix} \\ &= \sum_{hk\theta\kappa} \lambda(h)\lambda(k) X \begin{bmatrix} a & b & c \\ d & e & f \\ g & h & k \end{bmatrix} V \begin{pmatrix} c & f & k \\ \gamma & \phi & \kappa \end{pmatrix} V \begin{pmatrix} g & h & k \\ \eta & \theta & \kappa \end{pmatrix} V \begin{pmatrix} b & e & h \\ \beta & \epsilon & \theta \end{pmatrix} \quad (32) \end{aligned}$$

and the orthonormality rule for the X :

$$\begin{aligned} & \sum_{gh} \lambda(g)\lambda(h) X \begin{bmatrix} a & b & c \\ d & e & f \\ g & h & k \end{bmatrix} X \begin{bmatrix} a & b & c' \\ d & e & f' \\ g & h & k \end{bmatrix} \\ &= \lambda(c)^{-1}\lambda(f)^{-1}\delta_{cc'}\delta_{ff'}\delta(a,b,c)\delta(d,e,f)\delta(c,f,k). \quad (33) \end{aligned}$$

If we multiply (31) by

$$V \begin{pmatrix} c & f & k' \\ \gamma & \phi & \kappa' \end{pmatrix}$$

and sum over γ and ϕ we obtain equation (25) with X on the left-hand side replaced by $X\delta_{kk'}\delta_{\kappa\kappa'}$ and the second k , and κ on the right-hand side replaced by k' and κ' . Just as with equation (17) this result can be given a group-theoretic significance in terms of recoupling transformations (see FR, p. 60).

Finally, there is also an associative law for X which reads

$$\sum_{gh} (-1)^h \lambda(g)\lambda(h) X \begin{bmatrix} a & d & g \\ b & e & h \\ c & f & k \end{bmatrix} X \begin{bmatrix} a & d & g \\ e & b & h \\ l & m & k \end{bmatrix} = (-1)^{f+m} X \begin{bmatrix} a & b & c \\ e & d & f \\ l & m & k \end{bmatrix} \quad (34)$$

and can be deduced from equation (31).

5. DISCUSSION

We have now forged a mathematical tool and its use will be demonstrated in subsequent papers. The reader who is familiar with the corresponding one for the unitary unimodular group U_2 will have no difficulty in using it for himself already. Here I mention that our present theory is welded into the usual ligand field theory chiefly through equation (3), which expresses the coupling coefficients in terms of V , and equation (16) giving the three-representation recoupling coefficients in terms of W . Incidentally equations (16), (13) and (15) together with table 3 give implicitly the values of all these recoupling coefficients. We shall see in a later paper that the X are proportional to more complicated recoupling coefficients (as in FR, Chapter 12) and also to certain sums which occur in the theory of the vibration-induced electric dipole intensities of Laporte-forbidden electronic transitions in centrosymmetric ions. It will appear that the V , W and X are most useful in problems, such as the latter, where the states of interest are defined by coupling two or more sets of states of sub-systems each forming bases for irreducible representations, and which are complicated mainly because of the presence of these couplings and of summations over the components of irreducible representations. The relationship to methods directly involving coupling and recoupling coefficients will also be shown.

From our present viewpoint the most important difference between the representations of the octahedral group O and those of its associated spinor group O^* is that the direct product of two of the latter, but not of the former, may contain a repeated representation. Therefore if it proves possible at all usefully

to define V symbols for O^* they will be essentially more complicated and not at all a trivial generalization of those of the present paper. Hence our present method is not immediately applicable to general calculations with spin-orbit coupling. However it can be used in some cases and we shall see that general two-electron systems provide a straightforward example, spin functions with given S transforming as the irreducible representations A_1 or T_1 according to whether they represent singlets or triplets.

REFERENCES

- [1] FANO, U., and RACAH, G., 1959, *Irreducible Tensorial Sets* (Academic Press).
- [2] FROBENIUS, G., and SCHUR, I., 1906, *Sitzungsberichte der Akademie zu Berlin*, **1**, 186.

RESEARCH NOTES

Semiconductivity in organic molecular complexes

by Miss J. A. VAN DER HOEK, J. H. LUPINSKI and L. J. OOSTERHOFF

Division of Theoretical Organic Chemistry, Leiden University

(Received 24 February 1960)

Semiconductivity has been observed in charge-transfer complexes of large condensed aromatic hydrocarbons (or ketones) with halogens [1], of dimethyl-aniline with chloranil [2] and of paraphenylenediamines with quinones [3]. The electrical conductivity of coal is also ascribed to charge-transfer complexes [4].

Most of the above-mentioned complexes contain unpaired electrons as can be shown by electron spin resonance experiments [3, 5, 6]. A condition for the occurrence of unpaired electrons in such complexes seems to be that at least one of the complex-forming components can be rather easily transformed into a fairly stable radical ion.

Electron spin resonance was found in a large number of molecular compounds formed from donor molecules like 4, 4'-diaminodiphenyl (benzidine), 4, 4'-dimethylaminodiphenyl (tetramethylbenzidine) and acceptor molecules like iodine, bromine and tetranitromethane [7]. For some of these compounds the electrical conductivity (σ) has also been studied; the preliminary results are reported here (see table).

Complex†	n	$\sigma(\Omega^{-1} \text{cm}^{-1}, 300^\circ\text{K})$
Benzidine.nI ₂ [8]	1.35	3×10^{-6}
"	1.17	3×10^{-6}
"	1.50	4×10^{-6}
" ‡	1.50	5×10^{-3}
Benzidine.nBr ₂	0.96	4×10^{-10}
Benzidine.nC(NO ₂) ₄	0.38	5×10^{-6}
Benzidine.n(1, 3, 5-trinitrobenzene) [9]	1	3×10^{-9}
Tetramethylbenzidine.nI ₂	1.35	6×10^{-10}
Tetramethylbenzidine.nBr ₂ [10]	0.48	1×10^{-6}
"	0.51	3×10^{-6}

† Except in benzidine.n (1, 3, 5-trinitrobenzene) electron spin resonance was found in all complexes.

‡ Made in carbon tetrachloride.

Usually the complexes were made by mixing solutions of the components in benzene. The dark coloured precipitates were filtered, washed and dried. These complexes appeared to have a non-stoichiometrical composition represented by D.nA (D being the electron donor component while A is the electron acceptor).

In order to measure the electrical conductivity the powders were pressed ($10\ 000\ \text{kg/cm}^2$) into tablets, care being taken to remove the air from the sample. The resistance of the tablets of known dimensions was determined with a d.c. voltage. The accuracy of the measurements was not very great and no precautions have been taken with respect to surface conductivity. Therefore the results are not to be considered as accurate values, but as illustrations of the order of magnitude. At low temperatures electrical conductivity decreases; the benzidine. NI_2 complex appeared to have a conductivity of about $10^{-11}\ \Omega^{-1}\ \text{cm}^{-1}$ at 90°K .

Benzidine itself turned out to be an insulator at room temperature.

REFERENCES

- [1] AKAMATSU, H., INOKUCHI, H., and MATSUNAGA, Y., 1954, *Nature, Lond.*, **173**, 168.
- [2] ELY, D. D., INOKUCHI, H., 1957, *Proc. Third Biennial Carbon Conference*, Buffalo N.Y. (Pergamon Press).
- [3] BIJL, D., KAINER, H., and ROSE-INNES, A. C., 1959, *J. chem. Phys.*, **30**, 765.
- [4] SCHUYER, J., and KREVELEN, D. W. VAN, 1955, *Fuel*, **34**, 213.
- [5] KAINER, H., BIJL, D., and ROSE-INNES, A. C., 1954, *Naturwissenschaften*, **41**, 303.
- [6] MATSUNAGA, Y., 1959, *J. chem. Phys.*, **30**, 855.
- [7] BUCK, H. M., LUPINSKI, J. H., and OOSTERHOFF, L. J., 1958, *Mol. Phys.*, **1**, 196.
More details will be published shortly.
- [8] RICHTER, M. M., 1911, *Ber. dtsch. chem. Ges.*, **44**, 3466.
- [9] NOELTING, E., and SOMMERHOFF, E. O., 1906, *Ber. dtsch. chem. Ges.*, **39**, 77.
- [10] FRIES, K., 1906, *Liebigs Ann.*, **346**, 215.

Discrete sites in liquids†

by G. WILSE ROBINSON

Gates and Crellin Laboratories of Chemistry
California Institute of Technology
Pasadena, California

(Received 14 June 1960)

It has been clear for some time that spectral line shapes are important in the study of intermolecular interactions [1]. The first evidence that a *simple* relationship might exist between line shape and local structure in *dense* fluids arose through a comparison of the Hg 2537 Å spectrum in high density argon [2] with that of Hg in crystalline argon [3]. In the case of the fluid, a spectral doublet is observed (figure (a)). The relative intensities of the two components and their frequency positions were found to be density dependent.

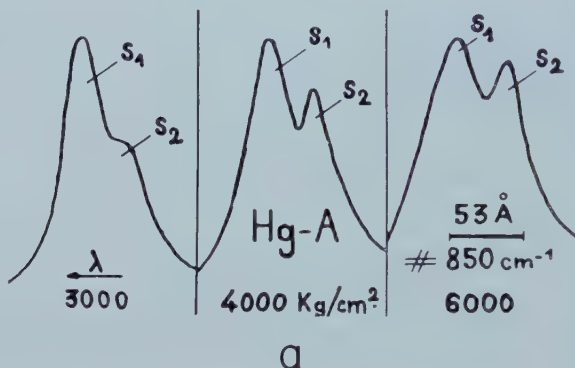
The solid phase spectrum shows a narrow triplet‡ whose mean line position corresponds almost exactly with the high frequency component of the fluid spectrum. These 'lines' are shifted from the free-atom line position 1200 cm^{-1} to higher energy. The substitutional site in crystalline argon is expected to be a highly repulsive one with respect to the Hg atom. This site, however, is energetically more stable with respect to the total local energy than are more attractive sites which must always be accompanied by local defects. This apparent anomaly is a fairly obvious result of the presence of a preponderance of argon–argon attractive interactions that resist local expansion or compression of the normal argon crystal structure. A 'squeezed Hg atom' spectrum characterized by the blue shift is the result. *In the high density fluid the presence of such a site indicates a strong tendency for the formation of argon clusters having internuclear distances and local density almost exactly the same as in the solid.*

The presence of the second broad line in the fluid spectrum is, at first sight, more puzzling. It was originally rationalized [3] on the basis of 'two different cluster configurations.' A more reasonable explanation is evident if it is assumed that the clusters are not very large, in which case the number of atoms on the cluster 'interfaces' may be of the same order as those in the cluster interiors. An atom at the interface is expected to have a different nearest-neighbour density and possibly different interaction distances and degrees of local fluctuations than an interior atom. The perturbations operating on the ground and excited states of Hg to cause the spectral shifts are probably of the 'van der Waals type'. Two pertinent features of these interactions are: (1) The interaction energies are roughly additive with respect to all neighbours; (2) the interaction energies fall off rapidly with distance with the result that nearest neighbours make by far the largest contribution to the interaction energy. The presence of Hg atoms in two different local environments therefore is expected to give rise to line doubling.

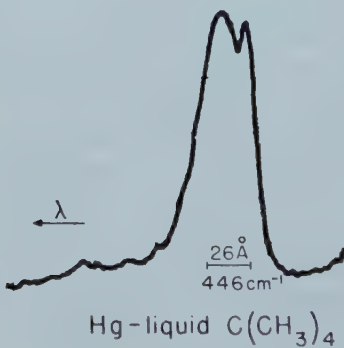
† Supported in part by the National Science Foundation. Contribution No. 2589.

‡ This triplet is very much narrower than the doublet splitting in the fluid spectrum. It has been explained [3] on the basis of removal of the 3-fold spatial degeneracy in the 3P_1 state of Hg by a slightly distorted cubic environment.

The change of relative intensity of the doublet components with density is consistent with the perfectly reasonable supposition that the average cluster size is density-dependent. This is in agreement with the results of x-ray diffraction in liquid argon [4], which show that the average nearest-neighbour distance remains sensibly constant throughout a 1.5-fold decrease in density above the triple point. The frequency shift of both doublet components with density is expected since (1) the non-nearest-neighbour contribution to the shift depends on density, but, more important, (2) fluctuations are expected to decrease the average nearest neighbour density by an amount dependent upon the fraction of holes (cluster interfaces?) in the fluid.



a



b

- (a) The 2537 Å absorption of Hg in argon gas at various densities up to the liquid density [2]. The density corresponding to 6000 kg/cm² is ~820 amagat while that of normal liquid argon is ~790 amagat and that of solid argon is ~910 amagat.
 (b) The 2537 Å absorption of Hg in liquid neopentane at 20°C.

A second experimental result† indicating discrete sites in liquids arises in the spectrum of Hg in liquid neopentane (figure (b)). A well-resolved doublet reminiscent of the Hg-argon spectrum is clearly present. Because of the large size of the neopentane molecule, the high-frequency component does not show a large repulsive blue shift as in fluid argon but is shifted very little from the free-atom position.

† Thanks are due to Dr. M. R. Wright for obtaining this spectrum.

At low densities the theory of spectral line shapes is reasonably simple, but at intermediate densities the theory becomes very complex. The theory is expected to become simple again in the high density region if, as suggested here, clustering is important. The study of spectral line shapes in very dense fluids might then shed light on the microscopic structure of these systems. It is important to realize that if the solute or solvent molecules deviate appreciably from spherical symmetry, large angular dependent forces may be present, the average over which would wash out any subtle line multiplicities.

REFERENCES

- [1] See, for example, CH'EN, S., and TAKEO, M., 1957, *Rev. mod. Phys.*, **29**, 20; KLEIN, C., and MARGENAU, H., 1959, *J. chem. Phys.*, **30**, 1556.
- [2] ROBIN, J., BERGEON, R., GALATRY, L., and VODAR, B., 1956, *Disc. Faraday Soc.*, **9**, 30; in particular, see figures 7 and 8.
- [3] McCARTY, M., Jr., and ROBINSON, G. W., 1959, *Mol. Phys.*, **2**, 415.
- [4] EISENSTEIN, A., and GINGRICH, N. S., 1942, *Phys. Rev.*, **62**, 261.

Intermolecular forces from optical spectra of impurities in molecular crystals†

by R. W. ZWANZIG

National Bureau of Standards, Washington 25, D.C., U.S.A.

(Received 11 December 1959)

A procedure is outlined by which one can get information about the effects of electronic excitation on the interactions between molecules. The absorption and emission spectra of impurities in molecular crystals, and specifically the mean positions and widths of the lines, are required as functions of temperature. A theory of M. Lax is used to relate mean position and width to intermolecular forces. The preliminary treatment of this problem by McCarty and Robinson is evaluated and extended: their procedure is expected to be valid for very narrow lines only.

McCarty and Robinson [1] have reported electronic absorption spectra of Hg, NH and C₂ in rare gas (Ar, Kr, Xe) matrices at 4·2°K. They attribute certain shifts in the spectra to the difference in interaction energy of the excited and the ground state impurity with the matrix. They correlate these shifts numerically on the basis of a simple model.

The work of McCarty and Robinson has introduced a new tool for the study of intermolecular forces, which enables one to obtain precise experimental information about the effects of electronic excitation on the interactions between atoms and molecules.

Their discussion, however, is based on certain assumptions which are not always satisfied. We point out in this article a more rigorous procedure for obtaining intermolecular force parameters from spectral data. This procedure requires considerably more experimental information than is now available—specifically, line positions and widths as functions of temperature in both emission and absorption—but it is capable of giving more, and more reliable, information about interactions.

Our analysis is a straightforward application of the theory developed by M. Lax [2] in his important article “The Franck-Condon Principle and its Application to Crystals”. In this article, Lax shows how to calculate the shapes of absorption and emission spectra of impurities in crystals, with emphasis on the role of lattice vibrations. (In a later review [3], Lax gives a more qualitative and pictorial treatment. Recently, Dexter [4] has also reviewed this subject.)

It should be noted that although Lax’s theory was aimed specifically at spectra of impurities in ionic crystals and homopolar semiconductors, and although the major application of his work has been to F-centres, it is equally applicable to impurities in molecular crystals. An important feature of his treatment is that the Hamiltonian for lattice vibrations should depend on the

† This research was carried out as part of the National Bureau of Standards Free Radicals Research Program, supported by the Department of the Army.

state of excitation of the impurity in a certain reasonably general way. The details of this dependence may vary from one substance to another, but the analysis of the Hamiltonian does not vary in any essential way.

In the following, we use a simplified form of Lax's theory. First we can avoid a great deal of trouble by seeking only the first and second moments of the spectral line (or mean position and the root-mean-square width of the line)†. If, as a result of future experiments, the actual shape of the line becomes of interest, a more refined application of Lax's theory must be made.

We also use the 'Condon' approximation, in which the dependence of the electric dipole matrix elements on lattice coordinates is neglected. This means that we can treat only strongly allowed transitions with confidence. If the transition is allowed entirely as a result of lattice vibrations, and is forbidden in the static non-deformable lattice, this is not a valid approximation at all.

Finally, we use what Lax calls the quasi-molecular viewpoint: "a complex system is simplified by neglecting all but a small number of coordinates . . .". One of the principal results of Lax's work is the elucidation of this viewpoint.

Consider a molecular crystal (the matrix) in which one of the molecules is replaced by an impurity. The lattice Hamiltonian of the pure matrix is H . When an impurity in its ground electronic state is substituted, the lattice Hamiltonian changes to $H + U_g$. When the impurity is excited this becomes $H + U_e$.

The perturbations U_g and U_e contain several contributions. First, there is a change in kinetic energy as a result of the substitution of one mass for another. This contribution occurs identically in U_g and U_e and is quadratic in momentum. The rest of the perturbation depends on molecular positions only, and may be expanded in power series; we get constant, linear, quadratic . . . contributions.

The terms which are quadratic in the momenta and coordinates give rise to changes in the lattice frequencies and possibly to changes in the character of the lattice normal modes. In the following, we neglect these and all higher-order terms.

We therefore use the linear approximation

$$U_g = E_g + \sum_j \mathbf{C}_g(j) \cdot (\mathbf{r}_j - \mathbf{r}_0) + \dots, \quad (1)$$

$$U_e = E_e + \sum_j \mathbf{C}_e(j) \cdot (\mathbf{r}_j - \mathbf{r}_0) + \dots \quad (2)$$

where \mathbf{r}_0 and \mathbf{r}_j are the displacements of the impurity and of its surrounding matrix molecules from their unperturbed equilibrium positions. The constant terms E_g and E_e represent the changes in energy of a static, non-deformable lattice as a result of substitution or excitation. The linear terms can be eliminated from the Hamiltonian by changing the equilibrium positions of the molecules. This 'lattice distortion effect' can be illustrated easily by considering a single normal mode oscillator,

$$\frac{1}{2} M\omega^2 Q^2 + AQ = \frac{1}{2} M\omega^2 \left(Q + \frac{A}{M\omega^2} \right)^2 - \frac{1}{2} \frac{A^2}{M\omega^2}. \quad (3)$$

† The reader is cautioned that the definitions of mean position and mean width which are used here are taken directly from Lax's article, and are not conventional. A factor of ν has been removed from the absorption coefficient, and a factor of ν^3 from the emission probability, before computing the 'mean position' and 'mean width'. Furthermore, the customary use of frequency of maximum intensity for mean position, and width at half intensity for mean width, depends on assumptions about the line shape which may not be satisfied.

The entire effect of a linear term is to displace the position of the minimum in the harmonic oscillator potential. Later in this article we shall show explicitly how the coefficients $\mathbf{C}_g(j)$ and $\mathbf{C}_e(j)$, and the energies E_g and E_e can be related to intermolecular potentials. In typical cases only the nearest neighbours of the impurity contribute significantly to the linear terms.

In the quasi-molecular viewpoint we treat each relative displacement $\mathbf{r}_j - \mathbf{r}_0$ as the normal coordinate of a fictitious oscillator with mass M and frequency $\bar{\omega}$. Of course this is not correct. Each $\mathbf{r}_j - \mathbf{r}_0$ is a linear superposition of all lattice normal modes, and these have a spread of frequencies. However, Lax shows how the correct and the quasi-molecular approaches can be reconciled. The mass M and frequency $\bar{\omega}$ have to be chosen according to a certain prescription (and may, in extreme cases, possess a temperature dependence).

One might guess that $\bar{\omega}$ should be fairly close to the average Debye cut-off frequency $\bar{\omega}_D$ for the lattice since very short wavelength (acoustic) lattice vibrations are involved in the relative motion of nearest neighbours. This guess is supported by a crude calculation in which the lattice is replaced by an elastic continuum and the Debye frequency spectra for longitudinal and transverse modes are used. Only the longitudinal modes are involved, and one gets $\bar{\omega} = 3\omega'/4$ where ω' is the cut-off for longitudinal waves. Since one generally knows only the average cut-off $\bar{\omega}_D$, and since $\omega' > \bar{\omega}_D$, the best one can do, other than to make a much more detailed calculation, is to use the crude value $\bar{\omega} \approx \bar{\omega}_D$ and to remember that this can be wrong by perhaps 25 per cent. If measurements of line widths are made as a function of temperature it is possible to get $\bar{\omega}$ experimentally: this will be made clear in the following discussion.

In the same crude calculation the effective mass M is a few per cent smaller than the mass of a matrix molecule. In view of all the approximations used in the calculation the difference is negligible.

The mean positions of the absorption and emission lines are then

$$(h\nu)_{\text{abs}} = E_e - E_g - \frac{Z}{M\bar{\omega}^2} C_g (C_e - C_g), \quad (4)$$

$$(h\nu)_{\text{em}} = E_e - E_g - \frac{Z}{M\bar{\omega}^2} C_e (C_e - C_g). \quad (5)$$

The energy difference $E_e - E_g$ depends on the kind of lattice, and Z is the number of nearest neighbours (twelve for a face-centred-cubic lattice). The distortion constants C_g and C_e do not depend on the kind of lattice. In principle M and $\bar{\omega}$ do, but in practice the preceding crude approximations for these quantities do not. The quantities C_g and C_e are defined by the equations

$$\mathbf{C}_g = C_g \frac{\mathbf{R}_j - \mathbf{R}_0}{|\mathbf{R}_j - \mathbf{R}_0|}, \quad \mathbf{C}_e = C_e \frac{\mathbf{R}_j - \mathbf{R}_0}{|\mathbf{R}_j - \mathbf{R}_0|}$$

(The vectors are directed radially out from the impurity to a nearest neighbour.) The mean square width is

$$\langle (h\nu - h\bar{\nu})^2 \rangle \equiv w^2 = Z \frac{\hbar}{2M\bar{\omega}} \coth \frac{\hbar\bar{\omega}}{2kT} \cdot (C_e - C_g)^2 \quad (6)$$

and should be the same for both emission and absorption.

In this approximation the mean positions of the spectral lines can depend implicitly on temperature for two reasons. The coupling constants C_g and C_e are functions of the lattice spacing, which changes with temperature according to

the coefficient of thermal expansion. Also, the effective frequency $\bar{\omega}$ may depend on temperature. However, if the latter effect is important, the quasi-molecular approach is not useful and a more detailed theory must be constructed. The root-mean-square line width also has an explicit temperature dependence: it is proportional to $(\coth \hbar \bar{\omega} / 2kT)^{1/2}$. At liquid helium temperatures this factor is very close to unity for virtually any matrix.

Before we get to our specific purpose, the interpretation of the parameters $E_e - E_g$, C_g and C_e in terms of intermolecular forces, let us consider how the more general aspects of the theory can be tested experimentally.

The theory contains three parameters which are characteristic of the impurity and its interaction with the matrix; a fourth parameter $\bar{\omega}$ has been related approximately to the Debye frequency. The theory connects three experimental quantities, $(h\bar{\nu})_{\text{abs}}$, $(h\bar{\nu})_{\text{em}}$ and w to the three parameters. Therefore, internal tests for consistency have to be devised. The temperature dependence of the line width and position should be measured so that the correct value of $\bar{\omega}$ can be obtained, its relation to $\bar{\omega}_D$ and its independence of temperature verified. Once $\bar{\omega}$ is known, the following prediction can be tested:

$$(h\bar{\nu})_{\text{em}} - (h\bar{\nu})_{\text{abs}} = \frac{2w^2}{\hbar \bar{\omega}}. \quad (7)$$

There do not seem to be any other tests which are independent of special assumptions about the parameters.

We turn now to the determination of intermolecular forces from spectral data. The problem here is to relate the parameters $E_e - E_g$, C_g and C_e to other parameters which are more commonly used to characterize intermolecular interactions. We shall assume that all interactions are additive in pairs, spherically symmetric, and obey the Lennard-Jones 6-12 potential. There is no reason why one cannot treat more general potentials, angular dependences, etc.; but our purposes are fully served here by using the above simplifications.

Let $V(R)$, $V_g(R)$ and $V_e(R)$ be the pair potentials for matrix-matrix, matrix-ground state impurity, and matrix-excited state impurity interactions respectively. Let \mathbf{R}_0 and \mathbf{R}_j be the equilibrium unperturbed lattice sites of the impurity and the j th matrix molecule, so their actual separation is $\mathbf{R}_j - \mathbf{R}_0 + \mathbf{r}_j - \mathbf{r}_0$. Then the perturbations are

$$U_g = \sum_j [V_g(\mathbf{R}_j - \mathbf{R}_0 + \mathbf{r}_j - \mathbf{r}_0) - V(\mathbf{R}_j - \mathbf{R}_0 + \mathbf{r}_j - \mathbf{r}_0)], \quad (8)$$

$$U_e = \sum_j [V_e(\mathbf{R}_j - \mathbf{R}_0 + \mathbf{r}_j - \mathbf{r}_0) - V(\mathbf{R}_j - \mathbf{R}_0 + \mathbf{r}_j - \mathbf{r}_0)] + \Delta, \quad (9)$$

where Δ is the energy of the transition in the isolated molecule, and the parameters occurring in the expansions are

$$E_e - E_g = \Delta + \sum_j [V_e(\mathbf{R}_j - \mathbf{R}_0) - V_g(\mathbf{R}_j - \mathbf{R}_0)], \quad (10)$$

$$C_g = V_g'(d) - V'(d), \quad (11)$$

$$C_e = V_e'(d) - V'(d). \quad (12)$$

The primes mean differentiation, d is the nearest-neighbour distance in the unperturbed lattice, and only nearest-neighbour contributions to C_e and C_g are kept.

For the pair potentials we use the Lennard-Jones function,

$$V(R) = \frac{\eta}{R^{12}} - \frac{\mu}{R^6}, \quad (13)$$

$$V_g(R) = \frac{\eta_g}{R^{12}} - \frac{\mu_g}{R^6}, \quad (14)$$

$$V_e(R) = \frac{\eta_e}{R^{12}} - \frac{\mu_e}{R^6}. \quad (15)$$

In a face-centred cubic lattice, for example, the sums over all neighbours in $E_e - E_g$ are:

$$E_e - E_g = \Delta + 12 \cdot 13 \frac{\eta_e - \eta_g}{d^{12}} - 14 \cdot 45 \frac{\mu_e - \mu_g}{d^6}. \quad (16)$$

The nearest-neighbour values of C_e and C_g are

$$C_g = -12 \frac{\eta_g - \eta}{d^{13}} + 6 \frac{\mu_g - \mu}{d^7}, \quad (17)$$

$$C_e = -12 \frac{\eta_e - \eta}{d^{13}} + 6 \frac{\mu_e - \mu}{d^7}. \quad (18)$$

Bearing in mind that the next-nearest neighbour separation is $\sqrt{2}d$, it can be verified that these contributions to C_e and C_g are an order of magnitude smaller than the nearest neighbour ones.

We have now introduced four new parameters η_g , η_e , μ_g , μ_e . (η and μ are assumed to be known for the pure matrix.) Even with very precise experimental data it is impossible to extract four independent quantities from three independent measurements. A complete analysis cannot be carried out unless further assumptions are made.

In the work of McCarty and Robinson the term

$$-\frac{Z}{M\bar{\omega}^2} C_g (C_e - C_g)$$

in $(h\nu)_{\text{abs}}$ is neglected. If the line width is very small then $C_e - C_g$ is small and the neglected term *may* be small. However this depends on the assumption that C_g itself is not unusually large. It is reasonable to expect this to be so in many cases: this distortion of the lattice due to substitution will often be much less than the distortion due to the excitation of the impurity. A precise numerical criterion for the neglect of this term cannot be given in general. Nevertheless, one can make some estimates with the McCarty-Robinson method, in which experimental values of $(h\nu)_{\text{abs}} \approx E_e - E_g$ are used to obtain Lennard-Jones potential parameters. These are then used to calculate $C_e - C_g$ and hence the line width. If the computed width agrees with experiment, the procedure is probably safe.

The treatment of McCarty and Robinson is based on a further assumption which allows the use of data for the same impurity in various matrices. This assumption takes the form of a combining law,

$$\eta_g = \sqrt{(\eta_{ig}\eta)}; \quad \mu_g = \sqrt{(\mu_{ig}\mu)}, \quad (19)$$

$$\eta_e = \sqrt{(\eta_{ie}\eta)}; \quad \mu_e = \sqrt{(\mu_{ie}\mu)} \quad (20)$$

where η_{ig} , μ_{ig} and η_{ie} , μ_{ie} are parameters characteristic of the ground and excited states of the impurity alone, and do not depend on the matrix. This combining

law is not the one commonly used in theories of the thermodynamic properties of gases [5]. Nevertheless, McCarty and Robinson succeeded in fitting data for three impurities in three matrices this way.

It is now quite easy to calculate the widths of the lines from which McCarty and Robinson obtained their Lennard-Jones parameters. Their article contains the numbers necessary to compute $C_g - C_r$, the masses are known and the Debye characteristic temperatures, related by $\bar{\omega}_D$ to $k\theta_D = \hbar\bar{\omega}_D$, are available [6]. Our equation (6) is used, and the results are given in the table. The measured shifts (measured transition energy minus the transition energy in the gas) are also given. It will be seen that in some cases the predicted widths are not at all small relative to the shifts: this casts doubt on the validity of McCarty and Robinson's approximations. (As a result of uncertainties in M and $\bar{\omega}$, our predicted widths can easily be in error by 25 per cent.) Unfortunately, McCarty and Robinson have not reported line widths, so the comparison with experiment cannot be made.

		Hg	NH	C_2
Ar	Shift Width	+ 1281 214 cm^{-1}	- 192 23 cm^{-1}	- 180 31 cm^{-1}
Kr	Shift Width	+ 796 183	- 264 12	(—) 17
Xe	Shift Width	+ 30 96	- 370 3	- 410 5

(The shifts are measured, and the widths calculated.)

We also make the test for internal consistency which is contained in equation (7), since they have reported values for $(h\nu)_{em} - (h\nu)_{abs}$ in two cases. The agreement is not good:

	NH—Ar	C_2 —Xe
Calculated	$19 cm^{-1}$	$1 cm^{-1}$
Measured	$6 cm^{-1}$	$50 cm^{-1}$

The arguments presented in this article are based on a sequence of approximations. These are:

(A) Quadratic and higher terms in the interaction of the impurity with the lattice have been neglected. These terms can cause 'trapped' or localized normal lattice modes around the impurity, with frequencies radically different from the lattice spectrum of the pure matrix. Such trapped modes can cause a substantial shift in frequency without appreciable broadening, and will invalidate our approach.

(B) If the linear approximation is valid, the use of the quasi-molecular picture may still be unsatisfactory. We have pointed out how this can be tested from the experimental data. A more detailed theoretical analysis of the linear approximation, correctly taking into account all lattice modes, has been made by Lax. But it is rather formal, and much harder to apply in actual cases.

(C) Even if the last two approximations are valid, one must still make assumptions about intermolecular forces. The use of the Lennard-Jones potential is undoubtedly correct in many cases, but the McCarty-Robinson combining law is questionable. Much more experimental data, and much more experimentation on fitting the data are needed.

REFERENCES

- [1] MCCARTY, JR., M., and ROBINSON, G. W., 1959, *Mol. Phys.*, **2**, 415.
- [2] LAX, M., 1952, *J. chem. Phys.*, **20**, 1752.
- [3] LAX, M., 1954, *Photoconductivity Conference held at Atlantic City* (New York: John Wiley and Sons), p. 111.
- [4] DEXTER, D. L., 1958, *Solid State Physics*, Vol. 6, edited by F. Seitz and D. Turnbull (New York: Academic Press, Inc.), p. 355.
- [5] HIRSCHFELDER, J. O., CURTISS, C. F., and BIRD, R. B., 1954, *Molecular Theory of Gases and Liquids* (New York: John Wiley and Sons), p. 168.
- [6] *Ibid.*, p. 1043.

Statistical mechanics of solid and liquid mixtures of ortho- and para-hydrogen: II

by AGNESSA BABLOYANTZ† and A. BELLEMANS‡

Faculty of Sciences, University of Brussels, Belgium

(Received 11 February 1960)

Various refinements are added to a previous theoretical calculation of the configurational free energy of condensed mixtures of *o*- and *p*-hydrogen, based on an oversimplified statistical model: (a) account is taken of the fact that the forces acting between *o*- and *p*-molecules are somewhat different and (b) the rigid lattice model previously used is replaced by an ensemble of Einstein oscillators. A better agreement with experiment is reached.

1. INTRODUCTION

The configurational free energy of liquid and solid hydrogen is a function of the fraction of ortho- and para-molecules; in a preceding paper (to be quoted as I) [1] we attempted to calculate this dependence theoretically for moderately low temperatures ($5 < T < 20^{\circ}\text{K}$) such that we are dealing with mixtures of two kinds of molecules in rotational states $l = 0$ and $l = 1$ respectively. The calculations were made (i) assuming that the intermolecular forces are strictly identical for neighbouring pairs 00, 01 and 11; (ii) for a rigid lattice model. Then, after subtraction of the ideal entropy of mixing, the configurational free energy can only vary with the mole fractions of molecules 0 and 1 on account of *directional intermolecular forces*. Treating this effect as a perturbation we found that the *excess free energy* with respect to a pure system of 0 molecules, could be expressed as

$$\Delta F_d = -Bx_1 - Cx_1^2, \quad (1.1)$$

where x_1 is the mole fraction of molecules 1 and the subscript *d* recalls that this part of the free energy is entirely related to directional forces§.

The experimental excess free energy ΔF is indeed of this form for mixtures of *o*-H₂ and *p*-H₂ [2]; however, the theoretical values of *B* and *C* calculated in I were much too small. So at the end of that paper we reconsidered our working hypotheses (i) and (ii) and suggested that (a) assumption (i) is not strictly true; (b) lattice vibrations should be taken into account.

The aim of the present paper is to report some new calculations where these effects have been included and to show that as expected the greater part of the discrepancy with experiment is eliminated. The effects (a) and (b) will be treated successively in § 2 and § 3. The numerical results will be discussed in § 4.

† Presently at The Naval Research Laboratory, University of Wisconsin.

‡ Associé au Fonds National de la Recherche Scientifique (F.N.R.S.).

§ We call here *excess free energy* the quantity

$$\Delta F = F(x_1) - F(0) - NkT\{(1-x_1)\ln(1-x_1) + x_1\ln x_1\}$$

where $F(x_1)$ is the configurational free energy of a mixture of mole fraction x_1 ; this terminology should not be confused with that used in the conventional theory of mixtures.

2. INFLUENCE OF ROTATIONAL MOTIONS ON INTERMOLECULAR FORCES

On account of their rotational motion molecules 1 have a slightly larger internuclear distance than molecules 0 and the corresponding difference of their electron clouds gives rise to small differences in the forces acting between pairs of 00, 01 and 11. Our aim in this section will be to estimate the contribution of this effect to the free energy.

In paper I the intermolecular potential was expanded in terms of zonal harmonics [3] and a set of coefficients $\zeta^{ll':m}(r)$ was introduced. The first of these $\zeta^{00:0}$ corresponds to central forces; all others relate to directional forces and ΔF_d is entirely due to them. Let us now introduce different sets of coefficients $\zeta_{AB}^{ll':m}(r)$ for each type of neighbouring pairs AB and look for their differences. As these will be small (less than one percent) we must care only for the central term $\zeta_{AB}^{00:0}$: indeed ΔF_d being already a small quantity, it is not affected significantly by such small differences in the coefficients $\zeta_{AB}^{ll':m}$.

We continue to assume in this section that the molecules 0 and 1 are randomly distributed on a rigid lattice. The contribution of the central interactions to the configurational free energy is then

$$F_0 = \frac{1}{2} N z \{ (1 - x_1)^2 \zeta_{00}^{00:0}(a) + 2x_1(1 - x_1) \zeta_{01}^{00:0}(a) + x_1^2 \zeta_{11}^{00:0}(a) \} \quad (2.1)$$

where a is the lattice spacing and z the number of nearest neighbours. The excess of F_0 over the corresponding quantity for an assembly of molecules 0, is

$$\begin{aligned} \Delta F_c = & \frac{1}{2} N z x_1 \{ \zeta_{11}^{00:0}(a) - \zeta_{00}^{00:0}(a) \} \\ & + N z x_1 (1 - x_1) \{ \zeta_{01}^{00:0}(a) - \frac{1}{2} \zeta_{00}^{00:0}(a) - \frac{1}{2} \zeta_{11}^{00:0}(a) \} \end{aligned} \quad (2.2)$$

(the subscript c recalls that this contribution is related to central forces).

To a reasonable approximation $\zeta^{00:0}(r)$ is made up of an attractive term ($\sim r^{-6}$) and a repulsive one ($\sim \exp -r$), both depending parametrically on the average internuclear distances of the interacting molecules. The term $\sim r^{-6}$ (i.e. the dispersion energy) is approximately equal to

$$-1.04 \times 10^{-11} / r^6 \text{ erg} \quad (2.3)$$

(r in angstroms) [4]; the numerical constant in (2.3) is roughly proportional to the product of the polarizabilities of the interacting molecules. Now the molecular polarizability α can be evaluated in two steps (Born-Oppenheimer approximation): first a function $\alpha(R)$ is derived for an arbitrary distance R of the nuclei; next the numerical value of α is computed for the actual vibrational-rotational state of the molecule. Calling R_e the equilibrium distance between the nuclei at rest we have

$$\alpha(R) = \alpha(R_e) \left\{ 1 + \left(\frac{d \ln \alpha}{dR} \right)_e (R - R_e) + \dots \right\}, \quad (2.4)$$

All molecules of the assembly are practically in their lowest vibrational state; further we neglect anharmonicity for our present purpose. It then follows that the average value $\overline{R - R_e}$ is zero for a (non-rotating) molecule 0; for a molecule 1 an elementary calculation shows that

$$\overline{R - R_e} = 2\hbar^2 / IKR_e = 4k\theta_{\text{rot}} / KR_e \quad (2.5)$$

where I is the moment of inertia of the molecule, K is the restoring constant between the nuclei and $k\theta_{\text{rot}} = \hbar^2/2I$. For hydrogen:

$$R_e = 0.74_1 \text{ \AA}, \quad K = 5.7_3 \times 10^{-11} \text{ erg/ \AA}^2, \quad \left(\frac{d \ln \alpha}{d R} \right)_e = 1.78_5 \text{ \AA}^{-1} \quad [5],$$

and the ratio of the polarizabilities of molecules 1 and 0 is found to be

$$\alpha_1/\alpha_0 = 1 + 2.32 \times 10^{-5} \theta_{\text{rot}}. \quad (2.6)$$

For H_2 ($\theta_{\text{rot}} = 85.4^\circ$) and D_2 ($\theta_{\text{rot}} = 42.7^\circ$) this ratio is equal to 1.0020 and 1.0010 respectively. The differences in the dispersion energy of pairs 00, 01 and 11 can now easily be estimated from (2.3) and (2.6), as (2.3) is roughly proportional to the product of the molecular polarizabilities. The same kind of calculation applies to the repulsive part of $\zeta_{AB}^{00:0}$ which following Nakamura [4] is approximately given by

$$48.5 \times 10^{-1.5330r} 10^{-11} \text{ erg} \frac{\sinh 1.77 \bar{R}_A}{1.77 \bar{R}_A} \frac{\sinh 1.77 \bar{R}_B}{1.77 \bar{R}_B} \quad (2.7)$$

where \bar{R}_A and \bar{R}_B are the average internuclear distances (in angstroms) of molecules A and B. For species 0 and 1 we have respectively

$$\sinh 1.77 \bar{R}_0 / 1.77 \bar{R}_0 = 1.331 \quad (\bar{R}_0 = R_e)$$

and

$$\sinh 1.77 \bar{R}_1 / 1.77 \bar{R}_1 = 1.311 \{1 + 0.90 \times 10^{-5} \theta_{\text{rot}}\} \quad (2.8)$$

on account of (2.4). The following expressions are then obtained for $\zeta_{AB}^{00:0}(r)$ by adding together the attractive and repulsive terms (2.3) and (2.7) and retaining first order corrections in θ_{rot} :

$$\begin{aligned} \zeta_{AB}^{00:0}(r) &= \left(83.5 + 10^{-1.5330r} - \frac{1.04}{r^6} \right) 10^{-11} \text{ erg}, \\ \zeta_{01}^{00:0}(r) &= \zeta_{00}^{00:0}(r) + \chi(r) \theta_{\text{rot}}, \\ \zeta_{11}^{00:0}(r) &= \zeta_{00}^{00:0}(r) + 2\chi(r) \theta_{\text{rot}}, \end{aligned} \quad (2.9)$$

where

$$\chi(r) = \left(75 \times 10^{-1.5330r} - \frac{2.42}{r^6} \right) 10^{-16} \text{ erg deg}^{-1}.$$

Substituting in (2.2) we get (by putting z equal to twelve)

$$\Delta F_c = 12N\chi(a)\theta_{\text{rot}}x_1. \quad (2.10)$$

The theoretical value of ΔF for the rigid lattice model is now the sum of ΔF_c and ΔF_d (this latter previously calculated in I). We shall postpone its discussion until § 4.

3. EFFECT OF LATTICE VIBRATIONS

We now abandon the rigid lattice model and replace it by an ensemble of Einstein oscillators with a unique frequency $\nu_0 = k\theta_{\text{vib}}/\hbar(\theta_{\text{vib}}: \text{Einstein characteristic temperature of the lattice})$. This model is much more realistic for liquids or solids than the rigid lattice and it allows us to include in ΔF the coupling between rotational and librational motions in a not too involved way. However, even for this simplified picture the calculations are exceedingly long and we shall omit them completely here†.

† They are given in detail in the Doctoral Thesis of one of us (A. Babloyantz), University of Brussels, 1959.

The general procedure for evaluating the configurational free energy of an assembly of molecules 0 and 1 is the same as in I: the directional interactions $\zeta^{ll':m}(r)$ (l or $l' > 0$) are treated as a perturbation; we limit ourselves to a second order calculation and keep coefficients $\zeta^{20:0}$ and $\zeta^{22:m}$ only; ($\zeta^{ll':m}$ vanishes for all odd values of l and l').[†] The only matrix elements involved in the calculations are relative to pairs of neighbouring molecules just as in I but now they refer to both rotational and vibrational states. These matrix elements depend parametrically on the average displacement of a molecule from its own site which is a function of θ_{vib} and M the molecular mass; its ratio to the lattice spacing a is expressible as

$$\mu = h/a(Mk\theta_{\text{vib}})^{1/2}. \quad (3.1)$$

All terms in μ and μ^2 have been collected in the calculation of ΔF . The numerical values of θ_{vib} for H_2 and D_2 have been estimated to be 44° and 42° respectively from specific heat data. As we limit ourselves to $T \leq 20^\circ\text{K}$ it is sufficient to assume that in the unperturbed system all molecules are in the lowest vibrational state. It then follows that all matrix elements involve but the lowest or the first excited vibrational wavefunction. The final expression of ΔF is of the same general form as for a rigid lattice but considerably longer and we shall not give it here. The numerical results alone will be quoted in the next section.

4. DISCUSSION

In the table we summarize the theoretical values of ΔF for H_2 and D_2 obtained from the three successive approximations:

(I) rigid lattice; identical intermolecular forces:

$$\Delta F_I \equiv \Delta F_d, \text{ (paper I);}$$

(II) rigid lattice; different intermolecular forces:

$$\Delta F_{II} \equiv \Delta F_d + \Delta F_c, \text{ (this paper, §2);}$$

(III) Einstein model; different intermolecular forces:

$$\Delta F_{III}, \text{ (this paper, §3).}$$

The available experimental data for ΔF are also given in the table.

It immediately appears that in any case ΔF_{II} and ΔF_{III} are much nearer to the experimental values than ΔF_I . For liquid H_2 , ΔF_{III} is in excellent agreement with ΔF_{exp} . This is also the case for liquid D_2 at the unique mole fraction $x_1 = 0.33$ where ΔF_{exp} is known; indeed we have at that point

$$\Delta F_{III} \approx -0.7 \text{ cal mole}^{-1}.$$

For solid H_2 the situation is less satisfactory: ΔF_{III} gives quite a good estimation of the quadratic term in x_1^2 but a rather poor one for the linear term; the reverse is true for ΔF_{II} .

It thus appears that the Einstein model works better for the liquid than for the solid state; this may be related to the fact that all correlations between the molecular displacements are neglected in such a model, a situation which is more likely to be approached in a liquid than in a solid.

[†] It was shown in I that $\zeta^{20:0}$ does not contribute to ΔF on account of the symmetry of the lattice; this is no more the case here because of the molecular oscillations.

The theoretical value of the excess energy ΔE has also been calculated; in the case of liquid H_2 at $20^\circ K$ we have

$$\Delta E_{III} = -2.1 x_1 - 3.0 x_1^2 \text{ cal mole}^{-1}.$$

to be compared to the experimental data :

$$\Delta E = -0.9 x_1 - 3.1 x_1^2 \text{ cal mole}^{-1},$$

$$\Delta E = -1.4 x_1 - 2.8 x_1^2 \text{ cal mole}^{-1},$$

obtained respectively from vapour pressure data [2] and energies of vaporization [6]. The agreement is less satisfactory than for ΔF_{III} at $20^\circ K$, but this is not surprising as the imperfections of the statistical model are usually emphasized by taking a derivative.

	ΔF in cal mole $^{-1}$
H_2 at $20.3^\circ K$ (liquid) $a = 4.05 \text{ \AA}$	$\Delta F_I = -0.05x_1 - 0.36x_1^2$ $\Delta F_{II} = -0.80x_1 - 0.36x_1^2$ $\Delta F_{III} = -1.0 x_1 - 1.0 x_1^2$ $\Delta F_{exp} = -0.89x_1 - 1.13x_1^2$ [2]
D_2 at $20^\circ K$ (liquid) $a = 3.80 \text{ \AA}$	$\Delta F_I = -0.22x_1 - 0.57x_1^2$ $\Delta F_{II} = -0.73x_1 - 0.57x_1^2$ $\Delta F_{III} = -1.6 x_1 - 1.3 x_1^2$ $\Delta F_{exp} = -0.6$ at $x_1 = 0.33$ ‡
H_2 at $13.8^\circ K$ (solid) $a = 3.80 \text{ \AA}$	$\Delta F_I = -0.11x_1 - 1.13x_1^2$ $\Delta F_{II} = -1.13x_1 - 1.13x_1^2$ $\Delta F_{III} = -2.7 x_1 - 2.8 x_1^2$ $\Delta F_{exp} = -0.7 x_1 - 2.6 x_1^2$ ‡

Theoretical and experimental values of ΔF for mixtures of
 $p\text{-H}_2$ — $o\text{-H}_2$ and $o\text{-D}_2$ — $p\text{-D}_2$ ‡.

x_1 : mole fraction of $o\text{-H}_2$ and $p\text{-D}_2$ respectively.

‡ Estimated from vapour pressure data [6].

To conclude we may say that a semi-quantitative agreement with experiment has been reached; we could not expect better than that in view of the simplified character of the statistical model and our quite inaccurate knowledge of intermolecular forces. An interesting fact is that the excess free energy ΔF is not solely related to directional interactions but also to a noticeable modification of the intermolecular forces by the rotational motions of the molecules. One of us has already stressed the influence of internal motions on intermolecular forces reflected in the thermodynamic properties of heavy isotopic molecules [7]. Here is another example of such an effect.

We want to thank Professor I. Prigogine for his constant interest in this work, and Mr. Harry Friedman for helpful discussions.

This research has been made possible through the support of The General Electric Research Laboratory, Schenectady, N.Y., through its European Office.

REFERENCES

- [1] BELLEMANS, A., and BABLOYANTZ, AGNESSA, 1959, *Mol. Phys.*, **2**, 169.
- [2] FRIEDMAN, HAROLD L., 1957, *J. chem. Phys.*, **27**, 220.
- [3] POPLE, J. A., 1953, *Disc. Faraday Soc.*, **15**, 35.
- [4] NAKAMURA, T., 1955, *Prog. theor. Phys., Osaka*, **14**, 135.
- [5] ISHIGURO, E., ARAI, T., KOTANI, M., and MIZUSHIMA, M., 1952, *Proc. phys. Soc. Lond. A*, **65**, 178.
- [6] WOOLLEY, H. W., SCOTT, R. B., and BRICKWEDDE, F. G., 1948, *J. Res. Nat. Bur. Stand.*, **41**, 379.
- [7] BELLEMANS, A., 1958, *Nuovo Cim.*, Suppl., **9**, 181.

The effect of paramagnetic molecules on the intensity of spin-forbidden absorption bands of aromatic molecules

by J. N. MURRELL

University Chemical Laboratory, Lensfield Road, Cambridge

(Received 15 January 1960)

It is shown that there are two possible mechanisms whereby a singlet-triplet absorption band of a molecule can gain intensity under the perturbing influence of a paramagnetic species. The first involves some mixing of the triplet state with the singlet states of the molecule. The second involves a mixing of the triplet state with charge-transfer states of the complex formed between the molecule and the paramagnetic species. It is shown that in the particular case of an alternant hydrocarbon, the first singlet-triplet absorption band is unlikely to gain intensity by the first of these mechanisms. It follows by elimination that the charge-transfer mechanism is the more important. The available experimental evidence supports this viewpoint.

1. INTRODUCTION

Evans [1] has shown that the weak absorption band of benzene occurring around 3300 Å, and first observed by Sklar [2], is associated with the presence of dissolved oxygen. It is fairly well established that the state giving rise to this band is the lowest triplet ($^3B_{1u}$). Evans has now shown that oxygen under pressure can bring out the first singlet-triplet absorption band of a large number of aromatic molecules [3]. He has also shown that nitric oxide will produce the same effect as oxygen [4].

The first explanation of this phenomenon was based on the spin-orbit interaction between the electronic states of the molecule, induced by the inhomogeneous field of the paramagnetic species [5, 6]. However, Stephen [7] has shown that the magnitude of the magnetic field of O_2 is insufficient to produce the observed effect. This is supported by the related work of Porter and Wright [8] who show that the quenching efficiency of a transition metal ion on the lifetime of the triplet state of naphthalene is uncorrelated with the magnetic moment of the ion.

An alternative explanation suggested by Evans [3] is that charge-transfer states between the organic molecule and the paramagnetic species are somehow responsible for the breakdown of the spin selection rules. This suggestion is supported by the fact that O_2 is known to give rise to charge-transfer absorption with organic molecules [9, 10], oxygen being a fairly strong electron acceptor.

In this paper the theoretical interpretation of the above experimental results will be examined. Two mechanisms for the breakdown of the spin selection rules for the electronic transitions will be proposed: one involving a mixing of the singlet and triplet states of the organic molecule, and one involving the mixing of the triplet state with charge-transfer states. The general theory will be described, and then this will be applied to the particular case of an alternant hydrocarbon.

2. GENERAL THEORY

We will begin by considering the simplest model which will illustrate the effect of a paramagnetic species (P) on the spin-forbidden electronic transitions of a molecule (R) which has a singlet ground state. The ground state of R will be written as a normalized Slater determinant, a function of the coordinates and spins of just two electrons as follows:

$$^1\psi_0^0 = |\vec{r}^0 \vec{r}^0|$$

r^0 is an α spin-orbital and \vec{r}^0 the corresponding β spin-orbital.

Typical excited states of R can be written

$$^1\psi_1^0 = \sqrt{\frac{1}{2}}(|\vec{r}^0 \vec{s}^0| - |\vec{r}^0 \vec{s}^0|),$$

$$^3\psi_2^1 = |\vec{r}^0 \vec{s}^0|,$$

$$^3\psi_2^0 = \sqrt{\frac{1}{2}}(|\vec{r}^0 \vec{s}^0| + |\vec{r}^0 \vec{s}^0|),$$

$$^3\psi_2^{-1} = |\vec{r}^0 \vec{s}^0|.$$

The perturbing molecule P will be taken to have a doublet ground state, a function of the coordinates and spin of just one electron:

$$^2\phi_0^{1/2} = a, \quad ^2\phi_0^{-1/2} = \bar{a}.$$

The two species are now brought together, and we inquire as to the nature of the states of the complex (which may or may not be stable with respect to the separate components). The orbitals r^0 , s^0 and a are not now orthogonal. To simplify the analysis it is convenient first to form new orbitals as follows:

$$\begin{aligned} a \\ r = (r^0 - S_{ra}a), \end{aligned}$$

and

$$s = (s^0 - S_{sa}a),$$

where S_{ra} is the overlap integral

$$S_{ra} = \langle r^0 | a \rangle.$$

These orbitals are orthogonal to the first order in the overlap between an orbital of R and one of P . As far as the theory developed in this paper is concerned they may be considered to be strictly orthogonal; this will become evident later.

The ground state of the complex, written in terms of the above orbitals, will have a zeroth order wave function

$$^2\theta_0^{1/2} = |\vec{r} \bar{a}|,$$

(we restrict our attention to the component having $S_z = \hbar/2$), and there will be excited states

$$^2\theta_1^{1/2} = \sqrt{\frac{1}{2}}(|\vec{r} \bar{s}a| - |\vec{r} s \bar{a}|),$$

and

$$^2\theta_2^{1/2} = \sqrt{\frac{1}{6}}(2|\vec{r} \bar{s}a| - |\vec{r} s \bar{a}| - |\vec{r} s a|).$$

Now combining a doublet with a triplet state gives rise to a doublet and a quartet state. That is, by combining the components of $^2\phi_0$ and $^3\psi_2$ one can construct two functions which have an eigenvalue of S_z equal to $\hbar/2$. The combination

${}^2\theta_2^{1/2}$, which is written above, is an eigenfunction of S^2 with eigenvalue $\frac{1}{2}(1 + \frac{1}{2})h^2$, that is, a component of a doublet. The function

$${}^4\theta_2^{1/2} = \sqrt{\frac{1}{3}}\{|rs\bar{a}| + |r\bar{s}a| + |\bar{r}s\bar{a}|\}$$

which is also an eigenfunction of S^2 , is one component of a quartet, which we are not concerned with further.

For very weak interaction between R and P , there are the following correlations:

$$\begin{aligned} {}^2\theta_0^{1/2} &\rightarrow {}^1\psi_0^0 \cdot {}^2\phi_0^{1/2}, \\ {}^2\theta_1^{1/2} &\rightarrow {}^1\psi_1^0 \cdot {}^2\phi_0^{1/2}, \\ {}^2\theta_2^{1/2} &\rightarrow \sqrt{\frac{2}{3}}[{}^3\psi_2^1 \cdot {}^2\phi_0^{1/2}] - \sqrt{\frac{1}{3}}[{}^3\psi_2^0 \cdot {}^2\phi_0^{1/2}]. \end{aligned}$$

Hence, relative to the energy of ${}^2\theta_0^{1/2}$, the energy of ${}^2\theta_1^{1/2}$ corresponds to that of the singlet excited state of R and that of ${}^2\theta_2^{1/2}$ corresponds to that of the energy of the triplet state of R .

In addition to the above wave functions we shall be interested in the charge-transfer states of the complex, a typical one being

$${}^2\theta_3^{1/2} = |ra\bar{a}|.$$

The energy of this charge-transfer state will be given in the usual way by the ionization potential of R , less the electron affinity of P , and less the coulombic energy associated with any charge separation involved in forming this state.

We now evaluate the matrix element of the dipole moment operator between the ground state and ${}^2\theta_2$ (which arises from the triplet state of R). It is found from the above wave functions that

$$\langle {}^2\theta_0^{1/2} | \mathbf{M} | {}^2\theta_2^{1/2} \rangle = 0.$$

It is therefore necessary to look further for the source of the intensity of the singlet-triplet absorption band. It will be shown that ${}^2\theta_2^{1/2}$ is not strictly an eigenfunction of the Hamiltonian for the complex, since there exist non-zero matrix elements of \mathcal{H} between ${}^2\theta_2^{1/2}$ and both ${}^2\theta_1^{1/2}$ and ${}^2\theta_3^{1/2}$. There are thus two mechanisms by which the singlet-triplet absorption band can pick up intensity. These two possibilities will be considered separately.

2.1. Intensity borrowing from the singlet state

From the wave function given above it can be seen that

$$\langle {}^2\theta_1^{1/2} | \mathcal{H} | {}^2\theta_2^{1/2} \rangle = \frac{\sqrt{3}}{2} (K_{ra} - K_{sa}), \quad (2.1)$$

where the K 's are two electron exchange integrals defined as

$$K_{ra} = \langle ra | G | ar \rangle = \int \int r(1) a(2) \frac{e^2}{r_{12}} a(1) r(2) d\tau_1 d\tau_2,$$

From first-order perturbation theory, it follows that the intensity of the singlet-triplet absorption band, that is borrowed from the singlet-singlet band of intensity I_{01} , is given by

$$I_{02} = \frac{3}{4} \frac{(K_{ra} - K_{sa})^2}{\Delta E_{12}^2} \cdot I_{01} \dagger. \quad (2.2)$$

ΔE_{12} is the singlet-triplet separation of R .

† A similar result has been obtained by Professor Hoijtink [11] although he does not define his orthogonal orbitals in the same way as is done in this paper. I am indebted to him for allowing me to see a copy of his paper on this topic prior to publication.

From our definition of the orbital r , the exchange integrals can be expanded as follows,

$$K_{ra} = \int \int (r^0 - S_{ra}a)(1)a(2) \frac{e^2}{r_{12}} a(1)(r^0 - S_{ra}a)(2) d\tau_1 d\tau_2,$$

and using the Mulliken approximation to the exchange integral [12] this reduces to

$$K_{ra} \approx \frac{S_{ra}^2}{4} (J_{rr}^0 + J_{aa}^0 - 2J_{ra}^0), \quad (2.3)$$

where the J^0 are two-electron Coulombic integrals between the orbitals of the unperturbed species,

$$J_{ra}^0 = \langle r^0 a | G | r^0 a \rangle.$$

It is seen that the intensity borrowed from the singlet state is proportional to the fourth power of the overlap integral between an orbital on R and one on P . In addition, its magnitude depends on the difference of the overlap integral between a ground state (r^0) and an excited state (s^0) orbital, and the orbital of the paramagnetic species. In general it is to be expected that excited state orbitals are blown up relative to those of the ground state, so that one expects $K_{sa} > K_{ra}$.

2.2. Intensity borrowed from the charge-transfer state

For the matrix element of the Hamiltonian between ${}^2\theta_2$ and ${}^2\theta_3$, we have

$$\langle {}^2\theta_2^{1/2} | \mathcal{H} | {}^2\theta_3^{1/2} \rangle = \sqrt{\frac{3}{2}} \{ H_{sa}^{\text{core}} + \langle rs | G | ra \rangle + \langle sa | G | aa \rangle - \langle rs | G | ar \rangle \}, \quad (2.4)$$

where $H_{sa}^{\text{core}} = \langle s | H^{\text{core}} | a \rangle$. H^{core} is made up of three terms: the potential due to R^{++} , the potential due to P^+ , and the kinetic energy operator (T). Writing $V(R^+)$ for the electrostatic field due to R^+ , and $V(P)$ that due to P , we can see that the above matrix element reduces to

$$\langle {}^2\theta_2^{1/2} | \mathcal{H} | {}^2\theta_3^{1/2} \rangle = \sqrt{\frac{3}{2}} \{ V_{sa}(R^+) + V_{sa}(P) + T_{sa} \} \dagger, \quad (2.5)$$

if the small term $\langle rs | G | ar \rangle$ is neglected.

The intensity of the singlet-triplet band which arises from this interaction is therefore given by

$$I_{02}' = \frac{(V_{sa}(R^+) + V_{sa}(P) + T_{sa})^2}{\Delta E_{23}^2} I_{03}, \quad (2.6)$$

where ΔE_{23} is the difference in energy between the triplet and charge-transfer state, and I_{03} is the intensity of the charge-transfer band. If P is a neutral species (say NO) then we can safely neglect $V_{sa}(P)$ in comparison with $V_{sa}(R^+)$ since the electrostatic field of P will fall off rapidly outside the electron cloud of P . However, this will not be so if P is an ion such as Cu^{++} .

The intensity of the charge-transfer band is proportional to the square of the transition moment

$$\langle {}^2\theta_0^{1/2} | \mathbf{M} | {}^2\theta_3^{1/2} \rangle = - \langle r | \mathbf{m} | a \rangle,$$

and is therefore itself proportional to the square of the overlap between an orbital on P and one on R . There are other sources of intensity of the charge transfer band of the same order of magnitude, which need not be discussed here [13]. It follows that I_{02}' like I_{02} is proportional to the fourth power of such an overlap.

† This type of expression, for the matrix elements occurring in the theory of charge-transfer spectra, has been discussed in more detail elsewhere [13].

From the analysis presented above there would appear to be little to choose between the two mechanisms proposed for the intensification of the singlet-triplet absorption band: both contributions to the intensity are of the fourth power in the overlap between orbitals on R and on P . It is therefore necessary to look to experiment for help in deciding between the two possible mechanisms, and this point will be returned to at the end of the paper.

It has been assumed in the theory presented so far, that the singlet, triplet and charge-transfer states lie sufficiently far apart, or that the interaction between them is sufficiently weak, for perturbation theory to be used. It would, of course, be possible for the triplet and charge-transfer states to be nearly degenerate. If this were the case the resulting states would be a more or less equal mixture of $^2\theta_2$ and $^2\theta_3$, and the two absorption bands, which may or may not overlap depending on the magnitude of the interaction term, would both be of the same order of intensity (of order I_{03}).

Likewise perturbation theory would break down if the singlet and charge-transfer states had about the same energy, for if this is the case, then the intensity of the charge-transfer band is likely to be increased enormously, and this intensity would in turn be passed on to the triplet band. In general, if perturbation theory breaks down, then the wave functions of the complex can only be obtained by diagonalizing the matrix of \mathcal{H} between the zeroth-order states that have been defined in this section.

So far we have considered the perturbation of the singlet-triplet transition by a molecule which has a doublet ground state. The mathematics for perturbation by a triplet state molecule (e.g. O_2) is very similar. It has been discussed in detail by Hoijtink [11], so will not be developed in this paper.

3. APPLICATION TO ALTERNANT HYDROCARBONS

Most of the available experimental results referring to the effect of paramagnetic molecules on singlet-triplet transition probabilities are concerned with aromatic hydrocarbons. The theoretical interpretation of the absorption spectra of these so called 'alternant' hydrocarbons (which gives good agreement with experiment) is simplified by the pairing properties of their molecular orbitals [14, 15]. In this section it will be shown how the same pairing properties simplify the theory developed in §2.

The π -molecular orbitals of the alternant hydrocarbon consisting of $2m$ conjugated atoms will be written in order of increasing energies,

$$m^0 \dots 2^0, 1^0, -1^0, -2^0, \dots -m^0$$

where 2^0 and 1^0 are the highest bonding, and -2^0 and -1^0 are the lowest antibonding orbitals. Using the zero overlap approximation, the coefficients in the l.c.a.o. approximation of the r th (bonding) and $-r$ th (antibonding) orbital are related by

$$\begin{aligned} r^0 &= \sum_{\mu}^{*} C_{\mu r} \phi_{\mu} + \sum_{\nu}^0 C_{\nu r} \phi_{\nu}, \\ -r^0 &= \sum_{\mu}^{*} C_{\mu r} \phi_{\mu} - \sum_{\nu}^0 C_{\nu r} \phi_{\nu}, \end{aligned}$$

where the first summation is over 'starred' atoms and the second over 'unstarred' atoms, such that no two atoms of the same set are directly bonded.

The lowest lying singlet excited states of these hydrocarbons have been interpreted using the following wave functions [14, 15] (using Clar's nomenclature):

$$^1\psi_0 = |m^0 \bar{m}^0 \dots 1^0 \bar{1}^0|,$$

$$^1\psi_p = ^1\chi_1^{-1},$$

$$^1\psi_\alpha = \sqrt{\frac{1}{2}}(^1\chi_1^{-2} - ^1\chi_2^{-1}),$$

$$^1\psi_\beta = \sqrt{\frac{1}{2}}(^1\chi_1^{-2} + ^1\chi_2^{-1}),$$

$$^1\psi_{\beta'} = ^1\chi_2^{-2}$$

$^1\chi_r^{-s}$ represents a singlet function obtained from $^1\psi_0$ by exciting an electron from the bonding orbital r^0 to the antibonding orbital $-s^0$, e.g.

$$^1\chi_1^{-1} = \sqrt{\frac{1}{2}}\{|m^0 \bar{m}^0 \dots 1^0 \bar{1}^0| - |m^0 \bar{m}^0 \dots \bar{1}^0 1^0|\}.$$

There are four low-lying triplet states corresponding to the singlet excited states that have just been described. A typical one will be

$$^3\psi_p = ^3\chi_1^{-1} = \begin{cases} |m^0 \bar{m}^0 \dots 1^0 \bar{1}^0|, \\ \sqrt{\frac{1}{2}}\{|m^0 \bar{m}^0 \dots 1^0 \bar{1}^0| + |m^0 \bar{m}^0 \dots \bar{1}^0 1^0|\}, \\ |m^0 \bar{m}^0 \dots \bar{1}^0 \bar{1}^0|. \end{cases}$$

We now examine the effect of a radical having a ground state wave function as before

$$2\phi_0^{1/2} = a, \quad 2\phi_0^{-1/2} = \bar{a}.$$

A more complicated many-electron wave function for the radical could have been chosen but it introduces nothing essentially new to the theory.

As in §2 we now form a set of nearly orthogonal orbitals

$$m, \dots, 2, 1, -1, -2, \dots, -m,$$

where

$$r = r^0 - S_{ra} \cdot a$$

and consider the states of the complex which are components of doublets having $S_z = \hbar/2$. For example,

$$^S\Omega_1^{-1} = \sqrt{\frac{1}{2}}\{|1, -\bar{1}, a| - |\bar{1}, -1, a|\},$$

$$^T\Omega_1^{-1} = \sqrt{\frac{1}{6}}\{2|1, -1, \bar{a}| - |1, -\bar{1}, a| - |\bar{1}, -1, a|\}.$$

The zeroth order excited states of the complex that we are interested in are then (leaving out the charge-transfer states for the moment):

$$^S\theta_p = ^S\Omega_1^{-1}; \quad ^T\theta_p = ^T\Omega_1^{-1}; \quad ^S\theta_\alpha = \sqrt{\frac{1}{2}}(^S\Omega_1^{-2} - ^S\Omega_2^{-1}) \text{ etc.}$$

The symbols S and T have been used to distinguish the states which correspond to the singlet and triplet states of the hydrocarbon, although they are of course all doublets. The matrix elements of \mathcal{H} between the above states can be evaluated from the general formula

$$\langle ^S\Omega_r s | \mathcal{H} | ^T\Omega_p q \rangle = \frac{\sqrt{3}}{2} \{ \delta_{qs} \langle pa | G | ar \rangle - \delta_{pq} \langle qa | G | as \rangle \}.$$

They are listed in table 1.

We now make use of the pairing properties of the molecular orbitals. From §2 we have

$$K_{1,a} \approx \frac{S_{1a}^2}{4} (J_{11}^0 + J_{aa}^0 - 2J_{1,a}^0),$$

and

$$K_{-1,a} \approx \frac{S_{-1a}^2}{4} (J_{-1,-1}^0 + J_{a,a}^0 - 2J_{-1,a}^0).$$

$s\theta_{\beta'}$

$s\theta_{\beta}$

$s\theta_{\alpha}$

$s\theta_p$

$T\theta_{\beta'}$	$\sqrt{\frac{3}{8}}\{K_{2,a} - K_{-2,a}\}$	$\sqrt{\frac{3}{8}}\{\langle 1,a G a,2\rangle - \langle -1,a G a,-2\rangle\}$	$\sqrt{\frac{3}{8}}\{\langle 1,a G \sigma,2\rangle + \langle -1,a G \sigma,-2\rangle\}$	0
$T\theta_{\beta}$	$\sqrt{\frac{3}{8}}\{\langle 1,a G a,2\rangle - \langle -1,a G a,-2\rangle\}$	$\sqrt{\frac{3}{4}}\{K_{1,a} + K_{2,a} - K_{-1,a} - K_{-2,a}\}$	$\sqrt{\frac{3}{4}}\{K_{1,a} - K_{2,a} + K_{-1,a} - K_{-2,a}\}$	$\sqrt{\frac{3}{8}}\{\langle 1,a G \sigma,2\rangle - \langle -1,a G \sigma,-2\rangle\}$
$T\theta_{\alpha}$	$\sqrt{\frac{3}{8}}\{\langle 1,a G a,2\rangle + \langle -1,a G a,-2\rangle\}$	$\sqrt{\frac{3}{4}}\{K_{1,a} - K_{2,a} + K_{-1,a} - K_{-2,a}\}$	$\sqrt{\frac{3}{4}}\{K_{1,a} + K_{2,a} - K_{-1,a} - K_{-2,a}\}$	$-\sqrt{\frac{3}{8}}\{\langle 1,a G a,2\rangle + \langle -1,a G a,-2\rangle\}$
$T\theta_p$	0	$-\sqrt{\frac{3}{8}}\{\langle 1,a G a,2\rangle - \langle -1,a G a,-2\rangle\}$	$-\sqrt{\frac{3}{8}}\{\langle 1,a G \sigma,2\rangle + \langle -1,a G \sigma,-2\rangle\}$	$\sqrt{\frac{3}{2}}\{K_{1,a} - K_{-1,a}\}$

Table 1. The matrix elements of the Hamiltonian between the zeroth order states of the complex.

If one neglects overlap between different atomic orbitals of the hydrocarbon (the approximation used in arriving at the orbitals r^0), then on expansion we have

$$\begin{aligned} J_{1,1}^0 = J_{-1,-1}^0 &= \sum_{\mu}^* \sum_{\mu'}^* C_{\mu 1}^2 C_{\mu' 1}^2 J_{\mu \mu'} \\ &\quad + \sum_{\nu}^0 \sum_{\nu'}^0 C_{\nu 1}^2 C_{\nu' 1}^2 J_{\nu \nu'} + 2 \sum_{\mu}^* \sum_{\nu}^0 C_{\mu 1}^2 C_{\nu 1}^2 J_{\mu \nu}, \end{aligned}$$

and

$$J_{1,a}^0 = J_{-1,a}^0 = \sum_{\mu}^* C_{\mu 1}^2 J_{\mu a} + \sum_{\nu}^0 C_{\nu 1}^2 J_{\nu a}.$$

However,

$$S_{1,a}^2 = \sum_{\mu}^* C_{\mu 1}^2 S_{\mu a}^2 + \sum_{\nu}^0 C_{\nu 1}^2 S_{\nu a}^2 + 2 \sum_{\mu}^* \sum_{\nu}^0 C_{\mu 1} C_{\nu 1} S_{\mu a} S_{\nu a},$$

whereas $S_{-1,a}^2$ is a similar expression but with the last term coming in with a negative sign. As a first approximation we shall drop this last term and take

$$S_{1,a}^2 = S_{-1,a}^2.$$

The justification for adopting this approximation is that terms in the last summation can be either positive or negative, and will tend to cancel one another out, whereas the terms in the first two summations are all positive. A particular case when the approximation will be very good will be if the orbital of the paramagnetic species is so small that for any one configuration of the complex it only overlaps with one atomic orbital of the hydrocarbon. A case when the approximation will be very poor will be if the orbital of P overlaps just two adjacent atomic orbitals of the hydrocarbon. However, adopting the suggested approximation we have

$$K_{1,a} = K_{-1,a},$$

and similarly

$$K_{2,a} = K_{-2,a}.$$

Likewise

$$\langle 1, a | G | a, 2 \rangle = \langle -1, a | G | a, -2 \rangle,$$

where from the Mulliken approximation

$$\langle 1, a | G | a, 2 \rangle \simeq \frac{S_{1,a} S_{2,a}}{4} (J_{1,2}^0 + J_{a,a}^0 - J_{1,a}^0 - J_{2,a}^0).$$

The matrix elements of the Hamiltonian then take the form given in table 2.

For the case of benzene, the p and β' states are described by the Göppert-Mayer and Sklar wave functions [16]

$$\psi_{\beta'} = \sqrt{\frac{1}{2}} \{ \chi_1^{-1} - \chi_2^{-2} \}, \quad \psi_p = \sqrt{\frac{1}{2}} \{ \chi_1^{-1} + \chi_2^{-2} \},$$

and in this case the matrix elements

$$\langle {}^S\theta_{\beta'} | \mathcal{H} | {}^T\theta_\alpha \rangle \quad \text{and} \quad \langle {}^T\theta_p | \mathcal{H} | {}^S\theta_\alpha \rangle$$

are also zero.

	${}^S\theta_{\beta'}$	${}^S\theta_\beta$	${}^T\theta_\alpha$	${}^S\theta_p$
${}^T\theta_{\beta'}$	0	0	$\sqrt{\frac{3}{2}} \langle 1, a G a, 2 \rangle$	0
${}^T\theta_\beta$	0	0	$\sqrt{\frac{3}{2}} \{ K_{1,a} - K_{2,a} \}$	0
${}^T\theta_\alpha$	$\sqrt{\frac{3}{2}} \langle 1, a G a, 2 \rangle$	$\sqrt{\frac{3}{2}} \{ K_{1,a} - K_{2,a} \}$	0	$-\sqrt{\frac{3}{2}} \langle 1, a G a, 2 \rangle$
${}^T\theta_p$	0	0	$-\sqrt{\frac{3}{2}} \langle 1, a G a, 2 \rangle$	0

Table 2. The matrix elements of the Hamiltonian with the approximations described in the text.

The lowest triplet level for the polyacenes, is predicted theoretically to correspond to the ${}^3\psi_p$ state [15]. This is probably true for alternant hydrocarbons in general. It is seen from the above matrices that the first singlet-triplet absorption band can borrow intensity only from the so-called α -band which arises from the transition ${}^1\psi_0 \rightarrow {}^1\psi_\alpha$. However, this band is usually very weak ($f \simeq 0.005$); the transition is indeed predicted to be forbidden if the simple wave functions described in this section are used. It follows that mechanism (a) of §2 is unlikely to contribute much intensity to the first singlet-triplet absorption bands of alternant hydrocarbons. In the case of benzene, not only is the ${}^1\psi_0 \rightarrow {}^1\psi_\alpha$ transition symmetry forbidden, but there are no non-zero matrix elements between ${}^T\theta_p$ and any of the S-states.

To examine the effect of the charge-transfer states we need the matrix element between the T-states and a typical charge-transfer state such as

$${}^{CT}\theta_1 = |1a\bar{a}|.$$

From §2 it follows that

$$\langle {}^T\Omega_r | \mathcal{H} | {}^{CT}\theta_k \rangle = \delta_{kr} \sqrt{\frac{3}{2}} \{ V_{sa}(R^+) + V_{sa}(P) + T_{sa} \},$$

there being small terms which can be neglected if $k \neq r$. It follows that the ${}^T\theta_p$ state will have a none-zero matrix element of \mathcal{H} with the lowest energy charge-transfer state (the one obtained by removing an electron from the highest bonding orbital of R). This will be true even in the case of benzene when we have to use

the Göppert-Mayer, Sklar wave functions. As far as mechanism (*b*) of §2 is concerned (and unlike mechanism (*a*)) alternant hydrocarbons do not therefore behave as a special case of the general theory.

4. DISCUSSION

Before we are able to calculate the intensity of the singlet-triplet absorption bands induced by paramagnetic molecules, we need to know more about the nature of the complex formed. If there is no stable complex then the singlet-triplet bands are induced only during a chance collision of the two species. To obtain the net intensity it is therefore necessary to average expressions (2.2) and (2.6) over all configurations which can be taken up during the chance collision. However, if a stable complex is formed, then one particular configuration may be much more stable than any of the others, and it is only necessary to evaluate the matrix element for just this one configuration. Dijkgraaf [17] has obtained an equilibrium constant $K_r(25^\circ\text{C}) = 0.6$ for the benzene-oxygen complex, but this is probably small enough for us to consider that the two species come together more or less as they would on chance contacts.

One might hope to decide whether the triplet-singlet or triplet-charge-transfer interactions are the more efficient in contributing to the intensity of the triplet band, by looking at the experimental results. That is, one would look for correlations between the intensity of the triplet band, and the energy and intensity of the α -band or the energy and intensity of the charge-transfer band. In practice, there is very little change in the intensity of the triplet band over a wide range of aromatic hydrocarbons [3]. There is also very little change in either the separation of the triplet and α -band, or in the intensity of the α -band, in this series. The energies of the charge-transfer bands are not easily measured as they only appear as tails to the more intense spin-allowed transitions of the hydrocarbon: their intensities are even more difficult to estimate. In short, there is so little variation over the series of hydrocarbons studied that no correlation with any of the most likely variables stand out in an obvious way.

There is, however, other evidence that the singlet-triplet interaction is not the important mechanism. On introducing a substituent into an aromatic hydrocarbon one not only destroys the pairing property of the molecular orbitals, but, in general, one increases the intensity of the α -band. Both these effects would tend to increase the intensity of the triplet band if mechanism (*a*) were important. In fact fluorobenzene gives a singlet-triplet band almost exactly as strong as that of benzene for the same pressure of oxygen [3], whereas the intensity of the α -band of fluorobenzene is six times as strong as that of benzene. Likewise the intensity of the triplet band in 9-methylanthracene is almost the same as that of anthracene [3].

The positive evidence in favour of the charge-transfer mechanism is slight; as Evans [3] has pointed out, acridine and 9-nitroanthracene give much weaker triplet bands than anthracene itself and this is to be correlated with the fact that they will be much weaker electron donors.

In this paper our attention has been focused on the intensity of the singlet-triplet absorption band. The theory can also be directly applied to give the probability of emission from the triplet state (the probability of absorption and emission being related through the Einstein coefficients.) In addition, however, the matrix elements we have derived will be of importance in the theory of the

radiationless transitions which can occur between the states of a molecule. Since internal conversion (a spin-allowed radiationless transition) is much more rapid than intersystem crossing (spin-forbidden), excitation of the molecule to any one of the excited singlet states will generally be transmitted to the triplet state via the lowest singlet state. It follows that for an alternant hydrocarbon in the presence of a paramagnetic molecule, we deduce:

(i) If the lowest singlet state is the α -state there will most likely be a radiationless transition to the p , β or β' -triplet states.

(ii) If the lowest singlet state is the p -state the radiationless transition is most likely to go to the triplet α -state.

Now theory predicts that the singlet and triplet α -states shall be nearly degenerate [15]. Moreover radiationless transitions go in such a direction that electronic energy is dissipated to the motion of the surrounding medium. It follows that if the p -state is the lowest singlet excited state and the α -triplet state is of higher energy, then there may be a rather small probability of populating the triplet states through light absorbed by the singlet states. Experimentally it would be interesting to compare the population of the triplet states, using the synchronised flash technique [8], for say naphthalene (α -singlet lowest) and pentacene (p -singlet lowest), in the presence of a transition metal ion.

Our analysis also suggests that the radiationless transition from the lowest triplet state to the ground state in the presence of paramagnetic molecules, is a second-order relaxation phenomenon, using the charge-transfer state as a virtual level.

The intensification of the singlet-triplet absorption band is to be associated with the formation of a complex between the molecule under consideration and the paramagnetic species. The exchange mechanism (*a*) can be considered to give rise to a covalent bond between the molecule in its triplet excited state and the paramagnetic species, whereas the charge-transfer mechanism (*b*) will give rise to an ionic bond. The two mechanisms are therefore to be considered as distinct in the same sense that ionic and covalent contributions can be distinguished in chemical bonding.

Finally, if a paramagnetic molecule intensifies the triplet band, should it not also change its energy? By perturbation theory, if I_{0r} is the intensity gained by the transition $\psi_0 \rightarrow \psi_r$ due to the mixing of ψ_r and ψ_s , then the change in energy of ψ_r due to this interaction is related to the gain in intensity by

$$\Delta E_r = (E_r - E_s) \frac{I_{0r}}{I_{0s}}.$$

From Evans' results [3], we calculate that if the benzene triplet were to gain all its intensity from the α -band there would be a shift of -7 cm^{-1} associated with the intensity which Evans measures. This would not be detectable in solution spectroscopy. If the intensity were gained from the charge transfer state the shift would probably be about the same order of magnitude.

The author wishes to thank Professor H. C. Longuet-Higgins, F.R.S., for interesting discussions on this topic.

REFERENCES

- [1] EVANS, D. F., 1956, *Nature, Lond.*, **178**, 534.
- [2] SKLAR, A. L., 1937, *J. chem. Phys.*, **5**, 669.
- [3] EVANS, D. F., 1957, *J. chem. Soc.*, 1351.
- [4] EVANS, D. F., 1957, *J. chem. Soc.*, 3885.
- [5] MCCLURE, D. S., 1949, *J. chem. Soc.*, **17**, 905.
- [6] YUSTER, P., and WEISSMAN, S. I., 1949, *J. chem. Phys.*, **17**, 1182.
- [7] STEPHEN, M. J. (private communication).
- [8] PORTER, G., and WRIGHT, M. R., 1959, *Faraday Soc. Disc.*, **27**, 18.
- [9] EVANS, D. F., 1953, *J. chem. Soc.*, 345.
- [10] MUNCK, A. U., and SCOTT, J. F., 1956, *Nature, Lond.*, **177**, 587.
- [11] HOIJTINK, G. J., 1960, *Mol. Phys.*, **3**, 7, 67.
- [12] MULLIKEN, R. S., 1949, *J. Chim. phys.*, **46**, 497.
- [13] MURRELL, J. N., 1959, *J. Amer. chem. Soc.*, **81**, 5037.
- [14] DEWAR, M. J. S., and LONGUET-HIGGINS, H. C., 1955, *Proc. phys. Soc. Lond. A*, **67**, 795.
- [15] POPLE, J. A., 1955, *Proc. phys. Soc. Lond. A*, **68**, 81.
- [16] GOPPERT-MAYER, M., and SKLAR, A. L., 1938, *J. chem. Phys.*, **6**, 645.
- [17] DIJKGRAAF, C. (unpublished). The result is published in *Chemical Constitution* by J. A. A. Ketelaar (Elsevier, 1958).

The absorption spectra of permanganate, manganate and related oxyions

by A. CARRINGTON† and D. S. SCHONLAND

The University of Southampton, Southampton

(Received 12 February 1960)

The visible and ultra-violet absorption spectra of transition metal oxyanions are discussed in terms of a level scheme originally proposed for permanganate and chromate by Ballhausen and Liehr [4]. This level scheme is extended to oxyions containing one or two unpaired electrons and by group theoretical arguments and dipole strength calculations is shown to be consistent with experiment.

The source of the intensity of the absorption bands is discussed and it is concluded that this arises primarily from transition dipole matrix elements between ligand orbitals in the ground and excited states.

1. INTRODUCTION

The differences which exist between the oxygen complexes and most other complexes of the transition metals are particularly apparent in their electronic absorption spectra. Ions of the transition metals in a low valency state usually show only weak absorption bands in the visible region of the spectrum, due to $d \rightarrow d$ transitions, and these are now well understood on the basis of ligand field theory [1]. Much more intense bands are found in the ultra-violet region of the spectrum and these have been described as 'charge transfer' bands, involving a movement of charge from the metal atom to the ligands or vice-versa [2].

In contrast, many of the tetrahedral oxyanions of the transition metals possess intense absorption bands in the visible and near ultra-violet. A tetrahedral ion does not possess a centre of symmetry and consequently there are no parity restrictions on the electronic transitions. This does not necessarily mean that $d \rightarrow d$ transitions will now give rise to intense bands since the matrix elements for electric dipole transitions between pure d levels still vanish. Non-vanishing matrix elements are only obtained (assuming we neglect metal $4p$ orbitals) if there is some mixing of the metal d orbitals with orbitals on the ligands and the intense absorption bands found for the MnO_4^2- ion for example might be taken to imply that this mixing is important. Thus one cannot for example treat MnO_4^2- as if it were a Mn^{6+} ion in a perturbing ligand field but must consider it from a general molecular orbital point of view.

2. MOLECULAR ORBITAL THEORY

The various L.C.A.O. molecular orbitals that can be formed for a tetrahedral XO_4 ion using $3d$, $4s$ and $4p$ orbitals on the central metal atom and $2p$ orbitals on the surrounding oxygen atoms have been discussed by Wolfsberg and Helmholz [3], hereafter referred to as WH. These molecular orbitals can be characterized by the irreducible representations of the tetrahedral symmetry group T_d to which

† Present address: Department of Theoretical Chemistry, University Chemical Laboratory, Lensfield Road, Cambridge.

they belong; the representations of particular interest to us are the triply degenerate T_1 and T_2 and the doubly degenerate E . If one introduces the coordinate system shown in figure 1, the corresponding molecular orbitals are characterized by saying that the T_1 orbitals transform like the components L_x , L_y , L_z of the orbital angular momentum under the operations of T_d , while the T_2 orbitals transform like x , y , z or yz , zx , xy and the E orbitals transform like $x^2 - y^2$ and $3z^2 - r^2$. WH showed that the T_1 orbitals are non-bonding combinations of oxygen orbitals, that the E orbitals are π -type combinations of $3d_{x^2-y^2}$ and $3d_{z^2}$ metal orbitals with oxygen orbitals and that the T_2 orbitals may contain both σ and π admixtures of oxygen orbitals with the metal $3d_{xy}$, $3d_{yz}$, $3d_{xz}$ and $4p_x$, $4p_y$, $4p_z$ orbitals (see figure 2). The explicit forms of these orbitals are discussed in section 4.



Figure 1. Coordinate system used to describe the molecular orbitals in a tetrahedral oxyanion MO_4^- . The direction cosines of the oxygen σ and π orbitals indicated in the figure are given by WH.

On the basis of a simple semi-empirical molecular orbital calculation WH concluded that the ground state configuration of the closed shell permanganate and chromate ions was $(a_1)^2(1t_2)^6(1e)^3(2t_2)^6(t_1)^6$ and that the first unoccupied level above the ground state was an anti-bonding t_2 level. They then explained the two bands observed in the permanganate and chromate spectra as due to electronic transitions into the anti-bonding t_2 level from the occupied t_1 and t_2 levels, and obtained tolerable agreement with the observed energies and oscillator strengths of these bands.

The details of the WH level scheme contain some surprising features and an alternative scheme, based on intuitive and chemical ideas of molecular orbital formation, has been proposed by Ballhausen and Liehr [4], hereafter referred to as BL. These authors describe the ground state of the permanganate and

chromate ions by the closed shell configuration . . . (t_1)⁶ and postulate that the first two unoccupied levels above the occupied t_1 level are anti-bonding orbitals of types e and t_2 respectively. They then explain the lower energy band in the permanganate and chromate spectra as due to a $t_1 \rightarrow e$ electronic transition and the higher energy band by a $t_1 \rightarrow t_2$ transition.

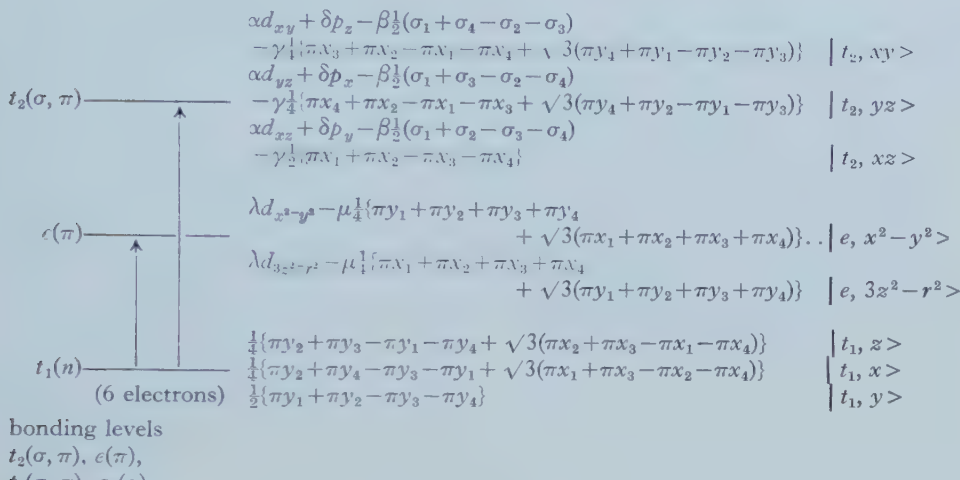


Figure 2. Orbital levels used and the corresponding molecular orbitals α , β , γ , δ , λ , μ are constants. πy_i , πx_i and σ_i are oxygen $2p$ orbitals whose orientations with respect to the coordinate system shown in figure 1 are given by WH.

Ion	Ground state	Transition	Energy (cm ⁻¹)	Oscillator strength	Dipole strength ($\times 10^{17}$ cm ²)
VO_4^{3-} (t_1) ⁶ : 1A_1	$t_1 \rightarrow e$	36 900	0.150	3.747
CrO_4^{2-} (t_1) ⁶ : 1A_1	$t_1 \rightarrow e$	26 810	0.089	3.060
		$t_1 \rightarrow t_2$	36 630	0.110	2.768
MnO_4^- (t_1) ⁶ : 1A_1	$t_1 \rightarrow e$	18 320	0.032	1.610
		$t_1 \rightarrow t_2$	32 210	0.070	2.003
MnO_4^{2-} (t_1) ⁶ e : 2E	$t_1 \rightarrow e$	16 530	0.025	1.394
		$t_1 \rightarrow t_2$	$\begin{cases} 22\ 940 \\ 28\ 490 \\ 33\ 440 \end{cases}$	Total 0.11-0.14	
MnO_4^{3-} (t_1) ⁶ e^2 : 3A_2	$t_1 \rightarrow e$	14 810	0.017	1.058
		$t_1 \rightarrow t_2$	30 800	0.112	3.352
FeO_4^{2-} (t_1) ⁶ e^2 : 3A_2	$t_1 \rightarrow e$	12 720	0.009	0.652
		$t_1 \rightarrow t_2$	19 600	0.035	1.646

Table 1. Summary of observed absorption spectra.

If one now extends these level schemes to describe ions like manganate and hypomanganate containing additional unpaired electrons it becomes possible to discriminate between them by making electron spin resonance measurements. If WH are right the unpaired electrons will go into triply degenerate t_2 orbital while BL would place them in a doubly degenerate e orbital and the electron

resonance properties of these orbitals are different. Preliminary measurements on amorphous alkaline glasses containing manganate, hypomanganate and ferrate ions appeared to be consistent with the WH scheme [5]. Subsequently it proved possible to make detailed measurements of the angular variation in the *g*-values and hyperfine splittings of these ions in diluted single crystals. The results of these measurements [6, 7] show quite unambiguously that the unpaired electrons are in a doubly degenerate *e* orbital, in agreement with the BL scheme. The analysis also suggests that the *e* orbital is largely concentrated in a *3d* orbital on the central metal atom while the higher lying *t*₂ orbital is spread over the whole molecule, again in agreement with the ideas of BL.

It is the purpose of this paper to show that the absorption spectra of these ions can also be explained on the BL level scheme. The details of the spectra are summarized in table 1, the last three columns of which show the energies of the absorption maxima, ν , in cm⁻¹, the oscillator strengths, f , and the corresponding dipole strengths, D , calculated from the formula $f = 1.085 \times 10^{11} \nu D$ [8]. The table also shows the postulated ground states of the ions and the electronic transitions associated with each band on the basis of the considerations of the next section.

3. GENERAL DISCUSSION OF THE ABSORPTION SPECTRA

We denote the components of the *t*₁ level by $|t_1, x\rangle$, $|t_1, y\rangle$, $|t_1, z\rangle$ transforming respectively like L_x , L_y , L_z under the operations of T_d and the components of the *e* and *t*₂ levels by $|e, x^2 - y^2\rangle$, $|e, 3z^2 - r^2\rangle$ and $|t_2, yz\rangle$, $|t_2, zx\rangle$, $|t_2, xy\rangle$, transforming under the operations of T_d like the combinations of *x*, *y*, *z* used to label them. The basic electric dipole matrix elements between these levels can then be expressed in terms of three quantities **a**, **b** and **c** by

$$\begin{aligned}\mathbf{a} &= \langle t_1, x|x|e, x^2 - y^2 \rangle = \langle t_1, y|y|e, x^2 - y^2 \rangle = (1/\sqrt{3})\langle t_1, x|x|e, 3z^2 - r^2 \rangle \\ &= -(1/\sqrt{3})\langle t_1, y|y|e, 3z^2 - r^2 \rangle = -\frac{1}{2}\langle t_1, z|z|e, x^2 - y^2 \rangle \\ \mathbf{b} &= \langle t_1, z|y|t_2, yz \rangle = -\langle t_1, z|x|t_2, zx \rangle = \langle t_1, x|z|t_2, zx \rangle \\ &= -\langle t_1, x|y|t_2, xy \rangle = \langle t_1, y|x|t_2, xy \rangle = -\langle t_1, y|z|t_2, yz \rangle \\ \mathbf{c} &= \langle t_2, yz|x|e, 3z^2 - r^2 \rangle = \langle t_2, zx|y|e, 3z^2 - r^2 \rangle = (1/\sqrt{3})\langle t_2, xz|y|e, x^2 - y^2 \rangle \\ &= -(1/\sqrt{3})\langle t_2, yz|x|e, x^2 - y^2 \rangle = -\frac{1}{2}\langle t_2, xy|z|e, 3z^2 - r^2 \rangle.\end{aligned}$$

The ions with which we are concerned have, on the BL level scheme, ground state configurations of the form $(t_1)^6(e)^n$ with $n = 0, 1$ or 2 and we have to consider transitions to the excited configurations $(t_1)^5(e)^{n+1}$, $(t_1)^5(e)^n t_2$ and $(t_1)^6(e)^{n-1} t_2$. The results of the calculations for the various values of n are summarized below.

(i) $n = 0$, Ions MnO₄⁻, CrO₄²⁻, VO₄³⁻

Here the ground state is $(t_1)^6 : ^1A_1$ and the electric dipole selection rule allows transitions to 1T_2 excited states. The two excited configurations $(t_1)^5 e$ and $(t_1)^5 t_2$ both give rise to just one 1T_2 state and the dipole strengths of the corresponding transitions are found to be $24\mathbf{a}^2$ and $12\mathbf{b}^2$ respectively.

The spectra of these ions should therefore show two distinct absorption bands corresponding to the two possible electronic transitions. This is the case for permanganate and chromate; in vanadate the lower energy transition is already so far into the ultra-violet that the higher energy transition cannot be observed.

(The dipole strengths given above are larger by a factor of 6 than the equivalent expressions of BL. These authors appear to have neglected to anti-symmetrize the six-electron wave functions that occur in these configurations.)

(ii) $n=1$, Ion MnO_4^{2-}

On the BL scheme the ground state of this ion is $(t_1)^6e: ^2E$ and transitions are allowed to both $2T_1$ and $2T_2$ excited states. It is found that the excited configurations $(t_1)^5(e)^2$ and $(t_1)^5et_2$ both contain two $2T_1$ and two $2T_2$ states, the sum of the dipole strengths for the four $t_1 \rightarrow e$ transitions, being $18\mathbf{a}^2$ and that for the four $t_1 \rightarrow t_2$ transitions being $12\mathbf{b}^2$. The various states of each excited configuration will be split apart by the Coulomb interactions of the electrons with separations that may be of the order of several thousand cm^{-1} so that one would expect to find a rather complicated absorption spectrum as is indeed the case. The observed spectrum shows four main absorption maxima and the bands overlap to such an extent that it is not possible to assign individual oscillator strengths to all of them.

Since the e orbital in the ground state is occupied by one electron an $e \rightarrow t_2$ transition is also possible. The dipole strength associated with this transition is $6\mathbf{c}^2$. As will be shown below the wave functions are such that this is very much smaller than the dipole strengths of the other transitions so that one expects this transition to produce a weak band in the absorption spectrum. The energy of the transition corresponds approximately to the energy difference between the e and t_2 levels and so, on the basis of the observed MnO_4^- spectrum, would be expected to have a value of about 14000 cm^{-1} . There is some evidence for the existence of a very weak band at 12600 cm^{-1} [9]. The spectrum of this ion is considered further below.

(iii) $n=2$. Ions MnO_4^{3-} , FeO_4^{2-}

Here the ground state configuration is $(t_1)^6(e)^2$ and the electron spin resonance results show that it has spin $S=1$ as one would expect. Accordingly the actual ground state is 3A_2 and electric dipole transitions are allowed only to 3T_1 excited states.

The transitions $t_1 \rightarrow e$ and $t_1 \rightarrow t_2$ give excited configurations $(t_1)^5(e)^3$ and $(t_1)^5(e)^2t_2$ respectively and it is found that from each of these configurations just one 3T_1 state can be formed which is coupled to the ground state by the electric dipole interaction. The corresponding dipole strengths are $12\mathbf{a}^2$ and $12\mathbf{b}^2$.

In addition the $e \rightarrow t_2$ transition should produce a weak absorption band with dipole strength $12\mathbf{c}^2$.

Thus the BL level scheme would predict a spectrum showing two main absorption bands with a third much weaker band. The two main bands in the ferrate and hypomanganate spectra are well resolved [10, 11] but no trace of the weak $e \rightarrow t_2$ band could be found. This is not surprising for from the energy differences of the main absorptions one would expect this weak band to lie well within the infra-red for ferrate, and to be obscured by the lower energy main band in the case of hypomanganate.

It appears therefore that the postulated level scheme is well able to supply a qualitative explanation of the observed spectra. The interpretation of the spectra for the ions with $(t_1)^6$ and $(t_1)^6(e)^2$ ground state configurations is straightforward and one can use the measured dipole strengths given in table 1 to deduce

the corresponding values of the matrix elements **a** and **b**. These are given in table 2, expressed in angstroms.

The spectrum of MnO_4^{2-} is more complicated. The first large peak occurs at $16\ 530\ \text{cm}^{-1}$, almost exactly half-way between the positions of the $t_1 \rightarrow e$ transitions in MnO_4^- and MnO_4^{3-} . If one assumes that in MnO_4^{2-} $|\mathbf{a}| = 0.088\ \text{\AA}$, the mean of $|\mathbf{a}|$ for MnO_4^- and MnO_4^{3-} , the total dipole strength associated with the $t_1 \rightarrow e$ transition is $18\mathbf{a}^2 = 1.394 \times 10^{-17}\ \text{cm}^2$ in exact agreement with the measured dipole strength of the $16\ 530\ \text{cm}^{-1}$ peak. It therefore seems possible that all the $t_1 \rightarrow e$ transitions in MnO_4^{2-} are combined in this single absorption band.

	VO_4^{3-}	CrO_4^{2-}	MnO_4^-	MnO_4^{3-}	FeO_4^{2-}
$ \mathbf{a} $	0.125	0.113	0.082	0.094	0.074
$ \mathbf{b} $	—	0.152	0.192	0.167	0.117

Table 2. Estimated values of $|\mathbf{a}|$ and $|\mathbf{b}|$ in angstroms.

The remaining three large absorptions in the spectrum overlap to such an extent that it is not possible to assign individual oscillator strengths to them; their combined oscillator strength lies between 0.11 and 0.14. Assuming that the mean energy of the $t_1 \rightarrow t_2$ transitions in manganate is $31\ 500\ \text{cm}^{-1}$ and that $|\mathbf{b}| = 0.148\ \text{\AA}$ (figures obtained by interpolating half-way between the corresponding values in permanganate and hypomanganate) one obtains an estimate of 0.09 for the total oscillator strength of the $t_1 \rightarrow t_2$ transitions in manganate which is in fair agreement with the value quoted above. The implications of the numerical values of the matrix elements **a**, **b** and **c** must now be considered.

4. TRANSITION DIPOLE MATRIX ELEMENTS

We will first discuss the $t_1 \rightarrow e$ transition in permanganate and the evaluation of the matrix element **a**. The $|e, x^2 - y^2\rangle$ molecular orbital can be represented by the expression (see figure 2)

$$|e, x^2 - y^2\rangle = \lambda d_{x^2-y^2} - \mu \frac{1}{4} \{ \pi y_1 + \pi y_2 + \pi y_3 + \pi y_4 + \sqrt{3}(\pi x_1 + \pi x_2 + \pi x_3 + \pi x_4) \}$$

the normalization condition being $\lambda^2 + \mu^2 - 2\lambda\mu G(e, \pi) = 1$. $G(e, \pi)$ is a 'group overlap integral', in this case the integral

$$\int d_{x^2-y^2} \cdot \frac{1}{4} \{ \pi y_1 + \pi y_2 + \pi y_3 + \pi y_4 + \sqrt{3}(\pi x_1 + \pi x_2 + \pi x_3 + \pi x_4) \} d\tau$$

The explicit forms of the non-bonding t_1 orbitals are fully determined by symmetry (figure 2) and by making use of the symmetry operation of T_d the matrix element **a** can be reduced to the expression

$$\mathbf{a} = \langle t_1, y | y | e, x^2 - y^2 \rangle = 2\lambda \langle \pi y_1 | y | d_{x^2-y^2} \rangle - \mu R / 2\sqrt{3} = \lambda I - \mu R / 2\sqrt{3}. \quad (1)$$

Here R is the length of the metal-oxygen bond and we have neglected integrals between oxygen orbitals on different atoms. We see that the value of **a**, and hence the dipole strength ($24\mathbf{a}^2$) of the transition, depends on three parameters, namely, the coefficient of π -admixture in the e orbital, the value of the 'charge-transfer' integral I , and the metal-oxygen bond length.

BL neglected the ligand admixture in the e orbital (i.e. took $\lambda = 1$, $\mu = 0$) and evaluated I using hydrogen-like radial wave functions with screened nuclear charges. One finds that for all the ions under discussion good agreement between the measured \mathbf{a} and the values of I calculated on this basis can be obtained with values of screening constants for the central metal and ligand orbitals close to those given by Slater's rules.

There is, however, a serious inconsistency in this approach for with the same wave functions the group overlap integral $G(e, \pi)$ turns out to be comparatively large (of the order of 0.4), and the assumption that ligand admixture can be disregarded is not justified. Indeed if overlap is as important as this the energy of the anti-bonding e level will be very high. It is this feature of a large overlap integral which is responsible for the results obtained by WH, namely that the bonding e level is very stable and that the anti-bonding e level is too high in energy to play any part in the absorption spectrum.

Values of the screening constants suggested by pure scaling of self-consistent field transition metal $3d$ wave functions [12] are considerably smaller than those given by Slater's rules and give rise to a much smaller value of the overlap integral $G(e, \pi)$. Qualitative evidence in favour of a small overlap is afforded both by the e.s.r. results which suggest that π admixture in the e orbital is small (but not negligible) and by the relatively low energy of this level. If the overlap is small the charge-transfer integral I will also be small and consequently most of the observed intensity in the $t_1 \rightarrow e$ transitions must come from the second term in (1). If one neglects $G(e, \pi)$ and I altogether the values of λ and μ required to account for the experimental value of \mathbf{a} in permanganate are 0.985 and 0.177 respectively and values of the same order of magnitude are obtained for the other ions. This small value of μ is in accord with the qualitative arguments used to derive it.

We will now consider the matrix element which arises in the $t_1 \rightarrow t_2$ transition. The problem again reduces to one of determining the orbital coefficients in the t_2 orbitals. If we simplify the problem by neglecting the metal $4p$ orbitals (WH found that this neglect had little effect on their calculated energies), one of the components of the t_2 triplet may be written

$$\begin{aligned} |t_2, yz\rangle = & \alpha d_{yz} - \beta \frac{1}{2}(\sigma_1 + \sigma_3 - \sigma_2 - \sigma_4) - \gamma \frac{1}{4}\{\pi x_4 + \pi x_2 - \pi x_1 - \pi x_3 \\ & + \sqrt{3}(\pi y_4 + \pi y_2 - \pi y_1 - \pi y_3)\} \end{aligned}$$

where the normalization condition is

$$\alpha^2 + \beta^2 + \gamma^2 - 2\alpha\beta G(t_2, \sigma) - 2\alpha\gamma G(t_2, \pi) = 1.$$

Here $G(t_2, \sigma)$ and $G(t_2, \pi)$ are σ - and π -type group overlap integrals. The matrix element \mathbf{b} can then be expressed as

$$\mathbf{b} = \langle t_1, z | y | t_2, yz \rangle = 2\alpha \langle \pi y_1 | y | d_{xy} \rangle - \gamma R/2 = 2\alpha I - \gamma R/2.$$

Here we have made use of the relationship between the integrals $\langle \pi y_1 | y | d_{xy} \rangle$ and $\langle \pi y_1 | y | d_{x^2-y^2} \rangle$ which follows from the angular dependence of the wave functions and their relative orientations. We see that the factors governing the magnitude of the matrix element \mathbf{b} are very similar to those discussed earlier for \mathbf{a} . While we may agree with BL that the t_2 orbital is likely to be mainly a σ -type orbital (electron resonance measurements suggest that it is spread over the whole molecule) this will not be relevant to the intensity of the $t_1 \rightarrow t_2$ transition if the charge-transfer integral I is unimportant. The intensity will depend on γ , the

coefficient of the π -combination in the t_2 orbital. This conclusion was also reached by WH. A value of 0.161 for γ is sufficient to account for the intensity of the $t_1 \rightarrow t_2$ transition in MnO_4^- .

Finally we consider the $e \rightarrow t_2$ transition in MnO_4^{2-} , MnO_4^{3-} and FeO_4^{2-} . Using the form already given for the e and t_2 orbitals, the matrix element c is given by the following expression

$$c = -\lambda\beta J - \lambda\gamma K + \gamma\mu R/2\sqrt{3}$$

where J and K are the charge-transfer integrals

$$(2/\sqrt{3})\langle\sigma_1|y|d_{x^2-y^2}\rangle \text{ and } (2/\sqrt{3})\langle\pi x_1|y|d_{x^2-y^2}\rangle$$

respectively. According to our previous arguments J and K are expected to be small and the third term contains the product of γ and μ , both of which are small. Hence one of the consequences of our previous discussion is that c will be small compared with a and b and we would not expect to see intense bands due to $e \rightarrow t_2$ transitions.

We have shown that the absorption spectra of $3d$ transition metal oxyions can be explained in a semi-quantitative fashion on the basis of the BL level scheme although our explanation of the observed intensities as due mainly to electron transitions amongst the ligand orbitals differs from the mechanism proposed by BL who supposed it to be entirely due to a charge transfer from ligand to central metal orbitals.

Further progress in the discussion of these ions must await reliable theoretical estimates of the values of the charge transfer and group overlap integrals. It might, however, be possible to learn more about the electron distribution in the e orbital by making e.s.r. measurements on manganate enriched with ^{17}O .

REFERENCES

- [1] GRIFFITH, J. S., and ORGEL, L. E., 1957, *Quart. Rev.*, **11**, 381.
- [2] ORGEL, L. E., 1954, *Quart. Rev.*, **8**, 422.
- [3] WOLFSBERG, M., and HELMHOLZ, L., 1952, *J. chem. Phys.*, **20**, 837.
- [4] BALLHAUSEN, C. J., and LIEHR, A. D., 1958, *J. mol. Spectroscopy*, **2**, 342.
- [5] CARRINGTON, A., INGRAM, D. J. E., SCHONLAND, D. S., and SYMONS, M. C. R., 1956, *J. chem. Soc.*, p. 4710.
- [6] CARRINGTON, A., INGRAM, D. J. E., LOTT, K. A. K., SCHONLAND, D. S., and SYMONS, M. C. R., 1960, *Proc. roy. Soc. A*, **254**, 101.
- [7] SCHONLAND, D. S., 1960, *Proc. roy. Soc. A*, **254**, 111.
- [8] MULLIKEN, R. S., and RIEKE, C. A., 1941, *Rep. Progr. Phys.*, **8**, 231.
- [9] CARRINGTON, A., 1959, Ph.D. Thesis, University of Southampton.
- [10] CARRINGTON, A., and SYMONS, M. C. R., 1956, *J. chem. Soc.*, p. 3373.
- [11] CARRINGTON, A., SCHONLAND, D. S., and SYMONS, M. C. R., 1957, *J. chem. Soc.*, p. 659.
- [12] HARTREE, D. R., 1957, *The Calculation of Atomic Structures* (London: Chapman and Hall).

Nuclear magnetic shielding and diamagnetic susceptibility of interacting hydrogen atoms

by T. W. MARSHALL and J. A. POPLE

National Physical Laboratory, Teddington, Middlesex

(Received 25 February 1960)

A quantum-mechanical study is made of the changes of the nuclear magnetic screening constant σ and the diamagnetic susceptibility χ of two interacting hydrogen atoms due to van der Waals and overlap interatomic forces (effects of electron spin being neglected). At large distances the calculations show that van der Waals forces decrease the nuclear screening but increase the diamagnetic susceptibility (in magnitude). As the internuclear distance is reduced the first effect of overlap forces is to increase the screening in the repulsive (electronic triplet) state but this is followed by a further reduction. Attractive overlap forces (as in the ground state of H_2) ultimately lead to an increase in screening.

1. INTRODUCTION

Proton magnetic resonance chemical shifts are known to be strongly influenced by molecular interaction. The large shifts to low field (reduction in screening) associated with hydrogen bonding and polar molecules have been interpreted in terms of the reduction of diamagnetic currents by strong intermolecular electric fields [1, 2, 3, 4]. Similar effects are also found, however, in non-associated liquids where the principal intermolecular forces are of the van der Waals and overlap repulsion types. Here there is little theoretical work beyond the suggestion of Stephen [2] that the rapidly fluctuating electric fields giving rise to van der Waals forces could be treated in the same way as electric fields due to neighbouring polar molecules.

In this paper we shall present a study of the magnetic effects of van der Waals and overlap forces for the simplest model system, two interacting hydrogen atoms where the complicating effects of electron spin are not considered. (For real hydrogen atoms, electron spin is important, of course, but it is not relevant if we are using H_2 as a model for more complex systems where spins are paired intramolecularly). In §2, it is shown that van der Waals interaction leads to a reduction of screening proportional to R^{-6} , and this is followed by a separate calculation of the effect of overlap forces in §3, both the molecular singlet and triplet states being considered (these corresponding to attractive and repulsive overlap forces respectively).

2. LONG-RANGE INTERATOMIC MAGNETIC EFFECTS

To investigate interatomic shielding effects at distances large enough for the overlap of electronic charge clouds to be neglected, we shall treat the external magnetic field, the magnetic field due to the nuclei and the electrostatic interaction

between atoms as simultaneous perturbations on a system of two isolated hydrogen atoms. By examining the cross-terms between these perturbations, we can study the effects of van der Waals forces on the magnetic susceptibility and the nuclear shielding as inverse power series in the internuclear distances. We shall evaluate the leading terms which are proportional to the inverse sixth power of the distance, as for the van der Waals energy.

To calculate the magnetic shielding constant of the nuclei, we need only evaluate the energy for the situation in which the external magnetic field H_0 and the nuclear magnetic moments are in the same direction, which will be taken as the z -axis. We shall consider the two cases of two hydrogen atoms separated by a distance R along the z and y axes. These will be referred to as the parallel and perpendicular calculations, respectively.

For large R , the magnetic environment of the electron in one atom will be treated as a uniform field H in the z -direction, together with the magnetic field due to its own nucleus. The field H will not be quite equal to H_0 because it also contains a contribution due to the magnetic field of the nucleus of the other atom. In fact

$$H - H_0 = \begin{cases} 2M/R^3a^3 & (||) \\ -M/R^3a^3 & (\perp) \end{cases}$$

where R is measured in units of the Bohr radius a . There will also be magnetic field gradients on one atom due to the magnetic moment of the other (proportional to R^{-4} , R^{-5} , ...). However, these will all be of symmetries which cannot give rise to a resultant field at the nucleus as far as leading terms are concerned.

The complete Hamiltonian to be used can be written in the form

$$\mathcal{H} = \mathcal{H}_{000} + \lambda \mathcal{H}_{100} + \mu \mathcal{H}_{010} + \nu \mathcal{H}_{001} + \mu^2 \mathcal{H}_{020} + \mu \nu \mathcal{H}_{011} + \nu^2 \mathcal{H}_{002}. \quad (2.2)$$

\mathcal{H}_{000} is the unperturbed Hamiltonian corresponding to infinite separation of the two atoms in the absence of magnetic effects. If all distances are measured in units of the Bohr radius and energies in units of e^2/a , and the lowest eigenvalue of \mathcal{H}_{000} taken to be zero, then

$$\mathcal{H}_{000} = -\frac{1}{2}\nabla_1^2 - \frac{1}{2}\nabla_2^2 - \tau_1^{-1} - \tau_2^{-1} + 1. \quad (2.3)$$

The term $\lambda \mathcal{H}_{100}$ represents the electrostatic dipole interaction between the atoms.

$$\lambda = R^{-3},$$

$$\mathcal{H}_{100} = r_1 r_2 P,$$

$$P_{||} = \frac{x_1 x_2 + y_1 y_2 - 2z_1 z_2}{r_1 r_2},$$

$$P_{\perp} = \frac{x_1 x_2 - 2y_1 y_2 + z_1 z_2}{r_1 r_2}, \quad (2.4)$$

where the electronic coordinates for each atom are referred to their respective nuclei as origins. Electrostatic terms of higher order are neglected in (2.2). This will not affect the calculation of the magnetic susceptibilities and screening constants to order R^{-6} .

The remaining terms in (2.2) represent the interaction of the electrons with the magnetic fields. They have the forms

$$\begin{aligned}\mu &= \frac{a\hbar H}{2mc}, & \nu &= \frac{M\hbar}{mca^2}, \\ \mathcal{H}_{010} &= \frac{1}{i} \left(\frac{\partial}{\partial \phi_1} + \frac{\partial}{\partial \phi_2} \right), \\ \mathcal{H}_{001} &= \frac{1}{i} \left(\frac{1}{r_1^3} \frac{\partial}{\partial \phi_1} + \frac{1}{r_2^3} \frac{\partial}{\partial \phi_2} \right), \\ \mathcal{H}_{020} &= \frac{1}{2}(r_1^{-2} \sin^2 \theta_1 + r_2^{-2} \sin^2 \theta_2), \\ \mathcal{H}_{011} &= r_1^{-1} \sin^2 \theta_1 + r_2^{-1} \sin^2 \theta_2, \\ \mathcal{H}_{002} &= \frac{1}{2}(r_1^{-4} \sin^2 \theta_1 + r_2^{-4} \sin^2 \theta_2).\end{aligned}\quad (2.5)$$

Here (r_1, θ_1, ϕ_1) and (r_2, θ_2, ϕ_2) are spherical polar coordinates for each atom with polar axes along the z -direction. M is the magnetic moment of each nucleus (supposed fixed along the z -axis). The expressions (2.5) arise from the superposition of the vector potentials appropriate to the field H and the fields due to the nuclei.

To study the effect of van der Waals forces on the magnetic susceptibility and nuclear shielding, we need to find the energy perturbation terms $\lambda^2 \mu^2$ and $\lambda^2 \mu \nu$. (Terms of lower order such as $\lambda \mu^2$, $\lambda \mu$, etc. turn out to be zero.) As we are not concerned with terms of order ν^2 at all, the Hamiltonian \mathcal{H}_{002} in (2.2) can be ignored. If the energy of the lowest state is expanded in orders of magnitude of λ, μ, ν

$$\mathcal{E} = \lambda^2 \mathcal{E}_{200} + \mu^2 \mathcal{E}_{020} + \mu \nu \mathcal{E}_{011} + \lambda^2 \mu^2 \mathcal{E}_{220} + \lambda^2 \mu \nu \mathcal{E}_{211} + \dots, \quad (2.6)$$

then $\lambda^2 \mathcal{E}_{200}$ is the usual van der Waals energy (R^{-6} term), $\mu^2 \mathcal{E}_{020}$ gives the unperturbed magnetic susceptibility of separated atoms and $\mu \nu \mathcal{E}_{211}$ gives the unperturbed shielding. $\lambda^2 \mu^2 \mathcal{E}_{220}$ and $\lambda^2 \mu \nu \mathcal{E}_{211}$ then give the leading corrections to the magnetic quantities due to the atomic interaction.

The calculation may be broken down into two parts using separate Hamiltonians

$$\mathcal{H}' = \mathcal{H}_{000} + \lambda \mathcal{H}_{100} + \mu \mathcal{H}_{010} + \nu \mathcal{H}_{001}, \quad (2.7)$$

$$\mathcal{H}'' = \mathcal{H}_{000} + \lambda \mathcal{H}_{100} + \mu^2 \mathcal{H}_{020} + \mu \nu \mathcal{H}_{011}. \quad (2.8)$$

The values of \mathcal{E}_{220} and \mathcal{E}_{211} for each Hamiltonian can be added to give the correct result for the full Hamiltonian \mathcal{H} . This is because in a complete perturbation calculation any cross-terms involving \mathcal{H}_{010} , \mathcal{H}_{001} on the one hand and \mathcal{H}_{020} , \mathcal{H}_{011} on the other would be of the third order in the pair of variables μ and ν and so could not contribute to the terms $\lambda^2 \mu^2$ and $\lambda^2 \mu \nu$ which we wish to find.

We first consider the Hamiltonian (2.7) and expand the corresponding wave function in powers of λ, μ, ν as follows

$$\psi' = \psi_{000} + \lambda \psi_{100} + \lambda^2 \psi_{200} + \lambda \mu \psi_{110} + \lambda \nu \psi_{101} + \dots \quad (2.9)$$

and set out to find the coefficient functions by variational procedures. There are no terms of the type ψ_{0mn} ($m, n > 0$) in (2.9) as the Hamiltonians \mathcal{H}_{010} and \mathcal{H}_{001} do not modify the wave functions of isolated atoms. We now have to minimize the integral $\int \psi'^* \mathcal{H}' \psi' d\tau$ subject to the orthogonality condition

$$\int \psi'^* \psi' d\tau = 1. \quad (2.10)$$

We proceed by minimizing the terms of lowest order in the energy integral first. The zero-order wave function is

$$\psi_{000} = \pi^{-1} \exp(-r_1 - r_2). \quad (2.11)$$

The function ψ_{100} clearly has to have the same symmetry as the perturbing Hamiltonian \mathcal{H}_{100} . It is therefore orthogonal to ψ_{000} and (2.10) is satisfied to first order in λ . We therefore find ψ_{100} by minimizing the energy term in λ^2

$$\mathcal{E}_{200} = (\psi_{000} | \mathcal{H}_{100} | \psi_{100}) + (\psi_{100} | \mathcal{H}_{100} | \psi_{000}) + (\psi_{100} | \mathcal{H}_{000} | \psi_{100}) \quad (2.12)$$

using the normal matrix notation. If ψ_{100} is taken in the form

$$\psi_{100} = \mathcal{H}_{100} \psi_{000} (a + br_1 + br_2) \quad (2.13)$$

and a and b are varied, minimization of (2.12) gives

$$a = -\frac{4}{13}, \quad b = -\frac{2}{13},$$

$$\mathcal{E}_{200} = -\frac{84}{13} = -6.46. \quad (2.14)$$

We next find ψ_{110}' by minimizing the term $\lambda^2 \mu^2$ in the energy integral. This is

$$\begin{aligned} \mathcal{E}_{220}' &= (\psi_{000} | \mathcal{H}_{100} | \psi_{120}') + (\psi_{120}' | \mathcal{H}_{100} | \psi_{000}) + (\psi_{100} | \mathcal{H}_{000} | \psi_{120}') \\ &\quad + (\psi_{120}' | \mathcal{H}_{000} | \psi_{100}) + (\psi_{100} | \mathcal{H}_{010} | \psi_{110}') + (\psi_{110}' | \mathcal{H}_{010} | \psi_{100}) \\ &\quad + (\psi_{110}' | \mathcal{H}_{000} | \psi_{110}'). \end{aligned} \quad (2.15)$$

Now if ψ_{100} were exact, it would satisfy the equation

$$\mathcal{H}_{000} \psi_{100} + \mathcal{H}_{100} \psi_{000} = 0. \quad (2.16)$$

If we suppose that our approximation (2.13) is accurate enough for this still to hold, (2.15) simplifies to

$$\mathcal{E}_{220}' = (\psi_{100} | \mathcal{H}_{010} | \psi_{110}') + (\psi_{110}' | \mathcal{H}_{010} | \psi_{100}) + (\psi_{110}' | \mathcal{H}_{000} | \psi_{110}'). \quad (2.17)$$

For the parallel calculation ψ_{110}' is identically zero for the wave function is axially symmetric about the direction of the magnetic field. For the perpendicular situation, the appropriate symmetry for ψ_{110}' is

$$\psi_{110}' = ig(r_1, r_2)(x_1 y_2 + y_1 x_2) \psi_{000}. \quad (2.18)$$

The optimum linear form for $g(r_1, r_2)$ is

$$g = -\frac{6}{169}(17 - 24r_1 - 24r_2) \quad (2.19)$$

giving

$$\mathcal{E}_{220}' = -25.60. \quad (2.20)$$

In a similar manner, an approximate form for ψ_{101}' can be found by minimizing the expression for \mathcal{E}_{202}' analogous to (2.17). The symmetry is the same and we find

$$\psi_{101}' = \frac{2i}{169}(139 - 15r_1 - 15r_2)(x_1 y_2 + y_1 x_2) \psi_{000}. \quad (2.21)$$

Knowing ψ_{110}' and ψ_{101}' , \mathcal{E}_{211}' can be calculated directly from

$$\begin{aligned} \mathcal{E}_{211}' &= (\psi_{100} | \mathcal{H}_{010} | \psi_{101}') + (\psi_{101}' | \mathcal{H}_{010} | \psi_{100}) + (\psi_{100} | \mathcal{H}_{001} | \psi_{110}') \\ &\quad + (\psi_{110}' | \mathcal{H}_{001} | \psi_{100}) + (\psi_{110}' | \mathcal{H}_{000} | \psi_{101}') + (\psi_{101}' | \mathcal{H}_{000} | \psi_{110}'); \end{aligned} \quad (2.22)$$

substituting from (2.18), (2.19) and (2.21), we obtain

$$\mathcal{E}_{211}' = -8.97. \quad (2.23)$$

We now consider the perturbation energies using the second Hamiltonian \mathcal{H}'' (equation (2.8)). In the absence of molecular interaction, the perturbation energies to order μ^2 and $\mu\nu$ are

$$\mathcal{E}_{020} = (\psi_{000} | \mathcal{H}_{020} | \psi_{000}) = 2, \quad (2.24)$$

$$\mathcal{E}_{011} = (\psi_{000} | \mathcal{H}_{011} | \psi_{000}) = \frac{4}{3}. \quad (2.25)$$

Corresponding wave function perturbations are solutions of

$$\mathcal{H}_{000}\psi_{020}'' + \mathcal{H}_{020}\psi_{000} = \mathcal{E}_{020}\psi_{000}, \quad (2.26)$$

$$H_{000}\psi_{011}'' + \mathcal{H}_{011}\psi_{000} = \mathcal{E}_{011}\psi_{000}. \quad (2.27)$$

We now require \mathcal{E}_{220}'' and \mathcal{E}_{011}'' . The complete expression for \mathcal{E}_{220}'' is

$$2(\psi_{120}'' | \mathcal{H}_{100} | \psi_{000}) + 2(\psi_{120}'' | \mathcal{H}_{000} | \psi_{100}) + 2(\psi_{200} | \mathcal{H}_{000} | \psi_{020}'') \\ + 2(\psi_{200} | \mathcal{H}_{020} | \psi_{000}) + 2(\psi_{100} | \mathcal{H}_{100} | \psi_{020}'') + (\psi_{100} | \mathcal{H}_{020} | \psi_{100}). \quad (2.28)$$

The first two terms cancel using (2.16). The second two terms simplify by (2.26) and, noting that

$$2(\psi_{200} | \psi_{000}) + (\psi_{100} | \psi_{100}) = 0 \quad (2.29)$$

by the normalization condition, we can write

$$\mathcal{E}_{220}'' = 2(\psi_{100} | \mathcal{H}_{100} | \psi_{020}'') + (\psi_{100} | \mathcal{H}_{020} - \mathcal{E}_{020} | \psi_{100}). \quad (2.30)$$

A similar argument gives

$$\mathcal{E}_{211}'' = 2(\psi_{100} | \mathcal{H}_{100} | \psi_{011}'') + (\psi_{100} | \mathcal{H}_{011} - \mathcal{E}_{011} | \psi_{100}). \quad (2.31)$$

The second matrix elements in these two equations can be evaluated directly using the previous approximation for ψ_{100} . The first terms can be evaluated using solutions of (2.26) and (2.27) as described in the Appendix.

The complete results (including \mathcal{E}' and \mathcal{E}'' terms) are

$$\mathcal{E}_{220} = \begin{cases} 115.74 & (||), \\ 142.95 & (\perp), \end{cases} \quad \mathcal{E}_{211} = \begin{cases} -28.79 & (||), \\ -33.34 & (\perp). \end{cases} \quad (2.32)$$

Combining with (2.24) and (2.25), we now have an expansion of \mathcal{E} in powers of R , H and M . To obtain the required expressions for magnetic susceptibility and screening constants, we have to convert this into an expansion in powers of R , H_0 and M using (2.1). The coefficient of H_0^2 is then $-\frac{1}{2}\chi$, where χ is the susceptibility (of the pair of atoms) and the coefficient of MH_0 is 2σ , where σ is the screening constant. The final results are

$$a^{-3}\chi_{||} = -\frac{\hbar^2}{m^2c^2a^2}(1 + 57.87R^{-6} + \dots), \\ a^{-3}\chi_{\perp} = -\frac{\hbar^2}{m^2c^2a^2}(1 + 71.47R^{-6} + \dots), \\ a^{-3}\chi_{av} = -\frac{\hbar^2}{m^2c^2a^2}(1 + 66.94R^{-6} + \dots), \quad (2.33)$$

and

$$\sigma_{||} = \frac{\hbar^2}{3m^2c^2a^2}(1 + 3R^{-3} - 21.59R^{-6} + \dots), \\ \sigma_{\perp} = \frac{\hbar^2}{3m^2c^2a^2}(1 - \frac{3}{2}R^{-3} - 25.00R^{-6} + \dots), \\ \sigma_{av} = \frac{\hbar^2}{3m^2c^2a^2}(1 - 23.86R^{-6} + \dots). \quad (2.34)$$

3. OVERLAP EFFECTS AND NUCLEAR SCREENING

To study the effect of overlap forces on the nuclear screening for two hydrogen atoms, it is necessary to use wave functions having full symmetry properties (symmetric in the electronic spatial coordinates for the singlet state and anti-symmetric for the triplet). A number of calculations of the screening constant for the hydrogen molecule at the equilibrium internuclear distance have been published, but these are mostly in a form which does not give the correct limiting answer at large separations and are therefore unsuitable for our purpose. Methods which are correct at infinite separation can be developed using gauge-invariant atomic orbitals as used by London [5] for the theory of magnetic susceptibilities and by one of the authors [6] and Hameka [7] for the theory of nuclear magnetic shielding. If the externally applied magnetic field is \mathbf{H} , the modified atomic orbital for atom s is

$$\chi_s(\mathbf{r}) = \phi_s(\mathbf{r}) \exp \left\{ -\frac{ie}{2\hbar c} \mathbf{r} \cdot (\mathbf{H} \wedge \mathbf{R}_s) \right\} \quad (3.1)$$

where $\phi_s(\mathbf{r})$ is the ordinary atomic orbital and \mathbf{R}_s is the position vector of the nucleus of atom s . We shall refer to the atoms as **a** and **b** and use the nucleus of **a** as origin for the position vectors (although in practice any point on the internuclear line will give the same final results).

In the absence of a magnetic field, the correct spatial wave functions $\Psi_s^{(0)}$ and $\Psi_t^{(0)}$ for the lowest singlet and triplet states at large separations are

$$\begin{aligned} \Psi_s^{(0)} &= N_s \{ \phi_a(1) \phi_b(2) + \phi_b(1) \phi_a(2) \}, \\ \Psi_t^{(0)} &= N_t \{ \phi_a(1) \phi_b(2) - \phi_b(1) \phi_a(2) \} \end{aligned} \quad (3.2)$$

where N_s and N_t are normalizing factors. The Heitler-London scheme for examining the effect of overlap is to assume the same wave functions at finite separations (with adjusted normalizing constants) and evaluate the expectation value of the energy. In the presence of a magnetic field \mathbf{H} , correct wave functions at infinite separation are

$$\begin{aligned} \Psi_s &= N_s \{ \chi_a(1) \chi_b(2) + \chi_b(1) \chi_a(2) \}, \\ \Psi_t &= N_t \{ \chi_a(1) \chi_b(2) - \chi_b(1) \chi_a(2) \}. \end{aligned} \quad (3.3)$$

We shall assume that these are suitable approximate functions at all separations. (The normalizing factors N_s and N_t depend on the magnetic field, but we may take them to be the same as in $\Psi_s^{(0)}$ and $\Psi_t^{(0)}$ for the same separation, for the change is found to be only of second order in H .)

In previous work [6, 7], some attempt has been made to correct wave functions such as (3.3) by allowing for mixing with other functions due to the magnetic field. Hameka [7] finds a considerable contribution to the screening from such a 'paramagnetic contribution' at the equilibrium separation, but this appears to be due to the use of excited state functions which are not orthogonal to the ground state function (because of the gauge factors). A more detailed study, which we shall not describe in detail, suggests that such contributions are really much smaller for the H_2 system and we shall not include them.

Our procedure therefore, is to pick out the terms which are first order in the external field H and the nuclear moments M_a and M_b in the energy integrals.

$$\mathcal{E}_s = (\Psi_s | \mathcal{H} | \Psi_s), \quad \mathcal{E}_t = (\Psi_t | \mathcal{H} | \Psi_t) \quad (3.4)$$

where \mathcal{H} is the complete Hamiltonian

$$\mathcal{H} = \frac{1}{2m} \sum_{i=1}^2 \left(\mathbf{p}_i + \frac{e}{c} \mathbf{A}(\mathbf{r}_i) \right)^2 + V, \quad (3.5)$$

V being the electrostatic potential energy. The vector potential \mathbf{A} is

$$\mathbf{A}(\mathbf{r}) = \frac{1}{2} \mathbf{H} \wedge \mathbf{r} + \frac{\mathbf{M}_a \wedge (\mathbf{r} - \mathbf{R}_a)}{|\mathbf{r} - \mathbf{R}_a|^3} + \frac{\mathbf{M}_b \wedge (\mathbf{r} - \mathbf{R}_b)}{|\mathbf{r} - \mathbf{R}_b|^3}. \quad (3.6)$$

The details are very similar to Hameka's calculation of the diamagnetic contribution, the principal difference being that we use Heitler-London functions. After averaging over directions of the field \mathbf{H} , the results are

$$\begin{aligned} \sigma_{\text{singlet}} &= \sigma_\infty (3I_1 + I_2 - I_5 + 2I_3S)/(1 + S^2), \\ \sigma_{\text{triplet}} &= \sigma_\infty (3I_1 + I_2 - I_5 - 2I_3S)/(1 - S^2), \end{aligned} \quad (3.7)$$

where $\sigma_\infty = e^2/3mc^2a$ and S, I_2, I_3 and I_5 are integrals given by

$$\begin{aligned} S &= \int \phi_a \phi_b d\tau, \\ I_1 &= \frac{1}{3} \int \phi_a^2 r_a^{-1} d\tau, \\ I_2 &= \int \phi_a^2 r_b^{-1} d\tau, \\ I_3 &= \int \phi_a \phi_b r_a^{-1} d\tau, \\ I_5 &= \int \phi_b^2 R z_a r_a^{-3} d\tau. \end{aligned} \quad (3.8)$$

and evaluated by Hameka [7]. Values of σ/σ_∞ calculated using (3.7) for a series of values of R are given in table 1.

R (atomic units)	$\sigma_{\text{singlet}}/\sigma_\infty$	$\sigma_{\text{triplet}}/\sigma_\infty$
1	1.5368	0.5429
1.4	1.3544	0.7847
1.5	1.3161	0.8228
2	1.1666	0.9380
3	1.0309	1.0000
4	1.0018	1.0043
5	0.9990	1.0020
6	0.9995	1.0007
7	0.9998	1.0002

Table 1. H_2 screening constants using Heitler-London functions.

The behaviour of σ is by no means simple, for whereas at distances of the order of the equilibrium distance (1.4 atomic units), the overlap forces cause an increase in the singlet shielding and a decrease for the triplet, at large distances the situation is reversed. The method predicts a value of 23.9×10^{-6} for the hydrogen molecule

(singlet state at $R = 1.4$ a.u.) compared with the accepted best value of 26.8×10^{-6} [8].

An improved theory can be obtained if we use hydrogen 1s orbitals of the form

$$\phi = (z^3/\pi)^{1/2} \exp(-zr) \quad (3.9)$$

(i.e. Wang-type wave functions), the parameter z being chosen to minimize the total energy. Hylleraas and Skavlem [9] found that a wave function with variable z for the helium atom ($R = 0$) gave a value of σ which agrees within about 0.25 per cent with the best available value.

The calculation with these modified atomic orbitals parallels closely that using Heitler-London functions. If $\sigma(z, R)$ is the screening constant using (3.7), (3.8) and (3.9) at distance R , then it is easily shown that

$$\sigma(z, R) = z\sigma(1, zR). \quad (3.10)$$

Hirschfelder and Linnett [10] have calculated the optimum values of z for various R in the case of the singlet state, but for the triplet they find it only for the more complicated 'Wang and Ionic' function. We have used these values in the calculations of σ from (3.10) shown in table 2. The results for the ground state of H_2 is now 26.5×10^{-6} which is very close to the best value.

R (atomic units)	$\sigma_{\text{singlet}}/\sigma_\infty$	R (atomic units)	$\sigma_{\text{triplet}}/\sigma_\infty$
0.719	2.14	1.228	0.442
1.235	1.60	1.724	0.716
1.40	1.49	1.973	0.792
1.537	1.40	2.190	0.857
1.848	1.26		

Table 2. H_2 screening constants using Wang functions.

For larger R , there appears to be no calculation of z for Wang functions of sufficient accuracy. However, a study of the asymptotic behaviour shows that $z_{\text{triplet}} > 1$ and $z_{\text{singlet}} < 1$ (R large) so that z itself shows the same cross-over behaviour as σ/σ_∞ (table 1). This means that the conclusion $\sigma_{\text{triplet}} > \sigma_{\text{singlet}}$ (large R) still applies with the more accurate Wang functions.

4. DISCUSSION

The calculations of § 2 give strong support to the view that van der Waals forces tend to reduce nuclear magnetic screening constants by an appreciable amount. At a separation of 4 atomic units (close to twice the van der Waals radius of hydrogen), the reduction according to equation (2.34) is about 10^{-7} (or 6 c/s at 60 Mc/s). For van der Waals interaction of hydrogen with heavier atoms, the value is likely to be larger.

The diamagnetic susceptibility, on the other hand, is increased (in magnitude) by van der Waals forces. This is in contrast with the effect of a static electric field on hydrogen atoms which reduces both the nuclear screening and the diamagnetic susceptibility. These results can be interpreted qualitatively in the following manner. For the hydrogen atom in an electric field, the principal

result is a hindering of diamagnetic electronic precession because the spherical symmetry of the potential field has been destroyed. This reduces both the screening and the susceptibility. For two interacting hydrogen atoms, there is a similar effect due to the fluctuating electric dipole field caused by the other atom, but there is an additional effect leading to an expansion of both atoms, so that the van der Waals dipoles are larger and the energy lowering greater. This expansion leads to an increase in diamagnetic susceptibility (proportional to \bar{r}^2) and a decrease in nuclear shielding (proportional to \bar{r}^{-1}). The net result is that there is a resultant increase in susceptibility.

R (atomic units)	$\sigma_{\text{singlet}}/\sigma_\infty$	$\sigma_{\text{triplet}}/\sigma_\infty$
3	0.9982	0.9473
4	0.9960	0.9985
5	0.9975	1.0005
6	0.9990	1.0002
7	0.9996	0.9998

Table 3. H_2 screening constants for combined van der Waals and overlap interactions.

At smaller separations, the overlap forces begin to affect the screening constant, leading to more complicated behaviour shown in table 3. (These values are obtained by adding the van der Waals R^{-6} term to the results of table 1.) As the atoms are brought together, the screening constant of the triplet (repulsive) state increases above that of the singlet (attractive) state. In the triplet state this corresponds qualitatively to the electrons being forced away from the overlap region and consequently closer to the nuclei. Closer still, however, there is a cross over and the dominant effect is a hindrance to precession due to interference of the electron clouds, leading to a reduction in σ_{triplet} . As R approaches zero, σ_{singlet} will tend to the screening constant for the helium atom.

These calculations suggest, therefore, that the screening contribution due to repulsive intermolecular forces can be of either sign, being positive for weak interaction and becoming large and negative for strong interaction. The net contribution to σ of both kinds of intermolecular force in the triplet state of H_2 is just positive for a small range of R , but is usually negative.

We are grateful to Miss P. M. Noyes for assistance with the calculations. We are also indebted to the Department of Scientific and Industrial Research for a Maintenance Grant to one of us (T.W.M.).

APPENDIX

In order to calculate the outstanding terms in (2.30) and (2.31), it is necessary to know ψ_{020}'' and ψ_{011}'' . Since the Hamiltonians \mathcal{H}_{020} and \mathcal{H}_{011} involve only one-electron operators, it is possible to find explicit forms. These are

$$\begin{aligned}\psi_{020}'' = & -\psi_{000}[F_{020}(r_1)(\sin^2 \theta_1 - \frac{2}{3}) + F_{020}(r_2)(\sin^2 \theta_2 - \frac{2}{3}) \\ & + \frac{2}{3}G_{020}(r_1) + \frac{2}{3}G_{020}(r_2)]\end{aligned}\quad (\text{A } 1)$$

and a similar expression for ψ_{011}'' . F and G are solutions of the differential equations :

$$\left(\frac{d}{dr} - \frac{1}{2} \frac{d^2}{dr^2} - \frac{1}{r} \frac{d}{dr} + \frac{3}{r^2} \right) F_{020} = \frac{1}{2} r^2, \quad (\text{A } 2)$$

$$\left(\frac{d}{dr} - \frac{1}{2} \frac{d^2}{dr^2} - \frac{1}{r} \frac{d}{dr} + \frac{3}{r^2} \right) F_{011} = \frac{1}{r}, \quad (\text{A } 3)$$

$$\left(\frac{d}{dr} - \frac{1}{2} \frac{d^2}{dr^2} - \frac{1}{r} \frac{d}{dr} \right) G_{020} = \frac{1}{2} r^2 - \frac{3}{2}, \quad (\text{A } 4)$$

$$\left(\frac{d}{dr} - \frac{1}{2} \frac{d^2}{dr^2} - \frac{1}{r} \frac{d}{dr} \right) G_{011} = \frac{1}{r} - 1. \quad (\text{A } 5)$$

In order to satisfy the normalization requirement, there is the further condition that

$$\int G_{020} r^2 \exp(-2r) dr = \int G_{011} r^2 \exp(-2r) dr = 0. \quad (\text{A } 6)$$

There are polynomial solutions of (A 2), (A 4) and (A 5) which satisfy (A 6). These are

$$\begin{aligned} F_{020} &= \frac{1}{6} r^3 + \frac{1}{4} r^2, \\ G_{020} &= \frac{1}{6} r^3 + \frac{1}{2} r^2 - \frac{11}{4}, \\ G_{011} &= -r + \frac{3}{2}, \end{aligned} \quad (\text{A } 7)$$

and correspond to energies $\mathcal{E}_{020} = 2$, $\mathcal{E}_{011} = \frac{4}{3}$.

It is now possible to calculate $2(\psi_{100} | \mathcal{H}_{100} | \psi_{020}'')$ directly. It has the value

$$\frac{1534 + 167B}{13} \quad (\text{A } 8)$$

(where $B = -2$ in the parallel case and 1 in the perpendicular case). F_{011} is more complicated, but we find it is possible to determine the value of $2(\psi_{100} | \mathcal{H}_{100} | \psi_{011}'')$ by using certain properties of F_{011} . If we put

$$F_m = \int \exp(-2r) r^m F_{011}(r) dr$$

we can find F_m for $m \geq 3$ which is all we shall need. For from (A 3) we can derive the difference equation

$$mF_{m+1} - \frac{1}{2}(m-2)(m+3)F_m = \frac{(m+1)^2}{2^{m+2}} \quad (\text{A } 9)$$

provided $F_{011}(r)$ satisfies the condition

$$Fr^{m+1} \exp(-2r) \rightarrow 0 \text{ as } r \rightarrow \infty \text{ and as } r \rightarrow 0. \quad (\text{A } 10)$$

Now we can find an F which satisfies both (A 10) and (A 3). It is :

$$\begin{aligned} F_{011}(r) &= \frac{2}{5C} \left[r^2 W_2(2, 6; 2r) \int_0^r \omega^3 \exp(-2\omega) W_1(2, 6; 2\omega) d\omega \right. \\ &\quad \left. + r^2 W_1(2, 6; 2r) \int_r^\infty \omega^3 \exp(-2\omega) W_2(2, 6; 2\omega) d\omega \right] \end{aligned} \quad (\text{A } 11)$$

where $W_1(2, 6; z)$ is that solution of the confluent hypergeometric equation

$$z \frac{d^2 W}{dz^2} + (6-z) \frac{dW}{dz} - 2W = 0$$

which is a power series :

$$1 + \frac{1}{3}z + \dots \text{ at the origin}$$

and which

$$\sim \frac{5C}{32} z^{-1} e^z$$

at ∞ (where C is a constant), while $W_2(2, 6; z)$ is another solution of the same equation which has the limiting behaviour:

$$W_2 \sim \begin{cases} \frac{1}{4} z^{-2} & \text{at } \infty, \\ \frac{C}{32} z^{-5} & \text{at the origin.} \end{cases}$$

Then the limiting behaviour of F given by (A 11) is:

$$F \sim \begin{cases} \frac{1}{2} r & \text{at the origin,} \\ \log r & \text{at } \infty, \end{cases}$$

and this certainly satisfies (A 10) for $m \geq 0$.

We therefore have

$$F_3 = \frac{3}{16}, \quad F_4 = \frac{7}{16}, \quad F_5 = \frac{79}{64}$$

and with these together with the explicit form for G_{011} given in (A 7) the remaining term is easily calculated. Its value is:

$$2(\psi_{100} | \mathcal{H}_{100} | \psi_{011''}) = -\frac{264}{13} + \frac{41B}{39}.$$

REFERENCES

- [1] SCHNEIDER, W. G., BERNSTEIN, H. J., and POPLE, J. A., 1958, *J. chem. Phys.*, **28**, 601.
- [2] STEPHEN, M. J., 1958, *Mol. Phys.*, **1**, 223.
- [3] BUCKINGHAM, A. D., 1960, *Canad. J. Chem.*, **38**, 300.
- [4] MARSHALL, T. W., and POPLE, J. A., 1958, *Mol. Phys.*, **1**, 199.
- [5] LONDON, F., 1937, *J. Phys. Radium*, **8**, 397.
- [6] POPLE, J. A., 1957, *Proc. roy. Soc. A*, **239**, 541.
- [7] HAMEKA, H. F., 1958, *Mol. Phys.*, **1**, 203.
- [8] RAMSEY, N. F., 1950, *Phys. Rev.*, **78**, 699.
- [9] HYLLERAAS and SKAVLEM, 1950, *Phys. Rev.*, **79**, 117.
- [10] HIRSCHFELDER, J. O., and LINNETT, J. W., 1951, *J. chem. Phys.*, **18**, 130.

High resolution nuclear-magnetic-resonance spectra of hydrocarbon groupings

IV. ABC spectra of vinyl compounds

by C. N. BANWELL and N. SHEPPARD

University Chemical Laboratory, Lensfield Road, Cambridge

(Received 5 February 1960)

The interpretation of ABC-type spectra is discussed in relation to several series of calculated spectra; some frequency and intensity sum rules are indicated.

The hydrogen spectra of some vinyl derivatives, $X \cdot CH=CH_2$ ($X=F, Cl, Br, O$ and C) have been analysed. It is shown that

$$J_{trans} \text{ (12 to 18 c/s)} > J_{cis} \text{ (4 to 12 c/s)} > J_{gem} \text{ (-3.5 to +2 c/s)},$$

and that a modified correlation holds between the J_{gem} coupling constants of CH_2 groups and the H-C-H angle in a range of molecules. All three coupling constants of the vinyl compounds decrease approximately linearly with the electronegativity of X ; these effects are probably transmitted through the sigma bonds. By contrast the difference between the chemical shift of the $=CH_2$ group and that of the $XHC=$ group is approximately linearly dependent on Taft's resonance parameter, σ_R , suggesting that the pi-electron distribution is principally concerned in this case.

1. INTRODUCTION

The three chemically non-equivalent hydrogen nuclei of a vinyl group give rise to nuclear magnetic resonance spectra of the type described as ABC in the notation of Bernstein *et al.* [1]. This means that the chemical shifts, δ , between the pairs of nuclei, when expressed in cycles per second (c/s), are of similar magnitude to the electron-coupled spin-spin interaction constants, J_{HH}' , expressed in the same units. The original aim of this investigation was to analyse the spectra of a series of vinyl compounds, $XCH=CH_2$, to find out how the chemical shifts and coupling constants depend on the nature of the adjacent atom, X , and on the stereochemical relationships of the hydrogen atoms. For this purpose spectra have been studied of substances in which X is C, O, F, Si, Cl and Br . In the course of the work certain more general aspects of the spectra of ABC type were explored. For ease of presentation these are discussed first in terms of selected series of calculated spectra.

A number of less well-resolved spectra of vinyl compounds have previously been analysed by Shimuzu *et al.* [2]. Also Fessenden and Waugh [3] have very recently published an analysis of the spectrum of styrene and of a number of other ABC spectra, and Gutowsky *et al.* [4] have published a detailed analysis of the spectrum of vinyl bromide. Fessenden and Waugh [3] have also considered some of the more general features of ABC spectra and have given formal proof of a number of relationships which we have also deduced and used in the present work.

2. GENERAL FEATURES OF ABC SPECTRA

2.1. Spectral regularities

The complete Hamiltonian for the three-nucleus ABC system has been given by Bernstein *et al.* [1]. In this system there are three nuclear shielding constants, σ_A , σ_B and σ_C , together with three coupling constants J_{AB} , J_{AC} and J_{BC} . The chemical shifts, δ_{AB} , δ_{AC} and δ_{BC} are given by $\sigma_A - \sigma_B$, etc. However, the detailed analysis given by these authors applies only to the case when the resonance of nucleus A is well removed from those of nuclei B and C so that δ_{AC} and δ_{AB} are much greater than δ_{BC} , J_{AB} , J_{AC} and J_{BC} . When this restriction is removed the diagonalization of the Hamiltonian involves the solution of two 3×3 matrices.

E_i	Total spin	ψ_i
E_1	+3/2	$\alpha\alpha\alpha$
E_2	+1/2	$c_{22}(\alpha\alpha\beta) + c_{23}(\alpha\beta\alpha) + c_{24}(\beta\alpha\alpha)$
E_3	+1/2	$c_{32}(\alpha\alpha\beta) + c_{33}(\alpha\beta\alpha) + c_{34}(\beta\alpha\alpha)$
E_4	+1/2	$c_{42}(\alpha\alpha\beta) + c_{43}(\alpha\beta\alpha) + c_{44}(\beta\alpha\alpha)$
E_5	-1/2	$c_{55}(\alpha\beta\beta) + c_{56}(\beta\alpha\beta) + c_{57}(\beta\beta\alpha)$
E_6	-1/2	$c_{65}(\alpha\beta\beta) + c_{66}(\beta\alpha\beta) + c_{67}(\beta\beta\alpha)$
E_7	-1/2	$c_{75}(\alpha\beta\beta) + c_{76}(\beta\alpha\beta) + c_{77}(\beta\beta\alpha)$
E_8	-3/2	$\beta\beta\beta$

Table 1. Eigenvalues and eigenfunctions for the ABC system.

Analytical diagonalization of the Hamiltonian for the ABC case leads to eight energy levels or eigenvalues, E_1 to E_8 , each associated with an eigenfunction ψ_1 to ψ_8 as set out in table 1. The eigenfunctions for levels E_2 to E_4 and E_5 to E_7 are combinations of the degenerate basic wave functions given in reference [1]. The eigenvectors, c_{ij} , are solutions of the simultaneous equations represented by:

$$\begin{bmatrix} H_{22} - E_r & H_{23} & H_{24} \\ H_{32} & H_{33} - E_r & H_{34} \\ H_{42} & H_{43} & H_{44} - E_r \end{bmatrix} \begin{bmatrix} c_{r2} \\ c_{r3} \\ c_{r4} \end{bmatrix} = 0 \quad (r=2, 3 \text{ and } 4)$$

and

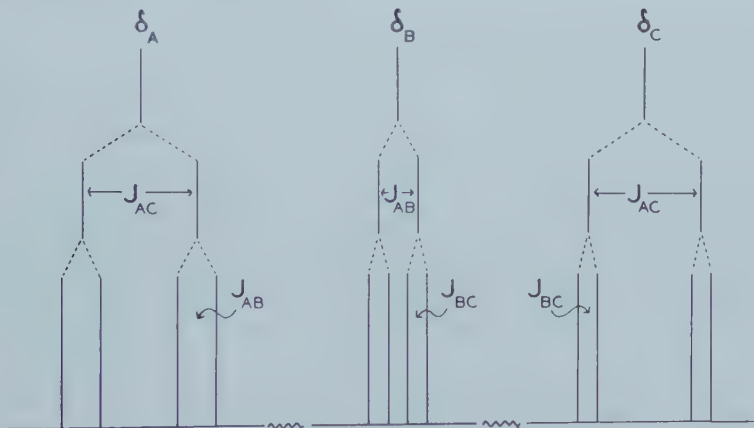
$$\begin{bmatrix} H_{55} - E_s & H_{56} & H_{57} \\ H_{65} & H_{66} - E_s & H_{67} \\ H_{75} & H_{76} & H_{77} - E_s \end{bmatrix} \begin{bmatrix} c_{s5} \\ c_{s6} \\ c_{s7} \end{bmatrix} = 0 \quad (s=5, 6 \text{ and } 7)$$

Transitions are allowed between the eigenvalues in which the change of total spin is ± 1 . The fifteen transitions set out in table 2 have to be considered, together with the transition probabilities which determine the relative intensities of the corresponding spectral lines. The lines are labelled, following reference [1], as A, B, or C transitions when the change of spin giving rise to the line is, in the unperturbed state (when the chemical shifts are much greater than the coupling constants) solely resident in the A, B, or C nucleus respectively, or as combination lines when all three nuclei change their spins simultaneously.

Transition	Frequency $\nu = \Delta E/h$	Relative intensity	Nucleus
1	$E_1 - E_2$	$(c_{22} + c_{23} + c_{24})^2$	C
2	$E_1 - E_3$	$(c_{32} + c_{33} + c_{34})^2$	B
3	$E_1 - E_4$	$(c_{42} + c_{43} + c_{44})^2$	A
4	$E_2 - E_5$	$[c_{22}(c_{55} + c_{56}) + c_{23}(c_{55} + c_{57}) + c_{24}(c_{56} + c_{57})]^2$	B
5	$E_2 - E_6$	$[c_{22}(c_{65} + c_{66}) + c_{23}(c_{65} + c_{67}) + c_{24}(c_{66} + c_{67})]^2$	A
6	$E_2 - E_7$	$[c_{22}(c_{75} + c_{76}) + c_{23}(c_{75} + c_{77}) + c_{24}(c_{76} + c_{77})]^2$	Comb.
7	$E_3 - E_5$	$[c_{32}(c_{55} + c_{56}) + c_{33}(c_{55} + c_{57}) + c_{34}(c_{56} + c_{57})]^2$	C
8	$E_3 - E_6$	$[c_{32}(c_{65} + c_{66}) + c_{33}(c_{65} + c_{67}) + c_{34}(c_{66} + c_{67})]^2$	Comb.
9	$E_3 - E_7$	$[c_{32}(c_{75} + c_{76}) + c_{33}(c_{75} + c_{77}) + c_{34}(c_{76} + c_{77})]^2$	A
10	$E_4 - E_5$	$[c_{42}(c_{55} + c_{56}) + c_{43}(c_{55} + c_{57}) + c_{44}(c_{56} + c_{57})]^2$	Comb.
11	$E_4 - E_6$	$[c_{42}(c_{65} + c_{66}) + c_{43}(c_{65} + c_{67}) + c_{44}(c_{66} + c_{67})]^2$	C
12	$E_4 - E_7$	$[c_{42}(c_{75} + c_{76}) + c_{43}(c_{75} + c_{77}) + c_{44}(c_{76} + c_{77})]^2$	B
13	$E_5 - E_8$	$(c_{55} + c_{56} + c_{57})^2$	A
14	$E_6 - E_8$	$(c_{65} + c_{66} + c_{67})^2$	B
15	$E_7 - E_8$	$(c_{75} + c_{76} + c_{77})^2$	C

Table 2. The allowed transitions for an ABC spectrum

In the simplest unperturbed case the complete spectrum consists of three groups of symmetrical quartets of lines all of the same intensity, the lines in each quartet being separated by the values of the coupling constants taken in pairs (figure 1). The three combination transitions occur with frequencies such that any pair of them is symmetrically situated about the centre of one of the quartets of lines. In the unperturbed case the intensities of the combination lines are zero, but they become observable in the more general case.

Figure 1. Unperturbed spectrum for three nuclei of spin $\frac{1}{2}$.

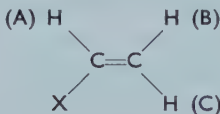
In a true ABC spectrum the interaction between the nuclei causes a redistribution of intensity in the spectrum so that the four lines corresponding to the transitions of a given nucleus are of unequal intensity. Furthermore the combination lines also often have appreciable strength which they acquire by sharing intensity with nearby 'fundamental' lines. While investigating empirically the manner in which the combination lines acquire intensity it was concluded that they only do so when (a) the two transitions have one energy level in common

and (b) the other energy levels are neighbouring ones associated with the same block of the overall Hamiltonian. Further consideration of this situation led to the conclusion that the sum of the intensities of all lines originating in allowed transitions between any two blocks of the Hamiltonian is the same as the sum of the intensities in the unperturbed case. This *intensity sum rule* has been independently derived and given formal proof by Fessenden and Waugh [3]. For ABC spectra it states $\sum I_{ii} = 3/4$ ($i=2, 3, 4$), $\sum I_{ij} = 3/2$ ($j=5, 6, 7$) and $\sum I_{js} = 3/4$, where I denotes the intensity of a transition and the unit of intensity is one per nucleus.

The positions of the lines in an ABC spectrum are such that the observed separations between pairs of lines in groups, A, B and C now differ from the actual coupling constants. Nevertheless the observed splittings are still repeated four times in the complete spectrum in a qualitatively similar manner to the unperturbed case, and the *sum* of the observed spacings is equal to the *sum* of the actual coupling constants. This latter rule follows from the fact that the sum of the roots of each determinantal block of the Hamiltonian is invariant [3].

2.2. Some calculated spectra of the ABC type

In the spectra of the vinyl compounds considered below the chemical shift between the methylene hydrogens (nuclei B and C) is usually fairly small in comparison with δ_{AB} and δ_{AC} , the lettering of the nuclei being given below:



We shall explore some of the features of such spectra by examining a few families of spectra calculated for regular changes of the parameters.

The intensity perturbation in a spectrum of this type is most noticeable in the overlapping BC part of the spectrum; the four lines due to nucleus A show only the usual effect of intensity enhancement towards the centre of gravity of the BC spectrum. However, it is also possible, under the condition that δ_{BC} is small, for two of the combination lines to lie close to, or within, the A quartet of lines and to gain measurable intensity at the expense of two of the 'fundamental' lines.

These effects are illustrated in figure 2 for the case when the A resonance is sufficiently far removed from those of the B and C nuclei for the spectrum to approximate to one of the XBC type. In this figure δ_{AB} is maintained constant while δ_{BC} is reduced, varying the overlap between the B and C resonances. This part of the spectrum can be seen to consist of two quartets of lines each of the two-nucleus type with symmetrical intensity patterns, each quartet corresponding to two B and two C lines. The relative intensities of the lines within a quartet are also similar to those for analogous spectra caused by a single pair of nuclei. The figure also shows the gain in intensity of the combination lines and consequent weakening of the fundamental lines in the A spectrum as δ_{BC} varies.

Figure 3 shows a series of calculated spectra obtained as the A lines are caused to approach the BC spectrum. As δ_{AB} (and δ_{AC}) decrease for a fixed value of δ_{BC} the perturbations of intensities and line separations become more pronounced. The spectra are actually calculated for $J_{AB}=5$, $J_{AC}=15$, $J_{BC}=1$, and $\delta_{BC}=2$ (in arbitrary units) while δ_{AB} is decreased in steps from 50 to 5. These figures

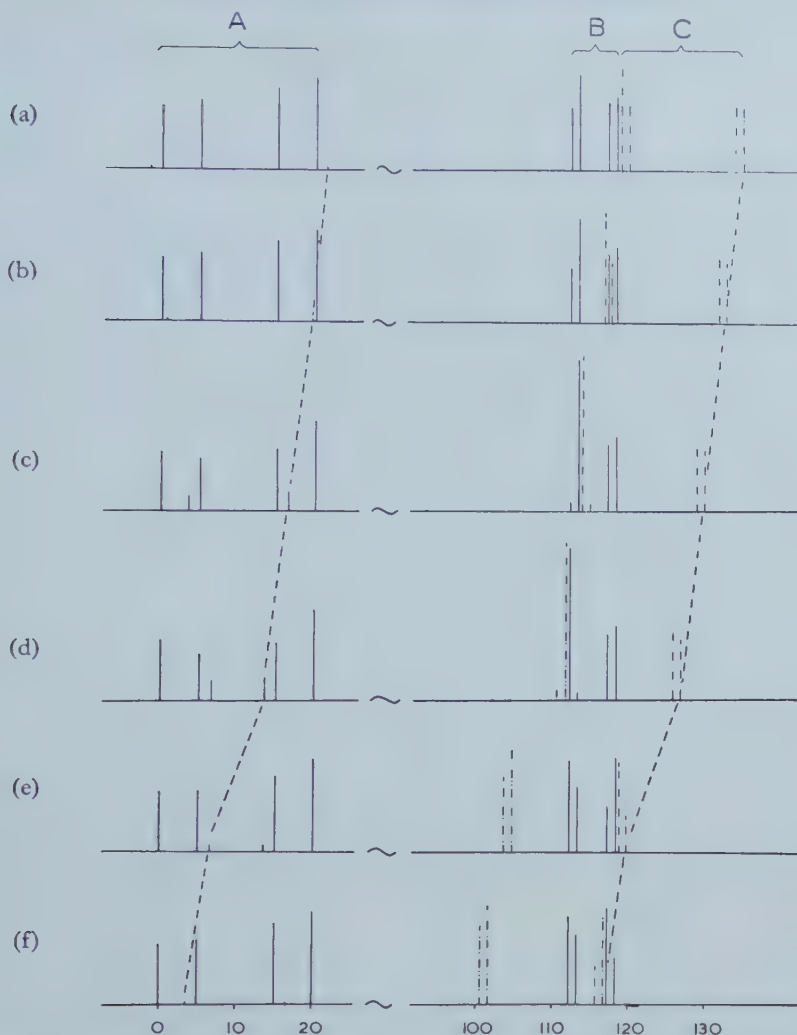


Figure 2. Change in the intensity pattern of ABC spectra for various values of δ_{BC} . δ_{AB} and the line separations due to the coupling constants are maintained constant. One dashed line connects the extreme lines of the C spectrum, the other one of the combination transitions, showing their parallel variations.

were chosen as being typical of the relative magnitudes found in the spectra of the vinyl compounds.

2.3. Alternative assignments of lines

Further examination of the spectrum shown in figure 3 (c) reveals that once the intensity of a combination line becomes comparable with that of a fundamental line, several reasonable alternative assignments of line frequencies could be made by inspection of the spectrum. Figure 4 shows that the symmetrical location of the combination bands with respect to the A group allows an exchange in trial assignments of fundamental and combination lines to be made within this group while still retaining three constant splittings throughout the spectrum by reassignment of the BC lines†. The three possible assignments that could be

† We are grateful to Professor J. S. Waugh and Dr. S. Castellano for pointing out this possibility to us; see also the discussion in the paper by Fessenden and Waugh [3].

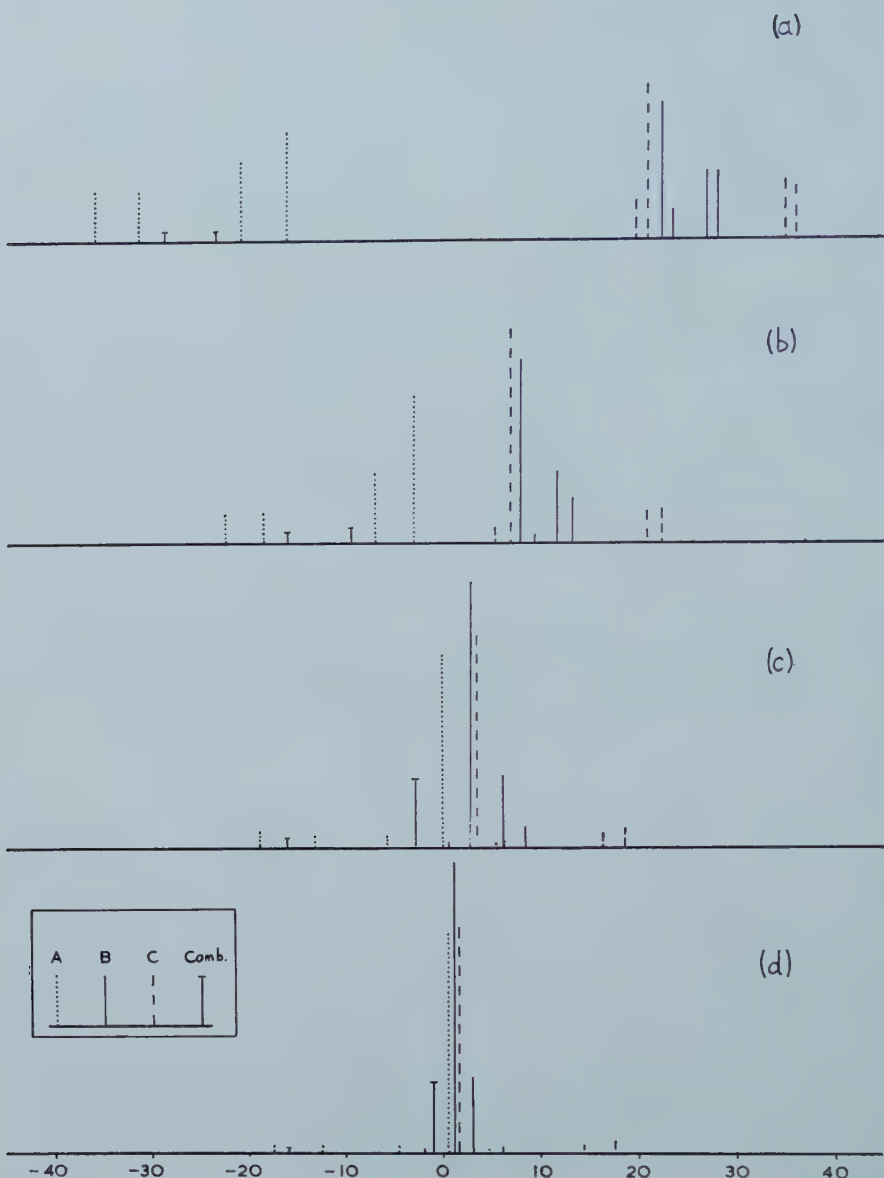


Figure 3. ABC spectra calculated for various values of δ_{AB} . $J_{AB}=5$, $J_{AC}=15$, $J_{BC}=1$, $\delta_{BC}=2$, and (a) $\delta_{AB}=50$, (b) $\delta_{AB}=20$, (c) $\delta_{AB}=10$, (d) $\delta_{AB}=5$.

made on the basis of the line frequencies are indicated. In a similar way the B and C lines and their symmetrically associated combination lines can in principle each be reassigned in two other ways, making seven possible assignments for the complete ABC spectrum. In practice, however, the third combination line is so weak for the values chosen for the parameters in the calculated spectra that the fundamental lines in the BC part of the spectrum can be selected without ambiguity. Of course, when all three combination lines are weak there is no ambiguity in assignment.

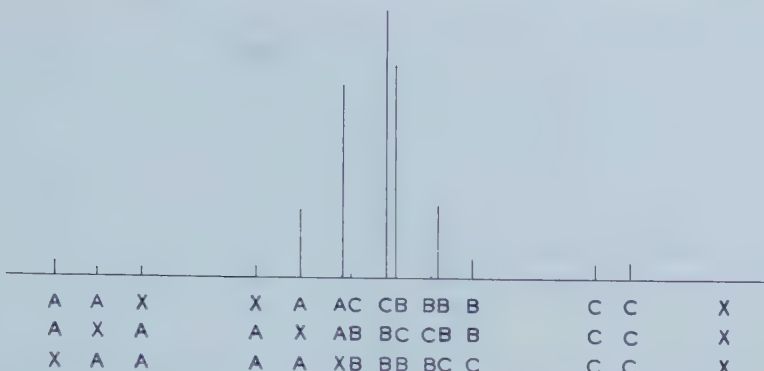


Figure 4. Figure 3 (c) redrawn so as to show the possible reassessments of line frequencies when the combination lines are of non-zero intensity.

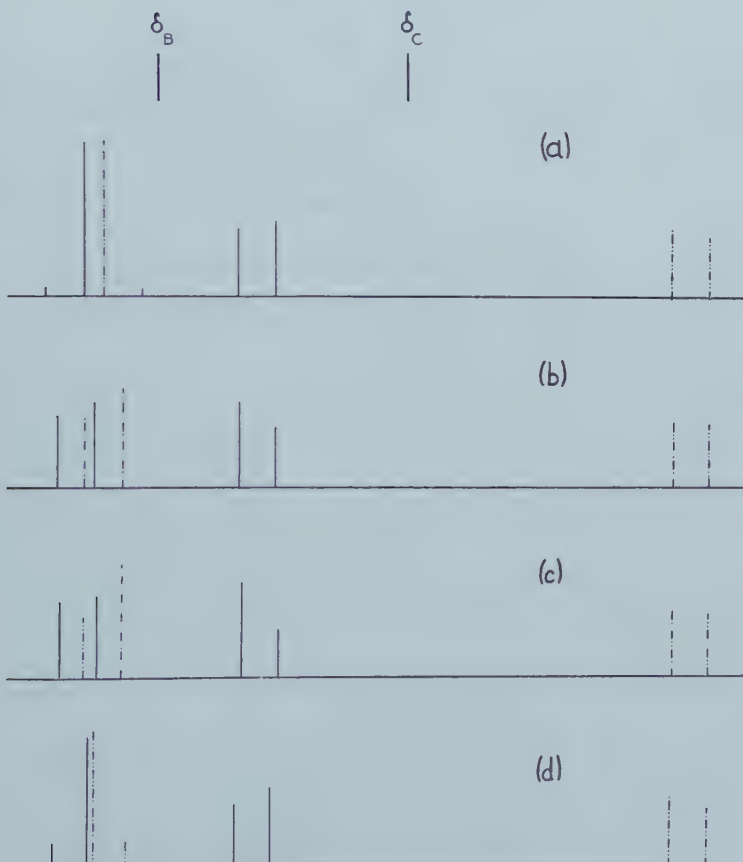


Figure 5. The B and C resonances of an ABC spectrum showing the intensity changes as the relative signs of coupling constants are varied. Spectra calculated for $\delta_{AB} = 99.5$, $\delta_{AC} = 105.0$, and (a) $J_{AB} = +4.7$, $J_{AC} = +15.4$, $J_{BC} = +1.0$; (b) $J_{AB} = -4.7$, $J_{AC} = +15.4$, $J_{BC} = +1.0$; (c) $J_{AB} = +4.7$, $J_{AC} = -15.4$, $J_{BC} = +1.0$; (d) $J_{AB} = +4.7$, $J_{AC} = +15.4$, $J_{BC} = -1.0$.

The seven assignments listed above each give a different set of numerical magnitudes for the parameters. One must, however, also consider possible alterations in the *signs* of coupling constants within any given numerical assignment. Only changes in relative signs of coupling constants affect the spectrum and hence there are four cases to be considered, viz. when all three coupling constants have the same sign, and when one of the three in turn is taken opposite in sign to the other two. The calculated spectra of figure 5 show how the intensity pattern of the BC spectrum of figure 2(c) changes if the four possible different combinations of relative signs of the coupling constants are taken. Because these spectra approximate to the XBC case it is seen that two pairs of the spectra are similar (for a true XBC system they would be identical) but that, as expected [5], different relative signs of J_{AB} and J_{AC} give markedly different spectra. It should be noted that the same magnitudes of the coupling constants with different relative signs give rise to slightly different spacings in the spectrum.

Altogether, therefore, 28 trial sets of parameters consistent with the frequencies can be chosen from the observed spectrum in the general case when all combination transitions have considerable intensity†.

3. THE ANALYSIS OF OBSERVED SPECTRA

The complete Hamiltonian for the ABC case involves the evaluation of two 3×3 determinants, and for the solution of these numerical methods have to be used. This implies that whereas it is a comparatively simple matter to derive a theoretical spectrum from a given set of chemical shift and coupling constant parameters the reverse procedure, i.e. the deduction of the parameters from an actually observed spectrum, cannot be carried out directly.

In order to overcome this difficulty we have drawn up a programme for use with the Cambridge electronic digital computer EDSAC 2. By means of this, attempts are made to fit the *frequencies* of the observed lines by successive approximations from a trial set of J and δ parameters chosen by inspection of the spectrum, the δ values being defined with respect to an arbitrarily chosen origin. When a best fit of frequencies has been obtained the computer calculates, and then prints out, both the frequencies and intensities of the complete spectrum together with the corresponding chemical shifts and coupling constants from which the spectrum is derived. A four-fold repetition of this process suffices to explore all possible sign combinations of the coupling constants. If the original inspection of the spectrum has led to a correct assignment of the lines, the frequencies of the lines in the final calculated spectra will agree closely with those observed; each of the four calculated spectra, however, usually shows a different intensity pattern, one of which agrees well with the observed intensities. This procedure sufficed to analyse most of the vinyl spectra.

In the more general case when combination lines cannot be distinguished from fundamental lines by inspection, the same type of analysis based on the fit of spectral frequencies could be carried straight through for all 28 cases.† This would however clearly be a procedure that is laborious and wasteful of computer time, and it becomes important to use intensity as well as frequency data in order to reduce the number of plausible alternative assignments. At this point we became aware of the intensity sum rule mentioned earlier and, like Fessenden

† Castellano and Waugh (personal communication) have recently proved that in the general case there are in fact 40 (and not 28) possible trial assignments.

X atom	Compound	Chemical shifts				Coupling constants [§]		
		$\delta_A \dagger$	δ_B	δ_C	Δ_1	Δ_2	J_{AB}^{cis}	$J_{AC}^{trans} \parallel$
F	Vinyl fluoride	-0.84	+1.30	+0.96	+1.13	-1.96	+4.7	12.8
	Vinyl methyl ether	-1.10	+1.43	+1.29	+1.36	-2.46	+6.8	14.4
	Divinyl ether	-1.06	+1.12	+0.81	+0.96	-2.02	+6.4	14.0
O	Vinyl chloride	-0.97	-0.11	-0.19	-0.15	-0.82	+7.2	14.9
	Vinyl bromide	-1.16	-0.70	-0.55	-0.63	-0.53	+7.1	15.0
	Vinyl benzene	-1.36	+0.12	-0.38	-0.13	-1.22	+10.9	17.5
Cl	Vinyl cyanide	-0.20	-0.72	-0.58	-0.65	+0.45	+11.8	+1.1
	Butene-1 \ddagger	—	—	—	—	-0.71	+10.4	18.0
	3,3-dimethylbutene-1†	—	—	—	—	-0.76	+10.8	+1.0
Br	3-methylbutene-1	-0.34	+0.56	+0.48	+0.52	-0.86	+10.4	+1.9
								+1.4
								+1.6

Notes: \dagger In p.p.m. relative to the resonance of ethylene as 0.00 which has the value of -3.9 with respect to cyclohexane (τ value 4.67); errors ± 0.05 p.p.m.

§ In cycles per second; errors ± 0.2 c/s.

$|J_{AC}^{trans}|$ is arbitrarily taken as positive; the other signs quoted for the same molecule are determined relative to this.

† Alexander [8]. No standard was quoted in this paper for the chemical shifts.

Table 3. Chemical shifts and couplings constants derived from analysis of the spectra of vinyl compounds

and Waugh [3], have found that its application often reduces the number of assignments by a factor of two or more. Even in the simpler cases where only four alternative sign combinations of coupling constants have to be considered, the sum rule will usually eliminate two of these by inspection even when apparent intensities are correct to only 10 or 15 per cent.

4. EXPERIMENTAL AND RESULTS

The nuclear-magnetic-resonance spectra of the vinyl compounds were obtained using a Varian V-4300B spectrometer operating at 40 Mc/s. The sample tubes were of 5 mm outside diameter and were spun in the magnetic field. The

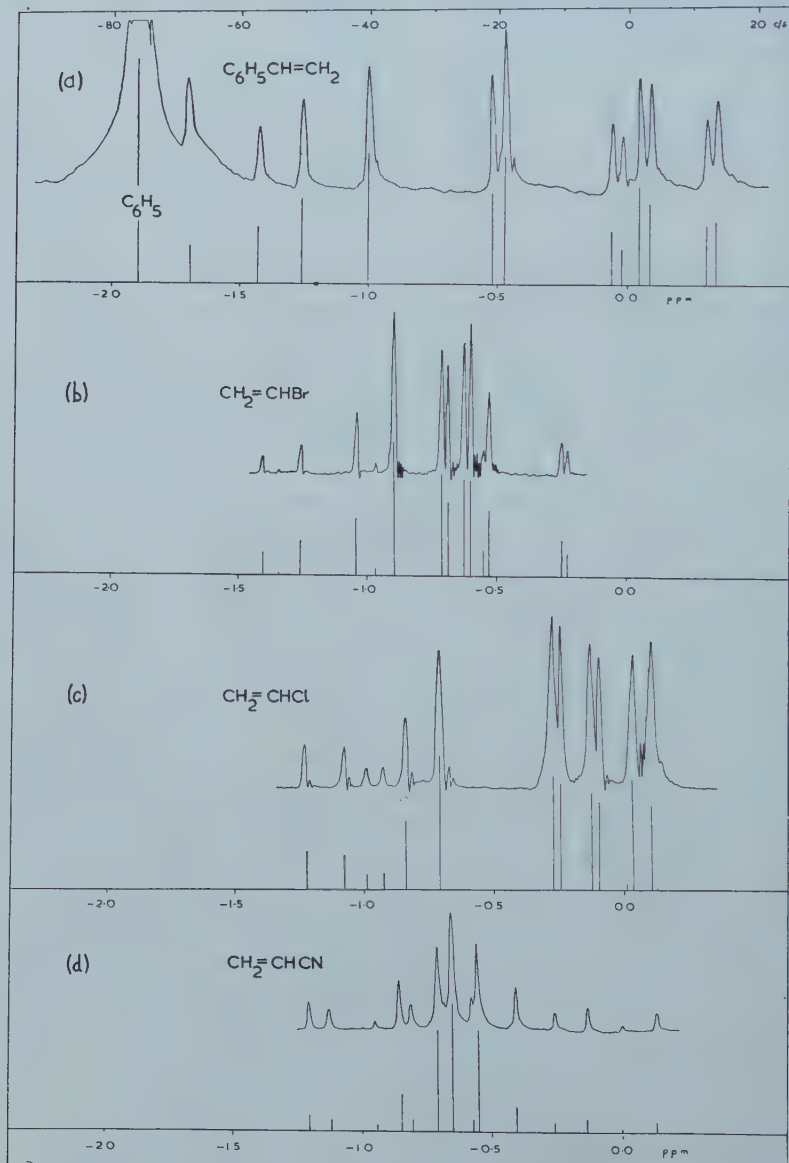


Figure 6. Observed and calculated spectra of the vinyl compounds studied at 40 Mc/s.
(a)-(d) are plotted on a uniform chemical shift scale.

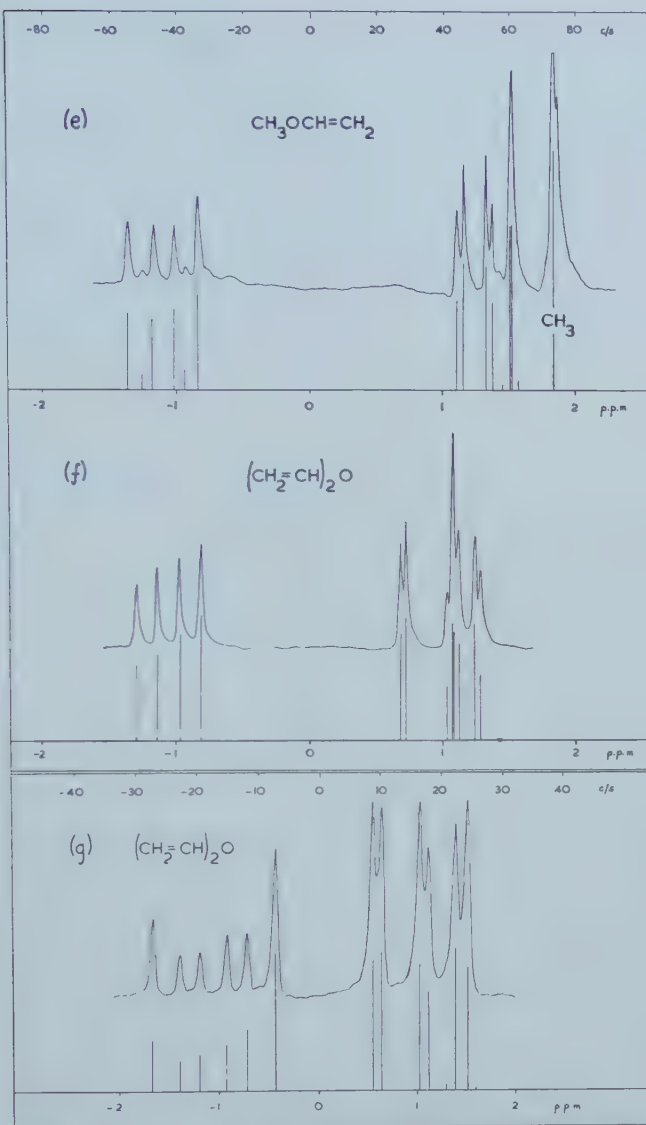


Figure 6 (continued). Observed and calculated spectra of the vinyl compounds studied. (e) and (f) are at 40 Mc/s plotted on a uniform chemical shift scale. (g) shows the agreement for divinyl ether at 16.2 Mc/s. 0.0 corresponds to the chemical shift of ethylene for all spectra, which has the value of -3.9 with respect to cyclohexane.

spectra were obtained in 10 per cent molar concentration in carbon tetrachloride and the line positions were measured relative to the resonance of 4 per cent cyclohexane added as an internal standard. Frequency measurements were made by the sideband technique of Arnold and Packard [6] using a Muirhead-Wigan Decade Oscillator Model D-695-A. It was found that the 40 Mc/s spectra of vinyl fluoride and of divinyl ether were insensitive to changes in the relative signs of coupling constants. These two compounds were further studied at 16.2 Mc/s, therefore, in order to establish the relative signs unambiguously.

Vinyl fluoride was analysed as an example of ABCX theory; full details of the analysis will be published later.

The results obtained from the analyses of the vinyl spectra are collected in table 3. The agreement between the observed and calculated spectra is illustrated in figure 6. These results show agreement to better than 0.5 c/s with those for vinyl bromide previously reported by Gutowsky *et al.* [4], and for styrene by Shimuzu *et al.* [2] and Fessenden and Waugh [3]. In the case of vinyl fluoride the 16.2 Mc/s results showed that the sign of J_{BC} is opposite to that assumed by Gutowsky *et al.* [4]. Also our analysis of the spectrum of vinyl chloride leads to a definite choice of -1.4 c/s for J_{BC} and not the alternative value of 0.1 c/s as favoured by these authors.

5. DISCUSSION OF RESULTS

5.1. The assignment of resonances to individual hydrogen atoms

The specific assignment of the chemical shifts or shielding parameters of the three resonances to the hydrogen atoms A, B, and C as they were labelled earlier does not follow from the analyses of the individual spectra. However an examination of the appropriate columns in table 3 shows that, whereas the first column of chemical shifts varies little in magnitude (except for the isolated case of vinyl cyanide) in the second and third columns considerable and roughly parallel changes occur in the chemical shifts. The latter observation in particular points strongly to the conclusion that the resonances listed in these two columns are those of the B and C hydrogen atoms of the terminal $C=CH_2$ group as their chemical shifts would be expected to change in unison. The A resonances are hence those listed in the first column.

The assignments of the last two columns to the individual B and C hydrogens is best made from the relative magnitudes of the coupling constants. It has been shown previously by Cohen *et al.* [7] that the inter-hydrogen coupling constant for *trans*-dichloroethylene (12.2 c/s) is considerably greater than the corresponding constant for *cis*-dichloroethylene (5.0 c/s). These two values are close to, though somewhat less than, the mean values (14.9 and 7.3 c/s) of the data recorded in the second and first columns of the coupling constant section of table 3; the assignment of these two columns respectively to J_{AC}^{trans} and J_{AB}^{cis} is therefore a convincing one. The rest of the assignments given in Table 3 follow from those already made. Our present choice of the relative magnitudes of the J_{AC}^{trans} , J_{AB}^{cis} , and J_{BC}^{gem} coupling constants agrees with that of Shimuzu *et al.* [2], Fessenden and Waugh [3] and Gutowsky *et al.* [4].

5.2. The relative magnitudes of the coupling constants

As a result of the above assignments we see from the last three columns of table 3 that experimentally J_{AC}^{trans} (12 to 18 c/s) > J_{AB}^{cis} (4 to 12 c/s) >> J_{BC}^{gem} (-3.5 to +2 c/s). It is of interest to compare the first two values with those recently calculated by Karplus [9] by quantum-mechanical methods. His value of J_{AC}^{trans} (11 c/s) and J_{AB}^{cis} (6 c/s) give a ratio of 1.9 which is in excellent agreement with 2.0, the ratio of the mean values recorded for the corresponding experimental data. However, the majority of the individual values recorded in table 3 lie about 50 per cent above the theoretical values, as do the corresponding results for substituted ethanes [10].

The coupling constants to be expected between the geminal protons of the CH_2 group have also been the subject of detailed theoretical calculations by Karplus and Anderson [11] for methane and, more recently, by Gutowsky *et al.* [4] for other than tetrahedral CH_2 angles. It appears that theoretically J_{gem} is very sensitive to changes in the CH_2 angle; it is calculated that as the CH_2 angle opens out the net coupling constant drops rapidly from a value of $\sim +12.5$ c/s for methane, to zero for an angle of 125° , and to negative values for angles wider than 125° .

For the vinyl compounds studied here the CH_2 angle would be expected to lie within a few degrees of the ideal value of 120° for sp^2 hybridization. For ethylene itself the most recent experimental determinations [12, 13] give the

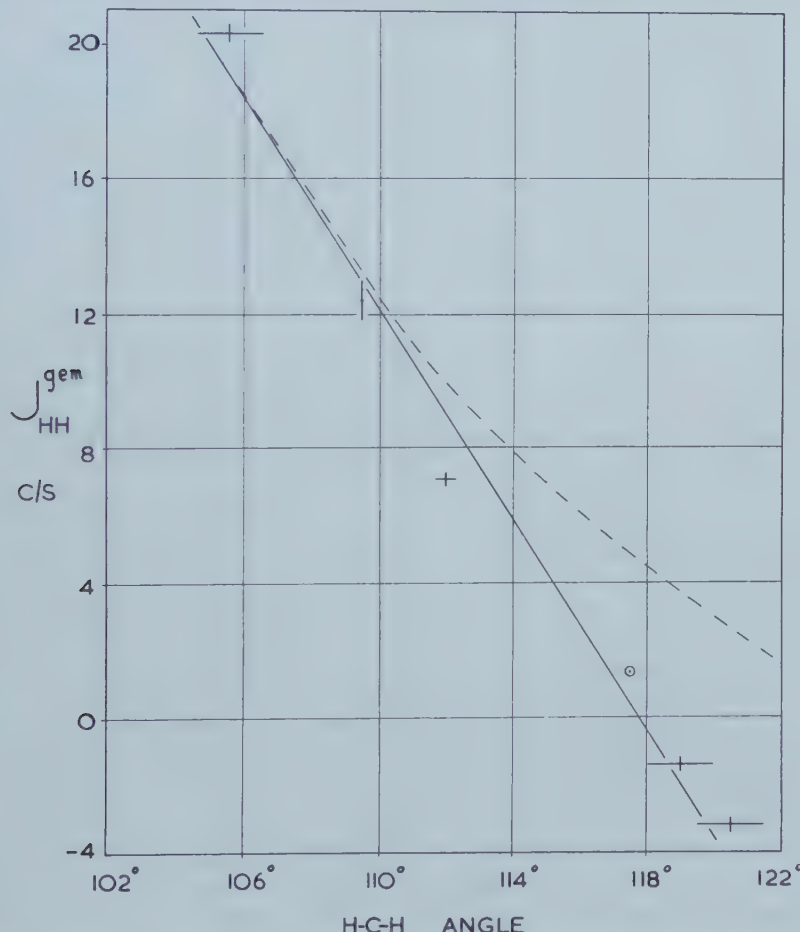


Figure 7. $J_{\text{EC}}^{\text{gem}}$ v. HCH angle. Experimental errors are indicated except that, where no error is quoted in the original paper, the error in angle is assumed to be $\pm 1^\circ$. \odot corresponds to the coupling constant assumed for ethylene. The other compounds shown, in order of decreasing coupling constant, are: Malononitrile, methane, methylene chloride, vinyl chloride, vinyl fluoride.

A recent microwave spectroscopic study (E. Hirota and Y. Morino, 1960, *Bull. Chem. Soc. Japan*, **33**, 158 and 705) has given the revised value of $108^\circ 42' \pm 1^\circ 22'$ for the HCH angle in malononitrile. The J_{gem} coupling constant for ethylene has also been measured directly as $+2.5$ c/s. (Sheppard and Truscott, unpublished work).

value of 117.5° . For vinyl fluoride an approximate value of 120.5° for the angle has been derived from a microwave determination [14] and for vinyl chloride the analogous value is reported to be 119° (see reference [4], footnote p. 1281). For none of the other vinyl derivatives do good experimental data appear to be available. Whatever are the precise values of the CH_2 angle in these vinyl derivatives, it is clear that there is good general agreement with the theoretical prediction in that the mean value of -1.4 c/s obtained experimentally for J_{gem} is much smaller than the presumably positive value of 12.4 c/s obtained for methane. In figure 7 we have replotted figure 10 of the paper by Gutowsky *et al.* [4] except that (i) with the exception of ethylene (see later) only those points have been retained in which both coupling constants and CH_2 angles have been measured experimentally for the same molecule, (ii) a point for vinyl chloride has been added and (iii) the point for vinyl fluoride has been moved to correspond to $J_{\text{gem}} = -3.2$ rather than $+3.2$ c/s as assumed previously. It is seen that there is now a smooth correlation between the two sets of experimental data and that the point for methylene chloride is no longer so abnormal. The deviation between the experimental and theoretical curves becomes more pronounced for CH_2 angles greater than 115° , but it is in this range of angles that the theoretical calculations are said to be less accurate [4]. Part of this deviation may be caused by the fact that most of the molecules studied experimentally have electronegative substituents whereas the calculations were carried out for a lone CH_2 group. On the other hand if the coupling constant for ethylene is assumed to be $\sim +1.4$, i.e. essentially the same as for the three alkyl substituted ethylenes listed in table 3, then this point also fits closely on the curve obtained from the other experimental data. In any case it is clear that, as suggested by Gutowsky *et al.* [4], there is a potentially very useful correlation between the J_{gem} coupling constant and the CH_2 angle.

It is also of interest to consider the trends in the values of the three coupling constants with the different atoms, X, attached to the vinyl group. For all three coupling constants the order of values is $\text{F} < \text{O} < \text{Br} < \text{Cl} < \text{C}$. Not only is this sequence qualitatively obeyed but the changes in coupling constants from one element to the next occur quantitatively in proportion as is shown by figure 8 where J_{cis} and J_{gem} are plotted against J_{trans} . It is seen that two satisfactorily straight lines are obtained. Thus the trends in value of the three coupling constants are closely correlated and probably depend on the same factor.

It seems probable that an operative factor is some electron-withdrawing or donating property of the atom (or group) X such as might be expressed in terms of the electronegativity† (E) or the Hammett-type σ constants as separated by Taft [17] into inductive (σ_I) and resonance (σ_R) contributions [18]. The lists of these parameters needed for the present purpose and for the subsequent discussion of the shielding constants are as follows:

$$(E) \quad \begin{array}{ccccc} \text{F} & > & \text{O} & > & \text{Cl} & > & \text{Br} & > & \text{C} \\ 3.9 & & 3.5 & & 3.15 & & 2.95 & & 2.6 \end{array}$$

$$(\sigma_I) \quad \begin{array}{ccccccccc} \text{CN} & > & \text{F} & > & \text{Cl} & > & \text{Br} & > & \text{OCH}_3 & > \text{Phenyl} & > \text{H} & > t\text{-butyl} \\ 0.59 & & 0.5 & & 0.47 & & 0.45 & & 0.23 & & 0.10 & & 0.0 & & -0.17 \end{array}$$

$$(\sigma_R) \quad \begin{array}{ccccccccc} \text{CN} & > & \text{H} & > & \text{Phenyl} & > & t\text{-butyl} & > & \text{Br} & > & \text{Cl} & > & \text{F} & > & \text{OCH}_3 \\ 0.07 & & 0.0 & & -0.09 & & -0.12 & & -0.22 & & -0.24 & & -0.44 & & -0.50 \end{array}$$

† The electronegativities we use are those given by Huggins [15], which differ slightly from the original values given by Pauling [16].

Comparison of these sequences with the observed order of coupling constants shows that the best correlation is with electronegativity, and that decreasing coupling constants go with increasing electronegativity. This is qualitatively as expected because a substituent atom with high electronegativity is expected to reduce electron densities around the various hydrogen atoms of the vinyl group; this in turn should lead to less interaction between nuclear and electron spins and therefore to lower coupling constants.

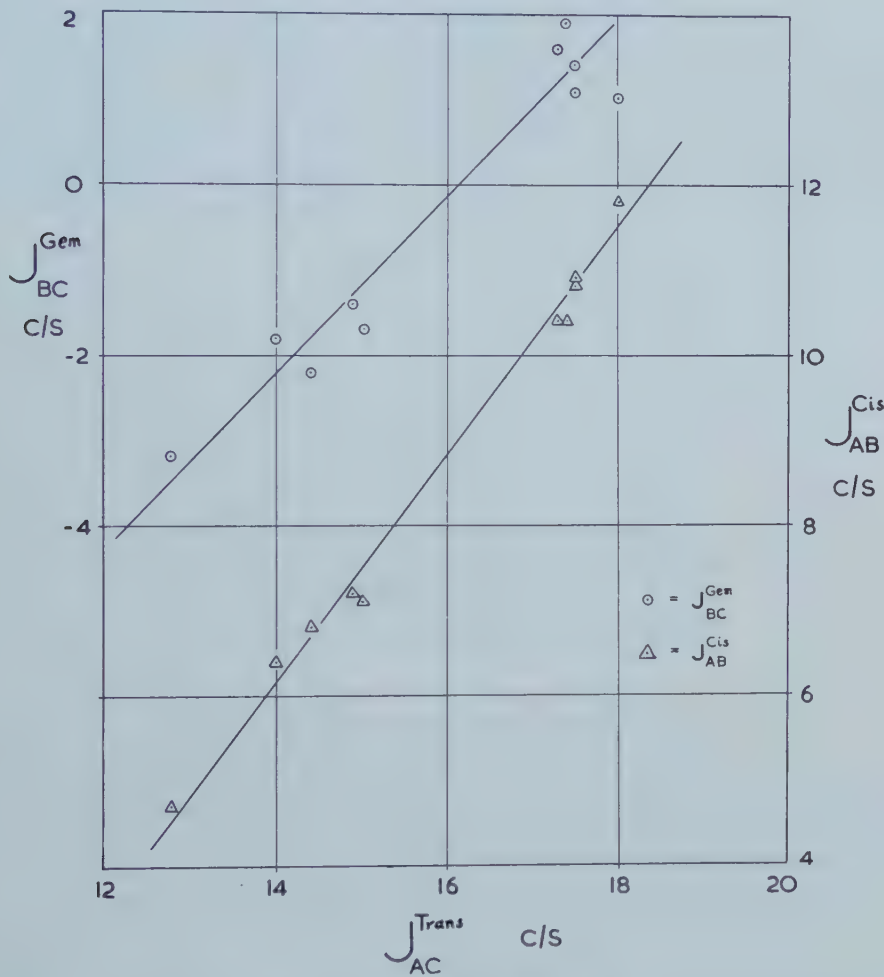


Figure 8. J_{AC}^{Trans} v. J_{AB}^{Cis} and J_{BC}^{Gem} .

Figure 9 shows quantitatively the variation of J_{trans} with electronegativity. For the other coupling constants the behaviour is very similar; in all cases the points for Cl and Br lie sufficiently far from the good straight lines that can be drawn through the points representing the elements of the first short period, to show that factors other than electronegativity affect the coupling constant to some degree.

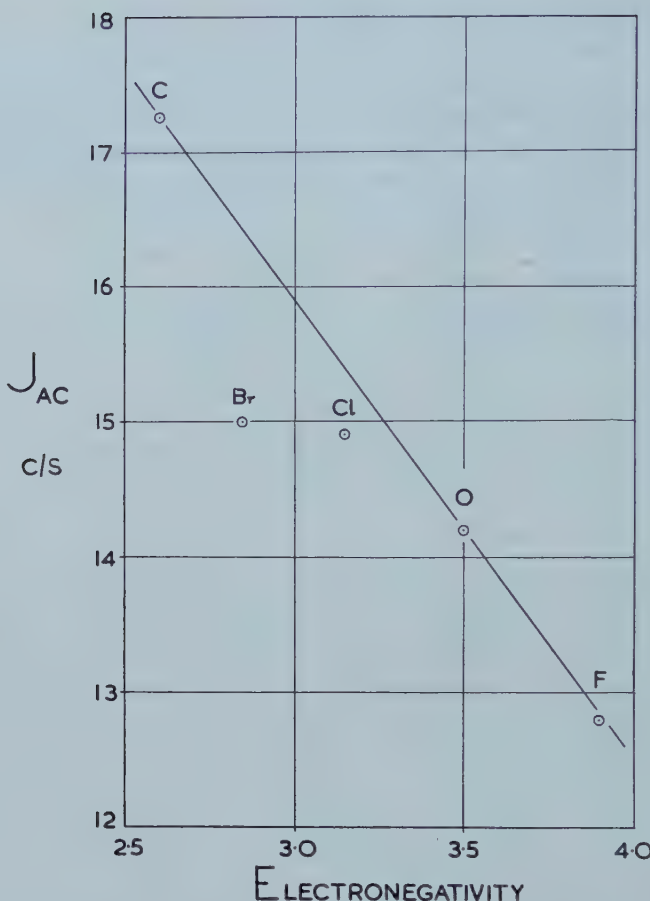


Figure 9. J_{AC}^{trans} v. Huggins' electronegativities [15].

5.3. The chemical shifts of the vinyl compounds

In this section we shall consider the changes that occur in the chemical shift parameters δ_A , $\frac{1}{2}(\delta_B + \delta_C) \dagger = \Delta_1$, and $\delta_A - \frac{1}{2}(\delta_B + \delta_C) = \Delta_2$ as the substituent X is changed. The appropriate values as well as the individual ones for δ_B and δ_C are listed in table 3 relative to the chemical shift of ethylene itself taken as zero.

It has been pointed out by Dailey and Shoolery [19] that for the ethyl derivatives $XCH_2 \cdot CH_3$ there is a general correlation between $\delta_{CH_2} - \delta_{CH_3}$ and the electronegativity of X. More recent data by Bothner-By and Naar-Colin [20] confirm this conclusion although the slope of the line connecting chemical shift with electronegativity seems to be somewhat different for the halogens ($X = F, Cl, Br, I$) and for the elements of the first short period (F, O, N). The latter difference is more pronounced for the isopropyl derivatives, $XCH(CH_3)_2$, and here $\delta_{CH_3} - \delta_{CH_2}$ is much less sensitive to the electronegativity of the halogen atom. Similar correlations hold for the chemical shifts of the individual CH_2 and CH groups that are adjacent to X atoms.

† The mean value of δ_B and δ_C is taken, as the chemical shifts of these two atoms vary closely in unison.

The order of the vinyl chemical shift parameters are:

$$\begin{aligned}\delta_A & \text{ CN} > \text{iso-Pr.} > \text{F} > \text{Cl} > \text{O(CH=CH}_2\text{)} \simeq \text{OCH}_3 > \text{Br} > \text{C}_6\text{H}_5 \\ \Delta_1 & \text{ OCH}_3 > \text{F} > \text{O(CH=CH}_2\text{)} > \text{iso-Pr.} > \text{C}_6\text{H}_5 \simeq \text{Cl} > \text{Br} \simeq \text{CN} \\ \Delta_2 & \text{ OCH}_3 > \text{O(CH=CH}_2\text{)} \simeq \text{F} > \text{C}_6\text{H}_5 \simeq \text{iso-Pr.} \simeq \text{Cl} > \text{Br} > \text{CN}\end{aligned}$$

It is seen that none of these orders are as expected for a correlation with electronegativity (see previous section). For example, the carbon-containing groups isopropyl, CN and C₆H₅ are all expected to have rather similar electronegativities [19] whereas for δ_A these occur at opposite ends of the series, and in the other two series they occur on either side of the halogens Cl and Br. Graphical plots of these experimental parameters confirm that there is little or at the best very poor correlation with electronegativity. The fact that the carbon-containing groups mentioned above have very different effects on the chemical shifts suggests that resonance effects associated with double or triple bonds may be of importance, and this is reasonable in view of the presence of π electrons in the vinyl compounds. π -electron effects can more often be successfully correlated with the σ_I and σ_R

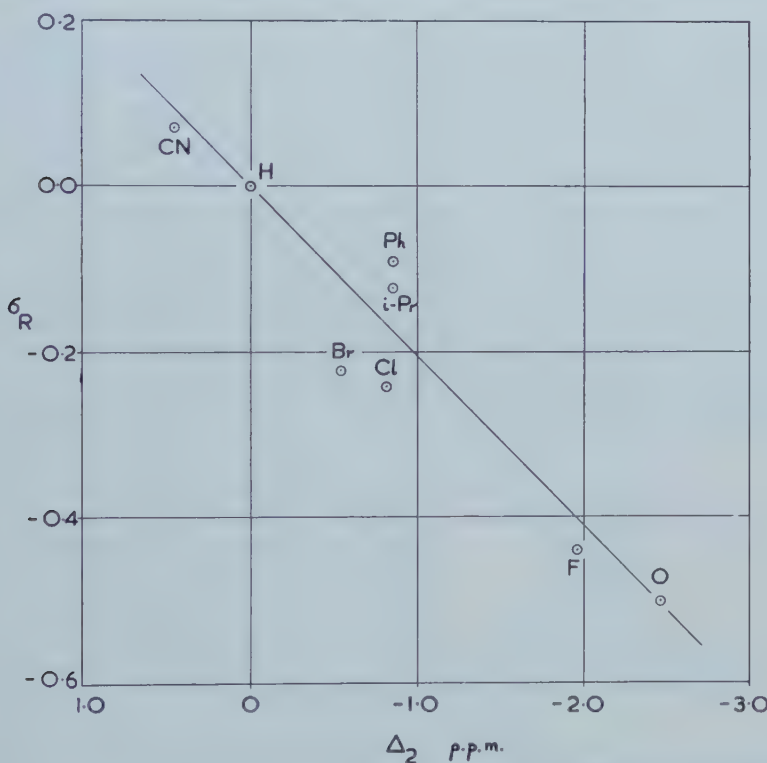
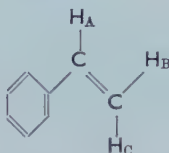


Figure 10. σ_R values [18] plotted against $\Delta_2 = \delta_A - \frac{1}{2}(\delta_B + \delta_C)$. The point for Ph = phenyl has been corrected for the diamagnetic anisotropy of the benzene ring (see text).

parameters listed in the previous section. In fact there is an approximate correlation of the sequence of σ_R values with both Δ_1 and Δ_2 if low σ_R values are assumed to go with high chemical shifts. Graphical exploration of such relationships revealed, as shown in figure 10, that the most successful correlation is between Δ_2 and σ_R . For Δ_1 the points for Cl and Br deviate considerably from an approximate straight-line relationship for the others. No reasonable correlation could

be found between δ_A and any of the above parameters. However the values of δ_A cover a surprisingly small range considering that this is the hydrogen nucleus nearest to X. Excluding CN, the range is only 20 c/s and including CN it is 45 c/s, whereas Δ_1 , for the more distant hydrogens, covers a range of about 90 c/s. It is possible that the experimentally observed values of δ_A are partially dependent on the cancellation of factors of opposite sign.

In figure 10 the value of Δ_2 for styrene is shown as -0.87 instead of -1.22 p.p.m. as given in table 3. The correction of +0.35 p.p.m. is applied to take account of the effect of diamagnetic circulation of the electrons in the benzene ring. Calculation shows that the A, B and C hydrogen nuclei in styrene are at distances from the centre of the ring of



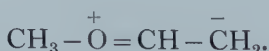
3.5, 4.9 and 3.8 Å, respectively and, assuming that conjugation retains the molecule in a planar configuration, the corrections to be applied to the observed chemical shifts of hydrogen nuclei at these distances are approximately [21] $\delta_A' = +0.7$, $\delta_B' = +0.2$, $\delta_C' = +0.5$ p.p.m. The correction to be applied to Δ_2 for styrene is, therefore $\Delta_2' = \delta_A' - \frac{1}{2}(\delta_B' + \delta_C') \sim +0.35$.

Another consequence of these correction terms is that the C resonance is expected to be at a considerably lower field than that of B, i.e. there should be an unusually large value of $\delta_B - \delta_C$ for styrene. Examination of the data of table 3 shows that the average value of $\delta_B - \delta_C$, excluding styrene, is less than +0.10 p.p.m.; for styrene the value is +0.50 p.p.m.

The σ_R parameters are derived from studies of substituted benzene rings where they are a measure of electron density. For an OCH_3 group attached to a benzene ring, the additional resonance structures are

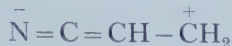


and for vinyl methyl ether the analogous structure is



It is seen that this leads primarily to an increase in electron density at the carbon atom of the terminal methylene group (and also presumably at the hydrogen nuclei) so that it approximates more to a saturated carbon atom. In addition the magnetically anisotropic π electrons of the $\text{C}=\text{C}$ group, which must be largely responsible for the low chemical shifts of olefinic hydrogen atoms, are now spread over two bonds. These two factors should both have the effect, as observed, of increasing the effective shielding and chemical shift of the methylene

hydrogens. The lowest value of Δ_1 and Δ_2 is given by the CN substituent for which σ_R is of the opposite sign and the resonance structure



is of a type which places a positive charge on the carbon atom of the terminal methylene group†.

A final general point is that whereas the values of coupling constants in these unsaturated molecules are, as expected, primarily dependent upon electron withdrawal within the sigma-electron framework, the chemical shifts are more intimately connected with the electron distribution in the pi-electron system.

One of us (C. N. B.) is grateful to the Department of Scientific and Industrial Research for a Research Studentship, and to Magdalene College, Cambridge for a Bye-Fellowship.

The spectrometer used was bought with a grant from the Wellcome Foundation, and thanks are due to the Hydrocarbon Research Group of the Institute of Petroleum for financial assistance.

We are grateful to Dr. M. V. Wilkes, F.R.S. of the University Mathematical Laboratory for enabling us to carry out calculations on the EDSAC 2 digital computer. We would like to acknowledge a very helpful discussion with Prof. J. S. Waugh and Dr. S. Castellano, and we are grateful to Dr. R. E. Richards, F.R.S. for communicating to us some of his results prior to publication.

Professor R. N. Haszeldine very kindly supplied the sample of vinyl fluoride.

REFERENCES

- [1] BERNSTEIN, H. J., POPLE, J. A., and SCHNEIDER, W. G., 1957, *Canad. J. Chem.*, **35**, 65.
- [2] SHIMUZU, T., MATSUOKA, S., HATTORI, S., and SENDA, K., 1959, *J. phys. Soc. Japan*, **14**, 683.
- [3] FESSENDEN, R. W., and WAUGH, J. S., 1959, *J. chem. Phys.*, **31**, 996.
- [4] GUTOWSKY, H. S., KARPLUS, M., and GRANT, D. M., 1959, *J. chem. Phys.*, **31**, 1278.
- [5] GUTOWSKY, H. S., HOLM, C. H., SAIKA, A., and WILLIAMS, G. A., 1957, *J. Amer. chem. Soc.*, **79**, 4596.
- [6] ARNOLD, J. T., and PACKARD, M. E., 1951, *J. chem. Phys.*, **19**, 1608.
- [7] COHEN, A. D., SHEPPARD, N., and TURNER, J. J., 1958, *Proc. chem. Soc.*, p. 118.
- [8] ALEXANDER, S., 1958, *J. chem. Phys.*, **28**, 358.
- [9] KARPLUS, M., 1959, *J. chem. Phys.*, **30**, 11.
- [10] SHEPPARD, N., and TURNER, J. J., 1959, *Proc. roy. Soc., A* **252**, 506.
- [11] KARPLUS, M., and ANDERSON, D. H., 1958, *J. chem. Phys.*, **30**, 6.
- [12] ALLEN, H. C., JNR., and PLYLER, E. K., 1958, *J. Amer. chem. Soc.*, **80**, 2673.
- [13] DOWLING, J. M., and STOICHEFF, B. P., 1959, *Canad. J. Phys.*, **37**, 703.
- [14] BAK, B., CHRISTENSEN, D., HANSEN-NYGAARD, L., and ROSTRUP-ANDERSON, J., 1958, *Spectrochim. Acta*, **13**, 120.
- [15] HUGGINS, M. L., 1953, *J. Amer. chem. Soc.*, **75**, 4123.
- [16] PAULING, L., 1948, *The Nature of the Chemical Bond* (Cornell University Press).
- [17] TAFT, R. W., JNR., 1956, *Steric Effects in Organic Chemistry*, Chap. XIII, Ed. Newman (New York: John Wiley & Sons, Inc.).
- [18] TAFT, R. W., JNR., 1957, *J. Amer. chem. Soc.*, **79**, 1045.
- [19] DAILEY, B. P., and SHOOLERY, J. N., 1955, *J. Amer. chem. Soc.*, **77**, 3977.
- [20] BOTHNER-BY, A. A., and NAAR-COLIN, C., 1958, *Ann. N.Y. Acad. Sci.*, **70**, 833.
- [21] JOHNSON, C. E., JNR., and BOVEY, F. A., 1958, *J. chem. Phys.*, **29**, 1012.

† Analogous qualitative conclusions concerning the relevance of these resonance structures to the chemical shifts of vinyl compounds have been reached by W. Brügel (paper presented at the Bologna meeting of the European Molecular Spectroscopy Group, September 1959).

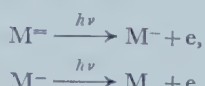
Polarization of electronic transitions in aromatic hydrocarbon molecules and their mono- and di-valent ions†

by G. J. HOIJTINK and P. J. ZANDSTRA

Chemical Laboratory of the Free University, Amsterdam

(Received 3 December 1959)

On irradiation of glassy solutions of aromatic hydrocarbon mono- and di-negative ions with ultra-violet light photo electron ejection occurs according to the reactions:



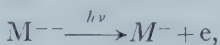
When one uses plane polarized light of a wavelength corresponding to an absorption band of the ion originally present, the solutions become permanently dichroitic. The differences in extinction of these dichroitic solutions for plane polarized light with its electric vector perpendicular and parallel to that of the primary light were plotted against the wave number of the absorbed light. From these diagrams the relative directions of polarization of the electronic transitions of some alternant aromatic hydrocarbon molecules and negative ions were determined. The absolute directions could be found by comparing the results obtained for the molecules with those of polarization measurements on the crystalline hydrocarbons reported in the literature.

1. INTRODUCTION

During the last few years the electronic absorption spectra of the mono- and di-valent negative [1, 2, 3, 4, 5] and positive ions [4, 5, 6] of various alternant aromatic hydrocarbons and 1, *n*-diphenylpolyenes have been investigated. The experiments provided information about the energies and dipole strengths of the electronic transitions. The purpose of the present investigation is to measure the directions of polarization of these electronic transitions. Since the positive and negative ions of alternant hydrocarbons have practically equal absorption spectra [4, 5, 6] we have restricted ourselves to a study of some alternant hydrocarbon negative ions.

2. DETERMINATION OF POLARIZATIONS OF ELECTRONIC TRANSITIONS

On irradiation with ultra-violet light of rigid solutions of aromatic hydrocarbon di-negative ions in 2-methyltetrahydrofuran electron ejection takes place according to the reaction:



the electrons being trapped in all probability by the alkali ions. In the same way irradiation of a rigid solution of the mono-negative ions leads to the formation of the corresponding molecules,



† Part of thesis by P. J. Zandstra, Free University, Amsterdam, 1959.

These investigations have been carried out under the auspices of the Netherlands Foundation for Chemical Research (S.O.N.) with financial aid from the Netherlands Organization for the Advancement of Pure Research (Z.W.O.).

Following Lewis *et al.* [7] this phenomenon was used in order to determine the directions of polarization of the electronic transitions in the molecule M and its mono- and di-negative ions, M^- and M^{--} . For that purpose the rigid solutions of the M^{--} ions were irradiated with plane polarized light of a wavelength corresponding to one of the ultra-violet absorption bands of M^{--} , which leads to dichroism of these solutions. Similarly, for the irradiation of the rigid solutions of the M^- ions plane polarized light of a wavelength of one of the ultra-violet absorption bands of M^- was used.

The irradiated solutions remain unchanged as long as the temperature is kept low enough—liquid air temperature—to prevent regeneration of the original substances.

Throughout these investigations we have confined ourselves to aromatic hydrocarbons with symmetry D_{2h} . Accordingly the allowed electronic transitions will be polarized along the mutually perpendicular symmetry axes x and y in the plane of the molecule or ion.

Let us now consider the case that the glassy solution is irradiated by plane polarized light of a wave length corresponding to an x -polarized transition of the original substance.

When about 50 per cent of the original substance is converted into the product substance, the extinctions are measured for light polarized parallel (E_{\parallel}) and perpendicular (E_{\perp}) to the electric vector of the primary exciting light and with the same direction of propagation. Then, since the x -axes of the product molecules or ions will be concentrated along a direction parallel to the electric vector of the primary exciting light and the remaining ions will have their y -axes concentrated along that direction, the following conditions hold:

Irradiation at an x -polarized transition of the original ion	Extinction difference $\Delta E = E_{\perp} - E_{\parallel}$	
	x -transition†	y -transition
Original substance	> 0	< 0
Product substance	< 0	> 0

† A quantitative treatment shows that for irradiation at an x -polarized transition of the original substance the effect on ΔE is twice as strong for x - as for y -polarized bands.

Measurements of the extinction differences thus provide information about the relative directions of polarization of the electronic transitions in the original and product substances. Since in view of the reaction $M^- \xrightarrow{h\nu} M + e$ rigid solutions of oriented molecules are obtainable, the correlations between the polarizations of the electronic transitions in molecules and ions can be studied. Absolute assignments are then possible by comparing the results with those obtained from measurements on molecular single or mixed crystals [8 to 13].

3. EXPERIMENTAL

3.1. Preparation of solutions of negative ions [2]

Since negative ions of unsaturated hydrocarbons are reactive to oxygen and moisture, their solutions must be prepared in vacuum. Our apparatus has been sketched in figure 1. When the cell has been carefully cleaned, evacuated, flamed out and filled with pure nitrogen, some milligrams of the hydrocarbons

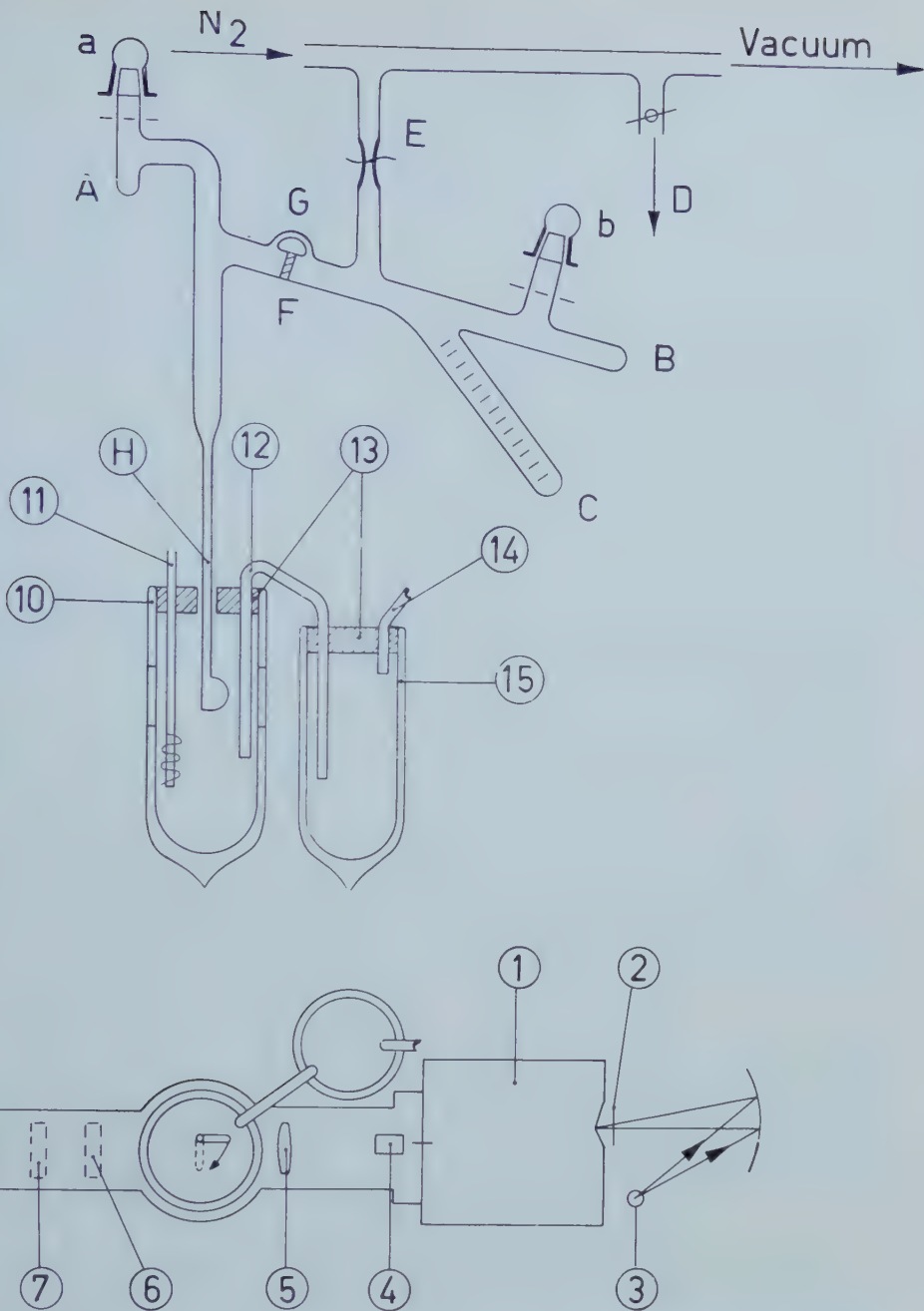


Figure 1. Apparatus for the preparation of the solutions of the hydrocarbon negative ions (upper diagram) and for the measurement of absorption and dichroism (lower diagram).

1 = monochromator with ultrasil prism (5–45 kK; Kipp L 27); 2 = chopper (127 Hz); 3 = light sources: tungsten bulb (5–25 kK), hydrogen discharge tube (25–40 kK); 4 = Glan-Thompson prism with ultra-violet lute, (aperture 17°; Halle); 5 = ultrasil lens ($f=50$ mm; $\phi=30$ mm; Halle); 6 = polarization foil (15–32 kK; Käsemann); 7 = glass-filters (Schott colour-filters and Zeiss mono-chromat-filters); 8 = ultrasil lens ($F=50$ mm; $\phi=20$ mm; Halle); 9 = detectors for absorption measurements: lead sulphide cell (5–13 kK; 61 SV; Philips), photo-multiplier (13–40 kK; VPUV 690 I; Maurer) or light source for irradiation: water-cooled high-pressure mercury arc (SP 500 Watt; Philips); 10 = ultrasil Dewar-vessel with unsilvered zone; 11 = heating element of 1 w; 12 = silvered siphon; 13 = cork stoppers; 14 = glass tube for pressure control. 15 = bulk Dewar vessel for liquid air.

and a piece of clean alkali metal are put into A and B, respectively. Tubes *a* and *b* are sealed off and the alkali metal is sublimed in vacuum onto the walls of B. After cooling the calibrated tube C with liquid air, about 10 ml of solvent are distilled from the storage bulb D into C. The cell is then sealed off at the capillary E.

The compound is dissolved in A and the solution obtained is poured into B, where the hydrocarbon, M, is reduced by the alkali metal, X, according to the reactions:



Of those hydrocarbons which have a relatively low reduction potential, only the mono-negative ions can be obtained. In case the reaction leads to the formation of the di-negative ion, the mono-negative ion may be prepared in the following way:

Half of the original solution is quantitatively reduced in B and subsequently combined with the remaining solution of hydrocarbon in A, so that the following reaction takes place:



This reaction proceeds quantitatively for all hydrocarbons investigated, except terphenyl. In the latter case the potentials for the addition of the first and second electron differ by only about 0.1 v, so that an excess of hydrocarbon molecules must be added.

To reduce decomposition of the very unstable ions of naphthalene, anthracene and pyrene, the reduction of these hydrocarbons was carried out at -80°C and the absorption measurements were performed directly after the preparation of the ions.

In all cases sodium was used as a reducing agent, except for the pyrene di-negative ions. The latter could be obtained to a measurable extent using potassium instead of sodium.

The glass filter F removes traces of metal and the connection G serves to equalize the pressure at both sides of the filter when the solution passes.

Dependent on the molecular extinctions the concentrations of the negative ions are varied between 10^{-3} and 10^{-5} moles-litre $^{-1}$. The ultrasil optical cell H has a thickness of 1 mm.

The hydrocarbon samples are from the same source as those used in previous investigations [2]. The solvent, 2-methyltetrahydrofuran (M.C.B.), which gives a rigid glass when cooled with liquid air, is purified by distillation from sodium in an atmosphere of nitrogen; then it is brought into the storage bulb D and stirred with sodium and anthracene in order to remove traces of oxygen.

3.2. Instruments and methods

The apparatus for the absorption measurements is drawn schematically in figure 1. The experiment was carried out with a single monochromator (1) with ultrasil prism, while a tungsten bulb and a hydrogen discharge tube served as light sources (3). A lead sulphide cell and a photomultiplier were used as detectors (9) in the spectral regions 5–13 kK and 13–40 kK, respectively. The light beam was chopped at 127 Hz (2) and the a.c. signal from the detector was amplified selectively and read from a milliammeter.

Ultrasil lenses (5 and 8), Dewar vessels (10) and absorption cells (H) and a Glan-Thompson polarizing prism with ultra-violet lute (4) enabled measurements from 5–40 kK.

3.2.1. Absorption spectra

Before starting the experiment the Dewar vessel (10) is filled with liquid air up to a level just below the optical path. The liquid air in (10) is kept boiling by a heating element of 1 w (11). The rising air cools the optical cell H sufficiently and prevents water vapour from condensing on the windows. At intervals the air in (10) is replenished by closing tube (14) so that the liquid air is siphoned over from the Dewar vessel (15) by its own vapour pressure. Transmittancies are measured with respect to the blank beam.

3.2.2. Dichroism

The detector is first replaced by a high-pressure mercury-arc and the glassy sample is now irradiated by the polarized light of one of the mercury lines. For that purpose suitable filters (7) and a polarization foil (6) are used. Since the polarization foil only polarizes between 15–32 kK, the mercury lines of higher energies cannot be employed for the irradiation. However, for the present purpose the 31·9 and 27·4 kK mercury lines are suitable except for the mono-negative ions of tetracene, which under this condition cannot be converted into the molecules.

For the mono- and di-negative ions the irradiation times, depending on the concentration and the hydrocarbons under investigation, varied between about 20 to 100, and 2 to 30 min, respectively. Upon longer irradiation of the rigid solutions of the di-negative ions, a fraction of the produced mono-negative ions might be converted into the molecules. For the irradiation times mentioned, however, this fraction is negligible.

When about half of the negative ions have been converted into the lower reduction stage, the filters and the polarization foil are removed and the mercury arc is replaced again by the detector. Thereupon the transmittances of the irradiated sample are measured at two positions of the polarizing prism (4), corresponding to a polarization perpendicular or parallel to that of the exciting mercury light. Both transmittances are measured at each setting of the prism of the monochromator.

3.3. Accuracy of the measurements

In the present type of single beam experiment the extinction is obtained from four readings. For extinction values between 0·2 and 1·5 the relative error is about 2 per cent in the spectral region 13–40 kK. In the 5–13 kK region, where a non-linear lead sulphide detector is used, it amounts to about 5 per cent. On the other hand the uncertainty in the concentration, due to irreproducible shrinkage of the solution upon cooling and to decomposition of the negative ions by traces of oxygen and moisture, suggests an absolute error in the molar extinctions of about 15 per cent.

For absorption bands of the product substance polarized parallel to the vector of the primary light the maximum value of the degree of polarization,

$$P = \frac{I_{\parallel} - I_{\perp}}{I_{\perp} + I_{\parallel}},$$

measured was 0·20–0·30 (theoretical value $\frac{1}{2}$) in all experiments.

The spectral band width was less than 0·1 kK in the whole spectral region investigated.

4. RESULTS

The experimental results are given in the figures 2-11. The molar extinctions are denoted by ϵ . In those cases where the concentrations are unknown the relative extinctions E have been used. As in the graphical representations of the absorption spectra ϵ/σ or E/σ are plotted against the wave number σ , the areas under the absorption bands are directly proportional to the dipole strengths.

The upper curves in the figures are the differential spectra in which $(E_{\perp} - E_{\parallel})/\sigma$ is plotted against σ . The relative directions of polarization of the electronic transitions in the original and product substances follow from the corresponding differences (table).

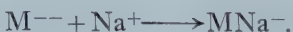
The absorption spectra of the ions in the 5-37 kK region have been measured in the rigid solutions at -180°C. The absorption spectra of the ions in the 37-42 kK region (25°C) and those of the molecules in the 5-42 kK region (-180°C) were taken from Weijland [4] and Clar [15], respectively.

5. DISCUSSION

Before entering into details about the polarizations of the transitions in the various hydrocarbons some accidental phenomena ought to receive attention first:

(a) In the absorption spectra of most negative ions absorption bands occur, which must be ascribed to decomposition of the original substances. These absorption bands resemble very closely those of the corresponding proton adducts MH^- , the spectra of which are investigated in this laboratory by Miss Velthorst [16]. In all probability the decomposition is due to the reaction of the negative ions with solvent molecules and possibly with traces of water.

(b) Even in the absence of decomposition products the solutions of the di-negative ions of anthracene on cooling display absorption bands which are very similar to those of the proton adducts MH^- . Contrary to the above-mentioned decomposition the absorption bands in this case disappear on heating. These bands are very likely due to a chemical association product formed according to the reaction:



On irradiation of the rigid solutions the absorption bands of the MNa^- ions remain unchanged.

5.1. Anthracene

From measurements on anthracene molecules in crystals [8, 9, 10, 11, 12] it is known that the first absorption band in the spectrum of the molecule is polarized along the shorter axis (y) and the second one along the longer axis (x). In relative sense this result is in agreement with Williams' work on the fluorescence polarization, who found that these two bands are polarized at right angles to each other [14].

From figure 2 it appears that the $\Delta E/\sigma$ values have the same sign for the y -polarized band of the molecule and the stronger bands at 14·0, 27·5 and 30·7 kK of the mono-negative ion. On the basis of the relations given in the table one may therefore conclude that these three bands are x -polarized. For the same reason the weaker absorption bands of the mono-negative ion at 10·9 and 25·2 kK must be y -polarized.

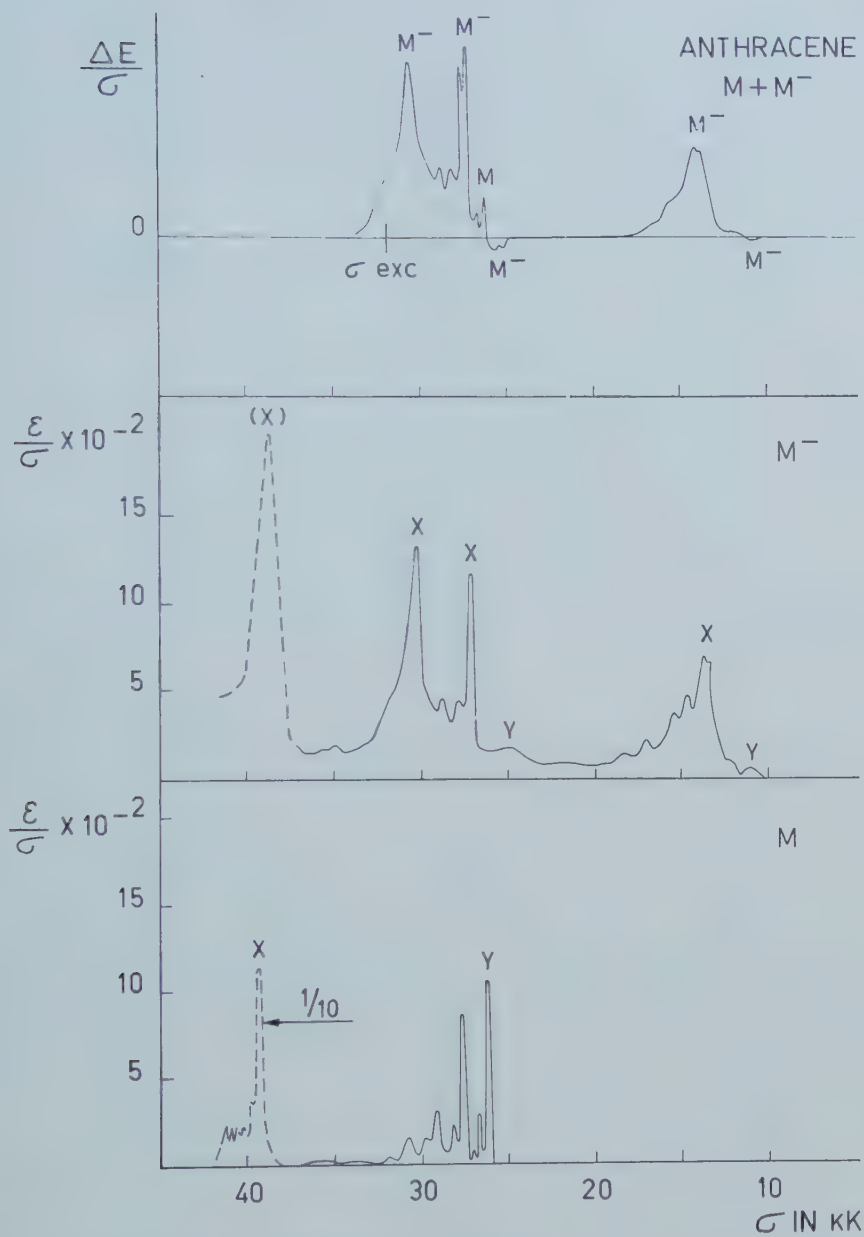


Figure 2. Differential and absorption spectra of anthracene molecules and mono-negative ions. In this and the following figures the directions of polarization are indicated at the heads of the absorption bands. The absorption spectra of the molecules were taken from Clar [15]. All spectra were measured at liquid air temperature, except the spectra of the ions above 37 kK. The latter, indicated by broken lines, were measured by Weijland [4] at 25°C. σ_{exc} = wave number of the mercury line (31.9 or 27.4 kK) used for photo-electron ejection.

In the 19-24 kK region no polarization is found. This indicates that the absorption observed in this region of the spectrum of the mono-negative ion must be due to some other species, probably the ion MH^- , which has a strong absorption in this region (16).

By analogy with the results obtained for the tetracene mono-negative ion the strong absorption band at 39 kK of the anthracene mono-negative ion lying beyond the limit of the present polarization measurements will in all probability be due to an x -polarized transition.

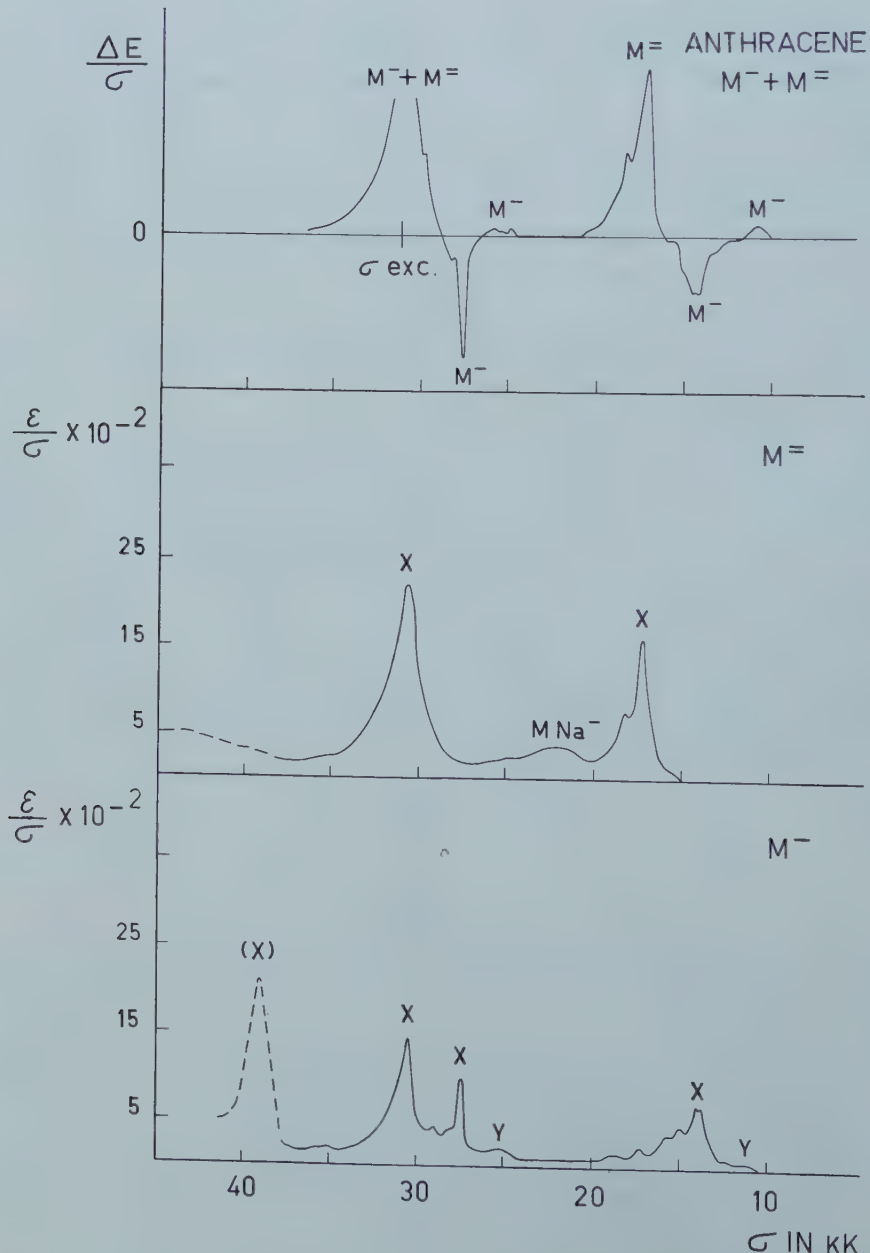


Figure 3. Differential and absorption spectra of anthracene mono- and di-negative ions (see text of figure 2).

Starting from the assignments given for the mono-negative ion the directions of polarization for the transitions in the di-negative ion can readily be derived from the differential spectrum shown in figure 3. Here the strong band at 17.1 kK of the di-negative ion has $\Delta E/\sigma$ values opposite to those of the σ -polarized bands at 27.5 kK of the mono-negative ion. Accordingly this band is also σ -polarized.

The $\Delta E/\sigma$ values at 31 kK, where absorption bands of both the mono- and di-negative ion are located, have the same sign as those of the first absorption band

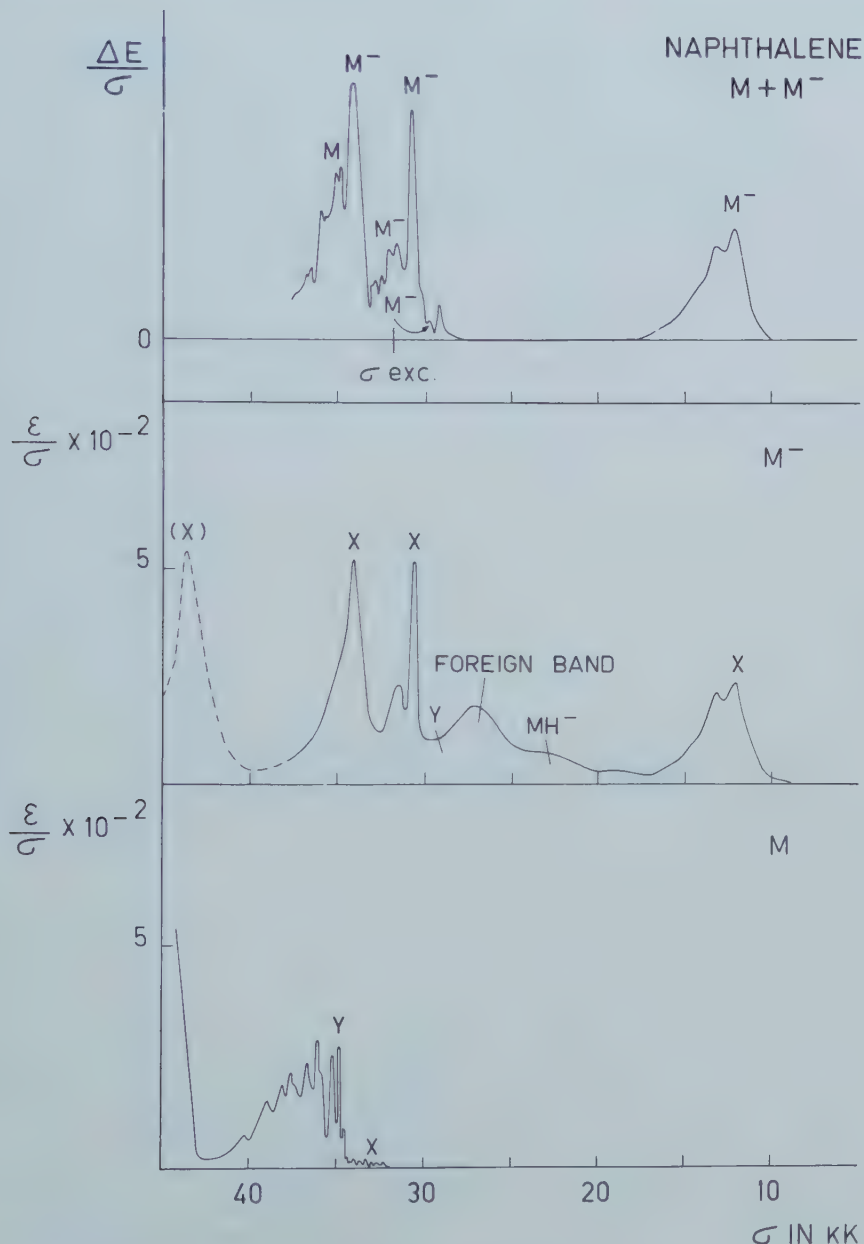


Figure 4. Differential and absorption spectra of naphthalene molecules and mono-negative ions (see text of figure 2).

of the di-negative ion. Here the absorption of the mono-negative ion is σ -polarized, so that it will give a negative contribution to the $\Delta E/\sigma$ value. The overall-effect is a positive value thus pointing to an x -polarization for the stronger absorption of the di-negative ion.

In the 20–25 kK region no polarization is observed, which implies that the absorption of the di-negative ion found in this region at -180°C must be due to some other substance, probably the covalent complex MNa^- .

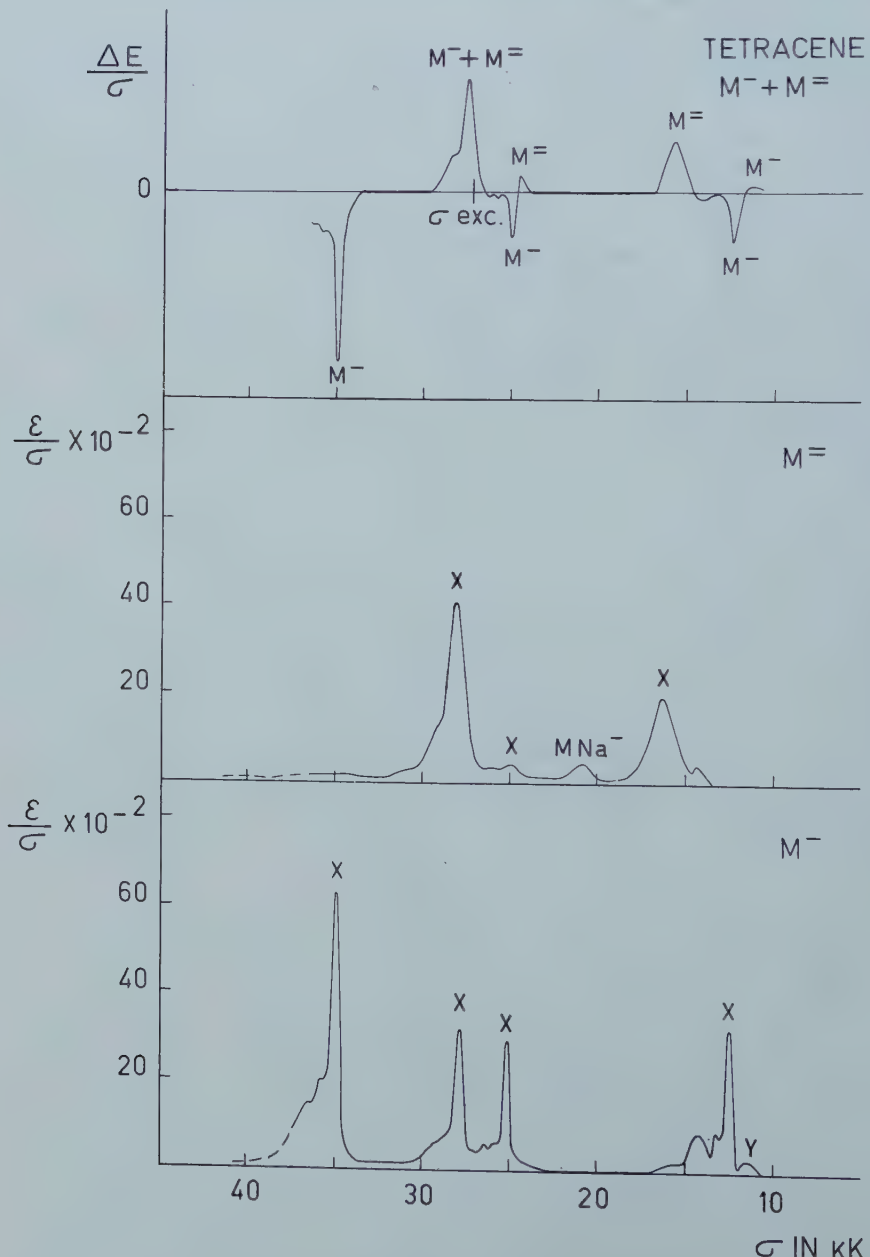


Figure 5. Differential and absorption spectra of tetracene mono- and di-negative ions (see text of figure 2).

The present investigations give no information about the occurrence of γ -polarized transitions in the di-negative ion. At any rate one may say that, by analogy with the results obtained for the mono-negative ion, these bands will be very weak and probably masked by the strong x -polarized bands.

5.2. Naphthalene

Experimental evidence indicates [9, 13] that the first weak absorption of the naphthalene molecules is polarized along the longer axis (x). The stronger

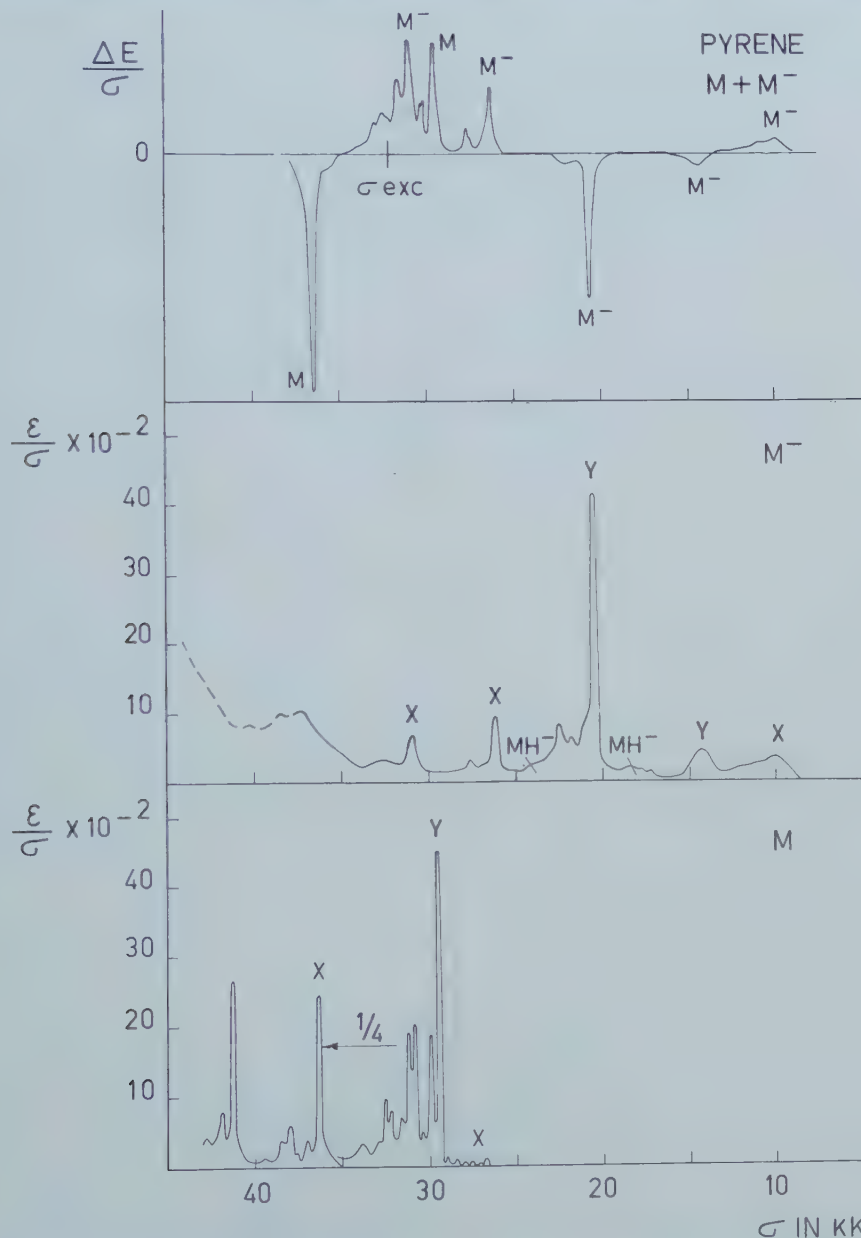


Figure 6. Differential and absorption spectra of pyrene molecules and mono-negative ions (see text of figure 2).

absorption in the 34–40 kK region is *y*-polarized. In our polarization experiments only the latter band could be measured. From figure 4 it becomes clear that the absorption bands at 12·2, 30·8 and 34·1 kK of the mono-negative ion are *x*-polarized, their $\Delta E/\sigma$ values having the same sign as those of the *y*-polarized absorption band of the molecule.

In the region 18–28 kK no polarization is found, which means that the absorption shown in this region of the spectrum of the mono-negative ion has to be

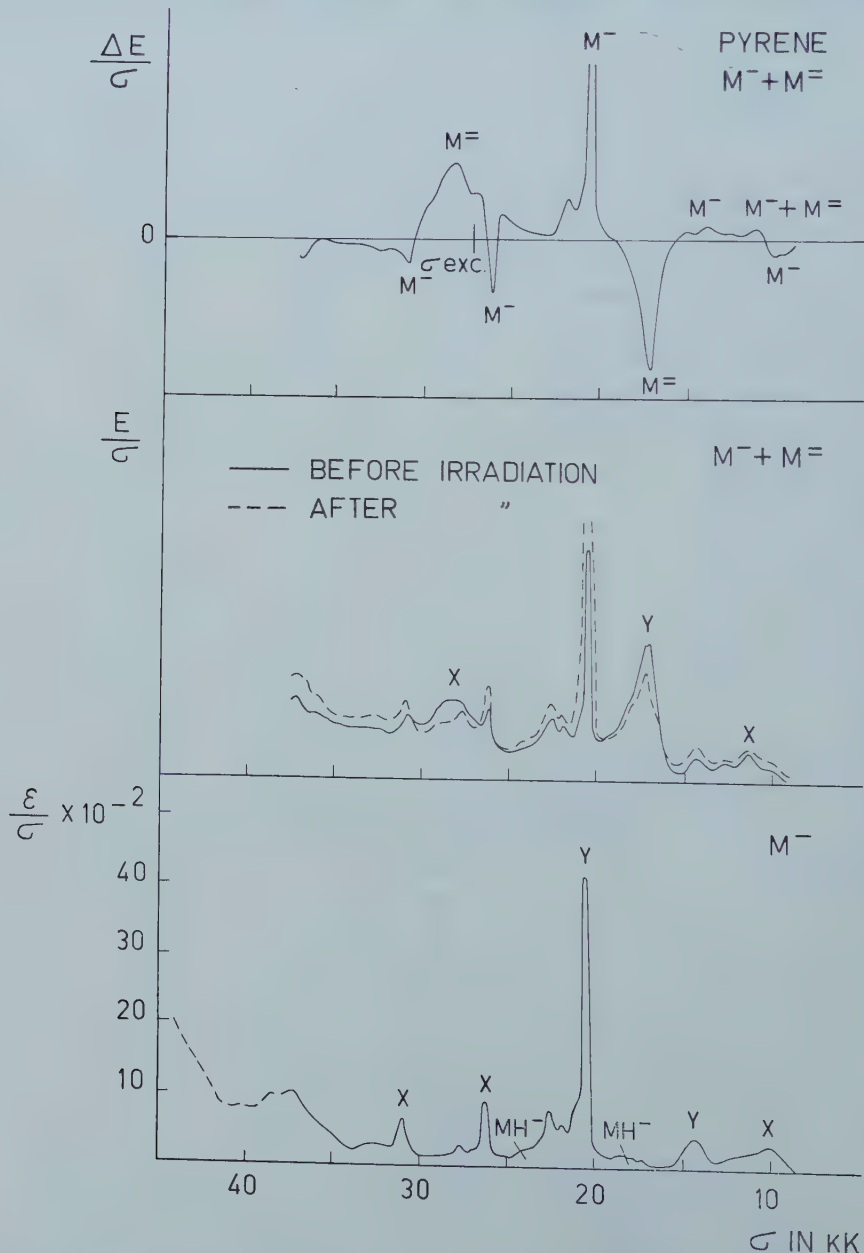


Figure 7. Differential and absorption spectra of pyrene mono- and di-negative ions. The absorption spectrum of the mixture of the mono- and di-negative ions, presented by the broken line have been measured after conversion of part of the di-negative ion by irradiation with the non-polarized 27·4 kK mercury line (see text of figure 2).

ascribed to some impurity. At least part of this absorption will be due to the presence of the ions MH^- , which strongly absorb in this region [16].

Just like in the case of the anthracene mono-negative ion, one might expect two weak y -polarized absorption bands in the spectrum of the naphthalene mono-negative ion. Actually no negative $\Delta E/\sigma$ values have been measured. However, the differential spectrum in the 29.2 to 30.5 kK region points to a depression of the $\Delta E/\sigma$ values in the rising part of the strong x -polarized band at 30.8 kK, which is very likely caused by the occurrence of a weak y -polarized band.

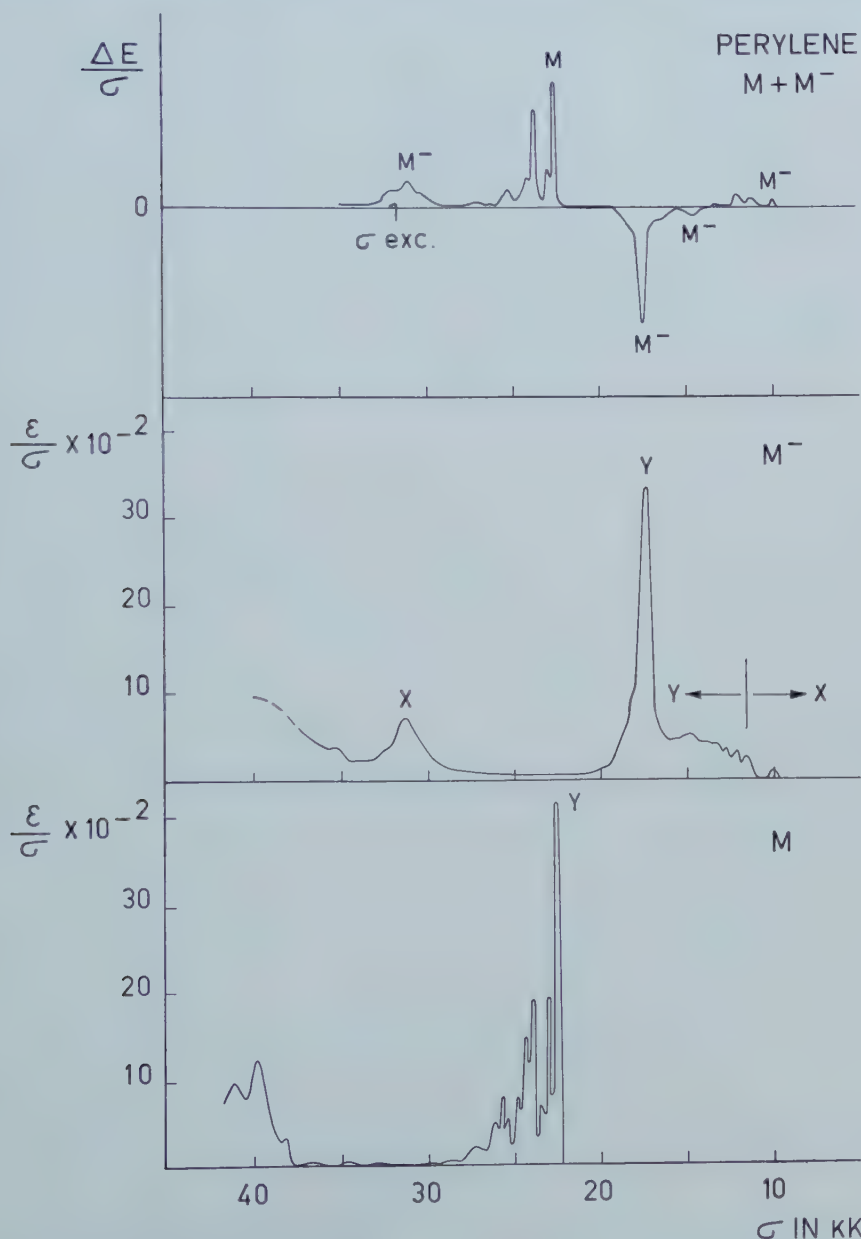


Figure 8. Differential and absorption spectra of perylene molecules and mono-negative ions (see text of figure 2).

In the spectrum of the mono-negative ion this band is obscured by the strong absorption of foreign substances†.

Unfortunately, owing to its low reduction potential the di-negative ion could not be obtained by reduction of naphthalene with alkali metal.

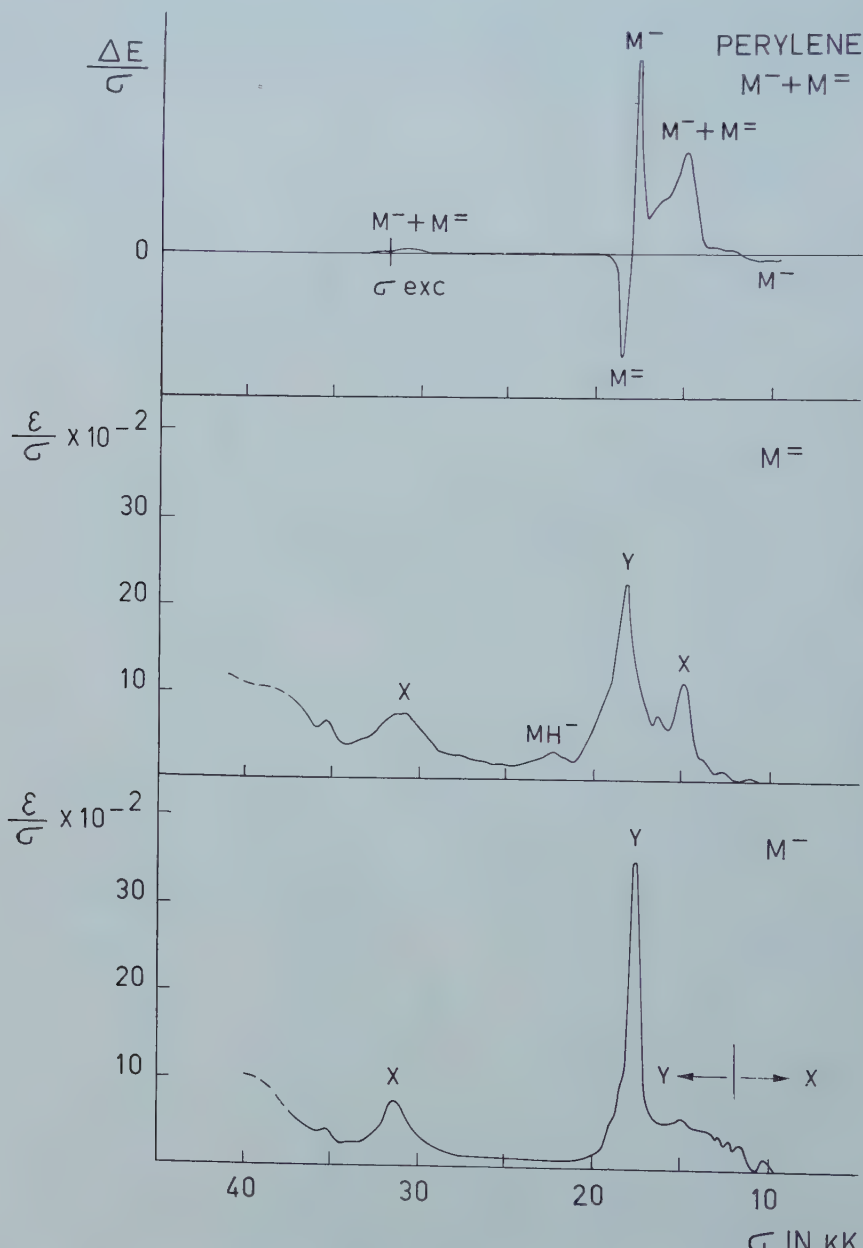


Figure 9. Differential and absorption spectra of perylene mono- and di-negative ions (see text of figure 2).

† Recent polarization experiments at higher concentrations by Miss Velthorst have shown a weak y -polarized absorption band to occur at 29.3 kK. The spectrum she obtained will be shown in the following paper [18].

5.3. Tetracene

Since the tetracene molecule could not be obtained on irradiation of the mono-negative ion no comparison can be made between the polarizations of the electronic transitions in the ions and those of the molecule, known from crystal measurements. The close similarity between the spectra of the ions of naphthalene, anthracene and tetracene, however, leaves no doubt that the four strong absorption bands in the spectrum of the mono-negative ion are polarized along the longer axis (*x*). From the differential spectrum in figure 5 it appears indeed

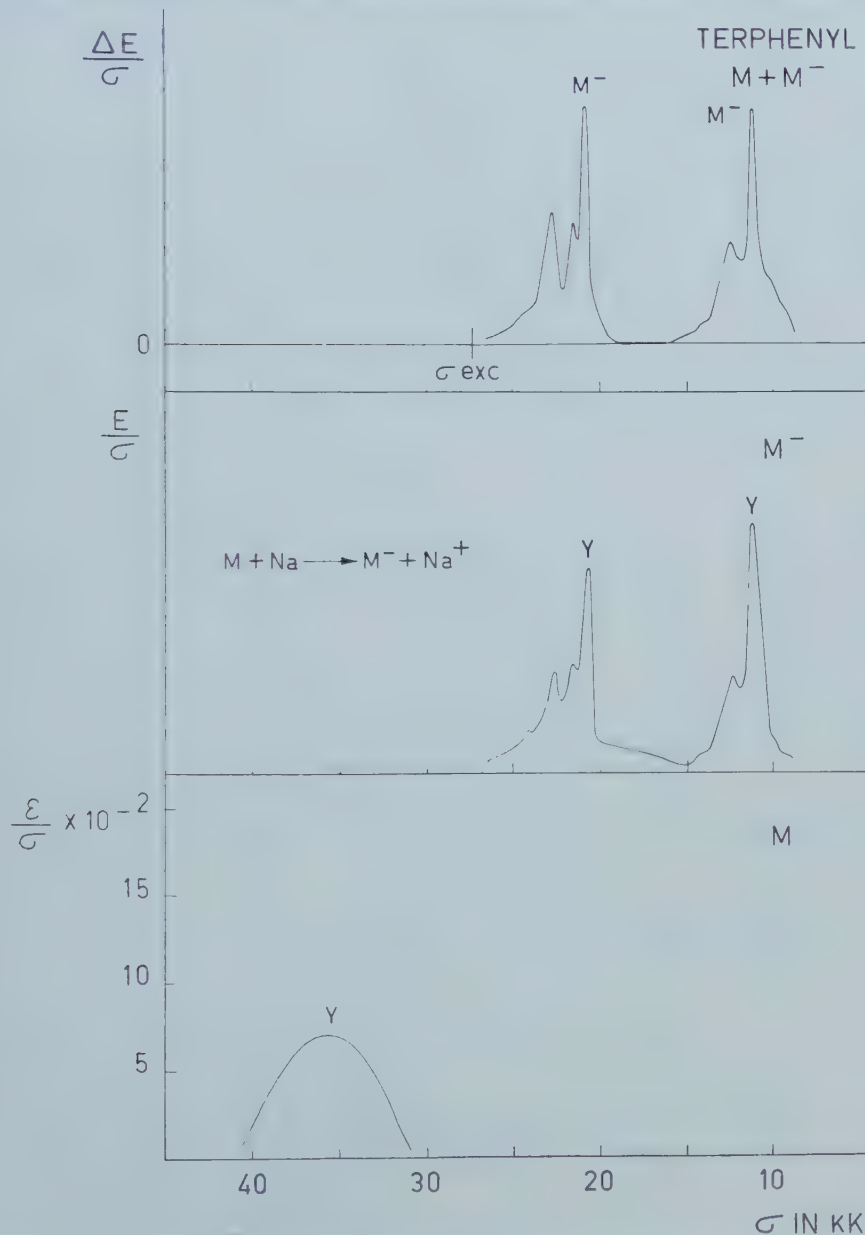


Figure 10. Differential and absorption spectra of terphenyl molecules and mono-negative ions (see text of figure 2).

that the signs of $\Delta E/\sigma$ of the 13.8, 25.3 and 35.3 kK bands are the same. The 16 kK band of the di-negative ion, the $\Delta E/\sigma$ value of which has opposite sign, must therefore be polarized along the same direction (x).

For the 27.8 kK band in the spectrum of the di-negative ion the same reasoning holds as in the case of anthracene. The positive sign of $\Delta E/\sigma$ at 27.8 kK is a result of a negative contribution of the 27.8 kK band of the mono-negative ion and a much stronger positive contribution of the absorption band of the di-negative ion. Accordingly the latter band must be x -polarized.

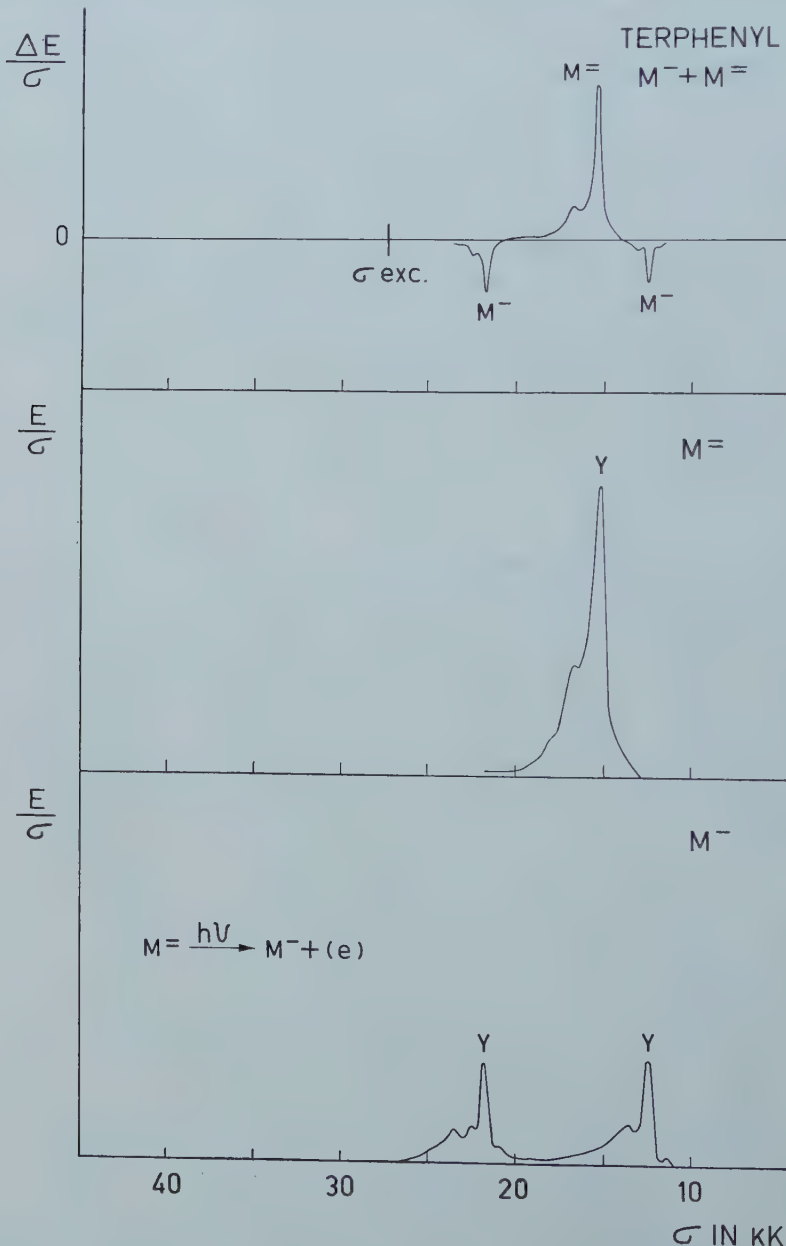


Figure 11. Differential and absorption spectra of terphenyl mono- and di-negative ions (see text of figure 2).

In contrast to anthracene in the spectrum of the tetracene mono-negative ion only one y -polarized absorption band is found, viz. the weak band at 11.6 kK. The second y -band is probably masked by the absorption bands in the 25–30 kK region.

In addition the differential spectrum exhibits a weak x -polarized absorption band of the di-negative ion at 24.8 kK.

The absence of polarization in the 17–24 kK region indicates that the absorption of the di-negative ion at 21 kK is due to some other species. Since this band occurs only in the low-temperature spectrum and disappears on warming it should be ascribed to the presence of a covalent complex MNa^- .

5.4. Pyrene

From the differential spectrum shown in figure 6 it appears that the absorption bands at 29–34 and 36.3 kK in the spectrum of the molecule are due to mutually perpendicularly polarized transitions, which will be called y - and x -polarized respectively. Williams has found from fluorescence polarization that the first very weak absorption band in the 27–29 kK region and the aforementioned bands have the same direction of polarization.

For this molecule Williams's results are not very convincing, however, the measured degrees of polarization being very small. Lyons and Morris [11] concluded from measurements on pyrene crystals that the first absorption is polarized along the shorter axis (x), of the molecule. As for the second band their results point more to a y - than to an x -polarization.

The strong resemblance between the spectra of aromatic hydrocarbons makes it very likely that the first two absorption bands have different polarizations (cf. naphthalene). Our results, combined with the absolute measurements of Lyons, lead to an x - an y - and an x -polarized band, respectively. Starting from this assignment the 14.3 and 20.5 kK bands in the spectrum of the mono-negative ion must be y -polarized, their $\Delta E/\sigma$ values having the same sign as those for the x -polarized band at 36.3 kK of the molecule. The residual bands of the mono-negative ion at 9.8, 26.2 and 30.9 kK, which have opposite $\Delta E/\sigma$ values, will be polarized along the shorter axis.

The weak absorption in the 17–19 and the 22–25 kK regions, where $\Delta E/\sigma$ is zero, have been ascribed to the occurrence of ions MH^- , probably due to proton addition by traces of water. This is confirmed by the fact that the addition of proton donor to the negative ion causes a strong absorption in this region [16].

Unfortunately the di-negative ion of pyrene could not be formed quantitatively. In figure 7 the spectrum is shown of a mixture of the mono- and di-negative ion. The stronger bands of the di-negative ion in this spectrum could be found easily by irradiation of the glassy solution, as is shown in the figure: the absorption bands due to the mono-negative ion increase in intensity, whereas the absorption bands which become lower on irradiation are due to the di-negative ion.

The small peak at 11.4 kK increases only slightly on irradiation, which indicates that an absorption band of the di-negative ion is superimposed on part of the x -band of mono-negative ion.

From the differential spectrum and the assignment given for the absorption bands of the mono-negative ion it immediately follows that the strong absorption band at 17.2 kK is polarized along the same axis as the strong band at 20.6 kK of

the mono-negative ion. The residual bands of the di-negative ion have opposite $\Delta E/\sigma$ values and are therefore *x*-polarized.

5.5. Perylene

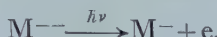
For the perylene molecules no crystal data are available. The analogy with pyrene, however, suggests the first absorption band in the spectrum of the molecule to be polarized along the longer axis (*y*).

The assignment of the absorption bands of the mono-negative and the di-negative ions immediately follow from the differential spectrum shown in figures 8 and 9, respectively. In the latter case a weak absorption is observed in the 21–24 kK region, which again must be ascribed to the presence of some proton adduct MH^- [16]. The low positive $\Delta E/\sigma$ values between 29 and 33 kK indicate that the $\Delta E/\sigma$ values for the absorption bands of the mono- and di-negative ion in this region have opposite signs, which implies that the corresponding transitions have the same directions of polarization.

5.6. Terphenyl

The differential spectra shown in figures 10 and 11 clearly indicate that the 15.4 kK band of the di-negative ion and the two strong bands of the mono-negative ion are due to transitions with the same polarization. Since from the experiments of Balk [2] it appeared that the intensities of the absorption bands strongly increase on going from terphenyl to quaterphenyl, the corresponding transitions will undoubtedly be polarized along the longer axis (*y*).

The polarization of the first absorption band of the molecule located in the 30–40 kK region could not be measured directly. As polarographic measurements have shown, the first and second reduction stages differ only slightly in standard potential (about 0.1 v), so that solutions of the mono-negative ion, without an observable concentration of the di-negative ion, can be obtained only in the presence of a large excess of the molecule. Consequently the extinction in the 30–40 kK region, where the first absorption band of the molecule is located, becomes too high to make measurements of the differential spectrum of the $M + M^-$ mixture possible in this region. Strong indication, however, that this absorption of the molecule is also *y*-polarized is obtained by the following experiments: The rigid solution of the di-negative ion is irradiated with non-polarized light during about 30 min. As a result, according to the reaction



nearly all the di-negative ions are converted into the mono-negative ions, whereas only a small fraction of the latter is converted into the molecules. Thereupon the irradiation is continued with polarized light for about two hours, after which the sign of $\Delta E/\sigma$ for the absorption band of the molecule was found to be opposite to that of the absorption bands of the mono-negative ion.

A comparison between the spectra of the mono-negative ion drawn in figures 10 and 11 reveals that the bands in figure 10 are located about 1 kK more towards the red than those in figure 11. The spectrum in figure 10 is obtained from a rigid solution of the mono-negative ion at liquid air temperature, whereas the spectrum in figure 11 is measured after irradiation of a rigid solution of the di-negative ion at the same temperature. Apart from the less apparent fine structure the spectrum of the mono-negative ion at room temperature appears to be identical with that shown in figure 11.

Further investigations by Dieleman [17] leave no doubt that the spectrum of the mono-negative ion at low temperature (in figure 10) arises from the free mono-negative ion, whereas the spectra of the ion at room temperature in 2-methyltetrahydrofuran as well as the spectrum shown in figure 11 are due to the associated form. When tetrahydrofuran [2] instead of 2-methyltetrahydrofuran is used as a solvent, the spectrum at room temperature looks like a superposition of the afore-mentioned spectra. Apparently in tetrahydrofuran at room temperature both forms are present. A more detailed discussion of these phenomena will be given in a separate paper [17].

The results obtained in this paper will be used in a forthcoming article dealing with the correlation between the electronic spectra of alternant aromatic hydrocarbon molecules and ions [18].

One of us (P.J.Z.) wishes to thank the Netherlands Foundation for Chemical Research (S.O.N.) and the Netherlands Organization for the Advancement of Pure Research (Z.W.O.) for the financial support which he received during these investigations.

The authors gratefully acknowledge the collaboration of Mr. J. Dieleman in part of these investigations.

REFERENCES

- [1] PAUL, D. E., LIPKIN, D., and WEISSMAN, S. I., 1956, *J. Amer. chem. Soc.*, **78**, 119.
- [2] BALK, P., 1957, Thesis, Free University, Amsterdam; BALK, P., HOIJTINK, G. J., and SCHREURS, J. W. H., 1957, *Rec. trav. chim. Pays-Bas*, **76**, 813.
- [3] BALK, P., de BRUIJN, S., and HOIJTINK, G. J., 1957, *Rec. trav. chim. Pays-Bas*, **76**, 907; 1958, *Mol. Phys.*, **1**, 151.
- [4] HOIJTINK, G. J., and WEIJLAND, W. P., 1957, *Rec. trav. chim. Pays-Bas*, **76**, 836; 1958, Hoijtink, G. J., *Colloque International sur le Calcul des Fonctions d'Ondes Moléculaires* (Paris: C.N.R.S.), p. 239; 1958, WEIJLAND, W. P., Thesis, Free University, Amsterdam.
- [5] VAN DER MEIJ, P. H., 1958, Thesis, Free University, Amsterdam; HOIJTINK, G. J., and VAN DER MEIJ, P. H., 1959, *Z. phys. Chem.*, **20**, 1.
- [6] KON, H., and BLOIS, M. S., 1958, *J. chem. Phys.*, **28**, 743; AALBERSBERG, W. IJ. HOIJTINK, G. J., MACKOR, E. L., and WEIJLAND, W. P., 1959, *J. chem. Soc.*, 3049, 3055. BENNEMA, P., HOIJTINK, G. J., LUPINSKI, J. H., OOSTERHOFF, L. J., SELIER, P., and VAN VOORST, J. D. W., *Mol. Phys.*, **2**, 431.
- [7] LEWIS, G. N., and LIPKIN, D., 1942, *J. Amer. chem. Soc.*, **64**, 2801; LEWIS, G. N., and BIGELEISEN, J., 1943, *J. Amer. chem. Soc.*, **65**, 520.
- [8] OBREIMOV, I. V., PRIKHOT'KO, A. F., and RODNIKOVA, I. V., *J. exp. theor. Phys.*, **18**, 409; PESTEIL, P., and BARBARON, M., 1954, *J. Phys. Radium*, **15**, 92; FERGUSON, J., and SCHNEIDER, W. G., 1958, *J. chem. Phys.*, **28**, 761; 1958, *Canad. J. Chem.*, **36**, 1070.
- [9] CRAIG, D. P., and HOBBINS, P. C., 1955, *J. chem. Soc.*, 539; CRAIG, D. P., and WALSH, J. R., 1958, *J. chem. Soc.*, 1613.
- [10] SIDMAN, J. W., 1956, *J. chem. Phys.*, **25**, 115, 122.
- [11] LYONS, L. E., and MORRIS, G. C., 1957, *J. chem. Soc.*, 2648, 3661.
- [12] BREE, A., and LYONS, L. E., 1956, *J. chem. Soc.*, 2662.
- [13] MCCLURE, D. S., 1954, *J. chem. Phys.*, **22**, 1668.
- [14] WILLIAMS, R., 1957, *J. chem. Soc.*, **26**, 1186.
- [15] CLAR, E., 1952, *Aromatische Kohlenwasserstoffe* (Göttingen: Springer Verlag).
- [16] HOIJTINK, G. J., and VELTHORST, N. H. (to be published).
- [17] DIELEMAN, J., and HOIJTINK, G. J. (to be published).
- [18] HOIJTINK, G. J., VELTHORST, N. H., and ZANDSTRA, P. J., 1960, *Mol. Phys.* (to be published).

The helix-coil transition in charged macromolecules

by BRUNO H. ZIMM

General Electric Research Laboratory,
Schenectady, New York†

and STUART A. RICE

Department of Chemistry and Institute for the Study of Metals,
University of Chicago, Chicago 37, Ill.

(Received 26 February 1960)

Starting from the Grand Partition Function and using matrix methods introduced previously, a formulation of the theory of helix-coil transitions in charged macromolecules is given. The theory is compared with experimental data for the system polyglutamic acid-dioxane-water-NaCl. If the parameter describing the extra difficulty associated with initiating a helical configuration is assigned the same value as for polybenzylglutamate, the calculations are in excellent agreement with experiment. An analysis of the physical significance of the Grand Partition Function leads to methods for determining the fraction of polymer in helical form, the equilibrium constant for the addition of a residue to an already formed helix, as well as the initiation parameter mentioned above. The value of the initiation parameter deduced from titration data on polyglutamic acid is in rough agreement with the value for polybenzylglutamate.

The nature of the approximations used is discussed briefly.

1. INTRODUCTION

It has now been established that a number of macromolecules possessing helical configurations in solution may undergo a transition to a different configuration. Of the possible examples, the most thoroughly investigated case is the molecular isomerization from α -helix to random coil characteristic of the synthetic polypeptides. For these substances the elegant studies of Doty and co-workers [1] have clearly shown the dependence of the transition upon the intimate details of the interactions within one polymer molecule, as well as the interactions of the polymer with solvent molecules. Previous work has dealt with the theory of the transition in uncharged polypeptides [2]. It is the purpose of the present note to extend these considerations to include the effects of electrostatic forces.

There are two aspects of the problem considered. First, it is pertinent to investigate how suitably defined molecular parameters may be deduced from experimental data. Second, it is necessary to construct a detailed theory in which the existence of the isomerization is predicted from the functional dependence and numerical values of these same molecular parameters. We shall discuss these two topics in the order indicated.

†Present address: Department of Chemistry, University of California, La Jolla.

2. EXPERIMENTAL EVALUATION OF PARAMETERS

The definition of appropriate molecular parameters requires specification of the system under investigation. We restrict attention to systems dilute in the polymeric component and consider only the interactions within one polymer molecule and between a polymer molecule and the various components of the solvent. We shall treat the solvent as a dielectric continuum. Each polymer consists of many identical sub-units, each of which may ionize, and each of which may also hydrogen bond to the appropriate other segment of the same chain to form an α -helix. A system of the type indicated may be conveniently described in terms of the semi-grand partition function [3]

$$\Xi = \sum_{\{c\}} \sum_{\{\eta\}} \exp\left(-\frac{W(\{c\}, \{\eta\})}{kT}\right) Q^0(\{c\}) \lambda \sum_i \eta_i \quad (1)$$

where η_i , which can be either 0 or 1, is an occupation variable specifying the charge state of site i , and c_i in the same fashion specifies the hydrogen bond state of site i . The internal partition function, $Q^0(\{c\})$ depends upon the positions of the chain sub-units, hydrogen bond energies, steric hindrances and any other relevant variables. Finally, the variable λ plays the role of the reciprocal of the absolute activity of the hydrogen ion (we take the macromolecule to be a polyacid for concreteness), and $W(\{c\}, \{\eta\})$ is the electrostatic energy corresponding to the skeletal configuration with $\{c\}$ hydrogen bonds and the charge distribution specified by $\{\eta\}$. Note that the summation of the occupation variable η_i over all sites is just the total charge on the polyion and the summation of c_i gives the total number of intact hydrogen bonds. The degree of ionization, α , is therefore seen to be

$$\alpha = \frac{1}{Z} \frac{\partial \ln \Xi}{\partial \ln \lambda} \quad (2)$$

where there are Z charge sites on the molecule. The absolute activity λ is related to the more familiar variables of pH and dissociation constant K_a^0 by

$$0.434 \ln \lambda = \text{pH} - pK_a^0. \quad (3)$$

Let us assume that the pure helix and pure coil could exist alone. These would then be characterized by partition functions Ξ_h and Ξ_c of the form indicated in equation (1). The degrees of ionization of these hypothetical forms would be

$$\alpha_h = \frac{1}{Z} \frac{\partial \ln \Xi_h}{\partial \ln \lambda}, \quad \alpha_c = \frac{1}{Z} \frac{\partial \ln \Xi_c}{\partial \ln \lambda}. \quad (4)$$

Consider for the moment the uncharged molecule, $\alpha=0$, and let s be the equilibrium constant for the addition to a section of helix of the appropriate segment from the adjacent section of randomly coiling chain. Then if it is assumed that when $\alpha=0$ the polymer molecule is completely in the helical form, it is seen that

$$(\Xi)_{\alpha=0} = s^Z \quad (5)$$

end effects being neglected. Then, by equations (2) and (4),

$$\ln m - \ln s = \int_{\lambda(0)}^{\lambda(\alpha)} \alpha d \ln \lambda, \quad (6)$$

$$\ln t_0 = \int_{\lambda(0)}^{\lambda(\alpha)} \alpha_c d \ln \lambda, \quad (7)$$

with

$$\mathfrak{m} = \Xi^{1/Z}, \quad \mathfrak{c}_0 = \Xi_c^{1/Z}, \quad \mathfrak{h}_0 = \Xi_h^{1/Z} \quad (8)$$

where m , c_0 and h_0 are the partition functions per residue of the mixed, pure coil and pure helix forms respectively. If the fully charged state is assumed to be in the pure randomly coiled configuration,

$$(\mathfrak{m})_{\alpha=1} = (\mathfrak{c}_0)_{\alpha=1} = 1 \quad (9)$$

and thereby

$$\ln s = \int_{\lambda(0)}^{\lambda(1)} (\alpha_c - \alpha) d \ln \lambda. \quad (10)$$

In equations (6), (7), (10) and (14) use is made of the limiting conditions at $\alpha = 0$,

$$\mathfrak{c}_0 = 1, \quad \mathfrak{h}_0 = 1,$$

which follow directly from the interpretation of the partition function in terms of the relative probabilities of finding various (charge) configurations and the use of the uncharged random coil and uncharged helix as reference states for Ξ_c and Ξ_h respectively. The titration curves for the pure helix and pure coil can in principle be calculated and can in practice be determined experimentally. The necessary extrapolations past the transition region into the domain of hypothetical stability are not difficult to perform.

The integrals may be most easily evaluated by the following device. The single integral is converted to a double integral by the introduction of a new variable. The double integral may then be transformed as follows:

$$\begin{aligned} \int_{\lambda(0)}^{\lambda(\alpha)} (\alpha_c - \alpha_h) d \ln \lambda &= \int_{\lambda(0)}^{\lambda(\alpha)} \int_{\alpha_h}^{\alpha_c} d\alpha d \ln \lambda \\ &= \int_{\ln \lambda(\alpha_h) - \ln(\alpha_c/1-\alpha_c)}^{\ln \lambda(\alpha_c) - \ln(\alpha_c/1-\alpha_c)} \int_{\alpha_h}^{\alpha_c} d\alpha d \left(\ln \lambda - \ln \frac{\alpha}{1-\alpha} \right) \end{aligned} \quad (11)$$

since the Jacobian of the transformation is unity. As can be seen in figure 1, a plot of $\ln \lambda - \ln(\alpha/1-\alpha)$ is much more nearly linear than a plot of α versus $\ln \lambda$ (see figure 2). Since the areas cut off by a line of constant λ on either plot are equal by virtue of equation (11) and the extrapolation of nearly linear curves is easier than that of non-linear curves, $\ln \lambda - \ln(\alpha/1-\alpha)$ is the more useful experimental variable. It is clear then that the determination of the titration curve of the polymer followed by interpolation of the portion characteristic of the pure coil and measurement of the area between the observed and the interpolated curves gives the value of the equilibrium constant s . The latter important quantity is a measure of the stability of the uncharged helix.

It is possible by similar methods to determine the fraction, ϑ , of intact hydrogen bonds in the helix. Two accessible experimental quantities are

$$s' = s \mathfrak{h}_0 / \mathfrak{c}_0, \quad (12)$$

$$\mathfrak{m}' = \mathfrak{m} / \mathfrak{c}_0. \quad (13)$$

By methods analogous to those used in the foregoing,

$$\ln s' = \int_{\lambda(0)}^{\lambda(1)} (\alpha_c - \alpha) d \ln \lambda = \int_{\lambda(0)}^{\lambda(\alpha)} (\alpha_c - \alpha_h) d \ln \lambda, \quad (14)$$

$$\ln \mathfrak{m}' = \int_{\lambda(\alpha)}^{\lambda(1)} (\alpha_c - \alpha) d \ln \lambda. \quad (15)$$

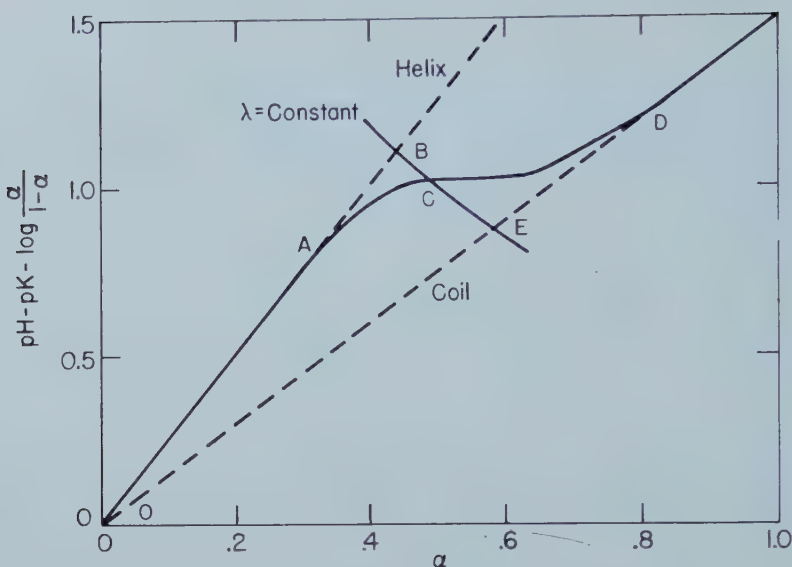


Figure 1. Construction for the determination of the thermodynamic parameters. The experimental titration curve OACD has been drawn through the data shown in figure 3 for polyglutamic acid in 0.0133 M salt. According to equations (10), (11), (14) and (15) the quantities $\log_{10} s$, $\log_{10} s'$ and $\log_{10} m'$ are given by the areas OACD, OACD-OBE, and CED respectively. The curve BCE is drawn for the particular case of $\lambda=1$, corresponding at point C on the experimental curve to $\alpha=0.49$.

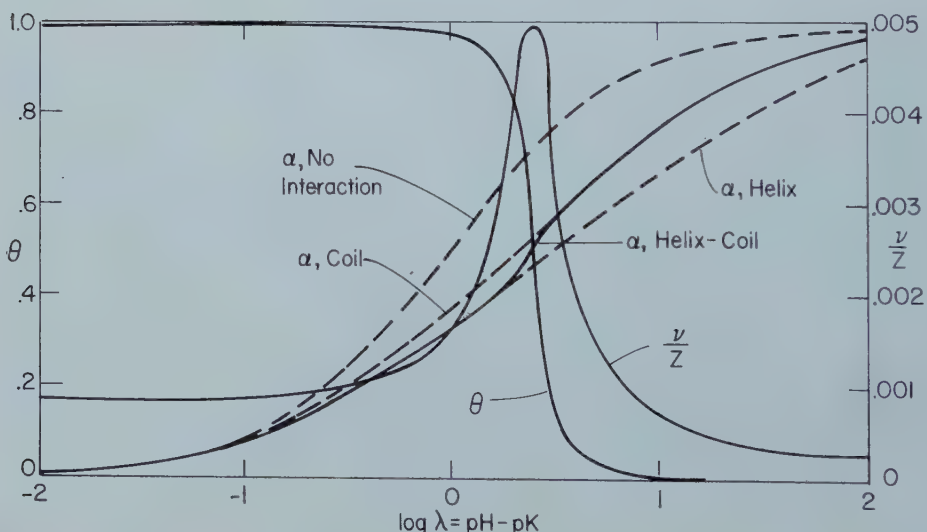


Figure 2. Theoretical results for our model of polyglutamic acid in 0.133 M salt in a dioxane-water mixture of dielectric constant 50. Shown are the titration curves of a mono-basic acid (no interaction), a perfect helix, a perfect random coil, and the equilibrium mixture of helix and coil; also shown are the fraction of internal hydrogen bonds, θ , and the frequency of alternation of random and helical sections, ν/Z . α , degree of ionization, λ , the reciprocal of the absolute activity of the hydrogen ion, ν , the number of helical sections in a chain of Z amino acid residues. $(\nu/Z) = \partial \ln m / \partial \ln \sigma$.

These integrals correspond to the areas shown in figure 1. For example, for the case illustrated in figure 1, $s = 1.355$, $s' = 1.02$, $\lambda = 1$, and $m' = 1.039$. The way in which these numbers can be put to use to determine the parameters characteristic of the transition will be discussed at a later point after we have introduced the necessary theoretical considerations.

Before closing this section it is pertinent to note that it is also possible to determine experimentally the fraction, v , of the polymer which is in the helical configuration. For, if the junction interactions between helical and coiled sections of the macromolecule are ignored, the partition function becomes

$$m^Z = (s \hbar_0)^k t_0^{Z-k} \quad (16)$$

where there are k residues in helix form. Using the definition $v = k/z$ and the definitions of equations (12) and (13),

$$\ln m = v \ln s + v \ln \hbar_0 + (1 - v) \ln t_0, \quad (17)$$

$$\ln m' = v \ln s', \quad (18)$$

whereby

$$\left(\frac{\partial \ln m}{\partial \ln s} \right)_\lambda = \frac{d \ln m'}{d \ln s'} = v. \quad (19)$$

3. THE MOLECULAR MODEL

In the last section it was seen that the equilibrium constant for the addition of a residue to a helical section could be determined from experimental data. It remains to be shown how this parameter enters the molecular theory and whether or not further deductions from experiment can be made.

The examination of the consequences of equation (1) requires an evaluation of the internal partition function $Q^0(\{c\})$. Consider the case of a polypeptide in the helical configuration. The partition function is the sum of the weighted probabilities of finding the macromolecule with some monomeric units in a random coil configuration and all others in a helical configuration. The weighting of particular configurations is in each case a Boltzmann factor with the exponent equal to the work required to create the specified state by breaking hydrogen bonds, overcoming steric hindrances, etc. In more descriptive language, the free energy of each hydrogen bond contributes to the stability of the helix. If a hydrogen bond is broken, the two amide groups which were previously severely restricted acquire an increased freedom of motion. If two adjacent hydrogen bonds are missing there is an extra increase in freedom over and above that achieved in the breaking of two separated hydrogen bonds. We can proceed in this manner to characterize the state of each hydrogen bond site in terms of interactions with other groups along the chain. The internal state of the macromolecule can thus be characterized by specifying the probabilities of occurrence of all possible arrangements of bonded and non-bonded sites.

Practical considerations, based upon the increased mathematical complexity involved in handling large numbers of simultaneously interacting sites, force the adoption of an approximation in which only small groups of sites interact as a unit. If the energy of interaction of a given site (which shall be called the central site) with its neighbours is truncated after the terms corresponding to say the x th neighbouring site, then the set of sites considered to interact forms a basic group from which the configuration of the entire polymer may be specified. The probability of finding the whole molecule in a given configuration is, in

fact, the product of the probabilities of finding the required local configurations of the $x+1$ interacting groups. The essence of the approximation inherent in truncating the interactions after x groups is that the total partition function is then constructed of the sub-partition functions for the interactions within the basic group. The basic groups are independent of one another. *This does not mean* that a given site is uncoupled from the rest of the molecule, but rather than interactions are reckoned group-wise, each site belonging to several groups and being respectively the central site, first neighbour, second neighbour, ... x th neighbour in the successive groups. The fact that each site belongs, in a different category, in several basic groups couples each site to all neighbours out to the truncation point. This is in the case cited the x th neighbour.

When charges are present, as in the present case, we proceed in the same way. From equation (1) it is seen that the weighting factor for each configuration must include both the energetic terms described above and the relevant electrostatic interactions. That is, the summation over configurations is made with a Boltzmann weighting factor of the total energy for each particular configuration. The partition function expressed in equation (1) thereby gives the electrical free energy of the polyion including those electrostatic effects which result from the helix-coil transition. This is, however, not the only contribution to the total change in free energy. Consideration must also be given the contribution to the Helmholtz free energy of the polyion by the free energy of the free hydrogen ions eligible to take part in neutralization of the acid groups of the polyion, by the electrical free energy due to interactions between portions of the net charge of the polyion and by the chemical free energy associated with the state of ionization of the polyion computed from a reference state in which the polyacid is completely undissociated. It may readily be shown [4] that the pH and degree of ionization, α , of a polyacid are related to the intrinsic acid dissociation constant, K_a^0 , and the electrostatic free energy by

$$0.434 \ln \lambda = \text{pH} - pK_a^0 = \frac{0.434}{ZkT} \frac{\partial A}{\partial \alpha}. \quad (20)$$

The free energy A also contains contributions from the non-electrostatic interactions which create the helical configuration, but only the electrostatic interactions are explicitly contained in the indicated derivative. Further progress requires the explicit evaluation of Ξ , a task to which we now turn.

In a previous paper [2] it has been shown that the internal hydrogen bonding of non-electrolytic polypeptides can be treated by the use of a model that includes nearest-neighbour interactions only. If it is assumed that only the hydrogen bonds characteristic of the α -helix can form, the internal bonding is completely described by the specification of the bond state of the oxygen of each amide group. A digit 1 is used to represent a bonded oxygen and 0 for an unbonded oxygen. Thus a state of the chain is described, with respect to internal hydrogen bonding, by a state number $\{c\}$ constructed from the occupation variables c_i and which is a sequence of ones and zeros, one apiece for each amide group. $Q^0(\{c\})$ is represented as a product of the following factors:

- (1) Unity for every 0 in the state number,
- (2) s for every 1 that follows a 1,
- (3) σs for every 1 that follows one or more 0's.

The equilibrium constant s was defined previously while σ is a factor less than unity representing the extra difficulty involved in the starting of a section of helix

compared to the extending of it. In the case of polybenzylglutamate the initiation parameter σ was in the neighbourhood of 10^{-4} .

The electrostatic part of the partition function is more complicated. As in the preceding, the electrolytic state number can be written as a sequence of 0's and 1's, indicating the absence or presence of charge on the corresponding segments of the chain. The electrostatic energy may be written in terms of the $\{\eta\}$ as

$$W(\{c\}, \{\eta\}) = \sum_{i>j} \frac{q^2}{DR_{ij}} \exp(-\kappa R_{ij}) \eta_i \eta_j \quad (21)$$

where we have assumed that the pair interaction potential is of the screened coulomb form. This form for the pair interaction potential has been justified by more detailed theories of poly-electrolyte solutions [5]. As usual, q is the charge per residue, D the dielectric constant, R_{ij} the separation of a pair of charges and κ the screening parameter is defined by

$$\kappa^2 = \frac{4\pi}{DkT} \sum_i n_i (z_i q)^2 \quad (22)$$

with n_i the concentration, z_i the valence of species i , and where the summation is to be taken over the counterions and small ions only.

The summation in equation (21) extends over all pairs of interacting charges. Following the lead of recent work in the theory of polyelectrolytes [4, 6] we consider electrostatic interactions between small numbers of near neighbouring sites only, accepting the necessary inaccuracies that arise from the neglect of the more numerous but weaker distant interactions. In the present case we retain the interactions of each charge with eight of its neighbours, four on each side. To estimate the error involved in this truncation we compare the contributions to $W(\{c\}, \{\eta\})$ of these four nearest neighbours on a polybenzylglutamate helix with the value obtained by summing the Debye Hückel potential out to infinity under the conditions appropriate to the experiments to be discussed later. If the solvent has a dielectric constant of 50, the four neighbour approximation accounts for 65 per cent of $W(\{c\}, \{\eta\})$ when the salt concentration is 0.133M NaCl, 90 per cent of the electrostatic energy is contributed when the salt concentration is 1.33M and at the lower concentration 0.0133M NaCl only 37 per cent of the electrostatic energy is contributed by the first four neighbours.

The inaccuracies generated by the truncation of the series of equation (21) are perhaps less important than the uncertainties arising from the choice of an appropriate dielectric constant. Although the bulk dielectric constant of a medium containing two-thirds water and one third dioxane is about 50, the medium immediately surrounding the polypeptide chain may be different because of selective concentration due to adsorption or salting-out effects; the saturation effects of the strong electric fields around ions are unknown, and in any case the polypeptide chain itself occupies a significant part of the space that the electric lines of force must traverse.

Although the figures provided above indicate an error of considerable magnitude in the absolute electrostatic energy, this is not the quantity of greatest interest since the transition depends upon the difference in energy of the two isomeric configurations. Since the errors will be in the same direction with both forms, a considerable compensation of errors is likely to result.

Thus, with some quantitative uncertainty in the fundamental formulae it is appropriate to choose models featuring simplicity rather than refinement. For

the structure of the polypeptide helix we use the parameters proposed by Pauling and Corey [7] for a helix with three to six residues per turn. It will be assumed that the side chains of the glutamic acid residues are extended straight out along the radii of the helix because of electrostatic repulsion. The charges are then located at 6.5 Å from the helix axis and at rotations of 100° apart with an axial translation of 1.5 Å per residue. The distances between one charge and its first six neighbours along the chain are 10.1 Å, 13.1 Å, 7.9 Å, 7.5 Å, 14.3 Å and 14.4 Å. It is clear that the first neighbours for charge interactions are the fourth and third neighbours along the skeleton. For the random form of the chain it will be assumed that the electrostatic forces favour a locally extended form of the chain with the backbone having 3.6 Å per residue. It will be further assumed that the charges are arranged around the chain in a helix of three residues per turn. The distance from the charges to the axis is 5 Å and the distances between one charge and each of its first three neighbours is about 10 Å, and the fourth neighbour is 16 Å away. Kinked configurations of the chain, although admittedly present to some extent, are nevertheless neglected by this model.

4. MATHEMATICAL METHOD

The natural method for the mathematical treatment of the problem as outlined above is the matrix analysis of the partition function first introduced by Kramers and Wannier [8], Montroll [9] and Lassetre and Howe [10]. This technique has previously been used for both parts of the problem separately.

We proceed by labelling the states of each segment with five binary digits. The first digit comes from the hydrogen bond occupation number and the others from the electrolytic state number corresponding to the charge on the segment in question and the three segments preceding it in the chain. The state vector then consists of the array of thirty-two statistical weights corresponding to the set of all values of the five digit binary numbers. With this labelling system, the first sixteen components of the state vector correspond to charge states of the random coil while the second sixteen components correspond to charge states of the α -helix. The interaction matrix, M , is of order 32×32 and may be partitioned into four 16×16 sub-matrices as shown:

$$M = \left(\begin{array}{c|c} C & J_1 \\ \hline \sigma s J_2 & H \end{array} \right) \quad (23)$$

where the sub-matrices C and H contain, respectively, only electrostatic interactions between random coil configurations or between helix configurations. The submatrices J_1 and J_2 contain the mixed helix-coil interactions. Since σ is small, the off diagonal matrices J_1 and J_2 may be considered to be perturbations. To proceed to find the dominant eigenvalue of M , let C and H be diagonalized by similarity transformations with matrices U and V ,

$$U^{-1}CU = \begin{bmatrix} t_0 & 0 & \dots \\ 0 & t_1 & & \\ \vdots & & \ddots & \\ & & & \ddots \end{bmatrix}, \quad (24)$$

$$V^{-1}HV = \begin{bmatrix} h_0 & 0 & \dots \\ 0 & h_1 & & \\ \vdots & & \ddots & \\ & & & \ddots \end{bmatrix}, \quad (25)$$

with the eigenvalues so ordered that \mathbf{t}_0 and \mathbf{h}_0 are the largest in their respective matrices. M may now be transformed by a similarity transformation with the matrices

$$\begin{pmatrix} U^{-1} & 0 \\ 0 & V^{-1} \end{pmatrix}, \quad \begin{pmatrix} U & 0 \\ 0 & V \end{pmatrix} \quad (26)$$

and the new matrix has the same eigenvalues as M . The dominant eigenvalue of M is denoted \mathbf{m} and is obtained from the secular equation of the transformed matrix by neglecting elements containing σ in all places except where they occur in parallel with the small but important elements $\mathbf{t}_0 - \mathbf{m}$ and $\mathbf{h}_0 - \mathbf{m}$. The secular equation reduces to

$$(\mathbf{t}_1 - \mathbf{m})(\mathbf{t}_2 - \mathbf{m}) \dots (\mathbf{h}_1 - \mathbf{m})(\mathbf{h}_2 - \mathbf{m}) \dots \begin{vmatrix} \mathbf{t}_0 - \mathbf{m} & \mathbf{l}_1 \\ \sigma s \mathbf{l}_2 & s \mathbf{h}_0 - \mathbf{m} \end{vmatrix} = 0 \quad (27)$$

where \mathbf{l}_1 and \mathbf{l}_2 are the upper left-hand corner elements of the transforms of J_1 and J_2 . \mathbf{l}_1 and \mathbf{l}_2 are related to the vectors \mathbf{u} , \mathbf{v} consisting of the first columns of U and V , and to \mathbf{u}^{-1} and \mathbf{v}^{-1} , the first rows of U^{-1} and V^{-1} , by

$$\mathbf{l}_1 = \mathbf{u}^{-1} J_1 \mathbf{v}, \quad \mathbf{l}_2 = \mathbf{v}^{-1} J_2 \mathbf{u}. \quad (28)$$

The elements of C , H , J_1 and J_2 depend upon the distance between segments in the indicated molecular configurations. For a given difference of number of segments, the intersegment distance is smallest in the helix and largest in the coil. Thus the elements of the interaction matrices are intermediate in size between the corresponding elements of C and H . Since all non-zero elements are positive and not very different from unity, it is consistent to approximate J_1 and J_2 by the average of C and H . This leads to the approximate formulae

$$\begin{aligned} \mathbf{l}_1 &= \frac{1}{2}(\mathbf{t}_0 + \mathbf{h}_0)(\mathbf{u}^{-1}\mathbf{v}), \\ \mathbf{l}_2 &= \frac{1}{2}(\mathbf{t}_0 + \mathbf{h}_0)(\mathbf{v}^{-1}\mathbf{u}). \end{aligned} \quad (29)$$

The principal eigenvalue of M is the largest root of equation (27), which is the larger root of the 2×2 determinant. With the approximation of equation (29) this is the larger value of

$$\mathbf{m} = \frac{1}{2}[\mathbf{t}_0 + s\mathbf{h}_0 \pm \{(\mathbf{t}_0 - s\mathbf{h}_0)^2 + \sigma s(\mathbf{t}_0 + \mathbf{h}_0)^2(\mathbf{u}^{-1}\mathbf{v})(\mathbf{v}^{-1}\mathbf{u})\}^{1/2}]. \quad (30)$$

As usual, the partition function is given by the Z th power of the dominant eigenvalue. In addition to equation (2) defining the degree of ionization, the fraction ν of segments whose oxygen atoms are involved in hydrogen bonds is

$$\vartheta = \frac{1}{Z} \frac{\partial \ln \Xi}{\partial \ln s} = \frac{\partial \ln \mathbf{m}}{\partial \ln s}. \quad (31)$$

Neither \mathbf{t}_0 , \mathbf{h}_0 nor the vectors \mathbf{u} , \mathbf{v} depend upon s , so that the differentiation of \mathbf{m} with respect to s presents no difficulties. The differentiation displayed in equation (2) requires the derivatives of \mathbf{t}_0 and \mathbf{h}_0 with respect to λ . These can be obtained from the matrix equations

$$\frac{\partial \mathbf{t}_0}{\partial \lambda} = \mathbf{u}^{-1} \left(\frac{\partial C}{\partial \lambda} \right) \mathbf{u}, \quad (32)$$

$$\frac{\partial \mathbf{h}_0}{\partial \lambda} = \mathbf{v}^{-1} \frac{\partial H}{\partial \lambda} \mathbf{v}. \quad (33)$$

5. CALCULATIONS AND RESULTS

The only elements of C and H that are non-zero are those whose indices in binary notation are of the form $C_{abcx, yabc}$ where x and y may be the same or different. The non-zero elements of C and H are the factors which enter the

corresponding term of the partition function when a segment in charge state x is added to a chain ending in four successive segments of charge states y, a, b, c . Included in these factors are the Boltzmann weights of the corresponding terms in the energy expression. For the purposes of numerical calculation we have taken $T=298^\circ\text{K}$, $D=50$. From equation (16) the reciprocal shielding length κ is 0.50, 0.158 and 0.050 \AA^{-1} for salt concentrations of 1.33 M, 0.133 M and 0.0133 M respectively.

As an example of the calculation of a typical element consider the case of 0.133 M salt. We shall construct $H_{1011,0101}$. This matrix element contains the following factors:

(1) λ for the missing hydrogen ion on the added segment ($x=1$), (2) the factor 0.8, the rounded-off value of the Boltzmann weight for the electrostatic interaction between the added charge and the charge on the next preceding segment at distance 10.1 \AA , (3) the factor 0.7, the Boltzmann weight for the interaction of the added charge and the charge on the third preceding segment at a distance of 7.9 \AA .

All other factors are unity since there are no charges on the second and fourth preceding segments and interactions beyond the fourth neighbour are neglected.

Neighbour number	1.33 M NaCl	0.133 M NaCl	0.0133 M NaCl
Helix			
1	0.99	0.8	0.51
2	1.00	0.9	0.64
3	0.97	0.7	0.39
4	0.97	0.6	0.36
Coil			
1, 2, 3	0.99	0.8	0.5
4	1.00	0.95	0.75

Table 1. Boltzmann factors for various neighbours at several salt concentrations.

The actual Boltzmann weights used are given in table 1. Each of the entries represents the interaction between a charge on the added segment and the charge on the indicated one of the four preceding segments. The principal eigenvalue and the left and right eigenvectors were found numerically for C and H for various values of λ by iteration on an arbitrary initial vector. The numerical work was carried out on an IBM 650 automatic computer. From the results obtained, the degrees of ionization were computed using equation (4), also by the use of the IBM 650. The results may be extended by the theorem of Lifson *et al.* [11] which states that the titration curve is symmetrical about its midpoint. Selected examples of the results are shown in table 2.

It should be noted that the course of the transition depends upon the value of the parameter s which expresses the stability of the internal hydrogen bonds. If s is either too large or too small the chain will remain in one or the other of its two forms at all degrees of ionization. To obtain the transition between configurations, s must be selected so that the helix and coil forms are of equal stability somewhere near the midpoint of the titration curve, i.e. $\epsilon_0 = sh_0$ at this point. Once s has been chosen α , v and all other quantities of interest are easily computed by equations (2), (30) and (31).

λ	1·33 M salt		0·133 M salt		0·0133 M salt	
	α coil	α helix	α coil	α helix	α coil	α helix
0·01	0·009894	0·009886	0·00980	0·00971	0·00957	0·00951
0·1	0·09046	0·08986	0·0823	0·0783	0·0710	0·0682
0·4	0·2822	0·2778	0·2263	0·2035	0·1672	0·1548
1·0	0·4926	0·4829	0·3711	0·3229	0·2510	0·2278
2·0	—	—	0·4949	0·4241	0·3210	0·2869
2·5	0·7055	0·6937	0·5354	0·4576	—	—
5·0	0·8263	0·8166	0·6575	0·5625	0·4180	0·3679
10·0	—	—	0·7660	0·6645	0·4930	0·4300
20·0	0·9497	0·9459	0·8524	0·7583	0·5682	0·4922
40·0	—	—	0·9139	0·8384	0·6422	0·5544
80·0	0·9869	0·9858	0·9527	0·9002	—	—
100·0	—	—	0·9614	0·9160	0·7361	0·6364
150·0	0·9929	0·9924	—	—	—	—
400·0	0·9974	0·9971	—	—	—	—

Table 2. Degree of dissociation, α , as a function of the reciprocal activity of hydrogen ion, $\lambda = 10(pH - pK)$.

6. DISCUSSION

It is convenient to separate the discussion of the results into several categories.

6.1. Form of the transition

The formulae of the preceding section show that the system under investigation can be analysed by separation into two parts: the calculation of the titration curve of a polyelectrolyte, and the calculation of the transition behaviour between two forms of the molecule. The transition is determined by the eigenvalue m' , which is the solution of an equation identical in form to the corresponding equation in the case of the uncharged polypeptide. This can be shown by rewriting equation (30) as follows:

$$m' = \frac{1}{2} [1 + s' \pm \{(1 - s')^2 + 4\sigma's'\}^{1/2}] \quad (34)$$

where m' and s' are defined by equations (12) and (13) and

$$\sigma' = \sigma(\mathbf{u}^{-1}\mathbf{v})(\mathbf{v}^{-1}\mathbf{u})(\epsilon_0 + h_0)^2 / 4\epsilon_0^2 h_0^2 \quad (35)$$

Equation (34) is identical with equation (22) of reference [2]. Thus the fact that the molecule is a polyelectrolyte introduces only one novel feature into the description of the transition. This is the presence of a new independent variable which may be taken either as the fraction of charged groups, α , or as λ , which is effectively the reciprocal of the hydrogen ion activity. This variable, however, affects the transition only in so far as it alters the canonical variable, s' .

The variable s' has a significance similar to that attached to s in the non-electrolyte case; s' can be thought of as the equilibrium constant for the addition of a segment, initially in the random form, to the end of a helical section, the molecule being allowed to ionize as it will. From the temperature variation of s' one can compute the net heat of such an addition, ΔH , by means of the equation

$$d\ln s'/dT = \Delta H/RT^2. \quad (36)$$

Data of Doty *et al.* [12] on polyglutamic acid show that the variation of s' with temperature is very slight. If σ is assumed to be approximately the same as the value for polybenzylglutamate [2], equation (36) leads to an estimate of only -50 cal/mol for the heat of addition of a segment to a helical section for polyglutamic acid in the mixture of water, dioxane, and NaCl studied by Doty *et al.* [12].

6.2. The transition and the titration curve

In figure 2 are shown the results of the calculation for 0.133 M salt, with σ assumed to be 10^{-4} and s adjusted to 1.114 , a value that causes the transition to take place in the neighbourhood of 50 per cent ionization. The transition causes a small anomaly in the titration curve. The frequency of alternation of helical and random regions goes through a maximum at the mid-point of the transition, just as in the case of a non-electrolyte; on the average, the maximum has a value of nearly one helical section in every two hundred segments.

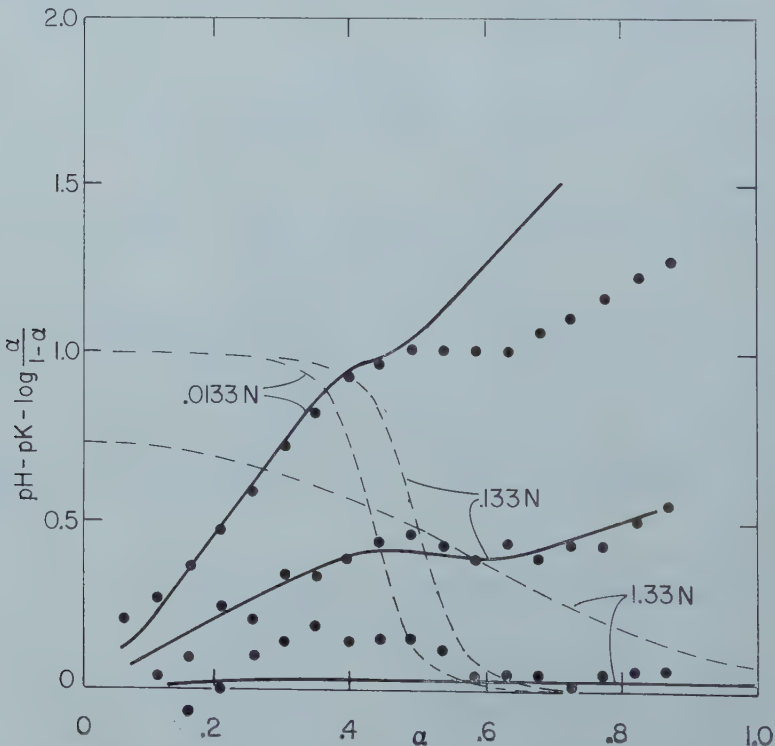


Figure 3. Titration curves plotted as the deviation from the mono-basic acid curve. Solid curves, theoretical titration curves. ●, A. Wada's data on polyglutamic acid (references [12] and [13]). Dashed curves, θ , the fraction of internal hydrogen bonds, calculated theoretically from equation (31) as a function of α .

Since the titration anomaly is rather small when plotted in the usual manner, it is helpful to adopt other representations of the curve that emphasize the changes produced by the transition. Such a representation is shown in figure 3, where the deviation of the pH from the ideal titration curve of a monobasic acid is plotted against the degree of ionization. Here the transition introduces a sigmoid region into the otherwise smoothly rising curve. The fact that the middle of the curve is nearly horizontal is an accidental result of the choice of parameters, and has no special significance.

Also shown in figure 3 are the titration data taken by Wada [13] on polyglutamic acid in various concentrations of salt. The parameter s has been adjusted to give the best agreement with these data. When one remembers that this is the *only* parameter that has been adjusted, the value of $\sigma = 10^{-1}$ having been taken from experiments on polybenzylglutamate in non-aqueous solvents [2], the agreement of the theory and experiment must be considered astonishingly good.

6.3. Titration curves of the individual forms

The agreement just noted between theory and experiment is the more remarkable in view of the approximations in the model. Inspection of figure 3 shows that we have succeeded in reproducing the experimental titration curves for the helical form almost exactly at the two lower salt concentrations, with some modest discrepancies at the highest salt concentration where the non-ideality is small anyway. Though the titration curve of the random form is reproduced somewhat less well, the discrepancies are still minor. It should be remembered that no adjustable parameters have entered these calculations, which are preliminary to and distinct from any discussion of the transition behaviour.

Let us recall the two principal approximations that have been made. These are truncation of the sum over the electrostatic interactions to four members, and the use of the linearized Debye-Hückel theory to represent the interactions. The effect of the first approximation has already been estimated (§ 2); the electrostatic interaction energy should be too small by about a factor of three in the case of 0.0133 M salt. The titration curve should therefore rise about three times more steeply in figure 3 than our calculations. On the other hand the linearization of the Poisson Boltzmann equation is also most serious at the lowest salt concentration, and might be expected to cause deviations in the opposite direction. It is known that in the neighbourhood of a highly charged macro-ion the electrostatic potential greatly exceeds kT , with the result that a thick atmosphere of counter ions surrounds the polymer. Therefore the internal ionic strength exceeds that of the bulk solution and the screening of the charges by the counter ions should be greater than calculated from the Debye-Hückel theory using the overall concentration of counter ions [5]. The magnitude of the counter ion association is dependent upon the geometry of the macromolecule. The calculations of Fuoss, Katchalsky and Lifson [14] for a rod lead to a predicted surface potential of $26kT/q$ for the case of no added external electrolyte. In contrast, the uniform sphere model of Wall and Berkowitz [15] leads to a maximum potential of $1.30kT/q$ in the presence of 0.133 M NaCl and $3.53kT/q$ in the presence of 0.0133 M NaCl. The Wall and Berkowitz model leads to a domain binding of 40–50 per cent whereas the rod geometry would have much more extensive counter ion clustering close to the macro-ion. In both cases the local

clustering is large enough that our neglect of the electrostatic interactions beyond the fourth neighbour may have providentially approximated more closely to the actual screening effects at low salt concentrations than our attempted use of the Debye-Hückel screening constant.

6.4. A simplified approximation

Since sixteenth-order matrices are cumbersome, and, as we have seen, only the principal eigenvalue and its derivatives are important to the results, it becomes interesting to examine the adequacy of simpler approximations. One such approximation consists of lumping the interactions of a charge with all of its neighbours together in one term, as if all the neighbouring charges were combined into a single charge at a single point. The distance of this point is then chosen so that the total electrostatic energy of the completely charged molecule is the same as without the lumping. This problem can then be described by a matrix of order two:

$$\begin{pmatrix} 1 & 1 \\ \lambda & \lambda u \end{pmatrix} \quad (37)$$

where

$$\mathbf{u} = \exp \left[\sum_{i \neq j} \frac{q^2}{DR_{ij}} \exp(-\kappa R_{ij}) \right]. \quad (38)$$

This mathematical problem has been treated extensively before [4, 6]. The degree of ionization, α , is given by

$$\alpha = \frac{\lambda[\mathbf{u} + (\lambda\mathbf{u}^2 - \mathbf{u} + 2)J^{-1/2}]}{\lambda\mathbf{u} + 1 + J^{1/2}} \quad (39)$$

$$J = (\lambda\mathbf{u} - 1)^2 + 4\lambda.$$

We have calculated a few values from this equation, cutting off the sum in equation (38) at the fourth term and using the values of table 1. The results, shown in table 3, are in remarkable agreement with the previous calculations, which used the matrix of sixteenth order.

Part of the explanation of this rather surprising agreement is probably to be found in table 4, where the distribution of charges derived from the sixteenth order matrix, is compared with the random distribution having the same average charge. The matrix distribution was calculated from the products of the corresponding elements in the left and right eigenvectors of the matrix H , which were automatically generated in the course of finding the eigenvalue. The numbers in the random column are simply the products of the probabilities of finding 0 or 1, 0.3355 and 0.6645 respectively. One is immediately struck by the degree to which the two distributions are in agreement. We may conclude that consideration of the detailed features of the charge distribution is not essential to obtaining reasonably accurate results, at least in this case where the individual potentials of interactions are not much larger than kT .

6.5. The determination of σ' from experimental data

From equation (34) we can derive the approximate relation

$$\frac{1}{\sigma'} = 16 \left(\frac{\partial^2 \mathbf{m}'}{\partial s'^2} \right)_{s'=1} \quad (40)$$

at $s' = 1$. By examination of figure 1 and equation (19) it is seen that

$$(\partial \ln \mathbf{m}' / \partial \ln s')$$

is determined by the ratio of the line segments CE and BE. A plot of this ratio

λ	Equation (33)	α_c	α_h	
		Sixteenth order matrix	Equation (33)	Sixteenth order matrix
0.133 M				
2.057	0.500	0.495	—	—
3.304	—	—	0.500	0.50
10	0.772	0.766	0.652	0.664
0.0133 M				
10.2	0.500	0.495	—	—
22.2	—	—	0.500	0.50

Table 3. Comparison of second and sixteenth-order matrix calculations.

Charge configuration†	Probability, matrix calculation	Probability, random distribution	Difference
0000	0.00844	0.01267	0.00423
0001	0.02401	0.02509	0.00108
0010	0.02124	0.02509	0.00385
0011	0.05229	0.04970	0.00259
0100	0.02124	0.02509	0.00385
0101	0.05593	0.04970	0.00623
0110	0.04641	0.04970	0.00329
0111	0.10600	0.09844	0.00756
1000	0.02401	0.02509	0.00108
1001	0.04953	0.04970	0.00017
1010	0.05593	0.04970	0.00623
1011	0.10012	0.09844	0.00168
1100	0.05231	0.04970	0.00261
1101	0.10012	0.09844	0.00168
1110	0.10600	0.09844	0.00756
1111	0.17642	0.19498	0.01856

†0 means no charge, 1 means a charge on one of four successive contiguous groups on one turn of the helical polypeptide.

Table 4. Comparison of exact charge distribution on helix with a random distribution (0.133 M salt, $\lambda = 10$, $\alpha = 0.6645$).

versus s' yields the desired second derivative as the slope at the point $s' = 1$. Figure 4 shows this method is applied to the data represented in figure 1 for the case of 0.0133 M NaCl; we find $\sigma' = 1.4 \times 10^{-3}$. This is to be compared with the value $\sigma = 10^{-4}$ assumed in the theoretical calculations and which was successful when the external salt concentration was 0.133 M NaCl. Uncertainties in the graphical work are probably too small to account for this discrepancy. We have no ready explanation for the disagreement.

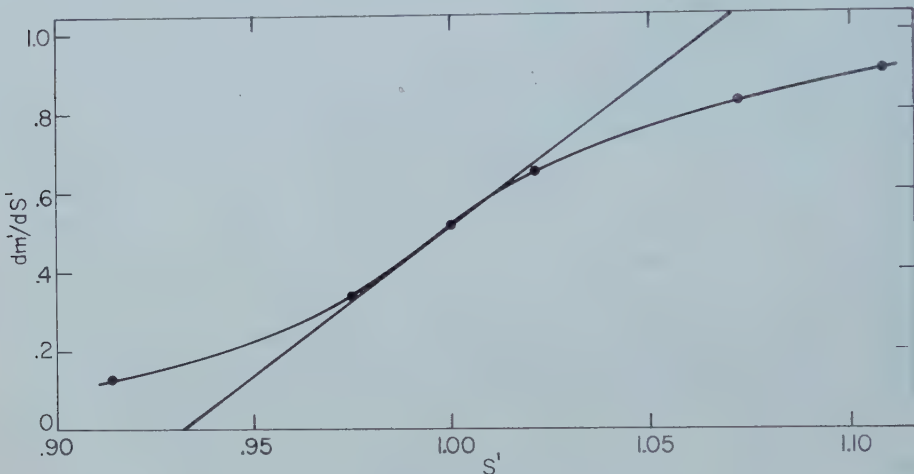


Figure 4. The evaluation of σ' from the slope of dm'/ds' versus s' ; the latter quantities are determined from the data for polyglutamic acid in 0.0133 M salt by means of the construction of figure 1.

6.6. Concluding remarks

In the calculations presented there is a direct analogy between the electrolytic and non-electrolytic transitions which has been exploited at several points. The comparison may be completed by noting that at constant temperature, the pH plays the role for the electrolytic case that the temperature plays for the uncharged polymer. As can be seen clearly from the results, the breadth of the transition depends upon the ionic strength of the medium. This solvent effect may also in principle be mimicked for uncharged polypeptides by the use of media in which the net heat of formation of the hydrogen bond differs with solvent composition.

This latter observation serves as an introduction to one of the subtler approximations of the theory. It has been assumed in the foregoing that the energy of a hydrogen bond is independent of both the charge state of the polyion and the ionic strength. It is not difficult to imagine that a hydrogen bond adjacent to a charge may differ in energy from one far from a charge. It is to be anticipated that such an effect is of secondary importance compared to our ignorance of the local dielectric constant and other pertinent variables.

The statistical theory of the transition offers no difficulties. It is the calculation of the electrostatic free energy of the polyion which is complex. This is due to the non-linearity of the Poisson-Boltzmann equation and the difficulties in handling the coordinate representation of the random coil configurations as well as to basic uncertainties in fundamental parameters. Good agreement between

experiment and theory was obtained. Even if this agreement is regarded as fortuitous, the combination of experimental analysis and statistical theory makes the titration curve a useful way of studying the energetics of the transition.

We would like to call attention to another treatment of this problem by Peller [16].

We wish to thank Miss Ann Warner for carrying out the numerical computations. Dr. J. K. Bragg suggested the perturbation procedure used in § 4.

We are greatly indebted to Dr. A. Wada for permitting the use of his unpublished data in figure 3.

REFERENCES

- [1] DOTY, P. M., HOLTZER, A. M., BRADBURY, A., and BLOUT, E., 1954, *J. Amer. chem. Soc.*, **76**, 4493; DOTY, P. M., and YANG, J. T., 1956, *J. Amer. Chem. Soc.*, **78**, 498.
- [2] ZIMM, B. H., and BRAGG, J. K., 1959, *J. chem. Phys.*, **31**, 526.
- [3] See for example, GUGGENHEIM, E. A., 1952, *Mixtures* (Oxford: University Press).
- [4] HARRIS, F. E., and RICE, S. A., 1954, *J. phys. Chem.*, **58**, 725.
- [5] HARRIS, F. E., and RICE, S. A., 1956, *J. chem. Phys.*, **25**, 955.
- [6] RICE, S. A., and HARRIS, F. E., 1956, *J. chem. Phys.*, **24**, 326.
- [7] PAULING, L., COREY, R., and BRANSON, 1951, *Proc. nat. Acad. Sci., Wash.*, **37**, 205.
- [8] KRAMERS, H. A., and WANNIER, G., 1940, *Phys. Rev.*, **60**, 1.
- [9] MONTROLL, E., 1942, *J. chem. Phys.*, **10**, 706.
- [10] LASETTRE, E. N., and HOWE, J. P., 1941, *J. chem. Phys.*, **9**, 747, 801.
- [11] LIFSON, S., KAUFMAN, B., and LIFSON, H., 1957, *J. chem. Phys.*, **27**, 1356.
- [12] DOTY, P. M., WADA, A., YANG, J. T., and BLOUT, E., 1957, *J. Polym. Sci.*, **23**, 851.
- [13] WADA, A. (to be published).
- [14] FUOSS, R. M., KATCHALSKY, A., and LIFSON, S., 1951, *Proc. nat. Acad. Sci., Wash.*, **37**, 579.
- [15] WALL, F. T., and BERKOWITZ, J., 1957, *J. chem. Phys.*, **26**, 114.
- [16] PELLER, L., 1959, *J. phys. Chem.*, **63**, 1194, 1199.

Helix-coil transformation and titration curve of poly-L-glutamic acid

by AKIYOSHI WADA

Department of Chemistry, Faculty of Science, Ochanomizu University
Bunkyo-ku, Tokyo, Japan

(Received 2 March 1960)

The titration curve of poly-L-glutamic acid was studied in connection with the helix-coil transformation.

In aqueous solution the transformation has its origin in the ionization of the polar group COOH in the side chain. Conversely the ionization and the titration curve of this molecule are affected by the change of the electrostatic interaction produced by its transformation.

It is shown in this report that the experimental result, the titration curve and its modified plot, can be divided into three sections, that is, the ionization of the perfect helix, the region of the helix-coil transformation, and the ionization of the perfect coil.

1. INTRODUCTION

A reversible conversion between two stable molecular forms, the α -helix and the random coil of a synthetic polypeptide in solution has recently been discovered by Doty, Yang, Blout, and their coworkers [1-3]. This conversion, the so-called helix-coil transformation, generally seems to have two types of mechanism. One is the case of the organic solvent in which two components, one of which stabilizes the helical form and other of which stabilizes the coiling form, are mixed. For instance, poly- γ -benzyl-L-glutamate that originally has a stable α -helical configuration in pure ethylene dichloride solution, is found to unfold into the random coiling form in about an 80 volume per cent mixture of dichloroacetic acid in ethylene dichloride. This phenomenon occurs when the dichloroacetic acid breaks the hydrogen bonds, of which there exist four per turn of the helix. It is these hydrogen bonds which stabilize the helical configuration.

The other mechanism, which will be considered in the present study, is the transformation of a polypeptide having ionizable residues in the side chain such as poly-L-glutamic acid (PGA). The PGA molecule has been shown to have the α -helical configuration in the low pH range ($pH < 5$) and to make the transformation to the random coil at a pH of around 5 [4]. The unfolding process is explained as follows. The dissociation of $-\text{COOH}$ in the side chain to $-\text{COO}^-$ and H^+ , which has given rise to an increase of pH in the solution, makes the α -helix unstable because the ionizable residues are distributed much more compactly in the α -helix than in the random coil and the electrostatic interaction leads to an intramolecular transformation from a less stable configuration to a more stable one [3, 5]. In addition to the above electrostatic effect, the helix will be less stable when the polar groups ionize and therefore rupture hydrogen bonds such as

$\text{—COOH} \cdots \text{HOOC}$ — between the side chains, because this kind of hydrogen bond is believed to be partially responsible for the stabilization of the helix [3].

From the above discussion it is clear that the unfolding of the α -helix in aqueous solution should bear a close relation to the ionization of the side chain. Consequently, the ionization of PGA will be affected by the helix-coil transformation to some extent and the titration curve of this polyelectrolyte will then be influenced.

As a brief outline the following picture can be given. In the low pH region, the titration curve will be that of the perfect α -helix. This titration curve will then be deformed when the helix-coil transformation occurs. After the completion of the transformation the titration curve of flexible chain polyelectrolyte will be produced.

This study will offer some useful information for the analysis of the titration curves of proteins since PGA has been considered to be a simplified model of these molecules. Actually several detailed studies have already been made of the protein molecule itself, relating the molecular configuration, ionization and titration curves [6]. In the protein molecules, however, many factors have to be taken into consideration because of the complicated configuration and the variety of the constituent amino acid residues.

2. MATERIAL AND EXPERIMENTAL METHOD

2.1. Material

Poly-L-glutamic acid: Poly- γ -benzyl-L-glutamate (PBG) synthesized by the Blout-Karlson method [7] was dissolved in dry benzene at 60°C. After dry hydrogen bromide bubbling the solution was allowed to stand for about 8 hours [8]. The resultant precipitate, a thick gel, was washed several times with ethyl ether and acetone and dissolved in 5 per cent NaHCO_3 aqueous solution. The solution was dialized against water and lyophilized. The result of the debenzylation was checked by ultra-violet absorption spectra and it was confirmed for the entire sample that the benzyl group does not constitute over 0.5 mole per cent.

The molecular weight of the sample was estimated from the intrinsic viscosity in 0.2 M NaCl aqueous solution of pH 7.3, with the $\log[\eta]$ vs. $\log M_w$ relation (where the absolute molecular weight is determined by light scattering measurement [4]) used for the calibration. All the data are given in table 1.

Starting PBG			PGA		
Polymer number	Initiator	M_w	Polymer number	$[\eta]^{\dagger}$	M_w^{\ddagger}
401	NaOMe	300000	401A	1.20	56000
402	NaOMe	230000	402A	1.06	50000
502	NaOMe	120000	502A	0.50	22000

† Measured in 0.2 M NaCl aq. at pH 7.3.

‡ Molecular weight for pure acid form.

Table 1. Summary of information on poly-L-glutamic acid (PGA) samples.

2.2. pH measurements

A potentiometric glass electrode pH meter model DG-3, accuracy ± 0.02 in pH scale, made by Denkishiki Kagakukeiki Research Laboratory was used for the pH measurements. To remove the undesirable effects of carbon dioxide in the air the measurement was made under a flow of nitrogen gas washed by conc. aq. KOH solution and saturated by solvent vapour. The temperature was controlled at $20^\circ \pm 0.5^\circ\text{C}$ by circulating water around the titration vessel. To see the effect of the ionic strength on the titration curve 2 M , 0.2 M and $0.01\text{ M}†$ aq. NaCl solutions were used as the solvents.

The volume of the alkali (NaOH) or acid (HCl) added was read by a micro burette. When the solution was titrated from the alkaline region by acid, the measurement was delayed until local gelation had completely disappeared ($30 \sim 60$ sec).

2.3. Optical rotation

Optical rotation was observed as a measure of the helix-coil transformation. The measurement was made at the wavelength of $589\text{ m}\mu$ with a Hitachi model AO-1 photoelectric polarimeter, the attachment of the photoelectric ultra-violet spectrometer model EPU-2.

3. EXPERIMENTAL RESULT AND DISCUSSION

The titration curve of PGA measured in 0.2 M NaCl aqueous solution is shown in figure 1. The titrations with HCl and NaOH, that is the forward and backward titrations, coincide when the volume change is taken into consideration.

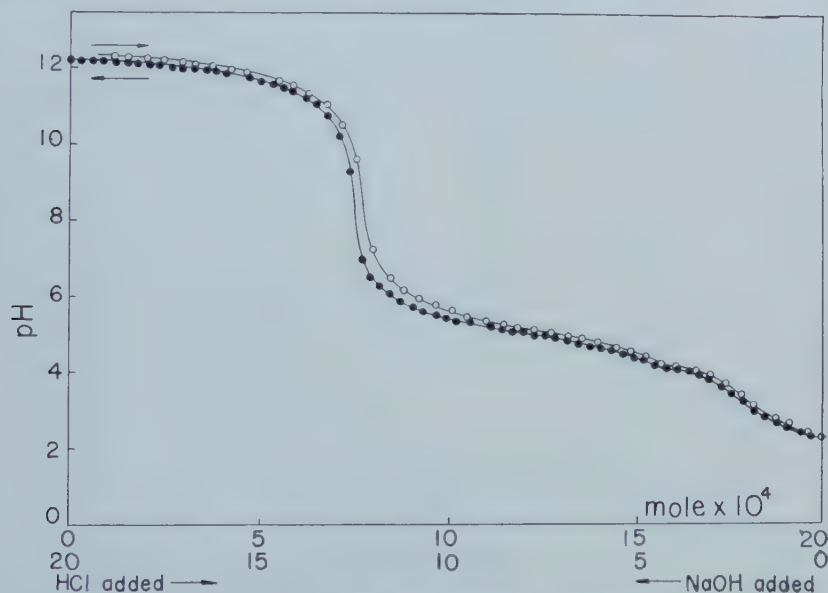


Figure 1. Titration curve of poly-L-glutamic acid (M_w : 22 000) in 0.2 M NaCl aqueous solution at 20°C .

The relation between the degree of ionization and pH is obtained by comparing the titration curve of the solution with that of the solvent as shown in figure 2.

† Average ionic strength. Actually it changes from 0.007 to 0.012 in the course of the titration.

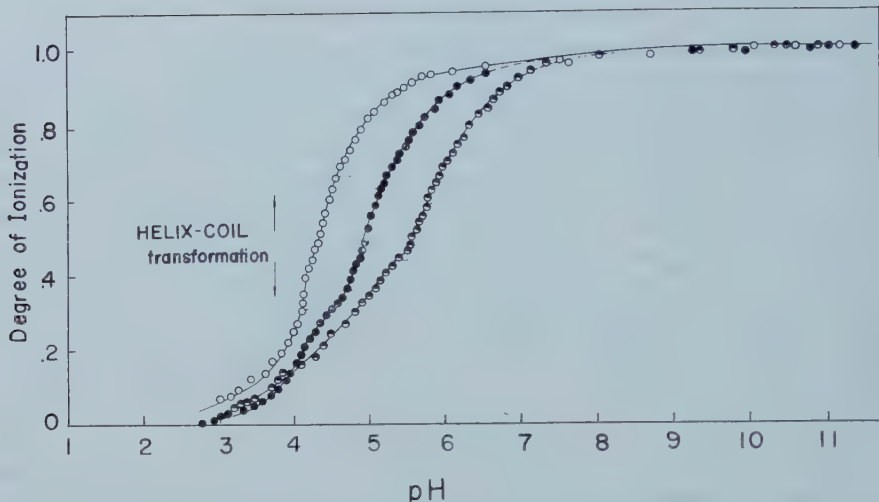


Figure 2. pH dependence of the degree of ionization of poly-L-glutamic acid ($M_w : 22\,000$) in 2 M, 0.2 M and 0.01 M NaCl aqueous solutions at 20°C.

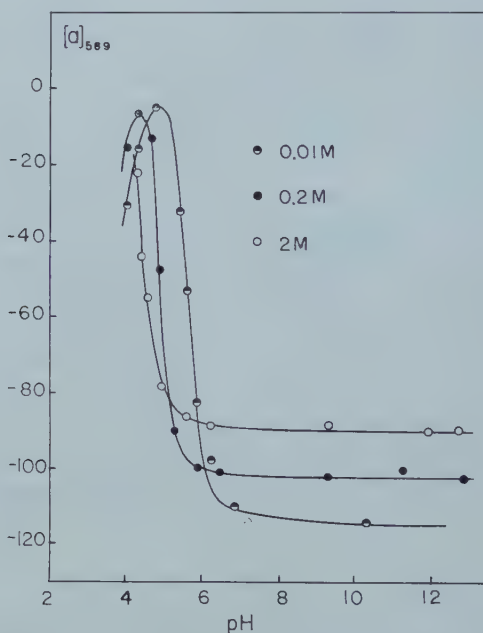


Figure 3. pH dependence of the specific rotation of poly-L-glutamic acid at 20°C at three ionic strength values.

The same kind of plots for the same material in 2 M and 0.01 M NaCl aqueous solution are also shown. Comparing these plots with the result of the optical rotation in figure 3, where the information on the transformation is given, the steep part of the curve which appears in the α vs. pH plot can be understood to be related to the helix-coil transformation as indicated in the figure. Here, because the plot is not appropriate to reveal the transformation, a modified plot was made as follows.

In general, the relation between pH and the degree of ionization, α , of a polyelectrolyte is given by

$$\text{pH} - \log(\alpha/1-\alpha) = pK_0 + 0.434 \cdot F(\alpha)/kT \quad (1)$$

where pK_0 is the intrinsic dissociation constant of the polar group in the polyelectrolyte. $F(\alpha)$ is a function of the degree of ionization and related to the electrostatic interaction between charged sites of a molecule. Physically this function may be interpreted as the increase in the electrostatic free energy when one more unit charge is added to the polyelectrolyte of degree of ionization α . The left side of the equation (1) can be obtained from the titration experiment and the right side, $pK_0 + 0.434 \cdot F(\alpha) \cdot kT$, can then be plotted against the degree of ionization. The modified plots as discussed above are shown in figure 4. The plots seem to give three steps 1, 2 and 3, separated by broken lines. For the time being the corresponding function $F(\alpha)$ for these steps are denoted $F_1(\alpha)$, $F_2(\alpha)$ and $F_3(\alpha)$.[†] $F_1(\alpha)$ corresponds to the charging process of the perfect α -helix and $F_3(\alpha)$ to that of the flexible chain polymer. The second region is related to the helix-coil transformation, which is also clear from the optical rotation measurement, and it should be an interesting subject for theoretical consideration.

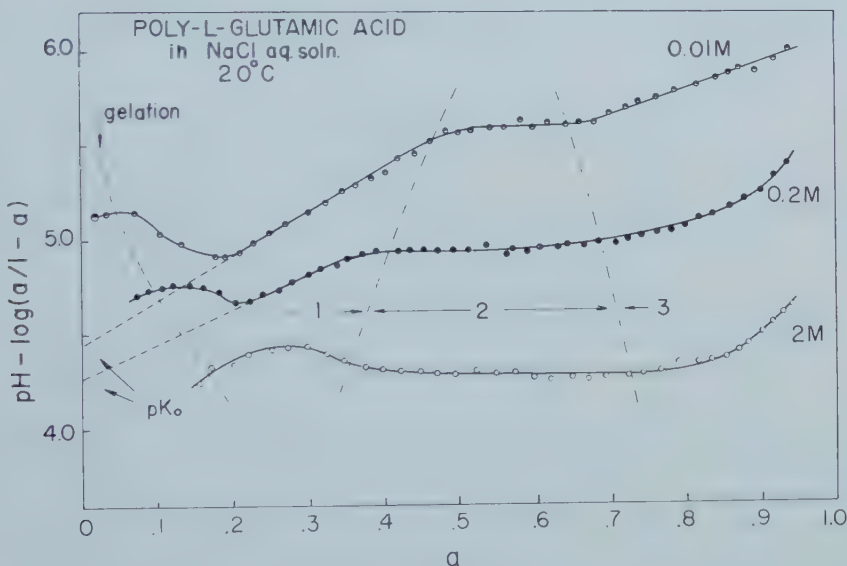


Figure 4. Modified titration curve for poly-L-glutamic acid at three ionic strength values at 20°C.

For $F_1(\alpha)$, when a cylindrical model and smeared-out charge distribution on its surface are assumed as the electrostatic model of the α -helix [9],

$$F_1(\alpha) = 2\alpha\rho(4\pi^2 b^2 l_0/D)K_0(\kappa b)/\kappa b K_1(\kappa b) \quad (2)$$

where l_0 is length of a segment, b the radius of the cylinder, K_0 , K_1 , are Bessel functions of the second kind, $\alpha\rho$ is the charge density on the helix surface, and κ is the inverse radius of the ion atmosphere.

[†] This separation will be a reasonable one when the perfect helix and the perfect coil exist as stable forms in the regions 1 and 3 respectively.

On the other hand the function $F_3(\alpha)$ is given by

$$F_3(\alpha) = \frac{2e^2}{D} \left[\frac{6}{\kappa h_0} - \left(\frac{8}{3\pi} \right)^{1/2} \cdot \frac{h_1}{2} \left(\frac{6}{\kappa h_0^2} \right)^2 \right] \quad (3)$$

with h_0 and h_1 , the root mean square end-to-end separations of the coil in the absence and in the presence of electrostatic interactions, respectively [10].

$F_1(\alpha)$ calculated from equation (2) can be compared with that obtained from the initial slope of the pH-log($\alpha/1-\alpha$) plot. Unfortunately the plot is not a straight line below about 0.2 degree of ionization. This deviation can be explained as due to the change in pK_0 itself owing to the inter and/or intramolecular hydrogen bonding between the side chains [6, 11]. (White gel which may be due to the association by the intermolecular hydrogen bonding often appeared in the titration vessel in the low pH range.) However, the deviation from the straight line was observed at a much higher pH than that at which the precipitation occurred. This reveals the presence of intramolecular hydrogen bonding between the side chain—COOH groups and the stabilization of the helical configuration by such hydrogen bonds is suggested. Now, excluding these regions, the extrapolation of the plot to zero degree of ionization gives 4.25 as the pK_0 in 0.2 M NaCl aq. solution and 4.45 in 0.01 M solution. These values seem to be more plausible than those obtained by other investigators [12]. From the slopes of these extrapolation lines, F_1/α can be determined as shown in table 2 where theoretical values calculated from equation (1) are compared with experiment.

Ionic strength	F_1/α (obs) kcal	F_1/α (calc) kcal†
0.01	3.20	7.92
0.2	2.40	3.72
2.0	—	1.44

† Radius of the cylinder is taken to be 7.4 Å.

Table 2. Observed and calculated values of F_1/α in the NaCl aq. solution of various ionic strengths.

On the other hand, the curves corresponding to $F_3(\alpha)$ seem to be qualitatively reasonable because the slope is smaller than that of the F_1/α 's, except in the region of a high degree of ionization where the experimental error becomes greater. As the electrostatic interaction should be smaller in the coiling form than in the helical one, which has a more compact configuration, it is theoretically required that the F_3/α must be smaller than F_1/α . Although F_3 was given in equation (2), further discussion of this aspect of the titration curve is better deferred since the actual titration behaviour of a polyelectrolyte with a flexible chain is known to be complex.

3.1. Effect of the ionic strength

The effect of the ionic strength on the titration curve and on its modified plot, which has already been shown in figures 2 and 4, is believed to originate in the change of electrostatic interaction due to the change in ionic shielding effect by the small ions. The relative agreement between observed and calculated values of F_1/α listed in table 2 is an indication that the effect of the ionic strength can be explained by such an idea.

3.2. Molecular weight dependence

The molecular weight dependence of the $\text{pH} - \log(\alpha / 1 - \alpha)$ plot was studied by three PGA samples of different molecular weight. No remarkable difference was found in the titration curves of these samples as shown in figure 5. It may be suggested that the helix-coil transformation will occur not on the molecular scale but on the scale of several tens of segments.

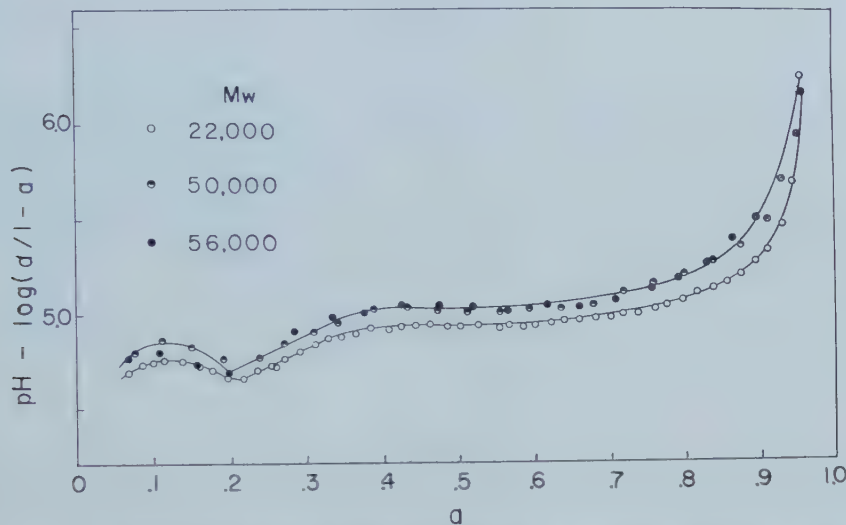


Figure 5. Modified titration curves for samples of different molecular weight poly-L-glutamic acid in 0.2 M NaCl aqueous solution at 20°C.

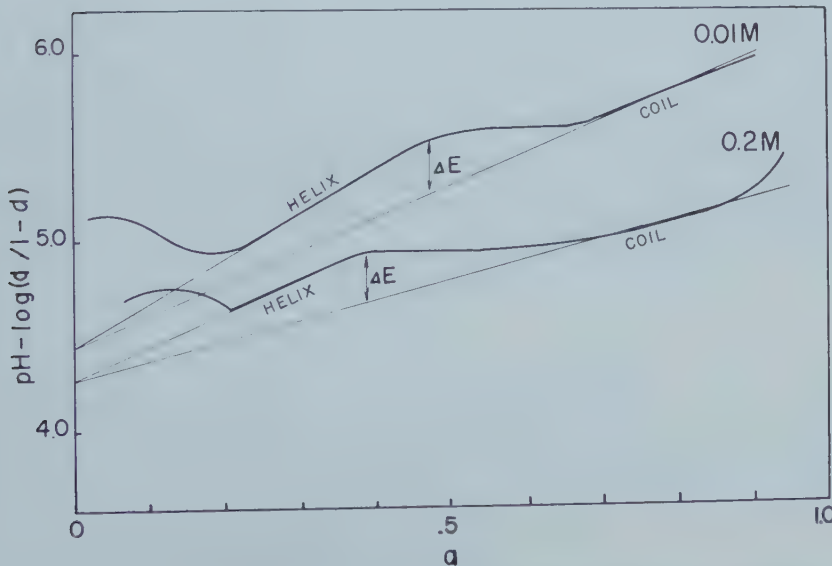


Figure 6. A graphic representation of the energy, ΔE , to initiate the unfolding of the perfect helix.

3.3. Energy needed to unfold the helix

The helix-coil transformation of the PGA molecule in aqueous solution has been postulated to occur when the electrostatic interaction predominates over the stability due to the intramolecular hydrogen bonding in the α -helix. The energy to initiate the unfolding of the α -helix can be estimated as shown in figure 6 from the modified plot. Both of the modified plots, 0·01 M and 0·2 M NaCl aq. solution, give 450~500 cal for that energy. The result seems to be of considerable interest since this value is of just the same order of magnitude as the energy of breaking of one peptide hydrogen bond in water. Here, the suggestion that the helix-coil transformation is an all-or-none process is denied.

The above discussion treats the problem in three separate parts. In other words, the discussion is based on the assumption that the perfect helix and coil can exist over a fairly wide pH range. A general and specific discussion must treat the problem of the unique model of the polypeptide chain in the open system including the helix-coil transformation, side chain hydrogen bondings, and small ion binding effect. Only from such an overall standpoint will the behaviour of the complicated function $F_2(\alpha)$ become clear.

We wish to express our indebtedness to Miss Kazuko Kimura for carrying out the pH measurements reported here.

REFERENCES

- [1] DOTY, P., HOLTZER, A. M., BRADBURY, J. H., and BLOUT, E. R., 1954, *J. Amer. chem. Soc.*, **76**, 4493.
- [2] DOTY, P., and YANG, J. T., 1956, *J. Amer. chem. Soc.*, **78**, 498.
- [3] DOTY, P., WADA, A., YANG, J. T., and BLOUT, E. R., 1957, *J. Polymer Sci.*, **23**, 851.
- [4] WADA, A., and DOTY, P. (unpublished data).
- [5] WADA, A., 1958, *J. chem. Soc. Japan*, **79**, 1393.
- [6] SCHERAGA, H. A., 1959, *Annu. Rev. phys. Chem.*, **10**, 191; TANFORD, C., 1958, *Symposium on Protein Chemistry*, edited by A. Neuberger (New York: John Wiley & Sons Inc.), p. 35.
- [7] BLOUT, E. R., and KARLSON, R. H., 1956, *J. Amer. chem. Soc.*, **78**, 941.
- [8] IDELSON, M., and BLOUT, E. R., 1958, *J. Amer. chem. Soc.*, **80**, 4631.
- [9] HILL, T. L., 1955, *Arch. biochem. biophys.*, **57**, 229.
- [10] KATCHALSKY, M., and LIFSON, S., 1953, *J. polymer. Sci.*, **11**, 409.
- [11] LASKOWSKI, and SCHERAGA, H. A., 1954, *J. Amer. chem. Soc.*, **76**, 6305.
- [12] COHN, E. J., and EDSALL, J. T., 1943, *Proteins, Amino Acids and Peptides* (New York: Reinhold Publishing Corp.).

The use of complex wiggle-beat patterns for the estimation of small splittings in NMR spectra

by J. J. TURNER

University Chemical Laboratory, Lensfield Road, Cambridge

(Received 24 August 1960)

The analysis of the 'wiggle-beat' patterns produced by rapid passage through simple NMR multiplets is modified and extended to permit analysis of beats from multiplets where adjacent signals are not equally separated and where the intensities are not necessarily in the ratio of the appropriate binomial coefficients. The simple example of mono-silane-d₁ (SiH₃D) is illustrated: $J_{HD} = 0.427 \pm 0.003$ c/s. Allowance is also made for the finite time of passage through the signal and the usefulness of this demonstrated by analysing the beat pattern from the asymmetric spectrum of a mixture of SiH₃D and SiH₄. In this way the SiH₄-SiH₃D chemical shift is estimated to be 0.0080 ± 0.0005 p.p.m., the SiH₄ resonance being to low field.

1. INTRODUCTION

If a single NMR signal is traversed rapidly, the main resonance is followed by a series of decaying oscillations [1]. Under these conditions of fairly rapid passage the pattern down the tail is described by

$$V(t) = V_0 \exp(-t/T_2) \cos \frac{1}{2}at^2,$$

where V_0 is the intensity of the signal at $t=0$, T_2 is the transverse relaxation time and a is the rate of change of the Larmor angular velocity in units of sec⁻² [1]. The more refined approach of Jacobsohn and Wangsness [2] modifies this result for conditions near the main resonance but in the work presented here this is not necessary since we examine the pattern fairly well down the tail.

If there are two or more closely spaced signals, interference between the decay patterns produces 'beats' [3]. Reilly [4] has shown that the beat pattern from a multiplet consisting of n closely spaced lines in which the intensities are given by the binomial coefficients is represented by

$$V(t) = 2^{n-1} V_0 \exp(-t/T_2) \cos \left\{ \frac{1}{2}at^2 - \frac{1}{2}(n-1)att_1 \right\} \cos^{n-1} \frac{1}{2}att_1, \quad (1)$$

for rapid passage. Here t_1 is the interval between adjacent signals and is related to the coupling constant (J) by

$$\frac{2\pi}{at_1} = \frac{1}{J}.$$

The first cosine term describes the oscillating decay pattern as for a single signal and the second cosine term gives the shape of the beat envelope. The separation between beat maxima in seconds is clearly equal to $1/J$. The exponential term merely imposes an overall decay on the pattern. Glick and Bothner-By [5] have used this 'wiggle-beat' method to estimate the coupling between the hydrocarbon groupings in ethyl and isopropyl compounds.

The derivation of equation (1) is of relevance to this paper and I present a method of obtaining it.

The decay patterns from an arbitrary series of individual signals can be approximated by

$$\left. \begin{aligned} V_0(t) &= V_0 \exp(-t/T_2) \cos \frac{1}{2}at^2, \\ V_1(t) &= V_1 \exp[-(t-t_1)/T_2] \cos \frac{1}{2}a(t-t_1)^2, \\ &\vdots \\ V_n(t) &= V_n \exp[-(t-t_n)/T_2] \cos \frac{1}{2}a(t-t_n)^2, \\ &\vdots \end{aligned} \right\} \quad (2)$$

The first signal is passed at time $t = 0$, the second at $t = t_1$, the $(n+1)$ th at $t = t_n$ and so on; V_0 , V_1 , V_n , etc. are the intensities of the signals. The resulting decay pattern is given by the sum $V_0(t) + V_1(t) + \dots + V_n(t) + \dots$. Suppose there are three lines in the spectrum, symmetrically placed with intensity ratio $1:2:1$; i.e. so that $t_2 = 2t_1$, $V_0 = V_2 = 1$ and $V_1 = 2$:

$$\begin{aligned} V(t) &= V_0(t) + V_1(t) + V_2(t) \\ &= V_0 \{ \exp(-t/T_2) \cos \frac{1}{2}at^2 + 2 \exp[-(t-t_1)/T_2] \cos \frac{1}{2}a(t-t_1)^2 \\ &\quad + \exp[-(t-2t_1)/T_2] \cos \frac{1}{2}a(t-2t_1)^2 \}. \end{aligned}$$

If t_1/T_2 is small,

$$\begin{aligned} V(t) &= V_0 \exp(-t/T_2) \{ \cos \frac{1}{2}at^2 + 2 \cos \frac{1}{2}a(t-t_1)^2 + \cos \frac{1}{2}a(t-2t_1)^2 \} \\ &= 2V_0 \exp(-t/T_2) \{ \cos(\frac{1}{2}at^2 - \frac{1}{2}att_1 + \frac{1}{4}at_1^2) \cos(\frac{1}{2}att_1 - \frac{3}{4}at_1^2) \\ &\quad + \cos(\frac{1}{2}at^2 - \frac{3}{2}att_1 + \frac{5}{4}at_1^2) \cos(\frac{1}{2}att_1 - \frac{3}{4}at_1^2) \}. \end{aligned}$$

If t_1 is very small, i.e. $\frac{1}{4}at_1^2 = \frac{3}{4}at_1^2 = \frac{5}{4}at_1^2 = 0$,

$$V(t) = 4V_0 \exp(-t/T_2) \cos(\frac{1}{2}at^2 - att_1) \cos^2 \frac{1}{2}att_1.$$

If there are n signals, similar trigonometric rearrangements lead to equation (1). This type of analysis therefore restricts measurements to simple beat patterns caused by signals satisfying three conditions:

- (a) Equal separations between adjacent lines,
- (b) Intensities in the ratio of the appropriate binomial coefficients, and
- (c) Very fast passage to allow neglect of t_n^2 .

This work describes a somewhat different analysis which renders unnecessary conditions (a) and (b); moreover allowance for finite t_n^2 (condition (c)) makes possible a more comprehensive analysis of the beat patterns produced by signals not satisfying (a) and (b).

2. BEAT ANALYSIS IN THE MORE GENERAL CASE

The signals are represented as in equations (2). The resulting decay pattern is again given by $V_0(t) + V_1(t) + \dots + V_n(t) + \dots$. Assuming once more that $\exp(t_n/T_2)$ is approximately unity†,

$$\begin{aligned} V(t) &= \exp(-t/T_2) \{ V_0 \cos \frac{1}{2}at^2 + V_1 \cos \frac{1}{2}a(t-t_1)^2 + \dots + V_n \cos \frac{1}{2}a(t-t_n)^2 + \dots \} \\ &= \exp(-t/T_2) \{ V_0 \cos \frac{1}{2}at^2 + V_1 \cos \frac{1}{2}at^2 \cos(att_1 - \frac{1}{2}at_1^2) + \dots \\ &\quad + V_n \cos \frac{1}{2}at^2 \cos(att_n - \frac{1}{2}at_n^2) + \dots + V_1 \sin \frac{1}{2}at^2 \sin(att_1 - \frac{1}{2}at_1^2) + \dots \\ &\quad + V_n \sin \frac{1}{2}at^2 \sin(att_n - \frac{1}{2}at_n^2) + \dots \} \\ &= \exp(-t/T_2) \{ P \cos \frac{1}{2}at^2 + Q \sin \frac{1}{2}at^2 \}, \end{aligned}$$

† In all the present experimental work t_n/T_2 was less than 0.05 so that $1 < \exp(t_n/T_2) < 1.05$.

where

$$P = V_0 + V_1 \cos(\text{att}_1 - \frac{1}{2} \text{at}_1^2) + \dots + V_n \cos(\text{att}_n - \frac{1}{2} \text{at}_n^2) + \dots$$

and

$$\begin{aligned} Q = & V_1 \sin(\text{att}_1 - \frac{1}{2} \text{at}_1^2) + \dots + V_n \sin(\text{att}_n - \frac{1}{2} \text{at}_n^2) + \dots \\ \therefore V(t) = & \exp(-t/T_2)(P^2 + Q^2)^{1/2} \cos(\frac{1}{2} \text{at}^2 - \tan^{-1} Q/P). \end{aligned} \quad (3)$$

The term $\cos(\frac{1}{2} \text{at}^2 - \tan^{-1} Q/P)$ represents the decay pattern similar to that for a single signal and the term $(P^2 + Q^2)^{1/2}$ represents the beat envelope. It is easily verified that this gives the same result as the previous analysis for an equally separated group of signals with binomial intensities.

In order to estimate the beat envelope, therefore, the expression $(P^2 + Q^2)^{1/2}$ must be evaluated; the form of the answer can be seen immediately if the spectrum is very simple, but for complex spectra the expression must be evaluated numerically by making calculations for small increments in t . In order to calculate $(P^2 + Q^2)^{1/2}$ numerically a programme has been written for the electronic computer EDSAC 2 which calculates the value of the expression for slightly different values of att_1 in fractions of π ; the expression

$$\left[\begin{array}{l} \left\{ V_0 + V_1 \cos(2\pi X_1 t - \pi X_1 t_1) + \dots \right. \\ \left. + V_n \cos\left(2\pi X_1 t \left(\frac{X_n}{X_1}\right) - \pi X_1 t_1 \left(\frac{X_n}{X_1}\right)^2\right) + \dots \right\}^2 \\ + \left\{ V_1 \sin(2\pi X_1 t - \pi X_1 t_1) + \dots \right. \\ \left. + V_n \sin\left(2\pi X_1 t \left(\frac{X_n}{X_1}\right) - \pi X_1 t_1 \left(\frac{X_n}{X_1}\right)^2\right) + \dots \right\}^2 \end{array} \right]^{1/2}$$

is evaluated for values of $2X_1 t$ of 0.1, 0.2, 0.3, etc.: X_n represents the separation in c/s between the first signal and the $(n+1)$ th. In this way the theoretical beat pattern is obtained for any number of signals of any intensity. Moreover there is no need to assume that t_n is small, apart from the stipulation that $\exp(t_n/T_2) \approx 1$. Two examples of the application of this method will now be given.

3. BEAT PATTERN FROM SiH₃D†

The hydrogen resonance spectrum of this compound will clearly be a symmetrical 1:1:1 triplet, with small separation. In fact by sealing the gas under a pressure of about forty atmospheres in a 5 mm o.d. tube containing ½ ml of liquid cyclohexane it was possible to resolve the spectrum of the dissolved gas. The spectra of this compound and the mixture described in the next section were obtained at 40 Mc/s using a Varian Associates V-4300B spectrometer, and V-4012 12 in. electromagnet with flux stabilizer and sample spinning. Direct measurement of the triplet separation by the side-band technique gave a value of $J_{\text{HD}} = 0.45 \pm 0.03$ c/s.

For the 1:1:1 triplet, the expression $(P^2 + Q^2)^{1/2}$ is given by

$$\begin{aligned} & [\{1 + \cos(\text{att}_1 - \frac{1}{2} \text{at}_1^2) + \cos(2\text{att}_1 - 2\text{at}_1^2)\}^2 \\ & + \{\sin(\text{att}_1 - \frac{1}{2} \text{at}_1^2) + \sin(2\text{att}_1 - 2\text{at}_1^2)\}^2]^{1/2}. \end{aligned}$$

† Vaughan and Taylor [6] have examined beats for a 1:1:1 triplet (from CH₃—C≡CD) but present no complete analysis.

Owing to its simplicity this expression can be evaluated algebraically and gives

$$[1 + 4 \cos(at_1 - at_1^2) \cdot \cos \frac{1}{2}at_1^2 + 4 \cos^2(at_1 - at_1^2)]^{1/2}.$$

The form of this is clearly not independent of t_1^2 because of the $\cos \frac{1}{2}at_1^2$ term. (If it is assumed that $t_1 \approx 0$, $(P^2 + Q^2)^{1/2} = \pm [4 \cos^2 \frac{1}{2}at_1 - 1]$). Figure 1(a) shows the beat pattern from SiH_3D , obtained with a sweep rate of 0.07 c/s/sec. Figure 1(b) shows the computed theoretical beat pattern for a 1:1:1 triplet with $X_2 = 2X_1 = 2 \times 0.427$ c/s and $t_1 = 0.03$ sec; since t_1 is small the pattern is almost identical with that obtained if $t_1 = 0$. It is clear that the separation between the large maxima gives the value of X_1 accurately: $X_1 = 0.427 \pm 0.003$ c/s. Reilly [4] comments that the interval between the resonance peak and the first beat maximum is dependent on T_2 . Since, for the spectra presented here, T_2 is large, its effect on this interval is small and the resonance peak coincides almost exactly with the theoretical pattern at $t = 0$.

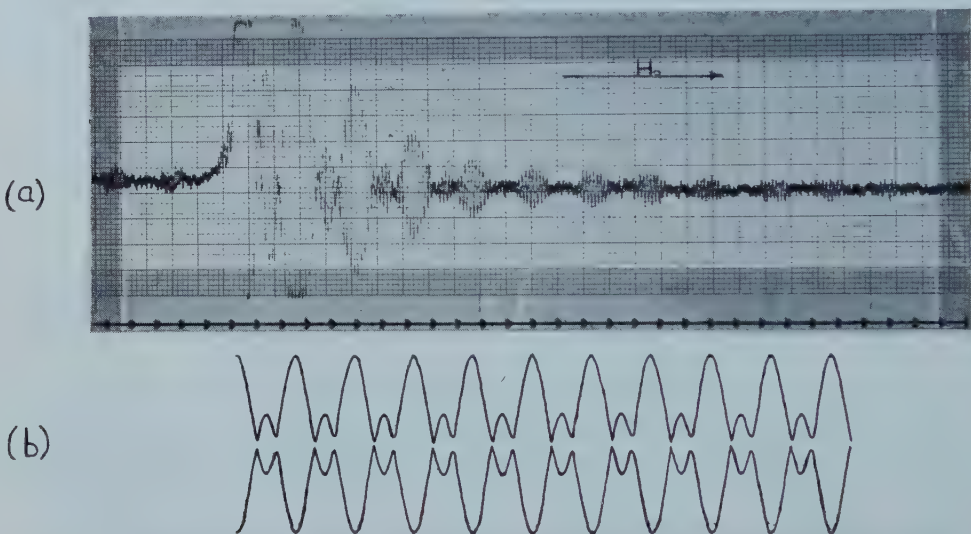


Figure 1. Experimental (a) and theoretical (b) beat patterns from SiH_3D with (a) obtained at a sweep rate of 0.07 c/s/sec, and (b) calculated for parameter values $X_2 = 2X_1 = 2 \times 0.427$; $V_0 = V_1 = V_2 = 1$; $t_1 = 0.03$.

4. BEAT PATTERN FROM A MIXTURE OF SiH_3D AND SiH_4

A mixture of one part of SiH_4 to four parts of SiH_3D was sealed under high pressure in a 5 mm o.d. tube containing liquid cyclohexane. Figure 2 shows the spectrum of the mixture under high resolution. It is clear that the SiH_4 resonance is very close to the low field member of the SiH_3D triplet. The beat pattern from this mixture is shown in figure 3 (a) and (b); 3 (a) is obtained by running through the signal in the direction of decreasing magnetic field and 3 (b) by scanning in the opposite direction, both sweep speeds being approximately 0.07 c/s/sec. The beat patterns are virtually identical apart from a constant intensity factor; this is because of the small t_1 value. It has been possible by analysing this pattern to obtain an accurate value of the $\text{SiH}_3\text{D}-\text{SiH}_4$ chemical shift.

The spectrum consists of a 1:1:1 triplet plus an extra line of intensity 1 somewhere near the low-field triplet line. No simple algebraic analysis is possible and computed patterns were obtained by putting $X_2 = 2X_1 = 2 \times 0.43$ c/s,

$t_1 = 0.03$ sec and giving X_3 various values near to zero. As long as t_1 is small, the increase and decrease patterns are identical in spite of the asymmetry in the spectrum. It was possible by comparing experimental and theoretical patterns to obtain a value for X_3 of 0.11 ± 0.03 . Figure 3 (c) shows the calculated pattern with $X_3 = 0.11$ c/s.

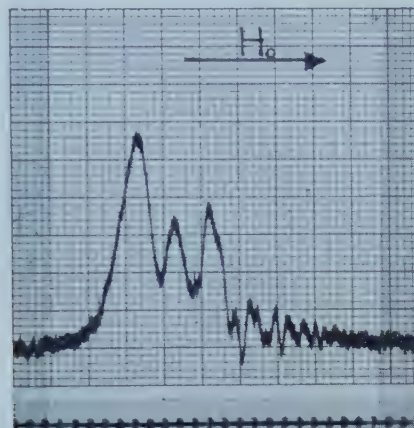


Figure 2. Experimental high resolution spectrum of a 4 : 1 molar mixture of SiH_3D and SiH_4 .

The asymmetry of the spectrum provides the justification for retaining the expressions involving t_1 since, as t_1 is increased, the beat pattern not only changes but becomes dependent on the direction of scan. This is very useful, since a considerably more accurate value of X_3 is obtained simply by slowing the sweep rate and examining the new beat patterns. Figure 4 illustrates this technique. Figures (a), (a'), (b), (b') show, at two different levels of amplification, the experimental patterns run with increasing (a), (a') and decreasing (b), (b') field at a speed of 0.7 c.s.⁻¹—the asymmetry in the pattern is clearly seen. Figure 4 (c → h) shows the theoretical patterns for the values of X_3 shown. By careful comparison it can be seen that X_3 is nearer to 0.11 (or 0.75 if decreasing)—figures 4 (e) and 4 (f)—than either 0.10 or 0.12 so that $X_3 = 0.11 \pm 0.01$ c/s and hence, given $X_1 = 0.43$, the $\text{SiH}_3\text{D}-\text{SiH}_4$ chemical shift is 0.32 ± 0.02 c/s, the SiH_4 resonance being to lower field.

The extreme sensitivity of the slow sweep patterns to the position of the fourth signal makes it virtually impossible to start the beat analysis with these patterns. Hence the technique of first performing an approximate analysis on the less sensitive fast sweep rate patterns.

As a considerable degree of accuracy is claimed for this chemical shift value, it is worth while to examine some possible sources of error.

(1) A 1 : 4 mixture of SiH_4 and SiH_3D results in a four-line spectrum, each line having approximately the same intensity. The error in the mixture ratio is probably less than 5 per cent but a series of spectra were computed with the SiH_4 peak having a relative intensity of 1.25 and 0.75, the other parameters having the values quoted previously. The effect of thus altering the SiH_4 peak intensity was negligible, the position of the beat maxima and minima being unaltered and their intensities only slightly modified.

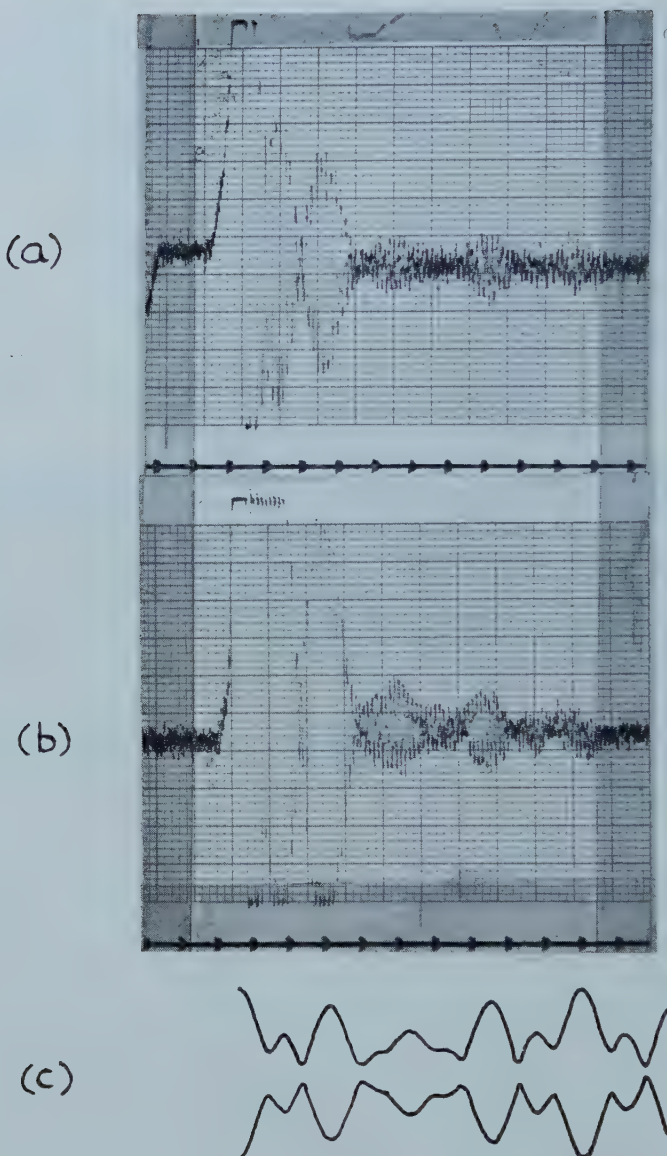


Figure 3. Experimental (a), (b) and theoretical (c) beat patterns from $\text{SiH}_3\text{D}/\text{SiH}_4$ mixture with (a) and (b) obtained by scanning in the direction of decreasing (a) and increasing (b) magnetic field, and (c) calculated for parameter values:

$$X_2 = 2X_1 = 2 \times 0.43; V_0 = V_1 = V_2 = V_3 = 1; t_1 = 0.03; X_3 = 0.11.$$

(2) As the calculations use a finite value of t_1 , it is necessary to know how an error in this parameter affects the spectrum. The sweep speed was estimated by scanning the spectrum of ethyl alcohol at the same rate and it is unlikely that t_1 for the slow runs is in error by more than 0.05 sec. Spectra were computed, for a 1:1:1+1 system, for t_1 having values 0.2 sec and 0.5 sec instead of 0.3 sec. The spectra with $t_1 = 0.2$ sec were indistinguishable from the corresponding ones with $t_1 = 0.3$ sec but there was a *slight* difference between spectra with $t_1 = 0.3$ sec and $t_1 = 0.5$ sec.

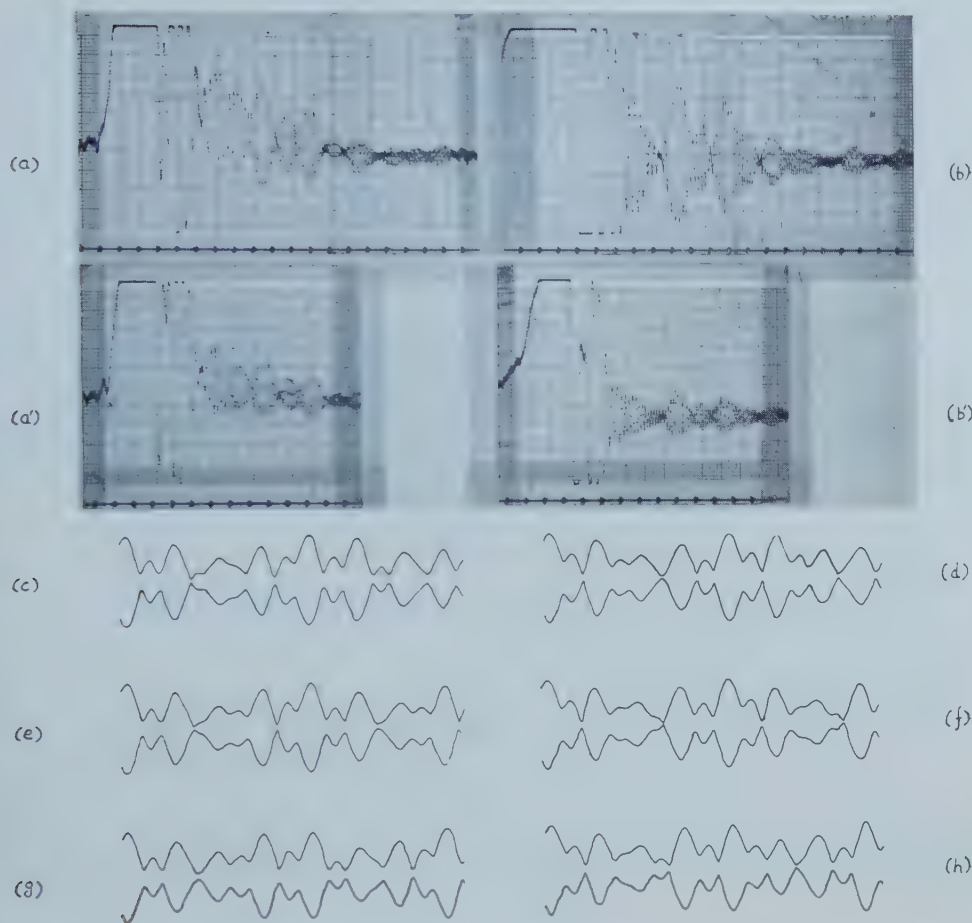


Figure 4. Experimental (a), (a'), (b), (b') and theoretical (c-h) beat patterns for $\text{SiH}_3\text{D}/\text{SiH}_4$ mixture with (a), (a'), (b), (b') obtained by scanning in the direction of increasing (a), (a') and decreasing (b), (b') magnetic field, and (c-h) calculated for parameter values: $X_2=2X_1=2 \times 0.43$; $V_0=V_1=V_2=V_3=1$; $t_1=0.3$; $X_3=0.10$ (c), 0.76 (d), 0.11 (e), 0.75 (f), 0.12 (g), 0.74 (h).

Points (1) and (2) show clearly that the beat pattern is much more sensitive to changes in the position of the SiH_4 resonance with respect to the SiH_3D triplet than either to its relative intensity or the sweep rate.

(3) Well down the tail of the beat pattern, where the exponential decay has only a slight effect, it is comparatively easy to compare the observed spectrum with the calculated pattern, but near the main resonance it is more difficult to estimate the correct relative intensities of the beat pattern. Rough calculations were performed to make allowance for such effects but this did not lead to any change in the value of X_3 and the intensities corresponded to a good approximation with the theoretical values. It would of course have been possible to modify the computer programme to allow for the exponential decay. This was thought unnecessary in view of the fact that the field quality is constantly changing so that the exponential factor varies in magnitude.

(4) As a final check on the method, the computer programme was modified to evaluate $\cos(\frac{1}{2}at^2 - \tan^{-1} Q/P)$ —actually the computer calculated $(P^2 + Q^2)^{-1/2}$ $(P \cos \frac{1}{2}at^2 + Q \sin \frac{1}{2}at^2)$ —and the calculated curves were identical in form to the wiggle pattern caused by a single resonance.

Thus it is possible to use complex beat patterns to evaluate separations within a non-symmetrical, non-binomial spectrum. This method has been extended to both pure SiHD₃ and a mixture of SiH₄ and SiHD₃ and the results are in the process of publication.

I should like to thank Dr. N. Sheppard for help and encouragement, Dr. E. A. V. Ebsworth for the preparation and sealing of the silicon compounds and Mr. D. Lynden-Bell for a useful discussion. I am also indebted to the Department of Scientific and Industrial Research for a research grant, King's College, Cambridge, for a Prize Fellowship and Dr. M. V. Wilkes, F.R.S., of the University Mathematical Laboratory, for computing facilities.

REFERENCES

- [1] BLOEMBERGEN, N., PURCELL, E. M., and POUND, R. V., 1948, *Phys. Rev.*, **73**, 679.
BLOEMBERGEN, N., 1948, *Nuclear Magnetic Relaxation* (The Hague: Nijhoff).
- [2] JACOBSON, B. A., and WANGNESS, R. K., 1948, *Phys. Rev.*, **73**, 942.
- [3] BENÉ, G. J., DENIS, P. M., and EXTERMANN, R. C., 1951, *Physica*, **17**, 308.
- [4] REILLY, C. A., 1956, *J. chem. Phys.*, **25**, 604.
- [5] GLICK, R. E., and BOTHNER-BY, A. A., 1956, *J. chem. Phys.*, **25**, 362.
- [6] VAUGHAN, W. R., and TAYLOR, R. C., 1959, *J. chem. Phys.*, **31**, 1425.

Fluorescence self-quenching in aromatic vapours; the role of excited dimers

by B. STEVENS and P. J. McCARTIN

Department of Chemistry, The University, Sheffield 10

(Received 22 July 1960)

At temperatures sufficiently high to produce an appreciable pressure of 9, 10-diphenylanthracene, perylene or pyrene, the quantum yield of fluorescence is found to be independent of vapour pressure. The negative temperature coefficient of self-quenching in anthracene vapour is explained in terms of the dissociation of an excited dimer which is also responsible for delayed fluorescence.

The pressure-dependence of the excited dimer lifetime at low pressures is shown to be consistent with a pressure-independent quenching constant if the second-order dissociation of the excited dimer becomes first-order at higher pressures.

1. INTRODUCTION

The efficient reversible quenching of excited aromatic molecules $^1F^*$ by the paramagnetic gases NO and O_2 is attributed [1] to a collision-induced inter-system crossing represented by



where 3F is the lowest triplet state of the aromatic molecule. Reversible quenching by diamagnetic molecules 1X is not observed since the corresponding process



would lead to a change in the overall spin angular momentum. A similar interpretation of triplet-state quenching by paramagnetic ions in solution has been recently given by Porter and Wright [2].

An important exception to this theory of reversible quenching is provided by self-quenching, which can have a high efficiency although the quenching molecule in this case is the singlet ground state. Investigations of self-quenching in solution [3] have shown that although the complexity of the phenomenon varies with the nature of the solute, dimeric association complexes play an important role, whilst the mechanisms recently put forward to account for delayed fluorescence [4] and the negative temperature-coefficient of self-quenching [5] in the vapour phase are also based on the existence of an excited dimer even at temperatures in excess of 300°C. The present investigation was undertaken with a view to establishing a detailed mechanism for self-quenching in the gas phase and relating this to the phenomenon of delayed fluorescence.

2. EXPERIMENTAL

The measured intensity $f(c)$ of fluorescence is related to the quantum yield of fluorescence $\gamma(c)$ at vapour concentration c by

$$f(c) = AI(c)\gamma(c) \quad (1)$$

where A is an instrumental constant assumed to be independent of concentration under the conditions of measurement [6] and $I(c)$, the intensity of absorbed radiation, is given by

$$I(c) = I_0[1 - \exp(-\epsilon cd)]. \quad (2)$$

I_0 is the incident light intensity, ϵ the extinction coefficient and d the absorption path of the fluorescent vapour. If quenching follows a Stern-Volmer mechanism then

$$\gamma(c) = 1/(1 + Kc) \quad (3)$$

where K is the self-quenching constant. Rearrangement of expressions (1), (2) and (3) provides the relationship

$$[1 - \exp(-\epsilon cd)]/f(c) = (1 + Kc)/AI_0 \quad (4)$$

and K is obtained as the slope/intercept ratio when the experimental quantity on the left-hand side of (4) is plotted against the vapour concentration c . In this way one of us [7] obtained

$K = 1280 \text{ l/mole}$ for anthracene at 300°C using the independently measured value

$$\epsilon_{10} = 2300 \text{ l/mole}^{-1} \text{ cm}^{-1} \text{ at } 366 \text{ m}\mu \text{ and } 300^\circ\text{C}.$$

More recently Härdtl and Scharmann [5] have measured K under conditions of complete light absorption when equation (4) becomes

$$1/f(c) = (1 + Kc)/AI_0 \quad (5)$$

and obtained the much lower values for anthracene given in the table. The difference is attributed to an error in the measured extinction coefficient for which these workers obtain the value

$$\epsilon = 6800 \text{ l/mole}^{-1} \text{ cm}^{-1} \text{ at } 366 \text{ m}\mu.$$

Molecule	$T^\circ\text{C}$	K (l/mole)	Reference
Anthracene	300	1280 ± 100	[7]
	280	370 ± 20	[5]
	310	300 ± 20	[5]
	340	240 ± 20	[5]
	230	630 ± 50	
	230	$\dagger 580 \pm 50$	
	256	$\dagger 510 \pm 50$	
	275	450 ± 30	
	323	310 ± 30	
	323	240 ± 30	
9, 10-diphenyl anthracene	300	1760 ± 200	[7]
	344	0 ± 40	This work
Perylene	378	0 ± 40	This work
Pyrene	390	0 ± 40	This work

† In presence of 100 mm CO₂.

Although this discrepancy in ϵ is not as serious as suggested, since the latter value corresponds to

$$\epsilon_{10} = 2900 \text{ l mole}^{-1} \text{ cm}^{-1},$$

it is nevertheless sufficient to account for the difference in quenching constants obtained.

The use of equation (5) restricts the lower concentration limit to that at which absorption of the incident radiation is complete whilst an upper limit is determined by the temperature required to prevent condensation together with the experimental difficulties in measuring fluorescence intensities at high temperatures and the possibility of thermal decomposition of the vapour itself. The use of equation (4) increases the available concentration range but introduces possible errors in the independent measurement of ϵ . It was therefore decided to measure the fraction of light absorbed and the fluorescence intensity simultaneously using the same cell.

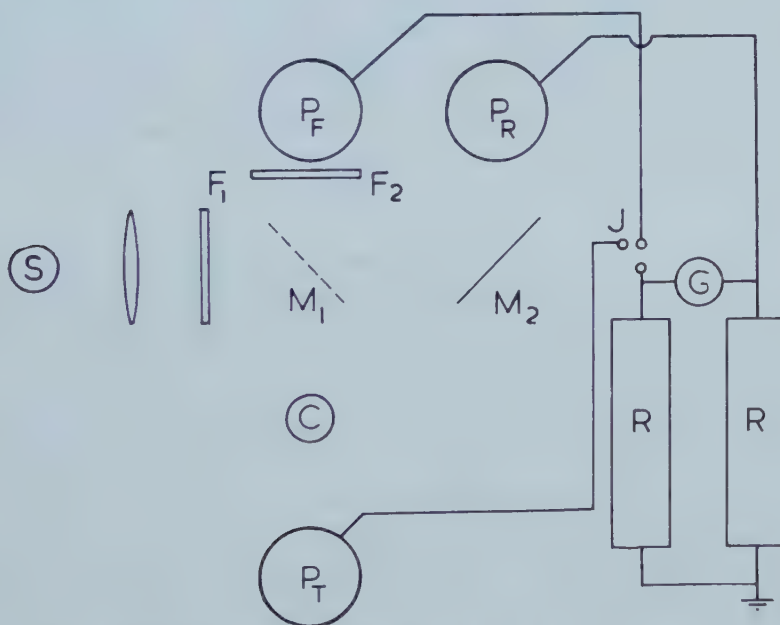


Figure 1. Plan of apparatus for self-quenching. S, Hg arc; M₁, half-silvered mirror; M₂, glass plate; F₁ and F₂, filters; P_F, P_R and P_T-RCA 931 A photomultipliers; J, switch; G, mirror galvanometer; R, decade resistances; C, cell.

Figure 1 shows a plan of the optical arrangement used and is self-explanatory. The pressure of vapour in the cell was controlled as previously described [8] and, by means of the switch J, the ratios of the transmitted light intensity or of the fluorescence intensity to the intensity of the reference beam could be measured almost simultaneously.

Some of the light reflected from the front of the cell was transmitted by the filter F₂ and contributed to the signal given by the photomultiplier P_F; a correction was applied to this signal by subtracting the signal at zero pressure. It was found that light reflected from the back surface of the cell was absorbed by the vapour so that the appropriate correction to the total signal P_F was impossible to assess; this reflection was therefore reduced to a minimum by inserting a blackened

aluminium plate pierced with a small hole to allow the intensity of transmitted light to be measured. The 365 m μ lines isolated from a stabilized 150 watt high-pressure mercury vapour lamp (Mazda MBL/D) were used to excite the fluorescence in each case.

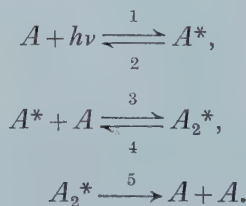
Anthracene (m.p. 217°C) was purified as previously described [9]; 9, 10-diphenyl anthracene (m.p. 248–250°C) was supplied by L. Light and Co. and not purified further. Light's pyrene (white puriss) was used without purification but their perylene was subjected to repeated chromatography on an activated alumina column and the final pure material melted at 269°C.

3. RESULTS

Excellent linear plots of $I(c)/f(c)$ against the vapour concentration c , calculated from published vapour pressure data [8, 10], were obtained for the compounds investigated; values of the self-quenching constants K given by the slope/intercept ratios are collected in the table together with previous data. The constants obtained for anthracene agree well with the results of Härdtl and Scharmann [5] whilst the conflicting data obtained previously for anthracene and 9, 10-diphenylanthracene [7] serve to illustrate the importance of simultaneous absorption and fluorescence intensity measurements when absorption is not complete.

4. DISCUSSION

The negative temperature-coefficient of self-quenching in anthracene vapour requires the presence of an energy-dependent process which competes with self-quenching. It has been suggested [5] that this is the dissociation of the electronically excited dimer A_2^* to regenerate anthracene molecules in the fluorescent and ground states A^* and A ; the same process is believed to be responsible for delayed fluorescence observed under similar conditions [4], and the overall photokinetic scheme may be written



Williams found that the lifetime τ_D of delayed anthracene fluorescence is inversely proportional to the anthracene pressure in the region 0.5 to 3.0 mm indicating that process 4 is second-order with

$$\tau_D = 1/k_4[A]. \quad (6)$$

If this is the case the quenching constant should also exhibit a pressure-dependence which was not observed in the pressure range employed (≥ 30 mm). However, extrapolation of τ_D to infinite pressure ($1/p = 0$) leads to the finite value (figure 4, ref. [4])

$$\tau_D \approx 1/(7 \times 10^3) \text{ sec at } 220^\circ\text{C},$$

which is inconsistent with equation (6) unless process 4 becomes first-order at higher pressures†; the decrease in τ_D observed in the presence of helium in the low pressure region is consistent with such an interpretation and the detailed kinetic scheme may be written

		rate constant at 220°C
$A + h\nu \longrightarrow A^*$	1.	
$A^* \longrightarrow A + h\nu'$	2.	$2.5 \times 10^8 \text{ sec}^{-1}$
$A^* + A \longrightarrow A_2^{*''}$	6.	$4.2 \times 10^{11} \text{ l mole}^{-1} \text{ sec}^{-1}$
$A_2^{*''} \longrightarrow A^* + A$	7.	$1.9 \times 10^8 \text{ sec}^{-1}$
$A_2^{*''} + A \longrightarrow A_2^* + A$	8.	$5.6 \times 10^{11} \text{ l mole}^{-1} \text{ sec}^{-1}$
$A_2^* + A \longrightarrow A_2^{*''} + A$	9.	$2.1 \times 10^7 \text{ l mole}^{-1} \text{ sec}^{-1}$
$A_2^* \longrightarrow A + A$	5.	$4.8 \times 10^3 \text{ sec}^{-1}$

where $A_2^{*''}$ denotes an excited dimer with sufficient vibrational energy to dissociate. Apart from the quenching process 5 this scheme was suggested by Williams to account for the increase in delayed fluorescence intensity with vapour pressure.

Expression (6) now becomes

$$\frac{1}{\tau_D} = \frac{k_7 k_9 [A]}{k_7 + k_8 [A]} \quad (7)$$

$\approx k_9 [A]$ at low pressures,

whence from the appropriate plot of Williams' data

$$k_9 = 2.1 \times 10^7 \text{ l mole}^{-1} \text{ sec}^{-1} \text{ at } 220^\circ\text{C}.$$

At infinite pressure

$$\frac{1}{\tau_D} = \frac{k_7 k_9}{k_8} \approx 7 \times 10^3 \text{ sec}^{-1} \text{ at } 220^\circ\text{C}$$

and

$$k_7 = 1.9 \times 10^8 \text{ sec}^{-1} \text{ at } 220^\circ\text{C}$$

if we assume that

$$k_8 = Z_8 = 5.6 \times 10^{11} \text{ l mole}^{-1} \text{ sec}^{-1} \text{ at } 220^\circ\text{C}.$$

(The collision number Z_8 is calculated from the simple kinetic theory expression using collision diameters of 8.0 Å and 12.0 Å for A and $A_2^{*''}$ respectively.)

Using these values of k_7 , k_8 and k_9 , $1/\tau_D$ calculated from equation (7) is plotted against $[A]$ on a logarithmic scale in figure 2. Since the lowest concentrations employed for self-quenching are of the order of 3×10^{-3} moles/l, except at the lowest temperatures where an inert gas is added, $k_8 [A] \geq 9k_7$ and process 4 may be treated as first-order in this region.

Under photostationary conditions processes 1, 2, 5–9 lead to the following expression for the overall quantum yield of fluorescence γ .

$$\frac{1}{\gamma} = 1 + \frac{k_5 k_6 k_8 [A]^2}{k_2 k_5 (k_7 + k_8 [A]) + k_2 k_7 k_9 [A]}$$

whence from (3) with $k_8 [A] \gg k_7$

$$K = \frac{k_5 k_6 k_8}{k_2 k_5 k_8 + k_2 k_7 k_9}. \quad (8)$$

† Preliminary investigations using the flash-photometric technique indicate that τ_D is independent of pressure for perylene and pyrene except at the lowest pressures. Unfortunately at the temperatures required to obtain a measurable intensity of delayed fluorescence in anthracene vapour, τ_D was too short for this to be resolved from the photoflash.

Equation (8) may be rearranged to

$$\left(\frac{\tau Z_6}{K} - 1 \right) = \frac{k_7 k_9}{k_5 k_8} \quad (9)$$

where

$$\tau = 1/k_2 \approx 4.0 \times 10^{-9} \text{ sec}$$

$$Z_6 = k_6 = 1.9 \times 10^{10} T^{1/2} \text{ l mole}^{-1} \text{ sec}^{-1},$$

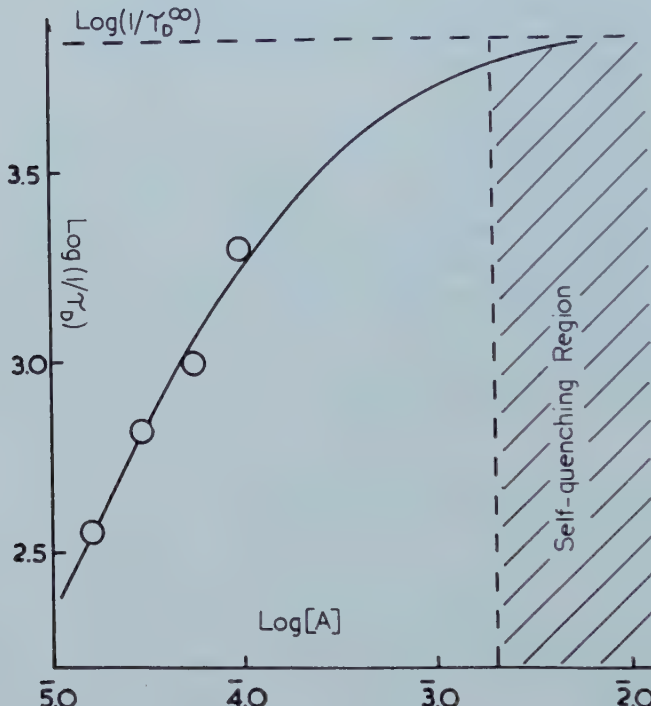


Figure 2. Plot of $\log(1/\tau_D^\infty)$ calculated from equation (7) as a function of anthracene vapour concentration. Circles represent Williams' data [4].

and from the plot of $\log(\tau Z_6/K - 1)$ against $1/T$ (figure 3) it is found that

$$\frac{k_7 k_9}{k_5 k_8} = 3.6 \times 10^3 \exp(-7600/RT). \quad (10)$$

Consequently $k_5 = 4.8 \times 10^3 \text{ sec}^{-1}$ at 220°C .

The activation energy in (10) is the difference in energy required for processes 4 (or 7 and 9) and 5, i.e.

$$E_4 - E_5 = 7.6 \text{ k cal.}$$

Since this is of the order of the energy of formation of the excited dimer which according to theoretical calculations is some few tenths of an electron volt [11], it seems probable that E_5 is very small or zero. If E_5 were appreciable process 5 would be expected to be very much slower in solution at room temperature whereas it is found to be some 10^5 times faster under these conditions [3]; this may be due to a solvent perturbation which reduces the symmetry restriction discussed below.

The relationship between self-quenching and delayed fluorescence in anthracene is illustrated by the potential energy diagram shown in figure 4. If the excited dimer is represented by the wave-function ψ_D^* which is a combination of the functions ψ_1^* and ψ_2 representing the colliding excited and unexcited molecules, i.e.

$$\psi_D^* = \psi_1^* \psi_2 \pm \psi_1 \psi_2^*, \quad (11)$$

the two states designated ${}^+_1A_2^*$ and ${}^-_1A_2^*$ arise depending on whether the + or - sign is operative in (11). Radiative transitions from the metastable ${}^-_1A_2^*$ state to the ground state are orbitally forbidden if the former has a centre of symmetry associated with a parallel orientation of the planar molecules [12], so that dimer emission will not be observed in the presence of the relatively efficient competing

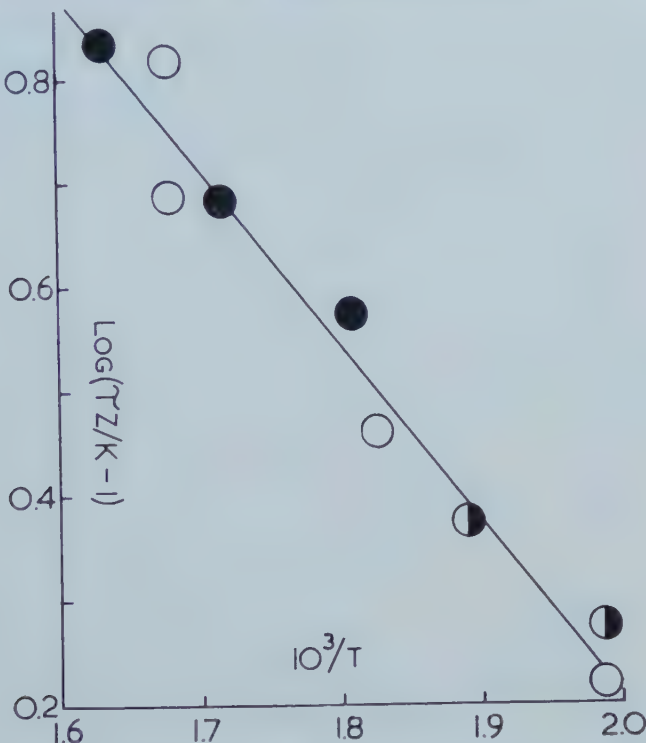


Figure 3. Arrhenius plot of anthracene self-quenching data according to equation (9). ●, data of Härdtl and Scharmann, ○, this work, ◐, 10 cm CO₂ added.

processes 4 and 5. Since it is unlikely that the energy of the repulsive ground state ${}^+_1A_2$ is sufficient at the inter-planar distance ($\sim 3 \text{ \AA}^{11}$) in ${}^-_1A_2^*$ to allow crossing of the two curves in this region, it is conceivable that the quenching process 5 involves a radiationless transition to the repulsive state (shown as ${}^+_3A_2$ in figure 4) which leads to the formation of triplet and ground state anthracene molecules; the low value of k_5 is consistent with such an intersystem crossing which is also forbidden by symmetry, and the overall quenching process can be regarded as



which is promoted by a collision of particularly long duration.

The absence of self-quenching in 9, 10-diphenylanthracene, perylene and pyrene indicates that $k_4 \gg k_5$ at the temperatures required to obtain appreciable vapour pressures. Since the lifetime of delayed fluorescence in perylene and pyrene vapours is of the order of that observed for anthracene [4], this inequality is almost certainly due to a very much smaller value of k_5 in these cases; indeed internal quenching of the excited pyrene dimer is so slow that dimer emission is observed in solution [13] with a decay constant of $5 \times 10^2 \text{ sec}^{-1}$ [14].

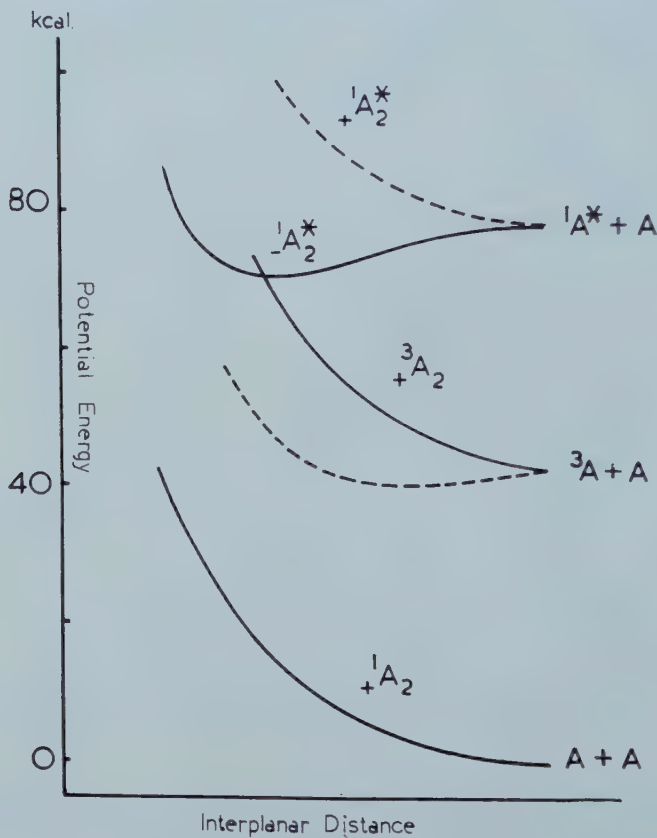


Figure 4. Potential energy diagram for anthracene dimer.

The persistence of the excited dimer in the gas phase at temperatures in excess of 200°C when it requires an activation energy of the order of 8 kcal for dissociation must be largely due to the very low efficiency of the collisional activation process 9. If the least favourable case of one contributing oscillator is assumed, then since

$$k_9 = P Z_9 \exp(-7600/RT) = 2.1 \times 10^7 \text{ mole}^{-1} \text{ sec}^{-1} \text{ at } 220^\circ\text{C},$$

the collisional activation efficiency $P \sim 0.1$. The alternative is a much higher activation energy for dissociation which at present is unlikely on theoretical grounds and which would require that $E_5 \gg 0$.

The authors would like to thank Professors H. C. Longuet-Higgins, F.R.S., and G. J. Hoijtink for constructive discussions; they also acknowledge a grant-in-aid from the Royal Society and a maintenance grant from D.S.I.R. (P.J.M.).

REFERENCES

- [1] TERENIN, A., 1943, *Acta phys.-chim. URSS.*, **18**, 210.
- [2] PORTER, G., and WRIGHT, M. R., 1959, *Disc. Faraday Soc.*, **27**, 18.
- [3] DAMMERS-DE KLERK, A., 1958, *Mol. Phys.*, **1**, 141.
- [4] WILLIAMS, R., 1958, *J. chem. Phys.*, **28**, 577.
- [5] HÄRDTL, K. H., and SCHARMANN, A., 1957, *Z. Naturforsch. A*, **12**, 715.
- [6] STEVENS, B., 1957, *Chem. Rev.*, **57**, 457.
- [7] STEVENS, B., 1955, *Trans. Faraday Soc.*, **51**, 610.
- [8] STEVENS, B., 1953, *J. chem. Soc.*, 2973.
- [9] VOGEL, I., 1951, *Practical Organic Chemistry*, 2nd ed (London: Longmans), p. 820.
- [10] INOKUCHI, H., SHIBA, S., HANADA, T., and AKAMATU, H., 1952, *Bull. chem. Soc. Japan*, **25**, 399.
- [11] HOIJTINK, G. J. (private communication).
- [12] HOIJTINK, G. J., 1960, *Z. Elektrochem.*, **64**, 156.
- [13] FÖRSTER, TH., and KASPER, K., 1955, *Z. Elektrochem.*, **59**, 976.
- [14] STEVENS, B., and HUTTON, E., 1960, *Nature, Lond.*, **186**, 1045.

Spin decoupling in high resolution proton magnetic resonance

by R. FREEMAN

Communication from National Physical Laboratory,
Teddington, Middlesex

(Received 23 June 1960)

A simple unit is described which can be incorporated in a high resolution nuclear magnetic resonance spectrometer to remove the spin coupling between two groups of hydrogen nuclei in the same molecule. Applied to the molecule of propionaldehyde, the method considerably simplifies the analysis of the high resolution spectrum measured at 60 Mc/s.

1. INTRODUCTION

When the difference between the resonance frequencies of two groups of magnetic nuclei is much greater than their electron coupled spin-spin interaction constant J , then this interaction may be destroyed by irradiating one of the groups of nuclei with a strong radio-frequency field. If at the same time, the spectrum of the second group is observed with the usual low radio-frequency power, the spin multiplet structure will be seen to collapse to a single line. Such 'double irradiation' or 'spin decoupling' experiments are commonly performed when the nuclei are of different isotopic species, and very useful information can be obtained in this way [1]. A theoretical treatment of such experiments has been given by Bloom and Shoolery [2].

The extension of this technique to two groups of chemically shifted hydrogen nuclei introduces some experimental difficulties since the strong decoupling radio-frequency is very close to the weak measuring radio-frequency. Anderson [3] was the first to demonstrate this double irradiation of protons. Considerable simplification of the equipment required is obtained by the use of the modulation sideband technique, and recently Itoh and Sato [4] have successfully used this method to decouple the CH_3 and CHO groups of acetaldehyde. The radio-frequency oscillator is set to a high power to 'stir up' the spin states of the CHO proton while the magnetic field is modulated at a frequency ω_m equal to the chemical shift between the groups, and the amplitude of modulation H_m is adjusted to make the effective radio-frequency field for the sideband response, $H_1(\gamma H_m/2\omega_m)$, small enough to record the CH_3 resonance without saturation. The doublet then becomes a single line. Inevitably this method superposes a sideband response of the strongly irradiated group on the signal being observed, this spurious signal being broadened by the high radio-frequency power. A simple way of eliminating this unwanted signal is to employ the detection system suggested by Pound [5, 6] where the sideband responses are observed by means of a lock-in detector operating at the field modulation frequency, instead of the d.c. detection system normally used in high resolution spectrometers. The use of this method in spin decoupling experiments is described below.

2. THE APPARATUS

To be of most use, a double irradiation equipment should be simple to operate and so designed that it can be plugged in to the commonly available types of high resolution spectrometer with as few alterations as possible. This section describes a unit which has been used in conjunction with a Varian V.4302, 60 Mc/s spectrometer to help elucidate high resolution spectra. It is essentially a conventional variable frequency lock-in detector and has been adapted from a diode demodulator circuit described by Chance *et al.* [7]. Figure 1 is a circuit diagram. The audio-frequency signal is fed to this unit from the diode detector of the spectrometer through an a.c. coupling. In the particular case of the Varian spectrometer the 'wide-line phase detector' switch position is used to give a low impedance output, and the oscilloscope input socket provides a convenient point from which to take the signal. An audio-frequency oscillator is required to provide modulation and reference signals, in the present experiment

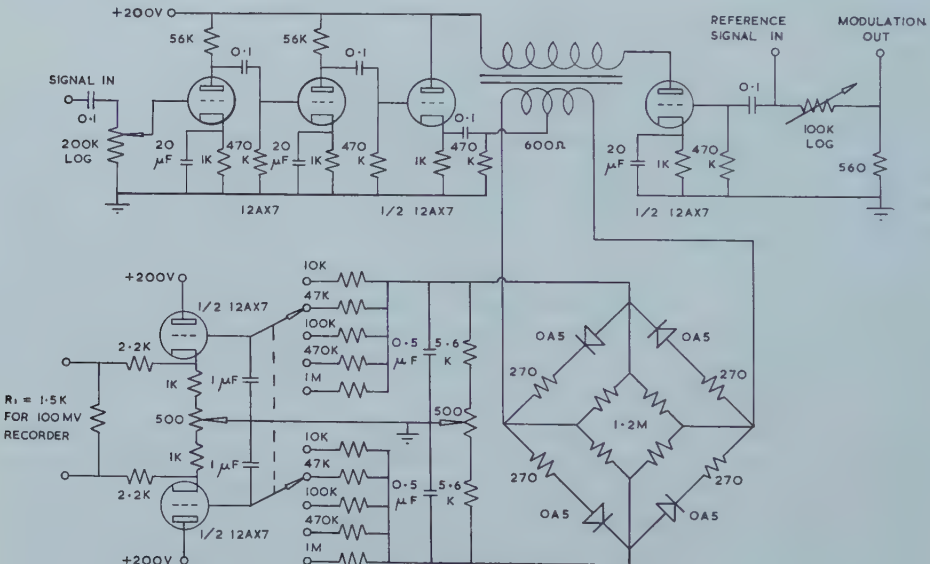


Figure 1. Circuit diagram.

a Hewlett Packard 300 CD oscillator has been used. The reference signal amplitude should be between one and two volts to ensure that the signal level is always less than the reference. A suitable amplitude of magnetic field modulation is selected by attenuating the reference signal and applying it to the field sweep coils (sockets are provided on the Varian Sweep Unit). This determines the effective radio-frequency level for the sideband response and must be set low enough to avoid saturation of the signal, detectable by the onset of line broadening. The unit will operate a recording potentiometer, and with $R_1 = 1.5$ K, a Varian 100 mv Graphic Recorder has been used. These four are the only inter-connections required, and when the unit is used with the Varian Spectrometer, they are all front panel connections and no internal modifications are required.

3. METHOD OF OPERATION

Spectra are first recorded conventionally and the chemical shifts measured by the modulation sideband technique. If the spectrum of a group A of hydrogen nuclei is to be observed while strongly irradiating a second group X, the X spectrum is centred on the oscilloscope trace and the radiofrequency power increased to meet the condition $\gamma H_1 \gg J_{AX}$. Field modulation at a frequency somewhat less than the AX chemical shift is then applied and the field swept slowly to display the normal A group resonance with the lock-in detector. These signals will usually have an admixture of dispersion mode; with the Varian spectrometer this can be removed by resetting the phase control on the radio-frequency receiver, otherwise a phase shifting network should be incorporated in either the modulation or reference signal circuits. When the modulation amplitude has been so reduced that the lines are not broadened by saturation, the recording should appear exactly as it did with the conventional detection system. Spin decoupling may then be accomplished by increasing the modulation frequency to equal the AX chemical shift.

For most spectra it is sufficient to sweep the magnetic field to display the A group resonance. Under these conditions the strong radio-frequency field passes through the X group resonance, the spin decoupling being most effective when the radio-frequency is centred on the X pattern of resonance lines. If the A group of lines extends over a large range of magnetic field, the decoupling may not always be complete at the extremes of the field sweep. A better method in that case is to centre the strong radio-frequency on the X group, switch off the field sweep and reduce field drift to a negligible amount, and display the A group spectrum by mechanically sweeping the audio-frequency modulation and reference signals. A synchronous electric motor can be used to drive the tuning condenser, and it is then an advantage to have an audio oscillator with a linear frequency scale.

4. A PRACTICAL APPLICATION

The high resolution spectrum of propionaldehyde has been chosen as an example of the use of this technique to elucidate spectra. This is an A_3B_2X molecule. Figure 2(a) shows the part of the spectrum arising from the CH_2 group and this seems at first sight to be a quadruplet with each component split into a triplet. The CH_3 group resonance is characteristic of an ethyl group where J/δ is not negligibly small, while the CHO group gives a simple triplet with $J = 1.3 \pm 0.1$ c.p.s. This suggests that the 'triplets' of the CH_2 spectrum are the result of a fortuitous matching of the second-order splitting with the small splitting from CHO. Although conventional analysis would be tedious, spin decoupling quickly confirms this hypothesis and figure 2(b) shows how the CH_2 spectrum appears when the CHO group is irradiated with a strong radio-frequency field. The amplitude of one of the rotating components of this field was calibrated by the method of Anderson [3] and found to be about 14 milligauss. In this particular example, a much smaller field would have been adequate to decouple CHO and CH_2 . When very strong radio-frequency fields are used there is a small discrepancy between the modulation frequency at which the best decoupling occurs and the chemical shift between the two groups [3].

The new CH_2 group spectrum can now be clearly recognized as typical of CH_2 in an ethyl group, and may be analysed by making use of the general calculation for the ethyl group by McGarvey and Slomp [8] or the third-order perturbation

treatment by Arnold [9] for ethanol undergoing rapid chemical exchange. Figure 2(c) is the theoretical spectrum for this group calculated for $J/\delta = 0.087$ and it fits the observed spectrum after spin decoupling reasonably well. The chemical shift between CH_2 and CH_3 was found to be 85.4 ± 0.5 c.p.s. and $J = 7.4 \pm 0.1$ c.p.s.

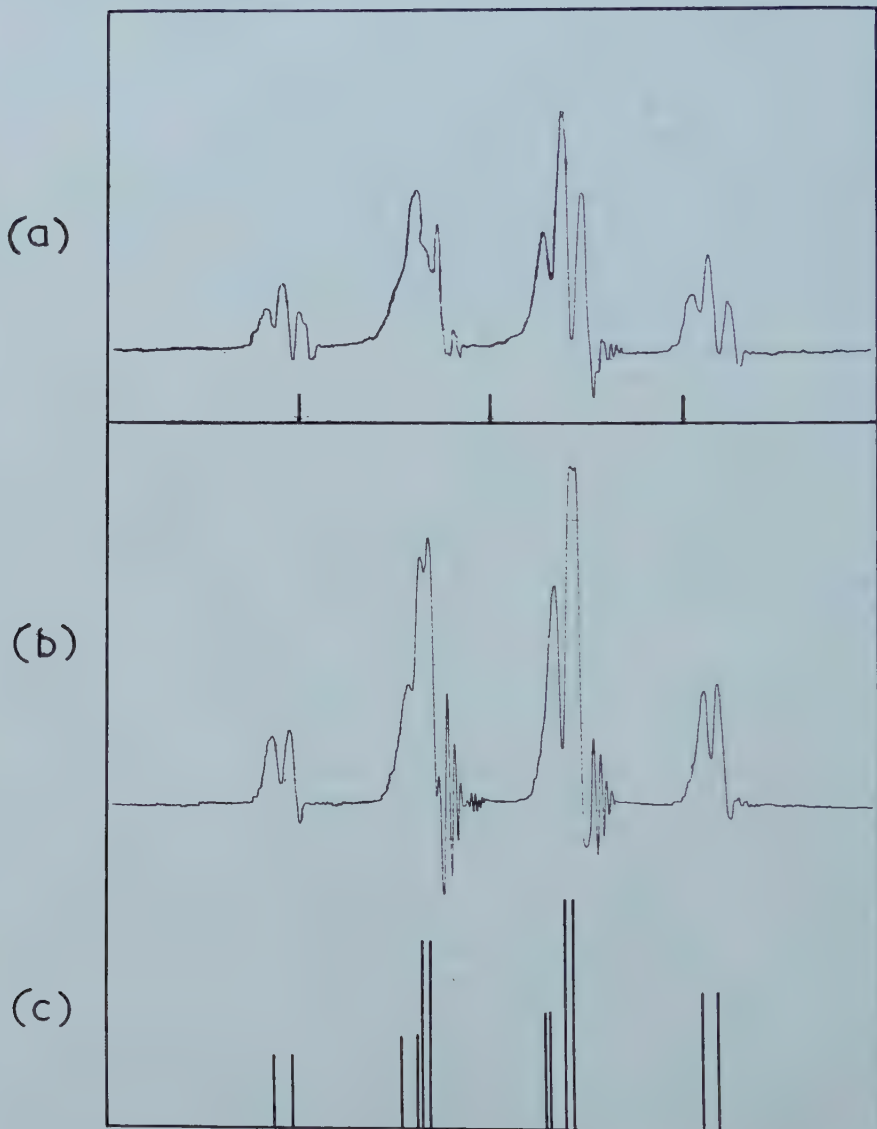


Figure 2. (a) Spectrum of CH_2 group in propionaldehyde, with markers at 10 c.p.s. (b) The same, when the aldehydic proton is being strongly irradiated. (c) Spectrum calculated with $J/\delta = 0.087$, and no coupling with the aldehydic proton.

The work described above has been carried out as part of the research programme of the National Physical Laboratory, and this paper is published by permission of the Director of the Laboratory.

The author wishes to acknowledge the kind interest of Dr. J. A. Pople, Dr. R. J. Abraham and Dr. T. P. Schaefer.

REFERENCES

- [1] ROYDEN, V., 1954, *Phys. Rev.*, **96**, 543.
- [2] BLOOM, A. L., and SHOOLERY, J. N., 1955, *Phys. Rev.*, **97**, 1261.
- [3] ANDERSON, W. A., 1956, *Phys. Rev.*, **102**, 151.
- [4] ITOH, J., and SATO, S., 1959, *J. phys. Soc. Japan*, **14**, 851.
- [5] POUND, R. V., 1957, *Rev. sci. Instrum.*, **28**, 966.
- [6] FREEMAN, R., and POUND, R. V., 1960, *Rev. sci. Instrum.*, **31**, 103.
- [7] CHANCE, B., *et al.*, 1949, *Waveforms*, M.I.T. Radiation Laboratory Series (McGraw-Hill).
- [8] McGARVEY, B. R., and SLOMP, G., 1959, *J. chem. Phys.*, **30**, 1586.
- [9] ARNOLD, J. T., 1956, *Phys. Rev.*, **102**, 136.

The calculation of dispersion forces

by L. SALEM†

Department of Theoretical Chemistry,
University Chemical Laboratory, Lensfield Road, Cambridge, England

(Received 21 June 1960)

By means of second-order perturbation theory and the use of the closure approximation, a simple closed formula is developed for the dispersion energy of interaction between spherical systems or molecules with axial symmetry. This expression contains an explicit two-electron correlation term. Agreement with experiment is most encouraging and is ascribed to the inclusion of this correlation term.

1. INTRODUCTION

The quantitative prediction of dispersion forces has long been recognized as a problem of major interest in the field of intermolecular forces. Margenau, in 1939 [1], and Pitzer twenty years later [2], have reviewed the state of the problem. It appears that results obtained from simple closed formulae are not as yet very satisfactory. Two main methods of approach have been widely used : second-order perturbation theory, and the variational method. Whatever the approach, it is always assumed that the interacting molecules (S and S' , say) are sufficiently far apart for electron exchange to be neglected and the total wave function for the composite system to be written as a product of antisymmetrized wave functions for the isolated molecules. Furthermore, both theories attempt to predict the first term only (the all-important one at large distances) in the multipole series expansion of the dispersion energy of interaction.

Using second-order perturbation theory, and the closure approximation [3], London [4] obtained the well-known formula for the induced dipole-induced dipole interaction term :

$$W = -\frac{3}{2D^6} \frac{\bar{U}\bar{U}'}{\bar{U} + \bar{U}'} \alpha\alpha', \quad (1)$$

$$W = -\frac{3}{4D^6} \bar{U}\alpha^2 \quad \text{if } S = S', \quad (1a)$$

where D is the distance (assumed large in comparison with the molecular size) between the two molecules, α is the static polarizability of molecule S and \bar{U} is some average or effective excitation energy. This is often chosen to be the ionization energy I . It is sometimes put equal to $h\nu$, the characteristic energy which provides the best one-term fit of the dispersion curve

$$\begin{aligned} \frac{\eta^2(\nu) - 1}{\eta^2(\nu) + 2} &= \frac{4\pi n}{3} \alpha(\nu) = \frac{4\pi n}{3} e^4 a_0 \sum_i \frac{f_i}{h^2 \nu_i^2 - h^2 \nu^2} \\ &\simeq \frac{4\pi n}{3} e^4 a_0 \frac{f}{h^2 \bar{\nu}^2 - h^2 \nu^2}, \end{aligned} \quad (2)$$

† Present address: Department of Chemistry, Harvard University, Cambridge, 38, Massachusetts, U.S.A.

in which $\eta(\nu)$ is the refractive index of S (assumed here to be non-polar), measured at the frequency ν , n the number of molecules S per cm^3 , a_0 the Bohr radius, h Planck's constant, f_i the oscillator strength of the i th transition of energy $h\nu_i$, and $f = (e^4 a_0)^{-1} (h\nu)^2 \alpha$ is the overall oscillator strength for the important transitions [1, 5].

The variational method (Slater and Kirkwood [6]) leads, in its simplest form, to the expression

$$W = -\frac{3}{2D^6} e^2 a_0^{1/2} \frac{\alpha\alpha'}{(\alpha/N)^{1/2} + (\alpha'/N')^{1/2}}, \quad (3)$$

$$W = -\frac{3}{4D^6} e^2 a_0^{1/2} N^{1/2} \alpha^{3/2} \quad \text{if } S = S', \quad (3a)$$

which applies to closed-shell systems only ; N is the number of electrons in the outer sub-shell of molecule S . (It is assumed that only this outermost sub-shell of electrons contributes to either α or W .) More elaborate formulae have been developed by Buckingham [7] and Donath [8]. Expressions (1) and (3) are identical if one chooses $N = f$ (and $\bar{U} = h\nu$) ; in fact (3) can be written as (1) with effective energies $\bar{U} = (\alpha/N)^{-1/2}$, $\bar{U}' = (\alpha'/N')^{-1/2}$.

A third formula, known as the Kirkwood-Müller formula [9, 10], can also be derived by the variational method :

$$W = \frac{6mc^2}{N_0 D^6} \frac{\alpha\alpha'}{\alpha/\chi_{\text{mol}}^{\text{dia}} + \alpha'/\chi_{\text{mol}}^{\text{dia}}}, \quad (4)$$

$$W = \frac{3mc^2}{N_0 D^6} \chi_{\text{mol}}^{\text{dia}} \alpha \quad \text{if } S = S', \quad (4a)$$

where N_0 is Avogadro's number, c the velocity of light, m the electron mass and

$$\chi_{\text{mol}}^{\text{dia}} = -\frac{N_0 e^2}{6mc^2} \sum_i \langle \mathbf{r}_i^2 \rangle_{\text{av}}. \quad (5)$$

For atoms, to which the application of (4) is usually limited, $\chi_{\text{mol}}^{\text{dia}}$ is simply the diamagnetic susceptibility per atom-gramme as given by the Langevin formula. For molecules (even 'spherical' ones), $\chi_{\text{mol}}^{\text{dia}}$ is the diamagnetic part of the total temperature-independent molar susceptibility ; (4) may therefore be used for molecules if this diamagnetic contribution can be evaluated, that is if both the total temperature-independent susceptibility and the temperature-independent paramagnetic term are known.

When applied to theoretical predictions of dispersion energies, these various formulae prove rather unsatisfactory. Generally, there is poor agreement with experiment. Both London's expression (1) and the Slater-Kirkwood expression (3) yield energies which are usually too small (see table 2), whereas the Kirkwood-Müller formula leads to values which are too large. In fact, for atoms with sp closed shells, effective values of \bar{U} (London formula) which lead to agreement with experiment are roughly twice the corresponding ionization energies ; in a similar manner, effective values of N (Slater-Kirkwood formula) are much larger than the actual number of electrons in the outer sub-shell. These results indicate that there are large contributions to dispersion forces from configurations, of high electronic repulsion energy, in which two or more electrons contribute to the net dipole moment of the molecule [2].

Vinti [11] pointed out long ago that the Slater-Kirkwood approximation, in which the total wave function for the closed-shell system is taken to be a product of individual-electron functions, each of which has spherical symmetry, failed

to give satisfactory results for calculated polarizabilities because of the neglect of electron correlation. He showed that one could obtain excellent agreement with experiment by including electron correlation explicitly. With a similar intention, and using second-order perturbation theory and the closure approximation, we derive here for W a simple expression which contains an explicit correlation term. This expression has the advantage of yielding satisfactory results when practicable. If the correlation term is neglected, our formula reduces to the Kirkwood–Müller expression.

2. DISPERSION ENERGY OF INTERACTION BETWEEN SPHERICAL SYSTEMS

The static polarizability of a spherical system (atom or ‘spherical’ molecule such as methane) is given by second-order perturbation theory :

$$\alpha = e^4 a_0 \sum_k' \frac{f(k)}{(\epsilon_k - \epsilon_0)^2} \quad (6)$$

(see, for instance, [12]), where

$$f(k) \equiv \frac{2}{3} \frac{\epsilon_k - \epsilon_0}{e^2 a_0} \langle 0 | \sum_i \mathbf{r}_i | k \rangle^2 \quad (7)$$

is the oscillator strength, averaged over all magnetic quantum numbers, of the $(0, k)$ electronic transition from the ground state $|0\rangle$, of electronic energy ϵ_0 , to some excited state $|k\rangle$ of energy ϵ_k ; \mathbf{r}_i refers to the electronic coordinates. The states $|0\rangle$ and $|k\rangle$ are defined by a set of quantum numbers from which the magnetic quantum number is missing. We now use the Unsöld closure approximation [3] : that is, we assume that all the important electronic transitions have nearly the same energy U . Hence

$$\alpha = \frac{2}{3} \frac{e^2}{U} \sum_k' \langle 0 | \sum_i \mathbf{r}_i | k \rangle^2 = \frac{2}{3} \frac{e^2}{U} \left\{ \langle 0 | (\sum_i \mathbf{r}_i)^2 | 0 \rangle - \langle 0 | \sum_i \mathbf{r}_i | 0 \rangle^2 \right\} \quad (8)$$

by the quantum-mechanical sum rule. If we choose our origin at the centre of gravity of electronic charge (this is simply the centre of symmetry for atoms or symmetrical molecules),

$$\alpha = \frac{2}{3} \frac{e^2}{U} \langle (\sum_i \mathbf{r}_i)^2 \rangle, \quad (9)$$

where $\langle (\sum_i \mathbf{r}_i)^2 \rangle$ refers to the expectation value of the operator $(\sum_i \mathbf{r}_i)^2$ in the ground state $|0\rangle$.

On the other hand, London’s fundamental formula for the dipole-dipole contribution to the dispersion energy between two molecules S and S' is

$$W = -\frac{3}{2} \frac{e^8 a_0^2}{D^6} \sum_k' \sum_{k'}' \frac{f(k)f'(k')}{(\epsilon_k + \epsilon_{k'} - \epsilon_0 - \epsilon_{0'})(\epsilon_k - \epsilon_0)(\epsilon_{k'} - \epsilon_0)}, \quad (10)$$

where the various states are defined as above. The closure approximation leads to

$$W = -\frac{2e^4}{3D^6} \frac{\langle (\sum_i \mathbf{r}_i)^2 \rangle \langle (\sum_{i'} \mathbf{r}_{i'})^2 \rangle}{U + U'} \quad (11)$$

where U is some average or effective energy for the transitions $(0, k)$. This expression was obtained by London, who then used equation (9) to eliminate the quantum-mechanical averages and keep the U ’s as empirical constants. Here we do precisely the contrary.

If we assume that \bar{U} , say, is the *same* average energy as that which occurs in the expression for the static polarizability α , given in (9), and that a similar argument applies to \bar{U}' , then the dispersion energy of interaction becomes

$$W = -\frac{e^2}{D^6} \frac{\alpha\alpha'}{\alpha/\langle(\sum_i \mathbf{r}_i)^2\rangle + \alpha'/\langle(\sum_{i'} \mathbf{r}_{i'})^2\rangle}, \quad (12)$$

$$W = -\frac{e^2}{2D^6} \langle(\sum_i \mathbf{r}_i)^2\rangle \alpha \quad \text{if } S=S'. \quad (12a)$$

These are the formulae we were seeking. (12) is also of the form (1), where the average energies \bar{U} and \bar{U}' are now defined by

$$\bar{U} = \frac{2}{3} e^2 \frac{\langle(\sum_i \mathbf{r}_i)^2\rangle}{\alpha}, \quad \bar{U}' = \frac{2}{3} e^2 \frac{\langle(\sum_{i'} \mathbf{r}_{i'})^2\rangle}{\alpha'}. \quad (13)$$

and the overall oscillator strengths corresponding to (2) are

$$f = \frac{4}{9a_0} \frac{\langle(\sum_i \mathbf{r}_i)^2\rangle^2}{\alpha}, \quad f' = \frac{4}{9a_0} \frac{\langle(\sum_{i'} \mathbf{r}_{i'})^2\rangle^2}{\alpha'}. \quad (14)$$

Thus, if one knows the polarizabilities α and α' , and the values of the quantum-mechanical averages

$$\langle(\sum_i \mathbf{r}_i)^2\rangle \quad \text{and} \quad \langle(\sum_{i'} \mathbf{r}_{i'})^2\rangle,$$

it is possible to calculate the dispersion energy of interaction between any two spherical systems S and S' . The quantity

$$\langle(\sum_i \mathbf{r}_i)^2\rangle = \sum_i \langle \mathbf{r}_i^2 \rangle + \sum_{i \neq j} \langle \mathbf{r}_i \cdot \mathbf{r}_j \rangle = -\frac{6mc^2}{N_0 e^2} \chi_{\text{mol}}^{\text{dia}} + \sum_{i \neq j} \langle \mathbf{r}_i \cdot \mathbf{r}_j \rangle \quad (15)$$

is made up of two terms: the sum of the mean square radii of all the electrons (readily obtained from the experimental value of $\chi_{\text{mol}}^{\text{dia}}$) which is positive, and a negative *correlation term*, which must be calculated. This term is very sensitive to the type of ground-state wave function chosen for the system, and vanishes for commonly used products of single-electron spherically symmetric wave functions.

If, in a rather crude approximation, this electron correlation term were neglected, the expression for the dispersion energy would reduce to

$$W = \frac{6mc^2}{N_0 D^6} \frac{\alpha\alpha'}{\alpha/\chi_{\text{mol}}^{\text{dia}} + \alpha'/\chi_{\text{mol}}^{\text{dia}'}}, \quad (4)$$

$$W = \frac{3mc^2}{N_0 D^6} \chi_{\text{mol}}^{\text{dia}} \alpha \quad \text{if } S=S'. \quad (4a)$$

These expressions are precisely the Kirkwood–Müller formulae; we see that they give only an *upper limit* to the true magnitude of the dispersion energy, since, in general,

$$\langle(\sum_i \mathbf{r}_i)^2\rangle \leq \sum_i \langle \mathbf{r}_i^2 \rangle. \quad (16)$$

This explains the fact that the Kirkwood–Müller formulae yield dispersion energies which are always too large [2]; the discrepancy between theory and experiment is mainly due to the neglect of correlation.

In practice, one uses the general formula (12) whenever possible. For systems for which the term $\sum_{i \neq j} \langle \mathbf{r}_i \cdot \mathbf{r}_j \rangle$ has not been evaluated, the Kirkwood–Müller formula is our best approximation. Numerical results and comparison with experimental data are given in §4.

3. DISPERSION ENERGY OF INTERACTION BETWEEN MOLECULES WITH AXIAL SYMMETRY

Consider now a molecule with axial symmetry in a Σ ground state. Second-order perturbation theory yields for the parallel and perpendicular components of the static polarizability

$$\left. \begin{aligned} \alpha_{\parallel} &= 3e^4 a_0 \sum'_{\text{states}} \frac{f(k)}{(\mathcal{E}_k - \mathcal{E}_0)^2} = 2e^2 \sum_{\text{states}} \frac{\langle 0 | \sum_i z_i | k \rangle^2}{\mathcal{E}_k - \mathcal{E}_0}, \\ \alpha_{\perp} &= 3e^4 a_0 \sum'_{\text{II states}} \frac{f(k)}{(\mathcal{E}_k - \mathcal{E}_0)^2} = 2e^2 \sum'_{\text{II states}} \frac{\langle 0 | \sum_i x_i | k \rangle^2}{\mathcal{E}_k - \mathcal{E}_0}, \end{aligned} \right\} \quad (17)$$

where the z -axis is the symmetry axis [13]. We use the quantum-mechanical sum rule and the closure approximation in the same manner as in §2, to define average energies

$$\bar{U}_{\parallel} = 2e^2 \frac{\langle (\sum_i z_i)^2 \rangle}{\alpha_{\parallel}}, \quad \bar{U}_{\perp} = 2e^2 \frac{\langle (\sum_i x_i)^2 \rangle}{\alpha_{\perp}} \quad (18)$$

and overall oscillator strengths

$$f_{\parallel} = \frac{4}{3a_0} \frac{\langle (\sum_i z_i)^2 \rangle^2}{\alpha_{\parallel}}, \quad f_{\perp} = \frac{4}{3a_0} \frac{\langle (\sum_i x_i)^2 \rangle^2}{\alpha_{\perp}} \quad (19)$$

for the parallel and perpendicular transitions, respectively. Once again, the origin of coordinates has been chosen at the centre of electronic charge so that both

$$\langle \sum_i z_i \rangle \quad \text{and} \quad \langle \sum_i x_i \rangle$$

vanish.

London [14] has calculated the dispersion energy of interaction between two molecules S and S' with axial symmetry, which he assumes to be three-dimensional anisotropic oscillators with fundamental frequencies $\bar{\nu}_{\parallel}$ and $\bar{\nu}_{\perp}$, $\bar{\nu}'_{\parallel}$ and $\bar{\nu}'_{\perp}$ respectively. The result, which corresponds to (11), is given in terms of the relative orientation of the oscillators as

$$W = -\frac{c(\theta, \phi; \theta', \phi')}{D^6}, \quad (20)$$

where θ and θ' are the angles which the two molecules make with a radial vector joining their centres, ϕ and ϕ' the azimuthal angles which the molecules make with an arbitrary plane passing through this radius vector, and D is the distance between the molecular centres; one has

$$\begin{aligned} c(\theta, \phi; \theta', \phi') &= (A - B - B' + C) \{ \sin \theta \sin \theta' \cos(\phi' - \phi) - 2 \cos \theta \cos \theta' \}^2 \\ &\quad + 3(B - C) \cos^2 \theta + 3(B' - C) \cos^2 \theta' + (B + B' + 4C), \end{aligned} \quad (21)$$

where the constants A , B , B' and C are defined in terms of the polarizabilities α_{\parallel} , α_{\perp} , α'_{\parallel} , α'_{\perp} and characteristic energies $h\bar{\nu}_{\parallel}$, $h\bar{\nu}_{\perp}$, $h\bar{\nu}'_{\parallel}$, $h\bar{\nu}'_{\perp}$.

If we now write $h\bar{\nu}_{\parallel} = \bar{U}_{\parallel}$, where \bar{U}_{\parallel} is given by (18), and similar expressions for the other characteristic energies, we obtain directly an expression for W in terms of the various polarizabilities and quantum-mechanical averages

$$\langle (\sum_i x_i)^2 \rangle, \quad \langle (\sum_i z_i)^2 \rangle,$$

etc. Both equations (20) and (21) are unchanged, but the constants A, B, B', C are now given by

$$\left. \begin{aligned} A &= \frac{e^2}{2} \frac{\alpha_{\parallel} \alpha_{\parallel}'}{\alpha_{\parallel}/\langle(\sum_i z_i)^2\rangle + \alpha_{\parallel}'/\langle(\sum_i z_i')^2\rangle}; & C &= \frac{e^2}{2} \frac{\alpha_{\perp} \alpha_{\perp}'}{\alpha_{\perp}/\langle(\sum_i x_i)^2\rangle + \alpha_{\perp}'/\langle(\sum_i x_i')^2\rangle}, \\ B &= \frac{e^2}{2} \frac{\alpha_{\parallel} \alpha_{\perp}'}{\alpha_{\parallel}/\langle(\sum_i z_i)^2\rangle + \alpha_{\perp}'/\langle(\sum_i x_i')^2\rangle}; & B' &= \frac{e^2}{2} \frac{\alpha_{\perp} \alpha_{\parallel}'}{\alpha_{\perp}/\langle(\sum_i x_i)^2\rangle + \alpha_{\parallel}'/\langle(\sum_i z_i')^2\rangle}. \end{aligned} \right\} \quad (22)$$

The use of these equations simply requires the knowledge of the various polarizabilities and quantum-mechanical averages; if these are known, one does not have to face the difficulty of estimating characteristic frequencies or resorting to new approximations, such as setting \bar{v}_{\parallel} equal to \bar{v}_{\perp} (de Boer [15]). This approximation, as we shall see, is not always justified; (18) shows that there is no *a priori* reason for \bar{U}_{\parallel} and \bar{U}_{\perp} to be equal.

As a first application of our results, let us consider the average over all orientations of the dispersion energy between two like molecules; (20) yields, when averaged over all orientations,

$$W_{av} = -\frac{2}{3D^6} \{A + 2(B + B') + 4C\}, \quad (23)$$

which, for $S=S'$, reduces to

$$W_{av} = -\frac{e^2}{6D^6} \left\{ (\alpha_{\parallel} + 2\alpha_{\perp}) (\langle(\sum_i z_i)^2\rangle + 2\langle(\sum_i x_i)^2\rangle) - \alpha_{\parallel} \alpha_{\perp} \frac{(\bar{U}_{\parallel} - \bar{U}_{\perp})^2}{\bar{U}_{\parallel} + \bar{U}_{\perp}} \right\} \quad (S=S'). \quad (23a)$$

Hence W_{av} is the sum of an ‘isotropic’ term and an ‘anisotropic’ term. Since \bar{U}_{\parallel} and \bar{U}_{\perp} , though not necessarily equal, are usually of the same order of magnitude, the anisotropic term, which is proportional to the square of a small difference, is negligible. (For H_2 and O_2 , for instance, this term is less than 2 per cent of the total contribution.) The dispersion energy can then be written in terms of the mean polarizability $\bar{\alpha} = (\alpha_{\parallel} + 2\alpha_{\perp})/3$ as

$$W_{av} = -\frac{e^2}{2D^6} \langle(\sum_i \mathbf{r}_i)^2\rangle \bar{\alpha} \quad (S=S') \quad (24a)$$

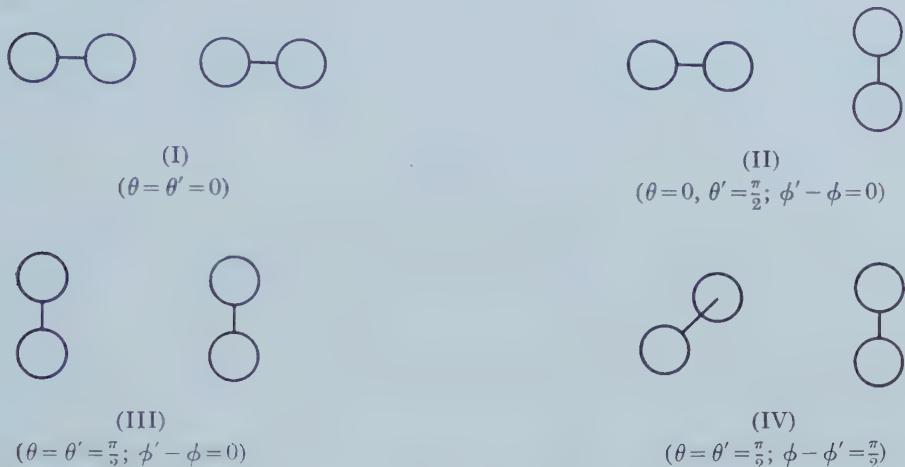
which is identical with the formula for two like spherical systems, (12a). In a similar fashion, the isotropic part of the dispersion energy between two unlike molecules is obtained from (23) by writing $\bar{U}_{\parallel} = \bar{U}_{\perp} = \bar{U}$ and $\bar{U}_{\parallel}' = \bar{U}_{\perp}' = \bar{U}'$; the result is

$$W_{av} = -\frac{e^2}{D^6} \frac{\bar{\alpha} \bar{\alpha}'}{\bar{\alpha}/\langle(\sum_i \mathbf{r}_i)^2\rangle + \bar{\alpha}'/\langle(\sum_i \mathbf{r}_i')^2\rangle} \quad (24)$$

which is identical with (12).

If, furthermore, electron correlation is neglected, the Kirkwood–Müller formulae are again obtained (mean polarizabilities, however, replacing the spherical polarizabilities of §2). However, in view of the additional assumptions already involved in the derivation of (24), any further approximation does not seem wise. Results derived from equations (23) and (24) are given in §4 for molecules for which $\langle(\sum_i \mathbf{r}_i)^2\rangle$ has been calculated for various ground-state wave functions.

Another interesting application concerns the prediction of W for various relative orientations of the two molecules. Four fundamental orientations are shown in the figure.



If the molecules are identical, equations (20), (21) and (22) yield

$$(I) \quad W = -\frac{e^2}{2D^6} [2\langle(\sum_i z_i)^2\rangle\alpha_{\parallel} + \langle(\sum_i x_i)^2\rangle\alpha_{\perp}], \quad (25a)$$

$$(II) \quad W = -\frac{e^2}{4D^6} \left[\langle(\sum_i x_i)^2\rangle\alpha_{\perp} + 10 \frac{\alpha_{\parallel}\alpha_{\perp}}{\alpha_{\parallel}/\langle(\sum_i z_i)^2\rangle + \alpha_{\perp}/\langle(\sum_i x_i)^2\rangle} \right], \quad (26a)$$

$$(III) \quad W = -\frac{e^2}{4D^6} [\langle(\sum_i z_i)^2\rangle\alpha_{\parallel} + 5\langle(\sum_i x_i)^2\rangle\alpha_{\perp}], \quad (27a)$$

$$(IV) \quad W = -\frac{e^2}{D^6} \left[\langle(\sum_i x_i)^2\rangle\alpha_{\perp} + \frac{\alpha_{\parallel}\alpha_{\perp}}{\alpha_{\parallel}/\langle(\sum_i z_i)^2\rangle + \alpha_{\perp}/\langle(\sum_i x_i)^2\rangle} \right]. \quad (28a)$$

The right-hand side of equation (25a), for instance, can be written

$$-(2\alpha_{\parallel}^2\bar{U}_{\parallel} + \alpha_{\perp}^2\bar{U}_{\perp})/4D^6;$$

there is evidently a significant error possible if one sets $\bar{U}_{\parallel} = \bar{U}_{\perp}$, since the neglected term is directly proportional to $(\bar{U}_{\parallel} - \bar{U}_{\perp})$. De Boer's approximation, therefore, is not justified for particular orientations of the two molecules.

Results obtained by these formulae are also given in the following section.

4. NUMERICAL RESULTS

Table 1 gives the polarizabilities and relevant data concerning the quantum-mechanical averages $\langle(\sum_i \mathbf{r}_i)^2\rangle$ (see equation (15)) for the H atom, the rare gases, CH_4 and two diatomic molecules, H_2 and O_2 . Theoretical polarizabilities have been chosen for systems for which accurate calculations have been performed. For the hydrogen molecule, Hirschfelder [16] calculated $\langle(\sum_i z_i)^2\rangle$ and $\langle(\sum_i x_i)^2\rangle$ for both Wang and Rosen functions; we have chosen the results for the latter. For the oxygen molecule, Kotani *et al.* [17] have calculated these averages for various elaborate ground-state wave functions. The tabulated

results are those for their best wave function, which includes $\sigma-\pi$ configuration interaction; this wave function enabled them to predict the oscillator strength of the Schumann-Runge bands within experimental error (see Bethke [18]). It is interesting to note that, whereas for the hydrogen molecule $\langle(\sum_i \mathbf{r}_i)^2\rangle$ and $\sum_i \langle\mathbf{r}_i^2\rangle$ do not differ very much (theoretical values calculated by Hirschfelder being 4.60 and 5.26 atomic units respectively), for the oxygen molecule (which has a triplet ground state) the calculations of Kotani *et al.* yield

$$\left. \begin{array}{l} \langle(\sum_i \mathbf{r}_i)^2\rangle = 12.6 \text{ a.u.}, \\ \sum_i \langle\mathbf{r}_i^2\rangle = 40.3 \text{ a.u.} \end{array} \right\} \quad (29)$$

so that neglect of the electron correlation term here would be catastrophic.

System	(1) $\alpha(\text{\AA}^3)$	$\langle(\sum_i \mathbf{r}_i)^2\rangle$		$\sum_{i \neq j} \langle\mathbf{r}_i \mathbf{r}_j\rangle$ (a.u.)
		$\chi_{\text{mol}}^{\text{dia}} \times 10^6$ c.g.s.	$\langle r^2 \rangle$	
H	0.667a	$\langle r^2 \rangle = 3$ a.u.)		0
He	0.206b,k	1.94e		-0.146j
Ne	0.398b	7.2e		-1.5j
A	1.63b	19.4e		—
Kr	2.48b	28e		—
Xe	4.01b	43e		—
CH ₄	2.60c	21.5f,g		—
H ₂	$\left\{ \begin{array}{l} (\alpha_{ }) \\ (\alpha_{\perp}) \end{array} \right. \begin{array}{l} 0.9476d \\ 0.6968d \end{array}$		$\left\{ \begin{array}{l} \langle(\sum_i z_i)^2\rangle = 1.56h \\ \langle(\sum_i x_i)^2\rangle = 1.52h \end{array} \right.$	
O ₂	$\left\{ \begin{array}{l} (\alpha_{ }) \\ (\alpha_{\perp}) \end{array} \right. \begin{array}{l} 2.35c \\ 1.21c \end{array}$		$\left\{ \begin{array}{l} \langle(\sum_i z_i)^2\rangle = 5.25i \\ \langle(\sum_i x_i)^2\rangle = 3.67i \end{array} \right.$	

(1) For transformation into atomic units, use the relation $1 \text{ \AA}^3 = 6.749 \text{ a.u.}$

(2) For obtaining $\sum_i \langle\mathbf{r}_i^2\rangle$ in atomic units, use the relation $\sum_i \langle\mathbf{r}_i^2\rangle \text{ (a.u.)} = -1.262 \times 10^6 \chi_{\text{mol}}^{\text{dia}}$ (c.g.s.)

a PAULING, L., and WILSON, E. B., 1935, *Introduction to Quantum Mechanics* (New York: McGraw-Hill), p. 185. b LANDOLT-BÖRNSTEIN, 1951, *Zahlenwerte und Functionen* (Berlin: Springer), Vol. I, Part 1, p. 401. c LANDOLT-BÖRNSTEIN, 1951, *Zahlenwerte und Functionen* (Berlin: Springer), Vol. I, Part 3, p. 510. d ISHIGURO, E., ARAI, T., MIZUSHIMA, M., and KOTANI, M., 1952 *Proc. phys. Soc. Lond. A*, **65**, 178. e LANDOLT-BÖRNSTEIN, 1951, *Zahlenwerte und Functionen* (Berlin: Springer), Vol. I, Part 1, p. 394. f WELTNER, W., 1956, *J. chem. Phys.*, **24**, 918. g WELTNER, W., 1958, *J. chem. Phys.*, **28**, 477. h HIRSCHFELDER, J. O., 1935, *J. chem. Phys.*, **3**, 555. i KOTANI, M., MIZUNO, Y., KAYAMA, K., and ISHIGURO, E., 1957, *J. Phys. Soc. Japan*, **12**, 707. j VINTI, J. P., 1932, *Phys. Rev.*, **41**, 813. k DALGARNO, A., and LYNN, N., 1957, *Proc. phys. Soc. Lond. A*, **70**, 802.

Table 1. Properties of atoms and molecules.

For the inert gases, the tabulated value of $\chi_{\text{mol}}^{\text{dia}}$ is simply the experimental diamagnetic susceptibility. In the case of methane, however, the tabulated value is the difference between the molar susceptibility and the paramagnetic temperature-independent term, as evaluated from experimental data by Weltner [19, 20]. It is an excellent agreement with the theoretically predicted value of Venkatachalam and Kabadi [21].

In table 2 we compare theoretical and experimental dispersion energies, the latter being obtained by fitting to experiment either Lennard-Jones 6-12 or modified Buckingham 6-exp. intermolecular potentials. In practice one compares coefficients of D^{-6} . Experimental coefficients based on either potential are proportional to $(D_m)^6$, where D_m is the intermolecular distance at the potential

Theoretical

System	L.-J. pot ⁽¹⁾	Experimental		London		Slater-Kirkwood		Accurate calcula- tions		Present calculations	
		L.-J. pot ⁽²⁾	Mod. Buck. pot	eqns. (1), (1 a)	eqns. (3), (3 a)	eqns. (3), (12 a) or (23), (23 a)	eqns. (4), (4 a) (Kirkwood- Müller)	eqns. (12), (12 a) or (23), (23 a)	eqns. (4), (4 a) (Kirkwood- Müller)	eqns. (12), (12 a) or (23), (23 a)	eqns. (4), (4 a) (Kirkwood- Müller)
H ₂ ↔H	—	—	—	7.58	—	—	—	6.499 ^{o,p}	6.75	6.75	6.75
He ₂ ↔He	1.644 ^a	1.644 ^a	2.43 ^a	1.31	1.29 ^m	1.74	1.50 ^q	1.60	1.70	1.70	1.70
Ne ₂ ↔Ne	10.4 ^b	9.70 ^c	9.08 ^h	4.30	4.88 ^m	8.10	—	10	—	12	—
A ₂ ↔A	107.7 ^e	114 ^e	104 ⁱ	52.6	57.9 ^m	67.0	—	—	—	135	—
Kr ₂ ↔Kr	214 ^e	242 ^e	254 ^j	108	112 ^m	125	—	—	—	295	—
Xe ₂ ↔Xe	606 ^e	587 ^e	481 ^h	246	243 ^m	259	—	—	—	730	—
A ₂ ↔He	—	12.17 ^{sf}	—	15.2 ^h	8.03	—	10.4	—	—	14.5 ^g	15.0
CH ₄ ↔CH ₄	265 ^d	271 ^c	214 ⁱ	110	117	155	—	—	—	237	—
H ₂ ₂ ↔H ₂	13.5 ^a	13.5 ^a	13.0 ^a	12.07	10.9 ^{gn}	13.04	—	12.1 (12.2) ^g	—	—	—
O ₂ ₂ ↔O ₂	117 ^e	114 ^g	78.7 ⁱ	38.85	41.6 ^m	—	—	66.9 (67.8) ^g	—	—	—
H ₂ ₂ ↔O ₂	—	36.63 ^{sf}	—	21.51	—	—	—	28.3 (28.5) ^g	—	—	—

(1) Experimental potential determined by fitting second virial coefficient data. (2) Experimental potential determined by fitting viscosity data. (3) The ionization potentials used here are those tabulated in [22]. (4) See equation (2). (5) From experimental Lennard-Jones potential determined by fitting thermal diffusion data for the gas mixture. (6) This particular value was obtained by fitting the dispersion curve with a two-term formula. (7) Calculated by equations (24) or (24₀) ($\bar{U} = \bar{I}^2 / \bar{I}$, assumed for both systems.) (8) Electron correlation neglected for the argon atom only. (9) For transformation into c.g.s. units, use the relation 1 a.u. = 0.9571 × 10⁻⁶⁰ ergs × cm⁶.

a MASON, E. A., and RICE, W. W., 1954, *J. chem. Phys.*, **22**, 522. b CORNER, J., 1948, *Trans. Faraday Soc.*, **44**, 914. (Potential fitted to both second virial coefficient data and crystal data.) c HIRSCHFELDER, J. O., CURTISS, C. F., and BIRD, R. B., 1954, *Molecular Theory of Gases and Liquids* (New York: John Wiley and Sons, Inc.), p. 1110. (When two different potentials are available for a given system, the first one has been chosen.) d BEATTIE, J. A., and STOCKMAYER, W. H., 1942, *J. chem. Phys.*, **10**, 473. e HOLBORG, L., and ORTO, J., 1922, *Z. Phys.*, **10**, 367. f SRIVASTAVA, B. N., and MADAN, M. P., 1953, *Proc. phys. Soc. Lond. A*, **66**, 278. g RAW, C. J. G., and ELLIS, C. P., 1958, *J. chem. Phys.*, **28**, 1198. h MASON, E. A., and RICE, W. E., 1954, *J. chem. Phys.*, **22**, 843. i DE ROCCO, A. G., and HALFORD, J. O., 1958, *J. chem. Phys.*, **28**, 1152. j MADAN, M. P., 1957, *J. chem. Phys.*, **27**, 113. k SRIVASTAVA, K. P., 1957, *J. chem. Phys.*, **26**, 579. l VANDERSLUCE, J. T., MASON, E. A., and MAISCH, W. G., 1959, *J. chem. Phys.*, **31**, 738. m MARGENAU, H., 1939, *Rev. mod. Phys.*, **11**, 1. n MARGENAU, H., 1943, *Phys. Rev.*, **64**, 131. o PAULING, L., and BEACH, J. Y., 1935, *Phys. Rev.*, **47**, 686. p HIRSCHFELDER, J. O., and LÖWDIN, P.-O., 1959, *Mol. Phys.*, **2**, 229. q DALGARNO, A., and LYNN, N., 1957, *Proc. phys. Soc. Lond. A*, **70**, 802.

Table 2. Experimental and theoretical D^6 coefficients (atomic units)⁽⁹⁾. (All coefficients are negative.)

minimum, and are therefore very sensitive to the value of D_m itself. Since the modified Buckingham potential contains, in addition to D_m , two other empirical parameters, there is a certain latitude in the choice of the set of values (and in particular of the value of D_m) which gives the best fit of the experimental data. Consequently coefficients of D^{-6} determined from this potential would seem slightly less reliable than those determined from Lennard-Jones potential curves; the coefficient for the $\text{He} \leftrightarrow \text{He}$ interaction, for instance, is certainly much too large.

For mixtures ($S \neq S'$) the only experimental coefficients which it is licit to compare to theoretical results are those calculated from force constants determined directly from experimental data, not from empirical combining laws for the force constants relative to the two components. Such potentials have been obtained for the argon-helium and hydrogen-oxygen systems.

As a matter of reference, theoretical coefficients obtained from the London and Slater-Kirkwood formulae have also been tabulated. The latter do not apply to H and O_2 , which are not closed-shell systems. Furthermore, for the $\text{H} \leftrightarrow \text{H}$ and $\text{He} \leftrightarrow \text{He}$ interactions, results of very accurate calculations are given.

Whenever it has been possible to apply our equations in the general form, without neglecting the electron correlation term, the theoretical D^{-6} coefficients are found to be in excellent agreement with experiment (or, in the $\text{H} \leftrightarrow \text{H}$ and $\text{He} \leftrightarrow \text{He}$ cases, with accurately calculated coefficients). For the $\text{O}_2 \leftrightarrow \text{O}_2$ system, however, the theoretical coefficient is slightly too small. But in this case one cannot attach too much significance to the experimental coefficients, since at short distances the experimental potential is only a rough average of several potentials of different energy, corresponding to the various possible relative orientations of the electron spin of the two molecules.

In other cases, we have resorted to the Kirkwood-Müller formulae (4) and (4a); as expected, the resulting interaction energies are appreciably larger than the experimental energies, except for methane. For this molecule, however, a spherical model gives a picture of the electron density which is far from satisfactory [23] and our result cannot bear much significance. For the argon, krypton and xenon gases, discrepancy between experiment and theory is primarily due to the neglect of the $\sum_{i \neq j} \langle \mathbf{r}_i \cdot \mathbf{r}_j \rangle$ term; values of this term necessary to bring about agreement with experiment (as given in the second column of table 2, say) are -3.82 , -6.35 and -10.6 a.u. respectively. These are certainly of the right order of magnitude since the corresponding theoretical values for helium and neon are -0.146 and -1.5 a.u. respectively (table 1).

Table 3, finally, gives the dispersion energy between two hydrogen molecules, and that between two oxygen molecules, for special orientations, as calculated from equations (25a) to (28a). Also tabulated are the corresponding results in de Boer's approximation, assuming

$$\bar{U}_{\parallel} = \bar{U}_{\perp} = \bar{U} \quad (30)$$

or

$$2 \frac{\langle (\sum z_i)^2 \rangle}{\alpha_{\parallel}} = 2 \frac{\langle (\sum x_i)^2 \rangle}{\alpha_{\perp}} = 2 \frac{\langle (\sum r_i)^2 \rangle}{3\bar{\alpha}}. \quad (31)$$

The values obtained from the 'rigorous' equations are less spread out about W_{av} than the approximate values. This seems to confirm recent calculations on

the $H_2 \leftrightarrow H_2$ system [24] which suggest that the variation of the dispersion energy with orientation is not as significant as previously assumed.

System	Relative orientation (figure 1)	General equations (25 a) to (28 a)	Isotropic approximation ($\bar{U}_\parallel = \bar{U}_\perp = \bar{U}$)
$H_2 \leftrightarrow H_2$	{ (I)	13.8	15.6
	(II)	12.4	12.7
	(III)	11.5	11.1
	(IV)	11.4	10.8
	W_{av}	12.1	12.2
$O_2 \leftrightarrow O_2$	{ (I)	98.5	112
	(II)	69.3	70.1
	(III)	58.3	57.4
	(IV)	54.7	51.5
	W_{av}	66.9	67.8

Table 3. Theoretical D^{-6} coefficients (a.u.) for special orientations. (All coefficients are negative.)

5. CONCLUSION

In conclusion, a net improvement over previous formulae is obtained by including an explicit electron correlation term. This is certainly because one has allowed for electron repulsion and accounted for the fact that atoms or molecules are actually less polarizable than would be expected on the basis of a simple independent-electron model (see for instance equations (9) and (16)). Furthermore, the only inaccuracy in our calculation is brought about by the use of the closure approximation and is largely eliminated by making the approximation for both polarizabilities and dispersion energy, and choosing as common average energy that which corresponds to the observed polarizabilities. At the present time, therefore, the precision of our results seems limited mainly by the difficulty of calculating $\sum_{i \neq j} \langle \mathbf{r}_i, \mathbf{r}_j \rangle$ for sufficiently accurate wave functions.

The author would like to thank Professor H. C. Longuet-Higgins, F.R.S. and Dr. L. E. Orgel for many helpful discussions on this problem and for their encouragement.

REFERENCES

- [1] MARGENAU, H., 1939, *Rev. mod. Phys.*, **11**, 1.
- [2] PITZER, K. S., 1959, *Advanc. chem. Phys.*, **2**, 59.
- [3] UNSÖLD, A., 1927, *Z. Phys.*, **43**, 563.
- [4] LONDON, F., 1930, *Z. phys. Chem. B*, **11**, 222.
- [5] MARGENAU, H., 1938, *J. chem. Phys.*, **6**, 896.
- [6] SLATER, J. C., and KIRKWOOD, J. G., 1931, *Phys. Rev.*, **37**, 682.
- [7] BUCKINGHAM, R. A., 1937, *Proc. roy. Soc. A*, **160**, 94, 113.
- [8] DONATH, W. E., 1958, Thesis, University of California.
- [9] KIRKWOOD, J. G., 1932, *Phys. Z.*, **33**, 57.
- [10] MÜLLER, A., 1936, *Proc. roy. Soc. A*, **154**, 624.
- [11] VINTI, J. P., 1932, *Phys. Rev.*, **41**, 813.
- [12] HIRSCHFELDER, J. O., CURTISS, C. F., and BIRD, R. B., 1954, *Molecular Theory of Gases and Liquids* (New York: John Wiley and Sons, Inc.), Chap 12, par. 6.

- [13] DALGARNO, A., and LEWIS, J. T., 1957, *Proc. roy. Soc. A*, **240**, 284.
- [14] LONDON, F., 1942, *J. phys. Chem.*, **46**, 305.
- [15] DE BOER, J., 1942, *Physica*, **9**, 363.
- [16] HIRSCHFELDER, J. O., 1935, *J. chem. Phys.*, **3**, 555.
- [17] KOTANI, M., MIZUNO, Y., KAYAMA, K., and ISHIGURO, E., 1957, *J. phys. Soc. Japan*, **12**, 707.
- [18] BETHKE, G. W., 1959, *J. chem. Phys.*, **31**, 669.
- [19] WELTNER, W., 1956, *J. chem. Phys.*, **24**, 918.
- [20] WELTNER, W., 1958, *J. chem. Phys.*, **28**, 477.
- [21] VENKATACHALAM, K. A., and KABADI, M. B., 1955, *J. phys. Chem.*, **59**, 740.
- [22] LANDOLT-BÖRNSTEIN, 1951, *Zahlenwerte und Functionen* (Berlin: Springer), Vol. I, Part 1, p. 211 and Part 3, p. 359.
- [23] MILLS, I. M., 1958, *Mol. Phys.*, **1**, 99.
- [24] BRITTON, F. R., and BEAN, D. T. W., 1955, *Canad. J. Phys.*, **33**, 668.

The effect of bond length variations in molecular orbital calculations of π -electron spectra—aniline

by T. E. PEACOCK

Chemistry Department, University College London†

(Received 14 July 1960)

The effect of bond length changes on ground and excited state energies is examined. The results are applied to aniline.

1. INTRODUCTION

In using semi-empirical self-consistent field molecular orbital theory with limited configuration interaction to calculate excited state energies it is generally assumed that the state energies are insensitive to small changes in bond lengths and overlap integrals. In this paper we show the extent to which these assumptions are justified. Using these assumptions we calculate the energies of the low excited (singlet) states in aniline, where there are considerable variations in both bond length and overlap integral due to the deviation by the nitrogen atom from a pure sp^2 valence state.

2. THE GROUND STATE ENERGY

The π electron energy of a molecule in the SCF m.o. theory is given by [1]

$$E = \text{tr } \mathbf{Rh} + \text{tr } \mathbf{Rf} = 2 \text{tr } \mathbf{Rf} + \text{tr } \mathbf{RG}$$

where $\mathbf{R} = \mathbf{T}\mathbf{T}^\dagger$ is the matrix whose columns are the coefficients of the atomic orbitals in the occupied m.o.'s. The charge and bond order matrix \mathbf{P} is therefore $2\mathbf{R}$. \mathbf{f} and \mathbf{G} are the matrices of the bare framework Hamiltonian and the total electron interaction operator [2] and \mathbf{h} is that of the SCF Hamiltonian.

We consider the variation in energy due to a small change in bond length $r_{ij} \rightarrow r_{ij} + \delta r$ of the bond $i-j$.

2.1. Change in f_{ij} ($= f_{ji}$)

It has been shown [3] that to a good approximation

$$f'_{ij} = \frac{S'_{ij}}{S_{ij}} \cdot f_{ij}$$

where S'_{ij} is the overlap integral when the distance $i-j$ is $r_{ij} + \delta r$.

For homonuclear bonds the overlap integral between two $2p\pi$ orbitals is given by [4]

$$S = \exp(-\rho/2) \left(1 + \frac{\rho}{2} + \frac{\rho^2}{10} + \frac{\rho^3}{120} \right)$$

where $\rho = Zr$, Z is the effective nuclear charge on atoms i and j , and r the interatomic distance (in atomic units). This gives

$$\frac{dS}{dr} = -\exp(-\rho/2) \left(\frac{\rho^2}{20r} + \frac{\rho^3}{40r} + \frac{\rho^4}{240r} \right).$$

† Now at Chemistry Department, King's College, London, W.C.2.

The change in the overlap integral S_{ij} due to a small change δr_{ij} is given by

$$\delta S_{ij} = \frac{dS_{ij}}{dr_{ij}} \delta r_{ij}.$$

Using the value of ρ for nearest neighbours in benzene, $dS/dr = -0.2036$ and $\delta S = -0.2036\delta r$.

For $\delta r = 0.2$ A.U., we obtain $\delta S = -0.040$, $\delta f = 0.37$ ev.

The change in one-electron energy ($= 2 \text{tr } \mathbf{R}\mathbf{f}$) is given by $2P_{ij}\delta f_{ij}$. In our example this gives $\delta E_1 = 0.506$ ev.

A similar argument applies when the hybridization of one or both atoms is changed by a small amount; to a first approximation a small change from sp^2 to sp^3 will slightly reduce the overlap integral and hence f_{ij} .

2.2. Change in G_{ij} ($= G_{ji}$)

For r_{ij} less than 2.8 \AA (~ 5.5 A.U.), we use Pariser and Parr's semi-empirical formula [5] to calculate the atomic Coulomb integrals γ_{ij} . For carbon-carbon bonds this is

$$\gamma_{ij} = 0.2157r_{ij}^{-2} - 2.625r_{ij} + 10.53 \quad (r \text{ in } \text{\AA})$$

giving

$$\delta\gamma_{ij} = \frac{d\gamma_{ij}}{dr_{ij}} \delta r_{ij} = (0.4314r_{ij} - 2.625)\delta r_{ij}.$$

For nearest neighbour bonds in benzenes $\delta\gamma_{ij} = -1.071\delta r$ ev (δr in A.U.). Now $G_{ij} = -R_{ij}\gamma_{ij}$ and so

$$\delta G_{ij} = -R_{ij}\delta\gamma_{ij}. \quad (1)$$

The change in two-electron energy ($= \text{tr } \mathbf{R}\mathbf{G}$) is $-\frac{1}{2}P_{ij}^2\delta\gamma_{ij}$. For benzene nearest neighbour bonds $\delta G_{ij} = 0.0357\delta r_{ij}$ and for $\delta r_{ij} = 0.2$ A.U., $\delta E_2 = 0.048$ ev.

δE_2 is negligible compared with δE_1 and can be ignored.

3. THE EXCITED STATE ENERGY

In the one-configuration approximation the transition energy E_{IJ} (for a singlet) is given by [2]

$$E_{IJ} = \epsilon_J - \epsilon_I - J_{IJ} + 2K_{IJ}$$

where ϵ_J and ϵ_I , J_{IJ} and K_{IJ} are orbital energies, coulomb and exchange integrals respectively.

Consider only the one-electron energy term; this can be rewritten as

$$E_{IJ} = \sum_{ij} (P_{ij}' - P_{ij}) f_{ij}$$

where \mathbf{P}' is the charge and bond order matrix for the excited configuration.

For a small change δt_{ij} in f_{ij} (and also f_{ji}) we have

$$\delta E_{IJ} = (P_{ij}' - P_{ij}) \delta f_{ij}.$$

Since $(P_{ij}' - P_{ij})$ is the difference in bond order P_{ij} in the excited and ground state, it will not usually be greater than one half (its maximum value in benzene) and hence the change in one electron energy will usually be less than $\frac{1}{2}\delta f_{ij}$.

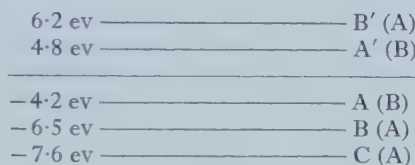
When one bond in benzene is stretched by 0.2 A.U. this gives $\delta E_{IJ} = 0.2$ ev. Bond length variations in aromatic hydrocarbons are usually within ± 0.1 A.U. which sets 0.1 ev for the maximum change in the transition energy. Since semi-empirical calculations rarely approach an accuracy better than this we may say that transition energies are insensitive to small changes in \mathbf{f} .

4. THE ANILINE MOLECULE

The aniline molecule is considered to be flat and the nitrogen of the amino group to be in an sp^2 valence state. There are therefore eight π electrons which occupy the lowest four of the seven available molecular orbitals.

An approximate self consistent ground state was calculated assuming parameter values used in previous calculations [6, 7, 8]. The excited state energies were calculated with interaction of seven singlet configurations

The symmetry of the molecule is C_{2v} and the three top occupied and the lowest two unoccupied molecular orbitals are shown in the figure. The orbitals are labelled (A) or (B) according to their symmetry or antisymmetry with respect to an in-plane two-fold rotation. The energies are given in electron volts about an arbitrary origin [6].



The excited state wave functions are given in the table. The first four belong to representation A of C_{2v} and the last three to B. The energies of the states are relative to the ground state. The symbol $\Phi_{AA'}$ means the singlet configuration in which one electron has been excited from m.o. A to A'.

The observed bands occur at 4.2 and 5.6 ev. Agreement of theory with experiment for the first band is excellent and for the second acceptable.

$\Psi_0 = 0.9862 \Phi_0 - 0.1625 \Phi_{BB'} - 0.0185 \Phi_{AA'} - 0.0228 \Phi_{CB'}$	$E_1^A = 4.3$ ev
$\Psi_1^A = 0.0428 \Phi_0 + 0.1309 \Phi_{BB'} + 0.9828 \Phi_{AA'} + 0.1234 \Phi_{CB'}$	$E_2^A = 7.6$ ev
$\Psi_2^A = 0.1284 \Phi_0 + 0.7065 \Phi_{BB'} - 0.1840 \Phi_{AA'} + 0.6712 \Phi_{CB'}$	$E_3^A = 10.1$ ev
$\Psi_3^A = 0.0945 \Phi_0 + 0.6762 \Phi_{BB'} - 0.0025 \Phi_{AA'} + 0.7306 \Phi_{CB'}$	$E_1^B = 4.3$ ev
$\Psi_1^B = 0.4489 \Phi_{BA} - 0.7795 \Phi_{AB} + 0.4368 \Phi_{CA}$	$E_2^B = 6.1$ ev
$\Psi_2^B = 0.6492 \Phi_{BA} + 0.6204 \Phi_{AB} + 0.4400 \Phi_{CA}$	$E_3^B = 8.3$ ev
$\Psi_3^B = 0.6140 \Phi_{BA} - 0.0860 \Phi_{AB} - 0.7846 \Phi_{CA}$	

We shall now show that the bond length disparities do not affect these conclusions. The exocyclic bond length is 1.47 Å as against the 'standard' length of 1.393 Å from which the integrals are calculated.

Using the methods of §2 and §3 the following estimates of the effect of this change on the ground and excited states are obtained

$$E_0 = 0.25 \text{ ev}, \quad E_1^A = -0.002 \text{ ev}, \quad E_1^B = E_2^B = 0.000 \text{ ev}.$$

The inclusion of a correction for change in bond length thus makes a small change to the ground state energy and no difference to the transition energies.

5. CONCLUSION

The spectrum of aniline calculated by the SCF m.o. theory with configuration interaction is in good agreement with experiment. Transition energies are insensitive to small changes in bond lengths and corresponding integrals. This is essentially a result of cancellation; similar estimates of the effect on ground state shows that all levels may experience significant *absolute* shifts although these will in general be less than 0.5 ev. It should be emphasized however, that these integrals are very sensitive to variations in bond length greater than 0.2 Å.

The author wishes to gratefully acknowledge many helpful discussions with Professor D. P. Craig of this College, also to Dr. R. McWeeny of University College of North Staffordshire for reading the manuscript and finally to Shell Research Ltd., for a research grant during the tenure of which this work was carried out.

REFERENCES

- [1] McWEENY, R., 1956, *Proc. roy. Soc. A*, **237**, 355.
- [2] ROOTHAAN, C. C. J., 1951, *Rev. mod. Phys.*, **23**, 69.
- [3] MULLIKEN, R. S., 1949, *J. Chim. phys.*, **46**, 497.
- [4] MULLIKEN, R. S., *et al.*, 1949, *J. chem. Phys.*, **17**, 1248.
- [5] PARISER, R., and PARR, R. G., 1953, *J. chem. Phys.*, **21**, 787.
- [6] MCWEENY, R., and PEACOCK, T. E., 1957, *Proc. phys. Soc. Lond. A*, **70**, 41.
- [7] PEACOCK, T. E., 1959, *J. chem. Soc.*, p. 3241.
- [8] PEACOCK, T. E., 1959, *J. chem. Soc.*, p. 3645.

Some investigations in the theory of open-shell ions

Part III. The calculation of matrix elements

by J. S. GRIFFITH

Department of Theoretical Chemistry, University Chemical Laboratory,
Lensfield Road, Cambridge

(Received 3 March 1960)

The use of V , W and X coefficients in calculations of matrix elements is shown. General formulae for all two-electron spin-orbit coupling matrices in an octahedral strong-field coupling scheme are deduced. The parametrization of the electrostatic energy in ligand field theory is discussed and the number of parameters required is given in various cases. The configuration f^2 in an octahedral strong-field scheme is treated in some detail and reasons for the anomalously low paramagnetism of PuF_6 are exposed, largely in contradiction to earlier views [13, 14]. Finally it is shown that expressions involving recoupling matrix elements, which occur in a scheme for calculating matrix elements of one-electron operators given by Tanabe and Kamimura [3], are proportional to W and X coefficients, thus considerably extending the scope of the latter work.

1. REDUCED MATRIX ELEMENTS

In Part II we defined and investigated the properties of V , W and X coefficients for certain finite groups and gave tables of their values for the octahedral group [1]. In this and a subsequent paper the use of these coefficients in actual calculations will be shown. The applications invariably depend on the following proposition. Let a , b , c be irreducible representations of a group G with components α , β , γ . Suppose the standard choice for their matrices to be real and that the direct product abc contains the unit representation at most once. Then if $|a\alpha\rangle$, T_β^b , $|c\gamma\rangle$ are kets and operators transforming according to these representations we have

$$\langle a\alpha | T_\beta^b | c\gamma \rangle = \langle a || T^b || c \rangle V \begin{pmatrix} a & b & c \\ \alpha & \beta & \gamma \end{pmatrix}, \quad (1)$$

with the reduced matrix element $\langle a || T^b || c \rangle$ independent of α , β and γ . This equation is the expression in our new notation of one which has already been used in ligand field theory [2, 3] and is the form which the Wigner-Eckart theorem (see, e.g. Fano and Racah [4], henceforward referred to as FR, chapter 14) takes in this case. The order of the representations in the V symbol is important and will always be taken as in equation (1). I adopt the double-barred notation for the reduced matrix element [3, 4] rather than Condon and Shortley's four dots notation [5] which I have used previously [2, 6, 7]. It follows from equation (1) that

$$\langle c || T^b || a \rangle = (-1)^{a+b+c} \overline{\langle a || T^b || c \rangle} \quad (2)$$

for Hermitian T^b , where $(-1)^a$ is -1 for $a = A_2$ or T_1 and is $+1$ otherwise (see Part II). Our definitions do not apply only for G the octahedral group but we consider only that case in the present paper.

2. IRREDUCIBLE PRODUCTS AND THEIR MATRIX ELEMENTS

Given two sets of operators T_η^g and U_θ^h transforming according to the irreducible representations g and h we define the irreducible products

$$(T^g \times U^h)_\kappa^k = \sum_{\eta\theta} \langle gh\eta\theta | ghk\kappa \rangle T_\eta^g U_\theta^h \\ = \lambda(k)^{1/2} \sum_{\eta\theta} V \begin{pmatrix} g & h & k \\ \eta & \theta & \kappa \end{pmatrix} T_\eta^g U_\theta^h. \quad (3)$$

Suppose now we have two independent systems with states $|a\alpha\rangle$, $|a'\alpha'\rangle$... and $|b\beta\rangle$, $|b'\beta'\rangle$..., etc., and that T_η^g operates only on states of the first system and U_θ^h only on those of the second. It then follows that the matrices of T^g and U^h between states which are products of those of the two systems can easily be simplified by equations such as

$$\langle a\alpha | \langle b\beta | T_\eta^g U_\theta^h | a'\alpha' \rangle | b'\beta' \rangle = \langle a\alpha | T_\eta^g | a'\alpha' \rangle \langle b\beta | U_\theta^h | b'\beta' \rangle.$$

Using this we can simplify the matrix of an irreducible product $T^g \times U^h$ within the coupled states

$$|abc\gamma\rangle = \sum_{\alpha\beta} \langle ab\alpha\beta | abc\gamma \rangle |a\alpha\rangle |b\beta\rangle.$$

In fact we have

$$\langle abc\gamma | (T^g \times U^h)_\kappa^k | a'b'c'\gamma' \rangle \\ = \sum_{\alpha\beta\alpha'\beta'\eta\theta} \langle abc\gamma | ab\alpha\beta \rangle \langle gh\eta\theta | ghk\kappa \rangle \langle a'b'\alpha'\beta' | a'b'c'\gamma' \rangle, \quad (4) \\ \langle a\alpha | T_\eta^g | a'\alpha' \rangle \langle b\beta | U_\theta^h | b'\beta' \rangle \\ = \lambda(c)^{1/2} \lambda(c')^{1/2} \lambda(k)^{1/2} \langle a | T^g | a' \rangle \langle b | U^h | b' \rangle X \begin{bmatrix} a & b & c \\ g & h & k \\ a' & b' & c' \end{bmatrix} V \begin{pmatrix} c & k & c' \\ \gamma & \kappa & \gamma' \end{pmatrix}$$

where we used equation (1) and also equation (31) of Part II. Equation (4) can be rewritten in terms of the reduced matrix element of the irreducible product as

$$\langle abc | (T^g \times U^h)^k | a'b'c' \rangle = \lambda(c)^{1/2} \lambda(c')^{1/2} \lambda(k)^{1/2} \langle a | T^g | a' \rangle \\ \langle b | U^h | b' \rangle X \begin{bmatrix} a & b & c \\ g & h & k \\ a' & b' & c' \end{bmatrix} \quad (5)$$

when it corresponds to FR, equation (15.4).

An important special case occurs when $g=h=T_1$. Dropping the superscripts, we can regard T_η and U_θ as vectors with components x , y and z and find

$$(T \times U)^{A_1} = \frac{1}{\sqrt{3}} \mathbf{T} \cdot \mathbf{U}. \quad (6)$$

Equation (4) then simplifies to

$$\langle abc\gamma | \mathbf{T} \cdot \mathbf{U} | a'b'c'\gamma' \rangle = (-1)^{a+b'+c+T_1} \delta_{cc'} \delta_{\gamma\gamma'} \langle a | T | a' \rangle \\ \langle b | U | b' \rangle W \begin{pmatrix} a' & b' & c \\ b & a & T_1 \end{pmatrix}. \quad (7)$$

3. SPIN-ORBIT COUPLING IN TWO-ELECTRON SYSTEMS

In the particular case of two-electron systems the eigenstates of \mathbf{S}^2 which span irreducible representations of the covering group of the three-dimensional

rotation group also do so for the octahedral group O. We can then use equation (7) by taking the kets $|a\alpha\rangle, \dots$ to refer to spin and $|b\beta\rangle, \dots$ to refer to space and \mathbf{T}, \mathbf{U} as a part $\mathbf{s}_i \cdot \mathbf{u}_i$ of the spin-orbit coupling energy.

The first application is to determine the form of the matrix of spin-orbit coupling between a pair of triplet terms, 3b and ${}^3b'$ for the various possible representations c which they have in common. Equation (7) shows this matrix to be a multiple of

$$(-1)^c \delta_{cc'} \delta_{\gamma\gamma'} W \begin{pmatrix} T_1 & b' & c \\ b & T_1 & T_1 \end{pmatrix} = \delta_{cc'} \delta_{\gamma\gamma'} P(c), \text{ say.}$$

As an example consider ${}^3b = {}^3T_1$ and ${}^3b' = {}^3T_2$. Then

$$P(c) = (-1)^c W \begin{pmatrix} T_1 & T_2 & c \\ T_1 & T_1 & T_1 \end{pmatrix}$$

whence from table 3 of Part II we find $P(E):P(T_1):P(T_2) = \sqrt{3}:1:-1$. Thus for triplet terms we have a new method of calculating the ratios of the c -numbers given in reference [6]. The phases of the coupling coefficients in the latter are the same as in the present series except for coupling of $T_2 T_1$ to E , $T_1 E$ to T_2 and ET_2 to T_1 , but not the same as in references [3, 7 or 8]. I did not realize when I wrote that paper [6] that I could choose my phases so that W is invariant to odd permutations of its columns.

Next we calculate the complete matrix of spin-orbit coupling in a scheme in which the basic states are built up by coupling together one-electron functions which form bases for irreducible spin and space representations. These states are simple products of a symmetric (antisymmetric) spin function with an antisymmetric (or symmetric) space function. The forms of the spin functions are well known and we readily obtain the reduced matrix elements of the spin vectors $\mathbf{s}(1)$ and $\mathbf{s}(2)$ for the two electrons as follows:

$$\begin{aligned} \langle 0 || s(1) || 0 \rangle &= \langle 0 || s(2) || 0 \rangle = 0 \\ \langle 1 || s(1) || 1 \rangle &= \langle 1 || s(2) || 1 \rangle = -\frac{1}{2}i\sqrt{6} \\ \langle 0 || s(1) || 1 \rangle &= -\langle 0 || s(2) || 1 \rangle = -\frac{1}{2}i\sqrt{3} \\ \langle 1 || s(1) || 0 \rangle &= -\langle 1 || s(2) || 0 \rangle = \frac{1}{2}i\sqrt{3}. \end{aligned} \quad (8)$$

Here 0 and 1 in the kets and bras give the value of S and the phases are chosen in accordance with those of references [1 and 6]. Note that the reduced matrix elements here derive from equation (1) and use real spin functions behaving like x, y, z under rotation rather than the usual ones quantized with respect to S_z .

Because of the antisymmetry of our total functions we can take the spin-orbit coupling in the form

$$\mathcal{H}_s = 2\mathbf{s}(1) \cdot \mathbf{u}(1). \quad (9)$$

Equations (8) for $s(1)$ can be contracted into the formula

$$\langle S || s(1) || S' \rangle = \frac{\sqrt{3}}{2} i(S + S')^{1/2} (-1)^{S'}. \quad (10)$$

Introducing (9) and (10) into (7) and setting $c = c'$ and $\gamma = \gamma'$ yields

$$\begin{aligned} &\langle^{2S+1}b\gamma | \mathcal{H}_s | ^{2S'+1}b'\gamma' \rangle \\ &= (-1)^{S+S'+b'+c+T_1} i\sqrt{3} (S + S')^{1/2} \langle b || u(1) || b' \rangle W \begin{pmatrix} S' & b' & c \\ b & S & T_1 \end{pmatrix} \end{aligned} \quad (11)$$

where we interpret S and S' as the numbers 0 or 1 or as A_1 or T_1 depending on their context. When $S=0$, $S'=1$, the right-hand side simplifies to

$$-i\lambda(b)^{-1/2}\delta_{bc}\langle b||u(1)||b'\rangle.$$

We now determine $\langle b||u(1)||b'\rangle$ in terms of reduced one-electron matrix elements for \mathbf{u} . Both $|b\beta\rangle$ and $|b'\beta'\rangle$ are built up by coupling together a pair of one-electron representations and a number of cases arise depending on the extent to which the four sets of one-electron functions concerned are distinct. For $|b\beta\rangle$ itself there are two possibilities, either the two constituent sets are the same or different. If they are both the one-electron set $|e\epsilon\rangle$, say, then a typical product set is

$$|e^2b\beta\rangle = \lambda(b)^{1/2} \sum_{\epsilon\phi} V \begin{pmatrix} e & e & b \\ \epsilon & \phi & \beta \end{pmatrix} |e\epsilon(1)\rangle |e\phi(2)\rangle \quad (12)$$

and forms part of a singlet or triplet spin state according to whether b is contained in the symmetrized or antisymmetrized square of e . If b is composed of two different one-electron sets, $|e\epsilon\rangle$ and $|f\phi\rangle$ say, then

$$|efb\beta\rangle = \frac{1}{\sqrt{2}} \lambda(b)^{1/2} \sum_{\epsilon\phi} V \begin{pmatrix} e & f & b \\ \epsilon & \phi & \beta \end{pmatrix} \{ |e\epsilon(1)\rangle |f\phi(2)\rangle + (-1)^S |f\phi(1)\rangle |e\epsilon(2)\rangle \} \quad (13)$$

where S is the spin.

Using (12) and (13) we can immediately obtain $\langle b||u(1)||b'\rangle$ in terms of one-electron elements. As an example consider matrix elements between e^2 and ef . We have

$$\begin{aligned} & \langle e^2b||u(1)||efb'\rangle V \begin{pmatrix} b & T_1 & b' \\ \beta & \theta & \beta' \end{pmatrix} = \langle e^2b\beta|u_\theta(1)|efb'\beta'\rangle \\ &= \frac{1}{\sqrt{2}} \lambda(b)^{1/2} \lambda(b')^{1/2} \sum_{\epsilon\phi\epsilon'\phi'} V \begin{pmatrix} e & e & b \\ \epsilon' & \phi' & \beta \end{pmatrix} V \begin{pmatrix} e & f & b' \\ \epsilon & \phi & \beta' \end{pmatrix} (-1)^{S'} \delta_{\phi'\epsilon} \langle e\epsilon'|u_\theta|f\phi\rangle \\ &= \frac{1}{\sqrt{2}} \lambda(b)^{1/2} \lambda(b')^{1/2} (-1)^{S'} \langle e||u||f\rangle \sum_{\epsilon\epsilon'\phi} V \begin{pmatrix} b & e & e \\ \beta & \epsilon' & \epsilon \end{pmatrix} V \begin{pmatrix} b' & e & f \\ \beta' & \epsilon & \phi \end{pmatrix} V \begin{pmatrix} T_1 & f & e \\ \theta & \phi & \epsilon' \end{pmatrix} \\ &= \frac{1}{\sqrt{2}} \lambda(b)^{1/2} \lambda(b')^{1/2} (-1)^{S'} \langle e||u||f\rangle W \begin{pmatrix} b & b' & T_1 \\ f & e & e \end{pmatrix} V \begin{pmatrix} b & b' & T_1 \\ \beta & \beta' & \theta \end{pmatrix} \end{aligned}$$

where we have used equation (18) of Part II. Hence we have to insert

$$\langle b||u(1)||b'\rangle = \frac{1}{\sqrt{2}} \lambda(b)^{1/2} \lambda(b')^{1/2} (-1)^{S'+b+b'+T_1} \langle e||u||f\rangle W \begin{pmatrix} b & b' & T_1 \\ f & e & e \end{pmatrix} \quad (14)$$

into equation (11). The other cases are dealt with in a precisely analogous way and we obtain the following four formulae which give a complete set of matrices of spin-orbit coupling for two-electron systems in terms of the reduced elements for one-electron functions:

$$\begin{aligned} & \langle e^{2S+1}bc|\mathcal{H}_s|e^{2S'+1}b'c\rangle \\ &= (-1)^{S+S'+b+b'+c} i\sqrt{3(S+S')}^{1/2} \lambda(b)^{1/2} \lambda(b')^{1/2} \langle e||u||e\rangle W \begin{pmatrix} b & b' & T_1 \\ e & e & e \end{pmatrix} W \begin{pmatrix} S' & b' & c \\ b & S & T_1 \end{pmatrix}, \\ & \langle e^{2S+1}bc|\mathcal{H}_s|ef^{2S'+1}b'c\rangle \\ &= \frac{1}{2} (-1)^{S+b+c} i\sqrt{6(S+S')}^{1/2} \lambda(b)^{1/2} \lambda(b')^{1/2} \langle e||u||f\rangle W \begin{pmatrix} b & b' & T_1 \\ f & e & e \end{pmatrix} W \begin{pmatrix} S' & b' & c \\ b & S & T_1 \end{pmatrix}, \end{aligned}$$

$$\begin{aligned}
 & \langle ef^{2S+1}bc | \mathcal{H}_s | ef^{2S'+1}b'c' \rangle \\
 &= \frac{1}{2}(-1)^{e+e+f}i\sqrt{3}(S+S')^{1/2}\lambda(b)^{1/2}\lambda(b')^{1/2}W\left(\begin{matrix} S' & b' & c \\ b & S & T_1 \end{matrix}\right) \\
 & \quad \left[(-1)^{S+S'+b+b'}\langle e||u||e \rangle W\left(\begin{matrix} b & b' & T_1 \\ e & e & f \end{matrix}\right) + \langle f||u||f \rangle W\left(\begin{matrix} b & b' & T_1 \\ f & f & e \end{matrix}\right) \right], \\
 & \langle ef^{2S+1}bc | \mathcal{H}_s | eg^{2S'+1}b'c' \rangle \\
 &= \frac{1}{2}(-1)^{S+S'+e+e+f}i\sqrt{3}(S+S')^{1/2}\lambda(b)^{1/2}\lambda(b')^{1/2}\langle f||u||g \rangle \\
 & \quad W\left(\begin{matrix} b & b' & T_1 \\ g & f & e \end{matrix}\right) W\left(\begin{matrix} S' & b' & c \\ b & S & T_1 \end{matrix}\right). \tag{15}
 \end{aligned}$$

The reduced matrix elements for $\mathbf{u} = \xi(r)\mathbf{l}$ are given in table 1 for p , d and f atomic orbitals and that table together with equations (15) give the spin-orbit matrices for any set of two-electron coupled states built up from s , p , d and f atomic orbitals. The resulting matrix for d^2 is identical with that derived from table 4 of reference [6], except for the consequences of the phase change mentioned earlier. In making this comparison remember that a change of order of coupling in equations (15) can sometimes produce a change of sign of the matrix element.

p	T_1	d	E	T_2
T_1	$-i\sqrt{6}$	E	0	$-2i\sqrt{3}$
		T_2	$-2i\sqrt{3}$	$i\sqrt{6}$
f	A_2	T_1	T_2	
A_2	0	0	$-2i\sqrt{3}$	
T_1	0	$\frac{3}{2}i\sqrt{6}$	$-\frac{3}{2}i\sqrt{10}$	
T_2	$2i\sqrt{3}$	$\frac{3}{2}i\sqrt{10}$	$-\frac{1}{2}i\sqrt{6}$	

Table 1. Reduced matrix elements of \mathbf{l} for p , d and f orbitals.

4. ELECTROSTATIC MATRIX ELEMENTS

It is convenient at this stage to interpose a discussion of the electrostatic energy. In the theory for spherical symmetry this two-electron operator is usually expanded as a sum of scalar products of irreducible one-electron tensor operators [9]. However, under the octahedral group these latter are no longer usually irreducible. We start by considering a set of atomic orbitals, using the same kind of treatment as in § 4 of Part I [10] and then as in that section pass on later to functions classified according to the representations of a finite group.

We first discuss the expansion of the electrostatic energy as a sum of products of one-electron operators. First we suppose we have a set of $(2l+1)$ states $|m\rangle$ which are eigenstates of \mathbf{l}^2 and l_z and ask what is an operator equivalent suitable to represent a general two-electron operator ρ within the set of simple product states $|m_1 m_2\rangle = |m_1\rangle|m_2\rangle$. Here the first ket in the product refers to

particle one and the second to particle two. An answer is an immediate generalization of equation (22) of Part I. We may use

$$X = \sum_{cc'\gamma\gamma'} Q_{\gamma\gamma'}^{cc'} \mathcal{L}_{-\gamma}^{(c)}(1) \mathcal{L}_{-\gamma'}^{(c')}(2) \quad (16)$$

where $\mathcal{L}_0^{(0)}=1$ and otherwise $\mathcal{L}^{(c)}(i)$ is the irreducible product of degree c of c orbital angular momentum vectors for the i th electron.

Assume now that $\rho = \bar{\rho} = \rho^*$ and $\rho(12) = \rho(21)$. Then using

$$\overline{\mathcal{L}_{\gamma}^{(c)}} = (-1)^c \mathcal{L}_{\gamma}^{(c)*} = (-1)^{\gamma} \mathcal{L}_{-\gamma}^{(c)}$$

we deduce that

$$Q_{\gamma\gamma'}^{cc'} = Q_{\gamma\gamma'}^{c'c}, \quad \overline{Q_{\gamma\gamma'}^{cc'}} = (-1)^{\gamma+\gamma'} Q_{-\gamma-\gamma'}^{cc'}$$

where $Q_{\gamma\gamma'}^{cc'} = 0$ when $c + c'$ is odd. If ρ is simply a function of the position of the two electrons, such as the electrostatic energy, we see by expressing our matrix elements in the Schrödinger representation that

$$\langle M_1 M_2 | \rho | M_3 M_4 \rangle = (-1)^{M_3 - M_1} \langle M_3 M_2 | \rho | M_1 M_4 \rangle.$$

The same equation holds for the matrix elements of X . We derive a condition on the Q by expanding the latter equation in terms of the reduced matrix elements of the $\mathcal{L}_{\gamma}^{(c)}$ and the \tilde{V} coefficients. The orthogonality relations for the \tilde{V} then enable us to deduce that $Q_{\gamma\gamma'}^{cc'} = (-1)^c Q_{\gamma\gamma'}^{c'c}$, so the $Q_{\gamma\gamma'}^{cc'}$ are zero unless both c and c' are even. It follows also that ρ determines the $Q_{\gamma\gamma'}^{cc'}$ uniquely.

Suppose now that ρ transforms as the unit representation Γ_1 of a symmetry group G , i.e. is an invariant of G . Write $h = X - \rho$. Then h has zero matrix elements within all our product states. Therefore so also has gh for g any element of G . This means that as $g\rho = \rho$, gX and X have the same matrix elements. But as the set of matrix elements of a quantity of the kind in equation (16) determine the $Q_{\gamma\gamma'}^{cc'}$ uniquely it follows that $gX = X$. So X is an invariant of G . As c and c' in (16) must both be even and $Q_{\gamma\gamma'}^{cc'} = Q_{\gamma\gamma'}^{c'c}$ we can deduce that the number of parameters necessary to specify a general invariant ρ within our product states is the number of times Γ_1 occurs in the symmetrized square of the symmetrized square of a set of functions transforming as $|lm\rangle$. We can write this $[[l]^2]^2$. For example if $l=2$ we have $[d]^2 = S + D + G$ and $[[d]^2]^2 = 3S + 4D + F + 4G + H + 2I + L$. If our symmetry group is the three-dimensional rotation group R_3 then $\Gamma_1 = S$ and we need three parameters. These are of course the Slater-Condon F_0 , F_2 and F_4 when ρ is the electrostatic energy. If it is the octahedral group, $\Gamma_1 = A_1$ and we need 10 parameters. For the latter group and $l=3$ we need 26 parameters.

A problem which is closely related to the preceding one and of much more interest is the following which we introduce via an example. We consider that d electrons in an octahedral complex are not in true d orbitals but merely in orbitals having the same transformation properties under the octahedral group. This may be made precise and more general by writing the transformation from lm to $l\Gamma_1 M_1$ quantization† as

$$|l\beta_1 \Gamma_1 M_1\rangle = \sum_m \langle lm | l\beta_1 \Gamma_1 M_1 \rangle |lm\rangle$$

where β_1 is introduced when necessary for large l to distinguish repeated Γ_1 . For simplicity the $|l\beta_1 \Gamma_1 M_1\rangle$ are taken to be real and we modify them by

† Here Γ_1 is no longer necessarily the unit representation.

multiplying them by a real invariant $a(\beta_1 \Gamma_1)$ which is independent of M_1 :

$$|l\beta_1 \Gamma_1 M_1\rangle' = a(\beta_1 \Gamma_1) |l\beta_1 \Gamma_1 M_1\rangle.$$

For $l=2$ this is what is meant by saying that d orbitals in an octahedral complex are not true d orbitals. We now show that it is formally equivalent to replacing the electrostatic energy V , which is an invariant of R_3 , by a corresponding operator V' which is only an invariant of the restricted symmetry group and to leaving the states $|lm\rangle$ unchanged.

The problem is to replace the multiplication of the kets $|l\beta_1 \Gamma_1 M_1\rangle$ by the quantities $a(\beta_1 \Gamma_1)$ which depend on β_1 and Γ_1 by multiplication by an invariant operator which is independent of them. We can then transform back to the lm scheme and will have established our result. To do this define

$$p(\beta \Gamma M) |l\beta' \Gamma' M'\rangle = \delta(\beta\beta') \delta(\Gamma\Gamma') \delta(MM') |l\beta' \Gamma' M'\rangle.$$

The $p(\beta \Gamma M)$ are projection operators and satisfy $\bar{p} = p^* = p$. Then we have

$$|l\beta_1 \Gamma_1 M_1\rangle' = A |l\beta_1 \Gamma_1 M_1\rangle,$$

where

$$A = \sum_{\beta \Gamma M} a(\beta \Gamma) p(\beta \Gamma M), \quad (17)$$

and $V' = A_1 A_2 V A_1 A_2$ is an invariant of the symmetry group, where A_i is the sum in (17) taken over projection operators operating only on kets for the i th electron. By expanding $\langle m_1 m_2 | V' | m_3 m_4 \rangle$ in the $l\Gamma_1 M_1$ scheme we easily deduce that V' possesses all the properties which gave us our restrictions on the $Q_{yy'}^{cc'}$ of equation (16). Therefore V' has an operator equivalent (16) with the same restrictions.

We next consider how our analysis is modified when we work entirely within the scheme provided by a finite group G for which V symbols are defined. Given an operator $f(\Gamma_1 M_1)$ which transforms as the M_1 component of a representation Γ_1 we have

$$\langle \alpha \Gamma M | f(\Gamma_1 M_1) | \alpha' \Gamma' M' \rangle = \langle \alpha || f || \alpha' \rangle V \begin{pmatrix} \Gamma & \Gamma_1 & \Gamma_1' \\ M & M_1 & M' \end{pmatrix}. \quad (18)$$

Equation (18) gives us exactly the same computational apparatus for G as we used for R_3 earlier in this section. Therefore the same results hold. In place of the $\mathcal{L}_y^{(r)}$ we can, if we wish, take unit operators $n(\Gamma_1 M_1)$ defined, for fixed $\alpha, \alpha', \Gamma, \Gamma'$, by $\langle \alpha || n || \alpha' \rangle = \delta_{\alpha \alpha'}$. As a simple example, for the octahedral group $[t_2]^2 = A_1 + E + T_2$ and hence we need three parameters for a general t_2^n configuration as pointed out by Stevens [11].

Our treatment is easily extended to cover the case when we have interactions amongst product states based on a set Σ of irreducible representations. Here we simply need a number of parameters equal to the number of times that the unit representation occurs in $[[\Sigma]^2]^2$. It is a consequence of this that the number of parameters needed to specify the electrostatic energy amongst products based on $2l+1$ orbitals which transform like $|lm\rangle$ under G but not necessarily under R_3 is the same as the number necessary to specify a general invariant, of the type considered earlier in the section, within the $|lm\rangle$. Therefore to specify the electrostatic interaction within a general $t_{2g}^m e_g^n$ set of configurations we need 10 parameters. Similarly for $a_{1u}^m t_{1u}^n t_{2u}^p$ we need 26. For d functions which are not 'true' d functions we need 23 and 26 for D_4 and D_3 respectively.

5. OFF-DIAGONAL MATRIX ELEMENTS FOR THE OCTAHEDRAL GROUP

In actual calculations we may need matrix elements of the electrostatic energy of the general type $\langle m_1 m_2 | V | m_3 m_4 \rangle$. We now obtain all of these for d and for f configurations both without and with the assumption that the constituent orbitals are 'true' d and f orbitals. This could be done via a sum of products of one-electron functions but it is actually easier just to determine the restrictions on the matrix elements directly by applying rotations and permutations of the constituent orbitals. We define real orbitals satisfying

$$\left. \begin{array}{l} \theta = |20\rangle \\ \epsilon = \frac{1}{2}\sqrt{2}(|22\rangle + |2-2\rangle) \end{array} \right\} \subseteq E \quad \left. \begin{array}{l} \xi = \frac{1}{2}i\sqrt{2}(|21\rangle + |2-1\rangle) \\ \eta = \frac{1}{2}\sqrt{2}(|2-1\rangle - |21\rangle) \\ \zeta = -\frac{1}{2}i\sqrt{2}(|22\rangle - |2-2\rangle) \end{array} \right\} \subseteq T_2$$

for d electrons and

$$\left. \begin{array}{l} \chi = \frac{1}{2}i\sqrt{2}(|3-2\rangle - |32\rangle) \subseteq A_2, \\ x = \frac{1}{4}(\sqrt{3}|31\rangle - \sqrt{3}|3-1\rangle - \sqrt{5}|33\rangle + \sqrt{5}|3-3\rangle) \\ y = -\frac{1}{4}i(\sqrt{3}|31\rangle + \sqrt{3}|3-1\rangle + \sqrt{5}|33\rangle + \sqrt{5}|3-3\rangle) \\ z = |30\rangle, \\ \xi = \frac{1}{4}(\sqrt{5}|31\rangle - \sqrt{5}|3-1\rangle + \sqrt{3}|33\rangle - \sqrt{3}|3-3\rangle), \\ \eta = \frac{1}{4}i(\sqrt{5}|31\rangle + \sqrt{5}|3-1\rangle - \sqrt{3}|33\rangle - \sqrt{3}|3-3\rangle), \\ \zeta = \frac{1}{2}\sqrt{2}(|32\rangle + |3-2\rangle) \end{array} \right\} \subseteq T_1, \quad \left. \begin{array}{l} \end{array} \right\} \subseteq T_2,$$

for f electrons. All the functions in the $l\Gamma_1 M_1$ scheme are real. For convenience of tabulation we also define

$$(ac; bd) \equiv \langle ab | V | cd \rangle$$

and have $(ac; bd)$ invariant to interchange of a with c , b with d or ac with bd . The calculation is now straightforward, but, at least for f electrons, a little lengthy. I illustrate it for d electrons.

First we derive some selection rules by classifying the orbitals by their behaviour under the group D_4 about OZ . $\xi, \eta, \zeta, \theta, \epsilon$ behave as $ex, -ey, b_2, a_1, b_1$, respectively under that group. Hence the 15 different products ac for the first electron form bases for representations of D_4 as follows:

$$\begin{aligned} & \frac{1}{\sqrt{2}}(\xi^2 + \eta^2), \xi^2, \theta^2, \epsilon^2 \subseteq A_1, \\ & \zeta\epsilon \subseteq A_2, \\ & \frac{1}{\sqrt{2}}(\xi^2 - \eta^2), \theta\epsilon \subseteq B_1, \\ & \xi\eta, \zeta\theta \subseteq B_2, \\ & \xi\theta, \eta\zeta, \xi\epsilon \subseteq Ex, \\ & \eta\theta, \zeta\xi, \eta\epsilon \subseteq Ey. \end{aligned} \tag{19}$$

We have omitted minus signs for Ex and Ey . The products bd for the second electron are classified in the same way and then because V belongs to the unit representation of D_4 we have $(ac; bd) = 0$ unless ac occurs in the same set as bd in (19). So the matrix of V breaks up into five completely non-interacting sub-matrices. We can also deduce relationships of the kind

$$(\xi^2; \theta^2) = (\eta^2; \theta^2), \quad (\xi^2, \theta\epsilon) = -(\eta^2, \theta\epsilon)$$

because $\xi^2 + \eta^2$ and θ^2 are A_1 but $\xi^2 - \eta^2$ and $\theta\epsilon$ are B_1 .

A_1, B_1	ξ^2	η^2	ζ^2	θ^2	ϵ^2	$\theta\epsilon$
$a = A + 4B + 3C$	$b = A - 2B + C$		$b = A - 2B + C$	$d + \frac{2}{\sqrt{3}} c = A + 2B + C$	$d = A - 2B + C$	$c = 2B\sqrt{3}$
$b = A - 2B + C$	$a = A + 4B + 3C$		$b = A - 2B + C$	$d + \frac{2}{\sqrt{3}} c = A + 2B + C$	$d = A - 2B + C$	$-c = -2B\sqrt{3}$
$b = A - 2B + C$			$a = A + 4B + 3C$	$d - \frac{1}{\sqrt{3}} c = A - 4B + C$	$d + \sqrt{3}c = A + 4B + C$	0
$d + \frac{2}{\sqrt{3}} c = A + 2B + C$	$d = A - 2B + C$		$d - \frac{1}{\sqrt{3}} c = A - 4B + C$	$c = A + 4B + 3C$	$c - 2f = A - 4B + C$	0
$d = A - 2B + C$			$d + \sqrt{3}c = A + 4B + C$	$e = A + 4B + 3C$	$e - 2f = A - 4B + C$	$e = A + 4B + 3C$
$c = 2B\sqrt{3}$			0	0	0	$f = 4B + C$

Table 2.

B_2	$\theta\xi$	$\xi\eta$
$\theta\xi$	$g + \sqrt{3}h = 4B + C$	$-2i = -2B\sqrt{3}$
$\xi\eta$	$-2i = -2B\sqrt{3}$	$j = 3B + C$

A_2	$\epsilon\xi$
$\epsilon\xi$	$g - \frac{1}{\sqrt{3}}h = C$
Ey	$\theta\eta$
$\theta\eta$	$g = B + C$
$\epsilon\eta$	$h = B\sqrt{3}$
$\zeta\xi$	$i = B\sqrt{3}$

Table 2 (continued). The expressions for the non-zero $(ab; cd) \equiv \langle ac|V|bd\rangle$ for d electrons, classified according to the representation of D_4 .

After this we progress by applying elements of O to matrix elements. For example

$$\begin{aligned} (\xi^2; \theta^2) &= C_4^x(\xi^2; \theta^2) \\ &= \frac{1}{4}(\xi^2; \theta^2) + \frac{3}{4}(\epsilon^2; \xi^2) + \frac{1}{2}\sqrt{3}(\xi^2; \theta\epsilon), \end{aligned}$$

i.e. $(\xi^2; \theta^2) = (\xi^2; \epsilon^2) + \frac{2}{3}\sqrt{3}(\xi^2; \theta\epsilon)$. Having determined sufficient relations of this type we then express the entire set of matrix elements in terms of 10 chosen parameters. This is shown in table 2, together with the expressions in terms of the Racah parameters A , B and C for the case in which the orbitals are actually d orbitals (largely as in reference [8]).

A_1, B_1	χ^2	z^2	ζ^2	x^2	y^2	ξ^2	η^2	$x\xi$	$y\eta$	$z\zeta$
χ^2	a	b	c	b	b	c	c	0	0	0
z^2	b	d	i	g	g	j	j	$-l$	l	0
ζ^2	c	i	e	j	j	h	h	$-k$	k	0
x^2	b	g	j	d	g	i	j	0	$-l$	l
y^2	b	g	j	g	d	j	i	l	0	$-l$
ξ^2	c	j	h	i	j	e	h	0	$-k$	k
η^2	c	j	h	j	i	h	e	k	0	$-k$
$x\xi$	0	$-l$	$-k$	0	l	0	k	f	m	m
$y\eta$	0	l	k	$-l$	0	$-k$	0	m	f	m
$z\zeta$	0	0	0	l	$-l$	k	$-k$	m	m	f

(Ey) Ex	$(-\chi\gamma)$ χ^x	$(\chi\eta)$ $\chi\xi$	$(-zx)$ yz	$(-\zeta\xi)$ $\eta\zeta$	$(x\zeta)$ $y\zeta$	$(z\xi)$ $z\eta$
$(-\chi\gamma)\chi x$	n	0	s	t	u	$-u$
$(\chi\eta)\chi\xi$	0	o	0	0	v	v
$(-zx)yz$	s	0	p	w	x	$-x$
$(-\zeta\xi)\eta\zeta$	t	0	w	q	y	$-y$
$(x\zeta)y\zeta$	u	v	x	y	r	z
$(z\xi)z\eta$	$-u$	v	$-x$	$-y$	z	r

A_2, B_2	$\chi\xi$	$x\eta$	$y\xi$	χz	xy	$\xi\eta$
$\chi\xi$	o	v	v	0	0	0
$x\eta$	v	r	z	u	x	y
$y\xi$	v	z	r	$-u$	$-x$	$-y$
χz	0	u	$-u$	n	s	t
xy	0	x	$-x$	s	p	w
$\xi\eta$	0	y	$-y$	t	w	q

Table 3. The non-zero $(ab; cd)$ for f electrons in terms of generalized parameters.

The calculation for f orbitals follows exactly the same course. Table 3 gives the matrix elements in terms of the 26 parameters and table 4 gives those parameters in terms of the quantities

$$\begin{aligned}E^0 &= F_0 - 10F_2 - 33F_4 - 286F_6, \\E^1 &= \frac{1}{9}(70F_2 + 231F_4 + 2002F_6), \\E^2 &= \frac{1}{9}(F_2 - 3F_4 + 7F_6), \\E^3 &= \frac{1}{3}(5F_2 + 6F_4 - 91F_6),\end{aligned}$$

introduced by Racah [12] for f electron configurations.

$$\begin{aligned}a &= E^0 + 3E^1 - 120E^2, \\b &= E^0 + E^1 + 80E^2 - 4E^3, \\c &= E^0 + E^1 - 40E^2 + 4E^3, \\d &= E^0 + 3E^1 + 24E^2, \\e &= E^0 + 3E^1 - 120E^2, \\f &= E^1 + 80E^2 + 2E^3, \\g &= E^0 + E^1 - 59\frac{1}{2}E^2 + \frac{1}{2}E^3, \\h &= E^0 + E^1 + 72\frac{1}{2}E^2 - 3\frac{1}{2}E^3, \\i &= E^0 + E^1 + 80E^2 - 4E^3, \\j &= E^0 + E^1 - 32\frac{1}{2}E^2 + 3\frac{1}{2}E^3, \\k &= \frac{\sqrt{15}}{2}(15E^2 - E^3), \\l &= -\frac{3\sqrt{15}}{2}(9E^2 + E^3), \\m &= -22\frac{1}{2}E^2 - 4\frac{1}{2}E^3, \\n &= E^1 + 80E^2 + 2E^3, \\o &= E^1 - 40E^2 - 2E^3, \\p &= E^1 - 59\frac{1}{2}E^2 - \frac{1}{4}E^3, \\q &= E^1 + 72\frac{1}{2}E^2 + \frac{7}{4}E^3, \\r &= E^1 - 32\frac{1}{2}E^2 - \frac{7}{4}E^3, \\s &= 9\sqrt{15}E^2, \\t &= \sqrt{15}(15E^2 + 2E^3), \\u &= 3E^3, \\v &= \sqrt{15}(15E^2 - E^3), \\w &= -22\frac{1}{2}E^2 + 3\frac{3}{4}E^3, \\x &= \frac{3\sqrt{15}}{2}(9E^2 - \frac{1}{2}E^3), \\y &= \frac{\sqrt{15}}{2}(15E^2 + \frac{1}{2}E^3), \\z &= -22\frac{1}{2}E^2 + \frac{3}{4}E^3.\end{aligned}$$

Table 4. The generalized parameters for f electrons expressed in terms of Racah's parameters E^i .

6. THE f^2 CONFIGURATION

Using the matrix elements in table 3 it is a straightforward matter to calculate the matrix of electrostatic energy for f^2 in terms of the 26 generalized parameters or the E^i . The results are given in table 5. They were checked by solving the associated secular equations in terms of the E^i and comparing with Racah [12]. The table, together with formulae (15) and table 1, give the complete matrices of electrostatic and spin-orbit coupling energies for f^2 . Part of the latter matrix is written out in table 6 and will now be used to discuss the magnetic properties of the f^2 configuration in an octahedral field.

1A_1	a_2^2	t_1^2	t_2^2	$t_1 t_2$
a_2^2	$E^0 + 3E^1 - 120E^2$ [a]	$\sqrt{3}(E^1 - 40E^2 - 2E^3)$ [o \sqrt{3}]	$\sqrt{3}(E^1 + 80E^2 + 2E^3)$ [n \sqrt{3}]	$\sqrt{3}(E^1 + 80E^2 + 2E^3)$ [n \sqrt{3}]
t_2^2	$\sqrt{3}(E^1 - 40E^2 - 2E^3)$ [o \sqrt{3}]	$E^0 + 5E^1 + 25E^2 + 3\frac{1}{2}E^3$ [e + 2q]	$3E^1 + 15E^2 - 1\frac{1}{2}E^3$ [f + 2r]	$3E^1 + 15E^2 - 1\frac{1}{2}E^3$ [f + 2r]
t_1^2	$\sqrt{3}(E^1 + 80E^2 + 2E^3)$ [n \sqrt{3}]	$3E^1 + 15E^2 - 1\frac{1}{2}E^3$ [f + 2r]	$E^0 + 5E^1 - 95E^2 - \frac{1}{2}E^3$ [d + 2p]	$E^0 + 5E^1 - 95E^2 - \frac{1}{2}E^3$ [d + 2p]
$^1A_2 = E^0 + 2E^1 + 70E^2 + 7E^3$				
$[i + f + 2w + 2z]$				

1E	t_1^2	t_2^2	$t_1 t_2$
t_1^2	$E^0 + 2E^1 + 83\frac{1}{2}E^2 + \frac{1}{4}E^3$ [d - p]	$112\frac{1}{2}E^2 + 3\frac{3}{4}E^3$ [i + f]	$\frac{9}{2}\sqrt{10}(9E^2 - \frac{1}{2}E^3)$ [x \sqrt{6}]
t_2^2	$112\frac{1}{2}E^2 + 3\frac{3}{4}E^3$ [i + f]	$E^0 + 2E^1 - 192\frac{1}{2}E^2 - 1\frac{3}{4}E^3$ [e - q]	$-\frac{3}{2}\sqrt{10}(15E^2 + \frac{1}{2}E^3)$ [-y \sqrt{6}]
$t_1 t_2$	$\frac{9}{2}\sqrt{10}(9E^2 - \frac{1}{2}E^3)$ [x \sqrt{6}]	$- \frac{3}{2}\sqrt{10}(15E^2 + \frac{1}{2}E^3)$ [-y \sqrt{6}]	$E^0 + 2E^1 + 205E^2 - 6\frac{1}{2}E^3$ [i + f - w - z]

1T_1	$a_2 t_2$	$t_1 t_2$
$a_2 t_2$	$E^0 + 2E^1 - 80E^2 + 2E^3$ [c + o]	$-\sqrt{30}(30E^2 + E^3)$ [-(t + v) \sqrt{2}]
$t_1 t_2$	$-\sqrt{30}(30E^2 + E^3)$ [-(t + v) \sqrt{2}]	$E^0 + 2E^1 - 110E^2 + E^3$ [j + r + w + m]

Table 5.

1T_2	a_2t_1	t_1^2	t_2^2	t_1t_2
a_2t_1	$E^0 + 2E^1 + 160E^2 - 2E^3$ [$b+n$]	$-18\sqrt{15}E^2$ [-2s]	$-2\sqrt{15}(15E^2 - E^3)$ [-2v]	$3\sqrt{2}E^3$ [$u\sqrt{2}$]
t_1^2	$-18\sqrt{15}E^2$ [-2s]	$E^0 + 2E^1 - 119E^2 + \frac{1}{4}E^3$	$-45E^2 - 3\frac{3}{4}E^3$	$\frac{3\sqrt{30}}{2} (18E^2 + \frac{1}{2}E^3)$
t_2^2	$-2\sqrt{15}(15E^2 - E^3)$	$-45E^2 - 3\frac{3}{4}E^3$	$E^0 + 2E^1 + 145E^2 - 1\frac{3}{4}E^3$	$\frac{\sqrt{30}}{2} (30E^2 - \frac{1}{2}E^3)$
t_1t_2	$3\sqrt{2}E^3$, [$u\sqrt{2}$]	$3\frac{\sqrt{30}}{2} (18E^2 + \frac{1}{2}E^3)$	$\frac{\sqrt{30}}{2} (30E^2 - \frac{1}{2}E^3)$	$E^0 + 2E^1 - 20E^2 + 2\frac{1}{2}E^3$
		$[(x-l)\sqrt{2}]$	$[(y+k)\sqrt{2}]$	$[(j+r-w-m)]$
			$[i-f+2w-2z]$	3F 3H
	${}^3A_2 = E^0$ ${}^3E = E^0 - 9E^3$			
3T_2	a_2t_1	t_1^2	t_2^2	t_1t_2
a_2t_1		$E^0 - 6E^3$	$3\sqrt{2}E^3$	
t_1t_2		$\frac{[b-n]}{3\sqrt{2}E^3}$ [$u\sqrt{2}$]	$\frac{[u\sqrt{2}]}{E^0 - 3E^3}$	$[j-r-w+m]$

Table 5 (continued).

3T_1	a_2t_2	t_1^2	t_2^2	t_1t_2
	$E^0 + 6E^3$	$-6E^3$	0	$-3\sqrt{30}E^3$
a_2t_2	$[c-o]$	$[-2u]$	$[0]$	$[(v-t)\sqrt{2}]$
t_1^2	$-6E^3$	$E^0 + \frac{3}{4}E^3$	$-5\frac{1}{4}E^3$	$\frac{9}{4}\sqrt{30}E^3$
t_2^2	$[-2n]$	$[\frac{g-p}{2}]$	$[\frac{m-z}{2}]$	$[-(x+l)\sqrt{2}]$
t_1t_2	0	$-\frac{5}{4}E^3$	$E^0 - \frac{5}{4}E^3$	$-\frac{3}{4}\sqrt{30}E^3$
	$[0]$	$[\frac{m-z}{2}]$	$[h-q]$	$[(k-y)\sqrt{2}]$
	$-3\sqrt{30}E^3$	$\frac{9}{4}\sqrt{30}E^3$	$E^0 + 13\frac{1}{2}E^3$	$E^0 + 13\frac{1}{2}E^3$
	$[(v-t)\sqrt{2}]$	$[-(x+l)\sqrt{2}]$		$[(j-r+w-m)]$

Table 5 (continued). The complete electrostatic matrix for f^2 in terms of the E^j and (in square brackets) in terms of generalized parameters.

Plutonium hexafluoride presumably has two f electrons [13]. The orbital energies are likely to be such that the t_1 orbitals lie far above the a_2 or t_2 orbitals [14]. It is rather obvious from tables 5 and 6 that whatever the value of $\Delta = E(t_2) - E(a_2)$ the lowest state will be of A_1 symmetry. It is probable that Δ is positive [14].

A_1	a_2^2	$a_2 t_2$	$\overbrace{^3T_1}^{t_2^2}$	$\overbrace{^1A_1}^{t_2^2}$
a_2^2	1A_1	3T_1		
$a_2 t_2$	3T_1			
t_2^2	$\overbrace{^3T_1}^{^1A_1}$			

E	$a_2 t_2$	$\overbrace{^3T_1}^{t_2^2}$	$\overbrace{^1E}^{t_2^2}$
$a_2 t_2$	3T_1	$\frac{1}{4}$	1
t_2^2	$\overbrace{^3T_1}^{^1E}$	1	$-\sqrt{2}$

T_1	$a_2 t_2$	t_2^2	3T_1
$a_2 t_2$	$\overbrace{^3T_1}^{^1T_1}$	$\overbrace{^3T_1}^{t_2^2}$	
t_2^2	$\overbrace{^3T_1}^{^1T_1}$		

T_2	$a_2 t_2$	t_2^2	3T_1
$a_2 t_2$	3T_1	$\frac{1}{4}$	1
t_2^2	$\overbrace{^3T_1}^{^1T_2}$	$-\sqrt{2}$	$\frac{1}{4}\sqrt{2}$

Table 6. Spin-orbit coupling matrices for the three lowest octahedral strong-field configurations contained in f^2 .

We now assume that only this A_1 state is thermally occupied and obtain an expression for its temperature-independent paramagnetic susceptibility. In terms of reduced matrix elements this is

$$\chi = \frac{8}{3} N \beta^2 \sum E_n^{-1} |\langle 0 | \{l(1) + 2s(1)\} | n \rangle|^2 \quad (20)$$

where n runs over all T_1 levels. The matrix elements of $l(1) + 2s(1)$ are easily worked out using the methods of §3 and are given in table 7. $|0\rangle$ is, to a good approximation a sum over the four A_1 states appearing in table 7. So apart from assuming values for E^i , ζ and Δ and obtaining a numerical value for χ , this completes the calculation.

A_1	T_1	$a_2 t_2$	t_2^2	3T_1
a_2^2	1A_1	0	$i\sqrt{6}$	0
$a_2 t_2$	3T_1	$-\frac{3}{4}i\sqrt{2}$	0	$i\sqrt{2}$
t_2^2	$\overbrace{^3T_1}^{^1A_1}$	$i\sqrt{2}$	0	$-\frac{3}{4}i\sqrt{2}$

Table 7. Reduced matrix elements $\langle A_1 | \{l(1) + 2s(1)\} | T_1 \rangle$ for the lowest states of f^2 in an octahedral field.

The observed susceptibility of PuF_6 is temperature-independent and corresponds to $\chi = 130 \times 10^{-6}$ for the two f electrons. The interpretation of this was discussed before (Griffith and Orgel [14]) using an inadmissibly simple model. The main defect was the neglect of the matrix element of spin-orbit coupling energy between $a_2^{21}A_1$ and $a_2t_2^3T_1$. The ground state was regarded as either $a_2^{21}A_1$ or $a_2t_2^3T_1A_1$ and in neither case was it possible to obtain as low a χ as 130×10^{-6} although the former state had the lower χ and it was concluded that it was in fact the ground state. It seems clear now that that view was incorrect and that the true ground state is a mixture, almost certainly containing substantial amounts of both $a_2^{21}A_1$ and $a_2t_2^3T_1$ and quite likely also $t_2^{23}T_1$. As an example if one neglects the upper 1A_1 and assumes these three A_1 states to have the same diagonal energies one finds

$$|0\rangle = \frac{\sqrt{3}}{\sqrt{10}} |a_2^{21}A_1\rangle - \frac{1}{\sqrt{2}} |a_2t_2^3T_1A_1\rangle - \frac{1}{\sqrt{5}} |t_2^{23}T_1A_1\rangle \quad (21)$$

with a calculated susceptibility of about 150×10^{-6} . Using the same parameters as in our previous paper the $t_2^{23}T_1$ does in fact only lie about 4000 cm^{-1} above a_2^{21} .

However, not knowing the parameters at all accurately, all we can usefully say is that a suitable mixture can give the low observed susceptibility whilst the pure $a_2^{21}A_1$ or pure $a_2t_2^3T_1A_1$ can not without unreasonable values of the parameters. There is no suggestion that (21) is necessarily at all close to the actual ground state. Qualitatively, however, we can say that the low value of χ appears to arise partly from the large repulsion between these two low-lying A_1 states and partly to the fact that the matrix elements of $l(1)+2s(1)$ to excited states partially cancel.

It is interesting to mention here calculations which have been made in the octahedral weak-field scheme on the f^2 configuration. They were restricted to the lowest level, 3H_4 [15, 16], of the configuration or at most the lowest term, 3H [17], but with either of those approximations the ground state still has A_1 symmetry.

7. TANABE AND KAMIMURA'S SCHEME OF CALCULATION

Tanabe and Kamimura ([3], hereafter referred to as TK) have given a discussion of the calculation by tensorial methods of matrix elements of one-electron operators between states of $t_2'''e''$ configurations, closely following Racah's treatment of atomic $l'''l''p$ configurations [18]. The matrix elements are shown to be proportional to recoupling coefficients or to sums of products of recoupling coefficients. In each case, however, they are also proportional to W or X coefficients as we see now.

First put $U^h = 1$, $h = A_1$, $g = k$ in equation (5). As $\langle b||U^h||b' \rangle$ is then equal to $\delta_{bb}\lambda(b)^{1/2}$ we find

$$\begin{aligned} \langle abc||T^g||a'b'c' \rangle &= (-1)^{a'+b+c+g}\delta_{bb}\lambda(c)^{1/2}\lambda(c')^{1/2}\langle a||T^g||a' \rangle \\ &\quad W\left(\begin{matrix} a' & b' & c' \\ c & g & a \end{matrix}\right). \end{aligned} \quad (22)$$

Because of the connection of W with recoupling coefficients (Part II, equation (16)), equation (22) is the same as TK 2.21 and 2.23. Equations TK 2.22

and 2.24 come similarly from (5) on putting $T^g = 1$. Actually the bracketted expressions defined in TK 2.23 and 2.24 satisfy

$$\begin{aligned} (dec[b]fea) &= (-1)^{a+b+d+e}\lambda(c)^{1/2}\lambda(a)^{1/2}W\begin{pmatrix} a & b & c \\ d & e & f \end{pmatrix}, \\ (edc[b]efa) &= (-1)^{a+c+d+f}(dec[b]fea), \end{aligned} \quad (23)$$

with our choice of phases for the constituent coupling coefficients.

In the evaluation of off-diagonal elements, more complicated recoupling coefficients appear (TK 2.37 and 2.39). These are easily shown to satisfy

$$[fde[b]kgh] = \lambda(e)^{1/2}\lambda(h)^{1/2}X\begin{bmatrix} E & b & T_2 \\ d & e & f \\ g & h & k \end{bmatrix} \quad (24)$$

for the octahedral group representations (TK 2.37) and

$$[S_1S_2S[1]S_3S_4S'] = (2S+1)(2S'+1)X\begin{bmatrix} S_4 & S_2 & \frac{1}{2} \\ S_3 & S_1 & \frac{1}{2} \\ S' & S & 1 \end{bmatrix} \quad (25)$$

for the spins (TK 2.39), the X of equation (24) being my X of Part II and of equation (25) being Racah's X . Incidentally the equation

$$\langle k, ab(c)(f)de|k, ad(g)(h)be \rangle = \lambda(c)^{1/2}\lambda(f)^{1/2}\lambda(g)^{1/2}\lambda(h)^{1/2}X\begin{bmatrix} a & b & c \\ d & e & f \\ g & h & k \end{bmatrix} \quad (26)$$

holds for the recoupling of k, a, b, d , four of our finite group representations. Equation (28) of Part II then connects the first and last forms of TK 2.37. (There are misprints: the last line of TK 2.37 lacks a Γ_2 and of TK 2.39 a tilda in the last W .)

The expression of Tanabe and Kamimura's symbols in terms of W and X has the advantage of revealing inherent symmetries which are otherwise hidden. From the point of view of applications it also greatly extends the scope of their paper for their tables only enable one to calculate within $t_2^m e^n$ configurations. However, configurations $c^m a^n$ for orbitals belonging to any pair of irreducible representations c and a can now be dealt with by simply replacing T_2 and E in (24) by c and a respectively, because we already calculated essentially all the X in Part II.

Finally note that Tanabe and Kamimura treat the spin-orbit coupling as a double tensor rather than, as in the present paper, an irreducible product. A double tensor $T_{\alpha\beta}^{ab}$ is defined with respect to two groups, G_1 and G_2 say, which are such that each element of G_1 commutes with each element of G_2 . a and b are irreducible representations of G_1 and G_2 respectively with components α and β . Then for fixed β , $T_{\alpha\beta}^{ab}$ is an irreducible tensor operator belonging to the representation a when operated on by elements of G_1 . A similar remark applies to G_2 . Suppose V symbols are defined for both G_1 and G_2 . Further suppose we have a system whose states are linearly dependent on simple products $|cd\gamma\delta\rangle = |c\gamma\rangle|d\delta\rangle$ of states for independent systems such that the elements of G_1 operate only on the $|c\gamma\rangle$ and those of G_2 only on the $|d\delta\rangle$. Then equation (1) is clearly generalizable to

$$\langle cd\gamma\delta|T_{\alpha\beta}^{ab}|c'd'\gamma'\delta'\rangle = \langle cd||T^{ab}||c'd'\rangle V\begin{pmatrix} c & a & c' \\ \gamma & \alpha & \gamma' \end{pmatrix} V\begin{pmatrix} d & b & d' \\ \delta & \beta & \delta' \end{pmatrix}, \quad (27)$$

and could be generalized further to deal with n mutually commuting groups $G_1 \dots G_n$ if one wished. The spin-orbit coupling can be treated as a linear form in the components of the double tensor

$$T_{\alpha\beta}{}^{1T_1} = \sum_i s_\alpha(i) u_\beta(i)$$

with G_1 the unitary unimodular group U_2 and G_2 the octahedral group which is, in effect, what Tanabe and Kamimura do. Equation (27) serves the same purpose as TK 2.13.

REFERENCES

- [1] GRIFFITH, J. S., 1960, *Mol. Phys.*, **3**, 285.
- [2] GRIFFITH, J. S., 1958, *Trans. Faraday Soc.*, **54**, 1109.
- [3] TANABE, Y., and KAMIMURA, H., 1958, *J. phys. Soc. Japan*, **13**, 394.
- [4] FANO, U., and RACAH, G., 1959, *Irreducible Tensorial Sets* (Academic Press).
- [5] CONDON, E. U., and SHORTLEY, G. H., 1951, *The Theory of Atomic Spectra* (Cambridge: University Press).
- [6] GRIFFITH, J. S., 1960, *Trans. Faraday Soc.*, **56**, 193.
- [7] GRIFFITH, J. S., *The Theory of Transition-Metal Ions* (Cambridge: University Press) (in the press).
- [8] TANABE, Y., and SUGANO, S., 1954, *J. phys. Soc. Japan*, **9**, 753.
- [9] RACAH, G., 1942, *Phys. Rev.*, **62**, 438.
- [10] GRIFFITH, J. S., 1960, *Mol. Phys.*, **3**, 79.
- [11] STEVENS, K. W. H., 1953, *Proc. roy. Soc. A*, **219**, 546.
- [12] RACAH, G., 1949, *Phys. Rev.*, **76**, 1352.
- [13] GRUEN, D. M., MALM, J. G., and WEINSTOCK, B., 1956, *J. chem. Phys.*, **24**, 905.
- [14] GRIFFITH, J. S., and ORGEL, L. E., 1957, *J. chem. Phys.*, **26**, 988.
- [15] PENNEY, W. G., and SCHLAPP, R., 1932, *Phys. Rev.*, **41**, 194.
- [16] HUTCHISON, C. A., and CANDELA, G. A., 1957, *J. chem. Phys.*, **27**, 707.
- [17] HERZFELD, C. M., and LEVINE, D. B., 1958, *J. Res. nat. Bur. Stand.*, **61**, 117.
- [18] RACAH, G., 1943, *Phys. Rev.*, **63**, 367.

Some investigations in the theory of open-shell ions

Part IV. The basis of intensity theory

by J. S. GRIFFITH

Department of Theoretical Chemistry, University Chemical Laboratory,
Lensfield Road, Cambridge†

(Received 25 April 1960)

The basis of the theory of electric dipole intensities in centrosymmetric ions is critically examined. It is shown that the physical assumptions of one current version [3, 4, 5] of this theory are mathematically inconsistent and the necessary revision of the theory is given. It is also pointed out that excitations from odd parity filled shells into the d shell should give a significant, and usually negative, contribution to the intensities.

1. INTRODUCTION

In this paper we examine critically the mathematical scheme usually used in the theory of intensities of centrosymmetric transition-metal ions. We discuss in detail only the theory for one d electron because all the essential points arise in this case and are rendered clearer because of the relative simplicity of the mathematics. n electron spectra will be discussed elsewhere.

The theory of the interaction between light waves and molecular systems is well known and has been often discussed for the special case of $d-d$ transitions. We can list five main possibilities for the origin of their intensities.

(1) Electric dipole intensity arising from mixing of odd parity states into d^n configurations under the influence of an environment which is not centrosymmetric. Environment here refers to that of the d electrons and the most discussed examples have been tetrahedral ions.

(2) Electric dipole intensity borrowed from parity-allowed electronic transitions through cooperation of odd parity vibrations. Unlike mechanism (1) this occurs in centrosymmetric ions and is usually supposed to be the main source of intensity for them. One quantum of an odd vibration is emitted or absorbed at the same time as the electronic transition.

(3) Electric dipole intensity borrowed from parity-allowed vibrational transitions. Here there is a change of at least one quantum of both an even and an odd vibration and the intensity arises largely from a difference in vibrational frequency in the upper and lower electronic states of the ion. This mechanism is not usually considered for these ions and does not seem likely to be responsible for any significant amount of the intensity.

(4) Magnetic dipole intensity. This is normally too small to be important for d^n systems.

(5) Electric quadrupole intensity is even smaller than (4).

The present paper is devoted to a discussion of the theoretical scheme usually used for mechanism (2), and we assume the reader to be familiar with it (Liehr

† Present address : John Harrison Laboratory of Chemistry, University of Pennsylvania, Philadelphia, U.S.A.

and Ballhausen [1, 2], Koide and Pryce [3], Koide [4], Pappalardo [5]). This scheme involves one in the evaluation of expressions like

$$S = \sum \{E(n) - E(X)\}^{-1} \langle X | \sum q(j) | n \rangle \langle n | \sum P(j) | Y \rangle + \sum \{E(n) - E(Y)\}^{-1} \langle X | \sum P(j) | n \rangle \langle n | \sum q(j) | Y \rangle, \quad (1)$$

for spin-allowed transitions. Analogous but more complicated expressions occur for forbidden transitions. Here $|X\rangle$ is the ground and $|Y\rangle$ the excited electronic state and $|n\rangle$ are odd-parity electronic states. P is a component of the electric dipole moment and q an electronic part of the nuclear-electronic interaction $\sum qQ$.

Koide *et al.* simplify (1) by assuming that the relevant excited states $|n\rangle$ all occur at the same energy E and obtain

$$S = [(E - E(X))^{-1} + (E - E(Y))^{-1}] \langle X | \sum P(i) \sum q(j) | Y \rangle. \quad (2)$$

(2) is then simplified further in ways which do not concern us here (Koide and Pryce [3], p. 619).

2. THE CLOSURE PROCEDURE

We first discuss the general problem of evaluating sums of the type†

$$\sum_n E_n^{-1} \langle X | b | n \rangle \langle n | c | Y \rangle. \quad (3)$$

With our applications in mind $|X\rangle$ and $|Y\rangle$ are states of a d^m configuration and b and c are sums of Hermitian one-electron operators, one being the electronic electric dipole moment operator and the other an electronic part of the coupling of the nuclear and electronic motions. The $|n\rangle$ are a complete orthonormal set. A method of estimating the sum which is often used is to assume that the important excited states $|n\rangle$ have all more or less the same energy E , whereupon one sums over n using $\sum_n |n\rangle \langle n| = 1$ to give $E^{-1} \langle X | bc | Y \rangle$. If the assumption is correct, the internal details of the 'important' states $|n\rangle$ are totally irrelevant to this argument and we need merely estimate their energy E .

It is actually customary to assume that these states belong, for the first transition series, to the configuration $3d^{m-1}4p$. It is natural to question whether the orbitals in a complex ion can usefully be taken to approximate at all closely to atomic $4p$ orbitals but we will not worry about this here. The assumption enables one, however, to obtain a value for E from atomic spectral data and to justify partially the earlier assumption by remarking that the electric dipole moment operator has its matrix elements which start from $3d^m$ going mainly to $3d^{m-1}4p$.

As used in calculations, the closure procedure is only strictly correct if there exists an orthonormal set of stationary states $|n\rangle$ and an energy E such that all the non-zero contributions to the sum (3) come from states $|n\rangle$ with energy E . We shall now investigate rather carefully the consequences of supposing this and the surprising fact will emerge that it is, in general, inconsistent with the earlier assumptions of this section. The closure procedure for calculating intensities in centrosymmetric ions is not only physically somewhat implausible but actually relies on a mathematical scheme which is internally inconsistent. Later, we see how to put at least the second matter right.

We now examine the properties of the sum (3) without the E_n^{-1} for fixed $|X\rangle$ and $|Y\rangle$. In general the sum in

$$\langle X | bc | Y \rangle = \sum \langle X | b | n \rangle \langle n | c | Y \rangle \quad (4)$$

† For clarity we take a discrete set of basic states $|n\rangle$.

contains an infinite number of non-zero terms. But if we take an orthonormal transform of the $|n\rangle$ which includes

$$|B\rangle = \sum_n \langle n | b | X \rangle |n\rangle / (\langle X | b^2 | X \rangle)^{1/2}, \quad (5)$$

(unless $\langle X | b^2 | X \rangle = 0$ when all terms of (4) are zero) then if $|B'\rangle$ is another member of the new set we find

$$\langle X | b | B' \rangle = \sum_n \langle X | b | n \rangle \langle n | B' \rangle = (\langle X | b^2 | X \rangle)^{1/2} \langle B | B' \rangle = 0.$$

So the sum (4) reduces to the single term

$$\langle X | bc | Y \rangle = \langle X | b | B \rangle \langle B | c | Y \rangle. \quad (6)$$

We have maximized the matrix element $\langle X | b | B \rangle$ at the expense, possibly, of $\langle B | c | Y \rangle$. Alternatively, defining

$$|C\rangle = \sum_n \langle n | c | Y \rangle |n\rangle / (\langle Y | c^2 | Y \rangle)^{1/2}, \quad (7)$$

we deduce

$$\langle X | bc | Y \rangle = \langle X | b | C \rangle \langle C | c | Y \rangle \quad (8)$$

maximizing the second matrix element. $|B\rangle$ and $|C\rangle$ are not necessarily the same and the expressions (6) and (8) are both equal to the more symmetrical

$$\langle X | b | B \rangle \langle B | C \rangle \langle C | c | Y \rangle$$

which leads to the Schwartz-type inequality

$$|\langle X | bc | Y \rangle|^2 \leq \langle X | b^2 | X \rangle \langle Y | c^2 | Y \rangle. \quad (7)$$

It is now clear that the only simple way in which the closure procedure can be strictly true is if either $|B\rangle$ or $|C\rangle$, but not necessarily both, can be taken to be one of the stationary states $|n\rangle$ of equation (3). It is usual to assume this for the one which maximizes the electric dipole matrix element.

3. GROUP-THEORETIC CONSIDERATIONS

We now suppose we have a centrosymmetric ion with a single electron making a transition between two real even parity orbitals forming the α, δ components of the irreducible representations a, d respectively of the octahedral group O for which V symbols have been defined according to §2 of Griffith [6] (hereafter referred to as Part II). We reject spin, i.e. we assume all functions to have the same m_s value. All the physically important points that I wish to make about the theory appear in the one-electron case. The restriction to the physically important octahedral group is merely for simplicity.

Let us take an orthonormal set of basic kets which breaks up into subsets, each subset forming a basis for an irreducible representation of O according to our standard choice of phase. We assume also that our two orbitals, $|X_\alpha\rangle$ and $|Y_\delta\rangle$ say, are part of this set and that O commutes with our Hamiltonian \mathcal{H} . The matrix element $\langle X | bc | Y \rangle$ becomes generalized to $\langle X_\alpha | q_\beta^b q_\gamma^c | Y_\delta \rangle$ where b, c are representation symbols and the Greek suffixes components. We suppose q_β^b and q_γ^c are real. For fixed α, β the equation (5) is replaced with the (non-normalized)

$$|B(\alpha\beta)\rangle = \sum_{ne\epsilon} \langle ne\epsilon | q_\beta^b | X_\alpha \rangle | ne\epsilon \rangle. \quad (10)$$

The simplification of this proceeds via reduced matrix elements and we have

$$\langle ne\epsilon | q_\beta^b | X_\alpha \rangle = \langle ne || q^b || X \rangle V \begin{pmatrix} e & b & a \\ \epsilon & \beta & \alpha \end{pmatrix}. \quad (11)$$

This gives

$$|B(\alpha\beta)\rangle = \sum_{e\epsilon} V\begin{pmatrix} e & b & a \\ \epsilon & \beta & \alpha \end{pmatrix} |Ne\epsilon\rangle \quad (12)$$

where

$$|Ne\epsilon\rangle = \sum_n \langle ne || q^b || X \rangle |ne\epsilon\rangle.$$

There is one ket $|Ne\epsilon\rangle$ for each irreducible representation e and each component ϵ , but the $|Ne\epsilon\rangle$ are the same for all choices of α and β . Naturally we are interested in a set of kets which are sufficient to construct the kets $|B\rangle$ of equation (10) for all α, β and the $|Ne\epsilon\rangle$ are such a set. Replacing them with normalized kets, $|e\epsilon\rangle$ say, we have

$$\begin{aligned} \langle X_\alpha | q_\beta^b q_\gamma^c | Y_\delta \rangle &= \sum_{e\epsilon} \langle X_\alpha | q_\beta^b | e\epsilon \rangle \langle e\epsilon | q_\gamma^c | Y_\delta \rangle \\ &= \sum_{e\epsilon} \langle X || q^b || e \rangle \langle \overline{Y} || q^c || e \rangle V\begin{pmatrix} a & b & e \\ \alpha & \beta & \epsilon \end{pmatrix} V\begin{pmatrix} d & c & e \\ \delta & \gamma & \epsilon \end{pmatrix}, \end{aligned}$$

instead of equation (6). We abbreviate this to

$$\langle X_\alpha | q_\beta^b q_\gamma^c | Y_\delta \rangle = \sum_{e\epsilon} A(e) V\begin{pmatrix} a & b & e \\ \alpha & \beta & \epsilon \end{pmatrix} V\begin{pmatrix} d & c & e \\ \delta & \gamma & \epsilon \end{pmatrix}. \quad (13)$$

(13) was obtained by maximizing the left-hand matrix elements in the sum over e and ϵ . If we maximize the right-hand ones we obtain an analogous equation which can be written

$$\langle X_\alpha | q_\beta^b q_\gamma^c | X_\delta \rangle = \sum_{e\epsilon} A'(e) V\begin{pmatrix} a & b & e \\ \alpha & \beta & \epsilon \end{pmatrix} V\begin{pmatrix} d & c & e \\ \delta & \gamma & \epsilon \end{pmatrix}.$$

We now use the general proposition that

$$\sum_{e\epsilon} R(e) V\begin{pmatrix} a & b & e \\ \alpha & \beta & \epsilon \end{pmatrix} V\begin{pmatrix} d & c & e \\ \delta & \gamma & \epsilon \end{pmatrix} = 0 \rightarrow R(e) = 0 \quad (14)$$

which follows at once from the orthonormality rules for the V (equation (II 4)) to deduce that $A'(e) = A(e)$.

In the calculation of intensity, one of the q is the electric dipole moment transforming as T_1 and the other is part of the Hamiltonian representing the coupling of electronic with nuclear motions. Both the q and the $|Ne\epsilon\rangle$ are odd. As the q are simply functions of position it follows that they commute. However the expression for the matrix elements of $q_\gamma^c q_\beta^b$ corresponding to (13) is

$$\begin{aligned} \langle X_\alpha | q_\gamma^c q_\beta^b | Y_\delta \rangle &= \sum_{e\epsilon} B(e) V\begin{pmatrix} a & c & e \\ \alpha & \gamma & \epsilon \end{pmatrix} V\begin{pmatrix} d & b & e \\ \delta & \beta & \epsilon \end{pmatrix} \\ &= \sum_{e\neq f} \lambda(f) B(e) W\begin{pmatrix} a & b & f \\ d & c & e \end{pmatrix} V\begin{pmatrix} a & b & f \\ \alpha & \beta & \phi \end{pmatrix} V\begin{pmatrix} d & c & f \\ \delta & \gamma & \phi \end{pmatrix}, \end{aligned} \quad (15)$$

where we have used equation (II 19). Because the q commute, this must be equal to the right-hand side of (13) which means, using (14), that

$$A(e) = \lambda(e) \sum_f B(f) W\begin{pmatrix} a & b & e \\ d & c & f \end{pmatrix}, \quad (16)$$

and similarly

$$B(f) = \lambda(f) \sum_e A(e) W\begin{pmatrix} a & b & e \\ d & c & f \end{pmatrix}, \quad (17)$$

the two equations being equivalent because of the orthonormality rules for the W (equation (II 21)).

A third method of analysing the matrix elements of $q_\beta^b q_\gamma^c$ is obtained by inverting equation (3) of Part III (Griffith [7]), to give

$$q_\beta^b q_\gamma^c = \sum_{g\eta} \lambda(g)^{1/2} V \begin{pmatrix} b & c & g \\ \beta & \gamma & \eta \end{pmatrix} (q^b \times q^c)_{\eta}^g, \quad (18)$$

whence

$$\langle X_\alpha | q_\beta^b q_\gamma^c | Y_\delta \rangle = \sum_{g\eta} C(g) V \begin{pmatrix} b & c & g \\ \beta & \gamma & \eta \end{pmatrix} V \begin{pmatrix} a & g & d \\ \alpha & \eta & \delta \end{pmatrix}, \quad (19)$$

where $C(g) = \lambda(g)^{1/2} \langle X || (q^b \times q^c)^g || Y \rangle$ is real. As before it follows from equation (II 19) that

$$A(e) = (-1)^{a+b+c} \lambda(e) \sum_g C(g) W \begin{pmatrix} d & c & e \\ b & a & g \end{pmatrix}. \quad (20)$$

It is clear now that there is nothing mathematically objectionable about making the physical assumption that in an equation such as (12) the $|Nee\rangle$ are all stationary states with energy E . What is not satisfactory is always to take the $|Nee\rangle$ to be p functions (or any T_{1u} functions) for $e=p$ in both of the expansions (13) and (15) and zero for $e \neq p$. For consider a transition $T_2 \rightarrow E$, i.e. a is a T_2 orbital and d an E orbital†. Then suppose q^b is the electric dipole moment, so $b=T_1$ and let $c=T_1$ or T_2 . If the non-zero $|Nee\rangle$ can only be T_{1u} orbitals, this means $A(e)$ and $B(e)$ are zero unless $e=T_1$. But (16) and (17) then imply

$$A(T_1) = 3B(T_1)W \begin{pmatrix} T_2 & T_1 & T_1 \\ E & c & T_1 \end{pmatrix} = 9A(T_1)W \begin{pmatrix} T_2 & T_1 & T_1 \\ E & c & T_1 \end{pmatrix}^2 = \frac{1}{4}A(T_1) \text{ or } \frac{3}{4}A(T_1)$$

according as to whether $c=T_1$ or T_2 . Hence we deduce that the matrix elements of $q_\beta^b q_\gamma^c$ and $q_\gamma^c q_\beta^b$ are all zero, even in the case when $b=c$. Naturally we do not want this to be true. The paradox derives from the joint assumption that $[q_\beta^b, q_\gamma^c] = 0$ and that only excited T_{1u} functions need be considered in an expansion such as (4). The commutation is obviously true so we are forced to throw away the second hypothesis. If we persist in our belief that, physically, the T_{1u} are the only important excited states then in evaluating the matrices of $q_\beta^b q_\gamma^c$ and $q_\gamma^c q_\beta^b$ we must reject that part which does not arise from T_{1u} functions for intermediate states. It is not difficult to do this. Consider the sum

$$S(\alpha\beta\gamma\delta) = \sum_{e\epsilon} E^{-1} \langle X_\alpha | q_\beta^b | Nee \rangle \langle Ne\epsilon | q_\gamma^c | Y_\delta \rangle + \sum_{e\epsilon} E_1^{-1} \langle X_\alpha | q_\gamma^c | N'e\epsilon \rangle \langle N'e\epsilon | q_\beta^b | Y_\delta \rangle. \quad (21)$$

A simple-minded application of the closure procedure leads to

$$S(\alpha\beta\gamma\delta) = \sum_{g\eta} (E^{-1} + E_1^{-1}) C(g) V \begin{pmatrix} b & c & g \\ \beta & \gamma & \eta \end{pmatrix} V \begin{pmatrix} d & a & g \\ \delta & \alpha & \eta \end{pmatrix} \quad (22)$$

in accordance with (19). However if only T_1 symmetry excited orbitals are considered then the scalar coefficient $(E^{-1} + E_1^{-1})C(g)$ becomes replaced by

$$E^{-1}\lambda(g)\lambda(T_1)W \begin{pmatrix} a & b & T_1 \\ c & d & g \end{pmatrix} \sum_{g'} C(g') W \begin{pmatrix} a & b & T_1 \\ c & d & g' \end{pmatrix} + E_1^{-1}\lambda(g)\lambda(T_1)W \begin{pmatrix} d & b & T_1 \\ c & a & g \end{pmatrix} \sum_{g'} (-1)^{g+g'} C(g') W \begin{pmatrix} d & b & T_1 \\ c & a & g' \end{pmatrix}. \quad (23)$$

† I am using capital letters for one-electron representations to avoid confusion. This is not normally to be recommended.

$\lambda(T_1)=3$ and the expression (23) is easily seen to be consistent with (22) by replacing T_1 by e and summing over e whereupon we recover $(E^{-1} + E_1^{-1})C(g)$.

In the literature expressions have been given [3, 5] for the $S(\alpha\beta\gamma\delta)$ of equation (22). Our present analysis shows how they should be corrected if one wishes to take only the contribution to them which arises from excited T_1 symmetry orbitals. One method is first to use equation (22) to derive the $C(g)$ from the given expressions (numerical or otherwise) for the S , then deduce the value of the expression (23) for each g and finally resubstitute it in equation (22) in place of $(E^{-1} + E_1^{-1})C(g)$. This gives the 'corrected' $S(\alpha\beta\gamma\delta)$.

Let us now consider as an example a $T_2 \rightarrow E$ transition mediated by one set of excited T_{1u} orbitals and put q_β^b as the electric dipole moment. For each of the two values of c ($= T_1$ or T_2) we have just two quantities occurring in (21) which are not group-theoretically determined. They can be taken as $E^{-1}A(T_1)$ and $E_1^{-1}B(T_1)$. So in order to calculate a one-electron intensity we must assign the values of (at least) four parameters. The matrix elements for an n electron system are all expressible in terms of the same combinations of reduced matrix elements as those for $n=1$, so provided we know the E and E_1 and the vibrational frequencies we have our intensities always dependent upon the two $A(T_1)$ and the two $B(T_1)$.

Especially in n electron spectra we are often interested in matrix elements between states each having the same occupancy of T_2 and E orbitals. For $n=1$ this means that $a=d$ in an equation such as (19). Then $|Y_\delta\rangle = |X_\delta\rangle$ and by taking the complex conjugate of (19) and interchanging α with δ we deduce a new equation identical but for the order of α and δ on the right-hand side. It then follows that

$$C(g) = (-1)^g C(g)$$

and so $C(g)=0$ if $g=A_2$ or T_1 .

4. INTERMEDIATE HOLE EXCITATIONS

In discussing the sums which occur in equation (1) it has been usual to suppose the $|n\rangle$ to be merely those states in which one or more d electrons have been excited into initially empty orbitals. However the $|n\rangle$ also include states in which one or more electrons from initially filled shells are excited into d or higher orbitals. So long as one assumes a strict crystal field model with atomic d and p orbitals, it may not matter too much neglecting intermediate states having holes in the inner shells. But as soon as one considers a molecular orbital model then they can be important. In particular, if, following Liehr and Ballhausen [1], we take $E(p) - E(d)$ from the observed strong absorption in the complex rather than as an atomic $p-d$ separation we are implicitly almost forced to suppose our intermediate T_{1u} orbitals to be mixtures of central ion p orbitals with ligand T_{1u} orbitals l , say. Then there will be doubly occupied orbitals

$$f = p \cos \theta + l \sin \theta \quad (24)$$

and empty orbitals

$$e = -p \sin \theta + l \cos \theta \quad (25)$$

both of which can contribute their share to the intensity.

The group-theoretic degeneracies which occur for both e and f and for our initial and final d orbitals are irrelevant to the point I am trying to make. For simplicity, therefore, suppose we have non-degenerate initial and final orbitals a

and d and that e and f are also spatially non-degenerate. Let \pm be used for spin affixes and consider a sum

$$S = \sum [E(n) - E(X)]^{-1} \langle X | q | n \rangle \langle n | P | Y \rangle + \sum [E(n) - E(Y)]^{-1} \langle X | P | n \rangle \langle n | q | Y \rangle \quad (26)$$

for a transition from a^+ to d^+ . Including the filled orbital f^2 we have $f^2 a^+$ for ground state and $f^2 d^+$ for excited state. There are two intermediate states, namely $f^2 e^+$ and $f^- a^+ d^+$. The others do not contribute owing to the orthogonality of the spin functions. It is immediately apparent that in a molecular orbital model hole and particle excitations can serve equally well in providing intermediate states. It is only on quantitative grounds that any neglect of hole excitations could be justified.

Actually the contribution of the holes to (26) tends to cancel out that of the particles. As a simple illustration let us neglect all but the orbital energies of the states. Also suppose

$$E(e) - E(d) = E(a) - E(f) = E \text{ say and put } E_1 = E(e) - E(a).$$

Further let $\langle a | q | l \rangle = \langle a | P | l \rangle = 0$. This is, of course, physically, unrealistic. Then S readily simplifies to

$$S = (E_1^{-1} \sin^2 \theta - E^{-1} \cos^2 \theta) \langle a | q | p \rangle \langle p | P | d \rangle + (E^{-1} \sin^2 \theta - E_1^{-1} \cos^2 \theta) \langle a | P | p \rangle \langle p | q | d \rangle$$

exhibiting the cancellation very clearly.

There is little point in pursuing this matter further here in general terms, except to say that the partial cancellation just demonstrated holds also for m -electron transitions. It is also to be noted that hole excitations must be considered in any attempt to use a closure argument in a molecular orbital theory. An alternative way of looking at this is to try to neglect the closed shells in describing our states. Then the relation $\sum |n\rangle \langle n| = 1$ includes states $|n\rangle$ with electrons in inner shell orbitals. But as these inner shells are already filled such states are forbidden by the exclusion principle which shows such a description to be incorrect. Finally, even in a strictly crystal field model we should consider not only intermediate states $3d \rightarrow 4p$ but also such ones as $3p \rightarrow 3d$.

Note added in proof.—A recent paper by Englman (*Mol. Phys.*, 1960, **3**, 48) gives some reasons for neglecting all A and B of § 3 except $A(T_1)$ with $c = T_1$.

REFERENCES

- [1] LIEHR, A. D., and BALLHAUSEN, C. J., 1957, *Phys. Rev.*, **106**, 1161.
- [2] BALLHAUSEN, C. J., and LIEHR, A. D., 1959, *Mol. Phys.*, **2**, 123.
- [3] KOIDE, S., and PRYCE, M. H. L., 1959, *Phil. Mag.*, **3**, 607.
- [4] KOIDE, S., 1959, *Phil. Mag.*, **4**, 243.
- [5] PAPPALARDO, R., 1959, *J. chem. Phys.*, **31**, 1050.
- [6] GRIFFITH, J. S., 1960, *Mol. Phys.*, **3**, 285.
- [7] GRIFFITH, J. S., 1960, *Mol. Phys.*, **3**, 457.

The proton resonance spectrum of *m*-dinitrobenzene, the AB₂ X system

by R. J. ABRAHAM

National Physical Laboratory, Teddington

E. O. BISHOP and R. E. RICHARDS

Physical Chemistry Laboratory, Oxford

(Received 14 March 1960)

The proton resonance spectrum of meta-dinitrobenzene is reported and analysed at 60 Mc/s as an AB₂ X spectrum and at 29.9200 Mc/s as an AB₂ C spectrum.

The matrix elements for both systems are given and from these the explicit functions for the transition energy levels and intensities for the AB₂ X system are derived.

It is practicable to determine the relative signs of only the two larger coupling constants in this case, and it was found from the spectrum at lower field that these have the same sign.

1. INTRODUCTION

The analysis of high resolution nuclear magnetic resonance spectra has been the subject of a number of recent publications [1-4]. This paper is concerned with the analysis and assignment of a further type of spectrum, the AB₂ X system (the nomenclature of Pople *et al.* [1] will be used here). Compounds of the type *m*-C₆H₄X₂ can give this type of spectrum and this is part of a study of the spectra of these compounds. Here, however, we are only concerned with the problem of the analysis of this type of spectrum.

2. ENERGY LEVELS, TRANSITION ENERGIES AND INTENSITIES FOR AB₂ X

The AB₂ X system can be described in terms of seven molecular quantities, four spin-spin coupling constants J_{AB} , J_{AX} , J_{BX} and J_{BB} , and three parameters H_A , H_B and H_X , which represent the magnetic fields at the three types of nucleus.

If H_0 is the applied magnetic field, we have

$$H_m = H_0(1 - \sigma_m)$$

where σ_m is a non-dimensional screening constant and the relative chemical shift (in c/s) between any pair of nuclei is

$$\delta_{mn} = \eta(H_m - H_n)$$

where $2\pi\eta$ is the gyromagnetic ratio of the nucleus considered.

The quantum rules leading to the transition energy levels and intensities are well known and will not be given here (see [1]).

The matrix elements of the Hamiltonian and basic wave functions for this system are given in table 1. As the coupling constant J_{BB} does not appear in the transition energies or intensities, the terms $+\frac{1}{4}J_{BB}$ and $-\frac{3}{4}J_{BB}$ have been omitted from the diagonal elements of the symmetric and anti-symmetric wave functions respectively.

Function ABBX	Diagonal matrix elements			Off diagonal elements
1 $S_2 \alpha\chi\alpha\alpha$	$\frac{1}{2}\eta(H_A + 2H_B + H_X)$	$+\frac{1}{4}(2J_{AB} + J_{AX} + 2J_{BX})$		
2 $1S_1 \alpha\chi\chi\beta$	$\frac{1}{2}\eta(H_A + 2H_B - H_X)$	$+\frac{1}{4}(2J_{AB} - J_{AX} - 2J_{BX})$		
3 $2S_1 \alpha 2^{-1/2}(\alpha\beta + \beta\alpha)\alpha$	$\frac{1}{2}\eta(H_A + H_X)$	$\frac{1}{4}J_{AX}$		
4 $3S_1 \beta\chi\alpha\alpha$	$\frac{1}{2}\eta(-H_A + 2H_B + H_X)$	$+\frac{1}{4}(-2J_{AB} - J_{AX} + 2J_{BX})$	$\mathcal{H}_{34} = \frac{J_{AB}}{\sqrt{2}}$	
5 $1S_0 \alpha 2^{-1/2}(\alpha\beta + \beta\alpha)\beta$	$\frac{1}{2}\eta(H_A - H_X)$	$-\frac{1}{4}J_{AX}$		
6 $2S_0 \beta\alpha\alpha\beta$	$\frac{1}{2}\eta(-H_A + 2H_B - H_X)$	$+\frac{1}{4}(-2J_{AB} + J_{AX} - 2J_{BX})$	$\mathcal{H}_{56} = \frac{J_{AB}}{\sqrt{2}}$	
7 $3S_0 \alpha\beta\beta\alpha$	$\frac{1}{2}\eta(H_A - 2H_B + H_X)$	$+\frac{1}{4}(-2J_{AB} + J_{AX} - 2J_{BX})$	$\mathcal{H}_{78} = \frac{J_{AB}}{\sqrt{2}}$	
8 $4S_0 \beta 2^{-1/2}(\alpha\beta + \beta\alpha)\alpha$	$\frac{1}{2}\eta(-H_A + H_X)$	$-\frac{1}{4}J_{AX}$		
9 $1S_{-1} \alpha\beta\beta\beta$	$\frac{1}{2}\eta(H_A - 2H_B - H_X)$	$+\frac{1}{4}(-2J_{AB} - J_{AX} + 2J_{BX})$	$\mathcal{H}_{910} = \frac{J_{AB}}{\sqrt{2}}$	
10 $2S_{-1} \beta 2^{-1/2}(\alpha\beta + \beta\alpha)\beta$	$\frac{1}{2}\eta(-H_A - H_X)$	$+\frac{1}{4}J_{AX}$		
11 $3S_{-1} \beta\beta\beta\alpha$	$\frac{1}{2}\eta(-H_A - 2H_B + H_X)$	$+\frac{1}{4}(2J_{AB} - J_{AX} - 2J_{BX})$		
12 $S_{-2} \beta\beta\beta\beta$	$\frac{1}{2}\eta(-H_A - 2H_B - H_X)$	$+\frac{1}{4}(2J_{AB} + J_{AX} + 2J_{BX})$		
13 $A_1 \alpha 2^{-1/2}(\alpha\beta - \beta\alpha)\alpha$	$\frac{1}{2}\eta(H_A + H_X)$	$+\frac{1}{4}J_{AX}$		
14 $1A_0 \alpha 2^{-1/2}(\alpha\beta - \beta\alpha)\beta$	$\frac{1}{2}\eta(H_A - H_X)$	$-\frac{1}{4}J_{AX}$		
15 $2A_0 \beta 2^{-1/2}(\alpha\beta - \beta\alpha)\alpha$	$\frac{1}{2}\eta(-H_A + H_X)$	$-\frac{1}{4}J_{AX}$		
16 $A_{-1} \beta 2^{-1/2}(\alpha\beta - \beta\alpha)\beta$	$\frac{1}{2}\eta(-H_A - H_X)$	$+\frac{1}{4}J_{AX}$		

Table 1. Basic functions and matrix elements for $AB_2 X$.

The basic wave functions of table 1 do not mix when (a) their total spin quantum number differs and (b) the functions are of different symmetry. These separations are shown by the full lines in table 1. Also as δ_{BX} and δ_{AX} are much larger than J_{BX} or J_{AX} the off diagonal terms involving J_{AX} and J_{BX} may be neglected, i.e. the states do not mix. These separations are shown by the dotted lines in table 1. These rules break the matrix down into a number of matrices no bigger than 2×2 . Thus the stationary state wave functions and the energy levels can be given explicitly in terms of the molecular quantities. The result of this calculation is shown in table 2. Combining this result with the usual selection rules [1] gives the transition energies and relative intensities (table 3). There is a total of 34 allowed transitions, of which 4 are of zero intensity. The remaining 30 transitions are given in table 3. They are classified in the usual manner, as A, B, X and combination bands.

Spectra of this type can be interpreted in one of two ways. One way is to consider the spectrum as an AB_2 spectrum perturbed by the X nucleus. From a knowledge of the transitions in the AB_2 case [5] and how these transitions split on introducing the X coupling, the spectrum can be interpreted. This, however, presupposes some knowledge of the coupling constants and chemical shifts

	Wave function	Energy
$2S_1'$	$2^{-1/2} \cos \theta^+ (\alpha\alpha\beta\alpha + \alpha\beta\alpha\alpha) + \sin \theta^+ (\beta\alpha\alpha\alpha)$	$\frac{1}{2}\eta (H_B + H_X) + \frac{1}{4} (-J_{AB} + J_{BX}) + C^-$
$3S_1'$	$-2^{-1/3} \sin \theta^+ (\alpha\alpha\beta\alpha + \alpha\beta\alpha\alpha) + \cos \theta^+ (\beta\alpha\alpha\alpha)$	$\frac{1}{3}\eta (H_B + H_X) + \frac{1}{4} (-J_{AB} + J_{BX}) - C^+$
$1S_0'$	$2^{-1/3} \cos \phi^+ (\alpha\alpha\beta\beta + \alpha\beta\alpha\beta) + \sin \phi^+ (\beta\alpha\alpha\beta)$	$\frac{1}{3}\eta (H_B - H_X) + \frac{1}{4} (-J_{AB} - J_{BX}) + D^+$
$2S_0'$	$-2^{-1/3} \sin \phi^+ (\alpha\alpha\beta\beta + \alpha\beta\alpha\beta) + \cos \phi^+ (\beta\alpha\alpha\beta)$	$\frac{1}{3}\eta (H_B - H_X) + \frac{1}{4} (-J_{AB} - J_{BX}) - D^+$
$3S_0'$	$\cos \phi^- (\alpha\beta\beta\alpha) + 2^{-1/2} \sin \phi^- (\beta\alpha\beta\alpha + \beta\beta\alpha\alpha)$	$\frac{1}{2}\eta (-H_B + H_X) + \frac{1}{4} (-J_{AB} - J_{BX}) + D^-$
$4S_0'$	$- \sin \phi^- (\alpha\beta\beta\alpha) + 2^{-1/2} \cos \phi^- (\beta\alpha\beta\alpha + \beta\beta\alpha\alpha)$	$\frac{1}{2}\eta (-H_B + H_X) + \frac{1}{4} (-J_{AB} - J_{BX}) - D^-$
$1S_{-1}'$	$\cos \theta^- (\alpha\beta\beta\beta) + 2^{-1/3} \sin \theta^- (\beta\alpha\beta\beta + \beta\beta\alpha\beta)$	$\frac{1}{3}\eta (-H_B - H_X) + \frac{1}{4} (-J_{AB} + J_{BX}) + C^+$
$2S_{-1}'$	$- \sin \theta^- (\alpha\beta\beta\beta) + 2^{-1/2} \cos \theta^- (\beta\alpha\beta\beta + \beta\beta\alpha\beta)$	$\frac{1}{2}\eta (-H_B - H_X) + \frac{1}{4} (-J_{AB} + J_{BX}) - C^-$
where	$C^+ \cos 2\theta^+ = \frac{1}{2}\eta (H_A - H_B) + \frac{1}{4} (J_{AB} + J_{AX} - J_{BX})$ $C^+ \sin 2\theta^+ = 2^{-1/2} J_{AB}$ $C^- \cos 2\theta^- = \frac{1}{2}\eta (H_A - H_B) - \frac{1}{4} (J_{AB} + J_{AX} - J_{BX})$ $C^- \sin 2\theta^- = 2^{-1/2} J_{AB}$ $D^+ \cos 2\phi^+ = \frac{1}{2}\eta (H_A - H_B) + \frac{1}{4} (J_{AB} - J_{AX} + J_{BX})$ $D^+ \sin 2\phi^+ = 2^{-1/2} J_{AB}$ $D^- \cos 2\phi^- = \frac{1}{2}\eta (H_A - H_B) - \frac{1}{4} (J_{AB} - J_{AX} + J_{BX})$ $D^- \sin 2\phi^- = 2^{-1/2} J_{AB}$	

Table 2. Stationary state wave functions and energies for AB_2X .

	Transition	Origin	Energy	Relative intensity
1	$3S_1' \rightarrow S_2$	A	$\frac{1}{2}\eta (H_A + H_B) + \frac{1}{4}(3J_{AB} + J_{AX} + J_{BX}) + C^+$	$(\cos \theta^+ - 2^{1/2} \sin \theta^+)^2$
2	$2S_0' \rightarrow 1S_1$	A	$\frac{1}{2}\eta (H_A + H_B) + \frac{1}{4}(3J_{AB} - J_{AX} - J_{BX}) + D^+$	$(\cos \phi^+ - 2^{1/2} \sin \phi^+)^2$
3	$4S_0' \rightarrow 2S_1'$	A	$\frac{1}{2}\eta (2H_B) + \frac{1}{2}J_{BX} + C^+ + D^-$	$[\cos \theta^+ \cos \phi^- + 2^{1/2} \sin (\theta^+ - \phi^-)]^2$
4	$2S_{-1}' \rightarrow 1S_0'$	A	$\frac{1}{2}\eta (2H_B) - \frac{1}{2}J_{BX} + D^+ + C^-$	$[\cos \phi^+ \cos \theta^- + 2^{1/2} \sin (\phi^+ - \theta^-)]^2$
5	$3S_{-1}' \rightarrow 3S_0'$	A	$\frac{1}{2}\eta (H_A + H_B) - \frac{1}{4}(3J_{AB} - J_{AX} - J_{BX}) + D^-$	$(\cos \phi^+ + 2^{1/2} \sin \phi^-)^2$
6	$S_{-2} \rightarrow 1S_{-1}'$	A	$\frac{1}{2}\eta (H_A + H_B) - \frac{1}{4}(3J_{AB} + J_{AX} + J_{BX}) + C^-$	$(\cos \theta^- + 2^{1/2} \sin \theta^-)^2$
7	$2a_0 \rightarrow a_1$	A	$\frac{1}{2}\eta (2H_A) + \frac{1}{2}J_{AX}$	1
8	$a_{-1} \rightarrow 1a_0$	A	$-\frac{1}{2}\eta (2H_A) - \frac{1}{2}J_{AX}$	1
9	$2S_1' \rightarrow S_2$	B	$\frac{1}{2}\eta (H_A + H_B) + \frac{1}{4}(3J_{AB} + J_{AX} + J_{BX}) - C^+$	$(2^{1/2} \cos \theta^+ + \sin \theta^+)^2$
10	$1S_0' \rightarrow 1S_1$	B	$\frac{1}{2}\eta (H_A + H_B) + \frac{1}{4}(3J_{AB} - J_{AX} - J_{BX}) - D^+$	$(2^{1/2} \cos \phi^+ + \sin \phi^+)^2$
11	$3S_0' \rightarrow 2S_1'$	B	$\frac{1}{2}\eta (2H_B) + \frac{1}{2}J_{BX} + C^+ - D^-$	$[2^{1/2} \cos (\theta^+ - \phi^-) + \cos \theta^+ \sin \phi^-]^2$
12	$4S_0' \rightarrow 3S_1'$	B	$\frac{1}{2}\eta (2H_B) + \frac{1}{2}J_{BX} - C^+ + D^-$	$[2^{1/2} \cos (\theta^+ - \phi^-) - \sin \theta^+ \cos \phi^-]^2$
13	$1S_{-1}' \rightarrow 1S_0'$	B	$\frac{1}{2}\eta (2H_B) - \frac{1}{2}J_{BX} + D^+ - C^-$	$[2^{1/2} \cos (\phi^+ - \phi^-) + \cos \phi^+ \sin \theta^-]^2$
14	$2S_{-1}' \rightarrow 2S_0'$	B	$\frac{1}{2}\eta (2H_B) - \frac{1}{2}J_{BX} - D^- + C^-$	$[2^{1/2} \cos (\phi^+ - \theta^-) - \sin \phi^+ \cos \theta^-]^2$
15	$3S_{-1}' \rightarrow 4S_0'$	B	$\frac{1}{2}\eta (H_A + H_B) - \frac{1}{4}(3J_{AB} - J_{AX} - J_{BX}) - D^-$	$(2^{1/2} \cos \phi^- - \sin \phi^+)^2$
16	$S_{-2} \rightarrow 2S_{-1}'$	B	$\frac{1}{2}\eta (H_A + H_B) - \frac{1}{4}(3J_{AB} + J_{AX} + J_{BX}) - C^-$	$(2^{1/2} \cos \theta^- - \sin \theta^+)^2$
17	$1S_1 \rightarrow S_2$	X	$\eta H_X + \frac{1}{2}(J_{AX} + 2J_{BX})$	1
18	$1S_0' \rightarrow 2S_1'$	X	$\eta H_X + \frac{1}{2}J_{BX} + C^+ - D^+$	$\cos^2(\theta^+ - \phi^+)$
19	$2S_0' \rightarrow 3S_1'$	X	$\eta H_X + \frac{1}{2}J_{BX} - C^+ + D^+$	$\cos^2(\theta^+ - \phi^+)$
20	$1S_{-1}' \rightarrow 3S_0'$	X	$\eta H_X - \frac{1}{2}J_{BX} + D^- - C^-$	$\cos^2(\theta^- - \phi^-)$
21	$2S_{-1}' \rightarrow 4S_0'$	X	$\eta H_X - \frac{1}{2}J_{BX} - D^- + C^-$	$\cos^2(\theta^- - \phi^-)$
22	$S_{-2} \rightarrow 3S_{-1}$	X	$\eta H_X - \frac{1}{2}(J_{AX} + 2J_{BX})$	1
23	$1a_0 \rightarrow a_1$	X	$\eta H_X + \frac{1}{2}J_{AX}$	1
24	$a_{-1} \rightarrow 2a_0$	X	$-\frac{1}{2}J_{AX}$	1
25	$2S_0' \rightarrow 2S_1'$	C	$\eta H_X + \frac{1}{2}J_{BX} + C^+ + D^+$	$\sin^2(\theta^+ - \phi^+)$
26	$1S_0' \rightarrow 3S_1'$	C	$\eta H_X + \frac{1}{2}J_{BX} - C^+ - D^+$	$\sin^2(\theta^+ - \phi^+)$
27	$3S_0' \rightarrow 3S_1'$	C	$\eta H_B + \frac{1}{2}J_{BX} - C^+ - D^-$	$[2^{1/2} \sin (\phi^+ - \theta^+) - \sin \theta^+ \sin \phi^+]^2$
28	$1S_{-1}' \rightarrow 2S_0'$	C	$\eta H_B - \frac{1}{2}J_{BX} - C^- - D^+$	$[2^{1/2} \sin (\theta^+ - \phi^+) - \sin \theta^- \sin \phi^+]^2$
29	$1S_{-1}' \rightarrow 4S_0'$	C	$\eta H_B - \frac{1}{2}J_{BX} - C^- - D^-$	$\sin^2(\theta^+ - \phi^-)$
30	$2S_{-1}' \rightarrow 3S_0'$	C	$-\frac{1}{2}J_{BX} + C^- + D^-$	$\sin^2(\theta^+ - \phi^-)$

Table 3. Transitions and relative intensities for AB_2X .

involved, in particular the magnitude of the ratio J_{AB} to δ_{AB} , as this ratio determines the appearance of the AB_2 spectrum.

The more general method, which will be used here, is to make use of the regularities which appear in the spectrum. Many pairs of lines have the same separation in two different groups, e.g. the A and B groups, although these separations are not usually simple functions of the coupling constants.

These relationships can be summarized as follows:

A group with B group	A group with X group	B group with X group
$1-3 = 9-12$	$1-2 = 17-19$	$9-10 = 17-18$
$2-4 = 10-14$	$3-4 = 18-21$	$11-13 = 18-20$
$3-5 = 11-15$	$5-6 = 20-22$	$12-14 = 19-21$
$4-6 = 13-16$	$7-8 = 23-24$	$15-16 = 21-22$

(1)

Without evaluating the actual separations, these relationships provide an immediate check on any possible assignment.

In order to obtain the molecular parameters, some further relationships are needed. These, which also help in assigning the spectrum, are as follows.

In the X group, we have

$$\begin{aligned}\eta H_X &= \frac{1}{2}(17+22) = \frac{1}{2}(23+24), \\ J_{AX} + 2J_{BX} &= 17-22, \\ J_{AX} &= 23-24, \\ J_{BX} &= \frac{1}{2}(18-20) + \frac{1}{2}(19-21).\end{aligned}\quad (2)$$

In the A group, the only simple expressions are

$$\begin{aligned}\eta H_A &= \frac{1}{2}(7+8), \\ J_{AX} &= 7-8,\end{aligned}\quad (3)$$

and in the B_2 group

$$\begin{aligned}\eta H_B &= \frac{1}{4}(11+12+13+14), \\ J_{BX} &= \frac{1}{2}(11-13) + \frac{1}{2}(12-14), \\ \text{and } \frac{3}{2}J_{AB} &= \frac{1}{2}(11-12) + (9-15) \\ &= \frac{1}{2}(13-14) + (10-16).\end{aligned}\quad (4)$$

With the aid of the above expressions, and those of equation (1), the spectrum can be interpreted completely.

The AB_2X spectrum, does give the relative signs of all the coupling constants, although only the X group depends upon the relative sign of J_{AB} . However a better check on the relative sign of J_{AB} was to consider the AB_2X spectrum at a lower applied magnetic field so that it now became an AB_2C system.

In the remaining sections, we will consider how this analysis is used to analyse a given spectrum.

3. THE AB_2C SYSTEM

The basic functions and matrix elements for AB_2C are the same as those in table 1, but with addition of certain other off diagonal elements. These are

$$\mathcal{H}_{2,4} = \mathcal{H}_{5,8} = \mathcal{H}_{9,11} = \mathcal{H}_{14,15} = \frac{1}{2}J_{AC},$$

$$\mathcal{H}_{6,7} = 0.$$

$$\mathcal{H}_{2,3} = \mathcal{H}_{5,7} = \mathcal{H}_{6,8} = \mathcal{H}_{10,11} = \sqrt{\frac{1}{2}}J_{BC}.$$

In order to calculate a spectrum from a given set of chemical shifts and coupling constants it is now necessary to solve two 3×3 and one 4×4 matrix blocks. The solid lines in table 1 indicate the separation of these matrices.

4. EXPERIMENTAL RESULTS

The spectra of meta dinitrobenzene in dioxane solution (0.600 g in 1 ml dioxane) are shown in figures 1 and 2 (a). The spectrum in figure 1 was measured

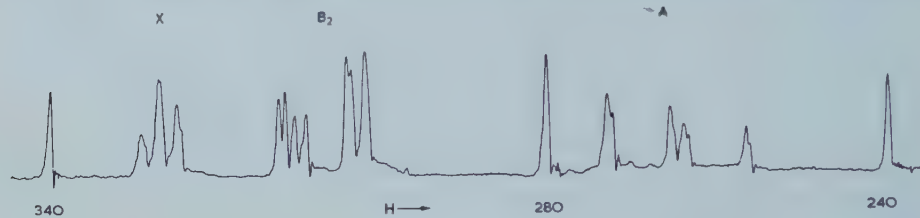


Figure 1. The proton resonance spectrum of meta dinitrobenzene in dioxane (0.6 g/ml) at 60 Mc/s.

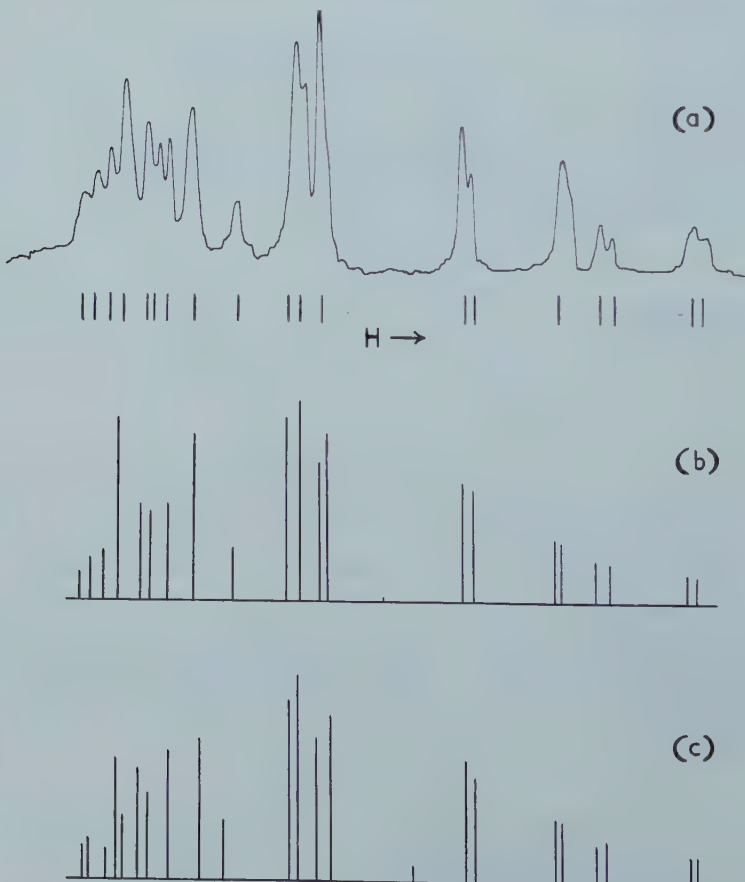


Figure 2. The proton resonance spectrum of meta dinitrobenzene in dioxane (0.6 g/ml) at 29.92 Mc/s. (a) Experimental trace; averaged experimental positions indicated beneath; (b) Theoretical spectrum, all J 's same sign; (c) Theoretical spectrum, J_{AB} and J_{BC} of different sign.

In the theoretical spectra, peaks closer than 0.3 c/s are coalesced.

with a Varian V-4300 spectrometer operating at 60 Mc/s. Figure 1 also shows the side bands of the dioxane solvent peak (in c/s) which were used to measure the spectrum. As higher energy transitions occur at lower applied magnetic fields, the direction of decreasing applied field will be taken as the positive direction. The observed energies (table 4) are the mean of the measurements for three runs. The three sets of measurements were reproducible to ± 0.1 c/s. The observed intensities were found by graphical integration of the area under the peaks. The intensities for the A, B₂ and X groups have been normalized separately.

Observed spectrum		Calculated spectra			
Energy	Relative intensity	(a) All J's positive Energy	Relative intensity	(b) J _{AX} negative Energy	Relative intensity
A transitions, relative to ηH_A					
7.66	3.03	7.53	1.43	7.48	1.45
7.20		7.05	1.45	7.10	1.44
0.22	1.89	0.22	1	0.22	1
-0.22		-0.22	1	-0.22	1
-1.28	1.77	-1.33	0.89	-1.43	0.90
-1.88		-1.84	0.89	-1.76	0.90
-8.68	1.31	-8.64	0.67	-8.69	0.65
-9.12		-9.11	0.66	-9.08	0.66
B ₂ transitions relative to ηH_B					
5.88	1.70	5.97	1.57	5.96	1.55
5.12	1.76	4.97	1.67	4.98	1.65
4.02	1.42	3.93	1.55	3.94	1.56
2.64	1.56	2.88	1.66	2.89	1.67
-2.28	4.52	-2.34	2.33	-2.34	2.34
-2.82		-2.89	2.43	-2.90	2.45
-4.54	5.02	-4.39	2.34	-4.37	2.33
-4.94		-4.96	2.45	-4.97	2.44
X transitions, relative to ηH_X					
2.20	1.72	2.30	1	2.24	1
1.72		1.82	1	1.86	1
0	3.69	{ 0.26	1	0.22	1
		{ 0.22	1	0.17	1
		{ -0.16	1	-0.16	1
		{ -0.22	1	-0.22	1
-1.76	2.58	-1.92	1	-1.86	1
-2.22		-2.30	1	-2.25	1

Table 4. Observed and calculated spectra for meta-dinitrobenzene at 60 Mc/s.

Figure 2 (a) shows the spectrum at 29.9200 Mc/s obtained on a permanent magnet high resolution spectrometer [6]. Dissolved oxygen had been removed from the sample by passage of nitrogen presaturated with dioxane. Table 5 shows the observed energies; there are so many overlapping lines that reliable quantitative values for the intensities could not be obtained.

Transition†		All J 's positive		$J_{AB}:J_{BC}$ different sign		Exptl. energies (c/s: ± 0.2)
		Energy (c/s)	Relative Intensity	Energy (c/s)	Relative intensity	
C	17	165.71	0.47	165.55	0.54	165.5
	19	164.94	0.70	165.07	0.71	164.7
	18	164.07	0.80	163.88	0.52	163.6
	23	163.17	0.97	163.17	0.99	162.7
	21	163.03	0.99	163.18	0.94	
	24	162.73	1.00	162.73	1.02	
	20	161.44	1.57	161.62	1.78	161.0
	22	160.76	1.43	160.96	1.39	160.5
B	9	159.52	1.58	159.51	2.07	159.6
	10	157.84	0.66	157.25	0.32	157.7
	11	157.60	2.02	157.33	1.93	
	13	155.00	0.84	155.66	0.96	154.6
	15	151.17	2.96	151.03	2.87	151.1
	12	150.29	3.20	150.42	3.28	150.3
	16	148.90	2.23	149.14	2.27	148.5
	14	148.38	2.69	148.20	2.61	
Comb. 25		144.41	0.07	142.46	0.23	
A	1	138.94	1.92	138.75	1.94	138.8
	2	138.17	1.79	138.09	1.66	138.1
	7	132.53	1.00	132.53	1.02	132.3
	8	132.09	0.97	132.09	0.99	
	3	129.72	0.67	129.70	0.62	129.4
	4	128.71	0.64	129.00	0.66	128.4
	5	123.29	0.45	123.18	0.45	123.0
	6	122.61	0.43	122.70	0.45	122.3

† This numbering applies to the 'all J 's positive' assignment only.

Table 5.

5. DISCUSSION

5.1. The 60 Mc/s spectrum

The assignment of the peaks in this spectrum is simplified by two factors. The groups do not overlap, thus the identification of the main groups is relatively easy. Also the values of the coupling constants in the benzene ring is known to be of the order of 7, 2 and 1 c/s for the ortho, meta and para proton coupling constants respectively [7].

Using this information the groups are easily assigned as X, B_2 and A, as shown in figure 1. Each group should have eight transitions. It can be seen that, although the A and B_2 groups do have eight resolved or nearly resolved transitions each, the X group has only five resolved transitions, the centre peak of the triplet consisting of four unresolved lines. The complete assignment follows from the

expressions (1) to (4) derived earlier. Two possible assignments are considered, according to the relative signs of J_{AX} and J_{BX} . These are:

(a) Assuming all positive coupling constants. Reading from left to right in figure 1:

A	1, 2	7, 8	3, 4	5, 6
B ₂	9, 11, 10, 13		15, 12, 16, 14	
X	17, 19		18, 21	20, 22
			23, 24	

(b) Assuming J_{AB} and J_{BX} positive, J_{AX} negative:

A	2, 1	8, 7	4, 3	6, 5
B ₂	9, 11, 10, 13		15, 12, 16, 14	
X	18, 17	21, 19	22, 20	
		24, 23		

The molecular parameters obtained from these assignments using expressions (2) to (4) are, in c/s:

$$\begin{aligned}\eta H_A &= 265.32, \quad \text{i.e. } \delta_{AB} = -41.40 \quad J_{AB} = 8.16, \\ \eta H_B &= 306.72, \quad \delta_{BX} = -20.04 \quad J_{BX} = 2.18, \\ \eta H_X &= 326.76, \quad \quad \quad J_{AX} = \pm 0.44,\end{aligned}$$

and the calculated energies and relative intensities for the two assignments are shown, with the observed ones, in table 4. It can be seen that both assignments fit the observed spectrum equally well, presumably due to the small size of J_{AX} .

The agreement between observed and calculated spectra could have been improved by considering second order terms of the form J_{BX}^2/δ_{BX} . However, this additional term is of approximately the same magnitude as the experimental error, and has therefore been neglected.

The calculated intensities for all the combination lines are vanishingly small and thus these lines have not been included in table 4. The small peak to high field of the B₂ group in figure 1 does not agree either in intensity or energy with any combination band and is therefore assigned to some impurity.

5.2. The 29.9200 Mc/s spectrum

The purpose of this part of the analysis is to find the relative signs of the two larger coupling constants, which are now J_{AB} and J_{BC} . The values for the coupling constants and chemical shifts obtained at 60 Mc/s were used to calculate theoretical spectra at 29.9200 Mc/s, for the case in which all J values are positive and for the case in which J_{AB} and J_{BC} are of opposite sign. For these calculations the following parameters were used:

$$\begin{aligned}\eta H_A &= 132.31; \quad \eta H_B = 152.95; \quad \eta H_C = 162.95 \text{ c/s}, \\ J_{AB} &= 8.16; \quad J_{AC} = 0.44; \quad J_{BC} = \pm 2.18 \text{ c/s}.\end{aligned}$$

The 4×4 and 3×3 matrices were solved with the aid of the Oxford University Mercury Ferranti Computer.

The two calculated spectra are shown in figures 2(b) and (c), and although they are rather similar, there is a sufficient difference of detail to permit a choice of the correct one. It is noted that the groups of lines due to transitions of the C and B nuclei have now moved very close together, although there is still no overlap between them.

The three transitions at lowest applied field show significant differences in the two calculated spectra. For all J values positive (spectrum 2b) they are approximately equidistant and their intensities increase towards the centre of the spectrum, as in the observed spectrum. For the J_{AB} and J_{AC} of different sign (spectrum 2c) the intensities and spacings are different, and the outer two lines are so close together that they could be scarcely resolved.

The position of the B transition at about 155 c./s relative to its two neighbours provides further evidence. In spectrum 2c it lies much nearer its low field neighbour than in spectra 2a and 2b.

The two strongest pairs of lines differ in their spacing. In spectrum 2c the high field pair is more widely separated than the low field pair, whereas in spectrum 2b the opposite occurs. In the observed spectrum only the low field line is easily split as would be expected if spectrum 2b was the correct one.

The combination line 25 is about half the strength of the highest field doublet components in spectrum 2c, and certainly ought to be observed. In spectrum 2b, however, it is very weak, and we were never able to detect it in the observed spectrum.

These differences all support the assignment of the same signs to both J_{AB} and J_{BC} and it is very probable that they are both positive. The value of J_{AC} is so small that a change in its sign would have a negligible effect on the spectrum, and so its relative sign cannot be obtained from these results.

The work at 60 Mc/s was started when R. J. A. was a post-doctoral fellow at the National Research Council of Canada, and he acknowledges with pleasure the assistance received from Dr. Bernstein.

We are grateful to the Hydrocarbon Research Group of the Institute of Petroleum and the Coal Board for grants in aid of apparatus. This work was done during the tenure of a D.S.I.R. Research Studentship by E. O. B.

REFERENCES

- [1] POPLE, J. A., SCHNEIDER, W. G., and BERNSTEIN, H. J., 1959, *High Resolution Nuclear Magnetic Resonance* (McGraw-Hill).
- [2] MCCONNELL, H. M., MCLEAN, A. D., and REILLY, C. A., 1955, *J. chem. Phys.*, **23**, 1152.
- [3] COHEN, A. D., and SHEPPARD, N., 1959, *Proc. roy. Soc. A*, **252**, 488.
- [4] MORTIMER, F. S., 1959, *J. mol. Spec.*, **3**, 335.
- [5] BERNSTEIN, H. J., POPLE, J. A., and SCHNEIDER, W. G., 1957, *Canad. J. Chem.*, **35**, 65.
- [6] LEANE, J. B., RICHARDS, R. E., and SCHAEFER, T. P., 1959, *J. sci. Instrum.*, **36**, 320.
- [7] GUTOWSKY, H. S., HOLM, C. H., SAIKA, A., and WILLIAMS, G. A., 1957, *J. Amer. chem. Soc.*, **79**, 4596.

Properties of the self-consistent field treatment of conjugated molecules

by H. H. GREENWOOD and T. H. J. HAYWARD

Imperial Chemical Industries Limited,
Billingham Division, Research Department

(Received 4 June 1960)

The polarizability properties of π electron systems are treated by the self-consistent field method, as modified by Pople for application to conjugated molecules. An analytical treatment of the π electron configuration of substituted hydrocarbons deduces certain universal symmetry properties of this method, and contains the Hückel treatment of inductive substituents as a simplified special case. Whereas the usual Hückel theory derives results by approximate perturbation methods, the treatment given here is formally exact. In a later section s.c.f. polarizability coefficients, as calculated on an Elliott 402 digital computer, are given for benzene, naphthalene, anthracene and phenanthrene, and the predictions of chemical properties are shown to be in better agreement with experiment than predictions derived from Hückel theory.

1. INTRODUCTION

Recent trends in the molecular orbital treatment of the electronic properties of conjugated molecules by means of the linear combination of atomic orbitals approximation have largely been associated with the employment of a more realistic Hamiltonian operator which includes interelectronic repulsion terms explicitly. Two main types of approach have been used, namely the self-consistent field [1] (s.c.f.) and the configuration interaction [2] (c.i.) methods. This paper deals exclusively with the former, and follows the presentation proposed by Pople [1] in simplifying, for application to conjugated molecules, the exact s.c.f. equations of Roothann [3].

One of the chief merits of the simpler Hückel theory resides in the adaptability to treatment by algebraic, as opposed to purely numerical methods, so that many properties may be understood or explained by analytical methods [4-8]. The basis of this work was laid by Coulson and Longuet-Higgins [8], since when various physical and chemical properties have been studied in terms of the analytical properties of the mathematical model. Examples are readily found in, for example, the fields of the ultra-violet spectroscopy and chemical reactions of conjugated molecules. Many properties, however, have been studied by means of first and second-order perturbation theory and are valid only to the extent that the sum over the remaining terms is negligible, though it appears that analytical properties of the sum itself may often be deduced [4, 9].

A few basic properties of the s.c.f. method as applied to alternant hydrocarbons have already been established. Pople [1] has shown that the charge density P_{rr} at each conjugated carbon atom is unity and has, in addition, deduced the symmetrical arrangement of energy levels about an appropriately chosen origin,

with a corresponding pairing of orbitals. Pople and Schofield [10] have derived expressions for the first-order perturbation coefficients in the s.c.f. method and have evaluated these for the case of benzene and similar molecules. McWeeny [11], in developing s.c.f. methods of calculation, has also dealt with the perturbation problem and has derived expressions based upon a steepest descent method applied to the density matrix for solving the s.c.f. equations.

The present paper is concerned with the properties of the s.c.f. solutions when a given atom in an alternant hydrocarbon is modified. As such it resembles in principle the well-known polarization techniques [8] used in Hückel theory for the treatment of inductive substituents. Unlike the Hückel case, however, where the properties are deduced by perturbation approximations, the properties deduced here are formally exact. The discussion will be restricted to properties relating largely to the ground-state electronic configuration. It is intended that spectroscopic and other similar topics will be dealt with in a subsequent paper.

Two theorems will be proved which relate to the solutions for substituted alternant hydrocarbons. As is well known, the s.c.f. equations are non-linear and, except where a high degree of geometric symmetry exists in the molecule, must be solved by an iterative process. The first theorem proves certain properties of the iterative steps for the modified system, when the configuration chosen to initiate the process is that of the unmodified parent hydrocarbon. The second theorem proves somewhat analogous properties of the s.c.f. equations themselves from a more fundamental view-point. No reference is made in the proof to methods of solving the equations, nor does the electron configuration of a parent molecule enter the argument. The theorem determines, in particular, the conditions which must be satisfied for the properties to hold, and indicates which of the various approximations involved in setting up the Hückel and s.c.f. equations give rise to known features of the theories based on these equations.

2. PROPERTIES OF THE S.C.F. FORMULATION

The procedure proposed by Pople for modifying Roothaan's s.c.f. equations for application to conjugated molecules will be followed. The modified equations take the well-known form [1]:

$$\sum_s F_{rs} c_{sj} = E_j c_{rj}, \quad (1)$$

$$F_{rr} = U_{rr} + \frac{1}{2} P_{rr} \gamma_{rr} + \sum_{t \neq r} (P_{tt} - Z_t) \gamma_{rt}, \quad (2)$$

$$F_{rs} = U_{rs} - \frac{1}{2} P_{rs} \gamma_{rs}, \quad (3)$$

$$P_{rs} = 2 \sum_{j'} c_{rj} c_{sj}, \quad (4)$$

$$\gamma_{rs} = (rs|G|rs), \quad (5)$$

where Z_t is the number of π electrons contributed by atom t for conjugation. Summations over j' , j'' and j will refer to occupied, unoccupied and the complete set of orbitals respectively. The matrix operators are defined in the basis of atomic orbitals ϕ_r from which molecular orbitals ψ_j are constructed, so that

$$\psi_j = \sum_r c_{rj} \phi_r.$$

Then \mathbf{U} is the core framework Hamiltonian, \mathbf{G} the electron interaction, \mathbf{F} the 'effective' Hamiltonian, and \mathbf{P} the bond order matrix. E_j and \mathbf{c}_j are corresponding eigenvalues and eigenvectors of \mathbf{F} . The matrix \mathbf{F} is quadratically

dependent on \mathbf{c} and the equations are non-linear and must be solved self-consistently. This is generally done by an iteration process in which the current \mathbf{c} matrix provides a \mathbf{P} for the formation of an \mathbf{F} matrix, using the given fixed matrices \mathbf{U} and \mathbf{G} . The new \mathbf{F} matrix is then diagonalized to provide a new \mathbf{c} for the next iteration.

Now Pople [1] has shown that for alternant hydrocarbons the energy levels are distributed symmetrically about the origin:

$$U_{CC} + \frac{1}{2}\gamma_{CC}$$

where C stands for a conjugated carbon atom. It is convenient for establishing theorem 1 to transform to this energy value as a new origin, so that the diagonal terms (2) become

$$F_{rr} = \delta U_r + \frac{1}{2}(P_{rr}\gamma_{rr} - \gamma_{CC}) + \sum_{t \neq r}(P_{tt} - Z_t)\gamma_{rt} \quad (6)$$

where $\delta U_r = U_{rr} - U_{CC}$ is an electronegativity difference between the r th atom and a normal conjugated carbon atom. Now, in alternant hydrocarbons the atom centres can be labelled as belonging to two sets, starred and unstarred, so that adjacent atoms never belong to the same set. Pople [1] has proved that for these hydrocarbons

$$P_{rs}^0 = \delta_{rs} \quad (r, s \text{ same set}). \quad (7)$$

Since, in addition

$$U_{rr}^0 = U_{CC}, \quad \text{i.e. } \delta U_{rr}^0 = 0, \quad (8)$$

$$\gamma_{rr}^0 = \gamma_{CC} \quad (9)$$

$$Z_t = 1, \quad (10)$$

for hydrocarbons, it follows that, for the chosen origin, $F_{rr}^0 = 0$. The zero superfix will be reserved for the s.c.f. solution of the unperturbed parent alternant hydrocarbon. The off-diagonal elements are then

$$F_{rs}^0 = U_{rs}^0 - \frac{1}{2}P_{rs}^0\gamma_{rs}, \quad (s \neq r) \quad (11)$$

with

$$U_{rs}^0 = 0 \quad (12)$$

for s, r non-neighbours.

The first theorem concerns the properties of the s.c.f. solutions obtained when the electronegativity term U_{rr} is modified from the carbon value U_{CC} . The modified atom will be labelled u so that the corresponding diagonal element of F is obtained by substituting $r = u$ in (6). It will be noted that the modification corresponds in the Hückel theory to a change in coulomb integral at the u th atom position, and in more general chemical terms to an inductive effect at the u th atom.

Theorem 1

Denote changes from the parent hydrocarbon due to changes $+\delta U_u$ and $-\delta U_u$ by + and - respectively. Then

- A. $\delta P_{rr}^{(n-1)}(+)= -\delta P_{rr}^{(n-1)}(-),$
- B. $P_{rs}^{(n-1)}(+)= -P_{rs}^{(n-1)}(-) \quad (r, s \text{ same set}),$
 $= +P_{rs}^{(n-1)}(-) \quad (r, s \text{ different sets}),$
- C. $E_i^{(n-1)}(+)= -E_i^{(n-1)}(-),$

where δP denotes the changes from the values in the parent hydrocarbon and

the $(n-1)$ superfix refers to the value after the $(n-1)$ th iteration. E_i are eigenvalues defined by (1).

Proof

The s.c.f. equations (1)–(5) may, after $n-1$ iterations, be written in the form

$$[\delta F_{rr}^{(n-1)} - E_i^{(n)}]c_{ir}^{(n)} + \sum_{s \neq r, \text{ same}} \delta F_{rs}^{(n-1)}c_{is}^{(n)} + \sum_{s \neq r, \text{ diff.}} (F_{rs}^0 + \delta F_{rs}^{(n-1)})c_{is}^{(n)} = 0 \quad (13)$$

where the summations refer to s and r in the same and different sets respectively, and where, by using (7) and (10) in (6)

$$\delta F_{uu}^{(n-1)} = \delta U_u + \frac{1}{2}\delta P_{uu}^{(n-1)}\gamma_{uu} + \sum_{t \neq u} \delta P_{ut}^{(n-1)}\gamma_{ut}, \quad (14)$$

$$\delta F_{rr}^{(n-1)} = \frac{1}{2}\delta P_{rr}^{(n-1)}\gamma_{rr} + \sum_{t \neq r} \delta P_{rt}^{(n-1)}\gamma_{rt} \quad (r \neq u), \quad (15)$$

$$\delta F_{rs}^{(n-1)} = -\frac{1}{2}\delta P_{rs}^{(n-1)}\gamma_{rs} \quad (r \neq s). \quad (16)$$

The proof now proceeds by way of the inductive assumption that conditions A and B hold for the $(n-1)$ th iteration. Then condition B states that

$$P_{rs}^{(n-1)}(+) = +P_{rs}^{(n-1)}(-) \quad (r, s \text{ different sets})$$

and yields immediately

$$\delta P_{rs}^{(n-1)}(+) = +\delta P_{rs}^{(n-1)}(-) \quad (r, s \text{ different sets}). \quad (17)$$

Also since by (7)

$$P_{rs}^0 = 0 \quad (r, s \text{ same set}, r \neq s),$$

it follows that

$$P_{rs}^{(n-1)} \equiv \delta P_{rs}^{(n-1)} \quad (r, s \text{ same set}, r \neq s)$$

so that condition B also yields

$$\delta P_{rs}^{(n-1)}(+) = -\delta P_{rs}^{(n-1)}(-) \quad (r, s \text{ same set}, r \neq s). \quad (18)$$

Applying the results (17) and (18) together with condition A, to equations (14), (15) and (16) yields

$$\delta F_{uu}^{(n-1)}(+) = -\delta F_{uu}^{(n-1)}(-), \quad (19)$$

$$\delta F_{rr}^{(n-1)}(+) = -\delta F_{rr}^{(n-1)}(-), \quad (20)$$

$$\delta F_{rs}^{(n-1)}(+) = -\delta F_{rs}^{(n-1)}(-) \quad (r, s \text{ different sets}) \quad (21)$$

$$= -\delta F_{rs}^{(n-1)}(-) \quad (r, s \text{ same set}). \quad (22)$$

Examination of the s.c.f. equations (13) in the light of the results obtained in (19) to (22) shows that to each $E_i^{(n)}$ for which there exists a solution $\mathbf{c}_i^{(n)}(+)$ for δU_u positive, there exists also a solution for δU_u equal and opposite in sign having the eigenvalue $-E_i^{(n)}$ and eigenvector $\mathbf{c}_i^{(n)}(-)$ which differs from $\mathbf{c}_i^{(n)}(+)$ in the signs of coefficients $c_{ir}^{(n)}$ associated with alternate atoms r . Condition C relating the eigenvalues $E_i^{(n)}(+)$ and $E_i^{(n)}(-)$ is clearly demonstrated in the analysis.

It is now necessary to establish the inductive assumption, which forms the basis of the above result, after the n th iteration. Therefore write

$$\begin{aligned} P_{rr}^{(n)}(+) &= 2 \sum_{j'} c_{rj}^{(n)}(+) c_{rj}^{(n)}(+) \\ &= 2 \sum_j c_{rj}^{(n)}(+) c_{rj}^{(n)}(+) - 2 \sum_{j''} c_{rj}^{(n)}(+) c_{rj}^{(n)}(+) \\ &= 2 - 2 \sum_{j''} c_{rj}^{(n)}(+) c_{rj}^{(n)}(+), \end{aligned}$$

since

$$\delta_{rs} = \sum c_{rj}^{(n)} c_{sj}^{(n)}. \quad (23)$$

But from the relation between the eigenvectors $\mathbf{c}_i^{(n)}(+)$ and $\mathbf{c}_i^{(n)}(-)$

$$P_{rr}^{(n)}(-) = 2 \sum_{j'} c_{rj}^{(n)}(-) c_{rj}^{(n)}(-) = 2 \sum_{j''} c_{rj}^{(n)}(+) c_{rj}^{(n)}(+) ;$$

$$\therefore P_{rr}^{(n)}(+) = 2 - P_{rr}^{(n)}(-)$$

$$\text{or } P_{rr}^{(n)}(+) - 1 = 1 - P_{rr}^{(n)}(-)$$

$$\text{or } \delta P_{rr}^{(n)}(+) = -\delta P_{rr}^{(n)}(-),$$

since $P_{rr}^0 = 1$; which therefore establishes condition A after the n th iteration. Now

$$\begin{aligned} P_{rs}^{(n)}(+) &= 2 \sum_{j'} c_{rj}^{(n)}(+) c_{sj}^{(n)}(+) \\ &= 2 \sum_j c_{rj}^{(n)}(+) c_{sj}^{(n)}(+) - 2 \sum_{j''} c_{rj}^{(n)}(+) c_{sj}^{(n)}(+) \\ &= -2 \sum_{j''} c_{rj}^{(n)}(+) c_{sj}^{(n)}(+) \end{aligned}$$

by (23). Also from the relations between the eigenvectors $\mathbf{c}_i^{(n)}(+)$ and $\mathbf{c}_i^{(n)}(-)$

$$2 \sum_{j'} c_{rj}^{(n)}(+) c_{sj}^{(n)}(+) = 2 \sum_{j'} c_{rj}^{(n)}(-) c_{sj}^{(n)}(-) \quad (r, s \text{ same set}, r \neq s)$$

$$\text{or} \quad = -2 \sum_{j'} c_{rj}^{(n)}(-) c_{sj}^{(n)}(-) \quad (r, s \text{ different sets});$$

$$\text{therefore} \quad \begin{aligned} P_{rs}^{(n)}(+) &= -P_{rs}^{(n)}(-) && (r, s \text{ same set}, r \neq s) \\ &= +P_{rs}^{(n)}(-) && (r, s \text{ different sets}), \end{aligned}$$

which establishes B after the n th iteration. Since the conditions A and B can be established for $n=1$ it follows that the theorem is proved. Then if the iteration process, which takes the unperturbed hydrocarbon configuration for the first step, converges, the theorem also applies to the s.c.f. solution.

It is advantageous at this stage to relate these results to the more familiar results obtained from the Hückel theory. The terms P_{rr} and P_{rs} (r, s neighbours) of the s.c.f. bond order matrix are analogous respectively to the Hückel charge density q_r at an atom and the bond order p_{rs} of the bond joining neighbouring atoms r and s . Denoting the change in coulomb integral in Hückel theory by δz_u , so that δz_u is analogous to δU_u in the s.c.f. formulation, the following Hückel expression [8]

$$\delta q_r = \frac{\partial q_r}{\partial \alpha_u} \delta z_u + \frac{1}{2} \frac{\partial^2 q_r}{\partial \alpha_u^2} \delta z_u^2 \quad (24)$$

is the conventional analogue of condition A. Since the second-order coefficient is zero [8] the relationship (24) has the same properties as condition A.

Similarly

$$\delta p_{rs} = \frac{\partial p_{rs}}{\partial \alpha_u} \delta z_u + \frac{1}{2} \frac{\partial^2 p_{rs}}{\partial \alpha_u^2} \delta z_u^2 \quad (25)$$

where now the first-order term is zero [8]. This then is the Hückel analogue of part of condition B where r and s are neighbours, and therefore belong to different sets. There appears to be no proof in the literature for Hückel theory analogous to condition C. It is possible, however, to obtain a more complete analogy, by considering the properties of the successive terms in the infinite expansions corresponding to (24) and (25) when the exact values of δq_r and δp_{rs} have precisely the same properties as the corresponding terms in the P matrix of the s.c.f. treatment [9]. It is more direct, however, to apply to Hückel theory the same technique, involving now no iterative process, as that used above for the

s.c.f. equations. Then precisely the same results are easily obtained for the simpler equations, namely conditions A, B and C where now q_r replaces P_{rr} , p_{rs} replaces P_{rs} , and ϵ_i the Hückel level replaces E_i . In this case p_{rs} ($r \neq s$) refers to all bond orders and not just those between nearest neighbours as in the usual Hückel treatment.

The second theorem establishes similar results as fundamental properties of the s.c.f. equations themselves, without reference to the solutions for parent molecules or to iterative processes of solution. The theorem is particularly concerned to determine the conditions under which these properties exist. Returning to the original form (1) to (5) of the s.c.f. equations, it is convenient to combine F_{rr} and F_{rs} to give the general matrix element

$$F_{rs} = V_{rs} - \frac{1}{2}P_{rs}\gamma_{rs} + \sum_t P_{rt}\gamma_{rt}\delta_{rs} \quad (26)$$

where

$$V_{rs} = U_{rs} + Z_r\gamma_{rr}\delta_{rs} - \sum_t Z_t\gamma_{rt}\delta_{rs} \quad (27)$$

and where the summations are now taken over all values of t including r and s .

Theorem 2

To every solution corresponding to a perturbation $+J_{uu}$ of the diagonal element V_{uu} there exists, for conditions to be determined, a conjugate solution corresponding to the perturbation $-J_{uu}$.

Proof

The s.c.f. equation (1) is equivalent to

$$F_{rs} = \sum_j c_{rj}E_jc_{sj} \quad (28)$$

where

$$\delta_{rs} = \sum_j c_{rj}c_{sj}, \quad (29)$$

the summation being taken over all values of j .

Now \mathbf{V} and γ are given, and the solution is expressed by the set of matrices \mathbf{c} , \mathbf{F} , \mathbf{E} and \mathbf{P} . Eliminate now \mathbf{P} using (4), (26), (28) and (29) to obtain

$$V_{rs} - \sum_{j'} c_{rj}c_{sj}\gamma_{rs} + \sum_t \sum_{j'} 2c_{tj}^2\gamma_{rt}\delta_{rs} - \sum_j c_{rj}E_jc_{sj} = 0 \quad (30)$$

where the summation j' , as in (4), is taken over occupied levels. Solution of (29) and (30) is equivalent to solution of the s.c.f. equations.

Apply now the perturbation

$$V_{rr} \longrightarrow V_{rr} + J_{rr}$$

and let \mathbf{c} , \mathbf{E} , etc. denote a solution for the perturbed system, so that

$$V_{rs} + J_{rr}\delta_{rs} - \sum_{j'} c_{rj}c_{sj}\gamma_{rs} + \sum_t \sum_{j'} 2c_{tj}^2\gamma_{rt}\delta_{rs} - \sum_j c_{rj}E_jc_{sj} = 0. \quad (31)$$

Consider now replacing in the left-hand side of (31)

$$\left. \begin{aligned} V_{rs} + J_{rr}\delta_{rs} &\text{ by } V_{rs} - J_{rr}\delta_{rs}, \\ c_{rj} &\text{ by } e_r c_{rj}^*, \\ E_j &\text{ by } M - E_j^*. \end{aligned} \right\} \quad (32)$$

The multipliers e_r are defined by reference to the starring scheme referred to above. In (32) $e_r = +1$ if atom r is starred and -1 if unstarred. M is a constant

to be determined later. The transformation $j \rightarrow j^*$ represents the interchange of the set of occupied orbitals with the set of unoccupied, the sets being equal in number since the number of occupied orbitals is half the complete set.

The left-hand side of (31) when subjected to the operations (32) becomes

$$\begin{aligned} \text{L.H.S.} &= V_{rs} - J_{rr}\delta_{rs} - e_r e_s \sum_{j''} c_{rj} c_{sj} \gamma_{rs} + \sum_t \sum_{j''} 2c_{tj}^2 \delta_{rt} \gamma_{rs} \\ &\quad - e_r e_s \sum_j c_{rj} M c_{sj} + e_r e_s \sum_j c_{rj} E_j c_{sj} \end{aligned} \quad (33)$$

$$\begin{aligned} &= V_{rs} - J_{rr}\delta_{rs} - e_r e_s \delta_{rs} \gamma_{rs} + e_r e_s \sum_{j'} c_{rj} c_{sj} \gamma_{rs} - \sum_t \sum_{j'} 2c_{tj}^2 \gamma_{rt} \delta_{rs} \\ &\quad + 2 \sum_t \gamma_{rt} \delta_{rs} - e_r e_s M \delta_{rs} + e_r e_s \sum_j c_{rj} E_j c_{sj}, \end{aligned} \quad (34)$$

since

$$\sum_{j'} + \sum_{j''} = \sum_j \quad \text{and} \quad \sum_j c_{rj} c_{sj} = \delta_{rs};$$

therefore

$$\begin{aligned} \text{L.H.S.} &= V_{rs} - \gamma_{rs} \delta_{rs} + 2 \sum_t \gamma_{rt} \delta_{rs} - M \delta_{rs} + e_r e_s V_{rs} \\ &= V_{rs} (1 + e_r e_s) + (2 \sum_t \gamma_{rt} - \gamma_{rr} - M) \delta_{rs}. \end{aligned} \quad (35)$$

To prove the theorem, it is only necessary to show that under conditions to be determined the new set of variables in (32) satisfy the same s.c.f. equations, i.e. (29) and (30), as the old set, since the different sets then give the required conjugate solutions defined by the relationships (32). Now

$$\sum_{j^*} c_{rj}^* c_{sj^*} = e_r e_s \sum_j c_{rj} c_{sj} = e_r e_s \delta_{rs} = \delta_{rs}$$

so that equation (29) is satisfied. To satisfy (30) requires that (35) shall be zero. Consider now the different cases

- (i) $e_r = -e_s$, $r \neq s$; then (35) is always zero,
- (ii) $e_r = e_s$, $r \neq s$; then (35) is zero if $V_{rs} = 0$,
- (iii) $e_r = e_s$, $r = s$; then (35) is zero if

$$2V_{rr} + 2 \sum_t \gamma_{rt} - \gamma_{rr} - M = 0. \quad (36)$$

Thus, given a solution to the s.c.f. equations for the perturbation $+J_{rr}$, it is possible to construct by means of the transformation (32) a solution, namely the conjugate solution of the equations for $-J_{rr}$, provided

- A. $V_{rs} = 0$ for $e_r = e_s$, $r \neq s$,
- B. $M = 2V_{rr} + 2 \sum_t \gamma_{rt} - \gamma_{rr}$ is independent of r ,

where \mathbf{V} is the unperturbed matrix. This establishes the proof of the theorem.

The theorem will now be applied to the case of alternant hydrocarbons. For this case $Z_i = 1$ for all conjugated carbon atoms so that V_{rs} in (27) is given by

$$V_{rs} = U_{rs} + Z_r \gamma_{rr} \delta_{rs} - \sum_t \gamma_{rt} \delta_{rs}.$$

In addition

$$U_{rr} = U_{CC} \quad \text{for all carbon atoms } r,$$

$$U_{rs} = U_{rs}^0 \quad \text{for neighbours } r \text{ and } s$$

$$= 0 \quad \text{for non-neighbours,}$$

$$\gamma_{rr} = \gamma_{CC} \quad \text{for all carbon atoms } r.$$

Condition A is clearly satisfied. Also on substitution

$$M = 2\{U_{CC} + \gamma_{CC} - \sum_t \gamma_{rt}\} + 2\sum_t \gamma_{rt} - \gamma_{rr}, \quad (37)$$

i.e.

$$M = 2U_{CC} + \gamma_{CC}.$$

Since M is independent of r , condition B is satisfied and conjugate solutions defined by (32) are obtained for alternant hydrocarbons.

3. DISCUSSION

The above analysis contains a number of corollaries which merit further consideration. It is, for example, interesting to consider the type of situation under which condition B is not satisfied. A simple case is exemplified by the molecule pyridine, where M is not independent of r , since V_{rr} takes the same value for the five carbon atoms, but a different value for the nitrogen atom. Different values may also be used for elements of the G matrix involving the nitrogen atom. The perturbation $+J_{rr}$ may now be applied to any diagonal element V_{rr} of pyridine, and the s.c.f. solution obtained. Since condition B is not satisfied there exists no conjugate solution for the perturbation $-J_{rr}$.

Another topic concerns additional information which may be deduced from condition A. It will be observed that no conditions are imposed on V_{rs} for the case $e_r = -e_s$, that is when r and s belong to different sets. This means that if the nearest-neighbour approximation

$$\left. \begin{array}{ll} U_{rs} = U_{rs}^0 & (r, s \text{ neighbours}) \\ = 0 & (r, s \text{ non-neighbours}) \end{array} \right\} \quad (38)$$

usually adopted for the \mathbf{U} matrix in the treatment of conjugated molecules, is relaxed to the approximation

$$\left. \begin{array}{ll} U_{rs} \neq 0 & (r, s \text{ different sets}), \\ U_{rs} = 0 & (r, s \text{ same set, } r \neq s), \end{array} \right\} \quad (39)$$

the properties of conjugate solutions are still retained. This result has bearing also upon the properties of the Hückel solutions for unperturbed alternant hydrocarbons. Thus the symmetry properties of the energy levels, the pairing of orbitals, and the uniform value $P_{rr} = 1$ for the charge densities will be obtained if the conventional nearest-neighbour approximation is relaxed to the condition corresponding to (39). It follows that these well-known properties will be lost if $U_{rs} \neq 0$ for some value of r and s belonging to the same set. Now the conventional Hückel theory, which uses the nearest-neighbour approximation (38), when applied to alternant hydrocarbons, is often said to possess self-consistent properties because the calculated charge densities at all atoms, which have the same coulomb integral, are all unity. But the pseudo-self-consistency is lost when condition (39) is no longer valid, though each atom is still associated with the same coulomb integral.

The derivation of the properties of the s.c.f. equations, exemplified by theorems 1 and 2, leads to a better understanding of the reasons for the success of the simple Hückel theory. The analysis shows that the non-linear s.c.f. equations in the form proposed by Pople, and the simpler Hückel equations, possess essentially similar properties with respect to modification of the coulomb integral of a given atom. Granted, then, the physical reliability of the more sophisticated s.c.f.

equations, it follows that Hückel theory must, from the analysis, produce mathematically, and therefore physically analogous descriptions. The only source of differences must lie in the magnitude of computed results derived from integrals and parameters obtained independently. This subject is dealt with in the next section. It seems equally certain that the analytical properties of the Hückel and s.c.f. equations towards variation of other molecular parameters are also analogous; this is true for bond parameters, though the proof will not be given here. There appears therefore to be a complete analytical correspondence between the two methods.

4. COMPUTATION OF POLARIZABILITY COEFFICIENTS

To obtain a numerical representation of the changes in the charge densities P_{rr} and bond orders P_{rs} in the s.c.f. approximation, due to a change δU_u in coulomb integral at the u th atom, the first non-zero coefficients in a Taylor expansion have been calculated. The atom-atom polarizability coefficients $\sigma_{r,u}$ and the atom-bond coefficients $\sigma_{rs,u}$ in the s.c.f. method will be defined by the equations

$$\left. \begin{aligned} \delta P_{rr} &= \sigma_{r,u} \delta U_u + O(\delta U_u^3), \\ \delta P_{rs} &= \sigma_{rs,u} (\delta U_u^2) + O(\delta U_u^4) \quad (r, s \text{ neighbours}), \end{aligned} \right\} \quad (40)$$

since, according to the theory given above, P_{rr} is an odd function and P_{rs} (r, s neighbours) an even function of δU_u . The suitability of these definitions follows both from the analytical dependence on δU_u , and from the correspondence with Hückel theory, where polarizability coefficients are similarly defined in the context of a similar analytical dependence. In the s.c.f. treatment the numerical values obtained for $\sigma_{r,u}$ and $\sigma_{rs,u}$ clearly depend upon values of the elements of the electron interaction matrix \mathbf{G} . In the results quoted below, matrix elements referring to two carbon atoms in the same ring have been given the values suggested by McWeeny and Peacock [12], namely

$$\begin{aligned} \gamma_{11} &= -2.380; & \gamma_{12} &= -1.503, \\ \gamma_{13} &= -1.148; & \gamma_{14} &= -1.044. \end{aligned}$$

The unit of energy here is -4.79 ev which is the value of F_{rs}^0 (equation (11)) for r and s neighbouring atoms in benzene. In terms of this unit the matrix element U_{rs}^0 between neighbouring carbon atoms, usually denoted by the symbol β , takes the value $U_{rs}^0 = \beta = 0.5$. Matrix elements corresponding to carbon atoms in different rings have been evaluated according to Pople's inverse distance prescription [1]. The change δU_u at atom u was expressed in the form

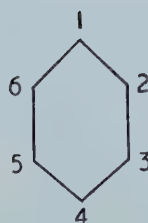
$$\delta U_u = k U_{rs}^0 \equiv k \beta \quad (41)$$

where k is a numerical parameter.

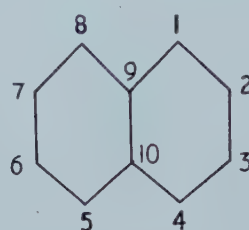
The polarizability coefficients have been derived in Hückel theory by two methods, namely by integral formulae based on functions of the minors of the secular determinant, and secondly by conventional perturbation methods [8]. Pople has developed a technique analogous to the latter method for the s.c.f. theory and has calculated polarizability coefficients for benzene, where, because of symmetry, the s.c.f. and Hückel molecular orbitals are identical [10]. The s.c.f. polarizability coefficients quoted below have been computed by an indirect method, namely by solving the s.c.f. equations for a few selected values of δU_u and deducing the coefficients of the Taylor expansions by differencing methods.

This approach was conditioned by the availability of an Elliott 402 digital computer which produced complete eigensolutions of the s.c.f. problem. Polarizability coefficients $\sigma_{r,u}$ for benzene, naphthalene, anthracene and phenanthrene are given in tables 1-4 in terms of β^{-1} . Values of the smaller second order coefficients $\sigma_{rs,u}$ have also been obtained, but will not be quoted here. Application to these prototype molecules is, in part, a preliminary test of the s.c.f. method itself, since unreasonable values, relative or absolute, or more especially, obvious failures to reproduce corresponding experimental properties, would raise doubts concerning its validity.

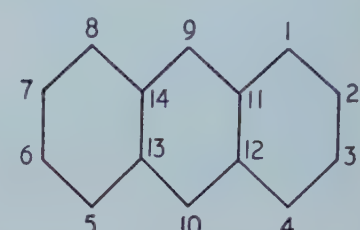
The numbering scheme used in the tables is as follows



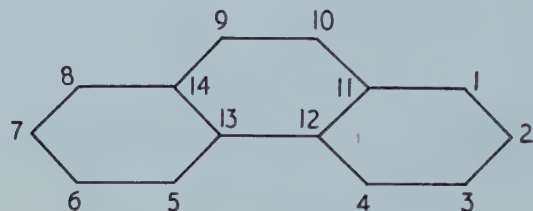
Benzene



Naphthalene



Anthracene



Phenanthrene

<i>r</i>	<i>u</i>	1
1		+0.279
2		-0.138
3		+0.030
4		-0.063

Table 1. Benzene $\sigma_{r,u} \times \beta$.

<i>r</i>	<i>u</i>	1	2
1		+0.293	-0.169
2		-0.168	+0.279
3		+0.035	-0.112
4		-0.079	+0.035
5		-0.002	+0.008
6		+0.009	-0.018
7		-0.014	+0.007
8		-0.006	-0.013
9		-0.090	+0.025
10		+0.023	-0.041

Table 2. Naphthalene $\sigma_{r,u} \times \beta$.

<i>r</i>	<i>u</i>	1	2	9
1		+0.282	-0.173	-0.004
2		-0.172	+0.270	-0.019
3		+0.036	-0.102	+0.012
4		-0.078	+0.036	-0.004
5		-0.000	+0.002	-0.004
6		+0.001	-0.008	+0.012
7		-0.003	+0.000	-0.019
8		+0.000	-0.003	-0.004
9		-0.004	-0.020	+0.305
10		-0.004	+0.011	-0.096
11		-0.074	+0.023	-0.116
12		+0.018	-0.033	+0.027
13		+0.008	-0.012	+0.027
14		-0.010	+0.010	-0.116

Table 3. Anthracene $\sigma_{r,u} \times \beta$.

<i>r</i>	<i>u</i>	1	2	3	4	10
1		+0.281	-0.155	+0.036	-0.070	-0.005
2		-0.155	+0.272	-0.121	+0.035	-0.008
3		+0.036	-0.121	+0.273	-0.153	+0.012
4		-0.069	+0.035	-0.154	+0.282	-0.000
5		+0.009	-0.008	+0.008	-0.029	+0.007
6		-0.006	+0.001	-0.010	+0.008	-0.022
7		+0.002	-0.008	+0.001	-0.007	+0.008
8		-0.006	+0.002	-0.007	+0.010	-0.015
9		-0.015	+0.008	-0.022	+0.008	-0.190
10		-0.005	-0.008	+0.011	-0.000	+0.276
11		-0.104	+0.029	-0.049	+0.026	-0.070
12		+0.027	-0.048	+0.031	-0.106	+0.023
13		-0.003	+0.011	-0.007	+0.006	-0.045
14		+0.008	-0.009	+0.010	-0.008	+9.929

Table 4. Phenanthrene $\sigma_{r,u} \times \beta$.

4.1. The computer programme

The computer programme solves the s.c.f. equations (1)–(5) by the iterative process briefly described earlier. The given fixed matrices **U** and **G** are stored permanently during the computation and form with the current **P** matrix a current **F** matrix. The latter is diagonalized by a Jacobi routine which yields simultaneously the complete set of eigenvalues **E** and eigenvectors **c**. A new **P** matrix is then computed according to equation (4) from the semi-matrix of eigenvectors which corresponds to occupied orbitals. Convergence was judged by the self-consistency obtained for successive **P** matrices or, more critically, successive eigensolutions. The **P** matrix chosen to initiate the iterative process was, in the present application, a Hückel solution obtained as part of the programme routine by diagonalisation of the fixed **U** matrix.

The convergence was improved by an extrapolation procedure described by Hartree [13]. Let x_0 , x_1 , x_2 be the values of an unknown, x , in three successive cycles of the process. Then, in general, if x_0 , x_1 , x_2 are moderately close to the true value of x ,

$$x_0 = x_2 - \frac{(x_2 - x_1)^2}{(x_0 - 2x_1 + x_2)}$$

will be much closer. Using the new x_{00} as starting value, two further cycles of iteration are carried out, giving a new set x_0, x_1, x_2 for computing a new x_{00} ; and so on. The method was programmed for application to each individual element of the \mathbf{P} matrix. The sequence x_{00} is a second-order process and gave improved convergence such that the number of iterations required was, in general, halved. Thus, to guarantee full accuracy to the third decimal place in elements of the \mathbf{P} matrix, twelve to fourteen iteration steps were required and, with the extrapolation routine included, six or seven. The results quoted in the tables were obtained by the last method.

It will be observed from the tables that the sum

$$\sum \sigma_{r,u}$$

taken over all atoms r in the given molecules, for the different atoms u , is found to be always zero or 0.001 apart from one case of 0.002. This provides a convincing check of the differencing procedure used for obtaining the $\sigma_{r,u}$'s individually from complete s.c.f. solutions of the corresponding perturbation problems, since the total charge must be constant. It will also be noted that $\sigma_{u,r} = \sigma_{r,u}$ with an error not exceeding 0.001. These equal coefficients were obtained independently from complete s.c.f. solutions in which the corresponding charges densities P_{uu} and P_{rr} , obtained from equal perturbations δU_r and δU_u , were themselves unequal, so that again the equality $\sigma_{u,r} = \sigma_{r,u}$ confirms the accuracy of the differencing procedure.

It was observed in the course of carrying through these calculations that a slope at the origin, calculated directly from a single displacement given by taking $k = \frac{1}{2}$ in equation (41), reproduced the $\sigma_{r,u}$'s with an error of order 0.001. With larger values, say $k = \frac{3}{4}$ or 1, the calculated slopes produced the $\sigma_{r,u}$'s with errors several times larger, whilst for values of k less than $\frac{1}{2}$, the small changes obtained provided calculated slopes of low accuracy. It seems, therefore, that, at least for alternant hydrocarbons, polarizability coefficients may be calculated to an accuracy of 0.001 from a single s.c.f. solution corresponding to $k = \frac{1}{2}$, with a considerable economy of effort.

5. DISCUSSION OF RESULTS

Examination of the tabulated results shows that the range of values obtained for the polarizability coefficients $\sigma_{r,u}$ is theoretically reasonable, and that the changes in the charge distributions resulting from application of these coefficients are substantially greater in the ring containing the perturbation than in more remote rings. In many ways the patterns of predicted changes in charge distribution obtained from these coefficients resembles those obtained from the simpler Hückel coefficients, though there are differences, described below, which appear to be chemically significant. It will be noted that the charges at positions ortho and para to the perturbed atom are, characteristically, modified more than the meta position, though the charge distribution is more even than that predicted by Hückel theory, as may be expected from the explicit introduction of electron repulsion terms. Similarly, the so-called law of alternating polarity is also reproduced, in that, in passing from the perturbed atom, the charge densities calculated from the tabulated polarizability coefficients alternate in magnitude at successive atoms. Unlike the corresponding results obtained by Hückel theory, however, the computed charge densities are not throughout

greater than, and less than unity at successive atoms. For example, taking the case $u=1$ in anthracene with $r=11, 9$ and 14 referring to successive atoms, the signs of $\sigma_{r,u}$ are all negative, whereas according to Hückel theory the coefficients $\pi_{r,u}$ with $r=11$ and 14 are likewise negative, but $\pi_{9,1}$ is positive. However, though negative in the s.c.f. treatment, $\sigma_{9,1}$ is smaller than $\sigma_{11,1}$ and $\sigma_{14,1}$ so that the alternation in absolute magnitudes is preserved. The conjugate coefficient $\sigma_{1,9}$ gives rise to the same property when $u=9$ and $r=11, 1$ and 2 . Examination of the tables shows that alternation in the signs of the $\sigma_{r,u}$'s associated with adjacent atoms may break down in this way for sequences involving nearest atoms in adjacent rings. It would seem that this property acquires chemical significance when applied to the angular molecule phenanthrene, and remedies a notable failure of Hückel theory in describing the nitration of phenanthridine as discussed by Coldwall and Walls [14]. With the N atom occupying position 10 of the phenanthrene structure, position 1 acquires substantially more π electron charge, according to Hückel perturbation theory than any other atom position [15], and should therefore be most active towards electrophilic attack. The charge at position 3 is also increased, though to a smaller extent; but a refinement [16, 14], which includes modification of coulomb integrals at positions adjacent to the N atom reduces the charge at atom 3. In proposing a theoretical interpretation of ionic attack, account should also be made of the magnitude of the polarizability term $\pi_{r,r}$ which at position 3 is small. In the refined Hückel treatment, position 1 retains the greatest π electron charge and a large polarizability term, and is still, therefore, predicted as the position most active towards electrophilic attack. Experiment shows, on the other hand, that the 1-nitro derivative, along with the 2- and 3-nitro derivatives are all minor constituents of the nitration reaction, and that the 4- and 5-derivatives are mainly obtained, with the 7-derivative in moderate yield. The predictions of Hückel theory are therefore not fulfilled experimentally, mainly through the very small yield of the 1-nitro derivative [14]. In the s.c.f. treatment atom 1 occupies a position with respect to the N substituent at atom 10, at which the alternation in the sign of the coefficients $\sigma_{r,u}$ breaks down. As a result s.c.f. theory predicts that π electron charge is withdrawn from atom 1, and not increased, as predicted by Hückel theory, by N substitution at position 10. It follows that, according to the s.c.f. treatment, atom position 1 is not favourably predisposed towards electrophilic attack, and the major deficiency of Hückel theory is thereby remedied. The susceptibilities of the remaining positions towards electrophilic attack, as observed experimentally, are also predicted reasonably well by the s.c.f. treatment, with, however, some overemphasis in the case of atom 3. This could be made more realistic by a refinement analogous to that adopted for the Hückel theory, as described above.

A further example of the improvement to be gained in describing chemical properties from the use of s.c.f. perturbation coefficients appears in application to the reactions of phenanthrene itself. Hückel theory predicts the 9, 10 meso positions as the most active, taken either together or individually, on the basis that the charge density is unity at all atom positions, and the self-polarizabilities $\pi_{r,r}$ are largest for $r=9$ and 10 . Experimentally, phenanthrene is hydrogenated, brominated and oxidized by chromic acid to give a 9, 10 disubstituted derivative as predicted by Hückel theory. On the other hand, certain reactions, such as sulphonation and acetylation, which involve ionic attack at a single atom position take place in the side rings at positions 2 and 3, which, according to Hückel

theory should be inactive. In the s.c.f. treatment the spread in the value of the self-polarizability coefficients $\sigma_{r,r}$ ($r = 1, 2, 3, 4, 9$) in phenanthrene is, according to the tables, much smaller than the spread in naphthalene ($r = 1, 2$) and anthracene ($r = 1, 2, 9$) and much less, proportionately, than the spread in the corresponding Hückel $\pi_{r,r}$ coefficients. For example, in the case of phenanthrene a difference of about 1 per cent is found in the calculated values of $\sigma_{r,r}$ for $r = 9, 2$ and 3 and the 9-meso position no longer carries the maximum value. Clearly, differences of this order of magnitude may depend more crucially upon the approximations used in computing individual integrals than upon factors determined by the topology of the molecule. The s.c.f. treatment therefore provides a better description of the observed activities of positions other than the 9, 10 bridge positions. That the small differences in computed polarizabilities should prevent the derivation of a well-defined description of the reactions of phenanthrene, probably reflects a genuine physical situation, that the various atom positions do not differ in their activities towards ionic attack as widely as in other molecules.

To summarize, the theoretical treatment given earlier, shows that the Hückel theory possesses similar analytical properties towards perturbations as those of the s.c.f. theory. The numerical computations of s.c.f. polarizabilities as given in the tables, show on the other hand a correspondence in proportionality with numerical values of Hückel polarizabilities for the different molecules examined. These two facts, taken together, account, in some measure, for the success of Hückel theory in describing chemical properties, such as the reactions of the molecules, and ground state properties such as the dipole moments. Where appreciable numerical differences occur between the two methods, the s.c.f. treatment appears to describe the observed properties more realistically.

Two other features, of a more general character, of the s.c.f. treatment used above, merit consideration. Firstly there exists the fundamental problem associated with the use 'atomic' orbitals ϕ_r for constructing molecular orbitals ψ_j for the variational problem. McWeeny [12] and other authors have pointed out that these orbitals, ϕ_r , are not strictly localized atomic orbitals, but contain a non-localized component due to modification by the orthogonalization procedure introduced by Lowdin [17]. It has been suggested that, for example, the calculation of dipole moments from elements of the \mathbf{P} matrix by a procedure analogous to that used in Hückel theory could, without further analysis produce misleading results. By the same argument, it is reasonable to enquire whether elements of the \mathbf{P} matrix can legitimately be used as criteria for describing the ionic reactions of conjugated molecules, on the assumption that these depend upon the charge distribution in the molecule. The justification is obviously to be found in the success obtained in applying numerical values, as described above. This then immediately raises the issue of whether electrophilic attack, for example, takes place preferentially at atom positions having a large excess of π electron charge, or whether the true criterion is the change in π electron energy due to polarization by the attacking charged reagent, since the charge density terms P_{rr} and self polarizabilities $\sigma_{r,r}$ are the leading terms of the Taylor expansion for this change. Correlation between numerical values of $P_{r,r}$ $\sigma_{r,r}$ and experimental results must be taken to support the latter interpretation.

The second feature concerns the application of digital computers to molecular calculations of this kind. On the Elliott 402 digital computer, the times for first

computing, and then printing, the Hückel eigensolution and **P** matrix for benzene, accurate to about eight decimal places, were about $1\frac{1}{2}$ min each. For naphthalene, the computing time was about 6 min, and the printing time 2 min. With faster machines, having a larger high-speed store, the computing time may easily be reduced by a factor of 10 or more. This clearly means that Hückel calculations by electronic computer are marginally justifiable and should soon be replaced as a standard form of M.O. calculation. The introduction of other methods, whether of the self-consistent field or configuration interaction variety, would benefit from a uniformity of formulation which would include, for example, an agreed procedure for obtaining the required integrals such as that proposed by Parr and Pariser [2]. Otherwise, arbitrariness in techniques could prove a serious impediment in comparing molecular properties as predicted theoretically.

REFERENCES

- [1] POPLE, J. A., 1953, *Trans. Faraday Soc.*, **49**, 1375.
- [2] PARR, R. G., and PARISER, R., 1953, *J. chem. Phys.*, **21**, 466, 767.
- [3] ROOTHAAN, C. C. J., 1951, *Rev. mod. Phys.*, **23**, 69.
- [4] FUKUI, K., YONEZAWA, T., and NAGATA, C., 1957, *J. chem. Phys.*, **26**, 831.
- [5] DEWAR, M. J. S., 1952, *J. Amer. chem. Soc.*, **74**, 3357.
- [6] GREENWOOD, H. H., 1952, *Trans. Faraday Soc.*, **48**, 585.
- [7] DEWAR, M. J. S., 1958, *Steric Effects in Conjugated Systems*, Chemical Society Symposium, p. 46.
- [8] COULSON, C. A., and LONGUET-HIGGINS, H. C., 1947, *Proc. roy. Soc. A*, **191**, 39; **192**, 16; 1948, *Ibid.*, **193**, 447.
- [9] GREENWOOD, H. H., 1952, *J. chem. Phys.*, **20**, 1333.
- [10] POPLE, J. A., and SCHOFIELD, P., 1955, *Proc. roy. Soc. A*, **233**, 233, 241.
- [11] MCWEENY, R., 1956, *Proc. roy. Soc. A*, **235**, 496; 1957, *Ibid.*, **237**, 355.
- [12] MCWEENY, R., and PEACOCK, T. E., 1957, *Proc. phys. Soc. Lond. A*, **70**, 41.
- [13] HARTREE, D. R., 1952, *Numerical Analysis* (Oxford: University Press), p. 192.
- [14] COLDWALL, A. G., and WALLS, L. P., 1952, *J. chem. Soc.*, p. 2156.
- [15] COULSON, C. A., and DAUDEL, R., 1955, *Dictionary of Values of Molecular Constants*, Vol. II.
- [16] COULSON, C. A., and LONGUET-HIGGINS, H. C., 1949, *J. chem. Soc.*, p. 971.
- [17] LÖWDIN, P. O., 1950, *J. chem. Phys.*, **18**, 365.

RESEARCH NOTE

**The nuclear magnetic resonance spectrum of
N-vinyl pyrrolidone**

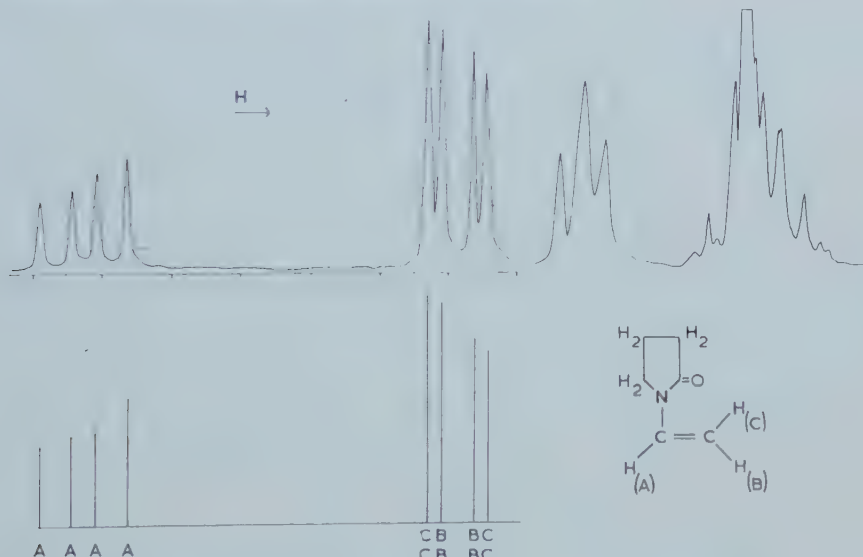
by C. N. BANWELL

University Chemical Laboratories, Lensfield Road, Cambridge

(Received 18 August 1960)

A study of the nuclear magnetic resonance spectra of several substituted ethylenes has shown [1] a linear relationship amongst the three coupling constants J_{trans} , J_{cis} and J_{gem} of these compounds, and between each constant and the electronegativity [2] of the immediate substituent to the vinyl radical when this is one of the first row elements carbon, oxygen or fluorine. Further, the internal chemical shift parameter $\Delta_2 = \delta_A - \frac{1}{2}(\delta_B + \delta_C)$ has been correlated with the resonance contribution [3], σ_R , to the Hammett σ constant of the substituent group.

A substance with a nitrogen-containing substituent, N-vinyl pyrrolidone, has now been examined under the same conditions as the series of reference [1].



Observed and calculated spectra of N-vinyl pyrrolidone at 40 Mc/s.
The graduations on the upper base line are at intervals of 20 c/sec.

The 40 Mc/s spectrum is shown in the figure together with a calculated spectrum based on the following chemical shifts and coupling constants:

$$\begin{aligned}\delta_A &= -1.63 \pm 0.05 \dagger \text{ p.p.m.} & J_{BC}^{gem} &= 0.0 \pm 0.2 \text{ c/sec}, \\ \delta_B &= +1.02 \pm 0.05 \dagger \text{ p.p.m.} & J_{AC}^{trans} \ddagger &= 15.9 \pm 0.2 \text{ c/sec}, \\ \delta_C &= +1.07 \pm 0.05 \dagger \text{ p.p.m.} & J_{AB}^{cis} &= \pm 9.2 \pm 0.2 \text{ c/sec}.\end{aligned}$$

† With reference to the resonance of ethylene as zero.

‡ Assumed positive.

The relative signs of J^{cis} and J^{trans} are indeterminate owing to the coincidence of pairs of B and C lines, and calculation shows that the ambiguity could not be resolved by studying the spectrum at lower applied fields. However, other experimental [1] and theoretical [4] studies point strongly to J^{cis} and J^{trans} being of the same sign. In particular this choice of relative sign places the data in good agreement with figures 8 and 9 of reference [1]. Thus, since the electronegativity of nitrogen is 3.05 [2] and the atom lies in the first row of the periodic table, figure 9 shows that J_{AC}^{trans} should be approximately +15.8 c/sec (observed 15.9 c/sec). Figure 8 indicates that a J_{AC}^{trans} of 15.9 c/sec should be associated with $J_{AB}^{cis} \approx 8.9$ and $J_{BC}^{gem} \approx -0.2$ c/sec, which are close to the observed values.

The two published values of σ_R for nitrogen-containing groups [3] differ widely. Thus for the unsubstituted —NH₂ radical, σ_R is reported to be -0.76, while for the charged —N⁺(CH₃)₃ group $\sigma_R \approx 0.0$. Figure 10 of reference [1] shows that the observed value of $\Delta_2 = -2.68$ p.p.m. for N-vinyl pyrrolidone is consistent with $\sigma_R = -0.55$. It is satisfactory that this falls between the two extremes quoted above and particularly that it lies nearer to the value for the uncharged group since it is likely that the availability of the lone pair electrons is similar in the —NH₂ and ring structures.

REFERENCES

- [1] BANWELL, C. N., and SHEPPARD, N., 1960, *Mol. Phys.*, **3**, 351.
- [2] HUGGINS, M. L., 1953, *J. Amer. chem. Soc.*, **75**, 4123.
- [3] TAFT, R. W., 1957, *J. Amer. chem. Soc.*, **79**, 1045.
- [4] KARPLUS, M., 1959, *J. chem. Phys.*, **30**, 11.

A semi-empirical theory of the electronic structure of ethylene with particular reference to the ionization potential†

by Y. I'HAYA

Department of Chemistry, Carnegie Institute of Technology,
Pittsburgh, Pennsylvania‡

(Received 9 June 1960)

The electronic structure of the ethylene molecule is scrutinized within the framework of the semi-empirical pi-electron theory. The lower electronic energy levels, twisting frequency, ionization potential and electron affinity are calculated without treating the so-called β parameter as empirical. A new approach for calculating the ionization potential is presented, in which an allowance is made for the change in the effective nuclear charge accompanying the actual ionization. The ionization potential is computed to be 10.757 ev, the observed value being 10.62 ev.

1. INTRODUCTION

Since the semi-empirical theory of electronic spectra and electronic structure of unsaturated molecules was presented by Pariser and Parr [1], the theoretical calculation of the vertical ionization potentials of such molecules within the framework of the pi-electron theory has remained a difficult question. There have been several papers which have treated, independently of electronic spectra, ionization potential increments of unsaturated molecules relative to a reference molecule [2], but there remains the question: can parameters obtained from the theory of electronic spectra be used to predict ionization potentials? Parr and Pariser [3], after they investigated the electronic structure of ethylene, showed that the ionization potential computed with the parameters which are optimum for the calculation of the electronic energy levels comes out much higher than the observed value.

The essential feature is that in the calculation of ionization potentials the core integrals over atomic orbitals of the type

$$\int \chi_a(1) H_{\text{core}}(1) \chi_a(1) dv(1)$$

no longer cancel out, while they cancel out in the formulation of the electronic spectra. Then the question is: is it correct to use the same core parameters for the calculations of the energies of both ground and ionized states? Put another way: is it correct to use fixed values of the effective nuclear charge for both states?

Recently, R. D. Brown and co-workers [4] presented a new approach for determining the molecular integrals, in which an allowance is made for the change in the effective nuclear charge of a nucleus accompanying the variation of the electron density around the nucleus. The present communication is intended

† Work supported by a grant from the Petroleum Research Fund of the American Chemical Society.

‡ Permanent address: Department of Chemistry, Tokyo University of Education, Tokyo, Japan.

to apply a similar idea to the calculation of the electronic structure of ethylene, and particularly to remove some of the uncertainties in the problem of the ionization potential.

2. THE ELECTRONIC SPECTRUM

Following Parr and Pariser [3], the starting anti-symmetrized wave functions of ethylene are:

$$\left. \begin{aligned} \Phi_1 &= (\phi_1 \bar{\phi}_1), \quad \Phi_2 = (\phi_2 \bar{\phi}_2), \quad \Phi_V = 2^{-1/2}[(\phi_1 \bar{\phi}_2) + (\phi_2 \bar{\phi}_1)] \text{ for singlet} \\ \text{and} \end{aligned} \right\} \quad (1)$$

$$\Phi_T = 2^{-1/2}[(\phi_1 \bar{\phi}_2) - (\phi_2 \bar{\phi}_1)] \quad \text{for triplet.}$$

Here $(\phi_1 \bar{\phi}_2)$, etc., stand for the Slater determinants constructed from molecular orbitals

$$\phi_1 = (2 + 2S)^{-1/2}(\chi_a + \chi_b), \quad \phi_2 = (2 - 2S)^{-1/2}(\chi_a - \chi_b), \quad (2)$$

with normalized Slater atomic $2p\pi$ orbitals χ_a and χ_b and overlap integral S .

Using the Hamiltonian operator,

$$H = H_{\text{core}}(1) + H_{\text{core}}(2) + \frac{e^2}{r_{12}} \quad (3)$$

the matrix elements of H between the various Φ functions are easily obtained in terms of integrals over molecular orbitals. As Moser, and Parr and Pariser have already suggested [3, 5] the following Mulliken-type approximation formulas [6] are convenient at the stage of expansion of the integrals over molecular orbitals into integrals over atomic orbitals:

$$(aa|ab) = \frac{1}{2}S [(aa|aa)_t + (aa|bb)], \quad (4)$$

$$(ab|ab) = \frac{1}{2}S^2 [(aa|aa)_t + (aa|bb)]. \quad (5)$$

Here the $(pq|rs)$ are the electronic repulsion integrals over atomic orbitals p, q, r , and s

$$(pq|rs) = \int \int \bar{\chi}_p(1) \bar{\chi}_r(2) \frac{e^2}{r_{12}} \chi_q(1) \chi_s(2) dv(1) dv(2) \quad (6)$$

and specifically $(aa|aa)_t$ stands for the one-centre repulsion integral which should be evaluated *theoretically*. This corresponds to the procedure in which the atoms-in-molecules correction for $(aa|aa)$ should be applied *before* the Mulliken-type approximations are made [3]†.

The complete formulas for the electronic energy levels relative to H_{11} are then obtained as follows: (cf. ref. [4])

$$\left. \begin{aligned} E_N &= H_{11} - (1 - S^2)^{-1}[2\beta + 2S\delta + [4(\beta + S\delta)^2 + K^2]^{1/2}], \\ E_V &= H_{11} - (1 - S^2)^{-1}[2\beta + 2S(1 - S)\delta - K], \\ E_T &= H_{11} - (1 - S^2)^{-1}[2\beta + 2S(1 - S)\delta + K], \\ E_Z &= H_{11} - (1 - S^2)^{-1}[2\beta + 2S\delta - [4(\beta + S\delta)^2 + K^2]^{1/2}]. \end{aligned} \right\} \quad (7)$$

Here

$$\left. \begin{aligned} H_{11} &= 2\alpha + 2\beta/(1 + S) + J + S(1 - S)(2 + S)\delta/(1 + S), \\ J &= \frac{1}{2}[(aa|aa) + (aa|bb)], \quad K = \frac{1}{2}[(aa|aa) - (aa|bb)], \\ \delta &= \frac{1}{2(1 - S^2)} [(aa|aa)_t - (aa|aa)], \end{aligned} \right\} \quad (8)$$

† If one applies the atoms-in-molecules correction *after* the Mulliken approximations are made, one obtains less satisfactory results (e.g. 8.47 ev for $N-V$ transition and 11.97 ev for ionization potential). Just which method is preferable on fundamental grounds is not clear.

α is a core integral over atomic orbitals

$$\alpha = \int \chi_a(1) H_{\text{core}}(1) \chi_a(1) dv(1) \quad (9)$$

and β is defined by [6]

$$\beta + S\alpha = \int \chi_a(1) H_{\text{core}}(1) \chi_b(1) dv(1). \quad (10)$$

The core Hamiltonian of equation (3) may be written as

$$H_{\text{core}}(1) = T(1) + U_a(1) + U_b(1) + \sum_H U_H(1) \quad (11)$$

where U_a and U_b are the potential due to the carbon atom a and b which are charged in the core, and U_H is a potential due to the attached hydrogen atom which is neutral in the core. The core integrals α and β of equations (9) and (10), then take out the following forms:

$$\alpha = -I_{2p} - (aa|bb) - (b:aa)_t - 2(H_1:aa)_t - 2(H_2:aa)_t, \quad (12)$$

$$\beta = -(a:ab)_t + S(a:bb)_t - (S/2)[(aa|aa)_t - (aa|bb)]. \quad (13)$$

Here I_{2p} is an appropriate atomic valence state ionization potential, and $(b:aa)_t$ and $(H_i:aa)_t$ are Coulomb penetration integrals between atomic orbital χ_a and neutral atoms a and H_i (H_1, H_2 denotes the hydrogen atoms attached to atom a and atom b , respectively); that is

$$(q:pp) = - \int Uq(1) \chi_p(1) \chi_p(1) dv(1). \quad (14)$$

In equation (13) the penetration integrals of the type $(H_i:pq)$ cancel out because we assume the following Mulliken-type approximation

$$(H_i:pq) = (Spq/2)[(H_i:pp) + (H_i:qq)]. \quad (15)$$

All penetration integrals are computed non-empirically using Slater orbitals with $Z=3.25$. The empirical value 10.842 ev for integral $(aa|aa)$ which was determined by Parks and Parr [7] from the atomic valence state consideration of carbon is used, while $(aa|bb)$ is determined in a way that it fits a parabola to two theoretical values calculated for 2.8 Å and 3.5 Å internuclear separations using Slater orbitals with effective charge $Z=3.25$ and one empirical value at $r=0$. The value 7.657 ev for $r=1.353$ Å is obtained by use of the empirical equation

$$(aa|bb) = 10.842 - 2.5924r + 0.1761r^2. \quad (16)$$

These values give $J=9.250$ and $K=1.593$ ev. The theoretical $(aa|aa)_t$ for Slater $2p\pi$ carbon atomic orbitals with $Z=3.25$ is 17.302 ev. This gives $\delta=3.498$ ev. Using these integrals and theoretical values for the penetration integrals, we get $\beta=-3.043$ ev.

The energy levels obtained from equation (7) are then as follows:

$$\left. \begin{aligned} E_N &= H_{11} - 0.311 \text{ ev}, \\ E_V - E_N &= 7.104 \text{ ev}, \\ E_T - E_N &= 3.680 \text{ ev}, \\ E_Z - E_N &= 9.736 \text{ ev}. \end{aligned} \right\} \quad (17)$$

Since the experimental value of the $N-V$ transition is probably 7.6 ev [8], the agreement is fairly good. The location of the lowest triplet state (E_T) has not

been definitely established. Several authors have assigned its location in the range 3.1 to 5.6 ev. The problem of the *N-T* transition will be discussed later.

3. THE TWISTING FREQUENCY OF ETHYLENE

The variation in the total energy, E_N , of the ground state when the CH_2 groups are little twisted one another will yield the twisting frequency. According to Parr *et al.* [3, 9], the twisting force constant, k , and the twisting frequency, ω , of the ground state ethylene are defined by

$$\left. \begin{aligned} k &= (\partial^2 E_N / \partial \theta^2)_{\theta=0} && \text{(in ev)} \\ \omega &= 560k^{1/2} && \text{(in cm}^{-1}\text{)} \end{aligned} \right\} \quad (18)$$

where θ is an angle between the major axis of the atomic orbital χ_a and χ_b .

In the planar configuration, the approximation $\Phi_N \approx \Phi_1$ is not so serious in the neighbourhood of the equilibrium position, because of the small contribution of Φ_2 to Φ_N shown above. Then the total energy will be the pi-electron energy H_{11} of equation (8) plus a core energy which is $(aa|bb)$ plus an angular independent term. The dependences of the basic quantities β and $(aa|bb)$ on the angle θ are given by

$$\left. \begin{aligned} \beta &= \beta_0 \cos \theta, & S &= S_0 \cos \theta, \\ (aa|bb) &= \cos^2 \theta (aa|bb)_0 + \sin^2 \theta (aa|bb)_{\pi/2}, \end{aligned} \right\} \quad (19)$$

where the subscripts 0 and $\pi/2$ denote angles between χ_a and χ_b . α depends on θ only through $(aa|bb)$ as can be seen from equation (12). The total energy then becomes

$$\begin{aligned} E_N = & 2\beta_0 \cos \theta / (1 + S_0 \cos \theta) - \frac{1}{2} \cos^2 \theta (aa|bb)_0 - \frac{1}{2} \sin^2 \theta (aa|bb)_{\pi/2} \\ & + S_0 \cos \theta (2 + S_0 \cos \theta) [(aa|aa)_t - (aa|aa)] / (1 + S_0 \cos \theta)^2 \\ & + \text{angular independent terms.} \end{aligned} \quad (20)$$

Thus equation (18) yields (omitting the subscripts in β_0 and S_0)

$$k = -2\beta/(1+S)^2 + [(aa|bb)_0 - (aa|bb)_{\pi/2}] - S[(aa|aa)_t - (aa|aa)]/(1+S)^3. \quad (21)$$

Using $(aa|bb)_{\pi/2} = 9.841$ for $r=0$, obtained from the value of Slater-Condon parameter [10], the value of $(aa|bb)_{\pi/2}$ is calculated to be 7.448 ev in the way described in the foregoing.

With this and the numerical values which are used in § 2, we get

$$\left. \begin{aligned} k &= 3.17 \text{ ev,} \\ \omega &= 998 \text{ cm}^{-1}, \end{aligned} \right\} \quad (22)$$

which well compares with the corresponding experimental values: $k = 3.36$ ev and $\omega = 1027 \text{ cm}^{-1}$ [11]. It should be added here that in the above calculation the effect of hyperconjugation, which is supposed to favour twisted ethylene, is not taken into consideration.

4. THE IONIZATION POTENTIAL AND ELECTRON AFFINITY

A method for calculating the ionization potential of ethylene will now be described. The total pi-electron energy of the ground state ethylene is

$$E(\text{C}_2\text{H}_4) = 2 \left(\alpha + \frac{\beta}{1+S} \right) + J + S(1-S)(2+S)\delta/(1+S) + \Delta E_N \quad (23)$$

where ΔE_N stands for $E_N - H_{11}$ of equation (7). For the C_2H_4^+ ion, on the other hand, the effective nuclear charge Z of each carbon atom may be presumed to be different from that of the ground state of ethylene. As will be discussed

below, both α and β (and also electron repulsion and penetration integrals) are functions of Z , so that use of the same α and β for both neutral and ionized molecules is wrong. Therefore we should write

$$E(C_2H_4^+) = \alpha^* + \beta^*/(1 + S^*) \quad (24)$$

where α^* and β^* have the same expressions of equation (12) and (13) respectively, but with different Z values. The formula for the first ionization potential then becomes

$$I = -2\alpha + \alpha^* - 2\beta/(1 + S) + \beta^*/(1 + S^*) - J - S(1 - S)(2 + S)\delta/(1 + S) + \Delta E_N. \quad (25)$$

The effective charge Z^* for a carbon atom in the ionized ethylene molecule is assumed to have the value 3.425, which is the mean of the Slater values for C and C^- [4]. Assuming that this increase in effective charge accompanies the actual ionization, we will get slightly different values of Coulomb integrals for the two states. To calculate the atomic valence state ionization potential I_{2p}^* in $C_2H_4^+$, the following empirical formula may be obtained from the values of the valence state ionization potentials of the isoelectronic series $C(Z=3.25, I=11.424 \text{ ev})$, $N^+(Z=4.25, I=28.885 \text{ ev})$ and $O^{2+}(Z=5.25, I=53.494 \text{ ev})$ [12]:

$$I_{2p} = 3.604Z^2 - 9.599Z + 4.5535. \quad (26)$$

This formula gives $I_{2p}^* = 13.954 \text{ ev}$ for $Z = 3.425$. All penetration integrals including hydrogen penetrations are evaluated theoretically using Slater orbitals for Z values of 3.250 and 3.425 (the same $a-b$ distance is assumed), and are listed in the table together with the electronic repulsion integrals. These values yield

Integral	$Z=3.250$	$Z=3.425$	$Z=3.075$
$(aa \mid aa)_t$	17.302	18.234	16.371
$(aa \mid aa)$	10.842 ^a	11.426 ^b	10.258 ^d
$(aa \mid bb)$	7.657 ^a	7.949 ^c	7.386 ^c
$(b: aa)_t$	0.744	0.600	0.936
$(H_1: aa)_t$	0.627	0.646	0.610
$(H_2: aa)_t$	0.020	0.022	0.020
S	0.264	0.235	0.298
α	-21.119	-23.839	-18.697
β	-3.043	-2.850	-3.283

a. Empirical value (see text). b. $10.842 \times \frac{3.425}{3.250}$. c. Evaluated in the same way as

shown in text, but with corresponding values of $(aa|aa)$. d. $10.842 \times \frac{3.075}{3.250}$.

Molecular integrals in ethylene (ev).

$\alpha = -21.119$, $\alpha^* = -23.829$ and $\beta^* = -2.850 \text{ ev}$. It should be noted that the value -21.119 ev is close to the value -20.972 ev obtained by Parks from a more complete consideration of the atomic valence states of the carbon atom.

The first ionization potential of ethylene can then be calculated from equation (25), which gives $I = 10.750 \text{ ev}$. This is a very satisfactory result indeed, compared with the observed value 10.62 ev [13] or 10.52 ev [14].

For comparison, if one assumes $\alpha^* = \alpha$ and $\beta^* = \beta$, as is customarily done, (that is $Z^* = Z$), equation (25) gives $I = 13.370$ ev. Further, if the Mulliken-type approximations

$$\chi_a(1)\chi_b(1) = (S_{ab}/2)[(\chi_a(1)\chi_a(1) + \chi_b(1)\chi_b(1))] \quad (27)$$

are used systematically before the atoms-in-molecules corrections are applied (this means $\delta = 0$ in equation (25)), one gets $I = 14.497$ ev with $E_V - E_N = 8.474$ and $E_T - E_N = 5.050$ ev.

A similar idea can be applied to the calculation of the electron affinity of ethylene. One can write the pi-electron energy of the $C_2H_4^-$ ion, in which there are two electrons in ϕ_1 , one in ϕ_2 of equation (2),

$$E(C_2H_4^-) = 3\alpha' \times \beta'(1 - 3S')/(1 - S'^2) + 3J' - K'/(1 - S'^2) \\ + S'(2 - 3S' - 3S'^2)\delta'/(1 + S'). \quad (28)$$

Here the various quantities are given by expressions like equations (8), (12) and (13), but again should be calculated with different effective nuclear charges Z' . The formula for the electron affinity comes out simply as the difference of equations (28) and (23):

$$A = 2\alpha - 3\alpha' + 2\beta/(1 + S) - (1 - 3S')\beta'/(1 - S'^2) + J - 3J' \\ + S(1 - S)(2 + S)\delta/(1 + S) - S'(1 - S')(2 + S')\delta'/(1 + S') \\ + 2S'^2\delta' + K'/(1 - S'^2) - \Delta_N. \quad (29)$$

After the manner of treating the ionization potential, the effective charge Z' for carbon atom in $C_2H_4^-$ ion is assumed to be 3.075, which corresponds to the mean of the Slater values for C^0 and C^- . The necessary integrals with $Z' = 3.075$ are evaluated by the same procedure as before, and are listed in the last column of the table. With these numerical values, equation (29) yields $A = -5.982$ ev.

5. DISCUSSION

It has been shown that the allowance made for the change of the effective nuclear charge accompanying the ionization can give a good account of both spectrum and ionization potential of ethylene, even in the form of the pi-electron theory. Without such allowance, Parr and Pariser [3] demonstrated that $I = 10.90$ ev is obtained if no atoms-in-molecules correction is made (at the sacrifice of the energy levels). This fact seems to suggest another fundamental problem but deviates from the present discussion.

Among several questions that still should be asked, the following three must be mentioned. How about the singlet-triplet split? How about the numerical value obtained for the electron affinity? Do or do not the 'sigma' electrons play significant roles?

Let us determine β , empirically this time, from molecular spectroscopic data, although its theoretical value was shown above to give quite satisfactory results. Assuming the 7.6 ev band of ethylene to be the $N-V$ transition, β_e must have the value -3.283 ev from equation (7), which compares favourably with $\beta_t = -3.043$ ev. Using this β_e , and values of β_e^* and β_e' reduced to theoretical value to 'empirical size' by a factor of β_t/β_e , similar calculations give:

$$\left. \begin{array}{l} E_N = H_{11} - 0.28 \text{ ev}, \quad k = 3.47 \text{ ev}, \\ (E_V - E_N = 7.60) \quad \omega = 1044 \text{ cm}^{-1}, \\ E_T - E_N = 4.18 \quad I = 10.76 \text{ ev}, \\ E_Z - E_N = 10.76 \quad A = -6.00 \text{ ev}. \end{array} \right\} \quad (30)$$

These are again good results, but no change in the singlet-triplet split is obtained.

The reason is that the theoretical expression for $(E_V - E_T)$ does not depend on β , and is exactly equal to $2K/(1 - S^2)$ as seen in equation (7).

Another treatment is as follows. Assuming Potts' [15] assignment of $(E_V - E_T) = 1.2$ to be correct, K can be determined to be 0.558 ev with $\beta = -3.918$ ev and $J = 10.284$ ev. In this case, one gets:

$$\left. \begin{array}{ll} E_N = H_{11} - 0.03 \text{ ev}, & k = 4.27 \text{ ev}, \\ (E_V - E_N) = 7.60 & \omega = 1584 \text{ cm}^{-1} \\ (E_T - E_N) = 6.40 & I = 12.14 \text{ ev}, \\ E_Z - E_N = 12.93 & A = -8.04 \text{ ev}. \end{array} \right\} \quad (31)$$

This is much less satisfactory than before.

In view of the fact that experimentally no conclusive work has yet been done in this connection, we would say tentatively that the calculations in the preceding sections and the empirical calculation (30) are both about right, so the location of the lowest triplet state should be around 4 ev. It might be added here that slightly different Z values would be expected for V and T states if the variational treatment could be performed, and these might give a different picture of the $V-T$ separation.

Concerning the electron affinity, unfortunately, the electron affinity of ethylene is experimentally unknown, while it may well be negative. The following facts support the method of calculation in § 4. (a) Neglecting the change in Z value from normal ethylene to ethylene negative ion, one obtains $A = +0.373$ ev. This value seems highly improbable. (b) The high negative value obtained suggests that ethylene in general has little tendency to function as an acceptor in the stage of both molecular association and chemical reaction. This agrees with experimental indications.

As for the sigma electrons, a more elaborate computation including sigma electrons has been almost finished and will be presented elsewhere. In the case of homonuclear unsaturated molecules like ethylene, it appears that: the effects of sigma electrons are not so great.

The author is indebted to Professor R. G. Parr for help with the manuscript.

REFERENCES

- [1] PARISER, R., and PARR, R. G., 1953, *J. chem. Phys.*, **21**, 466, 767.
- [2] HALL, G. G., 1952, *Proc. roy. Soc. A*, **213**, 102; POPLE, J. A., 1953, *Trans. Faraday Soc.*, **49**, 1375; HUSH, N. S., and POPLE, J. A., 1955, *Trans. Faraday Soc.*, **51**, 600; MATSEN, F. A., 1956, *J. chem. Phys.*, **24**, 602; HEDGES, R. M., and MATSEN, F. A., 1958, *J. chem. Phys.*, **28**, 950.
- [3] PARR, R. G., and PARISER, R., 1955, *J. chem. Phys.*, **23**, 711.
- [4] BROWN, R. D., and PENFOLD, A., 1957, *Trans. Faraday Soc.*, **53**, 397; BROWN, R. D., and HEFFERNAN, M. L., 1958, *Trans. Faraday Soc.*, **54**, 757.
- [5] MOSER, C. M., 1953, *J. chem. Phys.*, **21**, 2098.
- [6] MULLIKEN, R. S., 1949, *J. chem. Phys.*, **46**, 497.
- [7] PARKS, J. M., 1956, Ph.D. Thesis, Carnegie Institute of Technology; PARKS, J. M., and PARR, R. G., 1960, *J. chem. Phys.*, **32**, 1657.
- [8] WILKINSON, P. G., and JOHNSTON, J. L., 1950, *J. chem. Phys.*, **18**, 190.
- [9] PARR, R. G., and CRAWFORD, B. L., Jr., 1948, *J. chem. Phys.*, **16**, 526.
- [10] SKINNER, H. A., and PRITCHARD, H. O., 1953, *Trans. Faraday Soc.*, **49**, 1254.
- [11] ARNETT, R. L., and CRAWFORD, B. L., Jr., 1950, *J. chem. Phys.*, **18**, 118.
- [12] MOORE, C. E., Atomic Energy Levels, Nat. Bur. Stand., 1949–1952, Circular 467.
- [13] HONIG, R. E., 1948, *J. chem. Phys.*, **16**, 105.
- [14] WATANABE, K., 1954, *J. chem. Phys.*, **22**, 1564.
- [15] POTTS, W., 1953, Ph.D. Thesis, University of Chicago.

A further study on the electronic structure and spectrum of ethylene†

by Y. I'HAYA

Department of Chemistry, Carnegie Institute of Technology,
Pittsburgh, Pennsylvania‡

(Received 14 July 1960)

Calculations on the lower electronic states, ionization potential and electron affinity of ethylene are carried out by a semi-empirical ASMO method including configuration interaction. The carbon–carbon sigma bonding electrons are explicitly included. One-centre quantities for ethylene, ethylene negative ion and ethylene positive ion are evaluated from atomic valence-state energies, taking account of changes in effective nuclear charges of the corresponding states. Two-centre electronic repulsion integrals are determined by interpolation between theoretical values for distant nuclear separations and one-centre repulsion integrals obtained; two-centre core integrals are computed purely theoretically. Good agreement between calculated and observed values is obtained. Although preferential stabilization of the ion cannot be expected from sigma-pi configuration interaction, it is shown that the reorganization of the electronic sub-structure of the atom upon ionization plays a significant role.

1. INTRODUCTION

In the previous communication [1], it was shown that a theoretically calculated two-centre core integral β gives a reasonable picture of the electronic structure of ethylene even within the framework of the pi-electron theory. Furthermore, it was emphasized that allowance for the change in the effective nuclear charge of a nucleus accompanying the variation of the electron density around the nucleus plays an important part in determining the ionization potential. In this paper it is intended to examine how to take account of sigma electrons through a recipe which takes into account the sigma-pi configuration interaction.

For this purpose the ASMO-CI (antisymmetric molecular orbitals with configuration interaction) method modified to include the concept of atoms-in-molecules is useful. Among several papers which treat sigma-pi interaction in ethylene, Moser's purely theoretical calculation [2] should be noted. The results obtained were not very satisfactory; specifically the electronic transitions do not come out well, as is usual with the non-empirical ASMO method. This suggests the desirability of a semi-empirical calculation.

The problem of whether the pi- and sigma-electron pairs can be separately treated is a difficult question. If they could be separated, one could use the method of separated electron pairs presented by Parks and Parr [3]. This method gave successful results for the electronic structure of formaldehyde

† Work supported by a grant from the Petroleum Research Fund of the American Chemical Society to Carnegie Institute of Technology.

‡ Permanent address: Department of Chemistry, Faculty of Science, Tokyo University of Education, Tokyo, Japan.

[4], but in it sigma-pi interchange is ignored. In the present work similar procedures are employed, but sigma-pi interchange is included.

With the use of appropriate forms of the Hamiltonian operators for sigma and pi electrons and the corresponding core integrals, and the use of Mulliken-type approximations, the electronic energies of all configurational states may be expressed in terms of one- and two-centre core integrals and one-and two-centre electronic repulsion integrals. These features of the calculation are described in §2. Section 3 contains a method of obtaining one-centre integrals from complete consideration of atomic valence states, and §4 gives a recipe for calculating two-centre quantities. Results are given in §5. Comparison with previous work is also made in that section, and general conclusions are also stated.

2. ASMO-CI FORMULATION OF THE FOUR ELECTRON TREATMENT OF ETHYLENE

The procedure which will be described below is of the ASMO-CI type, and in it we explicitly consider no more than four electrons. These are carbon-carbon sigma and pi bonding electrons, the rest being relegated to a 'core' of charge +4 which is assumed to remain unchanged during all the excitations and even ionizations.

The appropriate molecular orbitals, in order of increasing energy, are

$$\left. \begin{array}{l} \chi_0 = (2+2S_o)^{-1/2}(a_o + b_o), \quad a_{1g}, \\ \chi_1 = (2+2S_\pi)^{-1/2}(a_\pi + b_\pi), \quad b_{3g}, \\ \chi_2 = (2-2S_\pi)^{-1/2}(a_\pi - b_\pi), \quad b_{2u}, \\ \chi_3 = (2-2S_o)^{-1/2}(a_o - b_o), \quad b_{1u}, \end{array} \right\} \quad (1)$$

with $a_o = (1/\sqrt{3})(a_s + \sqrt{2}a_z)$, and a like expression for b_o (sp^2 hybridization is assumed). Here a_s , a_z and a_π denote the $2s$, $2p_z$ and $2p_\pi$ atomic orbitals on atom a respectively, and S_i overlap integrals. The precise form of the atomic orbitals is not specified here—this provides a degree of freedom which is not commonly recognized.

The ground state of ethylene has ${}^1A_{1g}$ symmetry, to which the following eight (antisymmetrized) wave functions belong, provided that up to two-electron jump states are considered:

$$\left. \begin{array}{l} \Phi_1^N = (0\bar{0}1\bar{1}), \quad \Phi_2^N = (0\bar{0}2\bar{2}), \quad \Phi_3^N = (1\bar{1}2\bar{2}), \\ \Phi_4^N = \frac{1}{2}[(0\bar{1}2\bar{3}) + (1\bar{0}3\bar{2}) + (0\bar{2}1\bar{3}) + (2\bar{0}3\bar{1})], \\ \Phi_5^N = \frac{1}{2}[(0\bar{1}2\bar{3}) + (1\bar{0}2\bar{3}) + (0\bar{1}3\bar{2}) + (1\bar{0}3\bar{2})], \\ \Phi_6^N = (0\bar{0}3\bar{3}), \quad \Phi_7^N = (1\bar{1}3\bar{3}), \quad \Phi_8^N = (2\bar{2}3\bar{3}). \end{array} \right\} \quad (3)$$

Here $(0\bar{0}1\bar{1})$, etc., stand for Slater determinants constructed from the molecular orbitals of equation (1) (0 denotes χ_0 , and so on). On the other hand, there are four wave functions for the singlet and triplet states belonging to B_{1u} :

$$\left. \begin{array}{l} \Phi_1^V, T = \frac{1}{\sqrt{2}} [(0\bar{0}1\bar{2}) \pm (0\bar{0}2\bar{1})], \\ \Phi_2^V, T = \frac{1}{\sqrt{2}} [(2\bar{2}0\bar{3}) \pm (2\bar{2}3\bar{0})], \\ \Phi_3^V, T = \frac{1}{\sqrt{2}} [(1\bar{1}0\bar{3}) \pm (1\bar{1}3\bar{0})], \\ \Phi_4^V, T = \frac{1}{\sqrt{2}} [(3\bar{3}1\bar{2}) \pm (3\bar{3}2\bar{1})], \end{array} \right\} \quad (4)$$

where V (singlet) takes an upper sign and T (triplet) a lower sign. In addition to these, there are four configurations each for ${}^1, {}^3B_{2u}$ and ${}^1, {}^3B_{3g}$ states and three configurations for ${}^3A_{1g}$ states, which are not considered here.

To calculate the ionization potential and electron affinity, wave functions for the ground states of $C_2H_4^+$ and $C_2H_4^-$ ions are needed. For the former (${}^2B_{3u}$), there contribute five configurations.

$$\left. \begin{aligned} \Phi_1^I &= (0\bar{0}1), \quad \Phi_2^I = (2\bar{2}1), \quad \Phi_3^I = (3\bar{3}1), \\ \Phi_4^I &= \frac{1}{\sqrt{2}} [(0\bar{3}2) + (3\bar{0}2)], \\ \Phi_5^I &= \frac{1}{\sqrt{6}} [2(0\bar{2}3) + (0\bar{3}2) - (3\bar{0}2)]. \end{aligned} \right\} \quad (5)$$

For the latter (${}^2B_{2g}$) five configurations enter:

$$\left. \begin{aligned} \Phi_1^A &= (0\bar{0}1\bar{1}2), \quad \Phi_2^A = (0\bar{0}3\bar{3}2), \quad \Phi_3^A = (1\bar{1}3\bar{3}2), \\ \Phi_4^A &= \frac{1}{\sqrt{2}} [(2\bar{2}0\bar{3}1) + (2\bar{2}3\bar{0}1)], \\ \Phi_5^A &= \frac{1}{\sqrt{6}} [2(2\bar{2}0\bar{1}3) + (2\bar{2}0\bar{3}1) - (2\bar{2}3\bar{0}1)]. \end{aligned} \right\} \quad (6)$$

Final wave functions are expressed as

$$\Psi_i = \sum_j A_{ij} \Phi_j. \quad (7)$$

The Hamiltonian operator for the whole system may be written in the form

$$H = \sum_i H_{\text{core}} + 4(\zeta) + \frac{1}{2} \sum_{\zeta\eta} (e^2/r_{\zeta\eta}). \quad (8)$$

The matrix elements of H between the various Φ functions are easily obtained in terms of integrals over molecular orbitals [5]. The following Mulliken-type approximation formulas [6] for both sigma and pi orbitals are convenient at the stage of expansion of the integrals over molecular orbitals into integrals over atomic orbitals:

$$\left. \begin{aligned} (pp|pq) &= \frac{1}{2} S[(pp|pp) + (pp|qq)], \\ (pq|pq) &= \frac{1}{2} S^2[(pp|pp) + (pp|qq)], \end{aligned} \right\} \quad (9)$$

where

$$(pq|rs) = \int \int p^*(1) r^*(2) (e^2/r_{12}) q(1) s(2) dv(1) dv(2). \quad (10)$$

To evaluate core integrals of $H_{\text{core}} + 4$, we use

$$H_{\text{core}} + 4(\zeta) = H_{\pi-\text{core}} + 2(\zeta) - \mathbf{g}_\sigma(\zeta) \quad \text{for the pi electrons} \quad (11)$$

and

$$H_{\text{core}} + 4(\zeta) = H_{\sigma-\text{core}} + 2(\zeta) - \mathbf{g}_\pi(\zeta) \quad \text{for the sigma electrons.} \quad (12)$$

Here \mathbf{g} are Coulomb-exchange operators which take care of mutual interaction of the sigma and pi electrons; namely

$$\mathbf{g}_\sigma(\zeta) = \sum_{i=a,b} [\mathbf{j}_{i\sigma}(\zeta) - \frac{1}{2} \mathbf{k}_{i\sigma}(\zeta)] \quad (13)$$

$$\mathbf{g}_\pi(\zeta) = \sum_{i=a,b} [\mathbf{j}_{i\pi}(\zeta) - \frac{1}{2} \mathbf{k}_{i\pi}(\zeta)] \quad (14)$$

are, for example, defined by

$$\mathbf{j}_{i\sigma}(1)[a_\pi(1)] = \int i_\sigma^*(2) i_\sigma(2) (e^2/r_{12}) a_\pi(1) dv(2) \quad (15)$$

$$\mathbf{k}_{i\sigma}(1)[a_\pi(1)] = \int i_\sigma^*(2) a_\pi(2) (e^2/r_{12}) i_\sigma(1) dv(2). \quad (16)$$

Equations (11) and (12) may be regarded as defining $H_{\sigma-\text{core}}^{+2}$ and $H_{\sigma-\text{core}}^{-2}$.

The complete formulas for the electronic energy levels are then expressed in terms of the following quantities;

$$\alpha_\sigma = \int a_\sigma(1) H_{\sigma-\text{core}}^{+2}(1) a_\sigma(1) dv(1), \quad (17)$$

$$\beta_\sigma - S_\sigma \alpha_\sigma = \int a_\sigma(1) H_{\sigma-\text{core}}^{-2}(1) b_\sigma(1) dv(1), \quad (18)$$

$$\left. \begin{array}{l} J_\sigma \\ K_\sigma \end{array} \right\} = \frac{1}{2} [(a_\sigma a_\sigma | a_\sigma a_\sigma) \pm (a_\sigma a_\sigma | b_\sigma b_\sigma)] \quad (19)$$

and similar expressions for α_π , β_π , J_π , and K_π and

$$\left. \begin{array}{l} J_{\sigma\pi} \\ K_{\sigma\pi} \end{array} \right\} = \frac{1}{2} [(a_\sigma a_\sigma | a_\pi a_\pi) \pm (a_\sigma a_\sigma | b_\pi b_\pi)], \quad (20)$$

$$\left. \begin{array}{l} \omega \\ \mu \end{array} \right\} = \frac{1}{2} [(a_\pi a_\sigma | a_\pi a_\sigma) \pm (a_\pi a_\sigma | b_\pi b_\sigma)]. \quad (21)$$

It should be noted here that none of the above quantities takes the same numerical values for ionic states as for the neutral state, because we do *not* use the same atomic orbitals (the same Z values) for both states [1].

The following two sections are devoted to the evaluation of these basic integrals over atomic orbitals.

3. ONE-CENTRE INTEGRALS AND VALENCE STATE ENERGIES

To evaluate the one-centre quantities appearing in equations (17)–(21), we must: (1) obtain numerical values for non-hybridized valence-state energies from atomic spectroscopic data; (2) evaluate hybridized valence-state energies in terms of non-hybridized valence-state energies; (3) obtain simultaneous equations by expressing these energies in terms of Slater–Condon parameters; (4) solve the equations for a set of one-centre quantities.

In step (3), it is customarily assumed that: (a) the same atomic orbitals are used for both neutral atoms and ions; (b) each atom possesses a core which does not change under ionization or in going from one valence-state to another. The present point of view, already supported by a calculation of the ionization potential of ethylene [1], is that allowance should be made for the change in the effective charge under ionization. The same sort of treatment for atomic states should produce much more reliable numerical values for the one-centre quantities. Park's work [4] seems to support this view: a set of one-centre parameters obtained under assumptions (a) and (b) cannot produce exactly the valence state energies computed from atomic data. Although this is due partly to uncertainties in the atomic spectroscopic data, it seems to be evidence that the condition (a) should be relaxed at this stage.

Step (1) is tabulated in the Appendix. There the states of (C^0, p^4), which are experimentally unknown, need to be estimated. First, the Slater–Condon parameters are obtained empirically from the following experimental data for (C^0, sp^3) states [7]:

$$\left. \begin{array}{ll} {}^5S: & W_0 - K_{sp} - 10F_2 = 4.181 \text{ ev}, \\ {}^3D: & W_0 - F_2 = 7.944 \text{ ev}, \\ {}^3P: & W_0 + 5F_2 = 9.328 \text{ ev}, \\ {}^3S: & W_0 + 3K_{sp} - 10F_2 = 13.114 \text{ ev}. \end{array} \right\} \quad (22)$$

Interpolated data for 1D and 1P are intentionally omitted because of their possible errors. The method of least squares gives $W_0 = 8.323$ ev, $K_{sp} = 2.256$ ev, and $F_2 = 0.202$ ev. The ratio of the empirical W_0 obtained above to the theoretical $W_0 (= I_p - I_s - J_{ss} - J_{sp} + 2F_0)$ computed to be 9.822 ev from the theoretical Slater-Condon parameters given by Moffitt [8] is used as a factor, by which the individual theoretical values of parameters in W_0 are reduced to corresponding empirical values [4]. Using these parameters, one obtains

$$E(C^0, p^4; ^1S) = 21.583 \text{ ev}, \quad E(C^0, p^4; ^1D) = 19.765 \text{ ev}, \\ \text{and } E(C^0, p^4; ^3P) = 18.553 \text{ ev}.$$

With non-hybridized valence-state energies so obtained, step (3) is easily performed and gives theoretical hybridized valence-state energies shown in table 1. The energies (7) and (8) may contain small errors due to the use of K_{sp} value, and (9) contains another error due to the use of the (C^0, p^4) energy levels estimated above. Also (2) contains an error due to the extrapolated data [9]. However, none of these errors is considered to be more serious than the one involved in (3), where the estimation of the C^{-2} states causes uncertainties.

Valence state	Energy (ev)	Formulation†
(1) $C^0, t_1t_2\sigma^2; V_2$	6.673	$E + 2I_\sigma + j_{\sigma\sigma}$
(2) $C^{-1}, t_1t_2\sigma^2\pi; V_3$	4.787	$E + 2(I_\sigma + \Delta_\sigma) + (I_\pi + \Delta_\pi) + (Z^{-1}/Z^0)(j_{\sigma\sigma} + 2g_{\sigma\pi})$
(3) $C^{-2}, t_1t_2\sigma^2\pi^2; V_2$	(10.3)	$E + 2(I_\sigma + 2\Delta_\sigma) + 2(I_\pi + 2\Delta_\pi) + (Z^{-2}/Z^0) \times (j_{\sigma\sigma} + j_{\pi\pi} + 4g_{\sigma\pi})$
(4) $C^{+1}, t_1t_2\sigma; V_3$	19.679	$E + (I_\sigma - \Delta_\sigma)$
(5) $C^0, t_1t_2\sigma\pi; V_4$	8.261	$E + I_\sigma + I_\pi + g_{\sigma\pi}$
(6) $C^{-1}, t_1t_2\sigma\pi^2; V_3$	7.68	$E + (I_\sigma + \Delta_\sigma) + 2(I_\pi + \Delta_\pi) + (Z^{-1}/Z^0)(j_{\pi\pi} + 2g_{\sigma\pi})$
(7) $C^{+2}, t_1t_2; V_2$	46.817	E
(8) $C^{+1}, t_1t_2\pi; V_3$	22.929	$E + (I_\pi - \Delta_\pi)$
(9) $C^0, t_1t_2\pi^2; V_2$	12.807	$E + 2I_\pi + j_{\pi\pi}$

† For notation, see § 3.

Table 1. Hybridized carbon valence-state energies in terms of one-centre quantities.

In the last column of table 1, formulations of these valence-states are given in terms of one-centre quantities. A characteristic feature here is that while retaining the assumption (b) above we do not use the same orbitals for ions as for neutral atoms; the effective nuclear charge Z for C^1 , C^0 , and C^{+1} are assumed to be 2.90, 3.25 and 3.60 and so on [10]. All one-centre electronic repulsion integrals of the same kind, $j_{\sigma\sigma}$, $j_{\pi\pi}$ and $g_{\sigma\pi}$ (note $g_{\sigma\pi} = j_{\sigma\pi} - \frac{1}{2}k_{\sigma\pi}$) then come out to be proportional to their Z values. The one-centre core integral I_σ or α_σ has been found to change its value linearly in going from $Z = 2.90$ to 3.60 [1]. Assuming the same dependence on Z for I_σ , we use the empirical parameters Δ_π and Δ_σ to adjust the core integrals.

From eight simultaneous equations with eight unknown parameters (state (3) is omitted for the reason indicated above), one gets

$$\begin{aligned}I_\sigma &= -25.126 \text{ ev}, & j_{\sigma\sigma} &= 10.108 \text{ ev}, \\I_\pi &= -22.017, & j_{\pi\pi} &= 10.024, \\ \Delta_\sigma &= 2.012, & g_{\sigma\pi} &= 8.587, \\ \Delta_\pi &= 1.871, & (E = 46.817).\end{aligned}$$

With $K_{s,c} = K_{sp} = 2.2256 \text{ ev}$ and $K_{xy} = 3F_2 = 0.606 \text{ ev}$ obtained before, one finds $k_{\sigma\pi} = 1.156 \text{ ev}$ and also $j_{\sigma\pi} = 9.165 \text{ ev}$ from $g_{\sigma\pi}$. These parameters give the energy of the state (3) as 10.809 ev, which compares well with the value 10.3 ev derived from the spectroscopic data. Ambiguities in the process of determining values of one-centre quantities from atomic spectroscopic data are thus reduced by allowing a change in the effective nuclear charge upon ionization.

To calculate the one-centre repulsion integrals for C_2H_4^+ and C_2H_4^- ions, we only have to multiply the value obtained above by the appropriate ratio of the effective nuclear charges Z . The Z value for a carbon atom may be presumed to be 3.425 for a positive ion and 3.075 for a negative ion, which is the mean of the Slater values for C^0 and C^+ , and C^0 and C^- , respectively [1], the same effective charges for the 2s and 2p orbitals being assumed. The results are shown in table 2 in terms of quantities given in equations (19)–(21).

Integral†	$Z = 3.075$	$Z = 3.250$	$Z = 3.425$
J_σ	8.920	9.271	9.625
J_π	8.488	8.796	9.108
$J_{\sigma\pi}$	8.065	8.388	8.715
K_σ	0.645	0.837	1.027
K_π	0.996	1.229	1.457
$K_{\sigma\pi}$	0.608	0.777	0.944
ω	0.768	0.800	0.832
μ	0.326	0.356	0.386
α_σ	-24.120	-25.126	-26.132
α_π	-21.081	-22.017	-22.953
β_σ	-7.634	-8.445	-9.075
β_π	-3.040	-2.777	-2.532
$S_{\sigma\ddagger}$	0.796	0.773	0.744
$S_{\pi\ddagger}$	0.307	0.273	0.242

† For notation, see § 2.

‡ These are dimensionless.

Table 2. Integrals over atomic orbitals (ev).

4. TWO-CENTRE INTEGRALS

It has been suggested by several authors [1, 3, 11, 12] that theoretical values of two-centre electronic repulsion integrals are not the correct ones to use with one-centre integrals such as derived above, which values were determined to be consistent in a certain sense with Moffitt's atoms-in-molecules procedure [13]. It is therefore presumed that some kind of a *correlation* correction to the two-centre repulsion integrals (usually leading to lower values) is needed.

For obtaining these corrections, the Pariser and Parr-type method [11] is adopted: (1) calculate the two-centre repulsion integrals ($aa|bb$) theoretically for large values of the internuclear distances using Slater orbitals with corresponding effective nuclear charges mentioned before; (2) obtain the *actual* ($aa|bb$) for the equilibrium $a-b$ distances ($r=1.333 \text{ \AA}$) by smooth interpolation of the curve obtained down to $r=0$ to fit the one-centre integral ($aa|aa$) determined in the preceding section. To do this, it was found that using an equation of the form

$$mr + nr^2 = (aa|bb) - (aa|aa) \quad (23)$$

a reasonable result is obtained; the constants m and n are found by fitting the theoretical values of $r=3.2 \text{ \AA}$ and $r=4.0 \text{ \AA}$ for $(a_\sigma a_\sigma|b_\sigma b_\sigma)$ and $(a_\sigma a_\sigma|b_\pi b_\pi)$, and of $r=2.8 \text{ \AA}$ and $r=3.5 \text{ \AA}$ for $(a_\pi a_\pi|b_\pi b_\pi)$ and $(a_\pi a_\pi|b_\pi b_\sigma)$. The values of quantities in equations (19)–(21) are then obtained from these two-centre repulsion integrals with one-centre integrals determined before, and are listed in table 2.

Now the theoretical expressions for two-centre core integrals β_π and β_σ are easily obtained using

$$H_{\pi-\text{core}}^{+2}(\zeta) = T(\zeta) + V_{\pi a}(\zeta) + V_{\pi b}(\zeta) + \sum_i V_{Hi}(\zeta), \quad (24)$$

$$H_{\sigma-\text{core}}^{+2}(\zeta) = T(\zeta) + V_{\sigma a}(\zeta) + V_{\sigma b}(\zeta) + \sum_i V_{Hi}(\zeta), \quad (25)$$

where $T(\zeta)$ is the kinetic energy operator for electron ζ , $V(\zeta)$ gives a potential energy of attraction between electron ζ and the charged atom a or b , and $V_{Hi}(\zeta)$ denotes a potential due to a hydrogen atom [14]. For instance, one gets

$$\beta_\pi = -(A:a_\pi b_\pi) - (a_\pi a_\pi|a_\pi b_\pi) + S_\pi[(A:b_\pi b_\pi) + (a_\pi a_\pi|b_\pi b_\pi)]. \quad (26)$$

Here $(A:pq)$ is the penetration integral between atomic orbitals p, q and a neutral atom A :

$$(A:pq) = - \int U_A(1)p^*(1)q(1)dv(1). \quad (27)$$

The penetration integrals of the type $(H_i:pq)$ cancel out because we assume the Mulliken-type approximation

$$(H_i:pq) = (Spq/2)[(H_i:pp) + (H_i:qq)]. \quad (28)$$

On the other hand, the use of the corresponding approximation for $(A:a_\pi b_\pi)$ and $(a_\pi a_\pi/a_\pi b_\pi)$ probably would produce serious errors. We therefore adopted the *a priori* prescription that β_π should be calculated purely theoretically using the Slater-type atomic orbitals. Although this attitude seems to be somewhat inconsistent with the rest of the recipe which has been put down, the previous calculation [1] shows that β_π thus calculated purely theoretically can give good results for observables and also compares favourably with its alternative obtained empirically.

Assuming that the same line of discussion holds for β_σ , one gets the numerical values for both β_π and β_σ shown in table 2.

5. RESULTS AND DISCUSSION

The secular equations to be solved, 8×8 for $N(^1A_{1g})$, 5×5 for $I(^2B_{3u})$ and $A(^2B_{2g})$, and 4×4 for $V(^1B_{1u})$ and $T(^3B_{1u})$, were obtained from numerical values of integrals over atomic orbitals given in table 2. All secular equations

were solved on the IBM 650 Electronic Data Processing Machine at the Carnegie Institute of Technology. Table 3 gives the linear coefficients for the wave functions of five states and their energy depressions relative to energies for corresponding Φ_1 states.

	Ψ_N	Ψ_V	Ψ_T	Ψ_I	Ψ_A
Φ_1	0.9933	0.9986	0.9992	0.9990	0.9992
Φ_2	-0.0967	-0.0405	-0.0144	-0.0099	-0.0165
Φ_3	-0.0121	-0.0224	0.0275	-0.0322	0.0235
Φ_4	0.0389	-0.0239	-0.0255	-0.0135	-0.0170
Φ_5	0.0414			-0.0265	-0.0218
Φ_6	0.0117				
Φ_7	0.0232				
Φ_8	0.0044				
$-\Delta E^\dagger (\text{ev})$	0.3500	0.1571	0.0974	0.1264	0.0962

† Energy depression relative to corresponding Φ_1 state energy.

Table 3. Wave functions for various states in ethylene.

The results for the electronic spectrum of ethylene are shown in table 4, together with several others reported previously. The calculations of the first ionization potential and electron affinity were done by employing

$$\text{I.P.} = E(\Psi_I) - E(\Psi_N)$$

$$\text{E.A.} = E(\Psi_N) - E(\Psi_A) \quad (29)$$

and are listed in the bottom of table 4.

State	Obs.	AO [15]	ASMO [2]	Moffit [16]	Previous paper [1]	This paper I†	This paper II‡
$N(^1A_1)$	0.0	0.0	0.0	0.0	0.0	0.0	0.0
$V(^1B_{1u})$	7.6 [18]	8.6	11.42	7.3	7.10 ₄	7.94 ₁	7.82 ₇
$T(^3B_{1u})$	6.4? [19]	5.8	—	5.5	3.68 ₀	5.34 ₅	5.23 ₂
$Z(^1A_1)$	—	14.9	14.74	—	9.73 ₆	12.79 ₈	12.60 ₂
I.P.	10.62 [20]	—	—	—	10.75 ₀	10.93 ₉	10.82 ₈
E.A.	10.52 [21]	—	—	—	-5.98 ₂	-5.15 ₇	-5.06 ₄

† $\sigma-\pi$ interchange is included.

‡ $\sigma-\pi$ interchange is neglected.

Table 4. Electronic states of ethylene (ev).

It is clear that the present treatment including sigma electrons gives better result for the lower electronic transitions, in particular for $^3B_{1u}$ state, than the previous calculation in which the pi electron approximation was employed. Moser's calculation shows that the non-empirical ASMO-CI method produces

too high an $N \rightarrow V$ excitation (and also too large a singlet-triplet split) as usual. Considerable improvement for the $V-T$ split might be expected if different atomic orbitals (different Z values) were used for V and T states, as shown by Ohno and Ito [15]. Moffitt's [16] and Craig's [17] calculations treat only pi electrons (Craig also considers a change in $a-b$ distance and Z values between ground and excited states), and their predictions are not strictly comparable to those mentioned above.

As for the ionization potential and electron affinity of ethylene, there has been no theoretical calculation so far. The value obtained for the ionization potential is in good agreement with experimental values. From the fact that using the same Z value for both ground and excited states one gets too high an ionization potential (around 14 ev), it would seem clear that the present modification achieves a considerable improvement over the conventional ASMO method. Although the electron affinity of ethylene is experimentally unknown, there is evidence to support the method of calculation and the value obtained, as discussed in the previous paper [1].

The $\sigma-\pi$ interchange interaction, in general, causes larger energy intervals between the ground state and the excited states, as pointed out by several authors [15, 22]. The last column of table 4 shows that somewhat better agreement with observed spectrum is obtained if $\sigma-\pi$ interchange is neglected. The same tendency can be seen in the ionization potential and presumably also in the electron affinity. Anyway, the new configurations introduced by the inclusion of sigma electrons do not fall among the pure pi configurations (cf.[1]) but fall at much higher levels. Thus it may be stated that the $\sigma-\pi$ interaction is so small as to be negligible; the same conclusion as that of the non-empirical calculation [2].

Concerning the theoretical calculation of vertical ionization potentials, the usual procedure has been to suppose that the same atomic orbitals can be used for molecule and ion. Under this assumption, we get quite high ionization potentials around 14 ev as mentioned above. In the positive ion, the charge clouds must presumably be less spread out than those of the neutral atom due to the decrease in the electronic repulsion. Thus, in this paper, the adjustment of the effective nuclear charges in the exponents of the atomic orbitals is shown to be significant. Further preferential stabilization of the ion might be expected from $\sigma-\pi$ interaction, but this does not appear to be the case. This and the negligibility of the above interactions lead to the conclusion that allowing for the change for the effective nuclear charge in the ion, theoretical calculations of the ionization potentials for unsaturated hydrocarbons within the framework of the pi-electron theory should give good results.

I am greatly indebted to Professor Robert G. Parr for stimulating discussions and help with the manuscripts. It is also a pleasure to express my gratitude to him and other members of the quantum chemistry group for the hospitality shown during my stay at the Carnegie Institute of Technology.

APPENDIX

Valence state	Formulation†	Energy (ev)‡
$C^0 s^2xz; V_2$	$\frac{3}{4}E[{}^3P] + \frac{1}{4}E[{}^1D]$	0·316
$C^0 sxz^2; V_2$	$\frac{3}{8}E[{}^3D] + \frac{1}{8}E[{}^1D] + \frac{3}{8}E[{}^3P] + \frac{1}{8}E[{}^1P]$	9·851
$C^{-1} s^2xyz; V_3$	$\frac{1}{2}E[{}^4S] + \frac{1}{2}E[{}^2D]$	(-1·00)
$C^{-1} sx^2yz; V_3$	$\frac{1}{2}E[{}^4P] + \frac{1}{4}E[{}^2P] + \frac{1}{4}E[{}^2D]$	(7·68)
$C^{-2} s^2xy^2z; V_2$	$\frac{3}{4}E[{}^3P] + \frac{1}{4}E[{}^1D]$	((4·25))
$C^{-2} sxy^2z^2; V_2$	$\frac{3}{4}E[{}^3P] + \frac{1}{4}E[{}^1P]$	((11·85))
$C^{+1} sxz; V_3$	$\frac{1}{2}E[{}^4P] + \frac{1}{4}E[{}^2P] + \frac{1}{4}E[{}^2D]$	19·679
$C^0 sxyz; V_4$	$\frac{5}{16}E[{}^5S] + \frac{3}{16}E[{}^3S] + \frac{3}{8}E[{}^3D] + \frac{1}{8}E[{}^1D]$	8·261
$C^{+2} {}^1(sz); V_0$	$E[{}^1P]$	48·326
$C^{+2} {}^3(sx); V_0$	$E[{}^3P]$	42·124
$C^{+2} {}^3(zx); V_0$	$E[{}^3P]$	52·667
$E_s^0 (s^2)$	$E[{}^1S]$	35·640
$E_{zx}^0 (p^2)$	$\frac{7}{15}E[{}^1D] + \frac{8}{15}E[{}^1S]$	56·640
$C^{+1} {}^1(sz)y; V_1$	$\frac{3}{4}E[{}^2P] + \frac{1}{4}E[{}^2D]$	23·870
$C^{+1} {}^3(sx)y; V_1$	$\frac{1}{2}E[{}^2P] + \frac{1}{4}E[{}^2D] + \frac{2}{3}E[{}^4P]$	18·282
$C^{+1} {}^3(zx)y; V_1$	$\frac{1}{3}E[{}^2D] + \frac{2}{3}E[{}^4S]$	29·216
$E_s^0 (s^2p)$	$E[{}^2P]$	11·264
$E_{zx}^0 (p^3)$	$\frac{4}{5}E[{}^2P] + \frac{1}{5}E[{}^4S]$	31·725
$C^0 {}^1(sz)y^2; V_0$	$\frac{1}{2}E[{}^1D] + \frac{1}{2}E[{}^1P]$	13·490
$C^0 {}^3(sx)y^2; V_0$	$\frac{1}{2}E[{}^3P] + \frac{1}{2}E[{}^3D]$	8·636
$C^0 {}^3(zx)y^2; V_0$	$E[{}^3P]$	(18·553)
E_s^0	$\frac{2}{3}E[{}^1D] + \frac{1}{3}E[{}^1S]$	1·737
E_{zx}^0	$\frac{7}{15}E[{}^1D] + \frac{8}{15}E[{}^1S]$	(20·735)

† In the notation of term values, corresponding configurations are omitted. For instance, it should be read as $C^0 s^2xz; V_2$, $E[{}^3P; s^2p^2] + E[{}^1D; s^2p^2]$ and so on.

‡ While braces show that some error is involved due to the estimation of unknown term values, double braces indicate more serious uncertainties.

Non-hybridized carbon valence-state energies and their formulation in terms of atomic spectroscopic energies.

REFERENCES

- [1] I'HAYA, Y., 1960, *Mol. Phys.*, **3**, 513.
- [2] MOSER, C. M., 1953, *Trans. Faraday Soc.*, **49**, 1239.
- [3] PARKS, J. M., and PARR, R. G., 1958, *J. chem. Phys.*, **28**, 335.
- [4] PARKS, J. M., 1956, Thesis, Carnegie Institute of Technology; PARKS, J. M., and PARR, R. G., 1960, *J. chem. Phys.*, **32**, 1657.
- [5] CONDON, E. U., and SHORTLEY, G. H., 1957, *Theory of Atomic Structure* (New York : Cambridge University Press).
- [6] MULLIKEN, R. S., 1949, *J. chem. Phys.*, **46**, 497.
- [7] MOORE, C. E., *Atomic Energy Levels* (National Bureau of Standards, Circular 467, 1949-1952).
- [8] MOFFITT, W., 1950, *Proc. roy. Soc. A*, **202**, 534.
- [9] SKINNER, H. A., and PRITCHARD, H. O., 1953, *Trans. Faraday Soc.*, **49**, 1254; PRITCHARD, H. O., and SKINNER, H. A., 1955, *Chem. Rev.*, **55**, 745.
- [10] SLATER, J. C., 1932, *Phys. Rev.*, **42**, 33.
- [11] PARISER, R., and PARR, R. G., 1953, *J. chem. Phys.*, **21**, 767.
- [12] PARISER, R., 1956, *J. chem. Phys.*, **25**, 1112.
- [13] MOFFITT, W., 1951, *Proc. roy. Soc. A*, **210**, 245.
- [14] GOEPPERT-MOYER, M., and SKLAR, A. L., 1938, *J. chem. Phys.*, **6**, 645.

- [15] OHNO, K., and ITO, T., 1955, *J. chem. Phys.*, **23**, 1468.
- [16] MOFFITT, W., 1953, *Proc. roy. Soc. A*, **218**, 464.
- [17] CRAIG, D. P., 1950, *Proc. roy. Soc. A*, **200**, 474.
- [18] WILKINSON, P. G., and JOHNSTON, J. L., 1950, *J. chem. Phys.*, **18**, 190.
- [19] POTTS, W., 1953, Thesis, University of Chicago.
- [20] HONIG, R. E., 1948, *J. chem. Phys.*, **16**, 105.
- [21] WATANABE, K., 1954, *J. chem. Phys.*, **22**, 1564.
- [22] NIIRA, K., 1953, *J. phys. Soc. Japan*, **8**, 630.

Correlations between the electronic spectra of alternant hydrocarbon molecules and their mono- and di-valent ions†

II. Hydrocarbons with symmetry D_{2h}

by G. J. HOIJTINK, N. H. VELTHORST and P. J. ZANDSTRA‡

Chemical Laboratory of the Free University, Amsterdam

(Received 18 March 1960)

On the basis of a qualitative quantum mechanical theory of the energies and dipole strengths of the lower π -electronic transitions in alternant hydrocarbon molecules and their mono- and di-valent ions a comparison is made between the spectra in the 5–45 kK region of the molecules and ions of naphthalene, anthracene, tetracene, pyrene and perylene.

1. INTRODUCTION

In paper I [1] the correlations between the electronic spectra of the molecules and mono- and di-valent ions of benzene, coronene and triphenylene have been studied. These hydrocarbons with a three- or six-fold symmetry axis have in common that the highest bonding and lowest anti-bonding π -orbitals are two-fold degenerate. Further to these investigations, the correlations for alternant hydrocarbons with lower symmetry are considered in the present paper.

In previous work [2] it was shown that S.C.F.-M.O.-calculations of the energies and dipole strengths of π -electronic transitions in alternant hydrocarbon negative and positive ions of the same valency lead to exactly the same results, provided the nuclear framework is assumed to be the same for both ions and overlap between the atomic $2p_z$ functions is neglected. Recently McLachlan [3] arrived at the same conclusions. Experimentally it appears indeed that the electronic spectra of positive and negative ions of alternant hydrocarbons are practically identical [4]. As a consequence, just as in paper I, the study of the electronic spectra may be restricted to the molecules and their mono- and di-negative ions.

2. THEORETICAL PART

Following the usual procedure the π -electrons in a hydrocarbon molecule are considered to move in the fixed force field of their nuclei and the residual electrons, the so-called σ core. Hence the complete Hamiltonian for the π -electronic system becomes :

$$H = \sum_{\mu} h(\mu) + \sum_{\mu < \nu} \sum \frac{e^2}{r_{\mu\nu}} \quad (1)$$

† Part of Thesis by P. J. Zandstra, Free University, Amsterdam, 1959. These investigations have been carried out under the auspices of the Netherlands Foundation for Chemical Research (S.O.N.) and with financial aid from the Netherlands Organization for the Advancement of Pure Research (Z.W.O.).

‡ Present address: Department of Chemistry, Washington University, St. Louis, Mo.

where $h(\mu)$ stands for the energy operator of the electron μ moving in the field of the σ -core and $e^2/r_{\mu\nu}$ is the potential energy operator for the repulsion between the electrons μ and ν . Just as in paper I [1] the nuclear framework is assumed to be the same for the molecule and its mono- and di-valent ions, which seems to be a reasonable supposition for large π -electronic systems such as those in aromatic hydrocarbons. As a consequence, apart from the number of π -electrons, the Hamiltonian operator is the same for the molecule and its mono- and di-valent ions.

Using the L.C.A.O.-M.O. description the one-electron wave functions for a π -electron in a hydrocarbon molecule with $2n$ tervalent carbon atoms becomes :

$$\phi_j(\mu) = \sum_{s=1}^{2n} c_{s,j} \varphi_s(\mu); \quad j = 1, 2, \dots, 2n \quad (2)$$

in which $\varphi_s(\mu)$ describes the electron μ moving in the $2p_z$ -orbital at the s th carbon atom. In the scope of this approach the best solutions for the coefficients $c_{s,j}$ will be those obtained with the aid of S.C.F.-M.O.-calculations. For the present purpose, however, it is much more convenient to use one and the same set of M.O.'s both for the molecule and its mono- and di-valent ions. From calculations by other investigators [5] it appears that the S.C.F.-M.O.'s for the higher bonding and lower anti-bonding π -orbitals of alternant hydrocarbon molecules are nearly the same as the corresponding Hückel M.O.'s. Recent calculations by Colpa [6] have shown that the same holds true for the mono-valent ions. For this reason the Hückel M.O.'s will be used as a basis for the present study.

A further simplification is obtained by assuming that the energy relative to the ground state of an excited configuration described by one single anti-symmetrized product

$$\psi_V = |\phi_1 \bar{\phi}_1 \dots \phi_j \bar{\phi}_k \dots| \quad (3)$$

both for the molecule and its mono- and di-valent ions may be taken equal to the one-electron excitation energy

$$E_V = H_{V,V} - H_{N,N} = (x_j - x_k) \beta, \quad (4)$$

where x_j and x_k are the characteristic roots of the Hückel secular equation for the j th and k th π -orbital. Besides, configuration interaction will remain restricted to excited configurations with the same or nearly the same energies. For the molecules this comes to the procedure followed by Dewar and Longuet-Higgins [7], while for the mono- and di-valent ions it is closely analogous to previous treatments [8, 9].

As Coulson and Rushbrooke [10] have shown, the Hückel M.O.'s of alternant hydrocarbons obey the so-called pairing relations† :

$$c_{s,j} = \pm c_{s,m}; \quad m = 2n + 1 - j \quad (5)$$

where the + and - signs refer to odd and even numbered carbon atoms respectively. On the basis of these pairing properties it can be shown that,

† In S.C.F.-M.O.-calculations on alternant hydrocarbon molecules in the sense of Pariser-Parr and Pople (neglect of overlap between atomic orbitals, etc.) these pairing properties remain valid. For the mono- and di-valent ions, on the contrary, this pairing does no longer hold. In the latter case one finds that the bonding M.O.'s of the positive ion are paired with the anti-bonding M.O.'s of the corresponding negative ion and reverse [2, 3].

if the orbitals j and m , and k and l are paired, the following equalities hold :

$$K_{j,l} = \int \int \phi_j(\mu) \phi_l(\nu) \frac{e^2}{r_{\mu\nu}} \phi_j(\nu) \phi_l(\mu) d\tau_\mu d\tau_\nu = K_{k,m}, \quad (6)$$

$$\mathbf{M}_{j,l} = e \int \phi_j(\mu) \mathbf{r}_\mu \phi_l(\mu) d\tau_\mu = \mathbf{M}_{k,m}, \quad (7)$$

(where \mathbf{r}_μ denotes the position operator for the electron μ) and

$$x_j - x_l = x_k - x_m. \quad (8)$$

2.1. The hydrocarbon molecule

The ground and lower singlet excited states of the molecule may be described by the anti-symmetrized wave functions :

$$\psi_N = |\phi_1 \bar{\phi}_1 \dots \phi_k \bar{\phi}_k \dots \phi_n \bar{\phi}_n|, \quad (9)$$

$$n \rightarrow n+1 \quad \psi_A = \frac{1}{\sqrt{2}} \{ |\phi_1 \bar{\phi}_1 \dots \phi_k \bar{\phi}_k \dots \phi_n \bar{\phi}_{n+1}| + |\phi_1 \bar{\phi}_1 \dots \phi_k \bar{\phi}_k \dots \phi_{n+1} \bar{\phi}_n| \} \quad (10)$$

$$\left. \begin{array}{l} n \rightarrow l \\ k \rightarrow n+1 \end{array} \right\} \quad \psi_{B\pm} = \frac{1}{2} [\{ |\phi_1 \bar{\phi}_1 \dots \phi_k \bar{\phi}_{n+1} \dots \phi_n \bar{\phi}_n| + |\phi_1 \bar{\phi}_1 \dots \phi_{n+1} \bar{\phi}_k \dots \phi_n \bar{\phi}_n| \} \\ \pm \{ |\phi_1 \bar{\phi}_1 \dots \phi_k \bar{\phi}_k \dots \phi_n \bar{\phi}_l| + |\phi_1 \bar{\phi}_1 \dots \phi_k \bar{\phi}_k \dots \phi_l \bar{\phi}_n| \}] \quad (11)$$

where the + and - signs refer to the so-called plus and minus states [11].

Making use of (4)–(8) the transition energies and dipole strengths become :

$${}^1E_{A\pm} = (x_n - x_{n+1})\beta + K_{n,n+1}; \quad D_{N,A\pm} = 2 \frac{M^2_{n,n+1}}{e^2} = 2\mathcal{D}_{n,n+1}, \quad (12)$$

$${}^1E_{B\pm} = (x_n - x_l)\beta + K_{n+1,l} - K_{n,l}; \quad D_{N,B\pm} = 0, \quad (13)$$

$${}^1E_{B\pm} = (x_n - x_l)\beta + 3K_{n,l} - K_{n+1,l}; \quad D_{N,B\pm} = 4\mathcal{D}_{n,l}. \quad (14)$$

The transition dipole strength $D_{N,B\pm}$ vanishes only when overlap between the atomic orbitals is neglected. Since actually this overlap will have a small but finite value one may expect a strong and a weak absorption band due to the transitions $N \rightarrow {}^1B^+$ and $N \rightarrow {}^1B^-$.

2.2. The mono-negative ion

Within the scope of the present approach the mono-negative ions may be thought to be formed by adding one electron to the lowest anti-bonding orbital of the molecule. Accordingly, in addition to the electron excitations A and B , excitations occur from the lowest anti-bonding to empty π -orbitals. Hence the wave functions for the doublet ground and the lower doublet excited configurations become [8] :

$${}^2\psi_N = |\phi_k \bar{\phi}_k \phi_n \bar{\phi}_n \phi_{n+1}|, \quad (15)$$

$$n \rightarrow n+1 \quad {}^2\psi_A = |\phi_k \bar{\phi}_k \phi_n \bar{\phi}_{n+1} \phi_{n+1}|, \quad (16)$$

$$k \rightarrow n+1 \quad {}^2\psi_{B_1} = |\phi_k \bar{\phi}_{n+1} \phi_n \bar{\phi}_n \phi_{n+1}|, \quad (17)$$

$$n \rightarrow l \quad \left\{ \begin{array}{l} {}^2\psi_{B_2} = \frac{1}{\sqrt{2}} \{ |\phi_k \bar{\phi}_k \phi_n \bar{\phi}_l \phi_{n+1}| + |\phi_k \bar{\phi}_k \phi_l \bar{\phi}_n \phi_{n+1}| \}, \\ {}^2\psi_{B_3} = \frac{1}{\sqrt{6}} \{ 2|\phi_k \bar{\phi}_k \phi_n \bar{\phi}_{n+1} \phi_l| + |\phi_k \bar{\phi}_k \phi_n \bar{\phi}_l \phi_{n+1}| \\ - |\phi_k \bar{\phi}_k \phi_l \bar{\phi}_n \phi_{n+1}| \}, \end{array} \right. \quad (18)$$

$$l = 2n+1-k \quad \left\{ \begin{array}{l} {}^2\psi_{B_4} = \frac{1}{\sqrt{6}} \{ 2|\phi_k \bar{\phi}_k \phi_n \bar{\phi}_{n+1} \phi_l| + |\phi_k \bar{\phi}_k \phi_n \bar{\phi}_l \phi_{n+1}| \\ - |\phi_k \bar{\phi}_k \phi_l \bar{\phi}_n \phi_{n+1}| \}, \end{array} \right. \quad (19)$$

$$n+1 \rightarrow n+i \quad i \geq 2 \quad {}^2\psi_I = |\phi_k \bar{\phi}_k \phi_n \bar{\phi}_n \phi_{n+i}|. \quad (20)$$

Following the same procedure as for the molecules the energies and dipole strengths for the transitions in the mono-negative ion become :

$$^2E_A = (x_n - x_{n+1})\beta ; \quad D_{N,A} = \mathcal{D}_{n,n+1}, \quad (21)$$

$$^2E_{B_1} = (x_n - x_l)\beta ; \quad D_{N,B_1} = \mathcal{D}_{n,l} \quad (22)$$

$$^2E_{B_2} = (x_n - x_l)\beta + K_{n,l} ; \quad D_{N,B_2} = 2\mathcal{D}_{n,l} \quad (23)$$

$$^2E_{B_3} = (x_n - x_l)\beta + \frac{1}{3}\{2K_{n+1,l} + 2K_{n,n+1} - K_{n,l}\} ; \quad D_{N,B_3} = 0, \quad (24)$$

$$^2E_I = (x_{n+1} - x_{n+i})\beta ; \quad D_{N,I} = \mathcal{D}_{n+1,n+i}. \quad (25)$$

The matrix element for the interaction between the excited configurations B :

$$H_{B_1, B_2} = \frac{1}{\sqrt{2}}\{2K_{n,l} - K_{n+1,l}\}, \quad (26)$$

$$H_{B_1, B_3} = -\frac{\sqrt{3}}{\sqrt{2}}K_{n+1,l} \quad (27)$$

$$H_{B_2, B_3} = -\frac{1}{\sqrt{3}}\{K_{n,n+1} - K_{n+1,l}\}, \quad (28)$$

are far from negligible, so that configuration interaction ought to be taken into account.

Note : owing to the simplifications involved the matrix element (28) is two-thirds of the one which is obtained in the usual L.C.A.O.-M.O. treatment.

2.3. The di-negative ion

On the basis of the simplified model the di-negative ion is formed by adding two electrons to the lowest antibonding π -orbital of the molecule. As a consequence the transitions A cannot take place and the wave functions for the ground and lower singlet excited configurations become [9] :

$$^1\psi_N = |\phi_n \bar{\phi}_n \phi_{n+1} \bar{\phi}_{n+1}|, \quad (29)$$

$$n \rightarrow l \quad ^1\psi_B = \frac{1}{\sqrt{2}}\{|\phi_n \bar{\phi}_l \phi_{n+1} \bar{\phi}_{n+1}| + |\phi_l \bar{\phi}_n \phi_{n+1} \bar{\phi}_{n+1}|\}, \quad (30)$$

$$n+1 \rightarrow n+i \quad i \geq 2 \quad ^1\psi_I = \frac{1}{\sqrt{2}}\{|\phi_n \bar{\phi}_n \phi_{n+1} \bar{\phi}_{n+i}| + |\phi_n \bar{\phi}_n \phi_{n+i} \bar{\phi}_{n+1}|\}. \quad (31)$$

The transition energies and dipole strengths turn out to be :

$$^1E_B = (x_n - x_l)\beta + K_{n,l} ; \quad D_{N,B} = 2\mathcal{D}_{n,l} \quad (32)$$

$$^1E_I = (x_{n+1} - x_{n+i})\beta + K_{n+1,n+i} ; \quad D_{N,I} = 2\mathcal{D}_{n+1,n+i}. \quad (33)$$

2.4. Excited states of higher spin multiplicities

In the hydrocarbon molecule and its di-valent ion each singlet excited state is associated with a triplet state. The energy of the triplet state is always lower than the energy of the corresponding singlet state so that at least one triplet excited state will be located between the ground state and the lowest singlet excited state. In alternant aromatic hydrocarbon molecules this lowest triplet state will be of the type A or B^- , in the di-negative ion the lowest triplet will in all probability be of the category 3I .

In the mono-negative ion, on the other hand, only those doublet excited states are associated with states of higher spin multiplicity, i.e. quartet states, which belong to the categories B_2, B_3 , or to higher excited states. For transitions of the type B the corresponding quartet state is described by [8] :

$$^4\psi_B = \frac{1}{\sqrt{2}} \{ |\phi_k \bar{\phi}_k \phi_n \bar{\phi}_l \phi_{n-1}| - |\phi_k \bar{\phi}_k \phi_l \bar{\phi}_n \phi_{n+1}| - |\phi_k \bar{\phi}_k \phi_n \bar{\phi}_{n+1} \phi_l| \}. \quad (34)$$

Within the limitations of the present approach the energy of this state relative to the ground state becomes :

$$^4E_B = (x_n - x_l)\beta - \frac{2}{3}\{K_{n,l} + K_{n+1,l} - K_{n,n+1}\}. \quad (35)$$

This quartet state will in general be located above the lower doublet excited state (20) of type I .

2.5. Correlations between the spectra of molecules and ions

As Weijland [2] has shown the ratios between the exchange integrals $K_{n,n+1}$, $K_{n,l}$ and $K_{n+1,l}$ are roughly constant for the hydrocarbons considered in this paper. Using these average ratios one obtains for the transitions of the type B :

$$M : \quad ^1E_{B-} \approx (x_n - x_l)\beta - 0.8K_{n,l}; \quad D = 0, \quad (36)$$

$$^1E_{B+} \approx (x_n - x_l)\beta + 2.8K_{n,l}; \quad D = 4\mathcal{D}_{n,l}, \quad (37)$$

$$M^- : \quad ^2E_{B_a} \approx (x_n - x_l)\beta - K_{n,l}; \quad D \approx 0. \quad (38)$$

$$^2E_{B_1} \approx (x_n - x_l)\beta + 0.5K_{n,l}; \quad D \approx \mathcal{D}_{n,l}, \quad (39)$$

$$^2E_{B_c} \approx (x_n - x_l)\beta + 2.5K_{n,l}; \quad D \approx 2\mathcal{D}_{n,l}, \quad (40)$$

$$M^+ : \quad ^1E_B = (x_n - x_l)\beta + K_{n,l}; \quad D = 2\mathcal{D}_{n,l}. \quad (41)$$

The transition energies and dipole strengths of M^- have been calculated from (22)–(24) and (26)–(28) with the aid of configuration interaction. The results comprised in the equations (36)–(41) are shown diagrammatically in figure 1. From this figure as well as from the equations (12), (21), (25), and (33) one arrives at the following qualitative conclusions :

(1) Since the exchange integrals involved in the present calculations are always positive it can be seen from equations (12) and (21) that, on going from the molecule to its mono-valent ion, the absorption band A shifts to the red and its intensity is roughly halved.

(2) Similarly it follows from the equations (25) and (33) that on going from the mono- to the di-valent ion, the absorption band I , associated with an electron excitation $n+1 \rightarrow n+i$ shifts to the blue and becomes roughly twice as strong.

(3) The strongest absorption band of the type B in the spectrum of the mono-valent ion is located at about the same wave number as the strong absorption band B^+ in the spectrum of the molecule and has about half the intensity of the latter. In the spectrum of the di-valent ion one absorption band B occurs with about half the intensity of the band B^+ of the molecule.

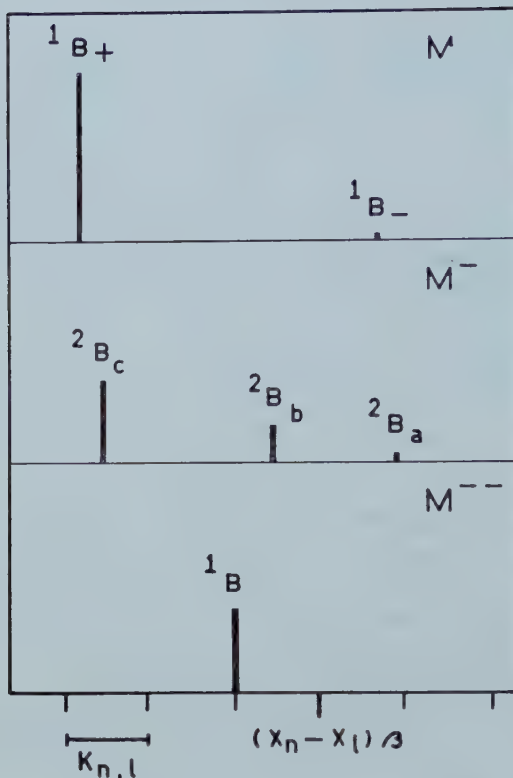


Figure 1. Relative positions and intensities of *B*-type transitions.

3. EXPERIMENTAL (In collaboration with R. van Hardeveld)

The absolute extinction values of recent absorption measurements on glassy solutions [12] of various hydrocarbon negative ions at liquid air temperature are rather uncertain owing to irreproducible shrinking of the glass. For that reason the spectra were also measured at room temperature, using tetrahydrofuran as a solvent. These spectra differ, in some respects, from those measured previously. In the first place the measurements could be extended into the 30–45 kK region by the use of quartz instead of pyrex optical cells. Furthermore by an improvement of the experimental techniques it was possible to exclude moisture and oxygen more rigorously.

Nevertheless in some cases the spectra still exhibit the characteristic absorption in the 20–25 kK region of the MH^- or MNa^- ion (see the discussion in a previous paper [12]). Since according to the polarization measurements the negative ions practically do not absorb in this region the absorption bands due to these impurities could be omitted. The residual curves at these wave numbers are indicated by broken lines.

The weak absorption band at 29.5 kK of the naphthalene mono-negative ion, which very recently has been found at liquid air temperature, is completely masked at room temperature by a broad absorption band due to some foreign species (see note on p. 384 of ref. [12]).

The spectra of the hydrocarbon molecules were measured using the same solvent as for the negative ions.

For more particulars we refer to previous papers [14].

4. DISCUSSION

Guided by the foregoing approach and the assignments of the spectra of the molecules given by other authors [5, 7, 11, 13] the spectra of the mono- and di-valent ions shown in the figures 3, 4, 5, 7 and 8 may now be elucidated. So far as not placed within brackets the directions of polarization x and y have been determined experimentally [12]. According to the usual convention the y -axis is chosen parallel to the central carbon–carbon bond(s).

4.1. The polyacenes

Owing to the symmetry D_{2h} of the polyacenes part of the π -electronic excitations are forbidden. The allowed excitations, in so far as they give rise to the absorption of light in the spectral region investigated, are indicated in figure 2.

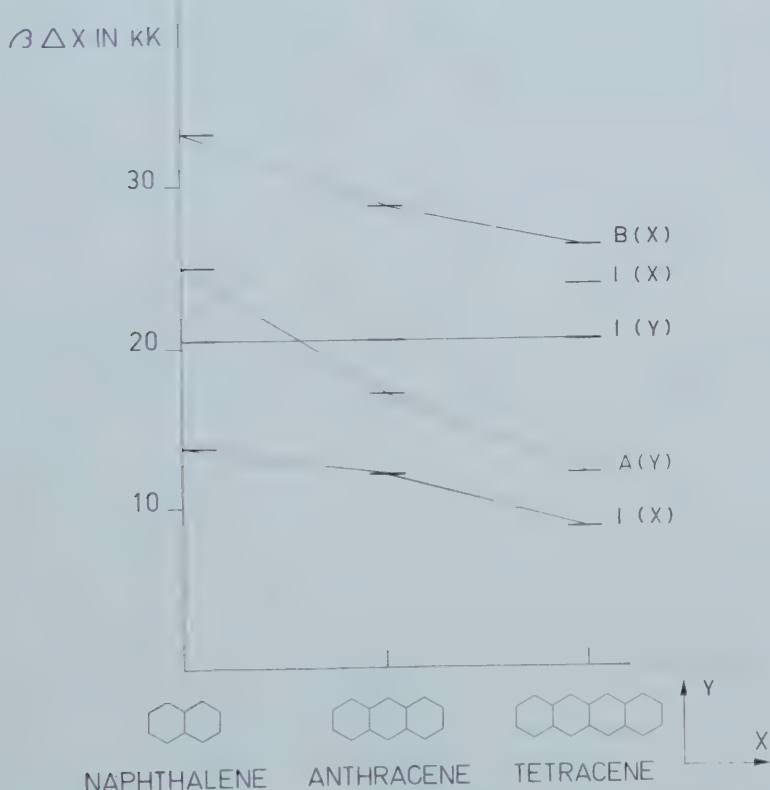


Figure 2. One-electron excitation energies for naphthalene, anthracene and tetracene ($\beta = -20.5$ kK).

For naphthalene and anthracene one may expect two I -type transitions, one x - and one y -polarized, and one or one set of B -type transitions. For tetracene a second x -polarized I -type transition enters. The dipole strength of this transition is very low; configuration interaction, however, may give rise to an absorption band with a low but observable intensity.

The y -polarized transitions A and I for the monovalent ion will be located rather close to each other, so that one may expect a strong interaction between the excited configurations. Since the dipole strengths of these two transitions

are of the same order of magnitude, configuration interaction will give rise to a stronger ($I+A$) and a weaker ($I-A$) absorption band, shifted to the blue and the red respectively.

The assignment of the spectra given in the figures 3, 4 and 5 is now self-evident.

The y -polarized absorptions are in general very weak. This is probably also the reason why in the polarization measurements only part of the y -polarized bands could be observed.

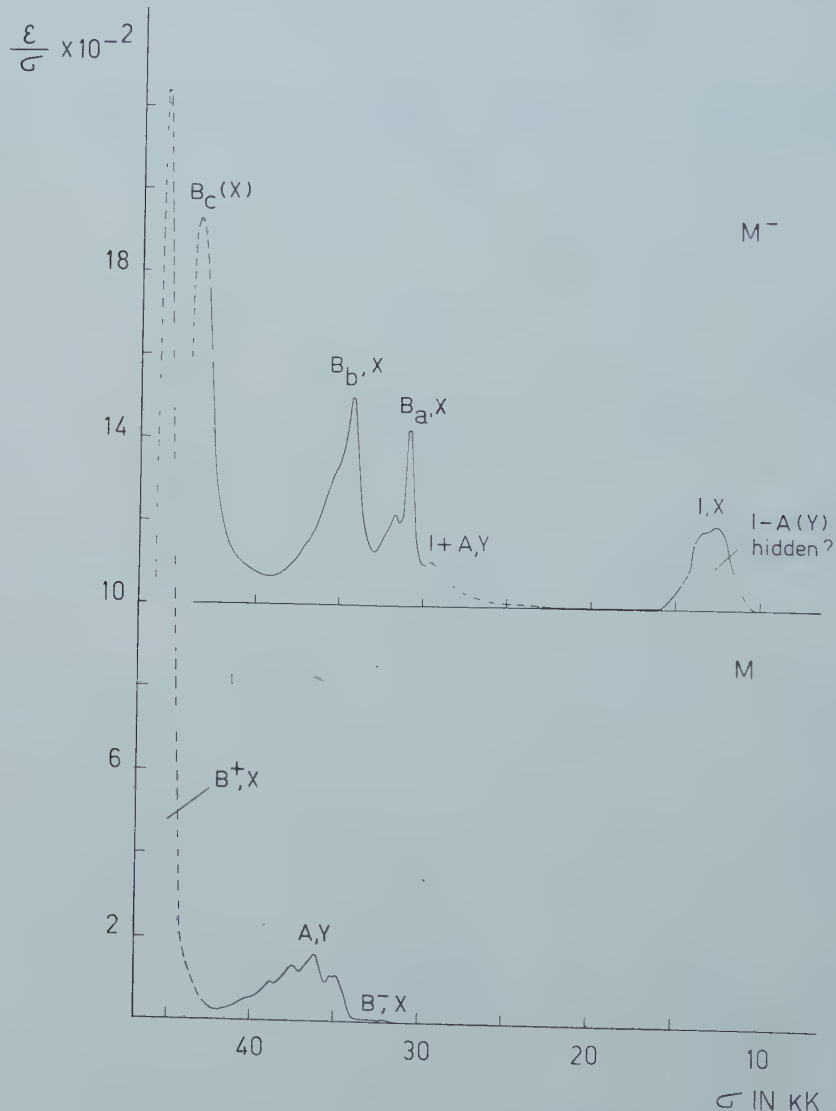


Figure 3. Absorption spectra of the naphthalene molecule and ion.

From a more quantitative treatment [8] one might expect the intensities of the y -polarized bands to be markedly higher. This divergence between the quantitative approach and experiment is also the reason why in our previous assignment [8] the absorption band of the mono-negative ion which is now ascribed to B_a was

erroneously attributed to the y -polarized transition ($I + A$). Since the experiment clearly points to an x -polarized transition there can be little doubt that this band is one of the three B -bands. Apparently this transition is much more probable than the present qualitative approach predicts. A more extended configuration interaction may lead to some improvement.

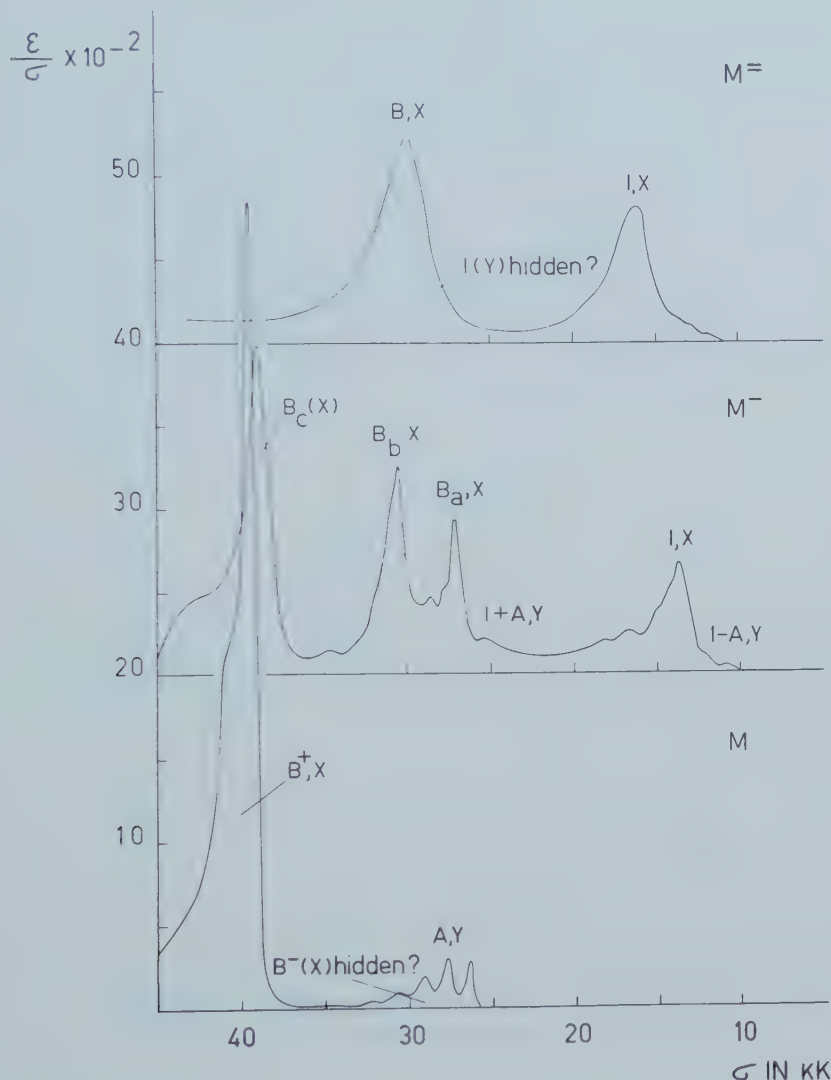


Figure 4. Absorption spectra of the anthracene molecule and ions.

Note: In our previous paper [8] a different value of the bond integral β was chosen for naphthalene than for the other aromatic hydrocarbons. It is worth noticing that on the basis of the present assignment the calculations for the naphthalene mono-negative ion using the same value of β as for the other negative ions, fit the experimental results reasonably well.

4.2. Pyrene and perylene

Contrary to the polyacenes, in the molecules and ions of the pericondensed hydrocarbons pyrene and perylene the y -polarized transitions are stronger than those polarized along the shorter x -axis. As a consequence the spectra of these systems look different from those of the polyacenes. Owing to the symmetry D_{2h} part of the π -electronic excitations are again forbidden. The allowed excitations

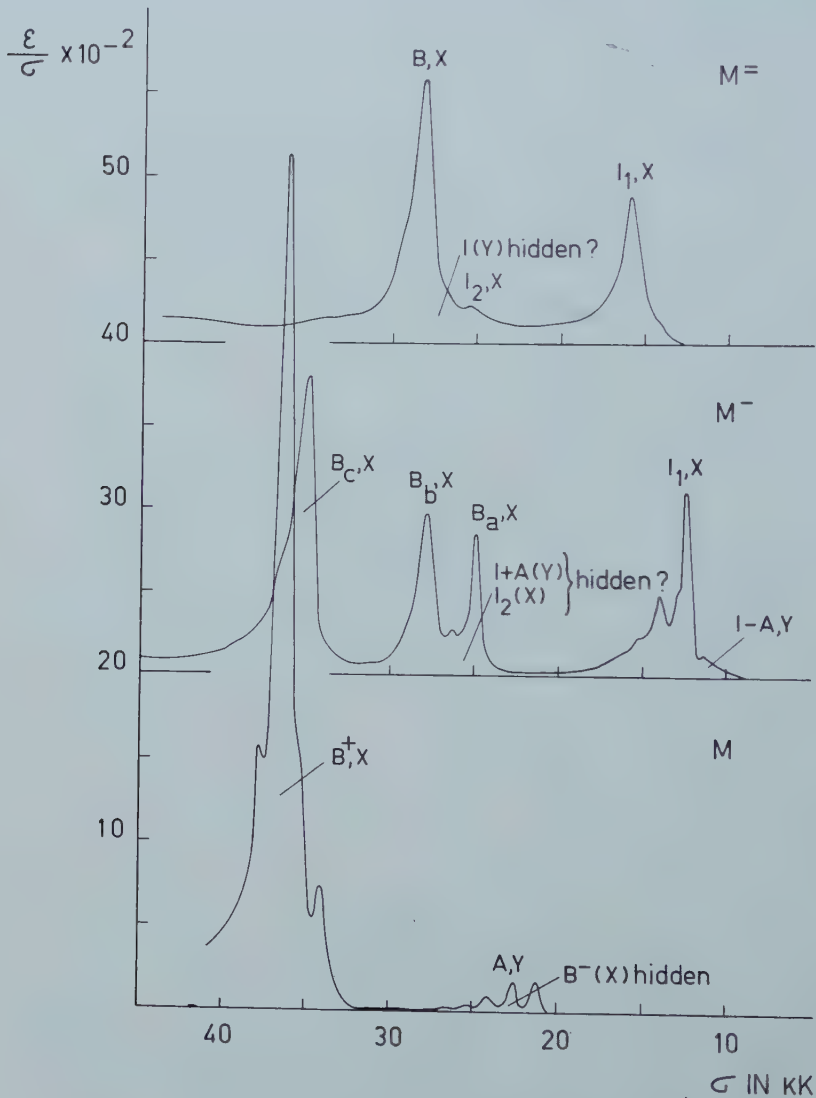


Figure 5. Absorption spectra of the tetracene molecule and ions.

have been drawn schematically in figure 6. Guided by this figure and the foregoing theoretical approach the assignment of the spectra in figures 8 and 9 presents no difficulties. Here two x -polarized I -type transitions occur with the same or nearly the same energies. Configuration interaction will therefore lead to a strong blue and a weak red absorption band of which only the stronger one appears to be visible in the spectra of the pyrene mono- and di-negative ion.

4.3. Fluorescence and phosphorescence of hydrocarbon ions

Various attempts to measure the fluorescence of the negative ions remained unsuccessful, except in the case of the pyrene and perylene negative ions, which show a strong emission in the visible. As has been pointed out elsewhere [12] this fluorescence is due to the presence of other species, probably the ions MH^- or MNa^- . This negative result is understandable since the first absorption bands of the negative ions are located in the red or in the near infra-red where owing to the lack of a sensitive detector the emission is not observable. It is also possible that, because of the small difference between the lowest excited state and the ground state, the excited state becomes deactivated by a rapid conversion into the vibrationally excited ground state.

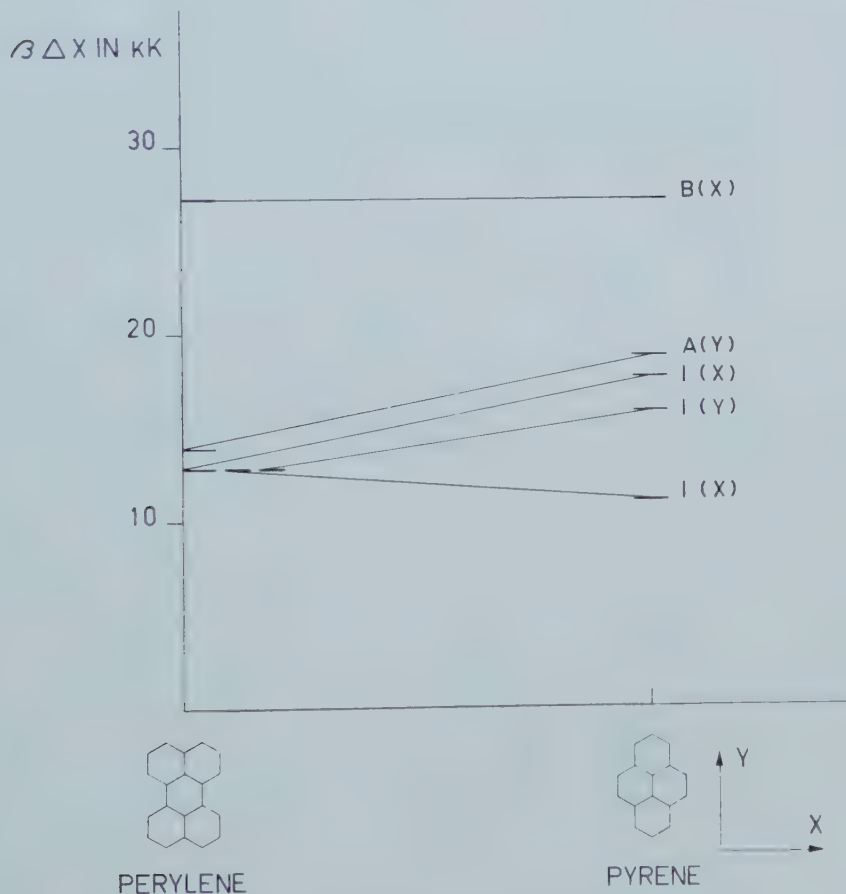


Figure 6. One-electron excitation energies for pyrene and perylene.

Glassy solutions of the negative ions show no phosphorescence either. For the di-negative ions this is not surprising as the lowest triplet will be located below the lowest singlet excited state, so that phosphorescence, if it occurred, would appear even farther in the infra-red than fluorescence.

For the mono-negative ions, on the contrary, the theory predicts a lowest quartet state of the type *B* which lies above one or more of the lower doublet excited states of the type *I*. If a quartet-doublet emission were to take place this would become observable in the visible. Apparently the population of the

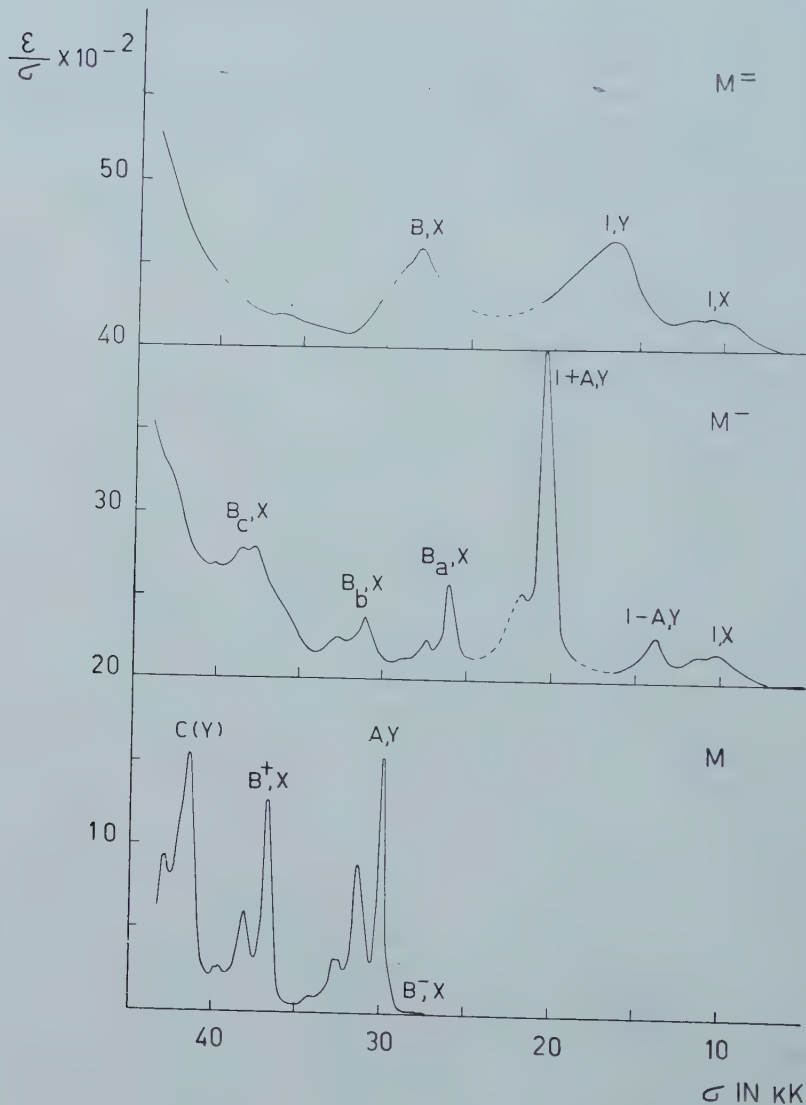


Figure 7. Absorption of the pyrene molecule and ions.

quartet state remains very low during irradiation, which in the scope of the Jablonski scheme [14] implies that the rate of internal conversion from the lowest quartet to lower-lying doublet states is at least of the same order of magnitude as the rate of population of the quartet state.

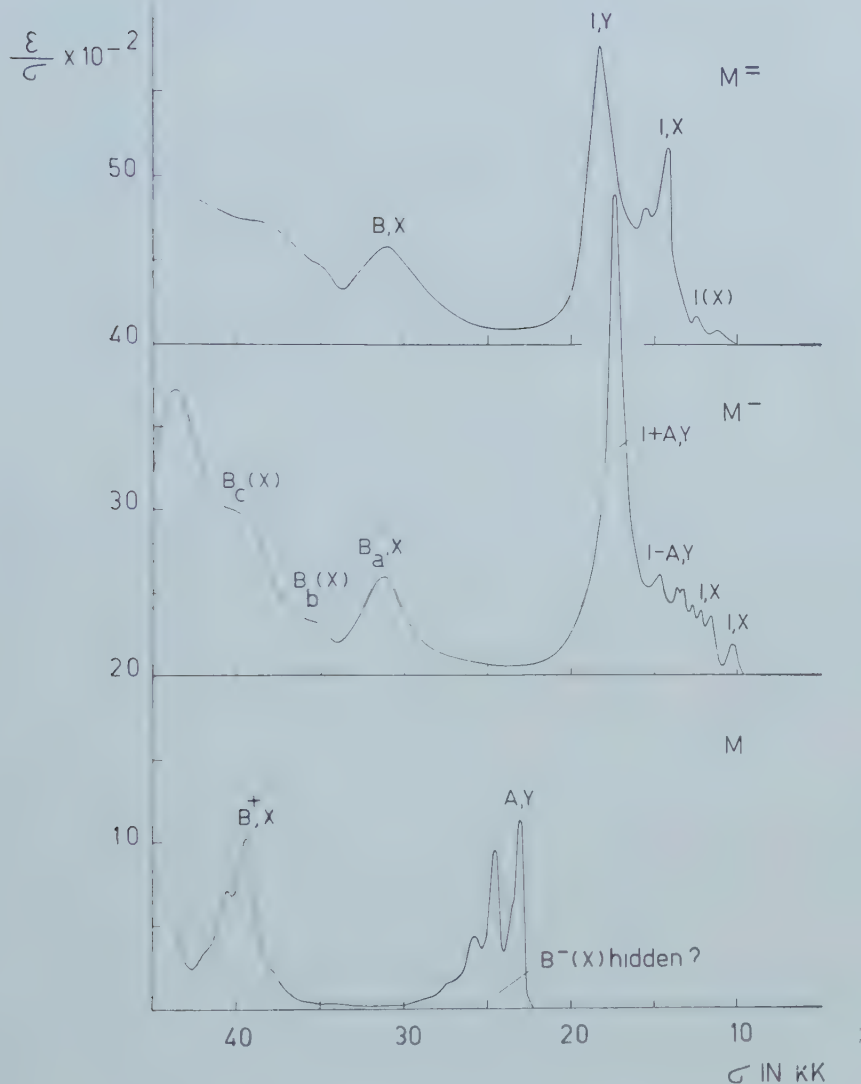


Figure 8. Absorption spectra of the perylene molecule and ions.

Two of the authors (N. H. V. and P. J. Z.) thank the Netherlands Organization for the Advancement of Pure Research (Z.W.O.) for financial aid during these investigations.

REFERENCES

- [1] HOIJTINK, G. J., 1959, *Mol. Phys.*, **2**, 85.
- [2] WEIJLAND, W. P., 1958, Thesis, Free University, Amsterdam; HOIJTINK, G. J., 1958, Colloque International sur le Calcul des Fonctions d'Onde Moléculaires, C.N.R.S., Paris.
- [3] McLACHLAN, A. D., 1959, *Mol. Phys.*, **2**, 271.
- [4] HOIJTINK, G. J., and WEIJLAND, W. P., 1957, *Rec. Trav. chim. Pays-Bas*, **76**, 836; AALBERSBERG, W. IJ., HOIJTINK, G. J., MACKOR, E. L., and WEIJLAND, W. P., 1959, *J. chem. Soc.*, 3049, 3055; BENNEMA, P., HOIJTINK, G. J., LUPINSKI, J. H., OOSTERHOFF, L. J., SELIER, P., and VAN VOORST, J. D. W., 1959, *Mol. Phys.*, **2**, 431.
- [5] PARISER, R., 1956, *J. chem. Phys.*, **24**, 50; POPPLE, J. A., 1955, *Proc. phys. Soc. Lond. A*, **68**, 81.
- [6] COLPA, J. P., Koninklijke/Shell Laboratorium, Amsterdam [private communication].
- [7] DEWAR, M. J. S., and LONGUET-HIGGINS, H. C., 1954, *Proc. phys. Soc. Lond. A*, **67**, 795.
- [8] BALK, P., DE BRUIJN, S., and HOIJTINK, G. J., 1957, *Rec. Trav. chim. Pays-Bas*, **76**, 908.
- [9] BALK, P., DE BRUIJN, S., and HOIJTINK, G. J., 1958, *Mol. Phys.*, **1**, 151.
- [10] COULSON, C. A., and RUSHBROOKE, G. S., 1940, *Proc. Camb. phil. Soc.*, **36**, 193.
- [11] PARISER, R., and PARR, R. G., 1953, *J. chem. Phys.*, **21**, 466, 767.
- [12] HOIJTINK, G. J., and ZANDSTRA, P. J., 1960, *Mol. Phys.*, **3**, 371.
- [13] MOFFITT, W., 1954, *J. chem. Phys.*, **22**, 320, 1820; PLATT, J. R., 1954, *J. chem. Phys.*, **22**, 1448 and related papers; HAM, N. S., and RUEDENBERG, K., 1956, *J. chem. Phys.*, **25**, 1.
- [14] JABLONSKI, A., 1935, *Z. Phys.*, **94**, 140.

The analysis of complex nuclear magnetic resonance spectra

I. Systems with one pair of strongly coupled nuclei

by J. A. POPLE and T. SCHAEFER†

National Physical Laboratory, Teddington

(Received 13 October 1960)

A general theory is presented of the high-resolution nuclear magnetic resonance spectra of systems in which two nuclei have a relative chemical shift comparable with their spin-coupling constant, all other relative chemical shifts being large. In the conventional notation such systems may be described as $ABR_pX_q\dots$, where $p, q\dots$ are small integers. All such systems can be handled within one theoretical scheme and the spectra, although possibly containing many lines, can be built up as the superposition of spectra of simpler types. The theory is illustrated by the analysis of the proton resonance spectrum of trans-crotonaldehyde which, in suitable solvents, is an example of ABR_3X .

1. INTRODUCTION

The analysis of high-resolution nuclear magnetic resonance spectra for molecules in which spin-coupling is not always small compared with chemical shifts is assisted by a schematic classification of spectra into types corresponding to certain simple nuclear groupings. A useful notation [1] is one in which different letters are used for chemically non-equivalent nuclei and consecutive letters refer specifically to nuclei between which spin-coupling constants are comparable with relative chemical shifts. Thus AB_2X_3 describes a system of three sets of nuclei with respectively one, two and three members, but the AB coupling constant is comparable with the AB chemical shift. The AX and BX coupling constants, on the other hand, are small compared with the AX and BX shifts, so that the NMR spectrum of the X-nuclei is well separated from that of A and B (or X may be a different nuclear species). If the nuclei all have spin $\frac{1}{2}$ (and we shall not consider nuclei of higher spin), the analysis of all AB_2X_3 groups proceeds similarly, although the molecules may differ greatly chemically.

A large number of spectral groupings have been analysed in various papers in the literature, usually by writing down a complete set of nuclear spin functions and diagonalizing the quantum-mechanical matrix of the appropriate spin Hamiltonian, using no-mixing and selection rules based on group theory and the symmetry of the molecule. All possible transitions between the resulting spin states are then listed. As the number of nuclei determining the spectrum increases, the total number of transitions increases rapidly and it is desirable to develop the theory in as systematic a manner as possible, showing where complex spectra can be treated in a composite manner, being built up of several spectra of a simpler type. This is possible, of course, for first-order spectra, where all chemical shifts are large compared with spin-coupling constants and simple multiplet rules frequently apply. In this paper we shall present a discussion of the

† Visiting Research Fellow, Summer 1960. Permanent address : Department of Chemistry, University of Manitoba, Winnipeg.

spectra of systems in which there are only two nuclei with strong coupling (i.e. comparable with their chemical shift), all others being well separated from each other. The simplest such cases are AB, ABX, $\text{ABX}_2\dots$, many of which have already been studied [1-5]. Our rather more general approach will show how these cases can be dealt with together and generalized to systems with more sets of nuclei such as ABR_pX_q where p and q are any small integers.

In § 4, the case ABR_3X is discussed in more detail as an example and illustrated by the proton resonance spectrum of trans-crotonaldehyde under conditions where the chemical shift between the A and B protons can be varied. This variation, like that of the external field can be used to determine relative signs of some of the coupling constants in the molecule [6].

2. THE ANALYSIS OF ABX_q SPECTRA

Complete analyses of ABX_q spectra for $q=1, 2, 3$ have already been presented. We reconsider them here, both to show how they can all be combined under an analysis for general q and as an introduction to methods applicable to more complex spectra to be developed in the next section.

The spin Hamiltonian (in cycles/sec) for an ABX_q system can be written

$$\mathcal{H} = \nu_A I_z(A) + \nu_B I_z(B) + \nu_X F_z(X) + J_{AB} \mathbf{I}(A) \cdot \mathbf{I}(B) + \mathbf{F}(X) \cdot [J_{AX} \mathbf{I}(A) + J_{BX} \mathbf{I}(B)] \quad (2.1)$$

where ν_A , ν_B and ν_X are the Larmor precession frequencies of A, B and X nuclei, J_{AB} , J_{AX} and J_{BX} the spin-coupling constants, and $\mathbf{F}(X)$ has been written for the total spin of all the X-nuclei.

$$\mathbf{F}(X) = \sum_{i=1}^q \mathbf{I}(\mathbf{X}_i). \quad (2.2)$$

The fact that all X-nuclei have the same chemical shift and the same coupling constants J_{AX} and J_{BX} means that only the total X-spin is significant, for it can be shown that the spectrum is independent of X-X coupling constants which can therefore be put equal to zero [7]. If all the nuclei are of the same species with magnetogyric ratio γ , the Larmor frequencies are related to the screening constants by

$$\left. \begin{array}{l} \nu_A = \gamma H_0 (1 - \sigma_A) / 2\pi, \\ \nu_B = \gamma H_0 (1 - \sigma_B) / 2\pi, \\ \nu_X = \gamma H_0 (1 - \sigma_X) / 2\pi, \end{array} \right\} \quad (2.2)$$

H_0 being the applied static field.

It is well known that the total spin component in the z -direction

$$F_z = I_z(A) + I_z(B) + F_z(X) \quad (2.3)$$

is a good quantum number, that is there is no mixing between spin functions with different values of F_z . Under the conditions we are considering (ABX_q rather than ABC_q), it is also true that $F_z(X)$ is a good quantum number and has a definite half-integral value in any stationary state. This means that terms in the Hamiltonian of the type $F_x(X) I_x(A)$, $F_y(X) I_y(A)$, etc. which only have off-diagonal matrix elements between functions with different $F_z(X)$ (specifying basic functions by their z -spin components) play no part in the calculation and can be ignored. The X-spin component $F_z(X)$ plays an important part in the theory

and for convenience we shall write it as x . We may then use an effective Hamiltonian

$$\mathcal{H} = [\nu_A + xJ_{AX}] I_z(A) + [\nu_B + xJ_{BX}] I_z(B) + x\nu_X + J_{AB} \mathbf{I}(A) \cdot \mathbf{I}(B). \quad (2.4)$$

The Hamiltonian (2.4) now depends on the X-nuclei only through the z -component of the X-spin. This has important consequences in simplifying the spectrum for, from the point of view of the A and B nuclei, coupling with the X-nuclei is merely equivalent to the experience of an additional magnetic field in the z -direction and leads to new 'effective Larmor frequencies' depending on x :

$$\left. \begin{aligned} \nu_A^*(x) &= \nu_A + xJ_{AX}, \\ \nu_B^*(x) &= \nu_B + xJ_{BX}. \end{aligned} \right\} \quad (2.5)$$

We can now solve the quantum-mechanical problem of the AB spin functions for a given x , using the Hamiltonian (2.4). This differs from the theory of an isolated AB pair only by replacing the Larmor frequencies ν_A and ν_B by the effective frequencies (2.5), so that there are four functions and energies as given in table 1.

	Wave function	Energy
1 _x	$\alpha\alpha$	$\frac{1}{2}\nu_A^*(x) + \frac{1}{2}\nu_B^*(x) + x\nu_X + \frac{1}{4}J_{AB}$
2 _x	$(\alpha\beta)\cos\theta_x + (\beta\alpha)\sin\theta_x$	$C_x + x\nu_X - \frac{1}{4}J_{AB}$
3 _x	$-(\alpha\beta)\sin\theta_x + (\beta\alpha)\cos\theta_x$	$-C_x + x\nu_X - \frac{1}{4}J_{AB}$
4 _x	$\beta\beta$	$-\frac{1}{2}\nu_A^*(x) - \frac{1}{2}\nu_B^*(x) + x\nu_X + \frac{1}{4}J_{AB}$

Table 1. AB wave functions and energy levels for given x in ABX_q systems.

The quantities θ_x and C_x in table 1 are both functions of the X-spin component x and are given by ($C_x > 0$, $0 \leq \theta_x < \pi$),

$$\left. \begin{aligned} C_x \cos 2\theta_x &= \frac{1}{2}(\nu_A^* - \nu_B^*), \\ C_x \sin 2\theta_x &= \frac{1}{2}J_{AB}, \end{aligned} \right\} \quad (2.6)$$

so that

$$\begin{aligned} C_x &= +\frac{1}{2}[(\nu_A^* - \nu_B^*)^2 + J_{AB}^2]^{1/2} \\ &= +\frac{1}{2}\{[(\nu_A - \nu_B) + x(J_{AX} - J_{BX})]^2 + J_{AB}^2\}^{1/2}. \end{aligned} \quad (2.7)$$

Although there is only one set of AB functions for each value of x there may be several corresponding X-functions. Thus if there are two X-nuclei ($q=2$), there is only one X-function corresponding to $x=1$ or $x=-1$ ($\alpha\alpha$ or $\beta\beta$) but there are two functions $((\alpha\beta + \beta\alpha)/\sqrt{2}$, $(\alpha\beta - \beta\alpha)/\sqrt{2}$) for $x=0$. For $q=3$, there are 1, 3, 3, 1 functions corresponding to the possible values $\frac{3}{2}$, $\frac{1}{2}$, $-\frac{1}{2}$, $-\frac{3}{2}$ of x . To distinguish between the different X-functions for a given x , we should have to specify additional quantum numbers such as the total X-spin, but these can always be chosen so that they do not change in any transition and need not be considered in detail.

Turning now to selection rules and the spectra that will actually be observed, we can consider AB- and X-transitions in turn. For the AB pair of nuclei, the selection rule is $\Delta F_z(AB) = \pm 1$, $\Delta x = 0$. Since x is the only way in which X-nuclei appear in the Hamiltonian, all AB transitions take place without any change in the spin arrangement of the X-nuclei. This means that the AB part of an ABX_q spectrum consists of a number of simple AB spectra (each consisting of four lines) for each possible value of x . The relative intensity of each such AB sub-spectrum will be determined by the number of X-states associated with the corresponding

value of x , which we shall write $n_q(x)$. For ABX_3 spectra, for example, there will be 1, 3, 3, 1 functions for $x = \frac{3}{2}, \frac{1}{2}, -\frac{1}{2}$ and $-\frac{3}{2}$. In general

$$n_q(x) = \frac{q!}{(\frac{1}{2}q-x)! (\frac{1}{2}q+x)!}. \quad (2.8)$$

The transition energies and intensities for each AB sub-spectrum are now easily obtained and are given in table 2.

Transition	Energy	Relative intensity
$3_x \rightarrow 1_x$	$\frac{1}{2}\nu_A^*(x) + \frac{1}{2}\nu_B^*(x) + C_x + \frac{1}{2}J_{AB}$	$n_q(x)\{1 - \sin 2\theta_x\}$
$4_x \rightarrow 2_x$	$\frac{1}{2}\nu_A^*(x) + \frac{1}{2}\nu_B^*(x) + C_x - \frac{1}{2}J_{AB}$	$n_q(x)\{1 + \sin 2\theta_x\}$
$2_x \rightarrow 1_x$	$\frac{1}{2}\nu_A^*(x) + \frac{1}{2}\nu_B^*(x) - C_x + \frac{1}{2}J_{AB}$	$n_q(x)\{1 + \sin 2\theta_x\}$
$4_x \rightarrow 3_x$	$\frac{1}{2}\nu_A^*(x) + \frac{1}{2}\nu_B^*(x) - C_x - \frac{1}{2}J_{AB}$	$n_q(x)\{1 - \sin 2\theta_x\}$

Table 2. Transition energies and intensities for two nuclei AB for given x in ABX_q systems.

The X-transitions can be discussed in a similar way. The selection rules are now $\Delta x = \pm 1$, $\Delta F_z(AB) = 0$ so that in any x -transition the total z -component of the AB spin is unchanged. But this can only take the values +1, 0 and -1. If $F_z(AB) = +1$, the AB wave function must be $\alpha\alpha$ before and after the transition, so that the z -spin component of the X-nuclei is changed by ± 1 in the presence of the $\alpha\alpha$ configuration of A and B. The A and B nuclei again give an effective field at the X-nuclei and the energy of the transition is clearly $\nu_X + \frac{1}{2}(J_{AX} + J_{BX})$. Similarly if $F_z(AB) = -1$, the only AB configuration is $\beta\beta$ and the corresponding X-transitions have energies $\nu_X - \frac{1}{2}(J_{AX} + J_{BX})$. This accounts for half of the possible AB states, so that half of the intensity of the X-spectrum will be concentrated in a simple doublet with separation equal to $(J_{AX} + J_{BX})$. These will be the strongest pair of lines in the X-spectrum and are usually picked out quite easily.

The remaining X-transitions occur with zero resultant z -spin in the AB set ($F_z(AB) = 0$) and are rather more complicated since the mixing of AB functions themselves is a function of x and is changed by the transition. Reference to table 1, shows that there will be four transitions in which x changes to $x+1$, the energies and intensities of which are given in table 3. Apart from the factor due to the mixing of AB functions, the intensity is also proportional to the number of X-transitions in which the z -component of the spin changes from x to $x+1$, (in the absence of the AB system) which we shall write $n_q(x \rightarrow x+1)$. For ABX_3 , for example, there are three transitions corresponding to $-\frac{3}{2} \rightarrow -\frac{1}{2}$, ($\beta\beta\beta \rightarrow \alpha\beta\beta$, $\beta\beta\beta \rightarrow \beta\alpha\beta$, $\beta\beta\beta \rightarrow \beta\beta\alpha$), six corresponding to $-\frac{1}{2} \rightarrow +\frac{1}{2}$, ($\alpha\beta\beta \rightarrow \alpha\beta\alpha$, $\alpha\beta\beta \rightarrow \alpha\alpha\beta$,

Transition	Energy	Relative intensity
$3_x \rightarrow 2_{x+1}$	$\nu_X + C_{x+1} + C_x$	$n_q(x \rightarrow x+1) \sin^2[\theta_{x+1} - \theta_x]$
$2_x \rightarrow 2_{x+1}$	$\nu_X + C_{x+1} - C_x$	$n_q(x \rightarrow x+1) \cos^2[\theta_{x+1} - \theta_x]$
$3_x \rightarrow 3_{x+1}$	$\nu_X - C_{x+1} + C_x$	$n_q(x \rightarrow x+1) \cos^2[\theta_{x+1} - \theta_x]$
$2_x \rightarrow 3_{x+1}$	$\nu_X - C_{x+1} - C_x$	$n_q(x \rightarrow x+1) \sin^2[\theta_{x+1} - \theta_x]$

Table 3. X-transitions ($x \rightarrow x+1$) for ABX_q systems with $F_z(AB) = 0$.

$\beta\alpha\beta \rightarrow \beta\alpha\alpha$, $\beta\alpha\beta \rightarrow \alpha\alpha\beta$, $\beta\beta\alpha \rightarrow \beta\alpha\alpha$, $\beta\beta\alpha \rightarrow \alpha\beta\alpha$) and three corresponding to $+\frac{1}{2} \rightarrow +\frac{3}{2}$, ($\beta\alpha\alpha \rightarrow \alpha\alpha\alpha$, $\alpha\beta\alpha \rightarrow \alpha\alpha\alpha$, $\alpha\alpha\beta \rightarrow \alpha\alpha\alpha$). In general,

$$n_q(x \rightarrow x+1) = \frac{q!}{(\frac{1}{2}q+x)! (\frac{1}{2}q-x-1)!}. \quad (2.9)$$

3. THE ANALYSIS OF ABR_pX_q SPECTRA

The method of calculating and interpreting ABX_q spectra developed in the previous section is easily extended to more complex systems in which there are several sets of equivalent nuclei, all well separated from each other and from AB and all satisfying the necessary conditions for coupling within the sets to be ignored. Rather than deal with a completely general case, we shall indicate in this section how systems with one additional set of nuclei can be handled. Such systems would be denoted by ABR_pX_q in the present notation.

Since the R and X spectra are both well separated from that of the AB nuclei, there will be effectively no mixing between functions with different z -components of spin $F_z(R)$ and $F_z(X)$. Following the simplified notation developed in the previous section, these quantities will be denoted by r and x . The effective Hamiltonian then has the form

$$\mathcal{H} = \nu_A^*(r, x) I_z(A) + \nu_B^*(r, x) I_z(B) + r\nu_R + x\nu_X + J_{AB} I(A) \cdot I(B) + rxJ_{RX}, \quad (3.1)$$

where A and B nuclei have effective Larmor frequencies now depending on both r and x :

$$\left. \begin{aligned} \nu_A^*(r, x) &= \nu_A + rJ_{AR} + xJ_{AX}, \\ \nu_B^*(r, x) &= \nu_B + rJ_{BR} + xJ_{BX}. \end{aligned} \right\} \quad (3.2)$$

The additional term rxJ_{RX} arises from coupling between R and X nuclei which again depends effectively only on the z -components of R- and X-spin.

There will be a set of four AB wave functions and energies for each pair of values of r and x . These summarized are in table 4, which is a direct extension of table 1. The quantities C_{rx} and θ_{rx} are defined by

$$\begin{aligned} C_{rx} \cos 2\theta_{rx} &= \frac{1}{2} [\nu_A^*(r, x) - \nu_B^*(r, x)] \\ &= \frac{1}{2} [(\nu_A - \nu_B) + r(J_{AR} - J_{BR}) + x(J_{AX} - J_{BX})], \end{aligned} \quad (3.3)$$

$$C_{rx} \sin 2\theta_{rx} = \frac{1}{2} J_{AB} \quad (C_{rx} > 0, \quad 0 \leq \theta_{rx} < \pi),$$

so that

$$C_{rx} = +\frac{1}{2}\{[(\nu_A - \nu_B) + r(J_{AR} - J_{BR}) + x(J_{AX} - J_{BX})]^2 + J_{AB}^2\}^{1/2}. \quad (3.4)$$

	Wave function	Energy
1_{rx}	$\alpha\alpha$	$\frac{1}{2}\nu_A^*(r, x) + \frac{1}{2}\nu_B^*(r, x) + r\nu_R + x\nu_X + \frac{1}{4}J_{AB} + rxJ_{RX}$
2_{rx}	$(\alpha\beta)\cos\theta_{rx} + (\beta\alpha)\sin\theta_{rx}$	$C_{rx} + r\nu_R + x\nu_X - \frac{1}{4}J_{AB} + rxJ_{RX}$
3_{rx}	$-(\alpha\beta)\sin\theta_{rx} + (\beta\alpha)\cos\theta_{rx}$	$-C_{rx} + r\nu_R + x\nu_X - \frac{1}{4}J_{AB} + rxJ_{RX}$
4_{rx}	$\beta\beta$	$-\frac{1}{2}\nu_A^*(r, x) - \frac{1}{2}\nu_B^*(r, x) + r\nu_R + x\nu_X + \frac{1}{4}J_{AB} + rxJ_{RX}$

Table 4. AB wave functions and energy levels for given x and r in ABR_pX_q systems.

Since r and x are unchanged in an AB transition, the AB spectrum will now consist of a superposition of a number of simple AB quartets, one for each value of r and x . There will be $(p+1)(q+1)$ such quartets in all. The transition energies will be just as in table 2, except that $\nu_A^*(x)$ $\nu_B^*(x)$, C_x and θ_x have to be replaced

by $\nu_A^*(r, x)$, $\nu_B^*(r, x)$, C_{rx} and θ_{rx} . The relative intensities will be proportional to $n_p(r)n_q(x)$, the number of R and X states with given r and x .

The X-spectrum can also be described in a manner which is a simple generalization of the previous spectrum for in X-transitions the R-spin r is conserved. The X-spectrum in ABR_pX_q , in fact, is a superposition of the X-spectra of $(p+1)$ different ABX_q systems, one for each value of the R-spin number r . Each of these will consist of a strong doublet ($F_z(AB) = \pm 1$) at $\nu_X + rJ_{RX} \pm \frac{1}{2}(J_{AX} + J_{BX})$ (the relative intensity of each line being $2^{q-1}qn_p(r)$ proportional to the total number of X-transitions and the number of R-states with spin component r). If there is no coupling between R and X, these doublets will all coincide at $\nu_X \pm \frac{1}{2}(J_{AX} + J_{BX})$. Further, for each value of r , there will be a set of $q(p+1)$ quartets $x \rightarrow x+1$ ($F_z(AB)=0$) as specified in table 5.

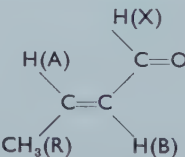
Transition	Energy	Relative intensity
$3_{rx} \rightarrow 2_{r, x+1}$	$\nu_X + rJ_{RX} + C_{r, x+1} + C_{rx}$	$n_p(r)n_q(x \rightarrow x+1)\sin^2(\theta_{r, x+1} - \theta_{rx})$
$2_{rx} \rightarrow 2_{r, x+1}$	$\nu_X + rJ_{RX} + C_{r, x+1} - C_{rx}$	$n_p(r)n_q(x \rightarrow x+1)\cos^2(\theta_{r, x+1} - \theta_{rx})$
$3_{rx} \rightarrow 3_{r, x+1}$	$\nu_X + rJ_{RX} - C_{r, x+1} + C_{rx}$	$n_p(r)n_q(x \rightarrow x+1)\cos^2(\theta_{r, x+1} - \theta_{rx})$
$2_{rx} \rightarrow 3_{r, x+1}$	$\nu_X + rJ_{RX} - C_{r, x+1} - C_{rx}$	$n_p(r)n_q(x \rightarrow x+1)\sin^2(\theta_{r, x+1} - \theta_{rx})$

Table 5. X-transitions ($x \rightarrow x+1$) for ABR_pX_q systems with $F_z(AB)=0$, $F_z(R)=r$.

The R-spectrum can be treated in a precisely similar manner simply by changing appropriate suffixes in the discussion of the X-spectrum.

4. THE PROTON RESONANCE SPECTRUM OF TRANS-CROTONALDEHYDE

As an example of the preceding discussion, we have measured and analysed the high-resolution proton resonance spectrum of trans-crotonaldehyde.



This is an example of an ABR_3X system with the above labelling of protons, if conditions are such that the AB chemical shift is small.

4.1. Experimental

The proton resonance spectra were measured for neat trans-crotonaldehyde and in 10 vol. per cent in benzene at 60 Mc/s on a Varian spectrometer. The trans-crotonaldehyde was a B.D.H. reagent. Although the chemical shifts were measured in the pure state, they are of minor interest here since they are strongly solvent dependent.

Calibrations were done using the sideband technique. A check was provided by superposing a peak from another part of the spectrum on chosen peaks. These peaks were then traversed, the frequency being adjusted for maximum intensity. For strong peaks, this procedure permitted the determination of peak separation to at least 0.2 c/s and often to 0.1 c/s. The centre of the CHO resonance was measured as 79.4 ± 0.2 c/s to low field of an external chloroform reference.

4.2. Results and discussion

The complete spectrum is not shown on one trace since the chemical shifts are relatively large. For the neat compound, the olefinic (AB) spectrum is shown in figure 1 and the methyl (R) and aldehyde (X) spectra in figure 2. The AB chemical shift is relatively large and the spectra are reasonably interpreted on the basis of first-order theory. Both the A and B protons are split into 1:3:3:1

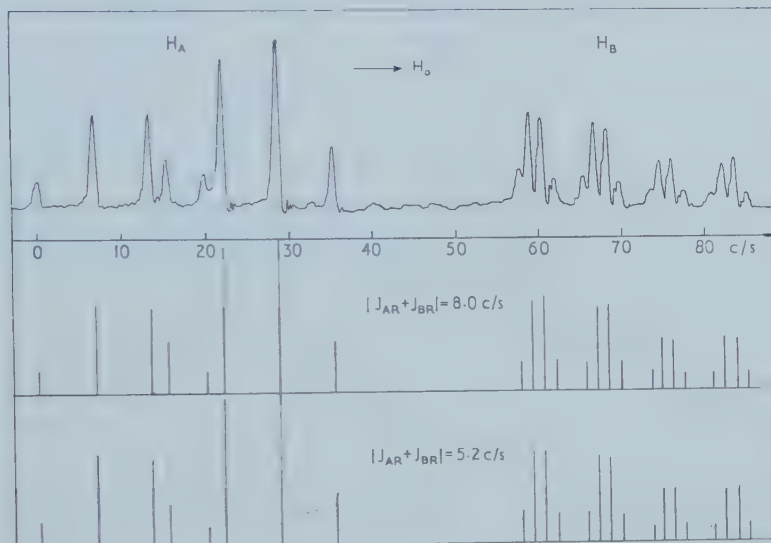


Figure 1. The observed spectrum of the AB (olefinic) protons in neat trans-crotonaldehyde together with the calculated spectra for the two assignments discussed in the text. The magnetic field increases from right to left.

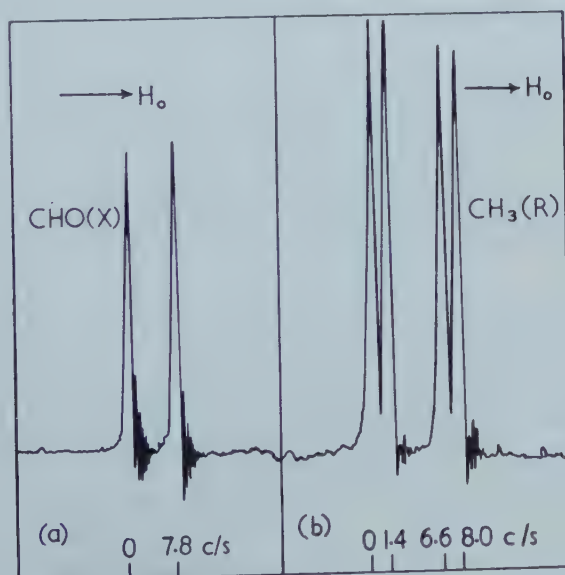


Figure 2. The observed spectra of (a) the X (aldehyde) proton and (b) the R (methyl) protons in neat trans-crotonaldehyde.

quartets by the methyl (R) group, but only the B-spectrum shows an additional doubling due to the aldehyde (X) proton. These splittings are, in fact, the basis of the AB assignment. Correspondingly, the X- and R-spectra show two and four sharp lines of equal intensity, as expected on the basis of first order theory if there is no AX or RX coupling (note the 'wiggles' with no noticeable beat in figure 2(a)).

First-order spectra are insufficient to determine the relative signs of spin-coupling constants, and in the present instance it is impossible to compare J_{AR} and J_{BR} without examining the spectra in more detail. Without a knowledge of the relative signs of J_{AR} and J_{BR} , there is an ambiguity in the assignment of peaks in the R region (figure 2(b)). We can set $|J_{AX} + J_{BX}| = 8.0$ c/s, the separation between the outer peaks or $|J_{AR} + J_{BR}| = 5.2$ c/s, the separation between the inner peaks. The two assignments correspond to equal or opposite signs for J_{AR} and J_{BR} .

This uncertainty can be removed by examining the spectrum to higher accuracy in the AB region as an ABR_3X system. This leads to a small change in the predicted intensity of some of the peaks. Figure 1 gives calculated spectra for both assignments (we shall not describe these calculations in detail as spectra in benzene solution to be described below provide a better example of ABR_3X). Distinguishing between the two requires an assessment of the relative intensities of lines about a cycle/sec apart which suggests that $|J_{AR} + J_{BR}| = 5.2$ c/s is correct. But the intensity difference is not large enough to be convincing.

Assuming that the larger proton spin-coupling constants are positive, the two assignments lead to the following sets of constants.

$$\begin{aligned} J_{AB} &= J_{HH}(\text{trans}) &= 15.6 \pm 0.2 \text{ c/s}, \\ J_{AR} &= J_{H, CH_3}(\text{gem}) &= 6.8 \pm 0.2 \text{ c/s}, \\ J_{BR} &= J_{H, CH_3}(\text{cis}) &= 1.2 \pm 0.2 \text{ c/s} \quad \text{or} \quad -1.6 \pm 0.2 \text{ c/s}, \\ J_{BX} &= J_{H_R, CHO} &= 7.8 \pm 0.2 \text{ c/s}, \\ J_{AX} &= J_{H_A, CHO} &= 0. \end{aligned}$$

The corresponding chemical shifts are ($\nu_0 = 60$ Mc/s):

$$\begin{aligned} \nu_0(\sigma_B - \sigma_A) &= 51.5 \pm 0.2 \text{ c/s}, \\ \nu_0(\sigma_B - \sigma_X) &= 204.3 \pm 0.3 \text{ c/s}, \\ \nu_0(\sigma_R - \sigma_B) &= 246.3 \pm 0.4 \text{ c/s}. \end{aligned}$$

In the solution in benzene, the AB chemical shift is substantially reduced and the spectrum then becomes a fuller example of an ABR_3X system and provides more conclusive evidence for the opposite sign of J_{AR} and J_{BR} (changes in spin-coupling constants due to solvents are usually very small). The relevant AB spectrum is shown in figure 4 and the R and X spectra in figure 3. From the methyl spectrum (figure 3(a)), it is immediately clear that the two large peaks (corresponding to methyl transitions with AB in the $\alpha\alpha$ or $\beta\beta$ states) are separated by 5.2 c/s rather than 8.0 c/s. This separation must be equal to $|J_{AR} + J_{BR}|$, confirming the previous suggestion that J_{AR} and J_{BR} have opposite signs.

The remaining features of the spectra shown in figures 3 and 4 can be interpreted in terms of the analysis of § 3 and used to determine the AB chemical shift.

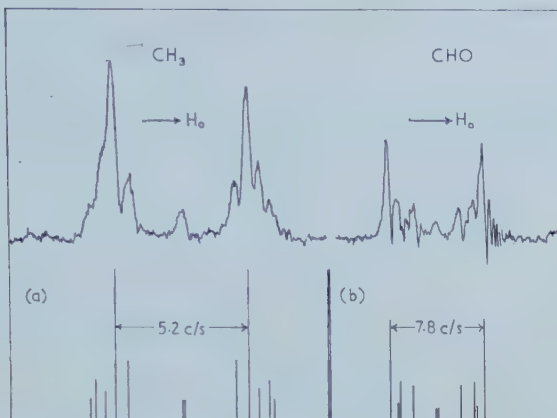


Figure 3. The observed and calculated spectra for the assignment $(J_{\text{AR}} + J_{\text{BR}}) = 5.2 \text{ c/s}$ for (a) the methyl protons and (b) the aldehyde proton in trans-crotonaldehyde at a concentration of 10 volume per cent in benzene.

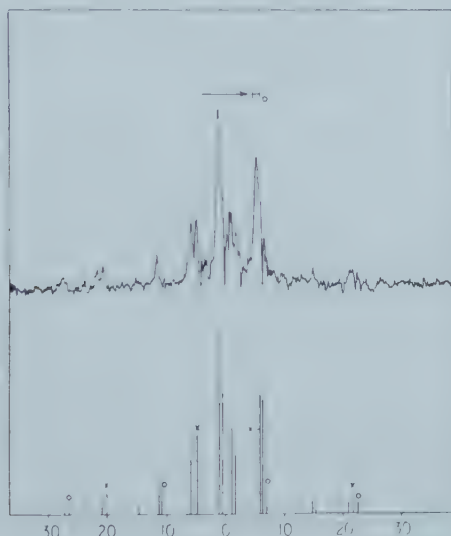


Figure 4. The observed and calculated spectrum for the assignment $(J_{\text{AR}} + J_{\text{BR}}) = 5.2 \text{ c/s}$ for the AB (olefinic) protons in trans-crotonaldehyde at a concentration of 10 volume per cent in benzene. The magnetic field increases from left to right.

Using the same coupling constants as for the neat compound (with the negative sign for J_{BR}), the value of $\nu_0(\sigma_B - \sigma_A)$ was taken to be 13.0 c/s after several trial calculations. The spin components r and x of the methyl and aldehyde protons can take values $\frac{3}{2}, \frac{1}{2}, -\frac{1}{2}, -\frac{3}{2}$ and $-\frac{1}{2}, -\frac{1}{2}$ respectively so that there will be eight C_{rx} parameters given by equation (3.4). These are (in c/s)

$$C_{\frac{3}{2}, \frac{1}{2}} = 13.36 \quad C_{\frac{1}{2}, -\frac{1}{2}} = 16.69$$

$$C_{\frac{1}{2}, \frac{1}{2}} = 10.25 \quad C_{\frac{1}{2}, -\frac{1}{2}} = 13.12$$

$$C_{-\frac{1}{2}, \frac{1}{2}} = 8.18 \quad C_{-\frac{1}{2}, -\frac{1}{2}} = 10.05$$

$$C_{-\frac{1}{2}, \frac{1}{2}} = 7.99 \quad C_{-\frac{1}{2}, -\frac{1}{2}} = 8.09$$

Apart from the two strong lines, the aldehyde proton (X) spectra should consist of four quartets as given by table 5 (one for each value of the methyl spin r). In fact only the inner members of each quartet are of appreciable intensity and these are shown in the calculated spectrum of figure 3 (b) which is in good agreement with the observed peaks. The central pair (which are not resolved) correspond to flipping the X-spin when the methyl group is in the state $\beta\beta\beta$.

In a similar manner, the methyl proton (R) spectrum should consist of six quartets (three for each state of the X-nucleus), but again the θ -angles are approximately equal and only the inner pairs of each quartet have appreciable intensity. The calculated spectrum is given in figure 3 (a) and the central (unresolved) pair is easily interpreted as the transition $-\frac{3}{2} \rightarrow -\frac{1}{2}$ in the presence of $x = +\frac{1}{2}$.

The olefinic (AB) spectrum in this molecule is a superposition of eight simple AB quartets corresponding to the four possible values of the methyl spin (r) and the two values of the aldehyde spin (x). All of these quartets should have J_{AB} as the common spacing between outer members. Figure 4 shows the spectrum calculated from the theory and indicates two of the quartets. Agreement with experiment is again satisfactory. It would, of course, be very difficult to analyse this part of the spectrum on its own without the additional information obtainable from the R- and X-spectra.

Certain other points about the details of these spectra are worth noting. The values of the coupling constants fall into the range obtained by other workers for similar compounds (3, 4, 5, 8, 9). In particular, Fessenden and Waugh's value of -1.8 c/s for J_{CH_3H} (cis) in trans-propenyl benzene can be compared with the present value of -1.6 c/s for trans-crotonaldehyde.

The effect of benzene on the relative chemical shift of the olefinic protons is striking, since it means that there is a preferential shift to high field of about 0.7 ppm for the A-proton in going from the neat compound to 10 per cent solution. Equally striking preferential benzene solvent shifts for particular protons have been found in vinyl bromide (6) and substituted benzenes (10). These effects are not fully understood and more systematic experimental work is in progress.

The work described above has been carried out as part of the research programme of the National Physical Laboratory, and this paper is published by permission of the Director of the Laboratory.

REFERENCES

- [1] BERNSTEIN, H. J., POPLE, J. A., and SCHNEIDER, W. G., 1957, *Canad. J. Chem.*, **35**, 65.
- [2] GUTOWSKY, H. S., HOLM, C. H., SAIKA, A., and WILLIAMS, G. A., 1957, *J. Amer. chem. Soc.*, **79**, 4596.
- [3] MORTIMER, F. S., 1959, *J. mol. Spectrosc.*, **3**, 335.
- [4] COHEN, A. D., and SHEPPARD, N., 1959, *Proc. roy. Soc. A*, **252**, 488.
- [5] FESSENDEN, R. W., and WAIGH, J. S., 1959, *J. chem. Phys.*, **30**, 944.
- [6] SCHAEFER, T., and SCHEIDER, W. G., *Canad. J. Chem.* (in the press).
- [7] GUTTOWSKY, H. S., MCCALL, D. W., and SLICHTER, C. P., 1953, *J. chem. Phys.*, **21**, 279.
- [8] BISHOP, E. O., and RICHARDS, R. E., 1960, *Mol. Phys.*, **3**, 114.
- [9] FRASER, R., 1960, *Canad. J. Chem.*, **38**, 549.
- [10] SCHAEFER T., and SCHNEIDER, W. G., 1960, *J. chem. Phys.*, **32**, 1218.

The analysis of complex nuclear magnetic resonance spectra II. Some further systems with one strong coupling constant

by P. DIEHL† and J. A. POPPLE
National Physical Laboratory, Teddington

(Received 13 October 1960)

The theoretical scheme described in Part I for the analysis of nuclear resonance spectra of the type ABX_q is extended to systems AB_2X_q where the symmetry is such that there is only one BX coupling constant. It is shown that these spectra can be interpreted in a systematic manner for all q . The spectra allow determination of the relative signs of all three coupling constants and can therefore be used to compare couplings between nuclei of different species (AX and BX) with the coupling between nuclei of the same species (AB). Further systems which could be studied by similar methods are indicated briefly.

1. INTRODUCTION

The previous paper [1] (Part I) discussed the high-resolution nuclear magnetic resonance spectra of groups of nuclei where there was only one pair of non-equivalent nuclei between which the spin-coupling was large compared with the chemical shift. In the conventional notation such systems may be denoted by $ABR_pX_q\dots$, A and B being the strongly coupled nuclei, and R_p , $X_q\dots$, being the other sets of equivalent nuclei all well separated and such that the coupling of all R-nuclei is the same to all nuclei within another set (and similarly with all X-nuclei, etc.). The theoretical spectra of systems of this type can all be calculated explicitly since the secular equations arising are never more than second order. In the present paper, we shall show how similar simplifications apply in certain other cases.

To see how this generalization is possible, let us return to the ABX_q systems considered previously [1]. It was shown that the quantum-mechanical problem was simplified because the total Hamiltonian effectively depends on the X-nuclei only through the z -component of the X-spin which was denoted by x . This becomes a good quantum number and it is possible to think of a set of AB states associated with each value of x . In this sub-problem, the effect of the X-nuclei is equivalent to replacing the Larmor frequencies ν_A and ν_B by effective frequencies $\nu_A^* = \nu_A + xJ_{AX}$ and $\nu_B^* = \nu_B + xJ_{BX}$.

This type of simplification does not depend on the complexity of the group of strongly coupled nuclei. Thus for $ABCX_q$, the z -component of the X-spin is well defined for each state and the quantum-mechanical problem reduces to that of $(q+1)$ ABC systems, which now, of course, involve 3×3 secular equations. Again, these sub-problems can be solved by introducing three effective frequencies ν_A^* , ν_B^* and ν_C^* . If B and C become equivalent, a further symmetry element is introduced and we have AB_2X_q where all BX coupling constants are the same. The energy levels and spectra for these systems can be dealt with explicitly and are described in the next section.

† Guest worker at N.P.L., summer 1960. Permanent address : Physics Department, University of Basle, Switzerland.

It should be emphasized that this simplified technique only applies if all BX coupling constants are identical. It does not apply, for example, to AB_2X_2 systems in which there are two BX constants as in pyridine [2]. It is useful to introduce a special notation for a set of nuclei which are not only chemically equivalent and have the same chemical shift but are also equally coupled to any particular nucleus in another set. Such sets will be referred to as magnetically equivalent [3] and denoted by an asterisk. In this sense, the three protons of a rapidly rotating methyl group are magnetically equivalent, whereas the two ortho protons in a monosubstituted benzene are not. In this notation, the systems to be considered are AB_2X_2^* or $\text{AB}_2^*\text{X}_2^*$.

2. THE ANALYSIS OF $\text{AB}_2^*\text{X}_q^*$ SPECTRA

It is well known that the spectra of any system of this type is independent of the coupling constants within the equivalent sets, so J_{BB} and J_{XX} may be put equal to zero. Using the same arguments as in Part I, we can immediately write an effective Hamiltonian

$$\mathcal{H} = [\nu_A + xJ_{\text{AX}}]I_z(A) + [\nu_B + xJ_{\text{BX}}][I_z(B_1) + I_z(B_2)] + x\nu_X + J_{\text{AB}}\mathbf{I}(A) \cdot [\mathbf{I}(B_1) + \mathbf{I}(B_2)]. \quad (2.1)$$

There will be no mixing between spin-functions corresponding to different values of x , and for each x , (2.1) is an AB_2 Hamiltonian with effective frequencies

$$\begin{aligned} \nu_A^* &= \nu_A + xJ_{\text{AX}} = \nu_0(1 - \sigma_A) + xJ_{\text{AX}}, \\ \nu_B^* &= \nu_B + xJ_{\text{BX}} = \nu_0(1 - \sigma_B) + xJ_{\text{BX}}. \end{aligned} \quad (2.2)$$

Using the well-known AB_2 theory, we can at once give the wave functions and energy levels for each value of x (table 1).

	Wave function	Energy
1 _x	$\alpha\alpha\alpha$	$\frac{1}{2}\nu_A^*(x) + \nu_B^*(x) + x\nu_X + \frac{1}{2}J_{\text{AB}}$
2 _x	$2^{-1/2}\cos\theta_x^+\alpha(\alpha\beta + \beta\alpha) + \sin\theta_x^+\beta\alpha\alpha$	$\frac{1}{2}\nu_B^*(x) + x\nu_X - \frac{1}{4}J_{\text{AB}} + C_x^+$
3 _x	$-2^{-1/2}\sin\theta_x^+\alpha(\alpha\beta + \beta\alpha) + \cos\theta_x^+\beta\alpha\alpha$	$\frac{1}{2}\nu_B^*(x) + x\nu_X - \frac{1}{4}J_{\text{AB}} - C_x^+$
4 _x	$\cos\theta_x^-\alpha\beta\beta + 2^{-1/2}\sin\theta_x^-\beta(\alpha\beta + \beta\alpha)$	$-\frac{1}{2}\nu_B^*(x) + x\nu_X - \frac{1}{4}J_{\text{AB}} + C_x^-$
5 _x	$-\sin\theta_x^-\alpha\beta\beta + 2^{-1/2}\cos\theta_x^-\beta(\alpha\beta + \beta\alpha)$	$-\frac{1}{2}\nu_B^*(x) + x\nu_X - \frac{1}{4}J_{\text{AB}} - C_x^-$
6 _x	$\beta\beta\beta$	$-\frac{1}{2}\nu_A^*(x) - \nu_B^*(x) + x\nu_X + \frac{1}{2}J_{\text{AB}}$
7 _x	$2^{-1/2}\alpha(\alpha\beta - \beta\alpha)$	$\frac{1}{2}\nu_A^*(x) + x\nu_X$
8 _x	$2^{-1/2}\beta(\alpha\beta - \beta\alpha)$	$-\frac{1}{2}\nu_A^*(x) + x\nu_X$

Table 1. AB_2^* wave functions and energy levels for given x in $\text{AB}_2^*\text{X}_q^*$ systems.

The quantities θ_x^+ , θ_x^- , C_x^+ , C_x^- , are given by
 $C_x^+ \cos 2\theta_x^+ = \frac{1}{2}[\nu_A^*(x) - \nu_B^*(x)] + \frac{1}{4}J_{\text{AB}} = \frac{1}{2}(\nu_A - \nu_B) + \frac{1}{2}x(J_{\text{AX}} - J_{\text{BX}}) + \frac{1}{4}J_{\text{AB}}$,
 $C_x^+ \sin 2\theta_x^+ = 2^{-1/2}J_{\text{AB}}$,
 $C_x^- \cos 2\theta_x^- = \frac{1}{2}[\nu_A^*(x) - \nu_B^*(x)] - \frac{1}{4}J_{\text{AB}} = \frac{1}{2}(\nu_A - \nu_B) + \frac{1}{2}x(J_{\text{AX}} - J_{\text{BX}}) - \frac{1}{4}J_{\text{AB}}$,
 $C_x^- \sin 2\theta_x^- = 2^{-1/2}J_{\text{AB}}$. (2.3)

As in Part I, the AB region has the selection rule $x=0$, so that this part of an $\text{AB}_2^*\text{X}_q^*$ spectrum consists of $(q+1)$ simple AB_2 spectra, one for each value of x . The relative intensities of these AB_2 sub-spectra are proportional to the number of states of the X-nuclei with this value of x .

$$n_q(x) = \frac{q!}{(\frac{1}{2}q-x)! (\frac{1}{2}q+x)!}. \quad (2.4)$$

Explicit expressions for transition energies and intensities are listed in table 2.

Transition	Energy	Relative intensity/ $n_q(x)$
$3_x \rightarrow 1_x$	$\frac{1}{2}\nu_A^*(x) + \frac{1}{2}\nu_B^*(x) + \frac{3}{4}J_{AB} + C_x^+$	$[2^{1/2} \sin \theta_x^+ - \cos \theta_x^+]^2$
$5_x \rightarrow 2_x$	$\nu_B^*(x) + C_x^+ + C_x^-$	$[2^{1/2} \sin(\theta_x^+ - \theta_x^-) + \cos \theta_x^+ \cos \theta_x^-]^2$
$8_x \rightarrow 7_x$	$\nu_A^*(x)$	1
$6_x \rightarrow 4_x$	$\frac{1}{2}\nu_A^*(x) + \frac{1}{2}\nu_B^*(x) - \frac{3}{4}J_{AB} + C_x^-$	$[2^{1/2} \sin \theta_x^- + \cos \theta_x^-]^2$
$4_x \rightarrow 2_x$	$\nu_B^*(x) + C_x^+ - C_x^-$	$[2^{1/2} \cos(\theta_x^+ - \theta_x^-) + \cos \theta_x^+ \sin \theta_x^-]^2$
$2_x \rightarrow 1_x$	$\frac{1}{2}\nu_A^*(x) + \frac{1}{2}\nu_B^*(x) + \frac{3}{4}J_{AB} - C_x^+$	$[2^{1/2} \cos \theta_x^+ + \sin \theta_x^+]^2$
$5_x \rightarrow 3_x$	$\nu_B^*(x) - C_x^+ + C_x^-$	$[2^{1/2} \cos(\theta_x^+ - \theta_x^-) - \sin \theta_x^+ \cos \theta_x^-]^2$
$6_x \rightarrow 5_x$	$\frac{1}{2}\nu_A^*(x) + \frac{1}{2}\nu_B^*(x) - \frac{3}{4}J_{AB} - C_x^-$	$[2^{1/2} \cos \theta_x^- - \sin \theta_x^-]^2$
$4_x \rightarrow 3_x$	$\nu_B^*(x) - C_x^+ - C_x^-$	$[2^{1/2} \sin(\theta_x^+ - \theta_x^-) + \sin \theta_x^+ \sin \theta_x^-]^2$

Table 2. AB transition energies and intensities for $AB_2^*X_q^*$ spectra for given x .

The X-transitions are rather more complicated and have to be found by reference to table 1, using the selection rule $\Delta x = \pm 1$, $\Delta F_2(AB_2) = 0$. In addition, X-transitions are only allowed if the symmetry of the AB_2 spin-function is left unchanged. Thus for the four AB_2 states

$$\alpha\alpha\alpha, \quad 2^{-1/2}\alpha(\alpha\beta - \beta\alpha), \quad 2^{-1/2}\beta(\alpha\beta - \beta\alpha), \quad \beta\beta\beta$$

the effect of the A and B nuclei is equivalent to an effective field at the X-nuclei and corresponding X-transitions have energies at

$$\nu_X + \frac{1}{2}J_{AX} + J_{BX}, \quad \nu_X + \frac{1}{2}J_{AX}, \quad \nu_X - \frac{1}{2}J_{AX}, \quad \nu_X - \frac{1}{2}J_{AX} - J_{BX}.$$

These account for half of the total X-intensity. For other AB_2 states, the mixing is changed by altering the X-spin and corresponding transition energies are derived from the state energies listed in table 1. Details of all X-transitions are given in table 3, the intensity factor $n_q(x \rightarrow x+1)$ being given as in Part I by

$$n_q(x \rightarrow x+1) = \frac{q!}{(\frac{1}{2}q+x)! (\frac{1}{2}q-x-1)!}. \quad (2.5)$$

Transition	Energy	Relative intensity/ $n_q(x \rightarrow x+1)$
$1_x \rightarrow 1_{x+1}$	$\nu_X + \frac{1}{2}J_{AX} + J_{BX}$	1
$7_x \rightarrow 7_{x+1}$	$\nu_X + \frac{1}{2}J_{AX}$	1
$8_x \rightarrow 8_{x+1}$	$\nu_X - \frac{1}{2}J_{AX}$	1
$6_x \rightarrow 6_{x+1}$	$\nu_X - \frac{1}{2}J_{AX} - J_{BX}$	1
$3_x \rightarrow 2_{x+1}$	$\nu_X + \frac{1}{2}J_{BX} + C_{x+1}^+ + C_x^+$	$\sin^2(\theta_{x+1}^+ - \theta_x^+)$
$2_x \rightarrow 2_{x+1}$	$\nu_X + \frac{1}{2}J_{BX} + C_{x+1}^+ - C_x^+$	$\cos^2(\theta_{x+1}^+ - \theta_x^+)$
$3_x \rightarrow 3_{x+1}$	$\nu_X + \frac{1}{2}J_{BX} - C_{x+1}^+ + C_x^+$	$\cos^2(\theta_{x+1}^+ - \theta_x^+)$
$2_x \rightarrow 3_{x+1}$	$\nu_X + \frac{1}{2}J_{BX} - C_{x+1}^+ - C_x^+$	$\sin^2(\theta_{x+1}^+ - \theta_x^+)$
$5_x \rightarrow 4_{x+1}$	$\nu_X - \frac{1}{2}J_{BX} + C_{x+1}^- + C_x^-$	$\sin^2(\theta_{x+1}^- - \theta_x^-)$
$4_x \rightarrow 4_{x+1}$	$\nu_X - \frac{1}{2}J_{BX} + C_{x+1}^- - C_x^-$	$\cos^2(\theta_{x+1}^- - \theta_x^-)$
$5_x \rightarrow 5_{x+1}$	$\nu_X - \frac{1}{2}J_{BX} - C_{x+1}^- + C_x^-$	$\cos^2(\theta_{x+1}^- - \theta_x^-)$
$4_x \rightarrow 5_{x+1}$	$\nu_X - \frac{1}{2}J_{BX} - C_{x+1}^- - C_x^-$	$\sin^2(\theta_{x+1}^- - \theta_x^-)$

Table 3. X-transitions ($x \rightarrow x+1$) for $AB_2^*X_q^*$ spectra.

The simplest systems to which this analysis is applicable are AB_2X for which $q=1$. This occurs for some symmetrical meta-disubstituted benzenes, an example having been studied by Abraham *et al.* [4]. According to the present analysis, the AB_2 part of the spectrum consists of two simple AB_2 spectra of the same total intensity but different apparent $J/\nu_0\delta$ ratios. These two sub-spectra can immediately be assigned to the AB_2 transitions in the presence of the two possible states (α, β) of the X-nucleus. The X-part of the AB_2X spectrum shows twelve lines as indicated in table 3. Four of these occur as two doublets with separations $J_{\text{AX}} + 2J_{\text{BX}}$ and J_{AX} centred on ν_{X} . Their intensity is half the total X-intensity. The remaining eight lines are centred as two quartets on $\nu_{\text{X}} \pm \frac{1}{2}J_{\text{BX}}$.

The spectra of $\text{AB}_2^*\text{X}_2^*$ systems ($q=2$) can be built up in a similar manner. The AB part now consists of three separate AB_2 spectra with relative intensities $1:2:1$ (corresponding to $x = -1, 0, +1$) and there are in all 20 lines in the X-spectrum (given by table 3 for $-1 \rightarrow 0$ and $0 \rightarrow +1$).

It is interesting to note that $\text{AB}_2^*\text{X}_q^*$ spectra can be used to determine the relative signs of all three coupling constants J_{AX} , J_{BX} and J_{AB} . The sign of J_{AB} relative to J_{BX} is deducible since the X-spectrum is not symmetric about ν_{X} and inspection of table 3 shows that changing the sign of J_{AB} interchanges C_x^+ and C_x^- and consequently inverts this asymmetry. This does not apply to the ABX_q systems discussed in Part I.

3. APPLICATION TO MORE COMPLEX SYSTEMS

The method of calculating spectra developed in Part I and used in the previous section can be extended to apply to many other systems. Additional sets of magnetically equivalent nuclei, with signals well separated from others, can be introduced. Thus $\text{AB}_2^*\text{R}_p^*\text{X}_q^*$ can be treated by specifying AB_2 states for each value of the z -component of R-spin (r) and X-spin (x). This is precisely analogous to the extension of ABX_q to ABR_pX_q described in detail in Part I.

Another extension would be to the general case $\text{AB}_n^*\text{X}_q^*$ where n is a general integer. Waugh and Dobbs [3] have described the analysis of AB_n systems in terms which only involve the solution of 2×2 secular equations. The AB part of an $\text{AB}_n^*\text{X}_q^*$ spectrum will consist of $(q+1)$ separate AB_n spectra, one for each value of the X-spin component x . The X-spectra could also be described by an extension of the methods used in this paper.

Most generally, the methods that have been outlined may be used to extend the discussion of any spectral system $\text{A}_m\text{B}_n\dots$ by adding additional sets of magnetically equivalent nuclei $\text{R}_p^*\text{X}_q^*\dots$ which give signals well separated from the other sets. The AB... parts of such $\text{A}_m\text{B}_n\dots\text{R}_p^*\text{X}_q^*\dots$ spectra consist of a superposition of $(p+1)(q+1)\dots$ separate $\text{A}_m\text{B}_n\dots$ spectra specified by the individual R, X... spin components r, x, \dots . These sub-spectra are each determined by effective Larmor frequencies

$$\nu_i^*(r, x, \dots) = \nu_i + rJ_{i\text{R}} + xJ_{i\text{X}} + \dots \quad (3.1)$$

They may, of course, be quite dissimilar. The R-spectrum of such a system would be obtained from a table of $\text{A}_m\text{B}_n\dots$ levels with effective frequencies together with selection rules $\Delta F_z(\text{A}_m\text{B}_n\dots) = 0$, $\Delta r = \pm 1$, $\Delta x = 0$, and any appropriate symmetry rules.

The work described above has been carried out as part of the research programme of the National Physical Laboratory, and this paper is published by permission of the Director of the Laboratory. Dr. P. Diehl gratefully acknowledges support given by the Swiss National Foundation for the Advancement of Science and by the University of Basle.

REFERENCES

- [1] POPLE, J. A., and SCHAEFER, T., 1961, *Mol. Phys.*, **3**, 547 (part I).
- [2] SCHNEIDER, W. G., BERNSTEIN, H. J., and POPLE, J. A., 1957, *Canad. J. Chem.*, **35**, 1487.
- [3] WAUGH, J. S., and DODDS, F. W., 1959, *J. chem. Phys.*, **31**, 1235.
- [4] ABRAHAM, R. J., BISHOP, E. O., and RICHARDS, R. E., 1960, *Mol. Phys.*, **3**, 485.

Equilibrium properties of crystalline argon, krypton and xenon

by E. A. GUGGENHEIM and M. L. McGlashan

Department of Chemistry, The University, Reading

(Received 10 October 1960)

By assuming an interaction energy for krypton and xenon of the same shape as that established for argon in an earlier paper and without introducing any adjustable parameters, values of the equilibrium properties of the crystals have been calculated which agree with the measured values to within the experimental accuracy or to within one per cent.

1. SCOPE

In a recently published paper [1] we used the experimental data on all the equilibrium properties of crystalline argon and experimental data on gaseous argon to derive the interaction energy between pairs of argon atoms as a function of their distance apart. This was found to be strikingly different from the commonly assumed 6:12 or other 6: n forms. In principle it should be possible to repeat this programme for krypton and xenon, but as experimental measurements on these two substances are less extensive such a detailed analysis as was made for argon seems not worthwhile. It is more profitable to proceed differently.

It is well known that argon, krypton and xenon conform with high accuracy to the principle of corresponding states as far as concerns the equilibrium properties of the fluid state. This implies that the curves of interaction energy plotted against distance have similar shapes. It is therefore interesting to assume tentatively that the interaction energy curves have exactly the same shape and on this assumption to calculate the properties of the crystal and see how good is the agreement between the values so calculated and the experimental values. This is the programme of the present paper. The three properties of the crystal investigated are the density (or molecular volume), the entropy and the energy each through the range of temperature from the triple point down to about 20°K. The agreement between calculated and measured values is striking.

2. NOTE ON CORRESPONDING STATES

We are assuming, as is usual in connection with the principle of corresponding states, that the curve of the interaction energy plotted against distance apart has the same shape for all the substances concerned, the energy scale being adjusted in direct proportion to the critical temperature and the distance scale in direct proportion to the cube root of the 'apparent' critical volume. By 'apparent' we mean estimated by application of the rule of the rectilinear diameter; this gives a well-defined and satisfactory scale for corresponding states regardless of whether or not there are complications in the behaviour of the fluid in the immediate neighbourhood of the critical point. For substances with monatomic molecules, such as we are here concerned with, this assumption, which we may

conveniently call that of 'corresponding interactions' leads to the usual results of the principle of corresponding states for the compression ratio pV/RT , the boiling-point temperature at corresponding pressures, the entropy of evaporation at corresponding temperatures, the molar volume of the liquid at corresponding temperatures, etc. These are all properties insensitive to the molecular mass. There are other properties, especially properties of the crystal, which are sensitive to the molecular mass. The indiscriminate application of the principle of corresponding states in a naïve form to such properties would lead to utterly false predictions. For example, the statement that the entropy of the crystal, measured relative to that at zero temperature, has the same value for the several substances at corresponding temperatures would have no theoretical basis and would be utterly contrary to experiment as shown in figure 1. In contrast to such incorrect naïve applications of the principle of corresponding states we shall assume 'corresponding interactions', from these calculate characteristic Einstein frequencies as a function of the lattice constant and thence calculate correct values for the entropy and other equilibrium properties.

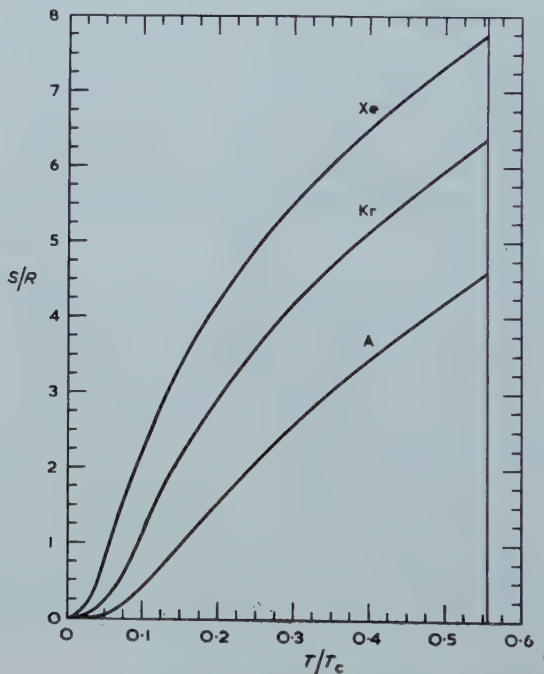


Figure 1. The entropy of solid argon, krypton, and xenon plotted against reduced temperature. In each case at the triple point T/T_c is between 0.555 and 0.560.

3. FORMULAE AND PARAMETERS

All the formulae used are given in our previous paper. We shall not repeat them but merely give in the table the values of the parameters for each substance. The values for argon are those described as set 4 in our previous paper. The values for krypton, xenon and neon were derived from the values for argon by use of the experimental values [2] of the critical temperature T_c and critical volume V_c . The values relating to neon are used in § 7. We wish to emphasize that there are no adjustable parameters.

	A	Kr	Xe	Ne
$T_c/^\circ\text{K}$	150·7	209·4	289·8	44·5
$V_c/\text{cm}^3 \text{mole}^{-1}$	75·3	92·1	118·8	41·7
$\epsilon/k^\circ\text{K}$	137·5	191·1	264·4	40·6
$10^{-2}\kappa/k^\circ\text{K}$	44·9	62·4	86·3	13·26
$10^{-3}\alpha/k^\circ\text{K}$	19·6	27·2	37·7	5·78
$10^{-4}\beta/k^\circ\text{K}$	1·96†	2·72	3·77	0·578
$\lambda/k^\circ\text{K}$	150·0	208·5	288·4	44·3
$r_0/\text{\AA}$	3·812	4·077	4·438	3·130

† In table 2 of our previous paper the printed value of β in set no. 4 (but not in set no. 5) is too large by a factor 10.

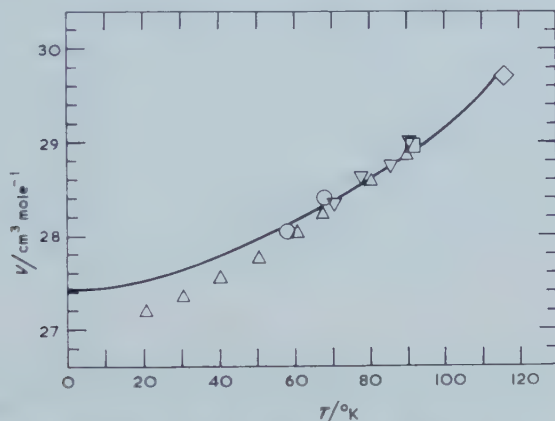


Figure 2. The molar volume of solid krypton plotted against temperature. The curve is that calculated as described in the text. ○ Cheesman and Soane [3]; □ Dobbs and Luszczynski [4]; △ Figgins and Smith [5] (x-ray); ▽ Figgins and Smith [5] (density); ◇ Clusius and Weigand [7].

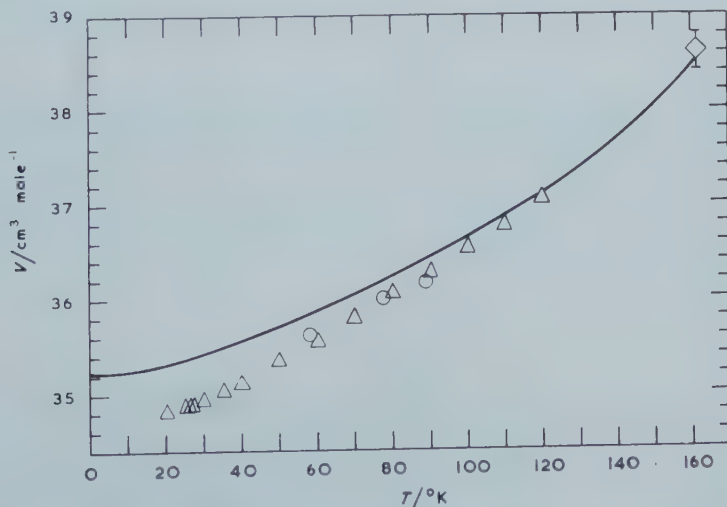


Figure 3. The molar volume of solid xenon plotted against temperature. The curve is that calculated as described in the text. ○ Cheesman and Soane [3]; △ Eatwell [6]; ◇ Clusius and Weigand [7].

4. VOLUME

The calculated molar volumes are compared with the experimental values in figures 2 and 3 for krypton and xenon respectively. Most of the experimental values are based on x-ray measurements. Of these, two values for krypton and three for xenon were obtained in this laboratory by Cheesman and Soane [3], while the remainder, namely one by Dobbs and Luszczynski [4] and eight by Figgins and Smith [5] for krypton, and fifteen by Eatwell [6] for xenon, were obtained at Queen Mary College. Earlier x-ray measurements are insufficiently precise to be worth mentioning. There are also four points for krypton obtained by Figgins and Smith [5] from direct density measurements.

We have also plotted values at the triple point obtained for each substance by combining the value of the molar volume of the liquid with Clusius and Weigand's [7] measurement of $d\bar{p}/dT$ along the melting curve which leads to an accurate value of the difference between molar volumes of liquid and crystal. For krypton the value of the molar volume of the liquid is obtained from the experimental measurements [8] with a slight extrapolation over a range of 10°K . Unfortunately, as stressed by Clusius and Weigand, there is no accurate experimental value for liquid xenon at or near the triple point. However, the principle of corresponding states applies to the liquid molar volumes of argon and krypton sufficiently accurately to give us confidence in applying the principle to liquid xenon. This leads to a molar volume of the liquid $44.2 \pm 0.2 \text{ cm}^3 \text{ mole}^{-1}$ and of the crystal $38.6 \pm 0.2 \text{ cm}^3 \text{ mole}^{-1}$. This value is plotted in figure 3.

For krypton there is agreement between our calculated values and the experimental values within the scatter of the latter from the triple point 115.95°K down to 60°K . At lower temperatures there are systematic deviations increasing to about 1 per cent at 20°K , presumably due to failure of the Einstein approximation. For xenon there is complete agreement at the triple point 161.36°K and at 120°K . Below 120°K there is a steadily increasing discrepancy reaching 1 per cent at about 60°K and about $1\frac{1}{2}$ per cent at 20°K .

5. ENTROPY

The comparison between calculated values of the entropy and experimental values obtained by integration of the measurements of Clusius and his collaborators [9, 10, 11] of the heat capacity is shown in figures 4 and 5. There is agreement within the experimental accuracy. We must however point out that the entropy gives no information concerning the important parameter ϵ . The calculated values of the entropy are most sensitive to the values of κ and α , less to those of λ and β .

6. ENTHALPY

At the low pressures, not exceeding one atmosphere, with which we are concerned the difference between enthalpy and energy is inappreciable. We accordingly compare calculated values of the energy with experimental values of the enthalpy. We take as zero energy that of infinitely dispersed atoms at rest. The comparison between calculated and experimental values of H/R is shown in figures 6 and 7. The experimental values used for heats of fusion and of evaporation, and for the heat capacities of crystal and liquid, are all those of

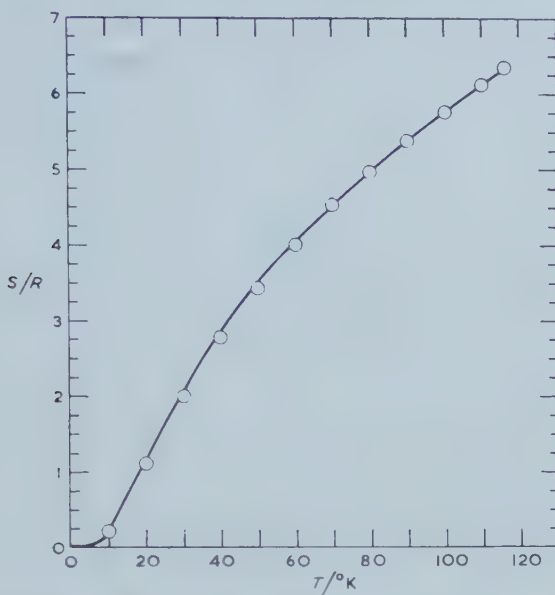


Figure 4. The entropy of solid krypton plotted against temperature. The curve is that calculated as described in the text. ○ experimental points.

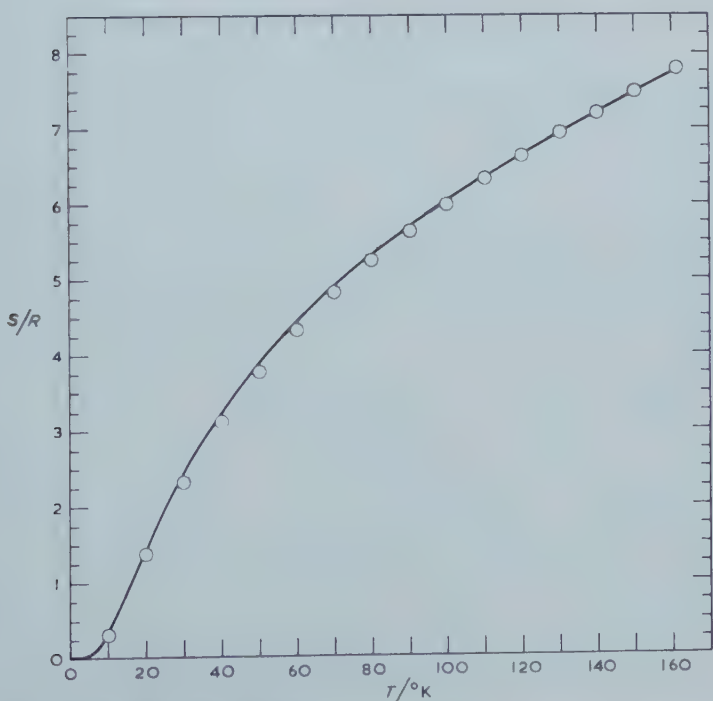


Figure 5. The entropy of solid xenon plotted against temperature. The curve is that calculated as described in the text. ○ experimental points.

Clusius and his collaborators [9, 10, 11]. There is also a correction for the deviation from ideality of the gas at a pressure of one atmosphere at the normal boiling point. This correction takes the form $P(B - TdB/dT)/\mathbf{R}$ where $P = 1 \text{ atm.}$ and B is the second virial coefficient. We estimate B and dB/dT from the formula [12]:

$$B/V_e = 0.458 - 1.123(T_e/T) - 0.435(T_e/T)^{5/2}.$$

In figure 6 relating to krypton we observe that the calculated values of H/\mathbf{R} lie systematically about 10°K below the experimental values. This discrepancy is just too large to be ignored. If it is a real discrepancy, i.e. due neither to

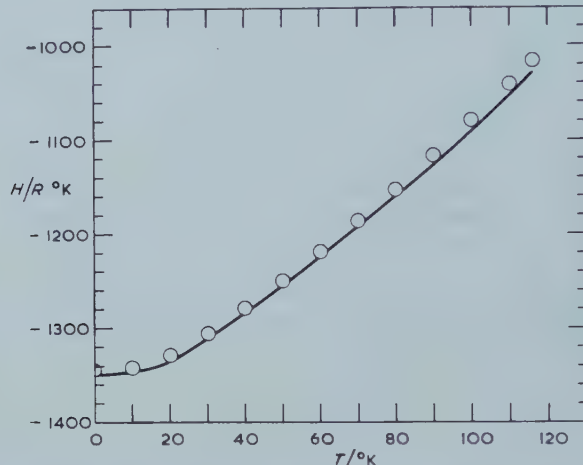


Figure 6. The enthalpy of solid krypton plotted against temperature. The curve is that calculated as explained in the text. ○ experimental points.

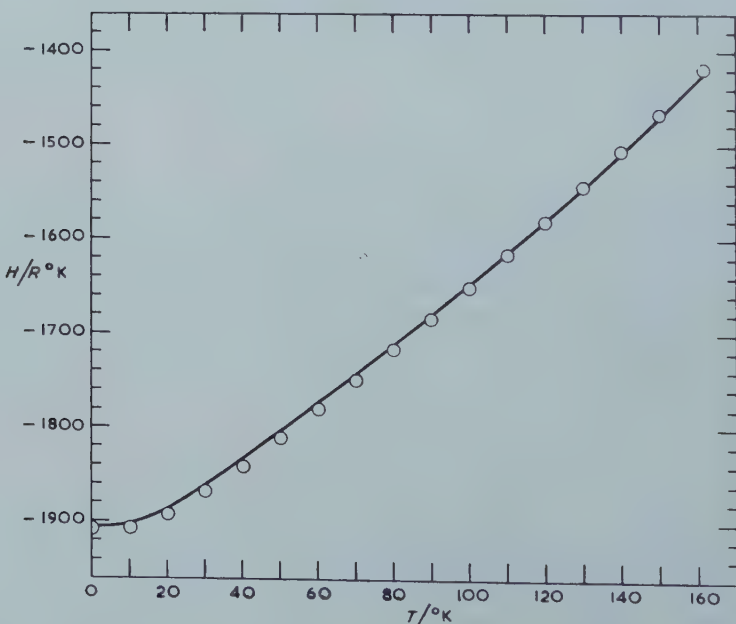


Figure 7. The enthalpy of solid xenon plotted against temperature. The curve is that calculated as explained in the text. ○ experimental points.

experimental error nor to computational error, it implies that the best value of ϵ for krypton is about one per cent smaller than the value given by 'corresponding interactions'. The values of λ , κ , α , β are not significant to better than one per cent. The small discrepancy might, on the other hand, be due to an error in an experimental quantity. The correction for deviation from ideality of the gas is a weak point because, while B is known with the requisite accuracy, the same cannot be said of dB/dT . However, the whole correction is estimated to be -10.8°K and we do not believe that this could be wrong by a factor 2. Moreover, if this were the source of the discrepancy, then there should be a parallel revision relating to xenon which would partly destroy the agreement between calculated and experimental values. The only other experimental quantity which might conceivably lead to an inaccuracy of as much as 10°K is the heat of evaporation $\Delta_e H$. Clusius, Kruis and Konnertz [10] give a value $\Delta_e H \cdot R = (1086 \pm 1.5)^\circ\text{K}$, thus claiming an accuracy of ± 0.15 per cent. This might be optimistic, but we are reluctant to believe that the experimental error could be six times as great. On the other hand, from the experimental values for argon and xenon the principle of corresponding states predicts for krypton the value $\Delta_e H \cdot R = (1094 \pm 4)^\circ\text{K}$. This would remove the discrepancy between the calculated and experimental values. It must however be remembered that, whereas we justifiably trust the principle of corresponding states for properties of the fluid state, we are not entitled to assume that it is exact. To sum up, all we can say with certainty is that the agreement between our calculated values of H and the experimental values is within one per cent for krypton. For xenon, as may be seen from figure 7, the agreement is appreciably better.

7. NEON

We may attempt similar calculations for neon using the parameter values given in the table but unfortunately the range of temperatures over which our approximations are valid is extremely short. If for example we perform a calculation for $R/r_0 = 1.01$ we find $h\nu/k = 47.3^\circ\text{K}$ and $T = 11.7^\circ\text{K}$ so that $h\nu/kT$ is too great for the Einstein model to be usable. If, on the other hand, we perform a calculation for $R/r_0 = 1.02$ we find $h\nu/k = 44.3^\circ\text{K}$ and $T = 19.5^\circ\text{K}$ so that $h\nu/kT$ is just tolerably large, but the thermal vibrations extend to values of r about 3.5 \AA , which is about as far as the assumed polynomial expression for the interaction energy is valid. The least unfavourable temperatures for the use of our formulae are close to 20°K .

We find at 19.50°K that the calculated value of the molar volume is $13.87 \text{ cm}^3 \text{ mole}^{-1}$. As far as we know there is no experimental value of the lattice constant or density at this temperature. At the triple point 24.57°K , however, Clusius [9] finds the value $13.98 \text{ cm}^3 \text{ mole}^{-1}$ by combining experimental values of the molar volume of the liquid and of dp/dT along the melting curve. We find at 19.50°K that the calculated value of S/R is 1.11 as compared with the experimental value 1.15 obtained by integration of Clusius' measurements [9] of the heat capacity. We cannot make a direct comparison between calculated and experimental values of H because we know of no experimental determination of either the heat of sublimation or the heat of evaporation. We can however use the experimental vapour pressure of the crystal to make a comparison between the calculated and experimental values of the chemical

potential μ which necessarily has the same value in the crystal and in the saturated vapour. In the crystal at low pressures μ is indistinguishable from F and is consequently given by formula (3.5) of our previous paper. In the vapour on the other hand μ is given in terms of the molar mass M and the experimental vapour pressure p by the formula [13]

$$\frac{\mu}{RT} = -\frac{5}{2} \ln \frac{T}{4.33_3^\circ K} - \frac{3}{2} \ln \frac{M}{g \text{ mole}^{-1}} + \ln \frac{p}{\text{atm}}$$

the correction for gas imperfection being negligible. We find at $19.50^\circ K$ that the calculated value of μ/RT is -11.7 as compared with the experimental value -11.9 obtained by use of the experimental value $p = 20.7 \text{ mm Hg}$ of Crommelin and Gibson [14].

8. DISCUSSION

For both krypton and xenon the agreement between calculated and measured values of the entropy and the enthalpy and consequently also of the free energy, is almost if not quite within the experimental accuracy from the triple-point temperature down to about $20^\circ K$. For the molar volume the agreement is less perfect and this is not surprising since the equilibrium molar volume is determined by minimizing the free energy. Hence a small inaccuracy in the shape of the assumed interaction energy curve or one due to the Einstein approximation will lead to a comparable small inaccuracy in the value of the minimum of the free energy but may well lead to a much greater inaccuracy in the position of this minimum. The agreement to within about 1 per cent between calculated and observed values of the molar volume is in our opinion satisfactory.

We are grateful to Professor G. O. Jones for letting us have unpublished details of experimental measurements.

REFERENCES

- [1] GUGGENHEIM, E. A., and McGLASHAN, M. L., 1960, *Proc. roy. Soc. A*, **255**, 456.
- [2] KOBE, K. A., and LYNN, R. E., 1953, *Chem. Rev.*, **52**, 117.
- [3] CHEESMAN, G. H., and SOANE, C. M., 1957, *Proc. phys. Soc. Lond.*, **70**, 700.
- [4] DOBBS, E. R., and LUSZCZYNSKI, K., 1955, *Conférence de Physique des basses températures* (Paris), p. 79.
- [5] FIGGINS, B. F., and SMITH, B. L., 1960, *Phil. Mag.*, **5**, 186.
- [6] Privately communicated by Professor G. O. Jones.
- [7] CLUSIUS, K., and WEIGAND, K., 1940, *Z. phys. Chem.*, **46**, 1.
- [8] MATHIAS, E., CROMMELIN, C. A., and MEIHUIZEN, J. J., 1937, *Physica*, **4**, 1200.
- [9] CLUSIUS, K., 1936, *Z. phys. Chem.*, B, **31**, 459.
- [10] CLUSIUS, K., KRUIS, A., and KONNERTZ, F., 1938, *Ann. Phys., Lpz.*, **33**, 642.
- [11] CLUSIUS, K., and RICCOPONI, L., 1937, *Z. phys. Chem. B*, **38**, 81.
- [12] McGLASHAN, M. L., and POTTER, D. J. B. (to be published).
- [13] GUGGENHEIM, E. A., 1957, *Thermodynamics* 3rd ed. (Amsterdam: North-Holland), p. 177.
- [14] CROMMELIN, C. A., and GIBSON, R. O., 1927, *Commun. Lab. Leiden*, no. 185b.

The properties of argon at its triple point

by E. A. GUGGENHEIM and M. L. McGlashan

Department of Chemistry, The University, Reading

(Received 10 October 1960)

Using the interaction energy between argon atoms deduced in a previous paper from the properties of the crystal and the gas and regarding the liquid as an approximately equimolar mixture of structures with coordination numbers $z=12$ and $z=8$ we have calculated the total energy of the liquid at the triple point in good agreement with experiment.

1. SCOPE

In a recently published paper [1] we have used the measured equilibrium properties of crystalline argon and the measured properties of gaseous argon to determine the dependence of the interaction energy between a pair of argon atoms on their distance apart. This dependence is strikingly different from the commonly assumed 6:12 or other 6: n forms. In the present paper we try to correlate this interaction energy with the equilibrium properties of liquid argon at its triple point. The most important of these properties are the enthalpy, which differs inappreciably from the energy, the entropy and the density. The temperature of the triple point is equal to the ratio of the enthalpy of fusion to the entropy of fusion; it is therefore not another independent quantity. Nor is the vapour pressure, since this is determined by equating the value of the Gibbs function in the condensed phase to that in the gas phase.

Since the equilibrium density of the liquid is determined by minimizing the free energy it is evident that conversely the value of the free energy is insensitive to the value of the density. It is therefore too much to hope that an accurate value of the density should be predictable from the interaction energy. We are sceptical of any claim to make such a prediction. The case of the crystal is different because the interaction energy has been chosen to give the correct value of the density at the triple point, and incidentally also at a temperature one half that of the triple point. We shall therefore perform calculations for the liquid assuming its density to have its experimental value and shall then verify that the free energy of the liquid at this density does not differ appreciably from the calculated minimum.

In order to discuss the energy (or enthalpy) and the entropy of the liquid we begin by recalling the description of a liquid given by Bernal [2] nearly a quarter of a century ago. Bernal pointed out that the configuration of a liquid composed of monatomic molecules can be usefully and adequately described by three parameters: the average number $\langle z \rangle$ of nearest neighbours of a chosen atom; the average distance $\langle r \rangle$ between an atom and its nearest neighbours; the average fluctuation λ of the interatomic distance r . These three quantities can be determined approximately by x-rays. Knowledge of $\langle z \rangle$ and $\langle r \rangle$ together with knowledge of the interaction energy should lead to a useful estimate of the enthalpy (or energy). The entropy is evidently related to

Bernal's λ but the impossibility of obtaining any quantitative relation has hitherto impeded further use of Bernal's description. We may state at once that we do not attempt to predict the entropy with sufficient accuracy to lead to quantitative predictions concerning the triple point. But by a slight change in the formulation of Bernal's description we are enabled to define unambiguously the entropy of disorder, and to make a crude estimate of its magnitude.

The available x-ray data on liquid argon lead [3] to a value of $\langle z \rangle$ estimated between 10 and 11, that is to say about midway between the values $z=12$ of a close packed structure and $z=8$ of a body centred structure. We take as our model of the liquid an equimolar mixture of these two structures. We then proceed as follows. From our previously determined interaction energy we calculate, at the experimental density of the liquid, the lattice energy and characteristic frequency and thence the enthalpy for each of the two crystalline structures defined by $z=12$ and $z=8$. We then take the mean of these two calculated enthalpies and obtain a value strikingly close to that of the liquid. It is this agreement which gives us confidence in the usefulness of our model.

For the entropy we begin by a similar procedure. Having calculated, at the experimental density of the liquid, the characteristic frequency we evaluate its contribution to the entropy for each of the two crystalline structures defined by $z=12$ and $z=8$. We take the mean of these and find that the actual entropy of the liquid exceeds this mean by $0.5\mathbf{R}$. This represents the entropy of mixing of the two structures or entropy of disorder. It is the quantity which Bernal denoted by ϕ . The accurate *a priori* prediction of this entropy of disorder is in our opinion a completely insoluble problem. At best we can by a crude argument show that $0.5\mathbf{R}$ is not an unreasonable value.

2. INTERACTION ENERGY

We begin by specifying the interaction energy which has been found to give excellent agreement with the observed equilibrium properties of the crystal, with the observed properties of the gas and for large distances with quantum theory.

We denote the distance apart of a pair of atoms by r and the distance at which the interaction energy is a minimum by r_0 . In the neighbourhood of this minimum we express the interaction energy w as a fourth degree polynomial in $(r-r_0)$, namely

$$w = -\epsilon + \kappa \left(\frac{r-r_0}{r_0} \right)^2 - \alpha \left(\frac{r-r_0}{r_0} \right)^3 + \beta \left(\frac{r-r_0}{r_0} \right)^4, \quad (2.1)$$

the five parameters having the values

$$r_0 = 3.812 \text{ \AA}, \quad \epsilon/k = 137.5^\circ\text{K}, \quad \kappa/k = 4.49 \times 10^3 \text{ }^\circ\text{K}, \quad \alpha/k = \beta/k = 1.96 \times 10^4 \text{ }^\circ\text{K}.$$

In interpreting the properties of the crystal it was assumed that (2.1) is accurate throughout the range 3.6 \AA to 4.15 \AA . For values of r exceeding 5.4 \AA the interaction energy was taken to be

$$w = -\lambda \left(\frac{r_0}{r} \right)^6. \quad (2.2)$$

with $\lambda/k = 150^\circ\text{K}$. Values of r between 4.15 \AA and 5.4 \AA are not relevant to the properties of the crystal. The interaction energy over this range required for computing the second virial coefficient was obtained by graphical interpolation

as shown in figure 1. At the top of this diagram is shown the range over which (2.1) has been used for the crystal. Immediately below are shown the ranges over which we assume the validity of (2.1) in our calculations relating to the liquid; there are two such ranges corresponding to the two coordination numbers $z=12$ and $z=8$.

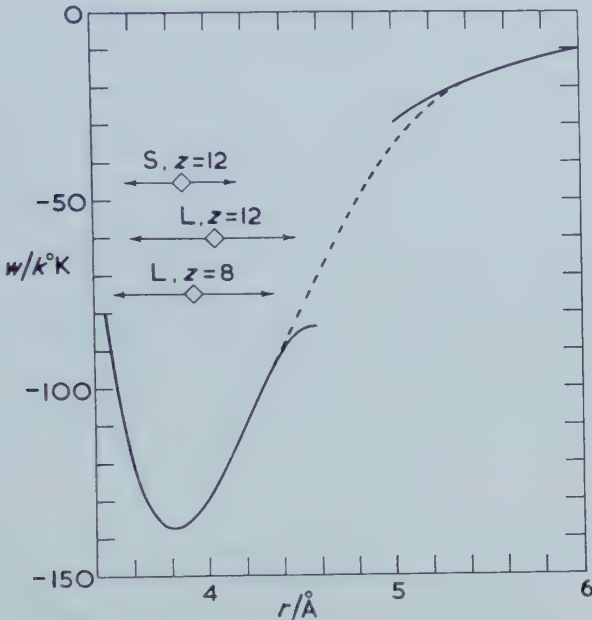


Figure 1. The interaction energy w plotted against the separation r of a pair of argon atoms.

3. EQUILIBRIUM PROPERTIES

In our previous paper we derived formulae for the several equilibrium properties of a face-centred cubic crystal. We shall now quote without derivation the formulae generalized for the three cubic structures, namely face-centred with $z=12$, body-centred with $z=8$ and simple with $z=6$. As previously we denote the mass of an atom by m and the distance between two lattice sites which are nearest neighbours by $R=r_0(1+\Delta)$.

According to Einstein's approximation for the acoustic modes of the crystal the characteristic frequency ν is given by

$$\frac{2\pi^2 m \nu^2 r_0^2}{z} = \frac{1}{3}\kappa(1+\Delta)^{-1}(1+3\Delta) - \alpha\Delta(1+\Delta)^{-1}(1+2\Delta) + 2\beta\Delta^2(1+\Delta)^{-1}(1+\frac{5}{3}\Delta) - 5\frac{C_{8,z}-z}{z}\lambda(1+\Delta)^{-8}. \quad (3.1)$$

The molar free energy F , the molar total energy U and the molar entropy S are given respectively by

$$\frac{F}{RT} = \frac{z}{2kT} \left\{ -\epsilon + \kappa\Delta^2 - \alpha\Delta^3 + \beta\Delta^4 - \frac{C_{6,z}-z}{z}\lambda(1+\Delta)^{-6} \right\} + 3 \ln(2 \sinh \frac{1}{2}x), \quad (3.2)$$

$$\frac{U}{RT} = \frac{z}{2kT} \left\{ -\epsilon + \kappa\Delta^2 - \alpha\Delta^3 + \beta\Delta^4 - \frac{C_{6,z}-z}{z}\lambda(1+\Delta)^{-6} \right\} + \frac{3}{2}x \coth \frac{1}{2}x, \quad (3.3)$$

$$\frac{S}{RT} = \frac{U-F}{RT} = \frac{3}{2}x \coth \frac{1}{2}x - 3 \ln(2 \sinh \frac{1}{2}x), \quad (3.4)$$

where $x = h\nu/kT$ and $C_{n,z}$ is the crystal potential constant [4] for power $-n$ in a cubic lattice with coordination number z . As usual U is taken as zero for infinitely dispersed atoms at rest and S is taken as zero for a crystal in the limit $T \rightarrow 0$.

The pressure p is given by

$$\begin{aligned} \frac{pV}{RT} &= -\frac{R}{3RT} \frac{\partial F}{\partial R} \\ &= -\frac{z}{6kT} \left\{ 2\kappa\Delta(1+\Delta) - 3\alpha\Delta^2(1+\Delta) + 4\beta\Delta^3(1+\Delta) + 6 \frac{C_{6,z}-z}{z} \lambda(1+\Delta)^{-6} \right\} \\ &\quad - \frac{3}{\pi^2 m v^2 r_0^2} \frac{1}{2} x \coth \frac{1}{2} x \left\{ \frac{2}{3} \kappa(1+\Delta)^{-1} - \alpha(1+\Delta)^{-1}(1+4\Delta+2\Delta^2) \right. \\ &\quad \left. + 4\beta\Delta(1+\Delta)^{-1}(1+3\Delta+\frac{5}{3}\Delta^2) + 40 \frac{C_{8,z}-z}{z} \lambda(1+\Delta)^{-8} \right\}, \end{aligned} \quad (3.5)$$

where V is the molar volume.

The molar volume V is related to the distance R between pairs of closest neighbours by

$$V = LR^3/\gamma_z \quad (3.6)$$

with $\gamma_{12} = \sqrt{2}$, $\gamma_8 = 3\sqrt{3}/4$, $\gamma_6 = 1$.

4. CALCULATIONS

We use formulae (3.1) and (3.3) to calculate the total energy as a function of the molar volume at the triple-point temperature $T_t = 83.78^\circ\text{K}$ taking $z = 12$, $z = 8$ and $z = 6$ in turn. The results for $z = 12$ and $z = 8$ are shown in figure 2

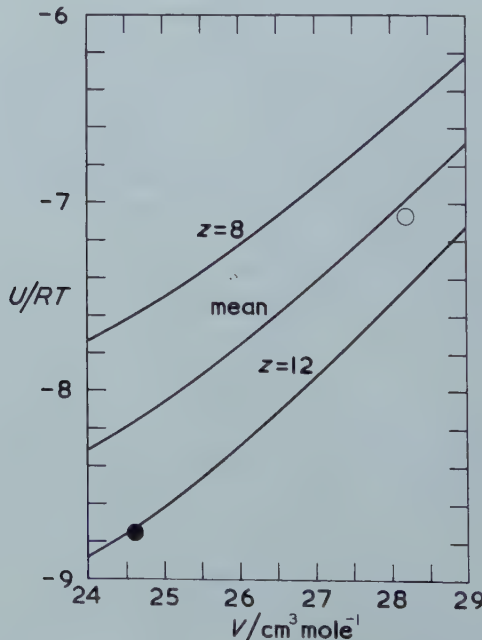


Figure 2. The energy of argon plotted against molar volume at the triple-point temperature.
 ● observed for the crystal ; ○ observed for the liquid.

At the volume equal to the experimental [5] triple-point volume of the liquid $28.2 \text{ cm}^3 \text{ mole}^{-1}$ the three calculated values of U/RT are -7.45 for $z=12$, -6.51 for $z=8$ and -4.50 for $z=6$. It is clear that the simple cubic structure, owing to its much higher energy, will not make an appreciable contribution to the structure of the liquid especially since the entropy of the simple cubic structure turns out to be considerably higher than that of the other two structures. An 'equimolar' mixture of $z=12$ and $z=8$ leads to $U/RT = -6.98$, which is strikingly close to the experimental value [5] for the liquid $U/RT = 7.06$. This agreement gives us confidence in our model. The slight difference of 0.08 is in the direction corresponding to a slight excess of the $z=12$ structures which has the lower energy. If then it is greater than the uncertainty of the calculation, it is in the right direction.

We use formulae (3.1) and (3.4) to make analogous calculations for the entropy as a function of molar volume at the triple point temperature. The results for $z=12$ and $z=8$ are shown in figure 3. At the experimental volume of the liquid $28.2 \text{ cm}^3 \text{ mole}^{-1}$ the calculated entropy is nearly the same for $z=12$ and $z=8$. The mean of these is less than the experimental entropy [5] of the liquid $6.30R$ by about $0.5R$. This difference is unambiguously the entropy of disorder which is superposed on the acoustic contribution of formula (3.4). We shall discuss this entropy of disorder in §5.

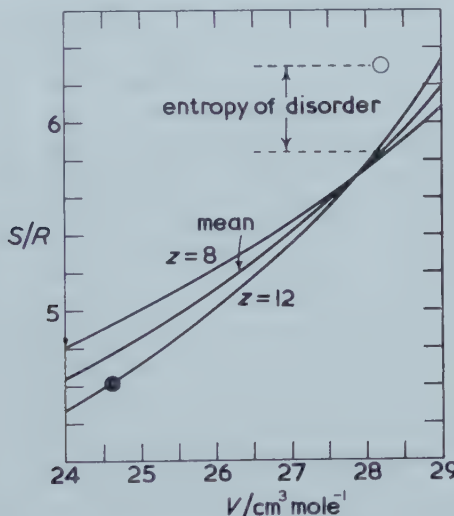


Figure 3. The entropy of argon plotted against molar volume at the triple-point temperature.
 ● observed for the crystal; ○ observed for the liquid.

We have used formulae (3.1) and (3.2) to calculate the free energy as a function of the molar volume at the triple-point temperature. The results are shown in figure 4 for $z=12$, for $z=8$ and the mean of these. We see that the calculated free energy is nearly independent of the volume as was to be expected, but we do not consider that our assumptions are sufficiently accurate for us to attach any reality to the shape, as opposed to the height of the curve. In particular we do not expect to predict the precise positions of a minimum nor of a maximum. By way of contrast we show in figure 5 the temperature dependence of F/RT when the volume is held constant at the experimental value for the liquid.

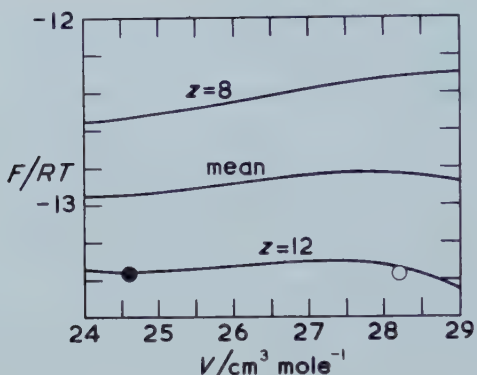


Figure 4. The free energy of argon plotted against the molar volume at the triple-point temperature. ● observed for the crystal; ○ observed for the liquid.

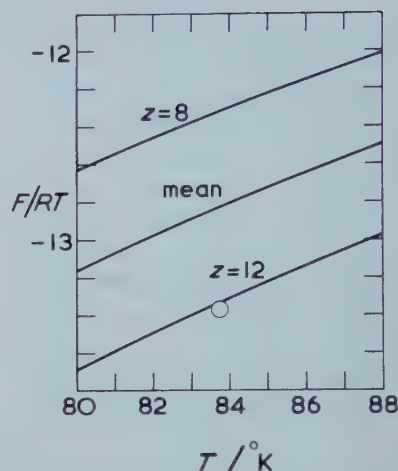


Figure 5. The free energy of argon plotted against temperature when the volume is fixed at $28.2 \text{ cm}^3 \text{ mole}^{-1}$. ○ observed at the triple point.

5. ENTROPY OF DISORDER

The quantity which we have defined as the entropy of disorder is, in agreement with Bernal's description, a measure of the disorder due to a mixing of crystal structures. We repeat that the accurate *a priori* evaluation of this entropy is in our opinion a completely insoluble problem. At the best we can by a crude argument show that the experimental value $0.5\mathbf{R}$ is not unreasonable. Here is the crude argument for what it is worth. A chosen atom may have 12 nearest neighbours or 8 or one of the intermediate numbers 9, 10, 11. Thus for each atom there are five alternative ways in which it can be surrounded. This might seem to lead to an entropy of disorder $\mathbf{R} \ln 5$ but this would be a gross overestimate because the manners of packing of the atoms are far from independent. Consequently all we can predict with confidence is that the entropy of disorder should be considerably less than $\mathbf{R} \ln 5 = 1.6\mathbf{R}$ and comparable with \mathbf{R} .

8. CONCLUSION

We have without any *ad hoc* assumptions calculated the correct value for the energy but have only roughly estimated the entropy of the liquid. This may seem a small achievement, but at least we believe that our treatment is more reasonable and our estimate more realistic than estimates based on counting the number of ways atoms can be arranged on a hypothetical, and certainly non-existent, lattice arrangement of cells. Our treatment is a natural extension of Bernal's. The progress of a quantitative nature is due to greatly improved knowledge of the atomic interaction energy.

REFERENCES

- [1] GUGGENHEIM, E. A., and McGLASHAN, M. L., 1960, *Proc. roy. Soc. A*, **255**, 456.
- [2] BERNAL, J. D., 1937, *Trans. Faraday Soc.*, **33**, 27.
- [3] EISENSTEIN, A., and GINGRICH, N. S., 1942, *Phys. Rev.*, **62**, 261.
- [4] (LENNARD-)JONES, J. E., and INGHAM, A. E., 1925, *Proc. roy. Soc. A*, **107**, 636.
- [5] DIN, F., 1956, *Thermodynamic Functions of Gases*, Vol. 2 (London: Butterworths).

Electron spin correlation and the ethane barrier

by HARRY G. HECHT†, DAVID M. GRANT
and HENRY EYRING

Department of Chemistry, University of Utah, Salt Lake City, Utah

(Received 19 August 1960)

The barrier to rotation in ethane is discussed in terms of hydrogen-hydrogen exchange integrals properly weighted by experimentally determined bond orders. Such bond orders are proportional to the spin correlation of delocalized electrons as determined from nuclear magnetic resonance spin-spin coupling constants. The calculated value of 2.3 kcal per mole determined for the rotational barrier in ethane in this study is in good agreement with the experimentally determined value of 2.7-3.0 kcal per mole.

1. INTRODUCTION

The problem of providing a suitable theoretical interpretation of the origin of barriers restricting free rotation about single bonds, the ethane barrier being the classic example, has troubled chemists and physicists for some time. Few problems have been as extensively investigated with as little success [1].

Consideration of this problem in terms of the perfect pairing approximation has been given by Eyring [2]. The energy for a given nuclear configuration can be written as

$$E = Q + \sum I_{ij}(\text{bonded}) - \frac{1}{2} \sum I_{kl}(\text{non-bonded}) \quad (1)$$

where Q is the coulomb integral, and I is a single exchange integral. Using this approximation, it was found that the only factor contributing to the ethane barrier is the exchange interaction of the hydrogen atoms between methyl groups. It was shown that the barrier resulting from such a calculation is only 0.36 kcal per mole, to be compared with the experimental value, 2.7-3.0 kcal per mole [3].

As sp^3 hybridized orbitals have axial symmetry in ethane, they cannot contribute to the rotational barrier. Contributions can arise from higher order hybridization effects, however, and have been discussed by Gorin *et al.* [4]. A non-axially symmetrical distribution of the electron density about the C-C bond can be produced by the proper admixture of $4f$ and $3d$ functions with the $2s$ and $2p$ atomic orbitals usually considered. These workers found that although the $3d$ orbital makes a larger contribution to the barrier than the $4f$, the differences in the energies of the orbitals concerned limit the effect of this contribution to the barrier from these calculations to 0.6 kcal per mole. More recently, Pauling [5] has considered such hybridization effects in a semi-quantitative way.

Eyring *et al.* [6] have suggested that *trans* delocalization of electrons in the staggered ethane structure would be energetically more favourable than electrons delocalized between *cis* hydrogen atoms in an eclipsed structure. Such an interaction qualitatively accounts for the rotational barrier in ethane, and suggests that bond structures other than the principal one contribute to make the staggered form of ethane most stable.

† This is an essential portion of a dissertation offered in partial fulfillment of the requirements for the Ph.D. degree.

An approximate valence bond calculation of the ethane barrier using a limited set of bond structures involving only *s* and *p* orbitals has been made by Harris and Harris [7]. The calculated barrier of 7.5 kcal per mole was not in close agreement with the experimental value, but was indicative that a more refined calculation may yield a value in better agreement using only the *s* and *p* orbitals.

2. NUCLEAR SPIN-SPIN COUPLING

A fine splitting of the spectral lines obtained under conditions of high resolution in nuclear magnetic resonance studies was observed by Gutowsky and McCall [8] and by Hahn and Maxwell [9]. The energy of such an interaction between the nuclei, *N* and *N'*, is given by [10]

$$E_{NN'} = J_{NN'} \mathbf{I}_N \cdot \mathbf{I}_{N'} \quad (2)$$

where \mathbf{I}_N and $\mathbf{I}_{N'}$ are the spin vectors of the two nuclei involved, and $J_{NN'}$ is the nuclear spin-spin coupling constant. The theoretical basis of this interaction has been given by Ramsey and Purcell [11] and by Ramsey [12], who have shown that it arises from an indirect coupling of the nuclear magnetic moments through the electrons in the molecule.

The energy of nuclear coupling can be obtained from a perturbation calculation using the complete Hamiltonian operator for interactions between the electrons and nuclei. Such calculations have shown that the Fermi contact interactions between electron spins in *s* orbitals and nuclear spins make the principal contribution to the nuclear spin-spin coupling [12, 13, 14].

McConnell [15] has shown that if only Fermi contact coupling is assumed, the nuclear spin-spin coupling constant for protons can be represented by the approximate formula,

$$J_{HH'} = \frac{16}{9} \beta^2 \gamma^2 h (\Delta E)^{-1} [\phi(0)]^4 \eta_{HH'}^2 \quad (3)$$

where $\phi(0)$ is the value of a hydrogen 1s atomic orbital at its centre, and $\eta_{HH'}$ is the bond order between the atoms *H* and *H'* (see equation (6)). Equation (3) further assumes a negligible value of all atomic orbitals (except local 1s orbitals) at the proton positions.

3. CALCULATION OF THE ETHANE BARRIER

In the molecular orbital calculations, a linear combination of atomic orbitals (LCAO) of the form,

$$\psi_s = \sum_N a_{Ns} \phi_N \quad (4)$$

is commonly used. ψ_s is the wave function for the molecular orbital, *s*, and ϕ_N is an atomic (or hybrid) orbital centred on nucleus *N* used in the construction of ψ_s . Using this wave function, the bonding energy is found to be [16]

$$E_{\text{bonding}} = \sum_{N < N'} \eta_{NN'} I_{NN'} \quad (5)$$

where $I_{NN'}$ is the exchange integral, $\int \phi_N H \phi_{N'} d\tau$, and

$$\eta_{NN'} = 2 \sum_s a_{Ns} a_{N's} \quad (6)$$

represents the bond order between the two nuclei, *N* and *N'*.

Using only sp^3 hybridization, the only interactions contributing to a barrier about the C-C bond axis are those between the hydrogen atoms in different methyl groups. Thus, equation (3) can be used to obtain

$$E_{\text{bonding}} = \sum_{H < H'} \frac{3(\Delta E)^{1/2} J_{HH'}^{1/2} I_{HH'}}{4\beta\gamma\hbar^{1/2}[\phi(0)]^2} + E'_{\text{bonding}} \quad (7)$$

where E'_{bonding} is the contribution to the energy of bonding of all interactions not effective in producing a barrier about the C-C bond. This becomes

$$E_{\text{bonding}} = \sum_{H < H'} \frac{J_{HH'}^{1/2} I_{HH'}}{(280)^{1/2}} + E'_{\text{bonding}} \quad (8)$$

by taking the bond order of the hydrogen molecule, whose nuclear spin-spin coupling constant is 280 c.p.s. [17], to be unity.

The integral, $I_{HH'}$, is approximated by neglecting the electronic repulsion terms and evaluating only the two-centred integrals involving the hydrogen atoms. The three-centred integrals involving two hydrogen atoms and one carbon atom are not considered in this treatment.

Explicit values of the nuclear spin-spin coupling constants in the various conformations are not determinable for ethane; nevertheless, reasonable values can be inferred. The values assigned to $J_{HH'}|_{180^\circ}$ and $J_{HH'}|_{60^\circ}$ are 11 c.p.s. and 5 c.p.s., respectively [18]. $J_{HH'}|_0$ is assumed to be about half $J_{HH'}|_{180^\circ}$ or 5.5 c.p.s., from the relative values of the *cis* and *trans* nuclear spin-spin coupling constants in ethylenic compounds [19]. (It should be noted that π bonds probably have little effect in this case [20].) $J_{HH'}|_{120^\circ}$ is not expected to differ greatly from $J_{HH'}|_{60^\circ}$ or $J_{HH'}|_0$ and will be taken as 5 c.p.s. [21, 22].

Referring to equation (8), the ethane barrier can be expressed as

$$\frac{1}{(280)^{1/2}} \{3J_{HH'}^{1/2} I_{HH'}|_{180^\circ} + 6J_{HH'}^{1/2} I_{HH'}|_{60^\circ} - 3J_{HH'}^{1/2} I_{HH'}|_0 - 6J_{HH'}^{1/2} I_{HH'}|_{120^\circ}\}. \quad (9)$$

A barrier of 2.3 kcal per mole results when the above values of the nuclear spin-spin coupling constants are used, together with the values of the approximate exchange integral as calculated for the several conformations. It should be noted that this calculation is very sensitive to the values of the nuclear spin-spin coupling constants chosen. The calculated value therefore suggests that a barrier of the proper magnitude can be realized from the hydrogen-hydrogen exchange interactions properly weighted by experimentally determined bond orders.

4. DISCUSSION

It is observed that the interactions in the above calculation are essentially the same as those previously considered by Eyring [2], in that they only involve hydrogen-hydrogen exchange terms. However, these terms have been weighted with experimentally determined bond orders obtained from nuclear magnetic resonance spin-spin coupling constants.

The fact that the magnitude of the nuclear spin-spin coupling constant is actually a measure of the extent if the correlation of the electron spins or bond order is readily seen by consideration of a physical interpretation given by Pople *et al.* [23] of the work of McConnell, to which reference has previously been made.

The nuclear spin-spin coupling constant between any two protons in a given molecule can be represented by

$$J_{HH'} = \left(\frac{8}{3}\beta\gamma\right)^2 h(\Delta E)^{-1} \sum_{s,t} \psi_s^*(H)\psi_t^*(H')\psi_t(H)\psi_s(H') \quad (10)$$

where $\psi_s(H)$ is the value of the molecular orbital, ψ_s , at the nucleus of the atom, H . If $P^{\alpha\alpha}(H, H')$ is written for the probability of there being two electrons with α spin simultaneously at nuclei H and H' , and $P^{\alpha\beta}(H, H')$ for the probability of there being an electron of α spin at nucleus H and an electron of β spin at nucleus H' , then equation (10) for $J_{HH'}$ is proportional to

$$P^{\alpha\beta}(H, H') - P^{\alpha\alpha}(H, H'). \quad (11)$$

In other words, the nuclear spin-spin coupling constant is proportional to the excess of electrons of β spin over electrons of α spin at nucleus H' , given that there is an electron of α spin at nucleus H . Thus, the magnitude of this constant measures the extent of the correlation of the electron spins, and thereby determines the extent of the deviation from perfect pairing.

Various experimental investigations have shown the approximate dependence of nuclear spin-spin coupling constants upon the geometrical configurations of molecules. It will be particularly noted from the magnitude of these constants that a greater degree of electron spin correlation (and greater bond order) exists between hydrogen atoms in the staggered rather than the eclipsed ethane molecule. This variation in the extent of the electron correlation with the conformation of the molecule has a very pronounced effect upon the size of the rotational barrier by determining the relative weights of the various hydrogen-hydrogen exchange interactions as indicated in equation (9). The calculations show that a rotational barrier of the proper magnitude is obtained by a weighting of the exchange terms in this manner. Experimental studies which will allow a more concrete assignment of values for the nuclear spin-spin coupling constants in the various conformations of interest are being undertaken in this laboratory.

We are indebted to the National Science Foundation for financial support under grants NSF G-11313 and NSF G-4234.

REFERENCES

- [1] For a recent comprehensive review of this problem, see WILSON, E. B., Jr., 1959, *Advances in Chemical Physics*, Vol. II, Ed. I. Prigogine (New York: Interscience Publishers, Inc.), p. 367.
- [2] EYRING, H., 1932, *J. Amer. chem. Soc.*, **54**, 3191.
- [3] See reference [1], p. 370.
- [4] GORIN, E., WALTER, J., and EYRING, H., 1939, *J. Amer. chem. Soc.*, **61**, 1876.
- [5] PAULING, L., 1958, *Proc. nat. Acad. Sci., Wash.*, **44**, 211.
- [6] EYRING, H., STEWART, G. H., and SMITH, R. P., 1958, *Proc. nat. Acad. Sci., Wash.*, **44**, 259.
- [7] HARRIS, G. M., and HARRIS, F. E., 1959, *J. chem. Phys.*, **31**, 1450; KARPLUS, M. (1960, *J. chem. Phys.*, **33**, 316), in a recent note published since this paper was submitted, obtained a rotational barrier which was less than 0.2 kcal per mole from similar valence bond considerations.
- [8] GUTOWSKY, H. S., and McCALL, D. W., 1951, *Phys. Rev.*, **82**, 748.
- [9] HAHN, E. L., and MAXWELL, D. E., 1951, *Phys. Rev.*, **84**, 1246.
- [10] GUTOWSKY, H. S., McCALL, D. W., and SLICHTER, C. P., 1953, *J. chem. Phys.*, **21**, 279.
- [11] RAMSEY, N. F., and PURCELL, E. M., 1952, *Phys. Rev.*, **85**, 143.

- [12] RAMSEY, N. F., 1953, *Phys. Rev.*, **91**, 303.
- [13] KARPLUS, M., ANDERSON, D. H., FARRAR, T. C., and GUTOWSKY, H. S., 1957, *J. chem. Phys.*, **27**, 597.
- [14] KARPLUS, M., 1959, *J. chem. Phys.*, **30**, 11.
- [15] McCONNELL, H. M., 1956, *J. chem. Phys.*, **24**, 460.
- [16] COULSON, C. A., 1939, *Proc. roy. Soc. A*, **169**, 413.
- [17] CARR, H. Y., and PURCELL, E. M., 1952, *Phys. Rev.*, **88**, 415.
- [18] POPLE, J. A., SCHNEIDER, W. G., and BERNSTEIN, H. J., 1957, *Canad. J. Chem.*, **35**, 1060.
- [19] POPLE, J. A., SCHNEIDER, W. G., and BERNSTEIN, H. J., 1959, *High Resolution Nuclear Magnetic Resonance* (New York: McGraw-Hill Book Co., Inc.), p. 193.
- [20] McCONNELL, H. M., 1957, *J. mol. Spectrosc.*, **1**, 11.
- [21] ANDERSON, W. A., 1956, *Phys. Rev.*, **102**, 151. (The fact that $J_{HH'}|_{120^\circ}$ and $J_{HH'}|_{0^\circ}$ were found to be the same in β -propiolactone should probably be thought of as quite accidental, possibly due to ring strain in this particular compound.)
- [22] MULLER, N., and PRITCHARD, D. E., 1959, *J. chem. Phys.*, **31**, 768.
- [23] POPLE, J. A., SCHNEIDER, W. G., and BERNSTEIN, H. J., 1959, *High Resolution Nuclear Magnetic Resonance* (New York: McGraw-Hill Book Co., Inc.), p. 190.

The proton resonance spectra of metal bis-cyclopentadienyls

by D. A. LEVY and L. E. ORGEL

Department of Theoretical Chemistry, University Chemical Laboratory,
Lensfield Road, Cambridge

(Received 26 September 1960)

The signs of the chemical shifts of the proton resonance frequencies in paramagnetic metallocenes are discussed.

The proton resonance spectra of the paramagnetic molecules $V(C_5H_5)_2$, $Cr(C_5H_5)_2$, $Mn(C_5H_5)_2$, $Co(C_5H_5)_2$ and $Ni(C_5H_5)_2$ present an interesting problem [1, 2]. As shown in table 1 the chemical shifts relative to protons in diamagnetic substances are considerable for the vanadium, chromium and nickel compounds, moderate for the manganese compound, and almost zero for the cobalt compound. While the shift is to high fields in the nickel and manganese derivatives it is in the opposite direction for those of vanadium and chromium.

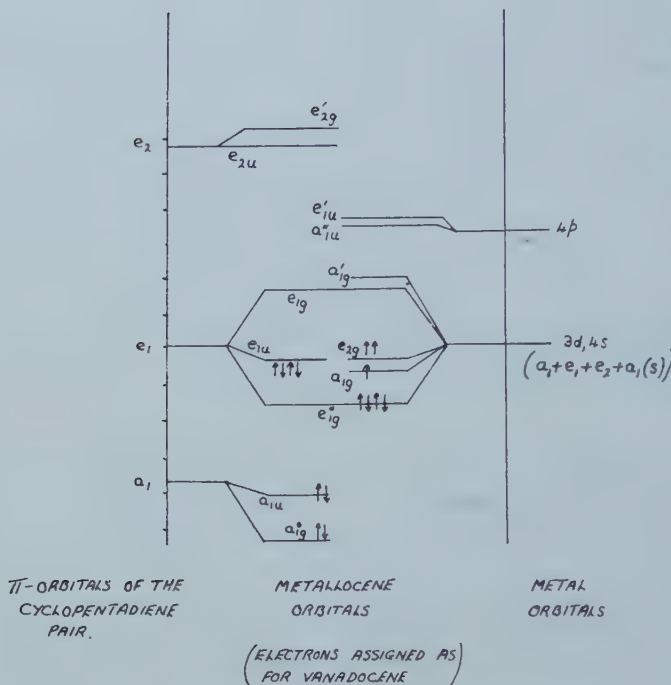
Compound	Proton resonance shift (per cent) + = to high field - = to low field	Net spin density on proton (unpaired electrons per carbon nucleus)
$V(C_5H_5)_2$	-0.026	-0.06
$Cr(C_5H_5)_2$	-0.029	-0.12
$Mn(C_5H_5)_2$	+0.012	+0.01
$Co(C_5H_5)_2$	+0.004	+0.004
$Ni(C_5H_5)_2$	+0.032	+0.14

Table 1. Proton resonance shifts and spin densities for bis-cyclopentadienyls.

In our discussion of this problem we shall adopt the energy level scheme suggested by Dunitz and Orgel [3] (figure). This energy level diagram was derived on the suppositions that:

- the strongest covalent bonding involves the e_{1g} orbitals of metal and ligands;
- there is an appreciable mixing of the $a_{1g} 3d$ orbital (the d_{z^2} orbital) and the $4s$ orbital under the influence of the non-spherical environment of the metal atom.

It is perhaps worth remarking that the a_{1g}' orbital might well be displaced above the e_{1g} orbital without invoking such extensive $d-s$ mixing if the molecule is appreciably polar, for in the transition-metal cations the $4s$ orbital is well above the $3d$ orbitals. We shall suppose that the electron configurations are those shown in table 2.



Energy-level diagram for metal bis-cyclopentadienyls.

	Preferred configuration	Alternative configuration
V	$(e_{2g})^2(a_{1g})^1$	—
Cr	$(e_{2g})^3(a_{1g})^1$ or $(e_{2g})^2(a_{1g})^2$	—
Mn	$(e_{2g})^2(a_{1g})^1(e_{1g})^2$	—
Fe	$(e_{2g})^4(a_{1g})^2$	—
Co	$(e_{2g})^4(a_{1g})^2(e_{1g})^1$	$(e_{2g})^4(a_{1g})^2(a_{1g}')^1$
Ni	$(e_{2g})^4(a_{1g})^2(e_{1g})^2$	$(e_{2g})^4(a_{1g})^2(a_{2g}')^1(e_{1g})^1$

Table 2. Electron configurations for bis-cyclopentadienyl compounds.

These configurations seem fairly certain for $\text{V}(\text{C}_5\text{H}_5)_2$, $\text{Cr}(\text{C}_5\text{H}_5)_2$ and $\text{Mn}(\text{C}_5\text{H}_5)_2$. We feel that we have chosen the most likely configurations for the cobalt and nickel compounds, but the alternative configuration, in particular for cobaltocene, which includes an unpaired *s* electron cannot be excluded.

Consider first the case of vanadocene where we have one electron in each of the a_{1g} and e_{2g} orbitals and none in e_{1g} orbitals. Delocalization of the a_{1g} and e_{2g} electrons inevitably leads to a spin density on the carbon atoms which has the same sign as that on the metal atom. If we may assume that the spin is transferred from carbon to hydrogen atoms with a change of direction, as is known to be the case in aromatic radicals [4, 5], then the spin density due to this delocalization process should lead to a high-field shift, in contradiction to the experimental result.

Two possible ways out of the dilemma suggest themselves, namely to propose a mechanism leading to a chemical shift which does not depend on the *s* electron contact term or alternatively to provide a spin delocalization mechanism which does not depend directly on the spreading out of the unpaired electrons into a molecular orbital including the carbon atoms. The former solution seems improbable in this particular example since the *g* tensor of $V(C_5H_5)_2$ is almost isotropic [6]. We shall see that the latter alternative, however, does provide a satisfactory solution of the problem.

One of us has suggested elsewhere a mechanism by means of which unpaired electrons in a non-binding orbital are able to polarize the spins of electrons in a bonding orbital of different symmetry [7]. This mechanism, which operates both in octahedral transition-metal complexes and in rare-earth compounds, should be effective in metal bis-cyclopentadienyls and we shall see that it leads to the correct qualitative conclusions about the signs of spin densities.

In order to preserve the theory in the form previously given, consider $V(C_5H_5)_2$ to be derived from the V^{2+} ion and two $(C_5H_5)^-$ rings. Then the major charge-transfer process involves electrons passing from the e_{1g} ring orbitals into the $e_{1g}d$ orbital. The transferred electrons may either have their spins parallel or antiparallel to those already present on the metal. More precisely we consider the basic electron configuration for vanadocene to correspond to a V^{2+} ion in the $d^3(a_{1g})^1(e_{2g})^1(e_{-2g})^1$ quartet state†, coupled to two closed-shell $C_5H_5^-$ anions. The transfer of an electron from the e_{1g} orbital on the rings to the metal ion then produces a $V^{+}d^4$ ion. If the electron transferred has its spin parallel to the three spins on the V^{2+} ion a unique state of the d^4 configuration is obtained, namely a 5E_1 state d^4 : $(a_{1g})^1(e_{2g})^1(e_{-2g})^1(e_{1g})^1$ 5E_1 (this is actually the $M_L=1$ component of the 5D state of the d^4 configuration). In terms of the usual Slater-Condon parameters this state has the electron repulsion energy $6F_0-21F_2-189F_4$.

The transfer of one electron with its spin 'antiparallel' to that of the metal ion does not lead to the latter being obtained in a unique state, for the configuration d^4 : $(a_{1g})^1(e_{2g})^1(e_{-2g})^1(\overline{e_{1g}})^1$ does not correspond to an eigenstate of the Hamiltonian of the atom in its environment of five-fold symmetry. A complete calculation of the effect of antiparallel spin-transfer would necessitate the evaluation of the energies and eigenfunctions of all the $M_L=1$, $M_S=1$ states of the atom and then the calculation of the extent of charge-transfer to each of them. We have not attempted this, but have made use of a form of second-order perturbation theory which should be applicable provided that the energy separation between the normal and charge-transfer configuration is large compared with the spread of the states involving the $(a_{1g})^1(e_{2g})^1(e_{-2g})^1(\overline{e_{1g}})^1$ configuration. The energy of this configuration is

$$6F_0-14F_2-119F_4$$

and if we treat it as though it gave rise to a single state we find the electronegativity for the transfer of electrons with parallel spin is 1.6 ev greater than that for electrons with anti-parallel spin. This supposes that the Slater-Condon parameters for the free atom [8] may be used for $V(C_5H_5)_2$, and hence probably overestimates the difference. The greater electron affinity for electrons with spin parallel to those of the metal ion, naturally induces a net spin of the opposite sign on the carbon atoms.

† We write e_{2g} and e_{-2g} to distinguish the components of the e_{2g} orbitals.

There is another equivalent way of looking at the same problem which is perhaps more realistic in covalent compounds. We suppose that $V(C_5H_5)_2$ is made up from a neutral vanadium atom and two cyclopentadienyl radicals by forming two covalent bonds using the e_{1g} orbitals. Then the exchange interaction of the unpaired a_{1g} and e_{2g} electrons polarizes the bond in a way exactly analogous to that by which a nuclear moment is supposed to polarize a covalent bond in the theory of spin-spin coupling constants [9]. This polarization leads to the transmission of a negative spin density to the carbon atoms.

The net spin-moment on the carbon atoms of $V(C_5H_5)_2$ is thus the result of a moment parallel to that on the metal ion brought about by electron delocalization and an oppositely directed moment due to spin polarization. Since delocalization occurs only through the secondary bonding orbitals (a_{1g} , e_{2g}) while polarization occurs through the strongly bonding e_{1g} orbitals it is not surprising that the spin-polarization effect is the larger.

Essentially the same conclusions apply in the case of $Cr(C_5H_5)_2$ although the details are rather more complicated. The average energies for e_{1g} electron transfer with parallel and antiparallel spin are shown in table 3 for the two possible ground states given in table 2. Again electron delocalization proceeds entirely through the a_{1g} and e_{2g} orbitals and is expected to be less important than spin polarization.

Energy of transfer state	Chromocene $(a_{1g})^2(e_{2g})^1(e_{-2g})^1$	Chromocene $(a_{1g})^1(e_{2g})^2(e_{-2g})^1$
Quartet	$10F_0 - 23F_2 - 165F_4$	$10F_0 - 19F_2 - 185F_4$
Low spin (mean)	$10F_0 - 17F_2 - 125F_4$	$10F_0 - 15F_2 - 135F_4$
Mean preferential electronegativity for high spin transfer	1.36 ev	1.21 ev

Table 3. Electron-transfer energies for chromocene.

It must be noted at this point that we have neglected a number of contributions to the spin polarization which arise through the use of the metal s (a_{1g}) and p orbitals (a_{1u} , e_{1u}). These are expected to be smaller than the d electron term, and to have the same sign. We shall see that they may be important in $Mn(C_5H_5)_2$.

In $Mn(C_5H_5)_2$ and $Ni(C_5H_5)_2$ the situation is quite different. All the available d orbitals are filled or occupied by one electron, and so electrons transferred to the metal ion d orbitals necessarily have their spins opposed to the metal ion spin. Thus the spins left behind on the carbon atoms are parallel to those on the metal. This is part of the usual delocalization of the unpaired electrons and leads, as we have already seen, to a high-field shift of the proton resonance in agreement with experiment.

In $Co(C_5H_5)_2$ both mechanisms operate since only one of the e_g antibonding orbitals is occupied. Since the experimental evidence suggests a very small spin density on the protons it is tempting to suppose that they have about equal magnitudes and opposite signs. However, this is not a quantitatively satisfactory

solution of the problem, since one would certainly expect the spin-delocalization effect to be larger than the polarization effect since both involve e_{1g} electrons. In fact, the electron affinity for a parallel electron transfer is $28F_0 - 47F_2 - 402F_4$, greater by 1.7 ev than for antiparallel transfer ($28F_0 - 41F_2 - 362F_4$), but now there are two antiparallel and only one parallel vacancy in the metal $e_{1g} d$ orbitals.

While this elementary theory accounts nicely for the qualitative observations it does not readily predict the relative magnitudes of the shifts. This is due in part to our incomplete knowledge of the electronic structure of the bis-cyclopentadienyls, in particular the way in which the degree of electron transfer varies from compound to compound.

Another unknown factor is the importance of the pseudo-contact contribution to the chemical shift in $\text{Co}(\text{C}_5\text{H}_5)_2$ and in $\text{Cr}(\text{C}_5\text{H}_5)_2$. McConnell's and Roberston's theory [10] shows that if the g tensor for the central atom is anisotropic there will be a pseudo-contact chemical shift given by

$$\sigma = \frac{\Delta H}{H_0} = \frac{1}{r^3} \cdot \frac{\beta^2 h S(S+1)}{27kT} (3 \cos^2 \chi - 1)(g_{\parallel} + 2g_{\perp})(g_{\parallel} - g_{\perp})$$

where S is the spin, χ the angle between the five-fold axis and the line joining the metal to the protons, r the metal-proton distance and g_{\parallel} and g_{\perp} are the g -values along and perpendicular to the five-fold axis. Now the g values are expected to be anisotropic when the lowest orbital state is degenerate as it may be in $\text{Co}(\text{C}_5\text{H}_5)_2$ and also in $\text{Cr}(\text{C}_5\text{H}_5)_2$. Unfortunately neither the paramagnetic resonance spectra nor the anisotropies of the magnetic susceptibility have been measured for these compounds, and so no estimate of this potentially large term can be made. Another factor which would require detailed consideration in a quantitative theory is the preferential antiparallel spin delocalization of paired metal a_{1g} or e_{2g} electrons in $\text{Cr}(\text{C}_5\text{H}_5)_2$, $\text{Co}(\text{C}_5\text{H}_5)_2$ and $\text{Ni}(\text{C}_5\text{H}_5)_2$. This should be less important than the e_{1g} electron delocalization, but is by no means negligible. It is not possible therefore to deduce anything about the electronic structures of $\text{Co}(\text{C}_5\text{H}_5)_2$ or $\text{Cr}(\text{C}_5\text{H}_5)_2$ from the magnitudes of the chemical shifts.

The small chemical shift in $\text{Mn}(\text{C}_5\text{H}_5)_2$ emphasizes again the limited involvement of the d electrons in bonding. Either the d electrons are scarcely delocalized at all or the delocalization shift is so small that it is largely cancelled by the shift in the opposite direction due to bonding involving the s and p electrons.

Finally we note that our conclusions would be altered in detail if the electronic configuration of $\text{Ni}(\text{C}_5\text{H}_5)_2$ were $(a_{1g})^2(e_{2g})^1(e_{1g})^1(a_{1g})^1$, but that the predicted sign of the shift would be unaltered.

REFERENCES

- [1] McCONNELL, H. M., and HOLM, C. A., 1957, *J. chem. Phys.*, **27**, 314.
- [2] McCONNELL, H. M., and HOLM, C. A., 1958, *J. chem. Phys.*, **28**, 750.
- [3] DUNITZ, J. D., and ORGEL, L. E., 1955, *J. chem. Phys.*, **23**, 1954.
- [4] McCONNELL, H. M., and CHESNUT, D. B., 1958, *J. chem. Phys.*, **28**, 107.
- [5] WEISSMAN, S. I., 1956, *J. chem. Phys.*, **25**, 890.
- [6] McCONNELL, H. M., PORTERFIELD, W. W., and ROBERTSON, R. E., 1959, *J. chem. Phys.*, **30**, 442.
- [7] ORGEL, L. E., 1959, *J. chem. Phys.*, **31**, 1617.
- [8] ORGEL, L. E., 1955, *J. chem. Phys.*, **23**, 1819.
- [9] POPLE, J. A., SCHNEIDER, W. G., and BERNSTEIN, H. J., 1959, *High Resolution Nuclear Magnetic Resonance* (New York: McGraw-Hill).
- [10] McCONNELL, H. M., and ROBERTSON, R. E., 1958, *J. chem. Phys.*, **29**, 1361.

The collisional stabilization of excited β -naphthylamine molecules by the paraffin hydrocarbons in the gas phase†

by B. STEVENS‡

The James Forrestal Research Center,
Princeton University, Princeton, New Jersey, U.S.A.

(Received 24 September 1960)

The transfer of vibrational energy from molecules of β -naphthylamine excited by the mercury lines at 2804 Å and 2652 Å to the homologous series of paraffin hydrocarbons up to *n*-hexane has been investigated in the gas phase at 180°C. Although the average amount of energy transferred collisionally increases with the complexity of the added gas by a factor of 5, the transfer efficiency expressed as an accommodation coefficient remains virtually unchanged.

A transfer mechanism based on the internal redistribution of vibrational energy within the collision complex is examined, in terms of which it is unnecessary to invoke vibration-vibration transfer except for pentane and hexane. The collision duration estimated on the basis of this model is well within an order of magnitude of that expected from collision diameters and relative velocities of the molecules concerned.

1. INTRODUCTION

Boudart and Dubois [1] have treated the collisional deactivation of vibrationally excited complex molecules as a multi-stage process and applied their results to Neporent's data [2] for the intensification of β -naphthylamine vapour fluorescence at various inert gas pressures. It was found that whilst the average amount of vibrational energy *E* transferred on collision generally increases with the complexity of the added gas, the transfer efficiency expressed as an accommodation coefficient *z* shows no such variation and appears to be quite specific; thus for He, H₂, CO₂, NH₃, CHCl₃ and *n*-C₅H₁₂, *z* has the respective values 0.2, 0.1, 0.5, 0.9, 0.5 and 0.2 at 2652 Å and 150°C.

Herman and Rubin [3] have recently treated the steady-state distribution of vibrational energy among the harmonic oscillators of frequency *v* temporarily adsorbed on a surface at temperature *T*. On the assumption that the rate constant for desorption *k*₁ is independent of the energy of the adsorbed oscillator, solution of the appropriate relaxation equations leads to the simple expression for the vibrational accommodation coefficient *α*_v,

$$1/\alpha_v = 1 + k_1/k_2(1 - \exp[-hv/kT]).$$

Since this expression, in which *k*₂ is the rate constant for change in vibrational state, is valid only for very weak interaction between surface and oscillator, i.e. for *hv/kT* ≥ 3, the dominant parameter is the residence time 1/*k*₁ during which energy exchange is possible.

† This work was supported by the United States Air Force under Contract No. AF 33(038)-23976 monitored by the Air Force Office of the Scientific Research and Development Command, Washington, D.C.

‡ Present address: Department of Chemistry, The University, Sheffield 10, England.

Under the prevailing experimental conditions [1, 2] the vibrational temperature of the β -naphthylamine 'surface' is of the order of 800°K which would require that the lowest natural frequency of the stabilizing molecule is not less than 1500 cm^{-1} if the condition for weak interaction is to be met. Clearly for polyatomic gases with low-frequency bending and twisting vibrations the interaction is far from weak and the problem requires a different approach.

For strong interaction the transfer of internal energy from vibrationally excited complex molecules has much in common with unimolecular reactions if it is considered as an intramolecular redistribution of vibrational energy within the complex during its lifetime. On the one hand, the reaction rate is determined by the time required for the activation energy to accumulate in a critical coordinate, whereas on the other, the amount of energy transferred to certain vibrations of the complex is a function of the time available. Again it is apparent that the residence time or collision duration is a dominant parameter (the relatively high efficiency of naphthalene in transferring energy from excited perylene molecules is attributed to prolonged collisions between the planar conjugated systems [4]), whilst the approach to an equilibrium distribution of vibrational energy throughout the collision complex should be favoured by low vibrational frequencies of the added gas which lead to strong interaction with the 'accommodating' molecule.

In so far as a collision can be defined, its duration is related to the range of intermolecular forces and the translational energy along the line of centres of the colliding molecules. Moreover, if one of the molecules is electronically excited there exists the possibility of resonance stabilization of the collision complex if the electronic energy levels of the other are suitably spaced. The vibrational energy transferred from an excited molecule of β -naphthylamine should therefore depend on the polarizability, dipole moment, mass, vibrational frequencies and electronic energy levels of the transferring species, whilst the transfer efficiency will be determined in addition by its heat capacity. Since it is impossible to vary these parameters independently it was decided to reduce them to a minimum by investigating the transfer of vibrational energy from β -naphthylamine to the paraffin hydrocarbons. This is done by measuring their effect on the fluorescence yield of the amine vapour excited by the mercury 2652 Å and 2804 Å lines as previously described [1, 2]; under these conditions the energy transferred to these transparent non-polar molecules should depend largely on their complexity and vibrational frequencies. The investigation of energy transfer in this way has recently been reviewed [14, 15].

2. EXPERIMENTAL

The apparatus and procedure have been described [1, 5]; β -naphthylamine from J. T. Baker Chemical Co. was purified by vacuum sublimation and the paraffin hydrocarbons supplied by the Esso Research and Engineering Co. were distilled twice *in vacuo* before use.

3. RESULTS

If F_X and F are the fluorescence intensities of β -naphthylamine vapour in the presence and absence of added gas X respectively, the relative intensification

of fluorescence F_x/F is due to

- (a) a change in the extinction coefficient of the absorbing vapour brought about by pressure broadening at the low amine pressure, and
- (b) an increase in the fluorescence yield of the amine due to collisional removal of its excess vibrational energy.

According to Neppen [2], the first of these effects is virtually independent of wavelength, and is responsible for the total observed intensification at 3660 Å

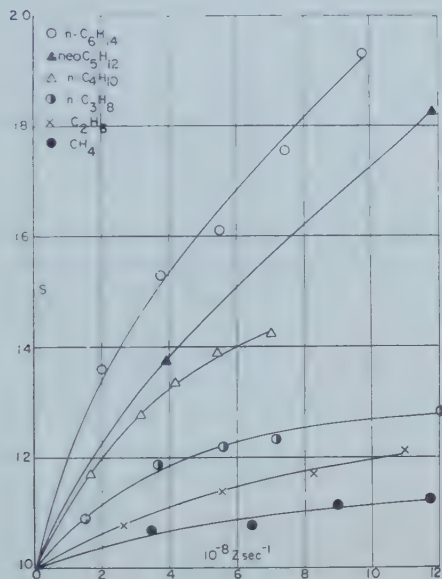


Figure 1. Stabilization curves for paraffin hydrocarbons at 180°C and 2804 Å.

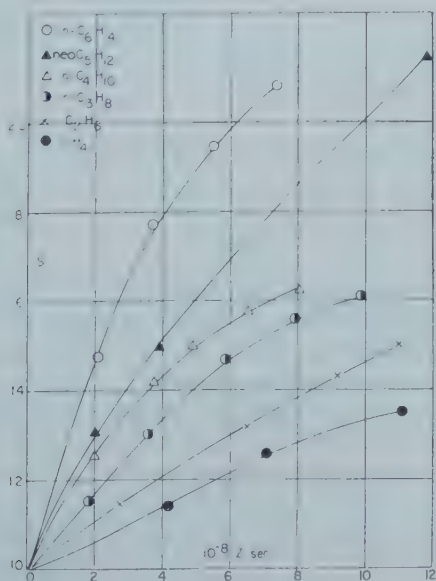


Figure 2. Stabilization curves for paraffin hydrocarbons at 180°C and 2652 Å.

where the amine has no excess vibrational energy. Consequently a correction for effect (a) is applied by comparing the relative intensification $(F_X/F)\lambda$ observed at the particular wavelength λ with that observed at 3660 Å [14]. The stabilization S given by

$$S = (F_X/F)\lambda / (F_X/F)_{3660}$$

is then a measure of effect (b).

S is plotted against the pressure of added gas X expressed as the collision frequency $Z\dagger$ in figures 1 ($\lambda=2804\text{ \AA}$) and 2 ($\lambda=2652\text{ \AA}$). In both cases the vapour temperature T was 180°C and the pressure of β -naphthylamine was sufficiently low (0.84 mm) to eliminate self-stabilization. Since the 0'-0" band in β -naphthylamine is at 29200 cm^{-1} [2], the excess vibrational energy ΔE excited by the 2804 \AA and 2652 \AA lines is 6460 cm^{-1} and 8460 cm^{-1} respectively; the corresponding vibrational temperatures given by [1]

$$T_{\text{vib}} = T + \Delta E / C_{\text{vib}}$$

where the vibrational heat capacity C_{vib} is 24 cm^{-1} ; c [2], are 722 K and 805 K.

As the result of collision between molecules of the amine M and the added gas X , an amount of vibrational energy E is removed from M , its vibrational temperature falls from $T_{1\text{ vib}}$ to $T_{2\text{ vib}}$ and the probability of internal conversion given by [1]

$$d = 2.5 \times 10^{12} \exp(-14200/RT_{\text{vib}})$$

is correspondingly reduced; this leads to an increase in the lifetime of M from τ_1 to τ_2 since

$$\tau = 1/(f+d)$$

where

$$\begin{aligned} 1/f &= \tau_0, \text{ the radiative lifetime of } M \\ &= 1.67 \times 10^{-8} \text{ sec [2].} \end{aligned}$$

The limiting slope of the stabilization curves in figures 1 and 2 is [1]

$$(dS/dZ)_{Z \rightarrow 0} = \tau_2 - \tau_1 \text{ sec}$$

which enables τ_2 and hence $T_{2\text{ vib}}$ to be calculated; consequently the amount of energy transferred at the first collision is

$$E = C_{\text{vib}}(T_{1\text{ vib}} - T_{2\text{ vib}}).$$

If C is the heat capacity of X at constant volume, α may be obtained from the expression [1]

$$\alpha = \frac{C_{\text{vib}} E}{C(\Delta E - E)}.$$

Values of E and α obtained in this way from the experimental stabilization curves are given in table 1 together with the corresponding lowest vibrational frequencies of the hydrocarbons used. The following points are noted.

- (a) Whilst E increases by a factor of at least 5 from methane to hexane, the transfer efficiency expressed as α remains virtually constant at 2652 \AA .
- (b) Although the data at 2804 \AA are less reliable, particularly for the smaller molecules since the relative intensification is lower, it is apparent that both E and α are smaller than at 2652 \AA but approach the values obtained at this wavelength as the complexity of X is increased.

† The collision diameters used are those appended by Rowlinson, 1954, *Quart. Rev. chem. Soc.*, **8**, 168.

- (c) The transfer data for neopentane agree well with that obtained from Neporent's data [2] for *n*-pentane. The independence of transfer efficiency on structure has previously been noted in the effect of similar molecules on the relaxation of nitrous oxide and ethylene [6].

Molecule	$\lambda = 2804 \text{ \AA}$		$\lambda = 2652 \text{ \AA}$		v_{\min}	v_{tors}
	$E (\text{cm}^{-1})$	α	$E (\text{cm}^{-1})$	α	cm^{-1}	cm^{-1}
CH_4	70	0.09	310	0.30	1306	—
C_2H_6	170	0.12	530	0.30	821	290
$n\text{-C}_3\text{H}_8$	340	0.16	790	0.30	375	202
$n\text{-C}_4\text{H}_{10}$	500	0.18	1130	0.34	432	200
$n\text{-C}_5\text{H}_{12}\dagger$	550	0.16	1350	0.33	—	200
neo- C_5H_{12}	760	0.23	1370	0.33	332	—
$n\text{-C}_6\text{H}_{14}$	1030	0.28	1750	0.38	—	200

† Neporent's data at 190°C [2].

Table 1. Energy transfer data for paraffin hydrocarbons at 180°C .

4. DISCUSSION

The quantity obtained from the experimental data is the average amount of vibrational energy E lost by the excited β -naphthylamine molecule at its first collision with X . This energy may be taken up in the translational, rotational and internal degrees of freedom of X and it would be desirable to factorize the molecular accommodation coefficient α into the corresponding components α_T , α_R and α_I , so that the physical properties of X which determine E and α could be ascertained. Since the transfer efficiency calculated in terms of the total heat capacity of X is virtually the same for the molecules investigated it is possible that the translational, rotational and vibrational modes of X are all involved in the transfer process; however the use of vibrotational or simply vibrational heat capacities would not change the relative magnitudes of α appreciably.

4.1. Vibration-translation transfer

Stabilization by helium [2] indicates that E can appear as translational energy of the colliding species; however, in accordance with the 'non-adiabatic collision' principle [7] the probability of vibration-translation transfer decreases rapidly with increasing molecular complexity in so far as this determines the collision duration, and its contribution to the overall effect considered here may be very small†. On the other hand, ultrasonic dispersion has not yet been observed in paraffin hydrocarbons higher than propane [8] due to extremely rapid equilibration of energy between translational and internal modes of these molecules themselves.

† Under the prevailing conditions the excited amine molecule undergoes a first-order radiationless transition with a frequency factor ν of $2.54 \times 10^{12} \text{ sec}^{-1}$ which according to Slater [9] is the average vibrational frequency of the excited molecule. For efficient vibration-translation transfer the collision duration should not therefore exceed $1/2\pi\nu$ or $7 \times 10^{-14} \text{ sec}$; this is at least one order of magnitude less than the collision durations estimated for the molecules considered here (table 3).

4.2. Vibration-rotation transfer

It has been concluded [1] that the rotational levels of the hydrogen molecule are inactive in the stabilization of β -naphthylamine. However, there is no reason to believe that this is the case for larger stabilizing molecules and Bowen and Veljkovic have suggested that rotational degrees of freedom play an important part in the stabilization of excited molecules of perylene by nitrogen, *p*-cymene, naphthalene and hexamethylbenzene [4].

4.3. Vibration-vibration transfer

It would be surprising if a part of the comparatively large amounts of vibrational energy lost by β -naphthylamine were not taken up internally particularly by the higher paraffins with low vibrational frequencies. If however the excitation of internal modes is the dominant process, it is difficult to see why neopentane should take up almost twice the energy transferred to propane in which the lowest vibrational frequency has virtually the same value. That E is several times greater than the lowest vibrational frequency in a number of cases indicates either that more than one quantum of vibrational energy is excited on collision or that the translational and rotational degrees of freedom play an important part.

It therefore appears that at the present time it is impossible to assess the extent to which the various degrees of freedom of the stabilizing molecule contribute to the overall effect observed, and until this can be achieved no reliable relationship between E , α and the vibrational frequencies of the stabilizing molecule can be established.

5. A COLLISION COMPLEX TRANSFER MECHANISM

In view of the facts that the amount of energy transferred depends on

- (a) the vibrational temperature of the excited β -naphthylamine molecule, and
- (b) the duration of the collision during which transfer takes place which accounts for the negative vapour temperature coefficient of E [1],

the following mechanism is examined with a view to relating E to these parameters:

- (i) the excited amine M and the stabilizing molecule X form a collision complex of duration t ; its formation is accompanied by the disappearance of three rotational and three translational degrees of freedom and the appearance of six 'transitional' vibrations of low frequency which arise from intermolecular forces;
- (ii) during the interval t an equilibrium redistribution of vibrational energy among all the vibrations of the complex is approached; since the interaction will be greatest between vibrations of lowest frequency [10], the equilibration of the transitional vibrations may be expected to precede that of the internal vibrations of X and the transfer of energy from M to X may be regarded as taking place via the transitional oscillators;
- (iii) the complex dissociates into its original constituents M and X after time t , the energy of the transitional oscillators appearing as rotational and translational energy not of the stabilising molecule alone but of both colliding partners.

On the basis of this mechanism, translational and rotational accommodation precede vibration-vibration transfer under conditions such that vibration-

translation transfer should be negligible according to the non-adiabatic collision principle; moreover, the accommodation coefficient is now related not only to the heat capacity of X but to the translational and rotational heat capacities of M , the importance of which has recently been noted by Neporent and Mirumyants [11].

Let us assume that s classical oscillators of heat capacity R are effective in removing the excess vibrational energy of M during collision as a result of which the vibrational temperature of M is reduced to $T_{2\text{vib}}$ given by

$$T_{2\text{vib}} = T + \Delta E / (C_{\text{vib}} + sR).$$

If all six transitional oscillators are effective for perfect translational and rotational accommodation in which case the vibrational temperature of M is reduced to

$$T'_{2\text{vib}} = T + \Delta E / (C_{\text{vib}} + 6R)$$

it is now possible to define a transrotational accommodation coefficient α_{TR} such that

$$\alpha_{TR} = \frac{(T_{1\text{vib}} - T_{2\text{vib}})}{(T_{1\text{vib}} - T'_{2\text{vib}})} = \frac{s(C_{\text{vib}} + 6R)}{6(C_{\text{vib}} + sR)}.$$

Values of s and α_{TR} obtained in this way from the stabilization curves in figures 1 and 2 are given in table 2, from which it is seen that it is unnecessary to invoke vibration-vibration transfer except in the case of hexane and of pentane at the shorter wavelength where $s > 6$; for these molecules the vibrational accommodation coefficients α_V are calculated from the energy transferred in excess of that required for $\alpha_{TR}=1$ and the appropriate internal heat capacity ($C_p - 3R$) of X . It is apparent that the transfer efficiency expressed as α_{TR} increases regularly with the complexity of the stabilizing molecule, whilst the accommodation coefficient for NH_3 which is included in table 2 for comparison is now no greater than that of propane or butane.

Molecule	$\lambda = 2804 \text{ \AA}$			$\lambda = 2652 \text{ \AA}$		
	s	α_{TR}	α_V	s	α_{TR}	α_V
CH_4	0.4	0.1	0	1.3	0.2	0
C_2H_6	0.9	0.2	0	2.2	0.4	0
$n\text{-C}_3\text{H}_8$	1.9	0.3	0	3.5	0.6	0
$n\text{-C}_4\text{H}_{10}$	2.9	0.5	0	4.3	0.7	0
neo- C_5H_{12}	4.7	0.8	0	6.6	1.0	0.02
$n\text{-C}_6\text{H}_{14}$	6.6	1.0	0.01	8.9	1.0	0.09
NH_3 †	—	—	—	4.3	0.7	0

† Neporent's data at 150°C [2].

Table 2. Number of classical oscillators s effective in collisional energy transfer.

6. THE COLLISION DURATION

Since a collision is defined in terms of the phenomenon for which it is responsible, an independent estimate of its duration t is neither easily made nor readily justifiable. In the present case t may be obtained from the energy transfer data on the basis of the mechanism proposed above if the further assumption is allowed that the rates of internal and external redistribution of vibrational energy

in M are the same. In this case, since the frequency of internal distribution of energy E is

$$2.54 \times 10^{12} \exp(-E/RT_{\text{vib}}) \text{ sec}^{-1}$$

the time $t(E)$ required for the transfer of energy E is given by

$$t(E) = 4.0 \times 10^{-13} \exp(+E/RT_{\text{vib}}) \text{ sec}^{-1}.$$

Molecule	$10^{13} t(E) \text{ sec}$		$10^{18} t(\sigma, V) \text{ sec}$
	2804 \AA	2652 \AA	
CH_4	4.5	6.8	6.1
C_2H_6	5.5	10	8.4
$n\text{-C}_3\text{H}_8$	7.8	16	10
$n\text{-C}_4\text{H}_{10}$	11	30	12
$\text{neo-C}_5\text{H}_{12}$	18	45	13
$n\text{-C}_6\text{H}_{14}$	31	90	14

Table 3. Collision duration $t(E)$ calculated from energy transfer data.

Values of $t(E)$ calculated in this way from the data in table 1 are given in table 3 together with $t(\sigma, V)$ obtained from the approximate expression [12]

$$t(\sigma, V) = \sigma_{MX}/V \text{ sec}$$

where σ_{MX} and V are the collision diameter and relative velocity of approach of the colliding molecules M and X . The agreement is well within an order of magnitude which is perhaps as much as can be expected, and the larger values of $t(E)$ estimated for the higher hydrocarbons might well be ascribed to 'wrestling' collisions [13].

The author would like to thank Mr. J. D. Lambert and Dr. P. G. Dickens for helpful discussions, and the Esso Research and Engineering Co. for a gift of hydrocarbons.

REFERENCES

- [1] BOUDART, M., and DUBOIS, J. T., 1955, *J. chem. Phys.*, **23**, 223.
- [2] NEPORENT, B. S., 1947, *J. phys. Chem. Moscow*, **21**, 1111; 1950, *Ibid.*, **24**, 1219.
- [3] HERMAN, R., and RUBIN, R. J., 1958, *J. chem. Phys.*, **29**, 591.
- [4] BOWEN, E. J., and VELJKOVIC, S., 1956, *Proc. roy. Soc. A*, **236**, 1.
- [5] DUBOIS, J. T., 1956, *J. chem. Phys.*, **25**, 178.
- [6] ARNOLD, J. W., MCCOUBREY, J. C., and UBBELOHDE, A. R., 1958, *Proc. roy. Soc. A*, **248**, 445.
- [7] ZENER, C., 1931, *Phys. Rev.*, **37**, 556.
- [8] LAMBERT, J. D., and SALTER, R., 1959, *Proc. roy. Soc. A*, **253**, 277.
- [9] SLATER, N. B., 1948, *Proc. roy. Soc. A*, **194**, 112.
- [10] SPONER, H., and TELLER, E., 1941, *Rev. mod. Phys.*, **13**, 75.
- [11] NEPORENT, B. S., and MIRUMYANTS, S. O., 1960, *Opt. Spectrosc.*, **8**, 336.
- [12] MASSEY, H. S. W., and BURHOP, E. H. S., 1952, *Electronic and Ionic Impact Phenomena* (Oxford: Clarendon Press).
- [13] MCCOUBREY, J. C., and MCGRATH, W. D., 1957, *Quart. Rev. chem. Soc.*, **11**, 87.
- [14] STEVENS, B., 1957, *Chem. Rev.*, **57**, 439.
- [15] STEVENS, B., and BOUDART, M., 1957, *Ann. N.Y. Acad. Sci.*, **67**, 570.

RESEARCH NOTES

The anomalous temperature dependence of the sound velocity in water

by J. SCHUYER

Centraal Laboratorium, Staatsmijnen in Limburg, Geleen, The Netherlands

(Received 14 April 1960)

The sound velocity in all liquids, except water, has a negative temperature coefficient. For non-associated compounds the following equation holds [1]:

$$\frac{1}{v} \frac{dv}{dT} = \frac{A}{\rho} \frac{dp}{dT}$$

where v , ρ and T represent the sound velocity, the density, and the temperature, respectively, and A is practically equal to 3 for these compounds. This relation can be derived [2, 3] from the potential energy u between the molecules:

$$u = -\frac{a}{r^6} + \frac{b}{r^n}$$

where r = intermolecular distance. From this derivation it follows [3] that

$$A = \frac{7+n}{6}.$$

The value of A for associated compounds is markedly lower, whereas water exhibits a striking exception to the above relation as the sound velocity in water increases with temperature to pass through a maximum at 74°C [4-6].

The anomalous temperature dependence of the sound velocity in water can be qualitatively described by introducing a temperature-dependent attraction term into the potential energy function:

$$u = -\frac{a_1}{r^6} - \frac{a_2}{Tr^6} + \frac{b}{r^n}. \quad (1)$$

This leads to the relation:

$$\frac{1}{v} \frac{dv}{dT} = \frac{n+7}{6} \frac{1}{\rho} \frac{dp}{dT} + \frac{7}{2n-12} \cdot \frac{x}{T} \quad (2)$$

where x is given by

$$\frac{a_1}{a_2} T = \frac{1-x}{x}.$$

The maximum in the $v-T$ curve of water is then due to the difference in sign between the two terms in the right-hand member of equation (2).

It is possible to give a quantitative interpretation if it is assumed that the attraction term

$$-\frac{a_1}{r^6}$$

in equation (1) is due to the combined effect of dispersion and induction forces, and the attraction term

$$-\frac{a_2}{Tr^6}$$

to dipole-dipole interaction. In that case a_1 and a_2 can be calculated [7] by:

$$a_1 = 11 \cdot 25 \cdot 10^{-24} p^{1/2} \alpha^{3/2} + 2\alpha\mu^2, \quad (3a)$$

$$a_2 = \frac{2\mu^4}{3k}, \quad (3b)$$

where p = number of electrons in the outermost shells, α = polarizability, μ = dipole moment and k = Boltzmann's constant.

In equation (3a) the Slater-Kirkwood approximation is used for computing the dispersion energy. Equation (3b) actually applies only if

$$\frac{\mu^2}{r^3} \ll kT;$$

since for water

$$\frac{\mu^2}{r^3}$$

is of the same order of magnitude as kT , this equation serves as an approximation only.

This interpretation of equation (1) implies that x represents the relative contribution of dipole-dipole interaction to the total attraction energy.

From equation (2) the experimental value of x can be derived, provided n is known. According to Altenburg [8] n is a function of p :

$$n = 8 + 0.288p(\pm 2).$$

For water ($p=8$) we therefore take $n=10$. If this value is used, the agreement between the values of x calculated from equation (2) and equation (3) respectively is surprisingly good (see table).

In substances similar to water, such as liquid ammonia [9] and hydrogen fluoride [10], the sound velocity does not show an anomalous temperature dependence. However, application of equation (2) to these compounds also leads to a satisfactory agreement with the calculated x -values (see table).

Compound	H ₂ O	NH ₃	HF
T (°K)	347	213	273
1 dv / v dT	0	-0.00319	-0.00495
1 dρ / ρ dT	-0.00059	-0.00187	-0.00226
p	8	8	8
n	10	10	10
α (Å ³)	1.48	2.21	2.46
μ (Debye units)	1.84	1.50	1.91
x [equation (3)]	0.68	0.47	0.58
x [equation (2)]	0.65	0.51	0.49

Computation of x .

According to equation (2), the anomaly of water can be attributed to its low thermal expansion coefficient. In view of the much higher coefficients for ammonia and hydrogen fluoride the temperatures at which a maximum can be expected are much lower than the melting points.

REFERENCES

- [1] RAMA RAO, M., 1940, *Indian J. Phys.*, **14**, 109.
- [2] ALTBURG, K., 1950, *Kolloidzschr.*, **117**, 153.
- [3] SCHUYER, J., 1959, *J. polymer Sci.*, **36**, 475.
- [4] WILLARD, G. W., 1947, *J. acoust. Soc. Amer.*, **19**, 235.
- [5] NEUMANN, E. A., 1947, *Proc. phys. Soc. Lond.*, **59**, 585.
- [6] SMITH, A. H., and LAWSON, A. W., 1954, *J. chem. Phys.*, **22**, 253.
- [7] See e.g. STUART, H. A., 1952, *Die Physik der Hochpolymeren*, Vol. I, Chapter I (Berlin, Göttingen, Heidelberg).
- [8] ALTBURG, K., 1959, *Habilitationsschrift* (Leipzig).
- [9] SCHUYER, J. (unpublished results).
- [10] LAGEMANN, R. T., and KNOWLES, C. H., 1960, *J. chem. Phys.*, **32**, 561.

Dynamical Jahn-Teller effect in molecules possessing one four-fold symmetry axis

by M. S. CHILD

University Chemical Laboratory, Lensfield Road, Cambridge

(Received 23 September 1960)

1. INTRODUCTION

Jahn and Teller [1] have shown that the components of a degenerate electronic state of symmetry Γ_e are coupled by terms linear in normal coordinates of symmetry Γ_q if the symmetrized product of Γ_e with itself contains Γ_q , i.e. if

$$[\Gamma_e^2] \text{ contains } \Gamma_q. \quad (1)$$

Renner [2] first showed that in such a case the Born-Oppenheimer method [3] must be generalized, by taking the total wave function to have the form

$$\Psi = \sum_t \psi_t \chi_t \quad (2)$$

where ψ_t and χ_t are electronic and vibrational functions respectively. Several authors [2, 4-6] have shown that this form for Ψ leads to a set of coupled equations for the many-component vibrational wave function χ :

$$\{(H_0 - E)\mathbf{I} + \mathbf{V}\} \chi = 0. \quad (3)$$

Here H_0 is the vibrational Hamiltonian, \mathbf{I} the unit matrix and the elements of the matrix \mathbf{V} are functions of the normal coordinates. These may be expanded as Taylor series and in the Jahn-Teller case only the linear terms are considered. Their form is determined by symmetry.

Table III of reference [1] shows which coordinates satisfy condition (1) for all point groups of chemical interest. One observes that:

- (a) linear molecules cannot show the Jahn-Teller effect;
- (b) for all axial point groups except C_4 , C_{4v} , C_{4h} , D_4 , D_{4h} and S_4 , vibrations of types a_1 and e interact with electronic motions of type e —a situation which has been discussed by several authors [4, 5];
- (c) for the above-mentioned groups (C_4 , etc.) vibrations of types a_1 and b mix the components of an electronic manifold of type e . This is the only case still to be considered, since an elegant study of the vibronic problems presented by molecules of cubic symmetry has also been published [7].

2. C_4 POINT GROUPS

Coupling terms in the a_1 coordinates may be neglected. They occur only on the diagonal of \mathbf{V} and merely produce a uniform depression of all the energy levels and the same change in the equilibrium values of the a_1 coordinates for both components of the electronic state.

If the electronic functions ψ_+ , ψ_- are chosen so that

$$C_4\psi_{\pm} = \pm i\psi_{\pm} \quad (4)$$

and if the coordinates Q_1 , Q_2 (with vibrational frequencies ω_1 , ω_2 and associated masses M_1 , M_2) have the symmetries given in the table, equation (3) reduces to

$$\{(H_0 - E)\mathbf{I} + k_1\sigma_1 Q_1 + k_2\sigma_2 Q_2\} \mathbf{\chi} = 0 \quad (5)$$

where k_1 , k_2 are constants and σ_1 , σ_2 the Pauli matrices

$$\sigma_1 = \begin{bmatrix} 0 & 1 \\ 1 & 0 \end{bmatrix}, \quad \sigma_2 = \begin{bmatrix} 0 & -i \\ i & 0 \end{bmatrix}.$$

Point group Q	C_4	C_{4v}	C_{4h}	D_4	D_{4h}	S_4
Q_1 Q_2	b	b_1 b_2	b_g	b_1 b_2	b_{1g} b_{2g}	b

If $k_1 = 0$, $k_2 = 0$, (5) has solutions which may be labelled $|n_1 n_2 \Lambda\rangle$ satisfying

$$H_0 |n_1 n_2 \Lambda\rangle = \{(n_1 + \frac{1}{2})\omega_1 + (n_2 + \frac{1}{2})\omega_2\} |n_1 n_2 \Lambda\rangle.$$

The symbol Λ takes the values ± 1 according as the vibrations are associated with ψ_{\pm} . For $k_1 \neq 0$, $k_2 \neq 0$ the solutions of (5) are taken as linear combinations of the $|n_1 n_2 \Lambda\rangle$.

The non-zero matrix elements connecting these functions are

$$\begin{aligned} \langle n_1 n_2 \pm 1 | k_1 \sigma_1 Q_1 | n_1 + 1 n_2 \mp 1 \rangle &= \hbar \sqrt{[(n_1 + 1)\Delta_1 \omega_1]}, \\ \langle n_1 n_2 \pm 1 | k_1 \sigma_1 Q_1 | n_1 - 1 n_2 \mp 1 \rangle &= \hbar \sqrt{(n_1 \Delta_1 \omega_1)}, \\ \langle n_1 n_2 \pm 1 | k_2 \sigma_2 Q_2 | n_1 n_2 + 1 \mp 1 \rangle &= \pm \hbar \sqrt{[(n_2 + 1)\Delta_2 \omega_2]}, \\ \langle n_1 n_2 \pm 1 | k_2 \sigma_2 Q_2 | n_1 n_2 - 1 \mp 1 \rangle &= \pm \hbar \sqrt{(n_2 \Delta_2 \omega_2)}, \end{aligned}$$

where

$$\Delta_i = \frac{k_i^2}{2M_i\omega_i^2\hbar} \quad (i=1 \text{ or } 2).$$

Ψ may therefore have either the form

$$\Psi = a_{00}|001\rangle + a_{10}|10-1\rangle + a_{01}|01-1\rangle + a_{20}|201\rangle + a_{11}|111\rangle + a_{02}|021\rangle + \dots \quad (6)$$

or an exactly equivalent one obtained by replacing Λ by $-\Lambda$. In both cases (5) reduces to the matrix equation

$$\begin{bmatrix} -\epsilon & \sqrt{(\Delta_1 \omega_1)} & \sqrt{(\Delta_2 \omega_2)} & 0 & 0 & 0 & \dots \\ \sqrt{(\Delta_1 \omega_1)} & \omega_1 - \epsilon & 0 & \sqrt{(2\Delta_1 \omega_1)} & -\sqrt{(\Delta_2 \omega_2)} & 0 & \dots \\ \sqrt{(\Delta_2 \omega_2)} & 0 & \omega_2 - \epsilon & 0 & \sqrt{(\Delta_1 \omega_1)} & \sqrt{(2\Delta_2 \omega_2)} & \dots \\ 0 & \sqrt{(2\Delta_1 \omega_1)} & 0 & 2\omega_1 - \epsilon & 0 & 0 & \dots \\ 0 & -\sqrt{(\Delta_2 \omega_2)} & \sqrt{(\Delta_1 \omega_1)} & 0 & \omega_1 + \omega_2 - \epsilon & 0 & \dots \\ 0 & 0 & \sqrt{(2\Delta_2 \omega_2)} & 0 & 0 & 2\omega_2 - \epsilon & \dots \\ \vdots & \vdots & \vdots & \vdots & \vdots & \vdots & \vdots \end{bmatrix} \begin{bmatrix} a_{00} \\ a_{10} \\ a_{01} \\ a_{20} \\ a_{11} \\ a_{02} \\ \vdots \end{bmatrix} = 0, \quad (7)$$

whose latent roots ϵ have the dimensions of a frequency. They are related to the roots E of (5) by

$$E = \hbar[\epsilon + \frac{1}{2}(\omega_1 + \omega_2)]. \quad (8)$$

Exact solutions of (7) require arduous numerical methods, but if Δ_1 , Δ_2 are small compared with ω_1 , ω_2 and $\omega_1 - \omega_2$, values of E may be obtained by second-order perturbation theory. To this degree of accuracy the solutions of (5) are

$$E = \hbar \left[(n_1 + \frac{1}{2})\omega_1 + (n_2 + \frac{1}{2})\omega_2 - (\Delta_1 + \Delta_2) + \frac{2\Delta_1\Delta_2}{\omega_1 - \omega_2} \left\{ n_1(n_2 + 1) - (n_1 + 1)n_2 \right\} \right]. \quad (9)$$

Expression (9) may be generalized to allow for interactions between p vibrations of type Q_1 and q vibrations of type Q_2 , specified by ω_{1i} , Δ_{1i} ($i = 1 \dots p$) and ω_{2j} , Δ_{2j} ($j = 1 \dots q$) respectively. In this case

$$E = \hbar \sum_{ij} \left[(n_{1i} + \frac{1}{2})\omega_{1i} + (n_{2j} + \frac{1}{2})\omega_{2j} - (\Delta_{1i} + \Delta_{2j}) + \frac{2\Delta_{1i}\Delta_{2j}}{(\omega_{1i} - \omega_{2j})} \left\{ n_{1i}(n_{2j} + 1) - (n_{1i} + 1)n_{2j} \right\} \right]. \quad (10)$$

In this approximation there is no Jahn-Teller coupling between vibrations of the same type.

I wish to thank Professor H. C. Longuet-Higgins for kindly suggesting this problem and for his help and discussions. I also gratefully acknowledge a grant from the Department of Industrial and Scientific Research.

REFERENCES

- [1] JAHN, H. A., and TELLER, E., 1937, *Proc. roy. Soc. A*, **161**, 220.
- [2] RENNER, E., 1934, *Z. Phys.*, **92**, 172.
- [3] BORN, M., and OPPENHEIMER, J. R., 1927, *Ann. Phys., Lpz.*, **84**, 457.
- [4] LONGUET-HIGGINS, H. C., ÖPIK, U., PRYCE, M. H. L., and SACK, R. A., 1958, *Proc. roy. Soc. A*, **244**, 1.
- [5] MOFFITT, W., and THORSON, W. R., 1958, 'Calcul des fonctions d'onde Moléculaire', Recueil de Mémoires, Centre Nationale de la Recherche Scientifique, November.
- [6] LONGUET-HIGGINS, H. C., 1960, *Advances in Spectroscopy*, Vol. 2, Ed. H. W. Thompson (in the press).
- [7] MOFFITT, W., and THORSON, W. R., 1957, *Phys. Rev.*, **108**, 1251.

Vibrational-electronic coupling in IrF_6 , OsCl_6^{2-} and IrCl_6^{2-}

by M. S. CHILD

Department of Theoretical Chemistry, University Chemical Laboratory,
Lensfield Road, Cambridge

(Received 13 October 1960)

A recent unsuccessful search for the dynamical Jahn-Teller effect in IrF_6 has been reported [1]. It is the purpose of this note to show why this effect is too small to be observed except under rather high resolution and to investigate the vibrationally induced coupling between different electronic states.

Weak bands in the absorption spectra of the hexafluorides of transition metals with outer electronic configurations $5d^1$ — $5d^4$ have been interpreted on the basis of ligand field theory [2]. The ligand field splitting is large and to a good approximation only those configurations involving electrons in the t_{2g} orbitals need be considered in calculating the lowest electronic energy levels. The calculations are simplified by using the isomorphism between t_{2g} and p orbitals [3]. One may therefore use the methods of atomic spectroscopy [4] to obtain terms, which are then split by spin-orbit coupling. The terms are labelled $^{2S+1}L'$ to indicate that their components are eigenfunctions of an effective orbital angular momentum operator \mathbf{L}'^2 . Similarly the states into which the terms are split by spin-orbit coupling are eigenfunctions of \mathbf{J}'^2 where

$$\mathbf{J}' = \mathbf{L}' + \mathbf{S}.$$

The components of a degenerate ground state may be mixed together by small changes in the nuclear configuration, in which case one may observe the Jahn-Teller effect [5]. There may also be a smaller effect due to coupling between the components of the ground and excited electronic states, with wave functions ψ_0 and ψ_e respectively. This coupling may be represented by functions V_{0e} of the normal coordinates. Let us consider linear terms in the mass-adjusted normal coordinates, Q_i , which have vibrational frequencies ω_i ; i.e.,

$$V_{0e} = \sum_i l_{ei} Q_i, \quad (1)$$

where l_{ei} are constants. The second-order correction to the m th vibrational energy level (E_{0m}) associated with ψ_0 due to interaction with a particular excited state ψ_e is

$$\Delta E_{0m}^e = \sum_n \frac{| \int X_{0m} V_{0e} X_{en} dQ |^2}{E_{0m} - E_{en}}. \quad (2)$$

The X 's are vibrational wave functions. If the energy difference $E_{0m} - E_{en}$

is approximately constant over the range for which the numerator on the right-hand side of (2) is large, we may use the closure property of the X_{en} and write

$$\Delta E'_{0m} \simeq \frac{\int |X_{0m} V_{0e}^2 X_{0m} dQ|^2}{E_0 - E_e}. \quad (3)$$

Taking

$$\begin{aligned} X_{0m} &= \prod_i \eta_{mi}(Q_i), \\ \Delta E'_{0m} &= \frac{\sum_i l_{ei}^2 \int \eta_{mi} Q_i^2 \eta_{mi} dQ_i}{E_0 - E_e} \\ &= \sum_i \frac{l_{ei}^2}{E_0 - E_e} \times \frac{\hbar}{\omega_i} (m_i + \frac{1}{2}). \end{aligned} \quad (4)$$

Vibrational-electronic coupling between the ground and excited states therefore leads to a small reduction in the apparent frequencies of vibration in those normal modes for which $l_{ei} \neq 0$. For this condition to be satisfied the ground and excited electronic states (with spatial symmetries Γ_0 and Γ_e respectively) must have the same spin multiplicity, and the direct product $\Gamma_0 \times \Gamma_e$ must contain the symmetry of the normal mode Q_i . This coupling will be most effective when the energy difference $E_0 - E_e$ is small. It will be important only if the much stronger Jahn-Teller coupling is absent.

(i) $5d^3 \text{IrF}_6$

The lowest term is $^4S'$ which is mixed with $^2P'$ by spin-orbit coupling to give a fourfold degenerate ground state (Γ_8) whose components have wave functions of the form:

$$\Psi = \sqrt{(1 - c^2)} \psi(^4S'_{3/2}) + c \psi(^2P'_{3/2}).$$

If $c = 0$ there can be no Jahn-Teller effect since the degeneracy arises only from the spin multiplicity and cannot be removed by changes in the nuclear configuration. There can be no vibronic coupling between the ground state $^4S'_{3/2}$ and the low-lying excited states $^2D'_{5/2, 3/2}$ and $^2P'_{3/2, 1/2}$. For $c \neq 0$ one predicts a dynamical Jahn-Teller effect in the e_g and t_{2g} normal modes, but the effect on the vibrational energy levels is proportional to c^2 . In IrF_6 , $c^2 = 0.1$ and so the effect is certainly small. The Raman spectrum of ReF_6 [6] (whose ground state is almost pure $^2P'_{3/2}$) shows rather diffuse peaks assigned to the e_g and t_{2g} vibrations, both of which are about 50 cm^{-1} lower than one would expect by comparison with the vibrational spectra of WF_6 [7] and PtF_6 [8]. From this one may estimate the strength of vibronic coupling in this type of molecule, and hence, using the value of c^2 , obtain an estimate of the Jahn-Teller splitting of the vibronic energy levels in IrF_6 . For both e_g and t_{2g} modes this splitting is about 5 cm^{-1} .

(ii) $5d^4 \text{PtF}_6$ and OsCl_6^{2-} ; $5d^5 \text{IrCl}_6^{2-}$

All these species have non-degenerate ground states and so cannot show the Jahn-Teller effect. But in all cases there may be vibrationally induced coupling between the ground state and a low-lying excited state, which would cause a small reduction ($\Delta\omega$) in the apparent vibrational frequencies in the normal modes e_g and t_{2g} . The order of magnitude of this effect in PtF_6 may be estimated by direct comparison with ReF_6 . The effect will be rather larger for OsCl_6^{2-} than for PtF_6 since the charge on the central ion is smaller. The

factor of 2·5 is adopted on the basis of a point charge model, which is also used to compare the effects in OsCl_6^{2-} and IrCl_6^{2-} . The values of $\Delta\omega$ are given in the table.

Species	Ground state	Interacting excited state		$\Delta\omega(e_g)$ (cm ⁻¹)	$\Delta\omega(t_{2g})$ (cm ⁻¹)
		Symmetry	Energy (cm ⁻¹)		
PtF ₆	A_2	$E + T_1$	5500†	2	4
OsCl_6^{2-}	A_2	$E + T_1$	$\sim 4000\ddagger$	5	10
IrCl_6^{2-}	Γ_6	Γ_8	$\sim 4000\ddagger$	10	10

† This value is taken from reference [2].

‡ These values are obtained by taking the one-electron spin-orbit coupling constant as $\zeta_d \sim 2700 \text{ cm}^{-1}$.

The author wishes to acknowledge the helpful discussions and advice from Professor H. C. Longuet-Higgins. He also gratefully acknowledges a Research Grant from the D.S.I.R.

REFERENCES

- [1] CLAUSSEN, H. H., and WEINSTOCK, B., 1960, *J. chem. Phys.*, **33**, 436.
- [2] MOFFITT, W., GOODMAN, G. L., FRED, M., and WEINSTOCK, B., 1959, *Mol. Phys.*, **2**, 109.
- [3] ABRAGAM, A., and PRYCE, M. H. L., 1951, *Proc. roy. Soc. A*, **205**, 135.
- [4] CONDON, E. U., and SHORTLEY, G. H., 1957, *The Theory of Atomic Spectra* (Cambridge University Press), Chapters VII and VIII.
- [5] JAHN, H., and TELLER, E., 1937, *Proc. roy. Soc. A*, **161**, 220.
- [6] GAUNT, J., 1954, *Trans. Faraday Soc.*, **50**, 209.
- [7] BURKE, T. G., SMITH, D. F., and NIELSEN, A. H., 1952, *J. chem. Phys.*, **20**, 447.
- [8] WEINSTOCK, B., CLAUSSEN, H. H., and MALM, J. G., 1960, *J. chem. Phys.*, **32**, 181.

Rotational isomerism in aldehydes

by R. J. ABRAHAM and J. A. POPLE

National Physical Laboratory Teddington

(Received 13 October 1960)

There have been many studies of rotational isomerism about carbon–carbon single bonds in ethane-like molecules such as 1,2 dichloroethane [1]. It is well known that the six bonds emanating from a C—C link take up a staggered rather than eclipsed position when viewed along the C—C axis and various isomeric possibilities in substituted ethanes can be classified accordingly. If one or both of the carbon atoms also form part of double bonds, it appears that a staggered configuration is again preferred if the double bond is treated as a pair of bent single bonds (one above and one below the plane of sp^2 hybridization) [2]. Thus in acetaldehyde, the equilibrium configuration is one in which the aldehyde (CHO) group is coplanar with the C—C single bond and one of the C—H bonds of the methyl group is cis or eclipsed with the carbonyl bond [3]. The structure can be illustrated schematically as in (1).



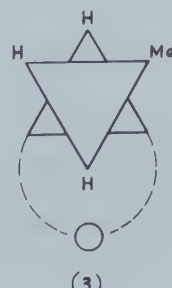
(1)

A similar configuration is found for the methyl group in propylene where the methyl group eclipses the C=C double bond [4]. In molecules such as chloroacetyl chloride $ClH_2C=COCl$ and chloroacetone $ClH_2C=COCH_3$, there is evidence for two isomeric forms with different configurations of the ClH_2C- group, one of them having the C—Cl bond approximately cis with the carbonyl group [5, 6].

Application of this rule to other aldehydes suggests that many such molecules may have distinguishable rotational isomers existing in equilibrium. A simple example is propionaldehyde which could be in either of the forms (2) or (3). If



(2)

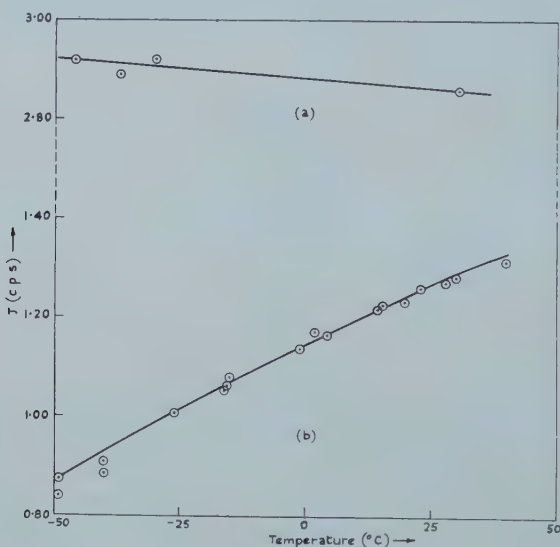


(3)

the forms differ in energy, the relative populations of the two configurations will depend on temperature and possibly on other environmental conditions.

Some evidence of the structure of aldehydes can be obtained from the proton magnetic resonance spectra, particularly the spin-coupling between the aldehyde proton and the protons on the α carbon atom. The coupling constants between protons attached to neighbouring carbon atoms are known to be sensitive to relative configuration and this has been used in studies of substituted ethanes [7, 8]. In molecules with single bonds, the trans H—H coupling J_t is generally much greater than the gauche J_g . This is supported theoretically [9] and it seems likely that a similar result applies in aldehydes. If the isomers are interconverting rapidly, the observed coupling constant will be the appropriately weighted average for the various forms. For acetaldehyde, this average will be $\frac{1}{3}(J_t + 2J_g)$ and should be temperature-independent.

The coupling constants between aldehyde and α -protons have been measured as a function of temperature for acetaldehyde and propionaldehyde (using a Varian 60 Mc/s NMR spectrometer and the 'wiggle-beat technique' [10]). The results are shown in the following figure.



The temperature-dependence of the coupling constants J_{CH-CHO} in
(a) acetaldehyde and (b) propionaldehyde.

The acetaldehyde value is practically independent of temperature as expected and the propionaldehyde value is smaller and increases with temperature. If J_t is greater than J_g this implies that (2) is the more stable form of propionaldehyde. If it is assumed that J_g and J_t have the same values in both molecules, it is possible to deduce J_g and J_t separately together with the enthalpy difference between the forms. It is found then that $J_g = 0.1$ c/s and $J_t = 8.3$ c/s and the enthalpy difference is 1.0 kcal/mole in favour of (2). The value of J_t is comparable with the value for trans-crotonaldehyde [11], where the molecule is probably entirely in one form.

Further details of work on these and other molecules will be given in a later publication.

The work described above has been carried out as part of the research programme of the National Physical Laboratory, and this paper is published by permission of the Director of the Laboratory.

REFERENCES

- [1] MIZUSHIMA, S., 1954, *Structure of Molecules and Internal Rotation* (Academic Press)
- [2] PAULING, L., 1958, *Proc. nat. Acad. Sci., Wash.*, **44**, 211.
- [3] KILB, R. W., LIN, C. C., and WILSON, E. B., 1957, *J. chem. Phys.*, **26**, 1695.
- [4] HERSCHBACH, D. R., and KRISHER, L. C., 1958, *J. chem. Phys.*, **28**, 728.
- [5] NAKAGAWA, I., ICHISHIMA, I., KURATANI, K., MIYAZAWA, T., SHIMANOUCHI, T., and MIZUSHIMA, S., 1952, *J. chem. Phys.*, **20**, 1720.
- [6] MIZUSHIMA, S., SHIMANOUCHI, T., MIYAZAWA, T., ICHISHIMA, I., KURATANI, K., NAKAGAWA, I., and SHIDO, N., 1953, *J. chem. Phys.*, **21**, 815.
- [7] GRAHAM, D. M., and WAUGH, J. S., 1958, *J. chem. Phys.*, **27**, 968.
- [8] SHEPPARD, N., and TURNER, J. J., 1959, *Proc. roy. Soc. A*, **252**, 506.
- [9] KARPLUS, M., 1959, *J. chem. Phys.*, **30**, 11.
- [10] BENE, G. J., DENIS, P. M., and EXTERMANN, R. C., 1951, *Physica*, **17**, 308.
- [11] POPLE, J. A., and SCHAEFER, T., 1960, *Mol. Phys.*, **3**, 547.

INDEX OF AUTHORS (WITH THE TITLES OF PAPERS)

- ABRAHAM, R. J., BISHOP, E. O., and RICHARDS, R. E.: The proton resonance spectrum of *m*-dinitrobenzene, the AB₂ X system, 485
- ABRAHAM, R. J., and POPEL, J. A.: Rotational isomerism in aldehydes, 609
- ANDREWS, A. L., and BUCKINGHAM, A. D.: The effect of strong electric and magnetic fields on the depolarization ratios of gases, 183
- ATHERTON, N. M., and WHIFFEN, D. H.: An electron spin resonance study of a γ -irradiated single crystal of glycollic acid, 1
- ATHERTON, N. M., and WHIFFEN, D. H.: Electron resonance study of the carboxylate hydroxy methyl radical ion, 103
- BABLOYANTZ, AGNESSA, and BELLEMANS, A.: Statistical mechanics of solid and liquid mixtures of ortho- and para-hydrogen. II, 314
- BADER, R. F. W.: An interpretation of potential interaction constants in terms of low-lying excited states, 137
- BANWELL, C. N.: The nuclear magnetic resonance spectrum of N-vinyl pyrrolidone, 511
- BANWELL, C. N., and SHEPPARD, N.: High resolution nuclear-magnetic-resonance spectra of hydrocarbon groupings. IV. ABC spectra of vinyl compounds, 251
- BELLEMANS, A., *see* BABLOYANTZ, AGNESSA.
- BELLEMANS, A., and STECKI, J.: On the surface tension of regular mixtures, 203
- BISHOP, E. O., *see* ABRAHAM, R. J.
- BISHOP, E. O., and RICHARDS, R. E.: High resolution hydrogen resonance spectra of some substituted ethylenes, 114
- BROWN, W. B., and ROWLINSON, J. S.: A thermodynamic discriminant for the Lennard-Jones potential, 33
- BUCKINGHAM, A. D., *see* ANDREWS, A. L.
- BUCKINGHAM, A. D., and LAWLEY, K. P.: Nuclear magnetic shielding of a hydrogen atom in (1) an electric field-gradient and (2) a cage, 219
- CARRINGTON, A.: The temperature-independent paramagnetism of permanganate and related complexes, 271
- CARRINGTON, A., DRAVNICKS, F., and SYMONS, M. C. R.: Studies of ion-solvent and ion-ion interactions using nuclear magnetic resonance spectroscopy, 174
- CARRINGTON, A., and SCHONLAND, D. S.: The absorption spectra of permanganate, manganate and related oxyions, 331
- CHILD, M. S.: Dynamical Jahn-Teller effect in molecules possessing one four-fold symmetry axis, 601
- CHILD, M. S.: Vibrational-electronic coupling in IrF₆, OsCl₆²⁻ and IrCl₆²⁻, 605
- COSSEE, P.: Magnetic properties of Co²⁺ ions in octahedral interstices of an oxide lattice, 125
- DALLINGA, G., SMIT, P. J., and MACKOR, E. L.: The redistribution of charge in naphthalene caused by methyl substitution. I. Partial rate factors for hydrogen-deuterium exchange in α , α - and β , β -dimethylnaphthalenes, 130
- DE GROOT, M. S., and VAN DER WAALS, J. H.: Paramagnetic resonance in phosphorescent aromatic hydrocarbons. II. Determination of zero-field splitting from solution spectra, 190
- DIEHL, P., and POPEL, J. A.: The analysis of complex nuclear magnetic resonance spectra. II. Some further systems with one strong coupling constant, 557
- DRAVNICKS, F., *see* CARRINGTON, A.
- ENGLMAN, R.: Some temperature dependent effects on the optical absorption line shape of paramagnetic ions, 23
- ENGLMAN, R.: Charge transfer states and optical absorption in octahedrally hydrated paramagnetic salts, 48
- EYRING, HENRY, *see* HECHT, HARRY, G.

- FREEMAN, R.: Spin decoupling in high resolution proton magnetic resonance, 435
- GASSER, R. P. H., and RICHARDS, R. E.: Cobalt nuclear resonance measurements of rate processes and a system in equilibrium, 163
- GLANSDORFF, P.: On a non-linear law of the irreversible phenomena with stationary constraints, 277
- GRANT, DAVID M., *see* HECHT, HARRY G.
- GREENWOOD, H. H., and HAYWARD, T. H. J.: Properties of the self-consistent field treatment of conjugated molecules, 495
- GRIFFITH, J. S.: Some investigations in the theory of open-shell ions. Part I. The spin-Hamiltonian, 79
- GRIFFITH, J. S.: Some investigations in the theory of open-shell ions. Part II. V , W and X coefficients, 285
- GRIFFITH, J. S.: Some investigations in the theory of open-shell ions. Part III. The calculation of matrix elements, 457
- GRIFFITH, J. S.: Some investigations in the theory of open shell ions. Part IV. The basis of intensity theory, 477
- GRIFFITHS, T. R., and SYMONS, M. C. R.: Ionic interactions in solutions of electrolytes as studied by ultra-violet spectroscopy, 90
- GUGGENHEIM, E. A., and McGlashan, M. L.: Equilibrium properties of crystalline argon, krypton and xenon, 563
- GUGGENHEIM, E. A., and McGlashan, M. L.: The properties of argon at its triple point, 571
- HATTON, J. V., and RICHARDS, R. E.: Solvent effects in the proton resonance spectra of dimethyl-formamide and dimethyl-acetamide, 253
- HAYWOOD, T. H. J., *see* GREENWOOD, H. H.
- HECHT, HARRY G., GRANT, DAVID M., EYRING, HENRY: Electron spin correlation and the ethane barrier, 577
- HOIJTINK, G. J.: The influence of paramagnetic molecules on singlet-triplet transitions, 67
- HOIJTINK, G. J., VELTHORST, N. H., and ZANDSTRA, P. J.: Correlations between the electronic spectra of alternant hydrocarbon molecules and their mono- and di-valent ions. II. Hydrocarbons with symmetry D_{2h} , 533
- HOIJTINK, G. J., and ZANDSTRA, P. J.: Polarization of electronic transitions in aromatic hydrocarbon molecules and their mono- and di-valent ions, 371
- HUTTON, E., *see* STEVENS, B.
- I'HAYA, Y.: A semi-empirical theory of the electronic structure of ethylene with particular reference to the ionization potential, 513
- JØRGENSEN, CHR. KLIKBÜLL: New interpretations of the orbital energy differences in hexafluorides, 201
- LAWLEY, K. P., *see* BUCKINGHAM, A. D.
- LEVY, D. A., and ORGEL, L. E.: The proton resonance spectra of metal bis-cyclopenta-dienyls, 583
- LUPINSKI, J. H., *see* VAN DER HOEK, J. A.
- MCCARTIN, P. J., *see* STEVENS, B.
- MACKOR, E. L., *see* DALLINGA, G.
- MACKOR, E. L., *see* MACLEAN, C.
- McGLASHAN, M. L., *see* GUGGENHEIM, E. A.
- MCLACHLAN, A. D.: Self-consistent field theory of the electron spin distribution in π -electron radicals, 233
- MACLEAN, C., and MACKOR, E. L.: The redistribution of charge in naphthalene caused by methyl substitution. II. The magnetic shielding of protons in α , α - and β , β -dimethylnaphthalenes, 223

- MARSHALL, T. W., and POPLE, J. A.: Nuclear magnetic shielding and diamagnetic susceptibility of interacting hydrogen atoms, 339
- MURRELL, J. N.: The effect of paramagnetic molecules on the intensity of spin-forbidden absorption bands of aromatic molecules, 319
- NAGAKURA, S.: Intramolecular charge-transfer absorption spectra of formamide and acrolein, 105
- NAGAKURA, S.: Ultra-violet absorption spectra and π -electron structures of nitro-methane and the nitromethyl anion, 152
- ORGEL, L. E., *see* LEVY, D. A.
- OOSTERHOFF, L. J., *see* VAN DER HOEK, J. A.
- PARSONAGE, N. G., and STAVELEY, L. A. K.: Thermodynamic properties of clathrates. II. The heat capacity and entropy of methane in the methane quinol clathrates, 59
- PEACOCK, T. E.: The effect of bond length variations in molecular orbital calculations of π -electron spectra—aniline, 453
- POPLE, J. A.: The Renner effect and spin-orbit coupling, 16
- POPLE, J. A., *see* ABRAHAM, R. J.
- POPLE, J. A., *see* DIEHL, P.
- POPLE, J. A., *see* MARSHALL, T. W.
- POPLE, J. A., and SCHAEFER, T.: The analysis of complex nuclear magnetic resonance spectra. I. Systems with one pair of strongly coupled nuclei, 547
- RICE, STUART A., *see* ZIMM, BRUNO H.
- RICHARDS, R. E., *see* ABRAHAM, R. J.
- RICHARDS, R. E., *see* BISHOP, E. O.
- RICHARDS, R. E., *see* GASSER, R. P. H.
- RICHARDS, R. E., *see* HATTON, J. V.
- ROBINSON, G. WILSE: Discrete sites in liquids, 301
- ROSENBAUM, J., and SYMONS, M. C. R.: Unstable intermediates. Part X. Aliphatic carbonium ions, 205
- ROWLINSON, J. S.: A test of the Lennard-Jones potential for nitrogen and methane, 265
- ROWLINSON, J. S., *see* BROWN, W. B.
- SALEM, L.: The calculation of dispersion forces, 441
- SCHAEFER, T., *see* POPLE, J. A.
- SCHONLAND, D. S., *see* CARRINGTON, A.
- SCHUYER, J.: The anomalous temperature dependence of the sound velocity in water, 597
- SHEPPARD, N., *see* BANWELL, C. N.
- SHEPPARD, N., and TURNER, J. J.: High-resolution nuclear-magnetic-resonance spectra of hydrocarbon groupings. III. An analysis of the spectrum of liquid propane using ^{13}CH satellites, 168
- SMIT, P. J., *see* DALLINGA, G.
- STAVELEY, L. A. K., *see* PARSONAGE, N. G.
- STECKI, J., *see* BELLEMANS, A.
- STEVENS, B.: The collisional stabilization of excited β -naphthylamine molecules by the paraffin hydrocarbons in the gas phase, 589
- STEVENS, B., and HUTTON, E.: The fluorescence and excitation spectra of anthracene vapour at low pressures, 71
- STEVENS, B., and McCARTIN, P. J.: Fluorescence self-quenching in aromatic vapours; the role of excited dimers, 425
- SYMONS, M. C. R., *see* CARRINGTON, A.
- SYMONS, M. C. R., *see* GRIFFITHS, T. R.
- SYMONS, M. C. R., *see* ROSENBAUM, J.
- TURNER, J. J.: The use of complex wiggle-beat patterns for the estimation of small splittings in NMR spectra, 417
- TURNER, J. J., *see* SHEPPARD, N.

- VAN DER HOEK, J. A., LUPINSKI, J. H., and OOSTERHOFF, L. J.: Semiconductivity in organic molecular complexes, 299
- VAN DER WAALS, J. H., *see* DE GROOT, M. S.
- VELTHORST, N. H., *see* HOIJTINK, G. J.
- WADA, AKITOSHI: Helix-coil transformation and titration curve of poly-L-glutamic acid, 409
- WHIFFEN, D. H., *see* ATHERTON, N. M.
- ZANDSTRA, P. J., *see* HOIJTINK, G. J.
- ZIMM, BRUNO H., and RICE, STUART A.: The helix-coil transition in charged macromolecules, 391
- ZWANZIG, R. W.: Intermolecular forces from optical spectra of impurities in molecular crystals, 305

DATE DUE

UIC-RECD APR 18 '86

UIC-RECD APR 23 '86

UIC-RECD APR 28 '86

UIC-RECD SEP 23 '91

**RENEWALS
996-2724**

DEMCO 38-297

THE UNI
3 8198 322 495 308

